

REVIEWS

Chemical Modifications of Proteins: History and Applications

Gary E. Means[†] and Robert E. Feeney^{*‡}

Department of Biochemistry, The Ohio State University, Columbus, Ohio 43210, and Department of Food Science and Technology, University of California, Davis, California 95616. Received October 19, 1989

With roots in ancient formulations, methods for the chemical derivatization of proteins continue to expand and develop. The creation of this new journal dealing exclusively with bioconjugate chemistry was barely conceivable just a few years ago. An explosion of interest in the subject during the last decade is, however, easily seen. The tremendous growth in both the number of publications and in the number of research groups involved in these kinds of studies has been promoted by both practical interests related, for example, in some cases to possible pharmacological or medical diagnostic applications and by interest in questions of fundamental biochemical structure and function.

Greatly improved understanding of established reagents and procedures and the development of many new, and more sophisticated, reagents and procedures have been facilitated by advances in the ancillary fields of organic chemistry, X-ray crystallography, and molecular biology. Whereas protein modification in the past often involved the same reagents and reactions commonly used in the organic chemistry of that time (i.e., acetylation, iodination, deamination, reaction with formaldehyde, etc.), those in most common use today have, by and large, been developed to meet the varied but relatively specific needs of the protein chemist. A large number of specialized reagents have been described: affinity labels, photoaffinity labels and other specifically designed site-directed reagents (1, 2), group-selective reagents which react exclusively (or at least predominantly) with one particular type of amino acid side chain (see below, especially Table II), and others that react relatively nonspecifically with a number of different side chains (3).

Reagents have been designed to preserve electrostatic charge (4, 5), to alter electrostatic charge (6), and to increase hydrophobicity (7, 8). Reagents and procedures have been developed to decrease immunogenicity (9, 10), to increase and decrease susceptibility to proteolysis (11-13), to increase UV or visible absorbancy (14), to introduce fluorescent labels (15, 16), spin labels (17), radiolabels (18-20), various metal ions (21), magnetic microspheres (22, 23), and electron-dense substituents (24), to increase the content of certain low-abundance nonradioactive isotopes (25), and to attach several different types of carbohydrate moieties (26-29), biotin (30), and a number of other biospecific recognition groups (i.e., avidin, streptavidin, antibodies, protein A, protein G, lectins, and others (31)). Procedures also have been developed to effect the cleavage of peptide chains (32, 33); to modify enzyme specificity (34); to modify the terminal hydroxyls of galactosyl residues in glycoproteins (35); to introduce intramo-

lecular and intermolecular cross-links, both to couple already associated species (36, 37); and to join various proteins, which might or might not otherwise associate, in order to combine the properties of both into a single molecule, e.g., to make protein-protein conjugates (38, 39), enzyme-linked antibodies (40, 41), immunotoxins (42, 43), and drug-protein conjugates (44). A large number of reagents that have been developed to serve these and a variety of other purposes are commercially available.

EARLY DEVELOPMENTS

The chemistry of proteins had its origin in the chemistry of the amino acids and only later concerned the amino acid side chains of intact proteins. For practical purposes, a variety of procedures for protein modification had been developed and used many years prior to any significant interest in or understanding of protein chemistry. For example, the use of formaldehyde and other agents in the tanning industry was apparently formulated entirely on the basis of empirical observations, without any real understanding of the reactions or of the chemical nature of the materials involved. Similar procedures were also employed successfully to convert a number of protein toxins, usually of bacterial origin, into toxoids, which retain some of the original antigenic determinants but are no longer toxic. Inoculations of toxoids are still widely employed to confer immunity against a number of serious bacterial diseases. Although still widely used, there is not much known about the manner by which formaldehyde converts toxins into toxoids.

Interest in quantitative determinations of proteins and their various constituent amino acids was a major impetus for many early studies of chemical modification. While a significant number of proteins had been crystallized by the 1920s, analytical values for individual amino acids were still quite poor well into the 1940s. Analytical data had, for example, revealed only one sulfur-containing amino acid, cystine, in naturally occurring proteins prior to the discovery of methionine in 1922. Threonine was not discovered until 3 years later.

Most of the procedures available at that time for the determination of individual amino acids were, of course, supplanted by the development of the far more convenient cation-exchanger amino acid analyzer in the 1950s. Slightly altered forms of some of those procedures, however, still find use today. Variations of the Van Slyke procedure for determining protein nitrogen, for example, are still sometimes useful for bringing about the selective deamination of proteins. Sodium nitroprusside, which was once used for spectrophotometric determinations of cysteine, also appears to be useful for the selective modification of protein thiol groups. Some much more recently developed procedures for protein modification, on the other

[†] The Ohio State University.

[‡] University of California.

Table I. Major Types of Affinity Labels

type	examples	target enzymes	reaction characteristics	refs cited
α -halocarbonyl RCOCH_2X	TPCK	chymotrypsin	addition to nucleophilic groups, especially His and Cys(SH), also COO-	58
	3-bromo-2-ketoglutarate	isocitrate dehydrogenase		59
	chloroacetol sulfate	triase phosphate isomerase		60
epoxide $\text{R}-\text{CH}-\text{CH}_2$ $\quad \quad \quad \diagup \quad \diagdown$ $\quad \quad \quad \text{O}$	1,2-anhydromannitol 6-phosphate glycidol phosphate	glucose 6-phosphate isomerase triase phosphate isomerase, enolase	addition to various nucleophilic groups, COO-, Cys(SH)	61 62
sulfonyl fluoride RSO_2F	5'-[(fluorosulfonyl)benzoyl]-adenosine	glutamine synthetase, etc.	addition to various nucleophilic groups, Cys(SH), Lys, His, etc.	63
aldehyde RCH=O	2',3'-dialdehydo-ATP	pyruvate carboxylase adenylate cyclase, etc.	synthesized by periodate oxidation of ATP, addition to amino groups especially in the presence of NaBH_4 , dialdehyde derivatives of other nucleotides and nucleosides may be employed similarly	64, 65
	pyridoxal phosphate	glycogen phosphorylase, glutamine synthetase, DNA polymerase, etc.	reaction with Lys in PLP and phosphate binding sites; irreversible, in the presence of NaBH_4 or $\text{NaBH}_3(\text{CN})$	66-68
azido RN_3 (photoaffinity labels)	8-azido-ATP	F1-ATPase	requires UV irradiation; by addition to nucleophiles and double bonds, insertion into C-H and O-H bonds, and other reactions	69
	5-azido-UDP	UDP-glucose, pyrophosphorylase		70

hand, have been shown to be useful for analytical determinations of certain amino acids in proteins. The use of water-soluble carbodiimides and certain nucleophiles to determine amounts of glutamine and asparagine, and of 2-hydroxy-5-nitrobenzyl bromide to determine tryptophan contents of proteins are possibly of special interest since the acid lability of those amino acids makes their determinations difficult by conventional amino acid analysis (45, 46). The use of TNBS¹ for the determination of amino groups (47) and DTNB for the determination of thiol groups (48) in intact proteins have also achieved special status as a result of their widespread use for such purposes.

By the end of World War II, interest had turned to determining particular amino acid residues necessary for the biological activities of proteins. That a particular amino acid residue in the active site of an enzyme might be identified on the basis of its reaction with selective chemical reagents was an idea developed during this period. Those interests and further careful scrutiny of the available methodology led to the publication of two important reviews of protein modification in 1947 (49, 50). The report of Balls and Jansen (51) showing that the inactivation of several proteases by diisopropyl fluorophosphate resulted from its reaction with a specific serine residue in each case was another milestone of this period.

Some of the earliest attempts to use chemical modification procedures to identify particular amino acid residues required for the biological activity of a protein were conducted in the laboratory of Heinz Fraenkel-Conrat (52-54). A few of those procedures are still used, with little change, to this day. However, these earlier studies were seriously hampered by the absence of sensitive and accurate procedures to determine the number and type(s) of amino acid residues undergoing modification and by the absence of effective micro and semimicro procedures to separate, purify, and characterize products. The studies of that period, nevertheless, provided important descriptions of procedures for use by other investigators and served as important steps to the later development of improved procedures.

Quantitative data on the extent of modification became more attainable with the increased availability of radio-

actively labeled reagents during the 1960s. Greater access to automated amino acid analyzers (55) and the development of effective ion-exchange and gel exclusion chromatography media at about the same time also facilitated the characterization of modified proteins, which led to a better understanding of many modification reagents and procedures. Various forms of micro gel electrophoresis also became commonplace in the same decade, and these greatly enhanced the ability to monitor the effects of modification on relatively small amounts of protein. The advent of an effective procedure for the routine determination of amino acid sequences, first described by Edman in 1956 (56), was also a major milestone. Although often considered routine today, these procedures were developed only after many years of effort and were essential for the characterization of various modification procedures.

SITE-SPECIFIC MODIFICATIONS

In 1962, Wofsey and co-workers (57) described a selective reaction of the *p*-arsonylbenzenediazonium ion with the antigen-combining site of a rabbit anti-*p*-azobenzene-*o*-arsenate antibody. This demonstration of affinity labeling was followed in about 1 year by the description of a highly selective reaction between chymotrypsin and a reactive substratelike compound, TPCK (58). The latter was shown to effect the modification of a particular histidine residue of chymotrypsin with the complete elimination of its catalytic activity. The selectivity of these and other affinity labels results from their resemblance to a substrate or ligand. Their strong affinity for a particular site concentrates a reactive group, like the chloromethyl ketone moiety of TPCK, at a specific site, where its reaction with a nearby amino acid side chain is promoted by mutual proximity. Subsequent to these reports, a very large number of affinity labeling reagents have been described. Affinity labeling is now one of the most important methods for identifying amino acid residues in enzyme active sites. Table I describes some of the most commonly used types of affinity labeling reagents and summarizes a few of their salient properties.

SIDE CHAIN SELECTIVE MODIFICATIONS

The use of the side chain selective reagents (i.e., those which react, under certain specified conditions, with a single or, at least, a limited number of side-chain groups in a fairly predictable manner) is, however, a simpler

¹ Abbreviations are as follows: trinitrobenzenesulfonic acid, TNBS; 5,5'-dithiobis(2-nitrobenzoic acid), DTNB; tosylphenylalanine chloromethyl ketone, TPCK; dithiothreitol, DTT; 1-ethyl-3-[3-(dimethylamino)propyl]carbodiimide, EDC.

Table II. Useful Side Chain Modification Reagents^a

side chain or group	reagent or procedure	optimum reaction pH, side chain selectivity, and other comments	refs cited
amino (Lys + α)	amidination (ethyl acetimidate)	pH ~9, no other side chains react, positive charge maintained, other imido esters are available, extent of modification may be determined with TNBS	4, 71
	reductive alkylation (formaldehyde + NaBH ₄ or NaBH ₃ CN)	pH ~9 with NaBH ₄ , pH ~7 with NaBH ₃ CN; reaction is much slower under the latter conditions; no other side chains react; positive charge maintained; other aldehydes and reducing agents may be used; extent of modification may be determined by amino acid analysis, the incorporation of radiolabel, or with TNBS	5, 25
	acylation (acetic anhydride)	pH ~8 and above, Tyr residues also modified, elimination of positive charge, extent of modification may be determined with TNBS	72
	(succinic anhydride)	same as above, Tyr residues undergo slow deacylation above pH ~5, replaces positive charges with negative charges	73
	trinitrobenzenesulfonate	pH ~8 and above, also reacts slowly with thiol groups, eliminates positive charge and introduces large hydrophobic substituent, extent of reaction may be determined spectrophotometrically	47, 74
carboxyl (Asp + Glu)	water-soluble carbodiimide + nucleophile (EDC + glycine ethyl ester)	pH ~4.5-5, some side reactions with Tyr and thiol groups, other carbodiimides are available, many other nucleophiles (amines) may be used to either maintain or alter the charge, extent of reaction may be determined by amino acid analysis or from incorporation of radiolabel	45, 75
guanidino (Arg)	dicarbonyls [2,3-butanedione, phenylglyoxal, and (p-hydroxyphenyl)glyoxal]	pH ~7 or higher, reaction promoted by borate buffer, no major side reactions; partially reversible upon dialysis, eliminates positive charge, extent of reaction can be determined from incorporation of radiolabel or by amino acid analysis, other dicarbonyl compounds can also be used (i.e., cyclohexanedione, glyoxal, etc.).	76-79
imidazole (His)	diethyl pyrocarbonate (ethoxyformic anhydride)	pH ~4-5, side reactions with Lys kept to minimum by low pH, extent of modification may be determined by spectrophotometric measurement, reversed in the presence of NH ₂ OH	80, 81
indole (Trp)	N-bromosuccinimide	usually pH ~4 or lower, higher pH values can be used; thiol groups are rapidly oxidized; Tyr and His react more slowly; extent of modification may be determined spectrophotometrically or by amino acid analysis	82
	2-hydroxy-5-nitrobenzyl bromide	pH <7.5, slight reaction with thiols, strong visible absorbance, can be used to determine the extent of reaction	83, 84
phenol (Tyr)	iodination (I ₃ ⁻ , chloramine T + I ⁻ , ICl, lactoperoxidase + I ⁻ , and H ₂ O ₂)	pH ~8 or higher, many different procedures and reagents, His also reacts but usually to a lesser extent, thiol groups are rapidly oxidized, both mono and diiodo derivatives are formed, the extent of reaction can be estimated spectrophotometrically or by amino acid analysis, widely used for radiolabeling of proteins	18, 85, 86
	tetranitromethane	pH ~8 or slightly higher, thiol groups are also rapidly oxidized, some nitration of Trp, extent of reaction may be determined spectrophotometrically or by amino acid analysis	87
thiol (Cys-SH)	carboxymethylation (iodo- and bromoacetate and iodo- and bromoacetamide)	pH ~7 or higher; no effect on other residues under appropriate conditions; Lys, His, Tyr and Met react slowly with excess reagent and long reaction times; extent of reaction may be determined with DTNB, by the incorporation of radiolabel, or by amino acid analysis	88, 89
	N-ethylmaleimide	pH ~6 or higher, reaction with Lys and His are much slower at pH 7 and usually of no importance, the extent of reaction may be determined from incorporation of radiolabel or by amino acid analysis	90, 91
	5,5'-dithiobis(2-nitrobenzoic acid) (Ellman's reagent)	pH ~7 or higher, no other side chains react, reversible in presence of excess low MW thiol, the extent of modification can be determined spectrophotometrically	48, 92
thioether (Met)	oxidation (H ₂ O ₂)	pH ~1 and higher, thiol groups also react very rapidly, reversed by treatment with low MW thiols, extent of modification may be determined by amino acid analysis after alkaline hydrolysis or by carboxymethylation followed acid hydrolysis	93

^a Many useful reagents have not been included due to space limitations. Descriptions of reaction conditions, outcomes and literature citations are also brief and incomplete for the same reason. More complete information is available in the references and other sources cited elsewhere in this review.

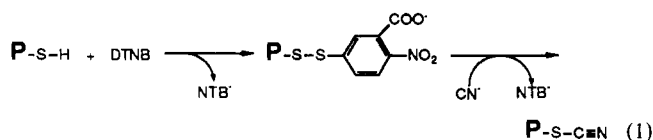
approach. At least for initial screening, it is still widely used to identify amino acid chains required for biological activity. Table II contains a list of some of the most commonly used and, in the authors' opinions, most useful group-selective reagents and brief descriptions of some of their important properties and applications.

The retention of biological activity after treatment with one of those reagents is usually good a priori evidence that the modified amino acid side chains are not required for that particular activity. Under appropriate conditions, each reagent normally reacts only with the indicated target side chain(s). Depending on the protein, the reagent, and the particular conditions, however, complete modification of all such side chains is not always obtained. In most cases, the extent of reaction can be determined by either direct spectrophotometric measurements, amino acid analyses, or the use of radioactive reagents. Indirect determinations can also be obtained from the number of unreacted amino acid residues, as determined either spectrophotometrically (e.g., amino groups by TNBS (47) or thiol groups by DTNB (48)) or by amino acid analysis. The extent of reaction can, of course, almost always be increased by the use of more vigorous reaction conditions, e.g., longer reaction times,

larger excesses of reagent, and the presence of urea or other denaturing agents. Using more severe conditions, however, is usually accompanied by some decrease in side-chain selectivity, greater risk of conformational change, and, sometimes, other disadvantages. Reaction with other than target side chains may be of little importance when activities are not affected.

A major loss of biological activity upon such treatment is often taken as evidence for the essentiality of the group modified. But this interpretation must be made with somewhat less conviction, owing to the possibility of unrecognized conformational changes or other subtle effects that may always accompany the modification of a protein. The latter are obviously of less concern when fewer side chains are modified and for those modifications that effect the least change in the size and character of side chains. Luckily, a reasonable number of reagents are available for some of the more important side chains, allowing some discretion as to the nature of the modifications that may be effected. Rat liver glycine methyltransferase, for example, is completely inactivated by reaction with excess DTNB (94). The inactivated enzyme is, however, almost completely reactivated by subsequent treatment with potassium cyanide which, presum-

ably, brings about the replacement of a relatively large and anionic 2-nitro-5-thiobenzoate moiety by a smaller cyano group with no formal charge, as follows:



A carboxymethyl moiety introduced by reaction with iodoacetate is also anionic but intermediate in size and effects only a partial loss of activity. The larger groups thus appear to block or otherwise perturb the active site, although none of the cysteine residues to which they are attached are really essential for catalytic activity.

Similar inactivations have been noted following the addition of large or charged groups to the cysteine residues of many enzymes that are either not inactivated or are only partially inactivated by the addition of smaller groups. 2-Nitro-5-thiocyanatobenzoic acid can be used to effect a direct, single-step addition of cyano moieties to thiol groups (95, 96), although its reactions are not quite as simple as they might initially seem (97). Another reagent, methyl methanethiosulfonate, can be used to attach relatively small, uncharged thiomethyl groups to cysteine residues, usually with comparable results (98).

As a general rule, modifications that have the least effect on side-chain character should have the least effect on protein structure and properties. Modifications of lysine residues that retain their usual cationic charge have, for example, generally been found to have relatively little effect on the biological activities and other properties of many proteins. Complete guanidination of the ϵ -amino groups in tuna heart cytochrome c thus has almost no effect on its UV-visible spectrum, its redox potential, or its activity in a standard succinate oxidase assay system (99). The catalytic activity of papain is also essentially unaffected by complete guanidination (100). Amidination or reductive alkylation of amino groups, both of which also retain the cationic charge, are generally preferred today, however, as both of those reactions take place under milder conditions (4, 5, 25).

SIDE-CHAIN REACTIVITIES

The reactivities of side-chain groups in proteins vary considerably depending on their locations and the influence of nearby residues with which they interact. Under appropriate conditions, differences in reactivity can be used to characterize the environments of such side-chain groups. Kaplan and co-workers (101, 102) and others (103, 104), for example, have developed procedures to determine the relative reactivities of certain types of side chains from the extent of their reaction with trace levels of one of several simple reagents. The intrinsic reactivity and pK_a of each reacting group can be determined by comparing its reaction to that of a simple model compound over a range of pH values.

For identical side-chain groups at different sequence positions, the observed differences in pK_a and reactivity are assumed to reflect differences in local environment. Side chains that experience a change in environment upon the binding of a ligand, complexation with another protein, a change in redox state, or the like can be identified by comparing the extent of their reaction in the two different states. This approach has been used primarily to evaluate the environments of the nucleophilic side chains—amino groups and histidine and tyrosine side chains—in proteins (105, 106).

Different local environments may either suppress or enhance the reactivities of individual side-chain groups. Unusually reactive side chains are usually relatively easy to distinguish from others on the basis of their reactivity and are, in many cases, also those required for biological activity. Rates of inactivation, which may differ from overall rates of modification, can be used in many cases to characterize the reactivity and, sometimes, the number of active site residues (107–109).

In many relatively simple cases, rates of inactivation can be correlated with those for the modification of one or more individual amino acid residues. The catalytic subunit of rabbit muscle cAMP-dependent protein kinase, for example, has only two thiol groups, and undergoes a biphasic reaction with DTNB (110). Its rapid inactivation under those conditions correlates with the initial, rapid phase of modification, which has been shown to reflect the reaction of one thiol group about 17 times faster than the other. In this and other cases where rates of inactivation exceed overall rates of modification, selectively labeled derivatives, modified only at the active site, can often be isolated and characterized (111–113).

Activities remaining at various stages of partial modification can also be used, in some cases, to estimate the number of essential residues according to a procedure first described by Tsou in 1962 (114). The decreased iron-binding capacity of chicken egg white ovotransferrin after partial modification by phenylglyoxal, for example, suggests an arginine residue is required for each of its two bound Fe^{3+} ions (76). In the more complicated case of transketolase, two arginine residues per dimer appear to be required for activity, but one appears to react with phenylglyoxal about 40 times faster than the other (115).

SPECTROSCOPIC AND FLUORESCENT LABELS

A number of important procedures requiring the incorporation of spectroscopic or fluorescent labels have been developed to characterize certain structural features of proteins. Fluorescence lifetimes and quantum yields of many different fluorescent groups and their sensitivities to quenching by acrylamide, iodide, and other substances can, for example, be used to evaluate environments in the vicinity of residues to which those groups have been attached (15, 116). Fluorescence energy transfer measurements are also widely employed to estimate distances between certain internal, or intrinsic, chromophores and various selectively introduced, extrinsic, fluorescent labels and, in some cases, between selectively introduced, extrinsic, donor-acceptor pairs (117, 118). Iodoacetamidofluorescein, dansyl chloride, and *N*-1-pyrenylmaleimide are three examples from a very large number of fluorescent labels that have been used for such purposes. Most may be considered to be analogues of commonly used group-selective reagents and their reaction characteristics may be predicted accordingly.

An extensive list of such reagents, with brief descriptions of their principal reaction and emission and excitation characteristics, has been presented by Haugland (119). Procedures to attach nitroxide moieties, for example the reaction of 4-(2,2,6,6-tetramethyl-1-oxypiperidin-4-yl)-2-(fluorosulfonyl)benzamide with chymotrypsin, have also been employed to obtain information concerning the protein environment and to detect conformational changes by EPR spectroscopy (17, 120).

CROSS-LINKING AND IMMOBILIZATION

Cross-linking of proteins and their immobilization, either by attachment to an insoluble support or by various other means, have a long and important history. The former

Table III. Homobifunctional and Heterobifunctional Protein Cross-Linking Agents^a

agent	description	refs cited
Homobifunctional		
glutaraldehyde	available as 25% aqueous solution, very effective reaction with amino groups and perhaps other nucleophilic groups, contains polymeric and other unknown materials, the nature of the reaction(s) are not known, slow progressive changes proceed long after the initial irreversible coupling	137
dimethyl suberimide (DMS)	a water-soluble solid; reacts only with amino groups and does not eliminate their cationic charge; reaction at pH 8 or above (optimal at pH ~9); $t_{1/2} \approx 46$ min at pH 8.5 and 25 °C; ~11-Å span; many related reagents with different spans, some readily cleavable, are available or can be easily synthesized	138, 139
disuccinimidyl suberate (DSS)	a water-insoluble solid; must usually be dissolved in DMSO or other water-miscible organic solvent; reacts with amino groups at pH 7 or above; reaction rates increase with pH; $t_{1/2} \approx 4-5$ h at pH 7; ~11-Å span; many related reagents with different spans; hydrophilic spacer arms, some cleavable and water-soluble; sulfosuccinimide esters are available	140, 141
bismaleimidoethane (BMH)	a water-insoluble solid, must usually be dissolved in DMF or other water-miscible organic liquid, reacts with thiol groups at pH ~6-8; ~16-Å span; many related reagents with different span lengths; more hydrophilic spacer arms and cleavable analogs are available	142, 143
<i>p</i> -phenylenemaleimide	a water-insoluble solid, must usually be dissolved in water-miscible organic solvent, reacts with thiol groups at pH ~6-8; ~12-Å span, ortho and meta isomer are also available, less stable than aliphatic maleimides	144-146
Heterobifunctional		
<i>m</i> -maleimidobenzoic acid <i>N</i> -hydroxysuccinimide ester (MBS)	a water-insoluble solid, must usually be dissolved in water-miscible organic liquid, initial reaction with amino group component at pH ~7-8 followed by coupling with thiol component at pH ~6-8, ~10-Å span, more water soluble sulfosuccinimide ester is also available	147, 148
<i>N</i> -succinimidyl 4-(<i>N</i> -maleimidomethyl)- cyclohexane-1-carboxylate (SMCC)	a water-insoluble solid, must usually be dissolved in water-miscible organic solvent, reaction characteristics very similar to those of MBS, ~12-Å span, more water soluble sulfosuccinimide ester is also available	149, 150
<i>N</i> -succinimidyl 3-(2-pyridyldithio)propionate (SPDP)	a water-insoluble solid, must usually be dissolved in a water-miscible organic solvent, initial reaction with the amino component at pH ~7-8.5 followed by either coupling to thiol component at pH 7 or above or treatment with DTT followed by coupling to maleimidylated protein, ~7-Å span	151, 152
2-iminothiolane ("Traut's reagent")	a water-soluble solid; reacts only with amino groups at pH 7-10 without eliminating their charge; reaction may be followed with DTNB; ~8-Å span; may be coupled directly to MBS-, SMCC- or SPDP-treated proteins	153, 154

^a Many more cross-linking agents have been described. Those included appear to be among the most widely used and most important at the present time. Please consult references in the text for additional examples.

is sometimes employed to increase the stability of proteins or of certain conformational relationships in proteins, to couple two or more different proteins (e.g., to join different activities into a single molecule), to identify or characterize the nature and extent of certain protein-protein interactions, and, in other cases, to determine distances between reactive groups in or between protein subunits (36, 37, 121-125). Proteins are sometimes immobilized to facilitate their reuse and their separation from other products and (in some cases) to increase their stability. A large number of different procedures, including physical as well as chemical procedures, have been developed to immobilize proteins, and many reviews, symposia proceedings, and books on this subject are available (126-130).

A large number of different types of cross-linking or, as they are sometimes called, bifunctional reagents have been described. They include so-called zero-length cross-linking agents that bring about the direct formation of covalent bonds between existing amino acid side chain groups. The use of water-soluble carbodiimides to bring about the formation of amide linkages between carboxyl groups of aspartate or glutamate and the ϵ -amino groups of lysine side chains appear to be the most prominent zero-length cross-linking agents (123, 131-133). Disulfide bonds obtained from existing thiol groups would also, presumably, be considered zero-length cross-links (134, 135). Such linkages appear to be formed only when the reacting groups are in close proximity.

Other cross-linking agents may be organized according to the type(s) of reactive groups, their side chain reactivity, their hydrophobicity or hydrophilicity, and the length or distance between the reactive groups; whether the two, or in some cases more (136), reactive groups are

the same or different (i.e., "homobifunctional" or "heterobifunctional" reagents), whether the structure connecting the reactive groups is readily cleavable, and whether the groups are membrane permeable or impermeable, and according to various other criteria. A list of the most widely used types of cross-linking agents and a few brief comments on some of their significant properties are presented in Table III. A much more extensive list of cross-linking agents has been presented by Ji (125).

The reactivities of cross-linking agents, except for one or two special cases, are very similar to those of the corresponding monofunctional reagents. The initial reaction with a protein is presumably, in most cases, a simple second-order process, not seriously affected by the second reactive group. The latter's reaction, however, is completely dependent on the availability of a second appropriate side chain which, for fast, efficient cross-linking, must be both nearby and in an appropriate orientation. Cross-linking agents with different lengths, different stereochemical configurations (some with little and others with a great deal of conformational flexibility), and with different side-chain specificities have been developed to fulfill different needs. Distances between potentially reactive side chains in the same or different subunits of some oligomeric proteins have, for example, been estimated by comparing rates and yields of cross-link formation with a series of cross-linking agents differing in length, stereochemical configuration, and side-chain reactivity (139, 155, 146).

The importance of side-chain proximity in these reactions is perhaps most evident in the case of cross-linking agents that undergo hydrolysis or some other inactivation process in addition to their cross-linking of proteins. The use of bifunctional imidoesters to characterize

oligomeric proteins, for example, is based on the formation of recognizable SDS gel electrophoretic patterns, reflecting the formation of cross-links between adjacent subunits (139, 138). Like the cross-links within a subunit, those between subunits are formed only when two amino groups are in close and appropriate proximity. Cross-links between other than adjacent subunits are largely precluded by the hydrolytic instability of the monofunctional imidoester intermediates. The importance of hydrolytic stability on yields of cross-linked products has been discussed by Staros (37, 156).

Of the 20 or so amino acid side chains normally present in proteins, ϵ -amino groups of lysine residues are usually among the most abundant and most accessible of the potentially reactive groups. A relatively large proportion of the most commonly used cross-linking agents are therefore amino group selective reagents (i.e., imidoesters, *N*-hydroxysuccinimide esters, activated aryl fluorides, etc.). Most of them, however, also undergo fairly rapid hydrolysis in addition to their reaction with amino groups, which, except for cases involving close proximity, seriously limits the yields that may be obtained. Glutaraldehyde, which does not hydrolyze or become otherwise inactivated over long periods of time, is widely used to immobilize enzymes by cross-linking and to stabilize their adsorption to or entrapment in various materials (157, 158). The nature of its reactions with proteins may involve some Schiff base formation but is clearly much more complicated than that and not completely understood (137, 159, 160).

The high reactivities of thiol groups with *N*-ethylmaleimide, iodoacetate, and many related α -halocarbonyl compounds has led to the development of many cross-linking agents containing comparable maleimide and α -halocarbonyl moieties. Under the conditions usually employed for cross-linking, the latter are much more stable to hydrolysis than the amino group reagents mentioned above and the yields of cross-linked products are, therefore, usually somewhat less dependent on side chain proximity (161, 162).

A large number of heterobifunctional cross-linking reagents have been developed which usually contain a thiol reactive and an amino group reactive moiety. *N*-Alkyl- or *N*-arylmaleimide and α -halocarbonyl groups are the most common of the former and *N*-hydroxysuccinimide esters appear to be the most common of the latter. To increase aqueous solubility, sodium salts of sulfonated *N*-hydroxysuccinimide esters are also commonly employed (163). In addition to the two reactive groups a variety of different types of connecting structures or spacer arms have been employed. The nature of the spacer arm may, of course, also have important consequences. Longer spacer arms are usually assumed to be more effective for coupling larger proteins or those where the potentially reactive side chains are sterically protected. The conformational flexibility, hydrophilicity or hydrophobicity, and the "cleavability" of the spacer arm are also important considerations. *N*-Alkylmaleimides are also generally more stable than their aryl counterparts (162, 164).

Photoactivatable heterobifunctional cross-linking agents are particularly useful for identifying interacting components in complicated biological systems (165). Wood and O'Dorisio (166), for example, used *N*-succinimidyl 4-azidobenzoate, *N*-succinimidyl 6-[(4'-azido-2'-nitrophenyl)-amino]hexanoate and two nonphotoactivatable homobifunctional cross-linking agents to identify vasoactive intestinal peptide receptors in human lymphoblasts by their

coupling to ^{125}I -labeled vasoactive intestinal peptide. A photoactive derivative of a *N*-formylated chemotactic peptide, prepared by reaction with the last mentioned photoactivatable agent, has also been used to characterize the *N*-formyl peptide receptors of human polymorphonuclear leukocytes (167).

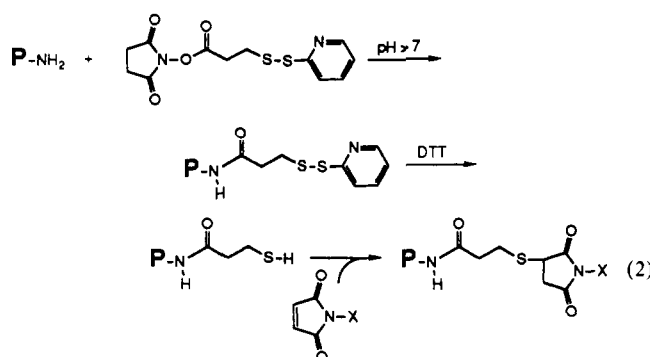
The initial reaction with photoactivatable cross-linking agents is usually conducted in the dark so that the photoreactive group is inert. Cross-linking is then initiated in a subsequent step involving exposure to light. Azido groups which are converted into a highly reactive nitrenes and diazo moieties (i.e., diazoacetyl, diazo ketones, etc.) which give even more reactive carbenes upon photoactivation are the most common photoactivatable groups in use at this time (2, 3). Being so reactive, both react relatively indiscriminately with OH, NH, CH, and C=C moieties in their vicinity and have short half-lives. Their reaction with surrounding solvent usually precludes reaction with groups not in their immediate vicinity and leads to quite low yields. The detection of cross-linked products thus often provides a good record of spatial relationships at the moment of photolysis but the yields are not adequate for most preparative purposes.

Heterobifunctional cross-linking agents are particularly useful for conjugating different proteins. The different side-chain reactivities of the two reactive groups, for example, usually permit the coupling to be carried out in a stepwise manner which allows, in some cases, for partial purification and, if desired, characterization of intermediates prior to the actual conjugation. Due to the hydrolytic instability of the most important groups directed at amino side chains, the first step usually involves addition of the cross-linker to the amino groups of one member of the future hybrid pair (which either has no thiol groups or where thiols, if present, are at least temporarily blocked). The removal of unreacted or hydrolyzed reagent and other unwanted substances is usually possible at this stage. The resulting derivative is then directly coupled via the introduced thiol-reactive maleimido or α -halocarbonyl group(s) to the thiol-containing member of the intended hybrid pair.

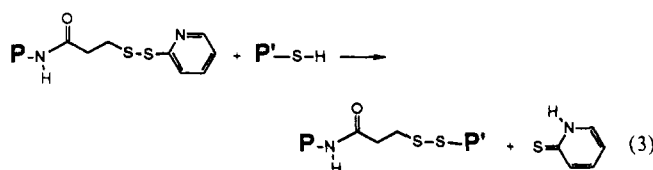
An artificial antibody-ricin conjugate, for example, has been prepared by treating ricin with *m*-maleimidobenzoyl *N*-hydroxysuccinimide ester and then incubating the resulting *m*-maleimidobenzoyl derivative with a partially reduced monoclonal antibody (148). The formation of unwanted homoprotein conjugates is precluded by such two-step procedures, and purification of the resulting hybrid conjugates by exclusion chromatography is usually rather easy since they should be significantly larger than any of their precursors. Iodoacetyl derivatives of avidin, alkaline phosphatase, and at least four other proteins are commercially available.

Several reagents have been employed to introduce thiol groups into proteins, which may then be employed for conjugation to other proteins or various other materials. *N*-Acetylhomocysteine thiolactone (168), (*S*-acetylthio)succinic anhydride (169), *S*-acetyl *N*-succinimidylthioacetate (170), 2-iminothiolane (153), and *N*-succinimidyl 3-(2-pyridyldithio)propionate (151), for example, can all be used under mildly alkaline conditions to introduce thiol groups into proteins. In the second and third cases, the acetyl moiety must subsequently be removed, usually by treatment with hydroxylamine, to release the thiol group and, in the last case, a small amount of DTT or some other simple thiol must be used to affect a comparable cleavage of the 2-pyridyl disulfide moiety. The resulting thiol groups potentially can be coupled to many

different maleimidyl or α -halocarbonyl groups including, for example, those of certain protein-maleimidyl conjugates as follows (171, 150):

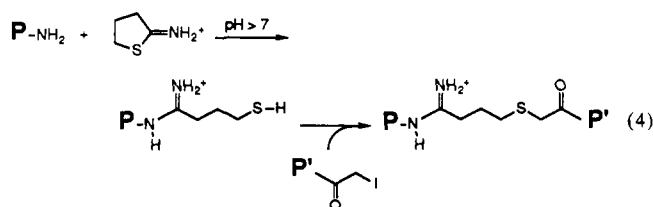


Even more important, probably, is the ability of the latter substituent to undergo direct coupling with the thiol groups of other proteins as follows (152, 172):



Several 2-pyridyl disulfide-protein conjugates are commercially available. The susceptibility of disulfide linkages to cleavage by low molecular weight thiols, however, appears to preclude many applications of such conjugates, including most of those involving exposure to physiological conditions.

2-Iminothiolane is probably the most important reagent for introducing thiol groups into proteins. It is quite water soluble, whereas the others really are not, it reacts rapidly with amino groups at pH 7 (or preferably a little above), and it does not require an additional activation step to effect release of the thiol moiety. It alone preserves the cationic charges of the modified amino groups. As with the other reagents used to introduce thiol groups, those introduced via reaction with 2-iminothiolane can be used to effect oxidative coupling to other protein thiols or may react with various maleimidyl or α -halocarbonyl groups, as follows (173, 154):



CONCLUSION

Space and time limitations have precluded the discussion of many important related subjects. We had hoped, in particular, to discuss the radiolabeling of proteins. Biotinylation also deserves serious discussion. We apologize to the many authors whose works we have failed to cite and particularly to those whose results we may have misinterpreted or misrepresented. We would also like to call the readers' attention to a number of reviews and books

on this subject, where more complete information can be obtained (174-183).

ACKNOWLEDGMENT

Financial support to GEM was received from Solar Energy Research Institute and to REF from U.S. National Institutes of Health Grant GM23817. The assistance of Shirley Miller in preparing the manuscript is greatly appreciated.

LITERATURE CITED

- (1) Colman, R. F. (1983) Affinity labeling of purine nucleotide sites of proteins. *Annu. Rev. Biochem.* **52**, 67-91.
- (2) Bayley, H. (1983) *Photogenerated Reagents in Biochemistry and Molecular Biology* Elsevier, New York.
- (3) Knowles, J. R. (1972) Photogenerated reagents for biological receptor-site labels. *Acc. Chem. Res.* **5**, 155-160.
- (4) Hunter, M. J. and Ludwig, M. L. (1962) The reaction of imidoesters with proteins and related small molecules. *J. Am. Chem. Soc.* **84**, 3491-3504.
- (5) Means, G. E. and Feeney, R. E. (1968) Reductive alkylation of amino groups in proteins. *Biochemistry* **7**, 1366-1371.
- (6) Goldstein, L., Leven, Y., and Katchalski, E. (1964) A water-insoluble polyanionic derivative of trypsin. II. Effect of the polyelectrolyte carrier on the kinetic behavior of bound trypsin. *Biochemistry* **3**, 1913-1919.
- (7) Nishikawa, A. H., Morita, R. Y., and Becker, R. R. (1968) Effects of the solvent medium on polyvalylribonuclease aggregation. *Biochemistry* **7**, 1506-1513.
- (8) Ampon, K. and Means, G. E. (1988) Immobilization of proteins on organic polymer beads. *Biotechnol. Bioeng.* **32**, 689-697.
- (9) Abuchowski, A., van Es, T., Palczuk, N. C., and Davis, F. F. (1977) Alteration of immunological properties of bovine serum albumin by covalent attachment of polyethylene glycol. *J. Biol. Chem.* **252**, 3578-3581.
- (10) Veronese, F. M., Largalolli, R., Boccu, E., Bengassi, C. A., and Schiavon, O. (1985) Surface modification of proteins. Activation of monomethoxy-polyethylene glycols by phenylchloroformates and modification of ribonuclease and superoxide dismutase. *Appl. Biochem. Biotechnol.* **11**, 141-152.
- (11) Raftery, M. A. and Cole, R. D. (1966) On the aminoethylation of proteins. *J. Biol. Chem.* **241**, 3457-3461.
- (12) Dixon, H. B. F. and Perham, R. N. (1968) Reversible blocking of amino groups with citraconic anhydride. *Biochem. J.* **109**, 312-314.
- (13) Rice, R. H., Means, G. E., and Brown, W. D. (1977) Stabilization of bovine trypsin by reductive methylation. *Biochem. Biophys. Acta* **492**, 316-321.
- (14) Parkinson, D. and Redshaw, J. D. (1984) Visible labeling of proteins for polyacrylamide gel electrophoresis with dansyl chloride. *Anal. Biochem.* **141**, 121-136.
- (15) Hudson, E. N. and Weber, G. (1973) Synthesis and characterization of two fluorescence sulfhydryl reagents. *Biochemistry* **12**, 4154-4161.
- (16) Weltman, J. K., Szaro, R. P., Frackelton, A. R., Dowben, R. M., Bunting, J. R., and Cathow, R. E. (1973) *N*-(3-Pyrene)maleimide: a long lifetime fluorescent sulfhydryl reagent. *J. Biol. Chem.* **248**, 3173-3177.
- (17) Berliner, L. J. and Wong, S. S. (1974) Spin-labeled sulfonyl fluorides as active site probes of protease structure. *J. Biol. Chem.* **249**, 1668-1682.
- (18) Hunter, W. M. and Greenwood, F. C. (1962) Preparation of I-131 labelled human growth hormone of high specific activity. *Nature* **194**, 492-496.
- (19) Rice, R. H. and Means, G. E. (1971) Radioactive labeling of protein in vitro. *J. Biol. Chem.* **246**, 831-832.
- (20) Bolton, A. E. and Hunter, W. M. (1973) The labelling of proteins to high specific radioactivities by conjugation to a ¹²⁵I-containing acylating agent. *Biochem. J.* **133**, 529-539.
- (21) Meares, C. F., McCall, M. J., Deshpande, S. V., DeNardo, S. J., and Goodwin, D. A. (1988) Chelate radiochemistry: Cleavable linkers lead to altered levels of radioactivity in the liver. *Int. J. Cancer* **2**, 99-102.

- (22) Langer, R. and Brown, E. (1985) Controlled release and magnetically modulated release systems for macromolecules. *Methods Enzymol.* 112, 399-422.
- (23) Senyei, D. and Widder, K. J. (1985) Biophysical drug targeting: Magnetically responsive albumin microspheres. *Methods Enzymol.* 112, 56-67.
- (24) Petsko, G. A. (1985) Preparation of heavy-atom derivatives. *Methods Enzymol.* 114, 147-156.
- (25) Jentoft, N. and Dearborn, D. G. (1979) Labeling of proteins by reductive methylation using sodium cyanoborohydride. *J. Biol. Chem.* 254, 4359-4365.
- (26) Maekawa, K. and Liener, I. E. (1960) Properties of the glucosylamidyl derivative of trypsin. *Arch. Biochem. Biophys.* 91, 101-107.
- (27) Lee, H. S., Sen, L. C., Clifford, A. J., Whitaker, J. R., and Feeney, R. E. (1979) Preparation and nutritional properties of caseins covalently modified with sugars. Reductive alkylation of lysines with glucose, fructose or lactose. *J. Agric. Food Chem.* 27, 1094-1098.
- (28) Chen, V. J. and Wold, F. (1984) Neoglycoproteins: preparation of noncovalent glycoproteins through high-affinity protein-(glycosyl) ligand complexes. *Biochemistry* 23, 3306-3311.
- (29) Wong, W. S. D., Kristjansson, M. M., Osuga, D. T., and Feeney, R. E. (1985) 1-Deoxyglycitulation of protein amino groups and their regeneration by periodate oxidation. *Int. J. Peptide Protein Res.* 26, 55-62.
- (30) Hofmann, K., Titus, G., Montibeller, J. A., and Finn, F. M. (1982) Avidin binding of carboxyl-substituted biotin analogues. *Biochemistry* 21, 978-984.
- (31) Wilchek, E. A. and Bayer, E. A. (1988) The avidin-biotin complex in bioanalytical applications. *Anal. Biochem.* 171, 1-32.
- (32) Gross, E. (1967) The cyanogen bromide reaction. *Methods Enzymol.* 11, 238-255.
- (33) Mahoney, W. C. and Hermodson, M. A. (1979) High-yield cleavage of tryptophan peptide bonds by *o*-iodosobenzoic acid. *Biochemistry* 18, 3810-3814.
- (34) Kaiser, E. T., Lawrence, D. S., and Rokita, S. E. (1985) The chemical modification of enzymatic specificity. *Annu. Rev. Biochem.* 54, 565-595.
- (35) Osuga, D. T., Feather, M. S., Shah, M. J., and Feeney, R. E. (1989) Modification of galactose and *N*-acetylgalactosamine residues by oxidation of C-6 hydroxyls to the aldehydes followed by reductive amination: Model systems and antifreeze glycoproteins. *J. Protein Chem.* 8, 519-528.
- (36) Han, K.-K., Richard, C., and Delacorte, A. (1984) Chemical cross-links of proteins by using bifunctional reagents. *Int. J. Biochem.* 16, 129-145.
- (37) Staros, J. V. (1988) Membrane-impermeant cross-linking reagents: Probes of structure and dynamics of membrane proteins. *Acc. Chem. Res.* 21, 435-441.
- (38) Poznansky, M. J. (1986) Tailoring Proteins for More Effective Use as Therapeutic Agents. In *Protein Tailoring for Food and Medical Uses* (R. E. Feeney and J. R. Whitaker, Eds.) pp 317-337, Marcel Dekker, New York.
- (39) Poznansky, M. (1988) Soluble enzyme conjugates: New possibilities for enzyme replacement therapy. *Methods Enzymol.* 137, 566-574.
- (40) Bode, C., Runge, M. S., Newell, J. B., Matsueda, G. R., and Haber, E. (1987) Characterization of an antibody-urokinase conjugate, a plasminogen activator targeted to fibrin. *J. Biol. Chem.* 262, 10819-10823.
- (41) Beyzavi, K., Hampton, S., Kwasowski, P., Fickling, S., Marks, V., and Clift, R. (1987) Comparison of horseradish peroxidase and alkaline phosphatase-labelled antibodies in enzyme immunoassays. *Ann. Clin. Biochem.* 24, 145-152.
- (42) Cumber, A. J., Forrester, J. A., Foxwell, B. M. J., Ross, W. C. J., and Thorpe, P. E. (1985) Preparation of antibody-toxin conjugates. *Methods Enzymol.* 112, 207-225.
- (43) Faulstich, H. and Fiume, L. (1985) Protein conjugates of fungal toxins. *Methods Enzymol.* 112, 225-237.
- (44) Urdahl, D. L. and Hakomori, S. (1980) Tumor-associated ganglio-*N*-triacylceramide target for antibody dependent, avidin mediated drug killing of tumor cells. *J. Biol. Chem.* 255, 10509-10516.
- (45) Hoare, D. G. and Koshland, D. E. (1967) A method for the quantitative modification and estimation of carboxylic acid groups in proteins. *J. Biol. Chem.* 242, 2447-2453.
- (46) Barman, T. E. and Koshland, D. E. (1967) A colorimetric procedure for the quantitative determination of tryptophan residues in protein. *J. Biol. Chem.* 242, 5771-5776.
- (47) Fields, R. (1972) The rapid determination of amino groups with TNBS. *Methods Enzymol.* 25, 464-468.
- (48) Ellman, G. L. (1959) Tissue sulfhydryl groups. *Arch. Biochem. Biophys.* 82, 70-77.
- (49) Olcott, H. S. and Fraenkel-Conrat, H. (1947) Specific group reagents for proteins. *Chem. Rev.* 41, 151-197.
- (50) Herriott, R. M. (1947) Reactions of native proteins with chemical reagents. *Adv. Protein Chem.* 3, 161-225.
- (51) Balls, A. K. and Jansen, E. F. (1952) Stoichiometric inhibition of chymotrypsin. *Adv. Enzymol.* 13, 321-343.
- (52) Fraenkel-Conrat, H., Bean, R. S., and Lineweaver, H. (1949) Essential groups for the interaction of ovomucoid (egg white trypsin inhibitor) and trypsin, and for tryptic activity. *J. Biol. Chem.* 177, 385-403.
- (53) Fraenkel-Conrat, H. and Olcott, H. S. (1948) The reaction of formaldehyde with proteins. V. Cross-linking between amino and primary amide or guanidyl groups. *J. Am. Chem. Soc.* 70, 2673-2684.
- (54) Fraenkel-Conrat, H. and Feeney, R. E. (1950) The metal-binding activity of conalbumin. *Arch. Biochem.* 29, 101-113.
- (55) Moore, S. and Stein, W. H. (1963) Chromatographic determination of amino acids by the use of automatic recording equipment. *Methods Enzymol.* 6, 819-831.
- (56) Edman, P. and Begg, G. (1967) A protein sequenator. *Eur. J. Biochem.* 1, 80-91.
- (57) Wofsy, L., Metzger, H., and Singer, S. J. (1962) Affinity labeling—A general method for labeling the active sites of antibody and enzyme molecules. *Biochemistry* 1, 1031-1039.
- (58) Schoellmann, G. and Shaw, E. (1963) Direct evidence for the presence of histidine in the active center of chymotrypsin. *Biochemistry* 2, 252-255.
- (59) Ehrlich, R. S. and Colman, R. F. (1987) Characterization of an active site peptide modified by the substrate analogue 3-bromo-2-ketoglutarate on a single chain of dimeric NADP⁺ dependent isocitrate dehydrogenase. *J. Biol. Chem.* 262, 12614-12619.
- (60) Hartman, F. C., LaMuraglia, C. M., Tomozawa, Y., and Wolfenden, R. (1975) The influence of pH on the interaction of inhibitors with triosephosphate isomerase and determination of the pK_a of the active-site carboxyl group. *Biochemistry* 14, 5274-5291.
- (61) O'Connell, E. L. and Rose, I. H. (1973) Affinity labeling of phosphoglucose isomerase by 1,2-anhydrohexitol-6-phosphates. *J. Biol. Chem.* 248, 2225-2231.
- (62) Schray, K. J., O'Connell, E. L., and Rose, I. A. (1973) Inactivation of muscle triose phosphate isomerase by D- and L-glycidolphosphate. *J. Biol. Chem.* 248, 2214-2218.
- (63) Pinkofsky, H. D., Ginsburg, A., Reardon, J., and Heinrikson, R. L. (1984) Lysyl residue 47 is near the subunit ATP-binding site of glutamine synthetase from *Escherichia coli*. *J. Biol. Chem.* 259, 9616-9622.
- (64) Easterbrook-Smith, B., Wallace, J. C., and Keech, D. B. (1976) Pyruvate carboxylase: Affinity labelling of the magnesium adenosine triphosphate binding site. *Eur. J. Biochem.* 62, 125-130.
- (65) Wescott, K. R., Olwin, B. B., and Storm, D. P. (1980) Inhibition of adenylate cyclase by the 2'-3'-dialdehyde of adenosine triphosphate. *J. Biol. Chem.* 255, 8767-8776.
- (66) Fischer, E. H., Kent, E. B., Snyder, E. R., and Krebs, E. G. (1958) The reaction of sodium borohydride with muscle phosphorylase. *J. Am. Chem. Soc.* 80, 2906-2907.
- (67) DiIanni, C. L. and Villafranca, J. J. (1989) Identification of amino acid residues modified by pyridoxal 5'-phosphate in *Escherichia coli* glutamine synthetase. *J. Biol. Chem.* 264, 8686-8691.
- (68) Basu, A., Kedar, P., Wilson, S., and Modek, M. J. (1989) Active-site modification of mammalian DNA polymerase β with pyridoxal 5'-phosphate. Mechanism of inhibition and

- identification of lysine 71 in the deoxynucleoside triphosphate binding pocket. *Biochemistry* **28**, 6305–6309.
- (69) Hollemans, M., Runswick, M. J., Fearnley, I. M., and Walker, J. E. (1983) The sites of labeling of the β -Subunit of bovine mitochondrial F1-ATPase with 8-azido-ATP. *J. Biol. Chem.* **258**, 9307–9313.
- (70) Drake, R. D., Evans, R. K., Wolf, M. J., Haley, B. E. (1989) Synthesis and properties of 5-azido-UDP-glucose. *J. Biol. Chem.* **264**, 11923–11933.
- (71) Wallace, C. J. A. and Harris, D. E. (1984) The preparation of fully N- ϵ -acetimidylated cytochrome c. *Biochem. J.* **217**, 589–594.
- (72) Grossberg, A. L. and Pressman, D. (1963) Effect of acetylation on the active site of several antihapten antibodies: Further evidence for the presence of tyrosine in each site. *Biochemistry* **2**, 90–96.
- (73) Buttkus, H., Clark, J. R., and Feeney, R. E. (1965) Chemical modifications of amino groups of transferrins: Ovotransferrin, human serum transferrin and human lactotransferrin. *Biochemistry* **4**, 998–1005.
- (74) Haynes, R., Osuga, D. T., and Feeney, R. E. (1967) Modification of amino groups in inhibitors of proteolytic enzymes. *Biochemistry* **6**, 541–547.
- (75) Huynh, Q. K. (1988) Evidence for a reactive α -carboxyl group (Glu-418) at the herbicide glyphosate binding site of 5-enolpyruvylshikimate-3-phosphate synthase from *Escherichia coli*. *J. Biol. Chem.* **263**, 11631–11635.
- (76) Rogers, T. B., Borresen, T., and Feeney, R. E. (1978) Chemical modification of the arginines in transferrins. *Biochemistry* **17**, 1105–1109.
- (77) Riordan, J. E. (1973) Functional arginine residues in carboxypeptidase A—modification with butanedione. *Biochemistry* **12**, 3915–3923.
- (78) Yamasaki, R. B., Vega, A., and Feeney, R. E. (1980) Modification of available arginine residues in proteins by *p*-hydroxyphenylglyoxal. *Anal. Biochem.* **109**, 32–40.
- (79) Kashner, J. S., Allen, K. E., Kasamo, K., and Slayman, C. W. (1986) Characterization of an essential arginine residue in the plasma membrane H⁺-ATPase of *Neurospora crassa*. *J. Biol. Chem.* **261**, 10808–10813.
- (80) Melchior, W. B. and Fahrney, D. (1970) Ethoxyformylation of proteins. Reaction of ethoxyformic anhydride with α -chymotrypsin, pepsin and pancreatic ribonuclease at pH 4. *Biochemistry* **9**, 251–258.
- (81) Dominici, P., Tancini, B., and Voltattorni, C. B. (1985) Chemical modification of pig kidney 3,4-dihydroxyphenylalanine decarboxylase with diethyl pyrocarbonate. *J. Biol. Chem.* **260**, 10583–10589.
- (82) Spande, T. F. and Witkop, B. (1967) Tryptophan involvement in the function of enzymes and protein hormones as determined by selective oxidation with *N*-bromosuccinimide. *Methods Enzymol.* **11**, 506–521.
- (83) Horton, H. R. and Koshland, D. E. (1972) Modification of proteins with active benzylhalides. *Methods Enzymol.* **25**, 468–482.
- (84) Horton, H. R. and Koshland, D. E. (1967) Reactions with reactive alkylhalides. *Methods Enzymol.* **11**, 556–565.
- (85) Morrison, M. (1970) Iodination of tyrosine: Isolation of lactoperoxidase (bovine). *Methods Enzymol.* **17**, 653–664.
- (86) Sinn, H. J., Schrank, H. H., Friedrich, E. A., Via, D. P., and Dresel, H. A. (1988) Radioiodination of proteins and lipoproteins using *N*-bromosuccinimide as oxidizing agent. *Anal. Biochem.* **170**, 186–192.
- (87) Sokolovsky, M., Riordan, J. F., and Vallee, B. L. (1966) Tetranitromethane. A reagent for the nitration of tyrosyl residues in proteins. *Biochemistry* **5**, 3582–3589.
- (88) Brake, J. M. and Wold, F. (1962) Carboxymethylation of yeast enolase. *Biochemistry* **1**, 386–391.
- (89) Crestfield, A. M., Moore, S., and Stein, W. H. (1963) The preparation and enzymatic hydrolysis of reduced and S-carboxymethylated proteins. *J. Biol. Chem.* **238**, 622–627.
- (90) Markham, G. D. and Satishchandran, C. (1988) Identification of the reactive sulfhydryl groups of S-adenosylmethionine synthetase. *J. Biol. Chem.* **263**, 8666–8670.
- (91) Lewis, C. T., Seyer, J. M., and Carlson, G. M. (1989) Cysteine 288: An essential hyperreactive thiol of cytosolic phosphoenolpyruvate carboxykinase (GTP). *J. Biol. Chem.* **264**, 27–33.
- (92) Fujioka, M., Takata, Y., Konishi, K., and Ogawa, H. (1987) Function and reactivity of sulfhydryl groups of rat liver glycine methyltransferase. *Biochemistry* **26**, 5696–5702.
- (93) Stauffer, C. E. and Etson, D. (1969) The effect on subtilisin activity of oxidizing a methionine residue. *J. Biol. Chem.* **244**, 5333–5338.
- (94) Fujioka, M., Takata, Y., Konishi, K., and Ogawa, H. (1987) Function and reactivity of sulfhydryl groups of rat liver glycine methyltransferase. *Biochemistry* **26**, 5696–5702.
- (95) Degani, Y., Neumann, H., and Patchornik, A. (1970) Selective cyanylation of sulfhydryl groups. *J. Am. Chem. Soc.* **92**, 6969–6976.
- (96) Dagani, Y. and Patchornik, A. (1974) Cyanylation of sulfhydryl groups by 2-nitro-5-thiocyanobenzoic acid. High yield modification and cleavage of peptides at cysteine residues. *Biochemistry* **13**, 1–11.
- (97) Kindman, L. A. and Jencks, W. P. (1981) Modification and inactivation of CoA transferase by 5-nitro-5-(thiocyanato)benzoate. *Biochemistry* **20**, 5183–5187.
- (98) Smith, D. J. and Kenyon, G. L. (1974) Nonessentiality of the active sulfhydryl group of rabbit muscle creatine kinase. *J. Biol. Chem.* **249**, 3317–3318.
- (99) Hettinger, T. P. and Harbury, H. A. (1965) Guanidinated cytochrome c. *Biochemistry* **4**, 2585–2589.
- (100) Shields, G. S., Hill, R. L., and Smith, E. L. Preparation and properties of guanidinated mercuripapain. *J. Biol. Chem.* **234**, 1747–1760.
- (101) Kaplan, H., Stevenson, K. J., and Hartley, B. S. (1971) Competitive labelling, a method for determining the reactivity of individual groups in proteins. *Biochem. J.* **124**, 289–299.
- (102) Duggleby, K. G. and Kaplan, H. (1975) A competitive labeling method for the determination of the chemical properties of solitary functional groups in proteins. *Biochemistry* **14**, 5168–5175.
- (103) Shewale, J. G. and Brew, K. (1982) Effects of Fe³⁺ binding on the microenvironments of individual amino groups in human serum transferrin as determined by differential kinetic labeling. *J. Biol. Chem.* **257**, 9406–9415.
- (104) Rieder, R. and Bosshard, H. R. (1980) Comparison of the binding sites on cytochrome c for cytochrome c oxidase, cytochrome bc₁ and cytochrome c₁. Differential acetylation of lysyl residues in free and complexed cytochrome c. *J. Biol. Chem.* **255**, 4732–4739.
- (105) Jackson, G. E. D. and Young, N. M. (1986) Determination of chemical properties of individual histidine and tyrosine residues of concanavalin A by competitive labelling with 1-fluoro-2,4-dinitrobenzene. *Biochemistry* **25**, 1657–1662.
- (106) Buechler, J. A., Vedvick, T. A., and Taylor, S. S. (1989) Differential labelling of the catalytic subunit of cAMP dependent protein kinase with acetic anhydride: substrate-induced conformational changes. *Biochemistry* **28**, 3018–3024.
- (107) Ray, W. J. and Koshland, D. E. (1961) A method for characterizing the type and numbers of groups involved in enzyme action. *J. Biol. Chem.* **236**, 1973–1979.
- (108) Redkar, V. D. and Kenkare, U. W. (1975) Effects of ligands on the reactivity of essential sulfhydryls in brain hexokinase. Possible interaction between substrate binding sites. *Biochemistry* **14**, 4704–4712.
- (109) Horiike, K., Tsuge, H., and McCormick, D. B. (1979) Evidence for an essential histidyl residue at the active site of pyridoxamine(pyridoxine)-5'-phosphate oxidase from rabbit liver. *J. Biol. Chem.* **254**, 6638–6643.
- (110) Jimenez, J. S., Kupfer, A., Gani, V., and Shaltiel, S. (1982) Conformational changes in the catalytic subunit of adenosine cyclic 3',5'-phosphate dependent protein kinase. Use for establishing a connection between one sulfhydryl group and the γ -subsite in the ATP site of this subunit. *Biochemistry* **21**, 1623–1630.
- (111) Ogawa, H., Okamoto, M., and Fujioka, M. (1979) Chemical modification of the active site sulfhydryl group of sac-

- charopine dehydrogenase (L-lysine-forming). *J. Biol. Chem.* **254**, 7030-7035.
- (112) First, E. H. and Taylor, J. J. (1989) Selective modification of the catalytic subunit of cAMP-dependent protein kinase with sulfhydryl-specific fluorescent probes. *Biochemistry* **28**, 3598-3605.
- (113) Makinen, A. L. and Nowak, T. (1989) A reactive cysteine in avian liver phosphoenolpyruvate carboxykinase. *J. Biol. Chem.* **264**, 12148-12157.
- (114) Tsou, Chen-Lu (1962) Kinetic determination of essential side chains in proteins. *Sci. Sin.* **11**, 1535-1558.
- (115) Kremer, A. B., Egan, R. M., and Sable, H. Z. (1980) The active site of transketolase two arginine residues are essential for activity. *J. Biol. Chem.* **255**, 2405-2410.
- (116) Lakowicz, J. R. (1983) *Principles of Fluorescence Spectroscopy* Plenum Press, New York.
- (117) Stryer, L. and Haugland, R. P. (1967) Energy transfer: A spectroscopic ruler. *Proc. Natl. Acad. Sci.* **58**, 719-726.
- (118) Stryer, L. (1978) Fluorescence energy transfer as a spectroscopic ruler. *Ann. Rev. Biochem.* **47**, 819-846.
- (119) Haugland, R. P. (1989) *Molecular Probes Handbook of Fluorescent Probes and Research Chemicals* Molecular Probes, Inc., Eugene, OR.
- (120) Berliner, L. J. (1976) *Spin Labels* Academic Press, New York.
- (121) Wold, F. (1972) Bifunctional reagents. *Methods Enzymol.* **25**, 623-651.
- (122) Wang, K. and Richards, F. M. (1974) An approach to nearest neighbor analysis of membrane proteins. *J. Biol. Chem.* **249**, 8005-8018.
- (123) Uy, R. and Wold, F. (1977) Introduction of artificial crosslinks into proteins. *Adv. Exp. Med. Biol.* **86A**, 169-186.
- (124) Das, M. and Fox, C. F. (1979) Chemical cross-linking in biology. *Annu. Rev. Biophys. Bioeng.* **8**, 165-193.
- (125) Ji, T. H. (1983) Bifunctional reagents. *Methods Enzymol.* **91**, 580-609.
- (126) Kennedy, J. F. and Cabral, J. M. S. (1983) In *Solid Phase Biochemistry* (W. H. Scouten, Ed.) pp 253-392, John Wiley, New York.
- (127) Laskin, A. I. (1985) *Enzymes and Immobilized Cells in Biotechnology* Benjamin/Cummings, Inc., Menlo Park, CA.
- (128) Hartmeir, W. (1986) *Immobilized Biocatalysts* Springer-Verlag, New York.
- (129) Mosbach, K. (1987) Immobilized enzymes and cells, part B. *Methods Enzymol.* **135**.
- (130) Mosbach, K. (1987) Immobilized enzymes and cells, part C. *Methods Enzymol.* **136**.
- (131) Weare, J. A. and Reichert, I. E. (1979) Studies with carbodiimide-cross-linked derivatives of bovine lutropin. I. The effects of specific group modifications on receptor site binding in testes. *J. Biol. Chem.* **254**, 6964-6971.
- (132) Waldmeyer, B. and Bosshard, H. R. (1985) Structure of an electron transfer complex. I. Covalent cross-linking of cytochrome c peroxidase and cytochrome c. *J. Biol. Chem.* **260**, 5184-5190.
- (133) Willing, A. H., Georgiadis, M. M., Rees, D. C., and Howard, J. B. (1989) Cross-linking of nitrogenase components structure and activity of the covalent complex. *J. Biol. Chem.* **264**, 8499-8503.
- (134) Korodi, I., Asboth, B., and Polgar, L. (1986) Disulfide bond formation between the active-site thiol and one of the several free thiol groups of chymopapain. *Biochemistry* **25**, 6895-6900.
- (135) Huston, E. E., Grammer, J. C., and Yount, R. G. (1988) Flexibility of the myosin heavy chain—Direct evidence that the region containing SH₁ and SH₂ can move 10 Å under the influence of nucleotide binding. *Biochemistry* **17**, 8945-8952.
- (136) Hiratsuka, T. (1988) Cross-linking of three heavy chain domains of myosin adenosinetriphosphatase with a trifunctional alkylating reagent. *Biochemistry* **27**, 4110-4114.
- (137) Peters, K. and Richards, F. M. (1977) Chemical cross-linking: Reagents and problems in studies of membrane structure. *Ann. Rev. Biochem.* **46**, 523-551.
- (138) Davies, G. E. and Stark, G. R. (1970) Use of dimethylsuberimide, a cross-linking reagent, in studying the subunit structure of oligomeric proteins. *Proc. Natl. Acad. Sci. U.S.A.* **66**, 651-656.
- (139) Dombradi, V., Hajdu, J., Bot, G., and Friedrich, P. (1980) Structural changes in glycogen phosphorylase as revealed by cross-linking with bifunctional diimides: phosphodephospho hybrid and phosphorylase a. *Biochemistry* **19**, 2295-2299.
- (140) Pilch, P. E. and Czech, M. P. (1979) Interaction of cross-linking agents with the insulin effector system of isolated cells. *J. Biol. Chem.* **254**, 3375-3381.
- (141) Staros, J. V., Lee, W. T., and Conrad, D. H. (1988) Membrane impermeant crosslinking reagents application to studies of the cell surface receptor for IgE. *Methods Enzymol.* **150**, 503-512.
- (142) Heilman, H. D. and Holzner, M. (1981) The spatial organization of the active sites of the bifunctional oligomeric enzyme tryptophan synthetase: Crosslinking by a novel method. *Biochem. Biophys. Res. Commun.* **99**, 1146-1152.
- (143) Sato, S. and Nakao, M. (1981) Cross-linking of intact erythrocyte membranes with a newly synthesized cleavable bifunctional reagent. *J. Biochem. (Tokyo)* **90**, 1177-1181.
- (144) Moore, J. E. and Ward, W. H. (1956) Cross-linking of bovine plasma albumin and wool keratin. *J. Am. Chem. Soc.* **78**, 2414-2418.
- (145) Hillel, Z. and Wu, C.-W. (1977) Subunit topography of RNA polymerase from *Escherichia coli*. A cross-linking study with bifunctional reagents. *Biochemistry* **16**, 3334-3342.
- (146) Hingorani, V. N., Tobias, D. T., Henderson, J. T., and Ho, Y.-K. (1988) Chemical crosslinking of bovine retinal transducin and cGMP phosphodiesterase. *J. Biol. Chem.* **263**, 6916-6926.
- (147) Kitagawa, T. and Aikawa, T. (1976) Enzyme coupled immunoassay of insulin using a novel coupling reagent. *J. Biochem. (Tokyo)* **79**, 233-236.
- (148) Youle, R. J. and Neville, D. M. (1980) Anti-thy 1.2 monoclonal antibody linked to ricin is a potent cell-type-specific toxin. *Proc. Natl. Acad. Sci. U.S.A.* **77**, 5483-5486.
- (149) Yoshitake, S., Yamada, Y., Ishikawa, E., and Masseyeff, R. (1979) Conjugation of glucose oxidase from *Aspergillus niger* and rabbit antibodies using *N*-hydroxysuccinimide ester of *N*-(4-carboxycyclohexylmethyl)maleimide. *Eur. J. Biochem.* **101**, 395-399.
- (150) Lambert, J. M., Senter, P. D., Young, A. Y. Y., Blattler, W. A., and Goldmacher, V. S. (1985) Purified immunotoxins that are reactive with human lymphoid cells. *J. Biol. Chem.* **260**, 12035-12041.
- (151) Carlsson, J., Drevin, H., and Axen, R. (1978) Protein thiolation and reversible protein-protein conjugation *N*-succinimidyl 3-(2-pyridyldithio) propionate, a new heterobifunctional reagent. *Biochem. J.* **173**, 723-737.
- (152) O'Keefe, D. O. and Draper, R. K. (1985) Characterization of a transferrin-diphtheria conjugate. *J. Biol. Chem.* **260**, 932-937.
- (153) Jue, R., Lambert, J. M., Pierce, L. R., and Traut, R. R. (1978) Addition of sulfhydryl groups to *Escherichia coli* ribosomes by protein modification with 2-iminothiolane (methyl 4-mercaptobutyrimide). *Biochemistry* **17**, 5399-5406.
- (154) Marsh, J. W. (1988) Antibody-mediated routing of diphtheria toxin in murine cells results in a highly efficacious immunotoxin. *J. Biol. Chem.* **263**, 15993-15999.
- (155) Cover, J. R., Lambert, J. M., Norman, C. M., and Traut, R. R. (1981) Identification of proteins at the subunit interface of the *Escherichia coli* ribosome by cross-linking with dimethyl 3,3'-dithiobis(propionimide). *Biochemistry* **20**, 2843-2852.
- (156) Staros, J. V., Wright, R. W., and Swingle, D. M. (1986) Enhancement by *N*-hydroxysulfosuccinimide of water-soluble carbodiimide modified coupling reactions. *Anal. Biochem.* **156**, 220-222.
- (157) Koyama, Y. and Taniguchi, A. (1986) Studies on chitin X. Homogeneous cross-linking of chitosan for enhanced cupric ion adsorption. *J. Appl. Polymer. Sci.* **31**, 1951-1954.
- (158) Golander, C.-G. and Eriksson, J. C. (1987) ESCA studies of the adsorption of polyethyleneimine and glutaraldehyde-

- reacted polyethyleneimine on polyethylene and mica surfaces. *J. Colloid Interface Sci.* **119**, 38–48.
- (159) Korn, A. H., Fearheller, S. H., and Filachione, E. M., Glutaraldehyde: Nature of the reagent. *J. Mol. Biol.* **65**, 525–529.
- (160) Kirkeby, S., Jakobsen, P., and Moe, D. (1987) Glutaraldehyde—"pure and impure". A spectroscopic investigation of two commercial glutaraldehyde solutions and their reaction products with amino acids. *Anal. Lett.* **20**, 303–315.
- (161) Gregory, J. D. (1955) The stability of *N*-ethylmaleimide and its reaction with sulfhydryl groups. *J. Am. Chem. Soc.* **77**, 3922–3923.
- (162) Knight, P. (1979) Hydrolysis of *p*-*N,N'*-phenylenebismaleimide and its adducts with cysteine. *Biochem. J.* **179**, 191–197.
- (163) Staros, J. V. (1982) *N*-Hydroxysulfosuccinimide active esters: Bis(*N*-hydroxysulfosuccinimide) esters of two dicarboxylic acids are hydrophilic, membrane-impermeant, protein cross-linkers. *Biochemistry* **21**, 3940–3955.
- (164) Yoshitake, S., Imagawa, M., Ishikawa, E., Niitsu, Y., Urushizaki, I., Nishiura, M., Kanazawa, R., Kurosaki, H., Tachibana, S., Nakazawa, N., and Ogawa, H. (1982) Mild and efficient conjugation of rabbit Fab' and horseradish peroxidase using a maleimide compound and its use for enzyme immunoassay. *J. Biochem.* **92**, 1413–1424.
- (165) Galardy, R. E., Craig, L. C., Jamieson, J. D., and Printz, M. P. (1974) Photoaffinity labeling of peptide hormone binding sites. *J. Biol. Chem.* **249**, 3510–3518.
- (166) Wood, C. L. and O'Dorisio, M. S. (1985) Covalent cross-linking of vasoactive intestinal polypeptide to its receptors on intact human lymphoblasts. *J. Biol. Chem.* **260**, 1243–1247.
- (167) Schmitt, M., Painter, R. G., Jesaitis, A. J., Preissner, K., Sklar, L. A., and Cochrane, C. G. (1983) Photoaffinity labeling of the *N*-formyl peptide receptor binding site of intact human polymorphonuclear leukocytes. *J. Biol. Chem.* **258**, 649–654.
- (168) Benesch, R. and Benesch, R. E. (1956) Formation of peptide bonds by aminolysis of homocysteine thiolactones. *J. Am. Chem. Soc.* **78**, 1597–1599.
- (169) Klotz, I. M. and Heiney, K. E. (1962) Introduction of sulfhydryl groups into proteins using acetylmercaptosuccinic anhydride. *Arch. Biochem. Biophys.* **96**, 605–612.
- (170) Julian, R., Duncan, S., Weston, P. D., and Wrigglesworth, R. (1983) A new reagent which may be used to introduce sulfhydryl groups into proteins, and its use in the preparation of conjugates for immunoassay. *Anal. Biochem.* **132**, 68–73.
- (171) Gitman, A. G., Kahane, I., and Loyter, A., (1985) Use of virus-attached antibodies or insulin molecules to mediate fusion between sendai virus envelopes and neuraminidase-treated cells. *Biochemistry* **24**, 2762–2768.
- (172) Gordon, R. D., Fieles, W. E., Schotland, D. L., Hogue-Angeletti, R., and Barchi, R. L. (1987) Topographical localization of the C-terminal regions of the voltage-dependent sodium channel from *Electrophorus electricus* using antibodies raised against a synthetic peptide. *Proc. Natl. Acad. Sci. U.S.A.* **84**, 308–312.
- (173) Senter, P. D., Saulnier, M. G., Schreiber, G. J., Hirschberg, D. L., Brown, J. P., Hellstrom, I., and Hellstrom, K. E. (1988) Anti-tumor effects of antibody-alkaline phosphatase conjugates in combination with etoposide phosphate. *Proc. Natl. Acad. Sci. U.S.A.* **85**, 4842–4846.
- (174) Hirs, C. H. W. (1967) Protein structure. *Methods Enzymol.* **11**.
- (175) Hirs, C. H. W. and Timasheff, S. N. (1983) Enzyme structure, part I. *Methods Enzymol.* **91**.
- (176) Baker, B. R. (1967) *Design of Active-Site-Directed Irreversible Enzyme Inhibitors* Wiley-Interscience, New York.
- (177) Means, G. E. and Feeney, R. E. (1971) *Chemical Modification of Proteins* Holden-Day, San Francisco, CA.
- (178) Glazer, A. N., Delange, R. J., and Sigman, D. S. (1975) *Chemical Modification of Proteins. Laboratory Techniques in Biochemistry and Molecular Biology* (T. S. Work and E. Work, Eds.) American Elsevier Publishing Co., New York.
- (179) Lundblad, R. L. and Noyes, C. M. (1984) *Chemical Reagents for Protein Modification* Vols. 1 and 2, CRC Press, Boca Raton, FL.
- (180) Widder, K. J. and Green, R. (1985) Drug and enzyme targeting, Part A. *Methods Enzymol.* **112**.
- (181) Pfleiderer, G. (1985) Chemical Modifications of Proteins. In *Modern Methods in Protein Chemistry* (H. Tschesche, Ed.) Walter de Gruyter, Berlin and New York.
- (182) Feeney, R. E. (1987) Chemical modification of proteins: Comments and perspectives. *Int. J. Pept. Protein Res.* **27**, 145–161.
- (183) Eyzaguirro, J. (1987) *Chemical Modification of Enzymes: Active Site Studies* John Wiley and Sons, New York.

TEACHING EDITORIAL

Recent Advances with Monoclonal Antibody Drug Targeting for the Treatment of Human Cancer¹

Gary A. Koppel

Lilly Research Laboratories, Indianapolis, Indiana 46285. Received August 21, 1989

I. INTRODUCTION

Drug targeting had its inception almost a century ago when the late Paul Ehrlich proposed that chemotherapeutic agents might be covalently joined to ligand substrates which had affinity for and selectivity to a target tissue such as malignant tumors. In addition, he suggested that antibodies or "magic bullets" as he described them might, in fact, be candidates for ligand substrates for drug targeting (2). This vision remained dormant for almost a century until the attendant technologies and support systems would be in place to begin to express this vision into a 20th century therapeutic modality.

During the past 15 years, there has been an exponential growth in the area of drug targeting as a result of the integration, interfacing, and coordination of the scientific disciplines represented by cell biology, recombinant technology, and chemistry (Figure 1). Within the area of cell biology, major advances have occurred in genetics, hybridoma technology, screening, and testing. In 1980, Benacerraf, Dausset, and Snell received the Nobel Prize in Medicine and Physiology for their pioneering efforts in elucidating the immune response gene network, that is the family of genes that dictate the ability of the mammalian immune system to respond to and process all immunogens (3). In the course of these important discoveries, the mouse became the representative immune system because of its prolific procreative behavior, physical size, and its brief gestation period. As a result, Snell had created the world's most sophisticated genetic library of inbred and recombinant strains of mice (4).

This family of mice became the instrument of knowledge that was utilized by Kohler and Milstein in their discovery of hybridoma technology. The discovery was of such magnitude that Kohler and Milstein, along with Jerne, were awarded the Nobel Prize in Medicine and Physiology in 1984, 9 years after their breakthrough (5, 6). Hybridoma technology allows the fusion of a normal immunological B cell committed to making antibody with a malignant myeloma partner, thus affording a hybrid cell with the genetic information of both immortality and antibody synthesis. Each cell is thus empowered to produce unlimited amounts of a single, or monoclonal, antibody (moab) (7). This discovery together with automated methods of screening and testing for the selective immunoreactivity of derived moab's accelerated the growth of the drug-targeting discipline.

Recombinant DNA technology has complemented and facilitated the growth of cell biology. The ability to rapidly identify, sequence, and clone genes of an antibody has led to the elucidation of the underlying mechanisms of antibody diversity (8). In addition, this powerful tool has allowed the construction of chimeric and humanized monoclonal antibodies which may reduce their immunogenicity in humans, either as native moab's or in the context of drug conjugates (9).

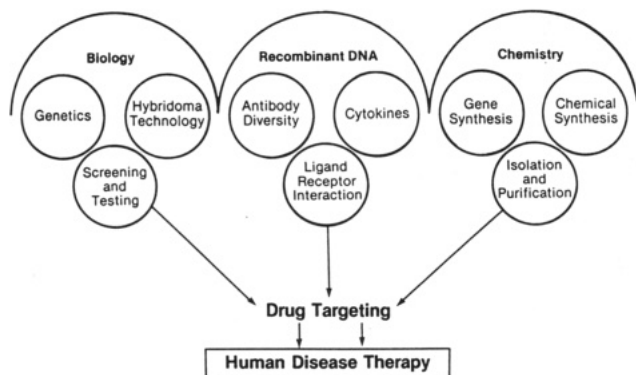
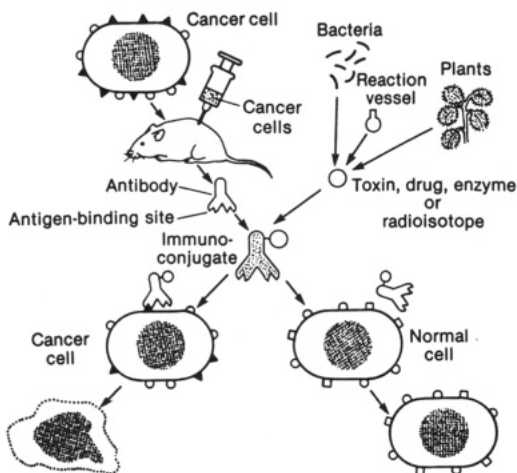
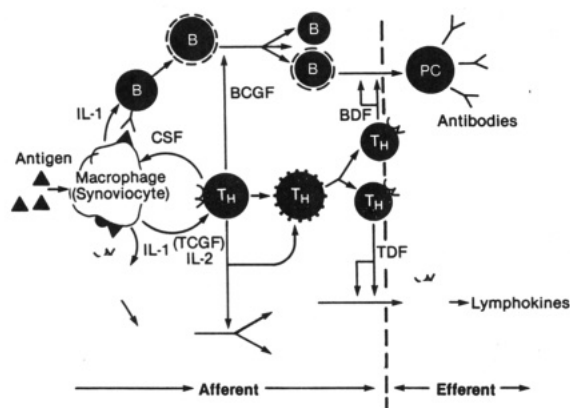
Finally, chemistry has catalyzed the growth rate of both cell and molecular biology. Through chemistry, the ability to rapidly synthesize DNA, peptides, linkers, and pharmacologic agents and to characterize and purify bioconjugates has been achieved. What has become apparent is the importance of chemistry in the design and synthesis of bioconjugates; indeed, the rate-determining step for the evolution of this program has been the "new chemistry" of drugs and linkages compatible with proteins and the incorporation of the drug/linkage onto the moab.

In summary, the three disciplines interface in creating a new dimension in the expression of biotechnology that has facilitated the emergence of monoclonal antibody drug targeting in the treatment of human cancer.

Conceptually, the process of drug targeting as proposed by Paul Ehrlich is illustrated in Figure 2. Since Ehrlich's vision of targeting, many investigators in the biological fields have tried to translate his dream into a reality. In order to build a foundation of understanding for moab-based targeting of drugs, this article will review the following in turn: (1) the immune system and antibody synthesis, (2) hybridoma technology and the generation of monoclonal antibodies, (3) chemical design and synthesis of modified targeting agents for attachment to moab's, and (4) the chemistry and biological activity of moab-drug conjugates.

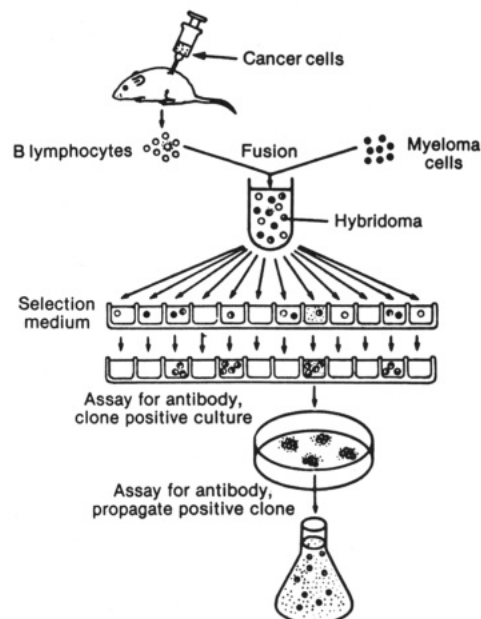
II. THE IMMUNE SYSTEM AND ANTIBODY SYNTHESIS

The cast of characters and the sequence of events that facilitate the activation of the immune response are illustrated in Figure 3. The macrophage or presenting cell takes up the antigen and presents it on its surface in the context of class II immune response gene products (10). This, in turn, determines the ability of the immune system to respond to the given antigen. Those clones of T cells (thymus-derived cells) designated as helpers (T_H) which express receptors for the antigen in the context of the class II self-determinant become activated through the synthesis and secretion of IL-1 (interleukin 1) (10). This cytokine, in turn, activates those clones of T_H cells to produce and express receptors for IL-2 (interleukin 2), a T cell growth factor which supports the growth of the autocrine T cell network. This highly sophisticated central pathway facilitates and supports the growth of both the humoral response represented by B cells (bone marrow derived cells committed to producing antibody) and the cell-mediated response represented by T cell mediated delayed type hypersensitivity (T_{DTH}) (10). The central pathway sustains the cell-mediated response by producing factors which support the growth and differentiation of the T cell mediating DTH, thus moving the process to the end stage effector function. Similarly, the central pathway activates the B cell response via the production

**Figure 1.****Figure 2.** Immunoconjugate-mediated site-directed therapy. Reproduced with the permission of R. John Collier and Donald A. Kaplan [(1984) *Sci. Am.* 251 (1), 56].**Figure 3.**

of growth and differentiating factors. As a result, the B cell recognizing the antigenic epitope matures to the end stage effector cell, the plasma B cell (PC), which secretes the antibody specific for the antigen at the incipient stage (10).

In addition to the utility of antibody in maintaining the survival of the organism, the antibody was recognized as an attractive candidate for ligand targeting. If one had the capability to intercept a specific plasma B cell clone and produce unlimited sources of moab, the moab's potential for recognizing and binding, selectively, to a given epitope, would make it the "universal ligand" in targeting. As a result of the Kohler/Milstein hybridoma breakthrough, the ability to select for and produce unlimited quantities of moab became a reality and thus fueled the research in the targeting program (5, 7).

**Figure 4.** Reproduced with the permission of R. John Collier and Donald A. Kaplan [(1984) *Sci. Am.* 251 (1), 56].

III. HYBRIDOMA TECHNOLOGY AND THE GENERATION OF MONOCLONAL ANTIBODIES

The process of producing a monoclonal antibody is illustrated in Figure 4. The human cancer tissue is presented as an antigen to the mammalian immune system. The mouse is the system of choice because hybridoma technology was developed within the context of mouse genetics (7). The immune system processes the cancer tissue and begins to make antibody as has been described. Monitoring to determine the reactivity against the cancer tissue is done by assaying serum against original cancer tissue (7). Once the animal is making polyclonal antibody against the target, plasma B cells are obtained by excising the spleen, harvesting the B cells, and fusing them with malignant myeloma cells (5, 7). The cells are then propagated in a medium in which only fused hybridoma cells can survive (e.g., a medium such as hypoxanthine/aminopterin/thymidine, which selects only for a survival pathway of fused hybridoma cells). The moab's derived from the surviving hybridoma cells are screened in a high-speed automated selection process against malignant and normal tissue. Those moab's that have good immunoreactivity against malignant tissue and minimal reactivity against normal tissue are selected and further evaluated as targeting ligands in the context of drug conjugates (5, 7).

Pursuant to understanding the chemistry of designing and developing conjugates, it is important to review the structure and the attendant biochemical characteristics of the antibody. A representation of an IgG class of antibody is illustrated in Figure 5 (11). The antibody is composed of identical heavy chains denoted by the subscript H which are joined by two disulfide linkages located in the "hinge region" of the antibody. Two identical light chains denoted by the subscript L are joined to the heavy chains by disulfide bonds connecting the constant portion of the light chain (C_L) to the heavy chain first constant region (C_{H1}). The amino terminus of each chain is located at the variable portions of both the heavy and light chains, V_H and V_L , respectively. The C terminus of the light chain is located at the C_L domain and that of the heavy chain is at the C_{H3} domain (11). The immunoreactivity of the moab is controlled by the variable

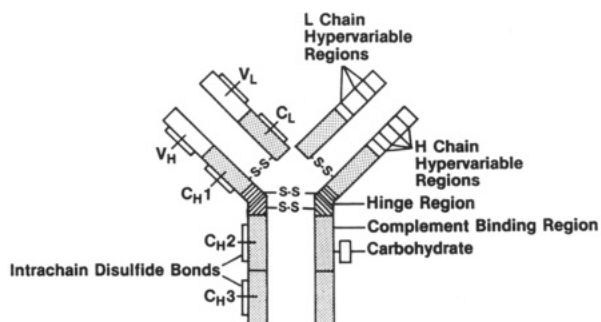


Figure 5.

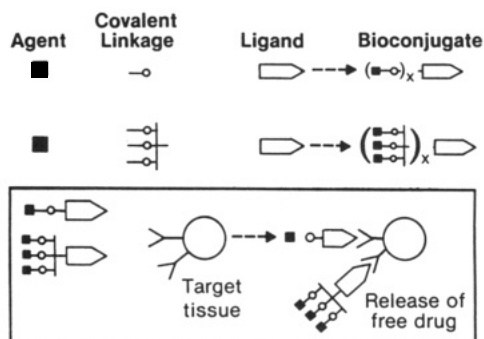


Figure 6. Design and synthesis of agent-linkage-ligand conjugate: (1) Agent-linkage-ligand construction expresses inherent biological activity or facilitates its release at the target site. (2) Agent and/or linkage amenable to stoichiometric determination within the context of the bioconjugate.

domains and is comprised of three peptide sequences in the hypervariable region of the light chain and four sequences in the heavy chain (11). The species characteristics of the moab are expressed both in the framework region of the variable domain as well as specific sequences of the C_H and C_L regions. In addition, classes of moab's such as IgM and IgE differ from IgA, IgD, and IgG by the addition of C_H4 domain at the C terminus (12). Finally, within species, classes and subclasses are characterized by subtle differences in C region sequences. The complement binding receptor and an N-glycosylated carbohydrate is located within the C_H2 domain. This fortuitous location of the sugar substrate provides a unique functionality for regioselectively incorporating drugs outside of the antigen-binding region. The importance of this linkage will be discussed later.

IV. THE CHEMICAL DESIGN AND SYNTHESIS OF MODIFIED TARGETING AGENTS FOR ATTACHMENT TO MOAB'S

In designing the bioconjugate, it is important to distinguish the integrity of the three components of a bioconjugate: the agent to be delivered, the covalent linkage, and the moab. The linkage must not diminish the biological activity of the modified agent nor compromise the moab's ability to target. Two general strategies for conjugating an agent to a moab are represented in Figure 6. In the first strategy, the modified agent is reacted directly with functional groups on the surface of the moab. In this process, the loading of the drug would be determined by the number of available attachment sites on the moab. Alternatively, one can engraft the agent onto a matrix substrate and then react this unit with the moab. In the second process, the amount of agent delivered can be increased without having to increase the number of covalent bonds to the moab (13). Regardless of which strategy is chosen, the chemistry of bioconjugate construction must be guided by the following tenets: (1) the

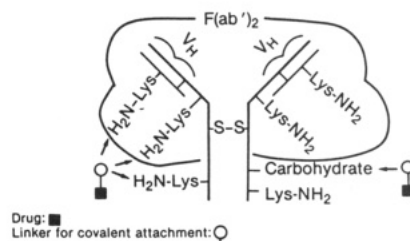


Figure 7. Moab sites of agent attachment and chemical methods for moab agent modification. Goals: (1) attach agent to moab without altering serological activity, (2) construct conjugate with retention of biological properties of agent, (3) construct conjugate with linkage that facilitates release of free drug at target site, (4) design of agent/linkage compatible with covalent attachment to $F(ab')_2$ fragment, (5) construct conjugate with minimal immunogenicity, and (6) synthesis of conjugate amenable to large-scale production.

attachment of agent to moab must be achieved without altering its immunoreactivity, (2) the conjugate must be constructed with a chemical linkage that will either allow the retention of the biologic properties of the agent or facilitate the release of the free drug at the target site, (3) the design of the agent/linkage chemistry should be compatible with covalent attachment to either the intact moab or its fragments, (4) the synthesis of the conjugate should be done in a manner that would minimize immunogenicity, and (5) the construction of the conjugate must be amenable to large-scale production (Figure 7).

The moab is attractive as a targeting ligand because (1) it has many potential sites of drug attachment and (2) it can maintain immunoreactivity even as subfragments. Represented in Figure 7 are the potential sites of covalent attachment on the intact moab and the proteolytic fragment, $F(ab')_2$ (14). The most accessible sites for drug attachment on the polypeptide chains are the ϵ amino groups of the lysine residues (approximately 90 lysines in a moab) and the carbohydrate moiety of the C_H2 domain (15). One can imagine oxidizing the carbohydrate to generate aldehyde functions from the *vic*-diols, which can react with various drug functionality such as hydrazides (16, 17). Drugs can be incorporated at the lysine residue through the construction of stable amide linkages. In addition, the lysine residues are important sites for drug attachment in the $F(ab')_2$ fragments since these have no carbohydrate.

Having reviewed the required characteristics of the bioconjugate and the sites of covalent attachment to the moab, it is appropriate to identify the representative chemical linkages that have been utilized in drug targeting. The succinate linkage has been employed in joining des-acetylvinblastine to the moab via an amide bond to the lysine amine (18, 19). This, of course, discourages release of the free drug from the conjugate (see Figure 8, entry 1).

The sulfhydryl-bearing A chains of the toxins ricin, diphtheria toxin, and abrin have been joined to the moab via disulfide linkages. For example, the moab has been reacted with the *N*-hydroxysuccinimide ester of 4-(2-pyridyldithio)butyric acid to introduce several latent thiols onto moab lysines. This, in turn, is reacted with the sulfhydryl-containing toxin to yield the moab conjugate as the disulfide. The lability of the disulfide bond and its resultant short half-life has encouraged the construction of hindered disulfides such as the α -methyl butyrate (see Figure 8, entry 2, $R = CH_3$). This minor change in the linkage enhanced the circulation half-life of the correspondingly linked moab-ricin A significantly (20, 21).

Linker	Agent
1. MoAB-Lys-NH-C(=O)-CH ₂ -CH ₂ -C(=O)-N-Lys-Agent	Vinblastine
2. MoAB-Lys-NH-C(=O)-CH ₂ -CH ₂ -S-S-Agent	Ricin A, Diphtheria toxin A, Abrin A
3. MoAB-Lys-NH-C(=O)-CH ₂ -CH ₂ -N-C(=O)-CH ₂ -N-Lys-Agent	Ricin A, Alkaline phosphatase
4. MoAB-Carbohydrate-C(=O)-N=N-C(=O)-Agent	Vinblastine hydrazide, Methotrexate hydrazide
5. MoAB-Lys-NH-C(=O)-N-C(=O)-N-Agent	Anthracycline
6. MoAB-Lys-NH-C(=O)-N(SiH ₃) ₃ -N-Agent	Indium and Yttrium chelates
7. MoAB-Lys-NH-C(=O)-C ₆ H ₄ -C(=O)-N=N-C(=O)-Agent	Metal chelates
8. MoAB-carbohydrate-C(=O)-N=N-C(=O)-Agent	Anthracycline

Figure 8. Chemical linkages for covalent attachment of agent to ligand.

An even more stable sulfhydryl-based moab/agent linkage has been achieved through formation of a thio-ether bond. The substrates ricin and alkaline phosphatase have been linked to moab in the following two-step procedure: (1) the lysine residue of either the substrate or the moab has been reacted with thiolane hydrochloride to give the 4-sulfhydrylbutyrimidate derivative and (2) sulfhydrylbutyrimidate has been joined to the complementary protein that bears a 4-(methylenemaleimido)cyclohexylcarboxamide via a conjugate addition of sulfur to maleimide (see Figure 8, entry 3) (22). The application of this linkage in the targeting of alkaline phosphatase for prodrug activation will be described in a later discussion (22).

Investigators at Cytogen and Lilly Research Laboratories have reported the oxidation of moab-carbohydrate and use of the resultant aldehydes for linkage of drug hydrazides (16, 17). Cytogen scientists have prepared the methotrexate hydrazone conjugate and Lilly Research investigators have synthesized the vinblastine hydrazone conjugate (see Figure 8, entry 4). The vinblastine hydrazone-moab conjugate will be described later in the review as an example of designing and developing conjugates in a structure-activity relationship based on human clinical feedback.

The anthracyclines, exemplified by adriamycin and daunomycin, are a family of oncolytics that have been very challenging as candidates for conjugation. The need for the release of the free drug in order to express its DNA-binding activity has required the development of labile linkages compatible with the functionality of the anthracyclines. Reisfeld and others have constructed the acid-labile aconitine amide linkage through the lysine amine of the moab and the amine group of the glycoside of the anthracycline (see Figure 8, entry 5) (23).

The importance of chemical linkers is most effectively highlighted in the targeting of radionuclides for both imaging and therapy. Historically, ¹²⁵I and ¹³¹I have been incorporated onto moab by iodination of the tyrosine residues (24). As imaging and therapy conjugates, the clinical data thus far have not been encouraging because of the rapid dehydrohalogenation of iodine. More recently, Meares has helped pioneer the construction of indium and yttrium conjugates through the development of nuclide chelate linkages (25). Investigators from Hybritech have utilized this technology in advancing the use of indium in imaging of solid tumors and then using the matched yttrium conjugate for therapy (see Figure 8, entry 6) (26). Most recently, investigators at NeoRx have reported

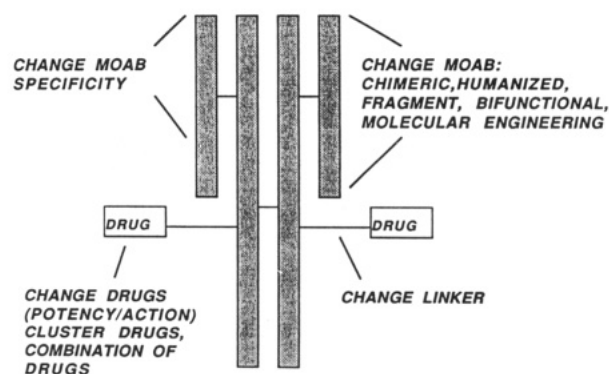


Figure 9. Structure-activity relationship: modification for moab-drug conjugates.

a radionuclide matched pair of technetium and rhenium for imaging and therapy, respectively. Thus, dosimetry data collected from the indium or technetium moab conjugate has allowed the therapy with the corresponding yttrium or rhenium moab conjugate. This has resulted in the first clinical response of a human solid tumor with a rhenium conjugate (27).

Offord and Rose at the University of Geneva as well as King at Rockefeller have reported the use of carboxybenzaldehyde as a linker for incorporating a ketone or aldehyde functionality onto the lysine amine of the protein (see Figure 8, entry 7) (28, 29). Offord and Rose have reported the construction of hydrazone conjugates via this linkage (29).

A complementary approach for modifying the carbohydrate aldehyde linkage has been one in which a hydrazide has been incorporated onto the moab for reaction with drugs containing carbonyl functions. Investigators at Cytogen have built in adipic dihydrazide linkage to join the oxidized carbohydrate of the moab to the ketone of an anthracycline via hydrazone linkages (30). Barton et al. at Lilly have utilized a reductive amination of the moab carbohydrate aldehyde with glutamic hydrazide and subsequently constructed a releasable attachment to an anthracycline via its ketone (see Figure 8, entry 8) (31).

As one begins to correlate the biological with the chemical components of a moab drug conjugate, it is clear that developing a medicinal chemistry structure-activity relationship (SAR) becomes a multidimensional challenge (illustrated in Figure 9) (32). As has been emphasized in earlier portions of this review, there are a variety of opportunities for independent structural modifications of the conjugate that are expressed in the framework of the moab, the linker, and the drug.

The quality of targeting of the conjugate to selective tissue can be achieved by changing either the specificity of the moab or simply its affinity (i.e., its on/off rate). If a human antibody response to the murine moab drug conjugate becomes a problem, the constant regions and the framework portion of the variable region can be replaced by human sequences through molecular engineering (8). In addition, if the intact moab with its attendant effector function domains such as complement binding present an innocent tissue bystander liability, fragments of the moab such as F(ab')₂ that no longer carry these domains can be synthesized and conjugated with drug (see Figure 9) (14).

The chemical linker is the heart of the conjugate. It determines the ability of the drug to express its activity either as an integral part of the conjugate or allows its release at a rate that is dictated by the chemistry. The

choice of a releasable or nonreleasable linkage as it impacts on the drug toxicity will be discussed specifically with respect to the moab-vinca conjugate in the next portion of this review.

V. THE CHEMISTRY AND BIOLOGICAL ACTIVITY OF MOAB-DRUG CONJUGATES

The oncolytic drug can be selected on the basis of a combination of its clinical effectiveness, its mode of action, and its potency against the tumor target. It is most important to understand that the parameters of biodistribution and local drug concentration may dramatically change a drug's profile as a conjugate compared to its unmodified form. As discussed before, the SAR that unfolds for a targeted drug is one that is multidimensional and dependent on a variety of structural changes, i.e., moab, linker, and drug. The ability to enhance the quality of the conjugate depends on the transmission of information from the clinic to the laboratory and applying this information to the preclinical model (see Figure 9) (32).

As an example of the design, the development, and the evaluation of a drug conjugate, I would like to describe a program that I have participated in, one that is generically representative of the drug-targeting efforts occurring at the many academic and industrial institutions throughout the world today. In this example, the importance of human clinical feedback is emphasized for adjusting the SAR and enhancing the efficacy of the drug conjugate.

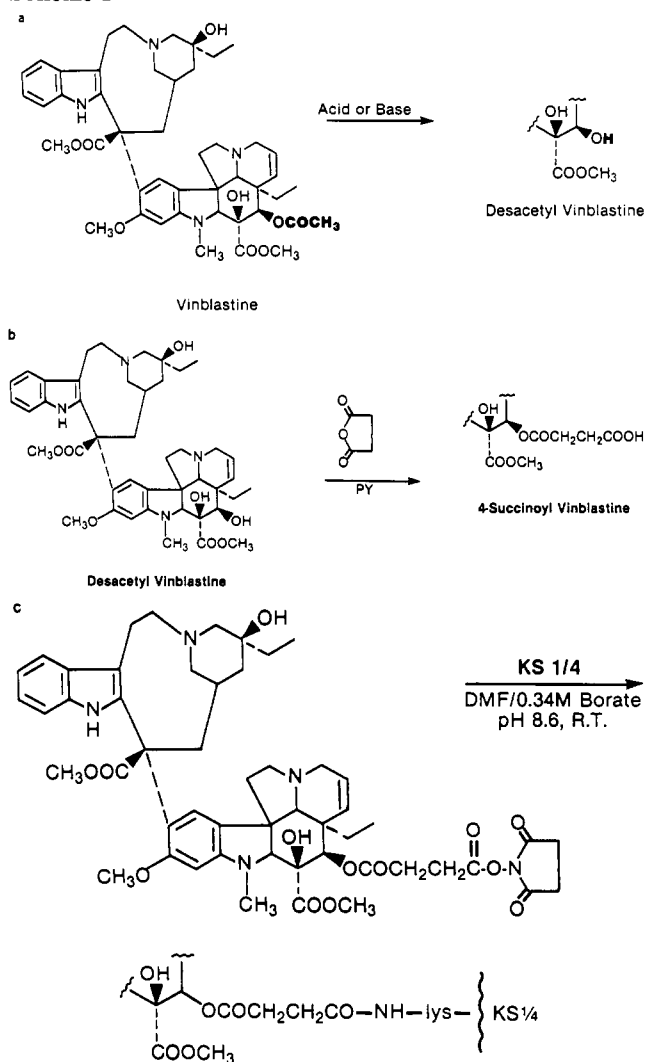
Our investigators at Lilly chose a vinca alkaloid for the designing of a moab-drug conjugate, partly because of our vast prior experience in chemical modification of the vincas and partly because of its biological potency for treatment of human cancer (33). The vinca substrate for conjugation was prepared by the reaction of vinblastine with acid or base effecting the deesterification of the 4-position of the vindoline component. This, in turn, was reacted with succinic anhydride to afford the 4-succinate of desacetylvinblastine (DAVLB), a substrate bearing the nonreleasing linker, succinate (see Scheme I, parts a and b) (18, 19). The choice of the succinate linker was made, initially, in order to evaluate the inherent activity of the vinca in the context of the conjugate, and to minimize the liability of free vinca.

The moab selected for targeting was identified as KS1/4, a murine moab developed by Walker in Reisfeld's laboratory at Scripps (34). The moab KS1/4 recognizes a tumor/epithelial associated antigen (40 KD) found in high epitope density on human adenocarcinomas (35). The primary target of this moab is lung and colorectal adenocarcinoma (36).

Pursuant to attaching the vinca to KS1/4, the DAVLB hemisuccinate was converted to its *N*-hydroxysuccinimide active ester. This, in turn, was reacted with KS1/4 in aqueous borate buffer in pH 8.6 at room temperature to afford, after a series of chromatographies, a 50% yield of the conjugate (see Scheme I, parts a-c) (16, 30, 45). Stoichiometric evaluation of the conjugate by ultraviolet spectrophotometry indicated a conjugation ratio of 4-6 drugs/moab (36). This chemical process and the corresponding biochemical purification proved to be reliable, reproducible, and amenable to large-scale production (36). The analytical profile that was developed for monitoring the quality of KS1/4-DAVLB and all our other drug conjugates is illustrated in Figure 10.

The difficulty with selecting a relevant *in vivo* animal model for evaluating the biological potential of a new moab-drug conjugate is that the targeting substrate recognizes "human epitopes". Consequently, a model had

Scheme I



to be created which would accommodate the pharmacology of the drug as part of a conjugate as well as the ability of the conjugate to target the human tumor tissue. The *in vivo* experimental system which has been widely utilized in evaluating drug conjugates has been the "athymic nude mouse" xenograft model. The inbred athymic mouse does not express a thymus; consequently, it is immunologically impotent and unable to reject tissue grafts such as malignant tumors from another species (38). The *in vivo* nude mouse human xenograft models that have been selected for our moab-drug conjugate evaluations are described in Figure 11 (32).

The traditional path for tracking antitumor potency of standard oncolytics has been in an *in vitro* potency assay measuring the ability of the agent to inhibit tumor growth. With respect to the drug conjugate KS1/4-DAVLB, which was constructed with a nonreleasing linker to minimize free drug, the *in vitro* assay measured the potency of the vinca in the context of the conjugate. Predictably, the *in vitro* assay showed the conjugate to be of a low potency, one whose IC_{50} was about 200-fold lower than that of vinblastine (Figure 12) (18b, 39). Clearly, the utility of targeting a low-potency conjugate could only be evaluated in an *in vivo* system, one that would allow the dramatic change in biodistribution to be expressed in tumor inhibition or regression.

In an *in vivo* nude mouse tumor xenograft model, which measures the effect of an agent against a P3UCLA human

SDS-PAGE(Reducing and Nonreducing Conditions)

Isoelectricfocusing Analysis

FPLC Chromatography(Superose12,MonoQ,MonoS)

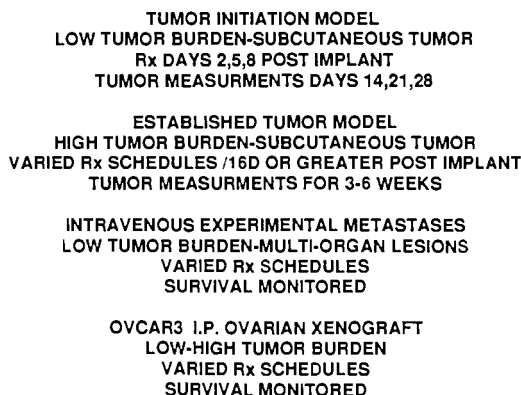
Functional ELISA- Immunoreactivity

Functional Flow Cytometry- Immunoreactivity

Laser Nephelometry-Total Mouse Ig

In Vitro Potency Analysis

Stability Studies

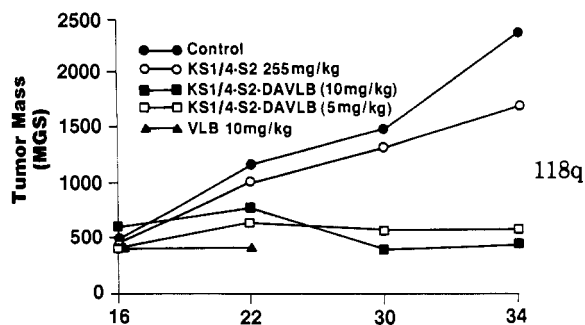
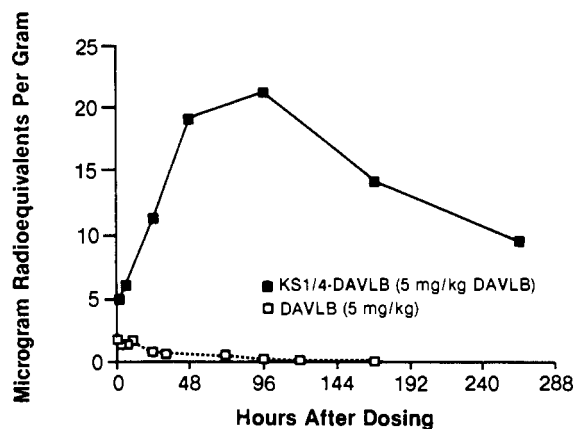
Figure 10. Analytical profile of moab-drug conjugates.**Figure 11.** Preclinical pharmacology: nude mice efficacy models.

Drug	Concentration ($\mu\text{g/ml}$)	% Inhibition vs. Control
VLB	.00015	0
VLB	.0015	80
VLB	.015	87
KS1/4-DAVLB	.1	8
KS1/4-DAVLB	.25	38
KS1/4-DAVLB	.5	71
KS1/4-DAVLB	2.5	84

Figure 12. In vitro potency analysis of vinblastine (VLB) and KS1/4-DAVLB (39a), as determined by a proliferation assay utilizing the P3A UCLA human lung adenocarcinoma cell line with a 72-h exposure to drug or monoclonal antibody-drug conjugate. All concentrations are in terms of vinca alkaloid content.

lung adenocarcinoma cell line, the KS1/4-DAVLB conjugate showed regression and inhibition of tumor growth at 10 and 5 mg/kg of vinca equivalent, respectively (see Figure 13) (39). This contrasts with the free drug vinblastine, which at 10 mg/kg was toxic to the mice. More importantly, the free KS1/4 showed no activity as did an irrelevant moab-DAVLB conjugate (data not shown) (39). Moreover, the vinca alkaloid mechanism of action is to inhibit the mitotic cell division in the G_2+VM phase by binding to tubulin and inhibiting its assembly (40). The KS1/4-DAVLB was equipotent to vinblastine with respect to tubulin binding in a cell-free tubulin assay carried out by Wilson (40).

As had been suggested by various investigators in the field of targeting, efficacy with a low-potency drug conjugate could be achieved if the concentration of drug in the tumor is enhanced by virtue of targeting. In order to more clearly define the mechanism of efficacy as well as establishing the "proof of targeting", a nude mouse was implanted with a P3UCLA tumor and treated with [^3H]DAVLB at 5 mg/kg and KS1/4-[^3H]DAVLB at 5

**Figure 13.** Effect of KS1/4-DAVLB on the growth of established xenografts (39a).**Figure 14.** Analysis of the biodistribution of tumor tissue of [^3H]DAVLB and KS1/4-[^3H]DAVLB in P3UCLA human lung xenograft bearing nude mice (41). The animals were sacrificed at the time points indicated for both free drug and conjugate-treated animals.

mg/kg of vinca equivalent. After 96 h postinjection, up to 7–8% of the total administered dose was found in the tumor tissue after dosing with KS1/4-DAVLB. In contrast, less than 0.3% of the dose was found in tumor tissue after dosing with free DAVLB (see Figure 14) (41).

After completing the preclinical biological evaluations in the mouse xenograft models and the preclinical toxicology evaluations in rodents and primates, the KS1/4-DAVLB conjugate was evaluated in the clinic. Twenty-two patients received KS1/4-DAVLB in a phase I trial. Of those, 13 received single iv infusions of conjugate at doses ranging from 40 to 240 mg. Nine patients received multiple iv infusions at a dose of 1.5 mg/kg every 2–3 days for up to nine doses (42).

A surprising and unpredicted dose-limiting duodenal toxicity presented itself at 250 mg during single-dose studies and at a cumulative dose of 400 mg during multiple-dose studies. The toxicity was reversible and no residual damage to the duodenum was observed. The toxicity did not appear to be vinca related. Studies by Schneck, Petersen, and Zimmerman suggested complement deposition in the inflamed duodenal tissue (43). Further studies are underway to more clearly define the mechanism of the gastrointestinal tract (GIT) toxicity.

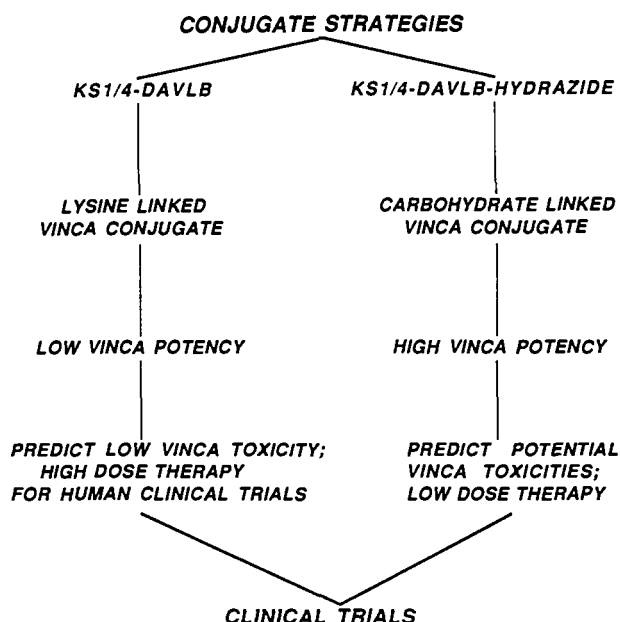
This human phase I study produced a significant amount of valuable information which is summarized in Figure 15. An extremely important observation was that there was significant tumor cell binding by KS1/4-DAVLB as evidenced by biopsied-tissue staining and evaluation. This, of course, supports the concept and process of targeting. In addition, there were no serious immunologic events that would be mediated by human antimouse antibody responses (HAMA) (42).

SUMMARY

1. GIT toxicity is the dose-limiting factor.
2. Iv morphine but not iv dexamethasone reduces toxicity.
3. In the studies conducted to date, multiple doses were administered without development of serious hypersensitivity or serum sickness reactions.
4. Pharmacokinetics are linear over the dose range studied and multiple-dosing schedules do not appear to change pharmacokinetic parameters.
5. significant tumor uptake and cell binding occur.
6. HAMA responses occurred in some but not all patients. The magnitude of response was not dose related.
7. Patients on morphine did not develop a significant HAMA response.

Figure 15.

Scheme II



As had been alluded to earlier in this review, the drug-targeting program enhances the complexity and the dynamics of the SAR evaluation; indeed, the essential human clinical information is of paramount importance in feeding back to the research aspects of the program in terms of modifying the drug, linker, and moab. The human data strongly suggested that the KS1/4-DAVLB was targeting to not only the tumor, but also to the GIT duodenal epithelium with a threshold toxicity level of 250 mg (42, 43). The conservative SAR strategy that had evolved with respect to the construction of KS1/4-DAVLB was to design a low-potency vinca conjugate with minimal risk of drug release. With the "new reality" of KS1/4-associated GIT toxicity at 250 mg, our SAR adjustment suggested a new drug conjugate profile. A high-potency vinca drug attached to the moab with a releasable linkage would reduce the amount of "KS1/4" in the conjugate that would have to be administered to achieve efficacy (see Scheme II) (32).

As outlined in Scheme III, the construction of the "high-potency" drug conjugate KS1/4-DAVLB-hyd was prepared by reacting desacetylvinblastine hydrazide (DAVLB-hyd) with the aldehyde-KS1/4 which has been prepared by periodate oxidation of the carbohydrate residues

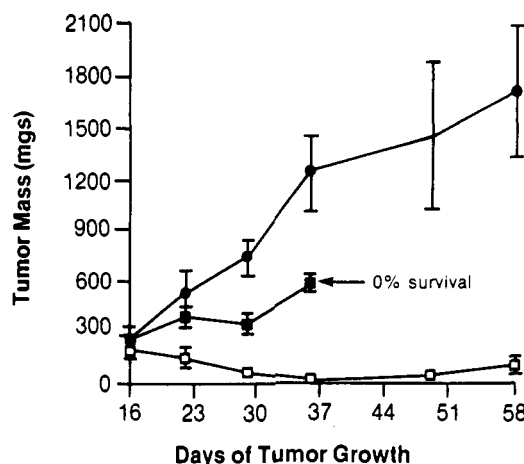
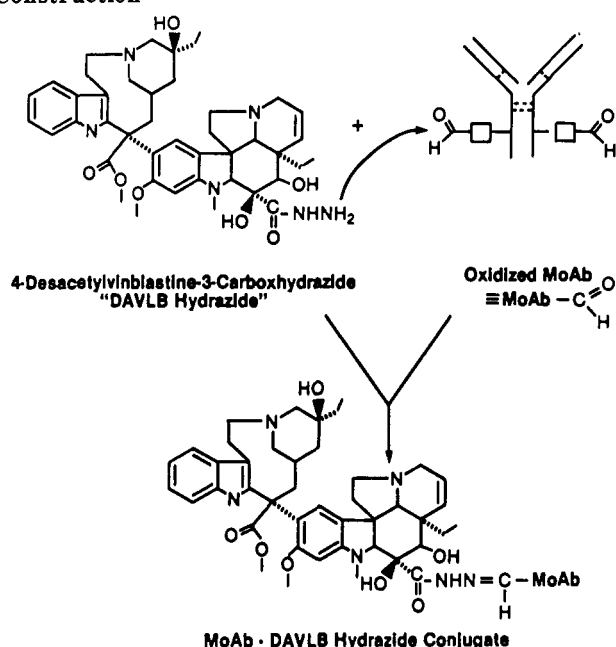


Figure 16. Effect of KS1/4-S2-DAVLB hydrazide (9) vs unjugated DAVLB hydrazide (6) on growth of established P3UCLA lung adenocarcinoma xenografts in nude mice (44): (□) 9 at 2 mg/kg (vinca content), (■) 6 at 2 mg/kg, (●) control. Each point is the mean \pm SE of $N = 5$ (treatment group) or $N = 10$ (control group).

Scheme III. Moab-DAVLB Hydrazide Conjugate Construction



of KS1/4 (see Scheme III) (44). The stoichiometry of the conjugate was 4-6 drugs/moab (44). The hydrazone-linked conjugate was predicted to be reasonably stable at pH 7.4 and release free vinca hydrazide in a microenvironment of pH 5.5 (44).

The prediction of the potency and efficacy profile of KS1/4-DAVLB-hyd in the nude mouse P3UCLA xenograft model was clearly demonstrated in Figure 16. As can be seen in the established high tumor burden model, the KS1/4-DAVLB-hyd effected regression of tumor at doses as low as 2 mg/kg in a six-dose protocol (44). The toxicology evaluation in rodents and primates has been completed and the human phase I clinical evaluation will occur in 1989.

VI. THE SYNTHESIS OF A MONOCLONAL ANTIBODY-ENZYME CONJUGATE FACILITATING SITE-SPECIFIC PRODRUG ACTIVATION

One of the most innovative applications of targeting has been in the area of enzyme-catalyzed prodrug activation.

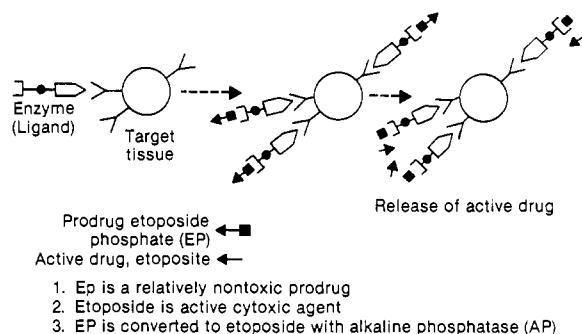
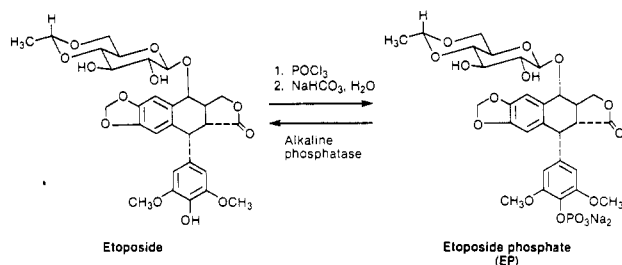


Figure 17. Enzyme-mediated, site-specific prodrug activation. Reproduced with the permission of P. D. Senter, M. G. Saulnier, G. J. Schreiber, D. L. Hirschberg, J. P. Brown, I. Hellstrom, K. E. Hellstrom [(1988) *Proc. Natl. Acad. Sci. U.S.A.* 85, 4842].

Scheme IV. Alkaline Phosphatase Mediated Conversion of Etoposide Phosphate to Etoposide (22)



vation (45). A number of investigators have been involved in this area. Most recently, a very elegant and promising study was reported by Senter et al. (22). They had envisioned etoposide phosphate (EP) as being an innocuous "prodrug" which could be activated, site specifically, with targeted alkaline phosphatase. EP was synthesized by reacting etoposide with phosphoryl chloride and sodium bicarbonate as illustrated in Scheme IV. EP's rapid conversion back to etoposide with alkaline phosphatase is also represented in Scheme IV (22).

Conceptually, the process of enzyme-targeted prodrug activation is depicted in Figure 17. The enzyme, once covalently linked to a moab and allowed to accumulate in target tissue, would convert a subsequently administered dose of EP to the "active" etoposide only within the microenvironment of the tumor (Figure 17). The advantage of this approach is that the enzyme, acting in a catalytic manner, can achieve the active conversion of a large molar excess of substrates. In addition, heterogeneous bystander tumors not bearing the target epitope can, in theory, experience the "overflow" effect of released drug (22).

The enzyme-moab conjugate was prepared by the following sequence: (1) the colorectal adenocarcinoma reactive mouse moab L6 was treated with iminothiolane hydrochloride to afford the sulfhydryl adduct, (2) the alkaline phosphatase was acylated with the *N*-hydroxysuccinimide active ester of 4-(methylenemaleimido)cyclohexylcarboxylic acid to afford the carboxamide, and (3) the two reactive substrates were joined in a 1,4-conjugate addition to afford a 1:1 adduct of the moab-alkaline phosphatase (AP), L6-AP (see Scheme V) (22).

The L6-AP/EP enzyme/prodrug system was evaluated in a nude mouse xenograft model implanted with the human colorectal cell line H3347. The animals were treated with conjugates 18–24 h before drug treatment. After drug dosing on days 9, 13, 17, and 20 after tumor

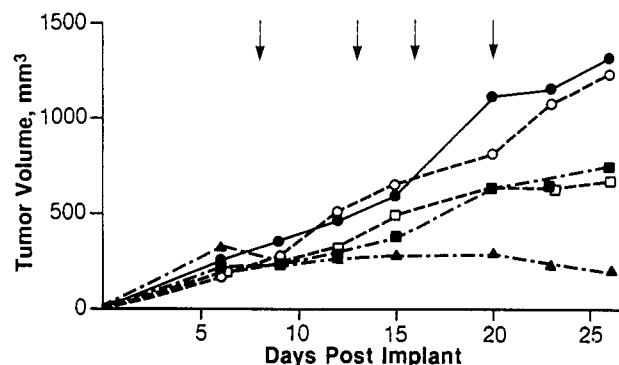
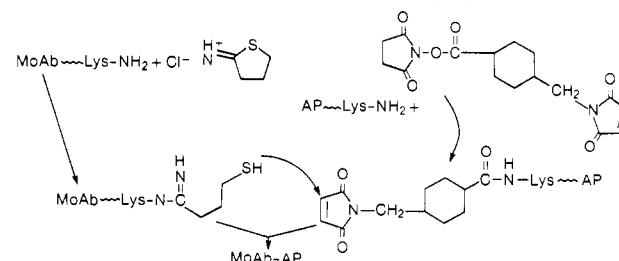


Figure 18. Moab-AP- and EP-mediated site-specific suppression of tumor growth (22). Effects of etoposide, EP, and conjugates plus EP on H3347 tumors in nude mice: (●) no treatment, (○) etoposide, (■) EP, (□) IF5-AP and EP, and (▲) LP-AP and EP. Arrows indicate drug treatment. Conjugates were administered 18–24 h earlier. Each group consisted of eight mice with bilateral tumors.

Scheme V. Construction of Moab-AP (22)



implant, tumor regression occurred only with the relevant combination L6-AP/EP (see Figure 18) (22).

The study by Senter and co-workers is important in that it demonstrates the potential utility of enzyme/prodrug targeting in human therapy. It is an impetus to design and develop other enzyme/prodrug systems which would be more applicable to human therapy.

VII. VISION OF 21ST CENTURY DRUG TARGETING THERAPY

As the drug-targeting community achieves its primary mission in demonstrating "proof of concept" in the treatment of human cancer, a 21st century vision could include the following: (1) the process of site-specific delivery as therapy could be applied to other diseases such as those of the cardiovascular and autoimmune system and AIDS; (2) the catalytic moabs (Abzymes) could be used in concert with agent targeting in site-specific "linker cleavage" and/or prodrug activation; (3) design of therapeutic bifunctional moab recognizing both agent and target could be applied to site-specific delivery; and (4) the construction of bifunctional moabs for activation and targeting of specific immune cells could be used in immunodeficient disease.

ACKNOWLEDGMENT

I would like to express my gratitude and appreciation to Dr. T. F. Bumol for his help and support during the preparation of this manuscript. I would also like to recognize the following interdisciplinary team in the design and development of the KS1/4-vinca conjugates at the Lilly Research Laboratories: Molecular Immunology Research, K. H. Armour, A. L. Baker, B. Barnickel, R. L. Barton, S. L. Briggs, G. J. Cullinan, K. L. Ford, D. Guttman-Carlisle, B. J. Houchins, B. L. Laguzza, C. L.

Nichols, R. A. Owens, W. L. Scott, M. R. Vorndran-Jones, G. A. Koppel (Group Leader); Monoclonal Antibody Research Group, L. D. Apelgren, S. R. Baker, K. R. Bigbee, S. V. DeHerd, D. C. Fix, R. L. Fouts, M. Gutowski, N. A. Hinson, D. A. Johnson, R. S. Maciak, P. Marder, J. J. Starling, D. M. Zimmerman, T. F. Bumol (Group Leader); Clinical Research, D. W. Schneck, B. H. Petersen; Toxicology Research, G. C. Todd, J. L. Zimmermann; Pharmacology, T. D. Lindstrom.

LITERATURE CITED

- (1) This review was presented as a lecture at the Dedicatory Symposia for the Journal of Bioconjugates at the American Chemical Society Meeting, Dallas, Texas, April 11, 1989.
- (2) The concept was presented as part of a lecture at the dedication of the Georg-Speyer-Haus, September 6, 1906; see: (1962) *Readings in Pharmacology* (Louis Shuster, Ed.) Little, Brown, and Company, Boston, MA.
- (3) (a) Benacerraf, B. and Germain, R. N. (1978) The immune response genes of the major histocompatibility complex. *Immunol. Rev.* 38, 70-119. (b) Benacerraf, B. (1982) Genetics and regulation of the immune response. *Natl. Cancer Inst. Monogr.* 60, 171-173. (c) Benacerraf, B. and Rock, K. L. (1984) The interaction between class II MHC molecules and antigens as a basis for Ir gene specificity. *Ann. Immunol. (Paris)* 135C (3), 386-389.
- (4) (a) McDevitt, H. O., Deak, B. D., Shreffler, D. C., Klein, J., Stimpfling, J. H., and Snell, G. D. (1972) Genetic control of the immune response. Mapping of the Ir-1 locus. *J. Exp. Med.* 135 (6), 1259-1278. (b) Snell, G. D. (1976) Recognition structures determined by the H-2 complex. *Transplant. Proc.* 8 (2), 147-156. (c) Snell, G. D. (1978) T cells, T cell recognition structures, and the major histocompatibility complex. *Immunol. Rev.* 38, 3-69. (d) Snell, G. D. (1979) Recent advances in histocompatibility immunogenetics. *Adv. Genet.* 20, 291-355. (e) Snell, G. D. (1980) The major histocompatibility complex: its evolution and involvement in cellular immunity. *Harvey Lect.* 74, 49-80. (f) Snell, G. D. (1981) Studies in histocompatibility. *Science* 213 (4504), 172-178. (g) Snell, G. D. (1981) The future of immunogenetics. *Prog. Clin. Biol. Res.* 45, 241-272.
- (5) Kohler, G., Howe, S. C., and Milstein, C. (1976) Fusion between immunoglobulin secreting and non-secreting myeloma cell lines. *Eur. J. Immunol.* 6, 292-295.
- (6) Kohler, G. (1985) Derivation and diversification of monoclonal antibodies. Nobel lecture. *Biosci. Rep.* 5 (7), 533-549.
- (7) Kohler, G. (1986) Derivation and diversification of monoclonal antibodies. *Science* 233 (4770), 1281-1286.
- (8) (a) Tonegawa, S. (1988) Nobel lecture in physiology or medicine—1987. Somatic generation of immune diversity. *In Vitro Cell Dev. Biol.* 24 (4), 253-265. (b) Tonegawa, S. (1979-1980) Somatic recombination and mosaic structure of immunoglobulin genes. *Harvey Lect.* 75, 61-83. (c) Tonegawa, S. (1988) Somatic generation of immune diversity. *Biosci. Rep.* 8 (1), 3-26. (d) Hood, L. (1988) Biotechnology and medicine of the future. *J. Am. Med. Assoc.* 259 (12), 1837-1844. (e) Perlmutter, R. M., Berson, B., Griffin, J. A., and Hood, L. (1985) Diversity in the germline antibody repertoire. Molecular evolution of the T15 VN gene family. *J. Exp. Med.* 162 (6), 1998-2016. (f) Perlmutter, R. M., Crews, S. T., Douglas, R., Sorensen, G., Johnson, N., Nivera, N., Gearhart, P. J., and Hood, L. (1984) The generation of diversity in phosphorylcholine-binding antibodies. *Adv. Immunol.* 35, 1-37.
- (9) (a) Marchitto, K. S., Kindsvogel, W. R., Beaumier, P. L., Fine, S. K., Gilbert, T., Levin, S. D., Woodhouse, C. S., and Morgan, A. C., Jr. (1989) Characterization of a human-mouse chimeric antibody reactive with a human melanoma associated antigen. *Prog. Clin. Biol. Res.* 288, 101-105. (b) Colcher, D., Milenic, D., Roselli, M., Raubitschek, A., Yarranton, G., King, D., Adair, J., Whittle, N., Bodmer, M., and Schlom, J. (1989) Characterization and biodistribution of recombinant and recombinant/chimeric constructs of monoclonal antibody B72.3. *Cancer Res.* 49 (7), 1738-1745. (c) Beidler, C. B., Ludwig, J. R., Cardenas, J., Phelps, J., Papworth, C. G., Melcher, E., Sierzega, M., Myers, L. J., Unger, B. W., Fisher, M., et al. (1988) Cloning and high level expression of a chimeric antibody with specificity for human carcinoembryonic antigen. *J. Immunol.* 141 (11), 4053-4060. (d) Shaw, D. R., Khazaeli, M. B., and LoBuglio, A. F. (1988) Mouse/human chimeric antibodies to a tumor-associated antigen: biologic activity of the four human IgG subclasses. *JNCI, J. Natl. Cancer Inst.* 80 (19), 1553-1559. (e) Stepkowski, Z., Sun, L. K., Shearman, C. W., Ghayeb, J., Daddona, P., and Loprowski, H. (1988) Biological activity of human-mouse IgG1, IgG2, IgG3, and IgG4 chimeric monoclonal antibodies with antitumor specificity. *Proc. Natl. Acad. Sci. U.S.A.* 85 (13), 4852-4856. (f) Sun, L. K., Curtis, P., Rakowicz-Szulczynska, E., Ghayeb, J., Chang, N., Morrison, S. L., and Koprowski, H. (1987) Chimeric antibody with human constant regions and mouse variable regions directed against carcinoma-associated antigen 17-1A. *Proc. Natl. Acad. Sci. U.S.A.* 84 (1), 214-218. (g) Shaw, D. R., Khazaeli, M. B., Sun, L. K., Ghayeb, J., Daddona, P. E., McKinney, S., and LoBuglio, A. F. (1987) Characterization of a mouse/human chimeric monoclonal antibody (17-1A) to a colon cancer tumor-associated antigen. *J. Immunol.* 138 (12), 4534-4538. (h) Liu, A. Y., Robinson, R. R., Murray, E. D., Jr., Ledbetter, J. A., Hellstrom, I., and Hellstrom, K. E. (1987) Production of a mouse-human chimeric monoclonal antibody to CD20 with potent Fc-dependent biologic activity. *J. Immunol.* 139 (10), 3521-3526. (i) Brown, B. A., Davis, G. L., Saltzberger-Muller, J., Simon, P., Ho, M. K., Shaw, P. S., Stone, B. A., Sands, H., and Moore, G. P. (1987) Tumor-specific genetically engineered murine/human chimeric monoclonal antibody. *Cancer Res.* 47 (13), 3577-3583. (j) Sahagan, B. G., Dorai, H., Saltzberger-Muller, J., Toneguzzo, F., Guindon, C. A., Lilly, S. P., McDonald, K. W., Morrissey, D. V., Stone, B. A., Davis, G. L., et al. (1986) A genetically engineered murine/human chimeric antibody retains specificity for human tumor-associated antigen. *J. Immunol.* 137 (3), 1066-1074. (k) Boulianne, G. L., Hozumi, N., and Shulman, M. J. (1984) Production of functional chimaeric mouse/human antibody. *Nature* 312 (5995), 643-646.
- (10) Benacerraf, B. (1985) Significance and biological function of class II MHC molecules. Rous-Whipple Award lecture. *Am. J. Pathol.* 120 (3), 334-343.
- (11) (a) Edelman, G. M., et al. (1969) Complete sequence of human IgG1. *Proc. Natl. Acad. Sci. U.S.A.* 63, 78. (b) Poljak, R. J. (1975) Three-dimensional structure, function and genetic control of immunoglobulin. *Nature* 256, 373. (c) Litman, G. W., Litman, R. S., Good, R. A., and Rosenberg, A. (1973) Molecular dissection of immunoglobulin G. Conformational interrelationships of the subunits of human immunoglobulin G. *Biochemistry* 12 (10), 2004-2011.
- (12) (a) Mathur, A., Lynch, R. G., and Kohler, G. (1988) The contribution of constant region domains to the binding of murine IgM to Fc mu receptors on T cells. *J. Immunol.* 140 (1), 143-147. (b) Dessein, A., Germain, R. N., Dorf, M. E., and Benacerraf, B. (1979) IgE responses of synthetic polypeptide antigens. I. Simultaneous Ir gene and isotype-specific regulation of IgE responses to L-glutamic acid60-L-alanine30-L-tyrosine10 (GAT). *J. Immunol.* 123 (1), 463-470. (c) Mendez, E., Frangione, B., and Franklin, E. C. (1973) Structure of immunoglobulin A. Amino acid sequence of cysteine-containing peptides from the J chain. *Biochemistry* 12 (6), 1119-1124. (d) Wolfenstein-Todel, C., Prelli, F., Frangione, B., and Franklin, E. C. (1973) Immunoglobulin A. Arrangement of disulfide bridges in the "hinge" region of an immunoglobulin lin A-1 human myeloma protein. *Biochemistry* 12 (25), 5195-5197.
- (13) Hurwitz, E., Wilchek, M., and Pitha, J. (1980) Soluble macromolecules as carriers for daunorubicin. *J. Appl. Biochem.* 2, 25-35.
- (14) (a) Lamoyi, E. (1986) Preparation of F(ab')₂ fragments from mouse IgG of various subclasses. *Methods Enzymol.* 121, 652-663. (b) Parr, D. M., Connell, G. E., Kells, D. I., and Hofmann, T. (1976) Fb'2, a new peptic fragment of human immunoglobulin G. *Biochem. J.* 155 (1), 31-36.

- (15) Parr, D. M. (1977) Fragments produced by digestion of human immunoglobulin G subclasses with pepsin in urea. *Biochem. J.* **165** (2), 303–308.
- (16) Bumol, T. F., Laguzza, B. C., Baker, A. L., Todd, G. C., Pohland, R. C., and Aepelgren, L. D. (1988) Studies on 9.2.27-4-desacetyl vinblastine-3-carboxyhydrazide (9.2.27-DAVLB-hydrazide): preclinical pharmacology and toxicology profiles for human melanoma therapy. *Abstracts of Papers, Third International Conference on Monoclonal Antibody Immunoconjugates for Cancer* p 19.
- (17) McKearn, T. J., Lopes, A. D., Radcliffe, R. D., Coughlin, D. J., Hrubiec, R. T., and Rodwell, J. D. (1988) In vivo efficacy of site-specific anti-folate monoclonal antibody conjugates. *Abstracts of Papers, Third International Conference on Monoclonal Antibody Immunoconjugates for Cancer* p 17.
- (18) (a) Rowland, G. F., Simmonds, R. G., Corvalan, J. R. F., et al. (1983) Monoclonal antibodies for targeted therapy with vindesine. *Protoplasma* **130**, 375. (b) Johnson, I. S., Spearman, M. E., Todd, G. C., Zimmerman, J. L., and Bumol, T. F. (1987) Monoclonal antibody drug conjugates for site-directed cancer chemotherapy: preclinical pharmacology and toxicology studies. *Cancer Treat. Rev.* **14** (3–4), 193–196. (c) Johnson, D. A. and Laguzza, B. C. (1987) Antitumor xenograft activity with a conjugate of a Vinca derivative and the squamous carcinoma-reactive monoclonal antibody PF1/D. *Cancer Res.* **47** (12), 3118–3122.
- (19) Johnson, I. S., Cullinan, G. J., Boder, G. B., Grindey, G. B., and Laguzza, B. C. (1987) Structural modifications of the vinca alkaloids. *Cancer Treat. Rev.* **14** (3–4), 407–410.
- (20) (a) Blakey, D. C. and Thorpe, D. C. (1983) An overview of therapy with immunotoxins containing ricin or its A Chain. *Antibody, Immunoconjugates, Radiopharm.* **1**, 1–16. (b) Vitetta, E. S. and Uhr, J. W. (1985) Immunotoxin. *Annu. Rev. Immunol.* **3**, 197–212. (c) Pastan, I., Willingham, M. C., and FitzGerald, D. J. P. (1986) Immunotoxins. *Cell* **47**, 641–648. (d) Laurent, G., Pris, J., and Farcet, J.-P. (1986) Effects of therapy with T101 ricin A-chain immunotoxin in two leukemia patients. *Blood* **67**, 1680–1687. (e) Spitler, L., del Rio, M., Khentigan, A., et al. (1987) Therapy of patients with malignant melanoma using a monoclonal antimelanoma antibody ricin A chain immunotoxin. *Cancer Res.* **47**, 1717–1723. (f) Thorpe, P. E., Wallace, P. M., Knowles, P. P., Relf, M. G., Brown, A. N., Watson, G. J., Knyba, R. E., Wawrzynczak, E. J. and Blakey, D. C. (1987) New coupling agents for the synthesis of immunotoxins containing a hindered disulfide bond with improved stability in vivo. *Cancer Res.* **47** (22), 5924–5931.
- (21) Worrell, N. R., Cumber, A. J., Parnell, G. D., Mirza, A., Forrester, J. A., and Ross, W. C. (1986) Effect of linkage variation of pharmacokinetics of ricin A chain-antibody conjugates in normal rats. *Anticancer Drug Des.* **1** (3), 179–188.
- (22) Senter, P. D., Saulnier, M. G., Schreiber, G. J., Hirschberg, D. L., Brown, J. P., Hellstrom, I., and Hellstrom, K. E. (1988) Anti-tumor effects of antibody-alkaline phosphatase conjugates in combination with etoposide phosphate. *Proc. Natl. Acad. Sci. U.S.A.* **85**, 4842–4846.
- (23) Yang, H. M. and Reisfeld, R. A. (1988) Pharmacokinetics and biodistribution of doxorubicin-monomoclonal antibody 9.2.27 conjugate. *Abstracts of Papers, Third International Conference on Monoclonal Antibody Immunoconjugates for Cancer* p 69.
- (24) (a) Murray, J. L., Rosenblum, M. G., Sobol, R. E., et al. (1985) Radioimmunoimaging in malignant melanoma with ¹¹¹In-labeled monoclonal antibody 96.5. *Cancer Res.* **45**, 2376–2381. (b) Murray, J. L., Rosenblum, M. G., Lamki, L., et al. (1987) Clinical parameters related to optimal tumor localization of indium-111-labeled mouse antimelanoma monoclonal antibody ZME-018. *J. Nucl. Med.* **28**, 25–33. (c) Epenetos, A. A., Munro, A. J., Stewart, S. et al. (1987) Antibody-guided irradiation of advanced ovarian cancer with intraperitoneally administered radiolabeled monoclonal antibodies. *J. Clin. Oncol.* **5**, 1890–1899. (d) DeNardo, S. J., DeNardo, G. L., O'Grady, L. F., et al. (1988) Pilot studies of radio-immunotherapy of B-cell lymphoma and leukemia using ¹³¹I-Lym-1 Monoclonal antibody. *Antibody, Immunoconjugates Radiopharm.* **1**, 17–33.
- (25) (a) Adams, G. P., DeNardo, S. J., Deshpande, S. V., DeNardo, G. L., Meares, C. F., McCall, M. J., and Epstein, A. L. (1989) Effect of mass of ¹¹¹In-benzyl-EDTA monoclonal antibody on hepatic uptake and processing in mice. *Cancer Res.* **49** (7), 1707–1711. (b) Meares, C. F., McCall, M. J., Deshpande, S. V., DeNardo, S. J., and Goodwin, D. A. (1988) Chelate radiochemistry: cleavable linkers lead to altered levels of radioactivity in the liver. *Int. J. Cancer.* **2**, 99–102. (c) Cole, W. C., DeNardo, S. J., Meares, C. F., McCall, M. J., DeNardo, G. L., Epstein, A. L., O'Brien, H. A., and Moi, M. K. (1987) Comparative serum stability of radiochelates for antibody radiopharmaceuticals. *J. Nucl. Med.* **28** (1), 83–90. (d) Haseman, M. K., Goodwin, D. A., Meares, C. F., Kaminski, M. S., Wensel, T. G., McCall, M. J., and Levy, R. (1986) Metabolizable ¹¹¹In chelate conjugated anti-idiotypic monoclonal antibody for radio-immunodetection of lymphoma in mice. *Eur. J. Nucl. Med.* **12** (9), 455–460. (e) Meares, C. F. (1986) Chelating agents for the binding of metal ions to antibodies. *Int. J. Radiat. Appl. Instrum.* **13** (4), 311–318. (f) Goodwin, D. A., Meares, C. F., McTigue, M., McCall, M. J., and Chaovapong, W. (1986) Metal decomposition rates of ¹¹¹In-DTPA and EDTA conjugates of monoclonal antibodies in vivo. *Nucl. Med. Commun.* **7** (11), 831–838. (g) Goodwin, D. A., Meares, C. F., David, G. F., McTigue, M., McCall, M. J., Frincke, J. M., Stone, M. R., Bartholomew, R. M., and Leung, J. P. (1986) Monoclonal antibodies as reversible equilibrium carriers of radiopharmaceuticals. *Int. J. Radiat. Appl. Instrum.* **13** (4), 383–391. (h) Reardan, D. T., Meares, C. F., Goodwin, D. A., McTigue, M., David, G. S., Stone, M. R., Leung, J. P., Bartholomew, R. M., and Frincke, J. M. (1985) Antibodies against metal chelates. *Nature* **316** (6025), 265–268. (i) Goodwin, D. A., Meares, C. F., DeRiemer, L. H., Diamanti, C. I., Goode, R. L., Baumert, J. E., Jr., Sartoris, D. J., Lantieri, R. L., and Fawcett, H. D. (1981) Clinical studies with In-111 BLEDTA, a tumor-imaging conjugate of bleomycin with a bifunctional chelating agent. *J. Nucl. Med.* **22** (9), 787–792. (j) Meares, C. F., McCall, M. J., Reardan, D. T., Goodwin, D. A., Diamanti, C. I., and McTigue, M. (1984) Conjugation of antibodies with bifunctional chelating agents: isothiocyanate and bromoacetamide reagents, methods of analysis, and subsequent addition of metal ions. *Anal. Biochem.* **142** (1), 68–78. (k) Baker, R. J., Diamanti, C. I., Goodwin, D. A., and Meares, C. F. (1981) Technetium-99 m complexes of EDTA analogs: studies of the radiochemistry and biodistribution. *Int. J. Nucl. Med. Biol.* **8** (2–3), 159–169.
- (26) Merchant, B., Schweighardt, S., Unger, M., and Frincke, J. (1989) Imaging of colorectal carcinoma with a ¹¹¹In-labeled anti-CEA murine monoclonal antibody, ZCE025. *Abstracts of Papers, Fourth International Conference on Monoclonal Antibody Immunoconjugates for Cancer* p 28.
- (27) Schroff, R., Hanelin, L., Vanderheyden, J.-L., Fer, M., Weiden, P., Breitz, H., Fisher, D., Abrams, P., Ratliff, B., Appelbaum, J., Morgan, C., Fritzberg, A. (1989) Preliminary clinical evaluation of a RE-186 labeled anti-CEA F(ab')₂ antibody fragment as a potential radioimmunotherapy agent. *Abstracts of Papers, Fourth International Conference on Monoclonal Antibody Immunoconjugates for Cancer* p 31.
- (28) King, T. P., Zhao, S. W., and Lam, T. (1986) Preparation of protein conjugates via intermolecular hydrazone linkage. *Biochemistry* **25** (19), 5774–5779.
- (29) (a) Offord, R. and Rose, K. (1987) European Patent Number 0243929. (b) Jones, R. M. and Offord, R. E. (1982) The proteinase-catalysed synthesis of peptide hydrazides. *Biochem. J.* **203** (1), 125–129. (c) Rose, K., DePury, H., and Offord, R. E. (1983) Rapid preparation of human insulin and insulin analogues in high yield by enzyme-assisted semi-synthesis. *Biochem. J.* **211** (3), 671–676. (d) Rose, K., Herrero, C., Proudfoot, A. E., Offord, R. E., and Wallace, C. J. (1988) Enzyme-assisted semisynthesis of polypeptide active esters and their use. *Biochem. J.* **249** (1), 83–88.
- (30) Coughlin, D. J., King, H. D., DeVirgilio, M., Greway, G., and Alvarez, V. (1989) Tumor localization of antitumor drug-antibody conjugates. Biodistribution of radiolabeled *N,N*-

- dimethyl adriamycin-B72.3 antibody conjugates with LS174T tumor xenografts in mice. *Abstracts of Papers American Chemical Society Meeting*, Dallas, Texas, Abstract No. 72, American Chemical Society, Washington, DC.
- (31) Barton, R., Starling, J., Hinson, A., Maciak, R., and Koppel, G. (1988) Adriamycin immunoconjugate designed to release free adriamycin from a linking moiety covalently bound to oxidized monoclonal antibody by reductive amination. *Abstracts of Papers, Third International Conference on Monoclonal Antibody Immunoconjugates for Cancer* p 78.
- (32) Figures 11, 17, and 22 were presented as part of an invited lecture, see: Bumol, T. F. (1989) Chemoimmunoconjugates for site-directed therapy of human adenocarcinomas. *Abstracts of Papers, Fourth International Conference on Monoclonal Antibody Immunoconjugates for Cancer* p 50.
- (33) Gorman, M., Neuss, N., and Cone, N. J. (1965) Vinca alkaloids. XVII. Chemistry of catharanthine. *J. Am. Chem. Soc.* 87 (1), 93-99.
- (34) Varki, N. M., Reisfeld, R. A., and Walker, L. E. (1984) Antigens associated with a human lung adenocarcinoma defined by monoclonal antibodies. *Cancer Res.* 44 (2), 681-687.
- (35) Strnad, J., Hamilton, A. E., Beavers, L. S., Gamboa, G. C., Apeltgren, L. D., Taber, L. D., Sportsman, J. R., Bumol, T. F., Sharp, J. D., and Gadske, R. A. (1989) Molecular cloning and characterization of a human adenocarcinoma/epithelial cell surface antigen complementary DNA. *Cancer Res.* 49 (2), 314-317.
- (36) Bumol, T. F., Marder, P., DeHerdt, S. V., Borowitz, M. J., and Apeltgren, L. D. (1988) Characterization of the human tumor and normal tissue reactivity of the KS1/4 monoclonal antibody. *Hybridoma* 7 (4), 407-415.
- (37) Baker, A. L., Bumol, T. F., and Conrad, P. C. (1988) Heterogeneity of monoclonal antibodies; implications for immunoconjugate preparation. *Abstracts of Papers, Third International Conference on Monoclonal Antibody Immunoconjugates for Cancer* p 93.
- (38) (a) Ueyama, Y. (1987) Utilization of nude mice in research on human cancer—screening system of anticancer agent using human tumor xenografts in nude mice. *Prog. Clin. Biol. Res.* 229, 287-310. (b) Garrett, A. J. and Franks, C. R. (1976) Letter: Cancer xenografts in nude mice. *Lancet* 1 (7952), 195. (c) Schmidt, M. and Good, R. A. (1976) Letter: Cancer xenografts in nude mice. *Lancet* 1 (7949), 39. (d) Fodstad, O., Aass, N., and Pihl, A. (1980) Response to chemotherapy of human, malignant melanoma xenografts in athymic, nude mice. *Int. J. Cancer* 25 (4), 453-458. (e) Mattern, J., Bak, M., Hahn, E. W., and Volm, M. (1988) Human tumor xenografts as model for drug testing. *Cancer Metastasis Rev.* 7 (3), 263-284. (f) Taetle, R., Jones, O. W., Honeysett, J. M., Abramson, I., Bradshaw, C., and Reid, S. (1987) Use of nude mouse xenografts as preclinical screens. Characterization of xenograft-derived melanoma cell lines. *Cancer* 60 (8), 1836-1841. (g) Taetle, R., Honeysett, J. M., Rosen, F., and Shoemaker, R. (1986) Use of nude mouse xenografts as preclinical drug screens. Further studies on in vitro growth of xenograft tumor colony-forming cells. *Cancer* 58 (9), 1969-1978.
- (39) (a) Bumol, T. F., Baker, A. L., Andrews, E. L., DeHerdt, S. V., Briggs, S. L., Spearman, M. E., and Apeltgren, L. D. (1988) *Antibody Mediated Delivery Systems* (John D. Rowell, Ed.) Marcel Dekker, Inc., New York, Basel. (b) Johnson, I. S., Spearman, M. E., Todd, G. C., Zimmerman, J. L., and Bumol, T. F. (1987) Monoclonal antibody drug conjugates for site-directed cancer chemotherapy: preclinical pharmacology and toxicology studies. *Cancer Treat. Rev.* 14 (3-4), 193-196. (c) Bumol, T. F., personal communication. Tumor mass measurements did not vary over 30% of the mean. Animals treated with KS1/4-DAVLB had tumor masses which were significantly different than control groups ($P < 0.001$ via Student's t test analysis).
- (40) (a) Wilson, L., Creswell, K. M., and Chin, D. (1975) The mechanism of action of vinblastine. Binding of [acetyl- ^3H]vinblastine to embryonic chick brain tubulin and tubulin from sea urchin sperm tail outer doublet microtubules. *Biochemistry* 14 (26), 5586-5592. (b) Wilson, L. (1975) Microtubules as drug receptors: pharmacological properties of microtubule protein. *Ann. N.Y. Acad. Sci.* 253, 213-31. (c) Hans, F. O., Dickerson, R. M., Wilson, L., and Owells, R. J. (1978) Differences in the binding properties of vinca alkaloids and colchicine to tubulin by varying protein sources and methodology. *Biochem. Pharmacol.* 27 (1), 71-76.
- (41) (a) Spearman, M. E., Goodwin, R. M., Apeltgren, L. D., and Bumol, T. F. (1987) Disposition of the monoclonal antibody-vinca alkaloid conjugate KS1/4-DAVLB (LY256787) and free 4-desacetylvinblastine in tumor-bearing nude mice. *J. Pharmacol. Exp. Ther.* 241 (2), 695-703. (b) Bumol, T. F., Parrish, H., DeHerdt, S. V., Spearman, M. E., Pohland, R., Borowitz, M. J., Briggs, S. L., Baker, A. L., Marder, P., and Apeltgren, L. D. (1987) *Immunological Approaches to the Diagnosis and Therapy of Breast Cancer* (Roberto L. Ceriani, Ed.) Plenum Press, New York.
- (42) Schneck, D. W., Petersen, B., Zimmerman, J., Butler, F., Dugan, W. (1989) Phase I studies with a monoclonal antibody vinca conjugate (MC,KS1/4-DAVLB) in patients with adenocarcinoma. *Abstracts of Papers, Fourth International Conference on Monoclonal Antibody Immunoconjugates for Cancer* p 58.
- (43) Zimmerman, J., Schneck, D. W., and Petersen, B. (1989) Treatment-related lesions observed in patients with adenocarcinoma administered single and multiple doses of a monoclonal antibody vinca conjugate (KS1/4-DAVLB). *Abstracts of Papers, Fourth International Conference on Monoclonal Antibody Immunoconjugates for Cancer* p 169.
- (44) Laguzza, B. C., Nichols, C. L., Briggs, S. L., Cullinan, G. J., Johnson, D. A., Starling, J. J., Baker, A. L., Bumol, T. F., Corvalan, J. R. (1989) New antitumor monoclonal antibody-vinca conjugates LY203625 and related compounds: design, preparation, and representative in vivo activity. *J. Med. Chem.* 32 (3), 548-555.
- (45) Springer, C. J., Antoniew, P., Bagshawe, K. D., Searle, F., Melton, R. G., and Sherwood, R. F. (1988) A novel approach to prodrug activation using a monoclonal antibody conjugated to carboxypeptidase G2. *Abstracts of Papers, Third International Conference on Monoclonal Antibody Immunoconjugates for Cancer* p 43.

ARTICLES

Preparation and Characterization of Conjugates of Recombinant CD4 and Deglycosylated Ricin A Chain Using Different Cross-Linkers

Victor Ghetie,[†] Mark A. Till,[†] Maria-Ana Ghetie,[†] Thomas Tucker,[†] Jim Porter,[§] Eric J. Patzer,[§] James A. Richardson,^{||} Jonathan W. Uhr,[†] and Ellen S. Vitetta^{*†}

Department of Microbiology and Division of Comparative Medicine, Department of Pathology, University of Texas Southwestern Medical Center, Dallas, Texas 75235, and Department of Medicinal and Analytical Chemistry, Genentech, Inc., South San Francisco, California 94080. Received June 1, 1989

In a previous study, we have demonstrated that conjugates containing soluble, recombinant human CD4 (rCD4) and the deglycosylated form of ricin A chain (dgA) (rCD4-dgA) effectively kill a human T cell line infected with the human immunodeficiency virus (HIV) in vitro. In contrast, such conjugates are 100-1000-fold less toxic to uninfected cells. In order to use a rCD4-dgA conjugate effectively in vivo, it was important to demonstrate that (1) it binds to and kills HIV-infected, but not uninfected, human cells, (2) it is stable in the circulation, and (3) it has an optimal therapeutic index (toxicity to animals versus toxicity to target cells). A major factor affecting the efficacy of such conjugates in vitro and in vivo is the nature of the cross-linker between the ligand (rCD4) and the toxin (dgA). In this report, we have prepared rCD4-dgA conjugates using three different cross-linkers. Different methods of purification have been compared by determining the optimal yield, purity, and retention of biological activity (i.e., binding to gp120 and dgA chain activity). The structure of these conjugates as well as their cytotoxicity to target cells in vitro has been analyzed. Finally, we have compared their pharmacokinetics, tissue localization, and toxicity in mice.

Conjugates of human recombinant CD4 (rCD4) and deglycosylated ricin A chain (dgA) (1) or a genetically engineered form of *Pseudomonas* exotoxin (PE₄₀) (2) represent potential new reagents for the therapy of patients infected with the human immunodeficiency virus (HIV). Such conjugates bind to HIV-infected cells by the interaction of rCD4 with the viral envelope glycoprotein, gp120. The conjugate is then internalized and the A chain or the *Pseudomonas* exotoxin inhibits protein synthesis. In this report, rCD4-dgA conjugates have been prepared with three different cross-linkers (SATA, *S*-(*N*-succinimidyl)thioacetate; SMCC, *N*-succinimidyl 4-(maleimidomethyl)cyclohexanecarboxylate; and SMPT, (*N*-succinimidylloxycarbonyl)- α -methyl- α -(2-pyridyldithio)toluene). Conjugates prepared with two of the cross-linkers (i.e., SMPT and SATA) contain disulfide bonds (hindered vs unhindered, respectively) between the rCD4 and dgA. The third, SMCC, contains a thioether bond. Different methods of purification using (i) affinity chromatography on Blue-Sepharose CL-4B and Sepharose-rgp120, (ii) molecular exclusion chromatography on Sephacryl S-200HR, and (iii) gel permeation on a TSK 3000 column for high-performance liquid chromatography have been com-

pared for optimal yields, purity, and gp120-binding activity. In addition, the in vitro toxicity of the conjugates to the HIV-infected human H9 cell line has been determined. Finally, their in vivo pharmacokinetics, tissue localization, and histopathology have been evaluated in mice. The data indicate that the cross-linker can affect in vivo tissue distribution, histopathology, and pharmacokinetics as well as in vitro cytotoxicity of rCD4-dgA. On the basis of these studies, the rCD4-dgA prepared with SMPT was selected for further preclinical testing since it is highly cytotoxic to HIV-1-infected cells in vitro, it is chemically stable, it has a long serum half-life, and most importantly, it does not cause pathologic lesions in life-sustaining organs.¹

EXPERIMENTAL PROCEDURES

Recombinant CD4 (rCD4). Recombinant CD4 containing amino acids 1-368 of the native protein was pre-

* To whom correspondence should be addressed: Department of Microbiology, University of Texas Southwestern Medical Center, 5323 Harry Hines Blvd., Dallas, Texas 75235.

[†] Department of Microbiology, University of Texas Southwestern Medical Center.

[§] Department of Medicinal and Analytical Chemistry, Genentech, Inc.

^{||} Division of Comparative Medicine, Department of Pathology, University of Texas Southwestern Medical Center.

¹ Abbreviations used in this paper: dgA, deglycosylated ricin A chain; DMF, dimethylformamide; DTNB, 5,5'-dithiobis(2-nitrobenzoic acid); DTT, dithiothreitol; FACS, fluorescence-activated cell sorter; FCS, fetal calf serum; HIV, human immunodeficiency virus; LD₅₀, dose killing 50% of the animals; OVA, ovalbumin; PBE, 0.1 M phosphate buffer with 0.003 M EDTA, pH 7.5; PBS, phosphate-buffered saline, pH 7.2; PBSA, phosphate-buffered saline containing 1% bovine serum albumin and 0.02% sodium azide; PE₄₀, *Pseudomonas* exotoxin-40; rCD4, recombinant CD4 antigen; rCD4-dgA, conjugate of rCD4 with dgA; rgp120, recombinant HIV glycoprotein gp120; SATA, *S*-(*N*-succinimidyl)thioacetate; SDS-PAGE, sodium dodecyl sulfate polyacrylamide gel electrophoresis; SMCC, *N*-succinimidyl 4-(maleimidomethyl)cyclohexanecarboxylate; SMPT, (*N*-succinimidylloxycarbonyl)- α -methyl- α -(2-pyridyldithio)toluene; *T*_{1/2}, half-life.

pared as previously described (3). The absorption coefficient ($A_{1\%}^{1\text{ cm}}$, 280 nm) and molecular mass used for rCD4 were 15 and 45 kDa, respectively. rCD4 was labeled with Na^{125}I (Amersham, UK) and the IODO-GEN reagent (Pierce, Rockville, IL) (4). The specific activity was approximately $1\ \mu\text{Ci}/\mu\text{g}$. rCD4 was also biotinylated with a 50-fold molar excess of the *N*-hydroxysuccinimide ester of biotin (Sigma, St. Louis, MO) (5).

Deglycosylated Ricin A Chain (dgA). Deglycosylated ricin A chain was purchased from Inland Laboratories (Austin, TX) and was prepared and characterized as previously described (6). The absorption coefficient and molecular mass of dgA are 7.7 and 32 kDa, respectively. Some dgA preparations were reduced with 5 mM dithiothreitol (DTT; Sigma, St. Louis, MO, final concentration) for 30 min at room temperature in the dark. The DTT was removed by gel filtration on Sephadex G-25M equilibrated with 0.1 M phosphate buffer containing 3 mM Na_2EDTA , pH 7.5 (PBE). The reduced dgA was further treated with Ellman's reagent [5,5'-dithiobis(2-nitrobenzoic acid) (DTNB); Pierce, Rockville, IL] dissolved in dimethylformamide (DMF; Pierce, Rockville, IL), at a final concentration of 2 mM for 30 min at room temperature. The Ellmanized dgA was separated from the reaction mixture by gel filtration on Sephadex G-25M in PBE. The Ellmanized dgA was labeled with Na^{125}I using the IODO-GEN reagent as described previously (7) and the specific activity was approximately $1\ \mu\text{Ci}/\mu\text{g}$.

dgA consists of two isomers, dgA₁ and dgA₂ (6). The separation of these isomers was accomplished with a Blue-Sepharose CL-4B column (20 × 0.8 cm; Pharmacia, Piscataway, NJ) equilibrated with 0.05 M PBE at pH 7.5. The bound dgA₁ + dgA₂ proteins were eluted with a continuous NaCl gradient (up to 0.5 M). Both dgA₁ and dgA₂ were eluted in two distinct chromatographic peaks; the last peak contained pure dgA₁.

Preparation of rCD4-dgA with the *S*-(*N*-Succinimidyl) Thioacetate (SATA) Cross-Linker. rCD4 (1 mL) dissolved in PBE, pH 7.5, at 4 mg/mL was mixed with 10 μL of SATA (Calbiochem, La Jolla, CA) (8) dissolved in DMF at 4.7 mg/mL (molar ratio SATA/rCD4 = 2.3) and the mixture was incubated at room temperature for 30 min. The derivatized rCD4 was separated from small molecules by gel filtration on Sephadex G-25M equilibrated with PBE. The thioacetylated rCD4 was deacetylated by treatment with 50 mM hydroxylamine (Sigma, St. Louis, MO; final concentration) at pH 7.5 and immediately mixed with the Ellmanized dgA solution at pH 7.5 in a molar ratio of dgA/rCD4 of 2. The protein concentration of both dgA and thiolated rCD4 solutions ranged between 2 and 3 mg/mL. After an incubation of 2 h at room temperature, the mixture was purified. In some experiments, one of the two proteins was labeled with Na^{125}I .

Preparation of rCD4-dgA with the (*N*-Succinimidyl)oxycarbonyl- α -methyl- α -(2-pyridyldithio)toluene (SMPT) Cross-Linker. rCD4 (1 mL) dissolved in PBE, pH 7.5, at 4 mg/mL was mixed with 10 μL of SMPT (9) dissolved in DMF at 10 mg/mL (molar ratio SMPT/rCD4 = 2.9) and the mixture was incubated at room temperature for 30 min. The derivatized rCD4 was separated from small molecules by gel filtration on Sephadex G-25M equilibrated with PBE and immediately mixed with freshly reduced dgA (non-Ellmanized) at pH 7.5 in a molar ratio of dgA/rCD4 of 2. The protein concentration of both reactants ranged between 1 and 2 mg/mL. After sterilization by passage through a 0.22- μm filter,

the mixture was incubated at room temperature for 48 h before purification. In some experiments, one of the two proteins was labeled with Na^{125}I .

Preparation of rCD4-dgA with the *N*-Succinimidyl 4-(Maleimidomethyl)cyclohexanecarboxylate (SMCC) Cross-Linker. rCD4 (1 mL) dissolved in PBE, pH 7.0, at 2 mg/mL was mixed with 10 μL of SMCC (Pierce, Rockville, IL) (10) dissolved in DMF at 10 mg/mL (molar ratio SMCC/rCD4 = 6.8) and the mixture was incubated at room temperature for 60 min. The derivatized rCD4 was separated from small molecules by gel filtration on Sephadex G-25M equilibrated with PBE, pH 6.0, and immediately mixed with freshly reduced dgA (non-Ellmanized) at pH 6.0 in a molar ratio of dgA/rCD4 of 2. The protein concentration of both reactants was 2 mg/mL. After 1 h of incubation at room temperature and 16 h at 4 °C, the mixture was purified.

Preparation and Purification of Conjugates Using Chicken Ovalbumin (OVA) and dgA. Control conjugates consisting of OVA (molecular mass 43 kDa; Sigma, St. Louis, MO) and dgA were prepared with SATA or SMPT by using procedures identical with those described for rCD4. The OVA-dgA mixtures were purified by chromatography on Blue-Sepharose CL-4B and Con A-Sepharose-4B (Pharmacia, Piscataway, NJ). The Con A-Sepharose-4B column (5 × 0.8 cm) was equilibrated with 0.02 M Tris-HCl buffer with 1 mM CaCl_2 , MgCl_2 , and MnCl_2 , pH 7.0, and the OVA-dgA conjugate was eluted with 0.25 M methyl α -D-mannoside in Tris-HCl buffer. These conjugates were used as controls in the *in vitro* cytotoxicity assay.

Molar Ratios of rCD4/dgA. The molar ratios of dgA chain to rCD4 were calculated from the specific radioactivities of [^{125}I]dgA or of [^{125}I]rCD4, respectively, and the following absorption coefficients: 7.7 for dgA, 15 for rCD4, and 12.0 for rCD4-dgA.

Chromatography on Blue-Sepharose CL-4B Columns. A 20 × 0.8 cm column containing 10 mL of gel with a binding capacity of 20 mg of dgA was used to purify rCD4-dgA. The column was equilibrated with 0.05 M PBE and eluted with a continuous NaCl gradient (up to 0.5 M) and a Pharmacia gradient maker filled with 50 mL of 0.05 M PBE and 50 mL of 0.5 M NaCl.

Affinity Chromatography on Sepharose-rgp120. The recombinant form of the viral envelope glycoprotein gp120 (rgp120; Genentech, Inc., South San Francisco, CA) was coupled to activated CH-Sepharose-4B (Pharmacia, Piscataway, NJ) according to the manufacturer's protocol at a final concentration of 0.8 mg of rgp120/mL of packed gel. The Sepharose-rgp120 bound 0.125 mg of rCD4/mg of rgp120. The rCD4 and rCD4-dgA conjugates bound to a Sepharose-rgp120 column (4 × 1.8 cm) were eluted with 0.1 M glycine buffer containing 0.15 M NaCl at pH 3.0.

Gel-Permeation High-Performance Liquid Chromatography (HPLC). Samples were applied either to an analytical 7.5 × 600 mm TSK 3000SW column (Spherogel, LKB, Bromma, Sweden) or to a preparative 21.5 × 600 mm TSK G3000SWG column (Ultropac, LKB, Bromma, Sweden) and separation was performed in PBE, pH 7.5, at a flow rate of 1 mL/min (Spherogel) and 3 mL/min (Ultropac). The retention times for the peaks were compared to those of standard protein of known molecular weight (Pharmacia, Piscataway, NJ).

Gel Filtration on Sephacryl S-200HR. Gel filtration was performed on a 80 × 1.8 cm column equilibrated with PBE. The column was calibrated with mouse F(ab')₂ (100 kDa), rCD4 (45 kDa), and dgA (32 kDa).

Sodium Dodecyl Sulfate Polyacrylamide Gel Electrophoresis (SDS-PAGE). rCD4, dgA, and rCD4-dgA conjugates were analyzed under both reducing and nonreducing conditions by SDS-PAGE using the Pharmacia Phast system with 8–25% gel gradient. The gels were stained with either 0.1% Phast gel blue R or with 0.4% silver nitrate according to the manufacturer's directions. The proportion of radioactivity present in the electrophoretic bands was determined by scanning densitometry of the autoradiograph following SDS-PAGE with a Bio-Rad (Model 620) videodensitometer (7). The following proteins were used as standards for the estimation of molecular weight (Pharmacia, Piscataway, NJ): α -lactalbumin (14.4 kDa), soybean trypsin inhibitor (20.1 kDa), carbonic anhydrase (30 kDa), OVA (43 kDa), bovine serum albumin (67 kDa), and phosphorylase b (94 kDa).

Determination of Sulfhydryl Groups. The number of SH groups introduced into rCD4 as well as the number of free SH groups in the rCD4-dgA conjugates were determined with DTNB (11).

Binding of rCD4 to Daudi Cells. The binding of rCD4 to Daudi cells was evaluated by a direct-binding assay using radiolabeled rCD4 or by an indirect assay with biotinylated rCD4 and fluorescein-avidin. Cells ($10^6/0.1$ mL) were treated with various amounts of [125 I]rCD4 (1–500 ng/0.1 mL) or biotinylated rCD4 (0.1–25 μ g/0.1 mL) for 3 h or 30 min, respectively, at 4 °C. After washing twice with cold phosphate-buffered saline (PBS) containing 10% fetal calf serum (FCS) and 0.1% sodium azide, the radioactivity of the cell pellet was measured (when radiolabeled rCD4 was used) or the cell suspension was treated with fluorescein-avidin (1–5 μ g/0.1 mL; Pierce, Rockville, NJ) for 15 min in ice. The cells were washed and analyzed on a fluorescence-activated cell sorter (FACS; Becton-Dickinson, Oxnard, CA).

rCD4 Competitive Binding Assay. The particle concentration fluorescence immunoassay utilized the instrumentation of the Pandex Screen Machine (Pandex Laboratories, Inc.) for the evaluation of solution-phase binding of rgp120 to rCD4. The assay was performed with 0.03 mL per well of rCD4 or conjugates of rCD4 titrated in a separate 96-well plate from 50 to 2 μ g/mL in PBS, pH 7.5; 1% BSA; and 0.02% azide (PBSA). rCD4-biotin (3 mL) at a concentration of 9 μ g/mL in PBSA was added followed by 0.03 mL of rgp120 at a concentration of 15 μ g/mL in PBSA. The reaction mixture was incubated for 3 h at room temperature with mixing. Free and bound rgp120 were immunoprecipitated from the reaction mixture with anti-rgp120 monoclonal antibodies (MoAbs) adsorbed to polystyrene beads. For the immunoprecipitation, 0.02 mL of these anti-rgp120 MoAb-coated beads were first added to a Pandex plate by the instrument. The reaction mixture (3 mL) was then transferred to the particles in the Pandex plate. Following a 15-min incubation, 0.02 mL of a streptavidin-phycoerythrin conjugate was added at a 1/50 dilution in PBSA. The plate was incubated in the dark for 15 min and then washed with PBS and 0.05% Tween 20, and the fluorescence intensity was determined.

In Vivo Elimination of rCD4-dgA Conjugates. The procedure previously described was used (7). Briefly, the conjugates were labeled with Na 125 I by the IODO-GEN technique and were injected into the retroorbital sinus of mice (approximately 4×10^6 cpm/5 μ g per animal). The 125 I levels were determined in heparinized samples (75 μ L) of blood at 5, 10, and 30 min and 1, 2, 4, and 8 h. The total radioactivity remaining in the blood was determined by counting aliquots in a γ -counter and as-

suming a total blood volume of 7% of the body weight (7). Acid-precipitable radioactivity was determined by precipitation of plasma aliquots with 10% trichloroacetic acid. The percentage of the injected radioactivity remaining in circulation was calculated as the percentage of acid-precipitable radioactivity injected. The half-lives ($T_{1/2}$) for both the α - (30 min) and β -phase (8 h) of clearance were determined graphically by extrapolation to zero of the percentage of acid-precipitable radioactivity vs time curves (12).

Organ Distribution of rCD4-dgA Conjugates. The organ distribution of radioiodinated proteins were determined following perfusion of anesthetized mice with PBS as previously described (7). Organs were removed, weighed, and counted in a γ -counter. A sample of the organs was minced with scissors and extracted with 0.5% Nonidet P-40, and the clarified extract was precipitated with 10% trichloroacetic acid. The percentages of acid-precipitable radioactivity were determined and the values were used to calculate the protein-bound radioactivity in various tissues. The capacity of the organ to accumulate the radiolabeled proteins was calculated by dividing the percent of the injected radioactive dose retained in the organ by the wet weight (g) of the organ.

In Vivo Stability of rCD4-dgA Conjugates. Radiolabeled conjugates (approximately 10^7 cpm/animal) were injected into mice and after 4 h the animals were exsanguinated with the heparinized blood was collected. The free and conjugated dgA in the plasma were precipitated with immunocomplexes prepared with rabbit anti-ricin A chain and goat anti-rabbit Ig (13). The precipitate was boiled in 1% SDS and electrophoresed on 12% SDS-polyacrylamide gel. Autoradiograms of the dried gels were scanned by using a Bio-Rad videodensitometer. The areas under the dgA and rCD4-dgA peaks were divided by the total area under both peaks to determine the percentage of radioactivity that corresponds to the released dgA. This value was used as a means of evaluating the in vivo splitting of the rCD4-dgA conjugates.

The functional activity of rCD4-dgA conjugates recovered from the blood was determined by performing a cytotoxicity assay on HIV-infected H9 cells. Mice were injected with radiolabeled SATA- or SMPT-linked conjugates with known specific radioactivity (approximately 5×10^4 cpm/ μ g). After 3 h, the animals were exsanguinated and the heparinated plasma containing a known amount of conjugate was compared in the in vitro cytotoxic assay to freshly thawed conjugates.

Incubation of rCD4-dgA Conjugates with Human Plasma. Conjugates were incubated at 50 μ g/mL with undiluted fresh human plasma or PBS for 16 h at 37 °C and then used in the cytotoxicity assay in parallel with freshly thawed conjugates.

In Vivo Toxicity Assay. Increasing amounts of rCD4-dgA conjugates were injected ip into three groups of four C3H/HEJ mice weighing 15 g and the LD $_{50}$ was calculated on the basis of deaths occurring within 10 days. For SMPT-linked rCD4-dgA conjugates, the assay was repeated twice with three groups of four BALB/c mice weighing 20 g. An average value for both C $_3$ H/HEJ and BALB/c mice was calculated.

Cell-Free Rabbit Reticulocyte Assay. This assay was carried out according to the procedure described by Press et al. as modified by Fulton et al. (6).

Pathology of Mice Injected with SATA- and SMPT-Derived Conjugates. Treatment groups consisted of four 25–32-g CAF $_1$ male mice which were inoculated intraperitoneally with a 1-mL solution contain-

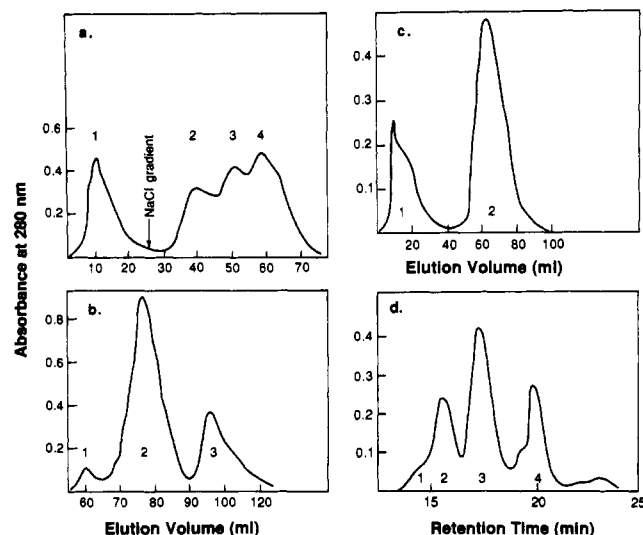


Figure 1. Purification of rCD4-dgA conjugates: (a) Blue-Sepharose CL-4B (SMPT-derived conjugate) (1) rCD4, (2) dgA₂, (3) rCD4-dgA, (4) dgA₁; (b) Sephacryl S-200HR (SATA-derived conjugate) (1) aggregated rCD4-dgA, (2) rCD4-dgA (molecular mass 80 kDa), (3) dgA; (c) Sepharose-rgp120 (SMPT-derived conjugate) (1) nonbound (dgA), (2) bound and eluted at pH 3.0 (rCD4-dgA); (d) TSK 3000SW (SMPT-derived conjugate) (1) aggregated rCD4-dgA, (2) rCD4-dgA (molecular mass 82 kDa), (3) rCD4, (4) dgA.

ing 5%, 10%, and 20% of the LD₅₀ of either SMPT-linked rCD4-dgA, SATA-linked rCD4-dgA, 20% of the LD₅₀ of dgA, or saline. Mice were sacrificed after 7 days by intraperitoneal injection of pentobarbital. Tissues were examined grossly and fixed in 10% buffered formalin. Liver, spleen, kidneys, lung, heart, brain, and appendicular and diaphragmatic muscle were embedded in paraffin, sectioned at 5 μ m and stained with hematoxylin and eosin. Lesions were scored subjectively as absent, minimal, mild, or marked and assigned grades of 0, 1, 2, or 3 and averaged for each group.

The Cytotoxicity of rCD4-dgA to HIV-Infected Human H9 Cells. This assay was performed as previously described (7). Briefly, serial dilutions of conjugates were plated in triplicate in 96-well microtiter plates in complete medium (RPMI, 12% FCS, and antibiotics). Cells were then added to a final concentration of 4×10^5 cells/mL and the plates were incubated for 36 h at 37 °C (5% CO₂). Cells were then pulsed for 6–8 h with 1 μ Ci of [³H]thymidine and harvested on a Titer-tek automatic harvester. [³H]thymidine incorporation was determined on an LKB β -counter. Results are expressed as a percentage of control (untreated cells). Thirteen separate experiments were performed, each using infected and uninfected human H9 cells.

RESULTS

Purification of rCD4-dgA Conjugates. For the purification of the crude conjugates, three methods were applied: (a) Blue-Sepharose/Sephacryl S-200HR, (b) Blue-Sepharose/Sepharose-rgp120, and (c) gel permeation by HPLC on TSK 3000 columns. By gradient chromatography on Blue-Sepharose (which binds dgA), the majority of the rCD4 was removed from the rCD4-dgA conjugate (rCD4 does not bind to Blue-Sepharose) (Figure 1). Irrespective of the cross-linker used for its preparation, the rCD4-dgA always eluted in the third peak and was flanked by dgA₁ and dgA₂ (Figure 1a). Most of the heavy molecular weight rCD4-dgA conjugates (molecular mass > 100 kDa) were tightly bound to the Blue-Sepharose and

Table I. Comparison among SATA-, SMPT-, and SMCC-Derived rCD4-dgA Conjugates

parameter	SATA	SMPT	SMCC
% yield ^a	19.5	17.5	20.8
% purity ^b	90.0	90.0	80.8
molecular composition (dgA/rCD4 ratio)	1.0	1.25 \pm 0.15	ND ^m
affinity for gp120 ($\times 10^{-9}$ M) ^c	4.4 \pm 0.5	4.9 \pm 0.2	ND
% stability in vitro ^d	53.0 \pm 7.0	36.0 \pm 6.0	ND
% stability of vivo ^e	18.6	4.4	1.0
half-life, min			
α -phase	45.0 \pm 10.0 ^f	60.0 \pm 11.0 ^f	40.0 ^h
β -phase	177.0 \pm 24.0 ^f	209.0 \pm 21.0 ^f	225.0 ^h
LD ₅₀ , μ g/g (mouse)	100.0	116.0 \pm 25.9	ND
inhibition of protein synthesis (IC ₅₀ $\times 10^{-11}$ M) ^j	1.6	1.2	>1000
cytotoxicity on HIV-infected H9 cells (IC ₅₀ $\times 10^{-10}$ M)	1.7 \pm 1.0 ^k	2.0 \pm 1.0 ^l	>5000

^a The amount of rCD4 in the conjugates (60% of the total protein) is expressed as the percentage of the initial amount of rCD4 used for preparation. Mean of four experiments. ^b After Blue-Sepharose CL-4B and Sephacryl S-200HR. Calculated by densitometry of silver-stained SDS-PAGE (nonreduced). ^c The affinity of rCD4 for gp120 was $4.1 \pm 0.5 \times 10^{-9}$ M (mean of three experiments). ^d Cytotoxic activity after 16-h incubation at 37 °C. The IC₅₀ of freshly thawed conjugate used in the same assay was taken as 100%. Mean of three experiments. ^e Percentage of free dgA chain released at 4 h after injection of the radiolabeled conjugate. ^f The α -phase is the first 30 min and the β -phase is the next 8 h. For dgA, α = 20 min; β = 228 min. For rCD4, α = 10 min; β = 105 min. ^g Mean of three experiments. ^h Mean of two experiments. ⁱ The LD₅₀ of dgA was 30 μ g/g (mouse). ^j Mean of three experiments. ^k Mean of five experiments. ^l Mean of eight experiments. ^m ND = Not determined.

therefore could only be eluted by a mixture of 0.05 M NaOH and 0.5 M NaCl. Residual dgA remaining in the rCD4-dgA preparations after Blue-Sepharose chromatography could be removed either by gel filtration on Sephacryl S-200HR (Figure 1b) or by affinity chromatography on Sepharose-rgp120 (Figure 1c). As shown by the chromatographic profiles (Figure 1b), gel filtration resulted in more extensive purification since some high molecular weight material could be further separated from the conjugate, which has an apparent molecular mass of 80 kDa. A partial purification (80% purity) can be achieved by a single-step purification procedure using HPLC with Spherogel TSK 3000SW column (Figure 1d) or Ultropac TSK G3000SWG column. If the HPLC separation was applied after the Blue-Sepharose chromatography, the rCD4-dgA conjugates have better purity than by using Sephacryl S-200HR since the TSK 3000SW columns facilitate the separation of rCD4-dgA from the rCD4. The yields and purity of the rCD4-dgA conjugates are presented in Table I.

Molecular Mass and Composition of the rCD4-dgA Conjugates. Irrespective of the cross-linker used to construct the conjugates, the final purified preparations had a rCD4/dgA ratio of approximately 1.0 (Table I) and molecular mass of 80–82 kDa as determined by gel filtration on Sephacryl S-200HR and HPLC. By SDS-PAGE analysis under nonreducing conditions, however, two electrophoretic bands of 75 and 92 kDa were present (Figure 2). The presence of rCD4 and dgA in each of the two electrophoretic bands was confirmed by electrophoresing rCD4-SMPT-dgA labeled either in the rCD4 or the dgA moiety with ¹²⁵I and preparing autoradiographs of the gels. Both electrophoretic species (75 and 92 kDa) were labeled irrespective of which moiety was

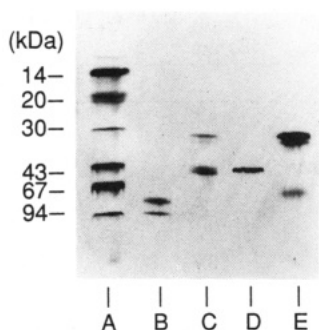


Figure 2. SDS-PAGE of rCD4-dgA and its protein components: (A) molecular weight standard, (B) rCD4-dgA prepared with SMPT (or SATA) from dgA or dgA₁, (C) rCD4-dgA reduced with 5% 2-mercaptoethanol, (D) rCD4 derivatized with SMPT (or SATA), (E) dgA.

labeled (data now shown). Both electrophoretic bands contained biologically active rCD4 since both bands specifically bound to Sepharose-rgp120 and eluted at pH 3.0 (Figure 1c). The simplest explanation for the existence of two forms of the rCD4-dgA is that one species contained one molecule of dgA/molecule of rCD4 (75 kDa) and the other contained two molecules of dgA/molecule of rCD4 (105 kDa). However, this explanation is considered unlikely on the basis of the lack of concordance between the measured (92 kDa) and calculated (105 kDa) molecular mass of the slower electrophoretic band, and, more importantly, because the ratio of dgA to rCD4 in both bands was 0.98 ± 0.02 . Another possible explanation for the existence of the protein doublet was that one species contained rCD4-dgA₁ (slow band) and the other contained rCD4-dgA₂ (fast band); however, this explanation was shown not to be the case by the finding that rCD4-SMPT-dgA prepared with purified dgA₁ also contained the same electrophoretic doublet (Figure 2, lane B). We, therefore, favor the explanation that there are two different sites on rCD4 which can be conjugated to dgA, leading to the formation of two types of conjugates, which have different molecular shapes and Stokes radii and run at different rates on SDS-polyacrylamide gels. Under reducing conditions, rCD4-dgA prepared with either SMPT or SATA, yielded two bands corresponding to rCD4 and dgA (Figure 2, lane C). As expected, the SMCC-derived conjugate was not reduced and maintained its unmodified electrophoretic doublet (data not shown).

Binding of rCD4 and Derivatives to rgp120. We have compared the binding of rCD4, SATA, or SMPT conjugates to rgp120 using an automated liquid-phase competitive binding assay.

The inhibition curves of rCD4 and the SATA and SMPT conjugates are illustrated in Figure 3. Although these curves are displaced slightly from one another, differences between curves are not statistically significant. These data also were used to calculate binding affinities (K_d) of rCD4 and the conjugates by Scatchard analysis using the software provided with the instrument (14). These results indicate that there is a small loss in affinity due to conjugation with SMPT, although this difference was within experimental error (Table I).

Cytotoxicity of rCD4-dgA Conjugates to HIV-Infected and Uninfected H9 Cells. In agreement with our previous report (1) using the SATA-linked conjugate, both rCD4-SMPT-dgA and rCD4-SATA-dgA were equally toxic to HIV-infected H9 cells in vitro (Figure 4 and Table I). In contrast, rCD4-SMCC-dgA was no more toxic than the control conjugate OVA-dgA (Table I) as predicted from previous reports that conjugates of anti-

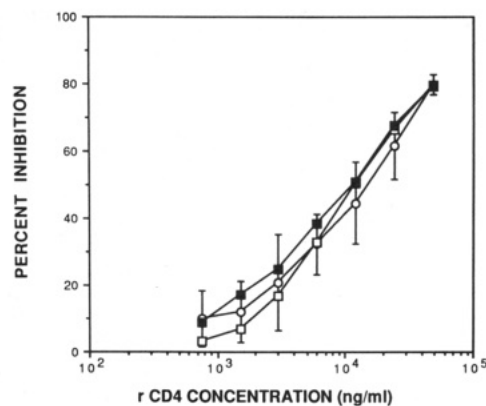


Figure 3. rCD4/rgp120 competitive binding assay. The percent inhibition of the fluorescent signal was calculated as $100\% \times (1 - [(sample - background)/(total signal - background)])$. The competitors were rCD4-SATA-dgA (■), rCD4-SMPT-dgA (□), and rCD4 (○). The binding of each conjugate was based on its rCD4 content. The bars indicate the SD for the rCD4 curve.

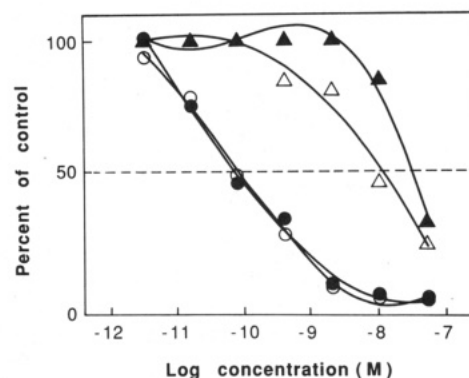


Figure 4. The toxicity of the three rCD4-dgA conjugates and OVA-dgA (control) to HIV-infected H9 cells: (○) rCD4-SMPT-dgA, (●) rCD4-SATA-dgA, (△) rCD4-SMCC-dgA, (▲) OVA-SMPT-dgA. One representative experiment of eight (SMPT) and five (SATA) trials is depicted.

bodies and ricin A chain are only toxic when a disulfide bond is present between the two components (15). None of the conjugates was toxic to uninfected H9 cells.

Binding of rCD4 to Daudi Cells. No significant binding of 125 I-labeled or biotinylated rCD4 to MHC class II⁺ human Daudi cells was observed ($K < 10^4 M^{-1}$). This indicates that neither rCD4 nor rCD4-dgA can bind to the cell-surface MHC class II antigens (16). These results are in agreement with our previous failure to kill Daudi cells with rCD4-SATA-dgA (1).

Stability of the rCD4-dgA Conjugates. The stability of the SATA- and SMPT-derived rCD4-dgA conjugates was tested by incubating the conjugates in fresh human plasma for 16 h at 37 °C prior to performing toxicity tests on HIV-infected human H9 cells. As shown in Table I, the cytotoxicity of both conjugates was reduced approximately 50% by incubation in human plasma at 37 °C for 16 h. The difference between the remaining cytotoxicity of SATA- and SMPT-derived conjugates is not statistically significant.

The dissociation of the rCD4-dgA conjugates in vivo was further studied by measuring the release of free dgA at 4 h after injection of the radiolabeled conjugate into normal mice. It should be noted that the mouse cells do not bind to rCD4-dgA and, hence, represent a good model for conjugate stability in a model where the conjugate is not specifically taken up by cells in vivo. Hence, following injection of rCD4-dgA, serum samples were collected and immunoprecipitated with rabbit anti-ricin A

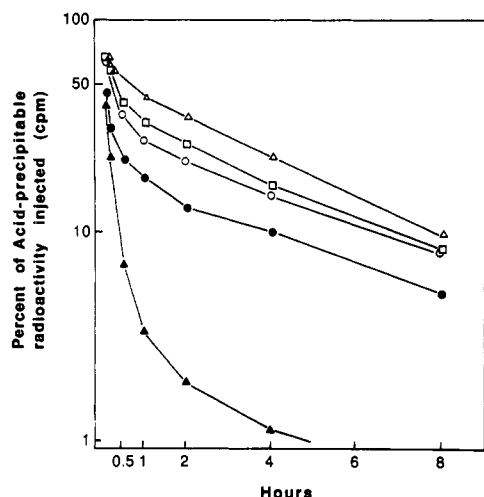


Figure 5. The elimination curves of rCD4-dgA conjugates and their protein components in mice (the results are from one experiment of three performed): (Δ) rCD4-SMPT-dgA, (□) rCD4-SATA-dgA, (○) rCD4-SMCC-dgA, (●) dgA, (▲) rCD4.

chain. Precipitates were analyzed by SDS-PAGE and autoradiography (see the Experimental Procedures). The results show that rCD4-SMPT-dgA broke down in vivo 4 times more slowly than rCD4-SATA-dgA (Table I) and that, as expected, rCD4-SMCC-dgA was the most stable (less than 1% released dgA).

When tested in a cytotoxicity assay on HIV-infected H9 cells, the plasma of mice collected 3 h (one half-life period) after injection of radiolabeled SATA- or SMPT-linked conjugates showed IC_{50} 's identical with those of freshly thawed conjugates (2×10^{-10} M).

Half-Life and Tissue Distribution of rCD4-dgA.

Plasma levels of radiolabeled rCD4-dgA injected into mice showed two major phases for elimination, namely, a rapid initial α -phase, which approached completion within 30 min, and a slower β -phase. Approximately 90% of all three conjugates were cleared in 8 h (Figure 5). There was no statistically significant differences among the $T_{1/2\beta}$ of the three conjugates. However, the SMPT-derived rCD4-dgA has a slightly longer half-life than the SATA-derived conjugate (Table I). This difference was not as great as would have been predicted from earlier studies using SMPT conjugates prepared with IgG and dgA (17). It should be noted that the half-life of rCD4 increases markedly in both phases (from 2- to 5-fold) after conjugation with dgA.

The tissue distribution of the labeled conjugates as determined by acid precipitability of extracts of various organs 1 h after injection of radiolabeled conjugates or their protein components is presented in Table II. From the results summarized in this table, the following conclusions could be drawn: (a) The rCD4-SMPT-dgA and rCD4-SMCC-dgA conjugates preferentially accumulated in the spleen at levels that were 3-fold higher than those of rCD4-SATA-dgA. (b) rCD4-SMCC-dgA concentrated in the liver, reaching levels approximately 3 times higher than those of the SATA-linked conjugates. (c) The rCD4-SATA-dgA conjugate showed lower accumulation in these organs (liver and spleen) than the other two conjugates but accumulated in the kidneys.

Toxicity of rCD4-dgA Conjugates. The capacity of various rCD4-dgA conjugates to inhibit protein synthesis was tested in a cell-free assay. The IC_{50} was 10^{-11} M for dgA, rCD4-SATA-dgA, and rCD4-SMPT-dgA and $>10^{-8}$ M for the SMCC-derived conjugate (Table I). The SMCC conjugate was not toxic in the assay because free

dgA could not be released by reduction. The LD_{50} of rCD4-SATA-dgA and rCD4-SMPT-dgA in mice were similar (Table I). The LD_{50} of the nontoxic conjugate rCD4-SMCC-dgA was not determined.

Tissue Reactivity in Mice. There were no gross lesions in the organs of any of the mice injected with 5%, 10%, or 20% of the LD_{50} dose. Microscopically, the liver, kidney, spleen, and brain from all animals were free of lesions.

Lesions were seen in the skeletal muscle of the proximal rear leg, diaphragm, and heart. The lesions varied in degree rather than in morphology (Table III). They consisted of myofibers which were fragmented, hyalinized, and often infiltrated and surrounded with macrophages and small numbers of neutrophils. The inflammatory cells infiltrate into the endomysium surrounding adjacent normal fibers. The inflammatory response was accompanied by proliferation of sarcoplasmic nuclei, and regenerating strap cells were documented admixed with the degenerating fibers in both the appendicular and diaphragmatic musculature. The lesions in the appendicular muscle were multifocal, frequently marked, and often concentrated within scattered muscle bundles, leaving other muscles unaffected. The lesions in appendicular skeletal muscle were consistently more prominent than those in the diaphragm or heart.

Myocardial lesions were widely scattered and were found in only four animals, two from each group treated with rCD4-SATA-dgA and with dgA. Myocardial lesions were minimal, usually focal, and restricted to one or two myofibers. The degenerated myofibers were hyalinized, stippled with basophilic granules, infiltrated with macrophages and neutrophils, and, in some sections, obliterated by infiltrates of macrophages. In none of the animals was there any evidence of heart failure.

DISCUSSION

The purpose of the present study was to generate and evaluate conjugates between rCD4 and dgA as potential therapeutic reagents for patients with HIV infections/AIDS. To this end, conjugates utilizing three different linkers were constructed and compared for their yield, purity, biochemical structure, in vitro activity, and in vivo behavior. Two of the conjugates were constructed with a disulfide bond between the rCD4 and dgA with the SATA or SMPT cross-linkers; the third was constructed with a thioether bond, by utilizing SMCC. The three cross-linkers derivatize the ϵ -amino groups on the rCD4 and utilize the natural SH or the cysteine of the dgA. For all three conjugates, the active group(s) were introduced by *N*-hydroxysuccinimide to establish an amide bond between the primary amino group(s) of rCD4 and the active group.

Biochemical analysis of the conjugates was performed and the results indicate that they were similar in size and content of rCD4 and dgA. Hence: (1) The three conjugates contained one molecule of rCD4 covalently linked to one molecule of dgA. The conjugates had apparent molecular masses of 80–82 kDa as determined by gel filtration and HPLC, but when analyzed by SDS-PAGE, they consisted of two forms with masses of 75 and 92 kDa. The 75- and 92-kDa species each contained a single rCD4 and a single dgA. The possibility that the doublet represents two rCD4-dgA conjugates with different amounts or types of dgA (dgA_1 and dgA_2) was excluded by appropriate experiments. This heteroclitic structure might be generated if the derivatized rCD4 contains two different populations of molecules. However, no heterogeneity of the rCD4 preparations was demonstrated by any technique, including isoelectric focusing (unpub-

Table II. Retention of Acid-Precipitable Radioactivity in Various Organs of Mice Injected with rCD4-dgA Conjugates and Their Components, rCD4 and dgA^a

organ	percent of injected acid-precipitable radioactivity retained per gram of organ (wet weight) 1 h after injection				
	rCD4-SATA-dgA	rCD4-SMPT-dgA	rCD4-SMCC-dgA	rCD4	dgA
kidneys	8.9	6.4	7.9	10.5	8.4
liver	3.7	5.4	10.8	1.6	1.8
spleen	2.8	8.9	7.8	1.1	1.7

^a Mean of two separate experiments.**Table III. Mean Scores for Myopathy in Mice Injected with rCD4-SMPT-dgA, rCD4-SATA-dgA, and dgA**

inoculum (% of LD ₅₀)	heart	diaphragm	appendicular skeletal muscle
rCD4-SMPT-dgA ^a			
5	0.00 ^a	0.00	0.00
10	0.00	0.25	1.25
20	0.00	0.00	1.75
rCD4-SATA-dgA ^a			
5	0.25	0.75	2.25
10	0.33 ^b	0.25	2.25
20	0.25	0.25	1.25
dgA ^b			
20	0.33	0.33	2.66
control	0.00	0.00	0.00

^a Mean lesion score for four animals. ^b Mean lesion score for three animals.

lished observations), suggesting that there are no significant differences in the distribution of the electric charges on the rCD4 molecules. (2) As determined by reduction and analysis of the two disulfide linked conjugates in a cell-free rabbit reticulocyte lysate assay, the dgA chains in the conjugates prepared with SATA and SMPT were as active as the dgA used to prepare them. (3) With different methods of purification, the final yield of each conjugate was approximately 20% and all three conjugates retained their gp120-binding activity. The purification of rCD4-dgA conjugates involved chromatography on Blue-Sepharose, a procedure previously used for the purification of ricin A chain containing immunotoxins (18). In our experiments, we have modified this basic technique using longer columns and applying a salt gradient with the aim of exploiting the ion-exchange property of Blue-Sepharose at pH 7.5. The combined properties of ion exchange and dgA-binding allowed the separation of rCD4-dgA conjugates in reasonable yield and with an acceptable degree of purity. A subsequent gel filtration on Sephacryl S-200HR or affinity chromatography on Sepharose-gp120, yielded rCD4-dgA preparations that were approximately 90% pure with traces of free dgA and rCD4 and some heavy molecular mass material. The greatest purity of the rCD4-SMPT-dgA conjugate (>95%) was achieved by combining Blue-Sepharose chromatography with HPLC on TSK G3000SWG.

Since these three rCD4-dgA conjugates were prepared for the purpose of killing HIV-infected cells, we next compared their cytotoxic activity for HIV-infected cells in vitro. The results indicate the following: (1) rCD4-dgA prepared with either SMPT or SATA killed HIV-infected H9 cells with identical potency (IC₅₀ = 1.7–2.0 × 10⁻¹⁰ M). rCD4-SMCC-dgA was no more toxic than an irrelevant conjugate (OVA-dgA) (>5 × 10⁻⁸ M) despite the fact that it displayed gp120-binding activity (data not shown). The two active conjugates were 1000-fold more toxic to HIV-infected cells than to uninfected cells and the control conjugate, OVA-dgA was not toxic to either infected or uninfected cells, confirming results of

our previous report (1). (2) As determined by binding analyses, the rCD4 molecule and the conjugates prepared with it did not bind to class II⁺ Daudi cells. Since class II molecules are the putative natural ligand for CD4, this demonstrates that while cell-bound CD4 can bind to cell-bound class II antigens (16), *soluble* rCD4 does not bind to cell-bound class II molecules. This finding is consistent with our previous report that rCD4-SATA-dgA does not kill Daudi cells even though an anti-class II-dgA conjugate was toxic in the same assay (1). (3) Stability tests of the rCD4-dgA conjugates in vitro (in human plasma) indicated that both the SATA- and SMPT-derived rCD4-dgA conjugates have similar chemical stability and that both lose approximately 50% of their cytotoxic potency after 16 h at 37 °C. However, in vivo (in mouse blood), the SMPT-linked conjugate was more stable than the SATA-linked conjugate, releasing 4 times less free dgA. This result is in agreement with a report by Thorpe et al. (17), who showed that an immunotoxin prepared with SMPT broke down in vivo 6 times more slowly than the corresponding immunotoxin prepared with 2-iminothiolane, a cross-linker which produces an unhindered disulfide bond as does SATA. SMPT generates a disulfide bond which is sterically hindered by the adjacent benzene ring and methyl groups, which protect the disulfide bond from the attack of thiolate anions such as glutathione, which can be present in tissues and blood.

Having determined that the SATA- and SMPT-linked conjugates were active in vitro, while the SMCC-linked conjugate was not, the in vivo behavior of the three conjugates was determined in mice. In these experiments, the SMCC-linked conjugate served as a control, i.e., a conjugate lacking a disulfide bond, which might be susceptible to thiol-mediated reduction. The results were as follows: (1) As determined by in vivo clearance experiments in mice, rCD4 was readily cleared with a $T_{1/2\alpha}$ of 10 min. Only 7% remained in the serum at 30 min. dgA also had a short $T_{1/2\alpha}$ of 20 min. At 30 min, 26% remained in the serum. In contrast, the rCD4-dgA conjugates had significantly longer $T_{1/2\alpha}$ s (40–60 min). At 30 minutes, more than 40% remained in the serum. Thus, the coupling of rCD4 to dgA gives rCD4 a significantly longer serum half-life. For all three conjugates, the percentage of protein remaining in circulation after 8 h was slightly under 10%. At this time, virtually all the rCD4 was cleared. The difference between the 8-h β -phase half-life of the SATA linked (177 min) and SMPT linked (209 min) conjugates is not statistically significant. (2) As determined by injecting the SATA- and SMPT-linked conjugates into mice and utilizing their sera 3 h later to kill HIV-infected H9 cells in vitro, there was no loss in activity of the remaining conjugate. This result suggests that both rCD4-dgA conjugates should maintain their cytotoxic activity for a period of time long enough to allow their reaction with circulating infected cells. (3) The LD₅₀s of the two active conjugates, rCD4-SATA-dgA and rCD4-SMPT-dgA, were 100 and 116 µg/g (mouse), respectively. This shows that, in comparison with the LD₅₀ of

IgG-dgA conjugates [15–20 $\mu\text{g/g}$ (mouse)] (17), the rCD4-dgA conjugates are 6-fold less toxic on a protein basis and 10-fold less toxic on a dgA basis. (4) Despite the fact that rCD4-dgA does not react with mouse tissues, both rCD4-SMPT-dgA and rCD4-SMCC-dgA localized in the spleen and liver while rCD4-SATA-dgA localized in the kidneys. It is unclear why the chemical linkage between rCD4 and dgA plays a role in the tissue localization of the conjugates, but irrespective of the explanation, these observations suggest that tissue damage could result with all three conjugates. Despite the fact that rCD4-SMPT-dgA localized in the spleen and liver and rCD4-SATA-dgA localized in the kidney, these organs showed no morphologic evidence of damage. Only skeletal muscle was affected by dgA and its derivatives. Myopathy was more prominent in the appendicular skeleton and diaphragm; the myocardium was least affected. The reason for this difference is unknown, but could represent intrinsic variations in the metabolism of the skeletal muscle from the appendicular skeleton, diaphragm, and heart.

Evidence of regeneration in sections of muscle from diaphragm and from the appendicular skeleton indicates that the myopathy is reversible. Myocardium does not regenerate after such damage, but the lesions in the myocardium were minimal, widely scattered and did not result in cardiac failure in any of the mice.

The use of SATA as opposed to SMPT to prepare the conjugates exacerbates the myopathy documented in the appendicular skeleton and diaphragm. In addition, the SATA-linked conjugate produced lesions in the heart. No cardiac lesions were detected in animals injected with rCD4-SMPT-dgA.

The results suggest that the rCD4-dgA conjugate prepared with SMPT is not toxic to cardiac myofibers and is less toxic to skeletal myofibers than rCD4-dgA prepared with SATA. No animal presented signs of cardiac failure either clinically or at necropsy.

Taken together, the results suggest that rCD4-dgA prepared with SMPT would be the conjugate of choice for further development as a therapeutic reagent for treating patients with AIDS.

ACKNOWLEDGMENT

We thank R. Nisi, P. May, D. Jones, B. K. Morrison, and Y. Chinn for technical assistance and G. A. Cheek, N. Stephens, M. Perkins-Mendro, and C. Baselski for secretarial assistance. We are grateful to Dr. S. Chamow and L. Riddle for assistance with the purification of rCD4 and Dr. P. E. Thorpe for his gift of the SMPT cross-linker and his invaluable suggestions for its use. We also thank Dr. Thorpe for his helpful comments concerning the manuscript. This work is supported by NIH Grants CA-28149, CA-41081, RR-00890, Texas Technologies Grant 18512 and a Grant from the Welch Foundation, Grant I-947. Mark A. Till is supported by Cancer Immunology Training Grant CA-09082.

LITERATURE CITED

- (1) Till, M., Ghetie, V., Gregory, T., Patzer, E., Porter, J. P., Uhr, J. W., Capon, D. J., and Vitetta, E. S. (1988) HIV-infected cells are killed by rCD4-ricin A chain. *Science* **242**, 1166–1168.
- (2) Chaudhary, V. K., Mizukami, T., Fuerst, T. R., FitzGerlad, D. J., Moss, B., Pastan, I., and Berger, E. A. (1988) Selective killing of HIV-infected cells by recombinant human CD4-Pseudomonas exotoxin hybrid protein. *Nature* **335**, 369–372.
- (3) Smith, D. H., Byrn, R. A., Marsters, S. A., Gregory, T., Groopman, J. E., and Capon, D. J. (1987) Blocking of HIV-1 infectivity by a soluble, secreted form of the CD4 antigen. *Science* **238**, 1704–1707.
- (4) Fraker, P. J., and Speck, J. C., Jr. (1978) Protein and cell membrane iodinations with a sparingly soluble chloramide, 1,3,4,6-tetrachloro-3a,6a-diphenylglycoluril. *Biochem. Biophys. Res. Commun.* **80**, 849–857.
- (5) Wojchowski, D. M., and Sytkowski, A. J. (1986) Hybridoma production by simplified avidin-mediated electrofusion. *J. Immunol. Methods* **90**, 173–177.
- (6) Fulton, R. J., Blakey, D. C., Knowles, P. P., Uhr, J. W., Thorpe, P. E., and Vitetta, E. S. (1986) Purification of ricin A1, A2, and B chains and characterization of their toxicity. *J. Biol. Chem.* **261**, 5314–5319.
- (7) Fulton, R. J., Tucker, T. F., Vitetta, E. S., and Uhr, J. W. (1988) Pharmacokinetics of tumor-reactive immunotoxins in tumor-bearing mice: effect of antibody valency and deglycosylation of the ricin A chain on clearance and tumor localization. *Can. Res.* **48**, 2618–2625.
- (8) Duncan, R. J., Weston, P. D., and Wrigglesworth, R. (1983) A new reagent which may be used to introduce sulfhydryl groups into proteins, and its use in the preparation of conjugates for immunoassay. *Anal. Biochem.* **132**, 68–73.
- (9) Thorpe, P. E., Wallace, P. M., Knowles, P. P., Relf, M. G., Brown, A. N. F., Watson, G. J., Knyba, R. E., Wawrzynczak, E. J., and Blakey, D. C. (1987) New coupling agents for the synthesis of immunotoxins containing a hindered disulfide bond with improved stability in vivo. *Can. Res.* **47**, 5924–5931.
- (10) Ishikawa, E., Imagawa, M., Hashida, S., Yoshitake, S., Hamaguchi, Y., and Ueno, T. (1983) Enzyme-labeling of antibodies and their fragments for enzyme immunoassay and immunohistochemical staining. *J. Immunol.* **4**, 209–327.
- (11) Ellman, G. L. (1959) Tissue sulfhydryl groups. *Arch. Biochem. Biophys.* **82**, 70–77.
- (12) Beeken, W. L., Volwiler, N., Goldsworthy, P. D., Garby, L. E., Reynolds, W. E., Stogsdill, R., and Stemler, R. S. (1962) I^{131} -Albumin catabolism and distribution in normal males. *J. Clin. Invest.* **40**, 1312–1332.
- (13) Tolleshaug, H., Goldstein, J. L., Schneider, W., and Brown, M. S. (1982) Post-translational processing of the LDL receptor and its genetic disruption in familial hypercholesterolemia. *Cell* **30**, 715–724.
- (14) Phillips, D. J., Wells, T. W., and Reimer, C. B. (1987) Estimation of association constants of 42 monoclonal antibodies to human IgG epitopes using a fluorescent sequential-saturation assay. *Immunol. Lett.* **17**, 159–160.
- (15) Blakey, D. C., Wawrzynczak, E. J., Wallace, P. M., and Thorpe, P. E. (1988) Antibody toxin conjugates: A perspective. In *Progress in Allergy (Monoclonal Antibody Therapy)* (H. Waldmann, Ed.) pp 50–90, Karger, Basel, Switzerland.
- (16) Doyle, C., and Strominger, J. L. (1987) Interaction between CD4 and class II MHC molecules mediates cell adhesion. *Nature* **330**, 256–259.
- (17) Thorpe, P. E., Wallace, P. M., Knowles, P. P., Relf, M. G., Brown, A. N. F., Watson, G. J., Blakey, D. C., and Newell, D. R. (1988) Improved anti-tumor effects of immunotoxins prepared with deglycosylated ricin A chain and hindered disulfide linkages. *Can. Res.* **48**, 6396–6403.
- (18) Knowles, P. P., and Thorpe, P. E. (1987) Purification of immunotoxins containing ricin A-chain and abrin A-chain using Blue Sepharose CL-6B. *Anal. Biochem.* **160**, 440–443.

Registry No. SATA, 76931-93-6; SMCC, 64987-85-5; SMPT, 123266-19-3.

Potential of Albumin Labeled with Nitroxides as a Contrast Agent for Magnetic Resonance Imaging and Spectroscopy

Hsiao-Chang Chan,^{†,‡} Keqin Sun,[§] Richard L. Magin,[†] and Harold M. Swartz^{*,†}

Bioacoustic Research Laboratory, Department of Electrical and Computer Engineering, Department of Biochemistry, and Departments of Medicine and Biophysics, University of Illinois, Champaign-Urbana, Urbana, Illinois 61801. Received June 17, 1989

The biological and physical properties of albumin and nitroxides make them attractive candidates as special purpose MRI contrast agents which could be used to study the intravascular compartment or specific targets in tissues. In this study, albumin-nitroxide complexes were prepared by reduction and alkylation of the disulfide bonds of the protein and characterized by electron spin resonance and ultraviolet absorption spectroscopy. An average of six nitroxides were bound covalently to each molecule of human serum albumin. The water proton relaxivity of the protein-bound nitroxide (at 20 MHz and 37 °C) was 4-fold greater than that of the free nitroxide. The digestion of the nitroxide-albumin complexes by cells or by trypsin decreased the relaxivity of the nitroxide-protein complex. The rate of reduction of albumin-bound nitroxide by cells was much slower than that of the free nitroxide but still was oxygen-sensitive (2-3-fold increase in the rate of reduction in the absence of oxygen).

The attachment of paramagnetic nitroxide free radicals to biomolecules has been an important biophysical tool for structural and functional studies in biological systems for more than 2 decades (1). The effect of the attachment of nitroxides to macromolecules on water-relaxation properties has been noted (2-5), and recently, nitroxides and their protein complexes have been suggested as contrast agents for magnetic resonance imaging and spectroscopy (MRI and MRS) (3-7).¹ This approach parallels the use of conjugates of albumin and paramagnetic metal ions as MRI contrast agents, which also has been investigated recently (11, 12). Although there are concerns regarding the antigenicity, toxicity, and slow excretion clearance of albumin, albumin with a paramagnetic species attached has several useful features that include provision of more optimum correlation times for relaxivity, a biodistribution primarily confined to the vascular space after intravenous administration (13), the ability to bind a wide variety of substances including monoclonal antibodies or specific receptors (14), and a rate of biodegradation of the complex which could be used as a potential additional parameter to measure metabolic function.

Although the relaxivity induced by nitroxides is usually less than that of many paramagnetic metals or metal chelates (8-10), nitroxides have some special features which make them attractive potential contrast agents. Nitroxides can be reduced by cells to their nonparamagnetic state at rates that reflect the metabolic condition of the cells (15); in particular, hypoxia increases the rate of reduc-

tion of nitroxides, and the rate of oxidation back to the nitroxides can be proportional to the concentration of oxygen (16). This metabolic responsiveness may enable nitroxides to provide contrast in MRI or MRS for various pathophysiological states characterized by hypoxia, e.g., cancer, ischemia, and inflammation (17).

Nitroxides can be attached to albumin covalently with a maleimide nitroxide which interacts principally with the single reactive sulfhydryl group of a native albumin molecule (1, 18-20). This method is easy, but the amount of nitroxide bound to each molecule of albumin is small, with a typical ratio of nitroxide to albumin of about 0.6 to 1 (2, 20). Chemical modifications of albumin with nitroxides have been reported which result in a higher ratio of nitroxides to albumin (3, 21); however, these preparations involve some special reagents and a certain degree of difficulty. In this study, we have used a relatively easy preparation which involves simple reduction of the disulfide bonds in albumin and the alkylation of the disulfide bonds with maleimide nitroxides; this allows the binding of several nitroxides to albumin. We report here on the relaxivity of the nitroxide-albumin complex and its interaction with two cell lines.

EXPERIMENTAL PROCEDURES

Materials. Human serum albumin (HSA, essentially fatty acid free), urea, chloroquine, and the nitroxide 3-maleimido-2,2,5,5-tetramethylpyrrolidine-*N*-oxyl (Mal-3) were purchased from Sigma Chemical Co. (St. Louis, MO). Cell culture media, serum, and trypsin were purchased from Gibco Laboratories (Grand Island, NY).

Preparation of Nitroxide-Labeled Albumin. The procedure involved reduction and alkylation of the disulfide bonds in albumin as described by Hunter and McDuffie (22) with some modification. The denaturing agent urea was added to an albumin solution (17.5 mg/mL) to a final concentration of 8 M, and the pH was adjusted to 8.2 with sodium carbonate. A solution of the reducing agent sodium thioglycolate (pH 8.2) then was added to a final concentration of 0.3 M, and the flask was immediately evacuated and filled with nitrogen. The mixture was left in the dark for 20 h at room temperature. The mixture then was put in dialysis tubing and

* Author to whom correspondence should be addressed: Dr. Harold M. Swartz, ESR Center at the University of Illinois, 190 Medical Sciences Building, 506 S. Mathews, Urbana, IL 61801.

[†] College of Medicine.

[‡] Bioacoustic Research Laboratory.

[§] Department of Biochemistry.

¹ Abbreviations: MRI and MRS, magnetic resonance imaging and spectroscopy; ESR, electron spin resonance; HSA, human serum albumin; Mal-3, 3-maleimido-2,2,5,5-tetramethylpyrrolidine-*N*-oxyl; TB cells, mixed cultures of thymus and bone marrow; CHO, Chinese hamster ovary.

dialyzed against 1 L of phosphate-buffered saline (PBS, pH 8.4) for 4 h at 4 °C with two changes of the buffer to eliminate the reducing agent. After dialysis the albumin solution was mixed with 10 mg of Mal-3, and the mixture was stirred for 24 h at 4 °C in a sealed vial flushed with nitrogen. The mixture was then dialyzed against PBS (pH 7.4) to remove unbound nitroxide.

Magnetic Resonance Measurements. All electron spin resonance (ESR) measurements were obtained at 9 GHz with a Varian E 109-E spectrometer equipped with a Varian gas flow temperature controller. The concentration of Mal-3 was determined by the double integration of ESR spectra with a Zenith Z-100 computer. The rate of reduction of nitroxide was calculated from the recorded initial linear decay of ESR signal intensity as a function of time.

The spin-lattice relaxation time (T_1) of the water protons were measured at 20 MHz on a Bruker PC/20 Minispec operating at 37 °C, using an inversion recovery pulse sequence.

UV Spectrophotometry. The concentration of HSA was measured on a 8415A diode-array spectrophotometer with the value of 6.0 for the specific absorption of a 1% solution through a path length of 1 cm (peak at 280 nm). Spectra were taken at wavelengths from 240 to 300 nm.

Cell Cultures. TB cells were established from mixed cultures of thymus and bone marrow from CFW/D mice (23). They were grown in McCoy's medium with 10% serum in a 150-cm³ flask. Chinese hamster ovary (CHO) cells were grown in suspension in a spinner flask (10⁶ cells/mL) with the same medium. To prepare samples for ESR measurements, 10⁷ cells were transferred to 100-mm petri dishes to grow as monolayers for 8 h, an aliquot of 5 mL of serum-free medium was substituted for the old medium at the end of the 8 h, and 0.25 mL of the nitroxide-albumin complex (1 mM Mal-3) was then added, and the samples were incubated for various periods of time at 37 °C. The treatment of cells with chloroquine was carried out by adding the agent (0.5 mM final concentration) 30 min prior to the addition of the nitroxide-albumin complex. After incubation, the cells were washed three times with PBS (pH 7.4). The cells were then exposed to 1 mL of 0.25% trypsin for 1 min. A 5-mL volume of medium with 10% serum was added to the trypsinized cells and the cell suspension was centrifuged at 500g for 5 min. The pelleted cells were transferred into gas-permeable Teflon tubing for ESR measurements. For measurements of relaxation times, 1.5×10^8 CHO cells per sample were taken from the spinner flask, and the pelleted cells were packed in a 7-mm NMR tube. A 0.2-mL sample of the nitroxide-albumin complex was added to make up the total volume of 0.6 mL.

Protein Digestion by Trypsin. The NMR sample was prepared by adding 0.2 mL of 0.25% trypsin to 0.4 mL of the nitroxide-albumin complex (0.17 mM of albumin) in a 7-mm NMR tube. A 70 μ L aliquot of the mixture was drawn into a glass capillary tube for study by ESR. The process of digestion at 37 °C was monitored by observing changes in the line widths of the spectra as a function of time.

RESULTS

ESR Characterization of the Complex. After exhaustive dialysis, the nitroxide-albumin complex had a broader and more complex ESR spectrum than the isotropic narrow spectrum of the free nitroxide (Figure 1), indicating that most of the nitroxides were motionally restricted due to binding to albumin. The concentration of bound

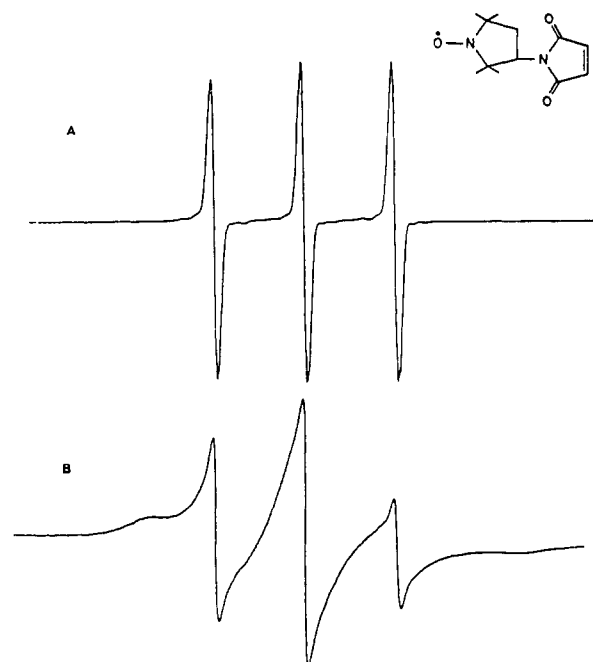


Figure 1. Binding of Mal-3 to albumin. The ESR spectrum of maleimide nitroxide (for structure see insert) in aqueous solution (A) and the ESR spectrum of Mal-3 covalently bound to albumin (B) are shown.

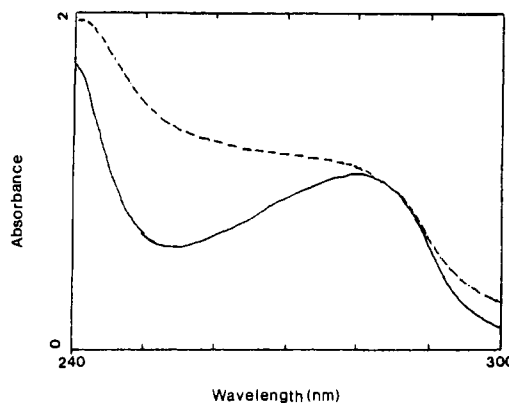


Figure 2. UV absorption of native albumin (—) and the albumin-nitroxide complex (---). The UV spectra indicate that there were structural changes in the albumin after reduction and alkylation of the disulfide bonds. The protein concentration for the two samples was identical.

nitroxide was 1.1 mM as measured by double integration of the ESR spectrum. In a control experiment, albumin was mixed with Mal-3 without reduction; these samples had ESR spectra indicating that a much lower proportion of Mal-3 was bound to albumin.

UV Characterization of the Complex. The protein concentration of the complex was 0.17 mM as determined by UV absorbance at 280 nm. The combined results of UV and ESR indicated that an average of six molecules of nitroxide were bound to each molecule of albumin. The altered UV spectrum of the complex (Figure 2) probably results from the unfolding of the polypeptide chains and the addition of nitroxides to albumin.

T_1 Measurements. The spin-lattice times (T_1) of Mal-3 and albumin-bound Mal-3 were measured and compared. The relaxivity ($\text{mM}^{-1} \text{s}^{-1}$) of the albumin-bound Mal-3, calculated by subtracting out the diamagnetic contribution of the protein and dividing by the concentration of the bound Mal-3 (over a range of concentrations, 0.1–5 mM), is $1.38 \text{ mM}^{-1} \text{s}^{-1}$. This value is about 4 times higher than the relaxivity of Mal-3 alone, $0.38 \text{ mM}^{-1} \text{s}^{-1}$.

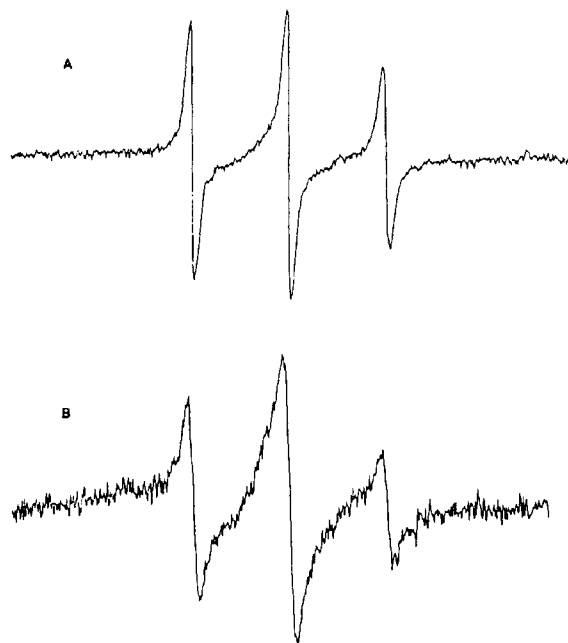


Figure 3. Interaction of the albumin-nitroxide complex with cells. The ESR spectrum of the albumin-nitroxide complex after incubation for more than 4 h with CHO cells (A) shows more isotropic motion than the ESR spectrum of the same nitroxide after incorporation into cells to which chloroquine has been introduced (B).

Interaction with Cells. The interaction of the nitroxide-albumin complex with cells was followed by both ESR spectroscopy and NMR relaxation measurements. The line width of the ESR spectrum of the nitroxide-albumin complex after incubation (2 h or longer) with either TB or CHO cell became narrower (Figure 3A), indicating greater motion of the nitroxide. This did not occur if the cells were treated with chloroquine (Figure 3B), an agent that inhibits proteolysis by raising the pH of lysosomes (24, 30, 31), indicating that the change in the spectrum of the nitroxide-albumin observed in untreated cells (Figure 3A) was due to digestion of the protein by the cells. The relaxation measurements were consistent with the interpretation, showing a 40% decrease in the relaxivity of the nitroxide-albumin complex after a 3-h incubation with CHO cells.

Digestion by Trypsin. In order to confirm that proteolysis could account for the changes described above, we studied the effect of the proteolytic enzyme trypsin (25). After the digestion of the nitroxide-albumin complex by trypsin, the ESR spectrum (Figure 4C) was similar to that of free Mal-3 (Figure 1A). The relaxivity of the digested complex was $0.58 \text{ mM}^{-1} \text{ s}^{-1}$, compared to $1.38 \text{ mM}^{-1} \text{ s}^{-1}$ for the undigested complex.

Reduction of Mal-3 by TB and CHO Cells. The reduction of albumin-bound Mal-3 by TB and CHO cells was studied in parallel to the study of the reduction of the free nitroxide (Table I). In both types of cells, free Mal-3 was reduced more rapidly than the albumin-bound nitroxide, and the rate of reduction of both free and bound Mal-3 increased under hypoxic conditions.

DISCUSSION

The relaxivity observed for the nitroxide-albumin complex is a factor of 4 greater than that for free Mal-3. Enhancement of relaxation due to binding of the paramagnetic species to albumin has been observed previously and the physical basis for such enhancement has been described (2, 4, 10, 26). The effect is attributed to

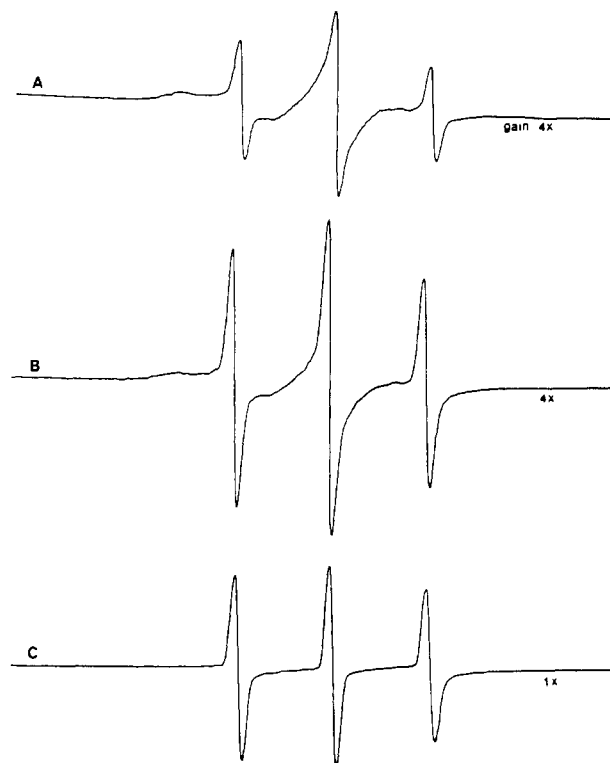


Figure 4. Effect of proteolysis (by trypsin) on ESR spectra of the albumin-nitroxide complex. The process is indicated by changes (decreases) in line width as a function of time of incubation: 1 min (A), 5 min (B), and 25 min (C). The receiver gains for each of the three spectra are indicated in the figure.

Table I. Reduction of Free and Albumin-Bound Mal-3 by TB and CHO Cells^a

	free		HSA-Mal-3	
	air	N ₂	air	N ₂
TB	23.0 ± 2.3	35.3 ± 0.4	0.5 ± 0.4	1.5 ± 0.5
CHO	6.0 ± 2.0	11.7 ± 3.4	0.4 ± 0.2	0.7 ± 0.1

^a Rates are initial rates in units of 10^6 molecules/min per cell. The results are given as mean ± SD from four independent measurements

the changes in correlation times, especially the rotational correlation time of the nitroxide. Binding free nitroxides to macromolecules such as albumin results in restricted motion or slower tumbling rate of the nitroxides. It has been demonstrated that the inner-sphere component, which is negligible for the rapidly tumbling, uncomplexed nitroxides, dominates the relaxivity of macromolecule-bound nitroxides (4). In this case, the overall correlation time (t_c) of the albumin-bound Mal-3 more closely approximates the time scale of the resonant (Larmor) frequency of water to give rise to more efficient proton relaxation. The relaxivity of $1.38 \text{ mM}^{-1} \text{ s}^{-1}$ for the nitroxide-albumin complex from the current study is fairly consistent with reported values (2, 4).

Water-soluble nitroxides previously have been shown to increase contrast in MRI and have been used to identify breaks in the blood-brain barrier (27) and to delineate renal structures (7) and tumors (28) in experimental animals. The albumin-nitroxide complex used in the current study has an enhanced relaxivity compared to free nitroxides and thus should be able to provide equivalent MRI contrast with a lower injected dose. Toxicity studies of nitroxides indicate relatively high LD₅₀ doses in rats (15–25 mmol/kg) and an apparent lack of induc-

tion of mutations in CHO cells (29). However, the toxicity of this albumin-nitroxide complex has not yet been evaluated.

The changes in ESR spectra and relaxation measurements over time in cell suspensions incubated with the albumin-nitroxide complex indicate that the complex can be digested, resulting in decreased relaxivity. This phenomenon might be exploited to extend MRS techniques to follow metabolic processes associated with cellular uptake and digestion of proteins. Similarly, the observation that the relaxivity of the albumin-nitroxide complex changes during the course of protein digestion raises the possibility of using such complexes as metabolically responsive, contrast-enhancing agents for detecting various pathological conditions, such as disorders of renal function, under which the rate of protein turn over is affected (32, 33).

Rapid metabolic conversion in vivo of nitroxides to non-paramagnetic states has been considered a disadvantage of nitroxides as MRI contrast agents. However, the finding that the rate of reduction of nitroxides responds to the metabolic state of the cells has led to the notion of using nitroxides as metabolically responsive MRI contrast agents (15, 16). The results from this study also indicate that the oxygen-dependent cellular reduction of the albumin-nitroxide complex could be exploited to provide contrast for pathophysiological hypoxic areas such as ischemic and neoplastic regions.

Biodistribution studies in rats have shown that albumin-metal chelate complexes remain largely in the intravascular space after iv injection (12, 13). Similar studies of the albumin-nitroxide complex must be performed. The potential antigenicity of this complex (an altered form of albumin) could be a drawback to in vivo use of the conjugate, and therefore the antigenicity as well as the toxicity and excretion rate of the complex should be carefully assessed. If these studies show that the albumin-nitroxide complex is safe and remains in the blood pool, it could be used in MR assessments of blood volume and tissue perfusion and diagnosis of ischemic and neoplastic disorders. In addition, the ability of albumin to bind antibodies and specific receptors (14) could be exploited to make such complexes target-specific contrast agents. Aggregation of albumin molecules into entities such as microspheres drastically changes their biodistribution; they are cleared rapidly from blood after iv injection and concentrated in the reticuloendothelial system (liver, spleen, and bone marrow) (34), and thus they also could be used to study the reticuloendothelial system.

ACKNOWLEDGMENT

We thank Maoxin Wu for preparing the cell cultures. This work was supported by NIH Grants CA 42388 and CA 40665. Hsiao Chang Chan received support from NIH Training Grant CA 09067. The ESR data were obtained at the University of Illinois ESR Research Center, supported by NIH Grant RR 01811.

LITERATURE CITED

- Stone, T. J., Buckman, T., Nordio, P. L., and McConnell, H. M. (1965) Spin-labeled biomolecules. *Proc. Natl. Acad. Sci. U.S.A.* **54**, 1010-1017.
- Polnaszek, C. F., and Bryant, R. G. (1984) Nitroxide radical induced solvent proton relaxation: measurement of localized translational diffusion. *J. Chem. Phys.* **81**, 4038-4045.
- Sosnovsky, G., Rao, N. U. M., Lukszo, J., and Brasch, R. C. (1986) Spin labeled bovine serum albumin, spin labeled bovine serum albumin chelating agents and their gadolinium complexes. *Z. Naturforsch.* **41b**, 1170-1177.
- Bennett, H. F., Brown, R. D., III, Koenig, S. H., and Swartz, H. M. (1987) Effects of nitroxides on the magnetic field and temperature dependence of $1/T_1$ of solvent water protons. *Magn. Reson. Med.* **4**, 93-111.
- Slane, J. M. K., Lai, C. S., and Hyde, J. S. (1986) A proton relaxation enhancement investigation of the binding of fatty acid spin labels to human serum albumin. *Magn. Reson. Med.* **3**, 699-706.
- Brasch, R. C. (1983) Work in progress: methods of contrast enhancement for NMR imaging and potential applications. *Radiology* **147**, 781-788.
- Brasch, R. C., London, D. A., Wesbey, G. E., Tozer, T., Nitecki, D., Williams, R., Doemeny, J., Tuck, L., and Lallemand, D. (1983) Work in progress: nuclear magnetic resonance study of a paramagnetic nitroxide contrast agent for enhancement of renal structures in experimental animals. *Radiology* **147**, 773-779.
- Wolf, G. L., Burnett, K. R., Goldstein, E. J., and Joseph, P. M. (1985) Contrast Agents for Magnetic Resonance Imaging. In *Magn. Resonance Annual* pp 231-266, Raven Press, New York.
- Kang, Y. S., Gore, J. C., and Armitage, I. M. (1984) Studies of factors affecting the design of NMR contrast agents: manganese in blood as a model system. *Magn. Reson. Med.* **1**, 396-409.
- Koenig, S. H., and Brown, R. D., III (1984) Relaxation of solvent protons by paramagnetic ions and its dependence on magnetic field and chemical environment: implication for NMR imaging. *Magn. Reson. Med.* **1**, 478-495.
- Lauffer, R. B., and Brady, T. (1985) Preparation and water relaxation properties of proteins labeled with paramagnetic metal chelates. *Magn. Reson. Imaging* **3**, 11-16.
- Ogan, M. D., Schmiedl, U., Moseley, M. E., Grodd, W., Paajanen, H., and Brasch, R. C. (1987) Albumin labeled with Gd-DTPA, an intravascular contrast-enhancing agent for magnetic resonance blood pool imaging: preparation and characterization. *Invest. Radiol.* **22**, 665-671.
- Schmiedl, U., Ogan, M., Paajanen, H., Marotti, M., Crook, L. E., Brito, A. C., and Brasch, R. C. (1987) Albumin labeled with Gd-DTPA as an intravascular, blood pool-enhancing agent for NMR imaging: biodistribution and imaging studies. *Radiology* **162**, 205-210.
- Peter, T. (1975) Serum Albumin. In *The Plasma Proteins* (F. W. Putnam, Ed.) pp 133-181, Academic Press, New York.
- Swartz, H. M., Chen, K., Pals, M., Sentjurs, M., and Morse, P. D., II (1986) Hypoxia sensitive NMR contrast agents. *Magn. Reson. Med.* **3**, 169-174.
- Chen, K., and Swartz, H. M. (1988) Oxidation of hydroxylamines to nitroxides spin labels in living cells. *Biochim. Biophys. Acta* **970**, 270-277.
- Swartz, H. M. (1989) Metabolically Responsive Contrast Agents. In *Advances in Magnetic Resonance Imaging* (E. Feig, Ed.) pp 49-71, Ablex Publishing Company, New Jersey.
- Griffith, O. H., and McConnell, H. M. (1966) A nitroxide-maleimide spin label. *Proc. Natl. Acad. Sci. U.S.A.* **55**, 8-11.
- Benga, G., and Strach, S. J. (1975) Interaction of the electron spin resonance spectra of nitroxide-maleimide-labeled proteins and the use of this technique in the study of albumin and biomembranes. *Biochim. Biophys. Acta* **400**, 69-79.
- Cornell, C. N., and Kaplan, L. J. (1978) Spin-labeled studies of the sulfhydryl environment in bovine plasma albumin. 1. The N-F transition and acid expansion. *Biochemistry* **17**, 1750-1754.
- Berliner, L. J., Ed. (1976) *Spin Labeling. Theory and Applications* Academic Press, New York.
- Hunter, M. J., and McDuffie, F. C. (1959) Molecular weight studies on human serum albumin after reduction and alkylation of disulfide bonds. *J. Am. Chem. Soc.* **81**, 1400-1406.

- (23) Ball, J. K., Huh, T. Y., and McCarter, J. A. (1959) On the distribution of epidermal papillomata in mice. *Br. J. Cancer* 18, 120-123.
- (24) Ohkuma, S., and Poole, B. (1978) Fluorescence probe measurement of the intralysosomal pH in living cells and the perturbation of pH by various agents. *Proc. Natl. Acad. Sci. U.S.A.* 75, 3327-3331.
- (25) Blackburn, S. (1976) *Enzyme Structure and Function* pp 105-141, Marcel Dekker, New York.
- (26) Wien, R. W., Morrisett, J. D., and McConnell, H. M. (1972) Spin-labeled-induced nuclear relaxation. Distances between bound saccharides, histidine-15, and tryptophan-123 on lysozyme in solution. *Biochemistry* 11, 3707-3716.
- (27) Brasch, R. C., Nitecki, D. E., Brant-Zawadzki, M., Enzmann, D. R., Wesby, G. E., Tozer, T. N., Tuck, L. D., Cann, C. E., Fike, J. R., and Sheldon, P. (1983) Brain nuclear magnetic resonance imaging enhanced by a paramagnetic nitroxide contrast agent: preliminary report. *Am. J. Radiol.* 141, 1019-1023.
- (28) Ehman, R. L., Wesbey, G. E., Moon, K. L., Williams, R. D., McNamara, M. T., Couet, W. R., Tozer, T. N., and Brasch, R. C. (1985) Enhanced MRI of tumors utilizing a new nitroxyl spin label contrast agent. *Magn. Reson. Imaging* 3, 89-97.
- (29) Afzal, V., Brasch, R. C., Nitecki, D. E., and Wolff, S. (1984) Nitroxyl spin label contrast enhancers for magnetic resonance imaging: studies of acute toxicity and mutagenesis. *Invest. Radiol.* 19, 549-552.
- (30) Segal, H. L., and Doyle, D. J., Eds. (1978) *Protein Turnover and Lysosome Function* Academic Press, New York.
- (31) Hershko, A., and Tomkins, G. (1971) Studies on the degradation of tyrosine aminotransferase in hepatoma cells in culture. *J. Biol. Chem.* 246, 710-714.
- (32) Schimke, R. T., and Doyle, D. (1970) Control of enzyme levels in animal tissues. *Annu. Rev. Biochem.* 39, 929-976.
- (33) Strober, W., Mogielnicki, R. P., and Waldmann, T. A. (1972) The Role of the Kidney in the Metabolism of Serum Proteins. *Protein Turnover* pp 25-41, Elsevier, Amsterdam.
- (34) Widder, D. J., Greif, W. L., Widder, K. J., Edelman, R. R., and Brady, T. J. (1987) Magnetite albumin microspheres: a new MR contrast material. *Am. J. Radiol.* 148, 339-404.
- Registry No.** Trypsin, 9002-07-7.

Site-Directed Chemical Modification and Cross-Linking of a Monoclonal Antibody Using Equilibrium Transfer Alkylating Cross-Link Reagents

Frederick A. Liberatore,^{*,†} Robert D. Comeau,[†] James M. McKearin,[†] Daniel A. Pearson,[†] Benjamin Q. Belonga III,[†] Stephen J. Brocchini,[‡] John Kath,[§] Terri Phillips,[§] Kira Oswell,[§] and Richard G. Lawton^{*,‡}

Medical Products Department, E. I. du Pont de Nemours and Company, 331 Treble Cove Road, North Billerica, Massachusetts 01862, and Department of Chemistry, University of Michigan, 2525 Chemistry Building, Ann Arbor, Michigan 48109. Received July 21, 1989

A new, more reactive group of protein cross-linkers in the class of equilibrium transfer alkylating cross-link (ETAC) reagents has been synthesized. These compounds include α,α -bis[(*p*-chlorophenyl)methyl]- and α,α -bis[(*p*-tolylsulfonyl)methyl]acetophenones substituted in the acetophenone ring with chloro, nitro, amino, and carboxyl groups and derivatives. Included are an ^{125}I -labeled ETAC reagent and a ^{111}In -labeled DTPA (diethylenetriaminepentaacetic acid) ETAC for site direction and biodistribution studies. These ETAC compounds were reacted with unreduced and partially reduced antibody under mild pH (pH 4-8) and room temperature conditions to give cross-linked structures. Examination of resultant cross-linked antibody via size-exclusion HPLC, sodium dodecyl sulfate (SDS) polyacrylamide gel electrophoresis, and an enzyme linked immunosorbent assay revealed that (1) both interantibody as well as intraantibody cross-linking had occurred; (2) the level of inter- and intraantibody cross-linking varied with the substituent on the ETAC; (3) the stability of the cross-links on the reducing SDS gels varied with substituents on the ETAC; (4) little if any immunoreactivity was lost after reaction with one of the more effective ETAC cross-linking compounds; (5) the ^{125}I -labeled ETAC sulfhydryl cross-linking in partially reduced antibody increased with pH whereas amine cross-linking with the unreduced antibody decreased with pH; (6) the optimum pH for sulfhydryl site direction was pH 5.0; (7) the ^{111}In DTPA ETAC labeled antibody had a biodistribution in CD1 mice similar to that of the ^{111}In bis cyclic anhydride DTPA labeled antibody.

The only *chemical* method that allows the identification of the tertiary and quaternary structure of proteins involves the use of organic hetero- and homobifunctional cross-linking reagents (1-4). These same reagents can be used to join similar or dissimilar proteins together

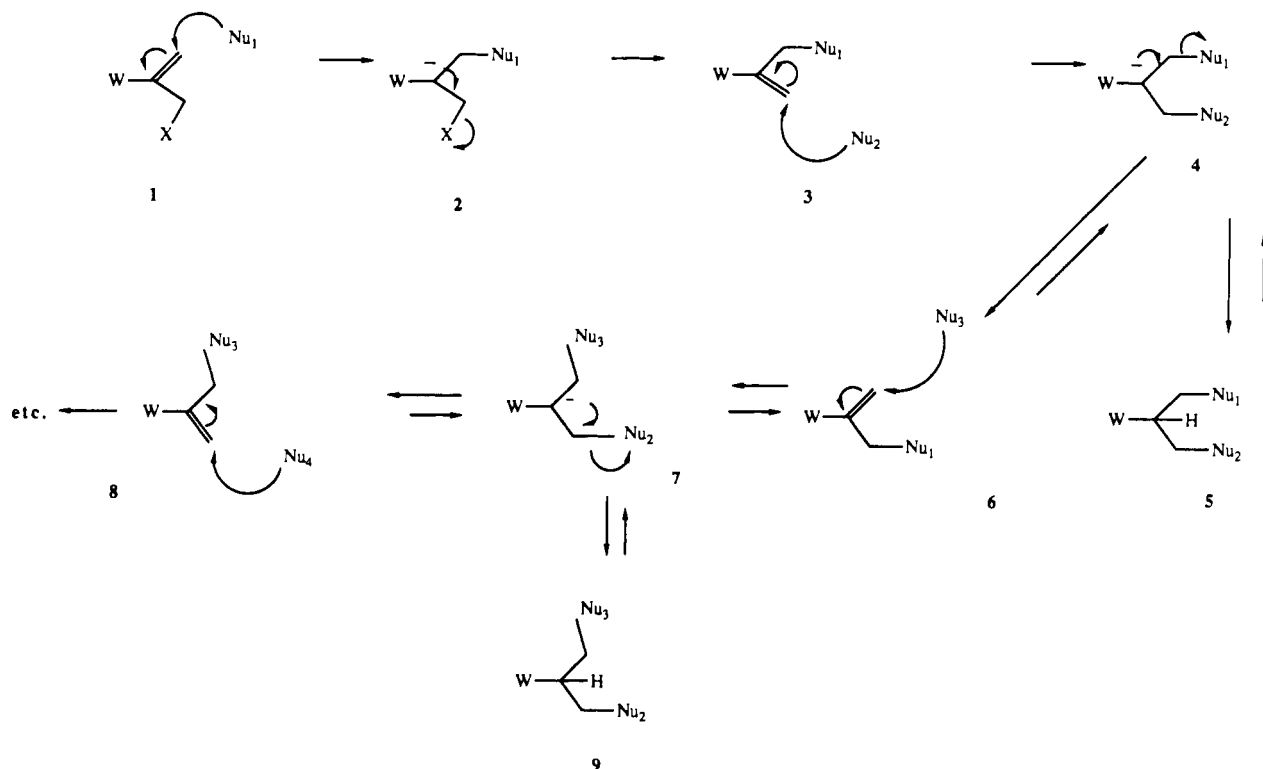
or to cross-link smaller molecules to a protein (5-8). Virtually all bifunctional cross-links described are believed to covalently couple to reactive functions through links that are nonreversible. However, one class of cross-linkers has been described whose members have the potential ability to transfer from the initial site of protein attachment to another reactive site to form a (relatively) more stable bond. These types of compounds have been given the acronym ETAC for equilibrium transfer alkylating cross-link (9). The original ETAC reagents consisted of

[†] E. I. du Pont de Nemours and Co.

[‡] University of Michigan.

[§] University of Michigan Undergraduate Research Participants.

Scheme I



a good leaving group (X) and an electron-withdrawing group (W), such as an ester, ketone, cyano, or *p*-nitrophenyl, conjugated to a double bond as shown with 1 in Scheme I. The protein cross-linking process was first demonstrated with W = *p*-nitrophenyl and X = N(CH₃)₃⁺ and X = SC₆H₃(NO₂)CO₂H, with ribonuclease. Recent reports in the literature (10, 11) describe the partial reduction of antibodies followed by chemical modification of the resultant sulfhydryl groups with probes of various types that covalently couple to one or both sulfhydryls, but these reagents do not bridge or reanneal the disulfide bridges.

The design of ETAC reagents provided a general class of protein-modification reagents based upon Michael addition/Michael elimination chemistry (Scheme I). This family of bifunctional reagents was fabricated so that nucleophilic residues on a protein chain would undergo the Michael addition process with the subsequent loss of a group to generate a new, previously latent, conjugated double bond (Scheme I, 1 → 2 → 3). A second Michael reaction is then possible, but now in either an intraprotein or an interprotein chain mode to yield a cross-linked protein (Scheme I, 3 → 4 → 5). An alternate pathway is available however. When the second nucleophilic protein residue undergoes the Michael addition, the transient intermediate anion formed by this process on the link connecting both the first and second residues (Scheme I, 4) can allow the release of the first residue by a retro-Michael process. This allows the transfer of the reagent moiety to the second protein residue with the simultaneous reformation of the conjugated double bond (Scheme I, 4 → 6). If the reagent can pivot and is close enough to interact with a third nucleophilic group on the protein, the process can continue (Scheme I, 6 → 7, etc.) allowing the reagent to transfer by a cascade of consecutive Michael reactions to eventually form the most thermodynamically stable cross-link. The reagent has the possibility of "walking", "skipping", or "jumping" along

the protein chain from one nucleophilic protein side chain to another. With functional groups such as amine, phenol, and carboxyl, the reagents never lose their alkylating capability. They transfer, through reverse Michael/Michael reactions, until addition of some group gives the (relatively) more stable links, usually from thiols adding to give thioether bridges. The reagents can be constructed easily, may contain multiple spectrophotometric probes, have water solubility, react under mild conditions, and can be joined to a wide variety of substances yet retain their alkylating and transfer potential.

A special feature of these reagents is that the cross-linking portion may bridge a span of very small distance. They may also contain elements which provide a mechanism for arresting the transfer process so that the mobile equilibrium can no longer take place. The alkylation cross-links between residues can then be identified by hydrolysis, amino acid analysis, and peptide-mapping techniques. Thus, the beginning studies provided a pathway for realizing the identification of equilibrium established cross-links on protein chains.

There are other applications and extensions of this modification technique to proteins that are especially attractive. If a protein contains natural disulfide links that can be reduced with significant retention of the tertiary structure, there is a chance, because of the equilibrium nature of the modification, that reagents of this type might "recross-link" or "reanneal" the original disulfide sites. Since the protein modification would be accomplished between cysteines that had been linked as cysteines in the original protein, there would be no necessary change in the kind and number of basic or acidic groups on the protein itself. Thus, reduction of a disulfide bond and the reestablishment of the link between the folds of the protein through an extra three-carbon bridge might be a minor perturbation of the system. If the activating function for the Michael reactions also contained an appropriate side chain, one could imagine the easy tethering

of a variety of spectrophotometric probes, pharmacologically active substances, and chemical reagents to this bridge. We have demonstrated this chemical modification technique and concept.

The nature of the ETAC type reaction suggested that the reannealing process might be accomplished under very mild conditions. However, the original reagents had a *p*-nitrophenyl activating group for the Michael reaction and were not reactive enough to insure rapid linking under mild conditions (9). In some proteins with certain functional groups, these original reagents required rather harsh conditions of pH and temperature for cross-linking. Our experience indicated that increased reactivity required masking in some fashion, so that the reagents would not undergo base- and free-radical-promoted polymerization and could be handled and used in the aqueous and highly nucleophilic environment required for the proteins. Perhaps most importantly, the former ETAC reagents did not have a design that easily allowed the addition of another complex functionality necessary for the attachment of the branching tether.

Thus, within the design of this new, more reactive family of cross-linking reagents, we were interested in adding structural elements for protein cross-linking probes with functions allowing the tethering of many different groups, especially chelating functions for the addition of radioactive metals. The new class of ETAC reagents has the general structure shown in Scheme II. They have an aromatic ketone function as a Michael activating group with substituents to allow various probes to be attached. The arylsulfonyl functions of the bis[(arylsulfonyl)methyl] group serve as effective leaving groups and assist in masking the latent double bond.

The application of these reannealing, cross-linking reagents to antibody chains was a natural, important, and unique extension of this chemistry. The new bridge created allows the tethering of a variety of biological probes (Scheme III). The ETAC pattern of reactivity with an unreduced as well as a partially reduced monoclonal antibody using a radioiodinated ETAC reagent is described. We also demonstrate the attachment of a chelating arm to one of these structures and complexation of a radioactive metal.

The biological applications of these tagged antibodies are outlined. In collaboration with others a similar ETAC reagent conjugated with a fluorescent probe has been created and reacted with monoclonal antibodies.¹

EXPERIMENTAL PROCEDURES

General Chemical Procedures. Melting points were determined in open glass capillary tubes using a Thomas-Hoover Uni-Melt melting point apparatus and are uncorrected. Infrared spectra were obtained on Perkin-Elmer 727B or 457 or Beckman 4240 spectrophotometers using the 1601 cm⁻¹ absorption of polystyrene as a standard reference. FT-IR spectra were obtained on Nicolet 60-SX or 5DX Fourier transform spectrophotometers. Transmittance minima are reported in reciprocal centimeters (cm⁻¹) and are characterized as strong (s), medium (m), weak (w), or broad (b) where pertinent. Proton magnetic resonance spectra were recorded at 60, 270, 300, or 360 MHz, on a Varian T-60A, Bruker IBM-AF, Bruker

AM-300, or Bruker WM-360 spectrometers, respectively. Broadband proton-decoupled carbon-13 nuclear magnetic resonance spectra were measured at 22.5, 67.5, 75.0, or 90.4 MHz on JEOL FX-90Q, Bruker IBM-AF, Bruker AM-300, or Bruker WM-360 spectrometers, respectively. Appropriate solvent resonances were consistently used as internal references. All magnetic resonance spectra are reported as δ values downfield from tetramethylsilane. Multiplicities of resonances are described as broad (b), singlet (s), doublet (d), triplet (t), quartet (q), or multiplet (m). Elemental analyses were performed by Spang Microanalytical Laboratories, Eagle Harbor, MI or by Guelph Chemical Laboratories Ltd., Guelph, Ontario, Canada. Slow addition of reagents to reaction mixtures was accomplished by a Harvard Scientific Model 901 infusion pump as noted. Preparative-scale medium-pressure chromatography was performed using a chromatograph assembled in the Michigan laboratory. Columns were either Lobar Lichroprep or manually packed with 0.040–0.063- μ m silica gel. An Altex Model 150 UV detector (254 nm) was used to monitor separations where appropriate. Flash chromatography was accomplished using EM grade 0.040–0.063- μ m silica gel. Conventional column chromatography was conducted with 40–200 mesh silica or Woelm Grade basic alumina. Analytical thin-layer chromatography was carried out on Merck silica gel 60 glass-backed, fluorescence-indicator plates. Plates were visualized with UV light and iodine, ceric ammonium molybdate stain, or ninhydrin. Cellulose plates were Eastman 13255 on polymer backing. Preparative-scale TLC utilized Analtech 1000- μ m or 2000- μ m plates.

The following solvents were purified or dried by distillation from the reagents indicated: chloroform, dichloromethane, trifluoroacetic anhydride, and toluene from phosphorus pentoxide; benzene, acetonitrile, and dimethyl sulfoxide from calcium hydride; pyridine from potassium hydroxide; methanol and ethanol from magnesium; tetrahydrofuran from sodium benzophenone ketyl; and dimethylformamide from phthalic anhydride. Solvents for column chromatography were distilled or HPLC grade. All other solvents were ACS reagent grade.

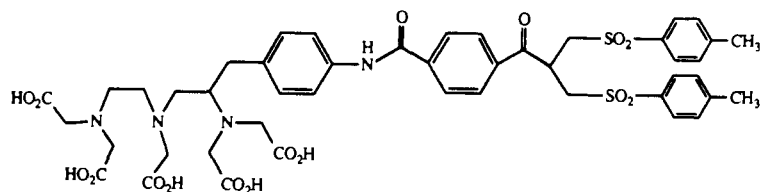
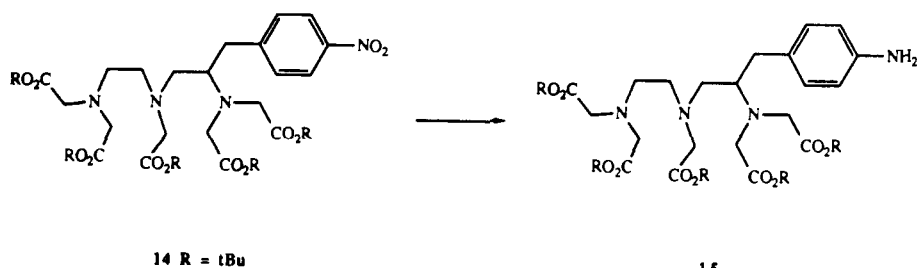
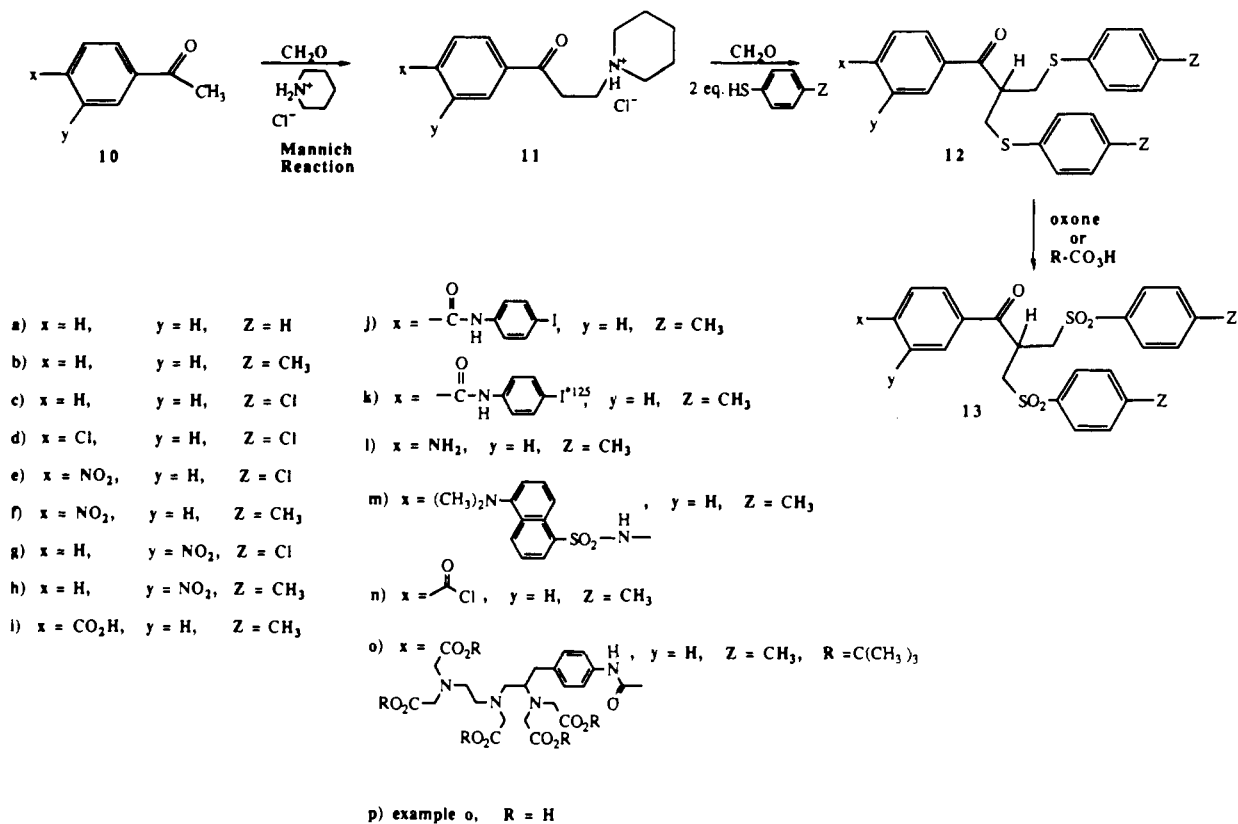
Mannich Salts. Mannich salts were prepared from the corresponding acetophenone by modifications of the procedure of Mannich (12) as given in ref 13.

***p*-Carboxy- β -piperidinopropiophenone Hydrochloride (11i).** *p*-Carboxyacetophenone (5.0 g, 31 mmol), paraformaldehyde (1.0 g, 91 mmol), and piperidine hydrochloride (3.67 g, 31 mmol) were suspended in 30 mL of absolute ethanol and heated at reflux with magnetic stirring overnight. During this time dissolution occurred. After cooling, the solution was diluted with acetone, yielding white crystals, mp 200 °C. Recrystallization from water yielded white needles, mp 214–215 °C, depressed upon mixture with starting material. The yield of 4.0 g (44%) was used without purification for the preparation of carboxy bis-sulfide 12i.

General Procedure for the Synthesis of Substituted Bis[(phenylthio)methyl]acetophenones (Scheme II, 12). The respective Mannich salt (11) was mixed with 2 equiv of thiol (thiophenol, *p*-chlorothiophenol, or *p*-thiocresol) and an excess of 37% formalin solution (10 mL, 0.03 mol of salt) in methanol (30 mL, 0.03 mol salt). This mixture was brought to reflux with stirring under a blanket of nitrogen. When the mixture became homogeneous, 2–3 drops of piperidine was added and the reaction mixture acquired a dark black or greenish-black color. As refluxing continues this color is lost. Within 1–2 h a

¹ del Rosario, R. B., Wahl, R. L., Brocchini, S. J., Lawton, R. G., and Smith, R. H. Sulfhydryl site-specific labeling and cross-linking of a monoclonal antibody by a fluorescent equilibrium transfer alkylation cross-link reagent. *Bioconjugate Chem.*, following paper in this issue.

Scheme II

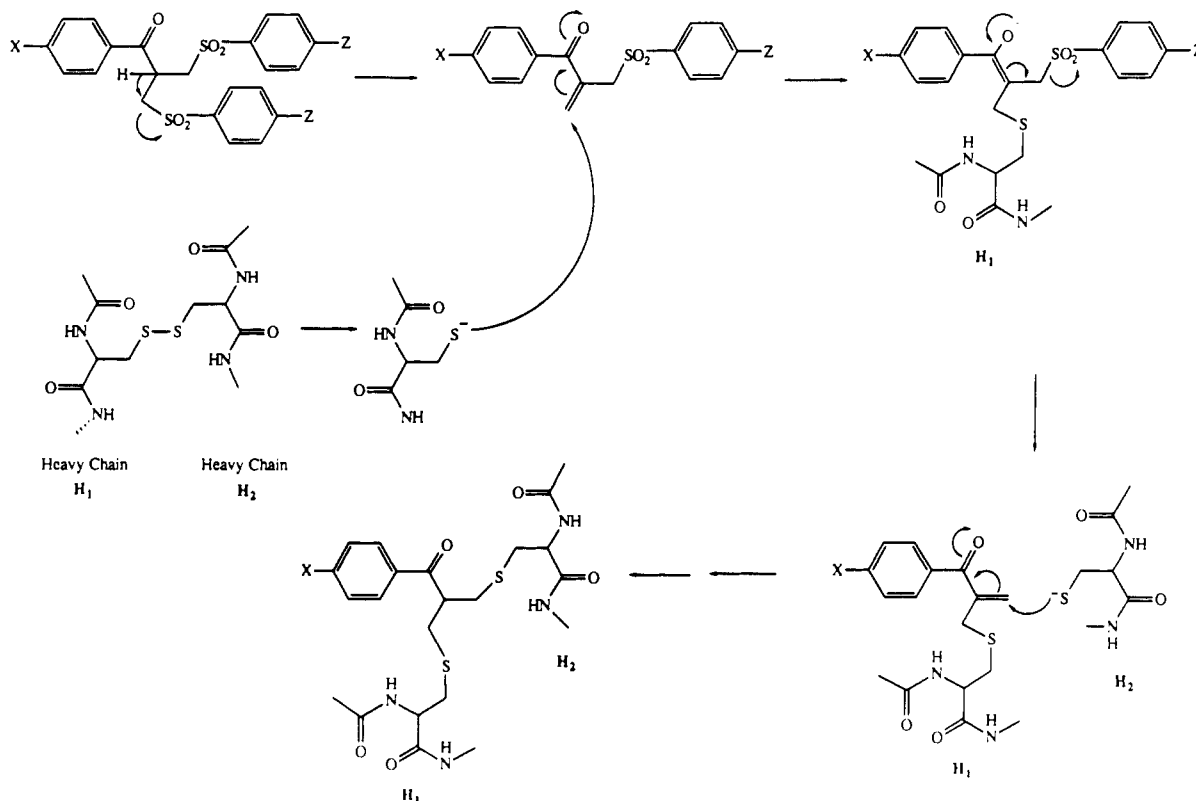


small amount of oil could be detected when the stirring was stopped. After refluxing for 24 h, a large amount of oil had formed. The solution was allowed to cool and the oil settled at the bottom of the flask. After the reaction mixture had cooled, methylene chloride was added to dissolve the oil and then an excess of water was added to form two layers. The layers were separated, and the methylene chloride layer was washed twice with 10% HCl, once with 5% bicarbonate, and once with brine. The methylene chloride solution was then dried with anhydrous sodium sulfate. After drying, the solvent was removed and an oil was obtained which crystallized with

either use of a high vacuum or vigorous scratching. This crude solid was crystallized from methanol or methanol with a trace amount of acetone to give the compounds listed below.

α,α -Bis[(phenylthio)methyl]acetophenone (12a). The Mannich salt β -piperidinopropiophenone hydrochloride (25.3 g, 0.10 mol) undergoes aldol and sequential Michael reactions with benzenethiol to give bis-sulfide 12a (30 g, 83%): ^1H NMR (CDCl_3 , 360 MHz) δ 3.24 (A2B2X, m, 4 H, $-\text{CH}_2-$), 4.4 (quintet, 1 H, $J = 5.7$ Hz, $-\text{CH}-$), 7.52 (m, 3 H), 7.58 (m, 6 H), 7.65 (m, 2 H), 7.71 (m, 4 H); ^{13}C NMR (CDCl_3 , 90.4 MHz) δ 202.16, 137.33,

Scheme III



133.02, 131.42, 129.52, 127.25, 127.08, 123.00, 122.78, 45.34, 35.63; mp 63–65 °C; R_f (solvent system) 0.45 (4:1 hexane/acetone). Anal. Calcd for $C_{22}H_{20}OS_2$: C, 72.49; H, 5.53. Found: C, 72.45; H, 5.66.

α,α -Bis[(*p*-tolylthio)methyl]acetophenone (12b). The Mannich salt β -piperidinopropiophenone hydrochloride (25.3 g, 0.10 mol) undergoes aldol and sequential Michael reactions with *p*-toluenethiol to give bis-sulfide 12b (28.2 g, 71.5%): 1H NMR ($CDCl_3$, 360 MHz) δ 2.11 (s, 6 H, $-CH_3$), 3.45 (A2B2X, 4 H, $-CH_2-$), 4.14 (quintet, 1 H, $J = 6.5$ Hz, $-CH-$), 7.08, 7.14 (AB q, 8 H, $J = 7.9$ Hz), 7.58–7.48 (m, 5 H); ^{13}C NMR ($CDCl_3$, 75 MHz) δ 202.16, 137.33, 133.02, 131.42, 129.52, 127.25, 127.08, 123.00, 122.78, 45.34, 35.63, 22.12; mp 63–65 °C; R_f (solvent system) 0.28 (4:1, hexane/acetone). Anal. Calcd for $C_{24}H_{24}OS_2$: C, 73.05; H, 6.04. Found: C, 73.50; H, 6.22.

α,α -Bis[(*p*-chlorophenylthio)methyl]acetophenone (12c). The Mannich salt β -piperidinopropiophenone hydrochloride (35.9 g, 0.14 mmol) undergoes aldol and sequential Michael reactions with *p*-chlorobenzenethiol to give bis-sulfide 12c (29.0 g, 67%). Crystallization from acetone/methanol yielded white crystals: 1H NMR ($CDCl_3$, 360 MHz) δ 3.52, 3.67 (A2B2X, 4 H, $-CH_2-$), 4.39 (quintet, 1 H, $J = 6.2$ Hz, $-CH-$), 7.76, 7.51 (AB q, 8 H, $J = 8.6$ Hz), 7.59 (m, 3 H), 7.40 (m, 2 H); ^{13}C NMR ($CDCl_3$, 75 MHz) δ 194.98, 141.21, 136.84, 134.43, 129.87, 129.82, 129.07, 128.46, 125.65, 55.11, 35.27; mp 78–79 °C; R_f (solvent system) 0.28 (4:1 hexane/acetone). Anal. Calcd for $C_{22}H_{18}Cl_2OS_2$: C, 55.23; H, 3.58. Found: C, 55.36; H, 3.50.

α,α -Bis[(*p*-chlorophenylthio)methyl]-*p*-chloroacetophenone (12d). The Mannich salt *p*-chloro- β -piperidinopropiophenone hydrochloride (28.8 g, 0.10 mmol) undergoes aldol and sequential Michael reactions with *p*-chlorobenzenethiol to give bis-sulfide 12d (29.0 g, 62%). Crystallization from acetone/methanol yielded white crystals: 1H NMR ($CDCl_3$, 360 MHz) δ 3.22 (A2B2X, 4 H,

$-CH_2-$), 3.71 (quintet, 1 H, $J = 6.7$ Hz, $-CH-$), 7.15, 7.23 (AB q, 8 H, $J = 8.8$ Hz), 7.35, 7.51 (AB q, 4 H, $J = 8.6$ Hz); ^{13}C NMR ($CDCl_3$, 75 MHz) δ 198.66, 148.65, 137.74, 134.55, 129.98, 129.80, 129.11, 128.24, 124.43, 58.36, 37.77; mp 102–105 °C; R_f (solvent system) 0.36 (4:1 hexane/acetone). Anal. Calcd for $C_{22}H_{17}Cl_3OS_2$: C, 56.48; H, 3.66. Found: C, 56.58; H, 3.66.

α,α -Bis[(*p*-chlorophenylthio)methyl]-4-nitroacetophenone (12e). The Mannich salt *p*-nitro- β -piperidinopropiophenone hydrochloride (35.9 g, 0.120 mol) undergoes aldol and sequential Michael reactions with *p*-chlorobenzenethiol to give bis-sulfide 12e (29.3 g, 51%): IR (phase, KBr, threshold for minima, 45% transmittance) 502.6, 701.0, 809.6, 822.2, 857.2, 1007.8, 1092.7, 1195.0, 1345.0, 1475.0, 1519.6, 1679.4 cm^{-1} ; 1H NMR ($CDCl_3$, 360 MHz) δ 3.24 (A2B2X, 4 H, $-CH_2-$), 3.79 (quintet, 1 H, $J = 6.8$ Hz, $-CH-$), 7.15, 7.23 (AB q, 8 H, $J = 8.6$ Hz), 7.71, 8.21 (AB q, 4 H, $J = 8.9$ Hz); ^{13}C NMR ($CDCl_3$, 75 MHz) δ 199.16, 150.52, 140.96, 133.43, 133.12, 131.92, 129.32, 129.25, 129.18, 123.89, 123.78, 46.14, 36.03; mp 104–106 °C; R_f (solvent system) 0.62 (4:1 hexane/acetone). Anal. Calcd for $C_{22}H_{17}Cl_2NO_3S_2$: C, 55.23; H, 3.58. Found: C, 55.36; H, 3.50.

α,α -Bis[(*p*-tolylthio)methyl]-4-nitroacetophenone (12f). The Mannich salt *p*-nitro- β -piperidinopropiophenone hydrochloride (26.6 g, 0.09 mol) undergoes aldol and sequential Michael reactions with *p*-tolyl mercaptan to give bis-sulfide 12f (20.24 g, 52%): IR (phase, KBr; threshold for minima, 45% transmittance) 1694.9, 1681.1, 1652.6, 1522.1, 1507.3, 1492.2, 1342.2, 1319.9, 1080.3, 806.5 cm^{-1} ; 1H NMR ($CDCl_3$, 360 MHz) δ 2.36 (s, 6 H, $-CH_3$), 3.19 (A2B2X, 4 H, $-CH_2-$), 3.79 (quintet, 1 H, $J = 6.8$ Hz), 7.06, 7.11 (AB q, 8 H, $J = 8.3$ Hz), 7.61, 8.13 (AB q, 4 H, $J = 8.9$ Hz); ^{13}C NMR ($CDCl_3$, 90.4 MHz) δ 199.76, 150.26, 141.20, 137.40, 131.46, 130.93, 129.91, 129.29, 123.59, 43.13, 36.40, 21.08; mp 91–93 °C; R_f (solvent system) 0.42 (4:1 hexane/acetone). Anal. Calcd for $C_{24}H_{23}NO_3S_2$: C, 65.88,

H, 5.30. Found: C, 65.66; H, 5.22.

α,α -Bis[[(*p*-chlorophenyl)thio]methyl]-*m*-nitroacetophenone (12g). The Mannich salt *m*-nitro- β -piperidinopropiophenone hydrochloride (10.0 g, 0.03 mol) undergoes aldol and sequential Michael reactions with *p*-chlorobenzenethiol to form bis-sulfide 12g (8.96 g, 56%): IR (phase, KBr) 1678.6, 1615.5, 1544.4, 1474.7, 1351.1, 1093.2, 1008.5, 809.2, 695.5, 668.2, 484.0 cm^{-1} ; ^1H NMR (CDCl_3 , 360 MHz) δ 3.25 (A2B2X, 4 H, $-\text{CH}_2-$), 3.80 (quintet, 1 H, $J = 7.6$ Hz), 7.15, 7.25 (AB q, 8 H, $J = 8.6$ Hz), 7.59 (t, 1 H, $J = 8.0$ Hz), 7.90 (d, 1 H, $J = 7.0$ Hz), 8.41 (m, 2 H); ^{13}C NMR (CDCl_3 , 90.4 MHz) δ 198.69, 148.40, 137.88, 133.57, 133.49, 132.89, 132.01, 129.88, 129.35, 127.68, 123.04, 45.66, 36.05; mp 88–88.5 $^\circ\text{C}$; R_f (solvent system) 0.31 (4:1 hexane/acetone). Anal. Calcd for $\text{C}_{22}\text{H}_{17}\text{Cl}_2\text{NO}_3\text{S}_2$: C, 55.23; H, 3.58. Found: C, 55.17; H, 3.45.

α,α -Bis[(*p*-tolylthio)methyl]-*m*-nitroacetophenone (12h). The Mannich salt of *m*-nitro- β -piperidinopropiophenone hydrochloride (11.4 g, 0.038 mol) undergoes aldol and sequential Michael reactions with *p*-tolyl mercaptan to form bis-sulfide 12h (11.2 g, 64%): IR (phase, KBr) 1684.2, 1527.6, 1491.4, 1437.8, 1411.7, 1348.2, 1258.6, 1219.7, 1084.6, 811.5, 732.1, 691.6, 672.3, 506.8 cm^{-1} ; ^1H NMR (CDCl_3 , 360 MHz) δ 2.33 (s, 6 H, $-\text{CH}_3$), 3.21 (A2B2X, 4 H, $-\text{CH}_2-$), 3.82 (quintet, 1 H, $J = 6.8$ Hz), 7.04, 7.09 (AB q, 8 H, $J = 8.2$ Hz), 7.52 (t, 1 H, $J = 8.0$ Hz), 7.89 (d, 1 H, $J = 7.8$ Hz), 8.23 (s, 1 H), 8.34 (d, 1 H, $J = 8.3$ Hz); ^{13}C NMR (CDCl_3 , 90.4 MHz) δ 199.44, 148.39, 138.26, 137.49, 133.78, 131.44, 130.75, 129.98, 129.66, 127.40, 123.20, 45.59, 36.47, 21.06; mp 81–84 $^\circ\text{C}$; R_f (solvent system) 0.30 (4:1 hexane/acetone). Anal. Calcd for $\text{C}_{24}\text{H}_{23}\text{NO}_3\text{S}_2$: C, 65.87; H, 5.30. Found: C, 65.66; H, 5.28.

4-[2,2-Bis[(*p*-tolylthio)methyl]acetyl]benzoic Acid (12i). The Mannich salt *p*-carboxy- β -piperidinopropiophenone hydrochloride (11i, 1.00 g, 3.4 mmol) undergoes aldol and sequential Michael addition reaction with *p*-thiocresol (0.86 g, 6.9 mmol), formaldehyde (37% solution, 1.90 mL, 23 mmol), and piperidine (0.47 mL, 4.77 mmol) at reflux to give bis-sulfide 12i (0.95 g, 65%, recrystallized from $\text{CH}_3\text{OH}/\text{H}_2\text{O}$, white needles): IR (phase, KBr; threshold for minima, 45% transmittance) 805, 1275, 1420, 1490, 1680, 1685, 2920, 3020 cm^{-1} ; ^1H NMR (CDCl_3 , 270 MHz) δ 2.36 (s, 6 H, $-\text{CH}_3$), 3.22 (m, 4 H, $-\text{CH}_2-$), 3.81 (q, 1 H, $-\text{CH}-$), 7.05, 7.14 (AB q, 8 H, $J = 8.0$ Hz), 7.60, 8.04 (AB q, 4 H, $J = 8.3$ Hz); ^{13}C NMR (CDCl_3 , 67.9 MHz) δ 200.31, 170.88, 140.40, 137.08, 132.77, 131.38, 130.91, 130.12, 129.68, 128.16, 45.72, 36.22, 20.92; mp 142–143 $^\circ\text{C}$; R_f (solvent system) 0.81 (7.5:1.5:1.0 chloroform/methanol/acetic acid).

General Procedure for the Oxidation of Substituted Bis[(phenylthio)methyl]acetophenones to Sulfones. One equivalent of the bis-sulfide was placed in 1:1 methanol/water with 6 equiv of Oxone (Du Pont, Wilmington, DE) (5 g of Oxone/25 mL of solution) and the suspension was stirred. The progress of the reaction was followed by TLC until completion (4–6 h). Chloroform was added to extract the sulfone and an excess of water was added to dissolve the residual salts, remaining Oxone, and other water-soluble side products. The chloroform layer was extracted twice with distilled water and then dried over anhydrous sodium sulfate. The solvent was removed under reduced pressure during which crystallization to a crude solid took place. The crude materials were recrystallized with 100% ethanol.

α,α -Bis[(*p*-chlorophenyl)sulfonyl]methyl]acetophenone (13c). Bis-sulfide 12c (2.0 g, 0.004 mol) was oxidized in a suspension of Oxone to give bis-sulfone 13c

(1.31 g, 75%): ^1H NMR (CDCl_3 , 360 MHz) δ 3.52, 3.67 (A2B2X, 4 H, $-\text{CH}_2-$), 4.39 (quintet, 1 H, $J = 6.2$ Hz), 7.40 (m, 2 H), 7.59 (m, 3 H), 7.51, 7.76 (AB q, 8 H, $J = 8.6$ Hz); ^{13}C NMR (CDCl_3 , 90.4 MHz) δ 194.98, 141.21, 136.84, 134.43, 129.87, 129.82, 129.07, 128.46, 125.65, 55.11, 35.27; mp 133–135 $^\circ\text{C}$. Anal. Calcd for $\text{C}_{22}\text{H}_{18}\text{Cl}_2\text{O}_5\text{S}_2$: C, 53.12; H, 3.65. Found: C, 53.12; H, 3.74.

α,α -Bis[(*p*-chlorophenyl)sulfonyl]methyl]-*p*-chloroacetophenone (13d). Bis-sulfide 12d (2.0 g, 0.0042 mol) was oxidized in a suspension of Oxone to give bis-sulfone 13d (1.51 g, 68%): ^1H NMR (CDCl_3 , 360 MHz) δ 3.47, 3.61 (A2B2X, 4 H, $-\text{CH}_2-$), 4.38 (quintet, 1 H, $J = 6.2$ Hz), 7.39, 7.61 (AB q, 4 H, $J = 9.2$ Hz), 7.53, 7.66 (AB q, 8 H, $J = 7.5$ Hz); ^{13}C NMR (CDCl_3 , 90.4 MHz) δ 194.18, 178.40, 141.29, 141.12, 136.80, 132.35, 129.87, 129.68, 129.38, 55.67, 35.05; mp 156–157 $^\circ\text{C}$. Anal. Calcd for $\text{C}_{22}\text{H}_{17}\text{Cl}_3\text{O}_5\text{S}_2$: C, 49.68; H, 3.22; S, 12.06. Found: C, 49.78; H, 3.24; S, 12.00.

α,α -Bis[(*p*-chlorophenyl)sulfonyl]methyl]-4-nitroacetophenone (13e). Bis-sulfide 12e (2.0 g, 0.004 mol) was oxidized in a suspension of Oxone to give bis-sulfone 13e (1.51 g, 69%): IR (phase, KBr) 1697.6, 1531.4, 1520.6, 1345.4, 1311.1, 1282.3, 1148.3, 1137.3, 1088.6, 1084.9, 772.2 cm^{-1} ; ^1H NMR (CDCl_3 , 360 MHz) δ 3.49 (2 H, d of d, A of A2B2X), 3.65 (2 H, d of d, B of A2B2X), 4.58 (m, 1 H, X of A2B2X, $J = 5.8$ Hz), 7.57, 7.79 (8 H, AB q, $J = 6.8$ Hz), 8.32, 8.00 (4 H, AB q, $J = 8.9$ Hz); ^{13}C NMR (CDCl_3 , 360 MHz) δ 194.92, 141.63, 138.97, 136.82, 130.10, 129.88, 129.69, 124.24, 56.13, 35.44; mp 190–192 $^\circ\text{C}$; R_f (solvent system) 0.28 (19:1 chloroform/methanol). Anal. Calcd for $\text{C}_{22}\text{H}_{17}\text{Cl}_2\text{NO}_7\text{S}_2$: C, 48.72; H, 3.16; S, 11.82. Found: C, 48.61; H, 3.06; S, 11.92.

α,α -Bis[(*p*-tolylsulfonyl)methyl]-4-nitroacetophenone (13f). Bis-sulfide 12f (5.0 g, 0.011 mol) was oxidized to give bis-sulfone 13f (4.95 g, 86%): IR (phase, KBr) 1692.8, 1522.9, 1345.7, 1333.4, 1313.5, 1305.0, 1294.8, 1272.5, 1158.9, 1135.8, 1084.5, 927.1, 853.8, 750.9, 743.4, 710.3, 573.8, 556.6, 523.7 cm^{-1} ; ^1H NMR (CDCl_3 , 360 MHz) δ 2.48 (s, 6 H, $-\text{CH}_3$), 3.54 (A2B2X, 4 H, $-\text{CH}_2-$), 4.46 (quintet, 1 H, $J = 8.9$ Hz), 7.37, 7.70 (AB q, 8 H, $J = 8.3$ Hz), 7.89, 8.24 (AB q, 4 H, $J = 8.9$ Hz); ^{13}C NMR (CDCl_3 , 90.4 MHz) δ 195.23, 145.76, 139.24, 135.46, 130.29, 129.78, 128.28, 124.01, 56.15, 35.72, 21.72; mp 168–169 $^\circ\text{C}$; R_f (solvent system) 0.07 (4:1 carbon tetrachloride/chloroform). Anal. Calcd for $\text{C}_{24}\text{H}_{23}\text{NO}_7\text{S}_2$: C, 57.47; H, 4.62; S, 12.79. Found: C, 57.43; H, 4.57; S, 12.54.

α,α -Bis[(*p*-chlorophenyl)sulfonyl]methyl]-*m*-nitroacetophenone (13g). Bis-sulfide 12g (5.0 g, 0.011 mol) was oxidized to give bis-sulfone 13g (3.25 g, 56%): IR (phase, KBr) 1684.9, 1576.5, 1536.9, 1473.8, 1399.1, 1349.4, 1319.0, 1305.0, 1273.8, 1261.3, 1146.1, 1089.7, 1084.2, 825.0, 768.6, 711.4; ^1H NMR (CDCl_3 , 360 MHz) δ 3.55 (m, 2 H, $-\text{CH}_2-$), 3.67 (m, A2B2X, 2 H, $-\text{CH}_2-$), 4.48 (quintet, 1 H, $J = 5.9$ Hz), 7.56, 7.78 (AB q, 8 H, $J = 8.6$ Hz), 7.70 (d of d, 1 H, $J = 8.0$ Hz), 8.16 (d, 1 H, $J = 7.9$ Hz), 8.46 (d, 1 H, $J = 8.2$ Hz), 8.54 (s, 1 H); ^{13}C NMR (CDCl_3 , 90.4 MHz) δ 194.28, 148.71, 141.64, 136.69, 135.83, 134.11, 130.44, 130.11, 129.65, 128.41, 123.35, 56.03, 35.35; mp 168–170 $^\circ\text{C}$; R_f (solvent system) 0.38 (19:1 chloroform/methanol). Anal. Calcd for $\text{C}_{22}\text{H}_{17}\text{NO}_7\text{S}_2$: C, 48.72; H, 3.16; S, 11.82. Found: C, 48.61; H, 3.06; S, 11.92.

α,α -Bis[(*p*-tolylsulfonyl)methyl]-*m*-nitroacetophenone (13h). Bis-sulfide 12h (1.0 g, 0.0023 mol) was oxidized to give bis-sulfone 13h (0.8 g, 70%): IR (phase, KBr; threshold for minima, 73% transmittance) 1693.4, 1531.3, 1407.6, 1349.6, 1316.1, 1306.4, 1291.4, 1274.4, 1267.9, 1151.9, 1087.2, 814.7, 770.2, 710.2, 666.4, 572.2, 557.9 cm^{-1} ; ^1H NMR (CDCl_3 , 360 MHz) δ 2.48 (s, 6 H, $-\text{CH}_3$),

3.58 (A2B2X, 4 H, $-\text{CH}_2-$), 4.35 (quintet, 1 H, $J = 6.8$ Hz), 7.38, 7.73 (AB q, 8 H, $J = 8.2$ Hz), 8.13 (d, 1 H, $J = 7.8$ Hz), 8.39 (m, 2 H); ^{13}C NMR (CDCl_3 , 90.4 MHz) δ 194.57, 148.53, 145.84, 136.00, 135.11, 134.24, 130.32, 130.24, 128.21, 128.16, 123.19, 56.01, 33.50, 21.73; mp 174–175 °C. Anal. Calcd for $\text{C}_{24}\text{H}_{23}\text{NO}_7\text{S}_2$: C, 57.47; H, 4.62; S, 12.79. Found: C, 57.34; H, 4.56; S, 12.84.

4-[2,2-Bis[(*p*-tolylsulfonyl)methyl]acetyl]benzoic Acid (13i). Bis-sulfide 12i (1.00 g, 2.30 mmol) was suspended in a 1:1 methanol/water solution (6.7 mL) and acetic acid (1.44 mL) was added. Hydrogen peroxide (30%, 1.4 mL) and sodium tungstate (100 mg, 0.3 mmol) were added and the heterogeneous solution was stirred at room temperature for 16 h. A white solid was filtered and dried in a vacuum desiccator to give 1.14 g (100% yield). A portion (500 mg) was recrystallized from water/methanol to give 344 mg of a white solid: IR (phase, KBr; threshold for minima, 45% transmittance) 520, 560, 570, 690, 720, 745, 755, 810, 820, 935, 1085, 1120, 1130, 1140, 1150, 1180, 1245, 1280, 1305, 1315, 1410, 1415, 1430, 1595, 1690, 1700, 2930, 2980 cm^{-1} ; ^1H NMR ($\text{THF}-d_6$; 270 MHz) δ 2.44 (s, 6 H, $-\text{CH}_3$), 3.56 (m, 4 H, $-\text{CH}_2-$), 4.16 (quintet, 1 H, $-\text{CH}-$, $J = 6.02$ Hz), 7.37, 7.62 (AB q, 8 H, $J = 7.99$ Hz), 7.55, 7.96 (AB q, 4 H, $J = 8.22$ Hz); ^{13}C NMR ($\text{THF}-d_6$, 67.9 MHz) δ 196.7, 167.28, 146.39, 139.58, 137.97, 136.55, 131.27, 131.06, 129.68, 129.61, 56.87, 37.59, 22.04; mp 174–175 °C; R_f (solvent system) 0.25 (9:1 chloroform/methanol). Anal. Calcd for $\text{C}_{25}\text{H}_{24}\text{O}_8\text{S}_2$: C, 59.98; H, 4.83; S, 12.81. Found: C, 59.82; H, 5.00; S, 12.76.

N-[4-[2,2-Bis[(*p*-tolylsulfonyl)methyl]acetyl]benzoyl]-4-iodoaniline (13j). Carboxy bis-sulfone 13i (100 mg, 0.20 mmol) was reacted overnight with thionyl chloride (500 μL) under a blanket of nitrogen. Thionyl chloride was removed in vacuo and the dark yellow solid was dissolved in dry methylene chloride (1 mL). The solvent was removed in vacuo and the yellow solid was dissolved in THF (2 mL). A solution of *p*-iodoaniline (42 mg, 0.19 mmol) and pyridine (17 μL , 16 mg, 0.21 mmol) in THF (1 mL) was treated dropwise (5 min) with the acid chloride solution at 25 °C. After stirring overnight, the solvent was removed in vacuo and the resulting oil was dissolved in methylene chloride (5 mL) and washed with 0.1 N HCl (2 \times 4 mL). The organic phase was dried over sodium sulfate and filtered, and the solvent was removed in vacuo to give 130 mg of foamy solid that was recrystallized from acetone to produce 94 mg of a white solid: 70% yield; IR (phase KBr; threshold for minima, 45% transmittance) 515, 570, 655, 665, 675, 715, 745, 820, 1050, 1090, 1145, 1240, 1290, 1300, 1310, 1390, 1405, 1485, 1500, 1520, 1590, 1660, 1695, 3360 cm^{-1} ; ^1H NMR ($\text{Me}_2\text{SO}-d_6$, 270 MHz) δ 2.42 (s, 6 H, $-\text{CH}_3$), 3.63 (d of d, 2 H, $J = 5.15$ Hz, $J = 14.5$ Hz), 3.76 (d of d, 2 H, $J = 7.14$ Hz, $J = 14.5$ Hz), 4.05 (m, 1 H, CH), 7.43, 7.75 (m, 14 H), 8.00 (d, 2 H, $J = 8.34$ Hz); ^{13}C NMR ($\text{Me}_2\text{SO}-d_6$, 67.5 MHz) δ 21.10, 35.14, 55.15, 87.76, 122.49, 127.78, 127.99, 130.09, 135.09, 136.85, 137.35, 138.72, 139.11, 145.14, 164.70, 195.58; mp 210–210.5 °C; R_f (solvent system) 0.54 (2:1 ethyl acetate/hexane). Anal. Calcd for $\text{C}_{31}\text{H}_{28}\text{INO}_6\text{S}_2$: C, 53.37; H, 4.02; N, 2.00; S, 9.14; I, 18.09. Found: C, 53.00; H, 4.15; N, 1.92; S, 9.44; I, 18.42.

N-[4-[2,2-Bis[(*p*-tolylsulfonyl)methyl]acetyl]benzoyl]-4-[^{125}I]iodoaniline (13k). *p*-[^{125}I]iodoaniline was prepared according to ref 14 with 29.6 mCi (1.09 GBq) of Na^{125}I , high pH (Du Pont-NEN, Boston, MA). The brown solid dissolved in methylene chloride (120 μL) was purified using a silica gel SepPak (Waters, Bedford, MA) column (eluant, 4:1 hexane/ethyl acetate). After passing 3 mL of the solvent through the column, the prod-

uct was eluted with a flush of pure ethyl acetate, analyzed on silica gel plates (1:1 hexane/ethyl acetate), and shown to coelute with authentic, cold *p*-iodoaniline (UV light and autoradiography visualized the product). Concentration under a gentle stream of N_2 resulted in a light brown solid containing 4.75 mCi (175.7 MBq) of ^{125}I . A solution of pyridine (4.3 μL , 4.2 mg, 0.05 mmol) dissolved in THF (500 μL) was added to the *p*-[^{125}I]iodoaniline. The acid chloride of carboxy ETAC 13i (25 mg, 0.05 mmol) was prepared as described for compound 13j, dissolved in THF (1 mL), and added to the pyridine/*p*-[^{125}I]iodoaniline solution prepared above. A solution of nonradioactive *p*-iodoaniline (9.5 mg, 0.40 mmol) dissolved in THF (500 μL) was also added to the reaction mixture. After swirling for 5 min, another lot of the acid chloride of carboxy ETAC 13i (20 mg, 0.04 mmol) in THF (500 μL) was added to the reaction mixture. After an additional 5 min, TLC (2:1, hexane/ethyl acetate) indicated that all of the *p*-iodoaniline had been converted to the desired product. The reaction mixture was concentrated under a gentle stream of N_2 and the resulting yellow glass was dissolved in chloroform (200 μL) and purified with a SepPac silica gel column eluted with 2:1 hexane/ethyl acetate. Radioactive impurities were eluted first followed by the desired product, which formed lustrous white crystals after sitting overnight at room temperature in a sealed ampule. The product was isolated by removing the solvent and drying the solid under a stream of N_2 , yielding 5.2 mg. The product was assayed by TLC (1:1 hexane/ethyl acetate), which showed a single UV and radioactive spot coincident with cold *p*-iodoaniline ETAC 13j (R_f 0.31). This solid was dissolved in Me_2SO (556 μL) and counted in a Capintek CRC-10R well counter. The radiochemical yield was 373.6 μCi (13.82 MBq, 1.26%), with a specific activity of 50.8 mCi (1.88 GBq)/mmol.

α,α -Bis[(*p*-tolylsulfonyl)methyl]-*p*-aminoacetophenone (13l). A suspension of α,α -bis[(*p*-tolylsulfonyl)methyl]-*p*-nitroacetophenone (13h, 1 g, 2 mmol) in 55 mL of 95% ethanol and 3 mL of acetic acid was added to 100 mg of 5% Pd/carbon. The mixture was hydrogenated at about 50 psi on a Parr shaker overnight. The solution was filtered through Celite and the cake was washed with methanol. The solvents were removed in vacuo. Trituration with methanol induced crystallization of light yellow crystals: ^1H NMR (CDCl_3 , 360 MHz) δ 2.04 (s, 6 H), 3.01 (b s, 2 H), 4.6 (A2B2X, m, 4 H), 4.96 (quintet, 1 H), 6.8, 7.25 (ABq, 4 H), 7.4, 7.7 (AB q, 8 H); ^{13}C NMR (CD_3OD , 67.9 MHz) δ 22.58, 24.19, 34.47, 53.30, 54.87, 129.26, 131.03, 136.54, 140.51, 168.60, 197.51; mp 170–173 °C; R_f (solvent system) 0.35 (9:1 chloroform/methanol). Anal. Calcd for $\text{C}_{24}\text{H}_{25}\text{NO}_6\text{S}_2$: C, 61.12; H, 5.34; N, 2.97. Found: C, 61.02; H, 5.40; N, 3.00.

N-[[5-(Dimethylamino)naphthyl]sulfonyl]- α,α -bis[(*p*-tolylsulfonyl)methyl]-*p*-aminoacetophenone (13m). A stirred solution of bis[(*p*-tolylsulfonyl)methyl]-*p*-aminoacetophenone (94 mg, 0.2 mmol) in dry pyridine (0.5 mL) was cooled in an ice bath and treated with a solution of dansyl chloride (54 mg, 0.2 mmol) in acetone (2 mL). After stirring overnight at room temperature the reaction mixture was diluted with 5 mL of H_2O and the orange-yellow gum was taken up in CHCl_3 . The chloroform layer was washed with saturated NaHCO_3 and dried over anhydrous sodium sulfate. The clear yellow oil that remained after the solvent was removed was triturated with methanol to yield 13m (88 mg, 62%) as a bright orange yellow solid: mp 182–185 °C; R_f (solvent system) 0.4 (9:1 chloroform/methanol), bright blue fluorescence. Anal. Calcd for $\text{C}_{36}\text{H}_{36}\text{N}_2\text{O}_7\text{S}_3$: C, 61.34; H, 5.34; N, 2.97.

5.15; N, 3.97. Found: C, 61.12; H, 5.29; N, 4.30.

N-[4-[2,2-Bis[(*p*-tolylsulfonyl)methyl]acetyl]benzoyl]-1-(*p*-aminobenzyl)diethylenetriaminepentaacetic Acid, Pentakis(*tert*-butyl ester) Hydrochloride (13o). Carboxy bis-sulfone 13i (34 mg, 0.068 mmol) was reacted with thionyl chloride (330 μ L, 538 mg, 4.52 mmol) at 50 °C for 2 h under a blanket of nitrogen. Thionyl chloride was removed in vacuo and the yellow foam was dissolved in methylene chloride (0.5 mL). The solvent was removed in vacuo and the yellow solid was dissolved in THF (5 mL) under a blanket of nitrogen. 1-(*p*-Aminobenzyl)diethylenetriaminepentaacetic acid, pentakis(*tert*-butyl ester), synthesized as described in ref 15 (53 mg, 0.068 mmol), was dissolved in THF (5 mL) under a blanket of nitrogen, and this solution was added dropwise to the acid chloride solution via a syringe at 25 °C. After 4.5 h the reaction was complete as analyzed by TLC. The solvent was removed in vacuo to give a yellow glass (79 mg, 92% yield): ^1H NMR (CDCl_3 , 270 MHz) δ 1.31 (m, 45 H), 2.4 (s, 6 H), 2.80 (b, 1 H), 3.00, 3.70 (m, 19 H), 4.15 (m, 1 H), 4.70 (b, 1 H), 7.00 (b, 2 H), 7.30 (d, 4 H, $J = 8.1$ Hz), 7.42 (b d, 2 H), 7.63 (d, 4 H, $J = 8.1$ Hz), 8.00 (b s, 2 H), 8.15 (b d, 2 H), 10.5 (b s, 1 H); ^{13}C NMR (CDCl_3 , 67.9 MHz) δ 21.61, 25.46, 27.93, 28.01, 34.17, 35.94, 49.63, 52.98, 53.50, 55.24, 56.93, 60.47, 67.79, 81.62, 82.00, 84.02, 121.75, 128.09, 128.19, 128.82, 129.00, 130.16, 132.35, 135.00, 135.58, 137.96, 139.75, 145.49, 164.91, 165.33, 170.01, 171.34, 194.71.

N-[4-[2,2-Bis[(*p*-tolylsulfonyl)methyl]acetyl]benzoyl]-1-(*p*-aminobenzyl)diethylenetriaminepentaacetic Acid (13p). Pentaester 13o (15 mg, 0.012 mmol) reacted with trifluoroacetic acid (0.5 mL) at 25 °C under a blanket of nitrogen for 2.5 h. The TFA was then removed in vacuo, resulting in a yellow glass which was dissolved in methanol (0.5 mL). The solvent was removed in vacuo to yield 13 mg (92% yield) of yellow glass: ^1H NMR (CD_3OD , 270 MHz) δ 2.53 (s, 6 H), 2.65 (m, 1 H), 3.19 (m, 3 H), 3.45, 3.85 (m, 17 H), 4.22 (m, 1 H), 4.60 (b s, 2 H), 7.34, 7.73 (AB q, 4 H, $J = 8.1$ Hz), 7.46, 7.66 (AB q, 4 H, $J = 8.3$ Hz), 7.66, 7.9 (AB q, 4 H, $J = 8.3$ Hz); ^{13}C NMR (CD_3OD , 67.9 MHz) δ 21.67, 34.54, 37.19, 49.94, 50.63, 53.21, 53.57, 54.98, 55.40, 56.40, 56.61, 57.21, 61.56, 122.80, 129.05, 129.41, 129.70, 130.80, 131.36, 135.29, 136.51, 136.63, 138.33, 138.49, 140.89, 147.16, 167.41, 169.09, 174.17, 175.44, 196.91.

1-(*p*-Nitrobenzyl)diethylenetriaminepentaacetic Acid, Pentakis(*tert*-butyl ester) (Scheme II, 14). 1-(*p*-Nitrobenzyl)diethylenetriamine trihydrochloride (1.11 g, 3.19 mmol) prepared as described in ref 15, 35.3 g (255 mmol) of potassium carbonate, and 3.84 g (23.1 mmol) of potassium iodide were placed in a dry 250-mL round-bottom flask and suspended in 100 mL of dry THF under nitrogen. *tert*-Butyl 2-bromoacetate (5.15 mL, 31.9 mmol) was added via a syringe and the reaction mixture was sonicated under an atmosphere of nitrogen for 72 h at 40 °C. The reaction mixture was taken up in 400 mL of ethyl acetate and 100 mL of water. The layers were separated, and the aqueous layer was extracted with an additional 100 mL of ethyl acetate. The organic layers were combined and dried over magnesium sulfate, filtered, and concentrated in vacuo to yield a brown oil. This was purified by flash chromatography on silica gel (2:8 ethyl acetate/hexane) to yield 1.81 g (70% yield) of a yellow oil: ^1H NMR (CDCl_3 , 270 MHz) δ 1.41 (s, 18 H), 1.42 (s, 9 H), 1.43 (s, 18 H), 2.35–2.5 (m, 1 H), 2.7–3.2 (m, 8 H), 3.30 (s, 2 H), 3.39 (s, 4 H), 3.41 (s, 4 H), 7.48 (d, 2 H, $J = 8.7$ Hz), 8.09 (d, 2 H, $J = 8.7$ Hz); ^{13}C NMR (CDCl_3 , 67.5 MHz) δ 28.1, 37.1, 52.1, 53.1, 53.4, 55.9, 56.2, 56.3,

62.7, 80.8, 80.9, 81.1, 123.2, 130.2, 146.4, 148.7, 170.1, 170.4, 171.0.

1-(*p*-Aminobenzyl)diethylenetriaminepentaacetic Acid, Pentakis(*tert*-butyl ester) (Scheme II, 15). 1-(*p*-Nitrobenzyl)diethylenetriaminepentaacetic acid, pentakis(*tert*-butyl ester) (1.41 g, 1.74 mmol) (Scheme II, 14) was dissolved in 40 mL of absolute ethanol in a 200-mL round-bottom flask and the atmosphere was flushed with nitrogen. Ten percent Pd/carbon (181 mg) was added and the atmosphere was evacuated and replaced with hydrogen three times. The reaction mixture was then stirred rapidly under 1 atm of H_2 for 18 h. At this time only product was detected by TLC (1:1 ethyl acetate/hexane, R_f 0.3). The reaction mixture was filtered through Celite and the ethanol was removed in vacuo to yield 1.39 g of a yellow oil (100% yield), which was pure by NMR: ^1H NMR (CDCl_3 , 270 MHz) δ 1.39 (s, 9 H), 1.42 (s, 18 H), 1.43 (s, 18 H), 2.4–3.15 (m, 9 H), 3.33 (s, 2 H), 3.37 (s, 4 H), 3.42 (s, 4 H), 6.55 (d, 2 H, $J = 8.2$ Hz), 6.96 (d, 2 H, $J = 8.2$ Hz); ^{13}C NMR (CDCl_3 , 67.5 MHz) δ 28.1, 36.2, 52.6, 53.0, 53.7, 55.0, 56.2, 63.2, 80.3, 80.4, 80.6, 115.4, 130.0, 130.5, 143.9, 170.6, 171.3.

Antibody Purification. The monoclonal antibody used in this study was B6.2, a mouse antihuman tumor monoclonal IgG₁ (16, 17), and was purified from ascites by 50% ammonium sulfate precipitation and cation-exchange chromatography utilizing the Pharmacia FPLC (fast protein–liquid chromatography) system and a Mono S column (18). Purity was determined by GF-250 (Du Pont, Wilmington, DE) SEC² HPLC and electrophoresis on 5–15% polyacrylamide SDS³ gels (19) under both reducing and nonreducing conditions. The hybridoma cells were supplied by Dr. J. Schlom (N.C.I.). Antibody concentration was determined with an extinction coefficient of 1.89 at 0.1% protein (280 nm) based on amino acid analysis.

Antibody Reduction. Partial reduction of the antibody (1–3 mg/mL in 0.1 M Na phosphate buffer, pH 8.0, 2 mM EDTA) was achieved by making the antibody solution 0.05 M in 2-mercaptoethanol followed by 45-min incubation at 37 °C. Excess reductant was removed and buffer exchange was accomplished by G-25 M Sephadex (Pharmacia, Piscataway, NJ) gel filtration on a 1 \times 40 cm column by loading 1–2 mL and collecting 1.5 mL/fraction. Sulfhydryl groups in the partially reduced antibody were quantitated with 2,2'-dithiodipyridine (20) and an extinction coefficient at 343 nm of 7600 1/M (21). The typical partially reduced antibody preparation resulted in 9–10 sulfhydryl groups/mol of antibody. All buffers and reagents used in this study were prepared in deionized water supplied from a Millipore (Bedford, MA) Milli-Q system. Me_2SO was used to dissolve the ETAC reagents prior to addition to the antibody. The 2,2'-dithiodipyridine (Aldrithiol-2) was obtained from Aldrich (Milwaukee, WI).

Structural Analysis. Modified antibody samples were analyzed on 5–15% polyacrylamide SDS gels (19) under reducing and nonreducing conditions using about 25 μ g of protein per lane. The samples were boiled 3 min prior to electrophoresis. High and low molecular weight standards were obtained from Bio-Rad (Richmond, CA). The protein bands in the Coomassie brilliant blue R-250 stained gels were scanned with a Hoefer GS300 densitometer, and the peaks were quantitated with a Hewlett-Packard 3392 integrator. On the reducing SDS gels, the ETAC

² Size-exclusion chromatography.

³ Sodium dodecyl sulfate.

cross-linked antibody was determined as the percent protein bands at or above 50 000 Da. On the nonreducing SDS gels, the ETAC cross-linked antibody was determined as the percent stained antibody at 150 000 Da. Since the antibody had been partially prerduced, only ETAC cross-links would prevent significant subunit separation during denaturation and subsequent electrophoresis.

Intermolecular antibody cross-linking was examined under native conditions using SEC HPLC on a Du Pont GF250 column equilibrated with 0.2 M sodium phosphate buffer, pH 7.0, monitoring absorption at 280 nm. Absorption peaks were quantitated with a Spectra-Physics 4200 integrator-recorder. New absorption peaks at greater than 150 000 Da by HPLC were quantitated as intermolecularly cross-linked antibody.

ETAC Modification. Antibody modification was accomplished by addition of 10 molar excess of ETAC to antibody (1 mg/mL) in 0.1 M phosphate, pH 7 and 8, 2 mM EDTA. Stock solutions of 10^{-3} M ETAC in Me_2SO were prepared so the final Me_2SO concentration with the antibody was less than 5% v/v. The reactions were incubated overnight at room temperature and then frozen at -20°C .

^{125}I -labeled ETAC 13k modifications were done with both partially reduced (sulfhydryl directed) and unreduced (amine directed) antibody at 1 mg/mL and a 20 molar excess of ^{125}I -labeled ETAC 13k in either 0.1 M sodium phosphate, pH 6 or 7, or 0.1 M sodium acetate, pH 4 or 5; all buffers were 2 mM in EDTA.

ETAC DTPA 13p modifications for both partially reduced (sulfhydryl directed) and unreduced (amine directed) antibody were done by reaction of 2.5 molar excess of ETAC DTPA 13p with 1 mg/mL antibody in sodium acetate, pH 5, 2 mM EDTA. The reactions were incubated overnight at room temperature, dialyzed against 0.1 M sodium phosphate, pH 7.0, and stored at -20°C .

Structural Analysis of ^{125}I -Labeled ETAC B6.2. The ^{125}I -labeled ETAC 13k modified antibody was analyzed by electrophoresis on 5–15% acrylamide SDS gels under reducing and nonreducing conditions. The gels were dried onto 3-mm Whatman paper in vacuo with a Hoefer SE 540 gel dryer and autoradiographed on Kodak (Rochester, NY) XAR5 film with an intensifying screen (Du Pont, Wilmington, DE) for 6–24 h. The stained bands were cut out and counted in a LKB 1282 γ -counter. The ^{125}I ETAC 13k molar incorporation/mol of antibody was calculated from the amount of ^{125}I in the dried gel. The molar incorporation of ^{125}I -labeled ETAC 13k in each stained protein band was determined from the specific activity (50.8 mCi/mmol, 1.88 GBq/mmol) of ^{125}I -labeled ETAC 13k.

^{111}In -Labeled ETAC DTPA B6.2. $^{111}\text{InCl}_3$ (Du Pont-NEN, Boston, MA) was mixed with an equal volume of 1 N HCl to dissolve the ^{111}In colloid and the pH was then adjusted with an equal volume of 1 M sodium acetate, pH 4.5. An equal volume of [^{111}In]indium acetate mixture was added to the DTPA ETAC 13p or bis cyclic anhydride DTPA antibody complex and incubated for 1 h at room temperature. The ^{111}In -labeled DTPA ETAC antibody was purified by SEC HPLC with a Du Pont GF250 column, monitoring absorption at 280 nm and radioactivity with a Nico MD3 Ratemeter and a NaI probe (Ludlum Measurements Inc., Sweetwater, TX). The column was equilibrated and eluted with 0.2 M sodium phosphate, pH 7.0, at a flow rate of 1 mL/min, collecting 0.5-mL fractions. Incorporation of 13p was calculated by multiplying the percent area under the ^{111}In -labeled DTPA

ETAC antibody peak from the SEC HPLC trace by the mol excess reacted with the antibody. In a typical preparation, 1.4 mol of DTPA ETAC 13p was incorporated per mol of partially reduced antibody when the reaction began with 2.5 mol of 13p per mol of partially reduced antibody.

Specific activity was determined by counting the ^{111}In radioactivity with a Capintec CRC 12 detector and measuring the protein in a Perkin-Elmer Lambda Array 3840 spectrophotometer. Typical specific activities for both the DTPA ETAC 13p and the bis cyclic anhydride DTPA modified antibodies were 5–10 mCi (185–370 MBq)/mg of antibody.

^{125}I -Labeled B6.2. Iodination of antibody was as previously described in ref 22. Briefly, the reaction involved 200 μg of Iodogen (Pierce, Rockford, IL) with 20 μg of antibody in 0.1 M sodium phosphate, pH 7.2, per 1 mCi (37 MBq) of ^{125}I for 2 min at room temperature. The reaction was terminated by separating the radiolabeled antibody from free iodine on a 10-mL BSA⁴-coated G-25 M column.

Immunoassays. The immunoactivity of the ETAC-modified antibodies was determined by ELISA⁶ and by a direct binding assay. The tissue culture of the human colorectal cell line LS174T used in the direct binding assay and the ELISA was described in ref 22.

ELISA. The antibody at an initial concentration of 40 $\mu\text{g}/\text{mL}$ was dissolved in 1% BSA/PBS (2.16 g of $\text{Na}_2\text{HPO}_4 \cdot 7\text{H}_2\text{O}$, 0.2 g of KH_2PO_4 , 8.0 g of NaCl, 0.2 g of KCl, 0.1 g of CaCl_2 , and 0.1 g of $\text{MgCl}_2 \cdot 6\text{H}_2\text{O}$ per liter of distilled water (23). Antibody (50 $\mu\text{L}/\text{well}$) was titrated 1:2 v/v with 1% BSA/PBS and then added to an LS174T tumor cell extract (24) coated microtiter plate (20 μg of cell extract in 100 μL of PBS/well, dried at 37°C overnight, blocked with 100 $\mu\text{L}/\text{well}$ of 5% BSA/PBS for 1 h at 37°C , and washed three times with 100 $\mu\text{L}/\text{well}$ of 1% BSA/PBS). After incubation for 1 h at 37°C , the liquid was removed, and the wells were washed three times with 100 μL of 1% BSA/PBS.

The second antibody, goat antimouse IgG heavy and light chains conjugated to horseradish peroxidase and absorbed against human serum (Kirkegaard and Perry, Gaithersburg, MD), was dissolved to 0.1 mg/mL in water and further diluted 1/1000 v/v with 1% BSA/PBS. The second antibody (50 μL) was added to each well, incubated for 1 h at 37°C , and then removed, and the wells were washed three times with 100 μL of 10 mM Tris-Cl, pH 8.0, containing 0.05% Tween 20 and 0.01% merthiolate (w/v). A solution (50 μL) of *o*-phenylenediamine (0.2%) w/v and 0.015% H_2O_2 v/v in a 65 mM sodium phosphate/17 mM citric acid buffer, pH 6.3, with 0.01% w/v merthiolate was added to each well. The plate was incubated 5–10 min at 37°C to allow color development. The reaction was quenched with 4.5 M sulfuric acid (50 $\mu\text{L}/\text{well}$). Absorption in the wells was measured in a Dynatech (Chantilly, VA) MR600 Microplate reader at 490 nm. Background 490-nm absorption was determined in wells which contained all reagents except the LS174T cell extract. The data was plotted as the logarithm of the reciprocal titer value versus the 490-nm absorption.

Direct Binding. The ^{111}In -labeled DTPA ETAC 13p modified antibody was assayed for immunoactivity prior to any animal studies by a direct binding assay. Dynatech Immulon 2 (Chantilly, VA) polystyrene 96-

⁴ Bovine serum albumin.

⁵ Polyacrylamide gel electrophoresis.

⁶ Enzyme linked immunosorbent assay.

well break-away plates were coated with titered LS174T cell extract diluted in PBS from 100 to 0.8 μ g per well and dried overnight at 37 °C. Following antigen coating, the wells were blocked with 100 μ L of 5% BSA/PBS for 1 h at 37 °C and then washed three times with 1% BSA/PBS. 111 In-labeled DTPA ETAC antibody and an 125 I-labeled antibody control were diluted in 1% BSA/PBS to a final concentration of 200 ng/mL. The antibody was allowed to bind for 60 min at 37 °C in a humidified incubator. The plates were washed three times with 1% BSA/PBS and the wells were counted in a LKB 1282 Compugamma γ -counter. The percent bound was expressed as a percentage of the total counts added to the wells.

Animal Studies. 111 In-labeled DTPA ETAC antibody, (2.5–10 μ Ci, 92.5–370 kBq) was injected into the lateral tail vein of CD1 mice weighing 26–49 g (Charles River Breeding Laboratories, Wilmington, MA). Animals were sacrificed by cervical dislocation at 24 h and the 111 In was measured in the blood, liver, and kidney with a γ -counter. The percent injected dose per gram of tissue (% ID/g) was calculated with the decay corrected to the time of injection.

RESULTS

Synthesis and Chemistry. The synthesis of these ETAC reagents was accomplished through the reaction of the Mannich base salt of an acetophenone with 2 equiv of a thiophenol and formaldehyde. The sequence appears to follow the process of retro-Michael reaction with loss of the amine group, thio-Michael addition, aldol condensation with formaldehyde, and elimination of water followed by the addition of the second thiol finally yielding the bis[(aryltio)methyl]acetophenones. These materials could then be easily oxidized to the corresponding bis[(arylsulfonyl)methyl]acetophenones with peracetic acid or Oxone (25). With use of these techniques the bis[(arylsulfonyl)methyl]-*p*-chloro-, -*p*-nitro-, -*m*-nitro-, and -*p*-carboxyacetophenones (13c,d,g,h,i) were synthesized.

In the sulfone compounds, chemical modification of the aromatic substitution sites was unexceptional. The nitro substituted bis-sulfone derivatives (13f–h) could be reduced to the corresponding amines with a palladium on carbon catalyst in ethanol with acetic acid. The amines so formed could be derivatized with acid chlorides, sulfonyl chlorides, and isocyanates (data for isocyanates not reported in this paper) using pyridine as a base for the reaction. Elimination of the sulfone functions did not appear significant under these conditions.

p-Carboxy derivative 13i could be converted to the acid chloride using thionyl chloride and this could in turn be processed to a wide variety of amide derivatives. These carboxy derivatives proved to be the most useful for construction of the radioactivity tagged linkers.

The pentakis(*tert*-butyl ester) of 1-(*p*-aminobenzyl)diethylenetriaminepentaacetic acid (Scheme II, 14) was synthesized by using a procedure analogous to that described in ref 15. 1-(*p*-Nitrobenzyl)diethylenetriamine hydrochloride was *N*-alkylated with bromo-*t*-butyl acetate in 70% yield to give the pentakis(*tert*-butyl ester) of 1-(*p*-nitrobenzyl)diethylenetriaminepentaacetic acid (Scheme II, 14). This reduced cleanly with hydrogen using palladium/carbon as the catalyst producing the *p*-aminobenzyl analogue (Scheme II, 15). This aromatic amine and ETAC acid chloride 13h reacted to yield DTPA-linked ETAC reagent 13o.

Models of Exchange Process. The exchange process and transfer cross-linking could be readily demonstrated in model reactions. For example, treatment of

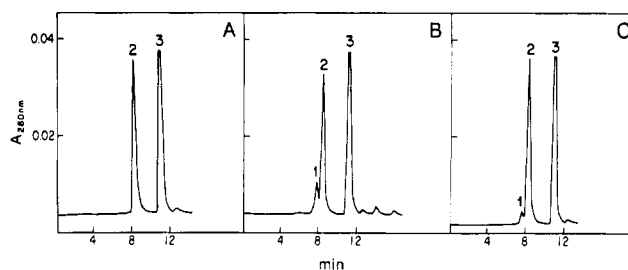


Figure 1. SEC HPLC of partially reduced antibody. A, no ETAC treatment; B, unreduced antibody; C, partially reduced antibody. B and C were reacted with a 10 molar excess of ETAC 13e at pH 8.0 for 24 h at room temperature. Analyses were done at 10 μ g of antibody on a Du Pont GF-250 column; Peak 1, intermolecularly cross-linked antibody; peak 2, antibody; peak 3, a buffer component.

bis[(*p*-tolylsulfonyl)methyl]-*p*-nitroacetophenone (13f) with *p*-chlorothiophenol in methanol with triethylamine or with sodium bicarbonate gave an almost quantitative yield of bis[[(*p*-chlorophenyl)thio]methyl]-*p*-nitroacetophenone (12e). The intermediate α -[(*p*-tolylsulfonyl)methyl]-*p*-nitrophenyl vinyl ketone was observed by NMR upon treatment of the α,α -bis[(*p*-tolylsulfonyl)methyl]-*p*-nitroacetophenone (13f) with triethylamine in chloroform. The vinyl proton singlets at δ 6.25 and 5.9 and the CH_2SO_2 singlet at δ 4.35 are diagnostic. Small amounts of unsaturated ketone could be observed by TLC when starting bis-sulfone 13f was allowed to stand in a polar solvent at room temperature for a short time. Reaction of *p*-nitro bis-sulfone 13e with acetylcysteine or glutathione in aqueous basic methanol also yielded the corresponding bis-thioether derivatives by the exchange process as evidenced by their isolation and characterization (NMR, MS) to be described in a future publication.

Evaluation of Antibody Partial Reduction and ETAC Cross-Linking. The antibody used in this study was a mouse monoclonal IgG1 with a classical antibody molecular structure of two identical heavy chains (50 000 Da) and two identical light chains (25 000 Da), which under native conditions, or when unreduced and electrophoresed on nonreducing gels, behave as an oligomeric protein of 150 000 Da. Partial reduction will result in various antibody intermediate species on nonreducing SDS gel electrophoresis.

Partial reduction of B6.2 typically resulted in, at most, 10 mol of sulfhydryl per mol of antibody as measured with the 2,2'-dithiodipyridine reagent. SEC HPLC analyses indicated that untreated antibody had only a trace of aggregate present (Figure 1A) whereas unreduced antibody treated with a 10 molar excess of ETAC 13e reagent had 18.3–20.6% interantibody cross-linking (Figure 1B). The partially reduced antibody treated with 10 molar excess of ETAC 13e had 2.4–5.7% interantibody cross-linking (Figure 1C).

Unreduced antibody represented amine modification as there are no free sulfhydryl groups in the unreduced antibody based on 2,2'-dithiodipyridine determinations. As shown in Table I, based on HPLC analyses, amine-based ETAC cross-linking of unreduced antibody (column 3) was greater than that observed for sulfhydryl based (partially reduced antibody) cross-linking (column 2). However it seems likely that both inter- and intrachain cross-linking of sulfhydryls would take place and thus less interantibody cross-linking would occur and be detected by the HPLC analyses. When the unreduced or partially reduced antibody was treated with ETAC 13c, 13l, or 13e at various pH's, less intermolecular antibody cross-

Table I. Inter- and Intraantibody ETAC Cross-Linking of Unreduced and Partially Reduced Antibody^a

ETAC	SEC HPLC ^b		gel electrophoresis	
	partially reduced	unreduced	reducing gel ^c	nonreducing gel ^d
13c	6.9	11.7	42	96.8
13e	5.7	18.3	37.8	44.6
13f	1.8	10.2	32.6	43.9
13l	2	1.9	trace	99.1
13i	5.9	8.8	36.4	80.9
13m	trace	trace	6.4	91.6
13h	12.3	17.7	14.8	59.3
	—	0 ^f	0 ^{e,f}	99.8 ^{e,f}
	trace ^f	—	0 ^f	50 ^f

^a All samples, unless otherwise indicated, were treated with a 10 molar excess of ETAC at room temperature, for 24 h, at pH 8.0.

^b SEC HPLC detected percentage of intermolecularly cross-linked antibody. ^c % SDS-PAGE^g stained bands greater than 50 000 Da on a reducing gel. Unless otherwise noted, the antibody was partially reduced as described. ^d % SDS-PAGE stained band at 150 000 Da on a nonreducing gel. Unless otherwise noted, the antibody was partially reduced as described. ^e No antibody prereluction. ^f No ETAC.

Table II. The pH Dependence of Interantibody ETAC Cross-Linking^a

ETAC	partially reduced antibody			unreduced antibody		
	pH 6.0	pH 7.0	pH 8.0	pH 6.0	pH 7.0	pH 8.0
13c	trace	1	4.5	1.3	10.0	17.2
13l	trace	trace	2.3	trace	2	2.6
13e	2.0	2.5	2.4	7.9	22.3	20.6

^a SEC HPLC quantitation of percent intermolecularly cross-linked antibody. All samples reacted with indicated ETAC at a 10 molar excess, overnight, at room temperature, at the pH indicated.

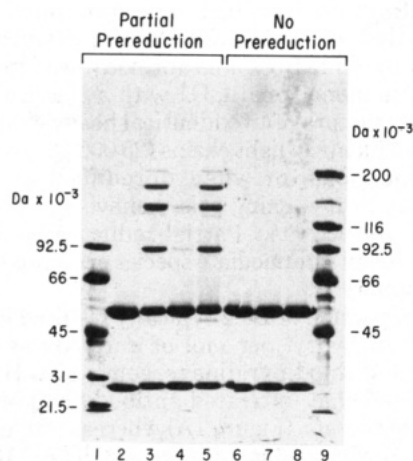


Figure 2. Reducing 5–15% polyacrylamide SDS gel electrophoresis of partially reduced and unreduced antibody treated with a 10 molar excess of ETAC at room temperature for 24 h at pH 8.0, 25 μ g of protein/lane. Lanes 2–5, partially reduced antibody; lanes 6–8 controls with no prereluction. Lane 1, low molecular weight standards; lane 2, partially reduced antibody and no ETAC; lane 3, ETAC 13c; lane 4, ETAC 13l; lane 5, ETAC 13m; lane 6, no prereluction of antibody and no ETAC; lane 7, ETAC 13c; lane 8, ETAC 13l; lane 9, high molecular weight standards.

linking was observed at lower pH values, based on SEC HPLC analyses. This data is summarized in Table II.

Reducing SDS gel electrophoresis of unreduced antibody (Figure 2, lane 6) and unreduced antibody reacted with ETAC 13c (Figure 2, lane 7) or ETAC 13l (Figure 2, lane 8) revealed little if any antibody cross-linking as only 25 000- and 50 000-Da protein bands were observed

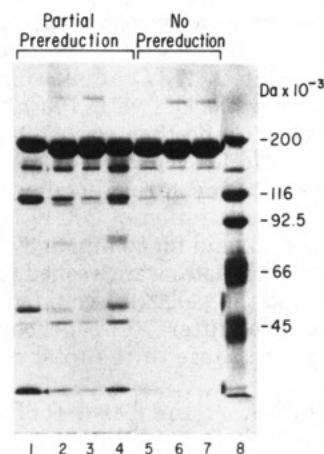


Figure 3. Nonreducing 5–15% polyacrylamide SDS gel electrophoresis of partially reduced and unreduced antibody reacted with ETAC as in Figure 2. Lanes 1–4, partially reduced antibody; lanes 5–7, controls with no prereluction. Lane 1, partially reduced antibody with no ETAC; lane 2, ETAC 13c; lane 3, ETAC 13l; lane 4, ETAC 13m; lane 5, no prereluction of antibody and no ETAC; lane 6, ETAC 13c; lane 7, ETAC 13l; lane 8, high molecular weight standards. For fuller details of the SDS gel electrophoresis see the Experimental Procedures.

(heavy and light chains). Reducing SDS gel electrophoresis of partially reduced antibody reacted with various ETACs presented a very different picture. Protein bands greater than 50 000 Da provided clear evidence of intraantibody cross-linking with ETAC 13c (Figure 2, lane 3) or ETAC 13m (Figure 2, lane 5). However, only traces of ETAC 13l cross-linking were detected (Figure 2, lane 4), while the control had no evidence of cross-linking (Figure 2, lane 2). The results for intraantibody cross-linking as measured by reducing SDS gels are summarized in Table I, column 4.

Nonreducing SDS gel electrophoresis of unreduced antibody resulted in a stained band at 150 000 Da and traces of lower molecular mass material (Figure 3, lane 5). This pattern was essentially the same for unreduced antibody reacted with ETAC 13c (Figure 3, lane 6) or ETAC 13l (Figure 3, lane 7). There was a trace of interantibody cross-linking evident for ETAC 13c and ETAC 13l shown as a protein band at greater than 150 000 Da molecular mass.

Nonreducing SDS gel electrophoresis of partially reduced antibody, prior to ETAC treatment, showed a dramatically different protein band pattern in the gel. The control shows individual light and heavy chains as well as intermediate species (Figure 3, lane 1). Treatment of partially reduced antibody with ETAC 13c (Figure 3, lane 2) and 13l (Figure 3, lane 3) clearly lessens the breakdown due to partial reduction, whereas ETAC 13m was not as effective a cross-linker of SH groups as determined by the greater quantitative antibody structural breakup evident on the gel (Figure 3, lane 4). The results of interantibody ETAC cross-linking of unreduced antibody as measured on nonreducing SDS gels are summarized in Table I, column 5.

The immunoreactivity of the ETAC-modified unreduced and partially reduced B6.2 antibody was qualitatively estimated with an ELISA. The unreduced ETAC 13c modified antibody appeared to bind antigen slightly less than the control (Figure 4A) whereas the partially reduced ETAC 13c modified antibody had essentially identical binding (Figure 4B). The amine-directed cross-linking (unreduced antibody) did not significantly compromise immunoreactivity, while the sulfhydryl-

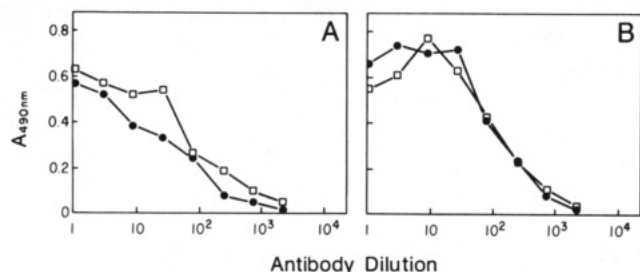


Figure 4. Antibody ELISA: A, antibody control (\square) and unreduced antibody treated with ETAC 13k (\bullet), 10 molar excess at room temperature for 24 h at pH 8.0; B, antibody control (\square) and partially reduced antibody treated with ETAC 13k (\bullet) as above.

Table III. Molar Incorporation of ^{125}I -Labeled ETAC 13k^a

pH	partially reduced antibody	unreduced antibody	ratio
7	2.52 ^b	0.95 ^b	2.65 ^c
6	0.98	0.44	2.22
5	1.03	0.24	4.29
4	1.41	0.09	15.16

^a A 20 molar excess of ^{125}I -labeled ETAC 13k was reacted with partially reduced and unreduced antibody at room temperature, overnight. Incorporation was calculated from the radioactivity detected in stained protein bands cut from a 5–15% acrylamide SDS gel electrophoresed under nonreducing conditions. ^b Values reported as mol ^{125}I -labeled ETAC 13k/mol antibody. ^c Ratio of mol of ^{125}I -labeled ETAC 13k partially reduced antibody/mol of ^{125}I -labeled ETAC 13k unreduced antibody.

directed ETAC 13k cross-linking (partially reduced antibody), presumably in the hinge region, did not compromise immunoreactivity at all.

^{125}I -Labeled ETAC 13k Incorporation into Antibody. Partially reduced and unreduced antibody was reacted with a 20 molar excess of ^{125}I -labeled ETAC 13k at pH 4–7. The molar incorporation was calculated by counting the stained protein bands from the SDS polyacrylamide gel. ^{125}I -labeled ETAC 13k reactivity with amines in the unreduced antibody was decreased by lowering the pH (Table III).

^{125}I -labeled ETAC 13k reactivity with partially reduced antibody represented modification of both amine and sulfhydryl groups. The greatest selectivity for sulfhydryl versus amine reactivity, as measured by the ratio of ^{125}I -labeled ETAC 13k incorporation into partially reduced antibody versus unreduced antibody, was achieved at pH 4 (Table III).

Kinetic Study. ^{125}I -labeled ETAC 13k reaction with partially reduced antibody could be followed by SDS gel electrophoresis and autoradiography or γ -counting. A kinetic study of ^{125}I -labeled ETAC 13k incorporation at pH 4–7 determined where the site directed modification of the antibody occurred. A 20 molar excess of ^{125}I -labeled ETAC 13k was reacted with partially reduced antibody at room temperature. The reaction was stopped by freezing samples in a dry ice/acetone bath and storing them frozen at -70°C until analyzed. Following gel electrophoresis and autoradiography, the dramatic equilibrium nature of this cross-linker was evident. The ^{125}I label had moved to the higher molecular mass protein bands over the time course at pH 7 (Figure 5). The stained protein bands were cut from the gel and counted, and the percentage of the total recovered ^{125}I was plotted versus each molecular mass at the 23-h time point (Figure 6).

At pH 7 and 6, 85% of the total radioactivity was found in the higher molecular mass bands of 150 000, 125 000

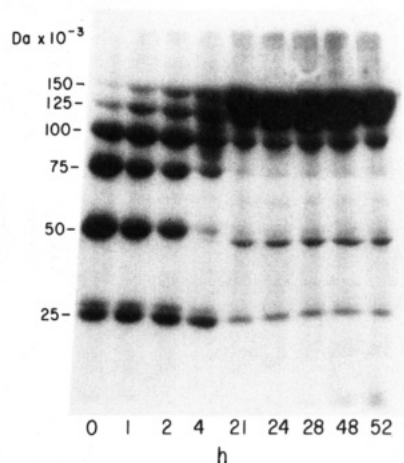


Figure 5. Autoradiograph of a nonreducing 5–15% polyacrylamide SDS gel using Kodak XAR5 film for 18 h. Reaction conditions: partially reduced antibody, 20 molar excess of ^{125}I -labeled ETAC 13k, pH 7, at room temperature. Reactions were stopped by freezing at -70°C with samples taken at 1, 2, 4, 21, 24, 28, 48, and 52 h.

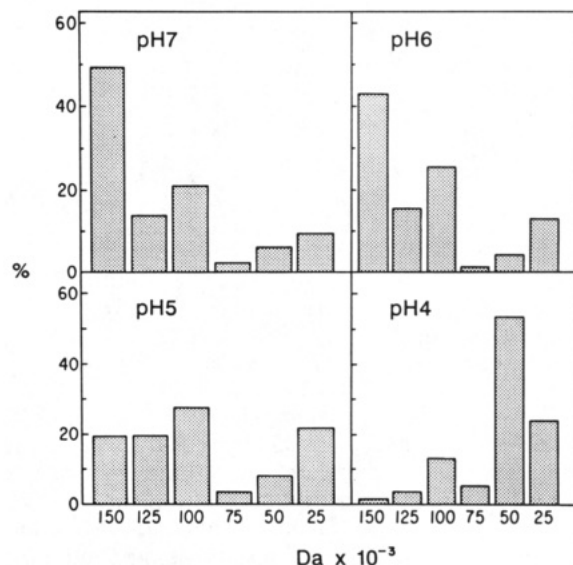


Figure 6. The percent of total radioactivity incorporated into stained protein bands at pH 4–7. Reaction conditions: partially reduced antibody, 20 molar excess of ^{125}I -labeled ETAC 13k, pH 4–7, overnight at room temperature.

and 100 000 Da. At pH 5, 65% of the total activity was in the same molecular mass range, while at pH 4 only 30% of the radioactivity was in that range.

The ^{125}I -labeled ETAC 13k incorporated in each molecular mass band was determined over the time course at pH 4 and 7 (Figure 7). The molecular distribution of ^{125}I -labeled ETAC 13k in the partially reduced antibody can be inferred from the various combinations of ^{125}I -labeled heavy and light chains. At pH 7, the ^{125}I was initially found in the 50 000-Da bands (heavy chain) and 25 000-Da bands (light chain). Over the time course, ^{125}I -labeled ETAC 13k was found more in the 150 000- and 125 000-Da bands, while decreasing in the 50 000- and 25 000-Da bands. Incorporation of ^{125}I -labeled ETAC 13k into the intermediate 100 000- and 75 000-Da bands remained constant over the time course. At pH 4, the ^{125}I -labeled ETAC 13k incorporation is very low with the majority of the label in the 50 000-Da band and very little in the 150 000- or 125 000-Da bands (Figure 7). The greatest ratio of sulfhydryl to amine ETAC reactivity was previously determined to be at pH 4. Unfortunately, the

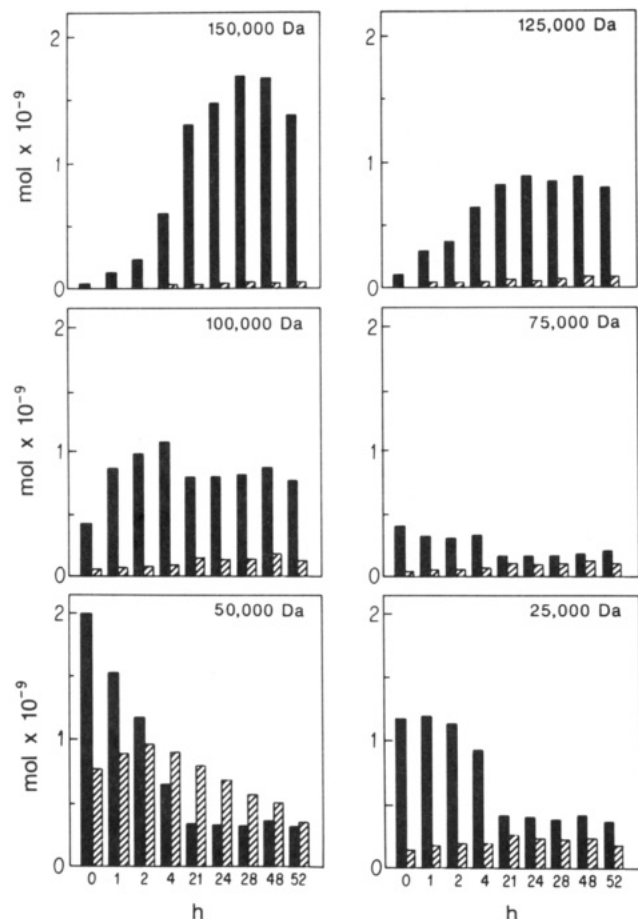


Figure 7. Time course of ¹²⁵I-labeled ETAC 13k incorporation into stained protein bands at pH 7 (solid) and 4 (hatched). Reaction conditions and samples taken as in Figure 6.

kinetic study indicated that at pH 4 the ¹²⁵I-labeled ETAC 13k was incorporated as intrachain cross-links in the heavy chain. Site-directed interchain (hinge region) cross-linking at pH 4 as measured by the radioactivity in the 100 000-, 125 000-, and 150 000-Da stained-protein bands was very low. Therefore, to obtain the maximum hinge region sulfhydryl site directed ETAC modification while minimizing amine modification, pH 5 was chosen for the reaction of DTPA ETAC 13p with the monoclonal antibody.

DTPA ETAC 13p Modification. The amine and sulfhydryl directed ¹¹¹In-labeled DTPA ETAC 13p antibodies were HPLC purified (Figure 8) and assayed for immunoreactivity by a direct binding assay and found to be as immunoreactive as an iodinated control antibody. When the material was injected into CD1 mice, the sulfhydryl-directed ¹¹¹In-labeled DTPA ETAC 13p antibody remained in the blood longer than the amine-directed ¹¹¹In-labeled DTPA ETAC 13p antibody or ¹¹¹In-labeled bis cyclic anhydride DTPA modified antibody. The ¹¹¹In-labeled bis cyclic anhydride DTPA modified antibody data was obtained from ref 26. The sulfhydryl-directed ¹¹¹In-labeled DTPA ETAC 13p antibody showed significantly higher liver accumulation at 24 h. Clearance occurred through the kidney, especially for the ¹¹¹In-labeled bis cyclic anhydride DTPA modified antibody and the amine-directed ¹¹¹In-labeled DTPA ETAC 13p antibody, which had a significantly higher kidney accumulation than the sulfhydryl-directed ¹¹¹In-labeled DTPA ETAC 13p antibody. Overall, the sulfhydryl-modified ¹¹¹In-labeled DTPA ETAC 13p antibody cleared more slowly from the blood and liver whereas the amine-mod-

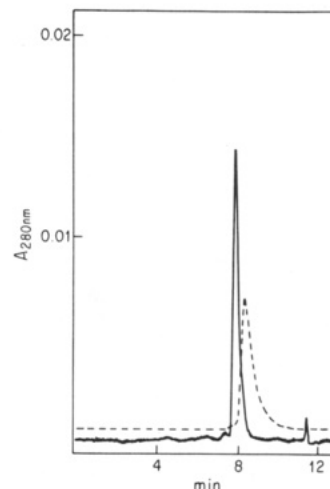


Figure 8. The SEC HPLC analysis of purified ¹¹¹In-labeled DTPA ETAC 13p antibody on a GF250 (Du Pont) column: ¹¹¹In trace (---), pen offset approximately 1 min, and absorbance at 280 nm (—).

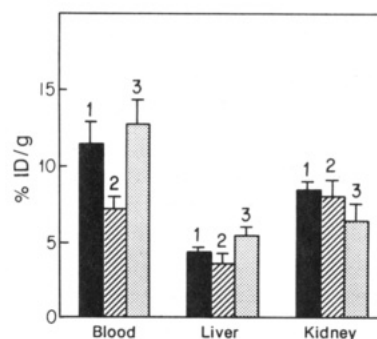


Figure 9. The percent injected dose/g tissue (% ID/g) determined for ¹¹¹In-labeled DTPA ETAC antibody and ¹¹¹In-labeled bis cyclic anhydride DTPA modified antibody in blood, liver, and kidney at 24 h: (1) ¹¹¹In-labeled bis cyclic anhydride DTPA modified antibody (from Brown et al., 1986); (2) unreduced, amine-directed ¹¹¹In-labeled DTPA ETAC 13p antibody; and (3) partially reduced, sulfhydryl-directed ¹¹¹In-labeled DTPA ETAC 13p antibody.

ified ¹¹¹In-labeled DTPA ETAC 13p antibody cleared more rapidly from the blood via the kidney (Figure 9).

DISCUSSION

The design of these ETAC reagents evolved from many trial structures. The keto group was chosen as the activating function for the ETAC reagents because of its significantly greater reactivity than ester, amide, or nitrophenyl groups and because it could be conveniently reduced in aqueous media to an alcohol function, thus preventing retro-Michael reactions and effectively trapping the cross-linker in the protein if that were necessary. Most other activating functions that have the appropriate reactivity do not allow this option. Reductive trapping is not necessary for SH alkylations in B6.2. The use of derivatives of acetophenone allowed easy synthesis of ETAC molecules with additional functions on the aromatic ring that could be used to append appropriate functionalities for radiolabeling. The sulfone group was used as the leaving group for synthetic convenience and for providing groups that serve simultaneously as latent functions for double bond development. These sulfone sites can be easily exchanged by a sequence involving retro-Michael of a sulfinic acid moiety, thiol addition to the conjugated double bond with subsequent retro-Michael of the remaining sulfone, followed by Michael addition of another

thiol to the new conjugated double bond. Finally, the bis-thioether formed can then be oxidized to the new bis-sulfone. This allows the synthesis of a wide variety of derivatives of these ETAC reagents from a single precursor.

We focused upon the synthetic linking of the ETAC moiety to radiolabeled and chelating groups through carboxyl ETAC **13i** reagent because of the poor nucleophilicity of the amine in the amino derivative. The chemistry and attachment of certain dye marker bioprobes will be discussed in future papers.¹

The monoclonal antibody used in this study, B6.2, does not have any free sulfhydryl groups in its native form based on 2,2'-dithiodipyridine analyses. ETAC cross-linking with unreduced antibody, as assayed via SEC HPLC and SDS gel electrophoresis, strongly suggests that available nucleophilic surface groups, in all likelihood the amino groups of lysine, have reacted with the ETAC reagents, resulting in inter- and intraantibody cross-linking. Since 10 mol of sulfhydryls were generated per mol of B6.2 and ETAC reactions were at a 10 molar excess of ETAC to antibody, then only 5 intraantibody cross-links per antibody molecule were possible. Our data shows the presence of cross-linked antibody at the low molar excesses used in the modification reactions (10^{-5} M ETAC and 10^{-6} M antibody). Classic protein cross-linking reactions with glutaraldehyde, dimethyl suberimidate, etc. involve millimolar levels of cross-linker to micromolar levels of protein. The ETAC reagents are more effective cross-linkers at low concentrations possibly due to their equilibrium-transfer characteristic.

The data suggest that, in contrast to the ETAC cross-linked to sulfhydryls, the ETAC cross-linked to the amine groups of lysine were lost on reducing SDS gels, presumably by transfer to the 2-mercaptoethanol in the SDS electrophoresis sample buffer (19), which was about 0.5 M in the prepared antibody samples prior to boiling and electrophoresis. We also observed the result of ^{125}I -labeled ETAC **13k** equilibrium transfer from 25 000- and 50 000-Da species (light and heavy chains) to intact antibody. At pH 4 a similar transfer did not occur. At the lower pH, the amine groups of lysine are protonated and the SH groups are poor nucleophiles, which makes the transfer of ETAC reagents very slow. ETAC transfer behavior from amine to sulfhydryl groups both in model compounds and in ribonuclease has been previously documented (9). Once the ETAC reagent had reacted with the sulfhydryl groups in partially reduced antibody, a relatively stable bond was formed. This was very evident in the higher molecular mass bands seen on the reducing SDS gels, which represented strong indirect evidence of cross-linking. The smaller amounts of cross-linked protein bands at 75 000 and 125 000 Da (one heavy and one light chain; two heavy and one light chain) suggested that some of the intraantibody cross-linking was occurring in the hinge region of the heavy chains. The disulfide bridges there are preferentially reduced (10, 11) and easily subject to further chemical modification with sulfhydryl modification reagents. In view of the equilibrium-transfer nature of these reagents, and their short length, it is probable that the cross-links formed in the partially reduced antibody do not significantly perturb the bridging domains found in the native molecular conformation.

The more rapid blood clearance of the amine-directed ^{111}In -labeled DTPA ETAC **13p** compared to the sulfhydryl-directed ^{111}In -labeled DTPA ETAC **13p** may be due to the presence of sulfhydryl groups of both protein and

nonprotein small molecules (especially glutathione) found in mouse plasma (27) at $96 \pm 11 \mu\text{M}$ and $18 \pm 3 \mu\text{M}$, respectively. The available sulfhydryl groups would be expected to react with and displace the amine-directed ^{111}In -labeled DTPA ETAC from the antibody. In the case of the smaller molecules, for example glutathione (307 Da), the resultant complex would be a radical alteration compared to the modification of a large molecule such as serum albumin, about 66 000 Da, containing about 1 sulfhydryl per mol (28). Enhanced kidney clearance of the ^{111}In -DTPA-ETAC-small molecule complexes would be expected and was observed. Although this explanation is reasonable, numerous other mechanisms operate in vivo for metabolizing organic compounds such as DTPA ETAC **13p** and heavy metals such as In. Their overall contribution to the metabolism and blood clearance of the ^{111}In -DTPA-ETAC-antibody complex is unknown.

Higher pH resulted in a generally greater level of ETAC cross-linking as seen in Table II. This was probably due to pH effects on both the sulfhydryl and lysine amino groups of the antibody as well as an activation of the ETACs. Deprotonation of the sulfhydryl and lysine amino groups will make them more reactive nucleophiles. The higher level of lysine amino based cross-linking was probably due to the fact that there are more lysines, about 86, per mol of B6.2 antibody than available cysteine sulfhydryls in the partially reduced antibody, about 10, based on 2,2'-dithiodipyridine analyses. Also, it is more likely that the charged lysine amino groups are mostly surface available, resulting in enhanced interantibody cross-linking, whereas the sulfhydryl groups derived from reduced cystine cross-links are mostly on the interior of the antibody, resulting in more intraantibody cross-linking which would not be detected by SEC HPLC. Higher pH also increases ETAC reactivity by enhancing the elimination of the sulfone moiety, yielding a molecule more readily subject to nucleophilic attack.

Various substitutions on both the sulfone leaving group and on the activating aromatic ketone group significantly influenced the ETAC cross-linking reaction. The *m*-amino aromatic ketone substituted ETACs **13l** and **13m** were very poor cross-linkers of the B6.2 antibody. This may be due to a chemical-electronic effect causing a reduced electrophilic character of the carbonyl of the acetophenone, or it may be a question of the electronics of the -SH cross-linking domain in the protein. The more electron-withdrawing ETACs **13c,e,f,h,i** are much more effective cross-linkers of this antibody.

Examination of ETAC cross-linked protein via SEC HPLC, SDS polyacrylamide gel electrophoresis, and ELISA revealed that (1) both interantibody as well as intraantibody cross-linking had occurred, (2) the level of interantibody and intraantibody cross-linking varied with the substituent on the ETAC, (3) the stability of the cross-links on the reducing SDS gels varied with substituents on the ETAC, and (4) little if any immunoreactivity was lost after reaction with one of the more effective ETAC cross-linking compounds.

The preservation of virtually all immunoreactivity after the reaction of partially reduced antibody with an ETAC is suggestive of their site direction away from the antigen binding site. This preservation of immunoreactivity is important in that modified ETACs can be used to conjugate chelators or other molecules in a site-directed fashion while simultaneously stabilizing the structure of the partially reduced antibody. This was demonstrated with the ^{111}In -labeled DTPA ETAC **13p** modified anti-

body in a biodistribution study. It should be noted that a double ETAC capable of four bifunctional bonds, i.e., two cross-links, would be useful for conjugating proteins and other molecules to one another in a site-directed fashion while stabilizing both molecules.

ACKNOWLEDGMENT

We acknowledge and appreciate the support of the National Science Foundation, Synthetic Organic and Natural Products Division, Grant CHE8421137 A02; NSF Instrumentation program; and the Colgate Palmolive Research Laboratories for summer research fellowships to R.G.L. We thank Dr. Stephen B. Haber for careful proofreading and useful criticism of this manuscript.

LITERATURE CITED

- (1) Wold, F. (1972) Bifunctional reagents. *Methods Enzymol.* **XXV**, 623-651.
- (2) Peters, K., and Richards, F. M. (1977) Chemical cross-linking: reagents and problems in studies of membrane structure. *Ann. Rev. Biochem.* **46**, 523-551.
- (3) Uy, R., and Wold, F. (1976) Covalent Linkage: II. Intramolecular Linkages. In *Biomedical Applications of Immobilized Enzymes and Proteins* (Thomas Ming Swi Chang, Ed.) pp 15-24, Plenum Publishing Corporation, New York.
- (4) Uy, R., and Wold, F. (1977) Introduction of artificial crosslinks into proteins. *Adv. Exp. Med. Biol.* **86A**, 169-186.
- (5) Han, K. K., Richard, C., and Delacourte, A. (1984) Chemical crosslinks of proteins by using bifunctional reagents. *Int. J. Biochem.* **16**, 129-145.
- (6) Ji, T. H. (1983) Bifunctional Reagents. *Methods Enzymol.* **91**, 580-609.
- (7) Das, M., and Fox, C. F. (1979) Chemical cross-linking in biology. *Ann. Rev. Biophys. Bioeng.* **8**, 165-193.
- (8) Fasold, H., Klappenberger, J., Meyer, C., and Remold, H. (1971) Bifunctional reagents for the crosslinking of proteins. *Angew. Chem., Int. Ed. Engl.* **10**, 795-801.
- (9) Mitra, S., and Lawton, R. G. (1979) Reagents for the cross-linking of proteins by equilibrium transfer alkylation. *J. Am. Chem. Soc.* **101**, 3097-3110.
- (10) Packard, B., Edidin, M., and Komoriya, A. (1986) Site-directed labeling of a monoclonal antibody: targeting to a disulfide bond. *Biochemistry* **25**, 3548-3552.
- (11) Morphy, J. R., Parker, D., Alexander, R., Bains, A., Carne, A. F., Eaton, M. A. W., Harrison, A., Millican, A., Phipps, A., Rhind, S. K., Titmas, R., and Weatherby, D. (1988) Antibody labeling with functionalized cyclam macrocycles. *J. Chem. Soc., Chem. Commun.* **3**, 156-158.
- (12) Mannich, C., and Lammering, D. (1922) Synthesis of β -keto bases from aliphatic-aromatic ketones, formaldehyde, and secondary amines. *Ber. Dtsch. Chem. Ges.* **55B**, 3510-3526.
- (13) Blicke, F. F. (1942) Mannich reaction. *Org. React.* **I**, 303-341.
- (14) Reiner, L., Keston, A. S., and Green, M. (1942) Absorption and distribution of insulin labeled with radioactive iodine. *Science* **96**, 362-363.
- (15) Brechbiel, M. W., Gansow, O. A., Atcher, R. W., Schlom, J., Esteban, J., Simpson, D. E., and Colcher, D. (1986) Synthesis of 1-(*p*-isothiocyanatobenzyl) derivatives of DTPA and EDTA. Antibody labeling and tumor-imaging studies. *Inorg. Chem.* **25**, 2772-2781.
- (16) Colcher, D., Horan Hand, P., Nuti, M., and Schlom, J. (1981) A spectrum of monoclonal antibodies reactive with human mammary tumor cells. *Proc. Natl. Acad. Sci. U.S.A.* **78**, 3199-3203.
- (17) Kufe, D. W., Nadler, L., Sargent, L., Shapiro, P., Austin, F., Colcher, D., and Schlom, J. (1983) Biological behavior of human breast-associated antigens expressed during cellular proliferation. *Cancer Res.* **43**, 851-857.
- (18) Burchiel, S. W. (1986) Purification and analysis of monoclonal antibodies by high-performance liquid chromatography. *Methods Enzymol.* **121**, 596-615.
- (19) Laemmli, U. K. (1970) Cleavage of the structural proteins during the assembly of the head of bacteriophage T4. *Nature* **227**, 680-685.
- (20) Grassetti, D. R., and Murray, J. F. (1967) Determination of sulfhydryl groups with 2,2'- or 4,4'-dithiodipyridine. *Arch. Biochem. Biophys.* **119**, 41-49.
- (21) Pedersen, A. O., and Jacobsen, J. (1980) Reactivity of the thiol group in human and bovine albumin at pH 3-9, as measured by exchange with 2,2'-dithiodipyridine. *Eur. J. Biochem.* **106**, 291-295.
- (22) Brown, B. A., Davis, G. L., Saltzgaber-Muller, J., Simon, P., Ho, M. K., Shaw, P. S., Stone, B. A., Sands, H., and Moore, G. P. (1987) Tumor-specific genetically engineered murine/human chimeric monoclonal antibody. *Cancer Res.* **47**, 3577-3583.
- (23) Dulbecco, R., and Vogt, M. (1954) Plaque formation and isolation of pure lines with poliomyelitis virus. *J. Exp. Med.* **98**, 167-182.
- (24) Colcher, D., Horan Hand, P., Teramoto, Y. A., Wunderlich, D., and Schlom, J. (1981) Use of monoclonal antibodies to define the diversity of mammary tumor viral gene products in virions and mammary tumors of the genus *Mus*. *Cancer Res.* **41**, 1451-1459.
- (25) Trost, B., and Curran, D. (1981) Chemoselective oxidation of sulfides to sulfones with potassium hydrogen peroxide. *Tetrahedron Lett.* **22**, 1287-1290.
- (26) Brown, B. A., Dearborn, C. B., Neacy, W. P., Sands, H., and Gallagher, B. M. (1986) Comparison of carbohydrate directed versus amine directed attachment of DTPA to murine monoclonal antibodies. *J. Labelled Compd. Radiopharm.* **23**, 1288-1290.
- (27) Ayers, F. C., Warner, G. L., Smith, K. L., and Lawrence, D. A. (1986) Fluorometric quantitation of cellular and non-protein thiols. *Anal. Biochem.* **154**, 186-193.
- (28) Janatova, J., Fuller, J. K., and Hunter, M. J. (1968) The heterogeneity of bovine albumin with respect to sulfhydryl and dimer content. *J. Biol. Chem.* **243**, 3612-3622.

Registry No. **10a**, 98-86-2; **10b**, 99-91-2; **10c**, 100-19-6; **10d**, 121-89-1; **10e**, 586-89-0; **11a**, 886-06-6; **11b**, 5250-05-5; **11c**, 893-53-8; **11d**, 32668-60-3; **11e**, 124242-84-8; **12a**, 124242-85-9; **12b**, 124242-86-0; **12c**, 124242-87-1; **12d**, 124242-88-2; **12e**, 124242-89-3; **12f**, 124242-90-6; **12g**, 124242-91-7; **12h**, 124242-92-8; **12i**, 124242-93-9; **13a**, 124242-94-0; **13b**, 58212-02-5; **13c**, 124242-95-1; **13d**, 124242-96-2; **13e**, 124242-97-3; **13f**, 124242-98-4; **13g**, 124242-99-5; **13h**, 123883-93-2; **13i**, 124243-00-1; **13j**, 124266-33-7; **13k**, 124266-34-8; **13l**, 124266-35-9; **13m**, 124266-36-0; **13n**, 124243-01-2; **13o**, 124243-02-3; **13p**, 124243-03-4; **14**, 124266-38-2; **15**, 124266-37-1; *p*-iodoaniline, 540-37-4; *p*-[¹²⁵I]iodoaniline, 77718-00-4; dansyl chloride, 605-65-2; 1-(*p*-nitrobenzyl)diethylenetriamine-3HCl, 124266-39-3; *tert*-butyl 2-bromoacetate, 5292-43-3; piperidine HCl, 6091-44-7; benzenethiol, 108-98-5; *p*-toluenethiol, 106-45-6; *p*-chlorobenzenethiol, 106-54-7.

Sulfhydryl Site-Specific Cross-Linking and Labeling of Monoclonal Antibodies by a Fluorescent Equilibrium Transfer Alkylation Cross-Link Reagent

Renato B. del Rosario,[†] Richard L. Wahl,^{*†} Stephen J. Brocchini,[‡] Richard G. Lawton,[‡] and Richard H. Smith[†]

Division of Nuclear Medicine, Department of Internal Medicine, University of Michigan Medical Center, Ann Arbor, Michigan 48109-0028, and Department of Chemistry, University of Michigan, Ann Arbor, Michigan 48109. Received July 20, 1989

The site-specific intramolecular cross-linking of sulfhydryls of monoclonal antibodies via a new class of "equilibrium transfer alkylation cross-link (ETAC) reagents" is described. Following complete or partial reduction of interchain disulfides with dithiothreitol (DTT), two murine IgG2a monoclonal antibodies, 225.28S and 5G6.4, were reacted with α,α -bis[(*p*-tolylsulfonyl)methyl]-*m*-aminoacetophenone (ETAC 1a) and a fluorescent conjugated derivative, sulforhodamine B *m*-(α,α -bis(*p*-tolylsulfonylmethyl)acetyl)anilide derivative (ETAC 1b). Reducing SDS-polyacrylamide gel electrophoresis analysis of the products from 1b indicated the formation of S-ETAC-S interchain heavy and light chain cross-links (~23-34% overall yield by video-camera densitometry) which do not undergo disulfide-thiol exchange with DTT at 100 °C. In contrast, no interchain cross-links were observed upon reaction of unreduced or reduced antibody wherein the thiols have been previously alkylated with iodoacetamide. These results indicated site-specific cross-linking of interchain sulfhydryls and places their distance within 3-4 Å. Flow cytometry of the ETAC 1b 5G6.4 cross-linked product using 77 IP3 human ovarian carcinoma target cells showed positive binding and retention of immunoreactivity. The in vivo biodistributions of ¹³¹I-labeled intact 5G6.4 and ¹²⁵I-labeled reduced 5G6.4 + ETAC 1a product in rats were essentially identical over a period of 24 h. The present study illustrates the potential applications of labelable ETAC reagents as thiol-specific probes for a wide variety of immunological studies.

The search for site-specific methods of introducing labels into monoclonal antibodies is currently an area of intense interest in immunochemical research. While traditional "random" methods of labeling are commonly achieved by conjugation to protein lysyl ϵ -amino groups (1-4) and radioiodination of tyrosines (5-7), more recent work has targeted carbohydrate (aldehyde) and sulfhydryl (cysteine) functionalities (8-10). A primary impetus for targeting these latter residues is that "tagging" is directed regiospecifically and away from the antigen combining regions. This may avoid unwanted chemical reactions which can arise from random labeling procedures and potentially may yield labeled antibodies with higher immunoreactivities. This feature is especially important in biochemical applications of immunoconjugates and radioimaging where diminishment of immunoreactivity can lead to poor target localization. Alkylation of reduced disulfides is particularly attractive because of the greater nucleophilicity of thiols over amines and the possibility for selective alkylation of different types of interchain disulfides (11-14).

A major limiting factor in the development of thiol-specific labeling techniques is the scarcity of thiol-reactive reagents. The recent synthesis of new N-substituted aromatic maleimide derivatives (9, 10) and crabescin (15) represent a promising class of organic compounds. We have recently reported our success with the sulfhydryl site-specific labeling of partially reduced monoclonal antibodies with biotin (16, 17). An additional caveat in thiol-directed labeling is that alkylation occurs with

concomitant and irreversible cleavage of interchain disulfide bonds. Cleavage of these covalent bonds may adversely affect not only the overall stability of the natural conformation of the antibody but can also diminish immunoreactivity if substantial dissociation of complementary heavy and light chains ensues. A plausible solution to this problem is design of reagents which carry the desired label and have thiol-specific cross-linking properties.

In this paper we describe the reactions of reduced disulfides of two murine monoclonal antibodies, 225.28S and 5G6.4, with a new class of cross-linking reagents characterized as "equilibrium transfer alkylation cross-link" (ETAC) reagents (18-20). The compounds in the present study are structurally and mechanistically similar to the earlier prototypes (18) and are designated in Figure 1. The insertion of ETAC 1 type compounds into reduced disulfide bonds of interchain IgG heavy chains is depicted in Scheme I. Compounds of type 1 are unique in that they possess an amine functionality on the aromatic ring attached to the bridge which serves as a chemical carrier for introduction of a desired label. We illustrate the potential of this structural feature with the synthesis of its rhodamine conjugate, 1b. Details of the syntheses and chemistry of the other structurally related extended ETAC compounds are described elsewhere (19).

EXPERIMENTAL PROCEDURES

α,α -Bis[(tolylsulfonyl)methyl]-*m*-aminoacetophenone (ETAC 1a). Bis[(*p*-tolylsulfonyl)methyl]-*m*-nitroacetophenone (20) (0.5 g, 1.0 mmol) was finely ground in a mortar and this fine powder was then dispersed in a solution of 25 mL of absolute ethanol and 1 mL of glacial acetic acid, forming a white suspension. This sus-

* To whom reprint requests should be addressed.

[†] University of Michigan Medical Center.

[‡] University of Michigan.

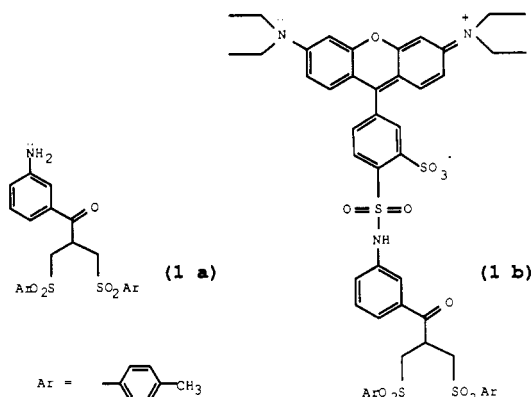


Figure 1. Chemical structures of ETAC compounds: α,α -bis[(*p*-tolylsulfonyl)methyl]-*m*-aminoacetophenone (**1a**) and tetraethylrhodamine derivative **1b**.

pension was added to a stirring suspension of 5% Pd/C (0.05 g) in 15 mL of absolute ethanol under a hydrogen atmosphere at ambient temperature. The reaction mixture was maintained under a slight positive pressure of hydrogen for 24 h as determined by a differential mineral oil manometer. The Pd/C catalyst was then filtered by gravity through Celite and the filtrate was roto-evaporated. Absolute ethanol (10–20 mL) was used to wash the filter cake, and the washings were added to the residue and again evaporated in vacuo, leaving 0.18 g (38%) of solid product (mp 143–144 °C). Less pure material was obtained if the Pd/C catalyst was allowed to soak in chloroform and then again filtered by gravity. The chloroform filtrate yielded material with very little difference by spectroscopic analyses and crude yields were increased to 70–75%. ETAC **1a**: IR (Nicolet 5DX and 5DX-B FT-IR) (KBr, cm^{-1}) 3473, 3378, 1683, 1596, 1291, 1149, 1085; ^1H NMR (Bruker WM 360 and AM 300 MHz, CDCl_3) δ 2.46 (s, 6 H), 3.54 (AB q, 4 H, $J_{\text{AB}} = 6.31, 6.28$ Hz), 4.26 (t, 1 H, $J = 6.27$ Hz), 6.82 (d, 1 H), 6.92 (d, 1 H), 7.00 (s, 1 H), 7.07 (t, 1 H, $J = 7.79$ Hz), 7.52 (AB q, 8 H, $J_{\text{AB}} = 8.02$ Hz); ^{13}C NMR (CDCl_3) δ 195.3, 147.1, 145.3, 135.4, 130.1, 129.1, 128.44, 128.38, 120.6, 118.2, 114.2, 55.3, 35.6, 20.7; MS (Finnigan 4021 GC-MS system) m/e (relative intensity, EI) 471 (M^{+} , 0.07), 278 (18.4), 246 (20.9), 160 (38.4), 155 (16.9), 139 (70.3), 120 (47.2), 91 (100.0).

Sulforhodamine B m -[α,α -Bis[(*p*-tolylsulfonyl)methyl]acetyl]anilide Derivatives (ETAC **1b).** α,α -Bis[(*p*-tolylsulfonyl)methyl]-*m*-aminoacetophenone (**1a**; 100 mg, 0.21 mmol) was dissolved in 2 mL of pyridine and to this solution was added 120 mg (0.20 mmol) of the sulfonyl chloride derivative of sulforhodamine B (Kodak). A trace of 4-(dimethylamino)pyridine was added and the mixture was stirred overnight at room temperature. A few drops of water was added and the mixture continued to stir for 2 h. The intensely colored solution was diluted with chloroform and treated with 10% HCl. The chloroform layer was washed with 10% HCl several times and then, after drying over anhydrous sodium sulfate, evaporated to give 130 mg of a dark purple foam after vacuum drying (0.01 mm) for 6 h. This material was essentially homogeneous by TLC in CHCl_3 /methanol (10/1), showing an intense orange-red fluorescent spot at R_f 0.43 and a trace of an orange fluorescent spot at R_f 0.64 believed to be the Michael elimination product from the bis-sulfone moiety. ETAC **1b**: ^1H NMR (CDCl_3) δ 1.28 (br t, 12 H), 2.48 (s, 6 H), 3.50 (m, 8 H) overlaps 3.54 (m, 4 H), 4.20 (p, 1 H), peaks at 6.62, 6.92, 7.00, 7.16 superimposed on 7.35 (A of AB q, 4 H), 7.65

(B of AB q, 4 H); FAB-MS (VG Instruments 702-50S) m/e (relative intensity, FAB) 1012 (MH^{+} , 13.0), 855 ($\text{MH}^{+} - \text{SO}_2\text{C}_6\text{H}_4\text{CH}_3$, 1.75).

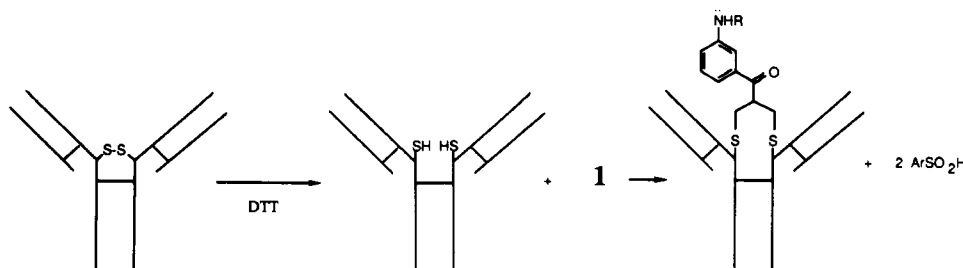
Isolation and Purification of 225.28S and 5G6.4. 225.28S is an IgG2ak murine monoclonal antibody reactive with the high molecular weight antigen of melanoma (21). Hybridoma cells producing this reagent were grown in pristane-primed (Aldrich) Balb/c mice as ascites and then purified by staphylococcal protein A chromatography (22). The antibody was eluted with 0.1 M citrate buffer (pH \approx 5) and directly reduced with DTT. 5G6.4 is an IgG2a murine monoclonal antibody with preferential reactivity with ovarian and other epithelial cancers and was similarly grown, purified, dialyzed, and concentrated against 0.1 M sodium phosphate buffer (pH \approx 7) (23). Protein concentrations were measured by using the method of Bradford with bovine serum albumin or bovine IgG (Bio-Rad) as reference standards (24). The purity and immunoreactivity of these preparations were regularly monitored by SDS-polyacrylamide gel electrophoresis conducted under reducing conditions and flow cytometry analysis using a Coulter Epics instrument.

Reductions and Reactions of Reduced Monoclonal Antibody with ETAC **1.** The procedure is illustrated for the reactions of 225.28S and ETAC **1b**. To 100 μL of 225.28S ($\sim 3.3 \times 10^{-5}$ M) was added by syringe 2 μL of DTT (Aldrich or Sigma, 1.71 M). The mixture was allowed to incubate at 37 °C for 2–3 h and chromatographed through a $5^3/4$ -in. glass pipet column containing ~ 2 mL of Sephadex G-25-150 which had been previously allowed to equilibrate in 0.05 M Tris-HCl (pH \approx 8). The reaction mixture was collected in ~ 200 – 250 - μL fractions into tubes each containing 15 μL of ETAC **1b** (0.026 M) dissolved in DMSO (Sigma). The tubes were allowed to incubate at 37 °C for ~ 3 h after vortexing and were subsequently examined for protein content qualitatively with Bradford's reagent (Bio-Rad). Fractions (normally 1 or 2) which gave a blue color were rechromatographed separately with a similar desalting column as above. The ETAC **1b** labeled 225.28S fraction eluted as a blue-violet band, leaving excess reagent at the origin of the column.

Reactions of partially reduced 5G6.4 (~ 50 – 70 :1 molar ratio of DTT to IgG2a, ~ 5 h) antibody with **1b** were similarly performed with the omission of the desalting step. Upon addition of an equimolar quantity of **1b** (to DTT), the mixture was vortexed and placed on a nutator for overnight incubation at room temperature. The reaction mixtures were then spun in a microfuge for 15 min to remove insoluble material prior to gel filtration chromatography.

Yields of cross-linked products were estimated by video-camera densitometry at the computer image analysis facility of the University of Michigan Medical Center. With this technique, the Coomassie blue content of each fragment (e.g. H2L2) in lane A of Figure 3 was measured as a function of optical density and obtained as integrated areas with a program which allows for variable background subtraction arising from nonuniform gel destaining. With use of the total integrated areas of heavy and light chains from a completely reduced sample of antibody, a correction factor to incorporate the difference of Coomassie blue staining for a heavy (H) chain and a light (L) chain was calculated for each gel in determining H and L contributions on areas of whole fragments. FPLC (fast protein–liquid chromatography) analysis of chromatographed product mixtures were run on a Pharmacia P-500 system equipped with a single or a series of

Scheme I. Intramolecular Cross-Linking of Interchain IgG Heavy Chain Thiols



two Superose 12 sizing columns with PBS (pH = 7.2) as eluting buffer and a flow rate of 24 mL/h.

SDS-Polyacrylamide Gel Electrophoresis (SDS-PAGE) Analysis (25). SDS-polyacrylamide gel electrophoresis was routinely performed with commercially available Pharmacia 8–25% polyacrylamide gradient gels on a Pharmacia Phast System. Sample preparation typically involved mixing 1 volume of protein sample with at least twice the volume of a Tris-HCl (pH \approx 6.8) buffer solution which contained 8% SDS (by weight), 20% glycerol (by weight), and 10% 2-mercaptoethanol (by volume) or DTT (0.67 M) for reducing SDS-PAGE. These mixtures were heated for 2–3 min in a boiling-water bath or incubated at 37 °C for 24 h prior to electrophoresis. (Both reaction conditions led to complete reduction and dissociation of heavy and light chains of intact monoclonal antibody.) Gels were stained with Coomassie blue.

Biodistribution of ^{131}I -Labeled 5G6.4 and ^{125}I -Labeled Reduced 5G6.4 + ETAC 1a in Rats. Approximately 40 μg ($\sim 3 \times 10^{-4}$ μmol) of 5G6.4 (Figure 4, lane B, E) and reduced 5G6.4 + ETAC 1a (Figure 4, lane B, F) were radioiodinated via the Iodogen (~ 20 μg ; $\sim 4.5 \times 10^{-2}$ μmol , ~ 20 min) method (6) with carrier free iodide (ICN Biomedicals), purified by anion-exchange chromatography (Bio-Rad AG-1-X8, 200–400 mesh), to give ^{131}I -labeled 5G6.4 ($\sim 8 \times 10^5$ mCi/ μmol) and ^{125}I -labeled 1a-alkylated 5G6.4 ($\sim 1.2 \times 10^7$ $\mu\text{Ci}/\mu\text{mol}$) which contained <1–2% free I^- as determined by iodine TLC (ITLC) on a Bioscan System 200 Imaging Scanner. The immunoreactivity of these radiolabeled preparations were in the highest range (40–60%) typically obtained for routine radioiodination of this antibody using a direct cell binding assay on 77 IP3 ovarian target cells ($\sim 58\%$ and $\sim 52\%$ specific binding for ^{131}I -labeled 5G6.4 and ^{125}I -labeled reduced 5G6.4 + 1a) (17). Size-exclusion radio-FPLC was performed with a Pharmacia Superose-12 column (24 mL/h, PBS eluant) equipped with a Gilson microfractionator. One-minute fractions were collected and the activity of each tube was measured on a Packard Minaxi 5000 automatic γ -counter. Radiochromatograms were constructed by plotting activity vs fraction number (Figure 6). Fifteen rats (~ 16 –17 g) were each iv injected with ~ 29 –31 mCi ($\sim 3.7 \times 10^{-6}$ μmol) of ^{131}I -labeled 5G6.4 and ~ 25 –28 mCi ($\sim 2.3 \times 10^{-6}$ μmol) of ^{125}I -labeled reduced 5G6.4 + ETAC 1a. Five rats were sacrificed after 1, 4, and 24 h postinjection and activities for liver, kidney, spleen, lung, leg muscle, small intestines, and blood on a per gram basis were measured (Figure 7).

RESULTS

The required reduction of the disulfide bonds of 225.28S and 5G6.4 was carried out with dithiothreitol (DTT) in either citrate or phosphate buffers. The initial strategy for reactions of reduced antibody with compounds 1 was to chromatograph the reduction mixture through Sepha-

dex G-25 directly into DMSO solutions of 1 with Tris-HCl or phosphate buffers as eluant. The extent of reduction was monitored by alkylation of generated thiols with iodoacetamide and examination of the products by SDS-PAGE in the absence of reducing agents. Complete reduction of all interchain disulfide bonds was effected by incubation of the IgG2a antibodies with ~ 1000 molar excess of DTT to protein for 2 h at 37 °C (Figure 2, lane B).

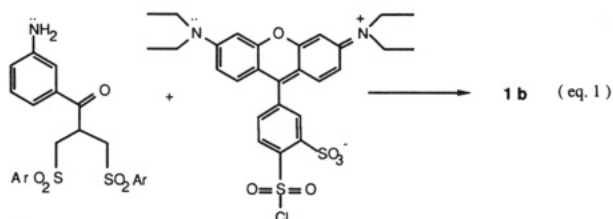
Cross-linking reactions of interchain thiols by ETAC reagents 1a,b were first examined for the IgG2a monoclonal antibody 225.28S. Preliminary experiments indicated that reoxidation of the reduced thiols of 225.28S was competitive (Figure 2, lanes G–N) under the conditions used for the cross-linking reaction. Figure 2 (lanes G–N) shows the nonreducing SDS-PAGE of the resulting product mixtures when samples of 225.28S in which all interchain disulfides have been reduced are chromatographed and allowed to air oxidize and then alkylated with iodoacetamide to block remaining thiols at varying time points (16). The product mixtures consisted of six bands which are assignable (with the migration taken from the top of the gel) to intact H2L2 (molecular weight ≈ 150 000) as well as successive degradations of H2L (≈ 125 000), H2 (≈ 100 000), HL (≈ 75 000), H (≈ 50 000), and L (≈ 25 000) chain fragments resulting from cleavage of interchain disulfide bonds. We thought that this would provide a good opportunity to test the reactivity of ETAC reagents toward neighboring protein thiols in the presence of their "natural" reannealing properties under these reduction conditions.

Whereas reducing (0.67 M DTT) SDS-PAGE of intact antibody at 100 °C for 2 min showed total cleavage of all interchain disulfide bonds, the ensuing cross-links remained stable under these conditions. The extent of cross-linking between interchain thiols was therefore conveniently assessed by reducing SDS-PAGE of the chromatographed cross-linked products. Identical results could also be obtained by incubation at 37 °C for 24 h prior to SDS-PAGE. (However, the higher temperature incubation gave sharper bands.) In addition, a control reduction of a large quantity of intact antibody using an identical DTT and SDS concentration was run alongside for comparison at all times.

Figure 2 (lane A) is illustrative of a typical SDS-PAGE analysis profile for the reaction product mixture obtained when 225.28S reduced with a ~ 1000 molar excess of DTT is chromatographed into a DMSO solution of α,α -bis[(*p*-tolylsulfonyl)methyl]-*m*-aminoacetophenone (ETAC 1a; ~ 200 molar excess over original antibody concentration) and incubated at 37 °C for ~ 3 h in Tris-HCl (pH = 8). The cross-linked species could easily be distinguished from heavy and light chain fragments since these latter two migrate furthest along the gel (migration is from top to bottom of gel as shown). Figure 2, lane A, shows the presence of three additional product

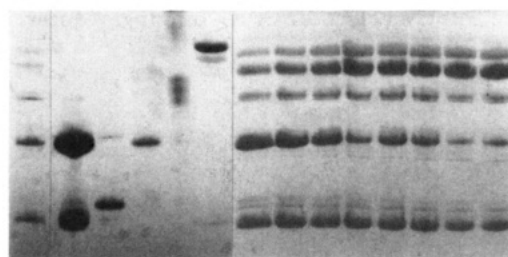
fragments clearly visible under denaturing and reducing (DTT) conditions. Comparison of these bands with completely reduced (lane B), unreduced (lane F) uncross-linked intact 225.28S, and molecular weight standards (lanes C–E) indicate that the cross-linked species are approximately in the molecular mass range spanned by the HL, H2, and H2L units (molecular weight $\approx 70\,000$ – $125\,000$). (The presence of an additional very faint band of mass approximately equal to that of H2L2 not visible in lane A of Figure 2 can sometimes be detected.) Furthermore, the order, spacing, and migration pattern for the cross-linked reaction product mixture (Figure 1, lane A) resembles those observed for nonreducing SDS-PAGE analysis (under identical conditions) of freshly prepared samples of reduced heavy and light chains of 225.28S which had been allowed to reanneal and were then alkylated with iodoacetamide (Figure 2, lanes G–N). The similarity suggests that the molecular mass of the product fragments are approximately 125 000, 100 000, and 75 000 and consistent with both H–H and H–L cross-links. The short distance span of ETAC 1 type reagents and the generally accepted hypothesis that heavy and light chains of an IgG molecule remain intimately associated by non-covalent attractions even after cleavage of all interchain disulfides suggests that the reaction products were intramolecularly cross-linked H2L2, H2L, H2, and HL antibody fragments (16, 26, 27). In this connection, we have also observed (by FPLC and SDS-PAGE) that reduced and iodoacetyl-alkylated heavy and light chains of antibody do not undergo complete dissociation except under strong denaturing conditions at elevated temperatures (16, 17).

For the purpose of ETAC labeling of monoclonal antibodies, it was important to know if attachment of a fairly bulky substituent to parent ETAC reagents (e.g. 1b) would affect the steric requirements of the desired interchain cross-linking reactions. Therefore, we chose to focus on the cross-linking reactions of ETAC 1b with 225.28S (and 5G6.4). The prototype fluorescent conjugate ETAC 1b was readily prepared by the N-sulfonylation of ETAC 1a by the sulfonyl chloride derivative of sulforhodamine B (eq 1). Reducing SDS-PAGE analysis of products from



the reactions of both reduced 225.28S and 5G6.4 with 1b gave very similar gel profiles. Lanes A and B of Figure 3 show the corresponding SDS-PAGE profile of the chromatographed product mixture when 225.28S reduced with ~ 1000 molar excess of DTT is chromatographed into DMSO solutions of ETAC 1b (~ 120 molar excess over IgG2a). As in the case for ETAC 1a, three bands are clearly evident in the expected region for cross-linked products (75 000–150 000 molecular weight range). Lane C of Figure 3 shows the control DTT reduction of intact 225.28S under identical SDS denaturing conditions.

Evidence for the thiol site specificity of the interchain cross-linking process by ETAC reagents came from studies of the reactions of unreduced 225.28S and a corresponding iodoacetamide-alkylated mixture of heavy and light chains with excess ETAC 1b. Lane D of Figure 3 shows the data profile of the chromatographed product mixture obtained when unreduced 225.28S was incu-



A B C D E F G H I J K L M N

Figure 2. Lane designations: A, reducing (DTT) SDS-PAGE analysis of the reaction product of ETAC 1a with 225.28S with complete reduction of all interchain disulfide bonds; B, intact 225.28S under identical reducing and SDS denaturing conditions; C, carbonic anhydrase (MW $\approx 29\,000$); D, bovine serum albumin (MW $\approx 67\,000$); E, phosphorylase B (MW $\approx 97\,000$); F, intact (unreduced) 225.28S under SDS denaturing conditions; G–N, SDS-PAGE (nonreducing media) analysis of chromatographed samples of 225.28S following reduction of all interchain disulfides and which were allowed to reoxidize and were alkylated with iodoacetamide at varying time points (~ 3 h).

bated with ~ 130 molar excess of ETAC 1b for 2 h at 37°C along with the control (Figure 3, lane E). The only bands observed are identical with those of heavy and light chain fragments while bands of higher mass were undetectable. Lanes F and G of Figure 3 show the reducing SDS-PAGE of the chromatographed final product mixture (after incubation with ETAC 1b) when 225.28S reduced with ~ 1000 molar excess of DTT was first quenched with excess iodoacetamide overnight at 4°C to block available thiols before chromatography into solutions of ETAC 1b. Again only bands arising from complete reduction of all interchain bands were observed. The stabilized ETAC 1 cross-links in 225.28S are therefore predominantly among neighboring thiols (18).

The relative quantities of cross-linked species in the reduced 225.28S + ETAC 1b (Figure 3, lane A) preparation were determined by video-camera densitometry and computer image analysis of the data profile. The integrated area of each band with mass $>50\,000$ (heavy chain, second band from the bottom of the gel) represented the quantity of cross-linked product of mass \approx the HL, H2, H2L, and H2L2 (very faint by visual inspection) mass with respect to the entire mixture of fragments. For lane A on Figure 3, this method gave $\sim 1.3\%$ (H2L2), $\sim 3.9\%$ (H2L), $\sim 9.2\%$ (H2), and $\sim 8.8\%$ (HL), which corresponded to a total yield of $\sim 23\%$ cross-linked products. The relative H and L chain content in each cross-linked species is proportional to percent area of cross-linked fragment \times fraction of H (or L) chains in a given fragment [e.g. $2H/[2 \times H/(\text{area of 1 heavy chain/area of 1 light chain}) + 2H]$ for H2L2 as corrected for the higher absorbance of H vs L; see the Experimental Procedures]. Summation of each contribution from H2L2, H2L, H2, and HL bands gives a $\sim 30\%$ yield for heavy and $\sim 15\%$ for light chains with respect to the total quantity of heavy and light chains in the product mixture ($\%H/\%L \approx 2$). Similarly, the proportion of heavy-heavy (H–H) and heavy-light (H–L) linkages can be estimated from the ratio of total area for H–H fragments/total area for H–L fragments. This calculation gives an H–H/H–L ratio ≈ 1 . The above ratios suggest that there is no large preference for heavy-heavy vs heavy-light cross-linking in reactions with completely reduced 225.28S although the number of cross-linked heavy chains is significantly higher than that of light chains.

Although the above experiments successfully demonstrated the thiol site specificity of ETAC 1 type com-

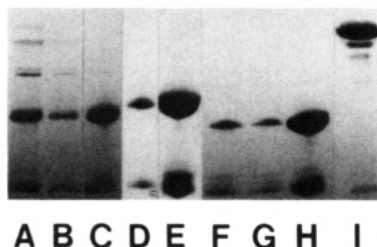


Figure 3. Lane designations: A and B, reducing (DTT) SDS-PAGE analysis of completely reduced 225.28S + ETAC 1b product mixture; C, intact 225.28S in the presence of an equivalent quantity of DTT and SDS (control); D, reducing (DTT) SDS-PAGE of unreduced 225.28S + ETAC 1b product mixture; E, control reduction of 225.28S for comparison to D; F and G, reducing (DTT) SDS-PAGE of reaction product mixtures from iodoacetamide-alkylated reduced 225.28S + ETAC 1b; H, control reduction of 225.28S for comparison to F and G; I, intact 225.28S.

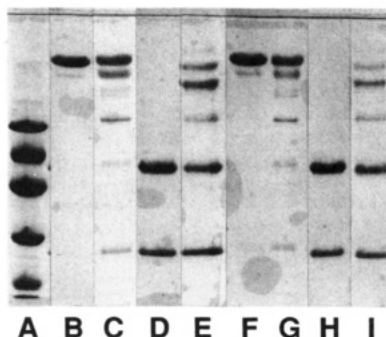


Figure 4. Lane designations: A, Pharmacia molecular mass standards were used (from top to bottom) were phosphorylase b (94 000), bovine serum albumin (67 000), ovalbumin (43 000), carbonic anhydrase (30 000), soybean trypsin inhibitor (20 100), a-lactalbumin (14 400); B, nonreducing SDS-PAGE of intact 5G6.4; C, nonreducing SDS-PAGE of reduced 5G6.4 + ETAC 1a product mixture; D, reducing SDS-PAGE of intact 5G6.4; E, reducing SDS-PAGE of reduced 5G6.4 + ETAC 1a product mixture; F-I, exact corresponding SDS-PAGE analysis for 5G6.4 and reduced 5G6.4 + ETAC 1b.

pounds, there were two practical limitations of the labeling procedure. First, the preparation and isolation of the cross-linked antibodies required chromatography at least twice and the quantity of ETAC reagent used always exceeded the actual amount needed for cross-linking. This was necessary to ensure that all reduced species from sizing chromatography were trapped by ETAC. The desalting chromatography step after DTT reduction also led to variable protein dilution and loss. It was also desirable to have a procedure that could be more easily adapted for scale up involving larger columns and longer periods of chromatography.

To address three issues we simplified the procedure by employing a strategy which involved a longer reduction period (~5 h) and lower DTT concentrations (~50–70 molar excess over IgG2a). The major difference was that a stoichiometric quantity of ETAC reagent (with respect to DTT concentration) was added after the reduction period and the mixture was allowed to incubate overnight at 37 °C prior to chromatography. Since 1a,b were only fairly soluble in aqueous DMSO solutions, the use of lower ETAC concentrations also minimized unwanted precipitation during the reaction.

Figure 4 depicts the nonreducing and reducing SDS-PAGE analysis of the product mixtures upon the application of this technique to the antiovarian IgG2a antibody 5G6.4 + ETAC 1a and 1b. Following reduction with a 70-fold molar excess of DTT, video-camera densitometry and image analysis of the product mixture from

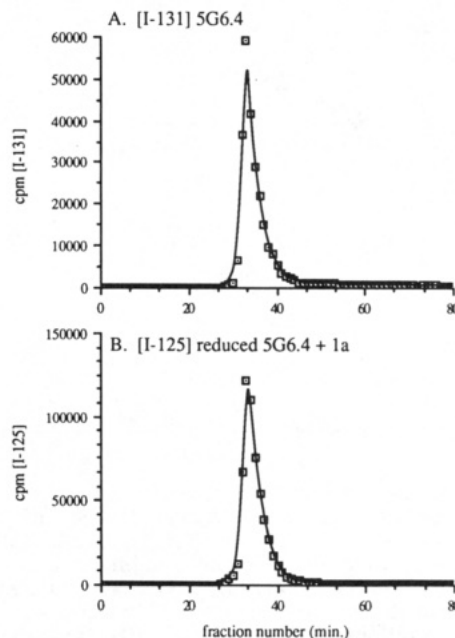


Figure 5. Size-exclusion radio-FPLC profile of radioiodinated 5G6.4 (A) and reduced 5G6.4 + ETAC 1a product B.

1b gave a ~34% yield of cross-linked products distributed among H2L2 (<1%), H2L (~7.3%), H2 (~18%), and HL (~8.9%) mass fragments. Calculations using arguments discussed above gave an H-H/H-L cross-linking ratio ≈ 2 with ~44% and ~13% yield, respectively, for heavy and light chain distribution. For ETAC 1a, the overall yield of cross-linked products was ~43% distributed among H2L2 (~1.3%), H2L (~12%), H2 (~22%), and HL (~7.2%) fragments with a H-H/H-L ratio ≈ 2 . Radioiodination of this reduced 5G6.4 + ETAC 1a product mixture at high specific activity (~80 mCi/mg) yielded a single peak by size-exclusion radio-FPLC with an elution time identical with that of radioiodinated intact 5G6.4 (Figure 5).

With the rhodamine ETAC 1b on hand and in view of the availability of 77 IP3 human ovarian carcinoma target cells (expressing an antigen recognized by the antiovarian monoclonal antibody 5G6.4) in our laboratories (28), we examined the binding characteristics of ETAC 1b cross-linked 5G6.4 preparations using flow cytometry analysis by measurement of fluorescence from both fluorescein (using a secondary antimouse antibody probe) and rhodamine independently. The results of these experiments are shown in Figure 6 and summarized in Table I. When the cells were separately incubated with intact 5G6.4 or 5G6.4 containing ~25% ETAC 1b cross-linked products and then probed with fluorescein IgG2a-specific antimouse antibody, no significant difference in the mean fluorescence was observed (Figure 6A). In another experiment, the rhodamine fluorescence of "active" and 5G6.4 "blocked" cells (Figure 6B) incubated with the ETAC 1b cross-linked 5G6.4 were compared. In spite of the relatively high red autofluorescence normally observed for 77 IP3 cells, an increase of ~30–40 fluorescent units (Table I) was clearly visible (Figure 6B) due to the 1b rhodamine conjugated 5G6.4 relative to the negative control used. These experiments qualitatively indicated that the ETAC 1b cross-linking procedure yielded immunoreactive rhodamine-labeled antibodies and that there did not appear to be a significant difference in immunoreactivity between the labeled and unlabeled antibody mixture.

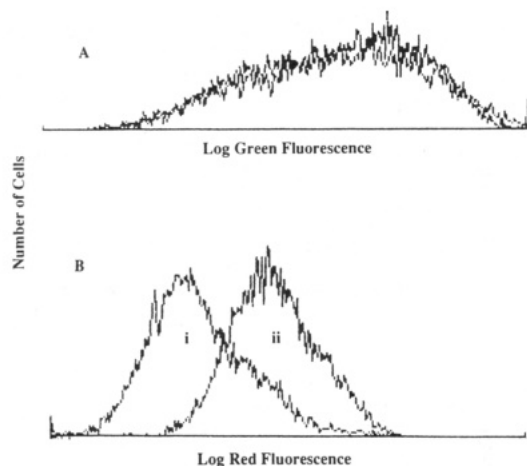


Figure 6. Flow cytometry of reduced 5G6.4 + ETAC 1b: (A) combined plots of observed green fluorescence from IP3 cells incubated separately with reduced 5G6.4 + 1b and intact 5G6.4 followed with fluorescein-IgG2a specific antimouse antibody (note superimposition of both plots). Fluorescence was measured with cells + buffer as a negative control and by using specific antibody concentrations of 10^{-6} $\mu\text{mol/mL}$. (B) Red (rhodamine) fluorescence data from IP3 cells preblocked with excess 5G6.4 (i) and unblocked cells (ii) following treatment with reduced 5G6.4 + 1b preparations.

Table I. Comparative Flow Cytometry Data for 5G6.4 and Reduced 5G6.4 + ETAC 1b

mean ("FITC") fluorescence	
5G6.4(untreated) ^a	156
1b-cross-linked 5G6.4	156
[1b-5G6.4], $\mu\text{g/mL}$	mean ("FITC") fluorescence
3	118 (unblocked)
3	81 (blocked)
30	124 (unblocked)
30	99 (blocked)

^a Results are the average of two flow runs employing 2–3 μg ($\sim 10^{-6}$ μmol) of 5G6.4 per $\sim 4 \times 10^6$ cells against background auto fluorescence (measured as 40–60 fluorescence units) from cells + buffer.

As an additional experiment to determine the effect of ETAC 1 cross-linking on the *in vivo* behavior of the modified antibody, a time-course comparison of the normal tissue and blood biodistribution of ^{131}I -labeled 5G6.4 (control) with ^{125}I -labeled reduced 5G6.4 + 1a was undertaken (Figure 7) in rats. The animal model study revealed no significant differences in tissue activity uptake over a period of 24 h. These results are consistent with no substantial alteration of the antibody structure under the reaction conditions of reduction and cross-linking.

DISCUSSION

X-ray crystallographic data of IgGs indicate the presence of "cavities" near the disulfides of the hinge region which are spacious enough to accommodate small organic molecules (or labels) without disruption of the tertiary protein structure (29, 30). The disulfide–thiol interchange cross-linking of sulfhydryls in the hinge region of an IgG2a monoclonal antibody by crabescien (15) as reported by Packard and co-workers lends support to this observation. Very recently, Brennan also exploited the high reactivity of reduced sulfhydryls in his preparation of F(ab)_2 –Ellman's reagent–thiol protected fragments from an IgG1 monoclonal antibody (31).

Over the past 10 years, the syntheses and reaction chemistry of equilibrium transfer alkylating crosslink reagents

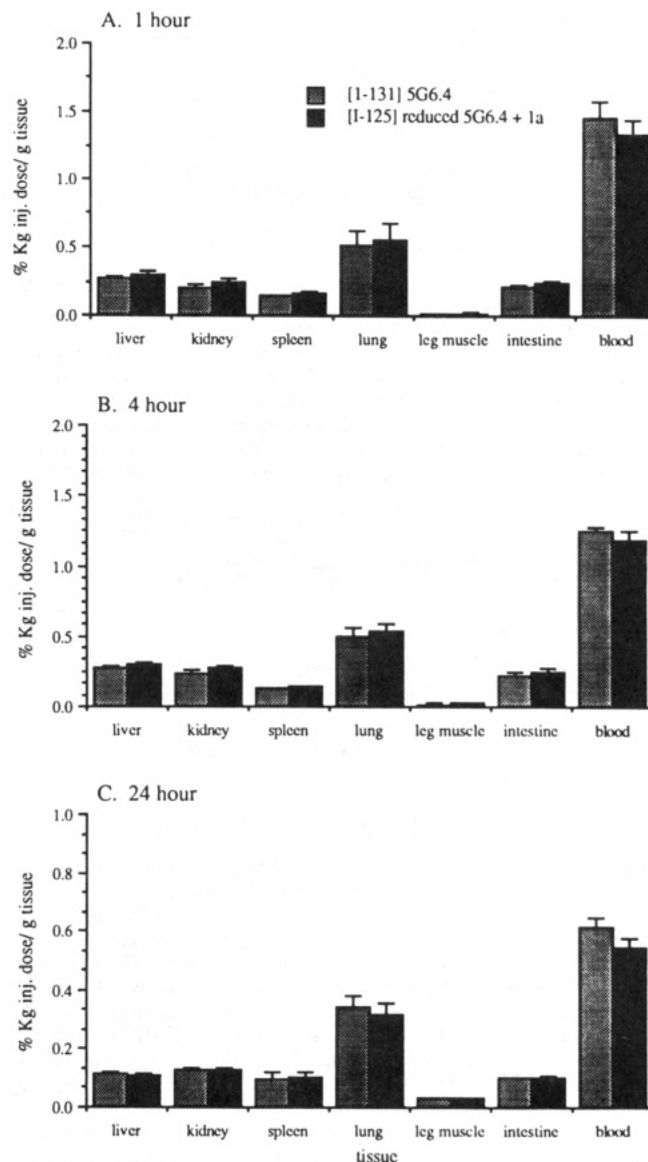
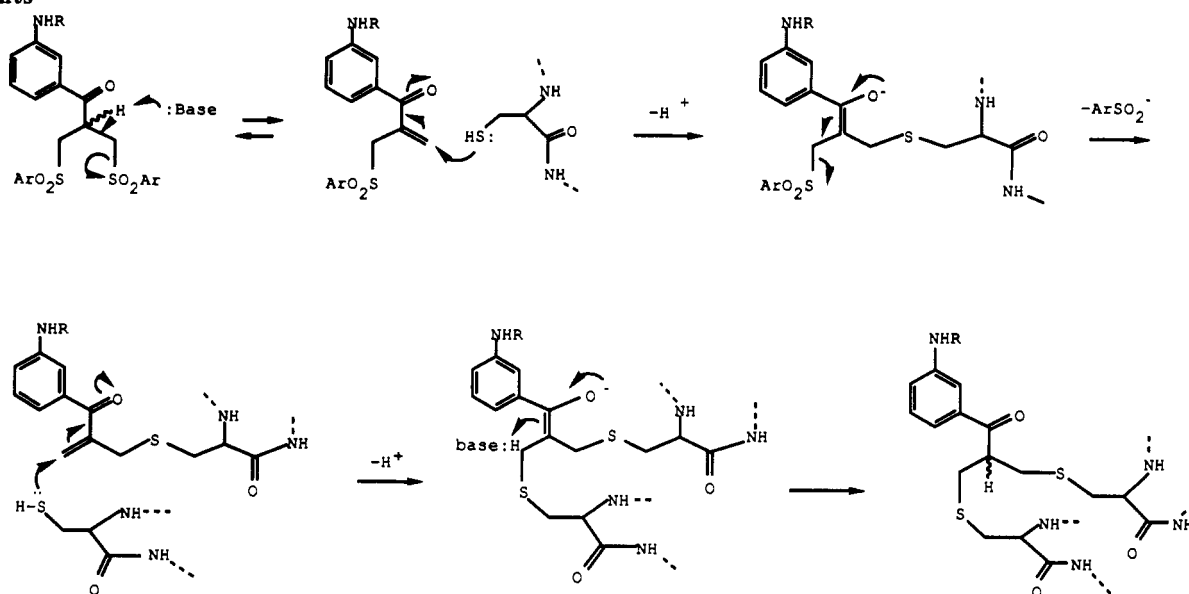


Figure 7. Biodistribution of reduced 5G6.4 + ETAC 1a product and 5G6.4 (control) at three time periods after iv injection. Values given are for $n = 5$ rats, with standard errors of the mean.

have been developed by Lawton and co-workers (18, 19). By virtue of their ability to undergo consecutive Michael and retro-Michael type reactions, these compounds can "skip" or "pivot" along a series of nucleophilic sites on a protein chain and can provide insight into the nature of the most stable cross-links as well as changes in conformation. Thus, the unlabeled ETACs are by themselves powerful molecular tools for studying protein structure. Earlier structural analogues of ETAC 1a,b have already been successfully utilized in a detailed study of intra- and intermolecular cross-linking of the unreduced and reduced forms of ribonuclease. This present study was undertaken in part to assess the potential applications of ETAC technology in labeling monoclonal antibodies and a fluorescent probe seemed most advantageous and efficient.

Previous work on earlier analogues of ETAC 1a,b and their reactions with small organic nitrogen (e.g. amines) and thiol nucleophiles demonstrated a clear kinetic preference for thiols (18). The cross-linking reactions of unreduced and reduced ribonuclease with these earlier compounds also manifested this selectively. A key observa-

Scheme II. Proposed Mechanistic Pathway for the Cross-Linking of Sulphydryls in Monoclonal Antibodies by ETAC Reagents

tion in the same study that bears on the present work was that a substantially higher degree of intermolecular cross-linking was obtained with completely reduced ribonuclease. A notable feature of the ETAC reagents is that even if they add to lysine ϵ -amino groups, at pH = 8 they have a high propensity to transfer to cysteine SH groups (18) since the protonated amine functions are good leaving groups in the retro-Michael process. The site-specific cross-linking of interchain sulphydryls in the monoclonal antibody 225.28S in the presence of a competitive reannealing process is clear evidence for the high reactivity of ETAC 1a,b toward thiols and the stability of these cross-links. The stability of these cross-links is also reflected by our ability to observe cross-link bands when SDS-PAGE was performed on samples which have been heated to 100 °C for 30 min.

The proposed reaction pathway for the cross-linking of sulphydryls from reduced cysteines with compound 1 is shown schematically in Scheme II (18, 19). By analogy with previously reported ETAC compounds, the process is thought to proceed via a sequence of Michael additions by thiol moieties. The cross-linking process is initiated by thiol attack on a 1,2-unsaturated ketone system formed from a base-catalyzed elimination of an aryl sulfone from 1. Upon subsequent elimination of an aryl sulfonate group from the ensuing enolate intermediate, a new 1,2-unsaturated enone is produced. The cross-linking is thus completed by a second thiol Michael addition. The ability of ETAC 1 type compounds to undergo essentially irreversible thiol cross-linking with high specificity (18) presents an advantage over labeling reagents which react via an active ester functionality with limited stability in protic aqueous media (1, 2).

The data of Figures 2 (lane A), 3 (lane A), and 4 (lanes E, I) are reminiscent of the earlier electrophoresis data obtained for the reactions of ETAC reagents with completely reduced ribonuclease (18). However, the interchain insertion of ETAC 1a,b reagents in sulphydryls of heavy and light chains in the monoclonal antibodies 225.28S and 5G6.4 is a significant finding because it was not clear at all prior to this work whether the addition of a three-carbon spacer would result in the formation of stable interchain S-ETAC-S cross-links in IgGs. The short span of an ETAC reagent is very similar to that of

1,3-dibromoacetone, which also alkylates thiols irreversibly and places the distance of the cross-linked nucleophilic sites within 3–4 Å (18, 19, 32). Comparison of the results of this work with that of Packard's crabscsein, which had a significantly longer (13 atoms) and relatively flexible bridge, suggests that reduction of interchain disulfides presumably leads to a conformation which is sufficiently accommodating to undergo varying lengths of cross-linking (15). The presence of a reactive amine function in the parent compound 1a capable of further chemical derivatization, coupled with the observed retention of immunoreactivity and in vivo behavior of cross-linked 5G6.4, makes the concept of ETAC-mediated disulfide bond reannealing an attractive and viable method for sulphydryl-targeted labeling of antibodies.

The data of Figures 2 (lane A), 3 (lane A), and 4 (lanes E, I) show that the high reactivity of ETAC 1 type compounds lead to both cross-linking between heavy-heavy and heavy-light chains. What was perhaps unusual from the gel profiles of Figures 2–4 was the absence of high molecular weight oligomers (MW > 150 000) or aggregates resulting from interantibody cross-linking as has been commonly observed with a number of cross-linkers, such as DTPA dianhydride, which link lysine amine residues (33). The absence of high molecular weight radiolabeled aggregates was also apparent in the radio-FPLC data of Figure 5. Since a large difference in the relative amounts of cross-linked products for the parent ETAC 1a and the rhodamine carrier 1b was not observed [Figures 2 (lane A), 3 (lane A), and 4 (lanes E, I)], the conjugation of labeled substituents to ETAC does not seem to affect the steric requirements or site preference of the cross-linking reactions to a significant extent. This implies that future applications of ETAC chemistry in site-specific labeling of monoclonal antibodies may largely depend on controlling the selectivity of the disulfide reduction or making the ETAC residues more site-selective (i.e. through modification of the sulfone moieties).

The modest yields of ETAC 1 cross-link products may in part arise from a competition from reoxidation of reduced intrachain thiols. Brennan and co-workers have already addressed this in their recent work on the synthesis of bispecific antibodies (31). Figure (lanes G–N) graphically illustrates the related interchain reoxidation

problem. Note that the relative diminishment of bands corresponding to heavy chain (second band from the gel bottom as shown) is accompanied by a concurrent increase in the intensity of a recombination band (fourth band from gel bottom). This observation is qualitatively in agreement with both experimental and kinetic modeling experiments on the reannealing of related IgG1 and IgG2a monoclonal antibodies and suggests a similar major reassembly mechanism involving $H + H = H_2 + 2L = H_2L_2$ for 225.28S (34).

Our experience indicated that ETAC in situ trapping of reduced sulfhydryls of monoclonal antibodies gave comparable results with those where reduced antibody was first separated from reductant prior to reaction with 1. Although we were initially concerned that this strategy could be complicated by side reactions involving undesired intermolecular reactions of reduced antibody, reducing agent, and ETAC reagents, we decided to pursue this latter scheme in part because independent model reaction studies of ETAC reagents with dithiols (e.g. DTT) suggested that formation of heterocyclic adducts resulting from intramolecular reactions were relatively facile in the presence of excess thiol (19). The success of this latter ETAC-quenching approach probably derives in part from the fact that in the actual cross-linking step the second Michael reaction (Scheme II) involves reaction in an intrachain mode of a conjugated double bond whose lifetime is too short for interchain reactions to occur. In conclusion, the present study demonstrates the feasibility of site-specific labeling of monoclonal antibodies using ETAC compounds and serves as a useful guide for directing future experiments with ETAC-mediated labeling of monoclonal antibodies.

ACKNOWLEDGMENT

The competent technical assistance of Andrew Kucharski, Patricia J. Scott, Gayle Ann Jackson, Anaira Clavo, and Martin Strnat is greatly appreciated. We also thank Jerry Hudson and Donald Wieland for helpful discussions, Diane Brede of the Dept. of Pathology for the flow cytometry measurements, and Will Jaynes of the image analysis facility at the University of Michigan Medical Center. Research was supported by the National Institutes of Health (Grants R.O.I. CA41531-02 and P.O.I. CA 42768-01A1) and the National Science Foundation (Grant CHE 8421137A02 and Instrumentation Program).

Registry No. 1a, 123883-91-0; 1b, 123883-92-1; bis[(p-tolylsulfonyl)methyl]-m-nitroacetophenone, 123883-93-2; rhodamine B sulfonyl chloride, 123883-94-3.

LITERATURE CITED

- Bolton, A. E., and Hunter, W. M. (1973) The labeling of proteins to high specific radioactivities by conjugation to a ^{125}I -containing acylating agent. *Biochem. J.* **133**, 529-539.
- Wilbur, D. S., Hadley, S. W., Hylarides, M. D., Abrams, P. G., Beaumier, P. A., Morgan, A. C., Reno, J. M., and Fritzberg, A. R. (1989) Development of a stable radiolabeling reagent to label monoclonal antibodies for radiotherapy of cancer. *J. Nucl. Med.* **30**, 216-226.
- Krejcarek, G. E. and Tucker, K. L. (1977) Covalent attachment of chelating groups to macromolecules. *Biochem. Biophys. Res. Commun.* **77**, 581-585.
- Halpern, S., Stern, P., Hagan, P., Chen, A., Frincke, J., Bartholomew, R., David, G., and Adams, T. (1983) Labeling of monoclonal antibodies with indium 111: technique and advantages compared to radiodine labeling. *Radioimmunoimaging and Radioimmunotherapy* (S. W. Burchiel, and B. A. Rhodes, Eds.) pp 197-205, Elsevier Science Publishing Co., Inc., New York.
- Greenwood, F. C., Hunter, W. H. (1963) The preparation of ^{131}I -labelled human growth hormone of high specific activity. *Biochem. J.* **89**, 114-123.
- Fraker, P. J., and Speck, J. C. (1978) Protein and all membrane iodinations with a sparingly soluble chloroamide, 1,3,4,6-tetrachloro-3L,6L-diphenylglycoline. *Biochem. Biophys. Res. Commun.* **80**, 849-857.
- Marchalonis, J. J. (1969) An enzymic method for the trace iodination of immunoglobulins and other proteins. *Biochem. J.* **118**, 299-305.
- Rodwell, J. C., Alvarez, V. L., Lee, C., Lopes, A. D., Goers, J. W. F., King, H. D., Powsner, H. J., and McKearn, T. J. (1986) Site-specific covalent modification of monoclonal antibodies: In vitro and in vivo evaluations. *Proc. Natl. Acad. Sci. U.S.A.* **83**, 2632.
- Srivastava, P. C., Knapp, F. F., Allred, J. F., and Buchsbaum, D. J. (1988) Monoclonal antibodies radiolabeled with N-(p-[^{125}I]iodophenyl)maleimide retain tumor uptake and show insignificant in vivo deiodination compared with [^{125}I]ICl radiolabeled MoAb. *J. Nucl. Med.* **29**, 836 (abstr.).
- Srivastava, P. C., Knapp, F. F., Dickson, D. R., and Allred, J. F. (1988) Design and synthesis of a new N-(p-[^{125}I]iodophenyl)maleimide "kit" for labeling monoclonal antibodies. *J. Nucl. Med.* **29**, 836 (abstr.).
- Hong, R., and Nisonoff, A. (1965) Relative labilities of two types of interchain disulfide bond of rabbit gamma G-immunoglobulin. *J. Biol. Chem.* **240**, 3883-3891.
- Palmer, J. L., Nisonoff, A., and Van Holde, K. E. (1963) Dissociation of rabbit gamma globulin into subunits by reduction and acidification. *Proc. Natl. Acad. Sci. U.S.A.* **50**, 314-321.
- Nisonoff, A., and Palmer, J. L. (1964) Hybridization of half-molecules of rabbit gamma globulin. *Science* **143**, 376-378.
- Mage, M. G., and Harrison, E. T. (1966) A comparison of the labile disulfide bonds of rabbit gamma G-immunoglobulin fragments. *Arch. Biochem. Biophys.* **113**, 709-717.
- Packard, B., Edidin, M., and Komoriya, A. (1986) Site-directed labeling of a monoclonal antibody: Targeting to a disulfide bond. *Biochemistry* **25**, 3548-3552.
- del Rosario, R. B., and Wahl, R. L. (1989) Site-specific radiolabeling of monoclonal antibodies with biotin/streptavidin. *J. Nucl. Med. Biol.* **16**, 525-529.
- del Rosario, R. B., and Wahl, R. L. Disulfide bond targeted radiolabeling: tumor specificity of a streptavidin-biotinylated monoclonal antibody complex. *Cancer Res.* In press.
- Mitra, S., and Lawton, R. G. (1979) Reagents for the cross-linking of proteins by equilibrium transfer alkylation. *J. Am. Chem. Soc.* **101**, 3097-3110.
- Brocchini, S. J., Eberle, M., and Lawton, R. G. (1988) Molecular yardsticks. Synthesis of extended equilibrium transfer alkylation cross-link reagents and their use in the formation of macrocycles. *J. Am. Chem. Soc.* **110**, 5211-5212.
- Liberatore, F. A., Comeau, R. D., McKearn, J. M., Pearson, D. A., Brocchini, S. J., Kath, J., Phillips, T., Oswell, K., and Lawton, R. G. Site directed modification and cross-linking of a monoclonal antibody using equilibrium transfer alkylation cross-link reagents. *Bioconjugate Chem.* preceding paper in this issue.
- Wilson, B. S., Imai, K., Natali, P. G., and Ferrone, S. (1981) Distribution and molecular characterization of a cell surface and cytoplasmic antigen detectable in human melanoma cells with monoclonal antibodies. *Int. J. Cancer* **28**, 293-300.
- Ey, P., Prowse, S., and Jenkins, C. (1978) Isolation of pure IgG1, IgG2a and IgG2b immunoglobulins from mouse serum using protein A sepharose. *Immunochemistry* **15**, 429-436.
- Wahl, R. L., Liebert, M., Biesman, B., Roberts, J., Jackson, G., Kronberg, S., and Laino, L. (1986) Production and characterization of a murine monoclonal antibody reactive with ovarian and other epithelial carcinomas. *Proc. AACR* **27**, 355 (abstr.).
- Bradford, M. (1976) A rapid and sensitive method for the quantitation of microgram quantities of protein utilizing the

- principle of protein-dye binding. *Anal. Biochem.* **72**, 248-255.
- (25) Laemmli, V. K. (1970) Cleavage of structural proteins during the assembly of the head of bacteriophage T4. *Nature* **222**, 680-685.
- (26) Roholt, O., Onoue, K., and Pressman, D. (1964) Specific combination of H and L chains of rabbit gamma-globulins. *Proc. Natl. Acad. Sci. U.S.A.* **51**, 173-178.
- (27) Sutton, J., Alden, J. R., and Easterbrook-Smith, S. B. (1984) The effects of cleavage of the inter-chain disulfide bonds of rabbit IgG on its ability to bind C1q. *Biochem. Biophys. Acta* **787**, 39-44.
- (28) Wahl, R. L., Liebert, M., Fisher, S., Sherman, P., Jackson, G., Laino, L., and Wissing, J. (1987) Radioimmunotherapy of human ovarian carcinoma xenografts: preliminary evaluation. *Proc. AACR* **28**, 384 (abstr.).
- (29) Amzel, L. M., and Poljak (1979) Three dimensional structure of immunoglobulins. In *Annual Review of Biochemistry* (E. E. Snell, P. D. Boyer, A. Meister, and C. C. Richardson, Eds.) Vol. 48, pp 961-967, Annual Reviews, Inc., Palo Alto, CA.
- (30) Davies, D. R., and Metzger, H. (1983) Structural basis of antibody function. In *Annual Review of Immunology* (W. E. Paul, C. G. Fathman, H. Metzger, Eds.) Vol. I, pp 87-117, Annual Reviews, Inc., Palo Alto, CA.
- (31) Brennan, M., Davison, P. F. and Paulus, H. (1985) Preparation of bispecific antibodies by chemical recombination of monoclonal immunoglobulin G1 fragments. *Science* **229**, 81-83.
- (32) Husain, S. S. and Lowe, G. J. (1968) Evidence for histidine in the active site of papain. *Biochem. J.* **108**, 855-859.
- (33) Paik, C. H., Ebbert, M. A., Murphy, P. R., Lassman, C. R., Reba, R. C., Eckelman, W. C., Pak, K. Y., Powe, J., Steplewski, Z., and Koprowski, H. (1983) Factors influencing DTPA conjugation with antibodies by cyclic DTPA anhydride. *J. Nucl. Med.* **24**, 1158-1163.
- (34) Sears, D. W., Mohrer, J., and Beychok, S. (1975) A kinetic study of the reoxidation of interchain disulfide bonds in a human immunoglobulin IgG1k. Correlation between sulfhydryl disappearance and intermediates in covalent assembly of H_2L_2 . *Proc. Natl. Acad. Sci. U.S.A.* **72**, 353-357.

Radiometal Labeling of Immunoproteins: Covalent Linkage of 2-(4-Isothiocyanatobenzyl)diethylenetriaminepentaacetic Acid Ligands to Immunoglobulin

Saed Mirzadeh,* Martin W. Brechbiel, Robert W. Atcher,[†] and Otto A. Gansow

Inorganic and Radioimmune Chemistry Section, Radiation Oncology Branch, National Cancer Institute, National Institutes of Health, Bethesda, Maryland 20892. Received July 27, 1989

A study was made of the covalent attachment of the bifunctional 2-(4-isothiocyanatobenzyl)diethylenetriaminetetraacetic acid family of chelate ligands to proteins for the purpose of labeling monoclonal antibodies with radiometals. The parameters and the chemical variables examined included pH, reaction period, temperature, and ligand and protein concentrations. It is shown that these variables, with the exception of protein concentration, have significant effects on the rate of protein conjugation. Conjugation of three monoclonal antibodies and human IgG under identical conditions showed only 17% variation. Finally, the effect of the concentration of conjugated IgG on radiolabeling yield was studied.

Attachment of radioactive metals to proteins by use of bifunctional chelate ligands (ligands) has expanded in use as an alternative to radiohalogenation (1-3) as the availability of these ligands has increased (4-7). The variety of metal isotopes with useful nuclear properties exceeds that of the halogen isotopes, giving the investigator greater flexibility in choosing a diagnostic or therapeutic agent. Further, the development of monoclonal antibodies (MoAb) has yielded an ideal vehicle for transporting radioactivity to living cells, perhaps the magic bullet long sought for use in medicine (8).

Derivatives of diethylenetriaminepentaacetic acid (DTPA) and ethylenediaminetetraacetic acid (EDTA) have been extensively used as ligands in recent years (9-15). The cyclic and mixed anhydrides DTPA (CA- and MA-

DTPA, respectively) react with immunoglobulins (predominately with ϵ -amino groups of lysine side chains) through one of the carboxylate groups of the ligand (5-7, 14), resulting in a net loss in the metal-binding capability of the ligand molecule. This problem is resolved in bifunctional ligands such as DTTA-azo-imidate [*N'*-[4-[[2-hydroxy-5-(iminomethoxymethyl)phenyl]azo]benzyl]diethylenetriaminetetraacetic acid] (15) and 2-(4-isothiocyanatobenzyl)-EDTA (SCN-Bzl-EDTA) or -DTPA (9-11), which contain a protein-binding group that is distinct from the metal-chelating group. In the latter cases the SCN group on these ligands reacts with ϵ -amino groups with formation of a thiourea group (9-11, 16, 17). As demonstrated in Figure 1a, the ligand portion of the molecule remains unchanged upon protein attachment, thus ensuring the expected stability of metal-ligand complex (metal chelate).

The CA- and MA-DTPA also have the potential for cross-linking of protein inter- and intramolecularly. In the case of the isothiocyanate linkage, no potential for

* To whom all correspondence should be addressed: NIH, 10/B3B69, 9000 Rockville Pike, Bethesda, MD 20892.

[†] Chemistry Division, Argonne National Laboratory, Argonne, IL 60439.

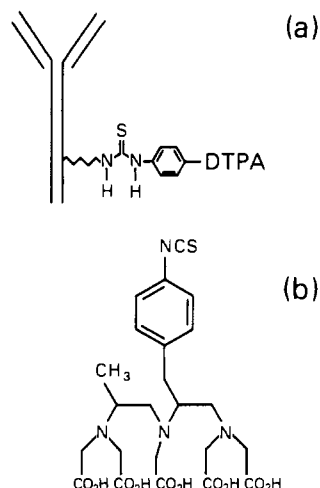


Figure 1. (a) Attachment of isothiocyanate group to protein via formation of a thiourea group with the ϵ -amino group of lysine side chain; (b) structure of 1M3B-DTPA.

cross-linking exists, thus the integrity of the protein molecules is more likely to be conserved. In addition, the coupling reaction does not involve the release of 4 equiv of H^+ per mole of ligand as does the hydrolysis of the dianhydride. Furthermore, the SCN-Bzl derivatives of EDTA or DTPA are relatively stable in aqueous solutions yet are adequately reactive to proteins. Importantly, they can be stored for long periods without noticeable degradation (9, 10).

Recently, we have reported a series of biodistribution studies of radiolabeled MoAb employing SCN-Bzl-EDTA, SCN-Bzl-DTPA, and various alkyl derivatives of SCN-Bzl-DTPA (12, 13). In this paper, a systematic study of the chemical factors which influence binding of the SCN-Bzl-DTPA family of ligands [specifically, ^{14}C -labeled 3-(4-isothiocyanatobenzyl)-6-methyldiethylenetriaminepentaacetic acid (1M3B-DTPA), Figure 1b] to proteins is presented. Variables explored included pH, reaction period, temperature, and ligand and protein concentrations. In addition, the effect of the concentration of chelate ligand conjugated IgG (conjugated IgG) on the ^{111}In -radiolabeling yield was also examined. Human IgG, a polyclonal protein with an average molecular weight of 150 kDa, was used as the protein model for these investigations. This choice was primarily based on the ready availability of this protein in high purity and high concentration. Finally, the direct applicability of the results and methodology presented in this work was demonstrated by results from conjugations of three clinically used MoAb's (B72.3, anti-Tac, UPC10) with the 1M3B-DTPA ligand. The immunoreactivity or the binding affinity of the chelate ligand modified MoAb to its antigenic target is an important criterion which deserves systematic study and discussion which are beyond the scope of the present work. In brief, we have shown that anti-Tac with two or less ligands per antibody retained its full binding affinity (12) and B72.3 retained its immunoreactivity when the ligand to protein ratio was less than one (9, 13). This compromise between the immunoreactivity and the number of ligands bonded to immunoproteins let us limit our study over a region of the ligand concentration which produced a practical ligand to protein ratio ≤ 4 .

All measurements of ligand binding are presented in terms of a final chelate ligand to protein molar ratio, (CL/P)_f, moles of ligands bound per mole of protein as determined by use of carbon-14 labeled ligands.

EXPERIMENTAL PROCEDURES

Materials, Reagents, and Instrumentation. To reduce the metal ion contamination, specifically the common metals [e.g. Fe(III), Zn(II), Cu(II)], plasticware (metal-free low protein binding polypropylene) was used in almost all protein work.

All reagents used were of analytical grade or better. In general, all buffers were prepared in 10 \times concentration in 2-L volumes. They were first filtered through 0.45- μ m cellulose nitrate filter papers (e.g. Whatman #D552), then passed through a column of Chelex-100 resin (2.5 \times 10 cm, preequilibrated with the same buffer, see below for specifications), and finally, prior to storage at 4 $^{\circ}C$, they were filtered through a 0.22- μ m sterile cellulose acetate membrane filtration unit (e.g. Corning 25942, Corning, NY). The composition of the buffers and reagents were as follows: HEPES [*N*-(2-Hydroxyethyl)piperazine-*N'*-ethanesulfonic acid] buffer, 50 mM in HEPES, 150 mM in NaCl, pH = 8.6; MES [2-(*N*-morpholino)ethanesulfonic acid] buffer, 20 mM in MES, 150 mM in NaCl, 0.05% NaN_3 , pH = 6.2; citrate buffer, 50 mM in sodium citrate, 150 mM in NaCl, 0.05% NaN_3 , pH = 5.5; phosphate buffer, 50 mM in KH_2PO_4 , the pH (6.7–8.3) was adjusted with the addition of 0.1 M NaOH; borate buffer, 50 mM with respect to both H_3BO_4 and KCl, the pH (8.0–10.3) was adjusted with the addition of 0.1 M of NaOH; NaCl reagent, 150 mM in NaCl, 0.05% NaN_3 ; Human IgG, GAMMAGARD, obtained from Travenol Laboratory, Inc. (Glendale, CA). The lyophilized IgG was rehydrated to produce a preparation 150 mM in NaCl (pH = 6.8) containing ~ 50 mg/mL of protein ($\sim 94\%$ IgG and $\sim 6\%$ human albumin). Bovine plasma γ -globulin (BSG γ) as protein standard was obtained from Bio-Rad Laboratories (Richmond, CA; catalogue #500-0005). Monoclonal antibodies anti-Tac and UPC10 were furnished by Dr. Thomas Waldmann (18) (Metabolism Branch, NCI, NIH), and B72.3 and BL3 were furnished by Dr. David Colcher (19) (Laboratory for Tumor Immunology and Biology, NCI, NIH). Tubular membrane for dialysis made of regenerated cellulose with a molecular weight cutoff (MWCO) of 12–14 kDa (Spectra/Por2, 10-mm flat width) was obtained from Spectrum Medical Industries (Los Angeles, CA). The dry membrane after treatment with EDTA to remove heavy metals was stored at 4 $^{\circ}C$ in a 0.05% solution of sodium azide. Chelex-100 resin was the Na^+ form, 100–200 mesh (Bio-Rad Laboratories). Resin was exhaustively washed with and stored in deionized H_2O . Size-exclusion columns for HPLC were Bio-Sil TSK-125, 250, and 400 series (Bio-Rad Laboratories). The protein microconcentrator used was a Centricon 30, MWCO = 30 kDa, Amicon Corp. (Danvers, MA). The HPLC used was a Model 2150/2152, LKB (Bromma, Sweden).

Ligand. ^{14}C -labeled 3-(4-isothiocyanatobenzyl)-6-methyldiethylenetriaminepentaacetic acid (1M3B-DTPA) was used as the ligand. A detailed description of synthetic methods of this compound and a procedure for ^{14}C synthesis is given by Brechbiel et al. (9, 10). The ^{14}C label was introduced by use of $Br^{14}CH_2CO_2H$ in the alkylation step of the synthesis. The tricesium salt of ^{14}C -1M3B-DTPA was stored over Drierite in a vacuum desiccator over a period of 1 year without any noticeable degradation in reactivity. As needed, 1.4 mg was dissolved in 100 μ L of H_2O to produce a 1.0×10^{-2} M solution of ligand. The specific activity of this batch (used throughout these studies) was 1.807×10^6 dpm/ μ mol, which was measured by correlating the ^{14}C counting rate (dpm) of a known volume of a ligand solution with ligand

concentration, as measured by UV absorption at 280 nm (9).

Radioactivity and Counting Methods. No-carrier-added ^{111}In (specific activity of about 50 mCi/ μg) was obtained from New England Nuclear/Du Pont (Boston, MA). The activity concentration was approximately 50 mCi/mL in 0.05 M HCl. The ^{111}In activity was quantitated by measuring its 171.3 (90.3%) and 245.4 (94.0%) KeV γ -rays in a NaI (T1) well type scintillation detector coupled to a multichannel analyzer (MCA). Samples of constant liquid geometry were counted for a duration sufficient to provide counting statistics of $\leq 2\%$. A gas ionization chamber (CRC-7, Capintec Instrument Inc., Ramsey, NJ) was used for gross activity measurements. A 1000-channel scintillation counter (LS5801, Beckman, Fullerton, CA) was used for quantitative determination of ^{14}C activity. Generally, a 50- μL aliquot of a sample containing ^{14}C was mixed with 10 mL of scintillation cocktail (Biofluor, NEN/Du Pont). The absolute disintegration of ^{14}C was determined by appropriate corrections for background and quench factor.

Protein Preparation and Measurement. The protein solutions were dialyzed against at least a 500-fold volume excess of HEPES buffer (or other buffers as needed) for 24 h. To deplete metal ion contaminants, Chelex-100 resin was added to the dialysates (~ 1 g/L). The protein concentrations were determined from UV absorption, at 280 nm. A value of 1.35 absorbance units per mg/mL was used for the extinction coefficient for IgG and the four monoclonal antibodies anti-Tac, UPC10, B72.3, and BL3. The SCN-Bzl-DTPA family of ligands also exhibits some absorption at this wavelength (due to the aromatic ring). Depending on the value of $(\text{CL}/\text{P})_f$, some corrections of the protein concentration were necessary (about 3% for every ligand per protein molecule of 150 kDa molecular weight).

The UV absorption method was compared with the bicinchoninic acid (BCA) colorimetric determination (20). The BCA assay is more sensitive than the UV method and can be used for determination of protein concentrations as low as a few $\mu\text{g}/\text{mL}$. This procedure is sensitive to temperature and reaction time and does not result in a linear Beer's law plot. The most convenient and reproducible conditions were found to be a 30-min incubation at 60 $^{\circ}\text{C}$. Typically, 100 μL of a protein solution (100 $\mu\text{g}/\text{mL}$) was added to 2 mL of a BCA working solution in a standard 1.3×10 cm Pyrex tube. The BCA working solution was freshly prepared by mixing 600 μL of solution A (4% $\text{CuSO}_4 \cdot 5\text{H}_2\text{O}$) with 30 mL of solution B (1% $\text{BCA} \cdot \text{Na}_2$, 2% $\text{Na}_2\text{CO}_3 \cdot \text{H}_2\text{O}$, 1.6% sodium tartrate, 0.4% NaOH , 0.95% NaHCO_3 , pH = 11.25). After a 30-min incubation at 60 $^{\circ}\text{C}$, the samples were quickly cooled to room temperature and their absorbance was measured vs a reagent blank at 562 nm. The protein standard bovine plasma γ -globulin in concentrations ranging from 20 to 200 $\mu\text{g}/\text{mL}$ in the same buffer as the other proteins, was used to construct the Beer's law plot.

Reaction of Isothiocyanatobenzyl-DTPA with IgG. In general, 2–4 mg of IgG in a concentration of about 10 mg/mL (in HEPES buffer, pH = 8.62, 200–400 μL in volume) was mixed with 2–10 μL of 1M3B-DTPA ligand solution (1×10^{-2} M in H_2O). The pH of the reaction mixture was measured by a semimicro glass electrode. The initial ligand-to-protein molar ratio, $(\text{CL}/\text{P})_i$, was determined by measuring the concentration of ligand in the reaction mixture. Typically, 20 μL of the reaction mixture was taken for ligand determination by ^{14}C counting. The protein concentration in the reaction mixture

was based on the protein measurement of an external standard which was prepared in parallel and was identical with the reaction mixture, but excluded the ligand. The reaction mixture was allowed to stand at room temperature for the desired period of time. The unconjugated or free ligand was separated from protein by serial dialysis. Typically, 2–4 mg of protein was dialyzed against 2×500 mL of citrate buffer for at least 12 h each time and then against NaCl reagent for a few hours. The $(\text{CL}/\text{P})_f$ of the conjugated IgG was then determined. In all experiments duplicate samples were used. The following describes the specific modifications to the above general procedure.

Effect of pH. The following reaction mixture was prepared. To 80 μL of protein stock solution (in 150 mM NaCl) containing 4 mg of protein was added 320 μL of the appropriate buffer of various pH values and 10.0 μL of the ligand solution. The pH of the reaction mixtures ranged from 6.75 to 10.1.

Effect of Reaction Period and Temperature. Reaction mixtures were prepared in a cold room at 5 $^{\circ}\text{C}$. At time zero, duplicate samples were placed in various temperature baths. At various time points, 300 μL of each reaction mixture was taken for the $(\text{CL}/\text{P})_f$ determination as described in the general procedure.

Effect of Concentration of Ligand. To 400 μL of IgG solution (10.0 mg/mL in HEPES buffer, pH = 8.62) were added various amounts of a ligand solution (3–50 μL), for $(\text{CL}/\text{P})_i$ ranging from 0.73 to 10.3. Then the total volume of the reaction mixture was adjusted to 460 μL with HEPES buffer. After this point the general assay procedure was followed.

Effect of Protein Concentration. By using sequential dilution, six IgG samples in concentrations ranging from 3.1 to 25.0 mg/mL in HEPES buffer were prepared from a stock solution of IgG (~ 50 mg/mL). Appropriate amounts of ligand solution were then added to each sample in order to keep the $(\text{CL}/\text{P})_i$ constant at 4.0 ± 0.2 . Then the volumes of the reaction mixtures were adjusted to 440 μL by the addition of HEPES buffer.

Although in these experiments membrane dialysis principally was used to isolate the free ligand from the conjugated IgG, two other methods, ultracentrifugation and size-exclusion HPLC, were also tested.

Ultracentrifugation was performed by using microcentrifugers with MWCO of 30 kDa and an active membrane surface area of 0.92 cm^2 . In this case the reaction was quenched by the addition of 1 mL of MES buffer followed by 20 min of centrifugation at 4200g at 4 $^{\circ}\text{C}$. To remove 99.9% of the unconjugated ligand the above step was repeated twice.

Purification of conjugated IgG from free ligand by size-exclusion HPLC was also explored. Excellent separation was achieved on a TSK-125 column. The eluent was MES buffer, pumped at a flow rate of 1 mL/min at room temperature. Chromatography was monitored at 280 nm. Under the above conditions, IgG eluted with a retention time of 6 min (almost at the column void volume) and the free ligand eluted at 11.2 min with FWHM = 2.0 min. Better than 85% of IgG was recovered in 4-mL volume when the initial reaction mixture contained about 1 mg of protein.

Procedure for ^{111}In Labeling of Conjugated IgG. An [^{111}In]Indium acetate solution was prepared at pH = 3.8–4.0 by addition of appropriate amounts of 2 M NaOAc to a $^{111}\text{InCl}_3/\text{HCl}$ mixture. Typically, 15 μL of the above mixture containing about 350 μCi of ^{111}In was added to a reaction vial containing 135 μL of a mixture of ligand-

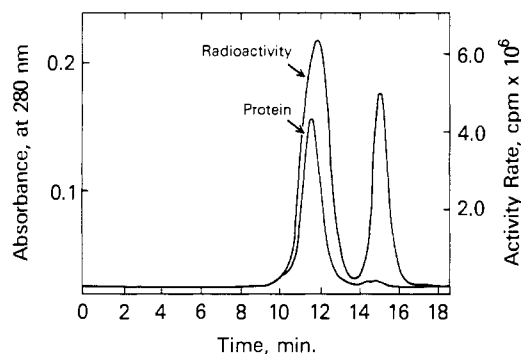


Figure 2. A typical HPLC chromatogram of ^{111}In -labeled [1M3B-DPTA]-IgG [conjugated IgG = 50 μg [(CL/P)_f = 0.23], unconjugated IgG = 450 μg ; ^{111}In activity \approx 350 μCi ; buffer = MES-Cl, pH = 6.2; flow rate = 1 mL/min; chart speed = 1 cm/min; pressure = 20 bar; TSK-400 size-exclusion column].

Table I. Comparison of Protein Concentration Measurements via UV Absorption at 280 nm and BCA Colorimetric Assay

protein	[protein], $\mu\text{g/mL}$		% difference ^a
	UV (280 nm)	BCA colorimetric ^b (562 nm)	
B72.3	242.5	245.9	1.4
BL3	222.2	229.5	3.2
anti-Tac	215.8	221.0	2.4
UPC10	234.3	238.1	1.6
IgG	238.1	264.9	10.1

^a Percent difference = $(\text{BCA} - \text{UV}) \times 100 / \text{BCA}$. ^b Vs primary external protein standards (see the Experimental Procedures).

conjugated and unconjugated IgG (total of 1 mg of protein in MES buffer). The pH of the reaction mixture was kept between 4.0 and 4.2. After 30 min, the reaction was quenched by raising the pH to about 6 by the addition of 10 μL of 2 M NaOAc followed by 3 μL of 10^{-2} M Na_2EDTA to scavenge any free ^{111}In . Subsequently, the radiolabeled protein was isolated from unreacted or free indium by HPLC employing a TSK-400 size-exclusion column. The HPLC was operated isocratically at pH = 6.2 (MES buffer) with 1.0 mL/min flow rate and was equipped with dual on-line UV and radioactivity detectors. Typically, 24 0.5-mL fractions were collected and the radiolabeling yield was determined as the ratio of the radioactivity of the protein peak to the total activity in all tubes. A representative chromatogram is shown in Figure 2.

Procedure for Purification of ^{111}In . ^{111}In activity was retained by cation-exchange resin from 8 M HBr (AG50Wx4, 2×20 mm, 100–200 mesh, pre-equilibrated with 8 M HBr). Under these conditions, excellent separations could be achieved from Co, Ni, Cu, and Zn. Subsequently, ^{111}In was eluted with 8 M HCl while a trace amount of Fe was strongly retained (21). The eluent was evaporated to dryness under an IR heat lamp and the ^{111}In activity was leached from the surface of the glass with 0.1 M HCl.

RESULTS AND DISCUSSION

As discussed in the introduction, the chelate ligand to protein molar ratio, (CL/P), was used as a measure of efficiency of ligand–protein binding. Obviously, determination of (CL/P) depends on the protein concentration and an accurate assay of protein is therefore necessary. The results of the protein assay by UV absorption and BCA colorimetric method are summarized in Table I. In addition to IgG, four monoclonal antibodies (anti-

Table II. Effect of Concentration of Chelate Ligand^a

[ligand], M	(CL/P) _i	(CL/P) _f	(CL/P) _{f/i}
3.88×10^{-5}	0.73	0.33	0.45
6.25×10^{-5}	1.17	0.55	0.47
1.17×10^{-4}	2.19	0.93	0.43
1.82×10^{-4}	3.41	1.42	0.42
2.42×10^{-4}	4.54	1.84	0.41
5.50×10^{-4}	10.3	3.71	0.36

^a [IgG] = $(4.6 \pm 0.2) \times 10^{-5}$ M (6.9 ± 0.3 mg/mL); reaction period = 17.3 h; pH = 8.62; temperature = 27 °C; volume of reaction = 460 μL .

Table III. Effect of Protein Concentration^a

[IgG]		(CL/P) _f
mg/mL	M	
2.43	1.62×10^{-5}	1.12
5.99	3.99×10^{-5}	1.29
9.27	6.18×10^{-5}	1.43
11.4	7.60×10^{-5}	1.45
21.9	1.46×10^{-4}	1.52
23.4	1.56×10^{-4}	1.58

^a (CL/P)_i = 4.0 ± 0.2 ; reaction period = 17.0 h; pH = 8.62; volume of reaction mixture = 440 μL ; temperature = 27 °C.

Table IV. Conjugation of Various Proteins^a

protein	[protein] _{rxn} , M	(CL/P) _i	(CL/P) _f	(CL/P) _{f/i}
IgG	5.19×10^{-5}	4.26	1.48	0.34
anti-Tac	4.79×10^{-5}	4.82	1.04	0.23
UPC10	5.21×10^{-5}	4.39	1.16	0.26
B72.3	5.39×10^{-5}	4.75	1.52	0.32
average	$(5.15 \pm 0.23) \times 10^{-5}$	4.56 ± 0.29	1.30 ± 0.15	0.29 ± 0.05

^a Reaction period = 16.1 h; temperature = 27 °C; volume of reaction mixture = 204 μL .

Table V. ^{111}In Labeling of Conjugated IgG: Effect of the Concentration of Conjugated IgG on Radiolabeling Yield at Constant ^{111}In Activity^a

[conj IgG], M	(CL/P) _f	% radiolabeling yield ^c	ratio of ^{111}In to conj IgG, $\mu\text{Ci}/\mu\text{g}$	% fraction of available sites occupied by ^{111}In atoms ^d
0.0 ^b	0.0	0.0	0.0	0.0
6.7×10^{-7}	0.23	69	4.8	31.0
1.3×10^{-6}	0.23	72	2.5	16.0
1.7×10^{-6}	0.23	89	2.5	16.0
3.3×10^{-6}	0.23	92	1.3	8.2
6.7×10^{-6}	0.23	93	0.65	4.1
1.3×10^{-5}	0.23	90	0.32	2.0
1.3×10^{-5}	0.35	92	0.32	1.4

^a Volume of reaction mixture = 150 μL ; the concentration of protein in the reaction mixture was adjusted to 1.3×10^{-5} M by the addition of unconjugated IgG; reaction period = 30 min; temperature = 27 °C; activity of ^{111}In \approx 350 μCi ; pH = 4.0–4.2.

^b 1.0 mg of unconjugated IgG. ^c See the text for definition.

^d Based on the specific activity of commercially available ^{111}In , see the Experimental Procedures.

Tac, UPC10, B72.3, and BL3) were also used in these comparative studies. The UV assays were only 2–3% lower than results obtained by BCA colorimetric assays for all four monoclonal proteins of 150-kDa molecular weight. However, in the case of the polyclonal human IgG (with the same average molecular weight) the difference was about 10%. The UV absorption bands are primarily due to the aromatic amino acids (e.g. tryptophan and tyrosine, ϵ = 5700 and 1300 $\text{M}^{-1} \text{cm}^{-1}$, respectively, at 280 nm). Proteins do not all have the same content of aromatic amino acid; consequently, two proteins at the same concentration may absorb to a different degree. As indi-

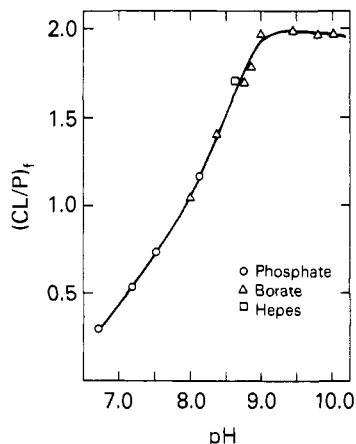


Figure 3. Variation of the final ligand-to-protein molar ratio, $(CL/P)_f$, as a function of pH [$(CL/P)_i = 3.9 \pm 0.4$; $[IgG]_{rxn} = 6.1 \times 10^{-5}$ M, 8.9 mg/mL; reaction period = 16.6 h, temperature = 27 °C].

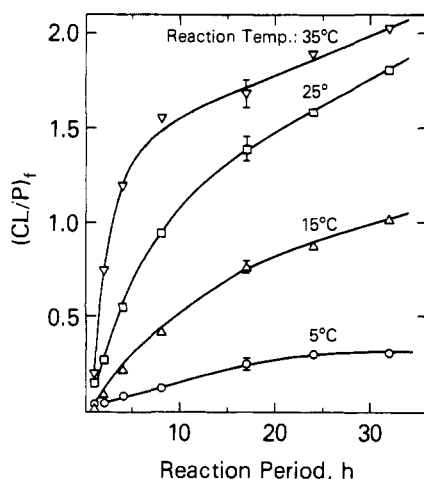


Figure 4. Effect of reaction period on $(CL/P)_f$ for various temperatures [$(CL/P)_i = 3.7$; $[IgG]_{rxn} = 5.7 \times 10^{-5}$ M; pH = 8.42].

ated above, no significant variations in UV assay of the four MoAb's were observed by using 1.35 absorbance units per mg/mL as the extinction coefficient.

As far as conjugation was concerned, no significant differences were observed among three methods, dialysis, ultracentrifugation, and size-exclusion HPLC, for isolation of free ligand from conjugated IgG. Inherently, dialysis is a slow process and requires a few days to obtain the final product.

Both centrifugation and HPLC methods are faster techniques and separation could be completed within a few hours. However, in subsequent radiolabeling of the conjugated-IgG samples prepared by these three methods, appreciable higher radiolabeling yield was obtained for the dialysis sample. Possibly, this is an indication of the effectiveness of serial dialysis in the removal of metal ion contaminants.

The results of binding of the SCN-Bzl-DTPA to the proteins illustrating the effect of pH, reaction period, temperature, and ligand and protein concentrations are presented in Tables II–V and Figures 3–6.

Effect of pH and Buffers. The results of these experiments, plotted in Figure 3, showed a simple and interpretable pattern. At $[IgG] = 6.1 \times 10^{-5}$ M, the $(CL/P)_f$ increased sharply from 0.29 to 1.96, as the pH of the reaction mixture increased from 6.71 to about 9. Above pH 9 (9.0–10.0), the $(CL/P)_f$ leveled off at 1.96 and remained rather independent of pH. The increase in $(CL/P)_f$ as a

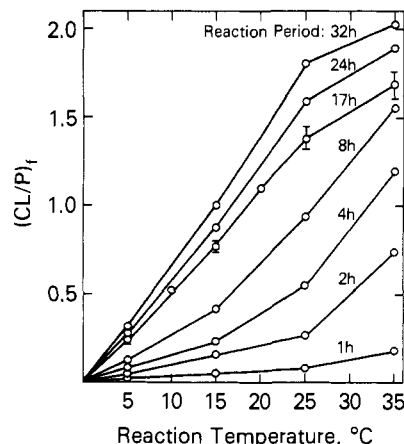


Figure 5. Effect of temperature on $(CL/P)_f$ for various reaction periods [$(CL/P)_i = 3.7$; $[IgG]_{rxn} = 5.7 \times 10^{-5}$ M; pH = 8.42].

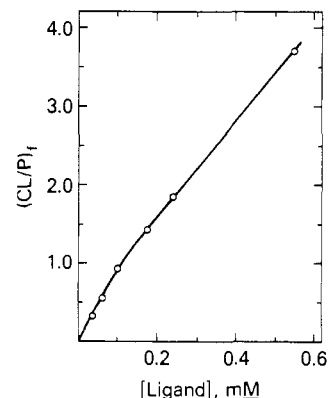


Figure 6. Variation of $(CL/P)_f$ as a function of the concentration of ligand (see Table II for conditions).

function of pH is likely due to the greater deprotonation of the ϵ -amino group of the lysines at higher pH values providing additional NH_2 sites for reaction with the isothiocyanate group. Degradation of isothiocyanate to thiourea at pH 9 and above (22, 23) could account for the pH-independent behavior of $(CL/P)_f$. The use of different buffers of equal ionic strength did not seem to have any significant effect on the rate of conjugation, as indicated in Figure 3.

Effects of Reaction Period and Temperature. In a series of parallel experiments, the effect of the reaction period was studied at 5, 15, 25, and 35 °C. Results are shown in Figure 4. All data points (except 17-h time points) represent the average of duplicate measurements. The data for the 17-h time points are the average of data from two independent experiments. At 25 °C, $(CL/P)_f$ increased rapidly to 0.94 within the first 8 h. Thereafter, from 8 to 32 h, $(CL/P)_f$ increased only 0.86 unit to 1.8. At 35 °C, the initial rate of the reaction was quite fast and $(CL/P)_f$ reached about 1.5 during the first 8 h. The effects of varying the temperature for different reaction periods are illustrated in Figure 5. The exponential dependence of the yield on temperature, which is expected for biomolecular reactions, is clearly suggested for reaction periods up to 17 h. However, for 17, 24, and 32 h this exponential dependence is less clear and a decreasing trend in $(CL/P)_f$ even can be seen at 35 °C.

The data describing the variation in yield as a function of temperature is important for two reasons. First, it markedly improves the kinetics of the reaction. Second, most antibodies are best maintained at lower tem-

perature until use, and these results could be used to optimize the conjugation temperature of various antibodies.

Effect of Concentration of Chelate Ligand. These data are summarized in Table II, and a plot of $(\text{CL}/\text{P})_f$ vs $[\text{ligand}]_{\text{rxn}}$ is shown in Figure 6. At $[\text{IgG}] = 6.9 \pm 0.3$ mg/mL, pH = 8.62, and reaction period of 17.3 h, a 14-fold increase in concentration of ligand from 3.9×10^{-5} to 5.5×10^{-4} M resulted in a 12-fold increase in $(\text{CL}/\text{P})_f$ from 0.33 to 3.71. The ratio of $(\text{CL}/\text{P})_f$ to $(\text{CL}/\text{P})_i$ ($(\text{CL}/\text{P})_{f/i}$, a measure of the linearity of the relationship) remains rather constant at 0.44 ± 0.03 when the $(\text{CL}/\text{P})_i$ increased from 0.73 to 4.54 (Table II, column 4), indicating first-order dependence of the reaction rate on the ligand concentration over this concentration range. At $(\text{CL}/\text{P})_i = 10.3$, the corresponding ratio dropped to 0.36; however, under the above conditions the saturation point of the lysines has not yet been observed. These data indicate that the reaction between IgG and 1M3B-SCN-Bzl-DTPA proceeds well at low initial ligand-to-protein ratio, in contrast to the reaction between protein and DTPA dianhydride or mixed anhydrides of DTPA, where a minimum of a 50-fold excess of ligand to protein is required to produce comparable results (6, 7). Moreover, the reaction between SCN-Bzl-DTPA and IgG can be allowed to proceed over a greater range of ligand concentrations since there is no possibility of cross-linkage.

Effect of Protein Concentration. At $(\text{CL}/\text{P})_i = 4.0 \pm 0.2$, pH = 8.62, and reaction period = 17.0 h, a 10-fold increase in the concentration of IgG from 2.4 to 23.4 mg/mL resulted in only a 1.4-fold increase in the $(\text{CL}/\text{P})_f$ from 1.12 to 1.58 (Table III). These results do not represent the first-order dependence of the reaction rate on the protein concentration.

Conjugation of Various Proteins. When IgG and three other monoclonal antibodies (anti-Tac, UPC10, and B72.3) were simultaneously conjugated under identical experimental conditions, no significant variation was observed in conjugation efficiencies (Table IV). An average value of 1.2 ± 0.3 for $(\text{CL}/\text{P})_f$ was obtained for the above proteins when concentrations of proteins in the reaction mixture were $(5.2 \pm 0.2) \times 10^{-5}$ M, with $(\text{CL}/\text{P})_i = 4.6 \pm 0.3$, and when the reactions were allowed to proceed for 17.0 h. This would indicate that it is possible to define a set of standard conditions for the reaction of SCN ligand with MoAb's.

Radiolabeling: Effect of the Concentration of 1M3B-DTPA-IgG on the Radiolabeling Yield at Constant ^{111}In Activity. Results of these experiments are summarized in Table V. When 1.0 mg of unconjugated IgG was used in the reaction, the radiolabeling yield was 0 (Table V, first row), indicative of the absence of non-specific binding of ^{111}In under our experimental conditions. The radiolabeling yield remained about 90% when the concentration of conjugated IgG [with $(\text{CL}/\text{P})_f = 0.23$] in the reaction mixture decreased over 1 order of magnitude from 1.3×10^{-5} to 1.7×10^{-6} M. Further decrease in concentration of conjugated IgG resulted in a decrease in radiolabeling yield. When the concentration of conjugated IgG was 6.7×10^{-6} M, the yield dropped to 69%. The ratio of activity (μCi) incorporated per microgram of protein also decreased from 4.8 to 0.32 as the concentration of conjugated protein increased from 6.7×10^{-7} to 1.3×10^{-5} M (Table V, column 4). It was not possible to attain a 100% radiolabeling yield under any conditions. In addition to acetate, two other weakly complexing ligands, iminodiacetic acid and citrate, were tested with no significant improvement of the labeling yield.

Use of a conjugated-IgG preparation with a 52% higher $(\text{CL}/\text{P})_f$ also did not result in a 100% yield (Table V, last row). An extensive purification of ^{111}In (by column chromatography, see the Experimental Procedures) resulted in a negligible increase in radiolabeling yield. Similar behavior has also been observed in the radiolabeling of various MoAb's.

SUMMARY

The foregoing results demonstrate the chemical factors which influenced binding of the SCN-Bzl-DTPA family of ligands (specifically, 1M3B-DTPA) to immunoglobulins. Variables explored included pH, reaction period, temperature, and ligand and protein concentration. These variables, with the exception of protein concentration, have significant effects on the rate of protein conjugation.

The effect of pH was demonstrated by a 7-fold increase in the labeling efficiency when pH was increased from 6.7 to 9.0. Above pH 9.0 the reaction rate was rather independent of pH. The kinetics of the reaction were studied at 5, 15, 25, and 35 °C. For reaction periods up to 17 h an exponential dependence of yield on temperature was obtained which was expected for a bimolecular reaction. This exponential dependence decreased over longer reaction periods and at higher temperatures. First-order dependence of the reaction rate on ligand concentration was obtained over a range from 3.0×10^{-5} to 5.5×10^{-4} M. A 10-fold increase in $[\text{IgG}]$, from 2.4 to 23.4 mg/mL, resulted in only a 1.4-fold increase in the $(\text{CL}/\text{P})_f$ from 1.12 to 1.58.

When IgG and three other monoclonal antibodies were simultaneously conjugated under identical experimental conditions, no significant variation was observed in conjugation efficiencies.

ACKNOWLEDGMENT

We wish to acknowledge Pierre St. Raymond and Jane Fitzgerald for their preliminary work in this field (unpublished data) and Drs. Tom McMurry and Robert Kozak for their critical review of the manuscript.

LITERATURE CITED

- Goldenberg, D. M., Edmund Kim, E., Deland, F. H., Bennett, S., and James Primus, F. (1980) Radioimmuno-detection of cancer with radioactive antibodies to carcinoembryonic antigen. *Cancer Res.* **40**, 2984-2992.
- Scheinberg, D. A., Strand, M., and Gansow, O. A. (1982) Tumor imaging with radioactive metal chelates conjugated to monoclonal antibodies. *Science* **215**, 1511-1513.
- Scheinberg, D. A. and Strand, M. (1982) Leukemic cell targeting and therapy by monoclonal antibody in mouse model system. *Cancer Res.* **42**, 44-49.
- Yeh, S. M., Sherman, D. G., and Meares, C. F. (1979) A new route to bifunctional chelating agents: Conversion of amino acids to analogs of ethylenedinitrilotetraacetic acid. *Anal. Biochem.* **100**, 152-159.
- Krejcarek, G. E. and Tucker, K. L. (1977) Covalent attachment of chelating groups to macromolecules. *Biochem. Biophys. Res. Commun.* **77**, 581-585.
- Gansow, O. A., Atcher, R. W., Link, D. C., et al. (1984) Generator-produced Bi-212; chelated to chemically modified monoclonal antibody for use in radiotherapy. *Amer. Chem. Soc. Symp. Ser.* **241**, 215-227.
- Hnatowich, D. J., Layne, W. W., and Childs, R. L. (1982) Preparation and labeling of DTPA-coupled albumin. *Int. J. Appl. Radiat. Isot.* **33**, 326-332.
- Kohler, C. and Milstein, C. (1975) Continuous cultures of fused cells secreting antibody of predefined specificity. *Nature* **256**, 495-499.

- (9) Brechbiel, M. W., Gansow, O. A., Atcher, R. W., Schlom, J., Esteban, J., Simpson, D. E., and Colcher, D. (1986) Synthesis of 1-(*p*-isothiocyanatobenzyl) derivatives of DTPA and EDTA. Antibody labeling and tumor-imaging studies. *Inorg. Chem.* **25**, 2772, 2781.
- (10) Brechbiel, M. W. (1988) *New Bifunctional Ligands for Radioimmunoimaging and Radioimmunotherapy* Ph. D. Thesis, The American University, Washington, D. C.
- (11) Meares, C. F., McCall, M. J., Reardon, D. T., Goodwin, D. A., Diamanti, C. I., and McTigue, M. (1984) Conjugation of antibodies with bifunctional chelating agents: Isothiocyanate and bromoacetamide reagents, methods of analysis, and subsequent addition of metal ions. *Anal. Biochem.* **142**, 68–78.
- (12) Kozak, R. W.; Raubitschek, A., Mirzadeh, S., Brechbiel, M. W., Junghaus, R., Gansow, O. A., and Waldmann, T. A. (1989) Nature of the bifunctional chelating agent used for radioimmunotherapy with yttrium-90 monoclonal antibodies: Critical factors in determining in vivo survival and organ toxicity. *Cancer Res.* **49**, 2639–2644.
- (13) Roselli, M., Schlom, J., Gansow, O. A., Raubitschek, A., Mirzadeh, S., Brechbiel, M. W., and Colcher, D. (1989) Comparative biodistributions of yttrium- and indium-labeled monoclonal antibody B72.3 in athymic mice bearing human colon carcinoma xenografts. *J. Nucl. Med.* **30**, 672–682.
- (14) Paik, C. H., Murphy, P. R., Eckelman, W. C., Volkert, W. A., and Reba, R. C. (1983) Optimization of DTPA mixed-anhydride reaction with antibodies at low concentration. *J. Nucl. Med.* **24**, 932–936.
- (15) Paik, C. H., Herman, E., Eckelman, W. C., and Reba, R. C. (1980) Synthesis, plasma clearance, and in vitro stability of protein containing a conjugated indium-111 chelate. *J. Radioanal. Chem.* **57**, 553–564.
- (16) Kawamura, A. (1969) in *Fluorescent Antibody Techniques and Their Applications* (Kawamura, A., Ed.) Chapter 3, University of Tokyo, Tokyo.
- (17) Mizusawa, E. A., Thompson, M. R., and Hawthorne, M. F. (1985) Synthesis and antibody-labeling studies with the *p*-isothiocyanatobenzene derivatives of 1,2-dicarba-closo-dodecaborane and the dodecahydro-7,8-dicarba-nido-undecaborate(1–) ion for neutron-capture therapy of human cancer. *Inorg. Chem.* **24**, 1911–1916.
- (18) Leonard, W. J., Depper, J. M., Robb, R. J., Waldmann, T. A., and Green, W. C. (1983) Characterization of the human receptor for T-cell growth factor. *Proc. Natl. Acad. Sci. U.S.A.* **80**, 6957–6961.
- (19) Colcher, D., Horan Hand, P., Nuti, M., and Schlom, J. (1981) A spectrum of monoclonal antibodies reactive with mammary tumor cells. *Proc. Natl. Acad. Sci. U.S.A.* **78**, 3199–3203.
- (20) Smith, P. K., Krohn, R. I., Hermanson, G. T., Mallia, A. K., Gartner, F. H., Provenzano, M. D., Fugimoto, E. K., Goeke, N. M., Olson, B. J., and Klenk, D. C. (1985) Measurement of protein using bicinchoninic acid. *Anal. Biochem.* **150**, 76–85.
- (21) Nelson, F., Murase, F., and Kraus, K. A. (1964) I. Cation exchange in concentrated HCl and HClO₄. *J. Chromatog.* **13**, 503.
- (22) Assony, S. J. (1961) The Chemistry of Isothiocyanates. In *The Chemistry of Organic Sulfur Compounds* (N. Kharasch and C. Y. Meyers, Eds.) pp 326–338, Pergamon Press, New York.
- (23) Satchell, D. P. N. and Satchell, R. S. (1975) Acylation by ketenes and isothiocyanates. A mechanistic comparison. *Chem. Soc. Rev.* **4**, 231–250.

Registry No. 1M3B-DTPA, 121806-84-6; ¹¹¹In, 15750-15-9.

Preparation and Characterization of Paramagnetic Polychelates and Their Protein Conjugates

Paul F. Sieving, Alan D. Watson, and Scott M. Rocklage*

Salutar, Incorporated, 428 Oakmead Parkway, Sunnyvale, California 94086. Received July 31, 1989

The gadolinium complexes of poly-L-lysine-poly(diethylenetriamine-*N,N,N',N'',N'''*-pentaacetic acid) (Gd-PL-DTPA) and poly-L-lysine-poly(1,4,7,10-tetraazacyclododecane-*N,N',N'',N'''*-tetraacetic acid) (Gd-PL-DOTA) and their conjugates with human serum albumin (HSA) have been prepared and characterized. Poly-L-lysine (PL, degree of polymerization ≈ 100) was N-acylated with a mixed anhydride of the chelating ligand (DTPA or DOTA). Sixty to ninety chelating groups per molecule of PL could be attached in this way. Following purification of the polychelate by size-exclusion chromatography, the gadolinium complexes were prepared by standard methods and conjugated to HSA with heterobifunctional cross-linking reagents. The molar relaxivities of these macromolecular species were 2-3-fold higher than those of the corresponding monomeric metal complexes ([Gd(DTPA)] and [Gd(DOTA)]). The conjugation conditions were optimized to produce conjugates containing 60-90 metal centers per molecule of HSA (ca. one polychelate per protein).

We are conducting a research program to investigate the feasibility of preparing derivatives of biologically active macromolecules containing a large number of covalently bound metal chelates. The utility of such species for producing target-specific contrast enhancement in mag-

netic resonance imaging (MRI), as well as for applications in nuclear medicine, is anticipated. The present system was proposed as a model of the physical and chemical properties of such systems in general. The polychelate approach was developed as a means of preserving

the biological activity of the targeting protein, consistent with the proposed high degree of loading with metal chelates.

Earlier attempts focused on direct attachment of chelates to proteins of interest (1, 2). These employed DTPA (diethylenetriamine-*N,N,N',N'',N'''*-pentaacetic acid) as the chelating group and utilized two different methods for attachment of DTPA to macromolecules. The mixed anhydride method (3) reduced the likelihood of cross-linking or polymerization of the macromolecular substrate, while the bicyclic anhydride method (4) offered the advantage of greater ease of use. Both methods, however, suffered from a common drawback when applied to direct modification of proteins. It was observed (5, 6) that increased levels of functional group modification of a protein, such as an antibody, resulted in a decrease in the biological activity of the protein. This compromise in biological activity was a serious limitation in view of the requirement for high metal loading of proteins when used as target specific MRI contrast agents (7-9). It is believed that a 50% reduction in T_1 relaxation time of water protons in the target tissue is the minimum requirement for an effective MRI contrast agent. Considering the affinity of antibodies for their antigens and the concentration of these antigens in the target tissues, each antibody molecule must carry many paramagnetic centers to bring about these levels of T_1 reduction. More recent efforts in this area (10, 11) have focused on the use of intermediary carriers of chelates as a means of overcoming this limitation. Although Manabe and co-workers prepared a polylysine-DTPA (PL-DTPA) species, the cyclic anhydride method was used and resulted in only ca. 40 DTPA groups per polylysine (PL) ($n = 109$). Torchilin et al. prepared PL-DTPA and PL-EDTA as well as their respective MAb conjugates. Although they used the mixed anhydride method, their method of conjugation was nonspecific and the end result was a conjugate that lacked structural definition.

Another drawback common to both methods, with or without the use of an intermediary carrier, arose from the chemical transformations employed in linking the chelate to the macromolecular substrate. Both of the methods described relied on the chemical modification of one of the carboxylate groups normally involved in metal binding and resulted in decreased chelate stability with respect to the monomeric chelates (12). Methods were developed to address this problem, particularly when applied to the radiolabeling of proteins by direct attachment of chelates (13). Meares et al. prepared and characterized a series of bifunctional chelators, based on macrocyclic ligands such as DOTA (1,4,7,10-tetraazacyclododecane-*N,N',N'',N'''*-tetraacetic acid), which featured the linking group attached to the backbone of the ligand. None of the coordination sites on these ligands were compromised, and full denticity was retained. The methods employed in the present work have not addressed this issue specifically; however, the use of DOTA in place of DTPA is expected to result in a lower rate of metal release in vivo. This improvement may well be sufficient to minimize metal loss for applications in which the agent is cleared from the body in under 48 h.

The present work is an extension of efforts to prepare intermediary carriers and incorporates some practical improvements as described below.

EXPERIMENTAL PROCEDURES

Reagents. DOTA was synthesized by published methods (14) and isolated as a zwitterion by precipitation from concentrated aqueous solution at pH 2.5 following ion-

exchange chromatography. All other reagents were purchased from commercial suppliers and used as received unless otherwise specified.

NMR Measurements. Proton nuclear magnetic resonance spectra were recorded on a Bruker AM250 spectrometer at an ambient temperature of $21 \pm 1^\circ\text{C}$. In the case of DOTA, the spectra were used to establish identity and estimate purity. In the case of PL-DTPA and PL-DOTA, the spectra were used to estimate the extent of acylation of PL by the mixed anhydride of the chelator via integration of the appropriate peaks.

Relaxivity Measurements. Relaxation times (T_1) in water of the title compounds were measured on a RADX Model 530 proton spin analyzer at 10 MHz, 37°C , for gadolinium concentrations of 0.04–2.0 mM. The data was fitted by nonlinear regression to the equation $T_1 = 1/A[\text{Gd}] + B$ to determine relaxivities, where A is the relaxivity and B is $1/T_1$ for pure water.

Titrimetric Measurements. The titration data were acquired with an automatic titrator system as previously described (15). In a typical measurement, a sample of one of the polychelate complexes (Gd-PL-DTPA or Gd-PL-DOTA), 20–50 mg/mL in water, was adjusted to pH 1, degassed to remove CO_2 , and titrated to pH 11.5 with 0.100 M KOH. The data were plotted as pH vs volume of titrant added, the first derivative (dpH/dvol) was taken, and the volume of titrant added between the two maxima in the pH range 9–11 was measured.

Directly Coupled Plasma Atomic Absorption (DCP-AA) Measurements. DCP-AA determinations of gadolinium concentration were performed on a Beckman SpectraSpan IV instrument.

Synthesis of DTPA Mixed Anhydride. A 25-mL round-bottom flask was fitted with a water condenser and charged with 1.622 g (4 mmol) of DTPA and 7.0 mL of acetonitrile (dried over 4-Å molecular sieves). Triethylamine (2.79 mL, 20 mmol) was added and the mixture was stirred magnetically under an atmosphere of nitrogen at 60°C for 1 h until homogeneous. This solution was cooled to -30°C under an atmosphere of nitrogen and stirred while adding 0.520 mL (4 mmol) of isobutyl chloroformate (IBCF) slowly over 5 min. The resultant slurry was stirred for 30 min at -30°C .

Synthesis of PL-DTPA. The mixed anhydride slurry was added slowly over 5 min to a solution of 0.250 g of poly-L-lysine hydrobromide (Sigma Chemical Company, degree of polymerization = 105, MW = 22 000) in 12.5 mL of 0.1 N sodium bicarbonate, pH 9.0, which was cooled in an ice bath. The resulting mixture was allowed to warm to room temperature and stirred for 6 h. The majority of the acetonitrile was removed by rotary evaporation at 60°C and the resulting aqueous solution was dialyzed in 12 500 MW cutoff tubing against 3.5 L of 0.02 M oxalic acid, pH 2.0, for 6 h at room temperature then against 3.5 L of 0.05 M sodium bicarbonate, pH 8.0, for 12 h at room temperature. Residual low molecular weight components were removed by gel filtration on Sephadex G-25 with UV detection at 254 nm, eluting with 10 mM sodium bicarbonate, 15 mM NaCl, pH 8.0. Lyophilization (10 μm , 24 h) afforded 0.532 g of white, amorphous solid. Analysis by ^1H NMR demonstrated 0.88 DTPA group per lysine residue, indicating that 88% of the lysine ϵ -amines were acylated.

Synthesis of Gd-PL-DTPA. PL-DTPA (0.100 g) was dissolved in 3.0 mL of standardized 50.1 mM GdCl_3 in 0.1 N HCl. The solution was adjusted to pH 7.0 with 7.0 N NaOH and stirred for 30 min at room temperature. A small aliquot of the solution tested positive for free Gd^{3+} when added to 1.0 mL of 10 μM arsenazo III in

acetate buffer, pH 4.0. A further 2 mg of PL-DTPA was added to the solution, and another aliquot tested negative for free Gd^{3+} . The relaxivity of the complex was determined to be $10.80 \text{ mM}^{-1} \text{ s}^{-1}$, on the basis of a DCP-AA determination of Gd concentration. Titrimetric determination of free ϵ -amines, in conjunction with the DCP data, confirmed 88% acylation of ϵ -amines with DTPA (% acylation = $([\text{Gd}]/[\text{Gd}] + [\text{RNH}_2]) \times 100$ and assuming that $[\text{Gd}] \approx [\text{DTPA}]$). HPLC analysis (column, Supelco C18 deactivated; mobile phase, 5 mM triethylammonium acetate, pH 6.8) demonstrated the absence (<1%) of free $[\text{Gd}(\text{DTPA})]$. The samples from nondestructive analyses were recombined with the stock solution and desalted by gel filtration on Sephadex G-25. Lyophilization afforded 0.135 g of white solid.

Synthesis of DOTA Mixed Anhydride. A 25-mL round-bottom flask was fitted with a water condenser and charged with 0.808 g (2 mmol) of DOTA and 5.0 mL of acetonitrile. Tetramethylguanidine (1.0 mL, 8 mmol) was added and the mixture was stirred until homogeneous (5 min). Stirring was discontinued and the solution was dried overnight over 4-Å molecular sieves. The solution was decanted from the sieves, placed under an atmosphere of nitrogen, cooled to -30°C , and stirred while adding 0.260 mL (2 mmol) of IBCF slowly over 5 min. The resultant slurry was stirred for 1 h at -30°C .

Synthesis of PL-DOTA. The slurry from above was added slowly over 5 min to a solution of 0.100 g of PL-HBr in 6.0 mL of 0.1 N sodium bicarbonate, pH 9.0, which was cooled in an ice bath. The resulting solution was allowed to warm to room temperature and was stirred for 6 h. The reaction mixture was worked up and purified as described for PL-DTPA, affording 0.183 g of white solid. Analysis by ^1H NMR demonstrated 0.68 DOTA group per lysine residue, indicating that 68% of the lysine ϵ -amines were acylated.

Synthesis of Gd-PL-DOTA. PL-DOTA (0.300 g) was dissolved in 5.0 mL of 50.1 mM GdCl_3 in 0.1 N HCl and adjusted to pH 7.0 with 7.0 N NaOH. After stirring for 1 h at room temperature, the solution tested negative for free Gd^{3+} . The mixture was maintained between pH 6.0 and 7.0 with 7.0 N NaOH, while additional 0.5-mL aliquots of 50.1 mM GdCl_3 were added at 1-h intervals until the solution tested positive for free Gd^{3+} . The solution was stirred overnight and 1-mg aliquots of PL-DOTA were added until the solution tested negative for free Gd^{3+} . The relaxivity of the complex was $13.03 \text{ mM}^{-1} \text{ s}^{-1}$. Data from titrimetry and DCP-AA confirmed 68% acylation of ϵ -amines with DOTA. HPLC analysis demonstrated the absence (<1%) of free Gd-DOTA. Desalting and lyophilization afforded 0.360 g of white solid.

Activation of HSA for Conjugation. HSA contains one native sulfhydryl residue, which was blocked by alkylation. HSA (1 g, 15 μmol) was dissolved in 50 mL of 0.05 M Tris-HCl, pH 8.0, in a 100-mL round-bottom flask. The flask was purged with dry nitrogen, sealed with a septum and wrapped with aluminum foil to exclude light. A solution of 15 mg (80 μmol) of iodoacetamide in 4.0 mL of 1.0 N NaOH was added by syringe through the septum and the mixture was stirred for 45 min at room temperature in the dark. The reaction mixture was dialyzed against 3.5 L of 0.05 M sodium bicarbonate, pH 8.0, for 12 h with a buffer change at 6 h. Lyophilization of the dialysate afforded 0.903 g of white fibers. The absence of free sulfhydryls in the preparation was demonstrated by the method of Ellman (16).

Thiol-blocked HSA (0.100 g) was dissolved in 50 mL of 50 mM triethanolamine, 7 mM monopotassium phos-

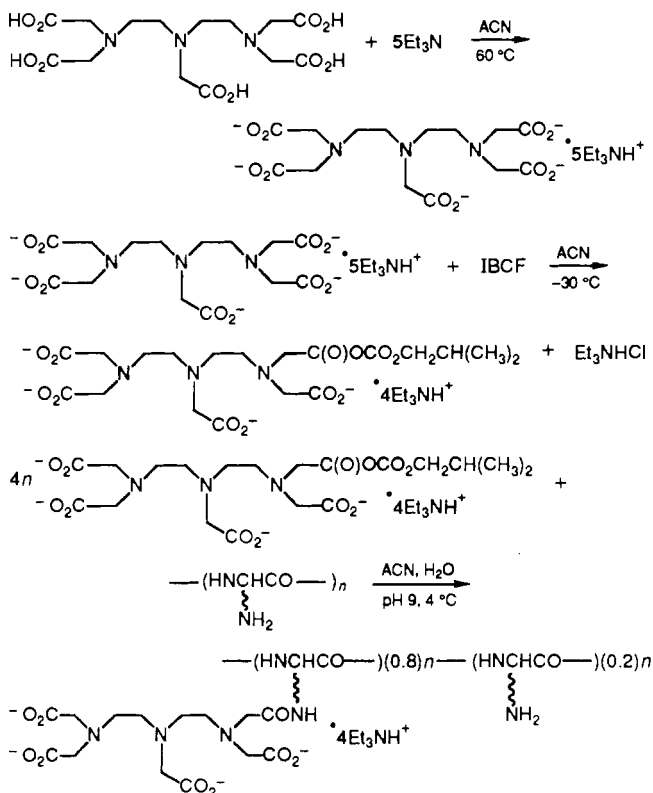
phate, 100 mM NaCl, 1 mM EDTA, pH 8.0. The solution was degassed for 10 min by stirring under vacuum and was covered with an atmosphere of nitrogen, and the flask was sealed with a septum and cooled to 4°C . A solution of 8.6 mg of 2-iminothiolane in 100 μL of 1 M triethanolamine hydrochloride, pH 8.0, was added by syringe through the septum and the mixture was stirred for 90 minutes at 4°C . The reaction mixture was dialyzed overnight against 3.5 L of 0.08 M sodium phosphate, 0.5 mg/mL EDTA, pH 8.0, with frequent buffer changes for the first few hours. Assay by the method of Ellman demonstrated 1.32 sulfhydryl residues per mole of HSA.

Activation of Gd-PL-DTPA or Gd-PL-DOTA for Conjugation to HSA. A 0.200-g sample of either Gd-PL-DTPA or Gd-PL-DOTA was dissolved in 18 mL of 8 mM sodium phosphate, pH 8.0, and the mixture was treated dropwise with a solution of 10.7 mg of *N*-succinimidyl 4-(*N*-maleimidomethyl)cyclohexane-1-carboxylate (SMCC) in 2.0 mL of DMSO, and stirred for 30 min. The reaction mixture was dialyzed overnight against 3.5 L of deionized water with frequent changes for the first few hours. Reaction of an aliquot of the dialysate with a known amount of 2-mercaptoethanol and measurement of the residual sulfhydryls by the method of Ellman, indicated 1.30 maleimide residues per mole of polychelate.

Conjugation of Polychelates to HSA. The solutions containing activated polychelate and activated HSA were combined and the mixture was stirred for 4 h at room temperature. Analysis of an aliquot by the method of Ellman indicated that over 90% of the thiols were consumed. The mixture was lyophilized, the residue was dissolved in 10 mL of deionized water and dialyzed for 6 h against 3.5 L of deionized water. The dialysate was fractionated by size-exclusion chromatography (SEC) on Sephacryl S-300 eluting with 10 mM NaH_2PO_4 , 15 mM NaCl, pH 8.0, and the fractions with a significant absorbance at 280 nm were pooled and lyophilized to yield 0.30 g of fibrous solid. The relaxivities of the conjugates were essentially the same as those of the polychelates from which they were prepared ($\sim 10 \text{ mM}^{-1} \text{ s}^{-1}$ for Gd-PL-DTPA-HSA, $\sim 13 \text{ mM}^{-1} \text{ s}^{-1}$ for Gd-PL-DOTA-HSA). Absorbance (280 nm) and DCP-AA data indicated that the metal content of the conjugates was 60–80 mol of Gd/mol of HSA.

RESULTS AND DISCUSSION

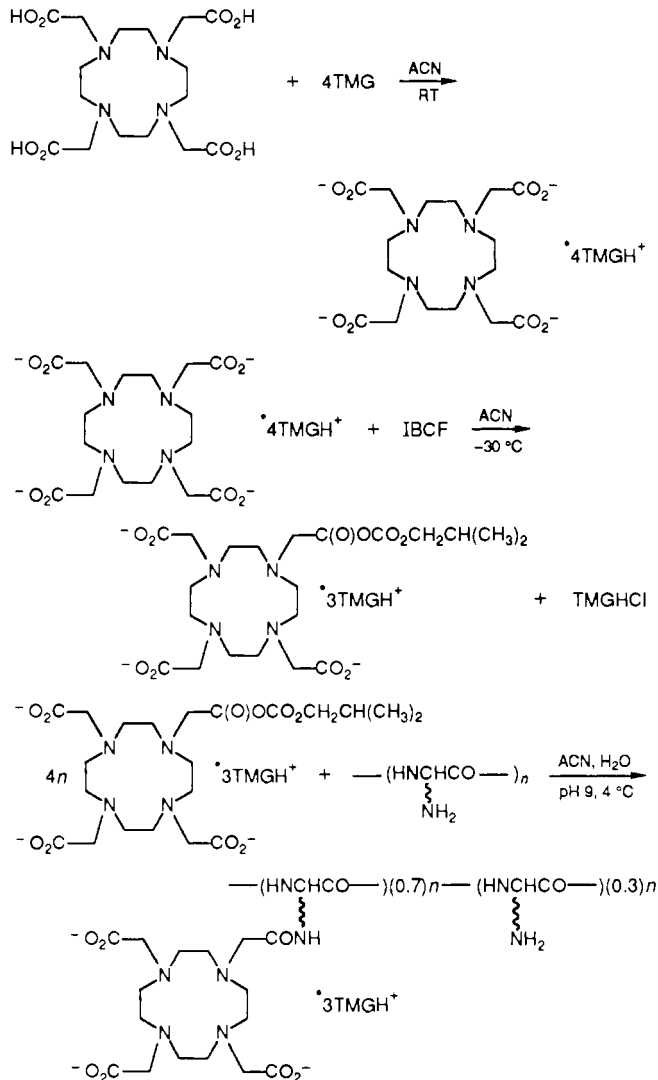
Synthesis of PL-DTPA and PL-DOTA. The syntheses of PL-DTPA and PL-DOTA are shown in Schemes I and II, respectively. The published procedure for preparation of DTPA mixed anhydride was revised to improve efficiency and reproducibility. Anhydrous grades of reagents (DTPA, triethylamine, acetonitrile) were used and the reaction was carried out under an atmosphere of nitrogen at low temperature to minimize hydrolytic decomposition of the mixed anhydride prior to reaction with polylysine. A series of experiments was carried out to determine a ratio of mixed anhydride to ϵ -amines required to achieve 80–90% acylation which left some amines available for subsequent conjugation reactions. A 4-fold molar excess of mixed anhydride with respect to ϵ -amines was satisfactory. Purification of the polychelate was effected by a combination of size-exclusion techniques. After evaporative removal of acetonitrile, the major impurities were excess DTPA, triethylamine, and isobutyl alcohol. It was found that dialysis at low pH (<3) was most effective at removing excess triethylamine, while higher pH (>6) was required to remove excess DTPA,

Scheme I. Synthesis of PL-DTPA

presumably due to its limited solubility at $\text{pH} \leq 3$. The progress of the sequential dialyses was monitored by ^1H NMR to optimize product recovery. Final purification by gel filtration on Sephadex G-25 served primarily as a desalting process (buffer exchange) as well as to remove residual DTPA, triethylamine, or isobutyl alcohol. The molecular weight of the starting PL was about 20 000, while that of the polychelate product was about 50 000.

DOTA was preferred to DTPA as the chelate component due to the greater thermodynamic and kinetic stabilities of its gadolinium complex (17, 18). Attempts to adapt the acylation procedure directly to DOTA were unsuccessful due to the difficulty in preparing an acetonitrile solution of a DOTA salt. Triethylamine was not a sufficiently strong base to deprotonate the two most basic sites on DOTA (demonstrated by ^1H NMR and titrimetry). Several other tertiary amine bases were evaluated to try to prepare an acetonitrile solution greater than 0.3 M in DOTA. Both 1,5-diazabicyclo[4.3.0]non-5-ene (DBN) and 1,1,3,3-tetramethylguanidine (TMG) were satisfactory. A minor impurity in the DBN ($\leq 5\%$), however, was sufficiently nucleophilic to either prevent formation, or promote decomposition, of the mixed anhydride intermediate. TMG did not exhibit this undesirable behavior. No heating was required to promote formation of the DOTA \cdot 4TMG. The reaction was exothermic and a homogeneous solution resulted almost immediately upon addition of stoichiometric TMG to the acetonitrile DOTA slurry.

The method employed in our laboratory to isolate DOTA as the free acid (zwitterion) afforded a solid product which was 9.3% water by Karl Fischer titration, corresponding approximately to a hydration state of $\text{DOTA} \cdot 2.5\text{H}_2\text{O}$. For this reason, the DOTA \cdot 4TMG solutions were dried over 4-Å molecular sieves for at least 6 h prior to treatment with IBCF. The remaining steps in preparation and purification of PL-DOTA parallel those for PL-DTPA very closely, although the maximum degree of acylation of PL

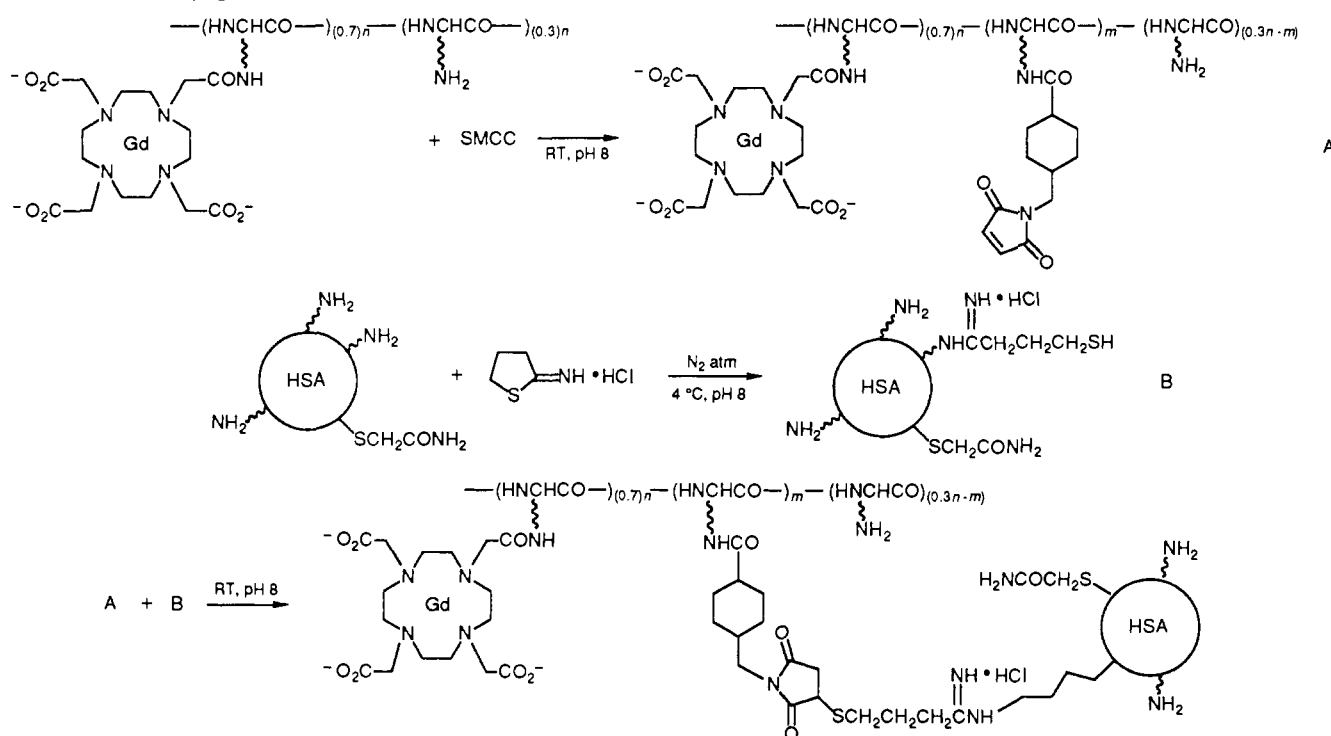
Scheme II. Synthesis of PL-DOTA

ϵ -amines with DOTA was 70–75%. This was achieved with 3.5–4-fold molar excess of DOTA mixed anhydride relative to amine and could not be increased, even with a 5–6-fold excess mixed anhydride. CPK models of the polychelates suggested that this was due to steric constraints inherent in the rigid, nonlinear structure of DOTA, leading to a greater effective bulk for DOTA compared to DTPA.

Preparation of the Gadolinium Complexes. The procedures for preparing Gd-PL-DTPA and Gd-PL-DOTA were essentially identical, with the notable exception of the time required for complete reaction. Preparation of Gd-PL-DTPA was essentially complete within 1 h, while preparation of Gd-PL-DOTA required 24–30 h. This observation is consistent with published reports (16) of the kinetic and thermodynamic properties of the respective monomeric complexes. The assay used to test for free Gd^{3+} allowed detection of a lower limit of 0.1 mM Gd^{3+} in the complexation solution, which represents 0.2% of total Gd^{3+} (50.1 mM). While the monoamides of both DTPA and DOTA have lower thermodynamic stability constants with Gd than do the corresponding acids, the complexes of Gd with DOTA amides are expected to be more stable than those with DTPA amides (19).

A spectrophotometric method for measuring the thermodynamic and kinetic stability of these polychelates and their protein conjugates is currently under development

Scheme III. Conjugation of Gd-PL-DOTA to HSA



in our laboratory. The polychelates, especially Gd-PL-DOTA, are not well-suited for the usual potentiometric methods of analysis. This is due to the presence of titratable functional groups not involved in chelation, as well as kinetic limitations. The method under development involves equilibrating the components of a competitive spectrophotometric titration at elevated temperature for several days prior to measurement to overcome these limitations. The results of these thermodynamic and kinetic measurements will be the subject of a separate report.

The relaxivities of solutions of the polychelate complexes containing a slight excess ($\sim 1\%$) of ligand were observed to be approximately 2.5-fold higher than those of the corresponding monomeric complexes ($[\text{Gd}(\text{DTPA})]$ and $[\text{Gd}(\text{DOTA})]$). The relaxivities (R_1) of $[\text{Gd}(\text{DTPA})]$ and $[\text{Gd}(\text{DOTA})]$ were measured at 10 MHz, 37 °C, and found to be 4.8 and 4.6 $\text{mM}^{-1} \text{s}^{-1}$, respectively, in the concentration range between 0.2 and 4.0 mM. Examination of the Solomon-Bloembergen equations, particularly the term for rotational correlation time, leads to the prediction of such an effect (20). Refinement of the equations to the extent that they can be used to predict the magnitude of such an effect, however, will depend on the accumulation of considerable experimental data. The increase in molecular weight from $[\text{Gd}(\text{DOTA})]$ to Gd-PL-DOTA (560 to 65 000) is approximately 2 orders of magnitude and brings about a 2.5-fold increase in the molar relaxivity of gadolinium.

The extent of acylation of PL ϵ -amines with DTPA or DOTA was measured by two techniques. The free ligand was analyzed by ^1H NMR, and following preparation of the complexes, titrimetric quantitation of amines was carried out. The assumption that only PL ϵ -amines were titratable was based on the presumption that all the backbone amines of the chelates were deprotonated above pH 4, due to their involvement in metal binding. For both polychelates, the two methods were in good agreement.

HPLC analyses of the polychelates, using methods developed to detect $[\text{Gd}(\text{DTPA})]$ and $[\text{Gd}(\text{DOTA})]$, consistently demonstrated very low levels ($<1\%$) of mono-

meric chelates in these preparations. Impurities in Gd-PL-DTPA were detected by post-HPLC column mixing of the column effluent with an equal volume of reagent containing 0.1 M HNO_3 and 1×10^{-4} M arsenazo III, pH 1.4, in a zero dead volume tee and measuring $[\text{Gd}(\text{arsenazo III})]$ in the resulting mixture (pH 1.5) by its absorbance at 658 nm (21). For the impurities in Gd-PL-DOTA, detection of chelated Gd was by fluorescence ($\text{Ex} = 277$ nm, $\text{Em} = 311$ nm) without acid digestion because of the prohibitively slow kinetics of decomplexation under the conditions employed for Gd-PL-DTPA. The polychelates were fully retained in the guard column and were not detected.

Conjugation of the Polychelates to HSA. Conjugation is described in Scheme III. Human serum albumin (HSA) was chosen as a model protein to demonstrate the conjugation of the polychelate to proteins in general. According to both amino acid sequence and other data (22), HSA contains approximately one sulfhydryl per mole when highly purified. Our measurements indicated the presence of 0.12 sulfhydryl per mole. This native residue was blocked prior to introduction of exogenous sulfhydryls for conjugation, in order to provide conjugates of well-defined structure. Published methods (23) were adapted for this purpose. Established procedures were also employed to introduce the sulfhydryls for conjugation (24). The reaction conditions were adjusted to afford one to two sulfhydryls per mole of HSA, on the basis of measurements of absorbance at 280 nm vs sulfhydryl measurement by the method of Ellman. The polychelates (Gd-PL-DTPA and Gd-PL-DOTA) were functionalized for conjugation by introduction of a maleimide group by the procedure developed by Yoshitake et al. (25). The reaction conditions were adjusted to afford one to two maleimide residues per mole of polychelate. The polychelate is the most valuable component in the present system; however, it is anticipated that future research will focus on systems where the protein is the more valuable component. Hence, conjugation conditions were developed which maximized efficiency of pro-

tein use. The activated derivatives of the polychelate and HSA were combined with the polychelate in 2-fold molar excess. Following suitable workup as described above, the conjugation reaction mixture was chromatographed on Sephacryl S-300 and the eluate was monitored at 280 nm. DCP-AA analysis of the collected fractions to monitor gadolinium elution, in conjunction with the UV detection, demonstrated that a conjugate containing from 60–80 mol of Gd/mol of HSA was eluted first, followed by excess polychelate and finally residual unreacted HSA. The molecular weight of a 1:1 HSA-polychelate conjugate was approximately 140 000 Da while the individual components ranged between 65 000 and 70 000 Da.

The molar relaxivity of gadolinium in the conjugates was essentially identical with that of the respective polychelates. The molecular weight had approximately doubled, a very small change relative to the 120-fold increase seen on going from monomeric to polymeric chelates.

CONCLUSION

It has been estimated (7–9) that in excess of 100 paramagnetic chelates per targeting protein will be required to bring about sufficient reduction in T_1 relaxation time to make possible the development of target-specific MRI contrast agents. The present system, with an average of 70 chelates per protein and a molar relaxivity 2.5 times higher than that of monomeric chelates, provides the equivalent of approximately 170 monomeric chelates per protein. This is a marked improvement over earlier results, and although the theoretical requirements cited may not be met, this system is certainly deserving of further experimental evaluation. Some of the physical and chemical properties of the conjugates have been determined. Preliminary animal biodistribution and imaging studies have been conducted and the results of these will be reported elsewhere. The extension of this method to other proteins with interesting biological activity is currently underway, as is the evaluation of the polychelates themselves, as potential contrast agents for MRI. It will be interesting to determine if the mechanical effects of targeting, such as immobilization of the agent at the target site, bring about further increases in molar relaxivity through effectively increasing the rotational correlation time. The polychelate approach described will allow the attachment of large numbers of chelates to a protein through a single covalent bond, with a minimum of functional modification of the protein. In addition, the use of DOTA as the chelate component provides at least some of the additional stability that will be required of an agent whose in vivo clearance half-life is 1–3 days. Choice of metal is also an important consideration in addressing this issue and will be based on both stability and toxicity considerations. For instance, although manganese is expected to form a less stable complex with DOTA than does gadolinium, manganese ion is expected to be excreted more readily, since it is found naturally in the body (26). The applicability of systems of this type to areas other than MRI, such as radioimmunotherapy (RIT) and radioimmunoscintigraphy (RIS), should not be overlooked. The use of such a system to radiolabel antibodies would allow significantly smaller amounts of antibody than are currently employed to deliver the necessary concentration of radionuclide. Combining the described polychelate approach with the methodology employed by Meares and co-workers (13) is likely to overcome some of the deficiencies apparent in current attempts to prepare targeted macromolecular diagnostic agents.

ACKNOWLEDGMENT

We thank Gene Jamieson and the analytical staff at Salutar, as well as David Love and Bill Cacheris, for their valuable contributions to this work.

LITERATURE CITED

- (1) Krejcarek, G. E. and Tucker, K. L. (1977) Covalent attachment of chelating groups to macromolecules. *Biochem. Biophys. Res. Commun.* **77**, 581.
- (2) Hnatowich, D. J., Layne, W. W., Childs, R. L., Lanteigne, D., Davis, M. S., Griffin, T. W., and Doherty, P. W. (1983) Radioactive labeling of antibody: A simple and efficient method. *Science* **220**, 613.
- (3) Paik, C. H., Murphy, P. R., Eckelman, W. C., Volkert, W. A., and Reba, R. C. (1983) Optimization of the DTPA mixed-anhydride reaction with antibodies at low concentrations. *J. Nucl. Med.* **24**, 932.
- (4) Paik, C. H., Ebbert, M. A., Murphy, P. R., Lassman, C. R., Reba, R. C., Eckelman, W. C., Pak, K. Y., Powe, J., Stepkowski, Z., and Koprowski, H. (1983) Factors influencing DTPA conjugation with antibodies by cyclic DTPA anhydride. *J. Nucl. Med.* **24**, 1158.
- (5) Curtet, C., Tellier, C., Bohy, J., Conti, M. L., Saccavini, J. C., Thredrez, P., Douillard, J. Y., Chatal, J. F., and Koprowski, H. (1986) Selective modification of NMR relaxation time in human colorectal carcinoma by using Gd(DTPA) conjugated with monoclonal antibody 19-9. *Proc. Natl. Acad. Sci. U.S.A.* **83**, 4277.
- (6) Scheinberg, D. A., Strand, M., and Gansow, O. A. (1982) Tumor imaging with radioactive metal chelates conjugated to monoclonal antibodies. *Science* **215**, 1511.
- (7) Unger, E. C., Totty, W. A., Neufeld, D. M., Otsuka, F. L., Murphy, W. A., Welch, M. S., Connett, J. M., and Philpott, G. W. (1985) Magnetic resonance imaging using gadolinium-labeled monoclonal antibody. *Invest. Radiol.* **20**, 693.
- (8) Manabe, Y., Longley, C., and Furmanski, P. (1986) High-level conjugation of chelating agents onto immunoglobulins: Use of an intermediary poly(L-Lysine)-DTPA carrier. *Biochim. Biophys. Acta* **883**, 460.
- (9) Eckelman, W. C., Tweedle, M., and Welch, M. J. (1988) NMR Enhancement With Gd Labeled Antibodies. In *Radiolabeled Monoclonal Antibodies for Imaging and Therapy* (S. C. Srivastava, Ed.) pp 571–579, Plenum Publishing Corporation, New York.
- (10) Aisen, A. M. and Schreve, P. (1986) Monoclonal antibodies labeled with polymeric paramagnetic ion chelates. *Magn. Reson. Med.* **3**, 336.
- (11) Torchilin, V. P., Klivanov, A. L., Nossiff, N. D., Slinkin, M. A., Strauss, H. W., Haber, E., Smirnov, V. N., and Khaw, B. A. (1987) Monoclonal antibody modification with chelate-linked high molecular weight polymers: Major increases in polyvalent cation binding without loss of antigen binding. *Hybridoma* **6**, 229.
- (12) Brechbiel, M. W., Gansow, O. A., Atcher, R. W., Schlom, J., Estaban, J., Simpson, R. E., and Colcher, D. (1986) Synthesis of 1-(p-isothiocyanatobenzyl) Derivatives of DTPA and EDTA. Antibody labeling and tumor-imaging studies. *Inorg. Chem.* **25**, 2772.
- (13) (a) Meares, C. F., McCall, M. J., Reardon, D. T., Goodwin, D. A., Diamanti, C. I., and McTigue, M. (1984) The conjugation of antibodies with bifunctional chelating agents: Isothiocyanate and bromoacetamide reagents, methods of analysis, and subsequent addition of metal ions. *Anal. Biochem.* **142**, 68. (b) Moi, M. K., Meares, C. F., McCall, M. J., Cole, V. C., and DeNardo, S. J. (1985) Copper chelates as probes of biological systems: Stable copper complexes with a macrocyclic bifunctional chelating agent. *Anal. Biochem.* **148**, 249. (c) Cole, W. C., DeNardo, S. J., Meares, C. F., McCall, M. J., DeNardo, G. L., Epstein, A. L., O'Brien, H. A., and Moi, M. K. (1986) Serum stability of ^{67}Cu chelates: Comparison with ^{111}In and ^{57}Co . *Nucl. Med. Biol.* **13**, 363. (d) Cole, W. C., DeNardo, S. J., Meares, C. F., McCall, M. J., DeNardo, G. L., Epstein, A. L., O'Brien, H. A., and Moi, M. K. (1987) Comparative serum stability of radiochelates for antibody

- radiopharmaceuticals. *J. Nucl. Med.* **28**, 83. (e) Deshpande, S. V., DeNardo, S. J., Meares, C. F., McCall, M. J., Adams, G. P., Moi, M. K., and DeNardo, G. L. (1988) ^{67}Cu -labeled monoclonal antibody Lym-1, a potential radiopharmaceutical for cancer therapy: Labeling and biodistribution in RAJI tumored mice. *J. Nucl. Med.* **29**, 217. (f) Moi, M. K., Meares, C. F., and DeNardo, S. J. (1988) The peptide way to macrocyclic bifunctional chelating agents: Synthesis of 2-(p)-nitro-benzylDOTA, and study of its yttrium (III) complex. *J. Amer. Chem. Soc.* **110**, 6266.
- (14) Desreux, J. F. (1980) Nuclear magnetic resonance spectroscopy of lanthanide complexes with a tetraacetic tetraaza macrocycle. Unusual conformation properties. *Inorg. Chem.* **19**, 1319.
- (15) Rocklage, S. M., Cacheris, W. P., Quay, S. C., Hahn, F. E., and Raymond, K. N. (1989) Manganese(II) *N,N'*-dipyridoxylethylenediamine-*N,N'*-diacetate 5,5'-Bis(phosphate). Synthesis and characterization of a paramagnetic chelate for magnetic resonance imaging enhancement. *Inorg. Chem.* **28**, 477.
- (16) Ellman, G. L. (1958) A colorimetric method for determining low concentrations of mercaptans. *Arch. Biochem. Biophys.* **74**, 443.
- (17) Magerstädt, M., Gansow, O. A., Brechbiel, M. W., Colcher, D., Baltzer, L., Knop, R. H., Girton, M. E., and Naegle, M. (1986) Gd(DOTA): An alternative to Gd(DTPA) as a $T_{1,2}$ relaxation agent for NMR imaging or spectroscopy. *Magn. Reson. Med.* **3**, 808.
- (18) Tweedle, M. F., Eaton, S. M., Eckelman, W. C., Gaughan, G. T., Hagan, J. J., Wedeking, P. W., and Yost, F. J. (1988) Comparative chemical structure and pharmacokinetics of MRI contrast agents. *Invest. Radiol.* **23**, S236.
- (19) Sherry, A. D., Brown, R. D., Gerald, C. F. G. C., Koenig, S. H., Kuan, K.-T., and Spiller, M. (1989) Synthesis and characterization of the gadolinium(3+) complex of DOTA-pyramide: A model DOTA-protein conjugate. *Inorg. Chem.* **28**, 620.
- (20) Lauffer, R. B. (1987) Paramagnetic metal complexes as water proton relaxation agents for NMR imaging: Theory and design. *Chem. Rev.* **87**, 901.
- (21) Cassidy, R. M., Elchuk, S., and Dasgupta, P. K. (1987) Performance of annular membrane and screen-tee reactors for postcolumn-reaction detection of metal ions separated by liquid chromatography. *Anal. Chem.* **59**, 85.
- (22) Hughes, W. L. (1947) An albumin fraction isolated from human plasma as a crystalline mercuric salt. *J. Am. Chem. Soc.* **69**, 1836.
- (23) May, S. W., Lee, L. G., Katopodis, A. G., Kuo, J.-Y., Wimalasena, K., and Thowsen, J. R. (1984) Rubredoxin from *Pseudomonas oleovorans*: Effects of chemical modification and metal substitution. *Biochemistry* **23**, 2187.
- (24) Jue, R., Lambert, J. M., Pierce, L. R., and Traut, R. R. (1978) Addition of sulfhydryl groups to *Escheria coli* ribosomes by protein modification with 2-iminothiolane (methyl-4-mercapto-butyrimidate). *Biochemistry* **17**(25), 5399.
- (25) Yoshitake, S., Imagawa, M., Ishikawa, E., Niitsu, Y., Urushizaki, I., Nishiura, M., Kanazawa, R., Kurosaki, H., Tachibana, S., Nakazawa, N., and Ogawa, H. (1982) Mild and efficient conjugation of rabbit Fab' and horseradish peroxidase using a maleimide compound and its use for enzyme immunoassay. *J. Biochem.* **92**, 1413.
- (26) Barbeau, A. (1984) Manganese and extrapyramidal disorders. *Neurotoxicology* **5** (1), 13.

Registry No. IBCF, 543-27-1; DOTA, 60239-18-1; TMG, 80-70-6; SMCC, 85060-00-0; DTPA, 67-43-6; DTPA mixed anhydride, 124098-80-2; DOTA mixed anhydride, 124098-82-4; Et_3N , 121-44-8; poly(L-lysine), 25104-18-1; poly(L-lysine) SRU, 38000-06-5.

Use of Maleimide-Thiol Coupling Chemistry for Efficient Syntheses of Oligonucleotide-Enzyme Conjugate Hybridization Probes

Soumitra S. Ghosh,* Philip M. Kao, Ann W. McCue, and Hugh L. Chappelle

SISKA Diagnostics, Inc., and Salk Institute Biotechnology/Industrial Associates, Inc., La Jolla, California 92037.
Received August 10, 1989

Two general methods which exploit the reactivity of sulfhydryl groups toward maleimides are described for the synthesis of oligonucleotide-enzyme conjugates for use as nonradioisotopic hybridization probes. In the first approach, 6-maleimidohexanoic acid succinimido ester was used to couple 5'-thiolated oligonucleotide to calf intestine alkaline phosphatase to provide a 1:1 conjugate in 80-85% yield. The second strategy employed *N,N'*-1,2-phenylenedimaleimide to cross-link thiolated horseradish peroxidase or β -galactosidase with a 5'-thiolated oligonucleotide in 58% and 65% yields, respectively. The oligonucleotide-alkaline phosphatase conjugate was able to detect 6 amol of target DNA in 4 h, while the horseradish peroxidase conjugate was found to be 40-fold lower in its sensitivity of detection by using dye precipitation assays.

In recent years, considerable interest has focused on exploiting the specificity of nucleic acid hybridization reactions for the diagnosis of genetic disorders and infectious diseases. The sensitivity of the technology has ben-

efited in great measure from the use of in vitro nucleic acid amplification procedures (1, 2) before detection by hybridization. Such target-directed amplification strategies are particularly essential for the detection of pathogens such as the HIV-1 virus, which are often present in immeasurably low titers in blood samples.

Traditionally, radioisotopes, such as ^{32}P , have been utilized as detection labels for nucleic acid probes in nucleic

* To whom correspondence should be addressed at SIBIA, P.O. Box 85200, San Diego, CA 92138-9216.

acid hybridization reactions. However, concerns about safety, short lifetimes, and cost have prompted the investigation of nonisotopic detection alternatives (3). Recently, we (4) and others (5–7) have demonstrated the efficacy of using enzymes as reporter groups in oligonucleotide probes. The signal amplification afforded by the enzyme component in these covalently linked conjugates results in sensitivities of detection equivalent to those of ^{32}P -labeled probes.

We have been interested in using the unique chemistry of the sulfhydryl group to develop a general methodology for covalently coupling signal-generating enzymes to oligonucleotides. Prior to our work, a ligation method was described for attaching oligonucleotides to nucleic acids, proteins, and peptides (8) based on the propensity of sulfhydryl groups to form disulfides. A drawback of this approach is the susceptibility of the disulfide bond to cleavage by thiols. This problem can be circumvented by using a stable thioether linkage, as exemplified by the synthesis of oligonucleotide-alkaline phosphatase conjugates using bromoacetyl-sulfhydryl coupling chemistry (6). This report presents alternate and extremely efficient conjugation approaches for the preparation of oligonucleotide-enzyme hybridization probes which utilize the high and rather specific reactivity of sulfhydryl groups for maleimides. The oligonucleotide-enzyme conjugates are capable of detecting complementary DNA sequences with high sensitivities with dye precipitation assays.

EXPERIMENTAL PROCEDURES

T4 polynucleotide kinase (EC 2.7.1.78) was obtained from New England Biolabs. Calf intestine alkaline phosphatase (EC 3.1.3.1., enzyme immunoassay grade) and β -galactosidase (EC 3.2.1.23., enzyme immunoassay grade) were purchased from Boehringer Mannheim, and $[\gamma\text{-}^{32}\text{P}]\text{ATP}$ was from ICN. Bovine serum albumin fraction V (BSA),¹ horseradish peroxidase (Type VII, EC 1.11.1.7), sodium dodecyl sulfate (SDS), and polyvinylpyrrolidone (PVP) were from Sigma. Bio-Gel P-100 fine and acrylamide were obtained from Bio-Rad, and DEAE-cellulose (DE-52) came from Whatman. *N*-(2-hydroxyethyl)piperazine-*N'*-ethanesulfonic acid (HEPES), 3-*N*-morpholinopropanesulfonic acid (MOPS), and 1-ethyl-3-[3-(dimethylamino)propyl]carbodiimide hydrochloride (EDC) were purchased from Calbiochem, and Sephadex G-75 was from Pharmacia. 2-Iminothiolane hydrochloride was obtained from Pierce and all other chemicals were purchased from Aldrich. Collodion bags (MW cutoff 25 000) and nitrocellulose filters were obtained from Schleicher and Schuell. Centricon-30 microconcentrators and Centriprep-30 concentrators (MW cutoff 30 000) were purchased from Amicon.

Plasmid pARV7A/2, constructed by inserting a cDNA copy of the HIV genome into the *EcoRI* site of pUC19 pBR322 (9), was obtained from D. Richman (University

of California, San Diego). Oligonucleotide HIV-300 (5'-TGGTCCTGTTCCATTGAACGTCTTATTATT-3') is complementary to the region coding for the HIV sequence in plasmid pARV7A/2. Plasmid pTBO61B was constructed by inserting a 0.9-kb *EcoRI* fragment containing the sequence of the hepatitis B surface antigen (HBsAg) into vector pBR322 (10). Oligonucleotide HBsAg-133 (5'-TGGCTCAGTTTACTAGTGCCATTTGTTTCAG-3') is complementary to the region coding for the hepatitis B surface antigen in plasmid pTBO61B. The oligonucleotides were synthesized on an Applied Biosystems 380A automated DNA synthesizer and were purified according to the reverse-phase chromatographic conditions described by Ghosh et al. (11). The purified oligonucleotides migrated as single bands on a 20% polyacrylamide gel. Enzymatic phosphorylation of the oligonucleotides at the 5'-terminus using T4 polynucleotide kinase and cold ATP or $[\gamma\text{-}^{32}\text{P}]\text{ATP}$ was performed according to the protocol of Maniatis et al. (12).

Preparation of 5'-Cystaminyl Oligonucleotide Derivative. Reaction tubes were silanized with a freshly prepared 5% solution of dichlorodimethylsilane in chloroform to prevent adhesion of the nucleic acids to the walls of the tubes. The 5'-cystaminyl derivative was prepared by the two-step procedure described by Chu et al. (13). Alternately, 5'-phosphorylated oligonucleotide (16 nmol) was treated with 3 mL of 0.1 M imidazole, 0.15 M EDC, 0.25 M cystamine, pH 6.00, at 23 °C for 16 h. The crude cystaminyl oligonucleotide derivative was isolated as a pellet by lithium chloride precipitation from an aqueous ethanol solution and used in the next step without further purification.

Reduction of 5'-Cystaminyl Oligonucleotide Derivative. Reduction of the disulfide linkage of the 5'-cystaminyl oligonucleotide derivative (~16 nmol) was effected by treatment with 2.5 mL of a degassed solution of 0.1 M DTT, 0.2 M HEPES, 1 mM EDTA, pH 7.7, for 1 h at 23 °C. The 5'-(mercaptoethyl)phosphoramidate oligonucleotide derivative was isolated from excess reagent with three consecutive lithium chloride/ethanol precipitations and used immediately in the conjugation reaction or in its reaction with *N,N'*-1,2-phenylenedimaleimide. It is essential to use degassed buffer in the subsequent step and keep the solution of the oligonucleotide derivative under an atmosphere of argon to prevent air oxidation of the terminal thiol group.

Preparation of Maleimide-Derivatized Oligonucleotide. 5'-(Mercaptoethyl)phosphoramidate oligonucleotide derivative (8 nmol) was dissolved in 2 mL of 0.2 M HEPES and 1 mM EDTA, pH 7.7, and then 0.016 mL of a 25 mM solution of *N,N'*-1,2-phenylenedimaleimide in CH_3CN was added. The reaction mixture was kept at 23 °C for 30 min and then ethanol precipitated two times. The maleimide-derivatized oligonucleotide was used immediately for the subsequent coupling step.

Derivatization of Calf Intestine Alkaline Phosphatase with 6-Maleimidohehexanoic Acid Succinimide Ester. 6-Maleimidohehexanoic acid succinimide ester (MHS) was prepared according to a literature procedure (14). Calf intestine alkaline phosphatase (11.3 mg, 81 nmol) in 1.13 mL of 3 M NaCl, 0.1 mM MgCl_2 , 0.1 mM ZnCl_2 , 30 mM triethanolamine, pH 7.6, was dialyzed against 0.1 M NaHCO_3 , 3 M NaCl, 0.02% NaN_3 at pH 8.5 with a collodion bag for a period of 3 h at 4 °C. A 50 molar excess of MHS (0.125 mL) as a 32 mM solution in CH_3CN (10% final concentration of CH_3CN in the reaction) was then added, and the reaction was allowed to proceed at 23 °C for 30 min. Excess reagent was then

¹ Abbreviations used are as follows: BSA, bovine serum albumin fraction V; SDS, sodium dodecyl sulfate; PVP, polyvinylpyrrolidone; DE-52, DEAE-cellulose; HEPES, *N*-(2-hydroxyethyl)piperazine-*N'*-ethanesulfonic acid; MOPS, 3-*N*-morpholinopropanesulfonic acid; EDC, 1-ethyl-3-[3-(dimethylamino)propyl]carbodiimide hydrochloride; DAB- NiCl_2 , 3,3'-diaminobenzidine hydrochloride-nickel chloride; NBT, nitroblue tetrazolium; BCIP, 5-bromo-4-chloro-3-indolyl phosphate; DMF, *N,N*-dimethylformamide; HBsAg, hepatitis B surface antigen; EDTA, ethylenediaminetetraacetic acid; MHS, 6-maleimidohehexanoic acid succinimide ester; DTT, dithiothreitol.

removed by dialysis against argon-degassed 50 mM MOPS, 0.1 M NaCl, pH 7.5, to provide a 1.60-mL solution of maleimide-derivatized alkaline phosphatase.

Preparation of Oligonucleotide-Alkaline Phosphatase Conjugate. A 1.60-mL aliquot of a 50 μ M solution of maleimide-derivatized calf intestine alkaline phosphatase in 50 mM MOPS, 0.1 M NaCl, pH 7.5, was added to 16 nmol of a 5'-(mercaptoethyl)phosphoramidate oligonucleotide derivative, and the conjugation reaction was allowed to proceed at 23 °C for 16 h. Gel filtration in a Bio-Rad P-100 column (1.5 \times 75 cm) at 4 °C using 0.05 M Tris, pH 8.5, as an eluant separated unreacted oligonucleotide from the enzyme-oligonucleotide conjugate and excess enzyme. The enzyme fractions were pooled and applied to a DEAE-cellulose column (1 \times 7.4 cm) equilibrated with 0.05 M Tris, pH 8.5, at 23 °C. The column was washed with 0.1 M Tris, pH 8.5 (15 mL), and a 40-mL salt gradient of 0–0.2 M NaCl in 0.1 M Tris, pH 8.5, followed by 40 mL of 0.2 M NaCl, 0.1 M Tris, pH 8.5, to elute free alkaline phosphatase. Pure oligonucleotide-alkaline phosphatase conjugate was obtained by elution with 0.5 M NaCl and 0.1 M Tris, pH 8.5. The conjugate fractions were combined, simultaneously dialyzed and concentrated with Centriprep-30 concentrators (Amicon), and stored in 0.1 M Tris, 0.1 M NaCl, pH 8.5, at 4 °C.

Thiolation of Horseradish Peroxidase. The thiolation of horseradish peroxidase was carried out by using a modification of a literature-described procedure (15). A 0.05-mL aliquot of a 0.12 M solution of 2-iminothiolane hydrochloride (6 μ mol) in 25 mM sodium borate, pH 9.00, was added to 0.28 mL of a 0.21 mM solution of horseradish peroxidase (60 nmol) in the same buffer. The reaction mixture was kept at 23 °C for 1 h and then excess reagent was removed by dialysis against 25 mM sodium borate, pH 9.00, at 4 °C.

Preparation of Oligonucleotide-Horseradish Peroxidase Conjugate. To ~8 nmol of maleimide-derivatized oligonucleotide in 2 mL of degassed 0.2 M HEPES, 1 mM EDTA, pH 7.7, was added 0.214 mL of a 0.19 mM solution of thiolated horseradish peroxidase (40 nmol) in 25 mM sodium borate, pH 9.00. The reaction mixture was kept under an argon atmosphere, and the conjugation was allowed to proceed for 16 h at 23 °C. A Sephadex G-75 column (1.5 \times 44 cm) was used to separate unreacted oligonucleotides from the mixture of conjugates and excess thiolated enzyme. The conjugates were then purified by DEAE ion-exchange chromatography with the conditions described in the previous section.

Preparation of Oligonucleotide- β -Galactosidase Conjugate. The conjugation of maleimide-derivatized oligonucleotides to β -galactosidase was performed under conditions identical with those for thiolated horseradish peroxidase. The purification of the conjugate was carried out following the protocol for the isolation of the oligonucleotide-alkaline phosphatase.

Alkaline Phosphatase Assay. The enzymatic activity of alkaline phosphatase and the oligonucleotide-alkaline phosphatase conjugates was assayed at 23 °C by following the hydrolysis of 0.1 mM *p*-nitrophenyl phosphate in 0.1 M Tris, 0.1 M NaCl, 0.01 M MgCl₂, pH 9.5, at 410 nm.

Horseradish Peroxidase Assay. The enzymatic activity of horseradish peroxidase and its conjugate was assayed with a 3,3'-diaminobenzidine hydrochloride-nickel chloride (DAB-NiCl₂) solution (0.5 mg/mL DAB in 0.05 M Tris, pH 7.6, containing 0.04% NiCl₂).

β -Galactosidase Assay. The enzymatic activity of β -galactosidase and its conjugate was assayed at 37 °C by

following the release of 4-nitrophenolate at 410 nm with a solution of 4-nitrophenyl- β -D-galactoside (1.57 mg/mL) in 50 mM potassium phosphate, 1 mM MgCl₂, 0.1 M 2-mercaptoethanol, pH 7.8.

Sensitivity of Conjugates for Nitrocellulose-Immobilized Target DNA: (i) Oligonucleotide-Alkaline Phosphatase Conjugate. Varying amounts of plasmid pARV7A/2, 1 μ g of *Escherichia coli* DNA, 100 ng of pBR322 and 10 μ g of human DNA were denatured under alkaline conditions at 65 °C (0.2 M NaOH, 15 min) and then neutralized with an equal volume of 2 M ammonium acetate. The DNA samples were immobilized onto a nitrocellulose membrane using a Schleicher and Schuell Minifold II slot-blot apparatus, and the nucleic acids were fixed to the nitrocellulose by UV radiation (16). The filter was prehybridized in 5 \times SSC, 0.5% BSA, 0.5% PVP, and 0.1% SDS for 10 min at 50 °C, followed by hybridization in the same buffer with 2 μ g/mL of oligonucleotide-alkaline phosphatase conjugate for 1 h at 50 °C. After three washes with 1 \times SSC containing 0.1% SDS at 23 °C and a stringency wash in the same buffer at 50 °C, the filter was rinsed three times with developing buffer (0.1 M Tris, 0.1 M NaCl, 0.01 M MgCl₂, pH 9.5). Color development was allowed to proceed for 4 h with 0.33 mg/mL nitroblue tetrazolium (NBT) and 0.16 mg/mL 5-bromo-3-chloro-3-indolyl phosphate (BCIP) in developing buffer containing 0.33% v/v DMF.

(ii) Oligonucleotide-Horseradish Peroxidase Conjugate. The prehybridization and hybridization steps were identical with the protocol described above. After the stringency wash at 50 °C, the filter was washed with 0.05 M Tris, pH 7.6. The detection assay was then carried out with DAB-NiCl₂ solution.

RESULTS

Preparation of Derivatized Oligonucleotides. A number of methods (13, 17–19) have been reported which describe the introduction of sulfhydryl groups at the termini of synthetic oligonucleotides. The strategy of Chu et al. (13) was used for modification of our oligonucleotide probes, since it conveniently allows ³²P labeling of the 5'-end of the nucleic acid, thereby enabling us to monitor the efficiencies of the conjugation reactions. In addition, the method has the advantage of permitting the functionalization of any unprotected oligonucleotide or RNA sequence which can be made available by chemical or enzymatic syntheses.

Thus, the 5'-cystaminyl oligonucleotide derivatives were obtained through conversion of the 5'-terminal phosphates to the activated phosphorimidazolides, followed by nucleophilic displacement of the leaving group with cystamine. The same modification was achieved in a single step with cystamine and EDC in imidazole buffer. Product analysis by 20% polyacrylamide gel electrophoresis indicated a 65–70% yield for both procedures (data not shown). Reduction of the disulfide linkage with DTT resulted in quantitative formation of the 5'-(mercaptoethyl)phosphoramidate oligonucleotide derivatives.

The thiolated oligonucleotides can be used directly in conjugation reactions with maleimide-modified enzymes (Figure 1). Alternately, the sulfhydryl groups can be functionalized with the bifunctional linker *N,N'*-1,2-phenylenedimaleimide to provide maleimide-derivatized oligonucleotides, thereby allowing the converse conjugation reaction with thiolated enzymes or enzymes possessing free cysteines (Figure 2). The reaction of 5'-(mercaptoethyl)phosphoramidate oligonucleotide derivatives with *N,N'*-1,2-phenylenedimaleimide was rapid and was essen-

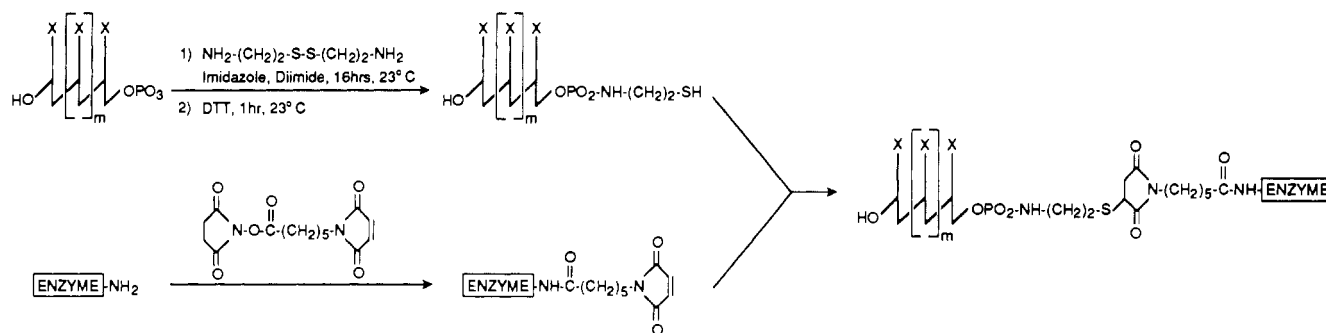


Figure 1. Conjugation of 5'-thiolated oligonucleotides with calf intestine alkaline phosphatase using 6-maleimido-hexanoic acid succinimido ester.

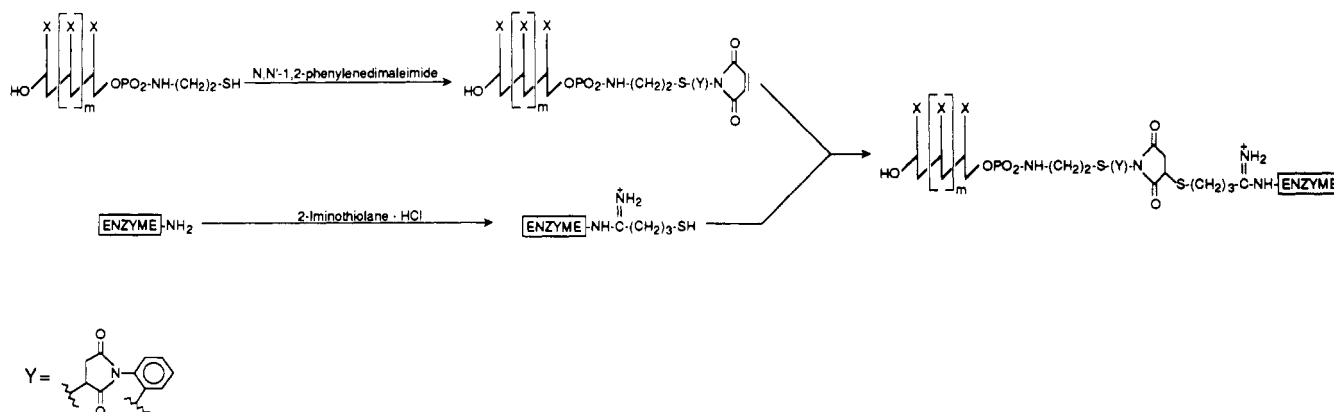


Figure 2. Cross-linking of oligonucleotides to enzyme using *N,N'*-1,2-phenylenedimaleimide.

tially complete in 30 min as determined by polyacrylamide gel analysis (data not shown).

Modification of Reporter Enzymes. Maleimide groups were introduced in calf intestine alkaline phosphatase by utilizing a 50-fold excess of the heterobifunctional linker 6-maleimido-hexanoic acid succinimido ester (MHS) (13). The extent of the modification was followed by treatment of the derivatized enzyme with excess DTT, followed by titration of the sulfhydryl groups with 5,5'-dithiobis(2-nitrobenzoic acid) (20). An average of 6.2 maleimide residues per enzyme molecule was estimated by this procedure.

Thiolation of horseradish peroxidase with 2-iminothiolane (15) was performed by using a modification of a literature procedure. The modified enzyme was found to possess an average of 1.9 sulfhydryl groups per mole of protein.

Synthesis of Oligonucleotide-Alkaline Phosphatase Conjugate. It is not essential to purify the 5'-(mercaptoethyl)phosphoramidate oligonucleotide derivative prior to the conjugation reaction, since unreacted phosphorylated oligonucleotides are inert toward maleimides. Typically, a 5-fold molar excess of maleimide-modified calf intestine alkaline phosphatase was reacted with 5'-(mercaptoethyl)phosphoramidate oligonucleotide derivative (Figure 1). Excess enzyme and conjugate were separated from the unreacted oligonucleotide with gel filtration (Figure 3A). The efficiency of the conjugation can be followed by ^{32}P labeling of the 5'-phosphorus of the oligonucleotide derivative. Since crude, thiolated oligonucleotides are used in the reaction, alkaline phosphatase hydrolysis of residual 5'-kinased oligonucleotides occurs in the conjugation step. Thus, a late-eluting, ^{32}P -labeled, inorganic phosphate peak is also observed in the cpm elution profile (not shown in Figure 3A). This allowed an independent determination of the efficiency of 5'-(mercaptoethyl)phosphoramidate oli-

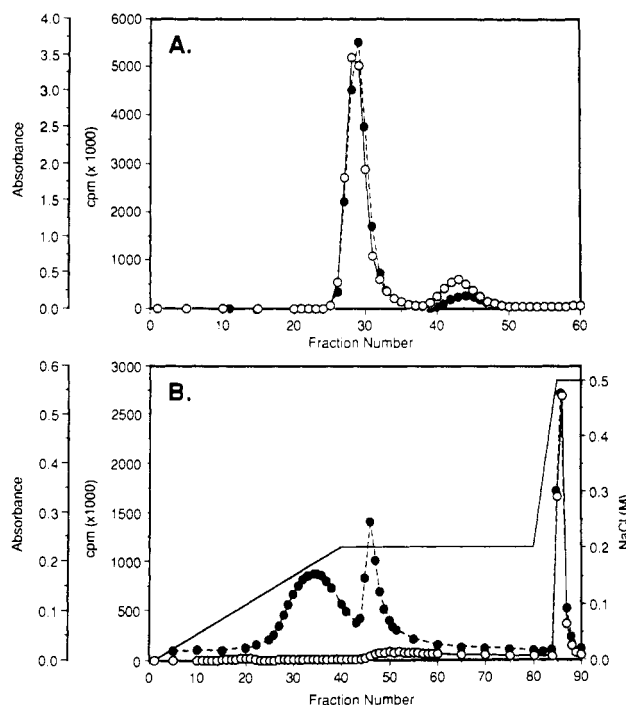


Figure 3. Purification of oligonucleotide-alkaline phosphatase conjugates: (A) Gel filtration chromatography of a conjugation reaction mixture on a Bio-Rad P-100 column [1.5 × 75 cm, 0.88 mL/reaction; (O) cpm; (●) absorbance], (B) ion-exchange chromatography of pooled reactions from the first peak in A on a DEAE-cellulose column (1 × 7.4 cm, 1.1 mL/reaction).

gonucleotide formation (~70%), which compares favorably with the results from the polyacrylamide gel electrophoresis discussed earlier. In addition, the distribution of radioactivity in the oligonucleotide-enzyme

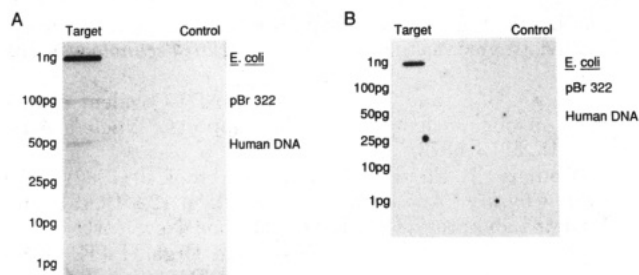


Figure 4. Detection of complementary target plasmid pARV7A/2 on nitrocellulose membranes: (A) Dilutions of the target plasmid and controls were immobilized on the membrane and hybridized with an HIV-300–alkaline phosphatase conjugate. Target DNA was visualized colorimetrically by using a dye precipitation assay. (B) the sensitivity of detection of target DNA using ^{32}P -labeled HIV-300 (4.4×10^6 cpm/nmol).

conjugate and unreacted 5'-(mercaptoethyl)phosphoramidate oligonucleotide peaks indicated an efficiency of 85% for the coupling reaction.

The appropriate protein fractions from the gel filtration step were subjected to DEAE-cellulose ion-exchange chromatography for the final purification of oligonucleotide-alkaline phosphatase conjugate. A combination of gradient and isocratic salt elutions successfully resolved the conjugate from two enzyme species, which presumably differ in their degree of modification with maleimide residues (see absorbance profile in Figure 3B). The conjugate was determined to have a composition of a 1:1 molar ratio of oligonucleotide and alkaline phosphatase by using the spectroscopic analysis of Li et al. (6). The conjugate was assayed colorimetrically with *p*-nitrophenyl phosphate and was found to retain 80–85% of the unmodified enzyme's activity.

Synthesis of Oligonucleotide–Horseradish Peroxidase Conjugate. A 5-fold excess of thiolated horseradish peroxidase was reacted with crude, ^{32}P -labeled, maleimide-derivatized oligonucleotide, and the conjugate was isolated by a combination of Sephadex G-75 gel filtration and DEAE-cellulose ion-exchange chromatography. Based on a 60% yield for the formation of the maleimide-derivatized oligonucleotide, the efficiency of the conjugation reaction was estimated to be 58% from the cpm elution profile of the gel filtration step. A DAB– NiCl_2 assay of the conjugate indicated a 70–75% retention of the original enzymatic activity.

Synthesis of Oligonucleotide– β -Galactosidase Conjugate. The coupling of β -galactosidase to maleimide-derivatized oligonucleotide was identical with the procedure described for horseradish peroxidase. The conjugate was isolated in 65% yield and was 75% as active as the unmodified enzyme.

Sensitivities of Conjugates in Detecting Complementary DNA Sequences. Figure 4A shows the sensitivity of the HIV-300–alkaline phosphatase conjugate for plasmid pARV7A/2 immobilized on a nitrocellulose membrane by using a dye precipitation assay. The conjugate detected 100 pg (12 amol) of target DNA in 1 h and was capable of detecting 50 pg (6 amol) with 4 h of color development. No cross-hybridization was observed with plasmid pBR322, *E. coli* DNA, or human genomic DNA, and filter background was completely absent. With use of the same hybridization conditions, ^{32}P -labeled HIV-300 detected 100 pg (12 amol) of target DNA after 18 h of autoradiography (Figure 4B).

Horseradish peroxidase was conjugated to oligonucleotide HBsAg-133 and was used as a probe for plasmid pTBO61B. The level of sensitivity was found to be 1 ng

(300 amol) with DAB– NiCl_2 for color development and was 40-fold higher than the limit of detection for the corresponding alkaline phosphatase conjugate.

We were unsuccessful in our attempts to use the HBsAg-133– β -galactosidase conjugate for the detection of nitrocellulose-immobilized target DNA. The conjugate exhibited a high nonspecific background for the membrane in an assay with 5-bromo-4-chloro-3-indolyl- β -D-galactopyranoside and nitroblue tetrazolium.

DISCUSSION

An important consideration in our choice of the conjugation chemistry was the ability to manipulate any oligonucleotide or RNA sequence, synthesized enzymatically or by solid phase procedure, for subsequent covalent attachment to the reporter enzymes. The procedure of Chu et al. (13) for the introduction of reactive thiol functionalities at the 5'-terminal phosphates of unprotected oligonucleotides was therefore well-suited for our purpose. In this respect, our previous paper (4) and this report differ from the other approaches (5–7), which require the use of linker-modified nucleotide analogues to replace one of the standard bases in the automated synthesis of the oligonucleotides. The linkers are functionalized with terminal amine groups, which provide a chemical handle for the conjugation chemistry.

The reaction of maleimides with sulfhydryl groups is fairly rapid compared to their reaction with amino and hydroxyl groups (21). We have exploited this reactivity to develop highly efficient methods for the conjugation of reporter enzymes to oligonucleotides. In the first strategy, calf intestine alkaline phosphatase was functionalized with maleimide groups and the heterobifunctional linker MHS and subsequently reacted with a 5'-(mercaptoethyl)phosphoramidate oligonucleotide derivative. Our choice of MHS was influenced by the presence of a suitable alkyl spacer in the reagent, thereby ensuring minimal interference of the reporter moiety in the hybridization reaction of the oligonucleotide–enzyme conjugate.

The second approach was designed for thiolated enzymes and enzymes with free cysteines and utilized *N,N'*-1,2-phenylenedimaleimide to effect the coupling with a 5'-(mercaptoethyl)phosphoramidate oligonucleotide derivative. Thiolated horseradish peroxidase and β -galactosidase were utilized in these conjugation reactions. Lower efficiencies of conjugation were obtained with this cross-linker when compared to the MHS-based procedure.

The conjugates retain greater than 70% of their original enzymatic activity and are stable indefinitely when stored at 4 °C. The oligonucleotide–alkaline phosphatase conjugate was extremely sensitive in nitrocellulose-based hybridization reactions, while the oligonucleotide–horseradish peroxidase conjugate was 40-fold less sensitive than its corresponding alkaline phosphatase conjugate. This observation is in accordance with our previous results using hydrazone-linked oligonucleotide–alkaline phosphatase and oligonucleotide–horseradish peroxidase conjugates (4).

The high sensitivities afforded by chemiluminescence have recently been exploited with acridinium ester labeled DNA probes (22), which were shown to detect target nucleic acid sequences in the 10^{-17} – 10^{-18} mol range. In contrast to the single chemiluminescent molecule per oligonucleotide probe in this system, the efficacy of oligonucleotide–enzyme conjugates derives from the signal amplification by the reporter group. Hence, even higher sensitivities of detection should be attainable with chemilumines-

cent substrates. Indeed, oligonucleotide-alkaline phosphatase conjugates have been demonstrated to detect 7×10^{-20} mol of target DNA when used in conjunction with the dioxetane-based chemiluminescent substrate AMPPD (23). Alternatively, the recently described, dual-enzyme, cascade amplification system (24) can be utilized as a colorimetric assay for the conjugates. We are currently focusing on the application of these sensitive methods with our alkaline phosphatase conjugates to the detection of target nucleic acids using a sandwich detection format.

ACKNOWLEDGMENT

We are indebted to Drs. Thomas Gingeras, Ulrich Merten, and Eoin Fahy for critical reading of the manuscript and to Linda Blonski, Claire Lynch, and Kris Blumeyer for technical assistance. We are grateful to Janice Doty for preparation of the manuscript.

LITERATURE CITED

- (1) Saiki, R. K., Scharf, S., Faloona, F., Mullis, K. B., Horn, G. T., Erlich, H. A., and Arnheim, N. (1985) Enzymatic amplification of β -globin genomic sequences and restriction site analysis for diagnosis of sickle cell anemia. *Science* **230**, 1350-1354.
- (2) Kwok, D. Y., Davis, G. R., Whitfield, K. M., Chappelle, H. L., DiMichele, L. J., and Gingeras, T. R. (1989) Transcription-based amplification system and detection of amplified human immunodeficiency virus type 1 with a bead-based sandwich hybridization format. *Proc. Natl. Acad. Sci. U.S.A.* **86**, 1173-1177.
- (3) For review, see: Matthews, J. A. and Kricka, L. J. (1988) Analytical strategies for the use of DNA probes. *Anal. Biochem.* **169**, 1-25.
- (4) Ghosh, S. S., Kao, P. M., and Kwok, D. Y. (1989) Synthesis of 5'-oligonucleotide hydrazide derivatives and their use in preparation of enzyme-nucleic acid hybridization probes. *Anal. Biochem.* **178**, 43-51.
- (5) Jablonski, E., Moomaw, E. W., Tullis, R. H., and Ruth, J. L. (1986) Preparation of oligodeoxynucleotide-alkaline phosphatase conjugates and their use as hybridization probes. *Nucleic Acids Res.* **14**, 6115-6128.
- (6) Li, P., Medon, P. P., Skingle, D. C., Lanser, J. A., and Symons, R. H. (1987) Enzyme-linked synthetic oligonucleotide probes: Non-radioactive detection of enterotoxigenic *Escherichia coli* in faecal specimens. *Nucleic Acids Res.* **15**, 5275-5287.
- (7) Urdea, M. S., Warner, B. D., Running, J. A., Stempien, M., Clyne, J., and Horn, T. (1988) A comparison of non-radioisotopic hybridization assay methods using fluorescent, chemiluminescent and enzyme labeled synthetic oligodeoxynucleotide probes. *Nucleic Acids Res.* **16**, 4937-4956.
- (8) Chu, B. C. F. and Orgel, L. E. (1988) Ligation of oligonucleotides to nucleic acids or proteins via disulfide bonds. *Nucleic Acids Res.* **16**, 3671-3691.
- (9) Luciw, P. A., Potter, S. J., Steimer, K., Dina, D., and Levy, J. A. (1984) Molecular cloning of AIDS-associated retrovirus. *Nature* **312**, 760-763.
- (10) Cregg, J. M., Tschopp, J. F., Stillman, C., Siegel, R., Akong, M., Craig, W. S., Buckholz, R. G., Madden, K. R., Kellaris, P. A., Davis, G. R., Smiley, B. L., Cruze, J., Torregrossa, R., Velicelebi, G., and Thill, G. P. (1987) High level expression and efficient assembly of hepatitis B surface antigen in the methylotrophic yeast, *Pichia pastoris*. *Bio/Technology* **5**, 479-485.
- (11) Ghosh, S. S. and Musso, G. M. (1987) Covalent attachment of oligonucleotides to solid supports. *Nucleic Acids Res.* **15**, 5353-5372.
- (12) Maniatis, T., Fritsch, E. F., and Sambrook, J. (1982) *Molecular Cloning: A Laboratory Manual*. p 122, Cold Spring Harbor Laboratory, Cold Spring Harbor, New York.
- (13) Chu, B. C. F., Kramer, F. R., and Orgel, L. E. (1986) Synthesis of an amplifiable reporter RNA for bioassays. *Nucleic Acids Res.* **14**, 5591-5603.
- (14) Keller, O. and Rudinger, J. (1975) Preparation and some properties of maleimido acids and maleoyl derivatives of peptides. *Helv. Chim. Acta* **58**, 531-541. MHS is commercially available from Boehringer Mannheim.
- (15) Ping, T. P., Li, Y., and Kochoumian, L. (1978) Preparation of protein conjugates via intermolecular disulfide bond formation. *Biochemistry* **17**, 1499-1506.
- (16) Church, G. M. and Gilbert, W. (1984) Genomic sequencing. *Proc. Natl. Acad. Sci. U.S.A.* **81**, 1991-1995.
- (17) Sproat, B. S., Beijer, B., Rider, P., and Neuner, P. (1987) The synthesis of protected 5'-mercapto-2',5'-dideoxyribonucleoside-3'-O-phosphoramidites; Uses of 5'-mercapto-oligodeoxyribonucleotides. *Nucleic Acids Res.* **15**, 4837-4848.
- (18) Zuckerman, R., Corey, D., and Schultz, P. (1987) Efficient methods for attachment of thiol specific probes to the 3'-ends of synthetic oligodeoxyribonucleotides. *Nucleic Acids Res.* **15**, 5305-5321.
- (19) Connolly, B. A. and Rider, P. (1985) Chemical synthesis of oligonucleotides containing a free sulphhydryl group and subsequent attachment of thiol specific probes. *Nucleic Acids Res.* **13**, 4485-4502.
- (20) Ellman, G. L. (1959) Tissue sulphhydryl groups. *Arch. Biochem. Biophys.* **82**, 70-77.
- (21) Ishikawa, E., Hamaguchi, Y., and Yoshitake, S. (1981) Enzyme Labeling with *N,N'*-o-Phenylenedimaleimide. In *Enzyme Immunoassay* (E. Ishikawa, T. Kawai, and K. Miyai, Eds.) pp 67-80, Igaku-Shoin, Tokyo.
- (22) Arnold, L. J., Hammond, P. W., Wiese, W. A., and Nelson, N. C. (1989) Assay formats involving acridinium-ester-labeled DNA probes. *Clin. Chem.* **35**, 1588-1594.
- (23) Bronstein, I., Voyta, J. C., and Edwards, B. (1989) A comparison of chemiluminescent and colorimetric substrates in a hepatitis B virus DNA hybridization assay. *Anal. Biochem.* **180**, 95-99.
- (24) Mize, P. D., Hoke, R. A., Linn, C. P., Reardon, J. E., and Schulte, T. H. (1989) Dual-enzyme cascade: An amplified method for the detection of alkaline phosphatase. *Anal. Biochem.* **179**, 229-235.

Registry No. Oligonucleotide HIV-300, 124041-88-9; oligonucleotide HBsAg-133, 124041-87-8; oligonucleotide HIV-300, 5'-cystaminyl derivative, 124041-92-5; oligonucleotide HBsAg-133, 5'-cystaminyl derivative, 124041-91-4; oligonucleotide HIV-300, 5'-(mercaptoethyl)phosphoramidate derivative, 124041-90-3; oligonucleotide HBsAg-133, 5'-(mercaptoethyl)phosphoramidate derivative, 124041-89-0; oligonucleotide HIV-300, 5'-(mercaptoethyl)phosphoramidate derivative reacted with *N,N'*-1,2-phenylenedimaleimide, 124041-94-7; oligonucleotide HBsAg-133, 5'-(mercaptoethyl)phosphoramidate derivative reacted with *N,N'*-1,2-phenylenedimaleimide, 124041-93-6; cystamine, 51-85-4; *N,N'*-phenylenedimaleimide, 13118-04-2.

Hydrazide Pharmaceuticals as Conjugates to Polyaldehyde Dextran: Syntheses, Characterization, and Stability

Ned D. Heindel,* Huiru Zhao, Jeffrey Leiby, Jacobus M. VanDongen, C. Jeffrey Lacey, Daniel A. Lima, Barakat Shabsoug, and John H. Buzby

Institute for Health Sciences and Department of Chemistry, Lehigh University, Bethlehem, Pennsylvania 18015.
Received October 16, 1989

The coupling of ellipticine and CI-921, two antineoplastic pharmaceuticals, to polyaldehyde dextran can be carried out under mild reaction conditions with novel acid hydrazides of the parent drugs. The resulting acyl hydrazones resist hydrolytic and enzymatic cleavage and offer a method for drug loading via dextran conjugates to monoclonal antibodies.

Numerous examples of the conjugation of antineoplastic pharmaceuticals to antibodies or to their fragments can be found in the burgeoning field of immunochemotherapy (1-3). Often these drug-to-antibody linkages involve the amino or carboxy functions on the glycoprotein bridging to counterpart carboxyl (or formyl) and amino moieties on the small molecule pharmaceutical (3-5).

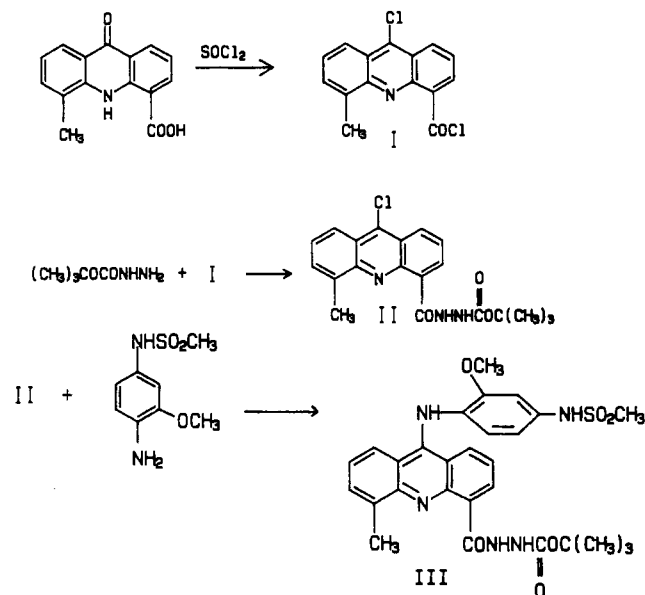
Recently, however, the chemical advantages of utilizing hydrazides in the conjugation process have been recognized. We have reported the synthesis of a no-carrier-added radioiodinated hydrazide which couples efficiently to carbonyl moieties (6). Others have noted that the very low pK of hydrazides (ca. 2.6) compared to that of primary amines (ca. 9-10) means that under mildly acidic conditions hydrazides can be linked to aldehydes without intervention of potentially competitive amino functions (7, 8). This chemistry has been exploited to permit conjugation of hydrazide anticancer agents to CHO moieties—often generated by oxidation of carbohydrate units on the antibody—with minimal intramolecular cross-linking by lysine residues on the glycoprotein (9-11). Furthermore, the acyl hydrazones thus generated are considerably more resistant to hydrolysis and do not require reduction for stabilization.

In this laboratory we have been developing the use of hydrazide-based pharmaceuticals and radiotracers as well as polyaldehyde dextran (PAD) as a macromolecular carrier for these agents (12, 13). Not only do drug-dextran conjugates offer a facile polymeric spacer for antibody attachment but they also offer a more soluble delivery form of the parent drug, which may now undergo tumor-affinic uptake by an endocytosis mechanism. Drug-to-PAD conjugates appear to offer therapeutic advantages in several cases (14, 15). In this study we have linked the antitumor agents CI-921 (Chart I) and two ellipticines (9-methoxy and 9-H, Chart II) as hydrazides onto PAD and have studied the stability of the conjugates.

EXPERIMENTAL PROCEDURES

Materials. Ellipticine and 9-methoxyellipticine were supplied by the Drug Development Branch, National Cancer Institute, NIH, Bethesda, MD. CI-921, also known as 9-[[2-methoxy-4-[(methylsulfonyl)amino]phenyl]amino]-*N*,5-dimethylacridine-4-carboxamide, was supplied by Parke-Davis Pharmaceuticals of Ann Arbor, MI. Clinical-grade dextran (40 kDa) was supplied by Pharmachem Corp., Bethlehem, PA. All other chemicals and solvents were of the highest purity commercial grade. Combustion analyses were supplied by Robertson Microana-

Scheme I. Synthesis of CI-921 Carbazate (III)



lytical Laboratory, Madison, NJ. ^1H NMR spectra were obtained in the indicated solvents on a JEOL FX90Q spectrophotometer. Melting points were obtained on either a Thomas-Hoover capillary or a Fisher-Johns melting point apparatus and are reported uncorrected.

Syntheses. *tert*-Butyl *N*-[[9-[[2-Methoxy-4-[(methylsulfonyl)amino]phenyl]amino]-5-methylacridin-4-yl]carbonyl]carbazate Hydrochloride (III). Intermediates in this pathway proved highly unstable and decomposed to red oils from initially isolated solids. The synthesis was continued in sequence until stable III was isolated (Scheme I).

5-Methyl-9-oxoacridan-4-carboxylic acid (1.51 g, 5.95 mmol) was dissolved in 20 mL of thionyl chloride containing one drop of dimethyl formamide and the solution was refluxed for 30 min (17). The volume was reduced to 5 mL and 15 mL of dry benzene was added. The mixture was again evaporated to about 5 mL, fresh benzene was added, and the flask contents were evaporated to dryness. The intermediate, yellow 5-methyl-9-chloroacridine-4-carbonyl chloride hydrochloride (I) (mp 143-146 °C) was used directly by immediate dissolution in 70 mL of dry methylene chloride. *tert*-Butyl carbazate (0.78 g, 5.9 mmol) was added as a single portion to the solution of I chilled in an ice-water bath. After 1 min of mixing, the methylene chloride was vacuum evaporated at room

Chart I. Structures of CI-921 and Analogues

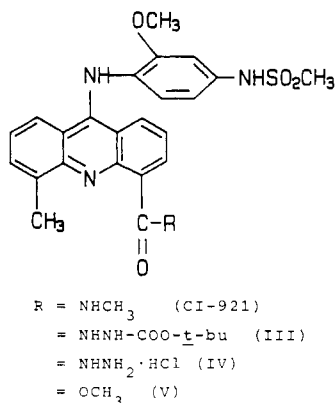
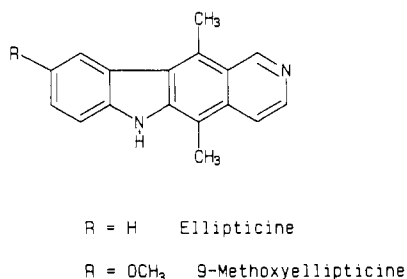


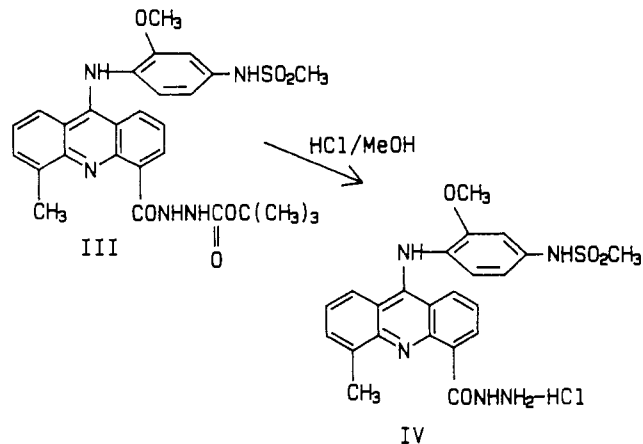
Chart II. Structures of Ellipticine and Methoxyellipticine



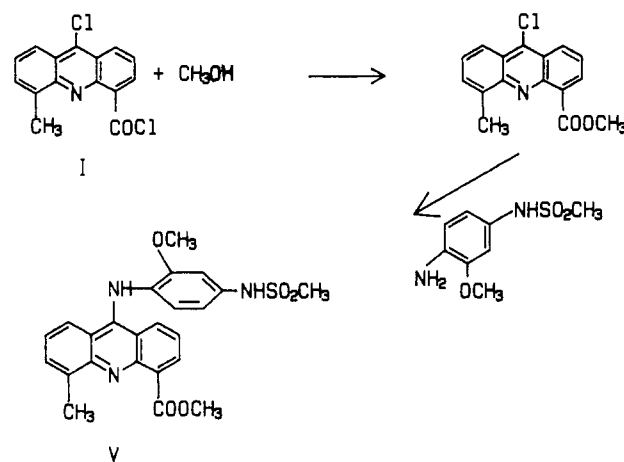
temperature and the labile *tert*-butyl *N'*-(5-methyl-9-chloroacridin-4-yl)carbonyl]carbazate hydrochloride (II) was dissolved in 50 mL of anhydrous methanol and employed directly in the condensation step with *N*-(4-amino-3-methoxyphenyl)methanesulfonamide (16) (1.29 g, 5.95 mmol) and 100 μL of concentrated hydrochloric acid. This slurry was refluxed for 20 min, the condenser was removed, and the solvent was evaporated to half-volume. Ethyl acetate (50 mL) was added and the resultant slurry was allowed to stand for 5 h prior to filtration. The isolated product (1.99 g) was shown by ^1H NMR to be a mixture of III and IV. Pure title product (*tert*-butyl carbazate III) was obtained as a red-orange solid by preparative thick (1000 μm) layer chromatography employing 9:4:1 chloroform-isopropyl alcohol-methanol as the moving phase. The product eluted just under the solvent front ($R_f \sim 0.8$) and all other impurities including the hydrazide ($R_f \sim 0.4$) were considerably less migratory: yield 0.122 g (3.4%) of a red-orange solid; mp 116–120 $^\circ\text{C}$; ^1H NMR ($\text{DMSO}-d_6$) δ 1.45 (s, 9H, *t*-Bu), 2.61 (s, 3 H, C-5 CH_3), 3.10 (s, 3 H, SO_2CH_3), 3.59 (s, 3 H, OCH_3), 7.01 (s, 2 H, ArH), 7.48 (m, 4 H, ArH), 7.89 (d, 1 H, ArH), 8.11 (d, 1 H, ArH), 8.55 (d, 1 H, ArH), 8.70 (d, 1 H, ArH), 9.28 (s, 1 H, NH), 10.15 (s, 1 H, NH), 11.21 (s, 1 H, NH). Anal. Calcd for $\text{C}_{28}\text{H}_{31}\text{N}_5\text{O}_6\text{S} \cdot \text{HCl}$: C, 55.85; H, 5.36; N, 11.63. Found: C, 55.73; H, 5.53; N, 11.43.

9-[[2-Methoxy-4-[(methylsulfonyl)amino]phenyl]amino]-5-methylacridine-4-carboxylic Acid Dihydrochloride (IV). This product could be obtained as a byproduct in the synthesis of III described above (R_f 0.40–0.45) but was best obtained by acid-catalyzed hydrolysis of purified carbazate III (Scheme II). A sample of 0.122 g (0.203 mmol) of III was dissolved in 1.0 mL of methanol and 15 mL of 2.0 M aqueous hydrochloric acid. This acidic, methanolic solution was allowed to stand at ambient temperature for 1 h and was evaporated in vacuo, and the resulting red solid was purified by preparative thick-layer chromatography on 1000- μm silica gel plates. The mobile phase was 10:2:1 chloroform-

Scheme II. Synthesis of CI-921 Hydrazide (IV)

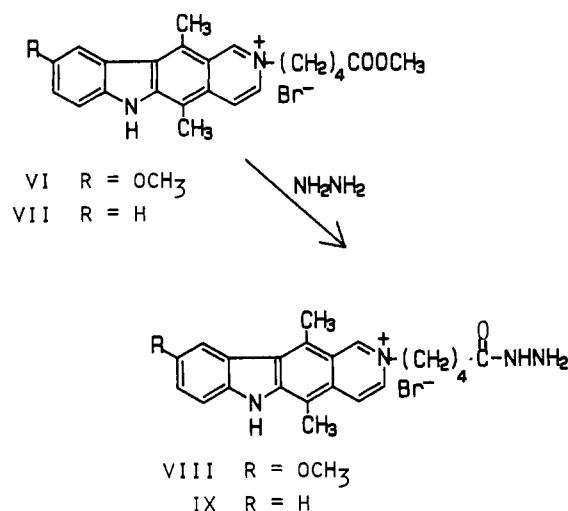


Scheme III. Synthesis of CI-921 Methyl Ester (V)



2-propanol-methanol (v:v:v) and the product was eluted as a sharp band at R_f 0.74. It was eluted from the silica gel in methanol, filtered, evaporated to dryness, and dried under vacuum for 2 h to yield 0.062 g (56%) of red-orange IV: mp 109.5–111.5 $^\circ\text{C}$; ^1NMR (CD_3OD) δ 2.81 (s, 3 H, C-5 CH_3), 3.09 (s, 3 H, SO_2CH_3), 3.58 (s, 3 H, OCH_3), 7.05 (m, 3 H, ArH), 7.50 (m, 3 H, ArH), 7.87 (d, 1 H, ArH), 8.10 (d, 1 H, ArH), and 8.55 (m, 2 H, ArH) (NH signals not visible in this solvent system); MS (FAB) $m/e = 465.9$ (calcd $m/e = 465.6$ for molecular ion of free base). Anal. Calcd for $\text{C}_{23}\text{H}_{23}\text{N}_5\text{O}_4\text{S} \cdot 2\text{HCl}$: Cl, 13.16. Found: Cl, 13.05.

Methyl 9-[[2-Methoxy-4-[(methylsulfonyl)amino]phenyl]amino]-5-methyl-4-acridinecarboxylate Hydrochloride (V). 5-Methyl-9-chloroacridine-4-carbonyl chloride hydrochloride (II) (prepared in situ by chlorination as described above from 1.51 g, 5.95 mmol of 5-methylacridone-4-carboxylic acid) was slurried in 50 mL of dry methanol with 5 mL of triethylamine for 1 h at room temperature (Scheme III). The yellow solid which formed, the methyl ester of the acridine, was filtered, washed with dry methanol, and suspended in 50 mL of dry methanol. *N*-(4-amino-3-methoxyphenyl)methanesulfonamide (1.29 g, 5.95 mmol) and one drop of concentrated hydrochloric acid were added to this suspension. The reaction mixture was distilled to 50% volume and 50 mL of ethyl acetate was added. The resulting slurry was allowed to stand at room temperature overnight. A tangerine solid (V) was filtered and washed with chloroform: yield 0.41 g (14%); mp 232–234 $^\circ\text{C}$ dec; ^1H NMR ($\text{DMSO}-d_6$) δ 2.61 (s, 3 H, C-5 CH_3), 3.05 (s, 3 H, SO_2CH_3), 3.50 (s, 3 H, OCH_3), 4.02 (s, 3 H, COOCH_3), 7.01

Scheme IV. Synthesis of Ellipticinium Hydrazides VIII and IX

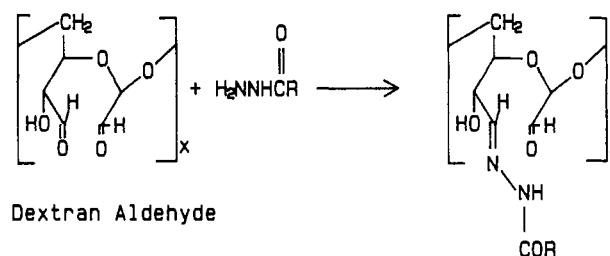
(s, 2 H, ArH), 7.19 (m, 4 H, ArH), 7.65 (d, 1 H, ArH), 7.85 (d, 1 H, ArH), 8.40 (d, 2 H, ArH), and 9.78 (s, 1 H, NH) (other NH signals not seen). Anal. Calcd for C₂₄H₂₄ClN₃O₅S^{1/2}·H₂O: C, 56.41; H, 4.93; N, 8.22. Found: C, 56.66; H, 4.82; N, 8.20.

2-(4-Methoxy-4-oxobutyl)-9-methoxyellipticinium Bromide (VI). A mixture of 9-methoxyellipticine (0.838 g, 3.04 mmol), methyl 5-bromopentanoate (3.41 g, 17.5 mmol), 2-propanol (48 mL), and dimethylformamide (16 mL) was refluxed for 72 h, cooled, and the precipitate was filtered and washed successively with 2-propanol and acetone. Evaporation of the combined mother liquors and washings to ca. 25 mL yielded, upon cooling, additional orange-brown crystals of 2-(4-methoxy-4-oxobutyl)-9-methoxyellipticinium bromide (VI) for a total of 1.02 g (71%), mp 200–202 °C (from CHCl₃). Anal. Calcd for C₂₄H₂₇BrN₂O₃: C, 61.15; H, 5.77; N, 5.94. Found: C, 60.99; H, 5.56; N, 5.78.

2-(4-Methoxy-4-oxobutyl)ellipticinium Bromide (VII). The above method with ellipticine (3.25 mmol) and methyl 5-bromopentanoate (18.2 mmol) gave VII (78%), mp 273–275 °C (from CHCl₃). Anal. Calcd for C₂₃H₂₅BrN₂O₂: C, 62.59; H, 5.71; N, 6.35. Found: C, 62.36; H, 5.51; N, 6.28.

2-(4-Hydrazino-4-oxobutyl)-9-methoxyellipticinium Bromide (VIII). A solution of 0.753 g (1.60 mmol) of VI in 80 mL of methanol was treated to the dropwise addition over 5 min of 4.5 mL of hydrazine hydrate (Scheme IV). The mixture was then stirred at room temperature for 48 h, concentrated to 15 mL, diluted with 60 mL of anhydrous benzene, and evaporated repeatedly (3×) in vacuo to 20 mL to remove residual water. The solid was taken up in a minimum volume of anhydrous methanol, the solution was chilled in ice, and ethyl ether was added dropwise to induce crystallization of 0.635 g (84%) of salt VIII: mp 174–177 °C; ¹H NMR (DMSO-d₆) δ 1.7–2.3 (m, 6 H, (CH₂)₃), 2.75 (s, 3 H, CH₃), 3.20 (s, 3 H, CH₃), 3.38 (br s, 2 H, NH₂), 3.91 (s, 3 H, CH₃O), 4.72 (br t, 2 H, CH₂N⁺), 7.2–8.6 (m, 5 H, ArH), 9.25 (br s, 1 H, NH), 10.06 (s, 1 H, C-1 H), and 11.95 (br s, 1 H, NH). Anal. Calcd for C₂₃H₂₇BrN₄O₂·H₂O: C, 56.44; H, 5.97; N, 11.44. Found: C, 56.78; H, 5.62; N, 11.03.

2-(4-Hydrazino-4-oxobutyl)ellipticinium Bromide (IX). Following the method for the preparation of VIII, the title compound was prepared from 0.206 g (0.467 mmol) of VII and 4.5 mL of hydrazine hydrate, in 50 mL of methanol. The product (IX) was precipitated

Scheme V. Conjugation of Hydrazides to Polyaldehyde Dextran

R may be for example CI 921 or Ellipticine

Table I. Conjugation of Drug to Polyaldehyde Dextran

molar ratio (hydrazide/ CHO)	drug	solvent	loading (mol of hydrazide/ mol of glucose)
0.04/1	IX	H ₂ O (H ⁺) ^a	0.02 ^d
0.10/1	IX	EtOH-H ₂ O (1:1)/H ⁺ ^a	0.06 ^d
0.14/1	IX	PBS buffer (pH 7.4) ^a	0.02 ^d
0.14/1	VIII	NaCl solution (H ⁺) ^a	0.03 ^d
0.14/1	IX	H ₂ O (H ⁺) ^a	0.04 ^d
0.14/1	IX	EtOH-H ₂ O (1:1)/H ⁺ ^a	0.09 ^e
0.21/1	IX	H ₂ O (H ⁺) ^b	0.08 ^e
0.21/1	IX	H ₂ O (H ⁺) ^c	0.13 ^e
0.21/1	VIII	H ₂ O (H ⁺) ^c	0.09 ^e
0.28/1	IX	H ₂ O (H ⁺) ^b	0.094 ^e
0.42/1	IX	H ₂ O (H ⁺) ^a	insoluble (H ₂ O)
0.07/1	IV	H ₂ O (H ⁺) ^a	0.04 ^d
0.10/1	IV ^f	H ₂ O (H ⁺) ^a	0.05 ^d
0.12/1	IV ^f	H ₂ O (H ⁺) ^a	0.08 ^d
0.14/1	IV	H ₂ O (H ⁺) ^a	0.15 ^e

^a Separation by dialysis. ^b Separation by Bio-gel P-60. ^c Separation by ultrafiltration. ^d Dissolved in both water and 0.01 M phosphate buffer (pH 7.35). ^e Soluble in water but not in 0.01 M phosphate buffer (pH 7.35). ^f Hydrazide IV generated in situ by cleavage of carbazate III.

from methanol by the dropwise addition of ether: yield 0.164 g (80%) of a red-orange solid; mp 203–206 °C (from methanol). Anal. Calcd for C₂₂H₂₅BrN₄O: C, 59.87; H, 5.72. Found: C, 60.19; H, 6.20.

Methods. Polyaldehyde dextran with approximately 0.36 formyl functions per glucose unit was prepared as reported from 40 kDa dextran (22).

Hydrazide Conjugations to Polyaldehyde Dextran. PAD was dissolved in distilled water and incubated with the requisite hydrazide IV, VIII, or IX with continuous stirring at ambient temperature at pH 4 (or in one case at pH 7.4 in PBS buffer) for 48 h (Scheme V). Several solvent media were employed (see Table I). Conjugates were purified by techniques previously described for dextran-drug conjugates (14, 22) involving either exhaustive dialysis against water, purification on a Bio-Gel P-60 column, or membrane ultrafiltration. Fractions eluted from the Bio-Gel P-60 column were tested by the anthrone reagent for carbohydrate and by UV absorption at the appropriate λ_{max} for the respective drugs. The conjugate product fraction was taken as that which tested positive in both monitoring methods. The drug-PAD conjugate was then lyophilized for analysis and storage. The degree of substitution of the drug/repeating glucose unit was determined by the UV absorbances at 447 nm for IV and at 305 nm for VIII and IX.

Indirect Hydrazide Conjugation with CI-921 Carbazate on PAD. CI-921 hydrazide (IV) was unstable and difficult to obtain in a pure, high-yield form. Thus, a convenient method was developed in which its carbazate precursor (III) was deblocked and conjugated in one

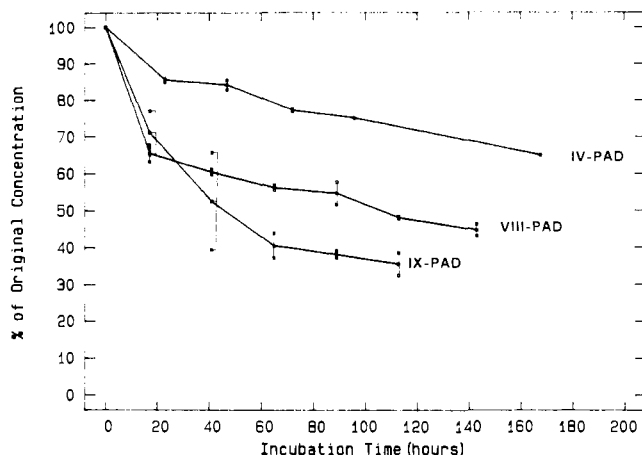


Figure 1. Hydrolyses of hydrazide conjugates to PAD (in PBS, pH 7.4, at 37 °C).

pot (see Table I). Carbazate hydrochloride III (20.0 mg, 0.033 mmol) was dissolved in 5 mL of 90% trifluoroacetic acid–10% water, stirred at ambient temperature for 20 min, and evaporated to dryness in vacuo. The residue was dissolved in 40 mL of distilled water, adjusted to pH 4, and added to 52.0 mg of PAD. The reaction was brought about by stirring/incubation at room temperature for 24 h and the conjugate was isolated by exhaustive dialysis against water (4 days, 2 changes of water/day) with subsequent lyophilization. The UV spectrum of the pure conjugate matched that of authentic CI-921 (16).

Hydrolytic and Enzymatic Cleavage of the PAD-Hydrazide Conjugates. The stability of the conjugates to hydrolysis in PBS (pH 7.4) was determined by incubating a selected hydrazide–PAD conjugate in PBS at 37 °C for the indicated times. Studies were performed on a IV–PAD conjugate with 0.07 drug/glucose unit, a VIII–PAD conjugate of 0.03 drug/glucose unit, and a IX–PAD conjugate of 0.04 drug/glucose unit at an effective concentration of 4 mg of conjugate in 10-mL fluid volume. The free-drug and dextran-bound-drug concentrations were determined by UV absorbance after separation in a centrifugal microconcentrator (molecular weight cutoff = 10 kDa) (Figure 1).

The stability of drug–PAD conjugates VIII and IX mentioned above to plasma enzymes was determined by incubating 5 mL of rat sera (freshly prepared and in one case 2-days old) and 10 mL of an aqueous solution (pH 7.4) of the requisite hydrazide–PAD conjugate containing 0.1% of sodium azide at 37 °C. Effective conjugate concentrations were 4 mg of each in 10 mL of fluid volume. One-milliliter aliquots were withdrawn at the indicated times, charged to a centrifuge tube, treated with 0.5 mL of a 10% solution of trichloroacetic acid, and spun. The supernatant from the resulting protein precipitation was transferred to a microconcentrator tube (molecular weight cutoff 10 kDa) and centrifuged. Free-drug and dextran-bound-drug concentrations were determined by UV analysis (Figure 2).

DISCUSSION

Ellipticine and its N-2-alkylated ellipticinium salts with wide structural variations on the isoquinoline ring have shown substantial activity against malignant cell lines from solid tumors in culture (18). Similar success has been reported with amsacrine species like CI-921 (19). Nevertheless the *in vivo* activity of both drug types has been marginal at best, occasioned at least in part by their

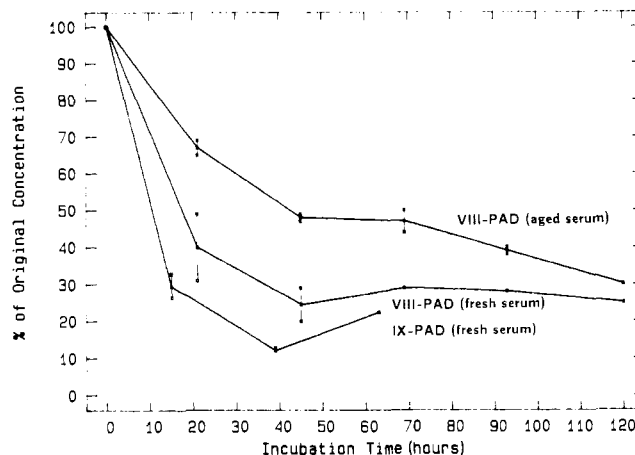


Figure 2. Enzymatic hydrolysis of hydrazide conjugates to PAD (in sera, pH 7.4, at 37 °C).

unfavorable biodistributions into solid tumors (20, 21). Coupling of ellipticine and CI-921 to polymeric or immunologically based carrier systems offers the prospect of improved tumor uptake.

While the syntheses of the ellipticinium hydrazides could be effected by directed hydrazinolysis of their corresponding esters, the synthesis of the CI-921 hydrazide in this fashion was impossible. Despite five attempts under varying reaction conditions, no clean, direct displacement of methyl ester V was capable of producing IV. Heating V with 0.5 M hydrazine hydrate in methanol for 24 h or even 4 h produced nearly total loss of starting material with concomitant conversion to a yellow solid displaying more than five spots on TLC. The reaction of CI-921 with 0.5 M hydrazine hydrate/methanol at reflux gave a similar mixture as did the reaction of CI-921 with *tert*-butyl carbazate and V with 0.5 M hydrazine standing at room temperature for 2 days. Refluxing V with 0.02 M hydrazine hydrate in methanol for 2 days or contact of V with 0.1 M hydrazine hydrate/methanol for 2 weeks at 4 °C resulted in total recovery of the starting material. Other related variations gave either complex mixtures or no evidence of reaction.

The successful approach to IV involved initial preparation of 5-methyl-9-chloroacridine-4-carbonyl chloride (I) and its condensation with an equimolar quantity of *tert*-butyl carbazate. This protected hydrazide II was reacted upon the C-9 position in a subsequent step with the pendant anilino moiety to give CI-921 carbazate III and the latter was deprotected to the target IV.

PAD was prepared by the periodate oxidation of dextran (22). We have observed, however, that it is essential to completely purify the PAD employed for hydrazide linking of iodate or periodate contaminants. No dextran hydrazones were formed when oxidizing impurities were present and model studies on the coupling of phenylacetylhydrazide to PAD contaminated by residual oxidant gave 1,2-bis(phenylacetyl)hydrazine, an observation supported by previous studies (16). Dimers were avoided if PAD was freed of iodate by exhaustive dialysis or by anion exchange.

Hydrazide conjugation load or degree of substitution upon the PAD was sensitive to the reactant ratios, expressed as moles of hydrazide employed per formyl equivalent on the PAD, as well as to solvent system and the purification method utilized. Membrane ultrafiltration, the most rapid purification technique studied, appears to yield a PAD with the highest loading. Ethanol–water reaction solvent at pH 4 was superior to water at pH 4,

while the higher pH of PBS detracted from loading efficiency. CI-921 hydrazide (IV) conjugated more efficiently than either ellipticine hydrazide and, in fact, the variation in which IV was produced in situ from III in the PAD-containing medium proved even more efficient and facile. The drug-PAD conjugates were readily soluble in both water and PBS (pH 7.35) but above a loading ratio of 0.08 mol of hydrazide/mol of glucose units the conjugates lost solubility in buffer. Attempts to produce the highest drug load from a 0.42/1 molar ratio of the reactants gave a conjugate which lost both water and buffer solubility. The degree of drug substitution could not be measured.

All conjugates demonstrated considerable resistance to hydrolysis in PBS and, in fact, the PAD conjugate of CI-921 hydrazide (IV) was the most resistant. 9-Methoxyellipticinium hydrazide VIII was 50% released by 100 h of incubation while CI-921 hydrazide (IV) was only 25% released. Under hydrolytic and enzymatic cleavage conditions there was a biphasic loss of drug from the conjugates. For example, VIII and IX (Figure 1) are first released with an initial half-life of ca. 1 day with a subsequent slower release half-life of ca. 15 days. Release of IV is slower and decidedly less biphasic. Similar biphasic scission rates are seen in the enzymatic cleavages (Figure 2), where the contrast between the more active enzymes in freshly drawn mouse sera and that allowed to stand for 48 h is evident.

An explanation for these biphasic rates may rest in the original structure of PAD which, by virtue of the lack of selectivity in the periodate oxidation which generates it from dextran, can have any paired combination of hydroxyls at carbons 2, 3, or 4 converted to formyl functions. Furthermore, there is no reason to expect the condensation of the hydrazide to take place upon any one of these CHO's specifically. It is therefore probable that hydrolytic and enzymic cleavage kinetics represent a complex function of loss from multiple sites of widely varying steric accessibility (23). It is interesting to note that this behavior is observed in the two hydrazide conjugates of the agents with extended pentamethylene side chains, i.e., VIII and IX, and virtually absent in the conjugate of IV. Clearly the hydrazide in IV at carbon 4 of an acridine, peri to a methyl at carbon 5, is a much more hindered function which may show greater selectivity in which formyl moiety on the PAD it initially attacks. This increased steric hindrance may be manifest in a slower and nearly monophasic cleavage of IV-PAD conjugates.

CONCLUSIONS

Hydrazides derived from the antineoplastic pharmaceuticals ellipticine and CI-921 form stable, soluble conjugates with formyl functions on polyaldehyde dextran. One can regulate the degree of substitution of the pharmaceutical on the biopolymer by control of the reaction ratios in the conjugation medium. Similarly, the specific choice of pharmaceutical can alter the release kinetics in vitro and in vivo, with the more hindered acridine-derived pharmaceutical showing the greater hydrolytic stability. Dextran conjugates of these agents and other closely related structures are under study, linked to tumor-associated monoclonal antibodies, for therapeutic drug targeting.

ACKNOWLEDGMENT

The Quaker Chemical Foundation provided fellowships to B.S. and H.Z. This work has been supported by

grants from the W. W. Smith Charitable Trust and the Brady Cancer Research Fund.

LITERATURE CITED

- (1) Ram, B. P. and Tyle, P. (1987) Immunoconjugates: applications in targeted drug delivery for cancer therapy. *Pharm. Res.* **4**, 181-188.
- (2) Kanellos, J., Pietersz, G. A., Cunningham, Z., and McKenzie, I. F. (1987) Anti-tumor activity of aminopterin-mono-clonal antibody conjugates. *Immunol. Cell Biol.* **65**, 483-493.
- (3) Borlinghaus, K. P., Fitzpatrick, D. A., Heindel, N. D., Mattis, J. A., Mease, B. A., Schray, K. J., Shealy, D. J., Walton, H. L., Jr., and Woo, D. V. (1987) Radiosensitizer conjugation to CA 19-9 monoclonal antibody. *Cancer Res.* **47**, 4071-4075.
- (4) Bumol, T. F., Baker, A. L., Andrews, E. L., DeHerdt, S. V., Briggs, S. L., Spearman, M. E., and Apelgren, L. D. (1988) KS1/4-DAVLB, A Monoclonal Antibody-Vinca Alkaloid Conjugate for Site-Directed Therapy of Epithelial Malignancies. *Antibody-Mediated Delivery Systems* (J. D. Rodwell, Ed.) pp 55-59, Dekker, New York.
- (5) Reisfeld, R. A. and Cheresch, D. A. (1985) Human tumor-associated antigens as targets for monoclonal antibody-mediated cancer therapy. *Cancer Surv.* **4**, 271-280.
- (6) Heindel, N. D. and Van Dort, M. (1985) Prosthetic group radioiodination at "no carrier added" level of carbonyl containing molecules. *J. Org. Chem.* **50**, 1988-1990.
- (7) Wilchek, M. and Bayer, E. A. (1987) Labeling glycoconjugates with hydrazide reagents. *Methods Enzymol.* **138**, 429.
- (8) O'Shannessy, D. J. (1988) Hydrazides as specific reagents for the labeling of glycoproteins. *ISBT Commun.* **3**, 4-6.
- (9) Bumol, T. F., Laguzza, B. C., DeHerdt, S. V., Andrews, E. L., Baker, A. L., Marder, P., Nichols, C. L., and Apelgren, L. D. (1987) Preclinical studies with DAVLB-hydrazide for site-directed therapy of human melanoma. (1987) *Second International Conference on Monoclonal Antibody Immunoconjugates for Cancer* (San Diego, CA) p 38, University of California—San Diego, San Diego, CA.
- (10) Trouet, A., Dejonghe, J. P., Collard, M. P., and Bhus-hana, R. K. (1987) Preparation of alkylvinblastines as anti-tumor agents. *Eur. Pat. Appl. EP 233,101*. [(1988) *Chem. Abstr.* **107**, 237105d].
- (11) Johnson, D. A. and Laguzza, B. C. (1987) Antitumor xenograft activity with a conjugate of a vinca derivative and the squamous carcinoma-reactive monoclonal antibody PF1/D. *Cancer Res.* **47**, 3118-3122.
- (12) Heindel, N. D. and Van Dort, M. (1985) Indirect iodinations with oxadiazoles precursors of hydrazides. *Org. Prep. Proc. Int.* **17**, 230-235.
- (13) Heindel, N. D., Zhao, H., Miller, M. R., Lautenslager, G. T., Nau, E. A., Burton, J. L., and Abel, J. H. (1988) Synthesis and conjugation of ellipticines for tumor cell targeting. *Pharm. Res.* **5**, S-63.
- (14) Takakura, Y., Takagi, A., Hashida, M., and Sezaki, H. (1987) Disposition and tumor localization of mitomycin C-dextran conjugates in mice. *Pharm. Res.* **4**, 293-300.
- (15) Hurwitz, E., Kashi, R., Arnon, R., Wilchek, M., and Sela, M. (1985) The covalent linking of two nucleotide analogs to antibodies. *J. Med. Chem.* **28**, 137-140.
- (16) Qureshi, S. Z. and Hasan, T. (1987) Detection and Spectrophotometric determination of anthranilohydrazide using periodic acid. *Acta Pharm. Jugosl.* **37**, 223-225.
- (17) Sample was a gift from Parke-Davis Co., Ann Arbor, MI.
- (18) Kansal, V. K. and Potier, P. (1986) The biogenetic, synthetic and biochemical aspects of ellipticine. *Tetrahedron* **42**, 2389-2408.
- (19) Denny, W. A., Atwell, G. J., and Baguley, B. C. (1984) Potential antitumor agents. 40. Orally active 4,5-disubstituted derivatives of amsacrine. *J. Med. Chem.* **27**, 363-367.
- (20) McNally, W., Whitfield, L., and Chang, T. (1987) Biodistribution of a radiolabeled amsacrine analog. *Proc. Annu. Meet. Am. Assoc. Cancer Res.* **28**, 434.
- (21) Heindel, N. D., Emrich, J. G., Woo, D. V., Garnes, K., Landvatter, S. W., Wilson, A. A., and Burns, H. D. (1986)

Syntheses and melanoma avidities of I-125 derivatives of ellipticine and *m*-Amsa. *J. Nucl. Med.* **27**, 1076.

- (22) Bernstein, A., Hurwitz, E., Maron, R., Arnon, R., Sela, M., and Wilchek, M. (1978) Higher antitumor efficacy of daunomycin linked to dextran. *J. Natl. Cancer Inst.* **60**, 379-383.
- (23) A reviewer has suggested another plausible explanation for the biphasic cleavage rates. An Amadori rearrangement, occurring during the syntheses of the hydrazide conjugates, might generate ketone hydrazones or other rearranged product(s) with different hydrolysis kinetics.

Registry No. I, 124536-15-8; II, 124536-16-9; III, 124536-17-0; IV, 124536-18-1; V, 124536-19-2; VI, 124536-20-5; VII, 124536-21-6; VIII, 124536-22-7; IX, 124536-23-8; *tert*-butyl carbazate, 870-46-2; *N*-(4-amino-3-methoxyphenyl)methanesulfonamide, 57165-06-7; 5-methyl-9-oxoacridan-4-carboxylic acid, 24782-66-9; 9-methoxyellipticine, 10371-86-5; ellipticine, 519-23-3; methyl 5-bromopentanoate, 5454-83-1; hydrazine, 302-01-2; 2,3-dialdehydodextran, 37317-99-0; IV dextran dialdehyde derivative, 124820-50-4; VIII dextran dialdehyde derivative, 124820-49-1; IX dextran dialdehyde derivative, 124820-48-0.

Photo-Cross-Linking of Psoralen-Derivatized Oligonucleoside Methylphosphonates to Single-Stranded DNA

Purshotam Bhan and Paul S. Miller*

Department of Biochemistry, School of Hygiene and Public Health, The Johns Hopkins University, 615 N. Wolfe St., Baltimore, Maryland 21205. Received August 21, 1989

The preparation of oligodeoxyribonucleoside methylphosphonates derivatized with 3-[(2-aminoethyl)carbamoyl]psoralen [(ae)CP] is described. These derivatized oligomers are capable of cross-linking with single-stranded DNA via formation of a photoadduct between the furan side of the psoralen ring and a thymidine of the target DNA when the oligomer-target duplex is irradiated with 365-nm light. The photoreactions of (ae)CP-derivatized methylphosphonate oligomers with single-stranded DNA targets in which the position of the psoralen-linking site is varied are characterized and compared to results obtained with oligomers derivatized with 4'-[[N-(aminoethyl)amino]methyl]-4,5',8-trimethylpsoralen [(ae)AMT]. It appears that the psoralen ring can stack on the terminal base pair formed between the oligomer and its target DNA or can intercalate between the last two base pairs of the oligomer-target duplex. Oligomers derivatized with (ae)CP cross-link efficiently to a thymidine located in the last base pair (n position) or 3' to the last base pair ($n + 1$ position) of the target, whereas the (ae)AMT-derivatized oligomers cross-link most efficiently to a thymidine located in the $n + 1$ position. The results show that both the extent and kinetics of cross-linking are influenced by the location of the psoralen-linking site in the oligomer-target duplex.

Psoralens, a class of naturally occurring photoreactive furocoumarins found in a variety of plants, were used as medicinal agents by the ancient Egyptians to treat the skin disorder vitiligo (1). In more recent times, these compounds have been used clinically in the treatment of a number of skin diseases including psoriasis (1) and cutaneous T-cell lymphoma (2).

Psoralens are planar molecules which are able to intercalate into double-stranded regions of DNA and RNA. Upon irradiation with long-wavelength ultraviolet light, the 3,4 and 4',5' double bonds of the pyrone or furan ring, respectively, can undergo 2+2 cycloadditions with the 5,6 double bond of pyrimidine nucleosides to form cyclobutane type monoadducts (3). If the psoralen has intercalated into a suitable site, the furan-side monoadducts can undergo a further cycloaddition reaction to form a cross-link between the two strands of the double-stranded nucleic acid. Thus psoralens have been found to be useful in mapping the secondary structure of large RNA molecules (4).

Psoralens, such as 8-methoxypsoralen, show a preference for cross-linking with -TpA- sequences in double-stranded DNA (5); however, their ability to specifically recognize long, unique nucleic acid sequences is limited. When conjugated to oligonucleotides or oligonucleotide analogues, either by attachment through linker arms or

by monoadduct formation with thymine bases of the oligomer, the psoralens can be targeted to specific sites in the nucleic acid (6-10). We have used this approach to prepare oligonucleoside methylphosphonates which are capable of cross-linking to complementary sequences on single-stranded DNA and RNA in a sequence-specific manner (11-13). The oligomer is conjugated through its 5'-phosphoryl group with 4'-[[N-(aminoethyl)amino]methyl]-4,5',8-trimethylpsoralen [(ae)AMT],¹ which, upon irradiation at 365 nm, forms a cyclobutane adduct between the pyrone ring of the (ae)AMT and a thymine or a cytosine base of the targeted nucleic acid.

The oligonucleoside methylphosphonates themselves are nuclease-resistant oligonucleotide analogues which are

¹ Abbreviations used: (ae)AMT, 4'-[[N-(2-aminoethyl)amino]methyl]-4,5',8-trimethylpsoralen; (ae)CP, 3-[(2-aminoethyl)carbamoyl]psoralen; 3-CP, 3-carboxypsoralen; CDI, 1-ethyl-3-[3-(dimethylamino)propyl]carbodiimide; DEAE, diethylaminoethyl; EDA, ethylenediamine; EDTA, ethylenediaminetetraacetic acid; PAGE, polyacrylamide gel electrophoresis; Tris-HCl, tris(hydroxymethyl)aminomethane hydrochloride; TLC, thin-layer chromatography; HPLC, high-performance liquid chromatography; TBE, 0.089 M Tris-borate, 0.002 M EDTA (pH 8.0); TEAB, triethylammonium bicarbonate buffer, CPG, control pore glass.

capable of entering mammalian cells intact and binding to complementary nucleic acid sequences (14, 15). It appears that psoralen-derivatized oligonucleoside methylphosphonates would be useful sequence-specific antisense reagents to study gene expression in cell culture. In addition, such oligomers could be used to study the mechanism of action of the antisense oligomers and to determine if the oligomers bind exclusively to their targeted nucleic acids within the cells.

In this paper we describe the synthesis and photoreactions of novel 3-[(2-aminoethyl)carbamoyl]psoralen [(ae)CP] derivatized oligonucleoside methylphosphonates. In contrast to (ae)AMT, the (ae)CP derivatives react via formation of furan-side photoadducts. The interactions of these oligomers with single-stranded DNA targets in which the position of the psoralen cross-linking site is varied are characterized and compared to results obtained with (ae)AMT-derivatized oligomers.

EXPERIMENTAL PROCEDURES

γ -[32 P]ATP was purchased from Amersham Inc. and T4 polynucleotide kinase was purchased from United States Biochemical Corp. Reagents for the synthesis of oligodeoxyribonucleotide methylphosphonates and oligodeoxyribonucleotides were purchased from American Bionetics Inc. 1-Ethyl-3-[3-(dimethylamino)propyl]carbodiimide (CDI) was obtained from Sigma Chemicals and 4,5',8-trimethylpsoralen was purchased from Aldrich Chemicals. SEP-PAK C-18 reversed-phase cartridges were obtained from Waters Associates. Wherever necessary, reactions were monitored by TLC on precoated thin layer (0.25 mm) silica gel 60 F-254 plates purchased from EM Reagents. Polyacrylamide gel electrophoresis was carried out on 20 cm \times 20 cm \times 0.75 mm gels containing 0.089 M Tris, 0.089 M boric acid, 0.2 mM EDTA, and 7 M urea (16). The gels were autoradiographed at -80°C and the film was scanned on a LKB Ultrosan XL Densitometer. Analytical and preparative HPLC was carried out on a Varian 5000 LC instrument at 254-nm detection with a Whatman Partisil ODS3-RAC II reversed-phase column. The column was eluted for 20 min with a linear gradient of 1%–50% acetonitrile in 0.1 M sodium phosphate buffer (pH 5.8) at a flow rate of 1.5 mL/min. All the reactions involving psoralens were performed in subdued light.

Synthesis of Oligodeoxyribonucleotides. Oligodeoxyribonucleotides were synthesized on CPG supports using β -cyanoethyl phosphoramidite chemistry (17). After the cleavage from the support and deprotection, the crude oligonucleotides were phosphorylated with [32 P]ATP and T4 polynucleotide kinase (18). The oligomers were next purified by polyacrylamide gel electrophoresis, extracted with 1 M TEAB, and desalted on a SEP-PAK cartridge (19). These purified 32 P-labeled phosphodiester targets were used for cross-linking experiments (vide infra).

Synthesis of Oligodeoxyribonucleoside Methylphosphonates. The methylphosphonate oligomers were synthesized on CPG supports with 5'-(dimethoxytrityl)nucleoside 3'-[(*N,N*-diisopropylamino)methyl]phosphoramidite monomers (20). The oligomers were deprotected, purified, and phosphorylated as previously described (18, 21).

Synthesis of 3-Carboxypsoralen. 3-Carboxypsoralen was synthesized from 2-hydroxy-4-methoxybenzaldehyde in eight steps according to the procedure of Worden et al. (22) and was obtained in 14% overall yield as a yellow powder: mp 258–261 $^\circ\text{C}$; 300-MHz ^1H NMR (CDCl_3) 6.95 (d, $J = 2.4$ Hz, 4'-H), 7.63 (s, 5-H), 7.80 (d, $J = 2.4$ Hz, 5'-H), 7.98 (s, 8-H), 9.05 ppm (s, 4-H).

Synthesis of 4'-[[*N*-(2-Aminoethyl)amino]methyl]-4,5',8-trimethylpsoralen Derivatives of Oligodeoxyribonucleoside Methylphosphonates. 4,5',8-Trimethylpsoralen was aminomethylated at the 4'-position (23) and was then converted to (ae)AMT as described by Lee et al. (11). The 5'-phosphorylated methylphosphonate oligomer (20 OD) was dissolved in 346 μL of 0.1 M imidazole buffer (pH 6.0). A solution of 1 M CDI (39 μL) was added and the reaction mixture was incubated at room temperature for 4 h. The mixture was diluted to 5 mL with 25 mM TEAB (pH 9.0) and purified with a SEP-PAK C-18 cartridge. The SEP-PAK was washed with 20 mL of 25 mM TEAB (pH 9.0) and the product was eluted with 50% acetonitrile in 100 mM TEAB (pH 9.0). The buffer was removed by evaporation at 37°C and the residue was lyophilized from water. The resulting 5'-imidazolide adduct was dissolved in 408 μL of 0.75 M lutidine hydrochloride buffer (pH 7.5) and a solution containing 51 μL of acetonitrile and 102 μL of 0.05 M (ae)AMT was added. The reaction was incubated at 37°C for 48 h and after dilution with 5 mL of 50% aqueous acetonitrile was chromatographed on DEAE-cellulose. The column was first washed with 50% acetonitrile (15 mL) and the product was eluted with 50% acetonitrile in 330 mM TEAB buffer. The product was further purified by preparative HPLC on a ODS 3-RAC II (4.5 mm \times 100 mm) column and was obtained in a 58% overall yield.

Synthesis of 3-Carboxypsoralen-Derivatized Oligodeoxyribonucleoside Methylphosphonates. The 5'-imidazolide adduct of the methylphosphonate oligomer (vide supra) was first converted to its 5'-aminoethyl amidate derivative (24). Typically, the 5'-imidazolide (10 OD) was dissolved in 160 μL of 0.75 M lutidine hydrochloride buffer and 70 μL of 1 M EDA in 0.4 M lutidine hydrochloride buffer (pH 7.5) was added. The reaction mixture was incubated at room temperature for 20 h, diluted to 5 mL with 25 mM TEAB, and loaded onto a SEP-PAK cartridge. The column was washed with 10 mL of 25 mM TEAB and the derivatized oligomer was eluted with 50% acetonitrile in 100 mM TEAB. Evaporation followed by lyophilization from water gave the 5'-aminoethyl amidate of the methylphosphonate oligomer. This adduct was dissolved in a mixture of 200 μL of 0.4 M lutidine hydrochloride buffer (pH 7.5) and 100 μL of acetonitrile. A solution containing 2 M CDI and 0.13 M 3-carboxypsoralen in 300 μL of 0.4 M lutidine hydrochloride was added and reaction was incubated at room temperature for 24 h. The mixture was diluted with 5 mL of 25 mM TEAB and applied to a SEP-PAK. The cartridge was washed with 10 mL of 25 mM TEAB and two 10-mL portions of 5% acetonitrile in 25 mM TEAB. The psoralen-derivatized oligomer was eluted with 3 mL of 50% acetonitrile in 100 mM TEAB and lyophilized. Final purification was done by polyacrylamide gel electrophoresis. The residue was dissolved in 10 μL of gel loading buffer which contained 80% formamide and 0.2% each of bromophenol blue and xylene cyanol in TBE buffer. The mixture was electrophoresed on a 15% polyacrylamide slab gel. The yellow area of the gel corresponding to the adduct was excised, crushed, and extracted with 1 M TEAB (5 \times 1 mL) at room temperature. The extract was diluted to 20 mL with water and passed through a SEP-PAK cartridge. The cartridge was washed with two 10-mL portions of 25 mM TEAB; the product was eluted with 50% acetonitrile in 100 mM TEAB and lyophilized from water.

Cross-Linking of Psoralen-Derivatized Oligodeoxyribonucleoside Methylphosphonates with Oli-

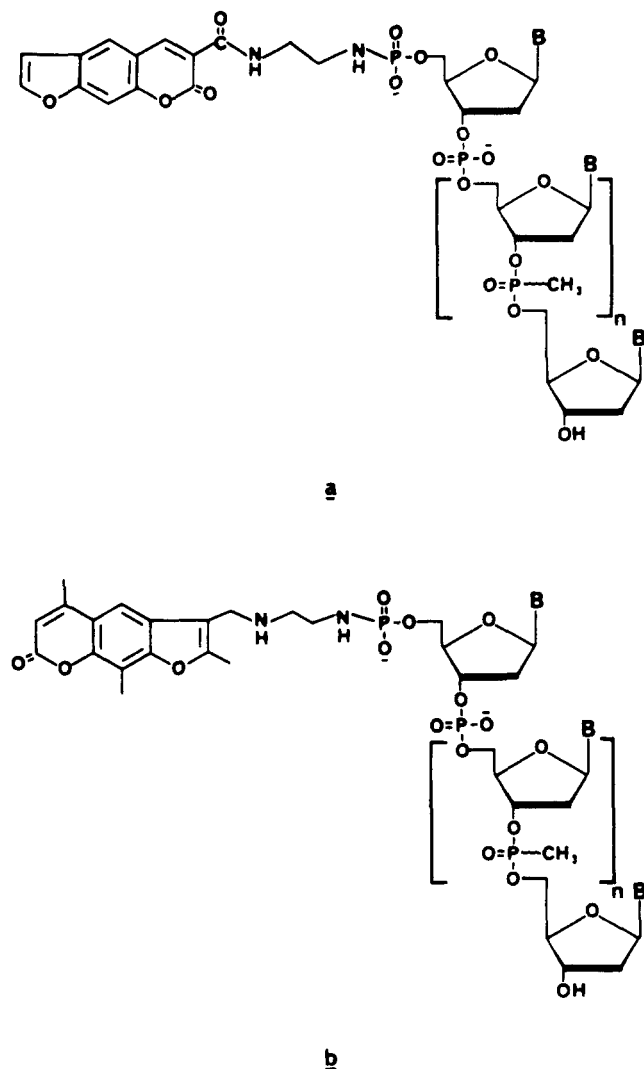


Figure 1. Structures of oligonucleoside methylphosphonates derivatized with (a) 3-[(2-aminoethyl)carbamoyl]psoralen or (b) 4'-[[N-(aminoethyl)amino]methyl]-4,5',8-trimethylpsoralen.

godeoxyribonucleotide Targets. A solution of $0.1 \mu\text{M}$ ^{32}P -labeled 21-mer target DNA and $10 \mu\text{M}$ of the psoralen-derivatized oligonucleoside methylphosphonate in $10 \mu\text{L}$ of water was preincubated in a borosilicate glass tube (Corning) at 4°C for 10 min. The solution was then irradiated at 365 nm for 0–30 min at an intensity of $0.83 \text{ J cm}^{-2} \text{ min}^{-1}$ in a thermostated water bath using an Ultra-Violet Products Inc. long-wavelength ultraviolet lamp. The reaction mixture was lyophilized; the residue dissolved in loading buffer and electrophoresed on a 15% acrylamide gel containing 7 M urea. The wet gel was autoradiographed. The extent of cross-linking was determined by scanning densitometry of the autoradiogram.

RESULTS

Psoralen-Derivatized Oligonucleoside Methylphosphonates and Their Oligodeoxyribonucleotide Targets. The structures of the psoralen-derivatized oligodeoxyribonucleoside methylphosphonates are shown in Figure 1. The oligomers are derivatized with either 3-carbamoylpsoralen (Figure 1a) or (aminomethyl)-trimethylpsoralen (Figure 1b) through ethylphosphoramidate linker arms. The first internucleotide bond at the 5' end of the oligomer is a phosphodiester linkage whereas the remaining internucleotide bonds are methylphosphonate linkages. Each methylphosphonate linkage can occur

in either the R_p or S_p configuration and thus each oligomer consists of 2^n diastereoisomers, where n is the number of methylphosphonate linkages. Previous experiments with (ae)AMT-derivatized methylphosphonates of the type shown in Figure 1b demonstrated that the methylphosphonate and phosphoramidate linkages are totally resistant to hydrolysis by endonucleases and by nucleases found in fetal bovine serum. The phosphodiester linkage is also quite resistant to endonuclease hydrolysis and has a half-life of approximately 48 h in serum-containing medium (12).

The single-stranded oligodeoxyribonucleotide targets and their complementary psoralen-derivatized methylphosphonate oligomers are shown at the bottom of Figure 2. The targets are 21 nucleotides in length and the psoralen-derivatized methylphosphonate oligomers are 9 nucleotides long. The binding site for the oligomer occupies positions 3–11 of the target. The position of the psoralen-linking site, which is a T residue in each target, varies for each of the targets. Thus the psoralen-linking site is located at $n + 1$ (nucleotide residue 12 of the target), n (nucleotide residue 11 of the target) or $n - 1$ (nucleotide residue 10 of the target), where n is defined as the position of the last base pair formed between the oligomer and the target.

The oligodeoxyribonucleotide targets were synthesized by using standard phosphoramidite chemistry on controlled pore glass supports and were end labeled with ^{32}P with polynucleotide kinase and $[^{32}\text{P}]\text{ATP}$. The methylphosphonate oligomers were synthesized on controlled pore glass supports using protected 5'-O-(dimethoxytrityl)nucleoside 3'-O-[(*N,N*-diisopropylamino)methyl]phosphonamidite synthons (20). After deprotection and purification (21), the oligomers were phosphorylated with polynucleotide kinase and ATP. The 5'-phosphorylated oligomers were converted to their imidazolidine derivatives by reaction with 1-ethyl-3-[3-(dimethylamino)propyl]carbodiimide in imidazole buffer at pH 6 (24). The imidazolidine, which was obtained in quantitative yield, was purified by reversed-phase chromatography on a SEP-PAK C-18 cartridge.

Oligomers derivatized with (ae)CP were prepared by first reacting the imidazolidine derivative of the 5'-phosphorylated oligomer with ethylenediamine in lutidine buffer at pH 7.5 (11). The resulting 5'-(aminoethyl)phosphoramidate oligomer was purified by reversed-phase chromatography and then reacted with 3-[(2-aminoethyl)carbamoyl]psoralen in the presence of 1-ethyl-3-[3-(dimethylamino)propyl]carbodiimide. The (ae)CP-oligomer was purified by preparative gel electrophoresis and was obtained in 25% overall yield.

Oligomers derivatized with (ae)AMT were prepared by reaction of the 5'-imidazolidine derivative with 4'-[[*N*-(aminoethyl)amino]methyl]-4,5',8-trimethylpsoralen in lutidine buffer. The (ae)AMT-oligomers were then purified by DEAE-cellulose chromatography and by preparative HPLC on a C-18 reversed-phase column. The overall yield of the (ae)AMT-oligomer, based on the amount of starting oligonucleoside methylphosphonate, was approximately 50%.

Cross-Linking Experiments with Psoralen-Derivatized Methylphosphonate Oligomers. A solution containing $0.1 \mu\text{M}$ ^{32}P -labeled target and $10 \mu\text{M}$ psoralen-derivatized oligomer was irradiated at 365 nm and the reaction mixture was subjected to polyacrylamide gel electrophoresis under denaturing conditions. As shown in Figure 3, target DNA cross-linked with oligomer has a lower mobility on the gel than the non-cross-linked target. Further irradiation of the reaction mixture at 254

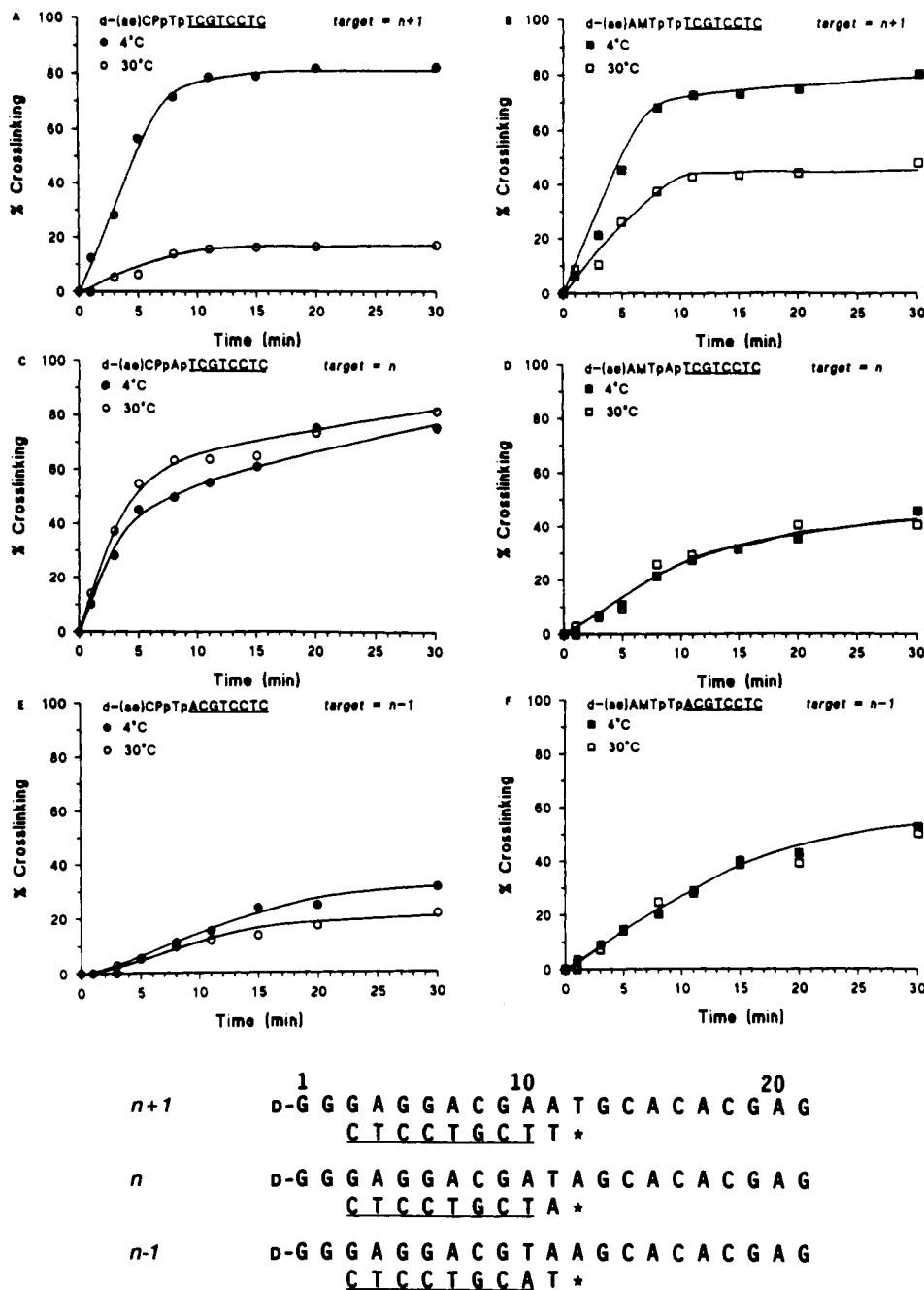


Figure 2. Kinetics of cross-linking of (ae)CP- or (ae)AMT-derivatized oligonucleoside methylphosphonates at 4 or 30 °C. The sequences of the oligomers and their single-stranded DNA targets are shown below the graphs. The asterisk represents the (ae)CP or (ae)AMT group.

nm results in disappearance of the cross-linked target and regeneration of the original target DNA (data not shown). The extent of cross-linking was determined from the autoradiogram by densitometry.

The kinetics of cross-linking at 4 °C and 30 °C were determined. Figure 2 shows the results when (ae)CP- or (ae)AMT-oligomers are irradiated with targets having the psoralen-linking site located at $n + 1$ (Figure 2A,B), n (Figure 2C,D), or $n - 1$ (Figure 2E,F). In the case of the $n + 1$ target, the cross-linking reaction is approximately linear over the first 10 min and does not increase beyond that point. The extent of cross-linking is the same at 4 °C for both the (ae)CP- and (ae)AMT-oligomers. At 30 °C the extent of cross-linking by d-(ae)AMTpTpTCGTCCTC is approximately 4-fold greater than that of d-(ae)CPpTpTCGTCCTC.

Unlike the $n + 1$ target, cross-linking with the n and $n - 1$ targets increases continuously over the 30-min observation period. In the case of the n target, cross-linking by (ae)CPpApTCGTCCTC is approximately 2.5-fold greater than that of (ae)AMTpApTCGTCCTC. The extent of cross-linking by each oligomer is essentially the same at both 4 and 30 °C. For the $n - 1$ target system, (ae)AMTpTpACGTCCTC cross-links about 1.5-fold more extensively than d-(ae)CPpTpACGTCCTC. Again the extent of cross-linking by both oligomers is essentially independent of the temperature of the cross-linking reaction.

DISCUSSION

Previous studies from our laboratory have shown that (ae)AMT-derivatized oligonucleoside methylphospho-

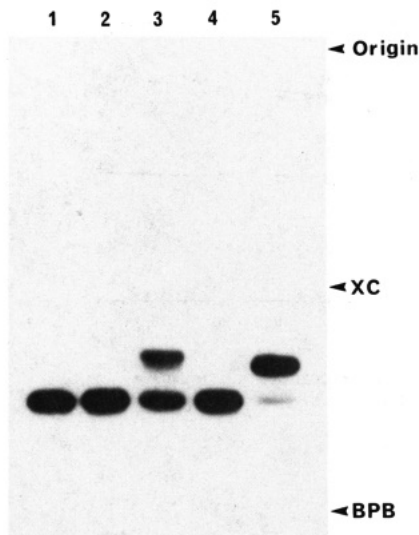


Figure 3. Cross-linking reactions between the n single-stranded DNA target and (ae)CPpApTCGTCCTC or (ae)AMT-pApTCGTCCTC after irradiation for 30 min at 30 °C: lane 1, 32 P-labeled target; lane 2, target plus (ae)AMT-oligomer not irradiated; lane 3, target plus (ae)AMT-oligomer irradiated for 30 min; lane 4, target plus (ae)CP-oligomer not irradiated; lane 5, target plus (ae)CP-oligomer irradiated for 30 min. The reaction mixtures were electrophoresed on a 15% polyacrylamide gel containing 7 M urea and the gel was autoradiographed. The top of the gel and the positions of the tracking dyes bromophenol blue (BPB) and xylene cyanol (XC) are indicated.

nates of the type shown in Figure 1b are capable of cross-linking with single-stranded DNA and RNA target nucleic acids. In this system cross-linking occurs via a photoinduced 2+2 cycloaddition reaction resulting in the formation of a cyclobutane adduct between the pyrone ring of the (ae)AMT group and a pyrimidine base of the target nucleic acid. Because the trimethylpsoralen moiety is tethered to the oligomer by the aminoethyl linker, furan side adduct formation with the target strand is not sterically feasible.

Studies on monoadduct formation between 4'-(hydroxyethyl)-4,5',8-trimethylpsoralen, 4,5',8-trimethylpsoralen, or 8-methoxypsoralen and double-stranded DNA have shown that adduct formation occurs mostly with the furan ring of the psoralen (25–27). Although theoretical calculations suggest that the pyrone double bond should be more reactive than the furan double bond (28), the preference for furan side adduct formation may result in part from unfavorable steric interactions between substituents at the 3- or 4-position of the pyrone ring and the 5-methyl group of thymine (26, 29). Thus it seemed possible that oligomers derivatized with a psoralen moiety restricted to forming furan monoadducts might be capable of efficiently forming cross-links with appropriate target nucleic acids. To test this possibility, we have prepared methylphosphonate oligomers derivatized with 3-carbamoylpsoralen (3-CP). The 3-CP group is linked via an aminoethyl linker arm to the 5' end of the oligomer through a phosphoramidate linkage as shown in Figure 1a.

Unlike 8-methoxypsoralen and the trimethylpsoralens, 3-carbethoxypsoralen forms only monoadducts with DNA (30). The furan-side adduct has the *cis-syn* configuration (31) which is the same configuration as the furan-side adducts formed by 8-methoxypsoralen (26). It appears that the 3-carbethoxy group sterically hinders formation of pyrone-side adducts. Thus 3-carbethoxypsoralen is not capable of forming inter-strand cross-links with DNA. Examination of computer-

generated molecular models, suggested that the aminoethyl linker arm should enable the furan ring of the psoralen moiety to form a *cis-syn* type cyclobutane adduct with suitably positioned pyrimidine nucleosides in the target strand.

The cross-linking studies were carried out with single-stranded 21-mer DNA targets. The site for adduct formation between the psoralen and the target, which we will call the psoralen-linking site, is a thymidine residue. Thymidine was chosen as the linking site because thymidine and uridine nucleosides show approximately 10–15-fold greater reactivity toward photoadduct formation with 8-methoxypsoralen, 3-carbethoxypsoralen, and oligomers derivatized with (ae)AMT than does cytosine (12, 31, 32).

In addition to examining the relative reactivities of pyrone versus furan adduct forming psoralen derivatives, we also wished to examine the effect of the position of the psoralen-linking site in the target on the kinetics and extent of cross-linking. Our previous studies with (ae)AMT-derivatized oligomers showed that the cross-linking reaction was mainly dependent upon the ability of the oligomer to bind to its complementary target sequence and upon the fidelity of the binding interaction (11–13). However, it also appeared that the location of the psoralen-linking site in the target and the sequence of the nucleotides surrounding the psoralen-linking site were important determinants of the extent of the cross-linking reaction.

In order to further investigate these possibilities, we have prepared the DNA target systems shown in Figure 2. In these systems, the psoralen-linking site is a T residue which is located at the $n + 1$, n , or $n - 1$ position of the target strand. Each oligomer should form equally stable duplexes with the target having five G–C base pairs and four A–T base pairs. Therefore any differences in the extent of cross-linking should reflect the change in the psoralen-linking site and not the stability of the oligomer–target duplex.

Cross-linking reactions were conveniently followed using polyacrylamide gel electrophoresis under denaturing conditions by observing the shift in mobility of the 32 P-labeled target DNA (see Figure 3). The rates and yields of cross-linking of the (ae)CP- and (ae)AMT-oligomers after 30 min of irradiation are summarized in Figure 2. Both (ae)CP- and (ae)AMT-oligomers undergo extensive photoadduct formation when bound to their complementary targets. The highest yields of cross-linking for both oligomers are observed to the $n + 1$ target at 4 °C. Thus for these two psoralens, photoadduct formation through the pyrone side or the furan side occurs with equal facility in this target system. Comparative studies with 8-methoxypsoralen, 5-methoxypsoralen, 5-methylisopsoralen, and 3-carbethoxypsoralen have shown that the extent of photoadduct formation is lowest for 3-carbethoxypsoralen (33). This low reactivity may result from the negligible association constant of the 3-carbethoxypsoralen with DNA and to the rapid photodegradation of the compound (31). It appears that these problems are overcome when 3-CP is attached to the oligomer. In this arrangement, formation of a duplex between the oligomer and its target brings the psoralen ring into close proximity with its binding site, thus enabling the psoralen to productively bind and react with a thymidine residue in the linking site.

Although the yield of photoadduct formation is high at 4 °C, it decreases dramatically for both oligomers when the temperature of the reaction is raised to 30 °C. The melting temperature of the duplex formed between d-



Figure 4. Schematic representation of the partial (upper) and full (lower) intercalation modes of the psoralen ring (represented by the rectangle) when psoralen-derivatized oligomers interact with their target DNAs.

TpTCGTCCTC and the target 21-mer is 33 °C at a total strand concentration of 2 μ M. A somewhat higher melting temperature would be expected for the oligomer-target duplex under conditions of the cross-linking experiments due to the higher concentration of the oligomer in the reaction mixtures. Thus this oligomer-target duplex would be expected to begin to melt at 30 °C. Examination of molecular models suggests that upon oligomer-target duplex formation, the psoralen ring can assume two different types of intercalated conformations as illustrated schematically in Figure 4. In order for cross-linking to occur when the psoralen linking site is in the $n + 1$ position, the psoralen ring must stack on the terminal base pair and intercalate between this base pair and the T residue at the $n + 1$ position. In this partial intercalation mode the alignment of the psoralen ring with the T residue would be expected to be sensitive to thermal perturbation and the effects of "end fraying" when the temperature of the duplex is raised. Under these conditions, the increased thermal motions imparted in the psoralen ring and the target would lead to reduced cross-linking at higher temperatures. The greater reduction in cross-linking for d-(ae)CPpTpTCGTCCTC versus d-(ae)AMTpTpTCGTCCTC may reflect the steric constraints imposed by the amide linkage on partial intercalation by the carbamoylpsoralen group.

In contrast to cross-linking at the $n + 1$ position, the rates and yields of cross-linking at the n and $n - 1$ positions are essentially the same at both 4 and 30 °C for both types of derivatized oligomers. The cross-linking reaction for both the n and $n - 1$ targets continues over the 30-min irradiation period. This behavior is in sharp contrast to that seen with the $n + 1$ target. In this case photoadduct formation increases linearly for the first 10 min of irradiation and then stops.

In the case of the n type target, cross-linking could occur when the psoralen is in either the partial-intercalation mode or in the full-intercalation mode, whereas cross-linking to the $n - 1$ target must occur via the full-intercalation mode. Duplexes formed when the psoralen is in the full-intercalation conformation would be expected to be less subject to thermal "end fraying" due to the added stability provided by the intercalated psoralen. The observation that cross-linking is not affected by increases in temperature for either the n and $n - 1$ target systems suggests that the psoralen cross-links when it is in the full-intercalation mode.

The greater extent of cross-linking by d-(ae)CPpApTCGTCCTC with the n target versus that of d-(ae)CPpTpACGTCCTC with the $n - 1$ target suggests that photoadduct formation occurs more readily to the 5'-face of the thymine in the n position than from the 3'-face of thymidine in the $n - 1$ position. This preference may result from restrictions on the conformational

flexibility of the intercalated psoralen ring imposed by the rigid carboxamide group of the linker arm of the (ae)CP-oligomers. It appears that such restrictions are less serious for the (ae)AMT-oligomers, which cross-link to the thymidine with equal efficiency in both the n and $n - 1$ targets. Such behavior is consistent with the expected greater flexibility of the aminoethyl linker arm of the (ae)AMT-oligomers. It is interesting to note that the psoralens when attached to the oligomers appear to show a preference for 3'-ApT binding sites in contrast to the behavior of free psoralens.

The extended kinetics of cross-linking observed for both the (ae)CP- and (ae)AMT-oligomers in the n and $n - 1$ targets is also consistent with the full-intercalation mode of psoralen binding. Free-psoralen derivatives undergo photodegradation in solution which leads to a loss of their ability to form photoadducts (5, 23, 31). It appears that psoralen is protected from such photodegradation when it is intercalated with nucleic acid bases (5, 23). The ability of the oligomers to continue to photocross-link with the n and $n - 1$ targets over a prolonged period of irradiation suggests that the psoralen rings of the oligomer are protected from photodegradation as a result of intercalation. On the other hand, partial intercalation of the psoralen ring results in less protection from photodegradation and thus the cross-linking reaction is over after 10 min of irradiation. Furthermore, the results suggest that psoralen-derivatized oligomers, once bound to their targets, do not exchange freely with unbound oligomer.

The results of our experiments show that both (ae)CP- and (ae)AMT-oligomers can cross-link efficiently with target single-strand DNA and that the extent of cross-linking can be controlled by selecting suitable psoralen-linking sites. In the case of (ae)CP-oligomers, efficient cross-linking occurs when the psoralen-linking site is located at either the n or $n + 1$ position of the target DNA. For (ae)AMT-oligomers the most efficient cross-linking occurs when the psoralen-linking site is located at the $n + 1$ position. Experiments are currently underway with single-stranded oligoribonucleotide targets in order to assess the parameters which affect cross-linking of psoralen-derivatized methylphosphonate oligomers to cellular RNAs. A better understanding of the factors which affect the interactions of photoreactive methylphosphonate oligomers with target nucleic acids are essential to designing antisense oligomers which can be used to study gene expression in mammalian cells.

ACKNOWLEDGMENT

This work was supported by grants from the National Institutes of Health (Grant GM 39127), the National Cancer Institute (Grant CA 42762), and the Department of Energy (Grant DE-FG02-88ER60636).

LITERATURE CITED

- Ben-Hur, E. (1984) The photochemistry and photobiology of furocoumarins (Psoralens). *Adv. Radiat. Biol.* 11, 132-171.
- Edelson, R., Berger, C., Gasparro, F., Jegasothy, B., Heald, P., Wintroub, B., Vonderheid, E., Knobler, R., Wolff, K., Plewig, G., McKiernan, G., Christiansen, I., Oseter, R. N. M., Honigsmann, H., Wilford, H., Kokoschka, E., Rehle, T., Perez, M., Stingl, G., and Laroche, L. (1987) Treatment of cutaneous T-cell lymphoma by extracorporeal photochemotherapy: Preliminary results. *N. Engl. J. Med.* 316, 297-303.
- Hearst, J. E. (1981) Psoralen photochemistry. *Annu. Rev. Biophys. Bioeng.* 10, 69-86.
- Cimino, G. D., Gamper, H. B., Isaacs, S. T., and Hearst, J. E. (1985) Psoralens as photoactive probes of nucleic acid struc-

- ture and function: Organic chemistry, photochemistry, and biochemistry. *Annu. Rev. Biochem.* **54**, 1151-1193.
- (5) Tessman, J. W., Isaacs, S. T., and Hearst, J. E. (1985) Photochemistry of the furan-side 8-methoxypsoralen-thymidine monoadduct inside the DNA helix. Conversion to diadduct and to pyrone-side monoadduct. *Biochemistry* **24**, 1669-1676.
 - (6) Houten, B. V., Gamper, H., Hearst, J. E., and Sancar, A. (1986) Construction of DNA substrates modified with psoralen at a unique site and study of the action mechanism of abc exonuclease on these uniformly modified substrates. *J. Biol. Chem.* **261**, 14135-14141.
 - (7) Houten, B. V., Gamper, H., Holbrook, S. R., Hearst, J. E., and Sancar, A. (1986) Action mechanism of ABC excision nuclease on a DNA substrate containing a psoralen crosslink at a defined position. *Proc. Natl. Acad. Sci. U.S.A.* **83**, 8077-8081.
 - (8) Cheng, A., Houten, B. V., Gamper, H. B., Sancar, A., and Hearst, J. E. (1988) Use of psoralen-modified oligonucleotides to trap three-stranded RecA-DNA Complexes and repair of these cross-linked complexes by ABC exonuclease. *J. Biol. Chem.* **263**, 15110-15117.
 - (9) Pieleles, U., and Englisch, U. (1989) Psoralen covalently linked to oligodeoxyribonucleotides: Synthesis, sequence specific recognition of DNA and Photo-cross-linking to pyrimidine residues of DNA. *Nucleic Acids Res.* **17**, 285-299.
 - (10) Teare, J., and Wollenzien, P. (1989) Specificity of the site directed psoralen addition to RNA. *Nucleic Acids Res.* **17**, 3359-3372.
 - (11) Lee, B. L., Murakami, A., Blake, K. R., Lin, S.-B., and Miller, P. S. (1988) Interaction of psoralen-derivatized oligodeoxyribonucleoside methylphosphonates with single-stranded DNA. *Biochemistry* **27**, 3197-3203.
 - (12) Kean, J. M., Murakami, A., Blake, K. R., Cushman, C. D., and Miller, P. S. (1988) Photochemical cross-linking of psoralen-derivatized oligonucleoside methylphosphonates to rabbit globin messenger RNA. *Biochemistry* **27**, 9113-9121.
 - (13) Lee, B. L., Blake, K. R., and Miller, P. S. (1988) Interaction of Psoralen-derivatized oligodeoxyribonucleoside methylphosphonates with synthetic DNA containing a promoter for T7 RNA polymerase. *Nucleic Acids Res.* **16**, 10681-10697.
 - (14) Miller, P. S. and Ts'o, P. O. P. (1988) Oligonucleotide inhibitors of gene expression in living cells: New opportunities in drug design. *Annu. Rep. Med. Chem.* **23**, 295-304.
 - (15) Miller, P. S. (1989) Nonionic Antisense Oligonucleotides. In *Oligonucleotides as Inhibitors of Gene Expression* (J. Cohen, Ed.) in press, The Macmillan Press Ltd, London.
 - (16) Maniatis, T., Fritsch, E. F., and Sambrook, J. (1982) *Molecular Cloning, A Laboratory Manual* pp 188-189, Cold Spring Harbor Laboratory: Cold Spring Harbor, NY.
 - (17) Sinha, N. D., Biernat, J., McManus, J., and Koster, H. (1984) Polymer support oligonucleotide synthesis XVIII: Use of β -cyano-ethyl-*N,N*-dialkylamino-/*N*-morpholino phosphoramidite of deoxynucleosides for the synthesis of DNA fragments simplifying deprotection and isolation of the final product. *Nucleic Acids Res.* **12**, 4539-4557.
 - (18) Murakami, A., Blake, K. R., and Miller, P. S. (1985) Characterization of sequence-specific oligodeoxyribonucleoside methylphosphonates and their interaction with rabbit globin mRNA. *Biochemistry* **24**, 4041-4046.
 - (19) Lo, K.-M., Jones, S. S., Hackett, N. R., and Khorana, H. G. (1984) Specific amino acid substitution in bacteriopsin: Replacement of a restriction fragment in the structural gene by synthetic DNA fragments containing altered codon. *Proc. Natl. Acad. Sci. U.S.A.* **81**, 2285-2289.
 - (20) Agrawal, S., and Goodchild, J. (1987) Oligodeoxynucleoside methylphosphonates: Synthesis and enzymic degradation. *Tetrahedron Lett.* **28**, 3539-3542.
 - (21) Miller, P. S., Reddy, M. P., Murakami, A., Blake, K. R., Lin, S.-B., and Agris, C. H. (1986) Solid-phase syntheses of oligodeoxyribonucleoside methylphosphonates. *Biochemistry* **25**, 5092-5097.
 - (22) Worden, L. R., Kaufman, K. D., Weis, J. A., and Schaff, T. K. (1969) Synthetic furocoumarins. IX. A new synthetic route to psoralen. *J. Org. Chem.* **34**, 2311-2313.
 - (23) Isaacs, S. T., Shen, C.-K. J., Hearst, J. E., and Rapoport, H. (1977) Synthesis and characterization of new psoralen derivatives with superior photoreactivity with DNA and RNA. *Biochemistry* **16**, 1058-1064.
 - (24) Chu, B. C. F. and Orgel, L. E. (1985) Nonenzymatic sequence-specific cleavage of single-stranded DNA. *Proc. Natl. Acad. Sci. U.S.A.* **82**, 963-967.
 - (25) Straub, K., Kanne, D., Hearst, J. E., and Rapoport, H. (1981) Isolation and characterization of pyrimidine-psoralen photoadducts from DNA. *J. Am. Chem. Soc.* **103**, 2347-2355.
 - (26) Kanne, D., Straub, K., Rapoport, H., and Hearst, J. E. (1982) Psoralen-deoxyribonucleic acid photoreaction. Characterization of the monoaddition products from 8-methoxypsoralen and 4,5',8-trimethylpsoralen. *Biochemistry* **21**, 861-871.
 - (27) Papadopoulos, D., Averbek, D., and Moustacchi, E. (1988) High levels of 4,5',8-trimethylpsoralen photoinduced furan-side monoadducts can block cross-link removal in normal human cells. *Photochem. Photobiol.* **47**, 321-326.
 - (28) Song, P.-S., Harter, M. L., Moore, T. A., and Herndon, W. C. (1971) Luminescence spectra and photocycloaddition of the excited coumarins to DNA bases. *Photochem. Photobiol.* **14**, 521-530.
 - (29) Kanne, D., Rapoport, H., and Hearst, J. E. (1984) 8-Methoxypsoralen-nucleic acid photoreaction. Effect of methyl substitution on pyrone vs furan photoaddition. *J. Med. Chem.* **27**, 531-534.
 - (30) Gaboriau, F., Vigny, P., Averbek, D., and Bisagni, E. (1981) Spectroscopic study of the dark interaction and of the photoreaction between a new monofunctional psoralen: 3-carbethoxy psoralen, and DNA. *Biochimie* **63**, 899-905.
 - (31) Moysan, A., Gaboriau, F., Vigny, P., Voituriez, L., and Cadet, J. (1986) Chemical structure of 3-carbethoxypsoralen-DNA photoadducts. *Biochimie* **68**, 787-795.
 - (32) Bachelier, J.-P., Thompson, J. F., Wegnez, M. R., and Hearst, J. E. (1981) Identification of the modified nucleotides produced by covalent photoaddition of hydroxymethyltrimethylpsoralen to RNA. *Nucleic Acids Res.* **9**, 2207-2222.
 - (33) Isaacs, S. T., Wieseahn, G., and Hallick, L. M. (1984) In vitro characterization of the reaction of four psoralen derivatives with DNA. *Natl. Cancer Inst. Monogr.* **66**, 21-30.

Registry No. $n + 1 \cdot (\text{ae})\text{CPpTpTCGTCCTC}$, 124242-47-3; $n \cdot (\text{ae})\text{CPpApTCGTCCTC}$, 124242-49-5; $n - 1 \cdot (\text{ae})\text{CPpTpACGTCCTC}$, 124266-25-7; $n + 1 \cdot (\text{ae})\text{AMTpTpTCGTCCTC}$, 124266-21-3; $n \cdot (\text{ae})\text{AMTpApTCGTCCTC}$, 124266-23-5; $n - 1 \cdot (\text{ae})\text{AMTpTpACGTCCTC}$, 124266-27-9.

Bioconjugate Chemistry

MARCH/APRIL, 1990
Volume 1, Number 2

© Copyright 1990 by the American Chemical Society

REVIEW

The Linkage of Cytotoxic Drugs to Monoclonal Antibodies for the Treatment of Cancer

Geoffrey A. Pietersz

Research Centre for Cancer and Transplantation, Department of Pathology, The University of Melbourne, Parkville, Victoria 3052, Australia. Received August 7, 1989

The search for selective chemotherapeutic agents for the eradication of infectious agents and cancer is of utmost importance. Most chemotherapeutic agents inhibit a critical metabolic pathway which is required for the target organism to survive (1, 2). In the case of bacterial infection, chemotherapeutic agents such as cephalosporins and antifolates interfere specifically with bacterial cell wall synthesis or bacterial dihydrofolate reductase (DHFR),¹ with little or no side effects to the host, while for some retroviruses, drugs acting on reverse transcriptase have been useful. A great challenge has been the search for a selective agent for the treatment of cancer where there are few differences between the biochemical pathways of cancer cells and normal cells (3). Indeed, most antineoplastic drugs inhibit metabolic pathways shared by both cancer and normal cell—the major differentiation being in the abnormal growth cycle of the cancer cell. Thus, rapidly proliferating cells in the hair follicles, bone marrow, and gastrointestinal tract are damaged by the antineoplastic agents. Several approaches have been used to produce antineoplastic agents with less side effects, such as design of analogues by chemical modification of

the parent drug (4), genetic engineering of antibiotic producing microorganisms (5), and production of prodrugs (6) which are activated in the target tissue. However, of the many hundreds of drugs tested for cancer (thousands at the National Cancer Institute) few have reached clinical usefulness—mainly because of nonspecific toxicity; i.e. they have a poor therapeutic index (7). Furthermore, many of the cytotoxic drugs currently in use are of little value in the commonest cancers, i.e. lung, colon, breast, and melanoma. There is clearly a major requirement for specific cytotoxic therapy which selectively kills tumor cells but spares normal cells. Can monoclonal antibodies convey such specificity to otherwise broadly cytotoxic drugs, and are such drug-antibody immunoconjugates the cancer treatment of the future?

With the discovery of tumor-associated antigens and their detection by monoclonal antibodies (MoAb), another approach for producing selective antineoplastic drugs could be used (8, 9). By covalently linking antineoplastic agents to MoAb reactive with tumor-associated antigens, these drugs can be targeted to the tumors (10). This concept was first suggested by Paul Ehrlich in the early 1900s (11). These drug-MoAb conjugates or immunoconjugates bind the tumor cells and are internalized and degraded in the lysosomes to release the drug or drug-peptide fragments which then act on the target—a particular enzyme, DNA, or RNA (12, 13). A number of tumor-associated antigens have now been identified and MoAbs have been produced for these (8, 9). Several drugs (10), toxins (14), radionuclides (15), immunomodulators (16, 17), and enzymes (18) have been attached to MoAbs, and their effects in vitro as well as in vivo in mice and humans have been studied. This review will concentrate on the various chemical methods utilized to produce drug-MoAb conjugates. No attempt will be made to describe the biological activity of the various conjugates.

¹ List of abbreviations: DHFR, dihydrofolate reductase; MoAb(s), monoclonal antibody(ies); MTX, methotrexate; CBL, chlorambucil; N-AcMEL, N-acetylmelphalan; Dm, daunomycin; Ad, adriamycin; CDI, carbodiimide; NHS, N-hydroxysuccinimide; Br-Dm, 14-bromodaunomycin; Br-Ida, 14-bromoidarubicin; CEA, carcinoembryonic antigen; HSA, human serum albumin; DTT, dithiothreitol; BSA, bovine serum albumin; SMPB, N-succinimidyl 4-(p-maleimidophenyl)butyrate; SPDP, N-succinimidyl 3-(2-pyridylthio)propionate; MBS, m-maleimido benzoic acid N-hydroxysuccinimide ester; Drug-COOH, drug containing a carboxyl group; MoAb-NH₂, amino group of monoclonal antibody; Drug-NH₂, drug containing an amino group; Dm-NH₂, daunomycin amino group; MEL, melphalan.

Table I. Commonly Used Chemical Transformations of Functional Groups of Drugs

functional group	reagent	new functional group	refs
OH	succinic anhydride	OCOCH ₂ CH ₂ COOH	23, 24
COOR ₁	hydrazine	CONHNH ₂	25, 26
COOH	CDI/NHS	active ester	27, 28
CH(OH)CH(OH)	periodate	aldehyde	29
CH(OH)CH(NH ₂)	periodate	aldehyde	30
NH ₂	SMPB	maleimide	31
	iodoacetic acid	COCH ₂ I	31
	active ester		
	succinic anhydride	NHCOCH ₂ CH ₂ COOH	32, 33
COCH ₃	bromine	COCH ₂ Br	34, 35

EARLY STUDIES ON IMMUNOCONJUGATES

The chemical methods used to couple cytotoxic drugs to MoAbs are similar to those used to couple small organic molecules to proteins such as bovine serum albumin for antibody production for immunoassay (19). In these cases vigorous reaction conditions could be used because no biological activity of the bovine serum albumin or hapten needed to be preserved. For immunoconjugate preparation mild conditions that do not denature the MoAb and interfere with the activity are essential. Some of the early work on immunoconjugate preparation was that of Mathe and colleagues in the mid-1950s, where methotrexate (MTX) was coupled to polyclonal rabbit antibodies raised against mouse leukaemia by diazotization of the MTX pterin amino group (20). Subsequently, in 1974 Davies' (21) group examined the conjugation of chlorambucil (CBL) to polyclonal antibodies and made the remarkable observation that noncovalently linked CBL was active in vitro and in vivo as a covalently linked drug! This aspect of drug-antibody, interaction should always be borne in mind—i.e. that drugs can associate noncovalently with antibodies and give the appearance of high activity and of many molecules of drug being bound to antibody in vitro. However, in vivo, such linkages are unstable, with the drugs transferring to other proteins and having potential toxic side effects. The main point, however, is that MoAbs carrying noncovalently bound drug may appear to be active in vitro but will not be in vivo, so attention has to be paid to the removal of non-conjugated drug. In these early studies the exact nature of the bonds between drug and antibody was not clear and sufficient quality control on conjugates was not apparent. In more recent studies sophisticated methods have been used to prepare drug-monoclonal antibody conjugates. Coupling agents such as glutaraldehyde and carbodiimides are still being used although with caution due to the difficulty of reproducing these couplings in other laboratories.

STRUCTURAL CONSIDERATIONS AND FUNCTIONAL GROUPS OF CYTOTOXIC DRUGS

Most cytotoxic agents are natural products or are produced by chemical synthesis, and from the biological activity of many analogues that have been produced, functional groups important for drug activity can be identified (22). However, such drugs will not always have appropriate functional groups for coupling to MoAbs, and the groups available may need to be transformed into more suitable functional groups by chemical modification (Table I). For example, hydroxy groups may be easily transformed to carboxyl groups by succinylation or carboxylic ester groups transformed to hydrazides with hydrazine. However, modification of the groups essential for biological activity on the drug before or during

Table II. Chemical Modification of Functional Groups of MoAb

group	reagent	new group	ref
NH ₂	SPDP	activated disulfide	37
	MBS	maleimide	38
	iminothiolane	SH	39
	iodoacetic acid	COCH ₂ I	40
SS	active ester		
	DTT	SH	41
	periodate	CHO	42
carbohydrate			

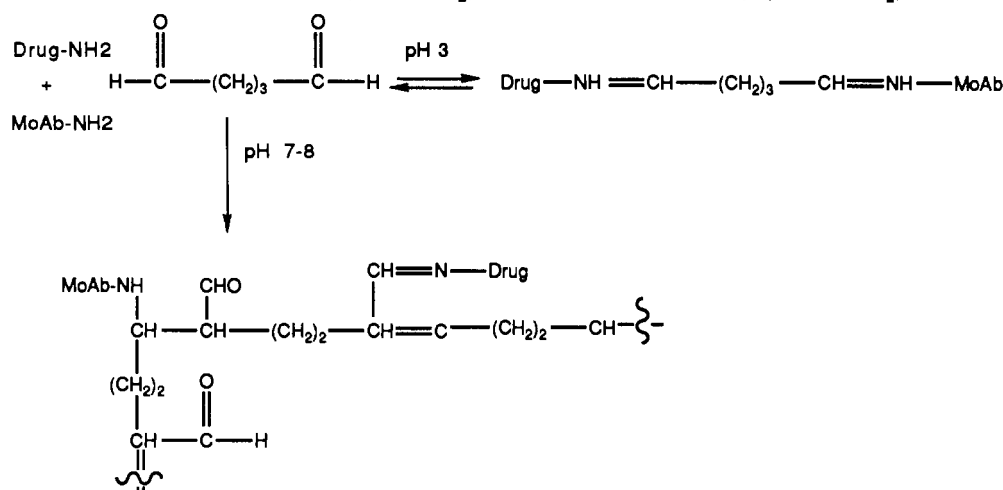
the coupling reaction will yield inactive conjugates, unless the drug is released when the immunoconjugate is degraded by the lysosomal enzymes. Several linkage strategies have been developed so that the drug is released after internalization and they will be discussed later. The release of the free drug may not always be necessary. Immunoconjugates of MTX made by reacting the γ -carboxyl active ester with MoAb retain the ability to inhibit DHFR, and it is therefore likely that any MTX-peptide fragments resulting from lysosomal digestion will also inhibit DHFR (12, 36). Furthermore, CBL (28) and *N*-acetylmelfalan (*N*-AcMEL) (27) both retain alkylating activity while conjugated to MoAb and may not need release of free drug. Therefore, the absolute necessity for the drug to be released may depend on the mechanism of action of the drug. If steric constraints do not effect the binding of drug to the target, then drug-peptide fragments released by lysosomal degradation will be active.

FUNCTIONAL GROUPS ON ANTIBODY MOLECULES

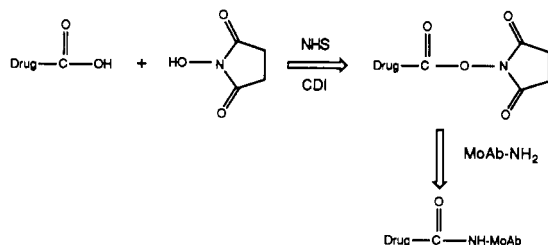
Monoclonal antibodies have a range of reactive groups that can be utilized for coupling to drugs. Some of these are involved in preserving the tertiary structure and binding to antigens. Extensive covalent modification of MoAb by drug may lead to loss of solubility and antibody activity. The extent of possible modification of MoAb by drug will depend on the particular MoAb. Therefore, once a suitable coupling procedure has been designed, it is necessary to measure the antibody activity and protein recovery after modification of the particular MoAb with different molar ratios of drug to MoAb, resulting in a different number of bound-drug residues. Reactive groups may be introduced onto MoAb by (a) use of heterobifunctional cross-linkers, (b) reaction with sodium periodate to create aldehyde groups by carbohydrate oxidation, or (c) reaction with dithiotreitol to reduce inherent disulfides to expose free sulfhydryl groups (Table II).

SELECTED METHODS FOR COUPLING DRUGS TO MOABS

Direct Linkage of Drug to MoAb. Glutaraldehyde. Glutaraldehyde is used to cross-link two amino groups. The exact mechanism of this reaction is complex, but there is evidence to show that an initial Michael addition of one amino group is involved followed by Schiff base formation with the other amino group and aldehyde (Scheme I) (43). The major problem associated with the use of this reagent is polymerization. Several approaches are available to reduce such unwanted side reactions by conducting the reactions in two stages—first mix glutaraldehyde with one reactant, remove the excess glutaraldehyde, and then react with the second component. Despite these obvious disadvantages, adriamycin (Ad) (30) and daunomycin (Dm) (44) have been conjugated to MoAbs with the use of glutaraldehyde. The Schiff base formed between the aldehyde and amino group may be stabilized with sodium borohydride or sodium cyanoborohydride.

Scheme I.^a Mechanism of Coupling of Drug (Drug-NH₂) to Monoclonal Antibody (MoAb-NH₂) with Glutaraldehyde

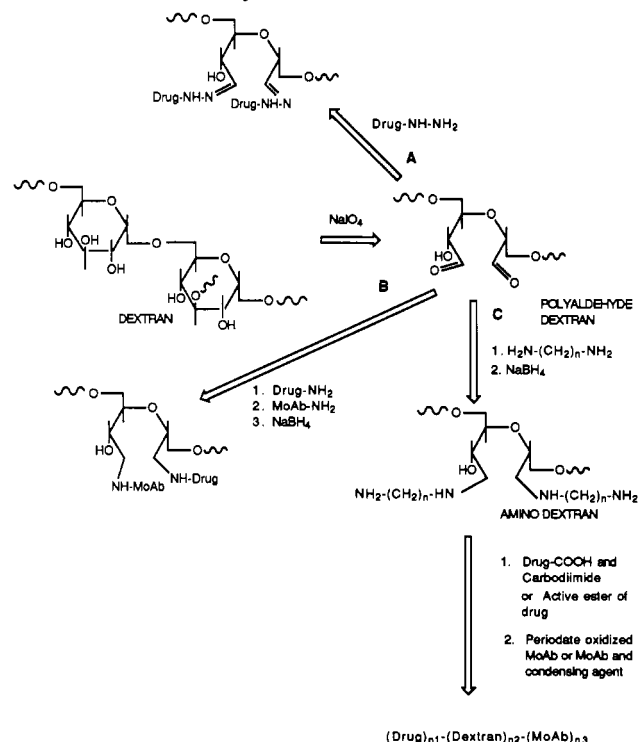
^a Under acidic conditions, Schiff bases are formed between antibody amino groups and aldehyde groups; at neutral or slightly basic pH a more complex reaction predominates.

Scheme II.^a Coupling of Monoclonal Antibody (MoAb-NH₂) to Active Ester Derivative of Drug (Drug-COOH)

^a The *N*-hydroxysuccinimide active ester reacts selectively with the basic amino groups of MoAb.

Carbodiimide (CDI). This condensing agent reacts with amino groups and carboxyl groups to form an amide bond, and as with glutaraldehyde, polymerization occurs during this reaction (45). Attempts have been made to reduce the polymerization by preforming the activated derivative and then reacting with the MoAb (46). A more attractive method of coupling carboxyl-containing drugs to MoAb is the use of active ester. CDIs have been used for coupling adriamycin (30), daunomycin (30), and methotrexate (36, 47) to MoAbs.

Active Ester. Esters formed between *N*-hydroxysuccinimide (NHS) and carboxylic acids react rapidly with amino groups and very slowly with water or hydroxy groups and has been the method of choice of coupling carboxylic acid containing drugs to MoAbs. Reaction of the active ester with an amino group gives rise to a stable amide linkage (Scheme II). Methotrexate (36, 48), chlorambucil (28), and *N*-acetylmelfalan (27) have been coupled by using the active-ester method. Methotrexate and aminopterin can be selectively activated at the γ -carboxyl group with equimolar amounts of NHS and CDI (36, 48, 49). Recent work by Endo et al. suggested the possible reaction of MTX active esters with hydroxy groups available on MoAb (50). The resulting ester linkages can be hydrolyzed with hydroxylamine. Hydroxylamine treatment of these conjugates results in greater selective cytotoxicity between antibody-reactive and nonreactive cells. Compounds with primary or secondary hydroxyl groups can also be coupled to MoAb by the active-ester method, by first reacting with succinic anhydride to form the hemisuccinate, followed by reaction with NHS and CDI. The solubility of the active esters may be increased by using the water-soluble *N*-hydroxysulfosuccinimide instead of NHS.

Scheme III.^a Coupling of Drugs to MoAbs via a Dextran Intermediary

^a Polyaldehyde dextran made by periodate oxidation of dextran may be sequentially reacted with drug and MoAb (path B), reacted with a diamine to introduce amino groups and then sequentially reacted with an activated drug and antibody (path C), or reacted with a drug hydrazide derivative (path A).

Hydrazide. Hydrazides can be readily prepared from carboxylic acids or esters with hydrazine and the hydrazides thus formed react readily with aldehydes under acidic conditions to form hydrazones (Scheme III, path A). Immunoglobulins have branched-chain carbohydrate at the hinge region and oxidation of this carbohydrate with periodate results in the production of aldehyde groups which can be reacted with a hydrazide derivative of the drug. Vinblastine (25) and methotrexate (26) have both been coupled to MoAb by using this procedure. The advantage of this method is the production of more immunoreactive conjugates than the active-ester method, due to site specific modification of MoAb.

Halocarbonyl. α -Halocarbonyl compounds are reactive with sulphydryl, amino, and carboxyl groups; for exam-

ple, 14-Bromodaunomycin (Br-Dm) (32, 34) and 14-bromoidarubicin (Br-Ida) (35) have been coupled to a variety of proteins. In the study where Br-Ida was used, the drug was linked via carboxylic groups and amino groups (35). The idarubicin immunoconjugates had excellent *in vivo* activity although Br-Dm coupled via sulfhydryl groups resulted in inactive immunoconjugates (32). The *N*-iodoacetyl derivative of Ad, when coupled to sulfhydryl groups of MoAb, resulted in conjugates with similar activity to the *N*-iodoacetyl adriamycin derivative *in vitro* (31). In a recent study by Umemoto et al., a peptide derivative of MTX was coupled to MoAb by reaction of an iodoacetyl derivative (51).

Miscellaneous. A number of other coupling procedures either unique to the particular drug or less widely used are available. Trenimon, an aziridinylquinone alkylating agent, was conjugated to a sulfhydryl-containing MoAb with retention of alkylating activity (52). Platinum salts have also been coupled to MoAb by simple mixing, even though the exact mechanism of coupling is not clear (53). The isocyanate derivative of chlorambucil has also been used to couple CBL to an anti-CEA MoAb (54).

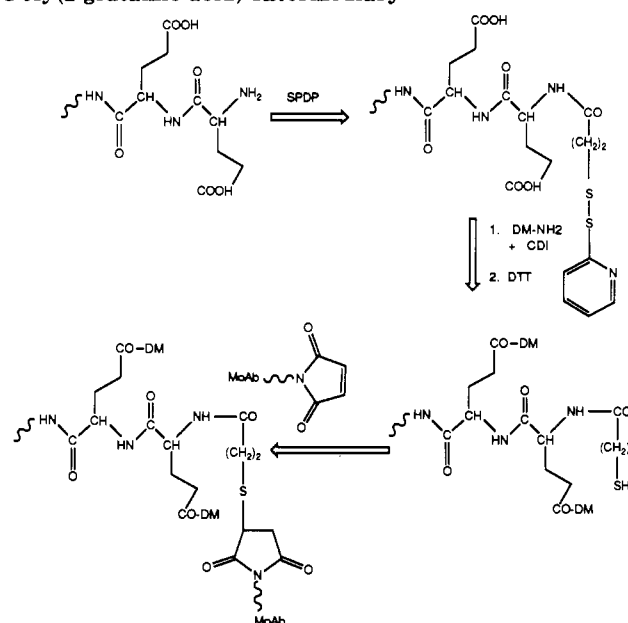
Linkage of Drug to MoAb via an Intermediary. To increase the number of drug molecules that can be carried by the MoAb, inert intermediaries have been used. The drug is reacted with the intermediary and the resulting complex is coupled to the MoAb. Several intermediaries have been used, including modified dextrans, polyamino acids, and human serum albumin.

Dextran. Dextran is a bacterial polysaccharide made up of α -D-glucopyranosyl units, and these dextrans can be derivatized in a variety of ways to introduce reactive groups and thereby be coupled to antibody (55). Polyaldehyde dextran, made by periodate oxidation, has been used as an intermediary for coupling cytosine arabinoside (29), bleomycin (56), daunomycin (57), adriamycin (58), and chlorin e_6 (59) to MoAbs (Scheme III, path B and C). Amino dextran synthesized from polyaldehyde dextran has been used to couple methotrexate to MoAb (60), resulting in an immunoconjugate with 23 residues of MTX per MoAb (Scheme III, path C).

Polyamino Acids. The property of poly(L-amino acids) such as poly(L-glutamic acid) and poly(L-aspartic acid) to be digested by enzymes has been utilized by using it as an intermediary for carrying large amounts of drug. These polyamino acids have been used extensively in drug delivery as a means of increasing the therapeutic index of drugs (61). Two approaches have been used to couple drugs to MoAbs via a polyamino acid carrier. Firstly, polyamino acid may be derivatized with a cross-linking agent at the α amino group followed by derivatization with drug and then linking to MoAb (Scheme IV) (62). An alternative procedure is to synthesize the poly(L-amino acid) by polymerization of a suitably functionalized monomer. The latter method was used by Kato et al. to introduce a thiol group onto polyglutamic acid for coupling to MoAb in the final step (63).

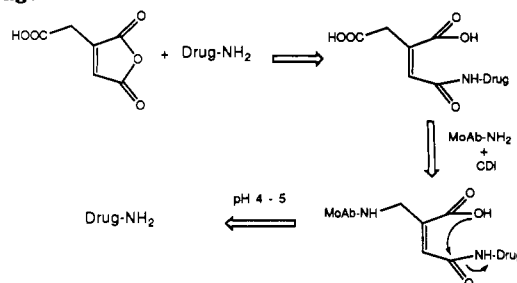
Human Serum Albumin. Human serum albumin (HSA) has also been used as an intermediary carrier for coupling methotrexate (64, 65) and mitomycin C (66) to monoclonal antibodies. In the approach by Garnett et al. (63), MTX was coupled to HSA with CDI and then reduced with DTT to expose the free thiol group on HSA and reacted with iodoacetylated MoAb. With this method, 38 residues of MTX were coupled to MoAb, and the resulting immunoconjugate was more active than free MTX. A serious problem in with the use of intermediaries is

Scheme IV.^a Linkage of Daunomycin to MoAb via a Poly(L-glutamic acid) Intermediary



^a Poly(L-glutamic acid) is activated at the amino terminal with SPDP, and the drug containing an amino group is coupled to poly(L-glutamic acid) with CDI. The reduced polymer is then reacted with an antibody substituted with a maleimide group.

Scheme V.^a Linkage of Drug (Drug-NH₂) to Monoclonal Antibody (MoAb-NH₂) via a *cis*-Aconityl Linkage



^a The basic amino group of the drug reacts with *cis*-aconitic anhydride to give a dicarboxylic acid, which can be selectively coupled by the carboxyl group to MoAb. Under acidic conditions the drug is liberated from the MoAb.

the possibility of obtaining conjugates with more than one carrier molecule per antibody molecule, which results in decreased yields.

Lysosome-Sensitive Linkers. The passage of antigen antibody complexes to the lysosome by endocytosis has led to the design of several linkages that are cleaved by either lysosomal enzymes or lower pH (4.5–5) to release free drug. Early work by Trouet et al. (67) demonstrated that the peptides LeuAlaLeu and AlaLeuAlaLeu when used as linkers between drug and BSA released the free drug when treated with lysosomal hydrolases. Several other linkers have been synthesized that have similar properties—e.g. GlyPheLeuGly (51). MTX has been coupled to MoAb with this linker. The use of *cis*-aconitic anhydride to link drugs to proteins was demonstrated by Shen et al. (68), where the *cis*-aconityl derivative of daunomycin was linked to poly(L-lysine). Exposure of these conjugates to pH 4.5–5 results in the release of drug (Scheme V). Immunoconjugates of daunomycin (69) and adriamycin (70) made by using this procedure have shown antitumor effects *in vitro* and *in vivo*. Several other linkers have been synthesized recently that may be utilized for coupling drugs to MoAbs (71).

Prodrug Approach. Immunoconjugates, once admin-

istered to animals, will circulate and eventually be removed from the circulation, presumably by the reticuloendothelial system. If the drug is not detoxified at this stage, drug toxicity will be seen. MTX immunoconjugates are more toxic than free MTX in animals, especially if given daily (26), presumably due to rapid clearance of MTX by the kidney and accumulation of immunoconjugate in the reticuloendothelial system. Alternatively, the drug may dissociate from the MoAb and harm nontumor tissue. With these in mind, the use of nontoxic prodrugs for immunoconjugation is an attractive concept. These prodrugs may be drugs with charged groups to prevent free diffusion across the cell membrane, defective by modification of groups involved in active transport, or requiring lysosomal cleavage for activation. This is an area that has not been explored even though *cis*-acotinyl derivatives and peptide derivatives of drugs may be considered as prodrugs. Melphalan was converted to *N*-acetylmelphalan by acetylation of the amino group, and this modification resulted in a 100-fold decrease in cytotoxicity due to defective transport (27). Conjugation of *N*-AcMEL to MoAb resulted in a conjugate 3-fold less toxic than melphalan. *N*-AcMEL conjugates were not toxic to mice at a dose of 16 mg/kg. However, *N*-AcMEL and MEL had an LD₅₀ of 115 and 6 mg/kg, respectively. Another method of utilizing prodrugs for targeting is their use in conjunction with enzyme—MoAb conjugates. Enzymes such as carboxypeptidase (72) or alkaline phosphatase (73) can be coupled to monoclonal antibodies and targeted to tumors and nontoxic prodrugs may be administered (64, 65). The prodrugs are transformed to the drug at the vicinity of the tumor and diffuse into the tumor. For enzyme targeting of this type, MoAbs to noninternalizing antigens are necessary. Careful consideration has to be given in choosing enzymes such that prodrugs are not activated in normal tissue by endogenous enzyme; therefore alkaline phosphatase is not an ideal choice. Another approach worth considering is the linking of photoactivatable moieties such as chlorin *e*₆ (59) and hematoporphyrin (74) to MoAbs. These agents are inactive until activated (cf. prodrugs) by light of a particular wavelength to emit singlet oxygen. Since singlet oxygen is a diffusible product, the conjugates do not need to be internalized and are capable of killing bystander cells lacking tumor antigen. Moreover, the light activation can also be directed to the tumor and thereby activate the photodrug locally, allowing MoAbs with slight cross-reactivity with healthy tissues to be used.

In Vitro Testing. Coupling of drug to MoAbs may lead to partial or complete loss of antibody activity and/or drug activity. Therefore both activities of the immunoconjugate should be carefully monitored at each step. Several approaches can be used to test for antibody activity and a review of this aspect is found in Pietersz et al. (10). The drug activity may be tested by using a cytotoxicity assay measuring the inhibition of DNA, RNA, or protein synthesis (10). The colorimetric tetrazolium assay (MTT) which utilized a yellow, water-soluble dye which is transformed to a blue formazan by live cells can also be used. For certain drugs such as alkylating agents and dihydrofolate reductase inhibitors, the functional integrity of the bound drug can be determined by measuring the drugs ability to alkylate 4-(4-nitrobenzyl)pyridine (28) or inhibit DHFR, respectively (36). The selectivity of immunoconjugates may be tested by comparing the inhibition of growth of antibody-reactive and nonreactive cell lines. However, lack of selectivity does not necessarily imply unsuitable conjugates (35). This point could be illustrated with reference to idarubicin-antibody con-

jugates, where specific conjugates are 5–10 times more active on the target cell line than the nonspecific conjugates. However, in vivo nonspecific conjugates do not show any antitumor effects, and no toxic effects due to the conjugates are apparent. The exact mechanism by which nonspecific conjugates demonstrate cytotoxicity in vitro is not known. These problems emphasize the need for more appropriate cytotoxicity and specificity assays that mimic the in vivo behavior of immunoconjugates. Suitability of immunoconjugates as specific antitumor agents will only be apparent from efficacy in preclinical studies using animal models (10). Despite certain drawbacks such as the inability to predict effects due to cross-reactivity of MoAb with normal human tissues, animal models can be extremely useful for the characterization of immunoconjugates. Ideally, preclinical testing should include tests for stability in vitro and in vivo, biodistribution studies using radiolabeled drug, and dose-responses studies to compare antitumor efficacy and toxicity.

CONCLUSION

This review has concentrated primarily on the chemical methods and strategies utilized for immunoconjugation of drugs. The techniques for coupling cytotoxic drugs to MoAbs have become increasingly more sophisticated, with the design of novel linkers and protecting groups which confer unique properties, such as stability in serum, with sensitivity to lysosomal or hydrolytic enzymes. The majority of drugs used in immunoconjugates have been limited to those commonly used in the clinic for the treatment of cancer and are not necessarily the most optimal for conjugation to antibodies. The conjugation of very cytotoxic, lower molecular weight compounds previously discarded due to their toxicity should now be investigated for immunoconjugation, as binding to antibody increases specificity and reduces the toxicity of such drugs. Such potent immunoconjugates may result in better antitumor efficacy by counteracting the low uptake of drug to the tumor. The access of immunoconjugates to the tumor is still a major problem and is a serious limitation for the treatment of larger tumors, but the production of small, single chain antibody molecules by genetic engineering techniques may overcome this. Because of the difficulty in delivery of large amounts of antibody to large tumours, the final place of immunoconjugate in the treatment of cancer may be in conjunction with other modes of therapy for treating minimum, residual disease in the adjuvant setting. However, this remains to be proven.

LITERATURE CITED

- (1975) *Antibiotics* (J. W. Corcoran and F. E. Hahn, Eds.) Vol. 111, Springer-Verlag; Berlin.
- (1981) *Molecular Actions and Targets for Cancer Chemotherapeutic Agents* (A. C. Sartorelli, J. S. Lazo, and J. R. Bertino, Eds.) Academic Press, New York.
- Weber, G. (1983) Biochemical strategy of cancer cells and the design of chemotherapy: G. H. A. Clowes Memorial Lecture. *Cancer Res.* 43, 3466–3492.
- (1980) *Anticancer Agents Based on Natural Product Models* (J. M. Cassady and J. D. Douros, Eds.) Vol. 16, Medicinal Chemistry, Academic Press, New York.
- Hutchinson, C. R., Borell, C. W., Olten, S. L., Stutzman-Engwall, K. J., and Wang, Y. (1989) Drug discovery and development through the genetic engineering of antibiotic-producing microorganisms. *J. Med. Chem.* 32, 929–937.
- Carl, P. L., Chakravarty, P. K., Katzenellenbogen, J. A., and Weber, M. J. (1980) Protease-activated "prodrugs" for cancer chemotherapy. *Proc. Natl. Acad. Sci. U.S.A.* 77, 2224–2228.

- (7) Double, J. A. and Bibby, M. C. (1989) Therapeutic index: A vital component in selection of anticancer agents for clinical trial. *JNCI, J. Natl. Cancer Inst.* 81, 988-994.
- (8) Smith, L. H. and Teng, N. N. H. (1987) Clinical applications of monoclonal antibodies in gynecologic oncology. *Cancer* 60, 2068-2074.
- (9) Teh, J. G., Stacker, S. A., Thomson, C. H., and McKenzie, I. F. C. (1985) The diagnosis of human tumours with monoclonal antibodies. *Cancer Surv.* 4, 149-184.
- (10) Pietersz, G. A., Kanellos, J., Smyth, M. J., Zalberg, J., and McKenzie, I. F. C. (1987) The use of monoclonal antibody conjugates for the diagnosis and treatment of cancer. *Immunol. Cell Biol.* 65 (2), 111-125.
- (11) Ehrlich, P. (1913) Chemotherapy, Proceedings of the 17th International Congress of Medicine. *The Collected Papers of Paul Ehrlich* (F. Himmelweit, Ed.) p 510, Pergamon Press, London.
- (12) Uadia, P., Blair, A. H., Ghose, T., and Ferrone, S. (1985) Uptake of methotrexate linked to polyclonal and monoclonal antimeelanoma antibodies by a human melanoma cell line. *JNCI, J. Natl. Cancer Inst.* 74, 29-35.
- (13) Garnett, M. C., Embleton, M. J., Jacobs, E., and Baldwin, R. W. (1985) Studies on the mechanism of action of an antibody-targeted drug-carrier conjugate. *Anti-cancer Drug Des.* 1, 3-12.
- (14) Frankel, A. E., Welsh, P. C., Ian Withers, D., and Schlossman, D. M. (1988) Immunotoxin Preparation and Testing in Vitro. In *Targeted Diagnosis and Therapy* (J. D. Rodwell, Ed.) pp 225-244, Marcel Dekker, New York.
- (15) Goldenberg, D. M., Goldenberg, H., and James Primus, F. (1987) Cancer Diagnosis and Therapy with Radiolabelled Antibodies. In *Immunoconjugates* (C-W. Vogel, Ed.) pp 259-280, Oxford University Press, New York.
- (16) Roche, A., Bailly, P., Midoux, P., and Monsigny, M. (1984) Selective macrophage activation by muramyl dipeptide bound to monoclonal antibodies specific for mouse tumour cells. *Cancer Immunol. Immunother.* 18, 155-159.
- (17) Obrist, R. and Sandberg, A. L. (1982) In vitro effects of antitumor antibody-chemotactic factor complexes. *Clin. Immunopathol.* 25, 91-102.
- (18) Lal, R. B., Brown, E. M., Seligmann, B. E., Edison, L. J., and Chused, T. M. (1985) Selective elimination of lymphocyte subpopulations by monoclonal antibody enzyme conjugates. *J. Immunol. Methods* 79, 307-318.
- (19) Erlanger, B. F. The preparation of antigenic hapten-carrier conjugates: A survey. *Methods Enzymol.* 70, 85-104.
- (20) Mathe, G., Loc, T. B., and Bernard, J. (1958) Effect sur la Leucemie 1210 de la souris d'une combinaison par diazotation d'A-methoptérine et de γ -globulins de hamsters porteurs de cette Leucemie par heterogreffe. *C. R. Acad. Sci. (Paris)* 246, 1626-1628.
- (21) Davies, D. A. L. (1974) The combined effect of drugs and tumor-specific antibodies in protection against a mouse lymphoma. *Cancer Res.* 34, 3040-3043.
- (22) Arcamone, F. (1981) *Doxorubicin Anticancer Antibiotics* Academic Press, New York.
- (23) Aboud-Pirak, E., Lesur, B., Bhushana Rao, K. S. P., Baurain, R., Trouet, A., and Schneider, Y. (1989) Cytotoxic activity of daunorubicin or vindesine conjugated to a monoclonal antibody on cultured MCF-7 breast carcinoma cells. *Biochem. Pharmacol.* 38, 641-648.
- (24) Rowland, G. F., Axton, C. A., Baldwin, R. W., Brown, J. P., Corvalan, J. R. F., Embleton, M. J., Gore, V. A., Hellstrom, I., Hellstrom, K. E., Jacobs, E., Marsden, C. H., Pimm, M. V., Simmonds, R. G., and Smith, W. (1985) Antitumor properties of vindesine monoclonal antibody conjugates. *Cancer Immunol. Immunother.* 19, 1-7.
- (25) Laguzza, B. C., Nichols, C. L., Briggs, S. L., Cullinan, G. J., Johnson, D. A., Starling, J. J., Baker, A. L., Bumol, T. F., and Corvolan, J. R. F. (1989) New antitumor monoclonal antibody-vinca conjugates LY203725 and related compounds: Design, preparation and representative in vivo activity. *J. Med. Chem.* 32, 548-555.
- (26) Ghose, T., Blair, A. H., Kralovec, J., Uadia, P. O., and Mammen, M. (1988) Synthesis and Testing of Antibody-Antifolate Conjugates for Drug Targeting. In *Targeted Diagnosis and Therapy* (J. D. Rodwell, Ed.) Vol. 1, pp 81-122, Marcel Dekker, New York.
- (27) Smyth, M. J., Pietersz, G. A., and McKenzie, I. F. C. (1987) Selective enhancement of antitumor activity of *N*-acetyl-melphalan upon conjugation to monoclonal antibodies. *Cancer Res.* 47, 62-69.
- (28) Smyth, M. J., Pietersz, G. A., Classon, B. J., and McKenzie, I. F. C. (1986) Specific targeting of chlorambucil to tumors with the use of monoclonal antibodies. *JNCI, J. Natl. Cancer Inst.* 76, 503-510.
- (29) Hurwitz, E., Kashi, R., Arnon, R., Wilchek, M., and Sela, M. (1985) The covalent linkage of two nucleotide analogues to antibodies. *J. Med. Chem.* 28, 137-140.
- (30) Hurwitz, E., Levy, R., Maron, R., Wilchek, M., Arnon, R., and Sela, M. (1975) The covalent binding of daunomycin and adriamycin to antibodies, with retention of both drug and antibody activities. *Cancer Res.* 35, 1175-1181.
- (31) Pietersz, G. A., Smyth, M. J., and McKenzie, I. F. C. (1988) The use of anthracycline antibody complexes for specific antitumor therapy. In *Targeted Diagnosis and Therapy*, (J. D. Rodwell, Ed.) Vol. 1, pp 25-53, Marcel Dekker, New York.
- (32) Gallego, J., Price, M. R., and Baldwin, R. W. (1984) Preparation of four daunomycin-monoclonal antibody 76IT/36 conjugates with anti-tumour activity. *Int. J. Cancer* 33, 737-744.
- (33) Cotter, T. G., Fecyc, T. D., and O'Malley, K. (1984) Monoclonal-antibody-mediated delivery of deacetylcolchicine to human peripheral blood neutrophils. *Biochem. Soc. Trans.* 12, 452.
- (34) Zunino, F., Gambetta, R., Vigevani, A., Penco, S., Geroni, C., and DiMarco, A. (1981) Biologic activity of daunorubicin linked to proteins via the methylketone side chain. *Tumori* 67, 521-524.
- (35) Pietersz, G. A., Smyth, M. J., and McKenzie, I. F. C. (1988) Immunochemotherapy of a murine thymoma with the use of idarubicin monoclonal antibody conjugates. *Cancer Res.* 48, 926-931.
- (36) Kulkarni, P. N., Blair, A. H., Ghose, T. I. (1981) Covalent binding of MTX to immunoglobulins and the effect of antibody-linked drug on tumor growth in vivo. *Cancer Res.* 41, 2700-2706.
- (37) Carlsson, J., Drevin, H., and Axen, R. (1978) Protein thiolation and reversible protein-protein conjugation *N*-succinimidyl 3-(2-pyridyldithio) propionate, a new heterobifunctional reagent. *Biochem. J.* 173, 723-737.
- (38) Kitagawa, T., Fujitake, T., Taniyama, H., and Aikawa, T. (1978) Enzyme immunoassay of viomycin. New cross-linking reagent for enzyme labelling and a preparation for antiserum to viomycin. *J. Biochem.* 83, 1493-1501.
- (39) Jue, R., Lombert, J. M., Pierce, L. R., and Traut, R. R. (1978) Addition of sulfhydryl groups to *Escherichia coli* ribosomes by protein modification with 2-iminothiolane (methyl 4-mercaptobutyrimidate). *Biochemistry* 17, 5399-5405.
- (40) Garnett, M. C., Embleton, M. J., Jacobs, E., and Baldwin, R. W. (1983) Preparation and properties of a drug-carrier-antibody conjugate showing selective antibody-directed cytotoxicity in vitro. *Int. J. Cancer* 31, 661-670.
- (41) Youle, R. J. and Neville, D. M., Jr. (1980) Anti-Thy 1.2 monoclonal antibody linked to ricin is a potent-cell-type specific toxin. *Proc. Natl. Acad. Sci. U.S.A.* 77, 5483-5486.
- (42) Rodwell, J. D., Alvarez, V. L., Lee, C., Lopes, A. D., Goers, J. W. F., King, H. D., Powsner, H. J., and McKearn, T. J. (1986) Site-specific covalent modification of monoclonal antibodies: In vitro and in vivo evaluations. *Proc. Natl. Acad. Sci. U.S.A.* 83, 2632-2626.
- (43) Peters, K. and Richards, F. M. (1977) Chemical cross-linking: Reagents and problems in studies of membrane structure. *Annu. Rev. Biochem.* 46, 523-551.
- (44) Belles-Isles, M. and Page, M. (1981) Anti-oncogenic proteins for targeting cytotoxic drugs. *Int. J. Immunopharmacol.* 3, 97-102.
- (45) Timkovich, R. (1977) Polymerization side reactions during protein modification with carbodiimide. *Biochem. Biophys. Res. Commun.* 74, 1463-1468.
- (46) Rowland, G. F. G., O'Neill, G. J., and Davies, D. A. L. (1975) Suppression of tumour growth in mice by a drug-an-

- tibody conjugate using a novel approach to linkage. *Nature* 255, 487-488.
- (47) Burstein, S. and Knapp, S. (1977) Chemotherapy of murine ovarian carcinoma by methotrexate antibody conjugate. *J. Med. Chem.* 20, 950-952.
- (48) Kanellos, J., Pietersz, G. A., and McKenzie, I. F. C. (1985) Studies of methotrexate-mono-clonal antibody conjugates for immunotherapy. *JNCI, J. Natl. Cancer Inst.* 75, 319-332.
- (49) Kanellos, J., Pietersz, G. A., Cunningham, Z., and McKenzie, I. F. C. (1987) Anti-tumour activity of aminopterin mono-clonal antibody conjugates; in vitro and in vivo comparison with methotrexate mono-clonal antibody conjugates. *Immunol. Cell Biol.* 65 (6), 483-493.
- (50) Endo, N., Takeda, Y., Umemoto, N., Kishida, K., Watanabe, K., Saito, M., Kato, Y., and Hara, T. (1988) Nature of linkage and mode of action of methotrexate conjugated with antitumor antibodies. Implications for future preparation of conjugates. *Cancer Res.* 48, 3330-3335.
- (51) Umemoto, N., Kato, Y., Endo, N., Takeda, Y., and Hara, T. (1989) Preparation and in vitro cytotoxicity of a methotrexate-anti-MM46 mono-clonal antibody conjugate via an oligopeptide spacer. *Int. J. Cancer* 43, 677-684.
- (52) Linford, J. H., Froese, G., Berczi, I., and Israels, L. G. (1974) An alkylating agent-globulin conjugate with both alkylating and antibody activity. *J. Natl. Cancer Inst.* 52, 1665-1667.
- (53) Hurwitz, E., Kashi, R., and Wilchek, M. (1982) Platinum-complexed antitumor immunoglobulins that specifically inhibit DNA synthesis of mouse tumor cells. *JNCI, J. Natl. Cancer Inst.* 69, 47-51.
- (54) Bernier, L. G., Page, M., Gaudreault, R. C., and Joly, L. P. (1984) A chlorambucil-anti-CEA conjugate cytotoxic for human colon adenocarcinoma cells in vitro. *Br. J. Cancer* 49, 245-246.
- (55) Hurwitz, E., Wilchek, M., and Pitha, J. (1980) Soluble macromolecules as carriers for daunorubicin. *J. Appl. Biochem.* 2, 25-35.
- (56) Manabe, Y., Tsubata, T., Haruta, Y., Okazaki, M., Haisa, S., Nakamura, K., and Kimura, I. (1983) Production of a mono-clonal antibody-bleomycin conjugate utilizing dextran-T-40 and the antigen targeting cytotoxicity of the conjugate. *Biochem. Biophys. Res. Commun.* 115, 1009-1014.
- (57) Tsukada, Y., Hurwitz, E., Kashi, R., Sela, M., Hibi, N., Hara, A., and Hirai, H. (1982) Chemotherapy by intravenous administration of conjugates of daunomycin with mono-clonal and conventional anti-rat α -fetoprotein antibodies. *Proc. Natl. Acad. Sci. U.S.A.* 79, 7896-7899.
- (58) Dillman, R. O., Shawler, D. L., Johnson, D. E., Meyer, D. L., Kozio, J. A., and Frincke, J. M. (1986) Preclinical trials with combinations and conjugates of T101 mono-clonal antibody and doxorubicin. *Cancer Res.* 46, 4886-4891.
- (59) Oseroff, A. R., Ohuoha, D., Hasan, T., Bommer, J. C., and Yarmush, M. L. (1986) Antibody-targeted photolysis: Selective photodestruction of human T-cell leukemia cells using mono-clonal antibody-chlorin e_6 conjugates. *Proc. Natl. Acad. Sci. U.S.A.* 83, 8744-8748.
- (60) Shih, L., Sharkey, R. M., Primus, F. J., and Goldenberg, D. M. (1988) Site-specific linkage of methotrexate to mono-clonal antibodies using an intermediate carrier. *Int. J. Cancer* 4, 832-839.
- (61) Zunino, F., Savi, G., Guiliani, F., Gambetta, R., Supino, R., Tinelli, S., and Pezzoni, G. (1981) Comparison of antitumor effects of daunorubicin covalently linked to poly-L-amino acid carriers. *Eur. J. Cancer Clin. Oncol.* 20, 421-425.
- (62) Tsukada, Y., Kato, Umemoto, N., Takeda, Y., Hara, T., and Hirai, H. (1984) An anti- α -fetoprotein antibody-daunorubicin conjugate with a novel poly-L-glutamic acid derivative as intermediate drug carrier. *JNCI, J. Natl. Cancer Inst.* 73, 721-729.
- (63) Kato, Y., Umemoto, N., Kayama, Y., Fukushima, H., Takeda, Y., Hara, T., and Tsukada, Y. (1984) A novel method of conjugation of daunomycin with antibody with a poly-L-glutamic acid derivative as intermediate drug carrier. An anti- α -fetoprotein antibody-daunomycin conjugate. *J. Med. Chem.* 27, 1602-1607.
- (64) Garnett, M. C. and Baldwin, R. M. (1986) An improved synthesis of a methotrexate-Albumin-79IT/36 mono-clonal antibody conjugate cytotoxic to human osteogenic sarcoma cell lines. *Cancer Res.* 46, 2407-2412.
- (65) Pietersz, G. A., Cunningham, Z., and McKenzie, I. F. C. (1988) Specific in vitro anti-tumour activity of methotrexate mono-clonal antibody conjugates prepared using human serum albumin as an intermediary. *Immunol. Cell Biol.* 66 (1), 43-49.
- (66) Umemoto, N., Kato, Y., Takeda, Y., Saito, M., Hara, T., Seto, M., and Takahashi, T. (1984) Conjugates of mitomycin C with the immunoglobulin M monomer fragment of a mono-clonal anti-MM46 immunoglobulin M antibody with or without serum albumin as intermediary. *J. Appl. Biochem.* 6, 297-307.
- (67) Trouet, A., Masquelier, M., Baurain, R., and Deprez-de Campeneere, D. (1982) A covalent linkage between daunorubicin and proteins that is stable in serum and reversible by lysosomal hydrolases, as required for a lysosomotropic drug-carrier conjugate: In vitro and in vivo studies. *Proc. Natl. Acad. Sci. U.S.A.* 79, 626-629.
- (68) Shen, W. C. and Ryser, J. P. (1981) *cis*-Aconityl spacer between daunomycin and macromolecular carriers: A model of pH-sensitive linkage releasing drug from a lysosomotropic conjugate. *Biochem. Biophys. Res. Commun.* 102, 1048-1054.
- (69) Diener, E., Diner, U. E., Sinha, A., Xie, S., and Vergidis, R. (1986) Specific immunosuppression by immunotoxins containing daunomycin. *Science* 231, 148-150.
- (70) Ming Yang, H. and Reisfeld, R. A. (1988) Pharmacokinetics and mechanism of action of a doxorubicin mono-clonal antibody 9.2.27 conjugate directed to a human melanoma proteoglycan. *JNCI, J. Natl. Cancer Inst.* 80, 1154-1159.
- (71) Srinivasachar, K. and Neville, D. M., Jr. (1989) New protein cross-linking reagents that are cleaved by mild acid. *Biochemistry* 28, 2501-2509.
- (72) Bagshawe, K. D., Springer, C. J., Melton, R. G., Antoni, P., Boden, J. A., Pedley, R. B., Burke, P., Sharma, S. K., Sherwood, R. F., Rogers, G. T., and Searle, F. (1989) Resistant choreocarcinoma xenograft growth delayed by antibody enzyme-conjugate activation of a prodrug. *Abstracts of Papers, the 4th International Conference on Mono-clonal Antibody Immunoconjugates for Cancer* (San Diego).
- (73) Senter, P. D., Saulnier, M. G., Schreiber, G. J., Hirschberg, D. L., Brown, J. P., Hellstrom, I., and Hellstrom, K. E. (1988) Antitumor effects of antibody-alkaline phosphatase conjugates in combination with etoposide phosphate. *Proc. Natl. Acad. Sci. U.S.A.* 85, 4842-4846.
- (74) Mew, D., Lum, V., Wat, C. K., Towers, G. H. N., Sun, C. H. C., Walter, R. J., Wright, W., Berns, M. W., and Levy, J. G. (1985) Ability of specific mono-clonal antibodies and conventional antisera conjugated to hematoporphyrin to label and kill selected cell lines subsequent to light activation. *Cancer Res.* 45, 4380-4386.

LETTERS

Synthesis of 1-(Aminooxy)-4-[(3-nitro-2-pyridyl)dithio]butane and 1-(Aminooxy)-4-[(3-nitro-2-pyridyl)dithio]but-2-ene, Novel Heterobifunctional Cross-Linking Reagents

1-(Aminooxy)-4-[(3-nitro-2-pyridyl)dithio]butane hydrochloride (1) and the related unsaturated compound 2 are stable alkoxyamino cross-linking reagents which react readily with ketones to give the corresponding alkoximes and which couple readily with thiolated proteins in aqueous media to provide stable protein conjugates.

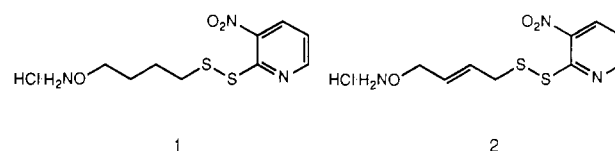
The most commonly employed procedures for attaching drugs to proteins involve thiolation of the protein using heterobifunctional cross-linking reagents such as SPDP [*N*-succinimidyl 3-(2-pyridyldithio)propionate] (1, 2) and subsequent coupling with a nucleophilic moiety of the drug. In the case of antibodies, procedures have been developed which call for periodate oxidation of the carbohydrate region of the antibody, subsequent reaction of the exposed aldehyde moieties with an amine, and reduction of the resultant imine with borohydride to yield stable alkylamino functionalized proteins (3).

As part of a program concerned with targeting of monoclonal antibody (MAb)-drug combinations for chemotherapeutic applications, we sought alternatives to currently employed strategies (2). Toward this end, the alkoxyamino compound 1-(aminooxy)-4-[(3-nitro-2-pyridyl)dithio]butane hydrochloride (1, Chart I) was prepared (vide supra) and found to react readily with the ketone moiety of adriamycin to produce a stable alkoxime (4). This drug-linker combination readily coupled with thiolated antibody (1) in neutral phosphate buffer solution to produce a disulfide-linked drug-antibody conjugate (Scheme I) which was found to be exceptionally stable, requiring exposure to strongly acidic media (aqueous phosphoric acid, ca. pH 2) to release the adriamycin (4).

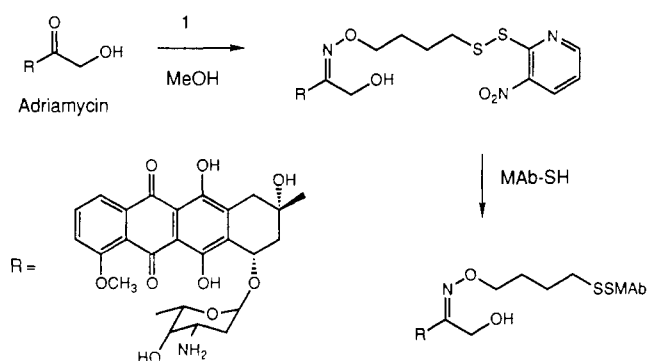
In addition, 1 was found to react with periodate-treated antibodies in aqueous solution (Scheme II) to produce the alkoximino-modified proteins (vide infra) not requiring further modification to improve their stability (Kaneko, T., and Webb, R., unpublished results).

The preparation of 1 proceeds as follows. The alkylation of the sodium salt of ethyl *N*-hydroxyacetimidate (3; NaH/THF, Chart II) with 1,4-dibromobutane gave bromide 4 (5) after fractional distillation to remove starting 3. Displacement of bromide 4 with potassium thioacetate in EtOH to give acetylthio compound 5 was followed by removal of the acetate (K_2CO_3 /MeOH) and the acetimidate (HCl/EtOH/ H_2O) to yield 1-(aminooxy)-4-mercaptobutane hydrochloride (6). Introduction of the (3-nitro-2-pyridyl)dithio group was accomplished by treatment of 6 in methanol with (methoxycarbonyl)sulfenyl chloride (6) to give crystalline 1-(aminooxy)-4-[(methoxycarbonyl)dithio]butane hydrochloride (7), which was stirred in methanol with 3-nitro-2-mercaptopyridine (7) to yield the desired alkylamino dithio compound 1. Compound 1 could be recrystallized from a mixture of meth-

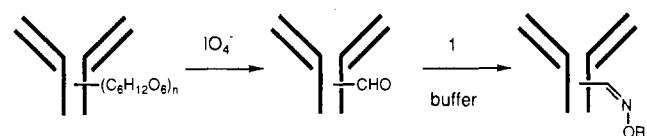
Chart I



Scheme I



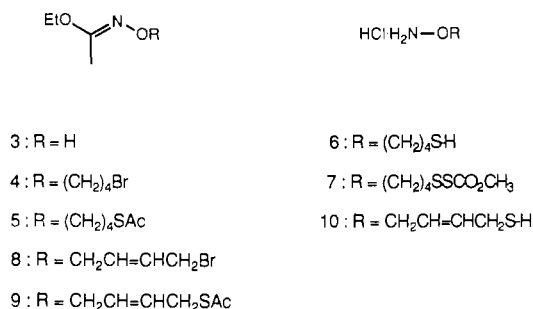
Scheme II



anol, ethyl acetate, and ether and was stable when stored at room temperature for several months. Unsaturated compound 2 was prepared in a similar fashion, i.e. by alkylation of 3 (NaH/THF) with 1,4-dibromo-(*E*)-but-2-ene to yield bromide 8 (Chart II); subsequent thioacetate displacement (KSAc/EtOH) giving 9, deprotection (K_2CO_3 /MeOH then aqueous HCl/EtOH) to thiol 10 and disulfide formation [(methoxycarbonyl)sulfenyl chloride/3-nitro-2-mercaptopyridine/MeOH] yielding 2. Both 1 and 2 could be reacted directly with carbonyl compounds or used as their corresponding free bases by first stirring with a slight excess of triethylamine in methanol.

Experimental Procedures. All solvents and reagents were employed as received, with the following exceptions: Aldrich anhydrous-grade tetrahydrofuran and anhydrous-grade hexane were used for reactions employing

Chart II



NaH; ethyl *N*-hydroxyacetimidate was obtained from Aldrich, and distilled from CaH_2 under nitrogen prior to use; (methoxycarbonyl)sulfonyl chloride was obtained from Fluka or prepared from (chlorocarbonyl)sulfonyl chloride (obtained from Aldrich) according to the procedure of Field and Ravichandran (6) and was distilled under argon prior to use; Sigma absolute methanol was employed as received after degassing with nitrogen. Thin-layer chromatography was performed on EM Science silica gel 60 F₂₅₄ using the following solvent systems: system A, 3:1 hexane/ethyl acetate; system B, 2:1 hexane/ethyl acetate; system C: 1:1 ethyl acetate/hexane. Proton and carbon-13 NMR spectra were obtained on a Varian 300 spectrometer at 300 and 75 MHz, respectively. Mass spectra and exact mass measurements were performed by the Analytical Research Department, Bristol-Myers-Squibb, Wallingford, CT. Elemental analyses were performed by Oneida Research Services, Whitesboro, NY. Values reported were within 0.4% of the theoretical values unless otherwise noted.

Ethyl *N*-[(4-Bromobutyl)oxy]acetimidate (4). A 3-L three-necked round-bottomed flask equipped with mechanical stirrer, addition funnel, and gas inlet, was oven-dried, flushed with nitrogen, and allowed to cool under nitrogen. It was then charged with NaH (20.40 g, 0.509 mol, 60% dispersion in oil). The NaH was washed twice with hexane, covered with tetrahydrofuran (1.6 L), and, with vigorous stirring, ethyl *N*-hydroxyacetimidate (3, 47.74 g, 0.463 mol) was added rapidly dropwise. Gas evolution was noted upon addition. After the addition was complete, the grey suspension was heated at reflux for 18 h. The suspension was then cooled and 1,4-dibromobutane (100.00 g, 0.463 mol) was added rapidly dropwise. After the addition was complete, the resulting suspension was refluxed for 2 days under nitrogen. Thin-layer chromatographic analysis of the reaction mixture indicated the presence of the starting acetimidate (R_f 0.4 in A) and the presence of a less polar product (R_f 0.6 in A). The mixture was cooled and treated with methanol (50 mL) followed by saturated aqueous NH_4Cl (200 mL). The tetrahydrofuran was removed in vacuo, and the slurry that remained was partitioned between ethyl acetate and water. The combined ethyl acetate layers were washed with brine, dried over MgSO_4 , filtered, and concentrated in vacuo to an oil which was distilled under vacuum to yield recovered ethyl *N*-hydroxyacetimidate [20 g, 19%, bp 35–40 °C (2 mmHg)], a mixed fraction (ca. 12 g), and 60 g (52%) of ethyl *N*-[(4-bromobutyl)oxy]acetimidate (4) as a colorless oil: bp 75–77 °C (2 mmHg); ^1H NMR (CDCl_3) δ 3.88 (q, J = 7 Hz, 2 H, OCH_2CH_3), 3.80 (t, J = 6 Hz, 2 H, NOCH_2), 3.33 (t, J = 6 Hz, 2 H, CH_2Br), 1.93 (m, 1 H, OCH_2CH_2), 1.84 (m, 1 H, OCH_2CH_2), 1.80 (s, 3 H, $\text{CH}_3(\text{EtO})=\text{N}$), 1.65 (m, 2 H, $\text{CH}_2\text{CH}_2\text{Br}$), 1.15 (t, J = 7 Hz, 3 H, OCH_2CH_3); ^{13}C NMR (CDCl_3) δ

161.79, 161.67 ($\text{CH}_3\text{C}(\text{OEt})=\text{N}$), 73.09, 72.49 (NOCH_2), 61.93, 61.86 ($\text{CH}_3\text{CH}_2\text{O}$), 33.41, 30.88, 29.59, 27.52, 25.51, 14.27, 13.40; IR (neat) 2980, 2941, 1647 (s), 1377 (s), 1306 (s), 1263, 1252, 1119, 1076, 978 cm^{-1} ; MS (DCI/methane) m/e 240 MH^+ + 2, 18), 238 (MH^+ , 19), 158 ($\text{MH}^+ - \text{Br}$, 60); exact mass calcd for $\text{C}_8\text{H}_{16}\text{NO}_2\text{Br}$ 237.0364, found 237.0358. Anal. ($\text{C}_8\text{H}_{16}\text{NO}_2\text{Br}$) C, H, N.

Ethyl *N*-[[4-(Acetylthio)butyl]oxy]acetimidate (5). A solution of ethyl *N*-[(4-bromobutyl)oxy]acetimidate (4, 34.00 g, 0.143 mol) in absolute ethanol (300 mL) was treated with potassium thioacetate (20.00 g, 0.175 mol) and the resulting yellow suspension heated at reflux for 1 h. Thin-layer chromatographic analysis of the reaction mixture revealed the absence of the starting bromide (R_f 0.6 in A) and the presence of the product thioacetate (R_f 0.5 in A). The mixture was cooled, filtered, and concentrated in vacuo, and the slurry was partitioned between ethyl acetate and water. The combined ethyl acetate layers were washed with saturated aqueous NaHCO_3 solution, water, and brine and then dried over MgSO_4 , filtered, and concentrated in vacuo. The oil remaining was distilled to yield 30 g (90%) of ethyl-*N*-[[4-(acetylthio)butyl]oxy]acetimidate (5) as a clear, yellow, foul-smelling liquid: bp 105–108 °C (2 mmHg); ^1H NMR (CDCl_3) δ 3.90 (q, J = 6 Hz, 2 H, OCH_2CH_3), 3.79 (t, J = 6 Hz, 2 H, NOCH_2), 2.81 (t, J = 6 Hz, 2 H, CH_2SAC), 2.22 (s, 3 H, CH_3COS), 1.81 (s, 3 H, $\text{CH}_3\text{C}(\text{OEt})=\text{N}$), 1.58 (br m, 4 H, CH_2CH_2), 1.16 (t, J = 6 Hz, 3 H, OCH_2CH_3); ^{13}C NMR (CDCl_3) δ 196.45 ($\text{SC}=\text{O}$), 162.74 and 162.66 ($\text{CH}_3\text{C}(\text{OEt})=\text{N}$), 73.55 and 73.05 (CH_2O), 62.35 and 62.32 ($\text{CH}_3\text{CH}_2\text{O}$), 30.73, 29.12, 28.81, 28.61, 28.23, 26.45, 25.74, 14.48, 13.66; IR (neat) 2990, 2945, 2875, 1700 (s, $\text{C}=\text{O}$), 1650, 1380, 1305 (s), 630 cm^{-1} ; MS (DCI/methane) m/e (relative abundance) 234 (MH^+ , 100); exact mass calcd for $\text{C}_{10}\text{H}_{19}\text{NO}_3\text{S}$ 233.1086, found 233.1084. Anal. ($\text{C}_{10}\text{H}_{19}\text{NO}_3\text{S}$) C, H, N, S.

1-(Aminoxy)-4-mercaptobutane Hydrochloride (6). A solution of ethyl *N*-[[4-(acetylthio)butyl]oxy]acetimidate (5, 35.00 g, 0.150 mol) in absolute methanol (100 mL) was thoroughly degassed with nitrogen and treated with anhydrous K_2CO_3 (20.00 g, 0.150 mol), and the resulting yellow suspension was stirred vigorously for 12 h. Thin-layer chromatographic analysis of the reaction mixture indicated the absence of the starting thioacetate 5 (R_f 0.5 in A) and presence of the product thiol (R_f 0.65 in A). The suspension was filtered and concentrated in vacuo to a yellow slurry, which was dissolved in ethanol and treated with concentrated aqueous HCl (30 mL), and the resulting mixture was heated on a steam bath for 1 h. The volatiles were removed in vacuo, and the residue was azeotroped with 4 successive volumes of absolute ethanol. The volatile amine was isolated as its hydrochloride by dissolution of the solid in aqueous NaHCO_3 , extraction with diethyl ether, and treatment of the ether solution slowly dropwise with HCl in diethyl ether (1.0 M) until no further solid had formed. The solid was collected by filtration, washed with hexane, and recrystallized from ethanol–hexane to yield 12.0 g (51%) of 1-(aminoxy)-4-mercaptobutane hydrochloride (6) as a white solid: mp 134 °C dec; ^1H NMR (CD_3OD) δ 5.08 (br s, 6 H, exch, NH_2 , SH, HCl), 3.85 (t, J = 6 Hz, 2 H, NOCH_2), 2.30 (t, J = 6 Hz, 2 H, CH_2S), 1.54 (m, complex, 2 H, OCH_2CH_2), 1.46 (m, complex, 2 H, $\text{CH}_2\text{CH}_2\text{S}$); ^{13}C NMR (CD_3OD) δ 76.39 (NOCH_2), 31.37 (CH_2S), 27.70 (OCH_2CH_2), 24.99 and 24.85 ($\text{CH}_2\text{CH}_2\text{S}$); IR (KBr) 3450 (br), 2980 (s), 2790, 1502, 1025 cm^{-1} ; MS (DCI) m/e (relative abundance) 122 (MH^+ , 45), 104 ($\text{MH}^+ - \text{NH}_3$, 12), 75 ($\text{MH}^+ - \text{N}_2\text{H}_2\text{O}$, P); exact mass calcd for $\text{C}_4\text{H}_{11}\text{NOS}$

122.0640, found 122.0638. Anal. ($C_4H_{11}NOS \cdot HCl$) C, H, N, S.

In separate runs, the intermediate ethyl *N*-[(4-mercaptobutyl)oxy]acetimidate could be isolated after treatment with K_2CO_3 in MeOH by partitioning of the residue between ethyl acetate and water. The combined ethyl acetate layers were washed with brine, dried over K_2CO_3 , and concentrated in vacuo to a light yellow liquid which was distilled to give ethyl *N*-[(4-mercaptobutyl)oxy]acetimidate as a clear, yellow, foul-smelling liquid: bp 65–67 °C (5 mmHg); 1H NMR ($CDCl_3$) δ 4.00 (q, $J = 6$ Hz, 2 H, OCH_2CH_3), 3.90 (t, $J = 6$ Hz, 2 H, OCH_2CH_2), 2.57 (q, $J = 7$ Hz, 2 H, CH_2S), 1.92 (s, 3 H, $CH_3C(OEt)=N$), 1.72 (m, 4 H, $OCH_2CH_2CH_2CH_2$), 1.35 (t, $J = 7$ Hz, 1 H, SH), 1.27 (t, $J = 6$ Hz, 3 H, OCH_2CH_3); ^{13}C NMR ($CDCl_3$) δ 162.75 ($CH_3C(OEt)=N$), 73.14 (OCH_2CH_3), 62.39, 30.93 (CH_2SH), 27.86 (CH_2CH_2SH), 24.68 (OCH_2CH_2), 14.51 (OCH_2CH_3), 13.72; MS (DCI/methane) m/e (relative abundance) 192 (MH^+ , P).

1-(Aminoxy)-4-[(methoxycarbonyl)dithio]butane Hydrochloride (7). A solution of (methoxycarbonyl)sulfonyl chloride (5 mL, 0.061 mol) in dry, degassed MeOH was cooled to 0 °C and treated with 1-(aminoxy)-4-mercaptobutane hydrochloride (6, 8.0 g, 0.045 mol), and the resulting yellow solution was stirred at 0 °C for 1 h (HCl gas evolution was noted). The yellow solution was then thoroughly degassed with N_2 , and the solvents were removed in vacuo. The white solid obtained was recrystallized from methanol/ CH_2Cl_2 /hexane to yield (in three crops) 5.4 g (75%) of 1-(aminoxy)-4-[(methoxycarbonyl)dithio]butane hydrochloride (7) as sharp-melting, white flakes: mp 107–108 °C; 1H NMR (CD_3OD) δ 4.6 (br s, exch, 6 H, NH_2 , HCl), 3.82 (t, $J = 6$ Hz, 2 H, $NOCH_2$), 3.63 (s, 3 H, OCH_3), 2.59 (t, $J = 6$ Hz, 2 H, CH_2S), 1.57 (m, 4 H, $OCH_2CH_2CH_2CH_2S$); ^{13}C NMR (CD_3OD) δ 172.10 ($SCOOCH_3$), 76.28 ($NOCH_2$), 56.45 (SCH_2), 39.78 (OCH_2CH_2), 27.52 (CH_2CH_2), 25.97 ($COOCH_3$); IR (CH_3OH) 3433 (br), 1737 (s, $C=O$), 1195, 1142 (s) cm^{-1} ; MS (DCI/methane) m/e (relative abundance) 212 (MH^+ , 22), 179 ($MH^+ - CH_3OH$, P); exact mass calcd for $C_6H_{13}NO_3S_2$ 211.0337, found 211.0335. Anal. ($C_6H_{13}NO_3S_2 \cdot HCl$) C, H, N, S, Cl.

1-(Aminoxy)-4-[(3-nitro-2-pyridyl)dithio]butane Hydrochloride (1). A solution of 1-(aminoxy)-4-[(methoxycarbonyl)dithio]butane hydrochloride (7, 1.50 g, 0.00949 mol) in dry, degassed methanol (30 mL) was treated with 3-nitro-2-mercaptopyridine (1.48 g, 0.00949 mol) and the resulting yellow solution was stirred under N_2 at room temperature. After 12 h, thin-layer chromatographic analysis of the reaction mixture revealed the absence of the starting material 7 (R_f 0.5 in B) and presence of the product pyridine 1 (R_f 0.4 in B). The mixture was filtered to remove unreacted 3-nitro-2-mercaptopyridine, and the product was precipitated by the addition of ethyl acetate and finally ether to yield 1.3 g (50%) of 1-(aminoxy)-4-[(3-nitro-2-pyridyl)dithio]butane hydrochloride (1) as a yellow solid. An analytical sample was obtained by recrystallization from MeOH/ethyl acetate/ether to give 1 as a white, crystalline solid: mp 134–135 °C; 1H NMR (CD_3OD) δ 8.85 (dd, $J = 1.5, 4.5$ Hz, 1 H, ArH), 8.59 (dd, $J = 1.5, 8$ Hz, 1 H, ArH), 7.49 (dd, $J = 4.5, 8$ Hz, 1 H, ArH), 4.88 (br s, exch, 6 H), 4.05 (t, $J = 6$ Hz, 2 H, CH_2ON), 2.91 (t, $J = 6$ Hz, 2 H, CH_2SS), 1.83 (m, 4 H, $OCH_2CH_2CH_2CH_2S$); ^{13}C NMR (CD_3OD) δ 158.25 (Ar), 155.71 (Ar), 144.96 (Ar), 135.83 (Ar), 123.28 (Ar), 76.31 (OCH_2CH_2), 38.91 (CH_2SS), 27.78 (CH_2CH_2SS), 26.20 (OCH_2CH_2); IR (KBr) 3434 (br), 2946, 1584, 1558, 1512, 1402, 1398 (s), 1342 (s), 744 cm^{-1} ; MS (DCI) m/e (relative abundance) 278 ($MH^+ + 2$, 10), 276 (MH^+ , P); exact

mass calcd for $C_9H_{13}N_3O_3S_2$ 276.0477, found 276.0473. Anal. ($C_9H_{13}N_3O_3S_2 \cdot HCl$) C, H, N, S, Cl.

Ethyl *N*-[(4-Bromo-(*E*)-but-2-enyl)oxy]acetimidate (8). A 3-L three-necked round-bottomed flask equipped with mechanical stirrer, addition funnel, and gas inlet was oven dried, flushed with nitrogen, and allowed to cool under nitrogen. It was then charged with NaH (18.80 g, 0.470 mol, 60% dispersion in oil). The NaH was washed twice with hexane and covered with tetrahydrofuran (1 L), and with vigorous stirring, ethyl *N*-hydroxyacetimidate (3, 43.82 g, 0.420 mol) was added rapidly dropwise. Gas evolution was noted upon addition. After the addition was complete, the grey suspension was heated at reflux for 18 h. The suspension was then cooled and 1,4-dibromo-2-butene (100.00 g, 0.470 mol) was added rapidly dropwise. After the addition was complete, the resulting suspension was refluxed for 2 days under nitrogen. Thin-layer chromatographic analysis of the reaction mixture indicated the presence of the starting acetimidate (R_f 0.4 in A) and the presence of a less polar product (R_f 0.7 in A). The mixture was cooled and treated with methanol (50 mL) followed by saturated aqueous NH_4Cl (200 mL). The tetrahydrofuran was removed in vacuo, and the slurry that remained was partitioned between ethyl acetate and water. The combined ethyl acetate layers were washed with brine, dried over $MgSO_4$, filtered, and concentrated in vacuo to an oil which was distilled under vacuum to yield recovered ethyl *N*-hydroxyacetimidate (3, 10.0 g, 23%) and 64.5 g (65%) of ethyl *N*-[(4-bromo-(*E*)-but-2-enyl)oxy]acetimidate (8) as a colorless oil: bp 70–72 °C (2 mmHg); 1H NMR ($CDCl_3$) δ 5.89 (m, 2 H, $OCH_2CH=CHCH_2$), 4.37 (m, 2 H, $NOCH_2$), 3.97 (q, $J = 6$ Hz, 2 H, OCH_2CH_3) overlapping 3.93 (m, 2 H, CH_2Br), 1.90 (s, 3 H, $CH_3(OEt)=N$), 1.23 (t, $J = 6$ Hz, 3 H, OCH_2CH_3); ^{13}C NMR ($CDCl_3$) δ 163.21 ($CH_3C(OEt)=N$), 132.15 ($OCH_2CH=CH$), 129.38 ($BrCH_2CH=CH$), 73.11 ($CH_3CH_2OC(CH_3)=N$), 62.53 (OCH_2), 32.30 ($BrCH_2$), 14.51 (OCH_2CH_3), 13.85 ($CH_3C(OEt)=N$); IR (neat) 2981, 1647 (s), 1378 (s), 1307 (s), 1207, 1119, 1095, 1062, 1027 (s), 969 cm^{-1} ; MS (DCI) m/e (relative abundance) 238 ($MH^+ + 2$, 75), 236 (MH^+ , 80), 156 ($MH^+ - HBr$, P); exact mass calcd for $C_8H_{14}NO_2Br$ 235.0208, found 235.0203. Anal. ($C_8H_{14}NO_2Br$) C, H, N.

Ethyl *N*-[[4-(Acetylthio)-(*E*)-but-2-enyl]oxy]acetimidate (9). A solution of ethyl *N*-[(4-bromo-(*E*)-but-2-enyl)oxy]acetimidate (8, 32.4 g, 0.137 mol) in absolute ethanol (200 mL) was treated with potassium thioacetate (16.0 g, 0.140 mol) and the resulting yellow suspension was heated at reflux for 1 h. Thin-layer chromatographic analysis of the reaction mixture revealed the absence of the starting bromide 8 (R_f 0.7 in A) and the presence of the more polar product thioacetate 9 (R_f 0.5 in A). The mixture was cooled, filtered, and concentrated in vacuo, and the slurry was partitioned between ethyl acetate and water. The combined ethyl acetate layers were washed with saturated aqueous $NaHCO_3$ solution, water, and brine and then dried over $MgSO_4$, filtered, and concentrated in vacuo. The oil remaining was chromatographed over SiO_2 eluting with 9:1 hexane/ethyl acetate to yield 30 g (90%) of ethyl *N*-[[4-(acetylthio)-(*E*)-but-2-enyl]oxy]acetimidate (9) as a clear, yellow, foul-smelling liquid: 1H NMR ($CDCl_3$) δ 5.75 (dt, $J = 6, 15$ Hz, 1 H, $CH=CHCH_2SAc$), 5.61 (dt, $J = 7, 15$ Hz, 1 H, $OCH_2CH=CH$), 2.80 (d, $J = 7$ Hz, 2 H, $OCH_2CH=CH$), 3.93 (q, $J = 7$ Hz, 2 H, $CH_3CH_2OC(CH_3)=N$), 3.47 (d, $J = 6$ Hz, 2 H, CH_2SAc), 2.26 (s, 3 H, $SCOCH_3$), 1.85 (s, 3 H, $CH_3C(OEt)=N$), 1.18 (t, $J = 7$ Hz, 3 H, OCH_2CH_3); ^{13}C NMR ($CDCl_3$) δ 194.88

(SCOCH₃), 162.36 (CH₃C(OEt)=N), 129.89 (CH=CH), 128.03 (CH=CH), 73.23 (CH₃CH₂OC(CH₃)=N), 62.09 (NOCH₂), 30.86 (CH₂SCO), 30.35 (CH₃COS), 14.30 (CH₃CH₂O), 13.56 (CH₃C(OEt)=N); IR (neat) 2981, 2933, 2866, 1695 (s, C=O), 1646 (s, C=N), 1378 (s), 1306 (s, NOCH₂), 1105, 1024, 969, 627 cm⁻¹; MS (DCI) *m/e* (relative abundance) 234 (MH⁺ + 2, 8), 232 (MH⁺, P), 190 (MH⁺ - COCH₃, 10), 156 (MH⁺ - SCOCH₃, 12), 129 (MH⁺ - CH₃C(OEt)=N, 38); exact mass calcd for C₁₀H₁₇NO₃S 231.0920, found 231.0928. Anal. (C₁₀H₁₉NO₃S) C, H, N, S.

1-(Aminooxy)-4-mercapto-(E)-but-2-ene Hydrochloride (10). A solution of ethyl N-[[4-(acetylthio)-(E)-but-2-enyl]oxy]acetimidate (9, 18.50 g, 0.0799 mol) in absolute methanol (100 mL) was thoroughly degassed with nitrogen and treated with anhydrous K₂CO₃ (20.00 g, 0.144 mol), and the resulting yellow suspension was stirred vigorously for 2 h. The suspension was filtered and concentrated in vacuo to a yellow slurry which was dissolved in ethanol (100 mL) and treated with concentrated aqueous HCl (10 mL), and the resulting mixture was heated on a steam bath for 1 h. The yellow solution was concentrated in vacuo, and the residue was azeotroped with 4 successive volumes of absolute ethanol. The slurry remaining was dissolved in water and washed with ether (3 × 50 mL), and the ether layers were discarded. The solution was then basified with 2 N NaOH to pH 10 and extracted exhaustively with diethyl ether. The combined ether layers were dried over MgSO₄, filtered, and treated slowly dropwise with HCl in diethyl ether (1.0 M) until no more solid had formed. The solid was collected by filtration, washed with hexane, dried in vacuo and recrystallized from ethanol-hexane to yield 9.0 g (60%) of 1-(aminooxy)-4-mercapto-(E)-but-2-ene hydrochloride (10) as a white solid: mp 134–136 °C dec; ¹H NMR (CD₃OD) δ 5.77 (m, 5 lines, 1 H, CH=CH), 5.54 (m, 5 lines, 1 H, CH=CH), 4.63 (br s, 6 H, exch, NH₂, SH, HCl), 4.31 (d, *J* = 6 Hz, 2 H, NOCH₂), 3.15 (d, *J* = 6 Hz, 2 H, CH₂S); ¹³C NMR (CD₃OD) δ 136.42 (NOCH₂CH=CH), 127.02 (CH=CHCH₂S), 76.43 (OCH₂), 41.35 (CH₂S); IR (KBr) 2953, 2665, 1402, 970 cm⁻¹; MS (DCI) *m/e* (relative abundance) 118 (MH⁺ - 2, P); exact mass calcd for C₄H₁₁NOS 120.0483, found 120.0485. Anal. (C₄H₁₁NOS·HCl) C, H, N, Cl.

1-(Aminooxy)-4-[(3-nitro-2-pyridyl)dithio]-(E)-but-2-ene Hydrochloride (2). A solution of 1-(aminooxy)-4-mercapto-(E)-but-2-ene hydrochloride (10, 2.00 g, 0.0088 mol) in dry, degassed (N₂) methanol (20 mL) was cooled to 0 °C under N₂ and treated with (methoxycarbonyl)sulfonyl chloride (0.72 mL, 0.0088 mol). The resulting light yellow solution was stirred for 15 min and then degassed with N₂ and concentrated in vacuo. The slurry remaining was dissolved in methanol (20 mL) and treated in one batch with 3-nitro-2-mercaptopyridine (1.40 g, 0.0088 mol). The resulting suspension was stirred under N₂ at room temperature for 2 h, at which time thin-layer chromatographic analysis of the reaction mixture revealed the absence of 3-nitro-2-mercaptopyridine (*R_f* 0.1 in C) and the presence of the product (*R_f* 0.2 in C). The solution

was filtered to remove a small amount of precipitate, and the filtrate was diluted with ethyl acetate and ether. The resulting light yellow solid was filtered, washed with ether, and dried in vacuo to yield 1.34 g (56%) of yellow, solid material. An analytical sample was obtained by recrystallization from methanol/ethyl acetate/ether to yield 1-(aminooxy)-4-[(3-nitro-2-pyridyl)dithio]-(E)-but-2-ene hydrochloride (2) as light yellow flakes: mp 135 °C (sharp); ¹H NMR (CD₃OD) δ 8.62 (dd, *J* = 1.5, 5 Hz, 1 H, ArH), 8.36 (dd, *J* = 1.5, 8.5 Hz, 1 H, ArH), 7.26 (dd, *J* = 5, 8.5 Hz, 1 H, ArH), 5.77 (m, complex (5 lines), 1 H, CH=CH), 5.40 (dt, *J* = 7, 12 Hz, 1 H, CH=CH), 4.19 (d, *J* = 6.5 Hz, 2 H, OCH₂), 3.32 (d, *J* = 7 Hz, 2 H, CH₂S); ¹³C NMR (CD₃OD) δ 160.49 (Ar), 158.23 (Ar), 138.36 (CH=CH), 138.21 (Ar), 129.89 (CH=CH), 78.78 (OCH₂), 43.11 (CH₂S); IR (KBr) 3433, 2942, 1585, 1558, 1521, 1396, 1342, 746 cm⁻¹; MS (DCI/methane) *m/e* (relative abundance) 274 (MH⁺ + 1, 95), 241 (MH⁺ - NH₂OH, P); exact mass calcd for C₉H₁₁N₃O₃S₂ 274.0320, found 274.0317. Anal. (C₉H₁₁N₃O₃S₂·HCl) C, H, N, S.

LITERATURE CITED

- (1) Carlsson, J., Drevin, H., and Axen, R. (1978) Protein Thiolation and Reversible Protein-Protein Conjugation. *Biochem. J.* 173 723–737.
- (2) Upeslakis, J., and Hinman, L. (1988) Chemical Modification of Antibodies for Cancer Chemotherapy. *Annu. Rep. Med. Chem.* 23, 151–160.
- (3) Rodwell, J., and McKearn, T. (1987) Antibody Conjugates for the Delivery of Compounds to Target Sites. US Patent 4,671,958.
- (4) Braslawsky, G., Fitzgerald, K., Edson, M., Daues, A., Kaneko, T., Webb, R., Knipe, J., and Greenfield, R. (1989) Internalization as a Requirement for MAb-Directed Cell Killing by ADM-Immunoconjugates. Presented at the 80th Annual Meeting of the American Association for Cancer Research, Abstract #4494.
- (5) Khomutov, A. R., and Khomutov, R. M. (1986) Aminooxythiothreitol—New Agent for Introducing Reactive Thiol Groups Into Nucleic Acids. *Bioorg. Khim.* 12 (6), 845–847. Bromide 4 is reported in this paper, but without experimental details.
- (6) Field, L., and Ravichandran, R. (1979) Organic Disulfides and Related Substances. 42. Synthesis and Properties of Some Tertiary Disulfides, Especially Involving Penicillamine. *J. Org. Chem.* 44 (15), 2624–2629.
- (7) Surrey, A. R., and Lindwall, H. G. (1940) The reaction of 2-Chloro-5-nitropyridine and Thiourea. *J. Am. Chem. Soc.* 62, 1697–1698.

Robert R. Webb II^{*,†} and Takushi Kaneko[‡]

Department of Antitumor Chemistry,
Bristol-Myers-Squibb, Pharmaceutical Research and
Development Division, 5 Research Parkway,
Wallingford, Connecticut 06492-7660
February 12, 1990

[†] Current address: Medicinal and Biomolecular Chemistry Department, Genentech Inc., 460 Pt. San Bruno Blvd., South San Francisco, CA 94038.

[‡] Current address: Pfizer Central Research, Groton, CT 06430.

ARTICLES

Attachment of Rhodosaminylanthracyclinone-Type Anthracyclines to the Hinge Region of Monoclonal Antibodies[†]

P. Hermentin,* R. Doenges, P. Gronski, K. Bosslet, H. P. Kraemer, D. Hoffmann, H. Zilg, A. Steinstraesser, A. Schwarz, L. Kuhlmann, G. Lüben, and F. R. Seiler

Behringwerke AG, D-3550 Marburg/Lahn, FRG. Received July 10, 1989

We have found that a maleimidobenzoyl spacer attached to OH-4' of the rhodosamine moiety of rhodosaminylanthracyclinone-type anthracyclines is most suitable for the attachment of these drugs to carriers, providing important advantages: The spacer is selectively and most readily introduced into the rhodosamine moiety of the drugs, is stable enough for proper handling of the derivatives, and can easily be attached to thiol groups of carrier systems such as reduced monoclonal antibodies. The anthracyclines can be liberated from the conjugates by mere hydrolysis, requiring neither hydrolytic enzymes nor acidic pH. Liberation of the drugs can, moreover, be affected by the presence of the appropriate substituents Z on the phenylene ring of the spacer, thus allowing slowed or enhanced liberation of the cytostatically active drug. The corresponding *p*-maleimidobenzoyl derivatives of β -rhodomycin I, *N,N*-dimethyldaunorubicin, and rodorubicin have been attached to thiol groups of the hinge region of reduced monoclonal antibody BW 494/32, directed against a pancreatic cancer associated glycoprotein antigen, resulting in MoAb BW 494/32 conjugates, carrying 4.8–6.8 mol of cytotoxic residues/mol of MoAb. Rodorubicin was similarly attached to MoAb BW 575/931/2, directed against a small cell lung cancer associated antigen and to MoAb BW 431/26, recognizing an epitope detectable on carcinoembryonic antigen. The results provide evidence that the newly developed method of coupling of anthracyclines to the hinge region of monoclonal antibodies may be of broader use.

The concept of delivering a toxic moiety by a carrier that binds specifically to foreign tissue in the body but not to the host tissue has largely focused on the attachment of cytotoxic drugs to tumor-localizing monoclonal antibodies.

In this way the concentration of the drug would be selectively enhanced in tumor tissue, while the systemic concentration would be reduced, thus diminishing the toxic side effects of chemotherapy.

A vast amount of literature has already accumulated, dealing with the problems and methods of drug conjugation to carriers, and has been extensively reviewed and discussed by Ghose and colleagues (1–3).

For antibody-mediated selective delivery of chemotherapeutic agents an ideal conjugation method should (a) not interfere with either the agent or antibody activity, (b) allow high incorporation of drug, (c) avoid formation of homopolymers of antibody or agent, (d) avoid aggregation of conjugate, and (e) be technically straightforward and reproducible (1).

[†] This paper is dedicated to Prof. Dr. R. U. Lemieux, University of Alberta, Edmonton, Alta, Canada, on the occasion of his 70th birthday. A preliminary report of this subject has been presented at the International Symposium on Immunotoxins, Durham, NC, June 9–11, 1988 (*Abstracts of Papers*; pp 60–62).

¹ The abbreviations used are as follows: MoAb, monoclonal antibody; PMBZ, *p*-maleimidobenzoyl; PBS, phosphate-buffered saline; SCLC, small cell lung cancer; CEA, carcinoembryonic antigen; Ag, antigen; HPLC, high-performance liquid chromatography; TLC, thin-layer chromatography; NMR, nuclear magnetic resonance; TMS, tetramethylsilane; OD, optical density.

Coupling of drugs to ϵ -amino groups of lysine residues or to carboxyl groups of aspartic and glutamic acid residues of immunoglobulins appears most attractive from a practical point of view. One has to take into account, however, that these amino and carboxyl groups are distributed across the entire immunoglobulin molecule. As a consequence, drugs may be linked to areas where they might interfere with antibody specificity, namely the antibody-combining site of the Fab fragments (4, 5).

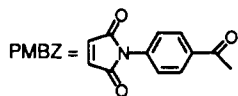
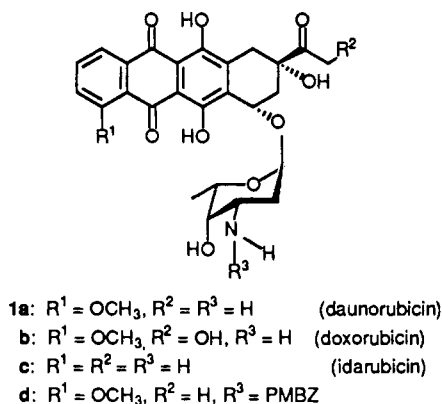
Although it is known that antibody specificity may be retained as long as drug conjugation does not exceed a certain level (6, 7), conjugation of drugs to areas remote from the antibody-combining site appears to be an attractive alternative (1, 2, 4, 5).

The approach we have focused on involves partial reduction of the immunoglobulin with mercaptoethanol or dithiothreitol (8, 9), which allows attachment of anthracycline maleimido derivatives to thiol groups of the hinge region (5).

In the anthracycline series, to our knowledge, daunorubicin (1a), doxorubicin (1b), and idarubicin (1c) (Scheme I) have thus far been coupled to antibody amino groups (a) via the amino group of the sugar (daunosamine) unit, (b) via the carbonyl function at C-13, or (c) via C-14 of the aglycon side chain. The methods developed in that regard have recently been reviewed (5).

Here we present a new method for the conjugation of rhodosaminylanthracyclinone-type anthracyclines, such as β -rhodomycin I (2a), *N,N*-dimethyldaunorubicin (3a), and rodorubicin (4a) (Scheme II), to monoclonal antibodies. These drugs, unlike daunorubicin (1a), doxorubicin (1b), and idarubicin (1c) (Scheme I), have neither a free amino group at their carbohydrate moiety(ies) nor

Scheme I. Daunorubicin and Related Structures



a side chain at C-9 of their aglycon that could be used to conjugate the drug. We have, however, found that the OH group of the sugar (rhodosamine) moiety can readily and regioselectively be acylated without affecting the OH groups of the aglycon (10), which we have exploited for the introduction of a *p*-maleimidobenzoyl spacer suitable for the attachment of the drug to the hinge region of monoclonal antibodies.

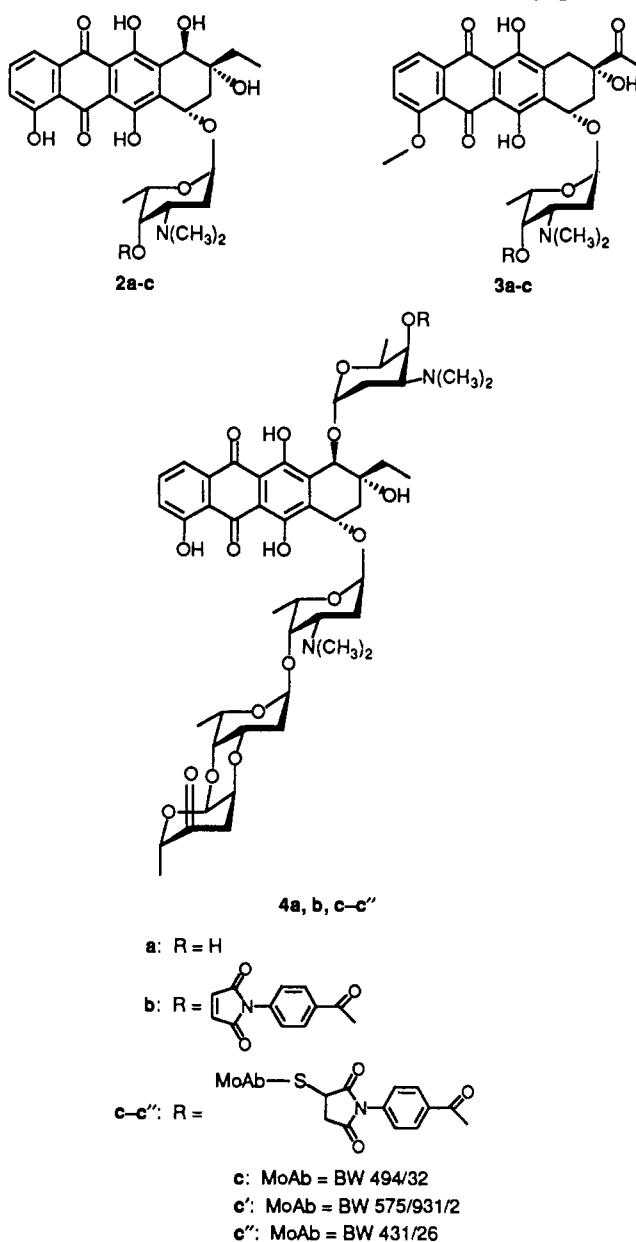
EXPERIMENTAL PROCEDURES

General Procedures. ^1H NMR spectra of chemical compounds were recorded at 90 MHz for the spacers or at 300 or 400 MHz for the anthracyclines with a JEOL FX 90 Q or a Bruker AC-300 or a Bruker AM-400 NMR spectrometer, respectively, using deuterated chloroform or deuterated dimethyl sulfoxide or a mixture of both as solvent and tetramethylsilane as internal standard. Chemical reactions were monitored by thin-layer chromatography on silica gel 60 plates F 254 (Merck), and spots were determined by their inherent color or by ultraviolet light.

Spacers. 4-Maleimidobenzoic acid, 2-chloro-4-maleimidobenzoic acid, and 2-acetoxy-4-maleimidobenzoic acid were prepared from 4-aminobenzoic acid, 2-chloro-4-aminobenzoic acid, and 2-hydroxy-4-aminobenzoic acid (Sigma), respectively, by reaction with maleic anhydride, similar to the procedure described by Yoshitake et al. (11). Briefly, the 4-aminobenzoic acids (36 mmol) were suspended in dry acetone (30 mL) and solubilized by the addition of dry methanol (5 mL). Then a solution of maleic anhydride (42 mmol) in dry acetone (10 mL) was added, and the precipitate which was formed was filtered off and dried in high vacuo. The precipitate (1 g) was treated with acetic anhydride (2 mL), containing anhydrous sodium acetate (170 mg), at 50 °C for 2 h. The clear solution formed was evaporated to dryness and stirred with water (30 mL) at 70 °C for 2 h. The precipitate which was formed was filtered off and dried in high vacuo. The ^1H NMR data were in agreement with the proposed structures. In each case the presence of the maleimido group was indicated by a singlet at around 7 ppm, integrating to two protons.

Activation of the Spacers. 4-Maleimidobenzoic acid, 2-chloro-4-maleimidobenzoic acid, 2-acetoxy-4-maleimidobenzoic acid (each prepared as described above), and 3-maleimidopropionic acid (Sigma) were reacted with thionyl chloride in anhydrous toluene at 120 °C for 3 h, as

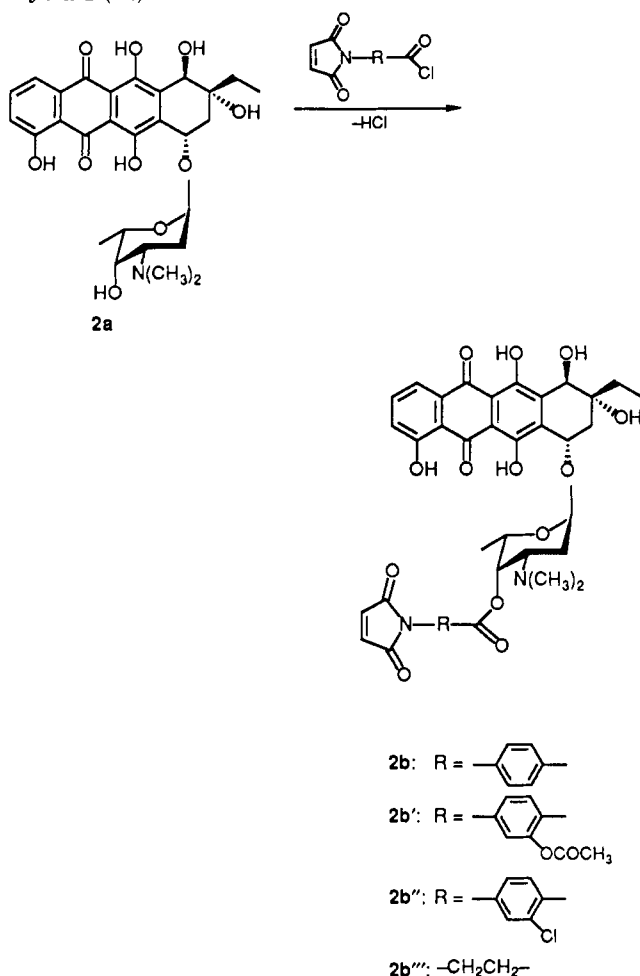
Scheme II. Structures of Compounds and Conjugates



described by Yoshitake et al. (11), to form the corresponding carboxyl chlorides. The solutions were evaporated to dryness, and the residues were dried in high vacuo and then kept at -30 °C until use.

Anthracyclines. *N,N*-Dimethyldaunorubicin (**3a**; Scheme II) was synthesized from daunorubicin (**1a**; Scheme I) (Farmitalia) according to Tong et al. (12). β -Rhodomycin I (**2a**; Scheme II) was prepared from β -rhodomycin II by acid hydrolysis (13). β -Rhodomycin II (13) and rodorubicin (**4a**; Scheme II) (14, 15) were kindly provided by Dr. H. G. Berscheid, Hoechst AG, Frankfurt/Main, FRG.

Introduction of Four Different Maleimido Spacers into β -Rhodomycin I (Scheme III). All four spacers, prepared as described above, were introduced into β -rhodomycin I (**2a**) in a two-phase (chloroform/water) solvent system in the presence of sodium bicarbonate, following a procedure described earlier (10), yielding **2b** ($R = \text{PMBZ}$, $Z = \text{H}$), **2b'** ($R = \text{PMBZ}$, $Z = \text{OCOCH}_3$), and **2b''** ($R = \text{PMBZ}$, $Z = \text{Cl}$), and **2b'''** ($R = -\text{CH}_2\text{CH}_2-$), respectively (Scheme III). The ^1H NMR data were in agreement with the proposed structures. The com-

Scheme III. Introduction of the Spacers into β -Rhodomycin I (2a)

pounds were kept at -30°C and were used for the experiments without further purification.

Introduction of a *p*-Maleimidobenzoyl Spacer into Drugs 2a, 3a, and 4a (Scheme II). β -Rhodomycin I (2a), *N,N*-dimethyl-daunorubicin (3a), and rodo-rubicin (4a) were each reacted with *p*-maleimidobenzoyl chloride, following the two-phase (chloroform/water) procedure (10). Briefly, the drugs (0.053 mmol, each) were dissolved in chloroform (10 mL) and saturated sodium bicarbonate (10 mL). A solution of *p*-maleimidobenzoyl chloride (0.076 mmol) in chloroform (3 mL) was added while the stirring was continued. The reaction was kept at ambient temperature in the dark and followed by TLC. After 16 h the organic phase was separated and evaporated to dryness, yielding the 4'-*O*-*p*-maleimidobenzoyl derivatives 2b, 3b, and 4b, respectively, which were kept at -30°C and used for the experiments without further purification.

2b: ^1H NMR (400 MHz, CDCl_3 , TMS) δ 13.61 (b s, 1 H, OH-11), 12.87 (b s, 1 H, OH-6), 12.10 (b s, 1 H, OH-4), 8.32 (d, 2 H, $J = 8.8$ Hz, phenylene: H-2, H-6), 7.88 (dd, 1 H, $J_{1,2} = 7.5$ Hz, $J_{1,3} = 1.0$ Hz, H-1), 7.71 (t, 1 H, $J_{1,2} = J_{2,3} = 8.0$ Hz, H-2), 7.53 (dd, 2 H, $J = 8.7$ Hz, phenylene: H-3, H-5), 7.33 (dd, 1 H, $J_{1,3} = 1.0$ Hz, $J_{2,3} = 7.4$ Hz, H-3), 6.88 (s, 2 H, maleimido-H), 5.67 (d, 1 H, $J_{1',2'} = 3.3$ Hz, H-1'), 5.57 (s, 1 H, H-4'), 5.18 (m, 1 H, H-7), 4.93 (s, 1 H, H-10), 4.33 (q, 1 H, $J_{5',6'} = 6.4$ Hz, H-5'), 2.36 (b s, 6 H, $\text{N}(\text{CH}_3)_2$), 2.23 (d, 1 H, $J_{8a,8b} = 15$ Hz, H-8b), 2.13 (dd, 1 H, $J_{7,8a} = 3.6$ Hz, $J_{8a,8b} = 15$ Hz, H-8a)

(superimposed by H-2'), 1.88 (m, 1 H, H-13 β), 1.78 (m, 1 H, H-13 α), 1.23 (d, 3 H, $J_{5',6'} = 6.4$ Hz, H₃-6'), 1.13 (t, 3 H, H₃-14).

3b: ^1H NMR (400 MHz, CDCl_3 , TMS) δ 14.01 (s, 1 H, OH-11), 13.28 (s, 1 H, OH-6), 8.21 (d, 2 H, $J = 8.3$ Hz, phenylene: H-2, H-6), 8.04 (d, 1 H, $J_{1,2} = 7.6$ Hz, H-1), 7.78 (t, 1 H, $J_{1,2} = J_{2,3} = 8.0$ Hz, H-2), 7.52 (d, 2 H, $J = 8.3$ Hz, phenylene: H-3, H-5), 7.39 (d, 1 H, $J_{2,3} = 8.4$ Hz, H-3), 6.89 (s, 2 H, maleimido-H), 5.70 (b s, 1 H, H-1'), 5.53 (b s, 1 H, H-4'), 5.34 (m, 1 H, H-7), 4.27 (q, 1 H, $J_{5',6'} = 6.3$ Hz, H-5'), 4.09 (s, 3 H, OCH_3), 3.25 (d, 1 H, H-10 β), 2.98 (d, 1 H, H-10 α), 2.44 (s, 3 H, H₃-14), 2.26 (s, 6 H, $\text{N}(\text{CH}_3)_2$), 1.21 (d, 3 H, $J_{5',6'} = 6.3$ Hz, H₃-6').

4b: ^1H NMR (400 MHz, CDCl_3 , TMS) δ 13.77 (b s, 1 H, OH-11), 12.86 (b s, 1 H, OH-6), 12.11 (b s, 1 H, OH-4), 8.17 (d, 2 H, $J = 8.7$ Hz, phenylene: H-2, H-6), 7.90 (d, 1 H, $J = 7.6$ Hz, H-1), 7.71 (t, 1 H, H-2), 7.50 (d, 2 H, $J = 8.7$ Hz, phenylene: H-3, H-5), 7.31 (dd, 1 H, $J_{1,3} = 1.0$ Hz, $J_{2,3} = 8.4$ Hz, H-3), 6.88 (s, 2 H, maleimido-H), 5.62 (b s, 1 H, H-4' of the spacers rhodosaminyl unit), 2.21 (b s, 12 H, $2 \times \text{N}(\text{CH}_3)_2$), 1.36 (d, 3 H), 1.30 (d, 3 H), 1.22 (d, 3 H), and 1.17 (d, 3 H) ($4 \times \text{H}_3$ -6' of four sugar units), 1.12 (t, 3 H, H₃-14).

Introduction of a *p*-Maleimidobenzoyl Spacer to the Amino Group of Daunorubicin. Daunorubicin (1a; Scheme I) was reacted with *p*-maleimidobenzoyl chloride under the conditions described above, resulting in a mixture of the corresponding O-substituted and N-substituted derivatives. Desired 3'-*N*-(*p*-maleimidobenzoyl)daunorubicin (1d; Scheme I) was purified by column chromatography on silica gel 60 (Merck 0.040–0.062 mm), using dichloromethane/methanol (95/5) as the solvent system (R_f 0.3). It is noteworthy that chromatography on silica gel of the O-substituted *p*-maleimidobenzoyl derivatives resulted in hydrolysis of the spacers (Hermentin et al., unpublished results).

1d: ^1H NMR (300 MHz, CDCl_3 , TMS) δ 13.97 (s, 1 H, OH-11), 13.23 (s, 1 H, OH-6), 8.01 (d, 1 H, $J_{1,2} = 7.7$ Hz, H-1), 7.79 (d, 2 H, $J = 8.5$ Hz, phenylene: H-2, H-6), 7.76 (t, 1 H, $J_{1,2} = J_{2,3} = 8.3$ Hz, H-2), 7.40 (d, 2 H, $J = 8.5$ Hz, phenylene: H-3, H-5), 7.36 (d, 1 H, $J_{2,3} = 8.7$ Hz, H-3), 6.84 (s, 2 H, maleimido-H), 6.63 (d, 1 H, $J_{\text{NH},3'} = 8.3$ Hz, NH), 5.53 (d, 1 H, $J_{1',2'} = 3$ Hz, H-1'), 5.23 (m, 1 H, H-7), 4.51 (s, 1 H, H-4'), 4.28 (q, 1 H, $J_{5',6'} = 6.4$ Hz, H-5'), 4.03 (s, 3 H, OCH_3), 3.22 (d, 1 H, $J_{10a,10b} = 19$ Hz, H-10b), 2.87 (d, 1 H, $J_{10a,10b} = 19$ Hz, H-10a), 2.43 (s, 3 H, H₃-14), 2.32 (d, 1 H, $J_{8a,8b} = 15$ Hz, H-8b), 2.11 (dd, 1 H, $J_{7,8a} = 4$ Hz, $J_{8a,8b} = 15$ Hz, H-8a), 1.31 (d, 3 H, $J_{5',6'} = 6.4$ Hz, H₃-6').

Stability of Various O-Linked Maleimidoacyl Spacers of β -Rhodomycin I. Compounds 2b–2b''' (Scheme III) were dissolved in acetonitrile at 1 mg/mL and diluted 100-fold with PBS, pH 7.2, such that the concentration of the anthracyclines was 10 $\mu\text{g/mL}$, each. The solutions were incubated in the dark at 37°C , and aliquots (20 μL , each) were examined by HPLC (Figures 1–3). The HPLC system consisted of a Perkin-Elmer ISS 100 Autosampler, a Gynkotheek 300 C pump, a Gynkotheek 250 B gradientformer, a 100×4 mm i.d. guard column combined with a 250×0.4 mm i.d. column, both filled with Lichrospher SI 100 RP 18 (100- μm particle size), and a Merck-Hitachi F 1000 fluorescence detector with the excitation and emission wavelength set at 495 and 560 nm, respectively. The sample constituents were eluted by using a 30-min linear acetonitrile gradient and a 10-min washout. The gradient consisted of a starting concentration of 10% acetonitrile/90% aqueous triethylamine (7% v/v) adjusted to pH 3.0 with phosphoric

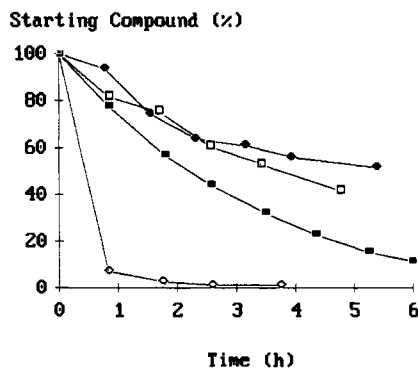


Figure 1. Stability of O-linked maleimidoacyl spacers of β -rhodomyacin I (**2a**) in PBS, pH 7.2, 37 °C (in presence of 1% acetonitrile): **2b**, \square ; **2b'**, \blacksquare ; **2b''**, \bullet ; **2b'''**, \circ .

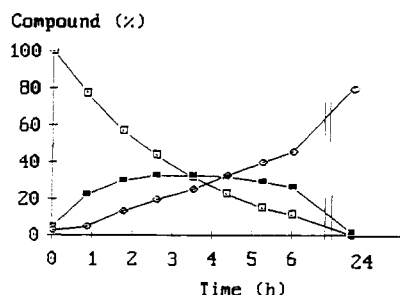


Figure 2. Hydrolysis of the spacer of compound **2b'** in PBS, pH 7.2, 37 °C (in presence of 1% acetonitrile): starting compound **2b'**, \square ; intermediate, \blacksquare ; product **2a**, \circ .

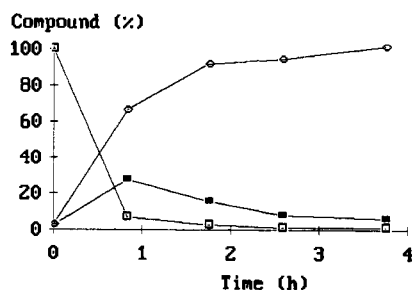


Figure 3. Hydrolysis of the spacer of compound **2b'''** in PBS, pH 7.2, 37 °C (in presence of 1% acetonitrile): starting compound **2b'''**, \square ; intermediate, \blacksquare ; product **2a**, \circ .

acid to a final concentration of 70% acetonitrile. The detector signal was recorded with a Perkin-Elmer LCI-100 integrator, and the peak areas of eluting compounds were calculated. The concentrations of compounds **2b**–**2b'''** (Scheme III) and their observed intermediate and hydrolysis products were expressed as a percentage of the initial peak area of the nonhydrolyzed compound (Figures 1–3).

Stability of an N-Linked *p*-Maleimidobenzoyl Spacer of Daunorubicin. Hydrolysis of 3'-*N*-(*p*-maleimidobenzoyl)daunorubicin (**1d**; Scheme I) was determined according to the procedure described above. Due to solubility problems of **1d** in PBS, the experiment was performed in the presence of 10% (instead of 1%) acetonitrile (Figure 4).

Conjugation of β -Rhodomyacin I (2a**), *N,N*-Dimethyldaunorubicin (**3a**), and Rodorubicin (**4a**) (Scheme II) to Monoclonal Antibody BW 494/32.** MoAb BW 494/32, directed against a pancreatic cancer associated glycoprotein antigen (**16**), was used as carrier system. The antibody was reduced by dithiothreitol, following the procedure outlined by Linford et al. (8), and maleimidobenzoyl derivatives **2b**, **3b**, and **4b** were attached to uncovered thiol groups of the hinge region, resulting in the cor-

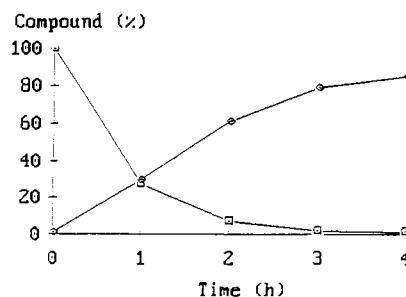


Figure 4. Stability of compound **1d** in PBS, pH 7.2, 37 °C (in presence of 10% acetonitrile): starting compound, \square ; carboxy-benzamido derivative, \circ .

responding conjugates β -rhodomyacin I–BW 494/32 (**2c**), *N,N*-dimethyldaunorubicin–BW 494/32 (**3c**), and rodorubicin–BW 494/32 (**4c**), respectively. Reaction scales, conjugation ratios, and yields are summarized in Table I. The conjugation may be generalized as follows.

A solution of the antibody (15 mg) in physiological saline, pH 7.2 (1 mL), was subjected to reduction by dithiothreitol (5 mg) for 30 min at ambient temperature. The reduced antibody was isolated by gel filtration over Sephadex G25 in physiological saline, pH 6.0, yielding 5 mL, which was diluted with dimethylformamide, pH 6.0 (1 mL). A solution of the maleimido derivative of the drug (0.005 mmol), dissolved in dimethylformamide (0.5 mL), was added and incubated in the dark for 1 h. The conjugates were purified by gel filtration over Sephadex G25 columns equilibrated and eluted with physiological saline, pH 7.2. The combined conjugate fractions (8 mL) were sterile filtered (filter with pore size 0.2 μ m) and kept frozen at –30 °C until use.

Conjugation of 4'-*O*-(*p*-Maleimidobenzoyl)rodorubicin (4b**; Scheme II) to Monoclonal Antibodies BW 575/931/2 and BW 431/26.** The conjugation was performed in analogy to the procedure described above, resulting in the corresponding conjugates rodorubicin–BW 575/931/2 (**4c'**) and rodorubicin–BW 431/26 (**4c''**) (Scheme II). Reaction scales, conjugation ratios, and yields are summarized in Table I.

Determination of Drug/Antibody Molar Ratios. Drug/antibody molar ratios of the conjugates were determined in physiological saline by measuring their absorbance at 495 and 280 nm. The measurements are summarized in Table I. The molar extinction coefficients of maleimido derivatives **2b**, **3b**, and **4b** (Scheme II), which were used for calculating the conjugation ratios, were determined in dimethylformamide at pH 6–7 and are summarized in Table II. Differences in extinction, resulting from differences in the solvents or from converting a maleimido group to a substituted succinimidyl group, as present in the conjugates, were neglected. The extinction coefficients of the antibodies were assumed to correlate with the extinction coefficients determined for human IgG (Table II), using the microkjeldahl method to determine the concentration of human IgG.

Specificity of MoAb BW 494/32 Conjugates **2c, **3c**, and **4c** (Scheme II) in Vitro.** The three MoAb BW 494/32 conjugates **2c** (β -rhodomyacin I–BW 494/32), **3c** (*N,N*-dimethyldaunorubicin–BW 494/32), and **4c** (rodorubicin–BW 494/32), were tested in Terasaki indirect immunofluorescence assays, as described elsewhere (17), against two Ag⁺ colon carcinoma cell lines (LoVo and DeTa). Rodorubicin–BW 575/931/2 (**4c'**), directed against a small cell lung cancer cell line, was used as a negative control. A small cell lung cancer cell line (GOT), reacting with MoAb BW 575/931/2, was used as a positive control for rodorubicin–BW 575/931/2 (**4c'**) and as a neg-

Table I. Photometric Evaluation of the Conjugates

conjugate	absorbance of the conjugates		absorbance of the protein content of the conjugates: 280 nm	conjugation ratio, (mol of drug/mol of antibody)	used for coupling, mg	amount of protein		
	495 nm	280 nm				isolated after coupling		
						mL	mg	% yield
2c	0.76	2.71	1.74	6.8	35	17	19.5	56
3c	0.52	2.74	1.92	4.8	30	15	18.9	63
4c	1.03	4.01	2.77	5.8	42	13	23.6	56
4c'	0.47	1.78	1.21	6.0	15	8.5	6.8	45
4c''	0.41	1.80	1.31	4.8	15	11	9.5	63

Table II. Molar Extinction Coefficients of Maleimido Derivatives 2b, 3b, and 4b and Conjugates 2c, 3c, and 4c-c''

compd	λ_{\max} , nm	molar extinction coefficient		solvent
		ϵ	ϵ_{495}	
2b	269	18 700	14 600	DMF
2c	280	355 000	99 300	saline
3b	276	20 500	13 000	DMF
3c	280	325 000	62 400	saline
4b	274	17 800	14 800	DMF
4c	280	331 000	85 800	saline
4c'	280	335 000	88 800	saline
4c''	280	313 000	71 000	saline
human IgG	280	228 000		saline

ative control for the MoAb BW 494/32 conjugates 2c, 3c, and 4c. All conjugates were shown to retain their specificities against the Ag⁺ cell lines.

Specificity of Rodorubicin Conjugates 4c, 4c', and 4c'' (Scheme II) in Vitro. The specificity of rodorubicin conjugates 4c, 4c', and 4c'' was evaluated with a double enzyme amplification ELISA, described by Stanley et al. (18). In brief, the antigens bearing the epitopes recognized by the respective MoAb were isolated from cell culture supernatants by using monoclonal immunoaffinity chromatography. Eluate (50 μ L) containing 10 ng of purified antigen was coated onto microtiter plates. The binding of the respective MoAb to the solid phase attached antigen was evaluated with a double enzyme, alcoholdehydrogenase and diaphorase, amplification system. Optical density was measured at 492 nm in a Titertek multi-scan. OD values exceeding the double standard deviation of the negative control were considered to be positive. The results are summarized in Table III.

Homogeneity of Rodorubicin Conjugates 4c, 4c', and 4c'' (Scheme II). Rodorubicin-BW 494/32 (4c), rodorubicin-BW 575/931/2 (4c'), and rodorubicin-BW 431/26 (4c'') were analyzed by high-performance gel permeation on a TSK G 3000 SW column with the eluant 0.07 mol/L sodium phosphate + 0.1 mol/L sodium chloride, pH 7.2, and detection at 280 and 490 nm. Eluting conjugate species were grouped into monomers, dimers + trimers, and aggregates (greater than trimers). The results are summarized in Table IV.

Liberation of Anthracyclines 2a, 3a, and 4a from Conjugates 2c, 3c, and 4c, Respectively (Scheme II, Figure 5). Solutions of MoAb BW 494/32-conjugates 2c, 3c, and 4c in physiological saline were incubated at 37 °C for up to 11 days. Aliquots of 140 μ L, each, were removed at time zero and on consecutive days and were kept frozen at -30 °C until analysis. Liberated β -rhodomycin I (2a), *N,N*-dimethyldaunorubicin (3a), and rodorubicin (4a) (Scheme II) were identified and determined by using an HPLC method described elsewhere (19). The compounds eluted at 2.8, 11.8, and 8.8 min, respectively, under the chromatographic conditions applied. The results are summarized in Figure 5.

Internalization of Rodorubicin-BW 494/32 (4c) into Cancer Cells in Vitro. Internalization of conjugate 4c into colon carcinoma (CoWi) cells in vitro was determined as described by Matzku et al. (20), using a mela-

noma cell line (M21) and a rodorubicin-BW 575/931/2 conjugate (4c') directed against a small cell lung cancer associated antigen as well as MoAb BW 494/32 alone as controls (Figure 6).

Cytotoxicity of Rodorubicin (4a), Rodorubicin-BW 494/32 (4c), and Rodorubicin-BW 431/26 (4c'') (Scheme II) in Vitro. The cytotoxicity was evaluated by incubating Ag⁺ (LoVo) cells and three Ag⁻ cell lines (L1210, GOT, and M21) with different concentrations of the immunoconjugate as well as of free rodorubicin as previously described (21). Short term (1 h) and long term (7 days) incubations were performed simultaneously to evaluate differences in membrane permeability and membrane binding. After in vitro growth for 14 days the total number of tumor cell colonies was counted with an automated image analysis system (FAS II, Bausch & Lomb) (Table V).

RESULTS

Evaluation of the Spacers. Hydrolysis of the spacers in PBS, pH 7.2, at 37 °C, was clearly apparent by HPLC analysis (Figure 1), indicating liberation of β -rhodomycin I (2a) from maleimido derivatives 2b-2b''' (Scheme III) either directly or via the corresponding carboxybenzamido intermediates which were formed by hydrolytic (nucleophilic) attack of the maleimido groups (see, e.g., Figure 2 for hydrolysis of 2b' and Figure 3 for hydrolysis of 2b''', respectively). An aliphatic 3-maleimidopropionyl spacer (in compound 2b''') proved to be the least stable (Figures 1 and 3), providing a half-life of 2b''' of ~30 min. With this spacer the formation of the carboxybenzamido intermediate was negligible due to the much faster liberation of β -rhodomycin I (2a) (Figure 3). In contrast, hydrolysis of 3'-*N*-(*p*-maleimidobenzoyl)daunorubicin (1d; Scheme I) led to the corresponding carboxybenzamido derivative as the only product (Figure 4), exhibiting a retention time of 24.0 min. The retention time of an authentic sample of daunorubicin (1a; Scheme I) was determined to 19.8 min, with the same HPLC conditions.

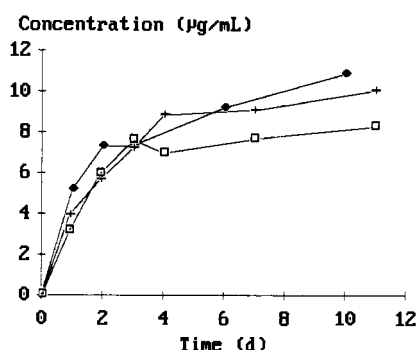
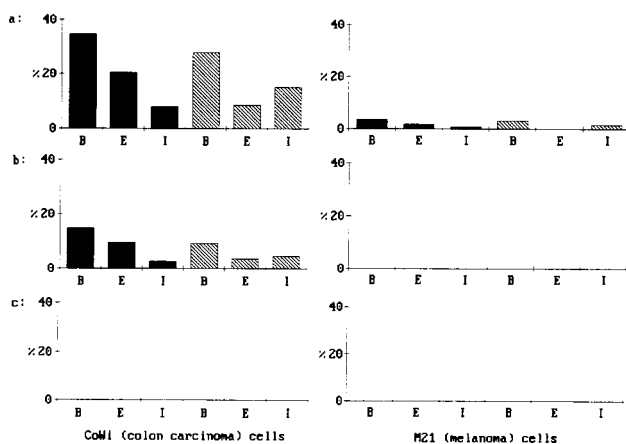
Evaluation of the Conjugates in Vitro. For the conjugates the conjugation ratios were calculated to be 4.8-6.8 (mol of drug/mol of antibody) (Table I), using the molar extinction coefficients summarized in Table II. The specificity of the different conjugates 4c (rodorubicin-BW 494/32), 4c' (rodorubicin-BW 575/931/2), and 4c'' (rodorubicin-BW 431/26) (Scheme II) was completely retained (Table III). All three conjugates consisted of a mixture of conjugate monomers (76-84%) and dimers + trimers (16-24%; the ratio of dimers/trimers usually was in the range of 10/1), while the presence of higher aggregates was negligible (Table IV). Half-life of liberation of anthracyclines 2a, 3a, and 4a from conjugates 2c, 3c, and 4c, respectively, was in the range of 1.5 days, each (Scheme II, Figure 5). As can be seen from Figure 6, the rodorubicin-BW 494/32 conjugate (4c) was efficiently internalized into CoWi (Ag⁺) cells in vitro (Figure 6a) whereas the nonspecific rodorubicin-BW 575/931/2 conjugate (4c') was neither bound nor internalized (Figure

Table III. Specificity of Rodorubicin Conjugates 4c-4c'' (Scheme II), Determined by Double Enzyme Amplification ELISA for the Evaluation of MoAb Binding to Solid Phase Attached Purified Antigens

antibody or conjugate	purified antigen preparation														
	pancreatic carcinoma cell-line associated mucin					SCLC associated mucin					carcinoembryonic antigen (CEA)				
	5000	500	50	5	0.5	5000	500	50	5	0.5	5000	500	50	5	0.5
BW 494/32	++	++	+	+	-	-	-	-	-	-	-	-	-	-	-
conjugate 4c	++	++	+	+	-	-	-	-	-	-	-	-	-	-	-
BW 575/931/2	-	-	-	-	-	++	+	+	-	-	-	-	-	-	-
conjugate 4c'	-	-	-	-	-	++	+	+	-	-	-	-	-	-	-
BW 431/26	-	-	-	-	-	-	-	-	-	-	++	++	++	+	-
conjugate 4c''	-	-	-	-	-	-	-	-	-	-	++	++	+	+	-

Table IV. Homogeneity of Rodorubicin-BW 494/32 (4c), Rodorubicin-BW 575/931/2 (4c'), and Rodorubicin-BW 431/26 (4c'') (Scheme II) as Determined by Gel Permeation

conjugate	conjugate species	frequency, % peak area at 280 nm
4c	monomers	76.2
	dimers + trimers	23.6
	aggregates	0.2
4c'	monomers	83.6
	dimers + trimers	16.2
	aggregates	0.2
4c''	monomers	81.3
	dimers + trimers	18.0
	aggregates	0.7

**Figure 5.** Liberation of anthracyclines 2a, 3a, and 4a from conjugates 2c, 3c, and 4c, respectively (Scheme II): □, liberation of 2a from 2c; +, liberation of 3a from 3c; ●, liberation of 4a from 4c.**Figure 6.** Internalization into cancer cells in vitro: a, rodorubicin-BW 494/32 (4c); b, MoAb BW 494/32; c, rodorubicin-BW 575/931/2 (4c'); B = bound, E = eluted, I = internalized; 4 °C, black bar; 37 °C, hatched bar.

6c). MoAb BW 494/32 alone was bound to CoWi cells to a lesser extent than conjugate 4c, and its internalization into CoWi cells was also comparably low (Figure 6b). Some nonspecific binding of conjugate 4c to M21 (Ag⁺)

melanoma cells was also detectable (Figure 6a), which might be attributable to hydrophobic interactions between the lipophilic drug and the cell membrane (Hermentin et al., unpublished results).

Conjugates 4c (rodorubicin-BW 494/32) and 4c'' (rodorubicin-BW 431/26) (Scheme II) were significantly less cytotoxic in vitro than free rodorubicin (4a), based on identical amounts of drug, in the 1 h incubation test (Table V). The conjugates appeared similarly cytotoxic as the free drug after incubation for 7 days, most likely due to hydrolytic liberation of cytostatically active rodorubicin (4a). There was, however, no indication for preferential cytotoxicity of rodorubicin conjugates 4c and 4c'' to human colon carcinoma (LoVo) cells expressing the appropriate antigen.

DISCUSSION

We have synthesized anthracycline-monoconal antibody conjugates (Scheme II) from which the cytostatically active drugs can again be released by mere hydrolysis under physiological conditions (Figure 5), requiring neither hydrolytic enzymes nor acidic pH. Our newly developed heterobifunctional spacers of choice, 4-maleimidobenzoyl chlorides, are regioselectively reacted with OH-4' of the rhodosamine moiety of anthracyclines (Schemes II and III). The maleimido derivatives formed are stable enough for proper handling and can easily be attached to thiol groups of carrier systems such as reduced monoclonal antibodies. Liberation of the free anthracycline from the maleimido derivative can be affected by the appropriate substituents Z of the phenylene ring of the spacer, thus allowing control of the rate of liberation of the cytostatically active drug (Figure 1).

An aliphatic maleimido spacer, on the other hand, is not stable enough for proper handling and in vivo application of corresponding conjugates, and therefore was not further developed.

The higher stability of the maleimidobenzoyl ester derivatives of β -rhodomycin I, 2b-2b'', in comparison to their aliphatic analogue 2b''' (Scheme III), may be due to reduced polarization of the carbonyl bond as a result of the positive mesomeric effect of the neighboring phenylene group. As can be seen from Figure 1, a 2-chloro substituent in the phenylene group somewhat slowed hydrolysis of the spacer bond, thus enhancing stability of the compound. A 2-acetoxy substituent, on the other hand, greatly enhanced susceptibility to hydrolysis, presumably as a result of the negative mesomeric and inductive effects of the acetoxy group on the neighboring carboxyl group, thus facilitating nucleophilic (hydrolytic) attack of the ester bond.

The *p*-maleimidobenzoyl spacer of compound 2b was chosen for further evaluation and was analogously introduced into other rhodosaminylanthracyclinone-type anthracyclines such as *N,N*-dimethyldaunorubicin (3a)

Table V. Cytotoxicity against LoVo (Ag⁺), L1210 (Ag⁻), GOT (Ag⁻), and M21 (Ag⁻) Cells in Vitro of Conjugates 4c and 4c'' (Scheme II) and of Rodorubicin (4a) after Incubation for 1 h or 7 Days, Expressed as 50% Inhibition of Tumor Growth (IC₅₀, µg/mL)^a

test substance	LoVo ⁺		L1210 ⁻		GOT ⁻		M21 ⁻	
	1 h	7 day	1 h	7 day	1 h	7 day	1 h	7 day
rodorubicin-BW 494/32 (4c)	>1	0.032	0.26	<0.004	>1	nd ^b	0.51	nd
rodorubicin-BW 431/26 (4c'')	0.61	nd	0.19	<0.04	nd	nd	0.33	nd
rodorubicin (4a)	0.2	0.025	0.010	0.003	0.015	nd	0.029	nd

^a LoVo, human colon carcinoma; L1210, mouse leukemia; GOT, human small cell lung cancer; M21, human melanoma. ^b nd = not determined.

and rodorubicin (4a) (Scheme II). Attachment of derivatives 2b, 3b, and 4b to MoAb BW 494/32 was performed at pH 6.0 in order to increase the solubility of the drugs by protonation of the dimethylamino groups. This was especially important for the conjugation of 4''-O-(p-methoxybenzoyl)rodorubicin (4b), which exhibited the highest lipophilicity as determined by its partition coefficient between water and *n*-octanol (22). For the same reason, the conjugation was performed in presence of dimethyl formamide, 20% (v,v), which did not hamper the antibody specificity, but provided conjugation ratios of 4.8–6.8 (mol of drug/mol of antibody) (Table I). Due to the presence of a hydrolysable spacer, the conjugates were kept frozen at -30 °C until use.

In contrast, as expected, the *p*-maleimidobenzoyl spacer proved stable when it was attached to an anthracycline by way of an amide linkage instead of an ester linkage. As can be seen from Figure 4, the amide linkage of 3'-N-(*p*-maleimidobenzoyl)daunorubicin (1d; Scheme I) could not be hydrolyzed and, as a consequence, daunorubicin (1a) could not be liberated from 1d. The observed disappearance of 1d has rather to be attributed to hydrolytic attack of the maleimido function, resulting in the corresponding carboxybenzamido derivative.

In order to evaluate our new method of coupling on a broader base, three different anthracyclines, i.e. β-rhodomyacin I (2a), *N,N*-dimethyldaunorubicin (3a), and rodorubicin (4a) (Scheme II), were coupled to MoAb BW 494/32 as our first choice carrier. The half-life of liberation of these anthracyclines from the corresponding conjugates 2c, 3c, and 4c, respectively (Figure 5), was estimated at approximately 1.5 days, under the assumption of first-order kinetics, which was regarded as slow enough for in vivo use. Rodorubicin (4a), our first choice drug, was further coupled to MoAb BW 575/931/2, directed against a small cell lung cancer associated antigen (23), and to MoAb BW 431/26, recognizing an epitope detectable on carcinoembryonic antigen (24). In every case, the conjugation ratio (mol of drug/mol of antibody) was between 4.8 and 6.8 (Table I; for molar extinction coefficients, see Table II) without observing any loss of MoAb specificity (Table III). The homogeneity of the three rodorubicin conjugates rodorubicin-BW 494/32 (4c), rodorubicin-BW 575/931/2 (4c'), and rodorubicin-BW 431/26 (4c'') (Scheme II) was somewhat impaired by the presence of conjugate oligomers (16–24%; mostly conjugate dimers) (Table IV). Their formation may be attributed to intermolecular recombination of hinge thiol groups to disulfide bonds and may be less prevalent if deoxygenated buffers and EDTA were used.

Rodorubicin-MoAb BW 494/32 (4c) was selected to be investigated in more detail, and the results may be summarized as follows. Conjugate 4c was efficiently internalized into CoWi tumor cells in vitro (Figure 6). It exhibited about 26-fold lower cytotoxicity toward L1210 mouse leukemic cells during short term (1 h) incubation in vitro than the free drug and approximated the cytotoxicity of free rodorubicin against L1210 cells after a long term (7

day) incubation period. As the half-life of hydrolytic liberation of the cytostatically active anthracyclines from the conjugates at 37 °C was estimated to be in the range of 1.5 days (Figure 5), practically all rodorubicin should be liberated from conjugates 4c and 4c'' after a 7 day incubation period, which could explain the killing of the antigen-negative cells (Table V). There was, however, no indication for preferential cytotoxicity of either conjugate 4c or 4c'' (Scheme II) toward human colon carcinoma (LoVo) cells expressing the appropriate antigen (Table V). This may be explained by our finding (Bosslet et al., unpublished results) that the number of epitopes per cell expressed by LoVo cells in vitro and recognized by the corresponding antibody (or conjugate) is approximately 100 000 for BW 494/32 and only about 30 000 for BW 431/26, which probably is too low to mediate any specific cytotoxicity in vitro. As the number of relevant epitopes expressed by LoVo cells in vivo may be about 10-fold higher than that found in vitro, based on the amounts of antigen isolated from human tumor xenografts (Bosslet et al., unpublished results), the conjugates are currently being tested in appropriate in vivo models. It may, however, be anticipated that an anthracycline of higher cytotoxicity than rodorubicin and a spacer of higher stability than *p*-maleimidobenzoyl should finally be chosen for further evaluation.

ACKNOWLEDGMENT

The authors are grateful to S. Muth for typing the manuscript. The skillful technical assistance of U. Maetze, H. Schmidt, and R. Frank has to be especially acknowledged.

LITERATURE CITED

- (1) Ghose, T. I., Blair, A. H., and Kulkarni, P. N. (1983) Preparation of antibody-linked cytotoxic agents. *Methods Enzymol.* 93, 280–333.
- (2) Blair, A. H., and Ghose, T. I. (1983) Linkage of cytotoxic agents to immunoglobulins. *J. Immunol. Methods* 59, 129–143.
- (3) Ghose, T., and Blair, A. H. (1987) The design of cytotoxic-agent-antibody conjugates. *Crit. Rev. Ther. Drug Carrier Syst.* 3, 263–359.
- (4) Hofstaetter, T., Gronski, P., and Seiler, F. R. (1984) Immunotoxins—Theoretical and practical aspects. *Behring Inst. Mitt.* 74, 113–121.
- (5) Hermentin, P., and Seiler, F. R. (1988) Investigations with monoclonal antibody drug (anthracycline) conjugates. *Behring Inst. Mitt.* 82, 197–215.
- (6) Kulkarni, P. N., Blair, A. H., and Ghose, T. I. (1981) Covalent binding of methotrexate to immunoglobulins and the effect of antibody-linked drug on tumor growth in vivo. *Cancer Res.* 41, 2700–2706.
- (7) Baldwin, R. W. (1985) Design and development of drug-monoclonal antibody 791T/36 conjugate for cancer therapy. *Dev. Oncol.* 38, 23–56.
- (8) Linford, J. H., Froese, G., Berczi, I., and Israels, L. G. (1974) An alkylating agent-globulin conjugate with both alkylating and antibody activity. *J. Natl. Cancer Inst.* 52, 1665–1667.

- (9) Youle, R. J., and Neville, D. M., Jr. (1980) Anti-Thy 1.2 monoclonal antibody linked to ricin is a potent cell-type-specific toxin. *Proc. Natl. Acad. Sci. U.S.A.* 77, 5483-5486.
- (10) Hermentin, P., Raab, E., Paal, M., Boettger, D., Berscheid, H. G., Gerken, M., and Kolar, C. (1989) Synthesis and structure elucidation of p-methoxybenzoyl derivatives of rhodomycins. *J. Carbohydr. Chem.* 8, 255-263.
- (11) Yoshitake, S., Yamada, Y., Ishikawa, E., and Masseyeff, R. (1979) Conjugation of glucose oxidase from *Aspergillus niger* and rabbit antibodies using *N*-hydroxysuccinimide ester of *N*-(4-carboxycyclohexylmethyl)-maleimide. *Eur. J. Biochem.* 101, 395-399.
- (12) Tong, G. L., Wu, H. Y., Smith, T. H., and Henry, D. W. (1979) Adriamycin analogues. 3. Synthesis of *N*-alkylated anthracyclines with enhanced efficacy and reduced cardiotoxicity. *J. Med. Chem.* 22, 912-918.
- (13) Brockmann, H., Waehnelt, T., and Niemeyer, J. (1969) Konstitution und Konfiguration von β -Rhodomycin II und β -Isorhodomycin II. *Tetrahedron Lett.* 415-419.
- (14) Huber, G., Berscheid, H. G., Fehlhaber, H.-W., and Kraemer, H. P. (1983) Anthracyclin-Derivative, ein Verfahren zu ihrer Herstellung und ihre Verwendung als Zytostatika. EP 0131942 A1.
- (15) Kraemer, H. P., and Sedlacek, H. H. (1988) Rodorubicin, a new tetraglycosidic anthracycline. *Behring Inst. Mitt.* 82, 216-230.
- (16) Bosslet, K., Kern, H. F., Kanzy, E. J., Steinstraesser, A., Schwarz, A., Lueben, G., Schorlemmer, H. U., and Sedlacek, H. H. (1986) A monoclonal antibody with binding and inhibiting activity towards human pancreatic carcinoma cells. I. Immunohistological and immunochemical characterization of a murine monoclonal antibody selecting for well differentiated adenocarcinomas of the pancreas. *Cancer Immunol. Immunother.* 23, 185-191.
- (17) Bosslet, K., Kurrle, R., Ax, W., and Sedlacek, H. H. (1983) Monoclonal murine antibodies with specificity for tissue culture lines of human squamous-cell carcinoma of the lung. *Cancer Detect. Prev.* 6, 181-184.
- (18) Stanley, C. J., Paris, F., Plumb, A., Webb, A., and Johanson, A. (1985) Enzyme amplification: a new technique for enhancing the speed and sensitivity of enzyme immunoassays. *Int. Comm. radiat. prot.* 3, 44-52.
- (19) Zilg, H. A., Kraemer, H. P., and Ronneberger, H. (1987) Pharmacokinetics of the anthracycline cytorhodin S in dogs. In *The Proceedings of the 3rd European Congress of Biopharmaceutics and Pharmacokinetics, Freiburg, FRG* (Aiche J. M. and Hirtz J., Ed.) Vol. II, pp 420-425, University Press of Clermont-Ferrand, France.
- (20) Matzku, S., Broecker, E.-B., Brueggen, J., Dippold, W., and Tilgen, W. (1986) Modes of binding and internalization of monoclonal antibodies to human melanoma cell lines. *Cancer Res.* 46, 3848-3854.
- (21) Kraemer, H. P., and Sedlacek, H. H. (1984) A modified screening system to select new cytostatic drugs. *Behring Inst. Mitt.* 74, 301-328.
- (22) Hoffmann, D., Sedlacek, H. H., Hermentin, P., Berscheid, H. G., Boettger, D., and Kraemer, H. P. (1990) Structure-activity relationship of anthracyclines in vitro. *J. Med. Chem.* 33, 166-171.
- (23) Bosslet, K., Kunze, W. P., Schwarz, A., Steinstraesser, A., and Sedlacek, H. H. (1987) Monoclonal antibodies (MAbs) suited for the immunoscintigraphic differential diagnosis of human lung carcinomas. *J. Steroid Biochem.* 28 (Suppl.), 2095.
- (24) Bosslet, K., Lueben, G., Schwarz, A., Hundt, E., Harthus, H. P., Seiler, F. R., Muhrer, C., Kloeppel, G., Kayser, K., and Sedlacek, H. H. (1985) Immunohistochemical localization and molecular characteristics of three monoclonal antibody-defined epitopes detectable on carcinoembryonic antigen (CEA). *Int. J. Cancer* 36, 75-84.

Sequence-Targeted Photochemical Modifications of Nucleic Acids by Complementary Oligonucleotides Covalently Linked to Porphyrins

Trung Le Doan,[†] Danièle Praseuth,[†] Loïc Perrouault,[†] Marcel Chassignol,[‡] Nguyen T. Thuong,[†] and Claude Hélène^{*,†}

Laboratoire de Biophysique, Muséum National d'Histoire Naturelle, INSERM U201, CNRS UA 481, 43 rue Cuvier, 75005 Paris, France, and Centre de Biophysique Moléculaire, CNRS, 45071 Orleans Cedex 02, France.

Received October 31, 1989

Porphyrins linked to oligonucleotides produce various types of photodamage on a complementary target DNA. The observed reactions include oxidation of guanine bases and cross-linking reactions of the oligonucleotide to its target sequence. Guanines located close to the porphyrin macrocycle were the most altered as compared to more remote guanines on the target sequence. No specific reaction was observed when the complexes were dissociated at temperatures above the melting temperature of the oligonucleotide-target hybrid. Both cross-linking and oxidation reactions accounted for ca. 60% modification of the target chains in the complex. Our results show that oligonucleotides covalently linked to porphyrins are efficient systems for inducing irreversible sequence-specific photodamage on a target DNA.

Synthetic oligonucleotides have been successfully used to control gene expression in various systems (For reviews see refs 1-3). However, in vivo applications of such oligonucleotides as antimessenger drugs face two main problems: (i) their poor penetration into cells and (ii) their susceptibility to nuclease degradation. Several strategies have been devised to cope with these problems. Oligonucleotides can be synthesized with a modified photodiester backbone so as to confer upon the whole molecule a better ability to cross cell membranes or to be protected from hydrolytic enzymes (4, 5). Another alternative is to synthesize oligonucleotides with the α -anomer form of the nucleosides instead of the natural β -anomer (see ref 6 for a review).

It was recently demonstrated that complexes of a messenger RNA and a complementary oligo- β -deoxynucleotide are specifically degraded by RNase H, a specific enzyme present in both prokaryotes and eukaryotes (7-10). These results constitute a strong basis for the understanding of the molecular mechanism of action of antimessenger oligodeoxynucleotides. Some of the oligonucleotide modifications (methylphosphonates, α -oligomers) that make them resistant to nucleases led to a loss of RNase H action on the mRNA-oligonucleotide hybrid (9, 10). This situation emphasized the need for developing oligonucleotides that could resist nuclease attack and induce local strand scission or chemical damage in their target. Such modified oligonucleotides could block enzymes involved in transcription or translation processes.

For several years our group has been actively engaged in designing active oligonucleotides that can specifically bind to a nucleic acid sequence and subsequently generate, in a controlled process, irreversible damage on the target sequence. Specific irreversible damage can be successfully produced on target sequences by using complementary oligonucleotides synthesized with the natural (β) or synthetic (α) anomers of nucleotides and covalently

linked to metal complexes of EDTA, phenanthroline, and porphyrin derivatives in dark reactions (see refs 1 and 6 for reviews). Photosensitizers such as proflavin and azido derivatives (azidophenacyl and azidoproflavine) attached to natural and α -oligonucleotides were also shown to induce specific photochemical reactions on complementary sequences in single-stranded (11, 12) and double-stranded (13, 14) DNA, but the yield of these reactions was rather low.

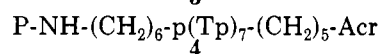
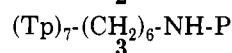
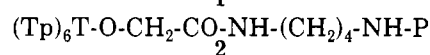
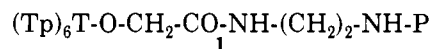
In this paper we present the results of a study of targeted photochemical reactions on DNA by complementary oligonucleotides linked to porphyrins. The reactions were found to be sequence-specific and the observed damage consisted mainly of cross-linking and oxidation reactions occurring predominantly on guanine bases of the target DNA. The yield of these reactions was much higher than that obtained with other photosensitizers.

EXPERIMENTAL PROCEDURES

A 27-mer oligonucleotide containing a stretch of adenines and whose sequence is



was used as a target for a series of porphyrin (P) substituted heptathymidylates



(where P stands for methylpyrroporphyrin XXI (Aldrich), p for a phosphate group, and Acr for 2-methoxy-6-chloro-9-aminoacridine). In all four compounds the carboxylic group of methylpyrroporphyrin XXI was attached to various linkers carrying an amine group to form an amide bond. In compounds 1 and 2, the linker was attached to the 3'-OH group of the 3'-terminal nucle-

[†] Muséum National d'Histoire Naturelle.

[‡] Centre de Biophysique Moléculaire.

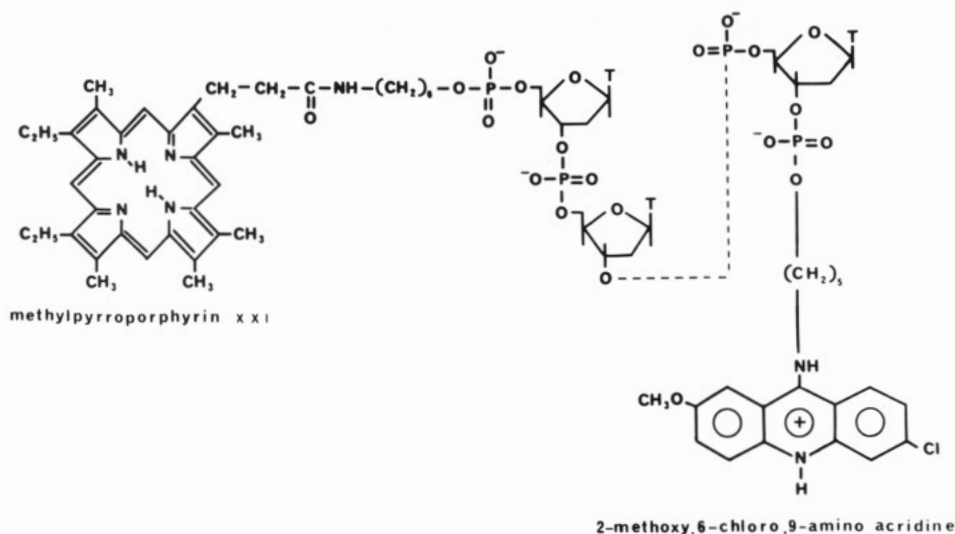


Figure 1. Schematic representation of compound 4 in which the porphyrin group is attached to the 5'-phosphate of the oligonucleotide and the acridine derivative to the 3'-phosphate via a pentamethylene linker. For compound 3, the porphyrin was linked to the 3'-phosphate while in 1 and 2, it was linked to the 3'-OH of the oligonucleotide. For more details on linker structure, see text.

side, without any intervening phosphate group. In compounds 3 and 4 the linker was attached to the 3' (3) or 5' (4) phosphate group of the terminal nucleotide. The detailed structure of compound 4 is shown in Figure 1. Synthesis of the oligonucleotides was carried out on either an Applied Biosystems or a Pharmacia automatic synthesizer. The synthesis of oligothymidylate-dye conjugates has been previously described (15, 16). Purification of the oligonucleotides was done either by liquid chromatography or by gel electrophoresis. The 27-mer fragment was 5'-end labeled with T_4 polynucleotide kinase and γ -[^{32}P]ATP (Amersham).

A standard procedure consisted of successive additions in an Eppendorf tube of 5'-labeled 27-mer DNA fragment (10 nM), the oligo(dT)₇-porphyrin derivative (10 μ M expressed as porphyrin concentration) in a final volume of 20 μ L containing 10 mM phosphate buffer, pH 7.4, and NaCl, usually at 0.25 M final concentration. The mixture was kept in the dark at 0 °C for 1 h. The DNA solution was then transferred into a small glass tube, and irradiation was carried out at 0 °C with the light of a high-pressure mercury lamp (200 W, OSRAM) filtered through a Pyrex glass plate ($\lambda > 300$ nm). The incident light intensity at the sample holder was measured with a Thermopile (Kipp and Zonen) to be approximately 180 mW/cm². After irradiation, the sample solution was frozen and lyophilized. To characterize alkali-labile sites produced on the DNA, samples were submitted to piperidine treatment. The reacted DNA was dissolved with 50 μ L of a 1 M piperidine solution and heated at 90 °C for 20 min followed by two cycles of washing with 50 μ L of water and lyophilization. The reacted product was then redissolved in 10 μ L of formamide-containing xylene cyanol dye and loaded on a polyacrylamide gel (20% acrylamide containing bisacrylamide, 1:40 (M/M), 7 M urea). Autoradiograms were obtained by exposing the gel to Fuji (X-ray) films with an intensifying screen at -80 °C overnight. Quantitative analysis of the reaction was carried out by excising the relevant bands from the gel and counting the corresponding radioactivity.

RESULTS

1. Analysis of Photoproducts by Gel Electrophoresis. The autoradiogram presented in Figure 2 shows the photoproducts formed after irradiation of the com-

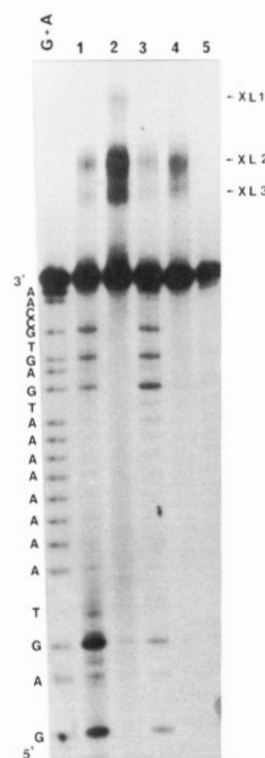


Figure 2. Autoradiogram of photoproducts obtained by irradiating the 27-mer fragment (10 nM) in the presence of oligo(dT)₇-porphyrin (10 μ M) in 10 mM sodium phosphate buffer, pH 7.4, containing 0.25 M NaCl. The left lane shows the (G + A) sequence. Part of the 27-mer sequence is shown on the left. Lanes 1 and 2: compound 3, before (lane 1) and after piperidine treatment (lane 2). Lanes 3 and 4: compound 4, before (lane 3) and after piperidine treatment (lane 4). Lane 5: unirradiated 27-mer.

plex of two oligo(dT)₇-porphyrins (3, lanes 1 and 2; and 4, lanes 3 and 4) with the target 27-mer whose (G + A) sequence is shown on the left side of the figure. At neutral pH, irradiation led to the production of new species (marked as XL₁, XL₂, and XL₃ in Figure 2) that migrated more slowly than the starting material (lanes 2 and 4). By analogy with what was previously observed with azido derivatives (11, 12), these species can be ascribed to products formed by photo-cross-linking of the oligonucle-

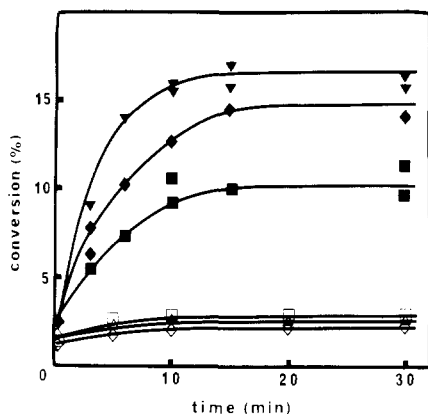


Figure 3. Dependence on the irradiation duration of cleavage yields at G(8) (\blacktriangledown), G(6) (\blacklozenge), and G(4) (\blacksquare) after irradiation followed by piperidine treatment of the 27-mer in the presence of 3. Experimental conditions are as in Figure 2. The three lower curves represent the cleavage yields at G(19) (upper), G(21) (middle), and G(23) (lower).

otide to the target matrix. The branched structure is expected to retard migration on the gels.

The irradiated samples were then treated with 1 M piperidine at 90 °C for 20 min in order to reveal alkali-labile sites (Figure 2, lanes 1 and 3). We observed that the cross-linked materials almost disappeared and that smaller fragments were produced that exhibited the same migration pattern as the fragments cleaved at guanine bases produced by reaction with dimethyl sulfate in the Maxam–Gilbert sequencing reaction. Some cleavage was also observed at adenines and thymines in the vicinity of the A_8 terminus located close to the porphyrin ring, assuming that a Watson–Crick double helix is formed. Compounds 1 and 2 exhibited the same pattern of photoproducts but with much lower yield (see below).

2. Specificity of the Photochemical Reaction. In Figure 2, lanes 1 and 2, the porphyrin moiety was attached at the 3'-end of the oligonucleotide and, as expected on the basis of an antiparallel orientation of the two strands, the main reactions occurred at G bases located on the 5'-side of the A_8 target sequence. The G bases on the opposite side (3'-side) were modified to a much lower extent. Conversely, when the porphyrin group was linked to the 5'-end of the oligonucleotide as in compound 4, the reaction occurred mostly at G bases of the 3'-side of the target (lane 3 of Figure 2). In a separate experiment with (dT)₈Acr we checked that the acridine dye (which was attached to the 3'-end of compound 4) was inactive under our experimental conditions (results not shown).

The reaction specificity could be analyzed further by comparing the yield of cleavage at the different guanines as a function of their distance from the reacting porphyrin center. This is illustrated in Figure 3 for compound 3, where the yields of cleavage after piperidine treatment of the two groups of guanines located on either side of the target A_8 sequence are presented as a function of irradiation time. The reaction leveled off after 15 min of irradiation, corresponding to a total incident dose of ~ 160 J/cm². This is very likely due to photodegradation of the dye at this irradiation dose. Such a photodegradation was observed by following the changes in absorption of the porphyrin ring under irradiation (data not shown). The much higher yield of cleavage at the 5'-guanines demonstrated the specificity reached with this system. As expected, the most modified G was G(8), the closest guanine to the photoactive group on the sequence. The cleavage yield decreased as one moved away from the reaction center on the 5'-side. For those guanines

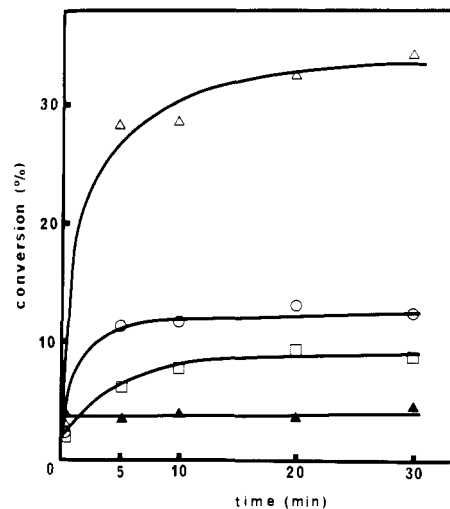


Figure 4. Cleavage yields at Gs on the 5'-side of the target oligonucleotide [G(8) + G(6) + G(4)] versus irradiation time after piperidine treatment of the reacted 27-mer in the presence of 1 (\square), 2 (\circ), and 3 (\triangle). Control experiment (\blacktriangle) consisted of irradiating the 27-mer in the absence of porphyrin-oligonucleotide derivative. All other conditions are as in Figure 2.

located on the 3'-side, the reaction yield was very low, 2–3% going from G(19) to G(23). It should be noted that the cleavage yields at the latter Gs were close to background figures obtained when the matrix was irradiated in the absence of the porphyrin conjugates and subsequently treated by piperidine (1–2%) (see Figure 4). Similar results were observed on a 32-mer DNA fragment that did not contain the A_8 sequence. A nonspecific weak cleavage (1–2% per G base) was observed at all Gs in the presence of 3.

3. Influence of the Linker Length and Structure.

The dramatic influence of the linker length and/or the chemical nature of the linker on the reaction efficiency is illustrated in Figure 4 for compounds 1–3. In compounds 1 and 2, the linker is directly attached to the 3'-OH of the terminal thymidine while in 3 and 4 it is linked to the terminal phosphate group (see the Experimental Procedures and Figure 1 for a detailed structure of 4). Among the four compounds tested in this study, the most reactive compound was compound 3. Two amide bonds are present in the linker structure of 1 and 2 instead of one as in 3 and 4. The short length of the linker coupled with restricted flexibility of the amide bonds may account for the observed low efficiencies of reactions of compounds 1 and 2. Compound 4 exhibited an efficiency comparable to that of 2. The lower reactivity of 4 as compared to that of 3 may be due to the site of attachment to the porphyrin group on the oligonucleotide (5'-end instead of 3'-end in 3), even though the presence of an acridine on the 3'-side provides a higher stability of the complex by intercalation of the acridine moiety within the duplex structure (1).

4. Quantitative Analysis of the Photochemical Reaction with Compound 3.

Irradiation of the complex under neutral pH conditions yielded three distinct cross-linked materials marked as XL₁, XL₂, and XL₃ in Figure 2. These cross-linked species and the material that migrated at the same position as the starting 27-mer fragment were excised from the gel; the reacted DNA was extracted and purified by ethanol precipitation. The recovered samples were submitted to piperidine treatment. Results are presented in Table I and Figure 5. The values in Table I represent the radioactivity of each

Table I. Quantitative Analysis of Photoproducts Formed after Irradiation (0 °C, 15 min) of the Complex (27-mer (10 nM)-oligo(dT)₇-porphyrin 3 (10 μM)) in 10 mM Phosphate Buffer, pH 7.4, NaCl 0.25 M, before and after Piperidine Treatment

		cross-linked 27-mer $\sum XL^b = 37$		
non-cross-linked 27-mer		XL ₁	XL ₂	XL ₃
63 ^a		3	21	13
After Piperidine Treatment				
XL ₁ ^c		0.17		
XL ₂		0.3	5.8	
XL ₃		0.4	1.1	3
27-mer	42	0.6	5.5	3.6
G(23)	1.8 ^d	0.05	0.3	0.4
G(21)	0.7	0.04	0.4	0.3
G(19)	0.4	0.07	0.3	0.5
A(10) to A(17)	1.25	0.17	0.45	0.6
G(8)	6.0	0.4	2.9	1.1
G(6)	2.9	0.3	1.4	1.1
G(4)	2.4	0.2	0.8	1.1
$\sum G(5')/\sum G(3')^e$	3.9	5.6	5.1	2.8

^a All values indicate the percentage of radioactivity in the corresponding bands extracted from the gel. ^b XL: cross-linked materials (see Figures 2 and 5). ^c Remaining cross-linked material after piperidine treatment. ^d Corrected values taking into account cleavage at G and A bases induced by piperidine treatment of the irradiated 27-mer in the absence of the oligonucleotide derivative. ^e Σ G(5') = G(8) + G(6) + G(4) and Σ G(3') = G(19) + G(21) + G(23).

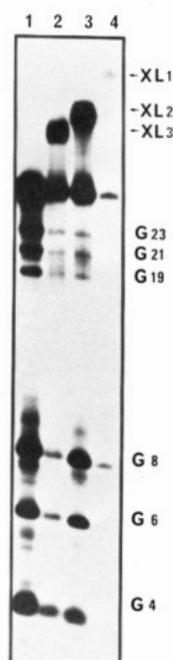


Figure 5. Autoradiogram of photoreacted 27-mer in the presence of 3 under the experimental conditions indicated in Figure 2. The material migrating as the 27-mer band (lane 1) and the cross-linked products XL₁ (lane 4), XL₂ (lane 3), and XL₃ (lane 2) were extracted from the gel and treated with piperidine before loading on the gel. The radioactivity in each lane reflects the yield of each photoproduct as detailed in Table I.

band as a percentage of the total radioactivity in the lane. The non-cross-linked material migrating as intact 27-mer yielded cleavage at guanines after piperidine treatment (Figure 5, lane 1, and first column of Table I). The data in Table I show that 25% of what migrated as the intact 27-mer in fact contained photooxidized guanines that were cleaved under alkaline conditions.

Under our experimental conditions, the yield of cross-linked products accounted for 37% of the original 27-

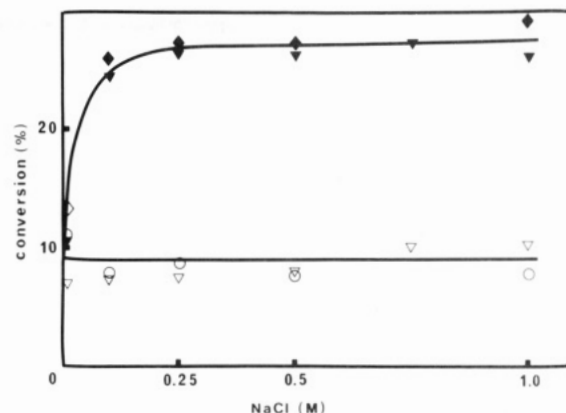


Figure 6. Influence of ionic concentration on the photochemical reaction of 3 with the 27-mer fragment after 15-min irradiation. Cleavage yield after piperidine treatment of the three Gs on the 5'-side (upper curve) and of the three Gs on the 3'-side (lower curve). NaCl (▼, ▽), NaClO₄ (◆, ○), in 10 mM sodium phosphate buffer pH 7.4.

mer. After piperidine treatment, there was about one-third of each of the cross-linked product left unmodified. The other two-thirds were converted into a product migrating as the starting material (27-mer) and shorter fragments cleaved predominantly at guanines (Figure 5, lanes 2–4). This result shows that piperidine treatment of the photo-cross-linked material led to cleavage of the 27-mer at photooxidized bases and/or bases involved in the cross-linking reactions (mostly guanines) and to cleavage of the covalent bond formed between bases and porphyrin, thereby releasing the cross-linked oligonucleotide from the 27-mer. In the latter case the resulting product, which migrates as an intact 27-mer, might contain altered bases that are not alkali-labile sites.

The specificity of the photochemical reaction is evidenced by comparing the yields of cleavage of the three Gs on the 5'-side to those located on the other side (last row of Table I). The results show that the probability of photochemical reaction is 3–5 times higher at the Gs located in the vicinity of the photosensitizer (5'-side) as compared to those located on the opposite side of the target sequence. When the mixture of 3 and the target was irradiated at a temperature (30 °C) at which the complex was dissociated, the ratio of cleavage yields at Gs on the 5'- and 3'-side was reduced to about 0.8. Assuming that cleavage of Gs on the 3'-side [G(19), G(21), and G(23)] represent the oxidative reaction due to diffusing species (see the Discussion), there results showed that in the cross-linked materials (37% of the starting matrix), ca. 20% contained oxidized Gs in their structure.

5. Influence of Ionic Concentration. The stability of complementary DNA duplexes is known to increase when the ionic concentration increases as a result of a reduction in the repulsive interactions between the two negatively charged phosphodiester backbones.²⁷ The dependence of the photosensitized reaction with ionic concentration is shown in Figure 6. It can be seen that the reaction yield of G modification on the 5'-side increased when salt concentration increased from 0.01 to 0.15 M and then remained constant up to 1.0 M NaCl (or NaClO₄). The yield of cleavage at the three Gs located on the 3'-side of the matrix remained constant over the whole concentration range of Na salts. This result demonstrates that the specific photosensitized reaction on the 5'-side is strongly dependent on the formation and stability of the oligonucleotide–target hybrid and the reactions at guanines on the 3'-side are not due to the formation of a triple helix involving two oligo(dT)s bound to the oli-

go(dA) sequence of the 27-mer. Such a triple helix would have been favored at high ionic concentration (14).

6. Influence of the Reaction Temperature. The temperature dependence of the photochemical reaction was studied with compound 4. In this compound the porphyrin group is attached to the 5'-end of the oligonucleotide and the acridine derivative to the 3'-end. Therefore the specific reaction occurs at G(19). The reaction yield as measured by the cleavage at G(19) after piperidine treatment decreased when the temperature increased with a half-transition at $\approx 18^\circ\text{C}$ (results not shown). Photo-cross-linking before piperidine treatment was abolished at high temperature and the half-transition also occurred at 18°C . In contrast, the nonspecific reactions at Gs on the 5'-side increased with temperature. In a previous work we studied the cleavage of a poly(dA) matrix in the dark by iron complexes of 3 and 4 (15). Melting temperatures of 17°C and 32°C were observed for the metal complexes of 3 and 4, respectively. These temperatures are certainly higher than those expected for the nonmetalated porphyrin due to the increased interaction provided by the positive charge brought by the Fe ion and more importantly by the effect of cooperative binding on the homopolynucleotide matrix.

DISCUSSION

This study shows that specific photochemical reactions can be targeted to specific DNA sequences by irradiating the complex formed by the target sequence with a complementary oligonucleotide tethered to a porphyrin group at the 3'- or 5'-end. These reactions involve bound porphyrin-oligonucleotide conjugates as reaction only occurred when the two molecules were hybridized, i.e., at high salt concentration and at temperatures lower than the melting temperature of the complex. Moreover, it was shown that the main reactions occurred on the side of the target sequence expected when the substrate and the porphyrin-oligonucleotide conjugate form a double helix with antiparallel orientation of the two strands. Both oxidation and cross-linking reactions were observed. Quantitative analysis of the photochemical reactions showed that under our experimental conditions, total damage, including oxidation and cross-linked products, accounted for ca. 60% of the target DNA for the most active derivative 3.

Porphyrins strongly absorb visible light and the produced excited states can react with various substrates including nucleic acid bases (17). When a porphyrin group is brought in close vicinity of a target DNA two types of photochemical events can be envisaged: (i) A direct reaction of the excited porphyrin (in its singlet or triplet state) with the substrate, e.g., an electron-transfer reaction from a guanine base yielding a G radical cation. (ii) The porphyrin excited states can react with oxygen, producing singlet oxygen $^1\text{O}_2$ or the superoxide anion $\text{O}_2^{\cdot-}$. The latter has been found to be rather inactive toward nucleic acid bases while $^1\text{O}_2$ reacts readily with guanine and to a lesser extent with thymine bases (18, 19). The observed alkali-labile sites at guanine bases in the target sequence could result from singlet-oxygen attack but also from decomposition of some peroxy form of the guanine radical cation. The fluorescence of some cationic porphyrins has been found to be quenched by poly(dG-C) and calf-thymus DNA (20), and this quenching has been ascribed to an electron-transfer reaction in the excited state. Photoreduction of hematoporphyrin has been observed in the presence of reductants such as ascorbate, pyrogallol, and catechol (21). Berg et al. (22) also proposed an electron-transfer reaction between thiopy-

ronine and guanine base, resulting in the formation of the radical cation $\text{G}^{\cdot+}$. The production of such radicals implies a close contact between donor and acceptor molecules. The photo-cross-linking reaction could result from a very localized reaction between radical species, in contrast to oxidation reactions involving diffusing species such as singlet oxygen. A mean diffusion pathway of singlet oxygen of 250 nm has been calculated from the diffusion constant ($2.5 \times 10^{-9} \text{ m}^2 \text{ s}^{-1}$) and the lifetime of singlet oxygen in water ($4 \mu\text{s}$ at 20°C). The alkali-induced cleavage reactions at guanine residues do not occur randomly. This is shown after piperidine treatment of the band migrating as the intact 27-mer (Figure 5, lane 1). Cleavage occurs predominantly on the 5'-side of the target sequence, indicating that modified guanines have been mostly produced in the immediate vicinity of the porphyrin ring. Porphyrins have been shown to produce singlet oxygen as a result of energy transfer from the triplet state (23, 24). Guanine bases located in the immediate vicinity of the porphyrin ring should react rapidly with singlet oxygen. A large excess of oligonucleotide-porphyrin conjugate over target DNA was used in most experiments. Singlet oxygen produced by unbound molecules is expected to react with guanine bases in a non-selective way. This is what was observed when the oligonucleotide-target hybrid was dissociated at temperatures above the melting temperature. All guanine bases were photooxidized both on the 5'- and the 3'-sides of the A_8 sequence although the reaction yield was lower than with the bound oligonucleotide. In contrast, the photo-cross-linking reaction leading to slowly migrating species on neutral polyacrylamide gels was abolished when the complex was dissociated. In summary, porphyrin-linked oligonucleotide lead to three types of reactions. Photo-cross-linking of porphyrin with nucleic acid bases and local photooxidation of bases by singlet oxygen are sequence-specific and occur only when the oligonucleotide is bound to its target sequence. Some further non-sequence-specific photooxidation of bases occurs mainly at guanines, due to singlet oxygen produced by unbound oligonucleotides and, possibly, by singlet oxygen generated from bound oligonucleotide and diffusing away from the porphyrin. Literature data indicate that photochemically modified Gs are effective blocking sites for various enzymes. Guanine oxidation mediated by singlet oxygen appears to generate efficient arrest sites for *Escherichia coli* DNA polymerase I (25, 26). Inhibition of DNA-dependent RNA synthesis by porphyrins has also been observed (27). Several photosensitizers have been shown to produce photodamage similar to those observed in our system. In a previous work we have shown that, under irradiation, proflavine induced both cross-linking and oxidation reactions occurring mainly at G bases (13). Piette and Moore (28) showed that damage photoinduced by proflavine blocked DNA polymerases on the reacted matrix. In the phenothiazine series, the genotoxic properties of chlorpromazine have been correlated with the ability to add covalently on to guanine bases of DNA (29). In model studies, Ciulla et al. (30) have isolated a photoadduct resulting from the coupling between the C(8) position of the deoxyguanosine and the C(2) position of the phenothiazine ring. The unreacted DNA was probed with DNA polymerase and the enzyme was found to stop one nucleotide before every guanine residue (29). Recently it has been reported that a specific photo-cross-linking reaction could be achieved with an oligonucleotide linked to a photoactivatable group, 4'-(aminoalkyl)-4,5',8-trimethylpsoralen (31). Photoadducts of psoralens with thymine bases have been demonstrated to be

efficient arrest sites for various enzymes including *E. coli* and T₄ DNA polymerases and reverse transcriptases (32, 33).

In conclusion, site-directed photodamage produced by porphyrins or other sensitizers coupled to oligonucleotides appears to provide a promising system for the selective inhibition of gene expression. Porphyrins can be covalently attached to nuclease-resistant oligonucleotides. This should make these oligonucleotides-porphyrin conjugates suitable for in vivo applications. Work is in progress in our laboratory on selective control of gene expression at replication, transcription, and translation levels using these new photoactive oligonucleotides.

ACKNOWLEDGMENT

This work was supported in part by Rhône-Poulenc-Santé, the Ligue Nationale Française contre le Cancer, and the Fondation pour la Recherche Médicale. We wish to thank Drs. J. Igolen and M. C. Gouyette, Institut Pasteur, Paris, for a gift of a sample of the 27-mer, and J. M. Kelly for helpful discussions.

LITERATURE CITED

- (1) Hélène, C. (1987) In *DNA-Ligand Interactions* (W. Guschlauer and W. Saenger, Eds.) pp 127-140, Plenum Publishing Corp., New York.
- (2) Stein, C. A., and Cohen, J. S. (1988) *Cancer Res.* 48, 2659-2668.
- (3) Toulmé, J. J., and Hélène, C. (1988) *Gene* 72, 51-58.
- (4) Miller, P. S., and Tso, P. O. P. (1987) *Anticancer Drug Des.* 2, 117-128.
- (5) Matsukura, M., Shinokuza, K., Zon, G., Mitsuya, H., Reitz, M., Cohen, J. S., and Broder, S. (1987) *Proc. Natl. Acad. Sci. U.S.A.* 84, 7706-7710.
- (6) Hélène, C., and Thuong, N. T. (1988) In *Nucleic Acids and Molecular Biology*, (F. Eckstein and D. M. J. Lilley, Eds.) Vol 2, pp 105-123, Springer Verlag, New York.
- (7) Minshull, J., and Hunt, T. (1986) *Nucleic Acids Res.* 14, 6433-6451.
- (8) Cazenave, C., Loreau, N., Thuong, N. T., Toulmé, J. J., and Hélène, C. (1987) *Nucleic Acids Res.* 15, 4717-4736.
- (9) Gagnor, C., Bertrand, J. R., Thenet, S., Lemaitre, M., Morvan, F., Rayner, B., Malvy, C., Lebleu, B., Imbach, J. L., and Paoletti, C. (1987) *Nucleic Acids Res.* 15, 10419-10436.
- (10) Cazenave, C., Stein, C. A., Loreau, N., Thuong, N. T., Neckers, L. M., Subasinghe, C., Hélène, C., Cohen, J. S., and Toulmé, J. J. (1989) *Nucleic Acids Res.* 17, 4255-4273.
- (11) Praseuth, D., Chassignol, M., Takusugi, M., Le Doan, T., Thuong, N. T., and Hélène, C. (1987) *J. Mol. Biol.* 196, 939-942.
- (12) Le Doan, T., Perrouault, L., Praseuth, D., Habbout, N., Decout, J. L., Thuong, N. T., Lhomme, J., and Hélène, C. (1987) *Nucleic Acids Res.* 15, 7749-7760.
- (13) Praseuth, D., Le Doan, T., Chassignol, M., Decout, J. L., Habbout, N., Lhomme, J., Thuong, N. T., and Hélène, C. (1988) *Biochemistry* 27, 3031-3038.
- (14) Praseuth, D., Perrouault, L., Le Doan, T., Chassignol, M., Thuong, N. T., and Hélène, C. (1988) *Proc. Natl. Acad. Sci. U.S.A.* 85, 1349-1353.
- (15) Le Doan, T., Perrouault, L., Hélène, C., Chassignol, M., and Thuong, N. T. (1986) *Biochemistry* 25, 6736-6739.
- (16) Asseline, U., Thuong, N. T., and Hélène, C. (1986) *Nucleosides Nucleotides* 5 (1), 45-63.
- (17) Jori, G., and Spikes, J. D. (1984) In *Topics in Photomedicine* (K. C. Smith, Ed.) pp 183-318, Plenum Press, New York.
- (18) Cadet, J., and Téoule, R. (1978) *Photochem. Photobiol.* 28, 661-667.
- (19) Kawanishi, S., Inoue, S., and Sano, S. (1986) *J. Biol. Chem.* 261, 6090-6095.
- (20) Kelly, J. M., and Murphy, M. J. (1985) *Nucleic Acids Res.* 13, 167-183.
- (21) Felix, C. C., Reszka, K., and Sealy, R. C. (1983) *Photochem. Photobiol.* 37, 141-147.
- (22) Berg, H. (1978) *Bioelectrochem. Bioenerg.* 5, 347-356.
- (23) Verlhac, J. B., Gaudemer, A., and Kraljic, I. (1984) *Nouv. J. Chim.* 45, 401-406.
- (24) Keir, W. F., Land, E. J., MacLennan, A. H., McGarvey, D. J., and Truscott, T. G. (1987) *Photochem. Photobiol.* 466, 587-589.
- (25) Decuyper-Debergh, D., Piette, J., Decuyper, J., and Van de Vorst, A. (1985) *Arch. Int. Physiol. Biochim.* 93, BP7.
- (26) Piette, J., Decuyper, J., and Van de Vorst, A. (1986) *J. Invest. Dermatol.* 102, 653-658.
- (27) Musser, D. A.; Datta-Gupta, N., and Fiel, R. J. (1980) *Biochem. Biol. Res. Commun.* 97, 918-925.
- (28) Piette, J., and Moore, P. D. (1982) *Photochem. Photobiol.* 35, 705-708.
- (29) Merville, M. P., Piette, J., Lopez, M., Decuyper, J., and Van de Vorst, A. (1984) *J. Biol. Chem.* 259, 15069-15077.
- (30) Ciulla, T. A., Epling, G. A., and Korchevar, I. E. (1986) *Photochem. Photobiol.* 43, 607-613.
- (31) Lee, B. L., Murakami, A., Blake, K. R., Lin, S. B., and Miller, P. S. (1988) *Biochemistry* 27, 3197-3203.
- (32) Piette, J. G., and Hearst, J. E. (1983) *Proc. Natl. Acad. Sci. U.S.A.* 80, 5540-5544.
- (33) Boyer, V., Moustacchi, E., and Sage, E. (1988) *Biochemistry* 27, 3011-3018.

Registry No. 1, 114436-49-6; 2, 112761-79-2; 3, 112726-40-6; 4, 114436-51-0; 27-mer oligonucleotide, 112603-07-3; G, 73-40-5; O₂, 7782-44-7.

A General Method for Highly Selective Cross-Linking of Unprotected Polypeptides via pH-Controlled Modification of N-Terminal α -Amino Groups

Ronald Wetzel,*† Roger Halualani, John T. Stults, and Clifford Quan

Departments of Protein Chemistry and Biomolecular Chemistry, Genentech, Inc., 460 Point San Bruno Boulevard, South San Francisco, California 94080. Received November 7, 1989

A method is described for the highly selective modification of the α -amino groups at the N-termini of unprotected peptides to form stable, modified peptide intermediates which can be covalently coupled to other molecules or to a solid support. Acylation with iodoacetic anhydride at pH 6.0 occurs with 90–98% selectivity for the α -amino group, depending on the N-terminal residue (as shown with a series of model hexapeptides containing a competing Lys residue). Although Cys residues must be protected (reversibly or irreversibly) before the anhydride reaction, there are no detectable side reactions of the α -amino moiety—of the reagent or of modified peptide—with the side chains of His, Met, or Lys. The reaction works well in denaturants, so that inhibitory effects of noncovalent structure can be minimized. In a second step the iodoacetyl-peptide can be reacted with a thiol group on a protein, on a solid chromatography matrix, on a spectroscopic probe, etc. This is illustrated by reaction of a series of N^{α} -iodoacetyl-peptides with murine interferon- γ , which contains a C-terminal Cys residue. Data are presented which suggest that this iodoacetic anhydride scheme is superior in selectivity for α -amino groups to conventional chemical approaches to cross-linking such as use of 2-iminothiolane or N -hydroxysuccinimide-activated carboxylic acid esters. The reaction is ideally suited for modifying peptide fragments, as pure species or as mixtures, derived from proteolytic or chemical fragmentation of proteins. Furthermore, polypeptides synthesized biosynthetically, for example via recombinant DNA techniques, can be cross-linked in this way. It should also be possible to confidently cross-link small amounts of proteinaceous biological factors, and thus develop affinity matrixes or make antibodies before the polypeptide of interest has been fully purified or structurally characterized.

Although chemical cross-linking of polypeptides, to another molecule or to a matrix, is an important and often-used step in the biological and biochemical study of peptides and proteins, there is no good general method available which does not require de novo synthesis of the polypeptide. One commonly used approach, for example, is to incorporate into a nonaqueous synthesis of the polypeptide an N- or C-terminal cysteine residue, which can subsequently be utilized as a reactive handle for cross-linking via a disulfide or thioether linkage (1). Such methods suffer from the disadvantage of requiring time and expertise to do the synthesis and, not incidentally, demand prior knowledge of the structure of the peptide of interest. Such a synthetic approach will sometimes present further problems, due to size or other limitations to chemical synthesis, such as the presence of a disulfide bond in the peptide. Mixtures of peptides, as in a protease digest of a protein, require separate synthesis of each peptide even for uses in which a mixture of cross-linked peptides might be adequate or desirable. The requirement of this conventional technology for de novo synthesis for control of the site of attachment is especially unfortunate in the present age of recombinant DNA based methods for polypeptide synthesis.

An alternative approach to de novo synthesis, in prin-

ciple, would be to utilize bifunctional cross-linking reagents to modify unprotected polypeptides in the aqueous phase. Although bifunctional cross-linking has been used with considerable practical success on proteins, the inherent lack of specificity of the available methods limits the control and confidence with which they can be used.

In theory, it should be possible to selectively modify the N-terminus of an unprotected peptide in aqueous solution by exploiting the differences between the pK_a values of its α -amino group (about 8.0) and the side chain amino groups of Lys (about 10.5) and Arg (about 12) (2, 3). This is particularly attractive since modification of the chain terminus should minimize interference of the cross-link with the amino acid side chains and their content of biological information. Such a modification should fulfill two requirements. First, the ratio of reactivities of the α -amino group to the amino groups of the side chains of Lys and Arg should be as high as possible. Second, the reactivity of the α -amino groups of different peptides should be independent of peptide sequence and composition, so that reaction conditions don't have to be customized for each peptide.

Stark (4) has shown that the reactivity of cyanate in the neutral pH range with a series of amino acids and short peptides exhibits a very good correlation with the pK_a values of their amino groups. This study showed that the relative reactivity between the α -amino group and the ϵ -amino group of AlaLys was based on both their pK_a difference and on the relative reaction rates of other model compounds. Stark concluded that α -amino groups

† Present address: Macromolecular Sciences Department, Smith Kline Beecham Pharmaceuticals, 709 Swedeland Road, P.O. Box 1539, King of Prussia, PA 19406-0939.

Table I. Selectivity^{a,2} of 2-IT for α -Amino Groups of N-Terminal Amino Acids

peptide	corrected rate, A_{412}/min	selectivity ratio ^a
AlaGly	0.027	4.5
AspGly	0.036	6
GluAla	0.066	11
GlyGly	0.174	29
HisGly	0.159	27
IleAsn	0.036	6
LeuGly	0.024	4
MetGly	0.063	11
PheGly	0.038	6
ProGly	0.029	5
SerGly	0.085	14
TrpGly	0.081	14
TyrGly	0.061	10
ValGly	0.013	2
AcGlyLysOCH ₃	0.006	(1)

^a Selectivity ratio is the rate of reaction of the α -amino group divided by the rate of reaction of the ϵ -amino group of lysine, as measured using the peptide AcGlyLysOCH₃.

of peptides should react about 100 times faster than the ϵ -amino group of Lys side chains when reacted at a pH at least 1 unit below the lower pK_a . This study was restricted to only three N-terminal amino acids (Thr, Ala, and Gly), all of which have relatively small side chains.

In contrast to this suggestion of uniform reactivity of peptide α -amino groups, Hunter and Ludwig (5) showed that, in reaction with methyl benzimidate, Gly reacts about 7 times faster than Phe at pH 9.5; taking into account their slightly different pK_a values, Gly was calculated to react about 12 times faster than Phe. The authors suggested that the different reactivities of the unprotonated forms of these amino acids derived from differences in steric access of reagent and/or in nucleophilicity. The authors also suggested that it was this inherent reactivity difference which accounts for observations (5–7) that reaction of insulin with amine-directed reagents generally leads to modification of the A chain terminus (Gly) but not the B chain terminus (Phe). These differential reactivities, not noted when insulin is reacted with cyanate (8), had previously been ascribed to inaccessibility of the B chain N-terminal Phe in the insulin tertiary structure. Thus it appears that selectivity for the α -amino group in the presence of other amino groups can vary both with the reagent and with the nature of the side chain on the N-terminal residue.

Selective modification of α -amino groups by pH control has also been reported for other acylating agents, such as aryl isothiocyanates (9). Most attempts to selectively react the N-termini of polypeptides, however, have been with acetic anhydride. For example, reaction of the peptide hormone glucagon with acetic anhydride at pH 5.5 generates two products, 70% acetylated only on the α -amino group of the N-terminal His residue and 30% diacetylated at the N-terminus plus the ϵ -amino group of Lys12 (10). Reaction of the 28 amino acid peptide desacetylthymosin α_1 with acetic anhydride gives the N-terminally acetylated peptide as about 90% of the product, even though the peptide contains four Lys residues (11). Larger polypeptides may be more difficult to selectively modify. Magee et al. (12) found that reaction with acetic anhydride exhibited little if any selectivity for the N-terminus of trypsinogen; a strategy of reversible protection of Lys residues was required to selectively modify the N-terminus.

In this paper we show that for two chemical groups widely used in the cross-linking of peptides, *N*-hy-

droxysuccinimide (NHS)¹ activated carboxylic acids and 2-iminothiolane (2-IT), pH-controlled selectivity² for a peptide's N-terminus is relatively poor. Furthermore, at least for 2-IT reactions, we show that peptide reactivities vary considerably with the nature of the N-terminal amino acid. We show that much better results can be obtained using a two-step procedure exploiting the high selectivity for α -amino groups of acid anhydrides. This simple method can be used to prepare peptides for cross-linking, in very good yields, from already existing peptides, and thus should be a useful general alternative to *de novo* peptide synthesis. In addition, the method may have some unique applications in modifying mixtures of peptides.

EXPERIMENTAL PROCEDURES

Materials. A series of 20 test hexapeptides were synthesized by building the pentapeptide sequence GAKQA on a solid phase, dividing the resin into 20 portions, and completing the synthesis with different N-terminal amino acids. After HF cleavage and deprotection, the peptides were purified by high-performance liquid chromatography (HPLC), lyophilized, and resuspended in water. Purity was assessed by analytical HPLC in two chromatographic systems. Identity was confirmed by mass spectrometry. Other peptides were also chemically synthesized, with the exception of *N* $^{\alpha}$ -desacetylthymosin α_1 [which was prepared by recombinant DNA methods (11)] and its trypsin fragments. Murine interferon-gamma (13) was provided by L. E. Burton (Genentech).

Dipeptides used in this study described in Table I were purchased from Sigma, as was 5,5'-dithiobis(2-nitrobenzoic acid) (DTNB). NHS, sulfosuccinimidyl acetate, 2-IT, and dicyclohexylcarbodiimide (DCC) were purchased from Pierce. Iodoacetic anhydride was purchased from Aldrich.

Methods. HPLC was performed on a Waters gradient system composed of Model 510 pumps and an automated gradient controller. Separations were on Vydak 5- μm C-18 reverse-phase columns. Two buffer systems were used, both employing Milli-Q-purified water as solvent A and acetonitrile as solvent B. In system I, 0.1% trifluoroacetic acid (Pierce) was included in both A and

¹ Abbreviations: DCC, dicyclohexylcarbodiimide; DTNB, 5,5'-dithiobis(2-nitrobenzoic acid); EDTA, ethylenediaminetetraacetic acid; FAB, fast atom bombardment; HPLC, high-performance liquid chromatography; 2-IT, 2-iminothiolane; MES, 2-(*N*-morpholino)ethanesulfonic acid; MS, mass spectrometer; NaOAc, sodium acetate; NHS, *N*-hydroxysuccinimide.

² For comparison of reagents we devised a "selectivity" value which would allow us to compare the qualities of reagents such as 2-IT, for which kinetic measurements can be made, with reagents such as acid anhydrides, where multiple additions of reagents are required, reactions are fast, and peptide and solvent compete for reagent. For the first class, selectivity is the ratio of the rate of reaction of the α -amino group to the rate for the ϵ -amino group. For the second class, selectivity is the ratio of all product molecules containing modified α -amino groups to those containing ϵ -amino groups (in each case regardless of whether or not they are also modified elsewhere); where uncharacterized side products exist, they are included in the denominator. In this latter method the selectivity clearly depends on how far the reaction is pushed; values will more closely reflect relative reaction rates if they are assessed on reaction mixtures containing substantial amounts of unreacted starting material. On the other hand, the object of this study is to devise an efficient synthetic strategy, so selectivity under practical conditions is also important. This is why there are two selectivities listed in Table II.

B. In system II, 5 mM heptafluorobutyric acid (Pierce) was included in both. System I was useful for initially identifying products, but for some peptides it could not be used to follow the progress of the reaction because iodoacetate coelutes with the peptide starting material. System II allowed us to follow the disappearance of starting material, except that with some peptides the disubstituted product co-elutes with starting material and thus cannot be quantified. Prep collection of modified peptides was performed with the TFA system, followed by lyophilization and resuspension in water. Iodoacetyl peptides were stable for at least 1 year stored at -20°C .

Mass spectra were obtained with a JEOL HX110HF/HX110HF tandem double-focusing mass spectrometer (MS), operating with a JEOL DA-5000 data system. Ionization by fast atom bombardment (FAB) with a 6 keV xenon beam produced positive ions that were analyzed at 10 keV accelerating voltage, 3000 resolution. Peptide products, purified by HPLC, were dried in vacuo and redissolved in water to a concentration of about 1 nmol/ μL . One microliter of this solution was added to 0.5 μL of nitrobenzyl alcohol on the probe tip and loaded into the MS. Nitrobenzyl alcohol was preferred as the matrix because the haloacetyl peptides did not produce intact MH^+ ions in glycerol, thioglycerol, or a 5:1 ratio of dithiothreitol/dithioerythritol. Conventional FAB spectra were produced by scanning MS-1 and acquiring data at detector 1. Daughter spectra were produced by selecting the ^{12}C isotope peak of the MH^+ ions with MS-1, passing it into a collision cell containing a pressure of helium sufficient to attenuate the parent ion beam to 25% of its original intensity, and measuring the MS-2 the fragmentation resulting from collision-induced dissociation.

Relative reaction rates of peptides with 2-IT were determined colorimetrically. For the dipeptide study summarized in Table I, peptides (3 mM) were mixed with 10 mM DTNB in 0.4 M sodium acetate (NaOAc), 1 mM ethylenediaminetetraacetic acid (EDTA), pH 5.4. A fresh stock solution of 100 mM 2-IT was prepared in the same buffer and held at 0°C . This stock solution was diluted 10-fold into the 0°C reaction mixture to give 10 mM 2-IT; the reaction was followed by generation of absorbance at 412 nm.

A stock solution of iodoacetic acid anhydride was prepared as follows. A fresh bottle of iodoacetic anhydride (Aldrich) was dissolved in its entirety in dry tetrahydrofuran (THF) to a concentration of 300–400 mM and stored at -20°C as aliquots in 1.5-mL Eppendorf tubes, which in turn were stored in 50-mL plastic, screw-top, conical tubes containing Drierite and sealed with Parafilm. Such tubes were not opened until equilibrated to room temperature. Stored in this way, reagents were stable for at least 9 months. This procedure was deemed necessary since in our hands iodoacetic anhydride proved unstable in its solid form under conditions in which portions of the stored solid were periodically removed.

Reaction of peptides with acid anhydrides was performed as follows. To a solution of the peptide (0.25–1 mM) in aqueous buffer at 0°C in a 1.5-mL polypropylene Eppendorf tube was added 1/100 volume of an approximately 300 mM solution of acid anhydride in dry THF. The sample was immediately vortexed. After 3 min, in which time reagent was depleted by a combination of reaction with peptide and hydrolysis, a fresh aliquot of anhydride in THF was added and the mixture was vortexed. This procedure was repeated until the reaction reached the desired level of completion, usually two

or three additions. Except where indicated in the text, reactions were done at pH 6.0 in 0.1 M 2-(*N*-morpholino)ethanesulfonic acid (MES).

Reactions were analyzed by adding a 10–20- μL aliquot of reaction mixture to 180–190 μL of HPLC buffer A. After vortexing, the solution was centrifuged (Eppendorf) and the supernatant was injected or transferred to vials for HPLC analysis.

The NHS ester of iodoacetic acid was prepared as follows. To a mixture of 6.4 g (34.4 mmol) of the free acid of iodoacetic acid and 3.9 g (33.9 mmol) of NHS in 120 mL of dried (3A molecular sieves) THF at room temperature was added, with stirring, a solution of 7.1 g (34.5 mmol) of DCC in 20 mL of dry THF over a 3–5 min period. The reaction mixture was stirred overnight with exclusion of light and then filtered and the precipitated dicyclohexylurea was washed with 20 mL of dry THF, which was added to the filtrate. The filtrate was reduced in volume on a rotary evaporator at about 40°C to about 40 mL, at which point a rapid crystallization occurred. After a few hours at 4°C the crystals were collected and recrystallized from about 70 mL of ethyl acetate/acetone by dissolving at 50°C and allowing to cool and stand at room temperature overnight. About 940 mg of material was obtained from the crystals obtained and another 1 g was obtained from crystallization of the dried filtrate of the first crystallization, for a total yield of 20%. The twice-crystallized material was characterized by MS as the NHS ester of iodoacetic acid. This was stored at 4°C over CaCl_2 .

Reaction with murine interferon-gamma was accomplished as follows. Five milligrams of the protein in 7 mL of pH 7.5 buffer was brought to 1 mM EDTA and 1 mM DTT and incubated for 1 h at room temperature. The resulting solution was dialyzed with two buffer changes over a period of 24 h against 100 mL of 10 mM NaOAc, 0.25 mM EDTA, pH 5.4. Portions (700 μL) of this solution were mixed with 80 μL of 1 M tris-HCl, 10 mM EDTA, pH 8 and with 70 μL of an aqueous stock solution (1–5 mM) of iodoacetyl peptide and the reaction mixture was incubated for 20 h at 37°C .

RESULTS

Table I lists selectivity ratios, indicating the preference for reaction at the N-terminal α -amino group to reaction at a Lys ϵ -amino group, for the reaction of 2-IT with a series of dipeptides with varying N-terminal residues. These ratios were calculated by dividing the rate of reaction of the dipeptide, determined colorimetrically as described in the methods, by the similarly determined rate for the dipeptide AcGlyLysOCH₃. When 2-IT reacts with an amino group, a sulfhydryl group is generated. Absorbance at 412 nm is developed in the assay by reaction of these released sulfhydryl groups with DTNB. Although the reaction of thiols with DTNB, just as the reaction of 2-IT with amino groups, is relatively slow at pH 5.7, we included a large concentration of DTNB to insure that this reporting reaction was fast compared to the reaction of amino groups with 2-IT. The table shows that in each case reaction at the α -amino group is favored over that of the ϵ -amino group, but that selectivity varies from a high of 29 for GlyGly to a low of 2 for ValGly, with most values falling in the range 4–14.

Figure 1 shows the result of reaction of the peptide FGAKQA with 2-IT at pH 5.8. Panel A shows the unreacted peptide. Panel B shows that, with approximately 26% of the peptide as yet unreacted, the reaction product is a mixture containing one major component and several minor ones. The main product, eluting at about

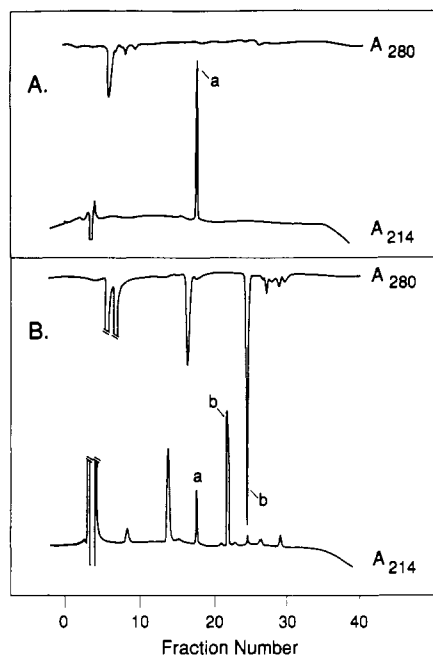


Figure 1. Reaction of FGAKQA with 2-IT. Panel A shows unreacted starting peptide (a). Panel B shows the mixture obtained after reaction of 0.4 mg/mL (0.62 mM) peptide with 10 mM 2-IT in 1 M NaOAc, 5 mM EDTA, pH 5.8, for 10 h at room temperature. The peak at 18 min is starting peptide (a). In the reaction mixture, none of the peaks eluting after 20 min are found in a mock reaction without peptide, and thus are assumed to be modified peptide. Products were not characterized. It can be seen that the main peptide product (b) has significant absorbance at 280 nm, the trace for which is offset about 3 min after the 214-nm trace. The chromatographic system is the same as that described in the legend to Figure 2.

22 min, represents 80% of the total reacted peptide (the peak at 14 min is associated with the reagent). This gives a *selectivity ratio*² [(monosubstituted + disubstituted/disubstituted) = (total reacted at α -amino/total reacted at ϵ -amino)] of $100/20 = 5$. This ratio is in good agreement with the value of 6 determined from the reactions of the dipeptides PheGly and AcGlyLysOCH₃ with 2-IT (Table I), suggesting that this colorimetric reaction with dipeptides can be considered diagnostic of the general reactivity of peptides with 2-IT.

Figure 2 shows the reaction of FGAKQA with two reagents which transfer an acetyl moiety. Panel A shows the reaction mixture with acetic anhydride (two additions of reagent; see the methods) at pH 6.0; with only 13% of the peptide left unreacted, 98% of what has reacted is acetylated on the α -amino group (peak b) and 2% is acetylated on both the α -amino group and on the ϵ -amino group of lysine (peak c; structure confirmed by MS analysis). This gives a selectivity ratio of $100/2 = 50$. Panel B shows the reaction with 4 mM sulfosuccinimidyl acetate in 0.1 M MES at room temperature for 1 h; with 15% of the peptide unreacted, 86% of the product mixture is only α -acetylated, while 14% is also reacted on the lysine side chain. This gives a selectivity ratio of $100/14 = 7$, which is comparable to the selectivity of 5–6 (see above) observed for reactions of N-terminal Phe peptides with 2-IT and is a factor of 7 less specific than the reaction of FGAKQA with acetic anhydride. Panel C shows the result of reacting iodoacetic anhydride with FGAKQA in 1.6 M NaOAc, pH 5.8; 43% of the product is N ^{α} -acetyl-FGAKQA, presumably derived from reaction with a mixed anhydride generated by rapid interchange of iodoacetic anhydride with the acetate buffer.

Figure 3 shows selected time points from a typical reac-

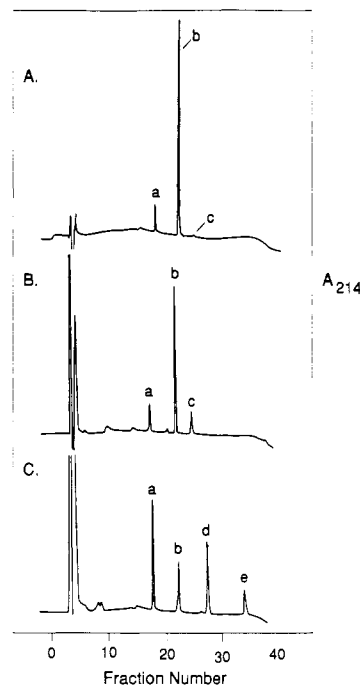


Figure 2. Formation of N ^{α} -acetyl-FGAKQA by acid anhydride reactions. FGAKQA (500 μ L, 0.4 mg/mL, 0.64 mM) was reacted under the following conditions. Panel A: 0.1 M MES buffer, pH 6.0, at 0 °C, three additions of 5 μ L each of \sim 350 mM acetic anhydride in THF. The small peak (a) at about 18 min is unreacted starting material, and the large peak (b) at about 22 min is the α -acetylated product. Panel B: 0.1 M MES buffer, pH 6.0, at room temperature, addition of sulfosuccinimidyl acetate to 4 mM and reaction for 1 h. The new peak (c) at about 25 min is the α,ϵ -diacylated peptide. Panel C: 1 M NaOAc, pH 5.8, at 0 °C, three additions of 5 μ L each of \sim 350 mM iodoacetic anhydride in THF. Coinjection with the reaction mixture from panel A confirms the identity of the 18- and 22-min peaks as unreacted (a) and α -acetylated (b) peptides. The peak (d) at 27 min is the α -iodoacetylated peptide and the peak (e) at 34 min is derived from the anhydride reagent. Samples were analyzed as described in the Experimental Procedures with a 1%/min gradient of acetonitrile in 0.1% trifluoroacetic acid with detection at 214 nm, full scale = 0.2 AU.

tion of iodoacetic anhydride with the hexapeptide SGAKQA in MES buffer. The figure shows the gradual conversion of the peak associated with starting peptide (peak b) to a main later-eluting peak (peak c), which was determined by MS analysis to be iodoacetylated on the N-terminus. After several reagent additions, a second product (peak a) appears; this was shown to be the diiodoacetylated product from reaction of the main product at the Lys ϵ -amino group. Both peaks exhibit absorbance at 280 nm, in contrast to the starting peptide, consistent with the addition of the iodoacetyl moiety (λ_{\max} for iodoacetic acid is 273 nm with $\log \epsilon = 2.66$). The peaks eluting at 10 and 43 min were shown to be associated with the reagent.

A series of 20 peptides of sequence X-GAKQA was synthesized in which X = each of the 20 standard biosynthetic amino acids, purified by HPLC and confirmed by MS analysis. Reaction of each peptide with iodoacetic anhydride was monitored by HPLC. Reactions were followed by both gradient systems described in the methods. For some peptides, reactions were quantified after two reagent additions in order to determine the selectivity ratio under favorable circumstances, i.e., with significant amounts (about 20%) of unreacted peptide present. In addition, all peptides were reacted with three reagent additions, conditions more useful synthetically, in which >95% of starting material is converted to products. The

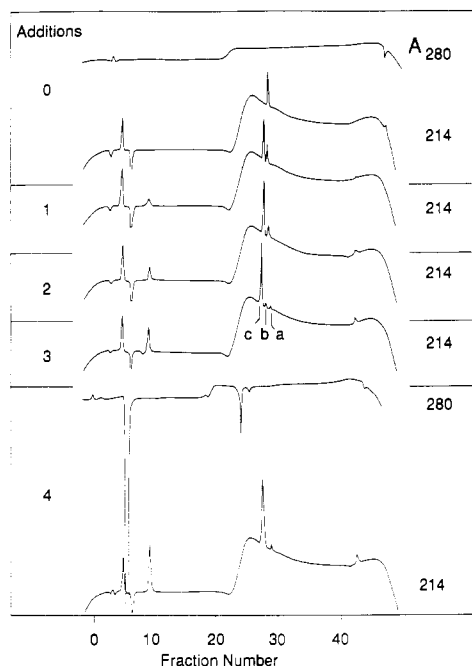


Figure 3. Progress of the reaction of iodoacetic anhydride with the peptide SGAKQA. Conditions are those described in the legend to Figure 2A. Before addition of reagent only one peak (b), for the starting peptide, is apparent in the A_{214} trace of HPLC fractionation of the reaction mixture. After one addition of reagent this peak is diminished to about 30% of its original height, and a new, earlier-eluting peak (c), corresponding to N - α -iodoacetylated peptide, is observed. After three additions only a small amount of starting material is left and the bulk of the product is monoacylated, but there is a third peak (a) eluting after starting material which is the α,ϵ -diacylated peptide. After four additions there is no starting peptide remaining. The A_{280} trace of the reaction mix after four additions shows that both product peaks absorb at 280 nm as expected (in this chromatogram, the A_{280} trace leads the A_{214} trace by about 3 min). The peaks at about 10 min and about 43 min are related to the iodoacetic anhydride reagent.

results of these measurements are listed in Table II. Percent yields of mono- and diacylated products were calculated as percentages of total product peptide absorbance; where percentages do not sum to 100, it indicates the corresponding amount of uncharacterized other peaks in the chromatogram. The table shows that, when reactions are not driven to complete loss of starting material, one obtains a range of selectivity ratios from 9 to 55, with most values at 18 or above.

For each of the 20 peptides, a reaction with iodoacetic anhydride was also conducted at pH 9 in sodium borate buffer. As expected, this gave a much greater amount of peptide product acylated on both the α - and the ϵ -amino groups and was useful in verifying the elution positions of the diacylated product in the pH 6.0 reaction mixtures. In some cases (indicated in Table II) reaction products were confirmed by tandem mass spectrometry (MS-MS) analysis. In this way it was possible to not only verify the molecular weights of the mono- and diiodoacetylated products of the Ala peptide but also to assign the acylation positions within the peptide product. Using MS-MS, the reaction products for the His and Met peptides, which theoretically could be alkylated on their side chains by iodoacetate, were confirmed to be unreacted on the side chains. In addition, the acylation position of the Pro peptide, whose α -amino group is a secondary amine and therefore of higher pK_a , was also confirmed by MS analysis to be the N-terminal α -amino group.

Table II. Selectivity^{a,2} of Iodoacetic Anhydride for α -Amino Groups of the Peptide X-GAKQA

X	three reagent additions			two additions: selectivity ^a
	% α -iodoacetyl	% diiodoacetyl	selectivity ^a	
Ala	87 ^b	10 ^b	10	
Arg	86	5	18	
Asn	82	6	15	
Asp	81	3	28	
CysSSCH ₂ CH ₂ OH	87	3	30	
Glu	79	7	12	
Gln	81	5	17	18
Gly	83	5	18	
His	70 ^b	23 ^b	4	16
Ile	76	10	9	
Leu	81	6	15	
Lys	88 ^b	12 ^b	8	
Met	97 ^b	3 ^b	33	40
Phe	77	3	27	33
Pro	74 ^b	3 ^b	26	37
Ser	77	13	7	55
Thr	86	6	15	50
Trp	80	8	11	23
Tyr	66	21	4	9
Val	78	11	8	18

^a Selectivity ratio is the sum of the mono- and diiodoacetylated peptide divided by the diiodoacetylated, which corresponds to the total α -iodoacetyl groups divided by the ϵ -iodoacetyl groups. ^b Structure verified by mass spectrometry.

Figure 4 shows the reactions of the peptide FGAKQA with reagents which transfer the iodoacetyl moiety, and thus is analogous to Figure 2C. Panel A shows the product (peak b), after two reagent additions, with iodoacetic anhydride. In this HPLC system the disubstituted product appears as a trailing shoulder on a peak (peak c) late in the chromatogram associated with reagent (as confirmed by panel B). The relative amounts of mono- and disubstituted products can be seen in the A_{280} trace. Adjusting the peak height of the disubstituted product to account for its content of two chromophores (using the factor 0.65 derived from analysis of the chromatogram in panel C), the product distribution when 11% of the starting material remains unreacted is 97% mono-substituted and 3% disubstituted, for a selectivity ratio of 33 (this number was confirmed by a similar analysis of another reaction mixture analyzed in HPLC system II, in which both reaction products can be quantified in the A_{214} trace). Panel C shows the reaction mixture with the NHS ester of iodoacetic acid, and the coinjection experiment shown in panel D confirms that the main products of this reaction are identical with the mono- (26 min) and disubstituted (33 min; see A_{280} trace) products with iodoacetic anhydride. The reaction mixture is qualitatively different, however, in the appearance of a new product (not characterized but not associated with reagent) at 23 min, as well as a much greater amount of disubstituted product (33 min). Even with the exclusion of the unidentified product, the selectivity ratio favoring α -substitution in this reaction is only 2, under conditions in which the extent of reaction, as judged by the 11% remaining unreacted peptide, is identical with the reaction in panel A. Thus for the iodoacetyl group, one sees an improvement in selectivity of a factor of $33/2 = 16.5$ comparing the acid anhydride to the NHS ester, an enhancement even better than that seen in the acetyl series (Figure 2).

Figure 5 shows the product of the reaction of a series of N^α -iodoacetyl-peptides with murine interferon-gamma, which contains a Cys residue at its C-terminus. The reaction is incomplete, even after a second cycle of

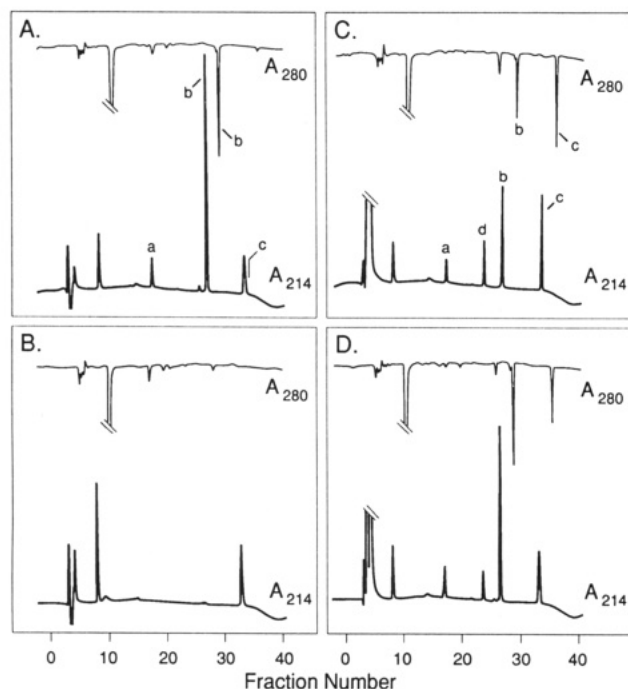


Figure 4. Iodoacetylation of FGAQQA. Panel A shows the reaction mixture of the peptide with iodoacetic anhydride under the reaction and chromatographic conditions described in the legend to Figure 2A, except that reaction was terminated after two reagent additions. Peak a is unreacted starting material and peak b is the N-terminally acylated product. The A₂₁₄ peak at about 34 min in panel A is predominantly derived from iodoacetic anhydride, as seen in panel B, a mock reaction mixture without peptide. However this peak contains a small trailing shoulder (c) which is the α,ϵ -diiodoacetyl-FGAQQA. Quantitation of this species is possible since it, but not the iodoacetic acid related material, also absorbs at 280 nm. Panel C shows the reaction mixture of 4 mM of the NHS ester of iodoacetic acid with FGAQQA at 25 °C after 1 h. The peak (a) at about 17 min is unreacted peptide, the peaks at 26 and 33 min are the α -mono- (b) and α,ϵ -diiodoacetylated (c) peptides, respectively, and the peak (d) at 23 min is unidentified but not seen in a mock reaction without peptide and so is presumed to be another peptide side product. As compared to iodoacetic anhydride, this reagent does not produce the decomposition product migrating at around 34 min. Panel D shows a coinjection of the reaction mixtures used to generate panels A and C. Note that all three products exhibit A₂₈₀. The A₂₁₄ trace leads the A₂₈₀ trace by 2–3 min.

reaction with fresh peptide; since precautions were taken to assure that the interferon Cys was fully reduced and available for reaction (see the Methods) incomplete reaction suggests that some of the molecules do not contain a C-terminal Cys. In fact, some preparations of this protein lack C-terminal residues due to a difficult to control limited proteolysis. The gel shows that the only product of each reaction is a discrete higher MW protein, whose migration retardation correlates with the MW of the reacting peptide. In a control experiment, human interferon-gamma, which contains no Cys, was shown to not react with N^α -iodoacetyl-peptide (data not shown).

DISCUSSION

In attempts to devise a general, highly selective cross-linking scheme for peptides, we initially investigated the use of 2-IT at a pH of 6 or below. However, as Table I and Figure 1 show, the selectivity of this reagent varies significantly depending on the N-terminal amino acid and for most amino acids is substantially lower than the factor of 100 found by Stark for the cyanate reaction (4). Since we had previously observed (11) a high selectivity

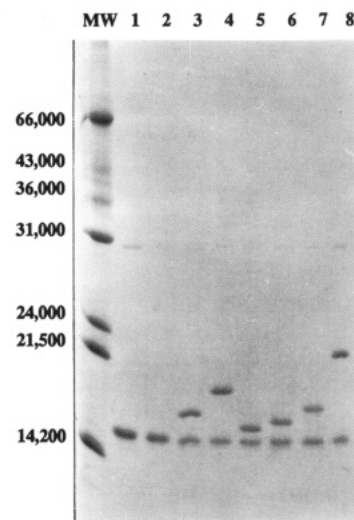


Figure 5. 12.5% SDS polyacrylamide gel on mixtures of reaction of a series of N^α -iodoacetyl-peptides with murine interferon-gamma (see the Methods). Aliquots of reaction mixtures were mixed with SDS-gel loading buffer containing 10 mM iodoacetamide, heat-denatured, and loaded onto the gel. The finished gel was stained with Coomassie Brilliant Blue. Lane 1 is unreacted interferon, and lane 2 shows the reaction product with iodoacetic acid. The other lanes show reaction with these iodoacetyl-peptides, all prep collected from HPLC before reaction: GRTQLQLTLNLF (lane 3), SRVSQRGLTLNLES-GRWR (lane 4), norleucine-FPTIPLSR (lane 5), EVVEEAEN (lane 6), SDAAVDTSEITTK (lane 7), SDAAVDTSEITTKDLKEKKEVVEEAEN (lane 8). The last peptide is N^α -desacetylthymosin α_1 , and the previous two are its main trypsin digestion products.

in the acetylation of the α -amino group of desacetylthymosin α_1 , a 28 amino acid peptide containing four Lys residues, it seemed that acid anhydrides might in general achieve selectivities more like that of cyanate. If true, reaction of a peptide with the anhydride of an α -haloacetic acid would generate an N-terminally derivatized intermediate which could subsequently be reacted with sulfhydryl groups of other molecules or matrices. To demonstrate that this strategy would be useful, we set about to address the following questions: (a) What are the selectivities for the reaction of iodoacetic anhydride for peptide α -amino groups and how do they compare to values for other bifunctional reagents, including other means of introducing the α -iodoacetyl moiety? (b) Is protection/deprotection of Cys residues feasible and are there any other potential side reactions of the α -iodoacetyl moiety with amino acid side chains? (c) Is the α -iodoacetamido moiety on a peptide sufficiently reactive to modify a sulfhydryl group on a macromolecule or solid support?

Selectivities.² Table II shows that selectivities for reaction of iodoacetic anhydride with a series of hexapeptides containing a competing Lys range from 9 to 55, substantially better than the 2-IT reaction (Table I and Figure 1) in degree of preference for the α -amino group and in uniformity with respect to N-terminal amino acids. Analysis of the data in Figures 2 and 4 (see the Results) suggests that α -amino group selectivities of acid anhydrides can be 10–20-fold higher than those of NHS-activated esters of the same acyl groups. Thus, 2-IT and NHS esters seem to behave relatively unselectively, while acid anhydrides are more highly selective for α -amino groups and discriminate less on the basis of N-terminal amino acid identity, qualities similar to those of cyanate (4).

For the acid anhydride reaction, the bulkiness of the

side chain of the N-terminal amino acid does not seem to greatly influence selectivity. Although the lowest observed selectivity of iodoacetic anhydride is for N-terminal Tyr, the values for the equally bulky Phe and Trp are much better. In fact, the low selectivity of Tyr probably derives not from its bulk but from its chemical nature. Under conditions designed to convert essentially all of the starting material (three reagent additions at pH 6), the Tyr and His peptides yield the lowest selectivity for the α -amino group (Table II). In contrast, His in a dipeptide exhibits *high* selectivity for the α -amino group when reacted with 2-IT (Table I). Examination of the course of the reactions of iodoacetic anhydride with HGAKQA and YGAKQA reveals that the reduced ratio of α -amino reactivity to ϵ -amino reactivity is not due to a decreased rate of reaction of the α -amino group *but rather to an increased rate of reaction of the ϵ -amino group of Lys*. This suggests that the His and Tyr residues of these peptides can catalyze the iodoacetylation of the Lys residues. This makes sense chemically, since both residues would be expected to undergo acylation on their side chains to yield unstable intermediate capable of transferring the acyl moiety to another group. In fact, a similar intramolecular interaction between the Tyr and His residues of angiotensin II has been postulated on the basis of the acetylation and deacetylation kinetics of these groups (14). This interpretation suggests that Tyr and His residues at other positions within a peptide may have similar effects. These catalytic transfers must be occurring intramolecularly, since the presence of HGAKQA in a mixed peptide reaction mixture does not alter the α/ϵ product ratio of FGAKQA with iodoacetic anhydride (data not shown). The relatively poor selectivity found by Desbuquois (10) for the acetylation of glucagon (see above) may thus in part be due to the presence of the His residue at the N-terminus of this peptide.

The above discussion suggests that selectivities may vary with amino acid composition of peptides. However, our studies suggest that with any particular peptide results will be better with acid anhydrides than with many other reagents. Further, reactions with a series of peptides containing up to four Lys or five Arg, for alkylation of murine interferon-gamma (Figure 5), gave the high selectivities expected from the number and pK_a values of their basic groups (data not shown), suggesting that one can reasonably expect most peptides to behave qualitatively as those described here.

Reactions of Amino Acid Side Chains. Three of the 20 amino acids normally used in ribosomal peptide synthesis, Cys, Met, and His, might be readily alkylated by the α -iodocarboxyl group, while the amino groups of Lys and the N-terminus are also reactive but require more stringent conditions (3). By incubation of our test peptides XGAKQA containing N-terminal His, Met, and Gly with iodoacetate under planned reaction conditions, we observed no detectable alkylation (data not shown). Furthermore, the reaction products of these peptides with iodoacetic anhydride were characterized by MS analysis and found to be iodoacetylated on the α -amino groups but not alkylated by a N^α -iodoacetamido moiety or by iodoacetate (Table II).

Since Cys residues of the peptide would almost certainly be alkylated under our reaction conditions, one must incorporate a Cys protection step into the procedure for peptides containing free Cys residues. Prior reaction of a Cys-containing peptide with a disulfide such as oxidized 2-mercaptoethanol or DTNB converts the Cys into a mixed disulfide incapable of being alkylated by

iodoacetate under reaction conditions (Table II), and the free sulfhydryl of the Cys can be regenerated by mild reduction after the iodoacetylation and subsequent cross-linking are completed (R.H. and R.W., unpublished).

Reaction with Sulfhydryl Groups. Although we have not characterized the reaction of N^α -iodoacetyl-peptides with thiol compounds in detail, we have conducted reactions with a number of different mercaptans. For example, reaction of 0.16 mM N^α -iodoacetyl-FGAKQA with 0.8 mM thiocholine in 0.1 M Tris HCl, 2 mM EDTA, pH 8.5 at 37 °C, goes to completion within 1 h. Complete reactions have also been achieved with cysteine, glutathione, and β -mercaptoethanol (data not shown). Finally, Figure 5 shows that a series of iodoacetyl-peptides varying considerably in size and amino acid composition can be efficiently attached to a sulfhydryl group of a macromolecule, in this case the Cys of murine interferon-gamma (13).

Practical Considerations. Acetylation of proteins has traditionally been done in NaOAc buffer at high concentration, because this buffer catalyzes the hydrolysis of the *O*-acetyltyrosine also formed from reaction with acetic anhydride (15). However, we found that these conditions gave poor results, for two reasons. First, use of 1 M NaOAc led to a mixture of iodoacetylated and acetylated peptides, presumably due to rapid generation of mixed acid anhydrides by reaction of acetate buffer with iodoacetic anhydride. Thus, when we reacted peptides with iodoacetic anhydride in 1.0 M NaOAc, pH 6.0, about half of the product formed was the peptide N-terminally modified with the acetyl, rather than α -iodoacetyl, group (Figure 1). Second, we found that high concentrations of acetate at pH 6 are so weakly buffering that the acid generated from hydrolysis of the anhydride reagent quickly lowers the pH to a point where no further reaction of amino groups with acid anhydride takes place; thus the standard acetate buffer is a poor choice even for reactions with acetic anhydride, since much more anhydride must be added to get a reasonable extent of reaction.

For these reasons we chose as a buffer MES, a sulfonic acid derivative which buffers well at pH 6.0 but is presumably too weakly nucleophilic to form significant amounts of mixed anhydride. Comparison of Figures 2C and 4A shows that MES buffer at pH 6 not only avoids the formation of acetylated side products in reactions with iodoacetic anhydride, but it also promotes the conversion of starting material much better than NaOAc at pH 6. Although we have not observed *O*-acetylation to be a problem in MES buffer, it would be simple to reverse this side reaction, were it to occur, by a subsequent incubation in concentrated acetate or another reagent (15).

In some cases it may be advantageous to carry out the iodoacetylation reaction in the presence of a protein denaturant. Reaction of FGAKQA with iodoacetic anhydride in 0.1 M MES, pH 6, in the presence of 5 M guanidine hydrochloride or 7 M urea, under conditions in which about 10% of the starting peptide is unreacted, gives a selectivity ratio of about 20 (data not shown). For the urea reaction, this extent of reaction was achieved with two reagent additions, each 1% of the reaction volume of ~ 350 mM anhydride (i.e., the usual conditions). For the guanidine hydrochloride reaction, two additions of 0.5% were required; two additions of 1% reagent gave a reaction mixture entirely depleted in starting material and enhanced in diacetylated peptide (thus giving lower selectivity). Presumably guanidine hydrochloride either slightly enhances the acetylation kinetics or inhibits the kinetics of hydrolytic breakdown of the reagent.

In general, reaction conditions, once optimized, can be used with different polypeptides and with some variation in other conditions. For best results, however, it is suggested that reagent excess, etc., be optimized on a test peptide for a given set of conditions. Use of anhydride from different sources or use of different buffers, pH conditions, or other solvent additives (like guanidine hydrochloride) may effect the extent to which a given amount of reagent acylates the polypeptide. Although the reaction conditions are surprisingly tolerant of changes in polypeptide concentration, we have observed increased conversion of starting material, and a corresponding decrease in the α/ϵ ratio of products (from 27 to 14), when polypeptide concentration is decreased from 600 to 60 μ M in the modification of FGAKQA with one 1% (vol) addition of reagent in 100 mM *N*-ethylmorpholine hydrochloride, pH 6.9.

The chemistry described in this paper should give yields of final product comparable to yields obtainable by de novo solid-phase synthesis of an appropriately derivatized peptide. It was designed primarily with the idea that resulting reaction mixtures could be used with no purification except elimination of excess iodoacetate, but it is also possible to purify the peptide products in the same way that peptides synthesized by organic chemistry methods are purified. Iodoacetylated peptides can be purified by HPLC and stored for at least 1 year in aqueous solution at -20°C without losing their capacity to alkylate sulfhydryl groups (data not shown). The reagent iodoacetic anhydride is commercially available, and stock solutions are stable when stored over drying agent at -20°C .

Potential Applications. One motivation for developing this chemistry is the increasing number of important polypeptides being made available in large amounts by recombinant DNA techniques. In addition, the method should be applicable to chemical or protease-generated fragmentation products of polypeptides; an especially attractive set of peptides are those derived from digestion with proteases with trypsin-like specificities, since the fragments will have no more than one Lys per fragment. There are many potential applications of this chemistry and the iodoacetylated peptides it can produce; among them are the following.

1. *Cross-Linking of a Polypeptide to a Carrier Molecule, Such as a Protein, for Use as an Immunogen to Raise Antibodies to the Polypeptide.* It is significant that for this and other applications to succeed the structure of the polypeptide need not be known, except that it must have a free N-terminus. For example one can imagine using this chemistry to make antibodies to a newly isolated peptide factor even before its structure has been assigned. It is also significant that the chemistry can be done effectively on mixtures of peptides. Thus, for example, it should be possible to test various fragmentation methods for their ability to generate highly immunogenic fragments of a protein, as might be useful in a search for a maximally effective polypeptide vaccine.

2. *Cross-Linking of a Polypeptide to a Solid Support for Use as an Affinity Column.* Although the acetyl group does not contribute much to the peptide as a spacer, it is equally possible to add the spacer to the matrix as part of the cross-linking chemistry. For example, we have reacted Lys-sepharose with 2-IT to generate a thiol sepharose with a spacer composed of both the tetramethylene arm of Lys and the trimethylene arm of cleaved 2-IT (R.W., unpublished). Here too there may be special advantages to being able to immobilize peptides of

unknown structure or mixtures of peptides. For example, one could immobilize the peptides derived from one or more proteolytic digests of a protein in order to make an immunoaffinity column specific for "linear epitope" antibodies to the protein.

3. *Modify Proteins or Other Molecules in Structure/Function Studies.* As shown above, iodoacetylated peptides can be reacted with Cys residues of proteins. When the Cys is not an N- or C-terminal residue, this would lead to novel branched polypeptides. Polypeptides modified with α -haloacetyl moieties may also prove to be useful as affinity labeling reagents, in analogy with this use of other α -halocarbonyl derivatives (16). Such reagents have potential as diagnostic tools for structure/function relationships and also as drugs.

4. *Tagging of Polypeptides with Reporter Groups for Biophysical and Other Studies.* It should be possible to label polypeptides with biotin, fluorescent probes, radioactive groups, etc., by using this chemistry. For example, radiolabeled polypeptides with reproducible properties could be prepared by synthesis of a stock of iodoacetylated polypeptide, which could be conveniently and safely synthesized and purified. When needed, small amounts could be reacted with radiolabeled groups such as [^{35}S]sodium sulfide or cysteine, the latter of which can be obtained at 600 Ci/mmol. Although selectivity of iodoacetic anhydride will probably be considerably lower in reactions with globular proteins, because of the likelihood of a large number of Lys residues, this method may compare favorably with other methods currently used to tag proteins.

5. *Cross-Linking of One Polypeptide to Another.* Cross-linking of one protein to another, for example, to tag an antibody with an enzyme as a reagent for ELISA, normally involves highly nonspecific chemistry and can result in poorly characterized, cross-linked peptide reagents with properties sometimes difficult to reproduce. Iodoacetylation may provide a more selective chemistry for preparing such reagents. N-Terminally iodoacetylated peptides can also be cross-linked to each other, for example, by reaction with a limiting amount of dithiol. One attractive possible application of this chemistry is the "random reassociation" of peptide fragments of a protein, which may be capable of generating, in a small percentage of the reaction mixture, molecules which contain a molecular surface which approximates the bioactive surface of the parent protein. Isolation and identification of such a peptide might rapidly provide leading evidence, for example, to the identity of the receptor binding site of a protein hormone. There are several reported examples of the reconstruction of antibody-binding sites of a protein by linking two discontinuous elements of the polypeptide chain in a single, relatively small peptide molecule (17, 18). Also supporting this idea is the work of Oas and Kim (19), who have recently shown that covalent association of two fragments of BPTI promotes noncovalent interactions to generate a cooperative folding unit structurally related to BPTI itself.

6. *Simplify Amino Acid Sequence Analysis of Peptides from MS Fragmentation Patterns.* N-Terminally iodoacetylated peptides can be used to prepare products containing a quaternary ammonium, charged group on the N-terminus; in the MS, such localizations of full positive charge generate spectra enriched in signals from fragments containing the positive charge (20). With a charge on the N-terminus derived from reaction of iodoacetylated peptides with thiocholine and other reagents, sequences can be read directly from the MS fragmenta-

tion pattern (R.H., J.S., and R.W., manuscript in preparation). In the tandem MS, fragmentation can be directed at any ion from a mixture of molecular species, so it may be possible to derivatize even small amounts of peptide and analyze the crude reaction mixture to obtain a sequence by this method.

ACKNOWLEDGMENT

We wish to thank John Burnier (Genentech), Bill Hancock (Genentech), Richard Vandlen (Genentech), Mark Loudon (Purdue), and Markus Graf (Ciba-Geigy, St. Aubin, Switzerland) for helpful suggestions and discussions and E. Rinderknecht and L. E. Burton for the murine interferon-gamma.

LITERATURE CITED

- (1) Green, N., Alexander, H., Olson, A., Sutcliffe, J. G., and Lerner, R. A. (1982) Immunogenic structure of the influenza virus hemagglutinin. *Cell* 28, 477-487.
- (2) Greenstein, J. P., and Winitz, M. (1961) *Chemistry of the Amino Acids* pp 486-488, Wiley, New York.
- (3) Means, G. E., and Feeney, R. E. (1971) *Chemical Modification of Proteins*, pp 14-15, 68-71, Holden-Day, San Francisco.
- (4) Stark, G. R. (1965) Reactions of cyanate with functional groups of proteins. III. Reactions with amino and carboxyl groups. *Biochemistry* 4, 1030-1036.
- (5) Hunter, M. J., and Ludwig, M. L. (1962) The reaction of imidoesters with proteins and related small molecules. *J. Am. Chem. Soc.* 84, 3491-3504.
- (6) Anderson, W. (1956) *C. R. Trav. Lab. Carlsberg, Ser. Chim.* 39, 104.
- (7) Evans, R. L., and Saroff, H. A. (1957) A physiologically active guanidinated derivative of insulin. *J. Biol. Chem.* 228, 295-304.
- (8) Cole, R. D. (1961) On the transformation of insulin in concentrated solutions of urea. *J. Biol. Chem.* 236, 2670-2671.
- (9) Bradbury, J. H., Howell, J. R., Johnson, R. N., and Warren, B. (1978) Introduction of a strong binding site for lanthanides at the N-terminus of peptides and ribonuclease. *Eur. J. Biochem.* 84, 503-511.
- (10) Desbuquois, B. (1975) Acetylglucagon: preparation and characterization. *Eur. J. Biochem.* 60, 335-347.
- (11) Wetzel, R., Heyneker, H. L., Goeddel, D. V., Jhurani, P., Shapiro, J., Crea, R., Low, T. L. K., McClure, J. E., Thurman, G. B., and Goldstein, A. L. (1981) Production of biologically active N^{α} -desacetylthymosin α_1 in *Escherichia coli* through expression of a chemically synthesized gene. In *Cellular Responses to Molecular Modulators; Miami Winter Symposium* (L. W. Mozes, W. A. Scott, J. Schultz, and R. Werner, Eds.) Vol. 18 pp 251-270, Academic Press, New York.
- (12) Magee, A. I., Grant, D. A. W., Hermon-Taylor, J., and Offord, R. E. (1981) Specific one-stage method for assay of enterokinase activity by release of radiolabelled activation peptides from α -[3 H]acetyl-trypsinogen and the effect of calcium ions on the enzyme activity. *Biochem. J.* 197, 239-244.
- (13) Gray, P. W., and Goeddel, D. V. (1983) Cloning and expression of murine immune interferon cDNA. *Proc. Natl. Acad. Sci. U.S.A.* 80, 5842-5846.
- (14) Moore, G. J. (1985) Kinetics of acetylation-deacetylation

- of angiotensin II. *Int. J. Pep. Protein Res.* 26, 469-481.
- (15) Riordan, J. F., and Vallee, B. L. (1967) *O*-Acetyltyrosine. *Methods Enzymol.* 11, 570-576.
 - (16) Murdock, G. L., Warren, J. C., and Sweet, F. (1988) Human placental estradiol 17 β -dehydrogenase: Evidence for inverted substrate orientation ("wrong-way" binding) at the active site. *Biochemistry* 27, 4452-4458.
 - (17) Atassi, M. Z., and Habeeb, A. F. S. A. (1977) In *Immunochemistry of Proteins* (M. Z. Atassi, Ed.), Vol. 2, pp 177-264, Plenum Press, New York.
 - (18) Geysen, H. M., Rodda, S. J., and Mason, T. J. (1986) A priori delineation of a peptide which mimics a discontinuous antigenic determinant. *Mol. Immunol.* 23, 709-715.
 - (19) Oas, T. G., and Kim, P. S. (1988) A peptide model of a protein folding intermediate. *Nature* 336, 42-48.
 - (20) Hopper, S., Johnson, R. S., Vath, J. E., and Biemann, K. (1989) Glutaredoxin from rabbit bone marrow: Purification, characterization, and amino acid sequence determined by tandem mass spectrometry. *J. Biol. Chem.* 264, 20438-20447.

Registry No. GRTQRLQLTLNLF, 125685-76-9; SRVSQR-GRLTLNLESGRWR, 125713-32-8; norleucine-FPTIPLSR, 125713-33-9; EVVEEAN, 69871-75-6; SDAAVDTSEITTK, 125685-77-0; SDAAVDTSEITTKDLKEKEVVEEAN, 125685-78-1; AGAKQA, 125685-79-2; RGAKQA, 125685-80-5; NGAKQA, 125685-81-6; BGAKQA, 125685-82-7; EGAKQA, 125685-84-9; QGAKQA, 125685-85-0; GGAKQA, 125685-86-1; HGAKQA, 125685-87-2; IGAKQA, 125685-88-3; LGAKQA, 125685-89-4; KGAKQA, 125685-90-7; MGAKQA, 125685-91-8; FGAKQA, 125685-92-9; PGAKQA, 125685-93-0; SGAKQA, 125713-34-0; TGAKQA, 125685-94-1; WGAKQA, 125685-95-2; YGAKQA, 125685-96-3; VGAKQA, 125685-97-4; α -iodoacetyl-AGAKQA, 125713-35-1; α -iodoacetyl-RGAKQA, 125713-36-2; α -iodoacetyl-NGAKQA, 125713-37-3; α -iodoacetyl-BGAKQA, 125713-38-4; α -iodoacetyl-EGAKQA, 125713-40-8; α -iodoacetyl-QGAKQA, 125713-41-9; α -iodoacetyl-GGAKQA, 125713-42-0; α -iodoacetyl-HGAKQA, 125713-43-1; α -iodoacetyl-IGAKQA, 125713-44-2; α -iodoacetyl-LGAKQA, 125713-45-3; α -iodoacetyl-KGAKQA, 125713-46-4; α -iodoacetyl-MGAKQA, 125713-47-5; α -iodoacetyl-FGAKQA, 125713-48-6; α -iodoacetyl-PGAKQA, 125713-49-7; α -iodoacetyl-SGAKQA, 125713-50-0; α -iodoacetyl-TGAKQA, 125713-51-1; α -iodoacetyl-WGAKQA, 125713-52-2; α -iodoacetyl-YGAKQA, 125713-53-3; α -iodoacetyl-VGAKQA, 125713-54-4; bis(iodoacetyl)-AGAKQA, 125713-55-5; bis(iodoacetyl)-RGAKQA, 125713-56-6; bis(iodoacetyl)-NGAKQA, 125713-57-7; bis(iodoacetyl)-BGAKQA, 125713-58-8; bis(iodoacetyl)-EGAKQA, 125713-60-2; bis(iodoacetyl)-QGAKQA, 125713-61-3; bis(iodoacetyl)-GGAKQA, 125713-62-4; bis(iodoacetyl)-HGAKQA, 125713-63-5; bis(iodoacetyl)-IGAKQA, 125713-64-6; bis(iodoacetyl)-LGAKQA, 125713-65-7; bis(iodoacetyl)-KGAKQA, 125713-66-8; bis(iodoacetyl)-MGAKQA, 125713-67-9; bis(iodoacetyl)-FGAKQA, 125713-68-0; bis(iodoacetyl)-PGAKQA, 125713-69-1; bis(iodoacetyl)-SGAKQA, 125713-70-4; bis(iodoacetyl)-TGAKQA, 125713-71-5; bis(iodoacetyl)-WGAKQA, 125713-72-6; bis(iodoacetyl)-YGAKQA, 125713-73-7; bis(iodoacetyl)-VGAKQA, 125713-74-8; AlaGly, 687-69-4; AspGly, 3790-51-0; GluAla, 21064-18-6; GlyGly, 556-50-3; HisGly, 2578-58-7; IleAsn, 59652-59-4; LeuGly, 686-50-0; MetGly, 14486-03-4; PheGly, 721-90-4; ProGly, 2578-57-6; SerGly, 687-63-8; TrpGly, 7360-09-0; TyrGly, 673-08-5; ValGly, 686-43-1; AcGlyLysOCH₃, 10236-44-9; CysSSCH₂CH₂OH, 125685-83-8; α -iodoacetyl-CysSSCH₂CH₂OH, 125713-39-5; bis(iodoacetyl)-CysSSCH₂CH₂OH, 125713-59-9; iodoacetic anhydride, 54907-61-8; 2-iminothiolane, 6539-14-6.

Cleavage of DNA by Electrochemically Activated Mn^{III} and Fe^{III} Complexes of *meso*-Tetrakis(*N*-methyl-4-pyridiniumyl)porphine

Marisol Rodriguez, Thomas Kodadek, Maritza Torres, and Allen J. Bard*

Department of Chemistry, The University of Texas at Austin, Austin, Texas 78712. Received December 12, 1989

Electrochemical methods were used to activate Mn^{III} and Fe^{III} complexes of *meso*-tetrakis(*N*-methyl-4-pyridiniumyl)porphine (H_2TMPyP) to cause cleavage of pBR322 DNA and to study their interaction with sonicated calf thymus DNA. Electrochemical reduction of $\text{Mn}^{\text{III}}\text{TMPyP}$ and $\text{Fe}^{\text{III}}\text{TMPyP}$ (at low concentrations) in the presence of O_2 was required to activate these complexes. However, $\text{Fe}^{\text{III}}\text{TMPyP}$ at 1×10^{-6} M produced DNA strand breakage without being electrochemically reduced. At low concentrations, $\text{Fe}^{\text{II}}\text{TMPyP}$ was more efficient at cleaving DNA than $\text{Mn}^{\text{II}}\text{TMPyP}$. Reduction of O_2 at a platinum electrode also produced some cleavage but to a much smaller extent. The oxidized form of $\text{Mn}^{\text{III}}\text{TMPyP}$ (charge 5+) has higher affinity for sonicated calf thymus (CT) DNA than the reduced form (charge 4+), as determined by the negative shift in E' for the voltammetric wave in the presence of DNA. Both forms of $\text{Fe}^{\text{III}}\text{TMPyP}$ (charge 4+) interact with DNA to about the same extent. Differential pulse voltammetry was used to determine binding constants (K) and binding-site sizes (s) of the interaction of these metalloporphyrins with sonicated CT DNA. The data were analyzed assuming both mobile and static equilibria. $\text{Mn}^{\text{III}}\text{TMPyP}$ binds to DNA (5 mM Tris, 50 mM NaCl, pH 7) with $K = 5 (\pm 2) \times 10^6 \text{ M}^{-1}$, $s = 3$ bp (mobile) or $K = 3.6 (\pm 0.3) \times 10^6 \text{ M}^{-1}$, $s = 4$ bp (static). $\text{Fe}^{\text{III}}\text{TMPyP}$ at that ionic strength caused DNA precipitation. At higher ionic strength (0.1 M Tris, 0.1 M NaCl, pH 7), $\text{Fe}^{\text{III}}\text{TMPyP}$ associates to DNA with $K = 4.4 (\pm 0.2) \times 10^4 \text{ M}^{-1}$, $s = 5$ bp (mobile) or $K = 1.9 (\pm 0.1) \times 10^4 \text{ M}^{-1}$, $s = 6$ bp (static).

INTRODUCTION

In the present work, we report cleavage of pBR322 DNA by electrochemical activation of manganese(III) and iron(III) complexes of *meso*-tetrakis(*N*-methyl-4-pyridiniumyl)porphine in presence of molecular oxygen. We also describe differential pulse voltammetric studies of the interaction of these metalloporphyrins with sonicated calf thymus DNA.

Several species, including metal ions and metal complexes, have been attached to DNA-interactive groups to produce DNA chain scission. For example Fe^{II} -EDTA covalently bound to methidium as an intercalator (1, 2), to oligonucleotides (3-6), and to oligopeptides/proteins (7-9) in the presence of O_2 and a reducing agent efficiently cleaves DNA. In a similar fashion some Fe^{III} -porphyrins associated with intercalators (10-13) and oligonucleotides (14, 15) produce DNA cleavage. A number of metal ions such as Fe^{II} , Cu^{I} , Co^{III} , and Mn^{II} are cofactors of bleomycin and induce DNA degradation in vitro (16-24). The DNA cleaving ability of $\text{Cu}(\text{phen})_2^+$ and other polypyridyl complexes of Co^{III} , Ru^{II} , Rh^{III} , Pt^{II} , Fe^{III} , Cr^{III} , and Mn^{II} have also been reported (25-35). Some of these metal complexes are activated by photoirradiation rather than by added chemical agents. Nuclease activity has been observed for Cu^{II} attached to peptides (36, 37), adriamycin (38), and camptothecin (39) and for various metal ions like Fe^{III} , Mn^{III} , Co^{III} , and Cu^{II} complexed to porphyrins (40-44). Similarly acridine orange, a DNA intercalator, linked to (diaminoethane)dichloroplatinum(II) can be photoactivated to nick DNA (45).

Thus the interactions of porphyrins and metalloporphyrins with DNA, especially those of cationic porphyrins, such as *meso*-tetrakis(*N*-methyl-4-pyridiniumyl)porphine (H_2TMPyP) and its metal complexes (46-58), are of interest. Especially important is the observed ten-

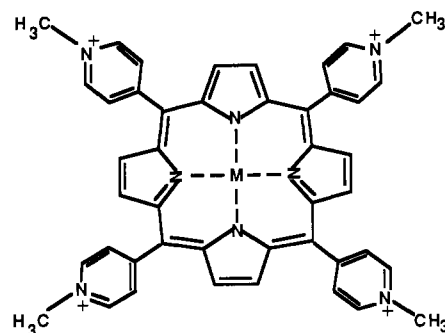


Figure 1. Structure of $\text{M}^{\text{III}}\text{TMPyP}$, $\text{M} = \text{Fe}, \text{Mn}$.

dency of some porphyrins to accumulate in malignant tumors and to cause tumor destruction after light irradiation (59-73). The water-soluble, tetracationic porphyrin H_2TMPyP is known to bind to DNA by intercalation with GC specificity (46-50) and to damage DNA upon photoillumination (44).

Studies have shown that metal complexes of TMPyP (Figure 1) also bind to DNA with binding modes dependent on the coordination number of the metal atom. The Mn^{III} , Fe^{III} , and Co^{III} complexes of TMPyP bind electrostatically in the minor groove at AT base pairs (47, 48, 54, 55). These metalloderivatives of TMPyP cleave DNA in the presence of O_2 and reducing and oxidizing agents, such as ascorbate, superoxide, and iodosobenzene (40). However, Fiel et al. (41) reported that $\text{Fe}^{\text{III}}\text{TMPyP}$ can nick DNA without any added activating agent. Praseuth et al. (44) reported that photoactivation of $\text{Co}^{\text{III}}\text{TMPyP}$ (but not $\text{Mn}^{\text{III}}\text{TMPyP}$) in the presence of O_2 can induce DNA cleavage. They showed that $\text{Fe}^{\text{III}}\text{TMPyP}$ can degrade DNA in a few minutes without light irradiation, but that the extent of degradation increased with exposure to light.

The mechanism of the chemically activated cleavage process includes the generation of a reduced form of oxygen produced in a redox reaction between the metal ion and oxygen. Several iron and manganese porphyrins in the presence of oxygen donor molecules such as iodobenzene, hypochloride, or alkyl hydroperoxides can catalyze oxidation of hydrocarbons through a high valent metal-oxo intermediate (74–78). The chemical activation of $\text{Mn}^{\text{III}}\text{TMPyP}$ and $\text{Fe}^{\text{III}}\text{TMPyP}$ has been suggested to occur through a similar mechanism. These activated metalloporphyrins are able to cause oxidative cleavage of the deoxyribose moiety and of DNA strands at the site of binding (40). Activated $\text{Fe}^{\text{III}}\text{TMPyP}$ has been found to cause base modification of the dinucleotide dTda (79).

It is thus well-established that these and other porphyrins and metalloporphyrins are very useful tools for probing nucleic acid structure, studying drug–DNA interactions, and detecting and destroying tumor and neoplastic tissue. $\text{Mn}^{\text{III}}\text{TMPyP}$ has been used in quantitative footprinting studies of neptrosin bound to a 139 base pair restriction fragment (80, 81) and as a selective magnetic resonance contrast agent for human tumors in mice (82).

In previous reports (83, 84) we showed that electrochemical methods can be used to study the interaction of small electroactive molecules with DNA. In those studies we used voltammetric data to determine the binding constant and binding-site size of tris-1,10-phenanthroline (phen) and tris-2,2'-bipyridine (bpy) complexes of Co^{III} and Fe^{II} with calf thymus (CT) DNA. In this report we show that electrochemical methods can be used to activate $\text{Mn}^{\text{III}}\text{TMPyP}$ and $\text{Fe}^{\text{III}}\text{TMPyP}$ in the presence of O_2 to cause DNA breakage. Differential pulse voltammetric data were used to obtain quantitative information about the interaction of these metalloporphyrins with sonicated CT DNA. We have chosen these metalloporphyrins for our initial studies, because they are water-soluble and easy to synthesize and their electrochemical behavior is well-understood (85–92). While this work was under way, degradation of oligodeoxynucleotides by electrochemically reduced Fe^{III} –bleomycin was reported in a brief communication by Van Atta and co-workers (93).

EXPERIMENTAL PROCEDURES

Materials. The manganese(III) and iron(III) complexes of H_2TMPyP were synthesized according to the procedure of Pasternack et al. (47) and their concentrations were determined spectrophotometrically with $\epsilon_{424} = 1.02 \times 10^5 \text{ M}^{-1} \text{ cm}^{-1}$ for $\text{Fe}^{\text{III}}\text{TMPyP}$ (55) and $\epsilon_{463} = 0.92 \times 10^5 \text{ M}^{-1} \text{ cm}^{-1}$ for $\text{Mn}^{\text{III}}\text{TMPyP}$ (94). Stock solutions were prepared with 5 mM Tris–HCl, 50 mM NaCl, pH 7 (buffer 1), or 0.1 M Tris–HCl, 0.1 M NaCl, pH 7 (buffer 2), and were stored in a refrigerator (4 °C) in the dark for no more than 3 days.

Calf thymus DNA was purchased from Sigma Chemical Co. (St. Louis, MO) and used without further purification (95). DNA stock solutions were prepared by dissolution overnight in the buffer. Calf thymus DNA was sonicated for 1 h at 0–5 °C with the sonicator on for 1 min and off for the same amount of time. The average size of fragments (600 bp) was obtained by gel electrophoresis using the *Hae* III digest of ϕX174 RF DNA as the standard. DNA concentration per nucleotide phosphate was determined by UV absorbance at 260 nm with $\epsilon_{260} = 6600 \text{ M}^{-1} \text{ cm}^{-1}$ (96). Stock solutions were stored at 4 °C and discarded after no more than 3 days.

pBR322 DNA was isolated from the *Escherichia coli* strain HB101 and purified according to the procedure of Maniatis (97). pBR322 was dissolved in 10 mM Tris–HCl, 1 mM EDTA buffer, pH 7.4, and stored at –20 °C.

All other chemicals were of reagent grade and used as received. Solutions were prepared with water that was purified by passage through a Millipore Milli-Q system.

Instrumentation. Voltammetric [cyclic voltammetric (CV) and differential pulse voltammetric (DPV)] studies and controlled-potential bulk electrolysis (BE) experiments were done with a Bioanalytical Systems (BAS) (West Lafayette, IN) Model BAS-100 electrochemical analyzer. DPV experiments were performed under the following conditions: pulse amplitude (PA), –50 mV; pulse width, 50 ms; sweep rate (v), 4 mV/s; sample width, 17 ms; and pulse period, 1 s.

Ultraviolet–visible absorption spectra were obtained on a Hewlett-Packard 8451 A diode-array spectrophotometer. The agarose gels were photographed with a Polaroid MP-4 camera and quantified by scanning densitometry.

CV and DPV Experiments. Voltammetric studies were carried out in a one-compartment cell, containing a Pt disk (area, 0.023 cm^2) working electrode, a Pt flag counter electrode, and a saturated calomel electrode (SCE) reference electrode. The working electrode surface was highly polished with $0.3 \mu\text{m}$ alumina paste (Buehler, Lake Bluff, IL) prior to each experiment.

Solutions were thoroughly deoxygenated, unless otherwise indicated, by bubbling with argon that had been previously saturated with water. During the data acquisition, an argon atmosphere was maintained over the solution in the cell. Before use, all glassware was silanized in 5% trimethylchlorosilane (Petrach Systems, Bristol, PA) in toluene. All the measurements were performed at 25 °C.

Bulk Electrolysis. To conserve the DNA it was necessary to do the bulk electrolysis experiments on a very small scale. Thus a microcell assembly (BAS Type MCA), consisting of an outer working electrode compartment and an inner compartment with a porous Vycor plug containing the reference and counter electrodes was used to electrolyze different amounts of the metalloporphyrins with pBR322 levels of $2 \mu\text{g}$. The reaction mixture was contained in the working electrode compartment and the other compartment held supporting electrolyte. The working solution compartment volume was $100 \mu\text{L}$.

The electrolysis was carried out in the dark for 12 h at –0.4 V for $\text{Mn}^{\text{III}}\text{TMPyP}$ and at –0.3 V for $\text{Fe}^{\text{III}}\text{TMPyP}$. During the electrolysis O_2 was bubbled into the supporting electrolyte. The working electrode was a Pt foil (area, 1 cm^2), the counter electrode was a Pt wire, and the reference was a SCE.

Gel Electrophoresis. A fraction ($20 \mu\text{L}$) of the reaction mixture and $5 \mu\text{L}$ of the loading buffer (bromophenyl blue dye and sucrose) were loaded into the wells of a 0.8% horizontal agarose gel containing $1 \mu\text{g}/\text{mL}$ ethidium bromide. The gel was electrophoresed at 5 V/cm for 5 h in 89 mM Tris, 89 mM boric acid, 2 mM EDTA buffer, pH 8. Samples containing pBR322 and metalloporphyrin that were not electrolyzed were incubated for a period of 2 h. The same results were obtained when they were incubated for 12 h. After electrophoresis, the DNA bands were visualized and photographed under ultraviolet light. Scanning densitometry of the photographic negatives was used to quantitate the amount of supercoiled circular (form I), open circular (form II), and linear (form III) species.

RESULTS

CV of $\text{Mn}^{\text{III}}\text{TMPyP}$ and $\text{Fe}^{\text{III}}\text{TMPyP}$. Figure 2 shows typical cyclic voltammograms of 0.50 mM $\text{Mn}^{\text{III}}\text{TMPyP}$ and 0.78 mM $\text{Fe}^{\text{III}}\text{TMPyP}$ in the absence and in the presence of molecular oxygen. In the absence of O_2 (Figure

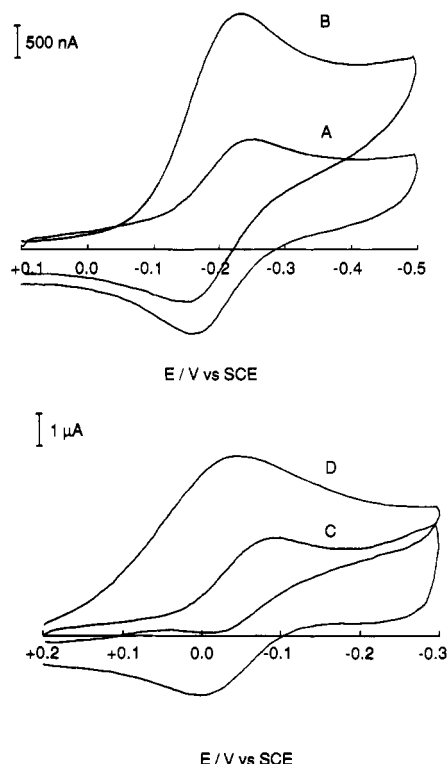


Figure 2. Cyclic voltammograms of (A, B) 0.50 mM Mn^{III} TMPyP and of (C, D) 0.78 mM Fe^{III} TMPyP, (A, C) in the absence and (B, D) in the presence of air (oxygen): sweep rate, 100 mV/s; supporting electrolyte, buffer 1.

Table I. Cyclic Voltammetric Data of Mn^{III} TMPyP in the Absence of Oxygen^a

v , mV s ⁻¹	E_{pc} , mV ^b	E_{pa} , mV	ΔE , mV	$E^{\circ'}$, mV	i_{pa}/i_{pc}
50	-249 (4)	-156 (5)	93	-203	0.9
100	-247 (5)	-159 (3)	88	-203	1.0
200	-250 (4)	-153 (3)	97	-202	1.0
500	-259 (3)	-146 (2)	113	-203	1.0

^a [Mn^{III} TMPyP] = 0.50 mM; supporting electrolyte, buffer 1.

^b Numbers in parentheses are standard deviations for three measurements.

Table II. Cyclic Voltammetric Data of Fe^{III} TMPyP in the Absence of Oxygen^a

v , mV s ⁻¹	E_{pc} , mV ^b	E_{pa} , mV	ΔE , mV	$E^{\circ'}$, mV	i_{pa}/i_{pc}
50	-91 (4)	3 (2)	94	-44	0.9
100	-90 (4)	3 (2)	93	-44	1.0
200	-92 (2)	2 (4)	94	-45	0.9
500	-97 (4)	5 (5)	102	-46	0.8

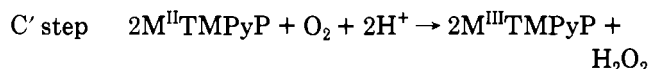
^a [Fe^{III} TMPyP] = 0.78 mM; supporting electrolyte, buffer 1. ^b Numbers in parentheses are standard deviations for three measurements.

2, parts A and C), reduction of M^{III} to M^{II} (M = Mn or Fe) occurs during the forward scan while the reoxidation of M^{II} occurs in the reverse scan. The cathodic and anodic peak potentials for the reduction and oxidation processes of Mn^{III} TMPyP were observed at E_{pc} = -245 mV and E_{pa} = -161 mV and of Fe^{III} TMPyP at E_{pc} = -90 mV and E_{pa} = 1 mV, respectively.

Voltammetric data obtained for both metalloporphyrins at different scan rates in the absence of oxygen are given in Tables I and II. For both compounds the cathodic peak potentials (E_{pc}) were slightly dependent on scan rate (v) and the separation of the anodic peak potential (E_{pa}) and E_{pc} (ΔE) was between 88 and 113 mV, suggesting quasireversible one-electron transfer reactions. The ratio of anodic to cathodic peak current ($i_{pa}/i_{pc} \approx 1$) indicated the absence of following reaction kinetic compli-

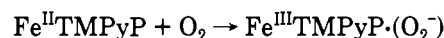
cations. The formal potential ($E^{\circ'}$), calculated as the average of E_{pc} and E_{pa} , was essentially independent of v , and for 50 mV/s $\leq v \leq 500$ mV/s, $E^{\circ'} = -202 (\pm 1)$ mV for Mn^{III} TMPyP and $E^{\circ'} = -44 (\pm 2)$ mV for Fe^{III} TMPyP.

In the presence of O₂ (Figure 2, parts B and D) $i_{pa}/i_{pc} < 1$, characteristic of an electrochemical catalytic mechanism (EC') in which the parent molecule M^{III} TMPyP is regenerated by reaction of the M^{II} form with O₂ as shown by the following formal overall reactions (85–89) (the actual species undergoing reaction and their charges depend upon the pH and the state of protonation, as discussed briefly in the discussion section):

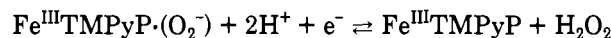
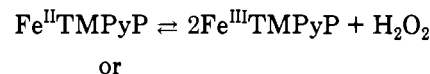
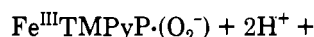


where M = Mn or Fe.

For Fe^{III} TMPyP, the reoxidation of the reduced form by oxygen-producing H₂O₂ occurs via an oxygen adduct in which the oxygen is bound axially to the metal (87, 88).



This adduct is then further reduced by another reduced metalloporphyrin or at the electrode.



Furthermore, H₂O₂ can be converted to H₂O.



The final product depends on the electrode material as well as on the concentration ratio of the metalloporphyrin to oxygen. At a glassy carbon electrode, oxygen is reduced primarily to H₂O₂, when the oxygen concentration is equal or higher than that of the metalloporphyrin (88, 90).

DPV of Mn^{III} TMPyP and Fe^{III} TMPyP in the Presence of Sonicated CT DNA. To study the interaction of the porphyrins with DNA, voltammetric studies of mixtures of the Fe^{III} and Mn^{III} species with different amounts of DNA were undertaken (83, 84). To conserve the pBR322 DNA, these studies were carried out with CT DNA. However under the solution conditions needed for the electrochemical studies, the addition of unmodified CT DNA caused precipitation of the porphyrins. Thus sonicated CT DNA, consisting of fragments with an average of 600 bp, were used, with low (0.1 mM) concentrations of the metal porphyrins. Typical differential pulse voltammograms of 0.1 mM Mn^{III} TMPyP and 0.1 mM Fe^{III} TMPyP in the absence of oxygen with and without sonicated CT DNA are shown in Figure 3. The average value of the peak potential (E_p^{av}) obtained by DPV in absence of CT DNA for 0.1 mM Mn^{III} TMPyP was -173 (± 7) mV and for 0.1 mM Fe^{III} TMPyP was -108 (± 8) mV, where the values in parentheses represent $\pm 2\sigma$ for five measurements.

The DPV peak potential (E_p) of a reversible reaction can be related to the formal potential ($E^{\circ'}$) by the following equation (98):

$$E^{\circ'} = E_p + \text{PA}/2 \quad (1)$$

where PA is the pulse amplitude. The $E^{\circ'}$ for Mn^{III}.

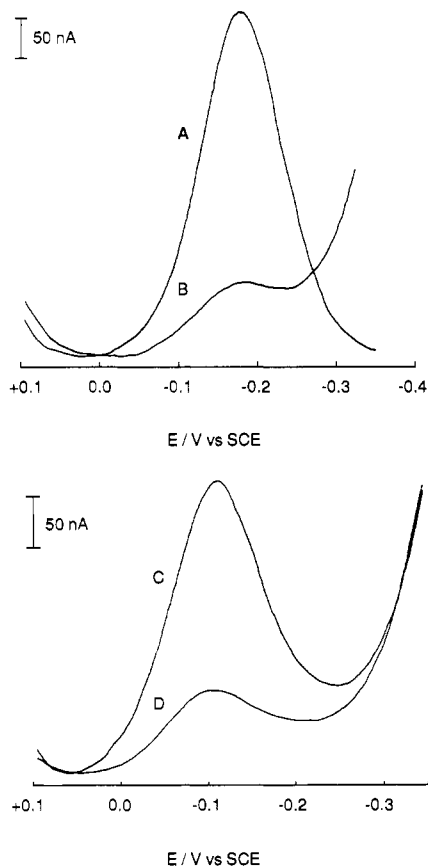


Figure 3. Differential pulse voltammograms of (A, B), 0.1 mM Mn^{III} TMPyP (buffer 1) and of (C, D) 0.1 mM Fe^{III} TMPyP (buffer 2), (A, C) in the absence of DNA and in the presence of sonicated CT DNA with (B) 0.8 mM NP, (D) 4.8 mM NP. Solutions were deoxygenated.

TMPyP calculated from this equation is -198 mV and for Fe^{III} TMPyP is -133 mV. The $E^{\circ'}$ obtained from DPV for Mn^{III} TMPyP is essentially the same as that found by CV, however that obtained by DPV for Fe^{III} TMPyP was significantly more negative. To explain this behavior we have to consider the different characteristic times (τ) of CV and DPV experiments. The time scale for a CV experiment (at $v = 100$ mV/s) is $\tau \approx RT/vF \approx 257$ ms [F is the faraday constant ($96,485$ C/eq) and R is the molar gas constant (8.314 J/mol $^{-1}$ K $^{-1}$)] while for a DPV experiment under the conditions here $\tau = 17$ ms. Therefore, for a system with heterogeneous electron transfer kinetic limitations as is the case for Fe^{III} TMPyP, more reversible behavior might be found with CV than with DPV.

The E_p^{av} of 0.1 mM Mn^{III} TMPyP in presence of sonicated CT DNA at 0.8 mM nucleotide phosphate (NP) was $-177 (\pm 8)$ mV. At the same supporting electrolyte concentration, Fe^{III} TMPyP caused DNA precipitation. To decrease its strong interaction with CT DNA, the salt concentration was increased and experiments were done in 0.1 M Tris-HCl, 0.1 M NaCl, pH 7, where no precipitation was observed. The E_p^{av} of 0.1 mM Fe^{III} TMPyP in presence of 4.8 mM NP was $-100 (\pm 4)$ mV. The effect of R , defined as $[\text{NP}]/[\text{M}^{\text{III}}\text{TMPyP}]$, on the DPV peak potential (E_p) of Mn^{III} TMPyP and Fe^{III} TMPyP is shown in Figure 4, parts A and B, respectively. The E_p^{av} , and therefore $E^{\circ'}_{\text{DPV}}$, of Mn^{III} TMPyP was practically unaffected by the addition of sonicated CT DNA for $0 < \text{NP} \leq 1$ mM, but at higher DNA concentration (e.g. $[\text{NP}] = 2.1$ mM), the E_p^{av} shifted to more negative values by 25 mV. This implies that the interaction of the oxidized Mn^{III} form with CT DNA is stronger than that of the

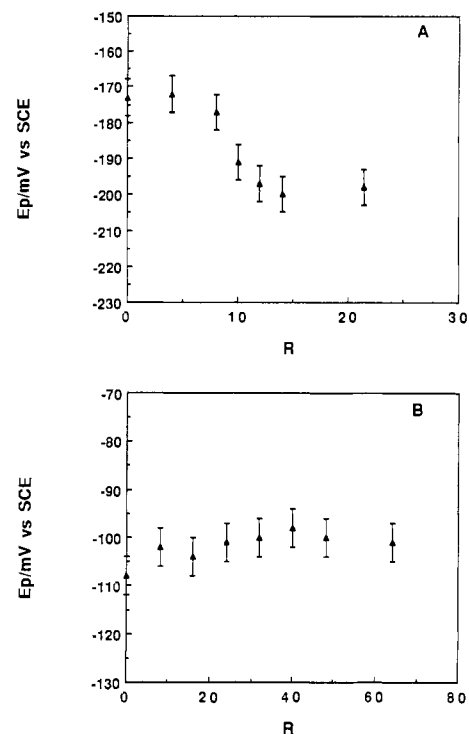


Figure 4. Effect of R ($[\text{NP}]/[\text{M}^{\text{III}}\text{TMPyP}]$) on the DPV peak potential (E_p) of (A) 0.1 mM Mn^{III} TMPyP (buffer 1) and (B) 0.1 mM Fe^{III} TMPyP (buffer 2).

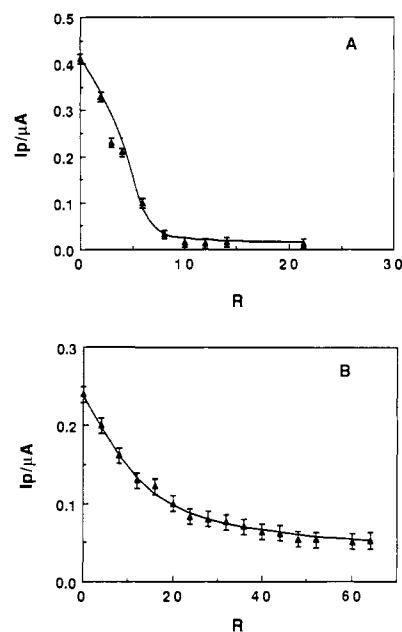


Figure 5. Titration curve of (A) 0.1 mM Mn^{III} TMPyP (buffer 1) and of (B) 0.1 mM Fe^{III} TMPyP (buffer 2) with sonicated CT DNA. Points represent the experimental data and solid curves represent the best fit obtained assuming mobile equilibria. Error bars correspond to $\pm 2\sigma$ for five measurements.

reduced Mn^{II} form. The E_p^{av} of Fe^{II} TMPyP in the presence of 4.8 mM NP shifted to more positive values by only 8 mV. This small shift, however, suggests that the reduced Fe^{II} form interacts with CT DNA slightly more strongly than the oxidized Fe^{III} form.

On the other hand, the peak current (i_p) measured for both compounds was greatly affected by the presence of DNA. For 0.1 mM Mn^{III} TMPyP, the i_p decreased to 8% and for 0.1 mM Fe^{III} TMPyP to 22% of that in the absence of DNA (Figure 3, parts B and D). The decrease of the currents at a given R value is a measure of the strength

Table III. Binding Constants (*K*) and Site Sizes (*s*) of 0.1 mM Mn^{III}TMPyP^a and 0.1 mM Fe^{III}TMPyP^b with Sonicated CT DNA Based on Titration Data

metalloporphyrin	model	experimental parameters ^c		best fit ^d			
		10 ⁶ <i>D_f</i> , cm ² /s	10 ⁹ <i>D_b</i> , cm ² /s	10 ⁶ <i>D_f</i> , cm ² /s	10 ⁹ <i>D_b</i> , cm ² /s	10 ⁻⁵ <i>K</i> , M ⁻¹	<i>s</i> , bp
Mn ^{III} TMPyP	mobile	0.9 (0.3)	0.8 (0.4)	0.9	0.4	50 (20)	3
	static	0.9 (0.3)	0.8 (0.4)	0.9	0.4	36 (3)	4
Fe ^{III} TMPyP	mobile	0.30 ^e (0.03)	5 (3)	0.3	2	0.44 (0.02)	5
	static	0.30 ^e (0.03)	5 (3)	0.3	4	0.19 (0.01)	6

^a Supporting electrolyte, buffer 1. ^b Supporting electrolyte, buffer 2. ^c Numbers in parentheses represent $\pm 2\sigma$ for five measurements. ^d Numbers in parentheses represent 95% of interval confidence of value determined by nonlinear-regression calculations. ^e This value differs from that found by CV and is probably not the actual free diffusion coefficient (see the text).

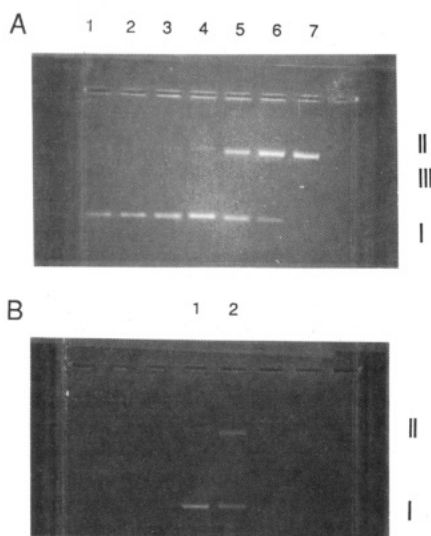


Figure 6. Electrochemically activated cleavage of pBR322 DNA with Mn^{III}TMPyP. (A) Electrolysis was carried out at -0.4 V for samples in lanes 5-7. Lane 1, pBR322 alone; lanes 2, 3, and 4, pBR322 and Mn^{III}TMPyP at concentrations of 1×10^{-8} , 1×10^{-7} , and 1×10^{-6} M, respectively; and lanes 5, 6, and 7, pBR322 and Mn^{III}TMPyP (electrochemically reduced) at concentrations of 1×10^{-8} , 1×10^{-7} , and 1×10^{-6} M, respectively. (B) Lane 1, pBR322 alone; and lane 2, pBR322 control (electrolyzed at a Pt cathode in oxygen-saturated solution at -0.4 V with no metalloporphyrin).

of interaction of these molecules with DNA. The current decreases because the diffusion of the metal complex, when bound to DNA, is much slower than when it is free in solution (83, 84).

The diffusion coefficients of the free metalloporphyrins were obtained in absence of sonicated CT DNA: Mn^{III}TMPyP, $D_f = 0.9 (\pm 0.3) \times 10^{-6}$ cm²/s; Fe^{III}TMPyP, $D_f = 3.0 (\pm 0.3) \times 10^{-7}$ cm²/s. The D_f of Fe^{III}TMPyP obtained by DPV is small compared to that obtained by CV ($D_f = 2.0 (\pm 0.2) \times 10^{-6}$ cm²/s). This suggests that kinetic factors play a role in the observed DPV peak height. However, these factors will affect the response in the presence of DNA in the same way, assuming the kinetics are not changed, so that the titration curves of DPV response vs the amount of DNA should still yield reasonable estimates of binding constants and site sizes. The bound diffusion coefficient (D_b) was obtained at the highest *R* possible (considering detection limits of the instrument and solubility of CT DNA) to make sure that the metalloporphyrins were bound to the DNA macromolecule. The bound diffusion coefficient calculated at *R* = 21 for Mn^{III}TMPyP was $D_b = 8 (\pm 4) \times 10^{-10}$ cm²/s and at *R* = 73 for Fe^{III}TMPyP was $D_b = 5 (\pm 3) \times 10^{-9}$ cm²/s.

The binding constant (*K*) and binding-site sizes (*s*) were calculated for both metalloporphyrins on the basis of both fast (mobile) and slow (static) equilibria with a titration curve in which the DPV peak current (*i_p*) was measured

at several *R* values. The interpretation of the changes in voltammetric behavior (*E*^o, *i_p*) due to the interaction of an electroactive species with DNA, as well as the approach used to fit the titration data, have been discussed in detail in previous publications (83, 84).

The titration curves of Mn^{III}TMPyP and Fe^{III}TMPyP with sonicated CT DNA are shown in Figure 5, parts A and B, respectively. For the titration of Mn^{III}TMPyP, the supporting electrolyte used was 5 mM Tris-HCl, 50 mM NaCl, pH 7, while for Fe^{III}TMPyP it was 0.1 M Tris-HCl, 0.1 M NaCl, pH 7. The solid curves represent the best fit for the mobile equilibria. Results of the nonlinear regression analysis of the titration data for both complexes are summarized in Table III.

Cleavage of pBR322 DNA. Electrochemical reduction of Mn^{III}TMPyP and Fe^{III}TMPyP, in the presence of oxygen, induced DNA cleavage. This electrochemical reductive activation parallels previous studies of porphyrins with chemical reductants (e.g., ascorbate, dithiothreitol, 2-mercaptoethanol, sodium hydrosulfite) (10-13, 40-42) but does not involve the addition of these reagents. Figure 6A shows the gel electrophoresis of pBR322 with different concentrations of Mn^{III}TMPyP. In lanes 2-4, Mn^{III}TMPyP was simply incubated with pBR322 DNA while in lanes 5-7 the reaction mixture was submitted to electrolysis at -0.4 V for 12 h. Production of the nicked open circular form II occurred only in lanes 5-7, where Mn^{III}TMPyP was electrochemically reduced. In lane 7, for example, there is complete conversion of the supercoiled form I to form II as well as some linear form III. To determine how much of this cleavage was really due to the reduction and therefore activation of Mn^{III}TMPyP, a control experiment was carried out in which an O₂-saturated solution of pBR322 was electrolyzed at -0.4 V. Oxygen reduction at the Pt cathode predominantly produces H₂O (99-102). Some DNA cleavage was observed in the control experiment (Figure 6B), however to a much smaller extent than when Mn^{III}TMPyP was present. To ascertain whether a small amount of H₂O₂ produced during the cathodic reduction of oxygen at this potential was responsible for the observed cleavage in the control experiment, a sample containing 2 μg of pBR322 was incubated for 12 h with 1.0 mM H₂O₂ and a piece of Pt metal. No cleavage was observed. This suggests that a small amount of cleavage might be promoted by some direct interaction of the DNA and oxygen at the Pt cathode. We did not consider it necessary to introduce a control experiment without oxygen, since the dependence of DNA scission on the presence of oxygen has been widely studied (10, 42).

Quantitative data of Figure 6 is expressed in terms of the percentages of forms I, II, and III in Table IV. Table IV also shows the number of single-strand breaks per DNA molecule (*S*). This value was calculated with the following equation (1):

$$S = -\ln \chi_I \quad (2)$$

Table IV. Results of pBR322 DNA Cleavage by Electrochemically Activated Mn^{III}TMPyP

lane	conditions ^a	electrolysis	% form I	% form II	% form III	S ^b
Figure 6A						
1	pBR322 alone	no	91	9	0	
2	pBR322, 0.01 μM Mn-P	no	90	10	0	
3	pBR322, 0.1 μM Mn-P	no	91	9	0	
4	pBR322, 1 μM Mn-P	no	91	9	0	
5	pBR322, 0.01 μM Mn-P	yes	50	50	0	0.60 (0.13)
6	pBR322, 0.1 μM Mn-P	yes	18	82	0	1.62 (1.15)
7	pBR322, 1 μM Mn-P	yes	0	96	4	4.54 (4.07)
Figure 6B						
1	pBR322 alone	no	90	10	0	
2	pBR322 alone	yes	57	43	0	0.46

^a Mn-P = Mn^{III}TMPyP. ^b Values in parentheses are the number of single strands produced by activated Mn^{III}TMPyP (*S* of control experiment was subtracted).

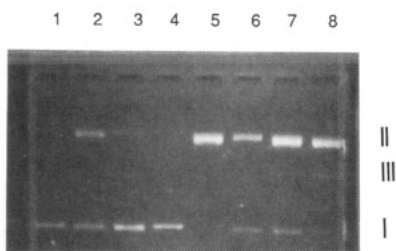


Figure 7. Electrochemically activated cleavage of pBR322 DNA with Fe^{III}TMPyP. Electrolysis was carried out at -0.3 V for samples in lanes 2, 6, 7, and 8. Lane 1, pBR322 alone; lane 2, pBR322 control (no Fe^{III}TMPyP); lanes 3, 4, and 5, pBR322 and Fe^{III}TMPyP at concentrations of 1×10^{-8} , 1×10^{-7} , and 1×10^{-6} M, respectively; and 5, 6, and 7, pBR322 and Mn^{III}-TMPyP (electrochemically reduced) at concentrations of 1×10^{-8} , 1×10^{-7} , and 1×10^{-6} M, respectively.

where χ_I is the fraction of form I. If form III was present, then *S* was obtained from eq 3 where χ_{II} is the fraction

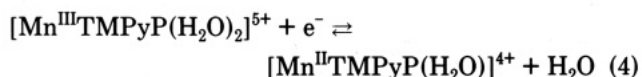
$$\chi_I + \chi_{II} = [1 - S(2h + 1)/2L]^{S/2} \quad (3)$$

of form II, *h* is the maximum space in base pairs between two nicks, required to produce form III (*h* = 16 base pairs) (103), and *L* is the total number of base pairs of pBR322 plasmid DNA (*L* = 4362 base pairs) (104). The *S* value reported was subtracted from that obtained for pBR322 DNA alone, in lane 1 of Figure 6, parts A and B. Numbers in parentheses are *S* values that account only for the catalytic effect of reduced Mn^{III}TMPyP (*S* of the control experiment was subtracted).

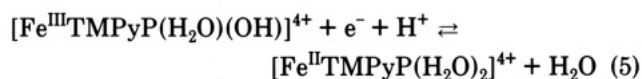
The gel electrophorogram of pBR322 with Fe^{III}-TMPyP is shown in Figure 7. In this gel, the control experiment was included in lane 2 and the electrolysis was done at -0.3 V for samples in lanes 6–8. The percent of forms I–III and the *S* values obtained from Figure 7 are given in Table V. At concentrations of complex of 1×10^{-8} and 1×10^{-7} M, formation of form II occurred only when Fe^{III}TMPyP was electrochemically reduced. However, 1×10^{-6} M Fe^{III}TMPyP was found to produce the same amount of cleavage in the absence of electrochemical reduction. In lane 5, 98% of form I was transformed to form II, and in lane 8, form I was totally converted to 97% form II and 3% form III.

DISCUSSION

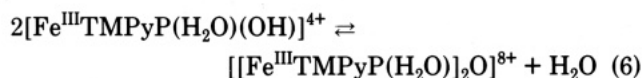
Voltammetric Studies of Mn^{III}TMPyP and Fe^{III}TMPyP. Mn^{III}TMPyP and its reduced form undergo several acid dissociation equilibria in aqueous solution. The identification of these species and the *pK* for these equilibria has been determined by Harriman et al. (94). At pH 7, the electrochemical reduction of Mn^{III}TMPyP can be described by eq 4. For Fe^{III}TMPyP the equilib-



ria of species in solution is somewhat more complicated and is not fully understood, because of simultaneous acid-base and dimerization equilibria that depend on concentration, ionic strength, and pH. The reduction of Fe^{III}-TMPyP can be expressed as



according to Kurihara et al. (89). At this pH, the following monomer-dimer equilibrium also occurs.



Several values appear in the literature for the magnitude of the dimerization constant, *K*_d: $2 \times 10^3 \text{ M}^{-1}$ by Forshey et al. (86), $9 \times 10^5 \text{ M}^{-1}$ by Pasternack et al. (105), $2.1 \times 10^3 \text{ M}^{-1}$ by Tondreau et al. (106), and $3 \times 10^5 \text{ M}^{-1}$ by Goff et al. (107).

The CV behavior of both metalloporphyrins is in agreement with that reported in the literature (85–92). The reduction of Fe^{III}TMPyP in phosphate buffer at pH 6.5–9.4 and at a glassy carbon electrode have been reported to show two cathodic peaks. The first corresponds to the reduction of the monomer form of Fe^{III}TMPyP and the second, at more negative potentials, to that of the dimeric form. The peak potential of the second peak was found between -0.45 and -0.55 V vs SCE. However, our CV of this compound in 5 mM Tris-HCl, 50 mM NaCl, pH 7, and at a Pt electrode only encompassed the first cathodic peak, because we used a Pt electrode which could not be used at potentials more negative than -0.6 V vs SCE due to background limitations (i.e., evolution of hydrogen).

As we pointed out earlier, the mode of interaction of these metalloporphyrins with DNA is electrostatic in nature. These complexes possess a high positive charge (5+ or 4+) and interact very strongly with the negative phosphate groups of the DNA backbone. On the basis of this type of interaction, we should expect a more positively charged species to have a higher affinity for DNA. Thus if the oxidized form of a redox couple had a higher positive charge than the reduced form, a difference in binding strength may arise, which would be reflected as a shift in *E*^{o'} to more negative values. In DPV, the *E*^{o'} (or *E*_p^{av}) of Mn^{III}TMPyP shifted 25 mV to more negative values, implying that the binding constant of the oxidized species (5+) to DNA is 2.7 times larger than that of the reduced species (4+). In the case of Fe^{III}-TMPyP, where both forms have charge 4+, the *E*^{o'} shifted

Table V. Results of pBR322 DNA Cleavage by Electrochemically Activated Fe^{III}TMPyP

lane	conditions ^a	electrolysis	% form I	% form II	% form III	S ^b
1	pBR322 alone	no	90	10	0	
2	pBR322 alone	yes	50	50	0	
3	pBR322, 0.01 μ M Fe-P	no	89	11	0	
4	pBR322, 0.1 μ M Fe-P	no	92	8	0	
5	pBR322, 1 μ M Fe-P	no	2	98	0	3.81 (3.22)
6	pBR322, 0.01 μ M Fe-P	yes	24	76	0	1.53 (0.94)
7	pBR322, 0.1 μ M Fe-P	yes	15	85	0	1.80 (1.11)
8	pBR322, 1 μ M Fe-P	yes	0	97	3	3.90 (3.21)

^a Fe-P = Fe^{III}TMPyP. ^b Values in parentheses are the number of single strands produced by activated Fe^{III}TMPyP (S of control experiment was subtracted).

only by 8 mV to more positive potentials, indicating no large differences in binding between the two forms and DNA. These thermodynamic arguments are somewhat compromised by the quasireversibility of the CV and DPV waves; however, the averaging procedure employed should give a good estimate of the formal potential. To obtain the binding constants we assumed reversibility of the systems, although some heterogeneous electron transfer limitations occur, especially in the case of Fe^{III}TMPyP, as discussed previously. For this case, we assumed that the electron-transfer kinetics of the Fe^{III}TMPyP is not affected by the presence of DNA as demonstrated by the absence of changes on the peak width at half-height of the DPV waves.

The DPV peak currents of both metalloporphyrins decreased drastically in presence of an excess of DNA. This decrease in the current is an indication of the degree of interaction of these complexes with DNA and was used to quantify the binding of these metalloporphyrins with CT DNA. The values of the binding constants obtained for sonicated CT DNA and Mn^{III}TMPyP in 5 mM Tris, 50 mM NaCl, pH 7, and Fe^{III}TMPyP in 0.1 M Tris, 0.1 M NaCl, pH 7, are larger than those reported for other DNA electrostatic binders such as Ru(bpy)₃²⁺, Fe(bpy)₃²⁺, and Co(bpy)₃²⁺ with native CT DNA. At 5 mM Tris, 50 mM NaCl, pH 7, Co(bpy)₃²⁺ has a binding constant for native CT DNA of 1.4×10^4 M⁻¹ (mobile equilibria), while the Ru(bpy)₃²⁺ and Fe(bpy)₃²⁺ affinity for CT DNA is negligible (83, 84, 108). Binding affinity studies of Ru(bpy)₃²⁺ and Fe(bpy)₃²⁺ with native CT DNA have been carried out at lower salt concentration (83, 84, 109). The binding-site sizes (*s*) found here compare quite well with those obtained for these bipyridyl complexes. The value of the binding constant for Fe^{III}TMPyP with sonicated CT DNA determined in this study ($K = 4.4 \times 10^4$ M⁻¹; mobile equilibria) is somewhat smaller than the one determined with native CT DNA by competition binding experiments using ethidium bromide ($K = 3.5 \times 10^5$ M⁻¹) (57) at the same ionic strength.

Cleavage of pBR322 DNA. As is evident from Figures 6 and 7, electrochemical reduction of Mn^{III}TMPyP and Fe^{III}TMPyP (at low concentrations) was essential to activate these complexes and cause DNA breakage. In the control experiment, as illustrated in Figure 6B, the reduction of oxygen also induced DNA degradation but to a lesser extent. H₂O₂, an expected intermediate of the reduction of oxygen, did not cause cleavage, even in the presence of Pt metal that would produce some hydroxyl radicals (110). Fe^{III}TMPyP (1×10^{-8} M), when electrochemically reduced, was more efficient at cleaving DNA than reduced Mn^{III}TMPyP. Fe^{III}TMPyP converted 85% of the form I to form II, while Mn^{III}TMPyP cut only 50%. At this concentration Mn^{III}TMPyP produced practically the same percentages of forms I and II as the control experiment, which means that the nicking observed was not due to activated Mn^{III}TMPyP.

At 1×10^{-6} M, Fe^{III}TMPyP caused DNA breakage with-

out being electrochemically reduced. This is consistent with the results reported by Fiel et al. (41). Ward et al. (40) attributed this phenomenon to the presence of reducing agents in the agarose. Possibly disproportionation of two Fe^{III}TMPyP molecules results in self-activation.

The long periods of time required for the activation of the metalloporphyrins via electrochemical reduction can be attributed to the slow mass transfer rates in the cell used, since the solutions were not stirred. Electrochemical activation, on the other hand, is a clean method which does not require addition of a reductant and thus makes the analysis of reaction products easier. It can also offer a wider range of potentials to activate molecules with different binding specificities which might not be activated by chemical methods and might also be useful in following formation and consumption of electroactive species to study reaction mechanisms.

CONCLUSION

We have shown that it is possible to use electrochemical methods to study the interaction of Mn^{III}TMPyP and Fe^{III}TMPyP with sonicated calf thymus DNA and to activate these complexes to produce pBR322 DNA cleavage. These results thus complement the earlier communication by Van Atta et al. (93) on electrochemical activation of the Fe^{III}-bleomycin complex.

ACKNOWLEDGMENT

We gratefully acknowledge the financial support from a National Science Foundation Minority Graduate Fellowship provided to M.R. and from NSF Grant CHE 8901450. We also thank Dr. Lawrence L. Poulsen for use of the computer-densitometric system.

LITERATURE CITED

- (1) Hertzberg, R. P., and Dervan, P. B. (1984) *Biochemistry* 23, 3934.
- (2) Dervan, P. B. (1986) *Science* 232, 464.
- (3) Chu, B. C. F., and Orgel, L. E. (1985) *Proc. Natl. Acad. Sci. U.S.A.* 82, 963.
- (4) Dreyer, G. B., and Dervan, P. B. (1985) *Proc. Natl. Acad. Sci. U.S.A.* 82, 968.
- (5) Boutorin, A. S., Vlassov, V. V., Kazakov, S. A., Kutiavin, I. V., and Podymnigov, M. A. (1984) *FEBS* 172, 43.
- (6) Moser, H. E., and Dervan, P. B. (1987) *Science* 238, 645.
- (7) Taylor, J. S., Schultz, P. G., and Dervan, P. B. (1984) *Tetrahedron* 40, 457.
- (8) Youngquist, R. S., and Dervan, P. B. (1985) *Proc. Natl. Acad. Sci. U.S.A.* 82, 2565.
- (9) Sluka, J. P., Horvath, S. J., Bruist, M. F., Simon, M. I., and Dervan, P. B. (1987) *Science* 238, 1129.
- (10) Lown, J. W., and Joshua, A. V. (1982) *J. Chem. Soc., Chem. Commun.* 1298.
- (11) Lown, J. W., Sondhi, S. M., Ong, C. W., Skorobogaty, A., Kishikawa, H., and Dabrowiak, J. C. (1986) *Biochemistry* 25, 5111.

- (12) Hashimoto, Y., Lee, C. S., Shudo, K., and Okamoto, T. (1983) *Tetrahedron Lett.* 24, 1523.
- (13) Hashimoto, Y., Iijima, H., Nozaki, Y., and Shudo, K. (1986) *Biochemistry* 25, 5103.
- (14) Le Doan, T., Perrouault, L., Hélène, C., Chassignol, M., and Thuong, N. T. (1986) *Biochemistry* 25, 6736.
- (15) Le Doan, T., Perrouault, L., Chassignol, M., Thuong, N. T., and Hélène, C. (1987) *Nucleic Acids Res.* 15, 8643.
- (16) Sausville, E. A., Stein, R. W., Peisach, J., and Horwitz, S. B. (1978) *Biochemistry* 17, 2746.
- (17) Sugiura, Y., Suzuki, T., Kuwahara, J., and Tanaka, H. (1982) *Biochem. Biophys. Res. Commun.* 105, 1511.
- (18) Burger, R. M., Peisach, J., and Horwitz, S. B. (1981) *J. Biol. Chem.* 256, 11636.
- (19) Ehrenfeld, G. M., Rodriguez, L. O., Hecht, S. M., Chang, C., Basus, V. J., and Oppenheimer, N. J. (1985) *Biochemistry* 24, 81.
- (20) Ehrenfeld, G. M., Shipley, J. B., Heimbrook, D. C., Sugiyama, H., Long, E. C., van Boom, J. H., van der Marel, G. A., Oppenheimer, N. J., and Hecht, S. M. (1987) *Biochemistry* 26, 931.
- (21) Chang, C. H., and Meares, C. F. (1984) *Biochemistry* 23, 2268.
- (22) Ehrenfeld, G. M., Murugesan, N., and Hecht, S. M. (1984) *Inorg. Chem.* 23, 1496.
- (23) Suzuki, T., Kuwahara, J., Goto, M., and Sugiura, Y. (1985) *Biochim. Biophys. Acta* 824, 330.
- (24) Stubbe, J., and Kozarich, J. W. (1987) *Chem. Rev.* 87, 1107.
- (25) Sigman, D. S. (1986) *Acc. Chem. Res.* 19, 180.
- (26) Marshall, L., Graham, D. R., Reich, K. A., and Sigman, D. S. (1981) *Biochemistry* 20, 244.
- (27) Que, B. G., Downey, K. M., and So, A. G. (1980) *Biochemistry* 19, 5987.
- (28) Chen, C. H. B., and Sigman, D. S. (1987) *Science* 237, 1197.
- (29) Barton, J. K., and Raphael, A. L. (1984) *J. Am. Chem. Soc.* 106, 2466.
- (30) Barton, J. K., and Raphael, A. L. (1985) *Proc. Natl. Acad. Sci. U.S.A.* 82, 6460.
- (31) Kelly, J. M., McConnell, D. J., Oh Vigin, C., Tossi, A. B., Mesmaeker, A. K. D., Masschelein, A., and Nasielski, J. (1987) *J. Chem. Soc., Chem. Commun.* 1821.
- (32) Basile, L. A., Raphael, A. L., and Barton, J. K. (1987) *J. Am. Chem. Soc.* 109, 7550.
- (33) Fleisher, M. B., Waterman, K. C., Turro, N. J., and Barton, J. K. (1986) *Inorg. Chem.* 25, 3551.
- (34) Chiou, S. H. (1984) *J. Biochem.* 96, 1307.
- (35) Howe-Grant, M., Wu, K. C., Bauer, W. R., and Lippard, S. J. (1976) *Biochemistry* 15, 4339.
- (36) Mack, D. P., Iverson, B. L., and Dervan, P. B. (1988) *J. Am. Chem. Soc.* 110, 7572.
- (37) Chiou, S. H. (1983) *J. Biochem.* 94, 1259.
- (38) Someya, A., and Tanaka, N. (1979) *J. Antibiot.* 32, 839.
- (39) Kuwahara, J., Suzuki, T., Funakoshi, K., and Sugiura, Y. (1986) *Biochemistry* 25, 1216.
- (40) Ward, B., Skorobogaty, A., and Dabrowiak, J. C. (1986) *Biochemistry* 25, 6875.
- (41) Fiel, R. J., Beerman, T. A., Mark, E. H., and Datta Gupta, N. (1982) *Biochem. Biophys. Res. Commun.* 107, 1067.
- (42) Aft, R. L., and Mueller, G. C. (1983) *J. Biol. Chem.* 258, 12069.
- (43) Groves, J. T., and Farrell, T. P. (1989) *J. Am. Chem. Soc.* 111, 4998.
- (44) Praseuth, D., Gaudemer, A., Verlhac, J. B., Kraljic, I., Sissoëff, J., and Guille, E. (1986) *Photochem. Photobiol.* 44, 717.
- (45) Bowler, B. E., Hollis, L. S., and Lippard, S. J. (1984) *J. Am. Chem. Soc.* 106, 6102.
- (46) Fiel, R. J., and Munson, B. R. (1980) *Nucleic Acids Res.* 8, 2835.
- (47) Pasternack, R. F., Gibbs, E. J., and Villafranca, J. J. (1983) *Biochemistry* 22, 2406.
- (48) Pasternack, R. F., Gibbs, E. J., and Villafranca, J. J. (1983) *Biochemistry* 22, 5409.
- (49) Kelly, J. M., Murphy, M. J., McConnell, D. J., and Oh Vigin, C. (1985) *Nucleic Acids Res.* 13, 167.
- (50) Banville, D. L., Marzilli, L. G., and Wilson, W. D. (1983) *Biochem. Biophys. Res. Commun.* 113, 148.
- (51) Fiel, R. J., Carvlin, M. J., Byrnes, R. W., and Mark, E. H. (1985) *Mol. Basis Cancer, Proc. Conf.*, Part B, 215.
- (52) McKinnie, R. E., Choi, J. D., Bell, J. W., Gibbs, E. J., and Pasternack, R. F. (1988) *J. Inorg. Biochem.* 32, 39.
- (53) Bromley, S. D., Ward, B. W., and Dabrowiak, J. C. (1986) *Nucleic Acids Res.* 14, 9133.
- (54) Ward, B., Skorobogaty, A., and Dabrowiak, J. C. (1986) *Biochemistry* 25, 7827.
- (55) Strickland, J. A., Banville, D. L., Wilson, W. D., and Marzilli, L. G. (1987) *Inorg. Chem.* 26, 3398.
- (56) Strickland, J. A., Marzilli, L. G., Gay, K. M., and Wilson, W. D. (1988) *Biochemistry* 27, 8870.
- (57) Sari, M. A., Battioni, J. P., Mansuy, D., and Le Pecq, J. B. (1986) *Biochem. Biophys. Res. Commun.* 141, 643.
- (58) Dougherty, G., Pilbrow, J. R., Skorobogaty, A., and Smith, T. D. (1985) *J. Chem. Soc., Faraday Trans. 2* 81, 1739.
- (59) Policard, A. (1924) *C. R. Soc. Biol.* 91, 1432.
- (60) Figge, F. h., Weiland, G. S., and Manganiello, L. O. (1948) *Proc. Soc. Exp. Biol.* 68, 640.
- (61) Rasmussen-Taxdal, D. S., Ward, G. E., and Figge, F. H. (1955) *Cancer* 8, 78.
- (62) Altman, K. F., and Solomol, K. (1960) *Nature* 187, 1124.
- (63) Winkelman, J. (1961) *J. Natl. Cancer Inst.* 27, 1369.
- (64) Kessel, D. (1984) *Photochem. Photobiol.* 39, 851.
- (65) Kessel, D. (1984) *Photochem. Photobiol.* 33, 1389.
- (66) van den Bergh, H. (1986) *Chem. Br.* 430.
- (67) Jori, G., and Spikes, J. D. (1984) In *Topics in Photomedicine* (K. C. Smith, Ed.) Plenum Press, New York.
- (68) Berns, M. W. (1984) *Hematoporphyrin Derivative Photoradiation Therapy of Cancer* Alan R. Liss Inc., New York.
- (69) Kessel, D. (1985) *Methods in Porphyrin Photosensitization* Plenum Press, New York.
- (70) Andreomi, A., and Cubbeddu, R. (1984) *Porphyrins in Tumor Phototherapy* Plenum Press, New York.
- (71) Doiron, D. R., and Gomer, C. J. (1984) *Porphyrin Localization and Treatment of Tumors* Alan R. Liss Inc., New York.
- (72) Winkelman, J. (1962) *Cancer Res.* 22, 589.
- (73) Amagasa, J. (1981) *Photochem. Photobiol.* 33, 947.
- (74) Bortolini, O., Ricci, M., Meunier, B., Friant, P., Ascone, L., and Goulou, J. (1986) *Nouv. J. Chim.* 10, 39.
- (75) Groves, J. T., and Nemo, T. G. (1983) *J. Am. Chem. Soc.* 105, 5786.
- (76) Groves, J. T., and Nemo, T. G. (1983) *J. Am. Chem. Soc.* 105, 6243.
- (77) Spreer, L. O., Leone, A., Maliyackel, A. C., Otvos, J. W., and Calvin, M. (1988) *Inorg. Chem.* 27, 2401.
- (78) Creager, S. E., Raybuck, S. A., and Murray, R. W. (1986) *J. Am. Chem. Soc.* 108, 4225.
- (79) Arakali, A. V., Byrnes, R., and Fiel, R. J. (1985) *Books of Abstracts Fourth Conversation in Biomolecular Stereodynamics* p 137, Adenine, Guilderland, NY.
- (80) Ward, B., Rehfuess, R., and Dabrowiak, J. C. (1987) *J. Biomol. Struct. Dyn.* 4, 685.
- (81) Dabrowiak, J. C., Ward, B., and Goodisman, J. (1989) *Biochemistry* 28, 3314.
- (82) Patronas, N. J., Cohen, J. S., Knop, R. H., Dwyer, A. J., Colcher, D., Lundy, J., Mornex, F., Hambright, P., Sohn, M., and Myers, C. E. (1986) *Cancer Treat. Rep.* 70, 391.
- (83) Carter, M. T., and Bard, A. J. (1987) *J. Am. Chem. Soc.* 109, 7528.
- (84) Carter, M. T., Rodriguez, M., and Bard, A. J. (1989) *J. Am. Chem. Soc.* 111, 8901.
- (85) Kuwana, T., Fujihara, M., Sunakawa, K., and Osa, T. (1978) *J. Electroanal. Chem.* 88, 299.
- (86) Forshey, P. A., and Kuwana, T. (1981) *Inorg. Chem.* 20, 693.
- (87) Forshey, P. A., Kuwana, T., Kobayashi, N., and Osa, T. (1982) *Adv. Chem. Ser.* 201, 601.
- (88) Forshey, P. A., and Kuwana, T. (1983) *Inorg. Chem.* 22, 699.
- (89) Kurihara, H., Arifuku, F., Ando, I., Saita, M., Nishino, R., and Ujimoto, K. (1982) *Bull. Chem. Soc. Jpn.* 55, 3515.
- (90) Kobayashi, N., Saiki, H., and Osa, T. (1985) *Chem. Lett.* 1917.
- (91) Harriman, A. (1984) *J. Chem. Soc., Dalton Trans.* 141.

- (92) Takahashi, K., Komura, T., and Imanaga, H. (1983) *Bull. Chem. Soc. Jpn.* 56, 3203.
- (93) Van Atta, R. B., Long, E. C., Hecht, S. M., van der Marel, G. A., and van Boom, J. H. (1989) *J. Am. Chem. Soc.* 111, 2722.
- (94) Harriman, A., and Porter, G. (1979) *J. Chem. Soc. Faraday Trans. 2* 75, 1532.
- (95) See the experimental section of ref 84.
- (96) Reichmann, M. E., Rice, S. A., Thomas, C. A., and Doty, P. (1954) *J. Am. Chem. Soc.* 76, 3047.
- (97) Maniatis, T., Fritsch, E. F., and Sambrook, J. (1982) *Molecular Cloning* Cold Spring Harbor Laboratory, New York.
- (98) Bard, A. J., and Faulkner, L. R. (1980) *Electrochemical Methods* p 194, Wiley, New York.
- (99) Sepa, D. B., Vojnovic, M. V., and Damjanovic, A. (1981) *Electrochim. Acta* 26 781.
- (100) Damjanovic, A., Genshaw, M. A., and O'M Bockris, J. (1967) *J. Electrochem. Soc.* 114, 466.
- (101) Damjanovic, A., Genshaw, M. A., and O'M Bockris, J. (1967) *J. Electrochem. Soc.* 114, 1107.
- (102) Hoare, J. P. (1967) In *Advances in Electrochemistry and Chemical Engineering* (P. Delahay, C. W. Tobias, Eds.) Vol. 6, p 201, Interscience, New York.
- (103) Freifelder, D. (1969) *Biopolymers* 7, 681.
- (104) Sutcliffe, J. G. (1978) *Cold Harbor Symp. Quant. Biol.* 43, 77.
- (105) Pasternack, R. F., Lee, H., Malek, P., and Spencer, C. (1977) *J. Inorg. Nucl. Chem.* 39, 1865.
- (106) Tondreau, G. A., and Wilkins, R. G. (1986) *Inorg. Chem.* 25, 2745.
- (107) Goff, H., and Morgan, L. O. (1976) *Inorg. Chem.* 15, 3181.
- (108) Kumar, C. V., Barton, J. K., and Turro, N. J. (1985) *J. Am. Chem. Soc.* 107, 5518.
- (109) Stradowski, C., Görner, H., Currell, L. J., and Schulte-Frohlinde, D. (1987) *Biopolymers* 26, 189.
- (110) Weiss, J. (1935) *Trans. Faraday Soc.* 31, 1547.

Synthesis of a Diaminedithiol Bifunctional Chelating Agent for Incorporation of Technetium-99m into Biomolecules¹

Kwamena E. Baidoo and Susan Z. Lever*

Division of Radiation Health Sciences, Department of Environmental Health Sciences, School of Hygiene and Public Health, The Johns Hopkins University, Baltimore, Maryland 21205-2179. Received January 16, 1990

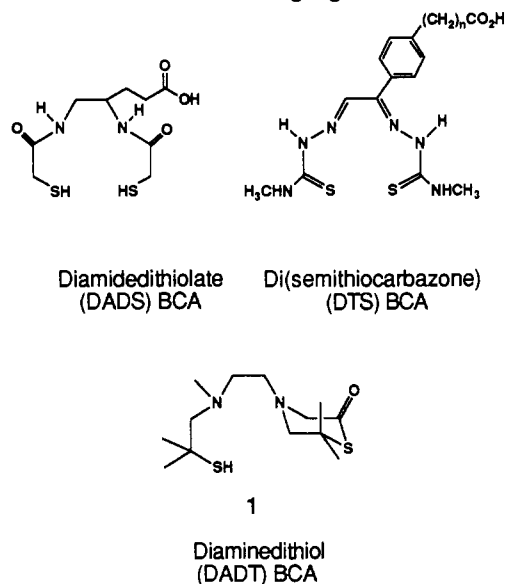
The synthesis of a bifunctional chelating agent (BCA), 1, based on the diaminedithiol (DADT) ligand system, is described. The six-step synthetic sequence has been accomplished in 16% overall yield, affording 1, which contains a thiolactone as a reactive moiety, which permits direct coupling to nucleophiles without the formation of byproducts. The reactivity of 1 toward benzylamine and subsequent labeling of the ligand with technetium-99m has been evaluated as a model for preparation of various bioconjugates. Both coupling and exchange labeling occur in high yield under mild conditions, and competition reactions with diethylenetriaminepentaacetic acid (DTPA) indicate the superior stability of the technetium-99m-DADT complex. Preparation of BCA 1 thus provides a new avenue into technetium-labeled radiopharmaceuticals.

Technetium-99m (^{99m}Tc) possesses the best characteristics for scintigraphic imaging among currently available radionuclides (1, 2). Its high photon yield per disintegration ensures good counting statistics and its monoenergetic γ photons (140 KeV) are ideally suited for planar and single photon emission computed tomography (SPECT) instrumentation. The short half-life of 6.02 h and lack of particulate emissions generally result in a low absorbed radiation dose to patients. In addition, ^{99m}Tc is inexpensive and is widely available in generator form.

Due to these properties, there is considerable interest in developing protein-based radiopharmaceuticals containing this radionuclide. Initial methods relied on the native protein to offer direct stabilization for reduced technetium; however, weak nonspecific labeling, colloidal contamination, protein denaturation, and loss of label in vivo can be problematic (2-6). The bifunctional chelate approach, which provides certain advantages (7-9), has been under investigation for the labeling of proteins with ^{99m}Tc. However, the bifunctional chelating agents (BCAs) available for use with other radionuclides have had only limited success with ^{99m}Tc. For example, attempts to utilize diethylenetriaminepentaacetic acid (DTPA) coupled proteins (10-13) result in labeled products which lack sufficient in vitro and in vivo stability (2, 14).

Newer chelates that form stable complexes with technetium have been synthetically modified into BCAs (Chart I). The diamidedisulfide (DADS) ligand system (15, 16) requires basic reaction conditions and higher temperatures for complex formation (17). In order to avoid these forcing conditions, preformed complexes have been coupled to the protein with a measure of success (18). The dithiosemicarbazone (CE-DTS) derivatives (19-21) require

Chart I. Bifunctional Chelating Agents for Technetium



acidic conditions for incorporation of ^{99m}Tc, which can lead to protein denaturation. In vivo, proteins labeled via this method show high liver and stomach radioactivity, suggesting label instability (21-23).

Diaminedithiol (DADT) ligands represent another chelate class that forms strong complexes with technetium (24-31). As in the DADS system, DADT ligands contain two thiol groups that exhibit high affinity for technetium. However, the two coordinating nitrogens are amines rather than amides; thus, their full coordinating potential is preserved. These properties of DADT ligands result in facile complex formation and exceptional complex stability.

Clearly, a BCA based on the DADT ligand system would permit efficient labeling of biomolecules, such as antibodies and other proteins, with ^{99m}Tc under mild conditions. In this report, we describe the complete synthesis of BCA 1 (32, 33) and its coupling reaction with ben-

* Address correspondence and requests for reprints to Susan Z. Lever, Ph.D., Department of Environmental Health Sciences, The Johns Hopkins University, School of Hygiene and Public Health, 2001 Hume Building, 615 N. Wolfe St., Baltimore, Maryland 21205-2179.

¹ Taken in part from the Ph.D. thesis of K.E.B., The Johns Hopkins University, 1988. A preliminary communication of a portion of this work has been published (ref 33).

zylamine. Incorporation of technetium into the coupled product **8** was performed under exchange-labeling conditions, and followed as a function of time. Stability of the major DADT complex was assessed in competition studies with diethylenetriaminepentaacetic acid (DTPA).

EXPERIMENTAL PROCEDURES

Solvents and chemicals were reagent grade and used as received. Dry tetrahydrofuran (THF) was prepared by predrying over anhydrous CaCl_2 followed by distillation over Na/benzophenone. [$^{99\text{m}}\text{Tc}$]glucoheptonate kits ("Glucoscan") were gifts from E. I. Du Pont de Nemours Co. Inc., N. Billerica, MA. [$^{99\text{m}}\text{Tc}$]NaTcO₄ was obtained as a saline solution from a $^{99}\text{Mo}/^{99\text{m}}\text{Tc}$ generator purchased from Cintichem/Union Carbide.

Melting points were determined with a Thomas-Hoover capillary melting point apparatus and are reported uncorrected. Spectrophotometric determinations were made on a Perkin-Elmer 399B infrared spectrophotometer. NMR spectra were recorded in deuteriochloroform solution with an NR80 FT-NMR spectrometer (IBM Instruments Inc.) operated at 80.06 MHz for protons (^1H) and 20.25 MHz for carbon-13 (^{13}C). Radioactivity was measured on a Capintec CRC-7 radioisotope dose calibrator. Elemental analyses were performed by Atlantic Microlabs, Norcross, GA. HPLC was performed on a Perkin-Elmer Series 2 instrument equipped with an LC-75 UV/visible detector; a 2-in. calcium fluoride flow-through scintillation detection system; EE & G/Ortec single-channel analyzer, amplifiers, and ratemeters; and a Hewlett-Packard HP 3392A integrating recorder.

Unless otherwise stated, all extractive workups utilized diethyl ether, and the organic extracts were dried over anhydrous Na_2SO_4 and filtered prior to concentration under reduced pressure.

Hexahydro-6,6,9,9-tetramethyl-1H-imidazo[2,1-*d*][1,2,5]dithiazepine (3). Sodium borohydride (17.5 g, 0.460 mol) was added in small portions to a solution of diiminedisulfide **2** (**34**) (44.5 g, 0.193 mol) in EtOH (2.80 L) and the mixture was stirred for 18 h at room temperature. Acetone (100 mL) was added to destroy the excess reducing agent, and after 15 min, volatile solvents were evaporated under reduced pressure. Aqueous sodium hydroxide (200 mL, 2.5 M) was added to the white residue. After extractive workup, the crude product was purified by short-path silica gel chromatography (ethyl acetate), followed by recrystallization from *n*-pentane to afford bicyclic amine **3** as a white, crystalline solid (36.3 g, 80%: mp 63–64 °C (lit. (35) mp 65 °C); IR (KBr) 3280 cm^{-1} (N–H); ^1H NMR δ 1.23–1.32 (m, 12 H), 1.9 (s, 1 H) 2.50–3.60 (m, 7 H); ^{13}C NMR δ 18.66, 24.79, 26.42, 28.28, 46.23, 58.56, 66.62, 91.23. Anal. Calcd ($\text{C}_{10}\text{H}_{20}\text{N}_2\text{S}_2$): C, 51.72; H, 8.68; N, 12.06; S, 27.54. Found: C, 51.42; H, 9.17; N, 11.95; S, 27.50.

Hexahydro-1,6,6,9,9-pentamethyl-1H-imidazo[2,1-*d*][1,2,5]dithiazepine (4). To a solution of **3** (4.0 g, 17 mmol) in acetonitrile (40 mL) was added 50% KF/Celite (6.0 g, 51 mmol) followed by methyl iodide (2.4 mL, 5.5 g, 40 mmol). The mixture was stirred at room temperature for 3 h and then filtered. Volatile solvents were removed by distillation under reduced pressure, aqueous sodium hydroxide (30 mL, 2.5 M) was added to the residue, and the mixture was extracted with ether (3 \times 25 mL). Additional product was obtained from the Celite filter cake by treatment with aqueous NaOH (25 mL, 2.5 M) followed by reextraction. The ether solution was treated at reflux with activated charcoal for 20 min, filtered, and evaporated under reduced pressure. Isolation by short-path silica gel chromatography (85:15 hexane/ethyl acetate) afforded **4** as a clear oil (3.95 g, 93%): mp

121–122 °C (2.4×10^{-3} Torr); IR (neat) no NH stretch at 3300 cm^{-1} ; ^1H NMR δ 1.22–1.32 (m, 12 H), 2.48–3.10 (m, 10 H); ^{13}C NMR δ 19.51, 24.41, 26.40, 27.92, 46.06, 54.16, 54.84, 66.88, 100.05. Anal. Calcd ($\text{C}_{11}\text{H}_{22}\text{N}_2\text{S}_2$): C, 53.65; H, 9.00; N, 11.37; S, 25.96. Found: C, 53.60; H, 8.94; N, 11.35; S, 26.00.

2,2,4,9,9-Pentamethyl-4,7-diaza-1,10-decanedithiol (5). To a stirred solution of **4** (15.0 g, 60.6 mmol) in dry THF (100 mL) under a slow stream of nitrogen was added LiAlH_4 (5.00 g, 132 mmol) in small portions. The mixture was refluxed for 18 h and cooled to room temperature. The reaction was externally cooled at 0 °C (ice bath) and quenched by slow, dropwise addition of saturated, aqueous NH_4Cl . The mixture was then quickly triturated with ethanol (4 \times 50 mL) and filtered. The filtrate was adjusted to pH 3–4 with aqueous hydrochloric acid (3 N), and volatile solvents were removed by evaporation under reduced pressure. Water (50 mL) was added to the residue and the mixture was brought up to pH 8 with aqueous sodium hydroxide (2.5 M). After extractive workup, the organic layers were concentrated to about 50 mL under reduced pressure and then applied to a 50-g silica gel column. The product was then eluted with ether. Concentration under reduced pressure and drying under high vacuum provided **5** as an oil: IR (neat) 3300 cm^{-1} (N–H), 2540 cm^{-1} (S–H); ^1H NMR δ 1.35 (s, 6 H), 1.37 (s, 6 H), 1.90 (br s, 3 H), 2.38 (s, 3 H), 2.48 (s, 2 H), 2.62 (s, 2 H), 2.71 (s, 4 H); ^{13}C NMR δ 30.48, 44.63, 45.26, 46.24, 48.40, 59.94, 63.74, 72.21. For long-term storage, the free base was converted to the hydrochloride salt by redissolution of the oil in ethanol (30 mL) followed by saturation with dry HCl gas. The resulting warm solution was cooled to room temperature and the product was precipitated with ether, filtered, washed, and dried under high vacuum to afford 5·2HCl as a white solid (14.54 g, 74%). Anal. Calcd ($\text{C}_{11}\text{H}_{26}\text{N}_2\text{S}_2\cdot 2\text{HCl}$): C, 40.75; H, 8.70; Cl, 21.57; N, 8.64; S, 19.72. Found: C, 40.92; H, 8.73; Cl, 21.94; N, 8.61; S, 19.75.

2,2,4,9,9-Pentamethyl-4,7-diaza-1,10-bis(*p*-methoxybenzyl)-1,10-dithiadecane (6). Aqueous sodium hydroxide (50 mL, 2.5 M) was added to a stirred solution of **5** (4.00 g, 12.4 mmol) in ethanol (60 mL). Neat *p*-methoxybenzyl chloride (8.80 g, 56.2 mmol) was added, and the stirring was continued for 1 h at room temperature. The ethanol was then distilled under reduced pressure. After extractive workup, the oily residue was redissolved in ethanol (10 mL). The mixture was adjusted to pH 2–3 with saturated ethanolic HCl. The warm mixture was cooled to room temperature and the product was precipitated with ether. The precipitate was filtered and washed with ether to yield 6·2HCl as a white powder (6.9 g, 76%). For subsequent use, the free base was regenerated by treatment of the salt with aqueous sodium hydroxide (2.5 M) followed by extraction with ether: IR (free base, neat) 3300 cm^{-1} (N–H); ^1H NMR (free base) δ 1.32 (s, 12 H), 1.6 (br s, 1 H), 2.36 (s, 3 H), 2.50 (s, 2 H), 2.57 (s, 2 H), 2.61 (s, 4 H), 3.66 (s, 2 H), 3.73 (s, 2 H), 3.77 (s, 6 H), 6.80, 7.24 (AB q, $J = 8.5$ Hz, 8 H); ^{13}C NMR (free base) δ 26.93, 27.24, 32.05, 44.79, 46.87, 47.63, 48.47, 55.11, 59.96, 60.11, 69.38, 113.78, 129.83, 130.38, 158.40. Anal. Calcd ($\text{C}_{27}\text{H}_{42}\text{N}_2\text{O}_2\text{S}_2$): C, 66.11; H, 8.63; N, 5.71; S, 13.03. Found: C, 65.99; H, 8.64; N, 5.68; S, 13.02.

2,2,4,9,9-Pentamethyl-4,7-diaza-7-(carbethoxymethyl)-1,10-bis(*p*-methoxybenzyl)-1,10-dithiadecane (7). A solution of **6** as the free base (20.0 g, 40.8 mmol) and ethyl bromoacetate (34.0 g, 203.7 mmol) in acetonitrile (75 mL) was heated at 44 °C for 3 h. Volatile solvents were removed by evaporation under reduced pres-

sure. The mixture was brought to pH 8–9 with aqueous NaOH (2.5 M) and then extracted with ether (3 × 50 mL). Excess ethyl bromoacetate was removed via a Kugelrohr apparatus (25 °C, 0.5 × 10⁻³ Torr). The residue was chromatographed on a short-path silica gel column (89.5:10:0.5 hexane/ethyl acetate/triethylamine) to yield **7** as a clear oil (13.0 g, 55%): IR (neat) 1730 cm⁻¹ (C=O); ¹H NMR δ 1.16–1.33 (m, 15 H), 2.34 (s, 3 H), 2.47–2.79 (m, 8 H), 3.56 (s, 2 H), 3.71 (s, 4 H), 3.77 (s, 6 H), 4.15 (q, 2 H), 6.80, 7.23 (AB q, *J* = 8.5 Hz, 8 H); ¹³C NMR δ 14.22, 26.71, 26.88, 32.14, 45.20, 47.62, 47.91, 54.54, 55.14, 56.74, 59.32, 59.97, 66.74, 69.47, 113.34, 129.37, 130.35, 158.45, 171.94. Anal. Calcd (C₃₁H₄₈N₂O₅S₂): C, 64.57; H, 8.39; N, 4.86; S 11.10. Found: C, 64.48; H, 8.42; N, 4.84; S, 11.05.

4-[2-[(2-Mercapto-2-methylpropyl)methylamino]-ethyl]-6,6-dimethyl-2-thiomorpholinone (1). Anhydrous hydrogen fluoride (5.85 g, 308 mmol) was condensed into a 100-mL Teflon round-bottom flask containing **7** (2.33 g, 4.04 mmol) and anisole (0.93 g, 8.5 mmol), at -78 °C (dry ice/acetone bath). After the addition was complete, the mixture was stirred for 1.5 h at 0 °C (ice bath) under a positive pressure of nitrogen. The HF was then flushed with a stream of nitrogen through two KOH traps in series. Water (10 mL) was added to the residue and the mixture was brought to pH 2–3 with aqueous NaOH (2.5 M). The mixture was then washed with ether (4 × 15 mL) and the aqueous layer was brought to pH 8. After extractive workup, the crude oily residue was chromatographed on a short-path silica gel column (90:10 hexane/ethyl acetate) to yield **1** as an oil (0.82 g, 70%): IR (neat) 1655 cm⁻¹ (C=O); ¹H NMR δ 1.32 (s, 6 H), 1.48 (s, 6 H), 2.08 (s, 1 H), 2.41 (s, 3 H), 2.47, 2.68 (2 s, 8 H), 3.32 (s, 2 H); ¹³C NMR δ 29.89, 30.46, 45.20, 46.23, 47.65, 56.00, 57.74, 65.14, 72.22, 199.00. Anal. Calcd (C₁₃H₂₆N₂O₂S₂): C, 53.80; H, 9.03; N, 9.65; S, 22.03. Found: C, 53.82; H, 8.79; N, 9.60; S, 22.04.

2,2,4,9,9-Pentamethyl-4,7-diaza-7-[(benzylcarbamoyl)methyl]-1,10-bis(*p*-methoxybenzyl)-1,10-dithiadecane (DADT-BzA) (8). A solution of **1** (200 mg, 0.691 mmol) and benzylamine (110 mg, 1.02 mmol) in acetonitrile (5 mL) was stirred at room temperature under nitrogen for 3 h. Concentration under reduced pressure gave a white residue, which was purified by preparative TLC on silica gel plates (2 × 2000 μm; 60:40 hexane/ethyl acetate) to give **8** as a colorless oil (222 mg, 81%): IR (free base, neat) 3260, 3160 cm⁻¹ (N–H); ¹H NMR (free base) δ 1.20 (s, 6 H), 1.28 (s, 6 H), 1.55 (br s, 2 H), 2.30 (s, 3 H), 2.34, (s, 8 H), 2.67 (m, 8 H), 3.38 (s, 2 H), 4.50 (d, *J* = 5.0 Hz, 2 H), 7.31 (s, 5 H), 7.8 (br s, 1 H). The product was stored as the dihydrochloride salt, prepared in the same manner as 5·2HCl. Anal. Calcd (C₂₀H₃₅N₃O₂·2HCl·0.5H₂O): C, 50.21; H, 8.00; Cl, 14.62; N, 8.78; S, 13.37. Found: C, 50.27; H, 8.05; Cl, 14.71; N, 8.50; S, 13.26.

Radiolabeling of 8. A solution of [^{99m}TcO₄]⁻ (20–50 mCi, 3 mL) was added to a "Glucosan" kit, containing sodium glucoheptonate and SnCl₂, mixed well, and allowed to stand for 15 min. Aliquots of this mixture containing [^{99m}Tc]glucoheptonate complex ([^{99m}Tc]GH) were added to solutions of **8**, to give a final DADT ligand concentration of 10⁻³ M in a total volume of 1 mL. The mixture was analyzed by reverse-phase HPLC using an Alltech C-18 Econosil column (6.5 × 250 mm) with MeOH/0.1 M ammonium formate solution (90:10) at a flow rate of 8 mL/min. Activity balances were measured by comparison of the total amount of radioactivity collected with that injected. Greater than 90% of activity was recov-

ered from the column, and no colloidal ^{99m}TcO₂ was detected. Within 10 min, 95% of the [^{99m}Tc]glucoheptonate complex was converted to two products (**9a** and **9b**) with retention times of 2.2 and 4.4 min, respectively. The composition of this product mixture varied as a function of time, and only the minor complex **9b** was observed from 25 min through the duration of the study (96 min).

Competition Experiments with DTPA. A stock solution containing DTPA (240 mM) and **8** (2 mM) was prepared. During exchange labeling [^{99m}Tc]glucoheptonate (0.5 mL, 6 mCi) as prepared above was added to an aliquot of the stock solution (0.5 mL). In a separate experiment, the major [^{99m}Tc]DADT-BzA complex was isolated and then challenged with DTPA by incubation with 0.1 M DTPA. The mixtures were incubated for up to 3 h at room temperature and analyzed periodically by reverse-phase HPLC as described above. The presence of [^{99m}Tc]DTPA was assessed by comparison of retention times of an authentic sample of [^{99m}Tc]DTPA.

RESULTS AND DISCUSSION

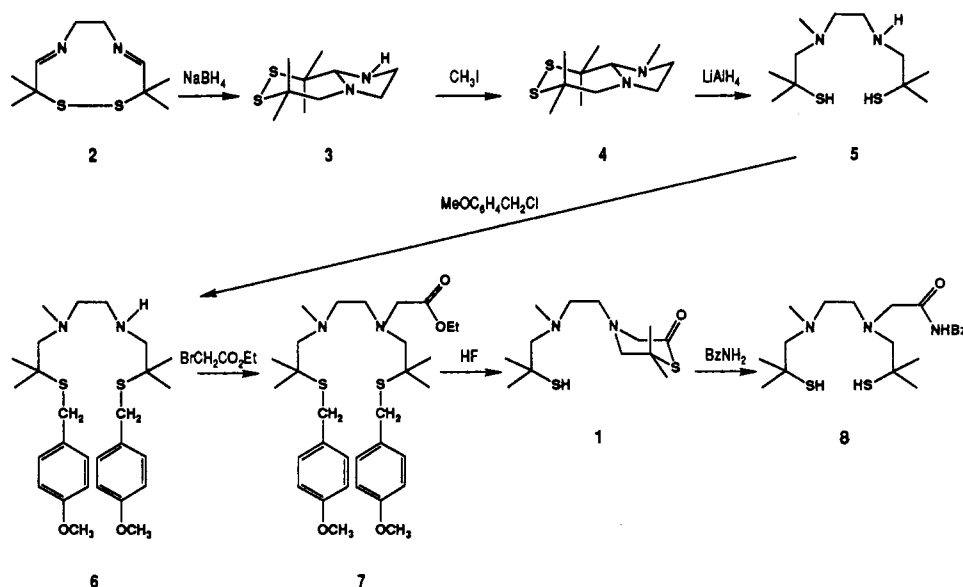
Our development of a BCA based upon the DADT ligand system focused upon the synthetic features needed for coupling of the ligand to the protein. Rather than utilize an external activating group, BCA **1** was selected as the synthetic target where the thioester is derived from a portion of the DADT ligand, and incorporation of an acetate side chain provides the balance of atoms needed to form the six-membered thiolactone. Thioesters are known to react with amine nucleophiles. Therefore, in order to prevent self-condensation from intra- or intermolecular amide formation, the secondary amine was protected with a methyl substituent.

The transformation of the parent DADT ligand to BCA **1** (Scheme I) therefore had to accommodate differentiation of each nitrogen to permit alkylation with nonequivalent groups. In addition, the thiol groups had to be protected throughout the alkylation reactions to prevent concomitant S-alkylation. Therefore, two features of the synthetic approach were key to the preparation of the target bifunctional chelating agent.

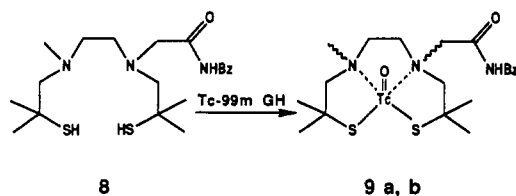
First, use of the mild reducing agent NaBH₄ (2 → 3) afforded the bicyclic intermediate **3**, where the two nitrogens were nonequivalent. In addition, the disulfide bond remained intact, serving as internal protection for the thiols. Of the two required alkylation steps, it was necessary to perform the methylation first, because the product is stable to the subsequent reduction step with lithium aluminum hydride (LiAlH₄). The alkylation of **3** with methyl iodide in the presence of 50% KF on Celite afforded **4** in excellent yield (93%). KF on Celite has been reported to aid S-, O-, and N-alkylations through extensive hydrogen bonding with the hydrogen atom bonded to the heteroatom (36). Cleavage of both rings of this bicyclic compound to the open-chained molecule was then accomplished with LiAlH₄ to permit elaboration of the other nitrogen. Acidification of the reaction mixture immediately after quenching is a requirement for isolation of high yields of **5**.

The second key feature of the synthesis utilized the acid-labile *p*-methoxybenzyl groups to selectively protect the thiols (5 → 6). Even though a large excess of *p*-methoxybenzyl chloride was used for the alkylation of the free thiols, there was no evidence of interfering N-alkylation when the reaction was conducted at room temperature. The resulting *p*-methoxybenzyl thioethers are stable under basic conditions and permit substitution on the secondary nitrogen with ethyl bromoacetate to afford precursor **7**.

Scheme I



Scheme II



Our initial route for the synthesis of BCA 1 from 7 entailed a three-step sequence of deprotection, ester hydrolysis, and condensation to give the thiolactone via an intermediate dithiol carboxylic acid. In practice, however, we found that the target thiolactone BCA 1 was obtained directly from the deprotection step. Since anhydrous HF does not promote simple ester hydrolysis, the reaction is likely to involve acid-catalyzed ester interchange of the free thiol and the ethyl ester. An analogy for this reaction can be drawn from the synthesis of a six-membered thiolactone from a benzyl-protected thiol carboxylic acid by Lumma and co-workers (37) using trifluoroacetic anhydride at reflux. The mechanism of this transformation was reported to involve acid-catalyzed debenzoylation with concomitant cyclization to generate the thiolactone.

With the target BCA in hand, its reactivity toward amine nucleophiles was tested by using benzylamine as a model (Scheme I). The reaction proceeded smoothly to yield the DADT-BzA adduct 8, and was practically complete in 3 h. The scope and limitations of the reaction of 1 with other nucleophiles is currently being assessed. For example, we have carried out coupling reactions with HSA in phosphate buffer and with the monoclonal antibody B72.3 in borate buffer in the presence of dimethylformamide (38). In both cases, coupling occurred readily. Therefore, under conditions required for coupling sensitive biomolecules, thiolactone 1 is sufficiently reactive.

Complexation of 8 with ^{99m}Tc was then investigated utilizing transchelation with [^{99m}Tc]glucoheptonate (Scheme II). Although direct labeling can also be used to achieve complex formation, many biological substrates are susceptible to damage by the relatively harsh reaction conditions used. Therefore, the mild conditions employed for ligand exchange represent a useful alternative approach to labeling with ^{99m}Tc . In addition,

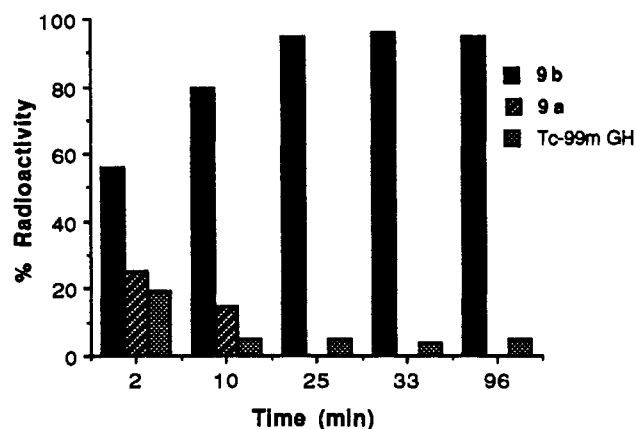


Figure 1. Composition of exchange labeling reaction mixture as a function of time.

tion, ligand exchange is preferred with respect to the labeling of proteins because it offers a mechanism to avoid labeling the weak binding sites on the native protein. As a consequence, an important criterion in the utility of ligands derived from BCA 1 is their ability to accept reduced ^{99m}Tc from labile complexes. Treatment of DADT-BzA 8 with preformed [^{99m}Tc]glucoheptonate ([^{99m}Tc]-GH) gave two [^{99m}Tc]DADT-BzA complexes (9a and 9b) as determined by HPLC. From activity balance measurements, the efficiency of labeling was >90% within 10 min and no colloidal $^{99m}\text{TcO}_2$ was detected. The two products, 9a and 9b, were obtained initially; however, by 25 min only 9b was observed (Figure 1). The formation of multiple products is not unexpected, due to the presence of the side chains, which upon complexation can be syn or anti to the $\text{Tc}=\text{O}$ core. Similar observations have been observed in other N-alkylated or C-alkylated DADT complexes. In the case of C-alkylated complexes, the ratio of products is usually 50:50 (31); whereas the ratio of products observed in N-alkylated complexes can vary from 80:20 to 96:4 (24, 26, 27, 30). In the case of the N-alkylated complexes the major complex, when characterized on the ^{99}Tc scale, has been shown to be the syn isomer (27, 30). This data indicates that the syn-anti pair of isomeric C-alkylation complexes are comparable in stability, and that the syn isomer in N-

alkylated complexes is relatively more stable than the corresponding anti isomer.

Since DTPA has been the most extensively used chelating agent for binding metals to proteins through the bifunctional chelate approach, we investigated the ability of the DADT-BzA ligand **8** to compete with DTPA for reduced technetium. A DTPA:DADT-BzA ratio of 120:1 was used under exchange-labeling conditions. Challenge experiments were also performed in which the isolated major [^{99m}Tc]DADT-BzA complex (**9b**) was incubated with 0.1 M DTPA. No evidence of the formation of a [^{99m}Tc]DTPA complex was found in these experiments during the 3-h incubation. These results indicate, as expected, that [^{99m}Tc]DADT-BzA is substantially more stable than [^{99m}Tc]DTPA. More detailed stability measurements using DADT ligands against other BCAs are underway.

The proposed structures for the complexes formed contain a [$\text{Tc}^{\text{V}}=\text{O}$] $^{3+}$ core, which is similar to those derived from mono- or unsubstituted DADT ligands. The two products are presumably isomeric in nature and are expected to be cationic. Support for this hypothesis is presently based on the crystal structure of the sole N,N'-disubstituted DADT- ^{99m}Tc complex reported to date (39). The synthesis and characterization of these complexes on the macroscopic ^{99m}Tc scale will authenticate the chelation of Tc by BCA 1 and allow structural determinations.

In a separate study, we have carried out preliminary studies using **1** for the preparation of ^{99m}Tc -labeled HSA and anticolorectal carcinoma antibody (B72.3) (38). BCA 1 can be coupled to both proteins under mild conditions, and exchange labeling proceeded efficiently. The ^{99m}Tc -labeled products were highly stable both in vitro and in vivo, with ^{99m}Tc labeling of only DADT sites, and not weak, nonspecific sites.

Thus, BCA 1 provides a new route to a variety of stable products containing technetium and serves as a versatile starting material for novel ^{99m}Tc radiopharmaceuticals.

ACKNOWLEDGMENT

This research was supported in part by USPHS Grants CA32845 and S07 RR05445. We also thank Kurt L. Loening, Director for Nomenclature of Chemical Abstracts Service, for assistance in naming **1**.

LITERATURE CITED

- Clarke, M. J., and Podbielski, L. (1987) Medical diagnostic imaging with complexes of ^{99m}Tc . *Coord. Chem. Rev.* 78, 253-331.
- Eckelman, W. C., and Paik, C. H. (1986) Comparison of Tc-99m and In-111 labeling of conjugated antibodies. *Nucl. Med. Biol. (Int. J. Radiat. Appl. Instrum. Part B)* 13, 335-343.
- Eckelman, W. C., Meinken, G., and Richards, P. (1971) Tc-99m-human serum albumin. *J. Nucl. Med.* 11, 707-710.
- Som, P., Rhodes, B. A., and Bell, W. R. (1975) Radiolabeled streptokinase and urokinase and their comparative biodistribution. *Thromb. Res.* 6, 247-253.
- Wong, D. W., Mishkin, T., and Lee, T. (1978) A rapid chemical method of labeling human plasma proteins with Tc-99m pertechnetate at pH 7.4. *Int. J. Appl. Radiat. Isot.* 29, 251-253.
- Rhodes, B. A., and Burchiel, S. W. (1983) Radiolabeling of antibodies with technetium-99m. In *Radioimmunoimaging and Radioimmunotherapy* (S. W. Burchiel and B. A. Rhodes, Eds.) pp 207-222, Elsevier Science Publishing Co., Inc., New York.
- Sunberg, M. W., Meares, C. F., Goodwin, D. A., and Diamanti, C. I. (1974) Chelating agents for the binding of metal ions to macromolecules. *Nature* 250, 587-588.
- Meares, C. F., and Wensel, T. G. (1984) Metal chelates as probes for biological systems. *Acc. Chem. Res.* 17, 202-209.
- Meares, C. F. (1986) Chelating agents for bonding of ions to antibodies. *Nucl. Med. Biol. (Int. J. Radiat. Appl. Instrum. Part B)* 13, 311-318.
- Khaw, B. A., Strauss, H. W., Carvallo, A., Locke, E., Gold, H. K., and Haber, E. (1982) Tc-99m labeling of antibodies to cardiac myosin Fab and to human fibrinogen. *J. Nucl. Med.* 23, 1011-1019.
- Lanteigne, D., and Hnatowich, D. J. (1984) The labeling of DTPA-coupled proteins. *Int. J. Appl. Radiat. Isot.* 35, 617-621.
- Paik, C. H., Phan, L. N. B., Hong, J. J., Sahami, M. S., Heald, S. C., Reba, R. C., Steigman, J., and Eckelman, W. C. (1985) The labeling of high affinity sites of antibodies with Tc-99m. *Nucl. Med. Biol.* 12, 3-8.
- Hnatowich, D. J. (1986) Labeled proteins in nuclear medicine—Current status. In *Current Applications in Radiopharmacology* (M. W. Billingham, Ed.) pp 257-270, Pergamon Press, Toronto, Canada.
- Fritzberg, A. R. (1987) Advances in Tc-99m labeling of antibodies. *Nucl. Med.* 26, 7-12.
- Jones, A. G., Davison, A., Latogola, M. R., Brodack, J. W., Orvig, C., Sohn, M., Toothaker, A. K., Lock, C. J. L., Franklin, K. J., Costello, C. E., Carr, S. A., Biemann, K., and Kaplan, M. L. (1982) Chemical and in vivo studies of the anion oxo[N,N'-ethylenebis(2-mercaptoacetimido)]technetate(V). *J. Nucl. Med.* 23, 801-809.
- Brenner, D., Davison, A., Lister-James, J., and Jones, A. G. (1984) Synthesis and characterization of a series of isomeric oxotechnetium(V) diamidodithiolates. *Inorg. Chem.* 23, 3793-3797.
- Byrne, E. F., and Tolman, G. L. (February 28, 1984) Bifunctional chelating agents. US patent 4 434 151.
- Fritzberg, A. R., Abrams, P. G., Beaumier, P. L., Kasina, S., Morgan, A. C. Rao, T., Reno, J. M., Sanderson, J. A., Srinivasan, A., Wilbur, D. S., and Vanderheyden, J.-L. (1988). Specific and stable labeling of antibodies with technetium-99m with a diamide dithiolate chelating agent. *Proc. Natl. Acad. Sci. U.S.A.* 85, 4025-4029.
- Yokoyama, A., Terauchi, Y., Horiuchi, K., Tanaka, H., Odori, T., Morita, R., Mori, T., and Torizuka, K. (1976) Technetium-99m-kethoxal-bis(thiosemicarbazone) complex with a tetravalent Tc-99m state and its excretion into the bile. *J. Nucl. Med.* 17, 816-819.
- Arano, Y., Yokoyama, A., Magata, Y., Horiuchi, K., Saji, H., and Torizuka, K. (1986) In the procurement of stable Tc-99m labeled protein using bifunctional chelating agent. *Appl. Radiat. Isot.* 37, 587-592.
- Arano, Y., Yokoyama, A., Magata, Y., Saji, H., Horiuchi, K., and Torizuka, K. (1986) Synthesis and evaluation of a new bifunctional chelating agent for Tc-99m labeling of proteins: *p*-carboxyethylphenylglyoxal-di-(*N*-methylthiosemicarbazone). *Nucl. Med. Biol.* 12, 425-430.
- Arano, Y., Yokoyama, A., Furukawa, T., Horiuchi, K., Yahata, T., Saji, H., Sakahara, H., Nakashima, T., Koizumi, M., Endo, K., and Torizuka, K. (1987) Technetium-99m-labeled monoclonal antibody with preserved immunoreactivity and high in vivo stability. *J. Nucl. Med.* 28, 1027-1033.
- Endo, L., Sakahara, H., Nakashima, T., Koizumi, M., Ohta, H., Kawamura, Y., Kunitatsu, M., Furukawa, T., Ohmomo, Y., Arano, Y., Nakamura, T., Tanaka, H., Kotoura, Y., Yamamuro, T., Hosoi, S., Toyama, S., Yokoyama, A., and Torizuka, K. (1987) Preparation and properties of antitumor monoclonal antibodies labeled with metallic radionuclides indium-111, gallium-67, and technetium-99m. *NCI Monogr.* 3, 135-140.
- Epps, L. A. (1984) The chemistry of neutral, lipid soluble technetium(V) complexes of aminoalcohols and aminothiols. Ph.D. Thesis, The Johns Hopkins University, Baltimore, Maryland.
- Kung, H. F., Molnar, M., Billings, J., Wicks, R., and Blau, M. (1984) Synthesis and biodistribution of neutral, lipid sol-

- uble Tc-99m complexes that cross the blood-brain barrier. *J. Nucl. Med.* 25, 326-332.
- (26) Lever, S. Z., Burns, H. D., Kervitsky, T. M., Goldfarb, H. W., Woo, D. V., Wong, D. F., Epps, L. A., Kramer, A. V., and Wagner, H. N., Jr. (1985) Design, preparation, and biodistribution of a technetium-99m triaminedithiol complex to assess regional cerebral blood flow. *J. Nucl. Med.* 26, 1287-1294.
- (27) Epps, L. A., Burns, H. D., Lever, S. Z., Goldfarb, H., and Wagner, H. N., Jr. (1987) Brain imaging agents: Synthesis and characterization of (*N*-piperidinyloxy)hexamethyl diaminedithiolate oxo technetium(V) complexes. *Appl. Radiat. Isot.* 38, 661-664.
- (28) Cheesman, E. H., Blanchette, M. A., Ganey, M. V., Maheu, E. J., Miller, S. J., and Watson, A. D. (1988) Technetium-99m ECD: Ester derivatized diaminedithiol Tc complexes for imaging brain perfusion. *J. Nucl. Med.* 29, 788 (Abstract).
- (29) Leveille, J., Demonceau, G., Rigo, P., DeRoo, M., Taillefer, R., Burgess, B. A., Morgan, R. A., and Walovitch, R. C. (1988) Brain tomographic imaging with Tc-99m-ethyl cysteinyl dimer (Tc-ECD): A new stable brain perfusion agent. *J. Nucl. Med.* 29, 758 (Abstract).
- (30) Lever, S. Z., Sun, S.-Y., Kaltovich, F., Scheffel, U., Goldfarb, H., Mahmood, A., Baidoo, K. E., and Wagner, H. N., Jr. (1988) Pulmonary accumulation of neutral alkyl-DADT-technetium complexes: Structure-biodistribution relationships. *J. Nucl. Med.* 29, 789 (Abstract).
- (31) Wei, Y., Liu, B.-L., and Kung, H. F. (1988) A study of the structure-stability relationship of technetium compounds. *J. Nucl. Med.* 29, 789 (Abstract).
- (32) Baidoo, K. E. (1988) Technetium-99m labeling of proteins. Ph.D. Thesis, The Johns Hopkins University, Baltimore, Maryland.
- (33) Lever, S. Z., Baidoo, K. E., Kramer, A. V., and Burns, H. D. (1988) Synthesis of a novel bifunctional chelate designed for labeling proteins with technetium-99m. *Tetrahedron Lett.* 29, 3219-3222.
- (34) Merz, K. W., and Specker, M. (1963) Kondensationsversuche mit 2,2,5,5-tetramethyl-3,4-dithiahexandial-(1,6). *Arch. Pharm.* 296, 427-438.
- (35) Joshua, A. V., Scott, J. R., Sondhi, S. M., Ball, R. G., and Lown, J. W. (1987) Transannular cyclization of 1,2-dithia-5,8-diazacyclodeca-4,8-dienes during borohydride reduction. *J. Org. Chem.* 52, 2447-2451.
- (36) Ando, T., and Yamawaki, J. (1979) Potassium fluoride on celite. A versatile reagent for C-, N-, O-, and S-alkylations. *Chem. Lett.* 45-46.
- (37) Lumma, W. C., Jr., Dutra, G. A., and Voeker, C. A. (1970) Synthesis of two benzothiacyclanones via a novel two-carbon ring expansion of thiolactones with vinylolithium. *J. Org. Chem.* 35, 3442-3444.
- (38) Baidoo, K. E., Scheffel, U., and Lever, S. Z. (1990) Technetium-99m labeling of proteins: Initial evaluation of a novel diaminedithiol bifunctional chelating agent. *Cancer Res. (Suppl.)* 50, 799s-803s.
- (39) Faggiani, R., Lock, C. J. L., Epps, L. A., Kramer, A. V., and Brune, D. (sic) Burns, H. D. (1988) (3,6-Dimethyl-3,6-diazaoctan-1,8-dithiolato- S^1, N^3, N^6, S^8)oxotechnetium(V) pertechnetate. *Acta Crystallogr. C* 44, 777-779.

Photoaffinity Heterobifunctional Cross-Linking Reagents Based on *N*-(Azidobenzoyl)tyrosines¹

Nobuyuki Imai,[†] Tadashi Kometani,[†] Peter J. Crocker,[†] Jean B. Bowdan,[†] Ayhan Demir,[†] Lori D. Dwyer,[‡] Dennis M. Mann,[‡] Thomas C. Vanaman,^{*,‡} and David S. Watt^{*,†}

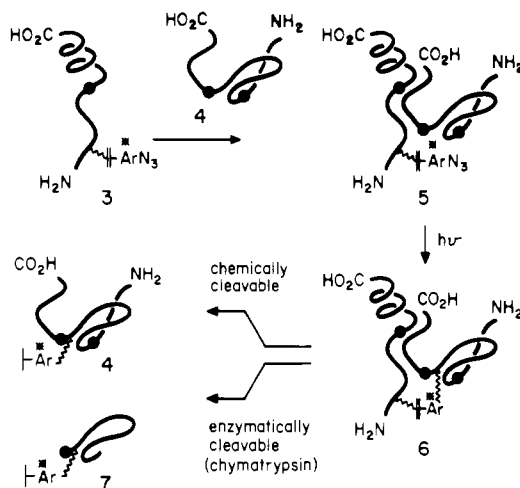
Departments of Chemistry and Biochemistry, University of Kentucky, Lexington, Kentucky 40506.

Received February 12, 1990

New heterobifunctional cross-linking reagents that possessed a photoactive terminus, an electrophilic terminus, and a linking arm between the two termini that had a radiolabeled, enzymatically cleavable bond were synthesized. In a model study, succinimidyl *N*-[*N'*-(4-azidobenzoyl)tyrosyl]- β -alanate (16A) was coupled to *n*-butylamine (a Lys surrogate), iodinated, and cleaved with chymotrypsin in the presence of tyrosylamide to afford the desired adduct *N*-(*N'*-(4-azidobenzoyl)-3-iodotyrosyl)tyrosinamide, thereby demonstrating the feasibility of the enzymatic cleavage. In a biochemical study, succinimidyl *N*-[*N'*-(3-azido-5-nitrobenzoyl)tyrosyl]- β -alanate (16C) was coupled to Lys-75 of calmodulin (CaM), and the radioiodinated monoadduct was successfully photo-cross-linked, in a calcium-dependent manner, to the human erythrocyte plasma membrane Ca^{2+} , Mg^{2+} -ATPase and to a synthetic fragment (M13) containing the CaM-binding region of myosin light-chain kinase. In the latter case, densitometry readings indicated 20% cross-linking efficiency.

The interaction of the ubiquitous calcium-binding protein calmodulin with a variety of other proteins including myosin light-chain kinase and membrane Ca^{2+} -pumping ATPases lies at the heart of certain regulatory events mediated by calcium ions and remains a topic of intense current interest (1-3). An effort to define these protein-protein interactions on a molecular level led to the construction of cross-linking reagents (4, 5) that possessed the following features: a radiolabel of high specific activity, an electrophilic succinimidyl ester terminus, and a photoactive aryl azide terminus. As an additional feature, an enzymatically cleavable linking arm connecting these termini was incorporated in the reagent with the expectation that a reagent with such a cleavable bond would permit the isolation of a fragment of the target protein in a cross-linking experiment as illustrated in the cartoon in Scheme I. In a study of two interacting proteins 2 and 4, reagent 1 would interact with a protein 2 to form a protein-reagent adduct 3. Subsequent binding of a second protein 4 and photolysis of complex 5 would lead to covalently cross-linked adduct

Scheme I. Cartoon Representation of a Cross-Linking Experiment



Legend: ArN_3 = aryl azide; \blacksquare = radio label; —|— = cleavable bond; \bullet = F, Y, K; \sim = covalent bond between reagent 1 and protein

6. Whereas chemical cleavage of a specific bond in the linking arm of 6 and SDS-PAGE separation would permit the identification of the entire protein 4 by autoradiography, the enzymatic cleavage, depicted in Scheme I for the case of chymotrypsin, would provide only a fragment 7 of target protein 4. Clearly, an enzymatically cleavable reagent of this type would be best suited for the delineation of binding sites between two purified proteins 3 and 4 in which the covalent attachment site in 3 was defined and in which enzymatic cleavage of the linking arm would provide a fragment that presumably could be separated and sequenced in order to define the binding site on protein 4. Before surmounting the separation problems necessary to reduce this notion to practice, it was necessary to synthesize heterobifunctional reagents of this type, test the feasibility of using these enzymatically cleavable reagents in model systems, and

* Authors to whom correspondence should be addressed.

[†] Department of Chemistry.

[‡] Department of Biochemistry.

¹ Part of this work was disclosed at the following meetings: Imai, N., Bowdan, J. B., Crocker, P. J., Watt, D. S., Vanaman, T. C., and Dwyer, L. D. Meeting of the American Chemical Society, Los Angeles, CA, September 1988 and Dwyer, L. D., Imai, N., Crocker, P. J., Mann, D. M., Watt, D. S., and Vanaman, T. C. FASEB Summer Research Conference on Calcium and Cell Function, Saxton's River, VT, July 1989.

² The abbreviations used are as follows: BOC-ON, 2-[[[*tert*-butoxycarbonyl]oxy]imino]-2-phenylacetonitrile; Et_3N , triethylamine; CaM, calmodulin; DCC, *N,N'*-dicyclohexylcarbodiimide; DMAP, 4-(dimethylamino)pyridine; DMSO, dimethyl sulfoxide; DSO, disuccinimidyl oxalate; EtOAc, ethyl acetate; EGTA, ethylene glycol bis(β -aminoethyl ether)-*N,N,N',N'*-tetraacetic acid; HEPES, 4-(2-hydroxyethyl)-1-piperazineethanesulfonic acid; HOAc, acetic acid; M13, a synthetic peptide containing the CaM-binding region of myosin light-chain kinase; TFA, trifluoroacetic acid; THF, tetrahydrofuran; TRIS, tris(hydroxymethyl)aminomethane.

perform preliminary experiments to verify that these reagents would effect a photochemical cross-link.

EXPERIMENTAL PROCEDURES

General Chemical Procedures. Infrared spectra were recorded on a Perkin-Elmer Model 1310 spectrometer. Nuclear magnetic resonance spectra were determined on a Varian EM390 or Gemini 200 MHz NMR spectrometer. Chemical shifts are reported in parts per million relative to tetramethylsilane as an internal standard. Mass spectra were determined on a VG ZAB spectrometer. Elemental analyses were performed by Atlantic Microlabs, Norcross, GA. Column chromatography using Macherey Nagel silica gel 60 is referred to as "chromatography on silica gel", preparative-layer chromatography on Macherey Nagel silica gel F254 is referred to as "chromatography on a silica gel plate", and the drying of an organic solution over anhydrous magnesium sulfate is simply indicated by the phrase "dried". The following experimental section contains detailed procedures only for the reagent that was successfully employed in biochemical cross-linking experiments (16C). Experimental data for other compounds appear in the supplementary material.

3-Azido-5-nitrobenzoic Acid (12C). To a solution of 2.00 g (9.46 mmol) of methyl 3,5-dinitrobenzoate (6) in 135 mL of acetone, 25 mL of acetic acid, and 25 mL of water at reflux was added 2.17 g (38.9 mmol) of iron in three portions at intervals of 20 min. After stirring at the reflux temperature for an additional 35 min, the mixture was cooled and filtered. The filtrate was adjusted to pH 8 with sodium carbonate, extracted with EtOAc,² washed with brine, and dried. The crude product was chromatographed on silica gel using 2:3 EtOAc-hexane to afford 0.71 g (38%) of methyl 3-amino-5-nitrobenzoate: mp 159–160 °C [lit (7, 8) mp 159–160 °C].

To a solution of 1.45 g (7.39 mmol) of methyl 3-amino-5-nitrobenzoate in 170 mL of water was added 17 mL of concentrated HCl at 0–5 °C. To this solution at 0 °C was slowly added 663 mg (9.61 mmol) of NaNO₂. The solution was stirred for 45 min at 0 °C, and 577 mg (8.87 mmol) of NaN₃ was slowly added. The mixture was stirred for 45 min at 0 °C and was extracted with EtOAc. The organic layer was washed with brine and dried. The product was chromatographed on silica gel using 2:3 EtOAc-hexane to afford 1.37 g (84%) of methyl 3-azido-5-nitrobenzoate: mp 93–94 °C; IR (KBr) 2114 (N₃), 1721 (CO) cm⁻¹; ¹H NMR (CDCl₃) δ 4.01 (s, 3, OCH₃), 8.01 (dd, *J* = 1.2, 2.2 Hz, 1, ArH), 8.04 (t, *J* = 2.2 Hz, 1, ArH), 8.60 (dd, *J* = 1.2, 2.2 Hz, 1, ArH). Anal. Calcd for C₈H₆N₄O₄: C, 43.25; H, 2.72. Found: C, 43.37; H, 2.87.

To a solution of 1.34 g (6.06 mmol) of methyl 3-azido-5-nitrobenzoate in 225 mL of MeOH was added 1.25 mL of water and 0.59 g (13.9 mmol) of lithium hydroxide monohydrate. The mixture was stirred for 7 h at 50 °C. The solution was acidified with 2 N aqueous HCl solution and extracted with EtOAc. The organic layer was washed with brine, dried, and concentrated to afford 1.41 g (100%) of 12C (9): mp 186–188 °C dec.

Succinimidyl 3-Azido-5-nitrobenzoate (13C). To a solution of 1.38 g (6.62 mmol) of 12C and 0.84 g (7.3 mmol) of *N*-hydroxysuccinimide in 50 mL of anhydrous THF was added 1.50 g (7.28 mmol) of DCC. The mixture was stirred for 16 h at 25 °C and filtered. The filtrate was concentrated, dissolved in EtOAc, washed with aqueous NaHCO₃ solution and brine, and dried. The solvent was removed to afford 1.98 g (98%) of 13C that was sufficiently pure to be used in the next reaction: mp 163–164 °C dec; IR (KBr) 2128 (N₃), 1809, 1788 (CON), 1743 (CO₂) cm⁻¹; ¹H NMR (CDCl₃) δ 2.96 (s, 4, CH₂CH₂), 8.07

(dd, *J* = 2.3 and 1.4 Hz, 1, ArH), 8.17 (t, *J* = 2.1 Hz, 1, ArH), 8.72 (dd, *J* = 2.0 and 1.4 Hz, 1, ArH); exact mass spectrum calcd for C₁₁H₇N₅O₆ 305.0396, found 305.0396.

Methyl *N*-[*N'*-(*tert*-Butoxycarbonyl)tyrosyl]-β-alanate (15). The procedure described for the preparation of 13C was repeated with 5.62 g (20 mmol) of *N*-(*tert*-butoxycarbonyl)tyrosine (14), 2.76 g (24 mmol) of *N*-hydroxysuccinimide, and 4.53 g (22 mmol) of DCC in 60 mL of anhydrous THF to afford, after stirring for 16 h at 25 °C, 5.98 g (79%) of succinimidyl *N*-(*tert*-butoxycarbonyl)tyrosine as white prisms: mp 183–184 °C (from EtOAc-hexane); IR (KBr) 3426 (OH), 3372 (NH), 1820, 1788 (CON of NHS), 1741 (CO₂NHS), 1683 (CO of BOC) cm⁻¹; ¹H NMR (DMSO-*d*₆) δ 1.32 (s, 9, C(CH₃)₃), 2.79 (s, 4, (CH₂)₂ of NHS), 2.72–3.12 (m, 2, CHCH₂), 4.25–4.62 (m, 1, CHCH₂), 6.68 and 7.13 (2 d, *J* = 8.1 Hz, 4, ArH), 7.53 (d, *J* = 8.1 Hz, 1, NH), 9.20 (s, 1, OH). Anal. Calcd for C₁₈H₂₂N₂O₇: C, 57.14; H, 5.86; N, 7.40. Found: C, 57.02; H, 5.94; N, 7.37.

To a solution of 5.98 g (15.8 mmol) of succinimidyl *N*-(*tert*-butoxycarbonyl)tyrosinate and 2.65 g (19.0 mmol) of methyl β-alanate hydrochloride in 60 mL of DMSO was added 3.19 g (31.6 mmol) of Et₃N. The mixture was stirred for 19 h at 50 °C, diluted with EtOAc, washed successively with dilute HCl solution and brine, and dried. The crude product was chromatographed on silica gel using 1:1 EtOAc-CHCl₃ to afford 3.83 g (66%) of 15: mp 104–106 °C; IR (KBr) 3348 (OH), 1732 (CO₂Me), 1698 (CON of BOC), 1664 (CON) cm⁻¹; ¹H NMR (CDCl₃) δ 1.37 (s, 9, C(CH₃)₃), 2.41 (t, *J* = 5.4 Hz, 2, MeO₂CCH₂), 2.93 (d, *J* = 6.3 Hz, 2, CHCH₂), 3.42 (t, *J* = 5.4 Hz, 2, MeO₂CCH₂CH₂), 3.66 (s, 3, OCH₃), 5.27 (d, *J* = 7.2 Hz, 1, CHCH₂), 6.58 (t, *J* = 6.3 Hz, 1, NH), 6.75 and 7.01 (2 d, *J* = 9 Hz, 4, ArH), 7.68 (br s, 1, OH). Anal. Calcd for C₁₈H₂₆N₂O₆: C, 59.00; H, 7.15. Found: C, 59.02; H, 7.18.

Succinimidyl *N*-[*N'*-(3-Azido-5-nitrobenzoyl)tyrosyl]-β-alanate (16C). To a solution of 1.1 g (3 mmol) of 15 in 20 mL of anhydrous MeOH was bubbled HCl gas for 5 min at 0 °C. The mixture was stirred for 2 h at 25 °C and concentrated to afford 856 mg (94%) of crude methyl *N*-tyrosyl-β-alanate hydrochloride: ¹H NMR (CD₃OD) δ 2.40 (t, *J* = 6.3 Hz, 2, MeO₂CCH₂), 2.96 (d, *J* = 7.2 Hz, 2, CHCH₂), 3.33 (t, *J* = 6.3 Hz, 2, MeO₂-CCH₂CH₂), 3.62 (s, 3, OCH₃), 3.95 (t, *J* = 7.2 Hz, 1, CHCH₂), 6.75 and 7.05 (2 d, *J* = 9 Hz, 4, ArH).

To a solution of 484 mg (1.60 mmol) of methyl *N*-tyrosyl-β-alanate hydrochloride and 406 mg (1.33 mmol) of 13C in 8 mL of DMSO was added 263 mg (2.66 mmol) of Et₃N. The mixture was stirred for 20 h at 25 °C, diluted with EtOAc, washed successively with dilute HCl solution and brine, and dried. The crude product was chromatographed on silica gel using 1:1 EtOAc-CHCl₃ to afford 368 mg (69%) of methyl *N*-[*N'*-(3-azido-5-nitrobenzoyl)tyrosyl]-β-alanate: mp 137–139 °C dec (EtOAc-hexane); IR (KBr) 3498 (OH), 3370, 3300 (NH), 2128 (N₃), 1734 (CO₂), 1643, 1628 (CON) cm⁻¹; ¹H NMR (DMSO-*d*₆) δ 2.46 (t, *J* = 7.0 Hz, 2, MeO₂CCH₂), 2.79–3.08 (m, 2, CHCH₂), 3.24–3.55 (m, 2, MeO₂CCH₂CH₂), 3.60 (s, 3, OCH₃), 4.55–4.74 (m, 1, CHCH₂), 6.63 and 7.11 (2 d, *J* = 8.3 Hz, 4, ArH of Tyr), 7.95 (d, *J* = 1.4 Hz, 1, ArH of ArN₃), 8.00 (t, *J* = 1.4 Hz, 1, ArH of ArN₃), 8.31 (t, *J* = 5.8 Hz, 1, CH₂NHCO), 8.43 (d, *J* = 1.4 Hz, 1, ArH of ArN₃), 9.12 (d, *J* = 6.8 Hz, 1, CHNHCO), 9.18 (s, 1, OH). Anal. Calcd for C₂₀H₂₀N₆O₇: C, 52.63; H, 4.42. Found: C, 52.73; H, 4.43.

To a solution of 137 mg (0.3 mmol) of methyl *N*-[*N'*-(3-azido-5-nitrobenzoyl)tyrosyl]-β-alanate in 3.6 mL of 1:5 water-MeOH was added 76 mg (1.8 mmol) of lithium

hydroxide monohydrate. The mixture was stirred for 18 h at 25 °C and concentrated. The residue was acidified with 2 N HCl solution. The solution was extracted with EtOAc, washed with brine, and dried. Concentration afforded 142 mg of crude *N*-[*N'*-(3-azido-5-nitrobenzoyl)tyrosyl]- β -alanine: mp 94–96 °C dec; IR (KBr) 3316 (OH), 2128 (N_3), 1719 (CO_2), 1647, 1620 (CON) cm^{-1} ; ^1H NMR (CD_3OD) δ 2.52 (t, $J = 6.8$ Hz, 2, HO_2CCH_2), 3.05 (d, $J = 9.0$ Hz, 2, CHCH_2), 3.23–3.73 (m, 2, $\text{HO}_2\text{CCH}_2\text{CH}_2$), 6.72 and 7.16 (2 d, $J = 8.1$ Hz, 4, ArH of Tyr), 7.77, 7.94, and 8.33 (3 s, 3, $\text{C}_6\text{H}_3(\text{NO}_2)\text{N}_3$).

The procedure described in the preparation of 13C was repeated with 118 mg (0.27 mmol) of *N*-[*N'*-(3-azido-5-nitrobenzoyl)tyrosyl]- β -alanine, 37 mg (0.32 mmol) of *N*-hydroxysuccinimide, and 55 mg (0.27 mmol) of DCC in 10 mL of anhydrous THF to afford, after stirring for 16.5 h at 25 °C, 117 mg (81%) of 16C: mp 142–145 °C dec (from EtOAc-hexane); IR (KBr) 3320 (NH), 2122 (N_3), 1813, 1780 (CON of NHS), 1731 (CO_2), 1640 (CONH).

Preparation of Calmodulin. CaM was isolated from bovine testes according to the procedure of Jamieson and Vanaman (10).

Preparation of Human Erythrocyte Plasma Membrane Ca^{2+} , Mg^{2+} -ATPase. Ca^{2+} , Mg^{2+} -ATPase was isolated from outdated human blood according to the procedure of Niggli et al. (11). Activity assays were performed by the method described by Niggli et al. (11) by using a colorimetric test for free phosphate.

Synthetic Fragment (M13) of Myosin Light-Chain Kinase Containing the CaM Binding Region. The peptide (12) called M13 was synthesized at the Macromolecular Structure Analysis Facility at the University of Kentucky, Lexington, KY with Biosearch 9600 peptide synthesizer.

Functionalization of CaM with Succinimidyl *N'*-[*N'*-(3-Azido-5-nitrobenzoyl)tyrosyl]- β -alanate (16C). A mixture containing 30 mM HEPES (pH 7.4), 10 μM CaM, 20 μM 16C dissolved in HPLC-grade acetonitrile (1 mg/mL) immediately prior to use, and either 2 mM CaCl_2 or 5 mM EGTA was incubated for 2 h at 25 °C, and the reaction was quenched by the addition of lysine to a final concentration of 10 mM. The modification of CaM was monitored by HPLC on a C-3 RPSC column (Altex). The calcium dependence of cross-linking was determined by substituting 2 mM EGTA for CaCl_2 in separate experiments. Separation of native and modified CaM was achieved with a gradient increasing from 25% to 45% acetonitrile in 10 mM sodium dihydrogen phosphate (pH 6.0) and 2 mM EGTA as described by Mann and Vanaman (13) and shown in Figure 1. The purified monoadduct of CaM and 16C was digested with *Staphylococcus aureus* V8 protease (Sigma) at a ratio of 1:20 V8/CaM in the presence of EGTA. Glutamate-specific cleavage was achieved by conducting the digest in ammonium bicarbonate buffer at pH 8.0. The peptides were separated with a Phenyl μ Bondpak HPLC (Waters) column using a 1%/min gradient of 0.05% TFA and 88% acetonitrile in 1% TFA. The single peptide exhibiting 310-nm absorbance characteristic of the nitroaryl azide was sequenced with an Applied Biosystems 477A peptide sequencer.

Preparation of ^{125}I -Labeled Monoadduct of CaM and Succinimidyl *N'*-[*N'*-(3-Azido-5-nitrobenzoyl)tyrosyl]- β -alanate (16C). Radioiodination of 100 μg of the monoadduct of CaM and reagent 16C was achieved with 100 μCi of sodium [^{125}I]iodide and Enzymobeads (Bio-Rad) according to the procedure supplied by Bio-Rad.

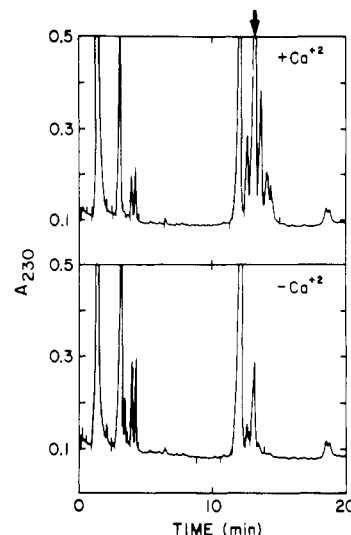


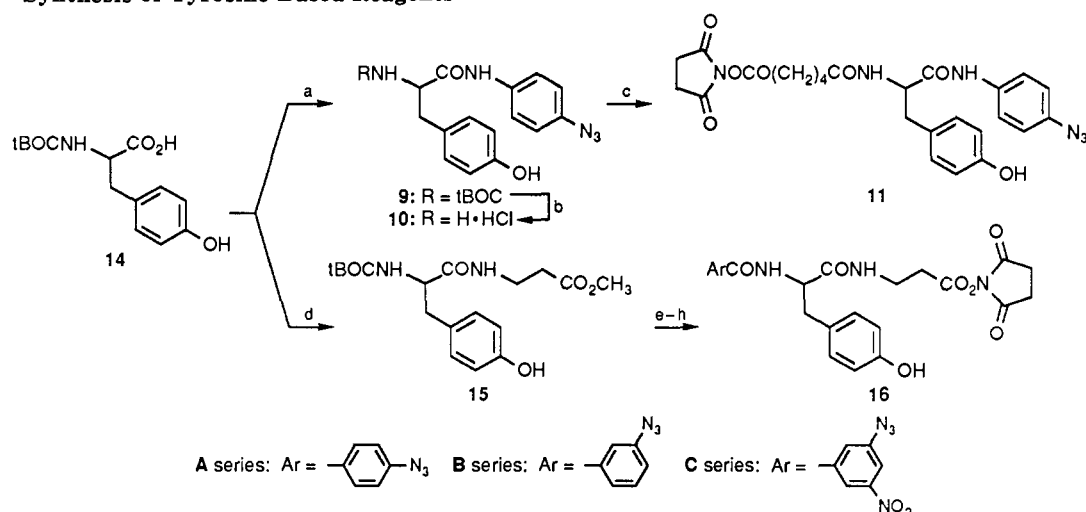
Figure 1. Reverse-phase HPLC profiles (C-3 column) of adducts of CaM and cross-linking reagent 16C: Upper trace in the presence of Ca^{2+} and lower trace in the absence of Ca^{2+} as monitored at 230 nm. The arrow denotes the Lys-75 monoadduct of CaM and 16C.

Photolabeling of Ca^{2+} , Mg^{2+} -ATPase with ^{125}I -Labeled Monoadduct of CaM and 16C. A solution of 0.7 μM Ca^{2+} , Mg^{2+} -ATPase was incubated with 2 μM of ^{125}I -labeled monoadduct of CaM and 16C (0.5 mCi/ μmol) in 30 mM HEPES (pH 7.4), 130 mM NaCl, 2 mM MgCl_2 , 100 μM CaCl_2 , 0.05% (v/v) Triton X-100, 5% (v/v) glycerol, and 0.5 mg/mL phosphatidylcholine. The calcium dependence of cross-linking was determined by substituting 2 mM EGTA for CaCl_2 in separate experiments. Solutions were photolyzed with a hand-held ultraviolet light with the glass face removed (4600 $\mu\text{W}/\text{cm}^2$, Model UVS-11, Ultra-violet Products, Inc.) at a distance of 4 cm for 1 min, suspended in a protein-solubilizing mixture of 65 mM Tris, 2% (w/v) SDS, 10% (v/v) glycerol, 5% (v/v) 2-mercaptoethanol, and 0.001% (w/v) bromophenol blue, and boiled for 5 min. The resulting solution was resolved on 7.5% SDS-PAGE, and the gel was silver-stained and autoradiographed for 48 h.

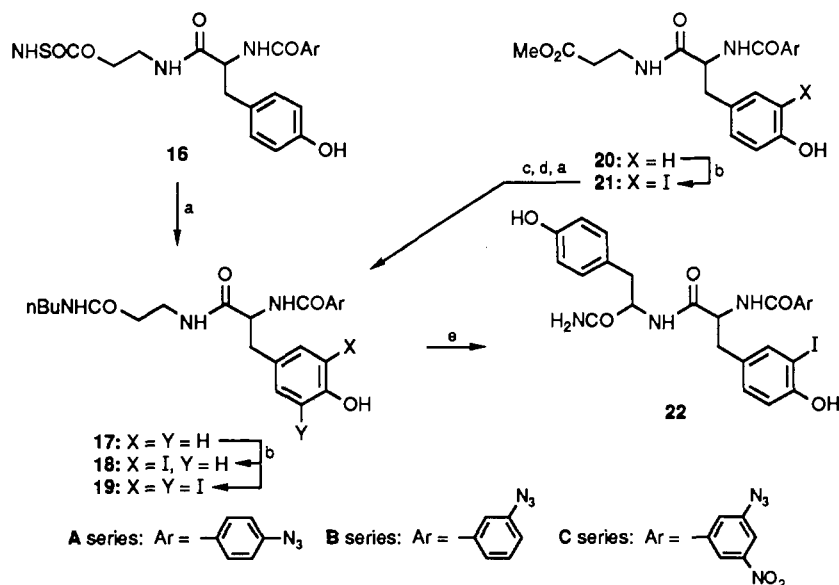
Photolabeling of the M13 Peptide. A solution of 4 μM monoadduct of CaM and 16C, 12 μM M13 peptide, and 2 mM CaCl_2 in 30 mM HEPES (pH 7.4) was photolyzed with a hand-held ultraviolet light as described above. The calcium dependence of cross-linking was again determined by substituting 2 mM EGTA for CaCl_2 in separate experiments. The photolyzed mixture was suspended in the protein-solubilizing mixture described above and boiled for 5 min. The product was resolved on 15% SDS-PAGE, and the gel was silver-stained.

RESULTS

Chemical Synthesis. After selecting tyrosine as the central structural element for these cross-linking reagents, we explored the addition of the photoactive aryl azide group at either the C-terminus or the N-terminus of tyrosine. As shown in Scheme II, the straightforward acylation of 4-azidoaniline (8) (14) with *N*-(*tert*-butoxycarbonyl)tyrosine, deblocking, and subsequent acylation with disuccinimidyl adipate furnished the potential cross-linking reagent 11 in which the C-terminus of the tyrosine residue held the photoactive portion of the reagent. As shown in Scheme II, incorporating the photoactive group at the N-terminus in the cross-linking reagents 16A, 16B, or 16C proceeded through a route that involved the acylation of β -alanine methyl ester with *N*-(*tert*-butoxy-

Scheme II.^a Synthesis of Tyrosine-Based Reagents

^a Legend for reagents: (a) DCC, 4-azidoaniline (8); (b) HCl, HOAc; (c) NHSOCO(CH₂)₄CO₂NHS, Et₃N; (d) NHS-OH, MeO₂CCH₂-CH₂NH₂·HCl, Et₃N; (e) HCl, MeOH; (f) ArCO₂NHS (13); (g) LiOH; (h) *N*-hydroxysuccinimide, DCC.

Scheme III.^a Model Studies for the Iodination and Enzymatic Cleavage

^a Legend for reagents: (a) *n*-BuNH₂; (b) NaI, chloramine T; (c) LiOH; (d) *N*-hydroxysuccinimide, DCC; (e) chymotrypsin, H₂NCOCH(NH₂)CH₂C₆H₄OH.

carbonyl)tyrosine, deblocking, and subsequent acylation with succinimide esters 13 of 4-azidobenzoic acid (12A), 3-azidobenzoic acid (12B), or 3-azido-5-nitrobenzoic acid (12C), respectively. An alternate route to succinimide esters 16 in which the acylation of tyrosine methyl ester with succinimide esters 13 preceded acylation with β -alanine methyl ester furnished the same products (16) but in poorer overall yield than the route shown in Scheme II. In comparison, cross-linking reagents 16 derived from azide-substituted benzoates were stable and readily purified whereas cross-linking reagent 11 derived from 4-azidoaniline (8) was produced in poor yield and was not readily generalized to incorporate other substituents such as a nitro group in the azidophenyl ring.

The electrophilic succinimide ester terminus in these reagents was expected to react with various nucleophilic groups in the target protein calmodulin. Since mammalian calmodulin lacked cysteine residues, the reactivity of succinimide esters with amino and hydroxyl groups was evaluated in a model study. Although succinimide esters are used routinely in reactions with amines (15–17), there was little precedent for the reactions of suc-

cinimide esters with alcohols. The alcoholysis of various succinimide esters afforded esters in good yields from primary alcohols, secondary alcohols, and phenols only if the alcohol component was used in excess (18). Under conditions useful for protein labeling, the cross-linking reagents were expected to exhibit selectivity for lysine residues rather than serine or threonine residues, a fact which we subsequently confirmed in studies using calmodulin.

As a model study for the radioiodination (19) and acylation processes needed for biochemical studies, the iodination (20, 21) of succinimide ester 16A followed by treatment with *n*-butylamine, a surrogate for a lysine residue, led, as shown in Scheme III, to a mixture of mono- and diiodinated products (18A and 19A) that could not be separated. For characterization purposes, the iodination of ester 20A, separation of the mono- and diiodinated esters, saponification, and coupling with *n*-butylamine furnished either pure 18A or 19A. Although iodinated amide 18A was not identical with the cross-linked adduct 6 in Scheme I in the sense that the azide group in 18A was still intact, we tested whether chymotrypsin

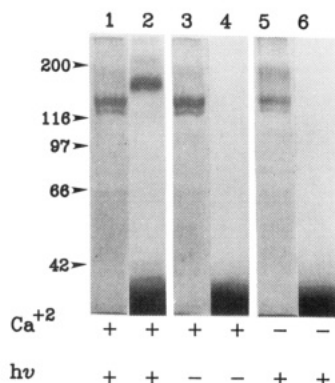


Figure 2. SDS-PAGE and autoradiograms of cross-linking experiments with CaM. Lanes 1, 3, and 5 correspond to the silver-stained gels, and lanes 2, 4, and 6 correspond to the autoradiograms of lanes 1, 3, and 5, respectively. Lanes 1 and 2 correspond to the photolysis of the ^{125}I -labeled CaM-16C monoadduct and Ca^{2+} , Mg^{2+} -ATPase in the presence of Ca^{2+} . Lanes 3 and 4 correspond to an experiment conducted in the absence of light, and lanes 5 and 6 correspond to an experiment conducted in the absence of Ca^{2+} . Less protein was used in lane 5, and this accounted for the reduced intensity of bands in this lane. Molecular weight markers are indicated at the left of lane 1.

would accept such a substrate. As shown in Scheme III, exposure of iodinated amide 18A to chymotrypsin in the presence of a nucleophile such as tyrosinamide (22) intercepted the acylated chymotrypsin intermediate and led to the isolation of the desired adduct 22A in 69% yield.

Functionalization of CaM with Succinimidyl N' -[N'' -(3-Azido-5-nitrobenzoyl)tyrosyl]- β -alanate (16C). CaM was treated with reagent 16C in the presence and absence of calcium chloride. In the presence of calcium, CaM underwent specific modification at Lys-75. Separation of native and modified CaM was achieved as described by Mann and Vanaman (13) and as shown in Figure 1. Under these conditions, 59% of the CaM was modified by 16C and the Lys-75 derivative (indicated by an arrow in Figure 1) comprised 78% of the modified CaM or 46% of the total CaM used in the experiment. The purified monoadduct of CaM and 16C was digested with *S. aureus* V8 protease (Sigma) and the single peptide exhibiting 310-nm absorbance characteristic of the nitroaryl azide was sequenced to confirm complete modification of Lys-75 (data not shown).

Photolabeling of Ca^{2+} , Mg^{2+} -ATPase with ^{125}I -Labeled Monoadduct of CaM and 16C. Irradiation of a solution of Ca^{2+} , Mg^{2+} -ATPase and ^{125}I -labeled monoadduct of CaM and 16C (0.5 mCi/ μmol) in the presence of calcium led, after separation on 7.5% SDS-PAGE and autoradiography, to the gels and autoradiograms in Figure 2. The calcium dependence of cross-linking was determined by substituting 2 mM EGTA for CaCl_2 in separate experiments. As shown in lanes 1 and 2, photolysis in the presence of Ca^{2+} yielded a radiolabeled band in the autoradiogram corresponding to a cross-linked species of CaM and Ca^{2+} , Mg^{2+} -ATPase having a M_r of approximately 150 kDa. In the absence of Ca^{2+} (lanes 5 and 6) or of photolysis (lanes 3 and 4), the radiolabeled band was absent, demonstrating that the formation of the cross-linked species required both Ca^{2+} and light.

Photolabeling of the M13 Peptide. Irradiation of a solution of monoadduct of CaM and 16C and the M13 peptide led, after separation on 15% SDS-PAGE and silver-staining, to the gel in Figure 3. Lane 1 shows the photolysis of the M13 peptide and the CaM-16C monoadduct in the presence of Ca^{2+} . The higher molecular weight band in Figure 3 is the cross-linked species. On the basis of the computed molecular weights of the cross-linked

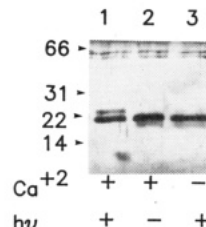


Figure 3. Silver-stained SDS-PAGE gel of cross-linking experiments with M13. Lane 1 corresponds to the photolysis of the CaM-16C monoadduct and M13 in the presence of Ca^{2+} . Lane 2 corresponds to an experiment conducted in the absence of light, and lane 3 corresponds to an experiment conducted in the absence of Ca^{2+} . Molecular weight markers are indicated at the left of lane 1.

species and CaM, there is a difference of ca. 2000 Da, and since the molecular weight of M13 is 1427 Da, this indicates that only one M13 is cross-linked per CaM molecule. An estimate of cross-linking efficiency was provided by densitometry that showed that ca. 20% of the CaM was cross-linked to M13. The high yield of photocross-linked species obviated, in this case, the need for radioisotopes. Lanes 2 and 3 demonstrate that the cross-linking is light and Ca^{2+} dependent, respectively.

DISCUSSION

New heterobifunctional cross-linking reagents that possessed a photoactive terminus, an electrophilic terminus, an ^{125}I -radiolabel, and an enzymatically cleavable linking arm between the two termini were synthesized and applied to cross-linking studies of calmodulin derivatized at Lys-75 and either the human erythrocyte plasma membrane Ca^{2+} , Mg^{2+} -ATPase or a synthetic fragment (M13) containing the CaM-binding region of myosin light-chain kinase. The selection of ^{125}I as the radiolabel was based on the availability of sodium iodide in high specific activity, the reasonable half-life, and the ease with which ^{125}I could be introduced in the cross-linking reagents late in the synthetic route. The neutral conditions necessary to preserve the succinimidyl ester functionality during radioiodination dictated the need for an activating phenolic hydroxyl group (20, 21). This need as well as the desire to incorporate an enzymatically cleavable bond led to the selection of a tyrosine residue as the spacer between the electrophilic and the photoactive termini. Reagents in which the photoactive aryl azide was attached to the N-terminus rather than the C-terminus of tyrosine were preferred on the basis of ease of synthesis and product stability. Model studies involving the successful coupling of one of these reagents (16A) with *n*-butylamine as a surrogate for a lysine residue, iodination, and chymotrypsin cleavage (22) in the presence of tyrosinamide, as shown in Scheme III, augured well for the proposed biochemical applications. This result, although promising, does not guarantee success in the biochemical system where steric bulk of the protein cross-linked through the azide may also play a role.

Preliminary studies indicated that reagents 16 were viable cross-linking reagents. Exposure of reagent 16C to calmodulin and subsequent HPLC purification provided a principal monoadduct of 16C and calmodulin. Trypsin digestion of this monoadduct and sequencing of the azide-bearing fragments indicated that 16C reacted preferentially at Lys-75 in calmodulin in a specific, calcium-dependent manner. This Lys-75 monoadduct of CaM and 16C retained 100% of the biological activity of calmodulin as established by activation of human erythrocyte plasma membrane Ca^{2+} , Mg^{2+} -ATPase (data not

shown). Radioiodination of the this monoadduct and photolysis in the presence of Ca^{2+} , Mg^{2+} -ATPase led to successful, calcium-dependent cross-linking as indicated by the gels and autoradiograms in Figure 2. A similar cross-linking experiment using the ^{125}I -labeled monoadduct of CaM and 16C and M13, a synthetic fragment of myosin light-chain kinase containing the CaM-binding region, also led to a successful, calcium-dependent cross-linking as shown in Figure 3. A detailed report of these latter studies will appear in due course. In summary, this study defined the structural parameters necessary for an enzymatically cleavable, heterobifunctional cross-linking reagent and demonstrated, in a preliminary fashion, the success of such a rationally designed reagent in two cross-linking experiments.

ACKNOWLEDGMENT

We thank the National Science Foundation (Grant CHE-8607441) for their financial support, K. Drauz and A. Bernd of Degussa AG for a generous gift of amino acids, NATO for a travel grant (Grant RG #0346/88) to D.S.W. and A.D., and the University of Kentucky for the purchase of bond issue equipment and for Faculty Grant Initiative Awards (to D.S.W. and T.C.V.).

Supplementary Material Available: Synthetic procedures and characteristic data (melting point, ^1H NMR, IR, MS, and analysis) for 9–11, 12A,B, 13B, 16A,B, 17A, 18A, 21A, and 22A (9 pages). Ordering information is given on any current masthead page.

LITERATURE CITED

- (1) Vanaman, T. C. (1980) *Calcium and Cell Function* (W. Y. Cheung, Ed.) Vol. 1., Chapter 3, Academic Press, New York.
- (2) Klee, C. B., and Vanaman, T. C. (1982) Calmodulin. *Adv. Protein Chem.* 35, 213–321.
- (3) Vanaman, T. C. (1983) Chemical approaches to the calmodulin system. *Methods Enzymol.* 102, 296–310.
- (4) Peters, K., and Richards, F. M. (1977) Chemical cross-linking: reagents and problems in studies of membrane structure. *Annu. Rev. Biochem.* 46, 523–551.
- (5) Bayley, H. (1983) *Photogenerated Reagents in Biochemistry and Molecular Biology* Elsevier, New York.
- (6) Crampton, M. R., and Khan, H. A. (1972) A spectroscopic study of the formation of isomeric Meisenheimer complexes from 1-methoxycarbonyl-3,5-dinitrobenzene. *J. Chem. Soc., Perkin Trans. 2*, 733–736.
- (7) Terpkko, M. O., and Heck, R. F. (1980) Palladium-catalyzed triethylammonium formate reductions. 3. Selective reduction of dinitroaromatic compounds. *J. Org. Chem.* 45, 4992–4993.
- (8) Ayyangar, N. R., Kalkote, U. R., Lugade, A. G., Nikrad, P. V., and Sharma, V. K. (1983) Partial reduction of dinitroarenes to nitroanilines with hydrazine hydrate. *Bull. Chem. Soc. Jpn.* 56, 3159–3164.
- (9) Myers, D. E., and Utter, M. F. (1981) The enzymatic synthesis of some potential photoaffinity analogs of benzoyl-coenzyme A. *Anal. Biochem.* 112, 23–29.
- (10) Jamieson, G. A., and Vanaman, T. C. (1979) Calcium-dependent affinity chromatography of calmodulin on an immobilized phenothiazine. *Biochem. Biophys. Res. Commun.* 90, 1048–1056.
- (11) Niggli, V., Zurini, M., and Carafoli, E. (1987) Purification, reconstitution, and molecular characterization of the Ca^{2+} pump of plasma membranes. *Methods Enzymol.* 139, 791–808.
- (12) Blumenthal, D. K., Takio, K., Edelman, A. M., Charbonneau, H., Titani, K., Walsh, K. A., and Krebs, E. G. (1985) Identification of the calmodulin-binding domain of skeletal muscle myosin light chain kinase. *Proc. Natl. Acad. Sci. U.S.A.* 82, 3187–3191.
- (13) Mann, D. M., and Vanaman, T. C. (1988) Modification of calmodulin on Lys-75 by carbamoylating nitrosoureas. *J. Biol. Chem.* 263, 11284–11290.
- (14) Smith, P. A. S., Hall, J. H., and Kan, R. O. (1962) The electronic character of the azido group attached to benzene rings. *J. Am. Chem. Soc.* 84, 485–489.
- (15) Cline, G. W., and Hanna, S. B. (1987) The aminolysis of *N*-hydroxysuccinimide esters. A structure-reactivity study. *J. Am. Chem. Soc.* 109, 3087–3091.
- (16) Anderson, G. W., Zimmerman, J. E., and Callahan, F. M. (1964) The use of esters of *N*-hydroxysuccinimide in peptide synthesis. *J. Am. Chem. Soc.* 86, 1839–1842.
- (17) Takeda, K., Sawada, I., Suzuki, A., and Ogura, H. (1983) A convenient synthesis of peptides using oxalates. *Tetrahedron Lett.* 24, 4451–4454.
- (18) Kometani, T., Watt, D. S., and Fitz, T. (1988) An esterification procedure using *N*-hydroxysuccinimidyl esters. *Toyama Kogyo Koto Senmon Gakko Kiyo* 22, 7–10 [(1989) *Chem. Abstr.* 110, 153854w].
- (19) Counsell, R. E., Smith, T. D., Ranade, V. V., Noronha, O. P. D., and Desai, P. (1973) Potential organ or tumor imaging agents. 11. Radioiodinated tyramines. *J. Med. Chem.* 16, 684–687.
- (20) Kometani, T., Watt, D. S., and Ji, T. (1985) Iodination of phenols using chloramine T and sodium iodide. *Tetrahedron Lett.* 2043–2046.
- (21) Kometani, T., Watt, D. S., Ji, T., and Fitz, T. (1985) An improved procedure for the iodination of phenols using sodium iodide and *tert*-butyl hypochlorite. *J. Org. Chem.* 50, 5384–5387.
- (22) Fink, A. L. (1973) The α -chymotrypsin-catalyzed hydrolysis of *N*-acetyl-L-tryptophan *p*-nitrophenyl esters in dimethyl sulfoxide at subzero temperatures. *Biochemistry* 12, 1736–1742.

Photoaffinity Heterobifunctional Cross-Linking Reagents Based on Azide-Substituted Salicylates

Nobuyuki Imai,[†] Lori D. Dwyer,[‡] Tadashi Kometani,[†] Tae Ji,[§] Thomas C. Vanaman,^{*,‡} and David S. Watt^{*,†}

Departments of Chemistry and Biochemistry, University of Kentucky, Lexington, Kentucky 40506, and Department of Biochemistry, University of Wyoming, Laramie, Wyoming 82071. Received August 28, 1989

Photoaffinity heterobifunctional cross-linking reagents are described that incorporate a 4-azidosalicylate group at one terminus and an *N*-hydroxysuccinimidyl ester at the other terminus with a "linking arm" of variable length separating the photoactive and electrophilic termini. Exposure of calmodulin (CaM) to succinimidyl *N*-[2-[(4-azidosalicyloxy)ethyl]suberamate (4C) led to monoadducts at Lys-21, Lys-75, and Lys-94. Separation of the monoadducts from CaM and polyadducts, radioiodination, and photolysis in the presence of human erythrocyte plasma membrane Ca^{2+} , Mg^{2+} -ATPase led to calcium-dependent cross-linking with 8% cross-linking efficiency.

Heterobifunctional photoaffinity cross-linking reagents are valuable probes for studying intermolecular associations among proteins (1-3) such as the ubiquitous calcium-binding protein calmodulin that plays an important regulatory role in a variety of biochemical processes.¹ Useful reagents of this type should possess four essential features: an electrophilic terminus capable of intercepting various nucleophilic amino acid residues; a "reporter group", such as an aryl azide or trifluoromethyl aryl diazine, capable of furnishing a reactive species that cross-links a second protein; a "linking arm" that connects the photoactive group and electrophilic terminus; and a radiolabel of sufficiently high specific activity to permit the detection of low concentrations of cross-linked biomolecules. Superimposed on these requirements are practical concerns that the radiolabels must be introduced late in the synthetic route to avoid, if possible, carrying radiolabeled intermediates through multistage transformations as well as concerns that the synthetic route must involve relatively few steps and originate with readily available materials. These requirements are fulfilled by new salicylate-based heterobifunctional reagents prepared in this study. Azide-substituted salicylates have been used previously as part of photoaffinity analogues of methotrexate (4, 5) and as part of heterobifunctional reagents (6, 7) different from those described here.

* Authors to whom correspondence should be addressed.

[†] Department of Chemistry, University of Kentucky.

[‡] Department of Biochemistry, University of Kentucky.

[§] Department of Biochemistry, University of Wyoming.

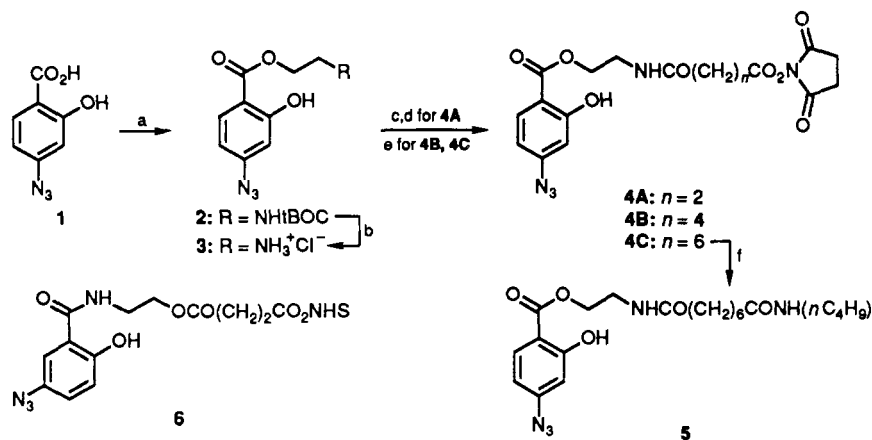
¹ Part of this work was disclosed at the following meetings: Federation of American Societies for Experimental Biology [Functional Group Orientation of Calmodulin as Determined by Heterobifunctional Reagents. L. D. Dwyer, D. M. Mann, D. S. Watt, and T. C. Vanaman, Las Vegas, NV, May 1988] and FASEB Summer Research Conference on Calcium and Cell Function [Use of Heterobifunctional Cross-linking Reagents to Map Structural and Functional Determinants on Calmodulin. L. D. Dwyer, N. Imai, P. J. Crocker, D. M. Mann, D. S. Watt, and T. C. Vanaman, Saxton's River, VT, July 1989].

EXPERIMENTAL PROCEDURES

General Chemical Procedures. Infrared spectra were recorded on a Perkin-Elmer Model 357 spectrometer. Nuclear magnetic resonance spectra were determined on a Varian 400-MHz or Gemini 200-MHz NMR spectrometer. Chemical shifts are reported in parts per million relative to tetramethylsilane as an internal standard. Mass spectra were determined on a VG ZAB spectrometer. Elemental analyses were performed by Atlantic Microlabs, Norcross, GA. Column chromatography using Macherey Nagel silica gel 60 is referred to as "chromatography on silica gel", preparative-layer chromatography on Macherey Nagel silica gel F254 is referred to as "chromatography on a silica gel plate", and the drying of an organic phase over anhydrous magnesium sulfate is simply indicated by the phrase "dried". The following experimental section contains detailed procedures for the reagents 4, one of which was successfully employed in biochemical cross-linking experiments. Experimental data for other compounds is available as supplementary material.

2-[(*tert*-Butoxycarbonyl)amino]ethanol. To a solution of 1.0 g (16 mmol) of ethanolamine and 2.4 g (25 mmol) of Et_3N^2 in 7.5 mL of dioxane and 7.5 mL of water was added 4.45 g (18 mmol) of BOC-ON. The mixture was stirred for 3 h at 25 °C. After cooling to 0 °C, the mixture was acidified with a 3 M HCl solution and extracted with EtOAc. The combined organic extracts were washed with brine and dried. The product was chromatographed on silica gel using 1:1 EtOAc-hexane to afford 1.58 g (60%) of 2-[(*tert*-butoxycarbonyl)amino]ethanol: IR (TF) 3400, 1700 cm^{-1} ; NMR (CDCl_3) δ 1.43 (s, 9, $(\text{CH}_3)_3$), 3.26 (q, $J = 6$ Hz, 2, CH_2), 3.48, (br s, 1, OH),

² The abbreviations used are as follows: BOC-ON, 2-[(*tert*-butoxycarbonyl)oxy]imino]-2-phenylacetoneitrile; Et_3N , triethylamine; CaM, calmodulin; DCC, *N,N'*-dicyclohexylcarbodiimide; DMSO, dimethyl sulfoxide; DSO, disuccinimidyl oxalate; EtOAc, ethyl acetate; EGTA, ethylene glycol bis(β -aminoethyl ether)-*N,N,N',N'*-tetraacetic acid; HEPES, 4-(2-hydroxyethyl)-1-piperazineethanesulfonic acid; HOAc, acetic acid; THF, tetrahydrofuran; NHS, *N*-hydroxysuccinimidyl; TRIS, tris(hydroxymethyl)aminomethane.

Scheme I^a

^a Reagents: (a) DCC, tBOCNHCH₂CH₂OH; (b) HCl; (c) succinic anhydride, Et₃N; (d) NHSOH, DCC; (e) NHSOC(O)-(CH₂)_nC(O)ONHS, Et₃N; (f) nBuNH₂.

3.67 (q, $J = 6$ Hz, 2, CH₂), 5.26 (br s, 1, NH). Anal. Calcd for C₇H₁₅NO₃: C, 52.16; H, 9.38. Found: C, 51.92; H, 9.43.

2-[(*tert*-Butoxycarbonyl)amino]ethyl 4-Azidosalicylate (2). To a solution of 111 mg (0.62 mmol) of 4-azidosalicylic acid (1) and 100 mg (0.62 mmol) of 2-[(*tert*-butoxycarbonyl)amino]ethanol in 2 mL of THF was added 141 mg (0.68 mmol) of DCC. The mixture was stirred for 15 h at 25 °C. The mixture was diluted with EtOAc and filtered. The filtrate was concentrated and chromatographed on silica gel in 1:2 EtOAc–hexane to afford 125 mg (61%) of (2): mp 111–112 °C (EtOAc–hexane); IR (KBr) 3340, 2100, 1670 cm⁻¹; NMR (CDCl₃) δ 1.41 (s, 9, C(CH₃)₃), 3.48 (q, $J = 6$ Hz, CH₂NH), 4.37 (t, $J = 6$ Hz, 2, OCH₂), 4.80 (br s, 1, NH), 6.45 (dd, $J = 2, 8$ Hz, 1, H-5), 6.55 (d, $J = 2$ Hz, 1, H-4), 7.71 (d, $J = 8$ Hz, 1, H-6), 10.72 (s, 1, OH). Anal. Calcd for C₁₄H₁₈O₅N₄: C, 52.17; H, 5.63. Found: C, 52.27; H, 5.66.

2-Aminoethyl 4-Azidosalicylate Hydrochloride (3). A solution of 3.5 g (11 mmol) of 2 in 20 mL of HOAc saturated with HCl gas was allowed to stand for 20 min at 25 °C. Ether was added to this mixture, and the precipitate was collected. The crystals were washed with ether and dried under reduced pressure to afford 2.44 g (87%) of 3: mp 201–202 °C (MeOH); IR (KBr) 3300–2500, 2130, 1660, 1620 cm⁻¹. Anal. Calcd for C₉H₁₁O₃N₄Cl: C, 41.79; H, 4.29. Found: C, 41.86; H, 4.33.

Succinimidyl N-[2-[(4-Azidosalicyloyl)oxy]ethyl]succinamate (4A). A solution of 200 mg (0.77 mmol) of 3, 77 mg (0.77 mmol) of succinic anhydride, and 78 mg (0.77 mmol) of Et₃N in 8 mL of DMSO was stirred for 3 h at 25 °C. The solution was diluted with EtOAc, washed with brine, and dried. The solvent was evaporated to afford 197 mg (79%) of an acid: IR (KBr) 3600–2500, 2100, 1710, 1665, 1640 cm⁻¹. Anal. Calcd for C₁₃H₁₄N₄O₆: C, 52.16; H, 9.38. Found: C, 51.92; H, 9.43.

To a suspension of 300 mg (0.93 mmol) of the above carboxylic acid and 107 mg (0.93 mmol) of *N*-hydroxysuccinimide in 10 mL of THF was added 192 mg (0.93 mmol) of DCC. The mixture was stirred for 15 h at 25 °C. The mixture was diluted with EtOAc and filtered. The filtrate was washed successively with 2% (w/v) NaHCO₃ solution and brine and dried. The residue was recrystallized from EtOAc–hexane to afford 297 mg (76%) of 4A: IR (KBr) 3280, 2103, 1810, 1778, 1725, 1645 cm⁻¹; NMR (CDCl₃) δ 2.61 (t, $J = 6.8$ Hz, 2, CH₂), 2.78 (s, 4, CH₂ of NHS), 2.97 (t, $J = 6.8$ Hz, 2, CH₂), 3.66 (q, $J = 5.3$ Hz, 2, CH₂NH), 4.41 (t, $J = 5.3$ Hz, 2, OCH₂), 6.13 (m, 1, NH), 6.53 (dd, $J = 8.6, 2.2$ Hz, 1, ArH), 6.61

(d, $J = 2.2$ Hz, 1, ArH), 7.80 (d, $J = 8.6$ Hz, 1, ArH), 10.81 (s, 1, OH). Anal. Calcd for C₁₇H₁₇N₅O₈: C, 48.69; H, 4.09. Found: C, 48.82; H, 4.13.

Succinimidyl N-[2-[(4-Azidosalicyloyl)oxy]ethyl]adipamate (4B). To a solution of 239 mg (0.70 mmol) of disuccinimidyl adipate and 200 mg (0.77 mmol) of 3 in 4 mL of DMSO was added a solution of 78 mg (0.77 mmol) of Et₃N in 2 mL of DMSO. The solution was stirred for 7 h at 25 °C, diluted with EtOAc, washed with brine, and dried. The product was chromatographed on silica gel using EtOAc to yield 137 mg (44%) of 4B: mp 110–111 °C (EtOAc–hexane); ¹H NMR (CDCl₃) δ 1.75 (m, 4, CH₂), 2.27 (t, $J = 6.8$ Hz, 2, CH₂COO), 2.62 (t, $J = 6.8$ Hz, 2, NHCOCH₂), 2.79 (s, 4, CH₂ of NHS), 3.67 (q, $J = 5.4$ Hz, 2, CH₂NH), 4.43 (t, $J = 5.4$ Hz, 2, OCH₂), 6.13 (m, 1, NH), 6.53 (dd, $J = 8.6, 2.2$ Hz, 1, ArH), 6.63 (d, $J = 2.2$ Hz, 1, ArH), 7.80 (d, $J = 8.6$ Hz, 1, ArH), 10.84 (s, 1, OH). Anal. Calcd for C₁₉H₂₁N₅O₈: C, 51.01; H, 4.73. Found: C, 51.09; H, 4.75.

Succinimidyl N-[2-[(4-Azidosalicyloyl)oxy]ethyl]suberamate (4C). To a solution of 129 mg (0.42 mmol) of disuccinimidyl suberate and 100 mg (0.39 mmol) of 3 in 4 mL of DMSO was added a solution of 39 mg (0.39 mmol) of Et₃N in 4 mL of DMSO. The solution was stirred for 12 h at 25 °C, diluted with EtOAc, washed successively with water and brine, and dried. The product was chromatographed on silica gel using EtOAc to afford 67 mg (40%) of 4C: mp 88–89 °C (EtOAc–hexane); IR (KBr) 3300, 2130, 1813, 1783, 1740, 1640 cm⁻¹; NMR (CDCl₃) δ 1.35 (m, 4, CH₂), 1.69 (m, 4, CH₂), 2.20 (t, $J = 7.3$ Hz, 2, CH₂COO), 2.58 (t, $J = 7.3$ Hz, 2, CH₂CONH), 2.81 (s, 4, CH₂ of NHS), 3.66 (q, $J = 5.6$ Hz, 2, CH₂NH), 4.43 (t, $J = 5.6$ Hz, 2, OCH₂), 5.99 (br s, 1, NH), 6.55 (dd, $J = 8.7, 2.2$ Hz, 1, ArH), 6.63 (d, $J = 2.2$ Hz, 1, ArH), 7.81 (d, $J = 8.7$ Hz, 1, ArH), 10.83 (s, 1, OH). Anal. Calcd for C₂₁H₂₅N₅O₈: C, 53.05; H, 5.30. Found: C, 53.05; H, 5.33.

Preparation of Calmodulin. CaM was isolated from bovine testes according to the procedure of Jamieson and Vanaman (8).

Preparation of Human Erythrocyte Plasma Membrane Ca²⁺, Mg²⁺-ATPase. Ca²⁺, Mg²⁺-ATPase was isolated from outdated human blood according to the procedure of Niggli et al. (9).

RESULTS

Chemical Synthesis. As shown in Scheme I, the salicylate derivatives 4B and 4C were prepared by coupling 4-azidosalicylic acid (1) with 2-[(*tert*-butoxycarbonyl)amino]ethanol, deprotection, and reaction with a bis-

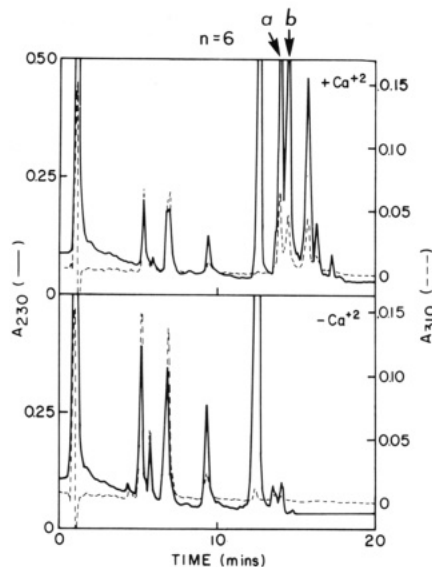


Figure 1. Reverse-phase HPLC profiles (C-3 column) of adducts of CaM and cross-linking reagent 4C in the presence and absence of Ca^{2+} as monitored at 230 and 310 nm. The latter wavelength indicated the presence of the aryl azide. Arrow "a" denotes the monoadduct at Lys-75, and arrow "b" denotes the inseparable monoadducts at Lys-21 and Lys-94.

(NHS ester). In the case of 4A, the final steps involved treating the intermediate amine 3 with succinic anhydride and activating the acid as the NHS ester.

Functionalization of CaM with Salicylate Reagents. CaM was treated with cross-linking reagents 4A, 4B, or 4C in the presence and absence of CaCl_2 . For example, the reagent 4C was dissolved in HPLC-grade acetonitrile at a concentration of 1 mg/mL immediately prior to use and was subsequently added to a mixture of 10 μM CaM, 30 μM HEPES (pH 7.4), and 2 mM CaCl_2 to a final concentration of 20 μM for the reagent 4C. The mixture was incubated at 25 $^\circ\text{C}$ for 2 h, and the reaction was quenched by the addition of Lys to a final concentration of 10 mM. To assess the calcium dependence of these reactions, 2 mM EGTA was used in place of the 2 mM CaCl_2 . The modification of CaM was monitored by HPLC on a C-3 RPSC column (Altex). Separation of native and modified CaM was achieved with a gradient increasing from 25% to 45% of acetonitrile in 10 mM sodium dihydrogen phosphate (pH 6.0) and 2 mM EGTA. The resulting traces for the modification of CaM with reagent 4C are shown in Figure 1, and the monoadducts at Lys-75 (arrow a) and at Lys-21 and Lys-94 (inseparable; arrow b) are identified in Figure 1. In the following photolabeling experiments, a mixture of these monoadducts (Lys-21, Lys-75, and Lys-94) was used, but in other photolabeling experiments (data not shown), it was possible to use just the Lys-75 monoadduct. Further purification of the CaM monoadducts and identification according to the procedure of Vanaman (10) will be described elsewhere.

Preparation of ^{125}I -Labeled Monoadduct of CaM and Reagent 4C. Radioiodination of 100 μg of a mixture of monoadducts (at Lys-21, Lys-75, and Lys-94) of CaM and reagent 4C was achieved with 200 μCi of [^{125}I]NaI and Enzymobeads (Bio-Rad) according to the procedure supplied by Bio-Rad.

Photolabeling Experiments. A solution of 1.5 μg of Ca^{2+} , Mg^{2+} -ATPase was incubated with 0.5 μg of ^{125}I -labeled monoadducts of CaM and reagent 4C (1.8 mCi/ μmol) in 30 mM HEPES (pH 7.4), 130 mM NaCl, 2 mM MgCl_2 , 0.05% Triton X-100, 5% glycerol, and 0.5 mg/

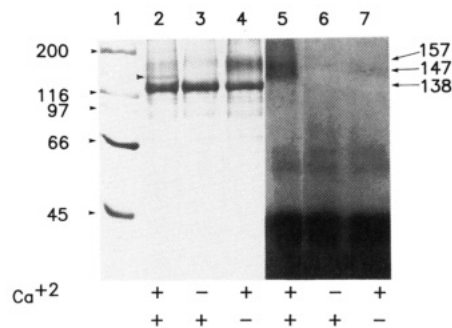


Figure 2. SDS-polyacrylamide gels and autoradiograms of cross-linking experiments. Lanes 1–4 correspond to the silver-stained gels and lanes 5–7 correspond to the autoradiograms of lanes 2–4, respectively. Lane 1 shows protein standards, whose molecular weights are indicated on the left margin. Lanes 2 and 5 correspond to the photolysis product of the ^{125}I -monoadducts of CaM and Ca^{2+} , Mg^{2+} -ATPase in the presence of 2mM CaCl_2 . The arrow at the left margin of lane 2 indicates the cross-linked adduct of CaM and Ca^{2+} , Mg^{2+} -ATPase. Lanes 3 and 6 show the gel and autoradiogram, respectively, of the same mixture without photolysis. Lanes 4 and 7 show the gel and autoradiogram, respectively, of the photolysis products in the presence of 2 mM EGTA. Arrows on the right indicate the position of Ca^{2+} , Mg^{2+} -ATPase (138 kDa) and the two cross-linked species at 147 and 157 kDa. The former corresponds to the band marked with an arrow in lane 2.

mL phosphatidyl choline containing either 0.1 mM CaCl_2 or 2 mM EGTA. The solution was photolyzed with a hand-held ultraviolet light with the glass face removed (4600 $\mu\text{W}/\text{cm}^2$, Model UVS-11, Ultra-violet Products, Inc.) at a distance of 4 cm for 1 min, suspended in a protein-solubilizing mixture of 65 mM TRIS-HCl, 2% SDS, 10% glycerol, 5% β -mercaptoethanol, and 0.001% bromophenol blue, and boiled for 5 min. Products were analyzed on a 7.5% SDS-PAGE gel, and the gel was dried, autoradiographed, resuspended, and silver-stained. Autoradiography was performed for 72 h. Figure 2 shows the results of these experiments. Cross-linking was seen only in the presence of calcium ion. The autoradiogram also shows the appearance of CaM dimer as well as an iodinated contaminant (55 kDa). Densitometry scans of the gel indicate a reproducible 8% cross-linking of the CaM and Ca^{2+} , Mg^{2+} -ATPase.

DISCUSSION

The selection of ^{125}I as the radiolabel and the decision to incorporate both the radiolabel and the azide group in the same aryl ring suggested the development of a heterobifunctional photoaffinity reagent based upon 4-aminosalicylic acid that possessed the necessary hydroxyl group needed for the activation of the aromatic ring (11, 12). The salicylate-based cross-linking reagents 4 in Scheme I met the basic requirements outlined earlier in that they possessed the capacity for radioiodination, a photoactive azide, and an electrophilic NHS ester group. Other related reagents, judged unsuitable as cross-linking reagents, such as succinimidyl *N*-[(4-azidophenoxy)carbonyl]methylsuberamate lacked the activating hydroxyl group and failed to iodinate under mild conditions, and reagents such as succinimidyl *N*-[(5-azido-3-hydroxyphenoxy)carbonyl]methylsuberamate proved too susceptible to nucleophilic substitution at the acyl group attached to the aryl azide residue rather than at the electrophilic NHS ester (see the supplementary material for the preparation of these reagents). The salicylate-based reagents also exhibited competition between the two electrophilic sites with *n*-butylamine as a Lys surrogate and gave both amide 5 and *N*-butyl-4-azido-2-hydroxybenzamide, the predominance of the former product warranted appli-

cation of the reagents 4 in experiments to functionalize CaM. In comparison with known salicylate-based cross-linking reagents, these reagents possessed an NHS electrophilic terminus instead of a maleimide (6), a photoactive aryl azide instead of an acyl azide (6), and a meta arrangement of the hydroxyl and azide groups instead of a para arrangement (7). This latter, seemingly trivial point was important in that it was noted that *p*-azidophenols, prepared in another connection (13), were considerably less stable than *m*-azidophenols and appeared to decompose thermally as well as photochemically. On this basis, it seemed reasonable that the meta-substituted reagents 4 would be potentially more effective cross-linking agents than the para-substituted reagent 6.

Calmodulin target enzymes were used as a forum in which to test the viability of the salicylate-based cross-linking reagents 4A–C. All of the salicylate-based reagents modified calmodulin in a calcium-dependent manner, although the specific modification site or sites varied from reagent to reagent as reported in detail elsewhere.³ For example, succinimidyl *N*-[2-[(4-azidosalicyloxy)oxy]ethyl]succinamate (4A) modified exclusively Lys-75, whereas succinimidyl *N*-[2-[(4-azidosalicyloxy)oxy]ethyl]suberate (4C) functionalized Lys-21, Lys-75, and Lys-94 of calmodulin to an equal extent. These results suggest an interesting spacial relationship between the hydrophobic binding site of calmodulin (14) that may bind the aryl portion of the reagents and the Lys residues in various domains of calmodulin.

In the actual photolysis experiments, it was also of interest that the length of the "linking arm" as well as the orientation of the azide and hydroxyl groups on the aryl ring influenced the cross-linking process. In these preliminary studies, it proved more convenient to perform the radioiodination on the monoadducts of calmodulin and the cross-linking reagent than to perform the radioiodination on the cross-linking reagent alone, modify calmodulin with this reagent, and purify the radiolabeled monoadducts. The outcome, in either case, was essentially the same with the exception of competitive radioiodination of Tyr residues in CaM during the former procedure. Photolysis of the ¹²⁵I-labeled monoadducts of 4A and calmodulin failed to cross-link the human erythrocyte plasma membrane Ca²⁺, Mg²⁺-ATPase whereas photolysis of the ¹²⁵I-labeled monoadducts of 4C and calmodulin successfully cross-linked this target enzyme in a calcium-dependent manner as shown in the autoradiograms of the SDS-PAGE gels in Figure 2. Appropriate controls (i.e., photolysis of the ¹²⁵I-labeled monoadducts of 4C and calmodulin in the presence of EGTA) established that the band in lane 2 (denoted by an arrow) of Figure 2 represented a true cross-linked species. The photolysis successfully produced a cross-linked species of approximately 147 kDa (lane 5 of Figure 2) that was detectable by both radioactivity and silver staining and that corresponded to the band marked in lane 2 with an arrow. Densitometry scans of the gel indicated a reproducible 8% cross-linking efficiency that compared favorably with other probes. A second, minor cross-linked species (157 kDa, lane 5 of Figure 2) of uncertain structure was also detected (by radioactivity only), consistent with literature reports (15). The isomeric reagent 6 (7) possessing a para arrangement of the azide and hydroxyl groups resulted in a remarkable 27% in cross-linking efficiency in studies using protein A and rabbit IgG (7).

On the basis of the current understanding of the pho-

tolysis of aryl azides (16, 17), it is unlikely that nitrene intermediates were the putative cross-linking agents in any of these cases. It is reasonable to suggest that a reactive *p*-iminoquinone intermediate may account for the success (7) noted with reagent 6 whereas a less reactive and more selective dehydroazepine intermediate in the present study may account for the 8% cross-linking efficiency encountered with reagent 4C. Photodeiodination (18) presumably disadvantaged both reagents 4 and 6, although the extent of this competitive process in each system was not determined. Other solutions to the problem of preparing efficient cross-linking reagents with photostable radiolabels will be described in due course.

ACKNOWLEDGMENT

We thank the National Science Foundation (Grant CHE-8607441) for financial support, Degussa AG for a generous gift of amino acids, and the University of Kentucky for the purchase of bond issue equipment.

Supplementary Material Available: Synthetic procedures and characteristic data for 8, 9, 10A–C, 12, 13, and 14A,B (5 pages). Ordering information is given on any current masthead page.

LITERATURE CITED

- (1) Bayley, H., and Knowles, J. R. (1977) Photoaffinity labeling. *Methods Enzymol.* 46, 69–114.
- (2) Chowdhry, V., and Westheimer, F. H. (1979) Photoaffinity labeling of biological systems. *Annu. Rev. Biochem.* 48, 293–325.
- (3) Bayley, H. (1983) *Photogenerated Reagents in Biochemistry and Molecular Biology* Elsevier, New York.
- (4) Price, E. M., Sams, L., Harpring, K. M., Kempton, R. J., and Freisheim, J. H. (1986) Photoaffinity analogues of methotrexate as probes for dihydrofolate reductase structure and function. *Biochem. Pharmacol.* 35, 4341–4343.
- (5) Price, E. M., Smith, P. L., Klein, T. E., and Freisheim, J. H. (1987) Photoaffinity analogues of methotrexate as folate antagonist binding probes. 1. Photoaffinity labeling of murine L1210 dihydrofolate reductase and amino acid sequence of the binding region. *Biochemistry* 26, 4751–4756.
- (6) Trommer, W. E., and Hendrick, M. (1973) Synthesis and properties of a new selective bifunctional cross-linking reagent. *Hoppe Seyler's Z. Physiol. Chem.* 356, 1455–1458.
- (7) Schwartz, M. A. (1985) A ¹²⁵I-radiolabel transfer crosslinking reagent with a novel cleavable group. *Anal. Biochem.* 149, 142–152.
- (8) Jamieson, G. A. and Vanaman, T. C. (1979) Calcium-dependent affinity chromatography of calmodulin on immobilized phenothiazine. *Biochem. Biophys. Res. Commun.* 90, 1048–1055.
- (9) Niggli, V., Zurini, M., and Carafoli, E. (1987) Purification, reconstitution, and molecular characteristics of the Ca²⁺ pump of plasma membranes. *Methods Enzymol.* 139, 791–808.
- (10) Vanaman, T. C. (1983) Chemical approaches to the calmodulin system. *Methods Enzymol.* 102, 296–310.
- (11) Kometani, T., Watt, D. S., and Ji, T. (1985) Iodination of phenols using chloramine T and sodium iodide. *Tetrahedron Lett.* 26, 2043–2046.
- (12) Kometani, T., Watt, D. S., Ji, T., and Fitz, T. (1985) An improved procedure for the iodination of phenols using sodium iodide and *tert*-butyl hypochlorite. *J. Org. Chem.* 50, 5384–5387.
- (13) Kawada, K., Dolence, E. K., Morita, H., Kometani, T., Watt, D. S., Balapure, A., Fitz, T. A., Orlicky, D. J., and Gerschenon, L. E. (1989) Prostaglandin photoaffinity probes: synthesis and biological activity of azide-substituted 16-phenoxo and 17-phenyl PGF_{2α} prostaglandins. *J. Med. Chem.* 32, 256–264.
- (14) Babu, Y. S., Sack, J. A., Greenbough, T. J., Bugg, C. E., Means, A. R., and Cook, W. J. (1985) Three-dimensional structure of calmodulin *Nature* 315, 37–40.

³ Dwyer, L. D., Imai, N., Crocker, P. J., Mann, D. M., Watt, D. S., and Vanaman, T. C., manuscript in preparation.

- (15) Carfoli, E., Zurini, M., Niggli, V., and Krebs, J. (1982) The calcium-transporting ATPase of erythrocytes. *Ann. N. Y. Acad. Sci.* 402, 304-306.
- (16) Torres, M. J., Zayas, J., and Platz, M. S. (1986) A formal CH insertion reaction of an aryl nitrene into an alkyl CH bond. Implications for photoaffinity labeling. *Tetrahedron Lett.* 27, 791-794.
- (17) Shields, C. J., Chrisope, D. R., Schuster, G. B., Dixon, A. J., Poliakoff, M., and Turner, J. J. (1987) Photochemistry of aryl azides: detection and characterization of a dehydroazepine by time-resolved infrared spectroscopy and flash photolysis at room temperature. *J. Am. Chem. Soc.* 109, 4723-4726.
- (18) Watt, D. S., Kawada, K., Leyva, E., and Platz, M. S. (1989) Exploratory photochemistry of iodinated aromatic azides. *Tetrahedron Lett.* 30, 899-902.

Biological Activity of Oligonucleotide–Poly(L-lysine) Conjugates: Mechanism of Cell Uptake

Jean-Paul Leonetti, Geneviève Degols, and Bernard Lebleu*

Laboratoire de Biochimie des Protéines, CNRS UA 1191, Université des Sciences et Techniques du Languedoc, Place E. Bataillon, 34060 Montpellier, France. Received December 28, 1989

We have previously shown that antisense oligomers linked to poly(L-lysine) (PLL) exhibit antiviral properties against vesicular stomatitis virus (VSV) at concentrations lower than 1 μ M. The conjugation to PLL provides an interesting alternative to natural or neutral oligomers to increase the biological effects of antisense oligomers. The internalization pathway of oligomer–PLL conjugates as compared to unconjugated oligomers has been studied in L929 cells. In parallel to their enhanced antiviral activity, PLL increases greatly the uptake of fluorescently tagged oligomers. This internalization follows a classical endocytic pathway and the oligomer has to be cleaved from PLL in the cell to exhibit an antiviral effect.

It has been established that small DNA sequences called "antisense oligonucleotides" are able to control negatively viral (1) or cellular (2) gene expression through formation of complementary hybrids with mRNAs or their precursors. Unmodified oligonucleotides (oligomers) are internalized in mammalian cultured cells through a saturable and energy-dependent process, possibly mediated by a receptor (3, 4). However oligomers are highly sensitive to nucleases present in the culture media and in many cases this uptake is too slow and/or inefficient to deliver functional oligomers at the appropriate concentration into cultured cells.

Nonionic methylphosphonate oligomers penetrate mammalian cells through passive diffusion across the membrane and are resistant to nuclease degradation; high concentrations (in the 50–100 μ M range) are nevertheless required to inhibit vesicular stomatitis virus (VSV) (5), human immunodeficiency virus (HIV) (6), or herpes virus multiplication (7).

Unmodified or phosphorothioate oligomers covalently linked to cholesterol (8) inhibit HIV at significantly lower concentrations than oligomers alone. This increased efficiency is most probably due to their enhanced uptake into cells (9).

Poly(L-lysine) (PLL), a well-known polycationic drug carrier (10), has been used to potentiate the antiviral effects of antisense oligomers directed against VSV (11), and more recently against HIV (12). A large decrease (100-fold or more) in the VSV titer was observed at antisense oligomers concentration lower than 1 μ M; this has to be compared with the inhibitions observed with unconjugated oligomers or oligomer analogues which act in a concentration range of 10–100 μ M.

In the present study we have investigated the internalization pathway of such conjugated oligomers, using fluorescently tagged oligomers, flow cytometry, and inhibitors of endocytosis. These results were compared to measurements of antiviral effects induced by the conjugates to ascertain the functional stability of the oligomer.

EXPERIMENTAL PROCEDURES

Materials. Media for cell culture were obtained from Eurobio (Paris, France) and sera were from Boehringer. PLL (14 000 mean MW) was supplied by Sigma, oligo-

mer synthesis reagents were from Milligen, and fluorescein *N*-hydroxysuccinimide ester was supplied by Boehringer.

Cell Cultures and Viruses. L929 cells were grown in minimal essential medium supplemented with 10% (v/v) fetal calf serum. VSV (Indiana strain) was grown in L929 cells and titrated by an end-point method (13). This method is easier to implement than plaque titration and gives similar results. Differences in VSV titers of more than 0.5 log unit are statistically considered as highly significant in this assay.

Oligomer Synthesis and Covalent Linkage to PLL. Oligomers were synthesized on a riboadenosine-derivatized support with a Bioscience Cyclone automatic DNA synthesizer and purified by reversed-phase chromatography. Covalent linkage of oligomers to PLL through an *N*-morpholine ring was achieved by periodic acid oxidation and borocyanohydride reduction of the 3'-end ribose, as previously described (14). The sequence CATTTT-GATTACTGTrA is complementary to the 5'-end sequence of VSV N protein mRNA (15) and the oligomer AACGT-TGAGGGGCATrA is complementary to the initiation codon and four downstream codons of the *c-myc* proto-oncogene mRNA (16).

Antiviral Experiments. L929 cells (2×10^5 /well in 24-well plates) were incubated for 2 h with oligomer–PLL conjugates (1 μ M usually) and infected with VSV at a multiplicity of infection (moi) of 1. The cells were frozen at -20°C 18 h after infection, and virus was titrated as described above.

Measurements of Oligomer Internalization. Detritylated 5'-end of the oligomer (uncleaved from synthesis support) was activated with carbonyldiimidazole and derivatized with diaminoethane according to Wachter et al. (1977). After cleavage from the column and deprotection, the oligomer was then fluorescently labeled with carboxyfluorescein *N*-hydroxysuccinimide ester (in 10-fold excess compared to the oligomer), in 10 mM Hepes, pH 8, 30% dimethylformamide. Free fluorescent dye was removed by several extractions with chloroform followed by reversed-phase HPLC chromatography. The fluorescently labeled oligomer was then linked to PLL as described above.

For flow cytometry analysis, L929 cells (2×10^5 /well

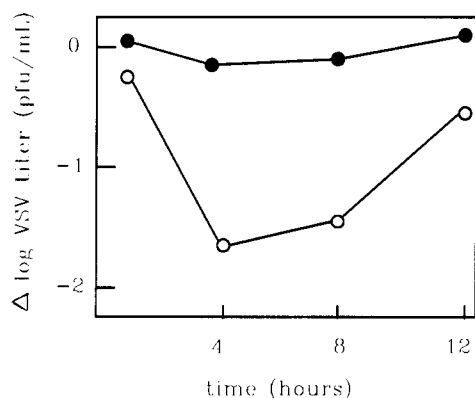


Figure 1. Stability of the antiviral effect promoted by oligomer-PLL conjugates: myc (●) or VSV (○) oligomer-PLL conjugates at 0.75 μ M concentration were added to L929 cells at the indicated time prior to VSV infection. The cells were frozen 18 h later and VSV titers were measured by a dilution method as described in the Experimental Procedures.

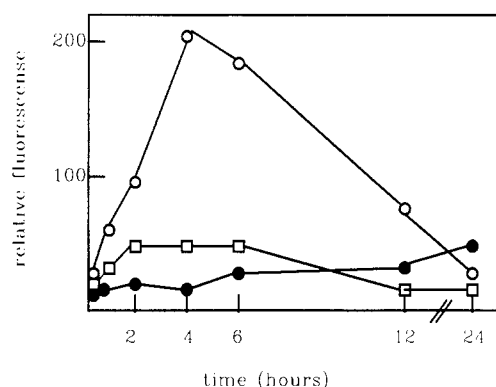


Figure 2. Kinetics of uptake of oligomer-PLL conjugates: Fluorescently tagged oligomers conjugated or not to PLL were added at 1 μ M concentration to L929 cells growing at 37 °C in 24-well plates. At the indicated time the cells were washed, treated with DNase I (20 units/mL), fixed, and submitted to flow cytometry analysis as described in the Experimental Procedures: (●) oligomer, (□) oligomer + 1 μ M PLL, (○) oligomer-PLL conjugate.

in 24-wells plate) were incubated at 37 °C with oligomers (1 μ M) linked or not to PLL. At various periods of time 20 units/mL DNase I was added in the culture medium for 10 min at 37 °C. The cells were then washed twice with PBS, scraped from the plates in PBS, 10 μ M EDTA and stored in PBS, 10 mM EDTA, 3% (v/v) paraformaldehyde prior to analysis on a fluorescence-activated cell sorter.

RESULTS

Kinetics of Oligomer-PLL Conjugate Uptake and Establishment of Antiviral Effects. An oligomer complementary to the 5'-end of VSV N protein mRNA promotes specific antiviral effects at concentrations lower than 1 μ M when linked to PLL (11), while PLL alone, noncomplementary oligomers, or oligomers not linked to PLL are inefficient in the same conditions. The kinetics of establishment of the antiviral effect was compared to the kinetics of uptake of the conjugates in L929 cells.

The antiviral effect rises to a maximum within 4 h after addition of the antisense oligomer-PLL conjugate in the culture medium and decreases progressively until 12 h (Figure 1). No reduction in the virus titer was observed with the noncomplementary myc oligomer. The antiviral effects attained with this approach protect cells from VSV-associated cytopathic effects only transiently; after

Table I. Cell Permeabilization by Poly(L-lysine) and Its Reversal by CaCl_2 ^a

PLL	CaCl_2 , mM	⁵¹ Cr release, cpm
–	0	782
+	0	1561
+	1	1599
+	5	658
+	10	655

^a L929 cells growing in 24-well plates were loaded with 20 μ Ci of ⁵¹Cr for 24 h. They were then washed with PBS and treated with 2 μ M PLL in presence or absence of 1, 5, or 10 mM CaCl_2 . Two hours later, ⁵¹Cr released in the culture medium was counted in the presence of liquid scintillator.

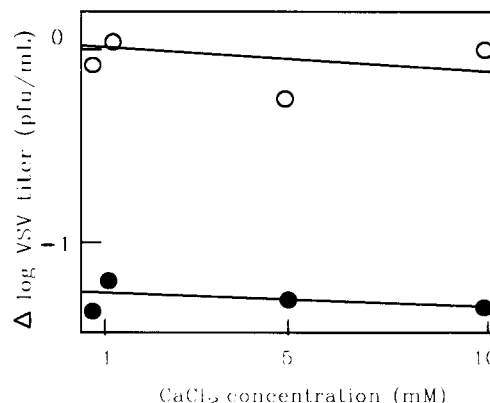


Figure 3. Effects of calcium on the antiviral activity of oligomer-PLL conjugates: PLL (○) or VSV oligomer-PLL conjugates (●) at 1 μ M concentration were added to L929 cells 2 h prior to VSV infection, in presence or absence of the indicated calcium concentration. The cells were frozen 18 h later and VSV titers were measured as described in the Experimental Procedures.

several viral multiplication cycles, cells lyse in line with incomplete eradication of VSV and with the expected degradation of antisense oligomers.

The uptake by L929 cells of fluorescently tagged oligomers linked to PLL is maximal between 4 and 8 h after their addition to the culture medium, as shown by flow cytometry analysis (Figure 2). After this time, the fluorescence associated with the cells decreases rapidly. The intracellular uptake by L929 cells of fluorescently tagged oligomers conjugated to PLL is faster and greatly increased as compared to that of unconjugated oligomers. In these experiments cells were treated with DNase I before flow cytometry analysis, in order to degrade all the fluorescently tagged oligomers associated only at the cell surface and in the culture medium.

Involvement of Cellular Membrane Permeabilization in the Antiviral Activity of Oligomer-PLL Conjugates. Naturally occurring or synthetic polycationic peptides induce permeabilization of cellular membranes (18). These damages can be reversed by divalent cations such as calcium, magnesium, and zinc (18). This cytotoxicity should be kept to a minimum when using low molecular weight PLL carrier at low concentration as it was done in all our studies. In order to evaluate any such effect, cells were loaded with ⁵¹Cr (Table I). Two hours after addition of 2 μ M PLL, measurement of ⁵¹Cr release in the medium reveals that the permeabilization of the cells incubated with PLL in these experimental conditions is only the double of control cells, e.g., barely significant. This effect of PLL is reversed by the addition of calcium salts in the culture medium. Although the permeabilization by 14 000 MW PLL is weak within this range of concentration, antiviral effects can poten-

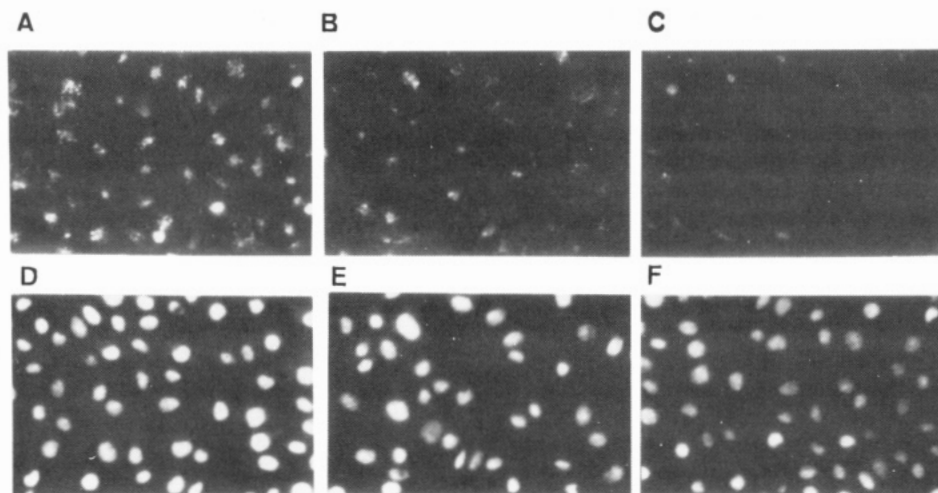


Figure 4. Uptake of fluorescently tagged oligomer-PLL conjugates at low temperature and in presence of metabolic inhibitors: L929 growing in 8-well microscopy chamber slides were incubated at 37 °C (A, D), 4 °C (C, F), or in presence of metabolic inhibitors (5 mM sodium azide, 50 mM deoxyglucose) (B, E), with 1 μ M fluorescently tagged oligomers conjugated to PLL. The cells were transferred 2 h later at 4 °C and treated for 1 h with DNase I (20 units/mL) and stained with Hoechst 33342. The cells were then washed with PBS, fixed at -20 °C in methanol, and observed by fluorescence microscopy. The cells were visualized for fluorescently tagged oligomer-PLL conjugates (A-C). The same cells were then visualized for Hoechst 33342 fluorescence (D-F).

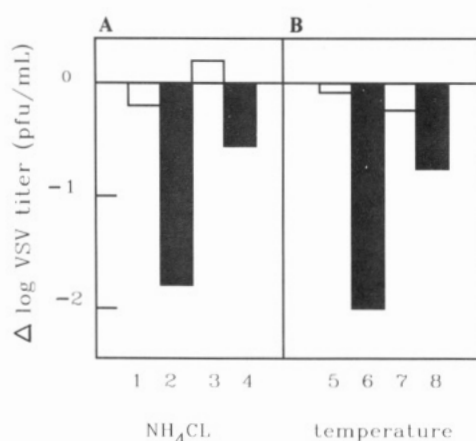


Figure 5. Effects of lysosomotropic amines and of low-temperature incubation on the antiviral activity of oligomer-PLL conjugates. (A) L929 cells growing in 24-well plates were incubated for 4 h at 4 °C (7, 8) or 37 °C (5, 6) with 1 μ M myc (□) or VSV (■) oligomer-PLL conjugate. The cells were then transferred at 4 °C, treated with DNase I (20 units/mL) for 1 h, put back at 37 °C, and infected with VSV at 1 moi. The cells were frozen 18 h later and VSV titers were measured as described in the Experimental Procedures. (B) L929 growing in 24-well plates with 4 mM NH₄Cl (3, 4) or without (1, 2) were incubated with myc (□) or VSV (■) oligomer-PLL conjugates at 1 μ M concentration and were infected 2 h later with VSV (1 moi). The cells were frozen 18 h later and VSV titers were measured as described in the Experimental Procedures.

tially be due in part to diffusion of the conjugate across the permeabilized cellular membrane.

To discriminate between such a pathway and endocytosis, the cells were incubated with the oligomer-PLL conjugates in the presence of calcium. The addition of 10 mM calcium in the culture medium abolishes the cellular permeabilization (Table I) but is not detrimental to the establishment of the antiviral effect (Figure 3).

Uptake of Oligomer-PLL Conjugates Involves an Endocytic Pathway. The internalization pathway of PLL linked to methotrexate was extensively studied by Ryser et al. (see ref 10 for a review). Its transport was shown to be energy dependent, and the cytotoxicity of the conjugate was inhibited by lysosomotropic amines.

In order to examine the internalization process of the oligomer-PLL conjugates, cells were incubated with flu-

Table II: Oligomer-Poly(D-lysine) Conjugates Do Not Promote Any Antiviral Effect^a

conditions	$\Delta \log$ VSV titer, pfu/mL
PLL	+0.2
VSV-PLL	-2.0
PDL	+0.4
VSV-PDL	+0.2

^a Oligomer-PLL or -PDL conjugates at 1 μ M concentration were added to L929 cells 2 h prior to VSV infection. Four hours after infection the culture media was changed to remove the conjugate. The cells were frozen 16 h later and VSV titers were measured as described in the Experimental Procedures.

orescently tagged oligomer linked to PLL under conditions known to modulate endocytosis, and the internalization was followed by microscopy. As shown in Figure 4, the uptake of the conjugates is decreased when the cells are incubated at 4 °C or with metabolic inhibitors such as sodium azide and deoxyglucose. When cells are preincubated at 4 °C with oligomer-PLL conjugates and treated with DNase I and the temperature is shifted to 37 °C before VSV infection, no reduction in the virus titer is observed (Figure 5). These results are consistent with the active process of transport described by Ryser et al. (19). Similarly the incubation of cells with oligomer-PLL conjugates in the presence of various lysosomotropic amines abolishes the antiviral effect (Figure 5 and data not shown).

An oligomer covalently linked to poly(D-lysine) (PDL), a carrier insensitive toward cellular protease degradation, is inefficient to promote an antiviral effect at the same concentration as an oligomer-PLL conjugate (Table II). Since PDL exhibits toxic effects on L929 cells at 1 μ M concentration, the medium was changed 4 h after its addition. Under these conditions no significant difference in the endocytosis of the conjugate can be observed by fluorescence microscopy.

DISCUSSION

PLL, a cationic macromolecular carrier, is efficiently transported into mammalian cultured cells by a process defined as a nonspecific adsorptive endocytosis (10). The uptake is preceded by nonspecific interactions on negatively charged molecules at the surface of the cell. It has been used to potentiate the uptake of various drugs

and macromolecules such as methotrexate and horseradish peroxidase (10–20).

We have conjugated this carrier to antisense oligomers complementary to the 5'-end of the VSV N protein mRNA, in order to potentiate the antiviral properties of the oligomer. More recently, similar approaches have proved to be successful in developing an antiproliferative activity with anti c-myc oligomers (Degols et al., manuscript in preparation) or to decrease the cytopathic effects of HIV-1 infection in MT4 cells (12).

In line with these observations, we now demonstrate directly that the uptake of fluorescently tagged oligomers is both accelerated and increased when conjugated to PLL as compared to oligomers alone or to a mixture of oligomers and PLL. The maximum uptake is attained after 4 h of exposure. However, after 4 h, the uptake of the oligomer-PLL conjugates decreases. The recycling of the conjugates at the cell surface and their degradation in the cells and/or the culture medium could potentially explain the decrease in fluorescence observed after 4 h of incubation.

To ascertain the integrity of the oligomers we measured the antiviral effect obtained with the conjugates under the same conditions. The magnitude of the antiviral effect increased to a maximum 4 h after addition of the conjugate and decreased slowly thereafter, in agreement with the kinetics of internalization.

PLL, as do other polycationic peptides, induces a permeabilization of the cellular membranes, which can be reversed by divalent cations (e.g. calcium, magnesium, etc.) (18). With 14 000 MW PLL, at 2 μ M, we only observed a slow increase of the permeability of L929 cells, which did not lead to cytotoxic effects. This is irrelevant to the antiviral activity of the conjugates since an increased calcium concentration in the culture medium inhibits the permeabilization without affecting the establishment of the antiviral effect.

In the same way, we observed that incubation at low temperature or in the presence of metabolic inhibitors abolishes the transport of the conjugates and their biological activities. These results are consistent with an active process of internalization as a prerequisite to their delivery into cells.

Although the covalent linkage of the oligomer to PLL increases the uptake of the conjugates, other effects of PLL cannot be excluded in the potentialization of their antiviral effects. PLL has been shown to increase the thermal stability of a poly(rI)-poly(rC) duplex and to stabilize polynucleotides toward nuclease degradation (21). We also observed a stabilization of the oligomer in cellular extracts when it was conjugated to PLL (data not shown).

Some experiments were done to elucidate if the conjugation to PLL is important to the action of the oligomers once inside the cell. With oligomers linked to PDL, a carrier insensitive to the degradation by proteases, no antiviral effect was observed. Moreover the incubation of cells with low NH_4Cl concentration (4 mM), a dose insufficient to inhibit VSV multiplication nonspecifically, decreases significantly the antiviral effect of the conjugates.

These results argue for endocytosis of the oligomer-PLL conjugates through the acidic compartments, where proteolysis of the carrier releases the oligomers. Nevertheless problems in the release from acidic compartments to cytoplasm or changes in the endocytic pathway mediated by the linkage to PDL or to the addition of NH_4Cl cannot be excluded.

Previous works of Loke et al. (3) and Yakubov et al. (4) suggest that oligomers at low concentration can be taken up by cells via receptors (about $1.2 \times 10^5/\text{L929}$ cells (4)), for which a 80-kDa protein, identified by affinity labeling with radioactive oligomers, is a good candidate. The nonspecific adsorptive endocytosis of PLL is not limited by the amount of cell surface receptors and allows higher capacity of binding; this could explain in part the increased efficiency of PLL-conjugated oligomers as compared to free oligomers.

For several years the use of antisense oligomers as artificial modulators of gene expression has been the object of a plethora of reports. Novel prospects are coming in now, such as interference with DNA-binding proteins through triple-helix formation or competition with double-stranded oligomers. Sensitivity to nucleases and limitations in the uptake of the oligomers by many cell lines have remained crucial problems. PLL conjugation thus constitutes an interesting alternative to increase the penetration of oligomers into cells and probably also to stabilize them against nucleases. However its efficiency is highly dependent on the cell lines and does not allow any specific targeting. Other alternatives therefore are under investigation in our group, such as encapsulation of the oligomers in liposomes.

ACKNOWLEDGMENT

We thank Dr. F. Favier for his expert assistance in flow cytometry experiments. This work has been supported by a fellowship of the Association pour la Recherche Contre le Cancer to G.D. and by research grants of the Centre National de la Recherche Scientifique, the Agence Nationale de Recherche sur le SIDA, and the Fédération Nationale des centres de Lutte contre le Cancer to B.L. J.P.L. is allocataire from the Ministère de la Recherche et de la Technologie.

LITERATURE CITED

- (1) Zamecnik, P., and Stephenson, M. (1978) Inhibition of Rous Sarcoma virus replication and cell transformation by a specific oligodeoxynucleotide. *Proc. Natl. Acad. Sci. U.S.A.* 75, 280–284.
- (2) Wickstrom, E. L., Bacon, T. A., Gonzalez, A., Freeman, D. L., Lyman, D. L., and Wickstrom, E. (1988) Human promyelocytic leukemia HL-60 cell proliferation and c-myc protein expression are inhibited by an anti-sense pentadecadeoxynucleotide. *Proc. Natl. Acad. Sci. U.S.A.* 79, 2181–2185.
- (3) Loke, S. L., Stein, C. A., Zhang, X. H., Mori, K., Nakanishi, M., Subasinghe, C., Cohen, J. S., and Neckers, L. M. (1989) Characterisation of oligonucleotide transport into living cells. *Proc. Natl. Acad. Sci. U.S.A.* 86, 3847–3848.
- (4) Yakubov, L. A., Deeva, E. A., Zarytova, V. F., Ivanova, E. M., Rytte, A. S., Yurchenko, L. V., and Vlassov, V. V. (1989) Mechanism of oligonucleotide uptake by cells: involvement of specific receptors? *Proc. Natl. Acad. Sci. U.S.A.* 86, 6454–6458.
- (5) Agris, C. H., Blake, K. R., Miller, P. S., Reddy, P., and Ts'o, P. O. P. (1986) Inhibition of vesicular stomatitis virus protein synthesis and infection by sequence specific oligodeoxynucleotide methylphosphonates. *Biochemistry* 25, 6268–6275.
- (6) Sarin, P. S., Agrawal, S., Civeira, M. P., Goodchild, J., Ikeuchi, T., and Zamecnik, P. C. (1988) Inhibition of acquired immunodeficiency syndrome virus by oligodeoxynucleoside methylphosphonates. *Proc. Natl. Acad. Sci. U.S.A.* 85, 7448–7451.
- (7) Smith, C. C., Aurelian, L., Reddy, M. P., Miller, P. S., and Ts'o, P. O. P. (1986) Antiviral effect of an oligo(nucleoside methylphosphonate) complementary to the splice junction of herpes simple virus type I immediate early pre-mRNA 4 and 5. *Proc. Natl. Acad. Sci. U.S.A.* 83, 3232–3236.

- (8) Letsinger, R. L., Zhang, G., Sun, D. K., Ikeuchi, T., and Sarin, P. (1989) Cholesteryl conjugated oligonucleotides: Synthesis, properties, and activity as inhibitors of replication of human immunodeficiency virus in cell culture. *Proc. Natl. Acad. Sci. U.S.A.* 86, 6553-6556.
- (9) Boutorin, A. S., Guskova, L. V., Ivanova, E. M., Kobetz, N. D., Zarytova, V. F., Rytte, A. S., Yurchenko, L. V., and Vlassov, V. V. (1989) Synthesis of alkylating oligonucleotide derivatives containing cholesterol or phenazinium residues at their 3'-terminus and their interaction within mammalian cells. *FEBS Lett.* 254, 129-132.
- (10) Ryser, H. J.-P., and Shen, W. C. (1978) Conjugation of methotrexate to poly(L-lysine) increase drug transport and overcome drug resistance in cultured cells. *Proc. Natl. Acad. Sci. U.S.A.* 75, 3867-3870.
- (11) Lemaitre, M., Bayard, B., and Lebleu, B. (1987) Specific antiviral activity of a poly(L-lysine)-conjugated oligodeoxyribonucleotide sequence complementary to vesicular stomatitis virus N protein mRNA initiation site. *Proc. Natl. Acad. Sci. U.S.A.* 84, 648-652.
- (12) Stevenson, M., and Iversen, P. L. (1989) Inhibition of human immunodeficiency virus type 1-mediated cytopathic effects of poly(L-lysine)-conjugated synthetic antisense oligodeoxyribonucleotides. *J. Gen. Virol.* 70, 673-682.
- (13) Milhaud, P. G., Silhol, M. Faure, T., and Milhaud, X. (1983) Numerical tables for the direct estimation of virus titers by the maximum likelihood method. *Ann. Virol. (Inst. Pasteur)* 134E, 405-416.
- (14) Leonetti, J. P., Rayner, B., Lemaitre, M., Gagnor, C., Milhaud, P. G., Imbach, J. L., and Lebleu, B. (1989) Antiviral activity of conjugate between poly(L-lysine) and synthetic oligodeoxyribonucleotides. *Gene* 72, 323-332.
- (15) Gallione, C. J., Greene, J. R., Iverson, L. E., and Rose, J. K. (1981) Nucleotide sequences of the mRNA's encoding the Vesicular Stomatitis Virus N and NS proteins. *J. Virol.* 39, 529-535.
- (16) Bernard, O., Cory, S., Gerondakis, S., Webb, E., and Adams, J. M. (1983) Sequence of the murine and human cellular myc oncogenes and two modes of myc transcription resulting from chromosome translocation in B lymphoid tumors. *EMBO J.* 2, 2375-2383.
- (17) Wachter, L., Jablonski, J.-A., and Ramachandran, K. L. (1986) A simple and efficient procedure for the synthesis of 5'-aminoalkyl oligodeoxynucleotides. *Nucleic Acids Res.* 14, 7985-7994.
- (18) Brashford, C. L., Alder, G. M., Menestrina, G., Micklem, K. J., Murphy, J. J., and Pasternak, C. A. (1986) Membrane damage by hemolytic viruses, toxins, complement, and other cytotoxic agents. *J. Biol. Chem.* 261, 9300-9308.
- (19) Ryser, H. J.-P., and Shen, W. C. (1986) Drug-poly(lysine) conjugates: Their potential for chemotherapy and for the study of endocytosis. *Targeting of Drugs and Synthetic Systems* (G. Gregoriadis, J. Senior and G. Poste, Eds.) pp 103-121, Plenum Press, New York.
- (20) Shen, W. C., and Ryser, H. J. P. (1978) Conjugation of poly-L-lysine to albumin and horseradish peroxidase: A novel method of enhancing the cellular uptake of proteins. *Proc. Natl. Acad. Sci. U.S.A.* 75, 1872-1876.
- (21) Levy, H. B., Baer, G., Baron, S., Bruckler, C. E., Gibbs, C. J., Iadarola, M. J., London, W. T., and Rice, J. (1975) A modified polyribonucleosinic-polycytidilic acid complex that induces interferon in primates. *J. Infect. Dis.* 132, 434-439.

Evaluation of Iodovinyl Antibody Conjugates: Comparison with a *p*-Iodobenzoyl Conjugate and Direct Radioiodination

Stephen W. Hadley* and D. Scott Wilbur

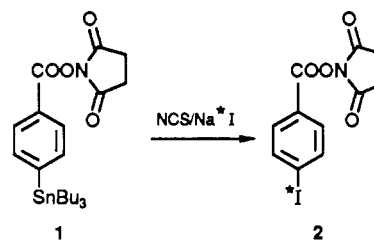
NeoRx Corporation, 410 W. Harrison Street, Seattle, Washington 98119. Received January 29, 1989

The preparations and conjugations of 2,3,5,6-tetrafluorophenyl 5- $^{125}\text{I}/^{131}\text{I}$ iodo-4-pentenoate (**7a**) and 2,3,5,6-tetrafluorophenyl 3,3-dimethyl-5- $^{125}\text{I}/^{131}\text{I}$ iodo-4-pentenoate (**7b**) to monoclonal antibodies are reported. Reagents **7a** and **7b** were prepared in high radiochemical yield by iododestannylation of their corresponding 5-tri-*n*-butylstannyl precursors. Radioiodinated antibody conjugates were prepared by reaction of **7a** or **7b** with the protein at basic pH. Evaluation of these conjugates by several in vitro procedures demonstrated that the radiolabel was attached to the antibody in a stable manner and that the conjugates maintained immunoreactivity. Comparative dual-isotope biodistribution studies of a monoclonal antibody Fab fragment conjugate of **7a** and **7b** with the same Fab fragment labeled with *N*-succinimidyl *p*- ^{131}I iodobenzoate (PIB, *p*-iodobenzoate, **2**) or directly radioiodinated have been carried out in tumor-bearing nude mice. Coinjection of the Fab conjugate of **7a** with the Fab conjugate of **2** demonstrated that the biodistributions were similar in most organs, except the neck tissue (thyroid-containing) and the stomach, which contained substantially increased levels of the **7a** label. Coinjection of the Fab conjugate of **7a** with the Fab fragment radioiodinated by using the chloramine-T method demonstrated that the biodistributions were remarkably similar, suggesting roughly equivalent in vivo deiodination of these labeled antibody fragments. Coinjection of the Fab conjugate of **7a** with the Fab conjugate of **7b** indicated that there was approximately a 2-fold reduction in the amount of in vivo deiodination of the **7b** conjugate as compared to the **7a** conjugate.

Radioiodinated monoclonal antibodies are being investigated for their application to the imaging and therapy of cancer (1-4). The standard method for producing radioiodinated monoclonal antibodies is direct attachment of the radioiodine to the protein. Direct protein radioiodination methods have been extensively studied (5). Generally, these methods employ oxidants, such as chloramine-T or Iodogen, for the generation of electrophilic iodine species which react principally with the activated aromatic ring of tyrosine amino acids of the protein (6). However, a significant problem affecting the diagnostic and therapeutic potential of directly radioiodinated antibodies is their susceptibility to in vivo deiodination. Presumably in vivo deiodinases are capable of recognizing the structural similarity between the thyroid hormones and iodinated tyrosines of the antibody or its catabolized fragments (7). Deiodination results in significant, undesirable accumulation of radioiodine in both the thyroid and stomach tissues. More important, however, is the potential for loss of radioactivity from that localized at tumors.

The in vivo instability of directly labeled antibodies has prompted the development of alternate methods of radioiodination which resist in vivo deiodination. For example, we have developed a protein radioiodination reagent, *N*-succinimidyl *p*-iodobenzoate (PIB, *p*-iodobenzoate, **2**), which employs a nonactivated, nonphenolic iodophenyl group to attach the radioiodine to the antibody in a stable manner (8). The PIB reagent (**2**) can be conveniently prepared in high specific activity by the radioiododestannylation of *N*-succinimidyl *p*-(tri-*n*-butylstannyl)benzoate (**1**), as shown in Scheme I. The PIB reagent (**2**) is then conjugated with antibody by acylation of the ϵ amino groups of the lysines on the surface of the antibody. In a similar manner, Zalutsky has reported *N*-succinimidyl *m*-(tri-*n*-butylstannyl)benzoate

Scheme I



(ATE, alkyl tin ester) as a protein radioiodination reagent (9). Antibodies labeled with either PIB (**2**) or ATE have been shown to undergo negligible, if any, in vivo deiodination.

Vinyl iodides are comparable to aryl iodides in terms of their chemical and biological stabilities and they are more stable than aliphatic iodides (10). Thus, a reasonable alternative to an iodophenyl group for the attachment of radioiodine to antibodies in a stable manner is an iodovinyl group. Indeed, iodovinyl moieties have been used in the development of new radiopharmaceuticals. For example, iodovinyl-substituted fatty acids have been studied for myocardial imaging (11), iodovinyl estradiols have been used to detect hormone dependent tumors (12), and iodovinyl glucose has been investigated for use in evaluating brain disorders (13). Reported herein are the results of an investigation involving two new protein radioiodination reagents: 2,3,5,6-tetrafluorophenyl 5-iodo-4-pentenoate (**7a**) and 2,3,5,6-tetrafluorophenyl 3,3-dimethyl-5-iodo-4-pentenoate (**7b**). In this investigation, the synthesis and radioiodination reactions used to prepare these reagents were studied. Evaluation of the radioiodination reagents included biodistribution studies comparing a Fab fragment labeled with **2**, **7a**, or **7b**, or directly labeled by the chloramine-T method. The

results obtained from the biodistribution studies have allowed comparison of the different radioiodination methods with respect to in vivo deiodination and tumor localization.

EXPERIMENTAL PROCEDURES

General Procedures. All compounds gave spectra in accord with their proposed structures. NMR spectra were obtained in CDCl_3 solution with a Varian Gemini-200 200-MHz instrument. The proton chemical shifts (δ) are reported in ppm downfield from internal Me_4Si (0.00 ppm). The carbon chemical shifts (δ) are reported in ppm downfield from Me_4Si ; $\delta(\text{Me}_4\text{Si}) = \delta(\text{CDCl}_3) - 77.0$ ppm. IR spectra were obtained on a Perkin-Elmer 1310 infrared spectrophotometer. Mass spectral data were obtained on a VG 7070H instrument operating in the EI mode or a VG 70SEQ instrument operating in the FAB mode.

In general, all reagents were reagent grade or better and were used as purchased. Toluene (anhydrous), THF (anhydrous), 4-pentynoic acid, 2,3,5,6-tetrafluorophenol, *N,N'*-dicyclohexylcarbodiimide, Et_3B , *N*-chlorosuccinimide, and Diazald were purchased from Aldrich Chemical Co. Bu_3SnH was purchased from Alfa Products and distilled prior to use. HPLC solvents were obtained as HPLC grade and were filtered (0.2 μm) prior to use. Phosphate-buffered saline (PBS) was purchased from Gibco Labs as Dulbecco's phosphate-buffered saline (#310-4190).

Radioiodine was obtained from Du Pont/NEN (North Billerica, MA). Iodine-125 was obtained as a Na^{125}I solution in 0.1 N NaOH (high concentration) at 17 Ci/mg in 2- and 5-mCi quantities. Iodine-131 was obtained as a Na^{131}I solution in 0.1 N NaOH (high concentration) at 7-12 Ci/mg in 5-mCi quantities.

Flash chromatography was performed with EM Science silica gel 60, 230-400 mesh. HPLC was conducted with Beckman Model 110B pumps, a Beckman Model 153 UV detector, a Beckman Model 170 radioisotope detector, and a Rheodyne Model 7125 injector. Spectrophotometric analyses were performed by UV detection at 254 nm and radiometric analyses were achieved by NaI scintillation optimized to the radionuclide used. Integration and plotting were accomplished by either an integrator/plotter (Hewlett-Packard, Model 3390) or a computer with a chromatographic software package (Dynamic Solutions, Maxima 820 workstation). Reverse-phase HPLC chromatography was run on a Whatman Partisphere C-18 column, 4.6 mm \times 12.5 cm, using a gradient solvent system operating at 1.0 mL/min. Solvent A in the gradient was 98% MeOH/2% H_2O (H_2O contained 1% HOAc). Solvent B was 10% MeOH/90% H_2O (H_2O contained 1% HOAc). The gradient began at 25% B. After 3 min the gradient was decreased in percent B over the next 7 min to 2% B and was held there for 10 min. With this gradient the retention times for the compounds were as follows: **6a** (20.0 min), **7a** (5.3, 5.6 min), **6b** (21.2 min), **7b** (9.6 min), and iodide (1.4 min, solvent front). Size-exclusion HPLC was performed on a Zorbax Bio-Series GF-250, 9.4 mm \times 24 cm, column (Du Pont) eluted with 0.2 M sodium phosphate, pH 6.8, at a flow rate of 1.0 mL/min.

Radiochemical purities of labeled proteins were determined by "instant" thin-layer chromatography (ITLC). Silica gel impregnated glass fiber strips (ITLC-Gelman) were activated by heating at 110 $^\circ\text{C}$ for 30 min prior to use. After elution, the plates were cut into small strips (horizontal) and were counted in a gamma counter (Packard Autogamma 5650) to detect radioactivity. Iodine-

125 samples were counted in plastic tubes with a 15-80 keV window, whereas iodine-131 samples were counted with a 260-470 keV window. Radiochemical purity, as determined by ITLC, was expressed as the percent of counts (cpm) on the bottom half (origin) of the strip divided by the total counts on the strip.

Synthesis of Methyl 4-Pentynoate (4a) and Methyl 3,3-Dimethyl-4-pentynoate (4b). To a solution of 4-pentynoic acid (**3a**, 510 mg, 5.2 mmol) in ether (7.5 mL) at 0 $^\circ\text{C}$ was added an ether solution of CH_2N_2 (**14**) until the faint yellow color of excess CH_2N_2 persisted. The reaction was stirred for 30 min, then the excess CH_2N_2 was quenched by the addition of acetic acid. The solution was extracted with saturated NaHCO_3 (2 \times 10 mL), washed with saturated NaCl (1 \times 10 mL), and dried over MgSO_4 . The solution was filtered and the ether was removed by simple distillation at atmospheric pressure to afford **4a** (545 mg, 94%) as a light yellow liquid: ^1H NMR δ 3.72 (s, 3 H), 2.55 (m, 4 H), 1.99 (t, $J = 2.5$ Hz, 1 H).

In a similar manner, **4b** was prepared from 3,3-dimethyl-4-pentynoic acid (**3b**) (**15**) (344 mg, 2.73 mmol) in 99% yield: ^1H NMR δ 3.70 (s, 2 H), 2.17 (s, 1 H), 1.36 (s, 6 H).

Synthesis of Methyl 5-(Tri-*n*-Butylstannyl)-4-pentenoate (5a). To a solution of **4a** (168 mg, 1.5 mmol) in anhydrous toluene (3.0 mL) under N_2 at 0 $^\circ\text{C}$ was added Bu_3SnH (0.40 mL, 1.5 mmol) followed by Et_3B (0.15 mL, 1.0 M solution in hexanes, 0.15 mmol) (**16**). After 3 h at 0 $^\circ\text{C}$ additional Bu_3SnH (0.20 mL, 0.75 mmol) was added. The resulting solution was allowed to warm to room temperature and stirred overnight. The solvents were evaporated under reduced pressure and the resulting oil was purified by flash chromatography (25 \times 150 mm), eluting with a step gradient of 100% hexanes, 5% EtOAc/hexanes, 10% EtOAc/hexanes, to afford **5a** (264 mg, 44%) as a 50/50 mixture of cis/trans isomers. ^1H NMR δ 6.47 (d of t, $J = 12, 7$ Hz, 0.5 H), 6.16-5.64 (m, 1.5 H), 3.69 (s, 1.5 H), 3.67 (s, 1.5 H), 2.60-2.25 (m, 4 H), 1.80-1.15 (m, 18 H), 0.92 (t, $J = 7$ Hz, 4.5 H), 0.89 (t, $J = 7$ Hz, 4.5 H); ^{13}C NMR δ 173.87, 173.52, 146.86, 146.61, 130.20, 128.94, 51.36, 51.30, 34.13, 33.26, 32.49, 31.96, 29.01, 28.90, 27.11, 27.06, 13.44, 9.98, 9.16.

Synthesis of 2,3,5,6-Tetrafluorophenyl 5-(Tri-*n*-butylstannyl)-4-pentenoate (6a). To a solution of **5a** (140 mg, 0.35 mmol) in EtOH (1.0 mL) was added a solution of KOH (208 mg, 3.7 mmol) in EtOH (1.0 mL), followed by H_2O (0.20 mL). The resulting solution was stirred at room temperature for 2 h. The solution volume was reduced to one-half the original volume by evaporation under reduced pressure. The residue was suspended in ether (10 mL) and acidified with 1.0 N HCl (4.0 mL, 4.0 mmol). The aqueous phase was separated and extracted with ether (2 \times 5 mL). The ether layers were combined, washed with saturated NaCl (1 \times 5 mL), and dried over MgSO_4 . The solution was filtered and the solvent was evaporated under reduced pressure to afford the crude acid as an oil. The crude acid was dissolved in anhydrous THF (3.0 mL), and 2,3,5,6-tetrafluorophenol (80 mg, 0.48 mmol) in THF (0.5 mL) was added, followed by *N,N'*-dicyclohexylcarbodiimide (101 mg, 0.49 mmol). The solution was stirred overnight at room temperature, during which time a white precipitate formed. The THF was evaporated under reduced pressure, CH_3CN was added, and the solution was filtered. The filtrate was evaporated under reduced pressure to afford an oil. The crude product was purified by flash chromatography (10 \times 170 mm), eluting with 5% EtOAc/hexanes, to afford

6a (118 mg, 63%) as a 50/50 mixture of *cis/trans* isomers: ^1H NMR δ 6.99 (m, 1 H), 6.54 (d of t, $J = 13$, 7 Hz, 0.5 H), 6.24–5.76 (m, 1.5 H), 2.87–2.40 (m, 4 H), 1.70–1.15 (m, 18 H), 0.92 (t, $J = 7$ Hz, 4.5 H), 0.88 (t, $J = 7$ Hz, 4.5 H); ^{13}C NMR δ 169.29, 169.04, 148.79 (m), 148.70 (m), 145.48, 145.34, 143.72 (m), 143.63 (m), 138.44 (m), 138.24 (m), 131.70, 130.33, 103.24 (t, $J = 23$ Hz), 103.17 (t, $J = 23$ Hz), 33.59, 32.68, 32.15, 31.75, 29.08, 28.96, 27.16, 13.49, 10.07, 9.26; IR (neat, thin film) 3090, 2960, 2920, 2870, 2850, 1790, 1645, 1600, 1530, 1490, 1180, 1100, 1080, 960 cm^{-1} ; MS (FAB) m/e 539 ($M + 1$, ^{120}Sn), 537 ($M + 1$, ^{118}Sn), 481 ($M + 1$, loss of butane, ^{120}Sn), 479 ($M + 1$, loss of butane, ^{118}Sn) amu.

Synthesis of Methyl 3,3-Dimethyl-5-(tri-*n*-butylstannyl)-4-pentenoate (5b). To a solution of **4b** (123 mg, 0.88 mmol) in anhydrous toluene (3.5 mL) under N_2 at 0 °C was added Bu_3SnH (0.30 mL, 0.95 mmol), followed by Et_3B (0.10 mL, 1.0 M solution in hexanes, 0.10 mmol). The resulting solution was allowed to warm to room temperature and stirred overnight. The solvents were evaporated under reduced pressure and the resulting oil was purified by flash chromatography (25 \times 150 mm), eluting with a step gradient of 100% hexanes, 5% EtOAc/hexanes, 10% EtOAc/hexanes, to afford **5b** (262 mg, 69%) as an oil: ^1H NMR δ 5.92 (AB, $\Delta\nu_{\text{AB}} = 11.8$ Hz, $J = 10$ Hz, 2 H), 3.62 (s, 3 H), 2.30 (s, 2 H), 1.60–1.20 (m, 18 H), 1.12 (s, 6 H), 0.89 (m, 9 H); ^{13}C NMR δ 172.57, 156.83, 122.47, 50.92, 46.50, 38.15, 28.88, 27.04, 26.75, 13.47, 9.23.

Synthesis of 2,3,5,6-Tetrafluorophenyl 3,3-Dimethyl-5-(tri-*n*-butylstannyl)-4-pentenoate (6b). To a solution of **5b** (150 mg, 0.35 mmol) in EtOH (2.0 mL) was added a solution of KOH (250 mg, 4.46 mmol), followed by H_2O (0.20 mL). The resulting solution was stirred at room temperature for 24 h. The solution volume was reduced to one-half the original volume by evaporation under reduced pressure. The residue was suspended in ether (10 mL) and acidified with 1.0 N HCl (4.5 mL, 4.5 mmol). The aqueous phase was separated and extracted with ether (2 \times 5 mL). The ether layers were combined, washed with saturated NaCl (1 \times 5 mL), and dried over MgSO_4 . The solution was filtered and the solvent was evaporated under reduced pressure to afford the crude acid as an oil. The crude acid was dissolved in anhydrous THF (3.0 mL), and 2,3,5,6-tetrafluorophenol (87 mg, 0.52 mmol) in THF (0.5 mL) was added, followed by N,N' -dicyclohexylcarbodiimide (107 mg, 0.52 mmol). The solution was stirred overnight at room temperature, during which time a white precipitate formed. The THF was evaporated under reduced pressure, CH_3CN was added and the solution was filtered. The filtrate was evaporated under reduced pressure to afford an oil. The crude product was purified by flash chromatography (10 \times 170 mm), eluting with 5% EtOAc/hexanes, to afford **6b** (125 mg, 69%) as an oil: ^1H NMR δ 6.97 (m, 1 H), 5.99 (AB, $\Delta\nu_{\text{AB}} = 12.3$ Hz, $J = 19$ Hz, 2 H), 2.64 (s, 2 H), 1.6–1.2 (m, 18 H), 1.22 (s, 6 H), 0.85 (t, $J = 7$ Hz, 9 H); ^{13}C NMR δ 167.71, 155.65, 148.76 (m), 143.72 (m), 138.51 (m), 123.79, 103.06 (t, $J = 23$ Hz), 45.69, 38.41, 28.89, 27.06, 26.70, 13.45, 9.24; IR (neat, thin film) 3080, 2960, 2920, 2870, 2850, 1790, 1645, 1595, 1525, 1490, 1180, 1090, 960 cm^{-1} ; MS (FAB) m/e 567 ($M + 1$, ^{120}Sn), 565 ($M + 1$, ^{118}Sn), 509 ($M + 1$, loss of butane, ^{120}Sn), 507 ($M + 1$, loss of butane, ^{118}Sn) amu.

Synthesis of 2,3,5,6-Tetrafluorophenyl 5-Iodo-4-pentenoate (7a) and 2,3,5,6-Tetrafluorophenyl 3,3-Dimethyl-5-iodo-4-pentenoate (7b). To a solution of **6a** (14 mg, 26 μmol) in CDCl_3 (0.4 mL) was added a solu-

tion of ICl (0.23 mL, 0.11 M solution in CDCl_3 , 25 μmol) until the faint purple color of excess ICl persisted. The crude product was purified by flash chromatography (5 \times 80 mm), eluting with 5% EtOAc/hexanes, to afford **7a** (6.4 mg, 66%) as a 50/50 mixture of *cis/trans* isomers: ^1H NMR δ 7.01 (m, 1 H), 6.59 (d of t, $J = 15$, 7 Hz, 0.5 H), 6.42–6.08 (m, 1.5 H), 2.95–2.70 (m, 2 H), 2.70–2.45 (m, 2 H); MS (EI) m/e 374 (M^+), 247, 209, 181, 167 amu.

In a similar manner **7b** was prepared from **6b** (19 mg, 35 μmol) in 74% yield: ^1H NMR δ 7.01 (m, 1 H), 6.69 (d, $J = 15$ Hz, 1 H), 6.20 (d, $J = 15$ Hz, 1 H), 2.66 (s, 2 H), 1.25 (s, 6 H); MS (EI) m/e 402 (M^+), 275, 237, 209, 195 amu.

Synthesis of 2,3,5,6-Tetrafluorophenyl 5-[^{125}I / ^{131}I]iodo-4-pentenoate (7a) and 2,3,5,6-Tetrafluorophenyl 3,3-Dimethyl-5-[^{125}I / ^{131}I]iodo-4-pentenoate (7b). Into a reaction vial fitted with a septum seal was placed a 25- μL solution containing either **6a** or **6b** (25 μg , 0.050 μmol) in 5% HOAc/MeOH, a 10- μL solution containing *N*-chlorosuccinimide (10 μg , 0.075 μmol) in MeOH, and 10 μL of PBS. To this mixture was added the desired quantity of Na^{125}I or Na^{131}I (up to 5 mCi, volume not to exceed 10 μL if diluted with PBS). After 5 min at room temperature the reaction was quenched by the addition of a 10- μL solution of NaHSO_3 (0.72 mg/mL $\text{Na}_2\text{S}_2\text{O}_5$ in H_2O , 0.075 μmol of NaHSO_3). An aliquot was removed for HPLC analysis.

Following this procedure, **7a** was prepared from **6a** and Na^{125}I (2 μL , 106 μCi) in 88% radiochemical yield as a 45/55 mixture of *cis/trans* isomers. Likewise, **7b** was prepared from **6b** and Na^{125}I (2 μL , 112 μCi) in 91% radiochemical yield as a single isomer.

The MeOH was carefully evaporated from the reaction mixture by passing a stream of N_2 gas through the reaction vial. To trap any volatile radioiodide, the N_2 gas was introduced into the vial by means of a needle inlet, and the vial was vented with a needle outlet attached to a 3 mL syringe barrel filled with granulated charcoal. The evaporated product was used without purification in the subsequent antibody conjugation reaction.

Preparation of NR-ML-05 Fab Labeled with [^{125}I]7a. To a vial containing [^{125}I]7a (850 μCi) was added a solution of NR-ML-05 Fab (500 μg in 56 μL PBS) in $\text{NaHCO}_3/\text{Na}_2\text{CO}_3$ buffer (100 μL , 1.0 M, pH 9.2). The reaction was incubated at 37 °C for 30 min and then quenched by the addition of a glycine solution (10 μL , 1 M glycine in 1.0 M $\text{NaHCO}_3/\text{Na}_2\text{CO}_3$, pH 9.2). The conjugate was purified with a Pharmacia PD-10 column eluted with PBS to afford 322 μCi (38%) of labeled NR-ML-05 Fab. The purity, as assessed by ITLC, was 98.7% and the specific activity was 0.73 $\mu\text{Ci}/\mu\text{g}$.

Preparation of NR-ML-05 Fab labeled with [^{131}I]7a or [^{125}I]7b was accomplished as described above. Preparation of NR-ML-05 Fab labeled with **2** is described elsewhere (8).

Direct Radioiodination of NR-ML-05 Fab. To a vial containing Na^{125}I (641 μCi), PBS (100 μL), and NR-ML-05 Fab (500 μg in 56 μL PBS) was added a solution of chloramine-T (10 μL of a 1.0 mg/mL solution in H_2O). After 5 min at room temperature the iodination reaction was quenched by the addition of NaHSO_3 (20 μL , 0.72 mg/mL $\text{Na}_2\text{S}_2\text{O}_5$ in H_2O). The crude, labeled material was immediately purified with a Pharmacia PD-10 column eluted with PBS to afford 496 μCi (77%) of labeled NR-ML-05 Fab. The purity, as assessed by ITLC, was 99.4% and the specific activity was 0.98 $\mu\text{Ci}/\mu\text{g}$.

Chemical Challenge Experiments. To test tubes containing 1.0 mL of either 12% TCA, 6 M urea, 10 mM dithiothreitol (DTT), 1.0 M (pH 9.2) sodium carbonate buffer, 95% ethanol, 1 M glycine in 1.0 M (pH 9.2) carbonate buffer, or PBS (control) was added 25 μ g of radiolabeled antibody. The samples were lightly vortexed and an aliquot was removed and analyzed by ITLC (80% MeOH) as the $t = 0$ time point. The tubes were then incubated at 37 °C for 24 h. Aliquots were periodically removed and analyzed by ITLC.

Serum Stability. Samples of freshly isolated human serum were filtered through 0.2- μ m filters and placed into sterile, capped culture tubes. Twenty-five micrograms of radioiodinated antibody were added to each 0.5-mL serum sample. Duplicate samples were lightly vortexed and an aliquot was removed and analyzed by ITLC (80% MeOH) as the $t = 0$ time point. The tubes were then incubated at 37 °C for several days. Aliquots were periodically removed and analyzed by ITLC.

Immunoreactivity Assessment. The immunoreactivities of the radioiodinated antibodies were determined from a cell-binding assay using a fixed labeled-antibody concentration and a varied number of antigen positive cells (17). Duplicate 110- μ L aliquots of 25, 20, 15, and 10×10^6 cells/mL were added to eight 0.5-mL tubes containing 55 μ L of assay buffer (PBS/11% BSA/0.1% sodium azide). To a ninth tube containing 55 μ L of assay buffer was added 110 μ L of the 25×10^6 cells/mL preparation, followed by 55 μ L of a 200 μ g/mL solution of unlabeled antibody. The tubes were mixed and incubated at 4 °C for 1 h. Then 55 μ L of a 160 ng/mL solution of radioiodinated antibody was added to each of the nine tubes. The tubes were incubated with mixing at 4 °C for 2 h. Aliquots (200 μ L) of the labeled antibody/cell reaction mixture were withdrawn from the tubes and overlaid onto an oil mixture (18). The overlaid oil tubes were cooled to 4 °C, centrifuged for 30 s, and cut through the oil layer to separate the cell pellet from the aqueous layer. The cut tubes were placed into 12 \times 75 mm glass tubes and counted in a gamma counter. The percent cell-bound radioactivity was calculated by dividing the counts associated with the cell pellet by the total counts. Duplicates were averaged and the percent nonspecifically bound radioactivity determined from the ninth tube was subtracted to give the percent specific binding. Adjustments to the percent specific binding were made according to the ITLC purities.

Average value obtained for immunoreactivity of NR-ML-05 Fab labeled with PIB (2) is $72 \pm 11\%$ ($n = 50$). The measured immunoreactivity of NR-ML-05 Fab labeled with 7a or 7b or directly labeled by using the chloramine-T method used in animal biodistribution studies described herein was within these bounds.

Biodistribution Studies. Female athymic nude mice (nu/nu) were obtained from Simonsen Laboratories, Inc., Gilroy, CA, and were used at 10–12 weeks of age. Tumor xenografts were produced by subcutaneous implantation of 2.5×10^6 A375 Met Mix cultured human melanoma tumor cells obtained from American Type Culture Collection, Rockville, MD (item no. ATCC CRL 1619). The tumor cells were grown for 7–10 days before use.

Biodistribution studies employed NR-ML-05 Fab labeled with 7a, 7b, or 2 or by the chloramine-T method, using either iodine-125 or iodine-131. NR-ML-05 is a murine IgG 2b monoclonal antibody which recognizes a 250-kDa proteoglycan antigen expressed on melanoma cells. Purified radioiodinated conjugates were coinjected into mice such that each animal received a 5- μ g dose of each radi-

olabeled preparation and a total of 10 μ g of injected protein.

Mice were injected intravenously via the lateral tail vein and sacrificed by cervical dislocation at prescribed times postinjection. Blood samples were obtained by retroorbital bleeding. Syringes were weighed before and after injection to determine the volume of conjugate injected. The activity per unit volume was calculated from standards. The animals were weighed (23.34 ± 1.61 g, $n = 24$) and marked for identification in all experiments. Twelve different tissues were evaluated: blood, tail (injection site), tumor, skin, muscle (thighs), lung, liver, spleen, stomach, neck including thyroid (the major portion of the muscle from the front of the neck), kidney (both), and intestine. The excised tissues were blotted, weighed, and counted in a dual-channel gamma counter. The raw counts were collected, and the contribution of iodine-131 counts to the iodine-125 window (spillover), as determined by iodine-131 standards, was subtracted from the iodine-125 counts and decay corrected. Summarized data include mean \pm SD of percent injected dose per gram, tissue-to-blood ratios, and tumor-to-tissue ratios.

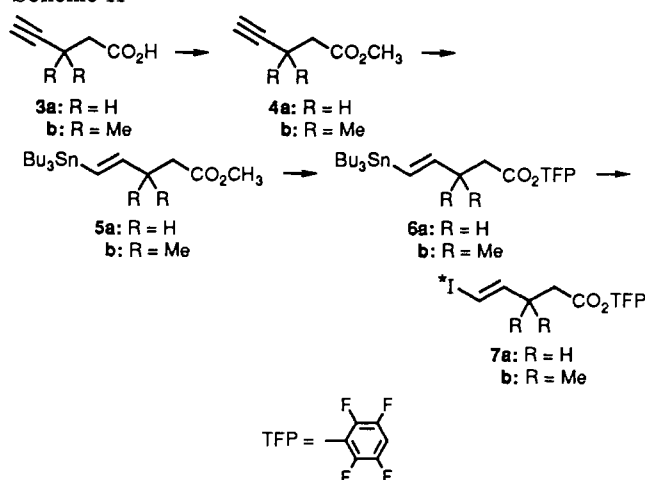
RESULTS

Chemistry. The first reagent selected for evaluation was 2,3,5,6-tetrafluorophenyl 5-iodo-4-pentenoate (7a). The design of this reagent was based on the stability of the iodine-carbon bond, which is influenced by the electronic nature of the carbon-carbon double bond. Since acylation chemistry was to be used to conjugate the reagent to antibody, it was deemed necessary to isolate the iodovinyl group from the acyl group by a minimum of two intervening saturated carbon atoms. In such a manner the electronic influence of the carbonyl group on the iodovinyl group would be minimized. In addition, reasoning that the placement of a quaternary carbon atom β to the carbonyl group and adjacent to the iodovinyl group might impart even greater stability to the iodine-carbon bond, we evaluated 2,3,5,6-tetrafluorophenyl 3,3-dimethyl-5-iodo-4-pentenoate (7b).

The method of choice to prepare radioiodinated compounds in high specific activity is to use organometallic reagents. Vinylboronic acids (19, 20), vinylmercurials (21, 22), and vinylstannanes (12) have been used to prepare the corresponding radioiodinated iodovinyl compounds, typically in high yield. Vinylstannanes were chosen for these studies since they can be conveniently prepared by hydrostannylation of the corresponding acetylenic compounds under relatively mild conditions. In addition, water-insoluble vinylstannanes would be less prone to conjugate to antibody, an advantage because it was desirable that the iodovinyl reagents not be purified from the vinyltin precursors prior to reaction with antibody. Avoiding purification of the iodovinyl reagents would simplify the labeling procedure and minimize handling of radioiodinated compounds.

Vinyltin active esters 6a and 6b were synthesized from the corresponding acetylenic carboxylic acids 3a and 3b as shown in Scheme 2. Treatment of 3a or 3b with excess CH_2N_2 afforded the methyl esters 4a or 4b. Introduction of a tri-*n*-butylstannyl group was accomplished by reaction of esters 4a or 4b with Bu_3SnH catalyzed by Et_3B (16) to afford 5a in 44% yield or 5b in 69% yield. Ester 5a was shown by ^1H and ^{13}C NMR to be a 50/50 mixture of cis and trans isomers, while ester 5b was shown to be a single isomer, presumably trans. Conversion of methyl ester 5a or 5b into its corresponding 2,3,5,6-tetrafluorophenyl (TFP) ester was accomplished by base-catalyzed hydrolysis followed by reaction of the interme-

Scheme II



diolate carboxylic acid with 2,3,5,6-tetrafluorophenol mediated by *N,N'*-dicyclohexylcarbodiimide to afford **6a** or **6b** in 63% or 69% yield, respectively.

Hydrostannylation of acids **3a** and **3b** was also investigated as a more direct approach to obtain the desired vinyltin active esters **6a** and **6b**. Unfortunately, reaction of **3a** or **3b** with excess Bu_3SnH in the presence of AIBN (23) or Et_3B afforded vinyltin-containing carboxylic acid derivatives, which proved more difficult to purify and characterize.

Authentic standards were synthesized to confirm the identities of radioiodinated compounds. Thus, vinyltin active esters **6a** and **6b** were treated with ICl in chloroform to provide iodovinyl active esters **7a** and **7b** in 66% and 74% yield, respectively. Simple iodovinyl active ester **7a** was shown by NMR to be a 50/50 mixture of *cis* and *trans* isomers. Dimethyl iodovinyl active ester **7b** was found to be exclusively a single isomer. A coupling constant of 15 Hz for the two vinyl protons indicated *trans* double bond geometry.

Radioiodination of the vinyltin active esters **6a** and **6b** was accomplished in methanol solution using *N*-chlorosuccinimide (NCS) and *nca* (*no carrier added*) $Na^{125}I$ (or $Na^{131}I$) to afford the desired labeled products **7a** and **7b** in yields ranging from 70% to 95%. Coinjection of the radiolabeled compounds and the corresponding standards on a reversed-phase HPLC system monitored by in-line UV and gamma detectors established the identity of the radiolabeled compounds. Also, HPLC analysis revealed that labeled **7a** was a 45/55 mixture of isomers, while labeled **7b** was a single isomer. The addition of 5% acetic acid to the methanol solution stabilized the reactive TFP esters toward hydrolysis and transesterification. Further, the addition of PBS to the reaction medium appeared to improve the reaction kinetics and the radiochemical yields. The reactions were quenched by the addition of a stoichiometric amount of $NaHSO_3$ based on the amount of NCS used. Quenching ensured that antibody was not exposed to electrophilic iodine species or excess oxidant during the conjugation reaction.

Reaction of either iodovinyl reagent **7a** or **7b** with several antibodies or their Fab fragments afforded corresponding radiolabeled conjugates in yields ranging from 25% to 50%. Several different buffers, pH values, and reaction temperatures were evaluated for the conjugation reaction. Optimum conjugation yields were obtained by incubation of **7a** or **7b** with the desired antibody in pH 9.2 sodium carbonate buffer at 37 °C for 30 min. The reaction was quenched by the addition of a glycine solu-

tion prior to purification of the crude conjugate by gel filtration. Radiochemical purities of the various iodovinyl conjugates were routinely in excess of 98.0%, as assessed by ITLC. Omission of the glycine quench afforded consistently lower radiochemical purities of the purified conjugates.

To improve the yield and kinetics of the conjugation reaction, we attempted to prepare the more reactive *N*-hydroxysuccinimide (NHS) ester of **7a**. While the corresponding NHS ester of the vinyltin TFP ester **6a** was successfully prepared, the NHS ester group proved to be too susceptible toward hydrolysis to survive the radioiodination conditions, and only the radioiodinated carboxylic acid was obtained.

In Vitro Analyses. Purified iodovinyl conjugates were analyzed by HPLC with a size-exclusion column. The column effluent was monitored by in-line UV and gamma detectors. The UV peak and the gamma peak coeluted, demonstrating that the radioactivity was associated with the protein. Furthermore, there was no apparent damage to the protein as a result of the radiolabeling, since there was an absence of high molecular weight aggregates, low molecular weight fragments, and peak tailing in the HPLC traces. Indeed, the HPLC profiles of the iodovinyl conjugates were indistinguishable from the HPLC profiles of unlabeled antibody and antibody labeled with PIB (2) or antibody directly labeled with chloramine-T.

The iodovinyl conjugates were analyzed by SDS-PAGE, reduced and nonreduced, combined with autoradiography. The SDS-PAGE protein bands corresponding to the iodovinyl conjugates were superimposable onto bands corresponding to antibody controls. Also, no additional bands were present in the iodovinyl lanes as compared to those of the controls. Autoradiography demonstrated that the radiolabel comigrated with the protein bands on the gel and that all radiolabel was associated with a protein band.

Chemical challenge studies were performed to evaluate whether unreacted iodovinyl reagents **7a** and **7b** or their corresponding carboxylic acids were nonspecifically associated with antibody or were bonded to a group other than an amine on the protein. In those experiments, the purified iodovinyl conjugates were exposed to a variety of chemical conditions, such as 12% TCA, 6 M urea, 95% ethanol, 10 mM dithiothreitol, 1 M glycine, and 1 M carbonate buffer, pH 9.2. The results demonstrated that the postchallenge purities were essentially equivalent to the prechallenge purities, suggesting that the radioiodine was covalently attached to the antibody in a stable manner.

The serum stabilities of the iodovinyl conjugates were also evaluated. Incubation of the conjugates at 37 °C in freshly prepared human serum demonstrated that there was no appreciable decrease in radioactivity associated with the antibody over several days.

The immunoreactivity of the iodovinyl conjugates was routinely determined prior to *in vivo* evaluation. In all cases, the immunoreactivity of the iodovinyl conjugates, as measured by a radiolabeled cell binding assay, was equivalent to the immunoreactivity of PIB (2) and chloramine-T-labeled controls.

Biodistribution Studies. To evaluate the stability of iodovinyl conjugates with respect to *in vivo* deiodination and tumor localization, several biodistribution studies were performed. The antibody selected for these studies was the Fab fragment of NR-ML-05, a murine antime-
lanoma antibody that recognizes a 250-kDa proteoglycan antigen expressed on melanoma cells. The biodistribu-

Table I. Tissue Distribution of Radioiodine at 4 and 20 h Postcoincubation of Iodovinyl NR-ML-05 Fab Conjugate, [¹²⁵I]-7a, and PIB NR-ML-05 Fab Conjugate, [¹³¹I]-2^{a-c}

tissue	4 h		20 h	
	[¹²⁵ I]-7a	[¹³¹ I]-2	[¹²⁵ I]-7a	[¹³¹ I]-2
blood	1.54 ± 0.16	1.27 ± 0.15	0.14 ± 0.04	0.13 ± 0.03
tail	2.08 ± 0.31	1.93 ± 0.33	0.16 ± 0.03	0.14 ± 0.05
tumor	4.79 ± 0.91	4.49 ± 0.90	2.44 ± 0.67	2.19 ± 0.67
skin	1.66 ± 0.29	1.28 ± 0.13	0.08 ± 0.03	0.04 ± 0.00
muscle	0.69 ± 0.18	0.53 ± 0.11	0.03 ± 0.00	0.01 ± 0.00
lung	1.94 ± 0.31	1.90 ± 0.39	0.32 ± 0.13	0.28 ± 0.12
liver	0.59 ± 0.11	0.51 ± 0.09	0.07 ± 0.01	0.03 ± 0.00
spleen	0.73 ± 0.06	0.44 ± 0.05	0.12 ± 0.03	0.01 ± 0.01
stomach	2.03 ± 0.21	0.48 ± 0.18	0.17 ± 0.08	0.03 ± 0.01
neck	1.90 ± 0.28	0.80 ± 0.10	1.30 ± 0.58	0.09 ± 0.03
kidney	6.32 ± 0.93	11.99 ± 2.00	0.16 ± 0.03	0.24 ± 0.03
intestine	0.50 ± 0.06	0.91 ± 0.29	0.03 ± 0.01	0.04 ± 0.01

^a Results were obtained from *n* = 4 mice per time point and are tabulated as mean ± SD of the percent injected dose/g. ^b The specific activity and radiochemical purity for [¹²⁵I]-7a and [¹³¹I]-2 conjugates were 0.73 μCi/μg, 98.7%, and 0.94 μCi/μg, 99.5%, respectively. ^c Tumor weights were 0.126 ± 0.039 g.

tion studies were performed in athymic nude mice bearing human A375 Met Mix tumor xenografts.

The first study compared the biodistribution of NR-ML-05 Fab labeled with the simple iodovinyl reagent 7a and NR-ML-05 Fab labeled with the PIB reagent (2). To make direct comparisons, the antibody was labeled with [¹²⁵I]-7a or [¹³¹I]-2, and the two preparations were subsequently combined and coinjected into the mice such that each animal received a 5-μg dose of each labeled preparation. Sacrifices of four animals were made at 4 and 20 h postinjection. The data obtained from the biodistribution study are presented in Table I. Equivalent tumor uptake was evident for both labels at both time points. However, significant differences in the biodistribution of the two labels were seen in the stomach, neck (thyroid), and kidney tissues. In the stomach tissue there was approximately a 5-fold greater accumulation of the iodovinyl label compared to the PIB label at both time points. Also, in the neck tissue there was a 2-fold greater accumulation of the iodovinyl label compared to that of the PIB label at the 4 h time point, and by 20 h, this differential increased to 14-fold. The 2-fold greater kidney uptake seen for the PIB label compared to that of the iodovinyl label at the 4 h time point was noteworthy.

A second study compared the biodistribution of NR-ML-05 Fab labeled with simple iodovinyl reagent 7a and NR-ML-05 Fab directly labeled by using the chloramine-T method. As in the previous study, direct comparisons were performed by coinjection of the [¹³¹I]iodovinyl conjugate of NR-ML-05 Fab and [¹²⁵I]NaI/chloramine-T labeled NR-ML-05 Fab. The data obtained from this biodistribution study are presented in Table II. The biodistributions of the two labels were remarkably similar in all tissues evaluated, including the tumor and kidney. Minor differences were seen in the biodistribution of the labels in the stomach and the neck tissues at both time points.

Finally, a third study compared the biodistribution of NR-ML-05 Fab labeled with simple iodovinyl 7a and NR-ML-05 Fab labeled with dimethyl iodovinyl reagent 7b. In this study, the mice were coinjected with the [¹³¹I]iodovinyl conjugate of NR-ML-05 Fab and the dimethyl [¹²⁵I]iodovinyl conjugate of NR-ML-05 Fab. The results from this study are presented in Table III. Equivalent tumor uptake was evident for both labels at both time points. However, there was approximately a 2-fold greater amount of iodovinyl label compared to the amount

Table II. Tissue Distribution of Radioiodine at 4 and 20 h Postcoincubation of Iodovinyl NR-ML-05 Fab Conjugate, [¹³¹I]-7a, and [¹²⁵I]iodide/Chloramine-T-Labeled NR-ML-05 Fab^{a-c}

tissue	4 h		20 h	
	[¹³¹ I]-7a	[¹²⁵ I]-Ch-T	[¹³¹ I]-7a	[¹²⁵ I]-Ch-T
blood	2.86 ± 0.24	2.55 ± 0.23	0.11 ± 0.01	0.09 ± 0.01
tail	2.79 ± 0.33	2.82 ± 0.33	0.13 ± 0.05	0.14 ± 0.05
tumor	4.40 ± 0.37	4.27 ± 0.42	1.38 ± 0.31	1.27 ± 0.27
skin	1.87 ± 0.35	1.86 ± 0.25	0.07 ± 0.01	0.06 ± 0.01
muscle	0.91 ± 0.07	1.02 ± 0.28	0.02 ± 0.00	0.02 ± 0.01
lung	2.73 ± 1.19	2.84 ± 0.88	0.21 ± 0.06	0.32 ± 0.13
liver	0.85 ± 0.05	0.84 ± 0.06	0.05 ± 0.00	0.04 ± 0.00
spleen	1.08 ± 0.07	1.20 ± 0.10	0.07 ± 0.04	0.06 ± 0.05
stomach	8.39 ± 1.65	10.21 ± 2.46	0.17 ± 0.07	0.18 ± 0.07
neck	3.80 ± 0.44	4.25 ± 0.58	1.73 ± 0.29	2.12 ± 0.39
kidney	6.16 ± 1.01	5.68 ± 1.03	0.11 ± 0.01	0.07 ± 0.00
intestine	0.77 ± 0.10	0.81 ± 0.12	0.03 ± 0.01	0.03 ± 0.01

^a Results were obtained from *n* = 4 mice per time point and are tabulated as mean ± SD of the percent injected dose/g. ^b The specific activity and radiochemical purity for [¹³¹I]-7a and [¹²⁵I]iodide/Ch-T conjugates were 0.76 μCi/μg, 98.0%, and 0.98 μCi/μg, 99.4%, respectively. ^c Tumor weights were 0.074 ± 0.017 g.

Table III. Tissue Distribution of Radioiodine at 4 and 20 h Postcoincubation of Iodovinyl NR-ML-05 Fab Conjugate, [¹³¹I]-7a, and Dimethyl Iodovinyl NR-ML-05 Fab Conjugate, [¹²⁵I]-7b^{a-c}

tissue	4 h		20 h	
	[¹³¹ I]-7a	[¹²⁵ I]-7b	[¹³¹ I]-7a	[¹²⁵ I]-7b
blood	3.42 ± 0.69	2.85 ± 0.41	0.12 ± 0.02	0.10 ± 0.02
tail	2.79 ± 1.01	2.61 ± 1.00	0.16 ± 0.08	0.19 ± 0.11
tumor	4.85 ± 0.34	5.00 ± 0.35	1.53 ± 0.56	1.79 ± 0.55
skin	1.80 ± 0.36	1.57 ± 0.18	0.07 ± 0.01	0.05 ± 0.01
muscle	1.09 ± 0.09	0.94 ± 0.12	0.03 ± 0.01	0.02 ± 0.01
lung	1.77 ± 0.34	1.74 ± 0.33	0.25 ± 0.18	0.34 ± 0.31
liver	0.84 ± 0.15	0.91 ± 0.12	0.05 ± 0.02	0.09 ± 0.01
spleen	1.17 ± 0.19	1.14 ± 0.09	0.05 ± 0.02	0.13 ± 0.04
stomach	9.13 ± 0.29	4.81 ± 0.24	0.33 ± 0.17	0.19 ± 0.10
neck	3.21 ± 0.95	2.07 ± 0.46	3.17 ± 1.32	1.58 ± 0.58
kidney	5.60 ± 0.13	6.34 ± 0.31	0.14 ± 0.04	0.11 ± 0.04
intestine	0.61 ± 0.10	0.55 ± 0.08	0.04 ± 0.01	0.03 ± 0.01

^a Results were obtained from *n* = 4 mice per time point and are tabulated as mean ± SD of the percent injected dose/g. ^b The specific activity and radiochemical purity for [¹³¹I]-7a and [¹²⁵I]-7b conjugates were 0.76 μCi/μg, 98.0%, and 0.19 μCi/μg, 99.0%, respectively. ^c Tumor weights were 0.074 ± 0.020 g.

of dimethyl iodovinyl label in the stomach at 4 h and in the neck (thyroid) at 20 h. In all other tissues evaluated the biodistributions of the labels were essentially equivalent.

DISCUSSION

Two iodovinyl protein radioiodination reagents 7a and 7b were prepared by radioiododestannylation of vinyltin active ester precursors 6a and 6b. The reactions are rapid and reproducibly afford high yields of the reagents 7a and 7b for either ¹²⁵I or ¹³¹I labeling at the nca levels. Precursor vinyltin active esters 6a and 6b were synthesized in three steps from the corresponding pentynoic acids 3a and 3b in 26% and 47% overall yield, respectively.

Reaction of 7a and 7b with NR-ML-05 Fab and other monoclonal antibodies or antibody fragments at basic pH afforded the desired antibody conjugates in yields ranging from 25% to 50%. The conjugation reaction was quenched by the addition of a glycine solution prior to gel filtration purification. The glycine quench ensured that the radiochemical purities of the purified antibody conjugates would consistently exceed 98% postpurification, as assessed by ITLC. The conjugation yields of 7a

and **7b** were routinely lower than the conjugation yields of **2**. These lower yields are probably due to a combination of the lower reactivity of a TFP active ester relative to an NHS active ester and to the more lipophilic, less soluble nature of **7a** and **7b** as compared to **2**. We had previously found that the corresponding TFP ester of **2** was much less reactive and substantially more lipophilic than the NHS ester of **2** (24).

The iodovinyl antibody conjugates were evaluated by several different *in vitro* procedures. The procedures included HPLC, SDS-PAGE combined with autoradiography, chemical challenge studies, serum stability studies, and immunoreactivity analysis. These studies demonstrated that the iodovinyl radiolabel was attached to the antibody in a stable manner. Also, the results demonstrated that the biological properties of the iodovinyl antibody conjugates, including immunoreactivity, were not compromised by the radiolabeling procedure.

Biodistribution studies were performed to determine the *in vivo* stability and tumor localization of an antibody fragment labeled with iodovinyl reagents **7a** and **7b** and to compare their biodistributions to the antibody fragment labeled with PIB (**2**) or directly labeled by using the chloramine-T method. Dual-label studies were performed to minimize animal to animal variability within the studies. Radioiodide is known to accumulate in the thyroid and to a lesser extent in the stomach (25). Therefore, preferential accumulation of either radiolabel in these tissues would suggest greater *in vivo* deiodination. The results suggested that there was a greater amount of deiodination of NR-ML-05 Fab labeled with simple iodovinyl reagent **7a**, as compared to NR-ML-05 Fab labeled with **2** (see Table I). The study suggested negligible *in vivo* deiodination of NR-ML-05 Fab labeled with **2**, consistent with our previous findings (8). The amount of deiodination of NR-ML-05 Fab directly labeled by using the chloramine-T method and NR-ML-05 Fab labeled with the simple iodovinyl reagent **7a** was almost equivalent (see Table II). This result is somewhat surprising, since one might anticipate that quite different metabolic pathways would be responsible for the loss of label in each case (26). The data suggests that there was approximately a 50% reduction in the amount of deiodination of NR-ML-05 Fab labeled with **7b**, as compared to that of NR-ML-05 Fab labeled with **7a**. Although not directly measured, the amount of *in vivo* deiodination of NR-ML-05 Fab labeled with **7b** appears to be approximately twice that of NR-ML-05 Fab labeled with **2**. Finally, the results of all the studies demonstrated that, regardless of the labeling method employed, essentially equivalent tumor localization was seen.

The stability of iodovinyl moieties has been demonstrated *in vivo* for the iodovinyl estradiols, where at 24 h postinjection in rats only 0.37% of the injected dose was found in the thyroid (12). Further, it has been reported that significant *in vivo* deiodination did not occur with iodovinyl fatty acids until 2 h after injection (11). It is not apparent whether it is the radioiodinated Fab conjugates of **7a** and **7b** or their lower molecular weight metabolites which are deiodinated *in vivo*. Deiodination of Fab labeled with **7b** was demonstrably less than that of Fab labeled with **7a**. Fab labeled with **7b**, the β,β -dimethylpentenoic acid derivative, might have more effectively resisted deiodination if metabolism via enzymatic β -oxidation occurred, as previously shown for branched fatty acids (27).

The preferential kidney uptake and/or retention of the PIB (**2**) label as compared to that of the simple iodovi-

nyl (**7a**) label seen in the first biodistribution study is interesting. Similar differences in kidney localization were found when another antibody, NR-LU-10 Fab, was labeled with **2** and compared to NR-LU-10 Fab labeled with either ATE or chloramine-T.¹ Antibody Fab fragments rapidly accumulate in the kidneys and are presumably metabolized in the same manner as other circulating proteins by renal cells. Renal cell metabolism of proteins results in complete degradation of the protein to the amino acid level (28). Since it is likely that renal cell uptake and protein metabolism of labeled NR-ML-05 Fab are not influenced by the labeling method, then a plausible explanation for the differential kidney uptake seen with the PIB label is that the PIB (**2**), iodovinyl (**7a**), dimethyl iodovinyl (**7b**), and chloramine-T metabolites of labeled NR-ML-05 Fab are released from, or are subsequently reabsorbed by, the renal cells at different rates.

In summary, Fab conjugates of the iodovinyl reagents **7a** and **7b** were immunocompetent and successfully targeted tumor *in vivo*. The Fab conjugate of dimethyl iodovinyl reagent **7b** was substantially more resistant to *in vivo* deiodination than directly labeled Fab or the Fab conjugate of the iodovinyl reagent **7a**. However, the Fab conjugate of the PIB reagent (**2**) was clearly more resistant to *in vivo* deiodination than the Fab conjugate of dimethyl iodovinyl reagent **7b**. It is important to recognize that these *in vivo* results were obtained with a Fab fragment and that studies with intact antibody or F(ab')₂ fragments may afford different results. However, one would predict that the relative propensity of each labeled conjugate to suffer *in vivo* deiodination, as observed in these Fab studies, would be similar for intact antibody or F(ab')₂ studies. However, the magnitude of the observed differences may vary. In addition, it should be noted that biodistribution studies performed with other antibodies and tumor models may afford different results, particularly in cases where antibody conjugates are actively internalized and metabolized by the tumor target.

ACKNOWLEDGMENT

We would like to thank Don Axworthy, Denise DuPont, Leah Grant, Dr. Mary Ann Gray, Cathy Jackson, Karen Poole, Joan Schroeder, and Carmen Soikowski for their efforts in obtaining the biodistribution, stability, and SDS-PAGE data presented herein. We would like to also thank Dr. Alan R. Fritzberg, Dr. A. Charles Morgan, Dr. Paul L. Beaumier, and Dr. Debra K. Leith for their discussions on the experiments and manuscript.

LITERATURE CITED

- (1) Lashford, L. S., Davies, A. G., Richardson, R. B., Bourne, S. P., Bullimore, J. A., Eckert, H., Kemshead, J. J., and Coakham, H. B. (1988) A Pilot Study of ¹³¹I Monoclonal Antibodies in the Therapy of Leptomeningeal Tumors. *Cancer* 61, 857-868.
- (2) Epenetos, A. A., Munro, A. T., Stewart, S., Rampling, R., Lambert, H. E., McKenzie, C. G., Soutter, P., Rahemtulla, A., Hooker, G., Sivolapenko, G. B., Snook, D., Courtenay-Luck, N., Dhorkia, B., Krauz, T., Taylor-Papadimitriou, J., Durbin, H., and Bodmer, W. F. (1987) Antibody Guided Irradiation of Advanced Ovarian Cancer with Intraperitoneally Administered Radiolabeled Monoclonal Antibodies. *J. Clin. Oncol.* 5, 1890-1899.
- (3) Colcher, D., Carrasquillo, J. A., Esteban, J. M., Sugarbaker, P., Reynolds, J. C., Siler, K., Bryant, G., Larson, S. M., and Scholm, J. (1987) Radiolabeled Monoclonal Antibody B72.3 Localization in Metastatic Lesions of Colorectal

¹ Wilbur, D. S., Hadley, S. W., Grant, L. M., and Hylarides, M. D., unpublished results.

- Cancer Patients. *Int. J. Radiat. Appl. Instrum. [B]* 14, 251-252.
- (4) Carrasquillo, J. A., Krohn, K. A., and Beaumier, P. B., McGuffin, R. W., Brown, J. P., Hellstrom, I., and Larson, S. M. (1984) Diagnosis of and Therapy for Solid Tumors with Radiolabeled Antibodies and Immune Fragments. *Cancer Treat. Rep.* 68, 317-328.
- (5) Regoeczi, E. (1984) Methods of Protein Iodination. In *Iodine Labeled Plasma Proteins* Vol. I, pp 35-102, CRC Press Inc., Boca Raton, FL.
- (6) Krohn, K. A., Knight, L. C., Harwig, J. F., and Welch, M. J. (1977) Differences in the Site of Iodination of Proteins Following Four Methods of Radioiodination. *Biochim. Biophys. Acta* 490, 497-505.
- (7) Engler, D., and Burger, A. G. (1984) The Deiodination of the Iodothyronines and of Their Derivatives in Man. *Endocr. Rev.* 5, 151-184.
- (8) Wilbur, D. S., Hadley, S. W., Hylarides, M. D., Abrams, P. G., Beaumier, P. A., Morgan, A. C., Reno, J. M., and Fritzberg, A. R. (1989) Development of a Stable Radioiodinating Reagent to Label Monoclonal Antibodies for Radiotherapy of Cancer. *J. Nucl. Med.* 30, 216-226.
- (9) Zalutsky, M. R., and Narula, A. S. (1987) A Method for the Radiohalogenation of Proteins Resulting in Decreased Thyroid Uptake of Radioiodine. *Int. J. Radiat. Appl. Instrum. [A]* 38, 1051-1055.
- (10) Coenen, H. H., Moerlein, S. M., and Stocklin, G. (1983) No-Carrier-Added Radiohalogenation Methods with Heavy Halogens. *Radiochim. Acta* 34, 47-68.
- (11) Knapp, F. F., Jr., Goodman, M. M., Kabalka, G. W., and Sastry, K. A. R. (1984) Synthesis and Evaluation of Radioiodinated (E)-18-Iodo-17-octadecenoic Acid as a Model Iodoalkenyl Fatty Acid for Myocardial Imaging. *J. Med. Chem.* 27, 94-97.
- (12) Hansen, R. N., Seitz, D. E., and Botarro, J. C. (1982) E-17- α -[¹²⁵I]iodovinylestradiol: An Estrogen-Receptor Seeking Radiopharmaceutical. *J. Nucl. Med.* 23, 431-436.
- (13) Goodman, M. M., Callahan, A. P., and Knapp, F. F. Jr. (1987) Design, Synthesis and Evaluation of 2-Deoxy-2-iodovinyl Branched Carbohydrates as Potential Brain Imaging Agents. *J. Labeled Compd.* 23, 243-245.
- (14) Black, T. H. (1983) The Preparation and Reactions of Diazomethane. *Aldrichimica Acta* 16, 3-10.
- (15) Cordes, C., Prelog, V., Troxler, E., and Westen, H. H. (1968) 190. Zur Kenntnis des Kohlenstoffringes; 1,1,6,6-Tetramethyl-cyclodecan und seine Derivate. *Helv. Chim. Acta* 51, 1663-1678.
- (16) Nozaki, K., Oshima, K., and Utimoto, K. (1987) Et₃B-Induced Radical Addition of R₃SnH to Acetylenes and Its Application to Cyclization Reaction. *J. Am. Chem. Soc.* 109, 2547-2549.
- (17) Lindmo, T., Boven, E., Cuttitta, F., Fedorko, J., and Bunn, P. A. Jr. (1984) Determination of the Immunoreactive Fraction of Radiolabeled Monoclonal Antibodies by Linear Extrapolation to Infinite Antigen Excess. *J. Immunol. Method.* 72, 77-89.
- (18) Beaumier, P. L., Neuzil, D., Yang, H. M., Noll, E. A., Kishore, R., Eary, J. F., Krohn, K. A., Nelp, W. B., Hellstrom, K. E., and Hellstrom, I. (1986) Immunoreactivity Assay for Labeled Anti-melanoma Monoclonal Antibodies. *J. Nucl. Med.* 27, 824-828.
- (19) Kabalka, G. W., Sastry, K. A. R., Gooch, E. E. (1982) Synthesis of Very High Specific Activity Radioiodinated and Radio-brominated Materials via Organoborane Chemistry. *J. Labelled Compd.* 19, 1506.
- (20) Knapp, F. F., Jr., Goodman, M. M., Callahan, A. P., Ferren, L. A., Kabalka, G. W., and Sastry, K. A. R. (1983) New Myocardial Imaging Agents; Stabilization of Radioiodine as a Terminal Vinyl Iodide Moiety on Tellurium Fatty Acids. *J. Med. Chem.* 26, 1293-1300.
- (21) Charleson, F. P., Flanagan, R. J., Synnes, E. I., and Weibe, L. I. (1984) Rapid No Carrier Added Radiolabeling Using Organomercury Compounds. *J. Labelled Compd.* 21, 1074-1075.
- (22) Flanagan, R. J., Charleson, F. P., Synnes, E. I., and Weibe, L. I. (1986) Radiolabeling with Organomercury Compounds: Part 2. High Specific Activity Synthesis of Iodine-125 and Iodine-131-6-iodocholest-5-en-3-beta-ol and its Tissue Distribution in Rats. *J. Nucl. Med.* 27, 1165-1171.
- (23) Corey, E. J., Ulrich, P., and Fitzpatrick, J. M. (1976) A Stereoselective Synthesis of (\pm)-11-Hydroxy-trans-8-decanoic Acid Lactone, a Naturally Occurring Macrolide from *Cephalosporium recifei*. *J. Am. Chem. Soc.* 98, 222-224.
- (24) Hadley, S. W., Grant, L. M., and Wilbur, D. S. (1987) Evaluation of Radioiodinations and Conjugations of 4-Iodobenzoates for Protein Labeling. *J. Nucl. Med.* 28, 725.
- (25) Zalutsky, M. R., and Narula, A. S. (1988) Radiohalogenation of a Monoclonal Antibody Using an N-Succinimidyl 3-(Tri-n-butylstannyl)benzoate Intermediate. *Cancer Res.* 48, 1446-1450.
- (26) Schulz, H. (1983) Metabolism of 4-Pentenoic Acid and Inhibition of Thiolase by Metabolites of 4-Pentenoic Acid. *Biochemistry* 22, 1827-1832.
- (27) Otto, C. A., Brown, L. E., and Scott, A. M. (1985) Radioiodinated Branched-Chain Fatty Acids: Substrates for Beta Oxidation? Concise Communication. *J. Nucl. Med.* 25, 75-80.
- (28) Maack, T., Park, C. H., and Camargo, M. J. F. (1985) Renal Filtration, Transport, and Metabolism of Proteins. *The Kidney: Physiology and Pathophysiology* (D. W. Sheldin, and G. Giebisch, Eds.) pp 1773-1802, Raven Press, New York.

Bioconjugate Chemistry

MAY/JUNE 1990
Volume 1, Number 3

© Copyright 1990 by the American Chemical Society

REVIEW

Conjugates of Oligonucleotides and Modified Oligonucleotides: A Review of Their Synthesis and Properties

John Goodchild

Worcester Foundation for Experimental Biology, 222 Maple Avenue, Shrewsbury, Massachusetts 01545.
Received February 21, 1990

Table of Contents

1. Introduction
2. Chemical Synthesis of Oligonucleotides
 - A. Strategies of Synthesis
 - B. Synthesis of Modified Oligonucleotides
 - (i) Methylphosphonates (1)
 - (ii) Phosphotriesters (2)
 - (iii) Phosphorothioates (3)
 - (iv) Phosphoramidates (4)
 - (v) Other Phosphate Modifications
 - (vi) Non-Phosphate Internucleoside Linkages
 - C. Synthesis of Conjugates
 - A. Incorporation of Conjugate and Linker Groups during Chemical Synthesis of Oligonucleotides
 - (i) Incorporation of Modified Nucleotides
 - (ii) Incorporation of Non-Nucleotides
 - B. Incorporation of Modified Nucleotides during Enzymatic Synthesis of Oligonucleotides
 - C. Postsynthetic Modification of Oligonucleotides
 - (i) Reactions of Primary Alkylamines
 - (ii) Reactions of Thiols
 - (iii) Reactions of Phosphates and Thiophosphates
 - (iv) Electrophilic Linkers
 - (v) Reactions at Naturally Occurring Sites in Nucleic Acids
 - D. Conjugate Groups
 - D. Conjugate Groups
4. Properties of Modified Oligonucleotides and Conjugates
 - A. The Effect of Modification on Oligonucleotide Hybridization
 - B. The Effect of Modification on Nuclease Resistance
 - C. Cellular Uptake of Modified Oligonucleotides

- D. Modified Antisense Oligonucleotides
5. Concluding Comments

1. INTRODUCTION

In the molecular processes of living things, nothing surpasses Watson-Crick base pairing in importance. It is fundamental to the events that define life: the storage, transmission, and translation of genetic information. The simplicity of these hydrogen-bonded bridges and the small number of bases involved gives a predictability to the interactions of nucleic acids that is unattainable as yet with other biological molecules.

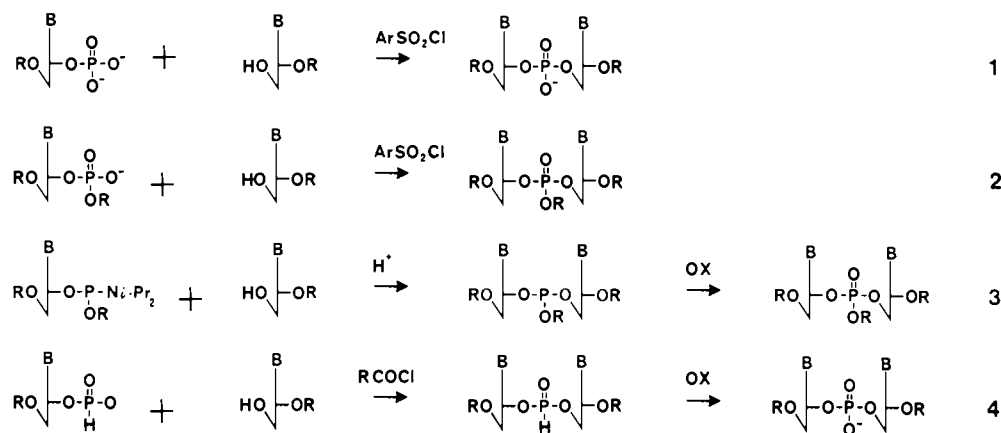
This applies even to the shortest oligonucleotides which hybridize like their larger relatives and can be viewed as informational molecules containing fragments of true genetic code. These are valuable models to investigate the physical and biological properties of DNA and RNA that would be intractable otherwise. Due to the limited number of bases used, oligonucleotides can contain the full range of functional groups and show similar chemical reactivity to true nucleic acids. This is useful for elucidation of the reactions of mutagens, carcinogens, and antitumor drugs with DNA and RNA.

As a result of their ability to base pair, oligonucleotides are used extensively in molecular biology as linkers, probes, and primers in such activities as sequencing, amplification by PCR, determination of secondary structure, engineering mutations, tailoring RNA with ribonuclease H, and assembling DNA constructs.

In other applications, "antisense" oligonucleotides can inhibit expression of viral or mRNA and, more recently, double-stranded DNA. Useful for genetic analysis, this also has potential for therapeutic application.

The recent demand for oligonucleotides resulted from improvements in their chemical synthesis that also made

Scheme I



available a wide range of conjugates. The few, simple derivatives of dinucleotides that were available at first have grown 10 times in length and can be festooned with a plethora of different pendant groups if so desired.

Not all modifications to oligonucleotides qualify as conjugates. In this review, a conjugate is considered to result from the coupling of two or more molecules with distinct properties so that some of the characteristics of each are retained in the product. An example is the union of an oligonucleotide with a fluorescent dye to give a fluorescent oligonucleotide. A distinction is drawn between conjugates and other modifications of oligonucleotides that do not result in such a combination of properties. However, the oligonucleotide component of the conjugate may itself be modified in other ways and may carry more than one conjugate group.

Conjugates may be designed to improve some already existing feature of the oligonucleotide, for example, the strength of hybridization or uptake by cells. More often, the oligonucleotide is endowed with some completely new property, either physical or chemical, while retaining its ability to base pair. In this way, new applications have been developed that were not possible previously.

Conjugate groups combined with oligonucleotides fall into three major categories.

1. Chemically Reactive Groups. Groups that cleave or cross-link with other nucleic acids or proteins are used to study interactions between these molecules and oligonucleotides, to modify or cleave nucleic acids at particular sites, and to create possible therapeutic agents.

2. Fluorescent or Chemiluminescent Groups. These are used in nonradioactive probes or primers for automated sequencing and in physical-chemistry studies including potentially powerful new applications involving combinations of different conjugates.

3. Groups Promoting Intermolecular Interactions. The best known example is probably biotin that binds to streptavidin. This has been used particularly as a reporter system for nonradioactive probes. Other examples are intercalating agents used to strengthen the hybridization of the oligonucleotide with its complement and polylysine used to enhance cellular uptake.

This review is divided into three main parts. The first two cover the chemical synthesis of modified oligonucleotides and conjugates and the third is concerned with their properties. This includes a discussion of antisense inhibition in general terms, but applications in areas such as diagnosis or genetic analysis are not covered here and the reader is referred to other sources.

2. CHEMICAL SYNTHESIS OF OLIGONUCLEOTIDES

Much of the chemistry described in this review has been developed around the methods for synthesizing oligonucleotides. These are introduced in section A only in sufficient detail to provide the necessary background for what follows.

The oligonucleotide component of a conjugate may contain all natural nucleotides or may itself be modified. Section B reviews methods for the synthesis of modified oligonucleotides.

A. Strategies of Synthesis. The impetus for the current interest in oligonucleotides derives from developments in two areas. Advances in molecular biology over the last decade or so created uses for these compounds while advances in chemical synthesis made them available for practical applications. A synthesis that took man-years of work in 1979 (1) could be done today in a few man-hours.

This resulted from improvements in two aspects of oligonucleotide synthesis. One was the development of solid supports that made possible the automation of the process and led to microprocessor-controlled synthesizers. The other was improvement in the synthesis of phosphate esters to give the coupling efficiencies of 98% and above that are necessary to take full advantage of the benefits that solid supports offer. The historical development of reactions used for nucleotide coupling is indicated in Scheme I and fuller accounts of oligonucleotide synthesis may be found in refs 2-5.

The first of these reactions is called the diester approach and was developed by Khorana (1). Ester formation was effected with dicyclohexylcarbodiimide or an aryl sulfonyl chloride. This coupling reaction is no longer used, but despite some shortcomings, the amide protecting groups developed for the bases and the dimethoxytrityl for 5'-OH are still standard.

This synthesis was improved by protecting the phosphate group to give the triester approach in reaction 2. This not only prevented side reactions but greatly facilitated workup and purification by enabling much larger scale and more rapid purification by chromatography on silica gel in organic solvents. With improved coupling reagents such as sulfonyl tetrazolides, this method was sufficiently efficient for solid support synthesis and is still used to some extent today (6).

The next improvement was to replace the reacting phosphate with a trivalent phosphite. Originally, a phosphorochloridite was used (7) but now the phosphoramidite in reaction 3 is preferred (8). Activation is by a mild

proton donor, usually triazole, and after each coupling reaction the phosphite is oxidized to the pentavalent level. This is the route employed most often today and permits synthesis of chain lengths considerably in excess of 100.

The fourth and most recent method (9, 10) returns to pentavalent phosphorus, this time a hydrogen phosphonate after which this approach is named and which was first recognized as a potential synthon some time ago (11). A carboxylic acid chloride is used as condensing agent. This method is comparable in efficiency to the previous one although it is generally considered inferior for very long sequences. It has the advantage that the oxidation step does not have to be performed after each coupling reaction but can be left until the end of the synthesis. This simplifies and speeds up the process but, more importantly, it facilitates the synthesis of modified oligonucleotides where sulfur, nitrogen, or other elements replace oxygen in the reaction at phosphorus.

These synthetic approaches have been adapted for use in the ribo series (12–14) and for nucleosides with unnatural L-sugars (15) or α -glycosidic linkages (16).

B. Synthesis of Modified Oligonucleotides. This section reviews some of the options that are available for modification of the oligonucleotide component within the conjugate. The consequences of these changes for biochemical properties are discussed in section 3.

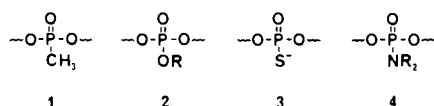
Modifications to the oligonucleotide have been employed most often for use in antisense inhibition where it is necessary for oligonucleotides to survive in cell cultures or other biological environments and also to cross the cell membrane. Nucleases are widespread and the lipophilic cell membrane is an effective barrier against passive diffusion of polyelectrolytes.

Often, modifications can be chosen to improve performance in both areas. For example, increasing lipophilicity to improve uptake is likely to decrease the rate of degradation by nucleases that are designed to degrade polyanions. The conjugate group itself may prove beneficial in these regards if it is lipophilic or otherwise inhibits the action of nucleases. As yet, the number of examples of conjugate groups combined with other modifications to the oligonucleotides is small but increasing rapidly.

Changes might be made at the bases, the sugars, the ends of the chain, or at the phosphate groups of the backbone. Those at the bases and sugars are generally the most difficult chemically and require the greatest amount of synthesis. In addition, they must not disrupt the ability of bases to form hydrogen bonds. One example is the use of α -nucleotides discussed later.

Modifications to the ends and backbone of the molecule are easier synthetically. Because the 5'-terminus is the most common site for conjugation, the phosphate groups are often available for further derivatization. As they are the site of action of nucleases and also carry the charges that inhibit cellular uptake, this presents the most direct approach to improvement in these areas.

The type of phosphate modification most studied is to replace or block the negatively charged oxygen atom to give structures 1–4. The syntheses of these and other modifications are discussed below.



(i) **Methylphosphonates (1).** These nonionic derivatives were introduced by Miller et al. in 1979 (17) and

are one of the most extensively studied classes of oligonucleotides because of their useful chemical and biological properties. Older methods for their synthesis were based on modifications of the triester approach (17–23). Following the introduction of phosphine reagents (24–26), solid-support synthesis based on phosphoramidite chemistry has become standard (27). Phosphoramidite reagents react as efficiently as the usual phosphoramidites and can be used interchangeably during automated synthesis to insert the uncharged linkage at any or all positions within the sequence. Products from this approach were found to give better melting curves than those from a synthesis based on triester type chemistry (28).

Because of the different nature of the backbone, special methods for their characterization have been developed (29). Like purification, this is still not as easy as with fully charged phosphodiester.

Only the methyl substituent on phosphorus has been investigated to any extent. A phenyl phosphonate was prepared early on (18) and a 4,4'-dimethoxytriphenylmethanephosphonate was obtained unexpectedly from an attempted Arbusov reaction (30). More recently, a (difluoromethyl)phosphonate was synthesized to mimic the polarity of the natural oxygen atom more closely (31).

(ii) **Phosphotriesters (2).** These compounds were used as nonionic analogues of oligonucleotides by Miller et al. before the methylphosphonates (32). They are more difficult to synthesize and, as a result, most studies have been limited to oligonucleotides containing only a single triester or only thymine bases.

The problem is the lability of the triester function during the basic conditions used in deblocking or cleaving from the solid support. Use of milder conditions (32, 33) or more labile amine protecting groups (34–37) or more stable triesters (38, 39) have not yet given a method as versatile as synthesis of the phosphonates.

Originally, methanol or ethanol in the presence of tosyl chloride was used to esterify internucleoside phosphates after each coupling in short sequences (32, 40, 41). Recently, it has been reported that this reagent can give complete triesterification of heterosequences as long as 10–20 bases following temporary protection of the amino groups with 9-fluorenylmethoxycarbonyl chloride (9-fluorenylmethyl carbonochloridate) in solution (36). This is the only method that gives extensively esterified products of this size. Methyl methanesulfonate has been used also as a methylating agent (42).

Different triesters have been introduced as the protecting groups during synthesis by the triester (43), phosphite (38, 39), or amidite (33, 34, 37, 44) approaches or by oxidation of hydrogen phosphonates with alcohols (45). In addition, transesterification in the presence of fluoride ions can replace aryl protecting groups on phosphate by alkyl to give more stable esters (41, 46–48).

Groups that have been used other than the usual methyl and ethyl include 1,1-dimethyl-2,2,2-trichloroethyl (38, 39, 43), isopropyl (33), neopentyl (48, 49), *n*-butyl (45), and 2,2,2-trifluoroethyl (37).

(iii) **Phosphorothioates (3).** Used extensively by Eckstein and his co-workers for the study of enzyme mechanisms, these derivatives are the closest to the natural nucleic acids in terms of structure and charge density. For reviews of their preparation and uses see refs 50–52. Both DNA and RNA polymerases accept the appropriate 5'-O-(1-thiotriphosphates) as substrates to give products containing just the R_p stereoisomers of phosphorus.

Chemical synthesis is also straightforward. Eck-

stein's use of elemental sulfur to oxidize dinucleoside phosphites is applicable to phosphoramidite synthesis on solid supports giving oligonucleotides with phosphorothioate linkages throughout or just at selected positions (50, 53, 54). A concern is that the phosphorothioate functions are subjected to an iodine oxidation step after each subsequent round of coupling which could lead to replacement of some sulfur by oxygen (55). In practice, phosphorothioate could still be isolated after 48 rounds of coupling (53) and NMR studies indicated that about one sulfur atom per molecule was lost to oxidation during the synthesis of a 20-mer (56).

Elemental sulfur can also be used for oxidation following the hydrogen phosphonate approach (45, 57–61). This offers some practical advantages over the phosphoramidite method where oxidation has to be performed after each coupling. The usual solvent for sulfur is carbon disulfide, which is volatile, malodorous, and troublesome in automated synthesizers, where the sulfur tends to form solid deposits. It is preferable to perform the oxidation just once manually at the end of the synthesis.

For synthesis of chimeric structures containing both phosphorothioates and phosphodiester in the backbone, treatment with sulfur partway through the synthesis is followed by further rounds of coupling and oxidation. This proved more successful with the phosphoramidite than the hydrogen phosphonate method. Unprotected phosphorothioates generated on sulfur treatment of hydrogen phosphonates survived subsequent coupling and oxidation cycles much less well than the blocked intermediates formed from phosphites (60).

(iv) *Phosphoramidates* (4). An appealing feature of phosphoramidates is the diverse range of amines that might be introduced. Given a good, general synthesis, this class of compounds should offer the greatest opportunity for structural variation. Substituents on the amine could include conjugate as well as nonconjugate groups. It might be desired to introduce just one phosphoramidate at a specific position or to modify all the phosphates with either the same or different substituents. Such precision and control is attainable with current synthetic methods.

A number of reactions for preparing phosphoramidates have been applied to oligonucleotides with greater or less success as discussed in ref 62. The preferred method uses an amine in the presence of carbon tetrachloride or iodine as the oxidant in the hydrogen phosphonate approach (45). By leaving this step until the end of the synthesis, phosphoramidate linkages are introduced throughout the sequence (15, 58, 63, 64). Alternatively, further rounds of coupling can be performed after amidation to generate a heterogeneous backbone (45, 61, 64). By alternating hydrogen phosphonate coupling steps with phosphoramidite, various unmodified and modified linkages can be inserted at specific sites throughout the sequence (61, 63).

Another attractive feature of phosphoramidates is that they may be readily converted to phosphodiester for characterization by the usual means (45, 64).

The P–N bond is hydrolyzed in acid and, unless the nitrogen is substituted, it is also too base labile to survive the deblocking reaction (64, 65). This bond is more labile in the ribo series (65). The oligonucleotide amidates made by this method are listed in Table I.

(v) *Other Phosphate Modifications*. The four types of phosphate modification discussed above have all been used fairly extensively to modify the properties of oligonucleotides or their conjugates. Other modifications that have been made but, for the most part, not yet studied

Table I. Amidates Made by the Hydrogen Phosphonate Approach

structure of the amine component	refs	structure of the amine component	refs
NHCH ₃	45, 64	NHCH ₂ CH ₂ -morpholinyl	63
NHC ₄ H ₉	45, 58, 62	NH(CH ₂) ₂ NHCO-cholesteryl	61
NHC ₈ H ₁₇	62	piperidinyl	45
NHC ₁₂ H ₂₅	62	morpholinyl	45, 58, 64
NH(CH ₂) ₂ OCH ₃	64	piperazinyl	58
N(CH ₃) ₂	62, 64	N-methylpiperazinyl	45
N(CH ₃)CH ₂ CH ₂ -N(CH ₃) ₂	63		

Table II. Modified Internucleoside Phosphates

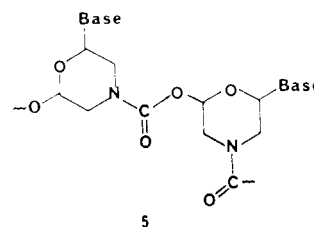
$\begin{array}{c} \text{B} \\ \\ -\text{A}-\text{P}-\text{C}- \\ \\ \text{D} \end{array}$				
A	B	C	D	refs
NH	O	O	O	66, 67
O	O	NH	O	67, 68
O	S	O	CH ₃	69
O	O	O	Se	53, 70
O	O	S	O	71
O	NPr	O	NEt ₂	72
O	S	O	NEt ₂	72
O	Se	O	NEt ₂	72
O	S	O	CH ₃	73
O	S	O	S	74
O	S	O	NHR	74
O	S	O	OPr	33, 75
O	S	O	OEt	44, 76
S	O	O	O	77
O	O	OPO ₃	O	67
CH ₂	O	O	O	78
S	O	O	O	79
S	S	O	O	79
O	O	S	CH ₃	267

Table III. Groups Used To Replace Internucleoside Phosphates

group	refs
-OCO-	85–88
-OCH ₂ CONH-	89
-OCH ₂ COO-	90
-OCONH-	89, 91–93
-OSiR ₂ O-	94–96

in this way are listed in Table II. Further examples include derivatives with pentavalent phosphorus (80, 81), but many more possibilities remain unsynthesized.

(vi) *Non-Phosphate Internucleoside Linkages*. In early work, the entire sugar phosphate backbone was replaced as in poly(1-vinyluracil) or in poly(acrylic acid) hydrazide derivatives (82–84). These suffered from solubility problems and spacing of the bases along the chain was different from that of natural nucleic acids. Most recent approaches have involved the less extensive modification in 5 (97) or replacing just the bridging phosphate by



the groups in Table III. As yet, synthesis of these types of compound is still at an early stage. Solubility in water is a common problem and hybridization is different from that of natural oligonucleotides in some cases.

3. SYNTHESIS OF CONJUGATES

Conjugate groups may be coupled to oligonucleotides either through sites present naturally in nucleic acids or through some other reactive linker group introduced specifically for the purpose. The naturally occurring groups that can be used are amino groups on the bases, hydroxyl groups on the sugars, and phosphate groups, both terminal and internal. Linker groups attached to the oligonucleotide for derivatization are most commonly primary amines, thiols, or aldehydes, but the possibilities are many. Often, the linker is attached to the oligonucleotide by a spacer arm either to facilitate coupling or to distance the conjugate group from the oligonucleotide.

Either the conjugate group or the linker may be introduced at one of three stages during oligonucleotide synthesis. These each have advantages and disadvantages.

1. The group can be attached to a nucleotide before incorporation into the growing chain. This approach can be used for either chemical or enzymatic synthesis of oligonucleotides.

2. Molecules other than nucleotides can be introduced during the synthesis of the oligonucleotide.

3. A linker or conjugate group can be attached to a natural nucleic acid or to a synthetic oligonucleotide after deblocking.

Sections A and B below describe incorporation during chemical or enzymatic synthesis, respectively. Section C covers coupling following synthesis and section D lists some conjugate groups that have been used.

A. Incorporation of Conjugate and Linker Groups during Chemical Synthesis of Oligonucleotides. From a synthetic point of view, incorporation of conjugates and linkers during the assembly of an oligonucleotide rather than afterward is the most rigorous approach. It gives greatest control over the number and location of the modifications; side reactions are minimized by the protecting groups on the nucleotides, and advantage is taken of the benefits of solid-support synthesis for workup and purification. Two strategies will be considered in which the conjugate group or linker may or may not be part of a nucleotide synthon. In both cases, the reactions are performed under anhydrous conditions, unlike the postsynthesis modifications described later, which are performed largely in aqueous solution.

(i) *Incorporation of Modified Nucleotides.* This approach is appealing for chemical synthesis as the nucleotide building block carrying the desired modifier can be introduced precisely at any internal or terminal position in the oligonucleotide with assurance that modification at that position is complete. As a result, concerns over the uniformity of the product and its identity should be less than those with some other methods. However, it is necessary to first prepare and purify the nucleotide, and the modifications must be able to withstand the coupling reaction and the rigors of acid and basic deblocking. In some cases, nonstandard protecting groups may be necessary. Probably as a result of the greater synthetic effort required, this approach has not been used as widely as others.

Substituents may be attached to nucleotides at the base, sugar, or phosphate residues, but ideally, changes should not interfere with hybridization. While there is potential for using phosphate-modified precursors such as substituted phosphonates or phosphotriesters, little work has been done in this regard other than with the simple blocking groups described in the previous section.

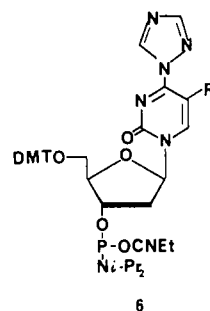
Two sites on bases which are easy to manipulate chemically without necessarily preventing base pairing are C(5)

Table IV. Linkers Incorporated into Oligonucleotides as Substituents on Pyrimidine Nucleoside Phosphoramidate Synthons

substituent	refs
At N(4) of dC	
(CH ₂) ₆ OH	98
(CH ₂)NHCO(CH ₂) ₆ NH ₂	99
At C(5) of dU	
(CH ₂) ₃ NH ₂	100-102
C=C(CH ₂) ₂ NH ₂	103
C=CCH ₂ NHCO(CH ₂) ₆ NH ₂	103
CH=CHCONH(CH ₂) ₆ NH ₂	104

of uracil and N(4) of cytosine, and several nucleotide phosphoramidite synthons have been prepared with protected linkers at these positions (Table IV).

The triazole leaving group introduced with reagent 6 can be displaced by various nucleophiles before the final

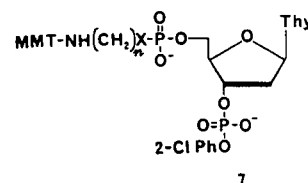


deblocking of the oligonucleotide (105-107). This might be used as a general-purpose reagent to minimize the synthetic effort necessary to introduce a variety of other groups or for the introduction of a group sensitive to the coupling or acidic detritylation steps.

In addition, a number of nucleotides already bearing conjugate groups at these positions have been used. Examples are EDTA, used in the generation of free radicals (108), and biotinyl, dinitrophenyl, pyrenyl, and dansyl reporter groups (109). 5-Bromo-2'-deoxyuridine has been incorporated by triester synthesis for its ability to cross-link with DNA-binding proteins on UV irradiation (111).

In the case of purines, C(8) of adenine was used as an attachment site for the photoactivatable cross-linking reagent psoralen (112).

Other nucleotide phosphoramidites have been prepared with O(5') of the sugar replaced by nitrogen or sulfur (113-115). Used in the final coupling, these give oligonucleotides with a thiol or primary amine at the 5'-end for subsequent reaction with electrophiles. For situations where a spacer was required between the 5'-amino and the oligonucleotide, nucleotide 7 was used with triester coupling (116).



Also in the triester series, protected thymidine 3',5'-diphosphate was used for the introduction of a terminal 5'-phosphate residue as a site for postsynthetic modification (117).

Unlike with solid-support synthesis, with the older solution-phase triester method nucleotides can be added to the 3'-end of the oligonucleotide. Nucleotides carrying

various 3'-bound conjugate groups or linkers have been introduced this way (117-120).

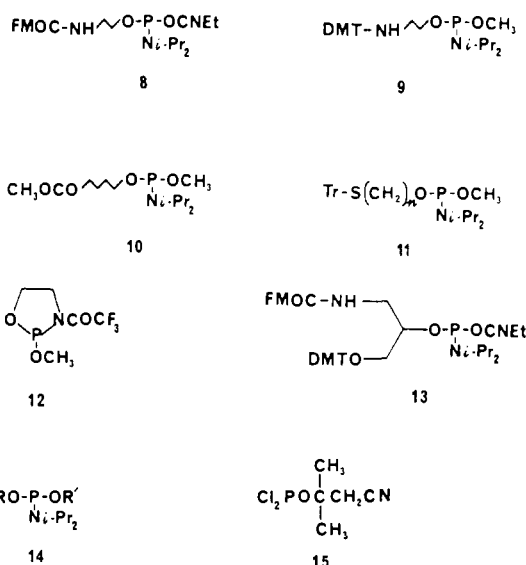
To accomplish this by solid-support synthesis, a special support bearing the modified nucleoside may be prepared as in the case of cytidine with an amine linker at N(4) (121).

(ii) *Incorporation of Non-Nucleotides.* A number of reagents other than nucleotides have been developed for incorporation during oligonucleotide synthesis. These are generally much simpler synthetic targets for the introduction of conjugates or linkers. They are used most commonly to couple a group at the 5'-end of an oligonucleotide while it is still fixed to the solid support. This reduces the potential for side reactions at the bases, which are still protected, and simplifies purification. The reagent must be soluble in an organic solvent suitable for the coupling reaction and, again, must withstand the deblocking procedure.

Most groups introduced in this way have been used to give, after deblocking, a nucleophilic linker for preparation of a conjugate. One reason for using nucleophiles is that many suitable electrophilic derivatives of the conjugate groups are available commercially.

Often, the same coupling chemistry is used for nucleotides and non-nucleotides so that the latter may be added from a spare reservoir of the synthesizer using the standard program.

Reagents 8-11 have a protected amine, thiol, or carboxyl at one end of a spacer and a phosphoramidite at the other (122-128). Reagent 12 is a cyclic analogue of



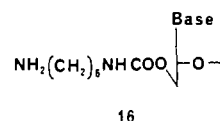
9 that uses the same nitrogen atom both as the leaving group and as the linker (129). These compounds can be used interchangeably with the standard nucleoside phosphoramidites. Analogous reagents are available for H-phosphonate (130) or triester synthesis (120, 131) or linking through a methylphosphonate (132). Hence, these groups can be incorporated readily during automated synthesis, whichever approach is employed, without the necessity for changing reagents. After deblocking, all give oligonucleotides with a nucleophilic linker at the 5'-end. Reagent 13, containing an additional protected hydroxyl function, can be used for multiple rounds of deblocking and coupling to increase the number of linker groups (153).

Phosphoramidite derivatives of biotin (133), acridine (134), and anthraquinone (135) have been used similarly and phosphate derivatives of acridine and tetramethyl-

rhodamine have been used for triester synthesis both by solid-support and solution-phase synthesis (131, 136).

During automated synthesis, reagents of general structure 14 or 15 can be used to phosphorylate or thiophosphorylate the 5'-hydroxyl group (118, 137-140) and a number of other reagents exist based on triester chemistry (141 and references therein). The phosphate can be used for modification at a later stage or it can be selectively deblocked before cleaving from the solid support and condensed, for example, with an alcohol in the presence of a sulfonyl triazolidine (142).

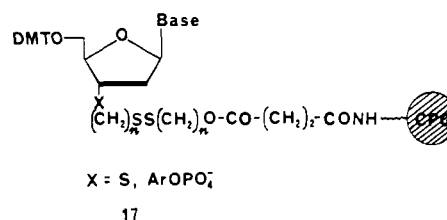
As an alternative to reactions at phosphorus, the 5'-hydroxyl group of support-bound oligonucleotide can be activated with carbonyldiimidazole for reaction with hexamethylenediamine to give carbamate 16 (143). Described



in section C below is the use of a vicinal diol as a linker. This can be introduced as a ribonucleotide joined 5'-5' during the final coupling of the synthesis (122).

Modifications at the 3'-end are less common due to the inaccessibility of this site in solid-support synthesis. The usual way to solve this problem is to use a support with the modification already built in. For example, polyamide or polypeptide chains synthesized on a support were used to initiate oligonucleotide synthesis to give conjugates with a 3'-polypeptide tail. Incorporation of lysine in the peptide furnished multiple amino linker sites for subsequent derivatization (144, 145).

The spacer between the nucleoside and the support can be designed so that on cleavage, a reactive nucleophile is generated at the end of the oligonucleotide. For example, support 17 gave a 3'-terminal thiol after ammo-



nia treatment followed by reduction (146, 147). To avoid the need for four such supports, a linker was developed to which the first nucleoside was added during the synthesis. On cleavage, this liberated a 3'-terminal amine from a carbamate (148).

Reactions at the 3'-end may be performed more readily during solution-phase synthesis. Examples are the condensation between a 3'-phosphate and the hydroxyl group of an acridine or phenanthroline derivative using triester chemistry (136, 149, 150).

A site amenable to ready modification during oligonucleotide synthesis is the internucleoside phosphate, particularly during the oxidation of intermediate phosphites or hydrogen phosphonates. Much of the work on conjugation here has been done by Letsinger and his co-workers, who have reported several methods for linking through phosphoramidates to prepare conjugates of phenanthridine and cholesterol (43, 61, 151). Other workers have introduced acridine by triesterification of unprotected internucleoside phosphates (136). Of these approaches, the most routine and widely applicable would seem to be generation of phosphoramidates during hydrogen phos-

Table V. Linker and Conjugate Groups Incorporated Enzymatically into Oligonucleotides as Substituents on Nucleotide Triphosphates

substituent	refs
At C(5) of (d)UTP	
naphthalene derivative	102
biotin	154-157
(CH ₂) ₁₂ NH ₂	157
CH=CHCH ₂ NH ₂	157
N ₃ ^a	158, 159
fluorescein	160
SCH ₃ ^b	161
At N(4) of (d)CTP	
(CH ₂) ₆ NH ₂	162
At C(4) of UTP	
S ^c	163, 164
At C(8) of ATP	
NH(CH ₂) ₆ NH ₂	157
2,4-dinitrobenzene ^d	165
At N(6) of ATP	
CH ₂ CONH(CH ₂) ₆ NH ₂	157

^a Used to cross-link with proteins. ^b Used in site-specific cleavage of DNA. ^c Used as a site for alkylation. ^d Used as a hapten.

phonate synthesis. This has been used to introduce a protected amino linker for postsynthetic derivatization (152).

Another easily accessible phosphate derivative is the phosphorothioate described previously. The sulfur atom reacts readily with alkylating reagents as will be discussed in section C.

Finally, the versatile trifunctional phosphoramidite 13 can be used in place of a nucleotide during synthesis to introduce one or more amine linkers into the backbone at any position (153).

B. Incorporation of Modified Nucleotides during Enzymatic Synthesis of Oligonucleotides. The strategy of incorporating modified nucleotides can be applied to enzymatic synthesis of oligo- or polynucleotides with or without a template. While the products are not subjected to the conditions of chemical synthesis and deblocking, this method generally gives less control over the sites of modification and is restricted by what is acceptable as a substrate for the enzyme.

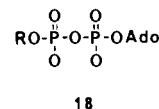
A variety of DNA and RNA polymerases have been used for this purpose, but those most commonly employed are *Escherichia coli* DNA polymerase I and terminal deoxynucleotidyl transferase. The former is used with a template either for internal incorporation of a modified nucleotide or for addition to the end of a presynthesized oligonucleotide. The latter enzyme is used without a template to add one or more nucleotides to the 3'-end.

Generally, the same positions on the nucleotides are modified as for the chemical syntheses discussed previously. These are C(4) and C(5) of pyrimidines and C(8) of purines and examples are given in Table V. Some of the more commonly used nucleoside triphosphates are commercially available.

T4 RNA ligase has been used to introduce a single, modified nucleotide at the 3'-end of RNA or DNA terminating with a ribonucleotide. The 3'-thiophosphoryl derivative of pCp gave the same phosphorothioate function whose chemical synthesis was described previously. Also incorporated was the fluorescent derivative with bimane attached to sulfur (166).

In the absence of ATP, T4 RNA ligase transfer the *non-nucleotide*-bearing phosphate from the ADP derivative 18 to the 3'-hydroxyl of an RNA (167). This has

been used to label RNA with various reporter molecules (168).



C. Postsynthetic Modifications of Oligonucleotides. Conjugate groups are usually introduced after the synthesis and deblocking of the oligonucleotide. This normally requires less effort than preparation of reagents for incorporation during synthesis but introduces other problems.

As oligonucleotides are polyionic, postsynthetic reactions are usually performed in water or an aqueous solvent in which the reagents must be sufficiently soluble and stable. This, in itself, is restricting as few synthetic, organic reactions are intended to be performed under these conditions.

As linkers are usually nucleophiles, unwanted reactions may occur at many internal sites in oligonucleotides. The separation of oligonucleotides with different numbers of conjugate groups is difficult as is their characterization, which is usually not attempted in any rigorous way and often not at all. The structure of the product is frequently assumed from the nature of the starting materials, particularly with conjugates of large, multifunctional molecules, where it is generally not possible to apply the more rigorous standards of organic chemistry. However, the reasons for making these compounds are usually for practical applications and, provided that they function as intended, then the precise number and location of the conjugate groups may not be crucial.

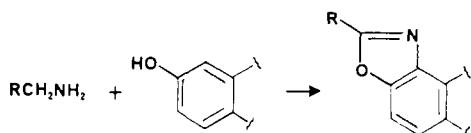
Postsynthetic reactions on oligonucleotides may be used to generate or modify linkers or to introduce the conjugate group. This section describes, in rather broad terms, the types of reactions that have been employed with various linker functions. The emphasis is on the nature of the bond-making reactions rather than particulars of individual cases. Subsections are devoted to coupling reactions used for different linker groups.

(i) *Reactions of Primary Alkylamines.* Primary alkylamines (and hydrazines) are among the most commonly used linkers because of their affinity for electrophiles. Usually, these are some activated form of a carboxylic acid such as the ester of *N*-hydroxysuccinimide that gives an amide (99, 100, 121, 122, 124, 130, 169-171). Other related species that have been used include nitrophenyl (126, 151, 172) and pentachlorophenyl esters (115), an acid anhydride (102, 173, 174), and sulfonyl chlorides (99, 102). Alternatively, the water-soluble 1-ethyl-3-[3-(dimethylamino)propyl]carbodiimide condensing reagent (EDC) can be used for amide formation with a carboxylic acid (170, 175). Formally, this reagent accomplishes a dehydration reaction in water.

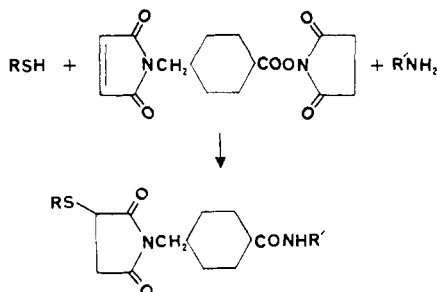
It was found with EDC that as many as 35-45% of the amide bonds formed were with the amines of the bases rather than with the intended linker. The *N*-hydroxysuccinimide ester gave less reaction at the bases but was also less efficient overall (170). This study was of reactions between oligonucleotides and carboxyl groups attached to solid matrixes, but extensive base modification was found also on EDC treatment of an oligonucleotide bearing a 5'-carboxyl group (127).

Chief among the reagents giving non-amide products are isothiocyanates that give thioureas (99, 113, 122, 130). Other reactions that have been used are hydrazone for-

Scheme II



Scheme III



mation with an aldehyde (176) and a less general reaction with nitrobenzodiazole fluoride (113, 122, 130). The unusual reaction in Scheme II brought about by horseradish peroxidase in the presence of hydrogen peroxide was used to introduce an intercalating agent (177).

A molecular adapter has been designed that will replace an amino linker with a thiol (121) while bromopyruvate was used to couple an amino linker with a thiol in a protein (178).

(ii) *Reactions of Thiols.* The chemistry of sulfur is more complex than that of nitrogen, and thiol linkers may be used in a greater variety of reactions than amines. As well as their nucleophilic properties, they bond readily to mercury and form disulfides with other thiols. In fact, disulfide formation can be a problem on storage (127).

In order to generate conjugates from two thiols by mixed disulfide formation, competing reactions to give symmetrical products must be suppressed. This is usually done by first forming a mixed disulfide between one thiol and 2-thiopyridine followed by an exchange reaction with the second thiol (127, 146, 179, 180). Alternatively, one of the thiols may be used in large excess (181).

A useful feature of disulfide formation is that it is readily reversed by treatment with dithiothreitol (DTT) or other mercaptans. This has been used to remove one-half of the conjugate after it has fulfilled its function (181) or to reversibly bind oligonucleotides to a solid matrix (127). Reversal of disulfide formation was used to generate thiol linkers from blocked disulfide precursors (121, 146, 179).

The most commonly used electrophilic groups for conjugation with thiol linkers are iodo- or bromoacetates and maleimides (121, 123, 130, 131), but some fluorescent markers proved troublesome by this approach (130). Immobilization on a solid support was claimed to be far superior with thiol as opposed to carboxyl or amine linkers (127).

By a type of Michael addition, the thiol on an oligonucleotide was linked with an amine in a one-pot reaction using the bifunctional reagent in Scheme III (182).

The affinity of thiols for mercury compounds was used for immobilization of an oligonucleotide on chloromercuribenzoate-derivatized agarose (127).

Another finding reflecting the more complex chemistry of sulfur is that a two-carbon spacer between sulfur and phosphate was unstable at pH 8 while longer ones were not (123, 146).

(iii) *Reactions of Phosphates and Thiophosphates.* Ter-

minal phosphates may be introduced during chemical synthesis, by enzymic phosphorylation or by β -elimination of a terminal ribonucleoside following periodate oxidation. Naturally derived material may already have a terminal phosphate. The only reactions used to form conjugates postsynthetically at phosphate are condensations with amines or alcohols to give phosphoramidates and esters. Thiophosphates are used in a different class of reactions with alkylating agents.

An early method from Khorana's laboratory for reaction at terminal phosphates was the formation of a phosphoramidate from aniline using dicyclohexylcarbodiimide (DCC) as the condensing reagent in a mixed solvent of water, dimethylformamide, and butanol (183). This is still basically the method used to modify oligonucleotides except that DCC has been replaced by water-soluble EDC (67, 184–186). Recently, cyanogen bromide has been used for the same purpose. This reagent may also be used to generate a variety of unusual internucleoside phosphate bridges by coupling contiguous oligonucleotides on a template in a form of chemical ligation (67, 185, 186).

Although they were not the first to use EDC with oligonucleotides, Chu et al. developed the protocol most commonly used of first preparing the phosphorimidazolide with EDC and reacting this with the amine or other nucleophile (187). This intermediate, used previously in chemical ligation (188), is faster than direct coupling of simple amines and permits the use of nucleophiles that would themselves react with EDC. Although side reactions at the bases do occur, they were considered to be minor under the conditions used. Other workers have reported that *N*-hydroxybenzotriazole is superior to imidazole for this purpose (67).

This approach has been used to attach a variety of linkers and conjugate groups to oligonucleotides (169, 170, 173, 179). Direct coupling to the amine without going through the intermediate phosphorimidazolide has been used also (67, 189). The reaction has been extended to nucleophiles other than amines and has been studied in some detail to minimize base modification (184).

Thiophosphate may be introduced during chemical synthesis or with polynucleotide kinase (190). The sulfur atoms at both terminal and internucleotide sites react at least 10^3 times faster than the other groups in nucleic acids with 2-chloroethylamines and so can be used for selective coupling (190). A variety of alkylating agents have been used to form conjugates in this way (118, 140, 150, 166, 191–194).

(iv) *Electrophilic Linkers.* Most examples of conjugate formation use a nucleophilic linker to react with some electrophilic reagent. Unwanted reactions may occur at other sites in nucleic acids which are predominantly nucleophilic in nature, particularly the bases. An electrophilic linker may be used providing that it does not undergo intramolecular coupling at these sites. There are a few examples of this approach, the electrophiles being carbonyl or activated carboxyl groups.

One of the earliest methods for labeling RNA with biotin used periodate to oxidize the 3'-terminal ribonucleoside to a dialdehyde that was reacted with a primary amine and reduced with borohydride (195). This has been used to label RNA with a number of fluorescent dyes and other agents (196–198). In the case of oligodeoxynucleotides, a terminal ribonucleotide can be introduced by 5'-5' coupling as the last step in synthesis (122). Steric hindrance around the reacting amino group may be troublesome in some cases with this method.

A single aldehyde function can be generated at the 5'-end by periodate oxidation of a vicinal diol introduced during synthesis. Reaction with an amine or hydrazine followed by reduction under very mild conditions did not show any competing side reactions and was particularly good for immobilization on a solid support (125).

Another electrophilic species was generated at the 5'-terminus by treatment of a carboxyl group with EDC in the presence of imidazole. This was used for amide formation (125).

(v) *Reactions at Naturally Occurring Sites in Nucleic Acids.* Unmodified oligonucleotides contain a number of reactive sites that are generally less potent than the synthetic linkers but which have been used for conjugation. For the most part, these are nucleophiles and include nitrogen functions on the bases, C(5) of pyrimidines, C(8) of purines, primary and secondary hydroxyl groups, and phosphomono- and diesters. Electrophilic substitution can also occur at some positions on the bases. Reactions at these sites are likely to lead to complex mixtures unless they can be controlled in some way. This may be acceptable for labeling of large DNA or RNA, where modification can be restricted to a very small fraction of nucleotides and the level of heterogeneity in the product is undetectable and irrelevant. The approach is less satisfactory for oligonucleotides where incomplete modification gives products with a spectrum of properties. Four of these reactions that are better defined chemically are given below.

The first uses a photoactivatable derivative of biotin carrying a phenyl azide that reacts with nucleic acid bases (199). This is used to label about only 1 in 50 bases in DNA so as not to impair hybridization and may therefore not be applicable to oligonucleotides.

In a second method, mercury at C(5) of pyrimidines, introduced by reaction with mercuric nitrate, was coupled with haptens bearing thiol groups (200).

Bisulfite adds across the 4,5-double bond of cytidine and encourages nucleophilic displacement of the amino group at C(4). This reaction is selective for single-stranded nucleic acids and has been used to introduce a number of substituents (178, 201, 202).

Finally, an electrophilic substitution occurs at C(8) of guanine in nucleic acids on reaction with *N*-acetoxy-2-aminofluorene to give a label for immunological detection (203, 204).

None of the above reactions can be used to modify an oligonucleotide in a controlled way other than by restricting to one or two the number of reacting nucleotides, thereby severely limiting the sequence. There are few examples where a more controlled approach is possible.

4-Thiouridine is a naturally occurring nucleoside that can be incorporated into oligonucleotides. It was shown that alkylation with α -haloacetamido derivatives or phenacyl bromides could be directed exclusively to the sulfur of this base to introduce a number of different conjugate groups (163, 164).

An example of a reaction restricted to a particular sequence involves introduction of psoralen onto thymidine only when it is flanked on the 3'-side by adenosine (205). This was possible because, on irradiation, psoralens preferentially cross-link double-stranded oligonucleotides at thymidine in the sequence 5'-TpA-3'. The reaction can be partially reversed on irradiation at a different wavelength to give, after strand separation, a single strand with the psoralen monoadduct of thymidine. This serves as a reactive probe that cross-links with its complementary sequence on irradiation.

Table VI. Groups Used in Conjugates of Oligonucleotides

groups	refs
Fluorescent Dyes	
fluoresceins	99, 103, 113, 114, 146, 157, 160, 163, 168, 198, 200, 208-211
tetramethylrhodamine	99, 113, 131, 168, 209, 211
Texas red	99, 113
pyrene	109, 210
bimane	130, 166, 192
mansyl	102
dansyl	109, 126, 191
proflavine	197
eosin	130, 163
naphthalene derivatives	123, 130
coumarin derivatives	130, 207
Intercalating Agents	
acridine	48, 49, 118, 134, 136, 149, 212-217
oxazolopyridocarbazole	177, 218
anthraquinone	135
phenanthridine	151
phenazine	219
Proteins	
peroxidases	99, 140, 176, 179, 220
IgG	179
alkaline phosphatases	99, 103, 121, 170
polylysine	130, 221-227
nucleases	147, 180, 228
Cross-Linking Agents	
alkylating agents	106, 119, 229-233
azidobenzenes	100, 163, 164, 190, 193, 196, 215
psoralen	112, 181, 182, 189, 205, 249
iodoacetamide	101
azidoproflavin	194
azidouracil	158, 159
platinum(II)	227, 234
Chain-Cleaving Agents	
EDTA/Fe ^{II}	108, 173, 174, 236-238
phenanthroline/Cu ^{II}	120, 150, 239, 240
porphyrin/Fe ^{II}	241, 242
Others	
biotin	107, 109, 110, 122, 124, 126, 130, 133, 142, 143, 145, 148, 154-157, 162, 168, 169, 171, 195, 199, 200, 202, 210, 243
solid matrixes	125, 127, 128, 140, 170, 175, 244, 245
dinitrophenyl	109, 165
trinitrophenyl	200
proxyl spin-label	191
fluorene	203, 204
isoluminol	99
digoxigenin	246
puromycin	247
DTPA (chelating agent)	182
phospholipid	248
cholesterol	61, 307

Finally, attention is drawn to an old reaction that has not been used for conjugation but which is unusual in that it permits selective reaction at oligonucleotide hydroxyl groups when more often it is the bases that react most readily. This is the reaction of acetic anhydride in water (206). No reaction was found at the bases and mixed-anhydride formation at phosphates is readily reversed. Thus, in the case of 5'-phosphorylated oligodeoxynucleotides, reaction occurred only on the 3'-hydroxyl group.

D. Conjugate Groups. Many of the conjugate groups used with oligonucleotides are given in Table VI. This is not an exhaustive list of the use of these compounds, particularly of probes where the literature is extensive. Rather, it is intended to indicate the nature of conjugates studied and to serve as a source of the methods for coupling different groups.

Included are some recent, more specific ways for immobilizing oligonucleotides on solid supports, but the older literature on this subject is not covered and may be obtained from the references cited.

There is a very large amount of literature on chemically reactive oligonucleotides, particularly on those bearing nitrogen mustard type alkylating groups. Reference has been given to a review plus a few more recent examples. No attempt is made here to discuss the chemical reactions of these compounds.

A choice that has to be made for each conjugate group is the length of the spacer used to link it to the oligonucleotide. This is particularly important in the case of an intercalating agent that has to interact with the helix. Here, a very small change in spacer length can influence the outcome, but chains of five or six carbon atoms were best (64, 177, 212, 213). For psoralen to cross-link with the opposite strand, a shorter spacer of two carbons was required, and yields fell six-fold if this were increased (249). For biotin or fluorescent tags that do not interact with the helix, a longer spacer of eleven or twelve atoms was preferable to minimize steric inhibition of hybridization (103, 127).

4. PROPERTIES OF MODIFIED OLIGONUCLEOTIDES AND CONJUGATES

The development of conjugates with new properties should improve existing techniques and lead to the development of new uses and ideas. Advances are being made in the areas of automated sequencing (113, 208) and non-radioactive probes (250) and in accurate chemical cleaving of DNA and RNA (101, 251–253). Chemically reactive probes can be used to place a tag on a particular base within an RNA (181) and have been used to demonstrate parallel helix formation (120, 194). Nonradiative energy transfer between oligonucleotides can be used to indicate their separation in solution (209, 220). This seems a particularly promising technique that could be applied in many different ways and has already been used to investigate the structure of the Holiday junction (211). The same principle has been used to investigate interactions of oligonucleotides with proteins (207).

It is beyond the scope of the present review to cover all the uses and developments involving oligonucleotides. Rather, the emphasis here will be on the biological properties of modified oligonucleotides, in particular the effect of modification on hybridization, stability, and cell uptake. The final section discusses antisense inhibition, which is the most demanding use of oligonucleotides, requiring that they find and hybridize with their complementary sequences inside cells. Again, the approach taken here is to examine the general consequences of modification rather than the particulars of individual cases.

A. The Effect of Modification on Oligonucleotide Hybridization. Modifications to the internucleoside phosphates can affect hybridization in a number of different ways, but it is important that they should not prevent base pairing. Reduction in charge density lessens electrostatic repulsion between the strands and should facilitate their association. This effect will be greatest at low salt concentrations, where the shielding of the charges is least. Steric interactions of substituents will normally destabilize the helix as, it has been suggested, will their electronic and other effects (254). These might include disruption of hydration of the helix. However, the grooves of the hybrid might also provide a more lipophilic environment for the sequestration of hydrophobic substituents, thereby promoting hybridization. Cases where stronger hybridization resulted on increas-

ing the lipophilicity of the substituent may be examples of such an effect (43, 62).

The relative contributions of all these factors are governed by external conditions such as salt concentration as well as intrinsic factors such as the length of the oligonucleotide, the degree of modification, the localization of a given modification relative to the ends or middle of the helix, and the sequence of bases around it (254). Thus, the consequences of a particular modification will vary from case to case. The complexity of this situation has prevented a clear understanding of the effects of phosphate modification on hybridization.

A complicating feature is the chirality of the phosphorus atom following modification. Absolute stereochemistry has been assigned by X-ray crystallography (255) and NMR (256, 257) and by enzymic (258–261) and chemical methods (33, 44, 76). A molecule with n chiral phosphorus atoms will consist of 2^n isomers, and one of the most challenging areas of oligonucleotide chemistry is the development of diastereospecific synthesis (262–267). Attempts to use diastereomerically pure starting materials in the usual synthetic approaches resulted in racemization (53, 73, 268, 269).

When small numbers of isomers are involved, resolution is possible by chromatography, and the pure diastereomers have been used for block condensation. This approach has been largely limited to the construction of short backbones with alternating unmodified and chiral phosphates or longer molecules with a single modification (46, 48, 270–272). Enzymatic synthesis of phosphorothioates gives the R_p isomer exclusively (50, 51, 273) and has enabled studies of polynucleotides with extensively modified, stereopure backbones (274). It is not yet possible to synthesize by chemical means diastereomerically pure chains of the length necessary for antisense inhibition.

In their early studies of uncharged methylphosphonates and triesters, Miller and Ts'o found that racemic di- to tetramers hybridized to unmodified strands with greater affinity than the parent phosphodiester (275, 276). While diastereoisomers of dimers differed from each other, both formed more stable hybrids than the natural, charged compounds and were less effected by salt concentration. This was attributed to the lack of charge-charge repulsion between the strands of the complex (17, 32). An adverse effect on hybridization as the size of the substituent increased from PCH_3 to POCH_3 to POCH_2CH_3 seemed to be due to steric interactions.

Similar improvements in hybridization were reported for other low molecular weight triesters and phosphoramidates (34, 43, 62). With substituted amidates, these included a positively charged backbone. In some cases, however, bulkier substituents improved rather than diminished hybridization.

When a single, uncharged group is incorporated into an oligonucleotide, a different effect is seen and the stability of the helix is unchanged (191, 271) or reduced in most situations (75, 254, 256, 277). Possibly the removal of a single charge out of many makes little difference to the overall electrostatic repulsion between the strands and the other destabilizing effects of substitution gain in relative importance. The difference between the diastereomers is more pronounced with greater destabilization when the substituent points into the major groove rather than away from the helix (75, 254, 256).

With longer, extensively modified oligonucleotides, the complexity of the mixture becomes much greater and as each diastereomer in a pair is slightly different, some het-

erogeneity in overall properties is expected. An uncharged octamer of thymidine with an ethyl phosphotriester backbone could be separated into fractions with different affinities for poly(dA) (40). The real test of these compounds, however, is the effect of extensive substitution on the properties of a longer heterosequence.

The hybrid of a 20-mer containing 18 methylphosphonates melted only 4 °C below the fully charged duplex with little broadening of the melting curve in 0.1 M salt (278). In another study, a 15-mer containing 11 phosphonate linkages melted 5 °C higher than the diester in 0.015 M salt and 8 °C lower in 0.15 M salt (64). Heterogeneity in hybridization would be reflected in a broadening of the melting curve which was not appreciable in either of these examples. From the limited data presently available, it would appear that, in practice, the complexity of the diastereomeric mixture does not greatly reduce or broaden the spectrum of affinity for the target sequence of phosphonates when compared to that of phosphodiester. That is not to say that higher melting would not result from the optimum, stereopure backbone.

At variance with these findings is the suggestion that methylphosphonates are inherently unsuitable for adopting a right-handed helical conformation so that melting temperature decrease to below 20 °C with chain lengths greater than four. Methyl triesters were not found to share this property and were proposed as superior antisense agents with high melting temperatures that are not influenced by the chirality of the phosphorus (36, 279). However, they hybridize poorly with RNA, which is the usual target for antisense inhibition (280).

Extensive substitution of longer oligonucleotides with various phosphoramidate linkages gave somewhat less stable hybrids than the phosphonates. Those derived from primary amines were superior to those from secondary amines (64). Cationic amidates showed a reversal in salt dependence and formed hybrids that were more stable in low salt than phosphodiester but less stable in high salt (63).

A common finding in many studies of noncharged phosphate modifications is that hybridization to RNA is less efficient than that to DNA (40, 43, 48, 63, 86, 174, 270, 280). It has been suggested in the case of ethyl phosphotriesters that this results from the inability to form an A type helix, where the loss of rotational freedom of the ethyl group is greater (40).

With a single phosphorothioate linkage, only the R_p isomer with sulfur pointing into the major groove destabilized the helix (281). Multiple phosphorothioate linkages, either all R_p or a racemic mixture, lowered the melting temperature by an amount that depended on the base composition of the oligonucleotide but was at least 7 °C for a 15-mer (56, 134, 274).

Modifications other than at internucleoside phosphate may also affect hybridization. α -Oligonucleotides, for example, hybridize with β -RNA and DNA by forming the usual Watson-Crick base pairs. In fact, these hybrids are considerably more stable than when both strands are β (243). Unlike natural duplexes, however, those with an α -chain have parallel strands (215, 216, 282, 283). An exception is the complex between α -oligothymidylic acid and β -poly(rA), which is antiparallel (239). This particular α -oligonucleotide is also unusual in that it can form a double-stranded helix with itself containing T·T base pairs (284). Similar parallel self-pairing was observed on neutralizing the phosphates of β -oligothymidylate as methyl triesters (42).

In an attempt to stabilize hybridization with very short oligonucleotides, Letsinger and Schott attached an intercalating agent to the phosphate group of TpT (151). This proved successful and, as discussed later, permits the use of shorter oligonucleotides than would otherwise be possible for antisense studies. The physical chemistry of these interactions has been investigated (165, 212, 213, 285) and it has been shown that an intercalating agent at the end of an oligonucleotide, especially the 3'-end, is more beneficial than on an internucleotide phosphate and that a second intercalating group offers no further advantage (136, 213).

α -Oligonucleotides and others with methylphosphonate or phosphotriester linkages also benefited from the addition of an intercalator (48, 64, 177, 215, 218). In these conjugates, two different mechanisms for stabilizing the duplex are combined. The only intercalator that has been combined with a phosphorothioate backbone was of somewhat uncertain efficacy (134). No stabilization was observed and, if confirmed in other cases, this may reflect steric effects of the larger sulfur atom at the site of intercalation.

B. The Effect of Modification on Nuclease Resistance. A number of studies have demonstrated degradation of unmodified oligonucleotides at greatly varying rates in different cells or in the serum-containing media used for cell culture. Survival times vary from minutes to days (56, 286-293). Consequently, it has been a goal in many approaches, particularly in the antisense field, to develop nuclease-resistant derivatives on the assumption that these will be more potent. Of course, there is the chance that they will also be more toxic because they survive longer.

It was recognized early on that the rate of degradation of RNA by exonucleases from snake venom and spleen was slowed considerably by phosphorothioate groups (294). The former enzyme can cleave the R_p diastereomer but not the S_p or adjacent R_pS_p or S_pS_p groups (53, 262, 295-297). In contrast, nucleases S1 and P1 are specific for the S_p isomer (53, 297, 298) while ribonucleases A and T2 do not distinguish between different configurations (296). With DNase I, sequence or base composition also effect the rate of digestion of phosphorothioate-substituted polynucleotides (274).

As a result, oligodeoxynucleotides with a high proportion of unresolved phosphorothioate groups are almost totally resistant to snake venom phosphodiesterase, are degraded 2-45 times more slowly than normal by S1 and P1 nucleases, and survive many times longer than unsubstituted oligonucleotides in human serum (56).

All other modifications to internucleoside phosphates that have been investigated also inhibit the action of nucleases. Most reports suggest complete resistance of phosphoramidate (43, 45, 58, 62), phosphonate (18, 270), or phosphotriester (32, 43, 299) linkages toward the nucleases that have been tested. An exception is the very slow rate of cleavage by snake venom or spleen phosphodiesterases of unsubstituted phosphoramidate observed for the sequence d(ApA) but not for TpT (43, 65). All N-substituted phosphoramidates were resistant. An early report of slow cleavage of one of the diastereomers of phosphonates by snake venom phosphodiesterase could not be confirmed (18, 270).

While the modified linkages themselves may be resistant, in oligonucleotides containing mixtures of modified and natural linkages, exonucleases that work progressively from one end of the chain can sometimes skip over an isolated phosphonate or triester linkage to cleave

the adjacent phosphodiester at a reduced rate (27, 270, 300). This may be more difficult if the phosphonate is near the end of the chain and the presence of two adjacent internal methylphosphonates in oligothymidylic acid blocked the progress of the enzyme much more effectively than just one (27, 300). Similarly, blocks of contiguous phosphorothioates at the ends of the chain gave resistance to exonucleases while conserving desirable properties of the unmodified backbone in between (56). Resistance to endonucleases may be improved by reducing runs of contiguous phosphodiesters, particularly below four (300).

Modifications at groups other than phosphate may also induce resistance to nucleases. α -Oligodeoxynucleotides, for example, proved far more stable than β -oligodeoxynucleotides in a number of different biological environments (291, 301). Also, the presence of a bulky group such as an intercalating agent or even methylthiophosphate at the appropriate end of an oligonucleotide can preempt exonuclease attack (134, 237, 291).

RNA was found to be more stable than DNA in nuclear cell extracts (302). Methylation of the 2'-hydroxyl group increases its resistance to nucleases (303).

Nucleases are not the only enzymes involved in the catabolism of oligonucleotides inside cells. In cultured fibroblasts, oligonucleoside ethyl phosphotriesters were broken down quite rapidly, probably following deethylation. Methylphosphonates survived much better but were slowly degraded by a pathway that may begin with deglycosylation (304).

C. Cellular Uptake of Modified Oligonucleotides. A problem common to uptake studies is the difficulty in distinguishing material inside the cell from that bound to the outer membrane. Few studies have managed to do this convincingly enough to eliminate doubt. Consequently, confidence in the literature concerning this subject is not as high as is desirable.

Despite their high charge density, oligonucleotides are taken up reasonably well by mammalian cells. This appears to be an energy-requiring process and may involve receptor proteins on the cell surface. Intracellular concentrations may rise to about 10% of those outside the cell within 15 min to 2 h (286, 290, 305, 306). Shorter oligonucleotides are taken up somewhat more rapidly and phosphorothioates are taken up more slowly than unmodified oligonucleotides (134). Lipophilic substituents such as intercalating agents or cholesterol facilitate uptake (216, 237, 307).

Uptake of uncharged methylphosphonates appears to be quite different. Intracellular levels of dimers to nonamers reached extracellular concentrations within 1.5 h (276). This would appear to be passive diffusion across the cell membrane. Prokaryotes have not been investigated extensively, but in contrast, *E. coli* cells were impermeable to chain lengths greater than four (308).

D. Modified Antisense Oligonucleotides. Oligonucleotides complementary to strategic regions of viral or messenger RNA's were first shown by Zamecnik and Stephenson to inhibit viral replication (309). The structures of these highly specific, biologically active compounds can be predicted from the sequence of the target RNA and are therefore useful for genetic analysis and attractive candidates for therapeutic agents. As they generally prevent expression of the sense strand, they have become known as antisense oligonucleotides. The object of this section is not to review the antisense approach or to discuss strategies for its use, as this has been done elsewhere (310, 311). Rather, attention will be focused

on the effects of chemical modification on activity.

Comparatively few true conjugates have been used for antisense studies so far although modifications to the backbone have been used extensively. These will play an increasingly important role in designing the next generation of compounds where components with particular properties will be required.

The factors that are usually assumed to limit the activity of antisense oligonucleotides are cellular uptake, resistance to nucleases, and the stability of the hybrid formed. Modifications are usually chosen to improve one or more of these properties, as discussed in the previous sections. Overall activity results from the interplay of these and other factors whose relative importance is generally not known. However, a steady improvement in activity has been achieved by using this rational approach that is encouraging for the future of designing conjugates to meet specified requirements.

The modifications to the backbone that have been used most extensively are those discussed in previous contexts: phosphorothioates, methylphosphonates, phosphoramidates, and phosphotriesters. Chimeric oligonucleotides with several modified linkages at each end have been more successful with phosphorothioates than methylphosphonates (28, 60, 278).

A fundamental difference between negatively charged phosphodiester or phosphorothioate and the uncharged derivatives is their acceptance by ribonuclease H. This enzyme degrades the RNA strand of an RNA/DNA duplex and has been shown to be an important factor for the activity of antisense oligonucleotides in a number of systems. In these cases, binding of oligonucleotide at any site on the RNA should lead to cleavage and irreversible inactivation. In situations where this enzyme is not available, oligonucleotides are thought to inhibit expression by passive steric blocking of translation or other events (hybridization arrest). The particular binding site is then of great importance. With mRNA, for example, it appears that oligonucleotides can be readily displaced by ribosomes and were only effective when bound to the 5'-capped end or, to a lesser extent, across the AUG initiator (312).

Ribonuclease H recognizes the charged, unmodified or phosphorothioate backbone in oligodeoxynucleotides but not the uncharged methylphosphonate or phosphoramidates (56, 249, 252, 300, 313–315). Thus, passive hybridization arrest is the only known mechanism open to the latter compounds and the target site may be of prime importance with these modifications. There is a suggestion, however, that methylphosphonates may be more resistant to displacement from the RNA by cellular factors which could be a property of the uncharged backbone and could improve activity by the passive hybridization mechanism (316).

The importance of the binding site is well illustrated by the α -deoxyoligonucleotides which, despite their good hybridizing ability, do not activate ribonuclease H and were found inactive as antisense agents except when complementary to the 5'-capped end of mRNA (223, 314, 317–320).

With chain lengths of 20, methylphosphonates, phosphorothioates, and phosphoramidates were found to reduce the concentration of oligonucleotide necessary for good viral inhibition from over 20 μ M to 5 μ M or less (58, 278). Perhaps because of their somewhat weaker hybridization, reducing their chain length to 15 reduced activity far more than with the unmodified series. [In another study, however, 15 was found to be the optimum chain length for phosphonates (331).] Methylphosphonates with

chain lengths of 10 or less may have to be used at concentrations of 100 μ M or higher to achieve good results. Even so, they are often more active than the unmodified compounds (276, 308, 316, 321–326). Inappropriate chain length or binding site might be among the reasons for poor or no activity found in other examples (28, 224, 314, 315, 327).

In the ribo series, both methylation of the 2'-hydroxyl group and phosphorothioate substitution were necessary for antiviral activity in one study (60). The 2'-O-methyl substituent alone does not permit ribonuclease H digestion of the complementary RNA (328).

With chemical modification, there is always the possibility of introducing unwanted biological properties. This was seen with the phosphorothioates, which can bind rather well to a number of proteins and inhibit certain enzymes (314, 329, 330). As a result, in some antiviral and other assays, inhibition was not restricted to antisense sequences (58, 61, 327, 331). In further studies, antisense effects were separated from other effects of phosphorothioates (332, 333).

Among the true conjugates are derivatives with acridine linked at the 3'-end to stabilize hybridization. This modification increases activity and permits the use of unusually short oligonucleotides (334–337).

Conjugates of polylysine were reported to lower the concentration necessary for good antiviral activity to 1 μ M or below (59, 221, 224–226). This more than compensates for the increase in mass of material required due to the doubling of molecular weight (the preferred molecular weight for the peptide is about the same as that of a 20-base oligonucleotide). This approach does not work in all cells and polylysine is toxic at higher concentrations (225).

Another group that, like polylysine, is intended to increase uptake is cholesterol. This has beneficial effects for both unmodified and phosphorothioate backbones as well as for alkylating derivatives (61, 307).

In 1967, Belikova et al. made a dinucleotide carrying an alkylating reagent for the modification of complementary sequences (119). This was probably the first example of what would now be called an antisense oligonucleotide. Reactive compounds of this type have been investigated extensively by groups in the USSR (229). In recent years, attention in the West also has turned to these and other derivatives in Table VI that can cross-link or cleave the target RNA or DNA. This has come about with the need to develop more potent derivatives to improve the potential for therapeutic applications. If hybridization is reversible, so one argument goes, then a higher concentration of the oligonucleotide is required in the cell to maintain the complex than if the process were not reversible. Hence oligonucleotides that irreversibly change the target may be more potent.

This was demonstrated using antisense oligonucleotides to inhibit replication of a single-stranded DNA by *E. coli* DNA polymerase I (227). The enzyme was not inhibited by an unmodified oligonucleotide hybridized to the template unless the two were cross-linked. Presumably, as the enzyme reads the DNA, it can displace hybridized oligonucleotide in its path but becomes stalled when the oligonucleotide is irreversibly bound to the template.

Despite the large body of chemical work in this area, there are only a few examples of the use of chemically reactive oligonucleotides as antisense agents either in vitro or in vivo. These include an early inhibition of IgG synthesis in cells (229). More recently, the photoactivated

cross-linker psoralen was attached to oligonucleoside methylphosphonates and found to increase their potency by 20–40-fold in antiviral or inhibition of translation assays (249, 326).

A concern in using reactive conjugates of this type is the possibility of nonspecific reaction with other cell components leading to toxicity or, alternatively, self-inactivation. The latter has been found to limit the use of EDTA attached to methylphosphonates due to autocleavage of the conjugate group by the free radicals it generates (174).

5. CONCLUDING COMMENTS

Much current research at the interface of biology and chemistry is directed at understanding and predicting the effect of molecular structure on biological activity. Oligonucleotides are particularly well-suited for this type of activity. This is because of the nature of their site of action. Unlike most active compounds, this is not some hydrophobic pocket on a protein with unique and unpredictable properties. Rather it is a nucleic acid whose precise sequence can be determined and whose interaction with the oligonucleotide can be predicted with some confidence.

The encouraging finding from the work reviewed here is just how robust this mechanism for base pairing is toward chemical modification. The nature of the backbone can be changed from anionic to uncharged or cationic, from hydrophilic to lipophilic without seriously interfering with hybridization. Attempts to improve antisense inhibition in a rational way by altering specific features of the molecule have successfully increased activity. This is promising for prospects of tailoring molecules to particular purposes. These include improving performance and utility in areas where oligonucleotides have already found application such as diagnosis, genetic analysis, automated sequencing, and many others. It also includes meeting the pharmacological requirements for possible future drug development.

Whether or not modified oligonucleotides and their conjugates have the necessary attributes for pharmaceutical use, it is clear that they provide an unusual opportunity for the rational design of useful molecules with specific properties.

ACKNOWLEDGMENT

I wish to thank Paul Zamecnik for his enthusiastic support and encouragement and the referees for valuable suggestions. This work was supported by a grant from the G. Harold and Leila Y. Mathers Foundation, by National Cooperative Drug Discovery Group for the treatment of AIDS Grant U 01 AI24846 from the National Cancer Institute and the National Institute of Allergy and Infectious Diseases, and by Cancer Center Support Grant P30 C 12708-18 from the National Cancer Institute.

LITERATURE CITED

- (1) Khorana, H. G. (1979) Total synthesis of a gene. *Science* 203, 614–625.
- (2) Gait, J. J. (Ed.) (1984) *Oligonucleotide Synthesis a Practical Approach* IRL Press, Washington DC.
- (3) Sonveaux, E. (1986) The Organic Chemistry Underlying DNA Synthesis. *Bioorg. Chem.* 14, 274–325.
- (4) (a) Narang, S. A. (Ed.) (1987) *Synthesis and Applications of DNA and RNA* Academic Press, Orlando, FL. (b) Engels, J. W. and Uhlmann, E. (1989) Gene Synthesis. *Angew. Chem., Int. Ed. Engl.* 28, 716–734.

- (5) Caruthers, M. H. (1989) Synthesis of Oligonucleotides and Oligonucleotide Analogues. In *Oligodeoxynucleotides, Antisense Inhibitors of Gene Expression* (J. Cohen, Ed.) pp 7-24, Macmillan Press, London.
- (6) Narang, S. A.; Brousseau, R.; Hsiung, H. M., and Michniewicz, J. J. (1980) Chemical Synthesis of Deoxyoligonucleotides by the Modified Triester Method. *Methods Enzymol.* 65, 610-620.
- (7) Letsinger, R. L., Finnan, J. L., Heavner, G. A., and Lunsford, W. B. (1975) Phosphite coupling procedure for generating internucleotide links. *J. Am. Chem. Soc.* 97, 3278-3279.
- (8) Beaucage, S. L., and Caruthers, M. H. (1981) Deoxynucleoside phosphoramidites—a new class of key intermediates for deoxypolynucleotide synthesis. *Tetrahedron Lett.* 22, 1859-1862.
- (9) Garegg, P. J., Lindh, I., Regberg, T., Stawinski, J., and Stromberg, R. (1986) Nucleoside H-phosphonates. IV. Automated Solid Phase Synthesis of Oligoribonucleotides by the Hydrogen Phosphonate Approach. *Tetrahedron Lett.* 27, 4055-4058.
- (10) Froehler, B. C., and Matteucci, M. D. (1986) Nucleotide H-phosphonates: Valuable Intermediates in the Synthesis of Deoxyoligonucleotides. *Tetrahedron Lett.* 27, 469-472.
- (11) Hall, R. H., Todd, A., and Webb, R. F. (1957) Nucleotides. Part XLI. Mixed anhydrides as intermediates in the synthesis of dinucleoside phosphates. *J. Chem. Soc.* 3291.
- (12) Ogilvie, K. K., Usman, N., Nicoghossian, K., and Cedergren, R. J. (1988) Total chemical synthesis of a 77-nucleotide-long RNA sequence having methionine-acceptance activity. *Proc. Natl. Acad. Sci. U.S.A.* 85, 5764-5768.
- (13) Tanaka, T., Tamatsukuri, S., and Ikehara, M. (1987) Solid phase synthesis of oligoribonucleotides using the *o*-nitrobenzyl group for 2'-hydroxyl protection and H-phosphonate chemistry. *Nucleic Acids Res.* 15, 7235-7248.
- (14) Brown, J. M., Christodoulou, C., Modak, A. S., Reese, C. B., and Serafinowska, H. T. (1989) Synthesis of the 3'-terminal half of alanine transfer ribonucleic acid (tRNA^{ala}) by the phosphotriester approach in solution. Part 2. *J. Chem. Soc. Perkin Trans. 1* 1751-1767.
- (15) Anderson, D. J., Reischer, R. J., Taylor, A. J., and Wechter, W. J. (1984) Preparation and characterization of oligonucleotides of D- and L-2'-deoxyuridine. *Nucleosides Nucleotides* 3, 499-512.
- (16) Morvan, F., Rayner, B., Leonetti, J.-P., and Imbach, J.-L. (1988) α -DNA VII. Solid phase synthesis of α -anomeric oligodeoxyribonucleotides. *Nucleic Acids Res.* 16, 833-847.
- (17) Miller, P. S., Yano, J., Yano, E., Carroll, C., Jayaraman, K., and Ts'o, P. O. P. (1979) Nonionic nucleic acid analogues. Synthesis and characterization of dideoxyribonucleoside methylphosphonates. *Biochemistry* 18, 5134-5143.
- (18) Agarwal, K. L., and Riftina, F. (1979) Synthesis and enzymatic properties of deoxyribonucleotides containing methyl and phenylphosphonate linkages. *Nucleic Acids Res.* 9, 3009-3023.
- (19) Jager, A., and Engels, J. (1981) Synthesis of methylphosphonate and methylphosphotriester analogues of 2',5'-adenylate trimers. *Nucleic Acids Res. symp. Ser.* 9, 149-152.
- (20) Miller, P. S., Agris, C. H., Blandin, M., Murakami, A., Reddy, M. P., Spitz, S. A., and Ts'o, P. O. P. (1983) Use of methylphosphonic dichloride for the synthesis of oligonucleoside methylphosphonates. *Nucleic Acids Res.* 11, 5189-5204.
- (21) Miller, P. S., Agris, C. H., Murakami, A., Reddy, M. P., Spitz, S. A., and Ts'o, P. O. P. (1983) Preparation of oligodeoxyribonucleoside methylphosphonates on a polystyrene support. *Nucleic Acids Res.* 11, 6225-6242.
- (22) Miller, P. S., Reddy, M. P., Murakami, A., Blake, K. R., Lin, S.-B., and Agris, C. H. (1986) Solid-phase syntheses of oligodeoxyribonucleoside methylphosphonates. *Biochemistry* 25, 5092-5097.
- (23) Marugg, J. E., de Vroom, E., Dreef, C. E., Tromp, M., van der Marel, G. A., and van Boom, J. H. (1986) Synthesis of nucleic acid methylphosphonates via the 1-hydroxybenzotriazole phosphotriester approach. *Nucleic Acids Res.* 14, 2171-2185.
- (24) Sinha, N. D., Grossbruchhaus, V., and Koster, H. (1983) A new synthesis of oligodeoxynucleoside methylphosphonates on control pore glass polymer support using phosphite approach. *Tetrahedron Lett.* 24, 877-880.
- (25) Dorman, M. A., Noble, S. A., McBride, L. J., and Caruthers, M. H. (1984) Synthesis of oligodeoxynucleotides and oligodeoxynucleotide analogues using phosphoramidite intermediates. *Tetrahedron* 40, 95-102.
- (26) Jager, A., and Engels, J. (1984) Synthesis of deoxynucleoside methylphosphonates via a phosphoramidite approach. *Tetrahedron Lett.* 25, 1437-1440.
- (27) Agrawal, S., and Goodchild, J. (1987) Oligodeoxynucleoside methylphosphonates: synthesis and enzymic degradation. *Tetrahedron Lett.* 28, 3539-3542.
- (28) Tidd, D. M., Hawley, P., Warenus, H. M., and Gibson, I. (1988) Evaluation of N-ras oncogene anti-sense, sense and nonsense sequence methylphosphonate oligonucleotide analogues. *Anti-Cancer Drug Des.* 3, 117-127.
- (29) Murakami, A., Blake, K. R., and Miller, P. S. (1985) Characterization of sequence-specific oligodeoxyribonucleoside methylphosphonates and their interaction with rabbit globin mRNA. *Biochemistry* 24, 4041-4046.
- (30) Stec, W. J., Zon, G., Egan, W., Byrd, R. A., Phillips, L. R., and Gallo, K. A. (1985) Solid-phase synthesis, separation and stereochemical aspects of P-chiral methane- and 4,4'-dimethoxytriphenylmethane phosphonate analogues of oligodeoxyribonucleotides. *J. Org. Chem.* 50, 3908-3913.
- (31) Bergstrom, D. E., and Shum, P. W. (1988) Synthesis and characterization of a new fluorine substituted nonionic dinucleoside phosphonate analogue, P-deoxy-P-(difluoromethyl)thymidyl(3'-5')thymidine. *J. Org. Chem.* 53, 3953-3958.
- (32) Miller, P. S., Fang, K. N., Kondo, N. S., and Ts'o, P. O. P. (1971) Synthesis and properties of adenine and thymidine nucleoside alkyl phosphotriesters, the neutral analogs of dinucleoside monophosphates. *J. Am. Chem. Soc.* 93, 6657-6665.
- (33) Stec, W., Zon, G., Gallo, K. A., and Byrd, R. A. (1985) Synthesis and absolute configuration of P-chiral O-isopropyl oligonucleotide triesters. *Tetrahedron Lett.* 26, 2191-2194.
- (34) Koole, L. H., van Genderen, M. H. P., Reiniers, R. G., and Buck, H. M. (1987) Enhanced stability of a Watson and Crick DNA duplex structure by methylation of the phosphate groups in one strand. *Proc. K. Ned. Akad. Wet. B* 90, 41-46.
- (35) Koole, L. H., Quaedflieg, J. L. M., Kuijpers, W. H. A., Broeders, N. L. H. L., Langermans, H. A., van Genderen, M. H. P., and Buck, H. M. (1988) A novel synthetic approach to phosphate-methylated DNA oligomers using 9-fluorenylmethoxycarbonyl (Fmoc) as temporary base amino protecting group. *Proc. K. Ned. Akad. Wet. B* 91, 205-209.
- (36) Moody, H. M., van Genderen, M. H. P., Koole, L. H., Kocken, H. J. M., Meijer, E. M., and Buck, H. M. (1989) Regioselective inhibition of DNA duplication by antisense phosphate-methylated oligodeoxynucleotides. *Nucleic Acids Res.* 12, 4769-4782.
- (37) Uznanski, B., Grajkowski, A., and Wilk, A. (1989) The isopropoxyacetic group for convenient base protection during solid-support synthesis of oligodeoxyribonucleotides and their triester analogs. *Nucleic Acids Res.* 12, 4863-4871.
- (38) Letsinger, R. L., Groody, E. P., and Tanaka, T. (1982) Use of trichlorodimethylethyl as a protecting group and tributylphosphine as a deprotecting agent in oligonucleotide synthesis. *J. Am. Chem. Soc.* 104, 6805-6806.
- (39) Letsinger, R. L., Groody, E. P., Lander, N., and Tanaka, T. (1984) Some developments in the phosphite triester method for synthesis of oligonucleotides. *Tetrahedron* 40, 137-143.
- (40) Pless, R. C., and Ts'o, P. O. P. (1977) Duplex formation of a nonionic olig(deoxythymidylate) analogue [heptadeoxythymidyl-(3'-5')-deoxythymidine heptaethyl ester (d-[Tp(Et)]₇) with poly(deoxyadenylate). Evaluation of the electrostatic interaction. *Biochemistry* 16, 1239-1250.
- (41) Ogilvie, K. K., and Beaucage, S. L. (1979) Fluoride ion promoted deprotection and transesterification in nucleotide triesters. *Nucleic Acids Res.* 7, 805-823.
- (42) Koole, L. H., van Genderen, M. H. P., and Buck, H. M. (1987) A parallel right-handed duplex of the hexamer

- d(TpTpTpTpTpT) with phosphate triester linkages. *J. Am. Chem. Soc.* 109, 3916–3921.
- (43) Letsinger, R. L., Bach, S. A., and Eadie, J. S. (1986) Effects of pendant groups at phosphorus on binding properties of d-ApA analogues. *Nucleic Acids Res.* 14, 3487–3499.
- (44) Gallo, K. A., Shao, K.-L., Phillips, L. R., Regan, J. B., Koziolkiewicz, M., Uznanski, B., Stec, W. J., and Zon, G. (1986) Alkyl phosphotriester modified oligodeoxyribonucleotides. V. Synthesis and absolute configuration of R_p and S_p diastereoisomers of an ethyl phosphotriester (Et) modified *EcoRI* recognition sequence, d[GGAA(Et)TTCC]. A synthetic approach to regio- and stereospecific ethylation-interference studies. *Nucleic Acids Res.* 18, 7405–7420.
- (45) Froehler, B. C. (1986) Deoxynucleoside H-phosphonate diester intermediates in the synthesis of internucleotide phosphate analogues. *Tetrahedron Lett.* 27, 5575–5578.
- (46) Miller, P. S.; Chandrasegaran, S.; Dow, D. L.; Pulford, S. M., and Kan, L. S. (1982) Synthesis and template properties of an ethyl phosphotriester modified decadeoxyribonucleotide. *Biochemistry* 21, 5468–5474.
- (47) Weinfeld, M., and Livingston, D. C. (1986) Synthesis and properties of oligodeoxyribonucleotides containing an ethylated internucleotide phosphate. *Biochemistry* 25, 5083–5091.
- (48) Durand, M., Maurizot, J. C., Asseline, U., Barbier, C., Thuong, N. T., and Helene, C. (1989) Oligothymidylates covalently linked to an acridine derivative and with modified phosphodiester backbone: circular dichroism studies of their interactions with complementary sequences. *Nucleic Acids Res.* 17, 1823–1837.
- (49) Lancelot, G., Guesnet, J.-L., Asseline, U., and Thuong, N. T. (1988) NMR studies of complex formation between the modified oligonucleotide d(T*CTGT) covalently linked to an acridine derivative and its complementary sequence d(GCACAGAA). *Biochemistry* 27, 1265–1273.
- (50) Eckstein, F. (1985) Nucleoside phosphorothioates. *Annu. Rev. Biochem.* 54, 367–402.
- (51) Eckstein, F., and Gish, G. (1989) Phosphorothioates in molecular biology. *Trends Biol. Sci.* 14, 97–100.
- (52) Stein, C. A. (1989) Phosphorothioate oligodeoxynucleotide analogues. In *Oligodeoxynucleotides. Antisense Inhibitors of Gene Expression* (J. Cohen, Ed.) pp 97–117, Macmillan Press, London.
- (53) Stec, W. J., Zon, G., Egan, W., and Stec, B. (1984) Automated solid phase synthesis, separation and stereochemistry of phosphorothioate analogues of oligodeoxyribonucleotides. *J. Am. Chem. Soc.* 106, 6077–6079.
- (54) Stec, W. J., Zon, G., and Uznanski, B. (1985) Reversed-phase high-performance liquid chromatographic separation of diastereomeric phosphorothioate analogues of oligodeoxyribonucleotides and other backbone-modified congeners of DNA. *J. Chromatogr.* 326, 263–280.
- (55) Connolly, B. A., Potter, B. V. L., Eckstein, F., Pingoud, A., and Grotjahn, L. (1984) Synthesis and characterization of an octanucleotide containing the *EcoRI* recognition sequence with a phosphorothioate group at the cleavage site. *Biochemistry* 23, 3443–3453.
- (56) Stein, C. A.; Subasinghe, C.; Shinozuka, K., and Cohen, J. S. (1988) Physicochemical properties of phosphorothioate oligodeoxynucleotides. *Nucleic Acids Res.* 16, 3209–3221.
- (57) Fujii, M., Ozaki, K., Kume, A., Sekine, M., and Hata, T. (1986) Acylphosphonates. 5. A new method for stereospecific generation of phosphorothioate via aroyl phosphonate intermediate. *Tetrahedron Lett.* 27, 935–938.
- (58) Agrawal, S., Goodchild, J., Civeira, M. P., Thornton, A. H., Sarin, P. S., and Zamecnik, P. C. (1988) Oligodeoxynucleoside Phosphoramidates and Phosphorothioates as Inhibitors of Human Immunodeficiency Virus. *Proc. Natl. Acad. Sci. U.S.A.* 85, 7079–7083.
- (59) Matsukura, M., Zon, G., Shinozuka, K., Stein, C. A., Mitsuya, H., Cohen, J. S., and Broder, S. (1988) Synthesis of phosphorothioate analogues of oligodeoxyribonucleotides and their antiviral activity against human immunodeficiency virus (HIV). *Gene* 72, 343–347.
- (60) Shibahara, S., Mukai, S., Morisawa, H., Nakashima, H., Kobayashi, S., and Yamamoto, N. (1989) Inhibition of human immunodeficiency virus (HIV-1) replication by synthetic oligo-RNA derivatives. *Nucleic Acids Res.* 17, 239–252.
- (61) Letsinger, R. L., Zhang, G., Sun, D. K., Ikeuchi, T., and Sarin, P. S. (1989) Cholesteryl-conjugated oligonucleotides: synthesis, properties, and activity as inhibitors of replication of human immunodeficiency virus in cell culture. *Proc. Natl. Acad. Sci. U.S.A.* 86, 6553–6556.
- (62) Jager, A., Levy, M. J., and Hecht, S. M. (1988) Oligonucleotide *N*-alkylphosphoramidates: synthesis and binding to polynucleotides. *Biochemistry* 27, 7237–7246.
- (63) Letsinger, R. L., Singman, C. N., Hestand, G., and Salunkhe, M. (1988) Cationic oligonucleotides. *J. Am. Chem. Soc.* 110, 4470–4471.
- (64) Froehler, B., Ng, P., and Matteucci, M. (1988) Phosphoramidate analogues of DNA: synthesis and thermal stability of heteroduplexes. *Nucleic Acids Res.* 16, 4831–4839.
- (65) Tomasz, J., and Simoncsits, A. (1981) On the stability of phosphodiester-amide internucleotide bond. *Tetrahedron Lett.* 22, 3905–3908.
- (66) Gromova, E. S., Elob, A. A., Kubareva, E. A., Metev, V. G., and Shabarova, Z. A. (1986) Interaction of *EcoRII* restriction and modification enzymes with synthetic fragments of DNA. IV. DNA duplexes with phosphamide and pyrophosphate internucleotide bonds—substrates for the study of single-strand breaks. *Mol. Biol.* 20, 29–40.
- (67) Shabarova, Z. A. (1988) Chemical development in the design of oligonucleotide probes for binding to DNA and RNA. *Biochimie* 70, 1323–1334.
- (68) Mag, M., and Engels, J. W. (1989) Synthesis and selective cleavage of oligodeoxyribonucleotides containing non-chiral internucleotide phosphoramidate linkages. *Nucleic Acids Res.* 17, 5973–5988.
- (69) Roelen, H. C. P. F., de Vroom, E., van der Marel, G. A., and van Boom, J. H. (1988) Synthesis of nucleic acid methylphosphonothioates. *Nucleic Acids Res.* 16, 7633–7645.
- (70) Nemer, M. J., and Ogilvie, K. K. (1980) Ribonucleotide analogues having novel internucleotide linkages. *Tetrahedron Lett.* 21, 4149–4152.
- (71) Nagyvary, J., Chladek, S., and Roe, J. (1970) The synthesis of 5' thioanalogs of polydeoxyribonucleotides. *Biochem. Biophys. Res. Commun.* 39, 878–882.
- (72) Nemer, M. J., and Ogilvie, K. K. (1980) Phosphoramidate analogues of diribonucleoside monophosphates. *Tetrahedron Lett.* 21, 4153–4154.
- (73) Niewiarowski, W., Lesnikowski, Z. J., Wilk, A., Guga, P., Okruszek, A., Uznanski, B., and Stec, W. (1987) Diastereomers of thymidine 3'-*O*-(methanephosphonothioate): synthesis, absolute configuration and reaction with 3'-methoxyacetylthymidine under conditions of triester approach to oligonucleotide synthesis. *Acta Biochim. Pol.* 34, 217–231.
- (74) Nielsen, J., Brill, W. K.-D., and Caruthers, M. H. (1988) Synthesis and characterization of dinucleoside phosphorodithioates. *Tetrahedron Lett.* 29, 2911–2914.
- (75) Lawrence, D. P., Wenqiao, C., Zon, G., Stec, W. J., Uznanski, B., and Broido, M. S. (1987) NMR studies of backbone-alkylated DNA: duplex stability, absolute stereochemistry, and chemical shift anomalies of prototypal isopropyl phosphotriester modified octanucleotides, (R_p, R_p)- and (S_p, S_p)-{d-[GGA(iPr)ATTCC]}₂ and -{d-[GGAA(iPr)TTCC]}₂. *J. Biomol. Struct. Dyn.* 4, 757–783.
- (76) Guga, P., Koziolkiewicz, M., Okruszek, A., Uznanski, B., and Stec, W. J. (1987) DNA-triesters—the synthesis and absolute configuration assignments at P-stereogenic centres. *Nucleosides Nucleotides* 6, 111–119.
- (77) Cosstick, R., and Vyle, J. S. (1988) Synthesis and phosphorus-sulphur bond cleavage of 3'-thiothymidyl(3'-5')thymidine. *J. Chem. Soc. Chem. Commun.* 992–993.
- (78) Jones, G. H., Albrecht, H. P., Damodaran, N. P., and Moffatt, J. G. (1970) Synthesis of isosteric phosphonate analogs of some biologically important phosphodiester. *J. Am. Chem. Soc.* 92, 5510–5511.
- (79) Cosstick, R., and Vyle, J. S. (1990) Synthesis and properties of dithymidine phosphate analogues containing 3'-thiothymidine. *Nucleic Acids Res.* 18, 829–835.
- (80) Koole, L. H., Moody, H. M., and Buck, H. M. (1986) Pentacoordinated phosphorus as the internucleoside linkage. Syn-

- thesis and ^{31}P NMR study of the pseudorotational dynamics. *Recl. Trav. Chim. Pays-Bas* 105, 196–197.
- (81) Koole, L. H., van Genderen, M. H. P., and Buck, H. M. (1988) Conformational transmission in nucleotides containing trigonal bipyramidal phosphorus as the internucleoside linkage. *J. Org. Chem.* 53, 5266–5272.
 - (82) Pitha, J., Pitha, P. M., and Ts'o, P. O. P. (1970) Poly (1-vinyluracil): the preparation and interactions with adenosine derivatives. *Biochim. Biophys. Acta* 204, 39–48.
 - (83) Pitha, P. M., and Michelson, A. M. (1970) Preparation and properties of poly (1-vinylcytosine). *Biochim. Biophys. Acta* 204, 381–388.
 - (84) Boulton, M. G., Jones, A. S., and Walker, R. T. (1971) Synthetic analogues of polynucleotides. VI. The synthesis of ribonucleoside dialdehyde derivatives of polyacrylic acid hydrazide and their interaction with polynucleotides. *Biochim. Biophys. Acta* 246, 197–205.
 - (85) Mertes, M. P., and Coates, E. A. (1969) Synthesis of carbonate analogs of dinucleotides. 3'-thymidinyl 5'-thymidinyl carbonate, 3'-thymidinyl 5'-(5-fluoro-2'-deoxyuridinyl)carbonate and 3'-(5-fluoro-2'-deoxyuridinyl) 5'-thymidinyl carbonate. *J. Med. Chem.* 154–157.
 - (86) Jones, D. S., and Tittensor, J. R. (1969) The preparation of dinucleoside carbonates. *J. Chem. Soc. Chem. Commun.* 1240.
 - (87) Tittensor, J. R. (1971) The preparation of nucleoside carbonates. *J. Chem. Soc. C* 2656–2662.
 - (88) Bleaney, R. C., Jones, A. S., and Walker, R. T. (1975) Synthetic analogue of polynucleotides. Part XIV. The synthesis of poly(3'-O-carboxymethyl-deoxycytidine) and its interaction with polyinosinic acid. *Nucleic Acids Res.* 2, 699–706.
 - (89) Gait, M. J., Jones, A. S., and Walker, R. T. (1974) Synthetic analogues of polynucleotides. Part XII. Synthesis of thymidine derivatives containing oxyacetamido- or an oxyformamido-linkage instead of a phosphodiester group. *J. Chem. Soc., Perkin Trans. 1* 1684–1686.
 - (90) Jones, A. S., MacCoss, M., and Walker, R. T. (1973) Synthetic analogues of polynucleotides. X. The synthesis of poly(3'-O-carboxymethyl-2'-deoxyadenosine) and its interaction with polynucleotides. *Biochim. Biophys. Acta* 365, 365–377.
 - (91) Mungall, W. S., and Kaiser, J. K. (1977) Carbamate analogues of oligonucleotides. *J. Org. Chem.* 42, 703–706.
 - (92) Stirchak, E. P., Summerton, J. E., and Weller, D. D. (1987) Uncharged stereoregular nucleic acid analogues. I. Synthesis of a cytosine-containing oligomer with carbamate internucleoside linkages. *J. Org. Chem.* 52, 4202–4206.
 - (93) Coull, J. M., Carlson, D. V., and Weith, H. L. (1987) Synthesis and characterization of a carbamate-linked oligonucleoside. *Tetrahedron Lett.* 28, 745–748.
 - (94) Ogilvie, K. K., and Cormier, J. F. (1986) Synthesis of a thymidine dinucleotide analogue containing an internucleoside silyl linkage. *Tetrahedron Lett.* 26, 4159–4162.
 - (95) Seliger, H., and Feger, G. (1987) Oligonucleotide analogues with dialkyl silyl internucleoside linkages. *Nucleosides Nucleotides* 6, 483–484.
 - (96) Cormier, J. F., and Ogilvie, K. K. (1988) Synthesis of hexanucleotide analogues containing diisopropylsilyl internucleoside linkages. *Nucleic Acids Res.* 16, 4583–4594.
 - (97) Stirchak, E. P., Summerton, J. E., and Weller, D. (1989) Uncharged stereoregular nucleic acid analogs: 2. Morpholino nucleoside oligomers with carbamate internucleoside linkages. *Nucleic Acids Res.* 17, 6129–6141.
 - (98) Horn, T., and Urdea, M. S. (1989) Forks and Combs and DNA: the synthesis of branched oligodeoxyribonucleotides. *Nucleic Acids Res.* 17, 6959–6967.
 - (99) Urdea, M. S., Warner, B. D., Running, J. A., Stempien, M., Clyne, J., and Horn, T. (1988) A comparison of non-radioisotope hybridization assay methods using fluorescent, chemiluminescent and labeled synthetic oligodeoxyribonucleotide probes. *Nucleic Acids Res.* 16, 4937–4956.
 - (100) Gibson, K. J., and Benkovic, S. J. (1987) Synthesis and application of derivatizable oligonucleotides. *Nucleic Acids Res.* 15, 6455–6467.
 - (101) Meyer, R. B., Jr., Tabone, J. C., Hurst, G. D., Smith, T. M., and Gamper, H. (1989) Efficient, specific cross-linking and cleavage of DNA by stable, synthetic complementary oligodeoxynucleotides. *J. Am. Chem. Soc.* 111, 8517–8519.
 - (102) Allen, D. J., Darke, P. L., and Benkovic, S. J. (1989) Fluorescent oligonucleotides and deoxynucleotide triphosphates: preparation and their interaction with the large (Klenow) fragment of *Escherichia coli* DNA polymerase I. *Biochemistry* 28, 4601–4607.
 - (103) Haralambidis, J., Chai, M., and Tregar, G. W. (1987) Preparation of base modified nucleosides suitable for nonradioactive label attachment and their incorporation into synthetic oligodeoxyribonucleotides. *Nucleic Acids Res.* 15, 4857–4876.
 - (104) Jablonski, E., Moomaw, E. W., Tullis, R. H., and Ruth, J. L. (1986) Preparation of oligodeoxynucleotide-alkaline phosphatase conjugates and their use as hybridization probes. *Nucleic Acids Res.* 14, 6115–6128.
 - (105) Sung, W. L. (1981) Synthesis of 4-triazolopyrimidinone nucleotide and its application in synthesis of 5-methylcytosine-containing oligodeoxyribonucleotides. *Nucleic Acids Res.* 9, 6139–6151.
 - (106) Webb, T. R., and Matteucci, M. D. (1986) Hybridization triggered cross-linking of deoxyoligonucleotides. *Nucleic Acids Res.* 14, 7661–7674.
 - (107) Le Brun, S., Duchange, N., Namane, A., Zakin, M. M., Huynh-Dinh, T., and Igolen, J. (1989) Simple chemical synthesis and hybridization properties of non-radioactive DNA probes. *Biochimie* 71, 319–324.
 - (108) Dreyer, G. B., and Dervan, P. B. (1985) Sequence-specific cleavage of single-stranded DNA: oligodeoxynucleotide-EDTA-Fe(II). *Proc. Natl. Acad. Sci. U.S.A.* 82, 968–972.
 - (109) Roget, A., Bazin, H., and Teoule, R. (1989) Synthesis and use of labelled nucleoside phosphoramidite building blocks bearing a reporter group: biotinyl, dinitrophenyl, pyrenyl and dansyl. *Nucleic Acids Res.* 17, 7643–7651.
 - (110) Urdea, M. S., Running, J. A., Horn, T., Clyne, J., Ku, L., and Warner, B. D. (1987) A novel method for the rapid detection of specific nucleotide sequences in crude biological samples without blotting or radioactivity; application to the analysis of hepatitis B virus in human serum. *Gene* 61, 253–264.
 - (111) Wolfes, H., Fliess, A., Winkler, F., and Pingoud, A. (1986) Cross-linking of bromodeoxyuridine-substituted oligonucleotides to the *EcoRI* and *EcoRV* restriction endonucleases. *Eur. J. Biochem.* 159, 267–273.
 - (112) Pielles, U., Sproat, B. S., Neuner, P., and Cramer, F. (1989) Preparation of a novel psoralen containing deoxyadenosine building block for the facile solid phase synthesis of psoralen-modified oligonucleotides for a sequence specific crosslink to a given target sequence. *Nucleic Acids Res.* 17, 8967–8978.
 - (113) Smith, L. M., Fung, S., Hunkapiller, M. W., Hunkapiller, T. J., and Hood, L. E. (1985) The synthesis of oligonucleotides containing an aliphatic amino group at the 5'-terminus: synthesis of fluorescent DNA primers for use in DNA sequence analysis. *Nucleic Acids Res.* 13, 2399–2412.
 - (114) Sproat, B. S., Beijer, B., Rider, P., and Neuner, P. (1987) The synthesis of protected 5'-mercapto-2',5'-dideoxyribonucleoside-3'-O-phosphoramidates; uses of 5'-mercapto-oligodeoxyribonucleotides. *Nucleic Acids Res.* 15, 4837–4848.
 - (115) Sproat, B. S., Beijer, B., and Rider, P. (1987) The synthesis of protected 5'-amino-2',5'-dideoxyribonucleoside-3'-phosphoramidites; applications of 5'-amino-oligodeoxyribonucleotides. *Nucleic Acids Res.* 15, 6181–6196.
 - (116) Tanaka, T., Sakata, T., Fujimoto, K., and Ikehara, M. (1987) Synthesis of oligodeoxyribonucleotides with aliphatic amino or phosphate group at the 5' end by the phosphotriester method on a polystyrene support. *Nucleic Acids Res.* 15, 6209–6224.
 - (117) Himmelsbach, F., and Pfeleiderer, W. (1982) Bis-(p-nitrophenylethyl)phosphoromono-chloridate, a new versatile phosphorylating agent. *Tetrahedron Lett.* 23, 4793–4796.
 - (118) Thong, N. T., and Chassignol, M. (1987) Synthèse et réactivité d'oligothymidylates substitués par un agent intercalant et un groupe thiophosphate. *Tetrahedron Lett.* 28, 4157–4160.

- (119) Belikova, A. M., Zarytova, V. F., and Grineva, N. I. (1967) Synthesis of ribonucleosides and diribonucleoside phosphates containing 2-chloroethylamine and nitrogen mustard residues. *Tetrahedron Lett.* 3557-3562.
- (120) Francois, J.-C., Saison-Behmoaras, T., Chassignol, M., Thuong, N. T., and Helene, C. (1989) Sequence-targeted cleavage of single- and double-stranded DNA by oligothymidylates covalently linked to 1,10-phenanthroline. *J. Biol. Chem.* 264, 5891-5898.
- (121) Li, P., Medon, P. P., Skingle, D. C., Lanser, J. A., and Symons, R. H. (1987) Enzyme-linked synthetic oligonucleotide probes: non-radioactive detection of enterotoxigenic *Escherichia coli* in faecal specimens. *Nucleic Acids Res.* 15, 5275-5287.
- (122) Agrawal, S., Christodoulou, C., and Gait, M. J. (1986) Efficient methods for attaching non-radioactive labels to the 5'-end of synthetic oligodeoxyribonucleotides. *Nucleic Acids Res.* 14, 6227-6245.
- (123) Connolly, B. A. (1985) Chemical synthesis of oligonucleotides containing a free sulphhydryl group and subsequent attachment of thiol specific probes. *Nucleic Acids Res.* 13, 4485-4502.
- (124) Coull, J. M., Weith, H. L., and Bischoff, R. (1986) A novel method for the introduction of an aliphatic primary amino group at the 5' terminus of synthetic oligonucleotides. *Tetrahedron Lett.* 27, 3991-3994.
- (125) Kremsky, J. N., Wooters, J. L., Dougherty, J. P., Meyers, R. E., Collins, M., and Brown, E. L. (1987) Immobilization of DNA via oligonucleotides containing an aldehyde or carboxylic acid group at the 5' terminus. *Nucleic Acids Res.* 15, 2891-2909.
- (126) Connolly, B. A. (1987) The synthesis of oligonucleotides containing a primary amino group at the 5'-terminus. *Nucleic Acids Res.* 15, 3131-3139.
- (127) Bischoff, R., Coull, J. M., and Regnier, F. E. (1987) Introduction of 5'-terminal functional groups into synthetic oligonucleotides for selective immobilization. *Anal. Biochem.* 164, 336-344.
- (128) Blanks, R., and McLaughlin, L. W. (1988) An oligonucleotide affinity column for the isolation of sequence specific DNA binding proteins. *Nucleic Acids Res.* 16, 10283-10299.
- (129) Connell, C., Fung, S., Heiner, C., Bridgham, J., Chakerian, V., Heron, E., Jones, B., Menchen, S., Mordan, W., Raff, M., Recknor, M., Smith, L., Springer, J., Woo, S. and Hunkapiller, M. (1987) Automated DNA sequence analysis. *BioTechniques* 5, 342-348.
- (130) Sinha, N. D., and Cook, R. M. (1988) The preparation and application of functionalized synthetic oligonucleotides: III. Use of H-phosphonate derivatives of protected amino-hexanol and mercapto-propanol or hexanol. *Nucleic Acids Res.* 16, 2659-2669.
- (131) Ansorge, W., Sproat, B. S., Stegemann, J., and Schwager, C. (1986) A non-radioactive automated method for DNA sequence determination. *J. Biochem. Biophys. Methods* 13, 315-323.
- (132) Agrawal, S. (1989) Preparation of functionalized oligonucleoside methylphosphonate suitable for non-radioactive label attachment. *Tetrahedron Lett.* 30, 7025-7028.
- (133) Alves, A. M., Holland, D., and Edge, M. D. (1989) A chemical method of labelling oligodeoxyribonucleotides with biotin: a single step procedure using a solid phase methodology. *Tetrahedron Lett.* 30, 3089-3092.
- (134) Stein, C. A., Mori, K., Loke, S. L., Subsinghe, C., Shinokuka, K., Cohen, J. S., and Neckers, L. M. (1988) Phosphorothioate and normal oligodeoxyribonucleotides with 5'-linked acridine: characterization and preliminary kinetics of cellular uptake. *Gene* 72, 333-341.
- (135) Mori, K., Subasinghe, C., and Cohen, J. S. (1989) Oligodeoxynucleotide analogs with 5'-linked anthraquinone. *FEBS Lett.* 249, 213-218.
- (136) Asseline, U., and Thuong, N. T. (1988) Oligothymidylates substitues par un derive de l'acridine en position 5', a la fois en position 5' et 3' ou sur un phosphate internucleotidique. *Nucleosides Nucleotides* 7, 431-455.
- (137) Marugg, J. E., Piel, N., McLaughlin, L. W., Tromp, M., Veeneman, G. H., van der Marel, G. A., and van Boom, J. H. (1984) Polymer supported DNA synthesis using hydroxybenzotriazole activated phosphotriester intermediates. *Nucleic Acids Res.* 12, 8639-8651.
- (138) Uhlmann, E., and Engels, J. (1986) Chemical 5'-phosphorylation of oligonucleotides valuable in automated DNA synthesis. *Tetrahedron Lett.* 27, 1023-1026.
- (139) Horn, T., and Urdea, M. S. (1986) A chemical 5'-phosphorylation of oligodeoxyribonucleotides. *DNA* 5, 421-426.
- (140) Horn, T., Allen, J. S., and Urdea, M. S. (1987) Solid supported chemical 5'-phosphorylation of oligodeoxyribonucleotides that can be monitored by trityl cation release: application to gene synthesis. *Nucleosides Nucleotides* 6, 335-340.
- (141) van der Marel, G. A., van Boeckel, C. A. A., Wille, G., and van Boom, J. H. (1982) A general method for the synthesis of 5'-monophosphates of DNA fragments via phosphotriester intermediates. *Nucleic Acids Res.* 10, 2337-2351.
- (142) Kempe, T., Sundquist, W. I., Chow, F., and Hu, S.-L. (1985) Chemical and enzymatic biotin labelling of oligodeoxyribonucleotides. *Nucleic Acids Res.* 13, 45-57.
- (143) Wachter, L., Jablonski, J., and Ramachandran, K. L. (1986) A simple and efficient procedure for the synthesis of 5'-aminoalkyl oligonucleotides. *Nucleic Acids Res.* 14, 7985-7994.
- (144) Haralambidis, J., Duncan, L., Angus, K., and Tregear, G. W. (1990) The synthesis of polyamide-oligonucleotide conjugate molecules. *Nucleic Acids Res.* 18, 493-499.
- (145) Haralambidis, J., Angus, K., Pownall, S., Duncan, L., Chai, M., and Tregear, G. W. (1990) The preparation of polyamide-oligonucleotide probes containing multiple non-radioactive labels. *Nucleic Acids Res.* 18, 501-505.
- (146) Zuckermann, R., Corey, D., and Schultz, P. (1987) Efficient methods for attachment of thiol specific probes to the 3'-ends of synthetic oligodeoxyribonucleotides. *Nucleic Acids Res.* 15, 5305-5321.
- (147) Corey, D. R., and Schultz, P. G. (1987) Generation of a hybrid sequence-specific single-stranded deoxyribonuclease. *Science* 238, 1401-1403.
- (148) Nelson, P. S., Frye, R. A., and Liu, E. (1989) Bifunctional oligonucleotide probes synthesized using a novel CPG support are able to detect single base pair mutations. *Nucleic Acids Res.* 17, 7187-7194.
- (149) Asseline, U., Thuong, N. T., and Helene, C. (1986) Oligothymidylates substitues en position 3' par un derive de l'acridine. *Nucleosides Nucleotides* 5, 45-63.
- (150) Francios, J.-C., Saison-Behmoaras, T., Chassignol, M., Thuong, N. T., Sun, J.-S., and Helene, C. (1988) Periodic cleavage of poly(dA) by oligothymidylates covalently linked to the 1,10-phenanthroline-copper complex. *Biochemistry* 27, 2272-2276.
- (151) Letsinger, R. L., and Schott, M. E. (1981) Selectivity in binding a phenanthridinium-dinucleotide derivative to homopolynucleotides. *J. Am. Chem. Soc.* 103, 7394-7396.
- (152) Agrawal, S., and Tang, J.-Y. (1990) Site specific functionalization of oligodeoxynucleotides for non-radioactive labelling. *Tetrahedron Lett.* 31, 1543-1546.
- (153) Nelson, P. S., Sherman-Gold, R., and Leon, R. (1989) A new and versatile reagent for incorporating multiple primary aliphatic amines into synthetic oligonucleotides. *Nucleic Acids Res.* 17, 7179-7186.
- (154) Langer, P. R., Waldrop, A. A., and Ward, D. (1981) Enzymatic synthesis of biotin-labeled polynucleotides: novel nucleic acid affinity probes. *Proc. Natl. Acad. Sci. U.S.A.* 78, 6633-6637.
- (155) Murasugi, A., and Wallace, R. B. (1984) Biotin-labeled oligonucleotides: enzymatic synthesis and use as hybridization probes. *DNA* 3, 269-277.
- (156) Shimkus, M., Levy, J., and Herman, T. (1985) A chemically cleavable biotinylated nucleotide: usefulness in the recovery of protein-DNA complexes from avidin affinity columns. *Proc. Natl. Acad. Sci. U.S.A.* 82, 2593-2597.
- (157) Kumar, A., Tchen, P., Rouillet, F., and Cohen, J. (1988) Nonradioactive labelling of synthetic oligonucleotide probes with terminal deoxynucleotidyl transferase. *Anal. Biochem.* 169, 376-382.
- (158) Evan, R. K., Johnson, J. D., and Haley, B. E. (1986) 5-Azido-2'-deoxyuridine 5'-triphosphate: a photoaffinity-labeling

- reagent and tool for the enzymatic synthesis of photoactive DNA. *Proc. Natl. Acad. Sci. U.S.A.* 83, 5382-5386.
- (159) Evans, R. K., and Haley, B. E. (1987) Synthesis and biological properties of 5-azido-2'-deoxyuridine 5'-triphosphate, a photoactive nucleotide suitable for making light-sensitive DNA. *Biochemistry* 26, 269-276.
- (160) Trainor, G. L., and Jensen, M. A. (1988) A procedure for the preparation of fluorescence-labeled DNA with terminal deoxynucleotidyl transferase. *Nucleic Acids Res.* 16, 11846.
- (161) Iveron, B. L., and Dervan, P. B. (1987) Nonenzymatic sequence-specific cleavage of single-stranded DNA to nucleotide resolution. DNA methyl thioether probes. *J. Am. Chem. Soc.* 109, 1241-1243.
- (162) Gillam, I. C., and Tener, G. M. (1986) *N*⁴-(6-Aminoheptyl)cytidine and -deoxycytidine nucleotides can be used to label DNA. *Anal. Biochem.* 157, 199-207.
- (163) Eshaghpour, H., Soll, D., and Crothers, D. M. (1979) Specific chemical labeling of DNA fragments. *Nucleic Acids Res.* 7, 1485-1495.
- (164) Stade, K., Rinke-Appel, J., and Brimacombe, R. (1989) Site-directed cross-linking of mRNA analogues to the *Escherichia coli* ribosome; identification of 30S ribosomal components that can be cross-linked to the mRNA at various points 5' with respect to the decoding site. *Nucleic Acids Res.* 17, 9889-9908.
- (165) Vincent, C., Tchen, P., Cohen-Solal, M., and Kourilsky, P. (1982) Synthesis of 8-(2,4-dinitrophenyl 2-6 aminoheptyl) amino-adenosine 5' triphosphate: biological properties and potential uses. *Nucleic Acids Res.* 10, 6787-6796.
- (166) Cosstick, R., McLaughlin, L. W., and Eckstein, F. (1984) Fluorescent labeling of tRNA and oligodeoxynucleotides using T4 RNA ligase. *Nucleic Acids Res.* 12, 1791-1810.
- (167) England, T. E., Gumpert, R. I., and Uhlenbeck, O. C. (1977) Dinucleoside pyrophosphates are substrates for T4-induced RNA ligase. *Proc. Natl. Acad. Sci. U.S.A.* 74, 4839-4842.
- (168) Richardson, R. W., and Gumpert, R. I. (1983) Biotin and fluorescent labeling of RNA using T4 RNA ligase. *Nucleic Acids Res.* 11, 6167-6184.
- (169) Chollet, A., and Kawashima, E. H. (1985) Biotin-labeled synthetic oligodeoxyribonucleotides: chemical synthesis and uses as hybridization probes. *Nucleic Acids Res.* 13, 1529-1541.
- (170) Ghosh, S. S., and Musso, G. F. (1987) Covalent attachment of oligonucleotides to solid supports. *Nucleic Acids Res.* 15, 5353-5372.
- (171) Ruby, S. W., and Abelson, J. (1988) An early hierarchic role of U1 small nuclear ribonucleoprotein in spliceosome assembly. *Science* 242, 1028-1035.
- (172) Letsinger, R. L., and Schott, M. E. (1981) Selectivity in binding a phenanthridinium-dinucleotide derivative to homopolynucleotides. *J. Am. Chem. Soc.* 103, 7394-7396.
- (173) Chu, B. C. F., and Orgel, L. E. (1985) Nonenzymatic sequence-specific cleavage of single-stranded DNA. *Proc. Natl. Acad. Sci. U.S.A.* 82, 963-967.
- (174) Lin, S.-B., Blake, K. R., Miller, P. S., and Ts'o, P. O. P. (1989) Use of EDTA derivatization to characterize interactions between oligodeoxyribonucleoside methylphosphonates and nucleic acids. *Biochemistry* 28, 1054-1061.
- (175) Gingeras, T. R., Kwok, D. Y., and Davis, G. R. (1987) Hybridization properties of immobilized nucleic acids. *Nucleic Acids Res.* 15, 5373-5390.
- (176) Ghosh, S. S., Kao, P. M., and Kwok, D. Y. (1989) Synthesis of 5'-oligonucleotide hydrazide derivatives and their use in preparation of enzyme-nucleic acid hybridization probes. *Anal. Biochem.* 178, 43-51.
- (177) Gautier, C., Morvan, F., Rayner, B., Huynh-Dinh, T., Igoen, J., Imbach, J.-L., Paoletti, C., and Paoletti, J. (1987) α -DNA IV: α -anomeric and β -anomeric tetrathymidylates covalently linked to intercalating oxazolopyridocarbazole. Synthesis, physicochemical properties and poly(rA) binding. *Nucleic Acids Res.* 15, 6625-6641.
- (178) Nitta, N., Kuge, O., Yui, S., Tsugawa, A., Negishi, K., and Hayatsu, H. (1984) A new reaction useful for chemical cross-linking between nucleic acids and proteins. *FEBS Lett.* 194-198.
- (179) Chu, B. C. F., and Orgel, L. E. (1988) Ligation of oligonucleotides to nucleic acids or proteins via disulfide bonds. *Nucleic Acids Res.* 16, 3671-3691.
- (180) Corey, D. R., Pei, D., and Schultz, P. G. (1989) Sequence-selective hydrolysis of duplex DNA by an oligonucleotide-directed nuclease. *J. Am. Chem. Soc.* 111, 8523-8525.
- (181) Teare, J., and Wollenzien, P. (1989) Specificity of site directed psoralen addition to RNA. *Nucleic Acids Res.* 17, 3359-3372.
- (182) Oser, A., Roth, W. K., and Valet, G. (1988) Sensitive non-radioactive dot-blot hybridization using DNA probes labelled with chelate group substituted psoralen and quantitative detection by europium ion fluorescence. *Nucleic Acids Res.* 16, 1181-1196.
- (183) Ralph, R. K., Young, R. J., and Khorana, H. G. (1962) The labelling of phosphomonoester end groups in amino acid acceptor ribonucleic acids and its use in the determination of nucleotide sequences. *J. Am. Chem. Soc.* 84, 1490-1491.
- (184) Ivanovskaya, M. G., Gottikh, M. B., and Shabarova, Z. A. (1987) Modification of oligo(poly)nucleotide phosphomonoester groups in aqueous solutions. *Nucleosides Nucleotides* 6, 913-934.
- (185) Sokolova, N. I., Ashirbekova, D. T., Dolinnaya, N. G., and Shabarova, Z. A. (1988) Chemical reactions within DNA duplexes. Cyanogen bromide as an effective oligodeoxyribonucleotide coupling agent. *FEBS Lett.* 232, 153-155.
- (186) Ferris, J. P., Huang, C.-H., and Hagan, W. J., Jr. (1989) *N*-Cyanimidazole and diimidazole imine: water-soluble condensing agents for the formation of the phosphodiester bond. *Nucleosides Nucleotides* 8, 407-414.
- (187) Chu, B. C. F., Wahl, G. M., and Orgel, L. E. (1983) Derivatization of unprotected polynucleotides. *Nucleic Acids Res.* 11, 6513-6529.
- (188) Shabarova, Z. A., Ivanovskaya, M. G., and Isagulants, M. G. (1983) DNA-like duplexes with repetitions: efficient template-guided polycondensation of decadeoxyribonucleotide imidazolidine. *FEBS Lett.* 154, 288-292.
- (189) Lee, B. L., Murakami, A., Blake, K. R., Lin, S.-B., and Miller, P. S. (1988) Interaction of psoralen-derivatized oligodeoxyribonucleoside methylphosphonates with single-stranded DNA. *Biochemistry* 27, 3197-3203.
- (190) Oshevski, S. I. (1982) Enzymatic transfer of ATP γ S thiophosphate onto the 5'-hydroxyl of an oligonucleotide as a route to reactive oligonucleotide derivatives. *FEBS Lett.* 143, 119-123.
- (191) Fidanza, J. A., and McLaughlin, L. W. (1989) Introduction of reporter groups at specific sites in DNA containing phosphorothioate diesters. *J. Am. Chem. Soc.* 111, 9117-9119.
- (192) Hodges, R. R., Conway, N. E., and McLaughlin, L. W. (1989) "Post-assay" covalent labeling of phosphorothioate-containing nucleic acids with multiple fluorescent markers. *Biochemistry* 28, 261-267.
- (193) Praseuth, D., Perrouault, L., Le Doan, T., Chassignol, M., Thuong, N., and Helene, C. (1988) Sequence-specific binding and photocrosslinking of α and β oligodeoxynucleotides to the major groove of DNA via triple-helix formation. *Proc. Natl. Acad. Sci. U.S.A.* 85, 1349-1353.
- (194) Le Doan, T., Perrouault, L., Praseuth, D., Habhou, N., Decout, J.-L., Thuong, N. T., Lhomme, J., and Helene, C. (1987) Sequence-specific recognition, photocrosslinking and cleavage of the DNA double helix by an oligo-[α]-thymidylate covalently linked to an azidoproflavine derivative. *Nucleic Acids Res.* 15, 7749-7760.
- (195) Broker, T. R., Angerer, L. M., Yen, P. H., Hershey, N. D., and Davidson, N. (1978) Electron microscopic visualization of tRNA genes with ferritin-avidin: biotin labels. *Nucleic Acids Res.* 5, 363-384.
- (196) Towbin, H., and Elson, D. (1978) A photoaffinity labeling study of the messenger RNA-binding region of *Escherichia coli* ribosomes. *Nucleic Acids Res.* 5, 3389-3407.
- (197) Schreiber, J. P., Hsiung, N., and Cantor, C. R. (1979) Fluorescence studies of the accessibility of the 3' ends of the ribosomal RNAs in *Escherichia coli* ribosomes and subunits. *Nucleic Acids Res.* 6, 181-193.

- (198) Stoffler-Meilicke, M., Stoffler, G., Odom, O. W., Zinn, A., Kramer, G. and Hardesty, B. (1981) Localization of 3' ends of 5S and 23S rRNAs in reconstituted subunits of *Escherichia coli* ribosomes. *Proc. Natl. Acad. Sci. U.S.A.* 78, 5538-5542.
- (199) Forster, A. C., McInnes, J. L., Skingle, D. C., and Symons, R. H. (1985) Nonradioactive hybridization probes prepared by the chemical labelling of DNA and RNA with a novel reagent, photobiotin. *Nucleic Acids Res.* 13, 745-761.
- (200) Hopman, A. H. N., Wiegant, J., Tesser, G. I., and Van Duijn, P. (1986) A non-radioactive *in situ* hybridization method based on mercurated nucleic acid probes and sulfhydryl-hapten ligands. *Nucleic Acids Res.* 14, 6471-6487.
- (201) Hayatsu, H. (1976) Reaction of cytidine with semicarbazide in the presence of bisulfite. A rapid modification specific for single-stranded polynucleotide. *Biochemistry* 15, 2677-2682.
- (202) Reisfeld, A., Rothenberg, J. M., Bayer, E. A., and Wilchek, M. (1987) Nonradioactive hybridization probes prepared by the reaction of biotin hydrazide with DNA. *Biochem. Biophys. Res. Commun.* 142, 519-526.
- (203) Tchen, P., Fuchs, R. P. P., Sage, E., and Leng, M. (1984) Chemically modified nucleic acids as immunodetectable probes in hybridization experiments. *Proc. Natl. Acad. Sci. U.S.A.* 81, 3466-3470.
- (204) Landegent, J. E., Jansen in de Wal, N., Baan, R. A., Hoelijmakers, J. H. J., and van der Ploeg, M. (1984) 2-Acetylaminofluorene-modified probes for the indirect hybridocytochemical detection of specific nucleic acid sequences. *Exp. Cell Res.* 153, 61-72.
- (205) Gamper, H. B., Cimino, G. D., and Hearst, J. E. (1987) Solution hybridization of crosslinkable DNA oligonucleotides to bacteriophage M13 DNA. Effects of secondary structure on hybridization kinetics and equilibria. *J. Mol. Biol.* 197, 349-362.
- (206) Stuart, A., and Khorana, H. G. (1963) The selective acetylation of terminal hydroxyl groups in deoxyribo-oligonucleotides. *J. Am. Chem. Soc.* 85, 2346-2347.
- (207) Heyduk, T., and Lee, J. C. (1990) Application of fluorescence energy transfer and polarization to monitor *Escherichia coli* cAMP receptor protein and *lac* promoter interaction. *Proc. Natl. Acad. Sci. U.S.A.* 87, 1744-1748.
- (208) Prober, J. M., Trainor, G. L., Dam, R. J., Hobbs, F. W., Robertson, C. W., Zagursky, R. J., Cocuzza, A. J., Jensen, M. A., and Baumeister, K. (1987) A system for rapid DNA sequencing with fluorescent chain-terminating dideoxyoligonucleotides. *Science* 238, 336-341.
- (209) Cardullo, R. A., Agrawal, S., Flores, C., Zamecnik, P. C., and Wolf, D. E. (1988) Detection of nucleic acid hybridization by nonradiative fluorescence resonance energy transfer. *Proc. Natl. Acad. Sci. U.S.A.* 85, 8790-8794.
- (210) Telser, J., Cruickshank, K. A., Morrison, L. E., and Netzel, T. L. (1989) Synthesis and characterization of DNA oligomers and duplexes containing covalently attached molecular labels: comparison of biotin, fluorescein and pyrene labels by thermodynamic and optical spectroscopic measurements. *J. Am. Chem. Soc.* 111, 6966-6976.
- (211) Murchie, A. I. H., Clegg, R. M., von Kitzing, E., Duckett, D. R., Diekmann, S., and Lilley, D. M. J. (1989) Fluorescence energy transfer shows that the four-way DNA junction is a right-handed cross of antiparallel molecules. *Nature (London)* 341, 763-766.
- (212) Asseline, U., Delarue, M., Lancelot, G., Toulme, F., Thuong, N. T., Montenay-Garestier, T., and Helene, C. (1984) Nucleic acid-binding molecules with high affinity and base sequence specificity: intercalating agents covalently linked to oligodeoxynucleotides. *Proc. Natl. Acad. Sci. U.S.A.* 81, 3297-3301.
- (213) Asseline, U., Toulme, F., Thuong, N. T., Delarue, M., Montenay-Garestier, T., and Helene, C. (1984) Oligodeoxynucleotides covalently linked to intercalating dyes as base sequence-specific ligands. Influence of dye attachment site. *EMBO J.* 3, 795-800.
- (214) Asseline, U., Thuong, N. T., and Helen, C. (1985) Oligonucleotides covalently linked to intercalating agents. *J. Biol. Chem.* 260, 8936-8941.
- (215) Praseuth, D., Chassignol, M., Takasugi, M., Le Doan, T., Thuong, N. T., and Helene, C. (1987) Double helices with parallel strands are formed by nuclease-resistant oligo-[α]-deoxynucleotides and oligo-[α]-deoxynucleotides covalently linked to an intercalating agent with complementary oligo-[β]-deoxynucleotides. *J. Mol. Biol.* 196, 939-942.
- (216) Sun, J., Asseline, U., Rouzaud, D., Montenay-Garestier, T., Thuong, N. T., and Helen, C. (1987) Oligo-[α]-deoxynucleotides covalently linked to an intercalating agent. Double helices with parallel strands are formed with complementary oligo-[β]-deoxynucleotides. *Nucleic Acids Res.* 15, 6149-6158.
- (217) Arnold, L. J., Jr., Hammond, P. W., Wiese, W. A., and Nelson, N. C. (1989) Assay formats involving acridinium-ester-labeled DNA probes. *Clin. Chem.* 35, 1588-1594.
- (218) Bazile, D., Gautier, C., Rayner, B., Imbach, J.-L., Paoletti, C., and Paoletti, J. (1989) α -DNA X: α and β tetrathymidylates covalently linked to oxazolopyridocarbazolium (OPC): comparative stabilization of oligo β -[dT]:oligo β -[dA] and oligo α -[dT]:oligo β -[dA] duplexes by the intercalating agent. *Nucleic Acids Res.* 17, 7749-7759.
- (219) Kutyavin, I. V., Podyminogin, M. A., Bazhina, Y. N., Fedorova, O. S., Knorre, D. G., Levina, A. S., Mamayev, S. V., and Zarytova, V. F. (1988) *N*-(2-Hydroxyethyl)phenazinium derivatives of oligonucleotides as effectors of the sequence-specific modification of nucleic acids with reactive oligonucleotide derivatives. *FEBS Lett.* 238, 35-38.
- (220) Heller, M. J., and Morrison, L. E. (1985) Chemiluminescent and fluorescent probes for DNA hybridization systems. In *Rapid Detection and Identification of Infectious Agents* (D. T. Kingsbury, Ed.) pp 245-256, Academic Press, Orlando, FL.
- (221) Lemaitre, M., Bayard, B., and Lebleu, B. (1987) Specific antiviral activity of a poly(L-lysine)-conjugated oligodeoxyribonucleotide sequence complementary to vesicular stomatitis virus N protein mRNA initiation site. *Proc. Natl. Acad. Sci. U.S.A.* 84, 648-652.
- (222) Lemaitre, M., Bisbal, C., Bayard, B., and Lebleu, B. (1987) Biological activities of oligonucleotides linked to poly(L-lysine). *Nucleosides Nucleotides* 6, 311-315.
- (223) Leonetti, J. P., Rayner, B., Lemaitre, M., Gagnor, C., Milhaud, P. G., Imbach, J.-L., and Lebleu, B. (1988) Antiviral activity of conjugates between poly(L-lysine) and synthetic oligodeoxyribonucleotides. *Gene* 72, 323-332.
- (224) Stevenson, M., and Iverson, P. L. (1989) Inhibition of human immunodeficiency virus type I-mediated cytopathic effects by poly(L-lysine)-conjugated synthetic antisense oligodeoxyribonucleotides. *J. Gen. Virol.* 70, 2673-2682.
- (225) Degols, G., Leonetti, J.-P., Gagnor, C., Lemaitre, M. and Lebleu, B. (1989) Antiviral activity and possible mechanisms of action of oligonucleotides-poly(L-lysine) conjugates targeted to vesicular stomatitis virus mRNA and genomic RNA. *Nucleic Acids Res.* 17, 9341-9350.
- (226) Westerman, P., Gross, B., and Hoinkis, G. (1989) Inhibition of expression of SV40 virus large T-antigen by antisense oligodeoxyribonucleotides. *Biomed. Biochim. Acta* 48, 85-93.
- (227) Chu, B. C. F., and Orgel, L. E. (1989) Inhibition of DNA synthesis by cross-linking the template to platinum-thiol derivatives of complementary oligonucleotides. *Nucleic Acids Res.* 17, 4783-4798.
- (228) Zuckermann, R. N., Corey, D. R., and Schultz, P. G. (1988) Site-selective cleavage of RNA by a hybrid enzyme. *J. Am. Chem. Soc.* 110, 1614-1615.
- (229) Knorre, D. G., and Vlassov, V. V. (1985) Complementary-addressed (sequence-specific) modification of nucleic acids. *Prog. Nucleic Acids Res. Mol. Biol.* 32, 291-320.
- (230) Fedorova, O. S., Knorre, D. G., Podust, L. M. and Zarytova, V. F. (1988) Complementary addressed modification of double-stranded DNA within a ternary complex. *FEBS Lett.* 228, 273-276.
- (231) Babkin, I. V., Butorin, A. S., Ivanova, E. M., and Rait, A. S. (1988) Chemical conversions of radioactive 4-(*N*-2-chloroethyl-*N*-methylamino)-benzyl-5'-[32 P]phosphamides of oligodeoxyribonucleotides in experiments in vivo. *Bio-khimiya* 53, 384-393.

- (232) Abramova, T. V., Vlassov, V. V., Lebedev, A. V., and Rytte, A. S. (1988) Complementary addressed modification of nucleic acids with the alkylating derivatives of oligothymidylate ethyl phosphotriesters. *FEBS Lett.* 236, 243-245.
- (233) Vlassov, V. V., Gaidamakov, S. A., Zarytova, V. F., Knorre, D. G., Levina, A. S., Nikonova, A. A., Podust, L. M., and Fedorova, O. S. (1988) Sequence-specific chemical modification of double-stranded DNA with alkylating oligodeoxyribonucleotide derivatives. *Gene* 72, 313-322.
- (234) Vlassov, V. V., Gorn, V. V., Ivanova, E. M., Kazakov, S. A., and Mamev, S. V. (1983) Complementary addressed modification of oligonucleotide d(pGpGpCpGpGpA) with platinum derivative of oligonucleotide d(pTpCpCpGpCpCpTpTpT). *FEBS Lett.* 162, 286-289.
- (235) Iverson, B. L., and Dervan, P. B. (1987) Nonenzymatic sequence-specific cleavage of single-stranded DNA to nucleotide resolution. DNA methyl thioether probes. *J. Am. Chem. Soc.* 109, 1241-1243.
- (236) Moser, H. E., and Dervan, P. B. (1987) Sequence-specific cleavage of double helical DNA by triplet helix formation. *Science* 238, 645-650.
- (237) Boidot-Forget, M., Chassignol, M., Takasugi, M., Thuong, N. T., and Helene, C. (1988) Site-specific cleavage of single-stranded and double-stranded DNA sequences by oligodeoxyribonucleotides covalently linked to an intercalating agent and an EDTA-Fe chelate. *Gene* 72, 361-371.
- (238) Povsic, T. J., and Dervan, P. B. (1989) Triple helix formation by oligonucleotides on DNA extended to the physiological pH range. *J. Am. Chem. Soc.* 111, 3059-3061.
- (239) Sun, J.-S., Francois, J.-C., Lavery, R., Saison-Behmoaras, T., Montenay-Garstier, T., Thuong, N. T., and Helen, C. (1988) Sequence-targeted cleavage of nucleic acids by oligo- α -thymidylate-phenanthroline conjugates: parallel and antiparallel double helices are formed with DNA and RNA respectively. *Biochemistry* 27, 6039-6045.
- (240) Chen, C. B., and Sigman, D. S. (1988) Sequence-specific scission of RNA by 1,10-phenanthroline-copper linked to deoxyoligonucleotides. *J. Am. Chem. Soc.* 110, 6570-6572.
- (241) Le Doan, T., Perrouault, L., Helen, C., Chassignol, M., and Thuong, N. T. (1986) Targeted Cleavage of Polynucleotides by complementary oligonucleotides covalently linked to iron-porphyrins. *Biochemistry* 25, 6736-6739.
- (242) Le Doan, T., Perrouault, L., Chassignol, M., Thuong, N. T., and Helen, C. (1987) Sequence-targeted chemical modifications of nucleic acids by complementary oligonucleotides covalently linked to porphyrins. *Nucleic Acids Res.* 15, 8643-8659.
- (243) Arai, H., Emson, P. C., Agrawal, S., Christodoulou, C., and Gait, M. J. (1988) In situ hybridization histochemistry: localisation of vasopressin mRNA in rat brain using a biotinylate oligonucleotide probe. *Mol. Brain Res.* 4, 63-69.
- (244) Ven Murthy, M. R., Bharucha, A. D., and Charbonneau, R. (1986) Preparation and biochemical manipulation of mRNAs and cDNAs on small oligo(dT)-cellulose discs. *Nucleic Acids Res.* 14, 7134.
- (245) Wolf, S. F., Haines, L., Fisch, J., Kremsky, J. N., Dougherty, J. P., and Jacobs, K. (1987) Rapid hybridization kinetics of DNA attached to submicron latex particles. *Nucleic Acids Res.* 15, 2911-2926.
- (246) Zischler, H., Nanda, I., Schafer, R., Schmid, M., and Epplen, J. T. (1989) Digoxigenated oligonucleotide probes specific for simple repeats in DNA fingerprinting and hybridization in situ. *Hum. Genet.* 82, 227-233.
- (247) Ramirez, F., Mandal, S. B., and Marecek, J. F. (1983) Synthesis of an oligonucleotide with a terminal puromycin. *Synthesis* 5, 443-444.
- (248) Ramirez, F., Mandal, S. B., and Marecek, J. F. (1982) Nucleotidophospholipids: oligonucleotide derivatives with membrane-recognition groups. *J. Am. Chem. Soc.* 104, 5483-5486.
- (249) Kean, J. M., Murakami, A., Blake, K. R., Cushman, C. D., and Miller, P. S. (1988) Photochemical cross-linking of psoralen-derivatized oligonucleoside methylphosphonates to rabbit globin messenger RNA. *Biochemistry* 27, 9113-9121.
- (250) Matthews, J. A., and Kricka, L. J. (1988) Analytical strategies for the use of DNA probes. *Anal. Biochem.* 169, 1-25.
- (251) Shibahara, S., Mukai, S., Nishihara, T., Inoue, H., Ohtsuka, E., and Morisawa, H. (1987) Site-directed cleavage of RNA. *Nucleic Acids Res.* 15, 4403-4415.
- (252) Agrawal, S., Mayrand, S., Zamecnik, P. C., and Pederson, T. Site-specific excision from RNA by RNase H and mixed-phosphate-backbone oligonucleotides. *Proc. Natl. Acad. Sci. U.S.A.*, in press.
- (253) Kim, S. C., Podhajska, A. J., and Szybalski, W. (1988) Cleaving DNA at any predetermined site with adapter-primers and class-IIS restriction enzymes. *Science* 240, 504-506.
- (254) Bower, M., Summers, M. F., Powell, C., Shinozuka, K., Regan, J. B., Zon, G., and Wilson, W. D. (1987) Oligodeoxyribonucleoside methylphosphonates. NMR and UV spectroscopic studies of R_p - R_p and S_p - S_p methylphosphonate (Me) modified duplexes of {d[GGAATTC]}₂. *Nucleic Acids Res.* 15, 4915-4930.
- (255) Chacko, K. K., Lindner, K., and Saenger, W. (1983) Molecular structure of deoxyadenylyl-3'-methylphosphonate-5'-thymidine dihydrate, (d-ApT·2H₂O), a dinucleoside monophosphate with neutral phosphodiester backbone. An X-ray crystal study. *Nucleic Acids Res.* 11, 2801-2814.
- (256) Summers, M. F., Powell, C., Egan, W., Byrd, R. A., Wilson, W. D., and Zon, G. (1986) Alkyl phosphotriester modified oligodeoxyribonucleotides. VI. NMR and UV spectroscopic studies of ethyl phosphotriester (Et) modified R_p - R_p and S_p - S_p duplexes, {d[GGAATTC]}₂. *Nucleic Acids Res.* 14, 7421-7436.
- (257) Kan, L.-S., Cheng, D. M., Chandrasegaran, S., Pramanik, P., and Miller, P. S. (1987) Structural and conformational studies on deoxyguanosyl-3',5'-deoxyadenosine monophosphate and its ethyl phosphotriester analogs—left-handed dimers. *J. Biomol. Struct. Dyn.* 4, 785-796.
- (258) Bryant, F. R., and Benkovic, S. J. (1979) Stereochemical course of the reaction catalyzed by 5'-nucleotide phosphodiesterase from snake venom. *Biochemistry* 18, 2825-2828.
- (259) Burgers, P. M. J., and Eckstein, F. (1979) Diastereomers of 5'-O-adenosyl 3'-O-uridyl phosphorothioate: chemical synthesis and enzymatic properties. *Biochemistry* 18, 592-596.
- (260) Potter, B. V. L., Romaniuk, P. J., and Eckstein, F. (1983) Stereochemical course of DNA hydrolysis by nuclease S1. *J. Biol. Chem.* 258, 1758-1773.
- (261) Potter, B. V. L., Connolly, B. A., and Eckstein, F. (1983) Synthesis and configurational analysis of a dinucleoside phosphate isotopically chiral at phosphorus. Stereochemical course of *Penicillium citrum* nuclease P1 reaction. *Biochemistry* 22, 1369-1377.
- (262) Lesnikowski, Z. J., Niewiarowski, W., Zielinski, W. S., and Stec, W. J. (1984) 2'-Deoxyribonucleoside 3'-aryl phosphoranilidates. Key intermediates in the stereospecific synthesis of 2'-deoxyribonucleoside cyclic 3',5'-phosphorothioates and dinucleoside(3'-5')-phosphorothioates. *Tetrahedron* 40, 15-32.
- (263) Fujii, M., Ozaki, K., Kume, A., Sekine, M., and Hata, T. (1986) Acylphosphonates. 6. Reaction mechanism of Zn/Me₃SiCl mediated conversion of 2,2,2-trichloroethoxycarbonylphosphonates to silyl phosphites. *Tetrahedron Lett.* 27, 3365-3368.
- (264) Lesnikowski, Z. J., Wolkani, P. J., and Stec, W. J. (1987) Stereospecific synthesis of (Rp)- and (Sp)-thymidylyl-(3',5')thymidylyl methanephosphonates. *Tetrahedron Lett.* 28, 5535-5538.
- (265) Fujii, M., Ozaki, K., Kume, A., Sekine, M., and Hata, T. (1986) Acylphosphonates. 5. A new method for stereospecific generation of phosphorothioate via aroylphosphonate intermediate. *Tetrahedron Lett.* 26, 935-938.
- (266) Lesnikowski, Z. J., Jaworska, M., and Stec, W. J. (1988) Stereoselective synthesis of P-homo-chiral oligo(thymidine methanephosphonates). *Nucleic Acids Res.* 16, 11675-11689.
- (267) Lebedev, A. V., Rife, J. P., Seligsohn, H. W., Wenzinger, G. R., and Wickstrom, E. (1990) Stereospecific coupling reaction for internucleotide methyl phosphonothioate linkage. *Tetrahedron Lett.* 31, 855-858.
- (268) Stec, W. J., and Zon, G. (1984) Stereochemical studies of the formation of chiral internucleotide linkages by phosphor-

- midite coupling in the synthesis of oligodeoxyribonucleotides. *Tetrahedron Lett.* 25, 5279-5282.
- (269) Lebedev, A. V., Wenzinger, G. R., and Wickstrom, E. (1990) A new DMAP-catalyzed phosphoramidite coupling reaction for synthesis of oligonucleotide methylphosphonate derivatives. *Tetrahedron Lett.* 31, 851-854.
- (270) Miller, P. S., Dreon, N., Pulford, S. M., and McParland, K. B. (1980) Oligothymidylate analogues having stereoregular, alternating methylphosphonate/phosphodiester backbones. Synthesis and physical studies. *J. Biol. Chem.* 255, 9659-9665.
- (271) Noble, S. A., Fisher, E. F., and Caruthers, M. H. (1984) Methylphosphonates as probes of protein-nucleic acid interactions. *Nucleic Acids Res.* 12, 3387-3404.
- (272) Callahan, L., Han, F.-S., Watt, W., Duchamp, D., Kezdy, F. J., and Agarwal, K. (1986) B- to Z-transition probed by oligonucleotides containing methylphosphonates. *Proc. Natl. Acad. Sci. U.S.A.* 83, 1617-1621.
- (273) Griffiths, A. D., Potter, B. V. L., and Eperon, I. C. (1987) Stereospecificity of nucleases towards phosphorothioate-substituted RNA: stereochemistry of transcription by T7 RNA polymerase. *Nucleic Acids Res.* 15, 4145-4162.
- (274) Latimer, L. J. P., Hampel, K., and Lee, J. S. (1989) Synthetic repeating sequence DNAs containing phosphorothioates: nuclease sensitivity and triplex formation. *Nucleic Acids Res.* 17, 1549-1561.
- (275) Miller, P. S., Barrett, J. C., and Ts'o, P. O. P. (1974) Synthesis of oligodeoxyribonucleotide ethyl phosphotriesters and their specific complex formation with transfer ribonucleic acid. *Biochemistry* 13, 4887-4896.
- (276) Miller, P. S., McParland, K. B., Jayaraman, K., and Ts'o, P. O. P. (1981) Biochemical and biological effects of nonionic nucleic acid methylphosphonates. *Biochemistry* 20, 1874-1880.
- (277) Pramanik, P., and Kan, L.-S. (1987) NMR study of the effect of sugar-phosphate backbone ethylation on the stability and conformation of DNA double helix. *Biochemistry* 26, 3807-3812.
- (278) Sarin, P. S., Agrawal, S., Civeira, M. P., Goodchild, J., Ikeuchi, T., and Zamecnik, P. C. (1988). Inhibition of Acquired Immunodeficiency Syndrome Virus by Oligodeoxynucleoside Methylphosphonates. *Proc. Natl. Acad. Sci. U.S.A.* 85, 7448-7451.
- (279) van Genderen, M. H. P., Koole, L. H., Merck, K. B., Meijer, E. M., Sluyterman, L. A. A. E., and Buck, H. M. (1987) Hybridization of phosphate-methylated and phosphonate oligonucleotides with natural DNA. Implications for the inhibition of replication and transcription processes. *Proc. K. Ned. Akad. Wet. B* 90, 155-159.
- (280) van Genderen, M. H. P., Koole, L. H., and Buck, H. M. (1988) Duplex stability of hybrids between phosphate-methylated DNA and natural RNA. *Proc. K. Ned. Akad. Wet. B* 91, 53-57.
- (281) LaPlanche, L. A., James, T. L., Powell, C., Wilson, W. D., Uznanski, B., Stec, W. J., Summers, M. F., and Zon, G. (1986) Phosphorothioate-modified oligodeoxyribonucleotides. III. NMR and UV spectroscopic studies of the Rp-Rp, Sp-Sp, and Rp-Sp duplexes, [d(GG_nAATTCC)]₂, derived from diastereomeric O-ethylphosphorothioates. *Nucleic Acids Res.* 14, 9081-9093.
- (282) Morvan, F., Rayner, B., Imbach, J.-L., Lee, M., Hartley, J. A., Chang, D.-K., and Lown, J. W. (1987) α -DNA-V. Parallel annealing, handedness and conformation of the duplex of the unnatural α -hexadeoxyribonucleotide α -[d(CpApTpGpCpG)] with its β -complement β -[d(GpTpApCpGpC)] deduced from high field ¹H-NMR. *Nucleic Acids Res.* 15, 7027-7044.
- (283) Gagnor, C., Rayner, B., Leonetti, J.-P., Imbach, J.-L., and Lebleu, B. (1989) α -DNA IX: parallel annealing of α -anomeric oligodeoxyribonucleotides to natural mRNA is required for interference in RNase H mediated hydrolysis and reverse transcription. *Nucleic Acids Res.* 17, 5107-5114.
- (284) Durand, M., Thuong, N. T., and Maurizot, J. C. (1989) Formation of a duplex structure by an α -octathymidylate: circular dichroism studies. *FEBS Lett.* 256, 175-178.
- (285) Lancelot, G., Asseline, U., Thuong, N. T., and Helene, C. (1985) Proton and phosphorus nuclear magnetic resonance studies of an oligothymidylate covalently linked to an acridine derivative and of its binding to complementary sequences. *Biochemistry* 24, 2521-2529.
- (286) Zamecnik, P. C., Goodchild, J., Taguchi, Y., and Sarin, P. S. (1986) Inhibition of Replication and Expression of Human T-cell Lymphotropic Virus Type III in Cultured Cells by Exogenous Synthetic Oligonucleotides Complementary to Viral RNA. *Proc. Natl. Acad. Sci. U.S.A.* 83, 4143-4146.
- (287) Wickstrom, E. L., Bacon, T. A., Gonzalez, A., Freeman, D. L., Lyman, G. H., and Wickstrom, E. (1988). Human Promyelocytic Leukemia HL-60 Cell Proliferation and c-myc Protein Expression are Inhibited by an Antisense Pentadecadeoxynucleotide Targeted Against c-myc mRNA. *Proc. Natl. Acad. Sci. U.S.A.* 85, 1028-1032.
- (288) Harel-Bellan, A., Ferris, D. K., Vinocour, M., Holt, J. T., and Farrar, W. L. (1988). Specific Inhibition of c-myc Protein Biosynthesis Using an Antisense Synthetic Deoxy-Oligonucleotide in Human T Lymphocytes. *J. Immunol.* 140, 2431-2435.
- (289) Holt, J. R., Redner, R. L., and Nienhuis, A. W. (1988). An Oligomer Complementary to c-myc mRNA Inhibits Proliferation of HL-60 Promyelocytic Cells and Induces Differentiation. *Mol. Cell. Biol.* 8, 963-973.
- (290) Goodchild, J., Letsinger, R. L., Sarin, P. S., Zamecnik, M., and Zamecnik, P. C. (1988) Inhibition of Replication and Expression of HIV-I in Tissue Culture by Oligodeoxynucleotide Hybridization Competition. In *Human Retroviruses, Cancer and AIDS: Approaches to Prevention and Therapy* (D. Bolognesi, Ed.) pp 423-438, Alan R. Liss, New York.
- (291) Cazenave, C., Chevrier, M., Thuong, N. T., and Helene, C. (1987). Rate of Degradation of [α]- and [β]-Oligodeoxynucleotides in *Xenopus* Oocytes. Implications for Antimessenger Strategies. *Nucleic Acids Res.* 15, 10507-10521.
- (292) Wickstrom, E. (1986) Oligodeoxynucleotide stability in subcellular extracts and culture media. *J. Biochem. Biophys. Methods* 13, 97-102.
- (293) Ceruzzi, M., and Draper, K. (1989) The intracellular and extracellular fate of oligodeoxyribonucleotides in tissue culture systems. *Nucleosides Nucleotides* 8, 815-818.
- (294) Matzura, H., and Eckstein, F. (1968) A polyribonucleotide containing alternating P=O and P=S linkages. *Eur. J. Biochem.* 3, 448-452.
- (295) Burgers, P. M. J., and Eckstein, F. (1978) Absolute configuration of the diastereomers of adenosine 5'-O-(1-thiotriphosphate): consequences for the stereochemistry of polymerization by DNA-dependent RNA polymerase from *Escherichia coli*. *Proc. Natl. Acad. Sci. U.S.A.* 75, 4798-4800.
- (296) Burgers, P. M. J. and Eckstein, F. (1979) Diastereomers of 5'-O-adenosyl 3'-O-uridyl phosphorothioate: chemical synthesis and enzymatic properties. *Biochemistry* 18, 592-596.
- (297) Potter, B. V. L., Connolly, B. A., and Eckstein, F. (1983) Synthesis and configurational analysis of a dinucleoside phosphate isotopically chiral at phosphorus. Stereochemical course of *Penicillium citrum* nuclease P1 reaction. *Biochemistry* 22, 1369-1377.
- (298) Potter, B. V. L., Romaniuk, P. J., and Eckstein, F. (1983) Stereochemical course of DNA hydrolysis by nuclease S1. *J. Biol. Chem.* 258, 1758-1760.
- (299) Jensen, D. E., and Reed, D. J. (1978) Reaction of DNA with alkylating agents. Quantitation of alkylation by ethylnitrosourea of oxygen and nitrogen sites on poly[dA-dT] including phosphotriester formation. *Biochemistry* 17, 5098-5107.
- (300) Quartin, R. S., Brakel, C. L., and Wetmur, J. G. (1989) Number and distribution of methylphosphonate linkages in oligodeoxynucleotides affect exo- and endonuclease sensitivity and ability to form RNase H substrates. *Nucleic Acids Res.* 17, 7253-7262.
- (301) Bacon, T. A., Morvan, F., Rayner, B., Imbach, J.-L., and Wickstrom, E. (1988) α -Oligodeoxynucleotide stability in serum, subcellular extracts and culture medium. *J. Biochem. Biophys. Methods* 16, 311-318.
- (302) Cotten, M., Schaffner, G., and Birnstiel, M. L. (1989) Ribozyme, antisense RNA, and antisense DNA inhibition of

- U7 small nuclear ribonucleoprotein-mediated histone pre-mRNA processing in vitro. *Mol. Cell. Biol.* 9, 4479-4487.
- (303) Dunlap, B. E., Friderici, K. H., and Rottman, F. (1971) 2'-O-Methyl polynucleotides as templates for cell-free amino acid incorporation. *Biochemistry* 10, 2581-2587.
- (304) Miller, P. S., Agris, C. H., Blake, K. R., Murakami, A., Spitz, S. A., Reddy, P. M., and Ts'o, P. O. P. (1983) Nonionic oligonucleotide analogs as new tools for studies on the structure and function of nucleic acids inside living cells. In *Nucleic Acids: The Vectors of Life* (B. Pullman, and J. Jortner, Eds.) pp 521-535, D. Reidel, Dordrecht, Netherlands.
- (305) Yakubov, L. A., Deeva, E. A., Zarytova, V. F., Ivanova, E. M., Rytte, A. S., Yurchenko, L. V., and Vlassov, V. V. (1989) Mechanism of oligonucleotide uptake by cells: involvement of specific receptors? *Proc. Natl. Acad. Sci. U.S.A.* 86, 6454-6458.
- (306) Loke, S. L., Stein, C. A., Zhang, X. H., Mori, K., Nakanishi, M., Subasinghe, C., Cohen, J. S., and Neckers, L. M. (1989) Characterization of oligonucleotide transport into living cells. *Proc. Natl. Acad. Sci. U.S.A.* 86, 3474-3478.
- (307) Boutorin, A. S., Gus'kova, L. V., Ivanova, E. M., Kobetz, N. D., Zarytova, V. F., Rytte, A. S., Yurchenko, L. V., and Vlassov, V. V. (1989) Synthesis of alkylating oligonucleotide derivatives containing cholesterol or phenazinium residues at their 3'-terminus and their interaction with DNA within mammalian cells. *FEBS Lett.* 254, 129-132.
- (308) Jayaraman, K., McParland, K., Miller, P., and Ts'o, P. O. P. (1981) Selective inhibition of *Escherichia coli* protein synthesis and growth by nonionic oligonucleotides complementary to the 3' end of 16S rRNA. *Proc. Natl. Acad. Sci. U.S.A.* 78, 1537-1541.
- (309) Zamecnik, P. C., and Stephenson, M. L. (1978) Inhibition of Rous Sarcoma Virus Replication and Cell Transformation by a Specific Oligodeoxynucleotide. *Proc. Natl. Acad. Sci. U.S.A.* 75, 280-284.
- (310) Stein, C. A., and Cohen, J. S. (1988) Oligodeoxynucleotides as inhibitors of gene expression: a review. *Cancer Res.* 48, 2659-2668.
- (311) Goodchild, J. (1989) Inhibition of gene expression by oligonucleotides. In *Oligodeoxynucleotides. Antisense Inhibitors of Gene Expression* (J. Cohen, Ed.) pp 53-77, Macmillan Press, London.
- (312) Goodchild, J., Carroll E., III, and Greenberg, J. R. (1988). Inhibition of Rabbit β -Globin Synthesis by Complementary Oligonucleotides: Identification of mRNA Sites Sensitive to Inhibition. *Arch. Biochem. Biophys.* 263, 401-409.
- (313) Furdon, P. J., Dominski, Z., and Kole, R. (1989) RNase H cleavage of RNA hybridized to oligonucleotides containing methylphosphonate, phosphorothioate and phosphodiester bonds. *Nucleic Acids Res.* 17, 9193-9204.
- (314) Cazenave, C., Stein, C. A., Loreau, N., Thuong, N. T., Neckers, L. M., Subasinghe, C., Helene, C., Cohen, J. S., and Toulme, J.-J. (1989) Comparative inhibition of rabbit globin mRNA by translation modified antisense oligodeoxynucleotides. *Nucleic Acids Res.* 17, 4255-4273.
- (315) Maher, L. J. and Dolnick, B. J. (1988) Comparative hybrid arrest by tandem antisense oligodeoxyribonucleotides or oligodeoxyribonucleoside methylphosphonates in a cell-free system. *Nucleic Acids Res.* 16, 3341-3358.
- (316) Blake, K. R., Murakami, A., Spitz, S. A., Glave, S. A., Reddy, M. P., Ts'o, P. O. P., and Miller, P. S. (1985) Hybridization Arrest of Globin Synthesis in Rabbit Reticulocyte Lysates and Cells by Oligodeoxyribonucleoside Methylphosphonates. *Biochemistry* 24, 6139-6145.
- (317) Gagnor, C., Bertrand, J.-R., Thenet, S., Lemaitre, M., Morvan, F., Rayner, B., Malvy, C., Lebleu, B., Imbach, J.-L., and Paoletti, C. (1987) α -DNA VI: Comparative Study of α - and β -Anomeric Oligodeoxyribonucleotides in Hybridization to mRNA and in Cell-free Translation Inhibition. *Nucleic Acids Res.* 15, 10419-10436.
- (318) Bloch, E., Lavignon, M., Bertrand, J.-R., Pognan, F., Morvan, F., Malvy, C., Rayner, B., Imbach, J.-L., and Paoletti, C. (1988) α -Anomeric DNA: β -RNA hybrids as new synthetic inhibitors of *Escherichia coli* RNase H, *Drosophila* embryo RNase H and M-MLV reverse transcriptase. *Gene* 72, 349-360.
- (319) Lavignon, M., Bertrand, J.-R., Rayner, B., Imbach, J.-L., Malvy, C., and Paoletti, C. (1989) Inhibition of Moloney murine leukemia virus reverse transcriptase by α -anomeric oligonucleotides. *Biochem. Biophys. Res. Commun.* 161, 1184-1190.
- (320) Bertrand, J.-R., Imbach, J.-L., Paoletti, C., and Malvy, C. (1989) Comparative activity of α - and β -anomeric oligonucleotides on rabbit β -globin synthesis: inhibitory effect of cap targeted α -oligonucleotides. *Biochem. Biophys. Res. Commun.* 164, 311-318.
- (321) Agris, C. H., Blake, K. R., Miller, P. S., Reddy, M. P., and Ts'o, P. O. P. (1986) Inhibition of Vesicular Stomatitis Virus Protein Synthesis and Infection by Sequence-Specific Oligodeoxyribonucleoside Methylphosphonates. *Biochemistry* 25, 6268-6275.
- (322) Smith, C. C., Aurelian, L., Reddy, M. P., Miller, P. S., and Ts'o, P. O. P. (1986). Antiviral Effect of an Oligo(nucleoside methylphosphonate) Complementary to the Splice Junction of Herpes Simplex Virus Type 1 Immediate Early Pre-mRNAs 4 and 5. *Biochemistry* 83, 2787-2791.
- (323) Zaia, J. A., Rossi, J. J., Murakawa, G. J., Spallone, P. A., Stephens, D. A., Kaplan, B. E., Eritja, R., Wallace, R. B., and Cantin, E. M. (1988) Inhibition of human immunodeficiency virus by using an oligonucleoside methylphosphonate targeted to the *tat-3* gene. *J. Virol.* 62, 3914-3917.
- (324) Yu, Z., Chen, D., Black, R. J., Blake, K., Ts'o, P. O. P., Miller, P., and Chang, E. H. (1989) Sequence specific inhibition of in vitro translation of mutated or normal *ras* p21. *J. Exp. Pathol.* 4, 97-108.
- (325) Brown, D., Yu, Z., Miller, P., Blake, K., Wei, C., Kung, H.-F., Black, R. J., Ts'o, P. O. P., and Chang, E. H. (1989) Modulation of *ras* expression by anti-sense, nonionic deoxy-oligonucleotide analogs. *Oncogene Res.* 4, 243-252.
- (326) Kulka, M., Smith, C. C., Aurelian, L., Fischelevich, R., Meade, K., Miller, P., and Ts'o, P. O. P. (1989) Site specificity of the inhibitory effects of oligo(nucleoside methylphosphonate)s complementary to the acceptor splice junction of herpes simplex virus type I immediate early mRNA 4. *Proc. Natl. Acad. Sci. U.S.A.* 86, 6868-6872.
- (327) Matsukura, M., Shinozuka, K., Zon, G., Mitsuya, H., Reitz, M., Cohen, J. S., and Broder, S. (1987). Phosphorothioate Analogs of Oligodeoxynucleotides: Inhibitors of Replication and Cytopathic Effects of Human Immunodeficiency Virus. *Proc. Natl. Acad. Sci. U.S.A.* 84, 7706-7710.
- (328) Lamond, A. I., Sproat, B., Ryder, U., and Hamm, J. (1989) Probing the structure and function of U2 snRNP with antisense oligonucleotides made of 2'OMe RNA. *Cell* 58, 383-390.
- (329) Majumdar, C., Stein, C. A., Cohen, J. S., Broder, S., and Wilson, S. H. (1989) Stepwise mechanism of HIV reverse transcriptase: primer function of phosphorothioate oligodeoxynucleotide. *Biochemistry* 28, 1340-1346.
- (330) Gao, W., Stein, C. A., Cohen, J. S., Dutschman, G. E., and Cheng, Y.-C. (1989) Effect of phosphorothioate homooligodeoxynucleotides on herpes simplex virus type 2-induced DNA polymerase. *J. Biol. Chem.* 264, 11521-11526.
- (331) Marcus-Sekura, C. J., Woerner, A. M., Shinozuka, K., Zon, G., and Quinnan, G. V. (1987) Comparative Inhibition of Chloramphenicol Acetyltransferase Gene Expression by Antisense Oligonucleotide Analogues having Alkyl Phosphotriester, Methylphosphonate, and Phosphorothioate Linkages. *Nucleic Acids Res.* 15, 5749-5763.
- (332) Matsukura, M., Zon, G., Shinozuka, K., Robert-Guroff, M., Shimada, T., Stein, C. A., Mitsuya, H., Wong-Staal, F., Cohen, J. S., and Broder, S. (1989) Regulation of viral expression of human immunodeficiency virus in vitro by an antisense phosphorothioate oligodeoxynucleotide against *rev* (*art/trs*) in chronically infected cells. *Proc. Natl. Acad. Sci. U.S.A.* 86, 4244-4248.
- (333) Agrawal, S., Ikeuchi, T., Sun, D., Sarin, P. S., Konopka, A., Maizel, J., and Zamecnik, P. C. (1989) Inhibition of human immunodeficiency virus in early infected and chronically infected cells by antisense oligodeoxynucleotides and their phosphorothioate analogues. *Proc. Natl. Acad. Sci. U.S.A.* 86, 7790-7794.
- (334) Toulme, J.-J., Krisch, H. M., Loreau, N., Thuong, N. T., and Helene, C. (1986) Specific Inhibition of mRNA Transla-

- tion by Complementary Oligonucleotides Covalently Linked to Intercalating Agents. *Proc. Natl. Acad. Sci. U.S.A.* 83, 1227-1231.
- (335) Cazenave, C., Loreau, N., Thuong, N. T., Toulme, J.-J., and Helene, C. (1987) Enzymatic Amplification of Translation Inhibition of Rabbit β -Globin mRNA Mediated by Antimessenger Oligodeoxynucleotides Covalently Linked to Intercalating Agents. *Nucleic Acids Res.* 15, 4717-4735.
- (336) Verspieren, P., Cornelissen, A. W. C. A., Thuong, N. T., Helene, C., and Toulme, J.-J. (1987) An acridine-linked oligodeoxynucleotide targeted to the common 5' end of trypanosome mRNAs kills cultured parasites. *Gene* 61, 307-315.
- (337) Zerial, A., Thuong, N. T., and Helene, C. (1987) Selective Inhibition of the Cytopathic Effect of Type A Influenza Viruses by Oligodeoxynucleotides Covalently Linked to an Intercalating Agent. *Nucleic Acids Res.* 15, 9909-9919.

TEACHING EDITORIAL

A Brief Guide to Nucleic Acid Chemistry

Paul S. Miller

Department of Biochemistry, School of Hygiene and Public Health, The Johns Hopkins University, 615 North Wolfe Street, Baltimore, Maryland 21205. Received January 19, 1990

STRUCTURE OF NUCLEIC ACIDS

Nucleic acids encode the genetic information of all living organisms and are intimately involved in the conversion of this information into cellular proteins and enzymes. Cellular nucleic acids are polymeric molecules which are composed of three basic units: a base, a sugar, and a phosphodiester group. The arrangement of these three groups to form either DNA or RNA is shown in Figure 1.

The nitrogenous, heterocyclic bases are derivatives of purine or pyrimidine. The four bases commonly found in DNA are adenine, guanine, cytosine, and thymine. These same bases are also found in RNA with the exception that thymine is replaced by uracil. In addition, a variety of modified bases, such as *N*⁴,*N*⁴-dimethyladenine and *N*⁷-methylguanine are found in messenger RNA, transfer RNA, and ribosomal RNA.

The bases are linked to 2'-deoxyribose in DNA or ribose in RNA via an *N*-glycosyl bond to form a nucleoside. The nucleosides are named according to the heterocyclic base which they contain. The nucleosides found in DNA are 2'-deoxyadenosine, 2'-deoxyguanosine, 2'-deoxycytidine, and thymidine. The nucleosides commonly found in RNA are adenosine, guanosine, cytidine, and uridine. 2'-*O*-Methylribosyl nucleosides are also found in RNA, particularly in messenger RNA and ribosomal RNA.

The nucleosides are linked together via phosphate ester groups to form the sugar phosphate backbone of the nucleic acid. Thus esterification of the 3'-hydroxyl of one nucleoside and the 5'-hydroxyl of the next nucleoside unit results in the formation of a 3'→5' internucleotide bond. This type of linkage is found in both DNA and RNA. In the case of RNA the internucleotide bond could also extend from the 2'-hydroxyl to form a 2'→5' internucleotide bond. Such 2'→5' linkages are found in certain oligoadenylates which are synthesized in mammalian cells in response to interferon (1).

A single phosphorylated nucleoside unit is called a nucleotide. The sequence of nucleotides within the nucleic acid chain determines the genetic information encoded by the nucleic acid. The purine bases, adenine and gua-

nine, can form hydrogen bonds with the pyrimidine bases, thymine (uracil in RNA) and cytosine, respectively (see Figure 2). The base pairs formed between these so-called complementary bases enable separate chains of nucleic acids to interact with one another. In DNA, separate nucleic acid strands form a double-helical structure in which the sugar phosphate backbones run in an antiparallel direction. Double-helical DNA, which usually exists in a right-handed, B-type conformation, can exist in a variety of conformational forms including left-handed helices (2). The particular conformation depends upon the nucleotide sequence and the environment of the DNA. DNA can also exist in a triple-stranded form in which three bases form a triad via hydrogen-bonding interactions as shown in Figure 2 (2, 3).

Although RNA is often thought of as a single-stranded molecule, self-complementary nucleotide sequences present within the single strand give rise to the formation of intramolecular helical regions. These intramolecular interactions can produce a tremendous variety of helical and looped structural regions and account for the secondary structure within RNA molecules. In addition to these secondary structural features, further folding and hydrogen-bonding interactions between bases in remote parts of the molecule give rise to a tertiary structure. The combination of these interactions results in overall three dimensional structure, whose complexity approaches that found in proteins. This complexity has been most clearly revealed in the structure of transfer RNA (4).

Nucleic acid structure has been elucidated at the atomic level of resolution by nuclear magnetic resonance spectroscopy and X-ray diffraction techniques. In addition to studying nucleic acid structure, recent X-ray experiments have been used to examine the interactions of proteins with nucleic acids. For example, the structures of the complex formed between the restriction enzyme *EcoR* I and a deoxyribonucleotide duplex, and of the complex formed by glutaminyl tRNA with its cognate aminoacyl synthetase have been determined (5, 6). Such studies promise to lead to further insights into how nucleic acids

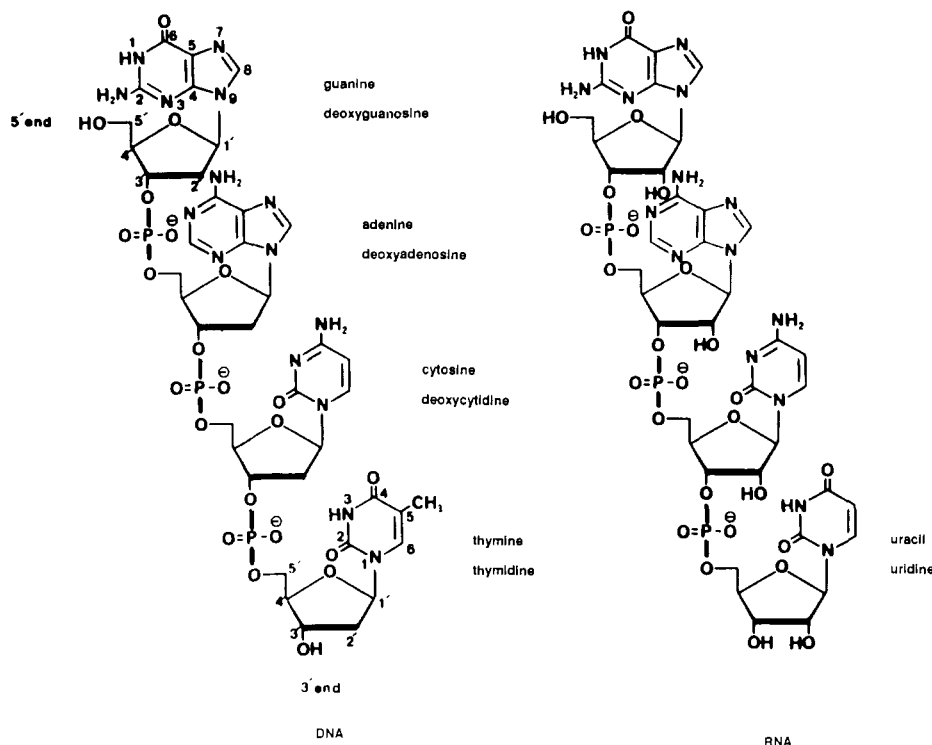


Figure 1. Structure of DNA and RNA.

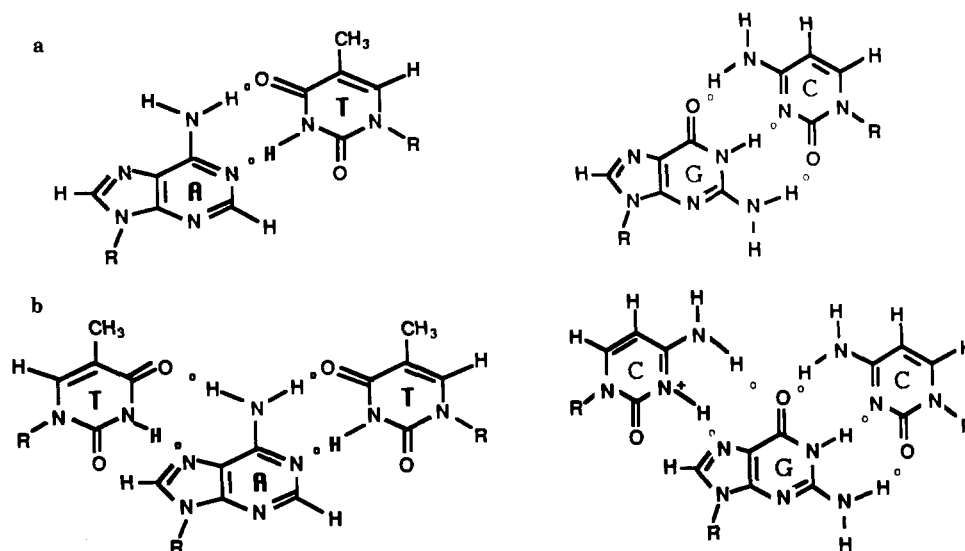


Figure 2. Watson-Crick base-pairing interactions between adenine and thymine and guanine and cytosine (a) and triple-strand hydrogen-bonding interactions (b).

function as repositories of genetic information.

CHEMISTRY OF NUCLEIC ACIDS

Nucleic acids can undergo a wide variety of reactions with chemical reagents, both man-made and naturally occurring (7). These reactions can take place at the bases, the sugars, and the phosphodiester internucleotide linkage. The heterocyclic bases can be modified by both nucleophilic and electrophilic reagents (8). The exocyclic amino groups of adenine, guanine, and cytosine are subject to deamination reactions. Reaction at the 5,6-double bonds of pyrimidines by nucleophiles such as hydrazine can ultimately lead to breakdown and loss of the pyrimidine ring. Alkylating agents such as dimethyl sulfate, alkyl nitrosoureas, epoxides, and nitrogen and sulfur mustards can react with ring nitrogens as well as the exocyclic nitrogens and oxygens of the bases. In addition, a variety of natural products such as aflatoxin and

mitomycin react with the nucleic acid bases. Adduct formation can seriously modify or even prevent hydrogen-bonding interactions between the bases which can ultimately lead to mutations and possibly to malignant cell transformation.

Modification of the bases can also lead to their excision from the nucleic acid. The *N*-glycosyl bond of deoxynucleosides in DNA is more labile than the corresponding bond in RNA. Treatment of DNA with acid, for example, results in loss of purine bases. Alkylation of adenine and guanine residues in DNA at the N-3 or N-7 positions produces adducts which can undergo spontaneous depurination.

The susceptibility of the bases to chemical modification depends to some extent upon the structure of the nucleic acid. Not surprisingly, single-stranded nucleic acids generally react more rapidly than double-stranded nucleic acids. In some cases the reactive site may be

involved in hydrogen-bonding interactions with a complementary base and therefore is not subject to modification. The differential reactivity of single- vs double-stranded nucleic acids has been exploited to study the secondary and tertiary structure of both deoxyribo- and ribonucleic acids (9, 10).

The nucleic acid bases can also undergo photochemical reactions (11). For example the 5,6-double bonds of adjacent thymine bases in the same strand of DNA can undergo a photocycloaddition reaction to form a cyclobutane adduct when DNA is irradiated with 254-nm UV light. Such adduct formation leads to distortions of the DNA helix.

The sugars of RNA can undergo reaction with alkylating agents to form 2'-O-alkyl ethers. The sugars are also subject to radical induced abstraction reactions and subsequent degradation. Hydroxyl radicals produced as a result of ionization radiation or drugs which react via radical intermediates, such as the bleomycins and neocarzinostatin, can abstract hydrogen atoms from the C-1', C-4', or C-5' positions of deoxyribose or ribose (12, 13). The sugar radicals which are produced as a result of these hydrogen-abstraction reactions undergo further oxidation and/or rearrangement which eventually leads to the destruction of the sugar skeleton and cleavage of the sugar phosphate backbone of the nucleic acid, producing strand breaks.

The phosphodiester internucleotide linkage of RNA is sensitive to base-catalyzed hydrolysis in aqueous solution, whereas that of DNA is stable under alkaline conditions. The base lability of the RNA internucleotide bond is due to the presence of the 2'-hydroxyl group which can participate in an intramolecular attack on the phosphate group, resulting in hydrolysis of the phosphate internucleotide bond.

The phosphodiester internucleotide bond can react with alkylating agents, resulting in the formation of alkylphosphotriesters (8). Phosphotriester formation creates a new chiral center in the nucleic acid backbone. Both R_p and S_p isomers are observed in these reactions. Alkyl phosphotriesters in DNA are stable to hydrolysis at physiological pH, although they can be cleaved by treatment with strong acid or base. In contrast, alkylphosphotriester groups in RNA are subject to rapid hydrolysis, even at neutral pH. This lability is due to intramolecular attack by the 2'-hydroxyl group of the sugar on the nonionic alkylphosphotriester group. Alkylphosphotriesters of oligonucleotides in which the 2'-OH is methylated are not subject to such hydrolysis (14).

As described above, abasic sites can be created in nucleic acids by degradation of pyrimidine bases with hydrazine or by depurination with acid or alkylating agents. When treated with base, the sugar phosphate linkages at these sites undergo β -elimination reactions resulting in cleavage of the backbone. It has been possible to develop conditions under which abasic sites can be created in a base-specific manner. This ability has led to the development of chemical procedures which can be used to determine the nucleotide sequence of DNA and RNA (15, 16).

In addition to being the subject of various chemical reactions, recent experiments have shown that certain RNA molecules are capable of catalyzing hydrolysis, transesterification, and polymerization reactions of other nucleic acids (17, 18). These catalytic RNAs are called ribozymes and appear to possess many of the catalytic properties previously associated only with enzymes. It appears that the catalytic properties of ribozymes are dependent upon

both the sequence and the secondary and tertiary structures of the RNA molecule.

CHEMICAL SYNTHESIS OF NUCLEIC ACIDS

The ability to synthesize oligonucleotides and oligonucleotide analogues of defined nucleotide sequence provides materials for a variety of physical and biochemical studies. Both single-stranded and double-stranded oligonucleotides serve as convenient and manageable models for studies on the structure and conformation of nucleic acids. Oligonucleotides are used as primers for nucleic acid polymerizing enzymes and are used to construct artificial genes for the preparation of proteins by recombinant DNA techniques. In addition, oligonucleotides are used as probes to detect and characterize cellular nucleic acid sequences and as such are finding increasing use as clinical, diagnostic tools (19). Recent studies suggest that oligonucleotides and oligonucleotide analogues may be used to control gene expression in living cells and show considerable potential for eventual use as antiviral and therapeutic agents (20). Such oligomers have been termed antisense oligonucleotides.

The chemical syntheses of oligonucleotides involve coupling a suitably protected nucleotide with another suitably protected nucleotide or oligonucleotide to form a 3'→5' internucleotide linkage between the two units (21, 22). Protecting groups are required on the exocyclic amino groups of the bases to prevent them from reacting under the coupling conditions. The most commonly used groups are the benzoyl group for the protection of the exocyclic amino groups of adenine and cytosine and the isobutyryl group for the protection of the amino group of guanine (see Figure 3a). Other groups such as the amidine and phenoxyacetyl protecting groups have also been used (23, 24). These protecting groups remain in place during the course of the synthesis and are removed from the completed oligomer at the end of the synthesis by treatment with aqueous ammonium hydroxide.

The hydroxyl groups of the sugars are protected in order to direct the incoming nucleotide unit to give the 3'→5' linkage. The 5'-hydroxyl is usually protected with a dimethoxytrityl group which can be selectively removed by acid treatment during the course of the synthesis. The synthesis of oligoribonucleotides presents special problems due to the presence of the 2'-hydroxyl group. This group is generally protected with an acetal protecting group such as the 4-methoxytetrahydropyran-4-yl group or with dimethyl-*tert*-butylsilyl group (25, 26). These protecting groups remain attached throughout the synthesis and are usually removed after the base-protecting groups have been removed. The acetal groups are removed by treatment with acid whereas the silyl protecting group can be removed by treatment with tetra-*n*-butylammonium fluoride in tetrahydrofuran solution.

Originally oligonucleotide syntheses were carried out in solution under anhydrous conditions employing nucleoside 3'- or 5'-monophosphates or phosphate diesters as synthons. The coupling reaction was effected by using a condensing reagent such as mesitylenesulfonyl chloride. These reactions, which required several hours to complete, resulted in the formation of oligomers containing phosphodiester or phosphotriester linkages. Because the coupling reactions were rather inefficient and were accompanied by the formation of a number of side products, time-consuming column chromatography was required after each coupling step to purify the desired product.

The efficiency of oligonucleotide syntheses was considerably improved with the advent of coupling proce-

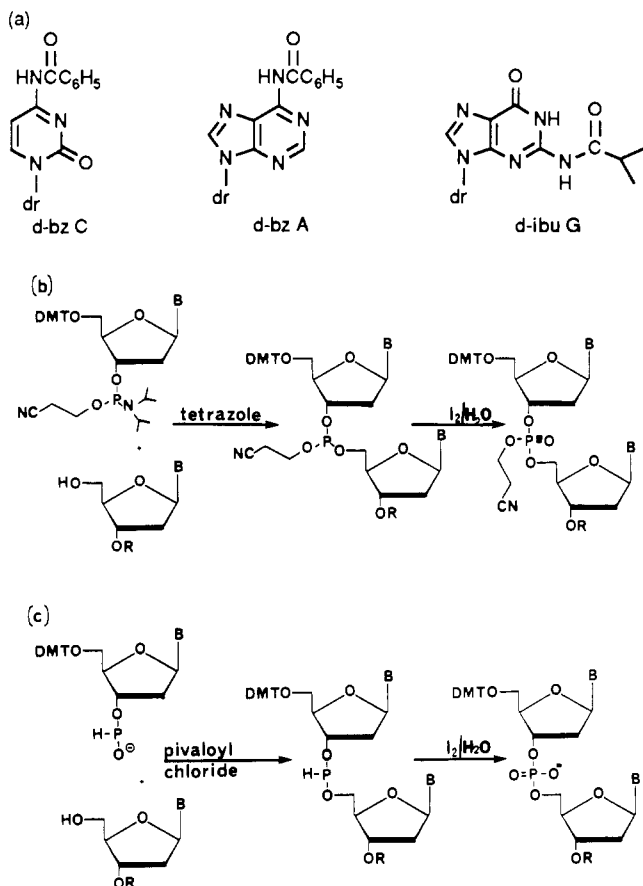


Figure 3. Base-protecting groups used in oligonucleotide synthesis (a). The symbol indicates 2'-deoxyribose. Synthesis of the internucleotide bond by the phosphoramidite method (b) and the H-phosphonate (c) method. The symbols B and R represent a protected base and controlled pore glass support, respectively.

dures using trivalent phosphorus chemistry (27). Two procedures are generally employed as shown in Figure 3. Protected nucleoside phosphoramidite synthons (Figure 3b) readily react with the 5'-hydroxyl of a nucleoside in the presence of tetrazole, which serves as both an acid catalyst for the reaction and forms a highly reactive nucleoside tetrazolidine phosphinite intermediate (28, 29). This coupling reaction, which proceeds to virtual completion in a matter of minutes at room temperature in the presence of a 10–20-fold excess of the phosphoramidite, yields a phosphite internucleotide linkage. The phosphite linkage is then oxidized quantitatively with aqueous iodine to give the β -(cyanoethyl)phosphotriester internucleotide bond. The β -cyanoethyl group remains in place during the course of the synthesis and is removed by the ammonium hydroxide treatment used to remove the base-protecting groups.

Protected nucleoside H-phosphonate synthons (Figure 3c) react with nucleoside 5'-hydroxyl groups when activated with a condensing agent such as pivaloyl chloride (30, 31). This coupling reaction proceeds with a yield of approximately 95–97% at room temperature. The resulting H-phosphonate internucleotide bond is readily and quantitatively converted to the phosphodiester internucleotide linkage by oxidation with aqueous iodine solution. The H-phosphonate linkage is a very versatile intermediate because it can be used to prepare variety of oligonucleotide analogues. Thus, for example, oxidation in the presence of elemental sulfur produces oligomers containing a phosphorothioate linkage (32), whereas oxida-

tion in the presence of amines gives oligomers with phosphoramidate linkages (33).

The coupling procedures described above enable the preparation of oligonucleotides on insoluble polymer supports (21, 22). In this methodology the nucleoside which occurs at the 3'-end of the oligomer chain is attached via a linker arm to a controlled pore glass support. The trityl group is removed from the nucleoside by treatment with dichloroacetic acid in methylene chloride and the first coupling reaction is carried out. After the coupling/oxidation step, excess reagent is removed by simply washing the support. The 5'-hydroxyl of any unreacted nucleoside is "capped" by acylation with acetic anhydride and the next round of detritylation and coupling is carried out. In this way the oligomer chain is built up one nucleotide at a time from the 3'- to the 5'-end. The entire procedure has been automated and a number of oligonucleotide synthesizers are commercially available which are capable of synthesizing oligomers over 100 nucleotides in length.

ACKNOWLEDGMENT

I wish to thank Dr. Lou-Sing Kan for providing the computer-generated drawings used in Figure 2.

LITERATURE CITED

- Brown, G. E., Lebleu, B., Kawakita, M., Shaila, S., Sen, G. C., and Lengyel, P. (1976) Increased Endonuclease Activity in an Extract from Mouse Ehrlich Ascites Tumor Cells Which Had Been Treated with a Partially Purified Interferon Preparation: Dependence on dsRNA. *Biochem. Biophys. Res. Commun.* 69, 114–122.
- Saenger, W. (1984) *Principles of Nucleic Acid Structure* Springer-Verlag, New York.
- Wells, R. D., Collier, D. A., Hanvey, J. C., Shimizu, M., and Wholrab, F. (1988) The Chemistry and Biology of Unusual DNA Structures Adopted by Oligopurine-Oligopyrimidine Sequences. *FASEB J.* 2, 2939–2949.
- Kim, S.-H., Quigley, G. J., Suddath, F. L., McPherson, A., Sneden, D., Kim, J. J., Weinzierl, J., and Rich, A. (1973) Three-Dimensional Structure of Yeast Phenylalanine Transfer RNA: Folding of the Polynucleotide Chain. *Science* 179, 285–288.
- Grable, H. W., and Rosenberg, J. M. (1986) Structure of the DNA-EcoR I Endonuclease Recognition Complex at 3 Å. *Science* 234, 1526–1541.
- Rould, M., Perona, J., Soll, D., and Steitz, T. (1989) Structure of *E. coli* Glutamyl-tRNA Synthetase Complexed with tRNA^{Glu} and ATP at 2.8 Å Resolution. *Science* 246, 1135–1142.
- Mizuno, Y. (1986) *The Organic Chemistry of Nucleic Acids* Elsevier, New York.
- Singer, B., and Grunberger (1983) *Molecular Biology of Mutagens and Carcinogens* Plenum Press, New York.
- Furlong, J. C., Sullivan, K. M., Murchie, A. I. H., Gough, G. W., and Lilley, D. M. J. (1989) Localized Chemical Hyperactivity in Supercoiled DNA: Evidence for Base Unpairing in Sequences that Induce Low-Salt Cruciform Extrusion. *Biochemistry* 28, 2009–2017.
- Ehresmann, C., Baudin, F., Mougél, M., Romby, P., Ebel, J.-P., and Ehresmann, B. (1987) Probing the Structure of RNAs in Solution. *Nucleic Acids Res.* 15, 9109–9128.
- Wang, S. Y. (1976) *Photochemistry and Photobiology of Nucleic Acids* Vol. I and II, Academic Press, New York.
- Kozarich, J., Worth, L., Jr., Frank, B., Christner, D., Vanderwall, D., and Stubbe, J. (1989) Sequence-Specific Isotope Effects on the Cleavage of DNA by Bleomycin. *Science* 245, 1396–1399.
- Lee, S. H., and Goldberg, I. H. (1989) Sequence-Specific, Strand-Selective, and Directional Binding of Neocarzinostatin Chromophore to Oligodeoxyribonucleotides. *Biochemistry* 28, 10109–10116.
- Miller, P. S., Braiterman, L. T., and Ts'o, P. O. P. (1977) Effects of a Trinucleotide Ethyl Phosphotriester, G^mp(Et)-

- G^mp(Et)U, on Mammalian Cells in Culture. *Biochemistry* 16, 1988-1996.
- (15) Maxam, A. M., and Gilbert, W. (1980) Sequencing End-Labeled DNA with Base-Specific Chemical Cleavages. *Methods Enzymol.* 65, 499-560.
- (16) Peattie, D. (1979) Direct Chemical Method for Sequencing RNA. *Proc. Natl. Acad. Sci. U.S.A.* 76, 1760-1764.
- (17) Cech, T. (1987) The Chemistry of Self-Splicing RNA and RNA Enzymes. *Science* 236, 1532-1539.
- (18) Uhlenbeck, O. (1989) A Small Catalytic Oligoribonucleotide. *Nature* 328, 596-600.
- (19) Wallace, R. B., Studencke, A. B., and Murasugi, A. (1985) *Biochimie* 67, 755-762.
- (20) Cohen, J. S. (1989) *Oligodeoxynucleotides. Antisense Inhibitors of Gene Expression. Topics in Molecular and Structural Biology* Vol. 12, MacMillan Press, London.
- (21) M. J. Gait, D. (1984) *Oligonucleotide Synthesis, a Practical Approach* IRL Press, Oxford.
- (22) Engels, J. W., and Uhlmann, E. (1989) Gene Synthesis. *Angew. Chem., Int. Ed. Engl.* 28, 716-734.
- (23) McBride, L. J., Kierzek, R., Beaucage, S. L., and Caruthers, M. H. (1986) Amidine Protecting Groups for Oligonucleotide Synthesis. *J. Am. Chem. Soc.* 108, 2040-2048.
- (24) Wu, T., Ogilvie, K. K., and Pon, R. T. (1989) Prevention of Chain Cleavage in the Chemical Synthesis of 2'-Silylated Oligoribonucleotides. *Nucleic Acids Res.* 17, 3501-3517.
- (25) Lehmann, C., Xu, Y.-Z., Christodoulou, C., Tan, Z.-K., and Gait, M. J. (1989) Solid Phase Synthesis of Oligoribonucleotides Using 9-Fluorenylmethoxycarbonyl (Fmoc) for 5'-Hydroxyl Protection. *Nucleic Acids Res.* 17, 2379-2390.
- (26) Ogilvie, K. K., Usman, N., Nicoghossian, K., and Cedergren, R. J. (1988) Total Chemical Synthesis of a 77-Nucleotide-Long RNA Sequence Having Methionine-Acceptance Activity. *Proc. Natl. Acad. Sci. U.S.A.* 85, 5764-5768.
- (27) Letsinger, R. L., Finnan, J. L., Heavner, G. A., and Lunsford, W. B. (1975) Phosphite Coupling Procedure for Generating Internucleotide Links. *J. Am. Chem. Soc.* 97, 3278-3279.
- (28) McBride, L. J., and Caruthers, M. H. (1983) An Investigation of Several Deoxynucleoside Phosphoramidites Useful for Synthesizing Deoxyoligonucleotides. *Tetrahedron Lett.* 24, 245-248.
- (29) Sinha, N., Biernat, J., McManus, J., and Koster, H. (1984) Polymer Support Oligonucleotide Synthesis XVIII: Use of β -Cyanoethyl-*N,N*-dialkylamino-*N*-morpholino Phosphoramidite of Deoxynucleosides for the Synthesis of DNA Fragments Simplifying Deprotection and Isolation of the Final Product. *Nucleic Acids Res.* 12, 4539-4557.
- (30) Garegg, P. J., Regberg, T., Stawinski, J., and Stromberg, R. (1987) Studies on the Synthesis of Oligonucleotides via the Hydrogenphosphonate Approach. *Nucleosides Nucleotides* 6, 283-286.
- (31) Froehler, B. C., and Matteucci, M. D. (1987) The Use of Nucleoside H-Phosphonates in the Synthesis of Deoxyoligonucleotides. *Nucleosides Nucleotides* 6, 287-291.
- (32) Stec, W. J., Zon, G., Egan, W., and Stec, B. (1984) Automated Solid Phase Synthesis, Separation, and Stereochemistry of Phosphorothioate Analogues of Oligodeoxyribonucleotides. *J. Am. Chem. Soc.* 108, 6077-6079.
- (33) Froehler, B., Ng, P., and Matteucci, M. (1988) Phosphoramidate Analogues of DNA: Synthesis and Thermal Stability of Heteroduplexes. *Nucleic Acids Res.* 16, 4831-4839.

ARTICLES

Labeling of Human IgG with Rhodium-105 Using a New Pentadentate Bifunctional Ligand

M. R. A. Pillai,* C. S. John,[†] and D. E. Troutner

Department of Chemistry, University of Missouri, Columbia, Missouri 65211. Received September 25, 1989

We report the labeling of human gamma globulin with the ^{105}Rh complex of a new pentadentate bifunctional ligand, 1,7-bis(2-hydroxybenzyl)-4-(*p*-aminobenzyl)diethylenetriamine. Complexes of this ligand with ^{105}Rh were prepared by refluxing rhodium carrier spiked with ^{105}Rh at pH 9 in bicarbonate buffer. The complex was treated with an excess concentration of thiophosgene to prepare the isothiocyanate derivative which was extracted into CHCl_3 . The CHCl_3 extract was dried and dissolved in DMF and reacted with a borate solution of human gamma globulin. Labeling yields were generally high and varied from 73% to 93%, depending upon the concentration of human gamma globulin and the isothiocyanate derivative of the complex used. The overall recovery of rhodium activity varied from 59% to 75% without taking into account activity lost due to decay. The conjugation reaction was complete by 4 h. From 0.4 to 8.5 atoms of Rh could be incorporated per molecule of protein by this method. The activated isothiocyanate complex did not show any degradation when stored at room temperature for up to 4 days and then used for conjugation.

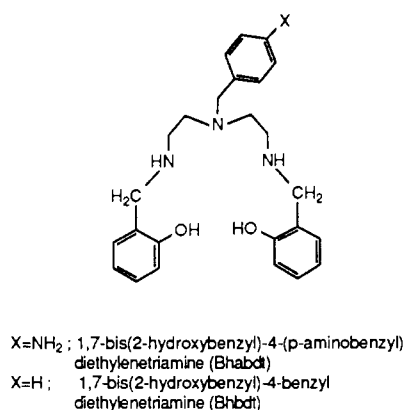
Because of its ideal radionuclidic properties, ^{105}Rh can be developed as a radiotherapeutic isotope (1). We have

* Permanent address: Isotope Division, B.A.R.C., Bombay 400 085, India.

[†] Radiopharmaceutical Chemistry, George Washington University, 2300 I Street, N.W., Washington, DC 20037.

demonstrated that ^{105}Rh can be attached to proteins through bifunctional chelating agents and that these methods are suitable for the labeling of antibodies with specific activities high enough for radioimmunotherapy (2, 3). In those studies we used tridentate bifunctional ligands derived from diethylenetriamine. One of our aims has been the development of a bifunctional ligand capable

Chart I



of chelating ¹⁰⁵Rh and also pure γ -emitting isotopes like ¹¹¹In or ^{99m}Tc for developing radioimmunoimaging agents for pretherapy studies to collect information regarding the pharmacokinetics of the labeled monoclonal antibody. Such information will help in determining the response of the tumor to treatment and also in radiation dosimetry calculations for determining the amount of radionuclide needed for therapy.

We have observed that ligands prepared by the reduction of the Schiff base formed by the condensation of salicylaldehyde with alkyldiamines complex ^{99m}Tc readily (4) and undertook the synthesis of a ligand with a similar structure to be used as a bifunctional ligand for the labeling of monoclonal antibodies with ¹⁰⁵Rh and ^{99m}Tc. Motekaitis et al. have reported the synthesis of a pentadentate ligand, 1,7-bis(2-hydroxybenzyl)-4-benzyl diethylenetriamine (5) and its complexation with Co^{II}. We reasoned that this ligand, if made bifunctional, would be suitable for both rhodium and technetium. Hence we have synthesized the bifunctional analogue 1,7-bis(2-hydroxybenzyl)-4-(p-aminobenzyl) diethylenetriamine (bhabdt) (Chart I). This paper describes the synthesis of this ligand and labeling of human gamma globulin with its ¹⁰⁵Rh complex. Complexation of this ligand with ^{99m}Tc and labeling of proteins is described elsewhere (6). We have also used the nonbifunctional ligand 1,7-bis(2-hydroxybenzyl)-4-benzyl diethylenetriamine (bhbdtd) (Chart I) to determine the nonspecific-labeling effects.

EXPERIMENTAL PROCEDURES

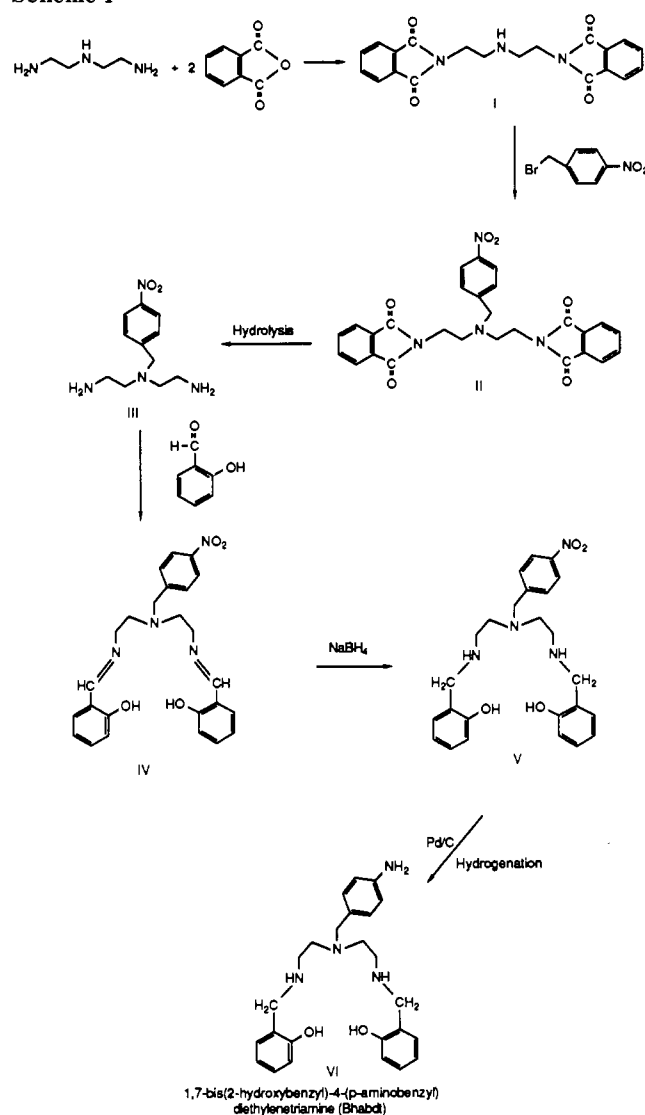
Reagents. Human gamma globulin (G-4386), Sephadex G75, and antihuman IgG (γ -chain specific) agarose (A-6656) were purchased from Sigma Chemical Co. The human gamma globulin supplied was reported to be >99% IgG and will be referred to hereafter as IgG. An average molecular weight of 150 000 has been used in all calculations. Thiophosgene and RhCl₃·3H₂O were from Aldrich Chemicals. All other reagents or solvents used were of reagent grade. Saline solution (0.9%) was prepared by dissolving 9 g of NaCl in 1 L of doubly distilled water. ¹⁰⁵Rh was prepared at the University of Missouri Research Reactor (MURR) and supplied as (RhCl₃·xH₂O)^{x-3}. Rhodium carrier used in these studies was prepared by dissolving RhCl₃·3H₂O in saline solution.

¹H and ¹³C NMR spectra were recorded on a JEOL FX 90Q spectrometer. Radioactivity was measured on a standard 5 × 5 cm NaI(Tl) well scintillation counter. Elemental analyses were done by Galbraith Laboratories, Knoxville, TN.

Synthesis. The ligand bhabdt was prepared by a six-step synthetic pathway as shown in Scheme I.

Step 1. 1,7-Dipthaloyldiethylenetriamine (I) was prepared as reported by Searle et al. (7).

Scheme I



Step 2. 4-(p-Nitrobenzyl)-1,7-dipthaloyldiethylenetriamine (II). To a round-bottomed flask were added 100 mL of absolute ethanol and 1.6 g (28 mmol) of KOH. The solution was heated until the KOH dissolved. I (10 g, 28 mmol) was added to the above solution and the mixture was refluxed for 2.5 h. p-Nitrobenzyl bromide (5.95 g, 28 mmol) was added to the mixture and refluxing continued for 16 h. At the end of this period the hot solution was filtered. Upon cooling of the filtrate, crystals of the product appeared (11.0 g), mp 129–130 °C. The compound was recrystallized from absolute ethanol: ¹H NMR (CDCl₃) δ (ppm) 2.6–2.9 (t, NCH₂, 4 H), 3.6–3.9 (m, NCH₂ + benzylic CH₂(OH)), 7.1–7.6 (m, aromatic, 12 H).

Step 3. 4-(p-Nitrobenzyl)diethylenetriamine (III). A round-bottomed flask was charged with 3.0 g of II and 60 mL of 6 M HCl. The mixture was heated at reflux for about 16 h. A clean solution was obtained, and upon cooling, a white solid appeared. The solid was filtered out and the filtrate was evaporated on a rotary evaporator to give a white solid (1.9 g, 91%), presumably the hydrochloride salt of III. This was neutralized with NaOH solution and extracted in CHCl₃ (3 × 10 mL). The organic layers were combined and evaporated to give an oil: ¹H NMR (CDCl₃) δ (ppm) 1.65 (s, NH₂, 4 H), 2.4–2.9 (m, NCH₂, 8 H), 3.7 (s, benzylic CH₂, 2 H), 7.3–8.3 (m, aromatic, 4 H).

Step 4. 1,7-Bis(salicylidene)-4-(*p*-nitrobenzyl)diethylenetriamine (IV). 4-(*p*-Nitrobenzyl)diethylenetriamine (III; 700 mg, 2.4 mmol) was dissolved in 50 mL of absolute ethanol in a 200-mL round-bottomed flask. Salicylaldehyde (720 mg, 5.9 mmol) was added in 50 mL of absolute ethanol and the mixture was refluxed for 18 h at room temperature. A bright yellow solution of the product was formed and was isolated as an oil by removing the solvent by vacuum distillation. The product was recrystallized from hot absolute ethanol: mp 86–88 °C; ^1H NMR (CDCl_3) δ (ppm) 2.8–3 (t, CH_2 , 4 H), 3.6–3.9 (m, CH_2 , 6 H), 6.8–8 (m, aromatic, 12 H), 8.2 (s, CH, 2 H); ^{13}C NMR (CDCl_3) δ (ppm) 55.27, 57.76, 58.68, 116.87, 118.55, 123.42, 128.90, 131.17, 132.20, 147.15, 160.97, 165.85.

Step 5. 1,7-Bis(2-hydroxybenzyl)-4-(*p*-nitrobenzyl)diethylenetriamine (V). Schiff base IV (2 g, 4.5 mmol) prepared as above was dissolved in 70 mL of absolute ethanol. NaBH_4 (0.3 g, 8.1 mmol) was added to the solution and the mixture was stirred for 2 h at room temperature. A white solid appeared which was washed with aqueous ethanol and filtered. The product was recrystallized from hot absolute ethanol: mp 108–110 °C; ^1H NMR (CDCl_3) δ (ppm) 2.6 (s, CH_2 , 8 H), 3.6 (s, 2 H), 3.9 (s, CH_2 , 4 H), 6.3 (br, amine, 2 H), 6.7–8.2 (m, aromatic, 12 H); ^{13}C NMR (CDCl_3) δ (ppm) 46.01, 52.45, 54.08, 58.85, 116.27, 118.98, 122.18, 123.69, 128.24, 128.73, 129.33, 146.61, 158.04. Anal. Calcd for $\text{C}_{25}\text{H}_{30}\text{N}_6\text{O}_4$: C, 66.67; H, 6.67; N, 12.44. Found: C, 66.18; H, 6.77; N, 12.44.

Step 6. 1,7-Bis(2-hydroxybenzyl)-4-(*p*-aminobenzyl)diethylenetriamine (bhabdt, VI). Nitro compound V (170 mg) prepared above was dissolved in 100 mL of absolute ethanol and 100 mg of palladium on activated charcoal (10% Pd) was added. The mixture was hydrogenated at 40 psi for 24 h. The catalyst was filtered and the ethanolic solution was used without further purification: ^1H NMR (CDCl_3) δ (ppm) 2.6 (s, CH_2 , 8 H), 3.4 (s, CH_2 , 2 H), 3.8 (s, CH_2 , 4 H), 6.4–7.2 (m, aromatic, 12 H); ^{13}C NMR (CDCl_3) δ (ppm) 46.06, 52.35, 53.48, 58.74, 115.08, 116.33, 118.87, 122.50, 128.35, 128.62, 130.03, 145.74, 158.31.

1,7-Bis(2-hydroxybenzyl)-4-benzyl-diethylenetriamine (Bhbdt). The synthesis of ligand bhbdtd is described by Motekaitis et al. (5). We have prepared the intermediate 1,7-bis(2-salicylidene)-4-benzyl-diethylenetriamine by following their procedure. The Schiff base obtained thus was reduced to the amine 1,7-bis(2-hydroxybenzyl)-4-benzyl-diethylenetriamine (bhbdtd) by using NaBH_4 instead of hydrogenation: ^1H NMR (CDCl_3) δ (ppm) 2.6 (s, CH_2 , 8 H), 3.4 (s, CH_2 , 2 H), 3.7 (s, CH_2 , 4 H), 6.5–7.2 (m, aromatic, 12 H); ^{13}C NMR (CDCl_3) δ (ppm) 46.01, 52.35, 53.75, 59.34, 116.27, 118.87, 127.38, 128.30, 128.51, 128.84.

Complexation. Complexation of bhabdt with rhodium was attempted at different concentrations of ligand as well as of carrier rhodium. Typically, 0.5 mL of sodium bicarbonate buffer (0.5 M, pH 9), 0.1 mL of ^{105}Rh (~ 15 MBq), and 0.05 mL of RhCl_3 (1.25×10^{-3} mmol) were mixed together and refluxed for about 10 min in a 10-mL round-bottomed flask fitted with a glass condenser over a boiling-water bath. An ethanolic solution of the ligand (0.5 mL, 1.5×10^{-3} mmol) was added to this and the mixture was further refluxed for 2 h. The solution turned yellow on refluxing.

The solution was cooled to room temperature and transferred to a 10-mL centrifuge tube. The color of the complex solution turns green on cooling. A portion of the solution (10 μL) was withdrawn and the remaining solution was centrifuged for 15 min. The clear supernatant solution was transferred to a clean vial. A 10- μL aliquot of this solution was also withdrawn and counted for radio-

activity in a NaI(Tl) scintillation counter after suitable modification of the geometry. By comparing the activity in 10 μL of the supernatant after centrifugation, the amount of activity lost as solid was calculated. The final concentration of rhodium in the complex solution was calculated by taking into account this loss of activity and the total volume after heating.

The ^{105}Rh complex of the nonconjugating ligand (bhbdtd) was also prepared similarly with 1×10^{-3} mmol of rhodium carrier and 1.25×10^{-3} mmol of ligand.

Complex yields were estimated by an MgO-adsorption technique (8). This method is based on the observation that inorganic rhodium complexes are adsorbed by MgO, leaving behind the organic complexes in solution. Typically 10 μL of the complex solution was diluted to 0.4 mL and about 50 mg of MgO powder (USP, light powder) was added and this was mixed over a vortex mixer for ~ 2 min followed by a 5-min centrifugation. The supernatant was separated, and both fractions were counted. The fraction of the activity in the supernatant can be used as an estimate of the amount of complex present.

Preparation of the Isothiocyanate Derivative. The isothiocyanate derivative of the complex was prepared by treating an aqueous solution of the complex with an excess of thiophosgene in CHCl_3 . The isothiocyanate derivative of the complex is referred to as the activated complex throughout this paper.

Typically 1 mL of the complex ($\sim 7 \times 10^{-4}$ mmol) prepared above was mixed with 0.1 mL (1.3×10^{-2} mmol) of thiophosgene diluted in CHCl_3 for 2–5 min over a vortex mixer. The bulk of the activity, which was presumed to be the activated complex, was transferred into the organic layer. The aqueous layer was carefully withdrawn into another test tube. The amount of activity transferred into the organic layer was calculated by counting a 10- μL aliquot of the aqueous layer before and after activation. The organic layer was dried under a stream of nitrogen gas to remove CHCl_3 and excess CSCl_2 . The dried activated complex was redissolved in 200 μL of DMF and used for conjugation.

Conjugation. IgG (15 mg, 10^{-4} mmol) dissolved in 2 mL of 0.1 M borate buffer, pH 9, in 0.15 M NaCl was mixed with 30 μL (10^{-4} mmol, in a typical run) of the DMF solution of the activated complex and the mixture was incubated at room temperature for 4–5 h.

Estimation of Conjugation Yield. The conjugation yields were estimated by gel-filtration chromatography. A 30×1.4 cm column was packed with presoaked Sephadex G75 gel and equilibrated by passing at least 100 mL of 0.15 M NaCl solution through it. The reaction mixture (0.1 mL) was applied to the top of the column and eluted with 0.15 M NaCl solution. Two-milliliter fractions were collected, and the activity was measured in a NaI(Tl) scintillation counter. Recovery from the column was monitored by counting an equal aliquot as applied to the column after dilution to 2 mL and by comparing it with the sum of activity eluted from the column. Activity associated with the protein peak was summed and compared to the total activity to estimate the yield of conjugation. Total activity recovered from the column was $94 \pm 4\%$ of the added activity.

Nonspecific Labeling. The following three types of nonspecific-labeling effects were studied.

The unactivated complex of bhabdt (5×10^{-5} mmol) was incubated with 1 mL of IgG solution (5×10^{-5} mmol) for 24 h and separated by gel-filtration chromatography.

The complex of the nonconjugating ligand bhbdtd was incubated with IgG as above.

Table I. Complexation Yields at Different Ratios of Rh/Bhabdt^a

[Rh] ^b × 10 ⁴ (I)	[bhabdt] × 10 ³ (II)	[bhabdt]/ [Rh] (III)	% activity in solution ^c (IV)	% complex in solution ^d (V)	% complex yield ^e (VI)	% activity in organic fraction ^f (VII)	% conjugation (VIII)	overall % yield ^g (IX)	% Rh/IgG incorporated ^h (X)	% affinity adsorption (XI)
12.5	1.25	1	85	91	78	82	87	61	1.7	60
5	1.25	2.5	91	90	82	85	92	71	0.8	63
2.5	1.25	5	88	85	75	79	90	62	0.4	66
	1.25	NCA ⁱ	95	87	83	76	92	66		60

^a All reactions used ~15 MBq of ¹⁰⁵Rh. Conjugation reactions were carried out with 5 × 10⁻⁵ M IgG and 1.4 × 10⁻⁴ M ligand. Rhodium concentrations varied from 0.4 × 10⁻⁴ to 2 × 10⁻⁴ M. ^b Total volume of reaction was 2.1 mL. ^c Estimated by centrifugation after complexation. ^d Estimated by MgO-adsorption technique. ^e VI = IV × V. ^f Percent activity in organic layer after activation. ^g IX = IV × VII × VIII. ^h X = (1.4/0.5) × (IX/III). ⁱ NCA = no carrier added.

Table II. Complexation Yields at Different Concentrations of Bhabdt and Rhodium^a

[Rh] ^b × 10 ⁴ (I)	[bhabdt] ^b × 10 ⁴ (II)	% activity in solution ^c (III)	% complex in solution ^d (IV)	% complex yield ^e (V)	activity in organic fraction ^f (VI)	% conjugation (VII)	overall % yield ^g (VIII)	Rh/IgG incorporated ^h (IX)	% affinity adsorption (X)
12.5	12.5	96	94	90	84	86	70	0.8	60
5	5	96	90	85	83	93	75	0.8	74
2.5	2.5	100	87	87	82	90	74	0.8	77
NCA	2.5	100	88	87	69	90	62		71

^a Rhodium to bhabdt ratio was kept constant at ~1 in all cases except for the no-carrier-added (NCA) reaction. Conjugation reactions were carried out with 5 × 10⁻⁵ M IgG and 5.6 × 10⁻⁵ M ligand. Rhodium concentration varied from 4.5 × 10⁻⁵ to 6.9 × 10⁻⁵ M except for the no-carrier-added reaction. ^b Total volume of reaction was 2.1 mL. ^c Estimated by centrifugation after complexation. ^d Estimated by MgO-adsorption technique. ^e V = III × IV. ^f Percent activity of organic layer after activation. ^g VIII = III × VI × VII. ^h IX = (5.6/5) × VIII.

The complex of bhabdt was also treated with thiophosgene under identical conditions as that of bhabdt and incubated with IgG in order to estimate any conjugation through functional groups other than the primary amine in the benzyl side chain. The complex (5 × 10⁻⁵ mmol) treated with CSCL₂ was mixed with 1 mL of IgG solution (5 × 10⁻⁵ mmol) and incubated for 24 h. The conjugation yield was estimated as before.

EDTA Challenge. Two milliliters of the gel filtration purified labeled protein equivalent to 4.5 × 10⁻⁵ mmol of the complex was mixed with 20 μL of 0.1 M EDTA solution and incubated for 24 h. The activities associated with the protein and EDTA fractions were estimated by gel-filtration chromatography.

Affinity Gel Adsorption. As another method of estimating yields, affinity chromatography was done on an anti-IgG agarose gel column. Two milliliters of the gel was packed into a syringe column and equilibrated with 20 mL of 0.01 M phosphate buffer, pH 7.2. Fifty microliters of the solution from the conjugation reaction mixture was applied to the top of the column. Nonbound fractions were collected in 10 mL of phosphate buffer. Bound IgG was eluted with 0.05 M acetic acid containing 0.2 M sodium acetate, pH ~5.5. One-milliliter fractions were collected in both cases, and activity was monitored on a NaI(Tl) γ-scintillation counter.

In other studies, 1 mL of the affinity gel was incubated with 25 μL (~0.2 mg of IgG) of the solution from the conjugation reaction for 15 min with gentle shaking. The gel was washed three times with 2 mL of phosphate buffer to remove unbound activity. After the third wash the gel was counted for radioactivity. A 25-μL aliquot of the original solution was also counted for radioactivity under identical geometry. The percentage retention of activity on the gel was calculated by comparing the activity in the gel with the total activity.

Conjugation Kinetics. The time dependence of the conjugation reaction was studied by incubating 80 μL of the activated complex (1.5 × 10⁻⁴ mmol) with 3 mL of IgG solution (1.5 × 10⁻⁵ mmol). Portions (100 μL) of this solution were withdrawn at different time intervals and conjugation yields were estimated by gel-filtration

chromatography.

Stability of the Activated Complex. Forty microliters of the CHCl₃ extract of the activated complex (~10⁻⁴ mmol) was dispensed in test tubes and dried under nitrogen. The tubes containing the activated complex were sealed and stored at room temperature. One reaction tube each was taken at different time intervals, the contents were dissolved in 50 μL of DMF, and 25 μL of this solution was added to 1 mL of an IgG solution (5 × 10⁻⁵ mmol). The conjugation reaction was carried out for 5 h and the conjugation yield was estimated by gel-filtration chromatography.

RESULTS

Complexation. Results of the complexation, conjugation, and affinity adsorption studies with different batches of complex are summarized in Tables I and II.

Table I gives the results of the complex prepared with different rhodium to ligand ratios. Bhabdt/Rh ratios varied from 1 to 5 in experiments with rhodium carrier. In the no-carrier-added experiment the ligand concentration was almost 10⁶ times higher than that of the rhodium. The amount of rhodium activity lost as solids varied from 5% to 15%. Column V of Table I gives the complexation yield estimated by the MgO-adsorption technique. The complex yield in solution after removal of the solids varied between 85% and 91%. The overall complex yields (column VI, Table I) were calculated by taking into account the activity in solution after removal of solids and the complex yield in solution and varied between 75% and 83%.

Table II gives the complexation yield studied for reactions carried out at different concentrations of bhabdt and rhodium. The bhabdt to rhodium ratio was kept constant at about 1 except for the reaction with no-carrier-added rhodium. The complexation reaction was clean in all these cases with greater than 96% of the activity in solution after centrifugation. The complex yield in solution varied between 87% and 94%. Overall complex yields varied between 85% and 90%.

The extractability of the complex in CHCl₃ varied from 20% to 35% in different batches. A back-extraction of

Table III. Conjugation Yields at Different Rhodium to Protein Ratios

[IgG] $\times 10^6$ (I)	[Rh] $\times 10^6$ (II)	[Rh]/ [IgG] (III)	% conjugation (IV)	atoms of Rh/molecule of IgG incorporated ^a (V)	% overall Rh yield ^b (VI)
50	25	0.5	91	0.5	74
50	50	1	93	0.9	75
50	100	2	93	1.9	75
50	250	5	92	4.6	74
50	500	10	85	8.5	69
50	50	1	91	0.9	74
20	50	2.5	87	1.8	70
10	50	5	84	4.2	68
5	50	10	73	7.3	59

^a $V = \text{III} \times \text{IV}$. ^b Overall yield includes losses during complexation and preparation of the activated complex.

the complex from the organic layer into saline gave 67% of the activity still remaining in the organic layer. However, the second extraction of the aqueous layer gave only 9% of the activity in organic layer. These results suggest the possibility of the presence of more than one species of complex in solution, one which was readily extracted and one which was not.

Tables I (column VII) and II (column VI) show the activity transferred to the organic layer during the reaction with thiophosgene. Note that only 0.1 mL of CHCl_3 was used for extraction as against 1 mL of complex solution. The bulk of the activity was transferred into the organic layer. As the extractability of the complex itself was not this high, the higher extractability seen after activation was assumed to be due to the higher partition coefficient of the activated complex. The partition coefficient of the isothiocyanate derivative of the complex was estimated by repeated back-extractions into saline and was found to be ~ 60 .

The rhodium complex of the nonconjugating ligand bbbdt showed 67% extraction into CHCl_3 , and after treatment with CSCl_2 , 75% extraction was observed.

Conjugation. Conjugation studies with complex prepared at different bbbdt to rhodium ratios and at different concentrations of rhodium showed high yields. Yields varied from 86% to 93% in these cases and were found to be independent of the complexation condition. Conjugation experiments with different bbbdt to rhodium ratios were done with a ligand/IgG ratio of 2.5/1. In these studies, since excess ligand was used for complexation, all the ligand was not utilized and there was free ligand present. The average number of rhodium atoms per IgG incorporated in these studies varied from 0.4 to 1.7, depending upon the initial rhodium concentration. The overall rhodium recovery at the end of the conjugation reaction varied from 61% to 71% without taking into account the activity lost due to decay.

In conjugation experiments with complexes in which the bbbdt to rhodium ratio was kept constant at 1 (Table II), the number of rhodium atoms incorporated per molecule of IgG varied from 0.8 to 0.9. Note that the rhodium to IgG ratio was kept constant at 1 in these experiments. The final rhodium recovery varied from 70% to 75%.

Table III gives the results of conjugation studies with different rhodium to IgG ratios at a constant IgG concentration. The conjugation yield varied from 85% to 93% and 0.5–8.5 rhodiums per IgG were incorporated. The overall rhodium yield in these studies varied from 69% to 75%, taking into account the activity lost in all steps. The concentration of complex was also kept con-

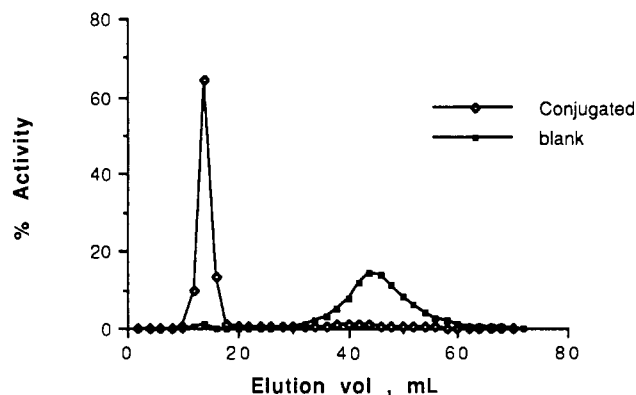


Figure 1. Gel filtration chromatography pattern of specifically and nonspecifically labeled IgG with the complexes of bbbdt on a Sephadex G75 column (30 \times 1.4 cm).

stant and the concentration of IgG varied. Rhodium to IgG ratios ranged from 1 to 10. The yield decreased from 91% to 73% when the IgG concentration was reduced from 5×10^{-5} to 5×10^{-6} mmol/mL. The number of rhodiums incorporated per IgG molecule varied from 0.9 to 7.3 in this set of experiments. The above results suggest that there is greater dependence on the concentration of IgG than on that of the activated complex for conjugation.

Figure 1 gives the gel filtration chromatography pattern of IgG incubated with activated and unactivated complexes of bbbdt. The nonspecific labeling obtained with the unactivated complex of bbbdt was less than 1%. The unactivated complex of the nonconjugating ligand bbbdt gave nonspecific labeling of about 3%. However, $\sim 30\%$ conjugation with IgG after reaction with thiophosgene was observed.

The results of EDTA-challenge studies show little exchange of rhodium between the labeled protein and EDTA. After a 24 h challenge study, 92% of the activity was still seen with the protein peak on chromatography. No separate peak was seen for EDTA or free complex when labeled-protein solution challenged with EDTA was rechromatographed.

Affinity chromatography of the labeled IgG from run 2 (Table II) gave 82% retention of the activity in the affinity column as against a 92% conjugation yield, indicating that $\sim 90\%$ of the labeled IgG was bound to the column. Labeled proteins from all the runs were not studied by affinity chromatography but instead by an affinity batch adsorption study which is less time consuming and has the advantage that multiple samples can be handled at a time. This method may not give the actual percentage of present but only an indication of the extent of labeling. The results of affinity adsorption studies are given as part of Tables I and II. Labeled IgG prepared in different batches showed greater than 61% adsorption to the affinity gel. The affinity adsorption for IgG from run 2 (Table II) was 73% as against 82% observed in affinity chromatography. The average of all the experiments listed in Tables I and II for the relative binding to the affinity gel compared to the gel filtration results is $75 \pm 10\%$, showing that the method can be used as a rough measure of whether or not conjugation has occurred. We also treated the unactivated complex of bbbdt with the affinity gel under similar condition and found that less than 5% of the activity was retained on the affinity gel after the third wash.

Figure 2 gives the kinetics of the conjugation reaction. Although the saturation was achieved at ~ 4 h, ~ 2 -h conjugation should be ideal, as the advantage gained by the

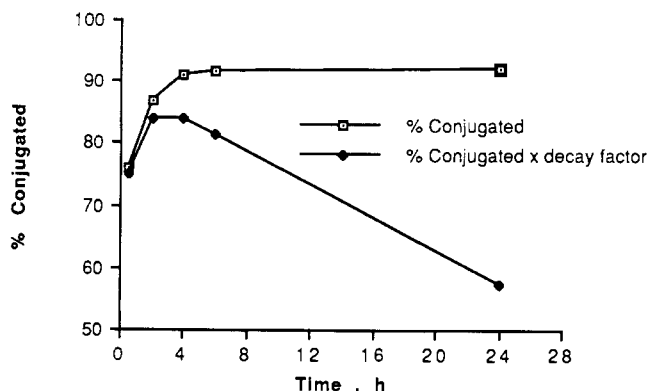


Figure 2. Kinetics of the conjugation reaction using 5×10^{-5} mmol of activated complex and IgG. Yield was estimated by gel-filtration chromatography.

Table IV. Stability of Dried Activated Complex after Storage at 4 °C^a

storage time, h	% conjugation	storage time, h	% conjugation
0	90	72	94
24	89	96	92
48	90		

^a The stored complex was redissolved in DMF and used to conjugate IgG. Concentrations of both protein and complex were $\sim 5 \times 10^{-5}$ M.

increase in conjugation is lost by the decay of activity.

Table IV gives the results of conjugation studies carried out with activated complex stored for different time intervals. No significant difference in conjugation was seen with activated complex stored up to 4 days.

DISCUSSION

These experiments show that bhabdt forms rhodium complexes which can be conjugated to IgG in high yield. From Tables I and II the yield of the complex itself was $83 \pm 5\%$, conversion of this complex to the isothiocyanate derivative was $90 \pm 5\%$, and the conjugation of this isothiocyanate derivative to IgG was $90 \pm 2\%$, giving an overall yield of $\sim 67\%$. Results shown in Tables III and IV are also consistent with these. Results from the four tables also show that from 0.4 to 8 atoms of rhodium can be incorporated per molecule of IgG. Although these experiments were done with rhodium spiked with ^{105}Rh , our goal was to show that proteins can be labeled with ^{105}Rh in specific activities high enough to produce radiotherapeutic agents. We have shown earlier (1) that ^{105}Rh can be produced at $>26 \times 10^6$ MBq/mmol from natural ruthenium targets irradiated in a flux of 8×10^{13} n/cm² s. That is a conservative estimate, allowing for a chemical recovery of only 50% and 2 days for processing and delivery and assuming that ruthenium impurities compete with rhodium for chelation sites. If one assumes further that an average of one rhodium (or impurity atom) can be added per antibody and that 1 half-life decay occurs during complexation, conjugation, and purification before use, labeling at greater than 74 MBq of ^{105}Rh /mg of antibody can be obtained, allowing treatment at the 3700-MBq level with less than 50 mg of antibody. Note again that these are conservative estimates. Use of 99%-enriched ^{104}Ru , irradiation in a flux of 4×10^{14} n/cm² s, and an average of two rhodiums per IgG would lead to specific activities of ~ 3000 MBq of ^{105}Rh /mg of IgG.

In order to treat a single patient with 3700 MBq, taking into account all the factors mentioned above, it would

be necessary to produce at EOB (end of bombardment) $\sim 37\,000$ MBq of ^{105}Rh . This amount could be decreased by decreasing the total time between EOB and patient use, by increasing the radiochemical yield during purification, and by increasing the overall conjugation yield.

The observation that the dried activated complex appears useful for at least 4 days after preparation suggests the possibility of a "kit" ready for reconstitution and conjugation. Again allowing for 1 half-life decay and $\sim 67\%$ yield, 11 000 MBq would be required for a kit providing 3700 MBq at time of use. Radiolytic damage during storage could reduce the effectiveness of the kit and require larger initial amounts.

We have not chemically characterized the rhodium complexes. Refosco et al. (9) have shown that the Schiff base forms of similar ligands form pentadentate complexes around the TcO^{3+} core with one hydroxy group trans to the oxo. We postulate a similar structure for these complexes, with a RhCl^{2+} core. However, there may be dinuclear species similar to those shown for Cu^{2+} (10).

X-ray structures done in this laboratory (11) for rhodium complexes with tetradentate, bis(bidentate), and tridentate amines show coordination of nitrogen atoms. We expect that the phenols are also coordinated. A similar structure is postulated (5) for Co^{II} complexes. However, there may also be species in which only three or four of the potential coordinating groups are utilized, leaving others free to form an isothiocyanate derivative. The blank experiments suggest that this may be true. While there was, as expected, very little apparent conjugation when complexes of bhabdt or bbbdt were used in the absence of thiophosgene, there was 30% conjugation when the complex of bbbdt was activated. We believe that in the absence of a *p*-aminobenzyl group, an uncoordinated phenol group may be activated and conjugated by means of a thiocarbamate (12). Similar results were obtained (13) with bis(salicylaldehyde) ligands of diaminopropane and 5-methyldipropylenetriamine.

These experiments were designed to prove the feasibility of using the ligand described here to couple rhodium to large proteins. They do not address the question of whether the use of DMF as a solvent and the conjugation itself lead to loss of immunoreactivity or the inertness of the complexes in vivo. Those experiments will follow later. They do confirm, however, our earlier work (2, 3) showing that rhodium can be linked to proteins by a preformed chelate method. They also suggest a simple and versatile scheme for synthesis of bifunctional pentadentate ligands with a wide range of linking groups and terminal coordinating groups.

ACKNOWLEDGMENT

Financial support for this work was provided by the Department of Energy (Grant No. DEFG02-86ER60400) and the University of Missouri Research Council. We wish to thank Dr. Alan Ketring and his colleagues at the University of Missouri Research Reactor and Dow Chemical Co. for the ^{105}Rh . A portion of this work was presented at the annual meeting of the Society of Nuclear Medicine, St. Louis, MO, June 1989.

LITERATURE CITED

- (1) Grazman, B., and Troutner, D. E. (1988) ^{105}Rh as a potential radiotherapeutic agent. *Appl. Radiat. Isot.* 39, 257-260.
- (2) John, C. S., Pillai, M. R. A., Lo, J. M., and Troutner, D. E. (1989) Labeling of proteins with ^{105}Rh . *Appl. Radiat. Isot.* 140, 701-705.
- (3) Pillai, M. R. A., Lo, J. M., John, C. S., and Troutner, D. E. (1989) Labeling of proteins using ^{105}Rh -4-(4-aminobenzyl)-diethylenetriamine. *Nucl. Med. and Biol.*, in press.

- (4) Pillai, M. R. A., John, C. S., Lo, J. M., and Troutner, D. E. (1989) Radiochemical studies of Tc-99m complexes of tetradentate amine-phenols. (Abstract) *J. Nucl. Med.* 30, 938.
- (5) Motekaitis, R. J., Martel, A. E., and Nelson, D. A. (1984) Formation and stabilities of cobalt(II) chelates of *N*-benzyl triamine Schiff bases and their dioxygen complexes. *Inorg. Chem.* 23, 275-283.
- (6) Troutner, D. E., Pillai, M. R. A., John, C. S., Lo, J. M., and Misellati, K. (1989) Pentadentate amine phenol complexes of ^{99m}Tc . (Abstract) *J. Nucl. Med. Allied Sci.* 33, 321.
- (7) Searle, G. H., Lincoln, S. F., Teague, S. G., and Rowe, D. (1979) Cobalt(III) complexes with 4-methyldiethylenetriamine [2,2'-methyliminodi(ethylamine)]: Their separation, characterization and reactions. *Aust. J. Chem.* 32, 519-536.
- (8) Lo, J. M., Pillai, M. R. A., John, C. S., and Troutner, D. E. (1989) Radiochemical purity evaluation of rhodium-105 complexes by magnesium oxide. *Appl. Radiat. Isot.*, in press.
- (9) Refosco, F., Tisato, F., Mazzi, U., Bandoli, G., and Nicolini (1988) Technetium(V) and rhenium(V) complexes with Schiff-base ligands containing the ONNNO donor atom set. Crystal structure of [*N,N'*-3-Azapentane-1,5-diylbis(salicylidineiminato)(3-)-*O,O',N,N',N''*]oxotechnetium(V). *J. Chem. Soc., Dalton Trans.* 611-615.
- (10) McKenzie, J. D., and Selvey, S. J. (1985) Copper(II) compounds with potentially quinquedentate ligand *N,N'*-bissalicylidene-1,5-diimino-3-azapentane, including an X-ray structure analysis of $[\text{Cu}_2(\text{C}_{18}\text{H}_{19}\text{N}_3\text{O}_2)_2] \cdot 2\text{C}_3\text{H}_6\text{O}$. *Inorg. Chem. Acta* 101, 127-133.
- (11) (a) Lynde, T. (1987) M.S. Thesis, University of Missouri.
(b) Ergun, G. (1989) Ph.D. Thesis, University of Missouri.
(c) John, C. S. (1988) personal communication.
- (12) Sharma, S. (1978) Thiophosgene in organic synthesis. *Synthesis* 803-820.
- (13) Misellati, K. (1989) Ph.D. Thesis, University of Missouri.

Immunoconjugate Design: A Predictive Approach for Coupling of Daunomycin to Monoclonal Antibodies

Ferenc Hudecz,[†] Helen Ross, Michael R. Price,* and Robert W. Baldwin

Cancer Research Campaign Laboratories, University of Nottingham, University Park, Nottingham NG7 2RD, U.K.
Received November 20, 1989

There is increasing interest in the development of daunomycin-antibody immunoconjugates for the targeting of drug to specific cells or tissues. To this end, we have examined the factors influencing the synthesis of daunomycin-monoclonal antibody conjugates linked covalently by an acid-labile *cis*-aconitic spacer (which is considered to aid drug release from immunoconjugates in the lysosomes and thus enhance their cytotoxic potential). A rapid and efficient procedure for the purification of drug from contaminants and stabilizers was first developed; conditions for the optimal preparation of *cis*-aconityldaunomycin were established; products were analyzed and identified by TLC and HPLC. The coupling of *cis*-aconityldaunomycin to antibody was accomplished by activating the modified drug with a carbodiimide before addition to antibody. Several factors were identified which influenced the efficiency of the conjugation; in particular, the compositional features of the antibody which determine its electrophoretic charge characteristics were of profound effect. However, by appropriate choice and control of buffer pH during conjugation, it was possible to define conditions resulting in the controlled substitution of antibody with drug. The consequent effects upon the cell-binding activity of immunoconjugates were established and related to the extent of substitution. The procedures described enable appropriate reaction conditions to be selected for the linkage of daunomycin to antibody (at set drug/antibody molar ratios) and in good yield, based upon consideration of the compositional and charge properties of the antibody.

Several strategies have been reported for the delivery of daunomycin to specific target cells. Daunomycin has been complexed to high molecular weight DNA (1), encapsulated in immunoliposomes (2), attached covalently to proteins such as hormones (3-5), enzymes (6), concanavalin A (7), casein (6), asialofetuin (6), histone (6), lactalbumin (5), serum albumin (6, 8, 9), ferritin (10), succinylated BSA¹ (11) or agglutinin (12), galactosylated HSA (1), and hapten-coupled ovalbumin (13), and conjugated

to polymers like poly[Lys] (14, 15), poly[Asp] (16), *N*-(2-hydroxypropyl)methacrylamide (HPMA) (17), poly[acryloyl-2-amido-2-(hydroxymethyl)-1,3-propanediol] (18), or

¹ Abbreviations (In order of appearance in the text): BSA, bovine serum albumin; HSA, human serum albumin; HPMA, *N*-(2-hydroxypropyl)methacrylamide; SPDP, *N*-succinimidyl 3-(2-pyridyldithio)propionate; MBS, *m*-maleimidobenzoic acid *N*-hydroxysuccinimide ester; cAD, *cis*-aconityldaunomycin; MoAb, monoclonal antibody; CMC, *N*-cyclohexyl-*N'*-(2-*N*-morpholinoethyl)carbodiimide methyl *p*-toluenesulfonate; EDC, *N*-ethyl-*N'*-[3-(dimethylamino)propyl]carbodiimide hydrochloride; PBS, phosphate-buffered saline, pH 7.3; MSR, molar substitution ratio; FITC, fluorescein isothiocyanate; Dau, daunomycin.

* To whom correspondence should be addressed.

[†] Present address: Department of Organic Chemistry, Eötvös, L. University, Budapest 112, P.O. Box 32, H-1518 Hungary.

dextran (19). Daunomycin has also been linked directly to cell-specific poly- or monoclonal antibodies (20, 21) or coupled to macromolecules such as HSA (22), dextran (23), HPMA (24), or poly[Glu] (25), which were then conjugated to antibodies to increase the degree of substitution with drug to enhance specific toxicity. More recent studies demonstrated that immunoconjugates containing daunomycin could be suitable not only for site-specific targeting, but also for modulating immune responses induced by immunoglobulin (26) or the T-cell mitogen concanavalin A (13).

The methods used for linking daunomycin to macromolecules have involved (a) cleavage of the bond between C-3 and C-4 of daunosamine producing carbonyl groups capable of reacting with the free amino groups of the protein (3, 5, 7, 10, 23, 27), (b) reaction at the amino group of the amino-sugar moiety (17, 24) using the cross-linking agents glutaraldehyde (8, 9, 19, 27, 28), carbodiimide (9, 25, 27), SPDP (21), and MBS (4), or (c) attachment to the methyl ketone side chain of the aglycon by nucleophilic substitution on its 14-bromo derivatives (6, 16, 21). Attachment of daunomycin was also achieved by the introduction of a peptidyl (11, 12, 18), maleyl (14), succinyl (15), or acid-labile *cis*-aconityl (13, 14, 21, 29) spacer. Although extensive work has been carried out with *cis*-aconityldaunomycin-monoclonal antibody (cAD-MoAb) conjugates, no systematic studies have been performed to define the optimal conditions with respect to coupling agent, reaction time, and concentration for their preparation.

In the present paper, we describe how a structurally defined cAD-MoAb conjugate can be synthesized and purified in a reproducible manner with an adequate yield and with a desired substitution ratio. The antibody reactivity of conjugates was also evaluated. This conjugation method was tested with two clinically relevant monoclonal antibodies, 791T/36 (30) and H65 (31), with different target cell specificities and chemical characteristics.

EXPERIMENTAL PROCEDURES

Materials. Daunomycin hydrochloride was obtained from Sigma or from May and Baker (Manchester, U.K.); *cis*-aconitic anhydride and *N*-cyclohexyl-*N'*-(2-*N*-morpholinoethyl)carbodiimide methyl *p*-toluenesulfonate (CMC) were from BDH (U.K.); *N*-ethyl-*N'*-(3-(dimethylamino)propyl)carbodiimide hydrochloride (EDC) was from Pierce.

Monoclonal Antibodies. The 791T/36 antibody (IgG2b) was obtained from a hybridoma produced by fusing spleen cells from a mouse immunized against the osteogenic sarcoma cell line 791T with the mouse myeloma cell line P3-NS1-Ag4 (30). The monoclonal antibody was purified from hybridoma tissue culture supernatant fluid by affinity chromatography using Sepharose-Protein A (Pharmacia, Uppsala, Sweden).

The H65 antibody (IgG1) reacting with CD5 antigen on normal and malignant human T cells (31) was purified from mouse ascites.

The antibodies 791T/36 and H65 were characterized by their amino acid compositions, isoelectric point values, and electrophoretic titration curves. Amino acid analyses were carried out on a LKB 4400 amino acid analyzer (LKB Biochrom, Cambridge, U.K.). The samples were subjected to hydrolysis with 6 M HCl in sealed tubes at 110 °C for 16 h. Isoelectric point determinations and titration curve analyses were performed by a PhastGel IEF 3-9 method using coomassie blue and silver staining procedures (Pharmacia, Uppsala, Sweden).

Preparation of *cis*-Aconityldaunomycin (cAD). Daunomycin hydrochloride and cAD samples were checked for purity by thin-layer chromatography (TLC), by elemental analysis, by IR spectroscopy, and by HPLC. TLC was done with silica gel containing fluorescent indicator (Polygram SIL G/UV₂₅₄, 0.25 mm Macherey-Nagel, FRG) on 3 × 5 cm precoated plastic sheets either in chloroform-methanol-water at 80:30:3 (by vol) (A) and in chloroform-ethanol-acetic acid at 70:20:15 (by vol) (B) systems in the case of daunomycin hydrochloride or in ethyl acetate-pyridine-acetic acid-water at 30:21:6:11 (by vol) (C) and in chloroform-methanol-acetonitrile-water at 50:50:14:12 (by vol) (D) systems in the case of cAD samples. Spots were detected with UV light and with 0.5% KMnO₄ solution in water.

Daunomycin hydrochloride preparations containing daunomycinone, daunosamine (Sigma, and May and Baker), and also mannitol (May and Baker) were purified by flash chromatography (32). Samples (20–100 mg) dissolved in the mixture (3–15 mL) of methanol-distilled water (1:1, v/v) were chromatographed on a 3.5 × 5 cm column of silica gel with average pore diameter of 60 Å (TLC standard grade without binder, Aldrich, U.K.) with chloroform-methanol-water at 80:30:3 (by vol) as eluent. Fractions (5–8 mL) were collected and analyzed by TLC. Fractions containing only daunomycin were pooled, evaporated, dissolved in distilled water, and freeze-dried (yield 65–80%). Purified daunomycin hydrochloride was stored in the dark at 4 °C.

cis-Aconityldaunomycin was prepared by using a modification of the method of Shen and Ryser (14). Purified daunomycin hydrochloride (50 mg–88.5 μmol) was dissolved in 6.0 mL of 0.1 N NaHCO₃/Na₂CO₃ buffer (pH 9.4) and cooled to 0 °C. A 70-mg portion (488 μmol) of *cis*-aconitic anhydride dissolved in 0.6 mL of anhydrous dioxane was added dropwise with vigorous stirring and a pH of 9.0 was maintained by addition of cold 0.5 N NaOH. When all the anhydride had been added, the reaction mixture was stirred at 0 °C for 15 min and the pH was kept between 9.0 and 9.2. To isolate the product, the cooled solution was acidified with cold 1.0 N HCl to pH 3. The precipitate formed was isolated by centrifugation at room temperature and redissolved in water, and the pH was adjusted to 6.8–7.4 with 0.2 N NaOH. The solution was then freeze-dried. The residue was stored in the dark at 4 °C. Samples for elemental analysis, melting point, and ε value determination were further purified on reversed-phase HPLC (yield 97.5%). Before conjugation, cAD was dissolved in distilled water (20 mg/mL) and extracted five times with a mixture of chloroform-methanol (95:5). The aqueous layer was evaporated and residue was dissolved in 1 mL of PBS and the cAD concentration was determined spectrophotometrically at 476 nm (ε = 8000).

Coupling of *cis*-Aconityldaunomycin to Monoclonal Antibody. Coupling was performed with either *N*-cyclohexyl-*N'*-(2-*N*-morpholinoethyl)carbodiimide methyl *p*-toluenesulfonate (CMC) (procedure A) or *N*-ethyl-*N'*-(3-(dimethylamino)propyl)carbodiimide hydrochloride (EDC) (procedure B) in PBS using a 1.5 times molar excess of carbodiimide. The coupling of activated cAD to antibodies was carried out with cAD/Ab at molar ratios between 30:1 and 100:1. After conjugation, the reaction mixture was centrifuged when necessary to remove any visible precipitate and the supernatant was applied to a Sephadex G-25 (medium grade) column equilibrated with PBS. The appropriate macromolecular peak as defined by UV detection at 275 nm was collected. The average ratio of molar substitution (MSR) was esti-

mated spectrophotometrically with the following formula:

$$\text{MSR} = (A_{476} 222200) / \{8000[A_{280} - (A_{476} Q)]\}$$

where A_{476} and A_{280} are the absorbances of the conjugate at 476 and 280 nm. The extinction coefficients of *cis*-aconityldaunomycin at 476 and 280 nm are 8000 and 5890 $\text{M}^{-1} \text{cm}^{-1}$, respectively, and Q is defined as $5890/8000 = 0.736$. The extinction coefficient of immunoglobulin at 280 nm is 222 200 $\text{M}^{-1} \text{cm}^{-1}$.

Procedure A. A 1.9–5.2 μmol portion (1.3–3.6 mg) of cAD in 86–216 μL of PBS was diluted with PBS, pH 6.0, to a final concentration of 0.25 mg/mL. The solution was stirred and treated with 2.85–7.8 μmol (1.2–3.3 mg) of CMC dissolved in 120–330 μL of distilled water (i.e. a 1.5 times molar excess of carbodiimide reagent). After stirring for 30 min at room temperature, 64.5 nmol (10 mg) of antibody in 1.2–2.9 mL of PBS was added to the solution and the pH was adjusted to 6.0, 8.0, or 9.0. The final concentration of antibody was 1.6 mg/mL. The reaction was allowed to proceed for 16 h at room temperature.

Procedure B. A 3.2–6.4- μmol portion (2.2–4.4 mg) of cAD was dissolved in 145–290 μL of PBS (at 15 mg/mL) and diluted with PBS, buffered to pH 7.0, 6.0, or 5.0. The stirred solution was treated with 4.8–9.6 μmol (0.92–1.94 mg) of EDC dissolved in 92–194 μL of distilled water. The reaction mixture was stirred for 30 min at room temperature and then 64.5 nmol (10 mg) of antibody in 1.2–2.9 mL of PBS was added and the pH was adjusted to 6.0, 8.0, or 9.0. The final concentration of antibody was 1.6–1.7 mg/mL. The reaction was allowed to stand for 3 h at room temperature.

HPLC Analysis of cAD–Antibody Conjugates. Instrumentation. The HPLC system consisted of one Model 302 and one Model 303 liquid delivery modules, a Model HM/HPLC Holochrome UV–visible detector, a Model 811 dynamic mixer, a Model 802 manometric module, a Model N1 recorder (all from Gilson France S.A., Villiers, France), a Model 7125 injector valve, and 100- μL and 200- μL sample loops (Rheodyne, Inc., Cotati, CA). A 25 cm \times 4.6 mm column and a 3 cm \times 4.6 mm Aquapore RP-300 guard column (Brownlee Labs, Inc., Santa Clara, CA) were used. Both columns contained spherical 7- μm silica (300 Å pore size) with a hydrophobic bonded phase.

Conditions. The mobile phase consisted of 0.2 M ammonium carbonate in water and of methanol (50:50, v/v). Ammonium carbonate solution was prepared daily with high-purity (Analar) salt and distilled, deionized water and was mixed with methanol 20 min before use. The injection volume was 100 μL containing 0.3 μg (0.53 nmol) of daunomycin and/or 0.3 μg (0.44 nmol) of cAD dissolved in eluent or 200 μL containing 1.3–4.7 μg (1.8–8.3 nmol) of cAD coupled to antibody in PBS. Daunomycin hydrochloride and cAD were used separately as standards and their retention times were determined. UV absorbance was monitored at a wavelength of 280 nm. All analyses were carried out at room temperature with a flow rate of 1.0 mL/min.

Assay of Conjugate Immunoreactivity. Cell-binding activity of conjugates was estimated by a flow cytometric competition assay essentially as previously described (33). Briefly, conjugates were diluted so that the equivalent of 4, 2, 1, or 0.5 μg of antibody were mixed with 1 μg of fluorescein-labeled antibody. A standard unlabeled antibody was tested in parallel with conjugates in each assay. After mixing of labeled and unlabeled anti-

Table I. TLC Chromatographic R_f Values of Daunomycin, Its Derivatives, and of Mannitol

compound	R_f value ^a			
	A	B	C	D
daunomycin hydrochloride	0.49	0.12	0.60	0.80
daunomycinone	0.80	0.86	0.87	0.91
<i>cis</i> -aconityldaunomycin	nt ^b	nt	0.44	0.54
daunosamine	0.00	0.00	0.00	0.00
mannitol	0.13	0.00	nt	nt

^a Solvent systems: A, chloroform–methanol–water 80:30:3 (by vol); B, chloroform–ethanol–acetic acid 70:20:15 (by vol); C, ethyl acetate–pyridine–acetic acid–water 30:21:6:11 (by vol); D, chloroform–methanol–acetonitrile–water 50:50:14:12 (by vol). ^b Nt = not tested.

bodies, 10^5 target cells expressing the appropriate antigen were added, and the mixture was incubated for 1 h at 4 °C. 791T/36 conjugates were tested on 791T cells and H65 conjugates were tested on MOLT-4 (MSKCC) cells; prior to use, target cells were fixed in 1% paraformaldehyde for 10 min.

Cell-bound fluorescence was quantitated with a FACS IV flow cytometer (Becton Dickinson). Under the conditions used (i.e. with antibody at saturation), the inhibition of binding of fluorescein-labeled antibody by non-fluorescent conjugate, or by standard antibody, is proportional to their binding activity; antibody activity of conjugate relative to standard antibody was determined by comparison of regression lines of antibody concentration plotted against the reciprocal of cellular fluorescence.

RESULTS

Synthesis and Characterization of *cis*-Aconityldaunomycin (cAD). Daunomycin hydrochloride preparations containing contaminants (daunosamine, daunomycinone, etc.) or stabilizers (e.g. mannitol) were purified by flash chromatography on a silica column by applying a chloroform–ethanol–water (80:30:3, by vol) solvent mixture as eluent. This procedure produced an efficient and rapid separation with simple apparatus and operation. After purification no contaminants were detected by TLC on silica gel in two independent solvent systems (Table I).

cAD was synthesized according to the literature (14) with modifications. In daunomycin, phenolic ionization occurs with the pK_a value near 10.0 and the ammonium group deprotonates with $\text{pK}_a = 8.6$ (34). In respect of these pK_a values, pH = 9.0 was selected for the preparation of cAD and strictly maintained by pH-stat during and after addition of *cis*-aconitic anhydride. The reaction was followed by TLC on silica gel in two independent solvent systems (Table I). In order to remove unreacted daunomycin, the aqueous solution of crude cAD was extracted with chloroform–methanol (95:5 v/v) to produce a homogeneous product (yield 97.5%). Further purification was performed on reversed-phase HPLC to prepare material for elemental analysis, melting point, and ϵ value determinations; the results were as follows: mp 215–225 °C; R_f values are detailed in Table I; UV λ_{max} (in PBS) = 476 nm ($\epsilon = 8000$). Anal. Calcd for $\text{C}_{33}\text{H}_{33}\text{O}_{15}\text{N}$ (683.635): C, 57.98; H, 4.87; N, 2.05. Found: C, 57.68; H, 4.82; N, 1.73. Although cAD showed only spot in TLC, it may contain two α - and β -monoamide isomers with carboxyl groups in *cis* position as hypothesized earlier (14). In order to investigate this, an HPLC method has been developed for quantitative analysis of cAD preparations. Chromatographic conditions were optimized to achieve base-line separation and high resolu-

Table II. Amino Acid Composition of Monoclonal Antibodies 791T/36 and H65

amino acid	monoclonal antibody		amino acid	monoclonal antibody	
	791T/36	H65		791T/36	H65
Asp/Asn	1.88 ^a	1.95	Leu	1.23	1.02
Glu/Gln	1.71	1.80	Ile	0.60	0.75
Thr	1.89	1.88	Met	0.23	0.18
Ser	2.17	1.70	Tyr	0.80	0.98
Pro	1.53	1.40	Phe	0.64	0.97
Gly	1.20	1.30	His	0.55	0.40
Ala	1.00	1.00	Lys	1.58	1.65
Val	1.17	1.22	Arg	1.02	0.46

^a Expressed as mol of amino acid/mol of alanine.

tion with an isocratic methanol–water–ammonium carbonate eluent system. The purified cAD dissolved in methanol was run on an Aquapore RP-300 column and two components with proper separation coefficient ($\alpha = 1.3$) were detected. On the basis of peak areas and assuming a common extinction coefficient for both components, the isomer composition of cAD samples was estimated to be 1:1.

Characterization of Monoclonal Antibodies (MoAb). The amino acid composition and charge characteristics of 791T/36 and H65 monoclonal antibodies were investigated so that the influence of their biochemical features with respect to the synthesis of *cis*-aconityldaunomycin–antibody conjugates could be established. The amino acid sequence of these proteins is not known.

The polypeptides were hydrolyzed to the constituent amino acids by standard procedures using acidic conditions (35). The results, expressed as molar ratio of each amino acid relative to alanine, are presented in Table II. These data indicate marked differences in the amino acid composition of the MoAbs. 791T/36 contains more Arg, Ser, and Leu, while the polypeptide chains of H65 are predominated by aromatic amino acids (Tyr, Phe, and Ile). Significant differences were noted by comparison of the basic amino acid residues (Lys + Arg + His). The elevated level of these residues in the 791T/36 antibody is accompanied by a slightly decreased amount of acidic amino acid residues (Asp/Asn + Glu/Gln).

The charge characteristics of the MoAbs were analyzed over a broad range of pH by isoelectric focusing in polyacrylamide gels (36). This technique has been used to determine the isoelectric points and electrophoretic titration curve of 791T/36 and H65. Figure 1 shows that the 791T/36 antibody preparation consisted of five major and one minor bands within a *pI* region from 7.7 to 8.6 (lane 2). It is evident from Figure 1 that H65 antibody was also found to display six bands with a range of isoelectric points from 6.3 to 6.7 (lane 1). It should be noted that in this case the *pI* range was somewhat less wide (with an average value of 6.5) than in the case of the 791T/36 antibody with a characteristic average *pI* value of 8.2. The multiple-band spectrum of various monoclonal antibodies has been demonstrated in the literature (e.g. ref 37). The origin of this phenomenon is likely to be due to posttranslational modification of biosynthetically homogeneous protein (glycosylation, etc.) or to lability after synthesis (deamidation, etc.), though this has not been investigated.

The comparison of the *pI* ranges and average *pI* values of 791T/36 and H65 demonstrates that these proteins are very different in their electrophoretic behavior. This observation was supported by their titration curve analysis. In our experiments, the electrophoretic mobility of these proteins throughout the gradient pH 3–9 was

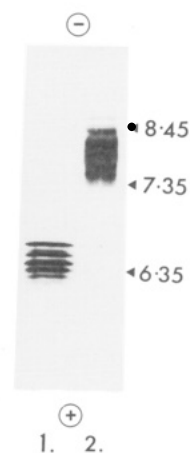


Figure 1. Monoclonal antibodies focused on PhastGel IEF 3-9. The gel was run according to the method in separation technique file number 100 using silver staining: lane 1, H65 monoclonal antibody; lane 2, 791T/36 monoclonal antibody.

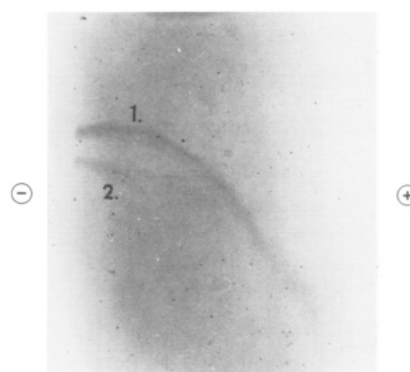


Figure 2. Electrophoretic titration of monoclonal antibodies on PhastGel IEF 3-9 with coomassie blue staining: curve 1, 791T/36 monoclonal antibody; curve 2, H65 monoclonal antibody.

investigated by running MoAbs individually or in a 1:1 (w/w) mixture. In the titration curve of the mixture of 791T/36 and H65, shown in Figure 2, both antibodies produced a fuzzy, but similar, patterns below their isoelectric point. Significant differences were recorded in the shape and position of bands above the *pI*, and this was attributed to a pronounced polycationic character of the 791T/36 antibody.

Preparation and Characterization of *cis*-Aconityldaunomycin–Monoclonal Antibody (cAD–MoAb) Conjugates. The coupling of cAD to proteins was achieved by a carbodiimide method in which one carboxyl group of the drug was linked to the ϵ -amino group of the lysine side chain of the antibody to provide covalent amide bonding. The synthesis of a conjugate was performed in two steps. First, the carboxyl groups of cAD were activated by water-soluble carbodiimide (either CMC or EDC) under identical conditions (i.e. 1.5 times molar excess of carbodiimide, temperature, concentration, reaction time). The pH dependence of this activation process was studied under a neutral (pH 7.0) or acidic (pH 6.0 or 5.0) environment. In the second step, the carboxyl-activated derivative was added to the amino component (protein) and the coupling reaction proceeded in acidic (pH 6.0) or in alkaline solution (pH 8.0 or 9.0). The conjugates composed of cAD and 791T/36 or H65 monoclonal antibody were purified by gel-filtration column chromatography and characterized by reversed-phase HPLC and by specific target cell binding activity. The synthetic procedures and the chemical properties of

Table III. Preparation and Characterization of cAD-791T/36 Conjugates

conjugate	prepn procedure	molar ratio of cAD/Ab (mol/mol)	coupling agent	pH		% yield	% free ^a cAD/Dau	MSR ^b
				activation	coupling			
1	A	30	CMC	6	8	85.5	<4.0	2.1
2	A	50	CMC	6	8	85.0	<3.0	2.9
3	A	50	CMC	6	9	90.0	<3.0	4.0
4	A	80	CMC	6	8	50.1 ^c	<4.0	5.0
5	B	50	EDC	7	9	95.0	<2.5	0.9
6	B	100	EDC	7	9	88.0	nt ^d	2.3
7	B	50	EDC	6	9	87.2	<3.0	4.6
8	B	100	EDC	6	9	93.0	1.9	9.1
9	B	50	EDC	6	8	90.6	2.9	2.5
10	B	100	EDC	6	8	39.4 ^c	<3.0	14.9
11	B	50	EDC	5	9	90.0	<3.0	8.8
12	B	100	EDC	5	9	84.7	<3.0	17.2

^a Determined by reversed-phase HPLC as described in the Experimental Procedures. ^b Average ratio of molar substitution. ^c Precipitation was observed. ^d Nt = not tested.

Table IV. Preparation and Characterization of cAD-H65 Conjugates

conjugate	prepn procedure	molar ratio of cAD/Ab (mol/mol)	coupling agent	pH		% yield	% free ^a cAD/Dau	MSR ^b
				activation	coupling			
1	A	50	CMC	6	8	82.0	nt ^c	1.7
2	A	100	CMC	6	8	91.7	<3.0	4.1
3	A	50	CMC	5	8	86.0	4.1	2.6
4	A	100	CMC	5	8	90.0	<4.0	8.4
5	A	100	CMC	5	6	83.6	nt	2.5
6	B	50	EDC	6	8	81.0	nt	2.2
7	B	100	EDC	6	8	97.0	2.2	11.9
8	B	50	EDC	5	8	86.0	2.8	3.4
9	B	75	EDC	5	8	99.0	2.3	12.7
10	B	100	EDC	5	8	98.5	2.7	29.0
11	B	50	EDC	5	6	95.4	nt	0.6
12	B	100	EDC	5	6	88.5	nt	4.0

^a Determined by reversed-phase HPLC as described in the Experimental Procedures. ^b Average ratio of molar substitution. ^c Nt = not tested.

conjugates are summarized in Tables III and IV. The results presented in these tables indicate that the amount of cAD incorporation into the protein conjugate depends on the ratio of cAD to MoAb used in the reaction mixture. The highest coupling efficacy quantitated by average molar substitution ratio (MSR) was obtained with a 100-fold molar excess of cAD over the protein. The choice of carbodiimide could also influence the composition of the conjugates. Under comparable conditions EDC-mediated synthesis of cAD-MoAb conjugates could lead to higher MSR values (Table IV, conjugates 6–8, 10, and 12). The activation of cAD proved to be favored at lower pH as demonstrated in Tables III and IV. cAD-791T/36 conjugated with high MSR (17.2) could be synthesized with a cAD intermediate prepared at pH 5.0. In contrast, the drug incorporation sharply decreased (MSR = 2.3) when this reaction was performed in neutral (pH 7.0) solution. A similar tendency was observed with cAD-H65 conjugates (Table IV, conjugates 7 and 10 or 2 and 4).

The pH sensitivity of the coupling step was also analyzed with cAD-791T/36 preparations. Conjugation at pH 8.0 resulted in lower drug incorporation as compared to coupling performed at pH 9.0 (Table III, conjugates 2 and 3 or 7 and 9) or nonreproducible amounts of precipitation (Table III, conjugates 4 and 10). It should be noted that no precipitate was observed during the synthesis of cAD-H65 conjugate under identical circumstances (Table IV, conjugate 7). The same findings could be demonstrated in the comparison of the cAD-791T/36 preparation (Table III, conjugate 4) with the cAD-H65 preparation (Table IV, conjugate 2). A heavy precipitate was formed in the course of the synthesis of cAD-791T/36 conjugate (yield 50.1%), while the reaction mixture remained clear after 16 h in case of cAD-H65 prepara-

tions (yield 91.7%) using even higher input molar ratio. These observations can be explained by the different charge characteristics of 791T/36 and H65. Isoelectric precipitation of cAD-791T/36 would occur at a pH 8.0, because the average pI of the antibody (pI = 8.2) is close to this value. No such phenomena would be expected with cAD-H65 preparations at this pH, due to the lower average isoelectric point of the antibody (pI = 6.2). An increase in pH of the coupling reaction (from pH 8.0 to 9.0) proved to be sufficient for precipitate-free synthesis of cAD-791T/36 conjugate (Table III, conjugate 8).

Following purification by gel filtration, HPLC was used to detect free anthracycline derivatives in the samples of cAD-MoAb conjugates. Quantitative analysis, performed on a reversed-phase column (pore size of 300 Å, isocratic elution), indicated no detectable amount of free daunomycin, but the presence of 1–5% of cAD could be demonstrated in the conjugates using peak-area measurement calibrated with appropriate standards.

To examine the retention of target cell binding activity, conjugates were tested in a competitive inhibition assay. With this, the capacity of conjugate to inhibit the binding of FITC-labeled 791T/36 antibody to 791T cells and FITC-labeled H65 antibody to MOLT-4 (MSKCC) cells was determined by flow cytometry and compared with the capacity of unlabeled antibody. As shown in Figure 3, cAD-791T/36 conjugates with low incorporation (MSR < 5) displayed greater binding activity than conjugates with a higher degree of substitution MSR > 10). The recovery of activity in conjugates belonging to the former group was between 25% and 65%, and with preparations of the latter group, recoveries of cell-binding activity less than 10% were recorded. In contrast, the cell-binding activity of H65 monoclonal antibody with the antigen-positive cell line was largely retained after

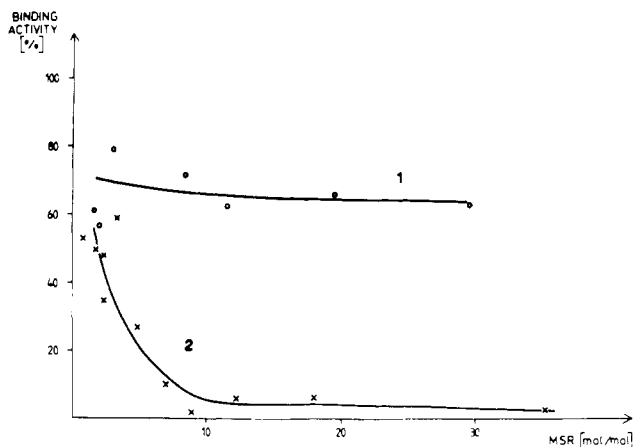


Figure 3. Correlation of antibody reactivity with mean substitution ratio in (1) H65 and (2) 791T/36 conjugates. Antibody reactivity is expressed as a percentage of the binding activity of unconjugated antibody to fixed cells expressing the appropriate antigen.

conjugation. As is indicated in Figure 3, a reduction in reactivity of 30–35% was observed with target cells, but this was almost independent, regardless of the degree of substitution achieved (up to 30 mol of cAD/mol of protein).

DISCUSSION

The clinical potential of daunomycin–MoAb conjugates includes the immunochemotherapy of cancer (29) and modulation of immune responses (13, 26). Many studies have demonstrated the specific toxicity of daunomycin or adriamycin on tumor cells when coupled to MoAb raised to tumor-associated antigens (38, 39). However, less emphasis has been directed toward the reliable and reproducible synthesis of anthracycline–MoAb conjugates. Attempts to compare the effect of various linkage between daunomycin and MoAb have been made (21), but no systematic studies were performed to optimize conjugation by using any particular method. One objective of this work has been to develop procedures suitable for the preparation of conjugates with predictable MSR and cell-binding activity. In order to achieve this, a model system was established, in which the *cis*-aconityl derivative of daunomycin and two MoAbs with different chemical characteristics were used.

Highly purified daunomycin, obtained following efficient and rapid flash chromatography, was reacted with *cis*-aconitic anhydride. In respect of the pK_a of ammonium and phenol groups of daunomycin, this reaction was kept under pH control to avoid decomposition (pH > 9.5) or low yield (pH < 9.0). Although cAD proved to be homogeneous on TLC, HPLC analysis revealed the presence of two isomers in a 1:1 molar ratio. Since these isomers could have different physicochemical properties, their isolation and characterization would be an appropriate objective in further experiments. Determination of the molar absorptivity of daunomycin in the $\lambda = 475$ –480-nm range varies from 9100 (40) to 11 500 $M^{-1} cm^{-1}$ (41) in the literature. It is generally accepted that the same molar absorptivity is relevant for cAD, but no experimental data have been reported. Our results with highly purified cAD did not support this assumption and a significantly lower ϵ value (8000 $M^{-1} cm^{-1}$) was determined.

Monoclonal antibodies used for these studies were characterized by their amino acid composition and charge properties. These results indicated pronounced structural differences between the two antibodies; 791T/36 proved to

have a polycationic character containing more Arg and less acidic amino acid residues (mean $pI = 8.2$), while H65 was found to be almost amphoteric (mean $pI = 6.5$).

A number of cAD–MoAb conjugates were prepared in order to analyze the dependence of coupling efficacy and target specific binding activity upon the physicochemical features of the drug and of the antibodies, and consequently upon the reaction conditions (i.e. coupling agent, cAD/protein input molar ratio, pH). The carbodiimide-mediated activation of cAD and the coupling procedure were studied separately. Our results clearly demonstrate that the efficacy of conjugation could be controlled by the input drug/protein ratio or by the choice of carbodiimide. These data also suggest that the degree of drug incorporation could be influenced dramatically by the ionization state of both cAD and monoclonal antibodies. The above studies led to the following conclusions: (1) cAD could be effectively activated by a carbodiimide at lower pH probably due to the protonation of one of the two carboxylate groups in the molecule. No data are available for the acidity of cAD. Acidity constants only for aconitic acid are known ($pK_{a1} = 2.8$, $pK_{a2} = 4.6$). (2) Coupling of activated cAD to monoclonal antibody could be optimized by performing this procedure at a pH above the average pI of the uncoupled antibody. As suggested by the comparison of our cAD–791T/36 and cAD–H65 studies, a reproducible synthetic strategy could be designed for each individual MoAb. It should be noted that the MSRs are not necessarily linearly related to the input cAD/MoAb ratios, probably due to some conformational changes during the sequential process of coupling. On the basis of these considerations, it is feasible to prepare cAD–MoAb conjugates with desired average molar substitution ratio. However, there are some limitations with this particular model system using cAD (which itself is a mixture of two isomers), which contains two types of carboxyl group with unknown relative reactivity.

With respect of the retention of cell-binding activity we determined that cAD–791T/36 conjugates differed from the cAD–H65 preparations. In the former group, the average molar substitution ratio was almost inversely proportional to the antibody reactivity, which may be related to the particular distribution of lysine residues within the Fab regions of the 791T/36 antibody. Similar observations have been made by other investigators using various monoclonal antibody–drug conjugates (20). cAD–H65 conjugates with high MSR were exceptionally active. The reason for this is unknown and further studies are required to determine whether domains exposed and/or generated by cAD attachment are more accessible for hydrophobic interaction with the target-cell surface following the binding of antibody to its target antigens. Alternatively, modification of the net charge of the conjugate compared with that of antibody may also influence the specific binding activity of conjugates, and it is further feasible that preferential substitution of H65 antibody in nonantigen binding regions of the protein may occur.

ACKNOWLEDGMENT

These studies were supported by the Cancer Research Campaign and the XOMA Corp. (Berkeley, CA). Support for F. Hudecz, provided by the Concern Foundation (Los Angeles, CA) is gratefully acknowledged. Thanks are expressed to M. Sekowski for providing purified 791T/36 antibody, to D. Hooi for expert technical assistance, and to the XOMA Corp. for providing purified H65 antibody.

LITERATURE CITED

- (1) Trouet, A., and Jolles, G. (1984) Targeting of daunorubicin by association with DNA or proteins: A review. *Semin. Oncol.* 11, 64-72.
- (2) Dhananjaya, K. V. R., and Antony, A. (1988) Cytotoxic activity of daunomycin and adriamycin encapsulated in immunoliposomes against avian myeloblastosis virus-infected cells. *J. Virol. Methods* 19, 131-140.
- (3) Varga, J. M., Asato, N., Lande, S., and Lerner, A. B. (1977) Melanotropin-daunomycin conjugate shows receptor-mediated cytotoxicity in cultured murine melanoma cells. *Nature* 267, 56-58.
- (4) Scott, D., and Ontjes, D. (1981) Biologically active conjugates of ACTH analogs containing daunorubicin. *Peptides: Synthesis, Structure and Function* (D. H. Rich, E. Gross, Eds.) pp 817-820, Pierce Chemical Co., Rockford, IL.
- (5) Kaneko, Y. (1981) Thyrotropin-daunomycin conjugate shows receptor mediated cytotoxicity in cultured thyroid cells. *Horm. Metab. Res.* 13, 110-114.
- (6) Zunino, F., Gambetta, R., Vigevari, A., Penco, S., Geroni, C., and DiMarco, A. (1981) Biologic activity of daunorubicin linked to proteins via the methylketone side chain. *Tumori* 67, 521-524.
- (7) Kitao, T., and Hattori, K. (1977) Concanavalin A as a carrier of daunomycin. *Nature* 265, 81-82.
- (8) Lagueux, J., Pagé, M., and Delorme, F. (1984) Daunorubicin-albumin copolymer targeting to leukemic cells in vitro and in vivo. *Semin. Oncol.* 11, 59-63.
- (9) Lyashenko, V. A., and Alexander, S. K. (1978) Antitumor properties and toxicity of carminomycin complex with protein. *Antibiotiki* 23, 1005-1009.
- (10) Williamson, J., Scott-Fininningan, T. J., Hardman, M. A., and Brown, J. R. (1981) Trypanocidal activity of daunorubicin and related compounds. *Nature* 292, 466-467.
- (11) Trouet, A., Masquelier, M., Baurain, R., and Deprez-De-Campeneere, D. (1982) A covalent linkage between daunorubicin and proteins that is stable in serum and reversible by lysosomal hydrolases, as required for a lysosomotropic drug-carrier conjugate: In vitro and in vivo studies. *Proc. Natl. Acad. Sci. U.S.A.* 79, 626-629.
- (12) Monsigny, M., Kieda, C., Roche, A. C., and Delmotte, F. (1980) Preparation and biological properties of a covalent antitumor drug-arm-carrier (DAC conjugates). *FEBS Lett.* 119, 181-186.
- (13) Diener, E., Diner, U. E., Sinha, A., Xie, S., and Vergidis, R. (1986) Specific immunosuppression by immunotoxins containing daunomycin. *Science* 231, 148-150.
- (14) Shen, W. C., and Ryser, H. J. P. (1981) *cis*-Aconityl spacer between daunomycin and macromolecular carriers: a model of pH-sensitive linkage releasing drug from lysosomotropic conjugate. *Biochem. Biophys. Res. Commun.* 102, 1048-1054.
- (15) Arnold, L. J., Dagan, A., and Kaplan, N. O. (1983) Poly-L-lysine as an Antineoplastic Agent and Tumor-Specific Drug Carrier. *Polymers in Biology and Medicine* Vol. 2, pp 89-112, Wiley, New York.
- (16) Zunino, F., Giuliani, F., Sovi, G., Dasdia, T., and Gambetta, R. (1982) Anti-tumor activity of daunorubicin linked to poly-L-aspartic acid. *Int. J. Cancer* 30, 465-470.
- (17) Duncan, R., Kopeckova-Rejmanova, P., Strohalm, J., Hume, I., Cable, H. C., Pohl, J., Lloyd, J. B., and Kopecek, J. (1987) Anticancer agents coupled to *N*-(2-hydroxypropyl)methacrylamide copolymers. I. Evaluation of daunomycin and puromycin conjugates in vitro. *Br. J. Cancer* 55, 165-174.
- (18) Daussin, F., Boschetti, E., Delmotte, F., and Monsigny, M. (1988) *p*-Benzylthiocarboamoyl-aspartyl-daunorubicin-substituted polytrisacryl. A new drug acid-labile arm-carrier conjugate. *Eur. J. Biochem.* 176, 625-628.
- (19) Bernstein, A., Hurwitz, E., Maron, R., Arnon, R., Sela, M., and Wilchek, M. (1978) Higher antitumor efficacy of daunomycin when linked to dextran. In vivo and in vitro studies. *JNCI, J. Natl. Cancer Inst.* 60, 379-384.
- (20) Ghose, T., and Blair, T. H. (1986) The design of cytotoxic-agent antibody conjugates. *Crit. Rev. Ther. Drug Carrier Sys.* 3, 263-359.
- (21) Gallego, J., Price, M. R., and Baldwin, R. W. (1984). Preparation of four daunomycin-monoclonal antibody 791T/36 conjugates with anti-tumor activity. *Int. J. Cancer*, 33, 737-744.
- (22) Ogunmuyiwa, Y., Clegg, J. A., Pimm, M. V., Price, M. R., and Baldwin, R. W. (1987) Comparative biodistribution of daunomycin-HSA-monoclonal antibody conjugates with different chemical linkages. *Br. J. Cancer* 56, 186.
- (23) Hurwitz, E., Maron, R., Bernstein, A., Wilchek, M., Sela, M., and Arnon, R. (1978). The effect in vivo of chemotherapeutic drug-antibody conjugates in two murine experimental tumor systems. *Int. J. Cancer* 21, 747-755.
- (24) Rihova, B., Kopeckova, P., Strohalm, J., Rossmann, P., Vetricka, V., and Kopecek, J. (1988). Antibody-directed affinity therapy applied to the immune system: in vivo effectiveness and limited toxicity of daunomycin conjugated to HPMA copolymers and targeting antibody. *Clin. Immunol. Immunopathol.* 46, 100-114.
- (25) Kato, Y., Umemoto, N., Kayama, Y., Fukushima, H., Takeda, Y., Hara, T., and Tsuduka, Y. (1984) A novel method of conjugation of daunomycin with antibody with a poly-L-glutamic acid derivative as intermediate drug carrier. An anti- α -fetoprotein antibody-daunomycin conjugate. *J. Med. Chem.* 27, 1602-1607.
- (26) Durrant, L. G., Robins, R. A., Marksman, R. A., Garnett, M. C., Ogunmuyiwa, Y., and Baldwin, R. W. (1989) Abrogation of antibody responses in rats to murine monoclonal antibody 791T/36 by treatment with daunomycin-*cis*-actonitryl-791T/36 conjugates. *Cancer Immunol. Immunother.* 28, 37-42.
- (27) Hurtwitz, E., Levy, R., Maron, R., Wilchek, M., Arnon, R., and Sela, M. (1975) The covalent binding of daunomycin and adriamycin to antibodies with retention of both drug and antibody activities. *Cancer Res.* 35, 1175-1181.
- (28) Lee, F. H., Berczi, I., Fujimoto, S., and Sehon, A. H. (1978) The use of antifibrin antibodies for the destruction of tumor cells. *Cancer Immunol. Immunother.* 5, 201-206.
- (29) Dillman, R. O., Johnson, D. E., Shawler, D. L., and Koziol, J. A. (1988). Superiority of an acid-labile daunorubicin-monoclonal antibody immunoconjugate compared to free drug. *Cancer Res.* 48, 6097-6102.
- (30) Embleton, M. J., Gunn, B., Byers, V. S., and Baldwin, R. W. (1981) Antitumor reactions of monoclonal antibody against a human osteogenic sarcoma cell line. *Br. J. Cancer* 43, 582-587.
- (31) Kernan, N. A., Knowles, R. W., Burns, M. J., Broxmeyer, H. E., Lu, L., Lee, H. M., Kawahata, R. T., Scannon, P. J., and Dupont, B. (1984) Specific inhibition of in vitro lymphocyte transformation by an anti-pan T cell (gp67) ricin A chain immunotoxin. *J. Immunol.* 133, 137-146.
- (32) Harwood, L. H. (1985) Flash Chromatography. *Aldrichimica Acta* 18, 25.
- (33) Robins, R. A., Laxton, R. R., Garnett, M., Price, M. R., and Baldwin, R. W. (1986) Measurement of tumour reactive antibody and antibody conjugate by competition, quantitated by flow cytometry. *J. Immunol. Methods* 90, 165-172.
- (34) Kiraly, R., Martin, R. B. (1982). Metal ion binding to daunorubicin and quinizarin. *Inorganica Chimica Acta* 67, 13-18.
- (35) Hill, R. L. (1965) Hydrolysis of proteins. *Adv. Protein Chem.* 20, 37-107.
- (36) Hamilton, R. G., Roebber, M., Reimer, C. B., and Rodkey, L. S. (1987) Isoelectric focusing-affinity immunoblot analysis of mouse monoclonal antibodies to the four human IgG subclasses. *Electrophoresis* 8, 127-134.
- (37) Hamilton, R. G., Reimer, C. B., and Rodkey, L. S. (1987) Quality control of murine monoclonal antibodies using isoelectric focusing affinity immunoblot analysis. *Hybridoma* 6, 205-217.
- (38) Yang, H. M., and Reisfeld, R. A. (1988). Doxorubicin conjugated with a monoclonal antibody directed to a human melanoma-associated proteoglycan suppresses the growth of established tumor xenografts in nude mice. *Proc. Natl. Acad. Sci. U.S.A.* 85, 1189-1193.

- (39) Pietersz, G. A., Smyth, M. F., Farquhar, I., and McKenzie, C. (1988). The use of anthracycline-antibody complexes for specific antitumor activity. *Antibody-Mediated Delivery Systems* (J. O. Rodwell, Ed.) pp 25-53, Marcel Dekker, New York.
- (40) Dzieduszyka, M., Stefanska, B., Borowski, E., and Martelli, S. (1986). "New *N*-amino acid derivatives of daunorubicin. *Farmaco* 41, 881-891.
- (41) Gabbay, E. J., Grier, D., Fingerle, R. E., Reimer, R., Levy, R., Pearce, S. W., and Wilson, W. D. (1976) Interaction specificity of the anthracyclines with deoxyribonucleic acid. *Biochemistry* 15, 2062-2070.

Registry No. Dau, 20830-81-3; cAD, 80445-77-8; Dau hydrochloride, 23541-50-6; *cis*-aconitic anhydride, 6318-55-4.

***N,N'*-Bis(2-hydroxybenzyl)-1-(4-bromoacetamidobenzyl)-1,2-ethylenediamine-*N,N'*-diacetic Acid: A New Bifunctional Chelate for Radiolabeling Antibodies**

Carla J. Mathias,[†] Yizhen Sun,[‡] Michael J. Welch,^{*,†} Judith M. Connett,[§] Gordon W. Philpott,[§] and Arthur E. Martell[‡]

Washington University School of Medicine, The Mallinckrodt Institute of Radiology, St. Louis, Missouri 63110, Department of Surgery, Jewish Hospital, St. Louis, Missouri 63110, and Texas A&M University, Department of Chemistry, College Station, Texas 77843. Received December 20, 1989

N,N'-Bis(2-hydroxybenzyl)-1-(4-bromoacetamidobenzyl)-1,2-ethylenediamine-*N,N'*-diacetic acid (BrΦHBED) was synthesized to bind trivalent metals with high stability constants and to bifunctionally link the radiometal with antibodies (Ab). This ligand has advantages over our previously reported *N*-(2-hydroxy-3,5-dimethylbenzyl)-*N'*-(2-hydroxy-5-bromoacetamidobenzyl)ethylenediamine-*N,N'*-diacetic acid (BrMe₂HBED). BrΦHBED has the protein coupling group BrCH₂CONH removed from the sterically hindered ring position with the addition of a benzyl group in the linker arm; this provides further distance between the protein and the chelate. We have also observed that the chelate was more stable than BrMe₂HBED, so it can be stored longer without loss of observed chemical properties. The improved chelate design allows for more rapid radiolabeling with [¹¹¹In]indium citrate (1 h at room temperature) with higher radiochemical yields. BrΦHBED was conjugated with an anticolorectal carcinoma monoclonal antibody (1A3) where radiolabeling yields of 75–90% were obtained and the antibody retained its immunoreactivity (ca. 90%) under all labeling conditions studied. Biodistribution studies in a hamster transplanted tumor (GW39) model demonstrated a high tumor uptake when compared to those of ¹²⁵I-1A3 or ¹¹¹In-DTPA cyclic anhydride-1A3. Blood clearance of ¹¹¹In-BrΦHBED-1A3 was rapid and combined with its high target uptake has higher target to nontarget ratios in vivo at various time intervals when compared with that of 1A3 radiolabeled with either ¹¹¹In-DTPA cyclic anhydride or ¹²⁵I.

Proteins and antibodies (Abs) have been radiolabeled with various radiometals (eg, ¹¹¹In, ^{67,68}Ga, ¹⁵³Gd, ⁶⁷Cu) with the use of bifunctional chelates (1–15). Although high radiolabeling yields can be obtained, because of slow nontarget tissue clearance in vivo, these radiolabeled Abs demonstrate less than the desired localization after a reasonable time. This high nontarget uptake coupled with relatively slow nontarget tissue clearance, may potentially mask Ab accumulation, in addition to the unnecessary radiation dose to the clearance organs. A bifunctional chelate that is capable of rapid clearance of the conjugated Ab from the blood and nontarget organs, does not interfere with the Ab immunoreactivity, and has a

very high metal stability constant would be ideal. Indium-111 has been widely utilized to radiolabel Abs; its 2.8 day physical half-life is sufficiently long to obtain high target to nontarget ratios and its medium energy γ-rays are reasonable for imaging with conventional nuclear medicine equipment. Diethylenetriaminepentaacetic acid (DTPA) cyclic anhydride has been utilized to bind ¹¹¹In to proteins and Abs (16–20); however, in vivo, the radiolabeled proteins have slow clearance and some or most of the radioactivity remains in the liver or kidneys (21, 22). Many investigators have described this incomplete clearance from the liver (intact antibody) or kidneys (antibody fragments) when ¹¹¹In-DTPA-conjugated Ab was used (23–26). Other approaches to radiolabeling antibodies which used functionalized DTPA or EDTA (ethylenediaminetetraacetic acid) to covalently attach the chelate to the antibody have been utilized with similar results (13–15, 27–32).

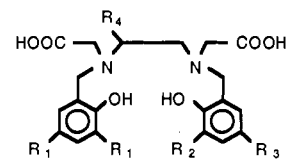
Recent work on in vivo biodistribution of the radiometal complexes of HBED [*N,N'*-bis(2-hydroxybenzyl)ethylenediamine-*N,N'*-diacetic acid] and its ana-

* Address correspondence to Michael J. Welch, Ph.D., The Edward Mallinckrodt Institute of Radiology, Washington University School of Medicine, 510 South Kingshighway Blvd., Box 8131, St. Louis, MO 63110.

[†] Washington University School of Medicine.

[‡] Texas A&M University.

[§] Jewish Hospital.

Chart I. Structural Comparison of the Parent Multidentate Ligands (33), BrMe₂HBED (40), and BrΦHBED


	R ₁	R ₂	R ₃	R ₄
HBED	H	H	H	H
Me ₄ HBED	CH ₃	CH ₃	CH ₃	H
BrMe ₂ HBED	CH ₃	H	NHCOCH ₂ Br	H
BrΦHBED	H	H	H	CH ₂ ΦNHCOCH ₂ Br

logues (alkyl groups added to the aromatic rings), where rapid liver and blood clearance was observed (33), led to the selection of a multidentate ligand, Me₄HBED, as the ligand to be derivatized for protein labeling (Chart I). This ligand was modified by functionalizing a benzene ring with NHCOCH₂Br to form an effective protein linking group (40), which forms a covalent bond between free amino groups in the protein (after alkylation) and the active bromoacetamido group (31, 34). Although this ligand (BrMe₂HBED) had characteristics superior to iodinated and ¹¹¹In-DTPA-labeled antibodies, it suffered from several deficiencies. Among these were the instability of BrMe₂HBED, along with the fact that long incubation times were needed to achieve high labeling yields. For this reason, we have developed the title compound, a new bifunctional chelate where the bromoacetamido group was situated on the ethylene backbone of the HBED structure at a greater distance from the chelating groups.

EXPERIMENTAL PROCEDURES

Materials and Methods. 4-Nitro-*D,L*-phenylalanine, salicylaldehyde, sodium borohydride, palladium on activated carbon (10%), borane-tetrahydrofuran complex (1.0 M solution in tetrahydrofuran), bis(trimethylsilyl)acetamide (BSA), trimethylsilyl bromoacetate, 2,4,6-collidine, and bromoacetyl bromide were purchased from Aldrich Chemical Co. and were used without further purification. Benzene and methanol were dried with 4A molecular sieves. Ethylene glycol dimethyl ether, and tetrahydrofuran were refluxed with LiAlH₄ and redistilled. 1-(4-Nitrobenzyl)ethylenediamine was prepared by the method of DeReimer et al. (14). [¹¹¹In]Indium chloride (50 mCi/mL in sodium chloride, pH 1–2) was provided by Mallinckrodt, Inc. Ultrapure sodium acetate, indium(III) acetate (99.99%), and indium(III) chloride (99.999%) were purchased (Morton Thiokol, Aesar, and Aldrich Chemical Co., respectively). Diethylenetriamine-pentaacetic acid (DTPA) anhydride was purchased (Sigma Chemical Co.) and dissolved in chloroform. Solutions of indium(III) were prepared by dissolving known amounts of either indium(III) acetate in glacial acetic acid or indium(III) chloride in hydrochloric acid (0.1 N). Buffer solutions were prepared with HPLC-grade water (>17 MΩ/cm; Milli-Q System, Millipore Division, Waters Associates). Solutions of sodium citrate, 0.1 M and 0.01 M, pH 8, and sodium acetate, 0.4 M and 0.04 M, pH 5, were used throughout. Phosphate-buffered saline (PBS) consisted of 137 mM sodium chloride, 8.1 mM sodium phosphate, 1.46 mM potassium phosphate, and 2.7 mM potassium chloride, pH = 7.3–7.4. Sephadex G-25 and G-50 (Sigma Chemical Co.) was utilized to prepare small volume (1–3 mL) spin columns (35). Bovine immunoglobulin G (IgG, Sigma Chemical Co.) was used to determine experimen-

tal conditions, initial radiolabeling efficacy, and conjugation efficiency. The monoclonal antibody (MAb) used in the animal studies, 1A3, is a murine MAb (IgG₁, κ), which binds to a lipid antigen found enriched in human colon cancer cells (36–38). Hybridoma cells producing 1A3 were grown as ascites in pristane-primed BALB/c mice. 1A3 was precipitated with 40% (NH₄)₂SO₄ and purified by Sephadex G-150 and DEAE Sephacryl chromatography. SDS-PAGE (7.5%) has shown that these MAbs are ca. 90% pure. The 1A3 was stored frozen (–80 °C) in PBS at ca. 7.5 mg/mL; prior to radiolabeling, the 1A3 solution was either washed in a small-volume spin column to effectively switch to the buffer appropriate to the exact conditions or radioiodinated in PBS. IgG was diluted in either 0.01 M citrate or 0.04 M acetate buffer.

The proton NMR spectra were recorded with a Varian XL-200 NMR spectrometer operating at 200 MHz, and chemical shifts were reported in ppm relative to tetramethylsilane. The mass spectra were obtained with VG analytical 70S high-resolution double-focusing magnetic-sector spectrometer, with an attached VG analytical 11/250J data system. The C, H, N analyses were performed by Galbraith Laboratories, Inc., Knoxville, TN.

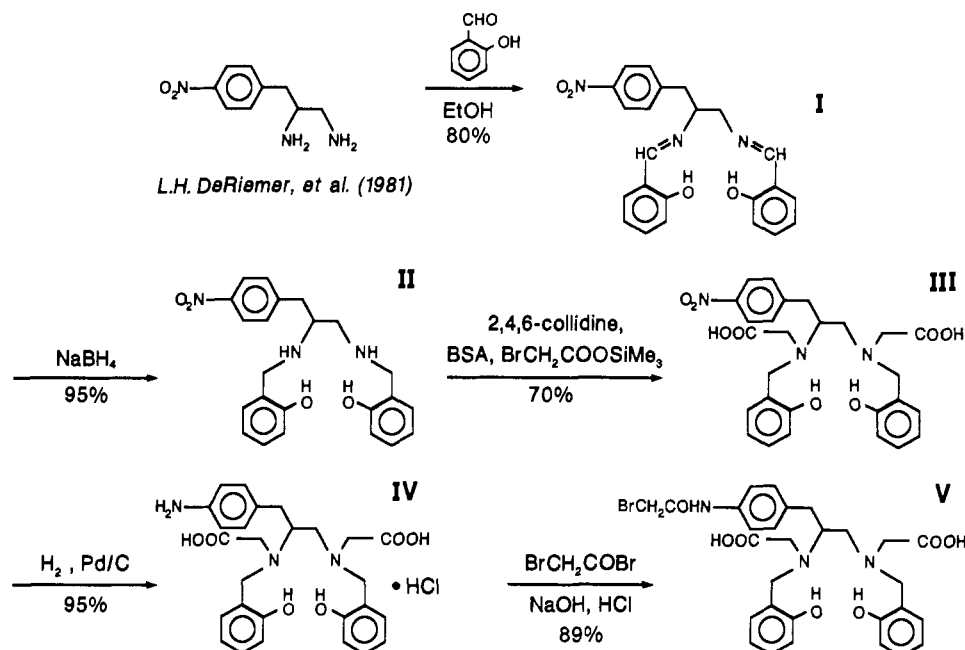
Synthesis of BrΦHBED was carried out as shown in Scheme I and as described.

1-(4-Nitrobenzyl)-*N,N'*-bis(2-hydroxybenzylidene)ethylenediamine (I) and 1-(4-Nitrobenzyl)-*N,N'*-bis(2-hydroxybenzyl)ethylenediamine (II). 1-(4-Nitrobenzyl)ethylenediamine (1.46 g, 7.5 mmol) was added to a solution of 1.83 g of salicylaldehyde (15 mmol) and 2 mL of absolute ethanol. After heating at 80 °C for 20 min, the reaction mixture was cooled with an ice-water bath. The yellow, crystalline product was collected by filtration, washed with absolute ethanol and dry ethyl ether, and vacuum dried under P₂O₅ overnight; 2.4 g of product was obtained (yield = 80%). ¹H NMR (in DMSO-*d*₆): 8.59 and 8.37 (s, s, 1 H, 1 H, —CH=N—), 8.16 (d, 2 H, 3-proton, and 5-proton of 4-nitrobenzyl), 7.55 (d, 2 H, 2-proton, and 6-proton of 4-nitrobenzyl), 6.8–7.5 (m, 8 H, 3,4,5,6-protons of the 2-hydroxybenzylidene), 3.3 and 4.0 (m, m, 5 H, —CH₂CHCH₂—) ppm.

A 3.54-g portion of the above Schiff base (I) was suspended in a solvent consisting of 25 mL of absolute ethanol and 25 mL of ethylene glycol dimethyl ether. It formed a bright yellow solid suspended in a yellow solution. To this suspension was added ca. 0.7 g of NaBH₄ portionwise. The reaction mixture was stirred at room temperature for 2 h (still pale yellow). The solvent was removed by distillation under reduced pressure. To the yellow oil which remained was added 20 mL of water and the product was extracted four times with 50 mL of CH₂Cl₂. The CH₂Cl₂ solutions were combined and decolorized with 2 g of activated charcoal. The mixture was warmed for 5–10 min. After filtration a nearly colorless CH₂Cl₂ solution was obtained. This solution was dried with anhydrous MgSO₄ for 24 h. After removal of MgSO₄·*x*H₂O and the solvent, 3.5 g of a pale yellow, oily product was obtained (yield = 95%). ¹H NMR (in CDCl₃): 8.12 (d, 2 H, 3-proton and 5-proton of 4-nitrobenzyl), 7.28 (d, 2 H, 2-proton, and 6-proton of 4-nitrobenzyl), 6.8–7.2 (m, 8 H, 3,4,5,6-protons of the 2-hydroxybenzyl), 3.9 and 2.6–3.1 (m, 5 H, —CH₂CHCH₂—) ppm.

1-(4-Nitrobenzyl)-*N,N'*-bis(2-hydroxybenzyl)ethylenediamine-*N,N'*-diacetic Acid (III). To 1.7 g (4.2 mmol) of 1-(4-nitrobenzyl)-*N,N'*-bis(2-hydroxybenzyl)ethylenediamine, under argon gas, was added 25–30 mL of BSA, and the reaction mixture was heated with a 60–70 °C oil bath for 2 h and then at 90 °C for 1 h. It was then

Scheme I



allowed to stand at room temperature for 16 h. The excess BSA was removed by distillation at 65 °C (25 mmHg). The byproduct (silylated acetamide) was removed at 45 °C (1 mmHg). To the yellow sticky residue were added 4 mL of dry benzene, 7 mL (43 mmol) of trimethylsilyl bromoacetate, and 5.5 mL (42 mmol) of 2,4,6-collidine, successively. The reaction mixture was heated in a 40–50 °C bath for 5 h and then allowed to stand at room temperature for 15 h.

The benzene, excess $\text{BrCH}_2\text{COOSiMe}_3$, and 2,4,6-collidine were removed by distillation under reduced pressure. To the residue was added 100 mL of 6 N HCl, the mixture was stirred at room temperature for 15 h, and a clear solution was obtained. Four portions of 50 mL of ethyl ether were used to extract the acidic byproduct. To the aqueous phase was added 50% aqueous NaOH to increase the pH to 11. Four portions of 50 mL of ether were used to extract the collidine and other basic impurities. The aqueous phase was separated and filtered, and 6 N HCl was then added to precipitate III at pH 8–9. The precipitation was complete at pH 2.5. This product was redissolved in an aqueous solution at pH 11 and reprecipitated at pH 2.5 with HCl. The product was collected by filtration, washed with 0.01 N HCl, and dried in a desiccator over P_2O_5 for 16 h; 1.69 g of pure product was obtained (yield = 77%). FAB MS (m/e): ($M + H$)⁺ = 524. Anal. Calcd for $\text{C}_{27}\text{H}_{29}\text{N}_3\text{O}_8 \cdot \text{H}_2\text{O}$: C, 59.89; H, 5.73; N, 7.76. Found: C, 60.02; H, 5.62; N, 7.36. The disodium salt was also prepared by recrystallization from an aqueous methanol solution. FAB MS (m/e) ($M + H$)⁺ = 546 and 568, which corresponds to the mono- and disodium salts. Anal. Calcd for $\text{C}_{27}\text{H}_{27}\text{N}_3\text{O}_8\text{Na}_2 \cdot 2.5\text{H}_2\text{O}$: C, 52.94; H, 5.23; N, 6.86. Found: C, 53.17; H, 5.78; N, 6.85.

1-(4-Aminobenzyl)-*N,N'*-bis(2-hydroxybenzyl)-ethylenediamine-*N,N'*-diacetic Acid (IV). To a 50-mL round-bottomed flask were added 20 mL of methanol and 0.21 g (0.4 mmol) of III. To this suspension was added 0.341 mL of 2.68 M NaOH, and a clear yellow solution was obtained. While the solution was covered with argon, 150 mg of 10% Pd/C was added. This reaction mixture was reacted with H_2 at 1 atm of pressure in an ice-water bath for 5 h until the calculated amount of H_2 was consumed. Under argon gas, 0.70 mL of 2.5 M HCl was then

added to the reaction mixture. The catalyst was removed by two successive filtrations with Whatman No. 42 filter paper. The filtrate was evaporated to near dryness over a water bath at 40 °C under reduced pressure.

^1H NMR (in D_2O) showed that the 8.0 ppm doublet of the nitrobenzyl group had disappeared and the two aminobenzyl doublets at about 6.8–7.4 ppm overlapped with the other aromatic protons peaks (yield > 95%). The aqueous solution is nearly colorless.

1-(4-Bromoacetamidobenzyl)-*N,N'*-bis(2-hydroxybenzyl)ethylenediamine-*N,N'*-diacetic Acid (V). About 0.4 mmol of the IV, the monohydrochloride salt, which was obtained from the catalytic hydrogenation of 0.21 g (0.4 mmol) of nitro compound III, was placed in a 25-mL beaker and was dissolved in 4 mL of water. About 1.2 mL of 1 M NaOH was added until the pH reached 7.5. Eight to nine portions of 20 μL of bromoacetyl bromide were added to the beaker, which was cooled by an ice-water bath. When the pH dropped below 7, additional 1 M NaOH was added. The reaction mixture was stirred thoroughly with a glass stirring rod. The solution was checked for the presence of the amino group with fluorescamine (39) until the test was negative.

When the reaction was complete, two 8-mL portions of ether were used to extract the excess bromoacetyl bromide. The aqueous phase was filtered and 2.5 M HCl was added dropwise to the solution until the pH was reduced to 2.5. The pale pink precipitate was filtered and washed successively with cold 0.01 M HCl and ether. It was vacuum dried over P_2O_5 at room temperature in a desiccator for 2–3 h; 0.22 g of product was obtained (yield = 89%). FAB MS (m/e): ($M + H$)⁺ = 614, the isotopic patterns show that this molecule contains one Br atom. Anal. Calcd for $\text{C}_{29}\text{H}_{32}\text{N}_3\text{O}_7\text{Br} \cdot 1/2\text{H}_2\text{O}$: C, 55.86; H, 5.30; N, 6.74. Found: C, 55.96; H, 5.42; N, 6.76.

Conjugation of Br Φ HBED with Ab. Br Φ HBED (V) was dissolved in 0.01 M citrate buffer (2 mg/mL) immediately prior to use. The pH of the 0.01 M and 0.1 M citrate buffer was varied from 5 to 8 to determine optimal conditions; the pH was maintained throughout the conjugation, radiolabeling, and purification procedures. The appropriate volume of Br Φ HBED solution was added to the Ab in 0.01 M citrate buffer (concentration > 2 mg/mL). The amounts of ligand (L) and Ab were var-

ied to achieve mole ratios varying from 1:1 to 100:1 (L:Ab). The Ab was incubated with Br Φ HBED at room temperature for 24 h. The unbound Br Φ HBED was removed from the conjugated Ab-Br Φ HBED by gel chromatography separation on a Sephadex G-50 spin column in 0.01 M citrate buffer. The separation was completed after a 7-min centrifugation (GLC-2B Sorvall centrifuge with HL-4 swinging-bucket rotor) at 1000g. The eluted Ab-Br Φ HBED conjugate was collected and the protein concentration was determined by colorimetric assay (Bio-Rad Protein Assay). The conjugated Ab can be stored at -80 °C for several months without decomposition as determined by radiolabeling efficiency. The conjugation efficiency was determined by titration of Br Φ HBED-IgG with indium(III) as described elsewhere (40).

Radiolabeling Br Φ HBED-Ab with ^{111}In was accomplished by mixing [^{111}In]indium chloride in citrate buffer (0.1 M, pH 8, less than 100 μL) with the purified, conjugated Ab. The labeling solution was incubated at room temperature for 1-24 h, when a final purification was carried out with an additional 1-mL Sephadex G-50 spin column (in 0.01 M citrate buffer). The ^{111}In -Br Φ HBED-Ab passed through the column while unbound ^{111}In remained on the gel bed. Control separations of [^{111}In]indium citrate alone, [^{111}In]indium citrate incubated with unconjugated Ab, and conjugated Ab alone were also carried out; [^{111}In]indium citrate does not elute, but Ab and/or conjugated Ab are collected with ca. 90% protein recovery (by colorimetric assay). Radiolabeling was measured as the fraction of radiolabeled material that eluted through the spin column from the total amount applied to the column.

Conjugation and radiolabeling with DTPA cyclic anhydride (0.5 mg/mL chloroform) was carried out by evaporating the desired amounts of the DTPA solution (23.8 $\mu\text{g}/\text{mg}$ Ab to obtain a 10:1 mole ratio) with nitrogen. The Ab (1 mg/200 mL in 0.04 M acetate buffer pH 5) was added to the tube with the ligand film and mixed gently. This reaction was allowed to proceed for 1 h at room temperature; after the incubation, the conjugated Ab was purified on a 1-mL Sephadex G-50 spin column equilibrated with 0.04 M acetate buffer, pH 5. The conjugated Ab was mixed with ^{111}In in 0.4 M acetate buffer (less than 100 μL of volume) and allowed to incubate at room temperature for 1 h. The ^{111}In -labeled Ab was collected in the eluent from an additional 1-mL Sephadex G-50 spin column in 0.04 M acetate buffer. The conjugation efficiency was determined by the isotope-dilution technique using indium(III) to which ^{111}In had been added (40).

Iodinated 1A3 was prepared by using a conventional lactoperoxidase (41) or iodogen technique (42). ^{125}I -1A3 was separated from unbound ^{125}I by use of a Sephadex G-25 spin column (35). With the use of this method, the specific activity of radiolabeled 1A3 after dilution with unlabeled 1A3 was 0.97 $\mu\text{Ci}/\mu\text{g}$ with 95% of the radioactivity recovered in a precipitable protein fraction (by TCA precipitation) (43).

An in vitro immunoreactivity assay (IRA) was developed so the immunoreactivity of each radiolabeled-1A3 preparation could be tested prior to in vivo use. The immunoreactive fraction of radiolabeled MAbs was determined by linear extrapolation to binding at infinite antigen excess (44) with the following conditions: GW39 human colon cancer cells (ca. 2.5×10^8) were implanted in the right thigh musculature of male Golden Syrian hamsters, tumors were harvested 10-14 days later, and single-cell suspensions were obtained by processing the tissue through wire-mesh screens. The isolated tumor

cells were stored in liquid nitrogen as a 50% cell suspension (v/v) in McCoy's 5A medium containing 10% dimethyl sulfoxide. Upon thawing, these cell suspensions were demonstrated to have more than 90% viability as determined by trypan blue dye exclusion. Significant decreases in cell viability were not observed over the course of this assay (4 h average). One concentration of labeled antibody (40 ng) and various dilutions of GW39 cells (range: 1.25×10^7 - 2.5×10^8) were incubated together for 1 h at 37 °C. Extensively washed cells were counted and the binding data were plotted.

Animal biodistribution experiments were carried out in 3-6 week old immunocompetent male Golden Syrian hamsters with GW39 human colon carcinoma tumors (45). Tumor cell suspensions (50%, v/v; 0.5 mL ca. 2.5×10^8 cells) were injected in the right thigh musculature of the hamsters and allowed to grow for 2-5 days before radiolabeled 1A3 was injected. The hamsters received KI in their drinking water (24 h prior) to block thyroid uptake of any unbound ^{125}I . Hamsters were cojected intracardially with 25 μg of ^{111}In -1A3, Br Φ HBED or DTPA conjugated, and 25 μg of ^{125}I -1A3. Tumors were harvested 3 or 5 days after the radiolabeled 1A3 injection. The entire tumor, bladder, heart, stomach, kidneys, spleen, and thyroid were removed, as well as samples of blood, skin, muscle, liver, lung, and intestine. All organs were rinsed in PBS, blotted, weighed, and then counted in an automated γ -scintillation NaI(Tl) well-type counter.

RESULTS

The procedure employed for the synthesis of the bifunctional ligand Br Φ HBED is somewhat different from that reported previously for BrMe $_2$ HBED (40), mostly due to the greater chemical stability of Br Φ HBED. The amino intermediate of BrMe $_2$ HBED formed by hydrogenation of the nitro precursor was not isolated and characterized, but was immediately acylated with BrCH $_2$ COBr to give the final product, which precipitated from acid solution. While stable in contact with acid, it undergoes perceptible deterioration when kept in aqueous solution at acylation pH (~ 7.5). Even in the acid form BrMe $_2$ HBED underwent slow decomposition when maintained for long periods of time (days) at room temperature. Therefore, it was not characterized by elemental analysis or by NMR (which would have required dissolution in alkaline D $_2$ O solution) but mass spectrometry provided the required criteria of purity (40). With respect to Br Φ HBED, the greater stability of intermediate amino compound IV made possible its isolation and characterization by NMR (see the Experimental Procedures). Also, the final product (V) (which was prepared by acylation of the amine with BrCH $_2$ COBr and finally isolated by precipitation with acid under the same conditions as those employed for the preparation of BrMe $_2$ HBED) was sufficiently stable for more complete characterization. While NMR was still preempted for solubility reasons, as in the previous case, it was possible to obtain an excellent elemental analysis, demonstrating the purity of the compound. The analytical results are further supported by mass spectral determination (FAB) showing two nearly equivalent peaks, the isotopic distribution of bromine, at mass $M + H^+ = 614$ and 616. There were no peaks which corresponded to the presence of two bromine atoms, demonstrating that additional O-acylation of the phenolic groups did not take place. Also, there were no bromine-free peaks corresponding to alkylation of the ligand by BrCH $_2$ COBr, followed by hydrolysis to a NHCH $_2$ COOH function.

The radiolabeling parameters were determined by evaluation with IgG or 1A3 in 0.01 M citrate buffer. The

Table I. Effect of pH on Radiolabeling^a of Br Φ HBED-IgG^b with [¹¹¹In]indium Citrate^c

pH	% radiolabeling
5	38.8 \pm 18.7
6	42.6 \pm 10.5
7	52.6 \pm 4.1
8	71.1 \pm 4.7

^a One hour at room temperature. ^b 10:1 mole ratio, 24-h incubation. ^c $\bar{X} \pm SD$, $n = 3$.

Table II. Effect of Conjugation Time on Radiolabeling of Br Φ HBED-IgG^a

L:Ab	% radiolabeled ($\bar{X} \pm SD$, $n = 3$)			
	1 h	3 h	8 h	24 h
0:1 ^b	1.88 \pm 0.11			
1:1				18.1 \pm 4.2
2:1	10.1 \pm 0.6	19.9 \pm 1.9	29.1 \pm 1.9	14.5 \pm 0.8
5:1				32.2 \pm 4.7
10:1	29 \pm 0.4	37.2 \pm 0.3	57.6 \pm 0.4	71.5 \pm 9.7
50:1				68.2 \pm 11.6
100:1	26.2 \pm 0.5	19.0 \pm 2.3	37.6 \pm 1.1	75.5 \pm 6.1

^a One-hour incubation time with [¹¹¹In]indium citrate (pH 8).

^b Unconjugated Ab was incubated with [¹¹¹In]indium citrate, conditions as described above.

effect of pH on the conjugation and radiolabeling efficiencies was examined and the optimum pH for the conjugation and radiolabeling was found to be pH 8 (Table I). The effect of incubation time (1, 3, 18, and 24 h at room temperature) for conjugation of Br Φ HBED with Ab on the radiolabeling efficiency was determined at pH 7–8 (Table II), as well as the effect of the amount of Br Φ HBED (mole ratio with respect to Ab; conjugated for 24 h at room temperature). A 1-h incubation (at room temperature) of [¹¹¹In] with Br Φ HBED-IgG (10:1, conjugated for 24 h at room temperature in 0.01 M citrate buffer, pH 8) was sufficient to achieve 75–90% radiolabeling; the efficiency was not improved with longer incubations, which were determined after 5, 18, and 24 h. The control Sephadex G-50 spin column separations demonstrate the effectiveness of these radiolabeling conditions; only 0.13 \pm 0.12% ($n = 3$) of the radioactivity is eluted when [¹¹¹In]indium citrate alone was applied, and when unconjugated Ab was incubated with [¹¹¹In]indium citrate only 1.88% of the radioactivity was recovered with the protein (Table II). The conjugation efficiency was determined by binding conjugated IgG with [¹¹¹In]indium at various specific activities. From the titration curves, assuming a 1:1 (M:L) relationship, 1.1 ($n = 2$) mol of Br Φ HBED conjugates with 1 mol of IgG when 10 mol of Br Φ HBED were used per mole of Ab. Under identical conditions, the conjugation efficiency of IgG with DTPA cyclic anhydride was determined to be 3.46 \pm 0.78 ($n = 4$).

The immunoreactivity (IR) values were determined from the plotted results of the cell-binding assay. The IR is the value of B/T at infinite dilution. For the example plotted in Figure 1 the radiolabeled 1A3 had an IR of 82%. A double reciprocal plot of the fraction of total added radioactivity bound to cells ($[T]/[B]$) as a function of the inverse cell concentration can also be plotted (Figure 1). In this case, the IR = (1/y intercept) \times 100, where the slope is a measure of the binding affinity. None of the described labeling techniques altered the binding affinity. The IR of [¹¹¹In]-Br Φ HBED-1A3 was compared with both [¹¹¹In]-BrMe₂HBED-1A3 and [¹¹¹In]-DTPA-1A3 (Figure 2). The effect on IR of the amount of ligand incubated with the Ab (mole ratio in reaction mixture) was also examined. Insignificant differences in IR were

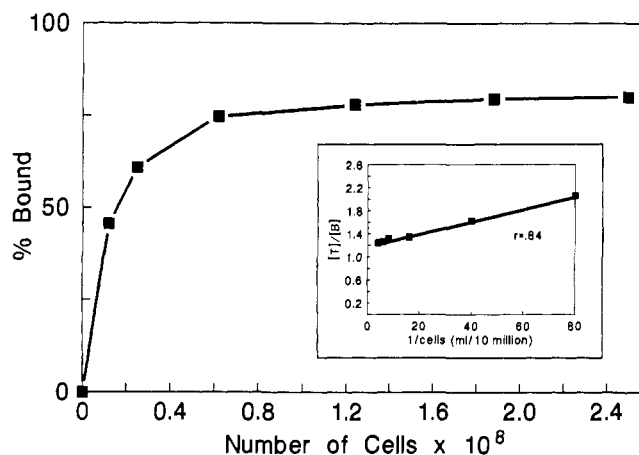


Figure 1. A representative plot to determine immunoreactivity of radiolabeled 1A3. The IR is the value B/T at infinite antigen concentration. The double reciprocal plot (inset) of cell binding ($[T]/[B]$) vs cell concentration ($1/\text{cell no.}$) is also shown. The IR can be calculated from the intercept and the binding affinity can be calculated from the slope.

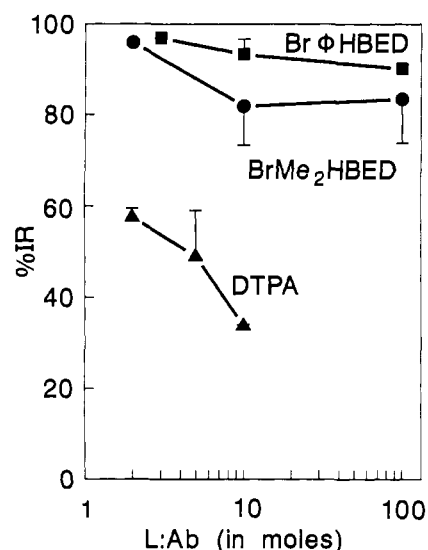


Figure 2. The effect of ligand concentration added to reaction mixture per mole of 1A3 on the in vitro immunoreactivity.

observed with Br Φ HBED-conjugated 1A3, and similarly with BrMe₂HBED-conjugated 1A3, however, DTPA-conjugated 1A3 exhibited marked reductions in IR as more ligand was utilized (Figure 2). Even when very low amounts of DTPA cyclic anhydride were added to Ab in the reaction mixture, the immunoreactivity is significantly lower than that of the Ab conjugated with Br Φ HBED.

Radiolabeled 1A3 was evaluated in the hamster tumor model. Biodistribution studies were carried out 3 or 5 days after coinjection of [¹¹¹In]-1A3 (DTPA or Br Φ HBED conjugated) and [¹²⁵I]-1A3 (50 μ g total Ab) in four separate experiments. The IR of [¹¹¹In]-Br Φ HBED-1A3 was 71–97%, that of [¹¹¹In]-DTPA-1A3 was 50–57%, and that of [¹²⁵I]-1A3 was 84–90%. The average percent injected dose per gram of tissue values were calculated and are presented in Tables III and IV for representative experiments. In the biodistribution experiments hamsters were studied 2 and 5 days after tumor implantation. The uptake of radiolabeled Ab has been correlated to tumor age and not tumor weight (47). The histological analysis of various age tumors suggests that the younger (2 day old) tumors have less fibrous capsule formation, similar to early metastatic tumor development, while older tumors

Table III. Biodistribution of ^{111}In -BrΦHBED-1A3 and ^{125}I -Radiolabeled 1A3 Coinjected in Hamsters with GW39 Tumors

	% ID/g ($X \pm \text{SD}$, $n = 5$): time since tumor implantation, time after injection			
	2 days, 3 days	2 days, 5 days	5 days, 3 days	5 days, 5 days
^{111}In -BrΦHBED-1A3 (IR = 97%)				
blood	1.57 ± 0.27	0.83 ± 0.04	1.92 ± 0.18	0.95 ± 0.17
tumor	7.94 ± 1.28	6.00 ± 0.83	4.63 ± 0.51	3.69 ± 0.35
liver	1.65 ± 0.13	1.47 ± 0.12	1.64 ± 0.23	1.50 ± 0.32
kidney	2.77 ± 0.32	2.80 ± 0.19	2.46 ± 1.21	2.81 ± 0.55
muscle	0.26 ± 0.07	0.23 ± 0.03	0.28 ± 0.02	0.24 ± 0.01
tumor/blood	5.15 ± 1.05	7.27 ± 0.99	2.43 ± 0.31	3.96 ± 0.59
tumor/muscle	28.16 ± 7.74	25.92 ± 1.62	16.37 ± 2.66	15.47 ± 1.70
^{125}I -1A3 (IR = 85%)				
blood	2.25 ± 0.36	1.46 ± 0.07	2.81 ± 0.26	1.70 ± 0.31
tumor	7.16 ± 1.35	4.34 ± 1.22	2.78 ± 0.77	2.09 ± 0.26
liver	0.63 ± 0.16	0.38 ± 0.07	0.65 ± 0.08	0.41 ± 0.08
kidney	0.44 ± 0.06	0.31 ± 0.01	0.46 ± 0.07	0.32 ± 0.04
muscle	0.16 ± 0.01	0.10 ± 0.01	0.18 ± 0.03	0.13 ± 0.01
tumor/blood	3.23 ± 0.74	2.98 ± 0.81	1.00 ± 0.33	1.27 ± 0.30
tumor/muscle	45.79 ± 13.14	43.07 ± 12.76	15.88 ± 5.73	16.67 ± 2.64
tumor weight (g)	0.553 ± 0.078	0.835 ± 0.081	0.895 ± 0.210	1.324 ± 0.542
tumor $P =$	>0.1	<0.05	<0.01	<0.001
blood $P =$	<0.01	<0.001	<0.001	<0.01

Table IV. Biodistribution of ^{111}In -DTPA-1A3 and ^{125}I -Radiolabeled 1A3 Coinjected in Hamsters with GW39 Tumors

	% ID/g ($X \pm \text{SD}$, $n = 5$): time since tumor implantation, time after injection			
	2 days, 3 days	2 days, 5 days	5 days, 3 days	5 days, 5 days
^{111}In -DTPA-1A3 (IR = 57%)				
blood	1.55 ± 0.07	0.80 ± 0.05	1.06 ± 0.04	0.56 ± 0.06
tumor	5.96 ± 0.62	4.50 ± 0.19	3.21 ± 0.33	2.70 ± 0.45
liver	1.44 ± 0.06	1.08 ± 0.15	1.29 ± 0.09	1.26 ± 0.19
kidney	2.84 ± 0.37	2.99 ± 0.22	4.14 ± 0.18	4.03 ± 0.70
muscle	0.27 ± 0.07	0.26 ± 0.03	0.27 ± 0.04	0.22 ± 0.02
tumor/blood	3.84 ± 0.36	5.66 ± 0.34	2.93 ± 0.17	4.91 ± 1.07
tumor/muscle	22.93 ± 4.72	17.30 ± 1.89	11.99 ± 2.34	12.00 ± 1.77
^{125}I -1A3 (IR = 90%)				
blood	3.29 ± 0.25	2.22 ± 0.17	3.15 ± 0.10	2.21 ± 0.26
tumor	8.25 ± 1.61	4.61 ± 0.38	3.10 ± 0.44	3.07 ± 0.50
liver	0.83 ± 0.10	0.47 ± 0.07	0.56 ± 0.06	0.41 ± 0.04
kidney	0.57 ± 0.08	0.37 ± 0.03	0.45 ± 0.11	0.35 ± 0.05
muscle	0.20 ± 0.04	0.14 ± 0.02	0.17 ± 0.03	0.12 ± 0.02
tumor/blood	2.50 ± 0.36	2.09 ± 0.27	0.98 ± 0.14	1.40 ± 0.27
tumor/muscle	40.94 ± 3.49	33.49 ± 5.45	18.20 ± 2.65	26.20 ± 2.58
tumor weight (g)	0.437 ± 0.068	0.552 ± 0.039	0.525 ± 0.103	1.42 ± 0.502
tumor $P =$	<0.02	>0.5	>0.5	<0.5
blood $P =$	<0.001	<0.001	<0.001	<0.001

(>4 days old) are perhaps a model for primary tumor evaluation.

DISCUSSION

The optimal radiolabeling conditions were derived from the experiments with BrΦHBED-conjugated IgG. The ligand was conjugated to Ab at a 10:1 mole ratio in 0.01 M citrate buffer (pH 8) incubated at room temperature for 24 h. The relatively high (70–90%) radiolabeling with [^{111}In]indium citrate was accomplished after a 1-h incubation at room temperature. These parameters provide a radiolabeled Ab with high retained immunoreactivity (ca. 90%) and a specific activity of 5 mCi/mg Ab can easily be obtained after purification.

Immunoreactivity with ^{111}In -BrΦHBED-1A3 is slightly greater than that of ^{111}In -BrMe₂HBED-1A3 and significantly greater than that of ^{111}In -DTPA-1A3 at similar attached ligands/mole Ab. Higher radiolabeling yields are obtained with 1:1 attachment of BrΦHBED than with DTPA, presumably due to the higher stability constant for BrΦHBED. Sufficient numbers of HBED-substituted analogues have been prepared and stability constants have been determined. A reasonable estimate of

the ^{111}In -BrΦHBED stability constant would be $\log K \approx 10^{31}$.

The conjugation efficiency with BrΦHBED (1.1) is less than that with DTPA cyclic anhydride (3.46), but slightly greater than that with BrMe₂HBED (0.8). The lower efficiency can be anticipated since bromoacetamide reactivity is less with amino groups than with SH groups (46) and because we are utilizing intact Ab. The greater reactivity compared to BrMe₂HBED is probably due to steric reasons.

The biodistribution of ^{111}In -BrΦHBED-1A3 compares favorably with ^{111}In -DTPA-1A3 and ^{125}I -1A3 (Tables III and IV). The absolute uptake of the ^{111}In -BrΦHBED-1A3 in tumor tissue is significantly greater than that of ^{111}In -DTPA-1A3 (in 2 day old tumors $p < 0.02$ at 3 and 5 days after injection, $p < 0.001$ 3 days after injection, <0.01 5 days after injection in 5 day old tumors). Also, ^{111}In -BrΦHBED-1A3 has decreased blood concentration when compared directly with iodinated Ab (Table III) and a more rapid blood clearance rate than ^{111}In -DTPA-1A3 ($p < 0.001$ in animals with 5 day old tumors), which provides a potentially improved bifunctional chelate for radiolabeling Ab. In considering the

clinical situation, the 5 day old tumor at injection is probably more representative of an established primary tumor whereas the 2 day old tumor may well represent early tumor metastases (47). Histological studies have previously shown (38) that by 5 days after implantation, tumor differentiation patterns are similar to those of 14 day old tumors.

¹¹¹In-BrΦHBED-1A3 exhibits advantages over DTPA cyclic anhydride conjugated Ab and/or iodinated Ab that include higher tumor/blood ratios (particularly at later times) and slower washout of tumor radioactivity. BrΦHBED has significant technical advantages over BrMe₂HBED as it can be stored (desiccated at -80 °C) for at least 20 months without loss of conjugation/radiolabeling efficiency. For the latter, the sensitivity of the compound was ascribed to the fact that it contains an oxidation-prone group, consisting of an NHCOCH₂Br function para to a phenolic group, and is thus similar in structure to many well-known antioxidants. Such a structure could probably explain the slow deterioration of the solid in contact with air. In the case of BrΦHBED, this situation does not exist, and long storage times without deterioration are possible. Finally, the shortened radiolabeling time (1 h) is vastly improved over the 24-h incubation required with BrMe₂HBED to achieve similar radiolabeling yields. The precursor, IV, of BrΦHBED could be functionalized by other activating groups to enable different coupling reactions to be carried out.

ACKNOWLEDGMENT

We thank Carl J. Germain and Martha B. Ruiz for their valuable assistance with IRA and Dr. T. R. Sharp for fast atom bombardment mass spectra analysis. This research was supported by NIH Grants CA-42925 and CA-44728.

LITERATURE CITED

- Meares, C. F., Goodwin, D. A., Leung, C. S. H., Girgis, A. Y., Silvester, D. J., Nunn, A. D., and Lavender, P. J. (1976) Covalent attachment of metal chelates to proteins: The stability in vivo and in vitro of the conjugate of albumin with a chelate of ¹¹¹indium. *Proc. Natl. Acad. Sci. U.S.A.* 73, 3803-3806.
- Khaw, B. A., Fallon, J. T., Strauss, H. W., and Haber, E. (1980) Myocardial infarct imaging of antibodies to canine cardiac myosin with indium-111-diethylenetriamine pentaacetic acid. *Science* 209, 295-297.
- Scheinberg, D. A., Strand, M., and Gansow, O. A. (1982) Tumor imaging with radioactive metal chelates conjugated to monoclonal antibodies. *Science* 215, 1511-1513.
- Ballou, B., Levine, G., Hakala, T. R., and Solter, D. (1979) Tumor location detected with radioactively labeled monoclonal antibody and external scintigraphy. *Science* 206, 844-847.
- Kozak, R. W., Atcher, R. W., Gansow, O. A., Friedman, A. M., Hines, J. J., and Waldmann, T. A. (1986) Bismuth-212-labeled anti-Tac monoclonal antibody: α-Particle-emitting radionuclides as modalities for radioimmunotherapy. *Proc. Natl. Acad. Sci. U.S.A.* 83, 474-478.
- Order, S. E., Klein, J. L., Lechner, P. K., Frincke, J., Lollo, C., and Carlo, D. J. (1986) ⁹⁰Yttrium antiferritin—A new therapeutic radiolabeled antibody. *Int. J. Radiat. Oncol. Biol. Phys.* 12, 277-281.
- Motta-Hennessy, C., Eccles, S. A., Dean, C., and Coghlan, G. (1985) Preparation of ⁶⁷Ga-labelled human IgG and its Fab fragments using desferoxamine as chelating agent. *Eur. J. Nucl. Med.* 11, 240-245.
- Hnatowich, D. J., Virzi, F., and Doherty, P. W. (1985) DTPA-coupled antibodies labeled with Yttrium-90. *J. Nucl. Med.* 26, 503-509.
- Cole, W. C., DeNardo, S. J., Meares, C. F., McCall, M. J., DeNardo, G. L., Epstein, A. L., O'Brien, H. A., and Moi, M. K. (1986) Serum stability of ⁶⁷Cu chelates: Comparison with ¹¹¹In and ⁵⁷Co. *Nucl. Med. Biol.* 13, 363-368.
- Pritchard, J. H., Ackerman, M., Tubis, M., and Blahd, W. H. (1976) Indium-111-labeled antibody heavy metal chelate conjugates: A potential alternative to radioiodination. *Proc. Soc. Exp. Biol. Med.* 151, 297-302.
- Lauffer, R. B., Brady, T. J., Brown, R. D., Baglin, C., and Koenig, S. H. (1986) ¹/T₁NMRD Profiles of solutions of Mn²⁺ and Gd³⁺ protein-chelate conjugates. *Magn. Reson. Med.* 3, 541-548.
- Unger, E. C., Totty, W. G., Neufeld, D. M., Otsuka, F. L., Murphy, W. A., Welch, M. J., Connett, J. M., and Philpott, G. W. (1985) Magnetic resonance imaging using gadolinium labeled monoclonal antibody. *Invest. Radiol.* 20, 693-700.
- Yeh, S. M., Sherman, D. G., and Meares, C. F. (1979) A new route to "bifunctional" chelating agents: conversion of amino acids to analogs of ethylenedinitrilotetraacetic acid. *Anal. Biochem.* 100, 152-159.
- DeRiemer, L. H., Meares, C. F., Goodwin, D. A., and Diamanti, C. J. (1981) BLEDTA II: Synthesis of a new tumor-visualizing derivative of CO(III)-bleomycin. *J. Labelled Compd. Radiopharm.* 18, 1517-1534.
- Sundberg, M. W., Meares, C. F., Goodwin, D. A., and Diamanti, C. I. (1974) Selective binding of metal ions to macromolecules using bifunctional analogs of EDTA. *J. Med. Chem.* 17, 1304-1307.
- Eckelman, W. C., Karesh, S. M., and Reba, R. C. (1975) New compounds: fatty acids and long chain hydrocarbon derivatives containing a strong chelating agent. *J. Pharm. Sci.* 64, 704-706.
- Krejcarek, G. E., and Tucker, K. L. (1977) Covalent attachment of chelating groups to macromolecules. *Biochem. Biophys. Res. Commun.* 77, 581-585.
- Hnatowich, D. J., Layne, W. W., and Childs, R. L. (1982) The preparation and labeling of DTPA-coupled albumin. *Int. J. Appl. Radiat. Isot.* 33, 327-332.
- Paik, C. H., Ebbert, M. A., Murphy, R. R., Lassman, C. R., Reba, R. C., Eckelman, W. C., Pak, K. Y., Powe, J., Steplewski, Z., and Koprowski, H. (1983) Factors influencing DTPA conjugation with antibodies by cyclic DTPA anhydride. *J. Nucl. Med.* 24, 1158-1163.
- Khaw, B. A., Cooney, J., Edgington, T., and Strauss, H. W. (1986) Differences in experimental tumor localization of dual-labeled monoclonal antibody. *J. Nucl. Med.* 27, 1293-1299.
- Otsuka, F. L., Cance, W. G., Dilley, W. G., Scott, R. W., Davie, J. M., Wells, J. A., and Welch, M. J. (1988) A potential new radiopharmaceutical for parathyroid imaging: Radiolabeled parathyroid-specific monoclonal antibody. II. Comparison of ¹²⁵I- and ¹¹¹In-labeled antibodies. *Nucl. Med. Biol.* 15, 305-311.
- Otsuka, F. L., Fleischman, J. B., and Welch, M. J. (1986) Comparative studies using ¹²⁵I- and ¹¹¹In-labeled monoclonal antibodies. *Nucl. Med. Biol.* 13, 325-334.
- Colcher, D., Zalutsky, M., Kaplan, W., Kufe, D., Austin, F., and Schlom, J. (1983) Radiolocalization of human mammary tumors in athymic mice by a monoclonal antibody. *Cancer Res.* 43, 736-742.
- Brown, B. A., Dearborn, C. B., Neacy, W. P., Sands, H., and Gallagher, B. M. (1986) Comparison of carbohydrate directed versus amine directed attachment of DTPA to murine monoclonal antibodies. *J. Labelled Compd. Radiopharm.* 23, 1288-1290.
- Covell, D. G., Barbet, J., Holten, O. D., Black, C. D. V., Parker, R. J., and Weinstein, J. N. (1986) Pharmacokinetics of monoclonal immunoglobulin G₁, F(ab')₂, and Fab' in mice. *Cancer Res.* 46, 3969-3978.
- Eger, R. R., Covell, D. G., Carrasquillo, J. A., Abrams, P. G., Foon, K. A., Reynolds, J. C., Schroff, R. W., Morgan, A. C., Larson, S. M., and Weinstein, J. N. (1987) Kinetic model for the biodistribution of an ¹¹¹In-labeled monoclonal antibody in humans. *Cancer Res.* 47, 3328-3336.

- (27) Najafi, A., Childs, R. L., and Hnatowich, D. J. (1984) Coupling antibody with DTPA—An alternative to the cyclic anhydride. *Int. J. Appl. Radiat. Isot.* 35, 554–557.
- (28) Leung, C. S. H., Meares, C. F., and Goodwin, D. A. (1978) The attachment of metal-chelating groups to proteins: Tagging of albumin by diazonium coupling and use of the products as radiopharmaceuticals. *Int. J. Appl. Radiat. Isot.* 29, 687–692.
- (29) Sundberg, M. W., Meares, C. F., Goodwin, D. A., and Diamanti, C. I. (1974) Chelating agents for the binding of metal ions to macromolecules. *Nature (London)* 250, 587–588.
- (30) Brechbiel, M. W., Gansow, O. A., Atcher, R. W., Schlom, J., Esteban, J., Simpson, D. E., and Colcher, D. (1986) Synthesis of 1-(p-isothiocyanatobenzyl) derivatives of DTPA and EDTA. Antibody labeling and tumor-imaging studies. *Inorg. Chem.* 25, 2772–2781.
- (31) Meares, C. F., McCall, M. J., Reardan, D. T., Goodwin, D. A., Diamanti, C. I., and McTigue, M. (1984) Conjugation of antibodies with bifunctional chelating agents: Isothiocyanate and bromoacetamide reagents, methods of analysis, and subsequent addition of metal ions. *Anal. Biochem.* 142, 68–78.
- (32) Yokoyama, K., Carrasquillo, J. A., Chang, A. E., Colcher, D., Roselli, M., Sugarbaker, P., Sindelar, W., Reynolds, J. C., Perentesis, P., Gansow, O. A., Francis, B., Adams, R., Finn, R., Schlom, J., and Larson, S. M. (1989) Differences in biodistribution of indium-111- and iodine-131-labeled B72.3 monoclonal antibodies in patients with colorectal cancer. *J. Nucl. Med.* 30, 320–327.
- (33) Mathias, C. J., Sun, Y., Welch, M. J., Green, M. A., Thomas, J. A., Wade, K. R., and Martell, A. E. (1988) Targeting radiopharmaceuticals: Comparative biodistribution studies of gallium and indium complexes of multidentate ligands. *Nucl. Med. Biol.* 15, 69–81.
- (34) Meares, C. F., and Wensel, T. G. (1984) Metal chelates as probes of biological systems. *Acc. Chem. Res.* 17, 202–209.
- (35) Leung, C. S. H., and Meares, C. F. (1977) Attachment of fluorescent metal chelates to macromolecules using “bifunctional” chelating agents. *Biochem. Biophys. Res. Commun.* 75, 149–155.
- (36) Connett, J. M., Fenwick, J. J., Timmcke, A. E., and Philpott, G. W. (1987) Characterization of the binding properties of murine monoclonal antibody (Mab)1A3, a newly described antibody displaying anti-human colon cancer selectivity. *Proc. Am. Assoc. Cancer Res.* 28, 352.
- (37) Connett, J. M., Inkster, M. D., Ruiz, M. B., and Philpott, G. W. (1988) Further characterization of murine monoclonal antibody (MAB)1A3, an antibody displaying anti-human colon cancer selectivity. *Proc. Am. Assoc. Cancer Res.* 29, 384.
- (38) Connett, J. M., Ruiz, M. B., Germain, C. J., Fenwick, J. J., and Philpott, G. W. (1989) In vitro and in vivo characterization studies of anti-human colon cancer monoclonal antibodies (Mab)1A3 and 5A4. *Proc. Am. Assoc. Cancer Res.* 30, 349.
- (39) Udenfriend, S., Stein, S., Bohlen, P., and Dairman, W. (1972) Fluorescamine: A reagent for assay of amino acids, peptides, proteins, and primary amines in the picomole range. *Science* 178, 871–872.
- (40) Mathias, C. J., Sun, Y., Connett, J. M., Philpott, G. W., Welch, M. J., and Martell, A. E. A new bifunctional chelate, BrMe₂HBED: An effective conjugate for radiometals and antibodies. *Inorg. Chem.*, in press.
- (41) Marchalonis, J. J. (1969) An enzymic method for the trace iodination of immunoglobulins and other proteins. *Biochem. J.* 113, 299–305.
- (42) Fraker, P. J., and Speck, J. C., Jr. (1978) Protein and cell membrane iodinations with a sparingly soluble chloroamide, 1,3,4,6-tetrachloro-3a,6a-diphenylglycoluril. *Biochem. Biophys. Res. Commun.* 80, 849–857.
- (43) Thach, R. E., and Newburger, M. A. (1972) *Research Techniques in Biochemical and Molecular Biology* W. A. Benjamin Inc., Menlo Park, CA.
- (44) Lindmo, T., Boven, E., Cuttitta, F., Fedorko, J., and Bunn, P. A., Jr. (1984) Determination of the immunoreactive fraction of radiolabeled monoclonal antibodies by linear extrapolation to binding at infinite antigen excess. *J. Immunol. Methods* 72, 77–89.
- (45) Goldenberg, D. M., Witte, S., and Elster, K. (1966) GW-39: A new human tumor serially transplantable in the golden hamster. *Transplantation* 4, 760–763.
- (46) Deshpande, S. V., DeNardo, S. J., Meares, C. F., McCall, M. J., Adams, G. P., and DeNardo, G. L. (1989) Effect of different linkages between chelates and monoclonal antibodies on levels of radioactivity in the liver. *Nucl. Med. Biol.* 16, 587–597.
- (47) Connett, J. M., Mathias, C., Welch, M. J., Zhu, X., and Philpott, G. W. (1989) Increased uptake of a unique radiolabeled anticolon cancer monoclonal antibody (Mab 1A3) in younger tumors in a human colon cancer (GW39) xenograft model. *Proc. Am. Assoc. Cancer Res.* 30, 359.

Registry No. I, 126926-43-0; II, 126926-44-1; III, 126926-45-2; III-2Na, 127063-51-8; IV·HCl, 126926-46-3; V, 126926-47-4; 1-(4-nitrobenzyl)ethylenediamine, 124888-28-4; salicylaldehyde, 90-02-8.

Preparation and Characterization of Immunoconjugates for Antibody-Targeted Photolysis

Scott L. Rakestraw,^{†,‡} Ronald G. Tompkins,[†] and Martin L. Yarmush^{*,†,§}

Department of Chemical and Biochemical Engineering and the Center for Advanced Biotechnology and Medicine, Rutgers University, Piscataway, New Jersey 08855, and Department of Surgery, Massachusetts General Hospital, Harvard Medical School, Boston, Massachusetts 02114. Received January 17, 1990

Monoclonal antibody (MAb)-dextran-tin(IV) chlorin e6 (SnCe6) immunoconjugates were prepared by a new technique involving the use of reducing, terminal-modified dextran carriers and site-specific modification of the Fc oligosaccharide moiety on the antibodies. Dextran carriers were synthesized to increase the number of SnCe6 molecules attached to a MAb. The dextran carriers were coupled to the MAb via a single, chain-terminal hydrazide group to prevent aggregation of MAbs. Conjugates were prepared with antimelanoma MAb 2.1 containing up to 18.9 SnCe6 molecules per MAb. Under neutral conditions, no hydrolysis of the hydrazone bond between the MAb and the dextran carrier could be detected, and the hydrazone was not stabilized by reduction with NaCNBH₃ or NaBH₄. Analysis of the purified immunoconjugates showed that approximately two dextran carrier chains were attached to a MAb regardless of the number of SnCe6 molecules linked to a dextran carrier. Site-specific covalent attachment of the SnCe6-dextran chains to the MAb was confirmed by SDS-PAGE. HPLC analysis of the conjugates gave a single species eluting in the range of 200-240 kDa. As determined by a competitive inhibition radioimmunoassay using viable SK-MEL-2 human malignant melanoma cells, the conjugates showed excellent retention of antigen-binding activity relative to unconjugated MAb.

INTRODUCTION

Methods for coupling active agents to antibodies can be grouped into two categories: (1) those which attach the agent directly to the antibody, and (2) those which rely on an intermediary for attachment. To date, most of the direct coupling procedures involve modification of amino acid side chains (1, 2). These approaches generally lack specificity of the coupling reaction in that the active agent cannot be directed to a particular site on the antibody. To exert control in this regard, direct methods which target the Fc oligosaccharide moiety of the antibody for coupling have been developed (3). While site-directed coupling to the heavy-chain carbohydrate has served to produce more well-defined immunoconjugates (4-6), the ratio of active agent to antibody is limited by the amount of periodate-oxidizable carbohydrate expressed by the immunoglobulin.

To increase the number of active agents coupled to each molecule of antibody, indirect attachment approaches have been developed. Most reported methods have linked the active agent of interest to a carrier biopolymer, followed by attachment of the resulting macromolecule to the immunoglobulin in a manner which does not offer site-directed control. Immunoconjugates prepared with carrier polymers such as poly amino acids (7), serum albumins (8), and dextran derivatives (9, 10) have been described. Recently, methods which attempted to combine the indirect carrier approach with site-directed control of the coupling reaction between carrier and antibody have been reported (11, 12). Attachment of a agent-

substituted dextran to the antibody was accomplished via Schiff base formation between the periodate-oxidized Fc oligosaccharide and an excess of free amino groups on the carrier dextran. No attempt, however, was made to limit the number of free amino groups on the carrier, raising the possibility of carrier-mediated cross-linking of antibodies to form high molecular weight aggregates. In addition, conjugation via Schiff base formation requires stabilization of the bond with reducing agents such as NaCNBH₃ or NaBH₄. Reductive stabilization of Schiff base bonds has been reported to often result in undesirable modification of some amino acids in the immunoglobulin (3).

The present work was undertaken to synthesize a monoclonal antibody (MAb)¹ immunoconjugate which (1) possessed a favorable active agent to antibody ratio by using the carrier approach, (2) demonstrated a site-directed coupling of the carrier by a single, chain-terminal group to the Fc carbohydrate moiety of the immunoglobulin, and (3) could be reproducibly prepared with retention of both active agent and antibody activity. By limiting the linkage of the antibody and carrier to a single area in each molecule, the possibility of carrier-mediated aggregate formation is reduced.

EXPERIMENTAL PROCEDURES

Chemicals. Unless noted otherwise, all organic chemicals were obtained from Aldrich (Milwaukee) and were used without further purification. Chlorin e6 was obtained

* Address correspondence and reprint requests to Dr. Martin L. Yarmush, Rutgers University, P.O. Box 909, Piscataway, NJ 08854.

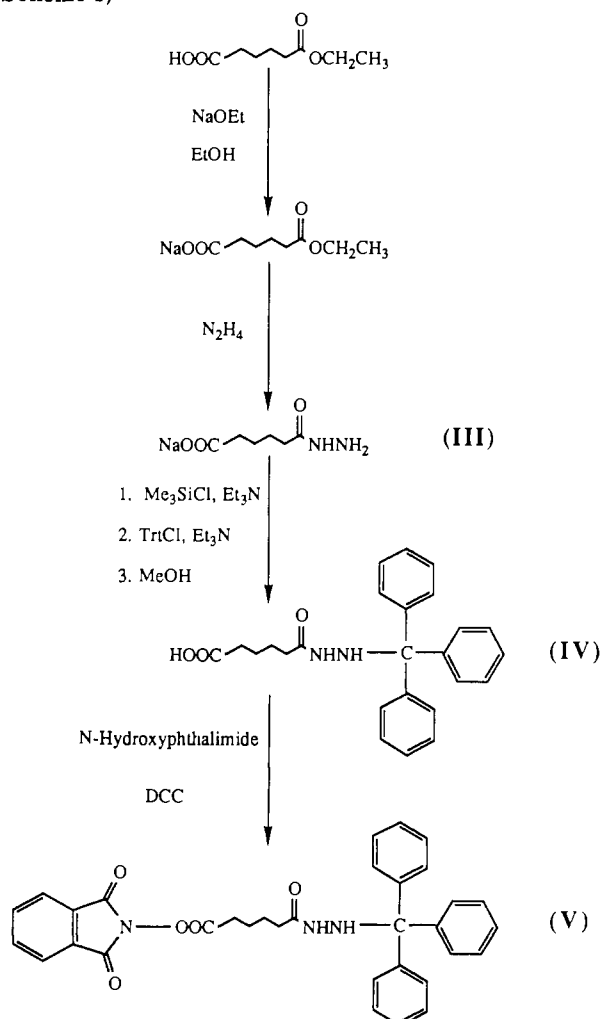
[†] Harvard Medical School.

[‡] Present address: E. I. du Pont de Nemours, Experimental Station, Wilmington, DE 19880-0304.

[§] Rutgers University.

¹ Abbreviations: MAb, monoclonal antibody; SnCe6, tin(IV) chlorin e6; DCC, dicyclohexylcarbodiimide; HOBT, *N*-hydroxybenzotriazole; EDAC, 1-ethyl-3-[3-(dimethylamino)propyl]carbodiimide; Trt, triphenylmethyl (trityl) group, DPBS, Dulbecco's phosphate-buffered saline; DMSO, dimethyl sulfoxide; DMF, dimethylformamide; BSA, bovine serum albumin; SDS-PAGE, sodium dodecyl sulfate-polyacrylamide gel electrophoresis.

Scheme II. Synthetic Scheme for the Preparation of the Trityl-Protected Active Ester Used To Block the Chain-Terminal Hydrazide Group on the Dextran Carrier (Scheme I)^a

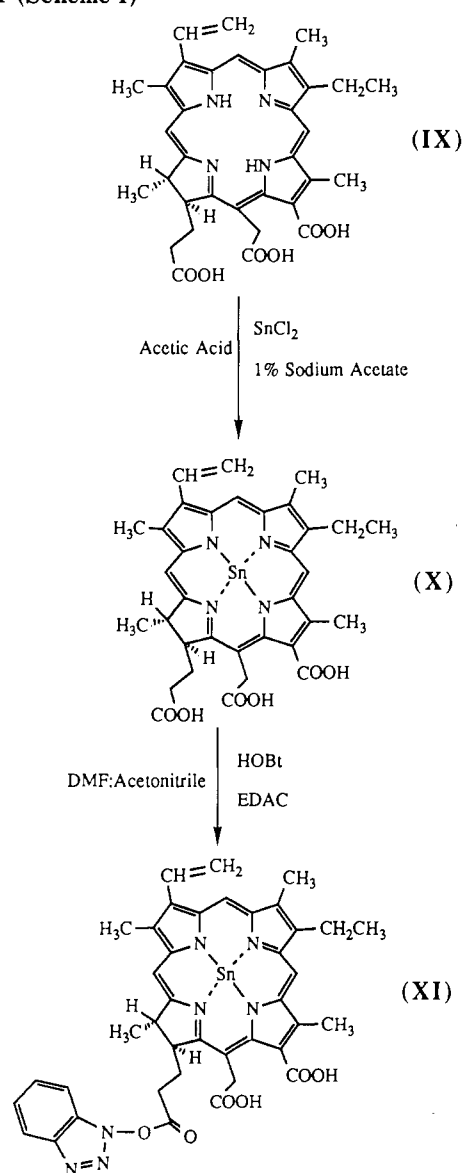


^a Roman numerals refer to the structures of compounds described in this paper and shown in the schemes.

refluxed in hydrazine hydrate (85%) for 1 h, poured into ethanol/ether (1:1), and evaporated to dryness in vacuo. The residue was treated with ethanol and vacuum evaporated until the odor of hydrazine could no longer be detected. The residue (III) was triturated with a mixture of ethanol and ether and collected (8.56 g, 92%, mp 149–151 °C dec).

Tritylhydrazo diformate IV was prepared by using a previously reported procedure with appropriate modifications (16). To a suspension of finely ground III (1.82 g, 10 mmol) in 20 mL of chloroform/acetonitrile (5:1) was added trimethylsilyl chloride (1.27 mL, 10 mmol). The mixture was refluxed for 2 h and cooled to room temperature, and triethylamine (2.79 mL, 20 mmol) and a solution of trityl chloride (2.79 g, 10 mmol) in 20 mL of chloroform were sequentially added. After stirring for 1 h, methanol (5 mL) was added with an additional 15 min of stirring to effect the hydrolysis of the trimethylsilyl ester. The light yellow solution was poured into ether and quickly washed with chilled 5% citric acid. The aqueous phase was discarded, and the organic phase was extracted twice with 1 N NaOH (50 mL). The combined alkaline extracts were cooled overnight at 4 °C and shaken with fresh ether (50 mL). Upon cooling of the separated aqueous layer to 0 °C and neutralization with glacial acetic acid, a dense white precipitate was formed.

Scheme III. Synthetic Scheme for the Preparation of the in Situ Active Ester of SnCe6 Used To Couple the Photosensitizer to Carbazate Groups on the Dextran Carrier (Scheme I)^a



^a The axial ligands associated with the central Sn ion have been omitted for clarity. The axial ligands are chloride anions for the anhydrous preparation of X, but are thought to be $(OH^-)_2$ when SnCe6 is dissolved in water. Roman numerals refer to the structures of compounds described in this paper and shown in the schemes.

The solid was resuspended in ethyl acetate (2 × 150 mL), washed with water, and dried over anhydrous $MgSO_4$. Rotary evaporation of the solvent yielded a gummy residue, which was dissolved in THF and slowly poured into rapidly stirred hexane to yield 1.75 g (44%) of a white solid (IV), which was used without further characterization.

To a solution of IV (1.75 g, 4.35 mmol) in dry THF (100 mL) was added N-hydroxyphthalimide (0.71 g, 4.36 mmol) followed by a solution of dicyclohexylcarbodiimide (896 mg, 4.35 mmol) in 20 mL of THF. The reaction contents were stirred for 20 h at room temperature, and the urea was removed by filtration. The filter cake was washed extensively with THF. Evaporation in vacuo of the combined filtrate and washes left a residue which was immediately taken up in chloroform (150 mL) and washed sequentially with saturated sodium bicarbonate

(2 × 100 mL), saturated NaCl (100 mL), and water (2 × 100 mL). The organic layer was dried over MgSO₄ and evaporated to a syrup which was slowly run into vigorously stirred hexane to yield V: 1.73 g; 73% yield; mp 168–170 °C; IR 1813, 1788, 1749, 1618 (C=O), 1534 (NH), 1490 (aryl) cm⁻¹; TLC on silica gel with a mobile phase of CH₂Cl₂/MeOH/acetic acid (9:1:trace) showed a single band at *R_f* 0.92. Theory: C, 72.4; H, 5.3; N, 7.7. Found: C, 71.8; H, 5.9; N, 7.8. A [³H]glycine analogue of V was prepared as described above by substituting tritiated glycine for the monohydrazide of adipic acid (III). The [³H]glycine analogue was used to label the position of the terminal hydrazide for structural studies.

(C) *Terminal Blocking of Hydrazinodextran II with the Protected Active Ester V.* The trityl-protected active ester V (530 mg, 0.97 mmol) was added to a solution of II (5.0 g, 0.14 mmol) in 25 mL of dry DMSO. The mixture was stirred for 3.5 h at room temperature during which time a slight, pale yellow tint developed due to release of *N*-hydroxyphthalimide upon reaction of the terminal hydrazide in II with the active ester. The reaction was terminated by pouring the contents into 500 mL of methanol, which caused precipitation of tritylhydrazinodextran VI. The product was collected by filtration and washed extensively with methanol. The filter cake was dissolved in deionized water (100 mL) and the solution was filtered to remove a small amount of insoluble material. The filtrate was dialyzed (tubing MWCO 12–14 kDa) versus several changes of deionized water for 2 days and lyophilized to yield 4.32 g (86.4%) of VI.

Digestion of purified VI with dextranase (17) for 30 min in 0.1 phosphate buffer, pH 6.0, at room temperature followed by TLC of the sugar fragments on silica gel plates (Analtech, Newark, DE) with ethyl acetate/methanol/water (4:2:1) produced three bands with anthrone detection (18): *R_f* 0.06 (smear), 0.20 (isomaltose), and 0.39 (glucose). A preparative plate was run and bands corresponding to the *R_f* values above were scraped from the plate. The compounds were eluted with excess mobile phase, and the solvent was evaporated to yield residues, which were dissolved in 60% perchloric acid. The *R_f* 0.06 band was the only fraction that exhibited the intense yellow color of the Trt cation. Trt content of the *R_f* 0.06 band (60% HClO₄; 430 nm, $\epsilon = 32\,000\text{ M}^{-1}\text{ cm}^{-1}$ for triphenylmethyl cation) was determined spectrophotometrically, and total carbohydrate content for each band was determined by using the anthrone assay (18).

To confirm the position of the hydrazide group in the dextran chain, a sample of II was reacted with the trityl-protected [³H]glycine active ester described previously. The resulting tritiated hydrazinodextran was digested for 30 min with 400 mM NaIO₄ at pH 6.5, and the digestion mixture was applied to a Sephadex G-25 column (2.5 × 40 cm) equilibrated with deionized water. The collected fractions were assayed for ³H content by liquid-scintillation counting and trityl content by acidification with 60% HClO₄ and spectrophotometry, and total carbohydrate content was determined by the anthrone method (18).

(D) *Preparation of (Tritylhydrazino)dextran trans-Carbonate (VII).* The cyclic *trans*-carbonate was prepared according to the general procedure of Doane et al. (19). A portion of VI (4.0 g) was dissolved in dry DMSO (40 mL) to which dioxane (4.8 mL) and triethylamine (20 mL) were subsequently added. The mixture was cooled in an ice bath under vigorous stirring while ethyl chloroformate (12 mL) was added dropwise over 4 min. The turbid mixture was stirred an additional 5 min, and the

product was precipitated by pouring into 1 L of rapidly stirred methanol. The solid was collected by filtration followed by extensive washing with fresh methanol. The product (VII) was air-dried on the filter after washing with ether: yield 3.92 g; IR 1810 (cyclic carbonate); 1752 (acyclic carbonate) cm⁻¹. The product was slightly soluble in water, but readily soluble in DMSO. The degree of substitution of the carbonate groups on the dextran chain was determined by acidic titration of VII that had been digested with barium hydroxide (19).

(E) *Conversion of VII to (Tritylhydrazino)dextran Carbazate (VIII) by Hydrazinolysis.* Dextran *trans*-carbonate VII (3.50 g) was ground to a fine powder and shaken with 30 mL of hydrazine hydrate (85%). The initial powder dissolved over the course of about 5 min, yielding a homogeneous solution, which was shaken for an additional minute, and poured into 1 L of methanol to effect precipitation of carbazate VIII. The solid was collected by filtration, washed with methanol, and air-dried on the filter. The white powder was dissolved in 100 mL of deionized water, dialyzed overnight versus several changes of deionized water, and lyophilized to yield 3.38 g. The infrared spectrum of the product showed a single strong carbonyl band at 1717 cm⁻¹ and the appearance of a new NH band at 1513 cm⁻¹. Addition of a drop of benzaldehyde to a solution of the product in 0.2 M acetate buffer, pH 4.75, containing 10% ethanol led to rapid formation of a precipitate, which was found to contain aromatic components by UV spectroscopy.

II. In Situ Preparation of the Tin(IV) Chlorin e6 Active Ester. The photosensitizer chlorin e6 was converted to its tin(IV) metallochlorin analogue and then activated for coupling to the side-chain carbazate groups on dextran carrier VIII. Activation of the SnCe6 was accomplished by in situ generation of an active ester by reaction with a carbodiimide and *N*-hydroxybenzotriazole in molar amounts equivalent to the amount of SnCe6 used. The in situ active ester (probable structure XI) was not isolated and characterized but used immediately to couple SnCe6 to the carrier.

(A) *Preparation of Tin(IV) Chlorin e6.* Chlorin e6 (IX; 500 mg, 0.837 mmol) was dissolved in 100 mL of 1% (w/w) anhydrous sodium acetate in glacial acetic acid and heated to 60 °C under nitrogen in darkness. Finely powdered SnCl₂ (1.0 g, 5.26 mmol) was charged into the reaction vessel with stirring. The incorporation of tin into the chlorin was followed by vis spectroscopy over the course of 1.5 h, during which time the red peak underwent a hypsochromic shift to 640 nm (pyridine) from the metal-free value of 664 nm (pyridine). Upon complete disappearance of the 664-nm peak, the reaction was cooled to room temperature with exposure to air (oxidation of Sn^{II} to Sn^{IV}) and poured into 1 L of chloroform. The dark green solution was extracted three times with 3 N HCl (300 mL) and twice with water (300 mL). The organic layer was evaporated in vacuo to dryness. The residue was dissolved in absolute ethanol (300 mL) and evaporated again in vacuo. The ethanol evaporation procedure was repeated twice more to strip any remaining water. The residue was triturated in hexane to produce dark blue-green plates, which were recrystallized from ethyl acetate to yield tin(IV) chlorin e6 dichloride (SnCe6; X): 391 mg; 59.5% yield; vis (pyridine) λ_{max} 415 nm; $\epsilon_{415} = 1.50 \times 10^5$; 640 nm $\epsilon_{640} = 6.00 \times 10^4$. TLC of the product on silica gel plates with 2.6-lutidine/water (6:4 v/v) in an atmosphere saturated with NH₃ vapor gave a single band at *R_f* 0.59. To facilitate quantitation, X was also prepared with a trace ¹¹³Sn γ -radiolabel in the manner described above using ¹¹³SnCl₆²⁻ (New England

Nuclear, Boston) prereduced with a small amount of magnesium metal in glacial acetic acid.

(B) *In Situ Generation of the SnCe6 Active Ester.* In order to produce the SnCe6 active ester, *N*-hydroxybenzotriazole (HOBt; 14 mg, 0.104 mmol) was initially added to a solution of SnCe6 (X; 30 mg, 0.042 mmol) in 1.0 mL of DMF and 700 μ L of acetonitrile. After 5 min, 1-ethyl-3-[3-(dimethylamino)propyl]carbodiimide (EDAC; 8 mg, 0.042 mmol) was added to initiate the reaction. The reaction was continued for 3 h in the dark at room temperature to generate XI, which was not isolated but used *in situ* in the next step to couple to dextran carbazate VIII.

III. Coupling of In Situ SnCe6 Active Ester XI to Dextran Carbazate VIII. In a separate vessel, a solution of the terminally protected carbazate VIII (120 mg, $\sim 3.43 \mu\text{mol}$) in 7.0 mL of dry DMSO was prepared just prior to the completion of the 3-h reaction time required for *in situ* generation of the chlorin active ester XI. Upon complete dissolution of VIII, the entire *in situ* active ester solution from above was added. The dark green mixture was allowed to react for 2 h in darkness at room temperature under tumbling agitation. Triethylamine (500 μ L) was then added, and the filtered reaction mixture was applied to a Sephadex G-50 column ($2.5 \times 45 \text{ cm}$) and eluted with deionized water. Two peaks showing strong absorbance at 634 nm (water) were observed. The first peak (XII), which eluted at the void volume and contained the majority of the green pigment, was collected for use in further reactions. The low molecular weight peak, which contained unbound X, was discarded.

To render excess side chain hydrazide groups on XII unreactive after coupling of the SnCe6, the remaining hydrazides were capped by reactions with excess acetaldehyde under reduction trapping conditions. To the pooled high molecular weight SnCe6-dextran fractions from above was added enough sodium acetate to bring the concentration to 300 mM. Cold acetaldehyde (2.0 mL, 35.8 mmol) was added, and the reaction mixture was adjusted to pH 5.0 with glacial acetic acid. Sodium cyanoborohydride was then added to a final concentration of 200 mM. The reaction was stirred at room temperature in the dark for 3 h. The pH, which changed rapidly at first due to consumption of protons by the reductive amination capping, was maintained at 5.0 by addition of acetic acid. Excess capping reagents were removed by extensive dialysis (tubing MWCO 12–14 kD) of the reaction solution against deionized water. The dialyzed material was lyophilized to yield 106 mg of a fluffy, green solid (XIII) readily soluble in water, DMSO, and neutral or alkaline buffers, but only slightly soluble in acidic buffers. The product was stored in darkness at -20°C until further use.

IV. Removal of the Chain-Terminal Trityl Blocking Group to Expose the Hydrazide Group. The lyophilized product from above (XIII; 100 mg) was dissolved in dry DMSO (5.0 mL), and trifluoroacetic acid (250 μ L) was added to cleave the chain-terminal trityl protection group. After 5 min, the reaction was terminated by addition of triethylamine (500 μ L), and the filtered mixture was eluted from a Sephadex G-50 column ($2.5 \times 45 \text{ cm}$) with deionized water. A single strong green peak (λ_{max} 405, 634 nm; XIV) eluted at the void volume followed by an intense yellow peak (λ_{max} 430 nm in 60% HClO_4 ; trityl cation) which eluted at the low molecular weight retention limit. The high molecular weight green peak was collected and lyophilized to yield 93 mg of SnCe6-dextran XIV, which was stored in the dark at -20°C until needed.

V. Coupling of SnCe6-Dextran to the Fc Carbohydrate Moiety in Antibodies. In preparation for coupling, the MAb (10 mg) was brought to a concentration of 5 mg/mL in 0.15 M acetate buffer, pH 4.75, by passage through a PD-10 desalting column (Pharmacia) followed by ultrafiltration as needed. Oxidation of the Fc carbohydrate moiety was performed as previously described with some modifications (3, 4). Sodium metaperiodate was added to the MAb solution to a final concentration of 20 mM. The oxidation was allowed to proceed in darkness for 15 min at room temperature, followed by the addition of ethylene glycol (50 μ L/mL MAb solution) with 15 min of further incubation to scavenge excess periodate. The oxidized MAb was purified by passage through PD-10 gel filtration column (Pharmacia) eluted with acetate buffer. Protein-containing fractions (determined by appreciable A_{280}) were pooled.

In a separate vessel, a solution of XIV (40 mg, $\sim 1.04 \mu\text{mol}$) in 1.0 mL of deionized water was prepared. This solution was added immediately to the oxidized MAb in acetate buffer and incubated for 48 h at 4°C in darkness. Following completion of the coupling, the reaction mixture was brought to pH 7.5 by dropwise addition of 1.0 M K_2HPO_4 . The immunoconjugates were purified by a two-step procedure. First, the coupling mixture was applied to a protein G-Sepharose column (Pharmacia) to remove unbound SnCe6-dextran XIV. After elution of the bound material with 0.15 M glycine pH 2.5 and immediate neutralization with 1.0 M K_2HPO_4 , unconjugated MAb was separated from the immunoconjugate by passage through a Sephacryl S-300 ($1.5 \times 25 \text{ cm}$) column. The high molecular weight conjugate fractions were pooled and dialyzed against PBS overnight at 4°C . The immunoconjugates were stable at 4°C for up to 1 week, and they could be stored frozen indefinitely at -70°C .

VI. Analysis of Immunoconjugates. Substitution ratios of SnCe6 per MAb were determined by γ -counting (^{113}Sn radiolabeled SnCe6) and A_{280} (MAb content). The measurement of MAb concentration was corrected for SnCe6-dextran absorbance at 280 nm with a standard curve produced from known concentrations of ^{113}Sn -labeled SnCe6-dextran. Conjugate structures were analyzed with SDS-PAGE (8–25% continuous gradient, mercaptoethanol) on a PHAST electrophoresis system (Pharmacia) with silver staining for protein visualization. Conjugate isoelectric points were determined with the same system using pI 3–9 gradient gels. HPLC of the purified conjugates was performed with a Du Pont Zorbax GF-250 column with 0.2 M phosphate buffer, pH 7.2 (1.0 mL/min).

The binding activity of the antimelanoma MAb 2.1 for its cell surface antigen (20) was measured by radioimmunoassay (RIA) (21) using ^{125}I -labeled MAb and a suspension of SK-MEL-2 human malignant melanoma cells (22). Previous results indicated that saturation of the available cell surface antigens occurred at a total MAb concentration of 20 nM for a suspension of 250 000 SK-MEL-2 cells. The binding activities of both the specific conjugate (antimelanoma 2.1-dextran-SnCe6) and the control conjugate (antilymphoma 2.130-dextran-SnCe6) were assessed by a competitive inhibition radioimmunoassay (21) in which increasing concentrations of the conjugates were incubated simultaneously with a nonsaturating amount (total MAb concentration of 10 nM) of unconjugated ^{125}I -labeled antimelanoma 2.1 and a suspension of 265 000 SK-MEL-2 melanoma cells. RIA data was plotted according to the following equation:

$$\frac{1}{I} = 1 + 1/KA$$

where I = percentage of inhibition expressed as a decimal, A = total molar concentration of the unlabeled inhibitor MAb, and K is the equilibrium affinity constant of the unlabeled MAb. Under conditions in which the total antibody concentration is sufficient to occupy all cell surface antigen, the slope of the inhibition curve $1/K$ is proportional to the average affinity constant of the inhibitor MAb relative to the ^{125}I -labeled reference MAb antimelanoma 2.1.

RESULTS

Synthesis of the SnCe6-Dextran Carrier. The synthetic schemes used in the present work are detailed in Schemes I-III. A reactive hydrazide group was added to the reducing terminus of dextran via reductive amination with a large excess of adipic acid dihydrazide in the presence of NaCNBH_3 . Titration of the unmodified reducing end in II using the dinitrosalicylate method (14) showed a 92% modification of the terminal aldehyde. Presumably, a hydrazone is formed by condensation of the dihydrazide with the small equilibrium amount of terminal acyclic aldehyde in dextran. The hydrazone is trapped to a hydrazide by reduction with NaCNBH_3 (23). The hydrazide group functions as the point of attachment of the dextran chain to the MAb.

To prevent modification of the chain-terminal hydrazide in II during the subsequent synthetic steps, a triphenylmethyl (Trt) protection group was introduced via an active ester of carboxypentanoic hydrazide (V, Scheme II). Digestion of purified VI with dextranase (17) followed by TLC of the sugar fragments on silica gel plates produced three bands of R_f 0.06 (smear, minor), 0.20 (isomaltose, major), and 0.39 (glucose, minor). The R_f 0.06 band was the only fraction that exhibited the intense yellow color of the Trt cation. Spectrophotometric measurement of the Trt content of the R_f 0.06 band combined with total carbohydrate content for each band yielded an average ratio of 125 mol of glucose per mol of Trt. This value was in good agreement with the number average molecular weight of 21.2 kDa (degree of polymerization = 131) previously determined by gel-permeation chromatography against dextran standards, suggesting that only one molecule of Trt was attached to each dextran chain.

To confirm the position of the hydrazide group in the dextran chain, a ^3H glycine analogue of the Trt-protected active ester was reacted with II. Periodate digestion of the tritiated analogue followed by chromatography of the fragments on Sephadex G-25 showed virtually all of the ^3H activity in the low molecular weight peak, while the bulk of the carbohydrate content was found in the void fractions (Figure 1). The observed chromatographic behavior can be explained by release of a low molecular weight tritiated fragment from the terminal glucose residue. Because the hydrazide group has been attached to the chain by reductive amination, the terminal glucose residue can no longer cyclize. Treatment of the chain with periodate cleaves the glucose subunit ring between the vicinal diols releasing C-3 as formic acid, and C-1 and C-2 as part of a tritiated low molecular weight fragment containing the trityl group. Although the remaining glucose subunits are also cleaved between the vicinal diol positions, the presence of the high molecular weight peak in the chromatogram of the digestion mixture (Figure 1) indicates that the dextran backbone remains intact.

Trt-protected hydrazinodextran VI was reacted with ethyl chloroformate in DMSO by using the general method of Doane and co-workers (19). The reaction yielded a mixture of cyclic and acyclic carbonates, which were evi-

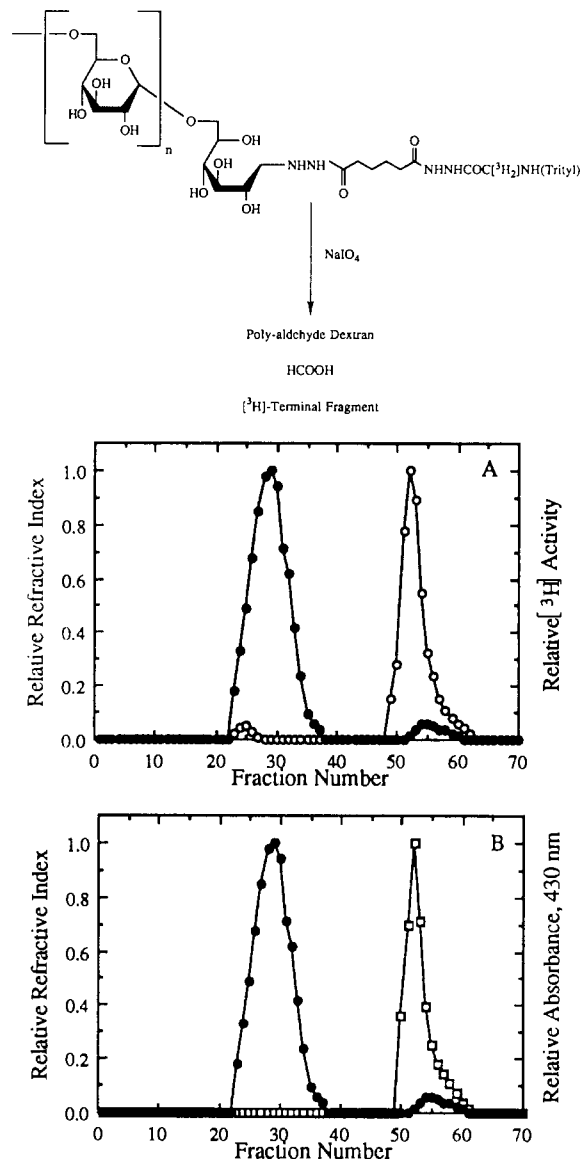


Figure 1. Chromatography of the mixture resulting from digestion of an ^3H -labeled analogue of the trityl-protected hydrazinodextran VI (Scheme I) with 400 mM NaIO_4 in pH 6.5 acetate buffer (reaction shown). The chromatograms were generated by passage of the digestion mixture through a Sephadex G-25 column (2.5×38 cm) equilibrated with deionized water. Fractions (5 mL) were collected, and each fraction was divided into three equal aliquots (1.67 mL). The refractive index of one aliquot was determined by an Abbe refractometer. The second aliquot was acidified with 60% perchloric acid and its absorbance at 430 nm was determined. The final aliquot was combined with 19 mL of liquid-scintillation cocktail (Hydrofluor, National Diagnostics) and ^3H content was determined. (A) A chromatogram of the refractive index (\bullet) and ^3H content (\circ) of each fraction is shown. Results are expressed relative to the maximum signal observed for each assay. (B) A chromatogram of the refractive index (\bullet) and absorbance at 430 nm (\square , in 60% HClO_4) of each fraction is shown. Results are expressed relative to the maximum signal observed for each assay.

cm^{-1}). In the present work, the dextran carbonate was found to have a total degree of substitution of 0.54 as determined by acidic back-titration of the sugar following barium hydroxide digestion (19). Treatment of dextran carbonate VII with hydrazine hydrate led to an immediate solvolysis of the carbonate groups with quantitative formation of a dextran carbamate (VIII). Evidence for the transformation was detected in the complete disappearance of the cyclic (1810 cm^{-1}) and acyclic (1752 cm^{-1}) carbonyl bands in the IR spectrum of the carbon-

ate with concurrent appearance of a single carbonyl band at 1717 cm^{-1} and a NH bending band at 1513 cm^{-1} in the spectrum of the carbazate.

SnCe6 was coupled to VIII by reaction with a SnCe6 active ester (XI) generated in situ in a separate vessel (Scheme III). The protocol reported in the current work gave five chlorins per chain based on an average molecular weight of the dextran chains of $\sim 35\text{ kDa}$. By varying the amount of in situ SnCe6 active ester XI reacted with each dextran chain in the coupling reaction, the ratio of SnCe6 per chain could be varied between 0.5 and 12.3 based on γ -counting of ^{113}Sn -labeled SnCe6. Introduction of Sn^{4+} into the chlorin macrocycle was observed to substantially increase the solubility of the SnCe6-dextran chains in aqueous buffers at modest loadings of SnCe6 per dextran chain. At ratios of SnCe6/dextran exceeding 10, the lyophilized material required dissolution in 0.10 M NaOH followed by dialysis into the working buffer of choice.

Coupling of SnCe6 to dextran carbazate VIII resulted in only partial coverage of the available hydrazide functions. Since the chain-terminal hydrazide was designed to be the sole point of linkage to MABs, excess hydrazide groups in the remainder of the chain were capped to render them unreactive. Capping was accomplished by a reductive ethylation of the spare hydrazides with excess acetaldehyde in the presence of NaCNBH_3 . The outcome of this procedure was measured by incubation of the purified XIII with an excess of benzaldehyde in 0.15 M acetate buffer, pH 4.75, containing 10% (v/v) ethanol. Prior to the reductive alkylation, rapid precipitation of the SnCe6-dextran chains was observed following benzaldehyde addition due to formation of hydrophobic phenyl hydrazones along the chain backbone. However, after the capping reaction, no precipitate was formed upon addition of benzaldehyde.

Finally, the Trt protecting group was removed from the terminal hydrazide group on the capped SnCe6-dextran chain by treatment with trifluoroacetic acid in dry DMSO. Elution of the reaction mixture on Sephadex G-50 with deionized water initially showed two bands. The rapidly eluting band contained all of the dark blue-green pigment present, whereas, the slower eluting band faded from deep yellow to colorless as it progressed down the column. The disappearance of the trailing yellow band can be explained by retardation of the trityl group due to hydrophobic interaction with the column packing. Initially, the cleaved Trt group comigrated with hydrophilic trifluoroacetic acid and thus displayed the characteristic yellow pigment of the Trt cation. As elution progressed, separation of the faster moving trifluoroacetic acid caused a shift of the equilibrium between Trt and its cation toward the uncharged species, which is colorless. The appearance of the slowly eluting yellow band provided evidence of deprotection of the chain-terminal hydrazide to yield XIV.

Preparation of Immunoconjugates. The MABs used in the present work (antimelanoma MAB 2.1 and antilymphoma 2.130) were stable to oxidation with 20 mM NaIO_4 . No evidence of precipitation of the MABs was ever observed in multiple preparations of immunoconjugates. Table I displays the various conjugates assembled from the MAB. Comparison of the SnCe6/MAB ratio with the SnCe6/dextran ratio showed that approximately two dextran carrier chains were able to be coupled to each antibody molecule. Coupling of the SnCe6-dextran to the MAB was always performed with the SnCe6-dextran present in at least 20-fold molar excess relative to the MAB. No attempts were made to prepare conju-

Table I. Conjugation Characteristics of MABs

MAB	sample no.	carrier SnCe6/dextran ratio ^a	immunoconjugate SnCe6/MAB ratio ^b	dextran chains per antibody	% conjugate yield ^c
2.1	1	0.9	1.7	1.89	31
	2	3.5	6.8	1.94	28
	3	5.5	11.2	2.04	27
	4	9.9	18.9	1.91	24
2.130 ^d	1	3.5	7.2	2.25	56

^a Determined by using ^{113}Sn Ce6 to prepare the SnCe6-dextran (dextran average $M_w \sim 35\text{ kDa}$). ^b Determined by using ^{113}Sn Ce6-dextran and A_{280} (MAB content) corrected for SnCe6-dextran absorbance. ^c Based on the amount of oxidized MAB used in the coupling reaction with ^{113}Sn Ce6-dextran. ^d MAB 2.130 is an antilymphoma MAB used as a nonbinding control antibody. MAB 2.1 is an antimelanoma MAB.

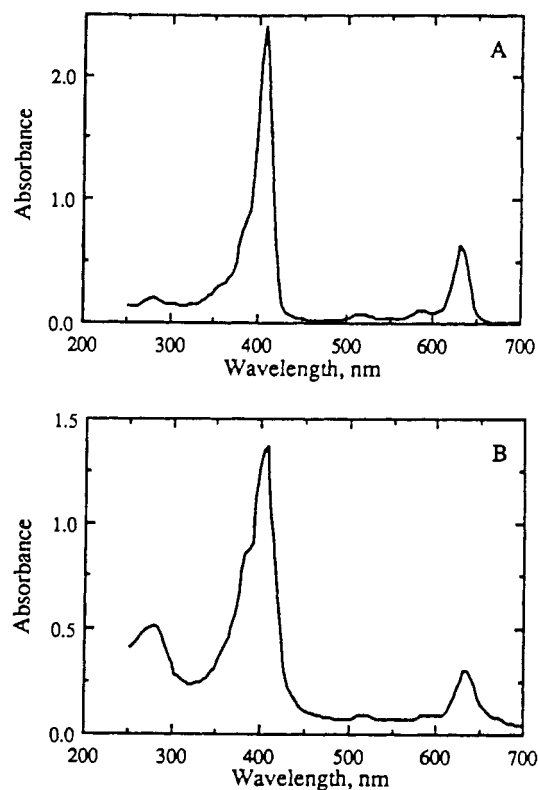


Figure 2. Optical absorption spectra of compounds used in the preparation of the immunoconjugates described in this paper: (A) A spectrum of unconjugated SnCe6 ($14.7\text{ }\mu\text{M}$) in DPBS, (B) a spectrum of an immunoconjugate (SnCe6/MAB molar ratio 11.2) in DPBS. The light path of the cuvette was 10 mm for both samples. Both the Soret band (409 nm) and the red band (634 nm) become broader with less pronounced absorbance as a result of conjugation. The Soret band also develops a shoulder at 378 nm and an isosbestic point at 390 nm .

gates with less of an excess of SnCe6-dextran in the coupling reaction mixture. Even at a 20-fold excess of SnCe6-dextran not all of the MAB was observed to form conjugate. However, for a particular MAB, the yield of conjugate did not appear to be significantly effected by the SnCe6/dextran molar ratio of the SnCe6-dextran used in the coupling (Table I). Instead, the yield of conjugate appears to be governed by the hydrazone equilibrium established between the hydrazide group on the carrier and the reactive aldehyde groups on the particular MAB.

Analysis of the Immunoconjugates. The spectrum of a typical conjugate is shown in Figure 2b. For comparison, the spectrum of free SnCe6 is illustrated in Figure 2a. Both the Soret and red bands showed were broad-

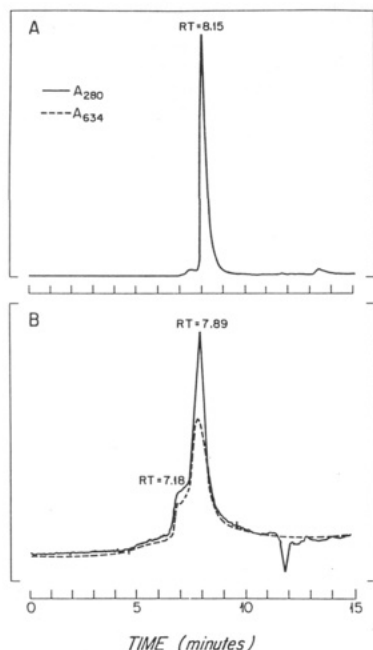


Figure 3. HPLC of antimalanoma 2.1 MAb and a purified antimalanoma MAb 2.1 immun conjugate (SnCe6/MAb molar ratio 6.8:1). The chromatograms were produced by elution of each sample from a Du Pont GF-250 column (0.8×25 cm) with 0.2 M phosphate buffer, pH 7.2, at 1.0 mL/min. (A) Unmodified MAb detected by A_{280} and (B) purified immun conjugate detected by A_{280} (solid line) and A_{634} (dotted line) are shown.

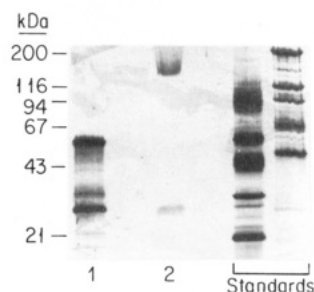


Figure 4. SDS-PAGE of antimalanoma MAb 2.1 and a purified antimalanoma MAb 2.1 immun conjugate (SnCe6/MAb molar ratio 6.8:1). A continuous gradient gel (8–25%) was used with silver staining for visualization of protein bands. Samples were prerduced with mercaptoethanol prior to migration on the gel. Lane 1 is the unmodified MAb 2.1 showing the characteristic light and heavy chain bands for IgG. Lane 2 shows the migration pattern for the purified immun conjugate. The modified immunoglobulin heavy chain in the conjugate (lane 2) was observed to be green prior to silver staining.

ened as a result of conjugation to the dextran carrier and MAb. In addition, the Soret band displayed a shoulder peak at 378 nm and an isosbestic point at 390 nm. Purified conjugates analyzed by HPLC were found to elute in a single peak corresponding to a molecular weight range of 200–240 kDa (Figure 3). Small amounts (<10%) of conjugates containing two MAbs per dextran chain were noted in some HPLC analyses.

In order to confirm covalent attachment of the SnCe6-Dextran chains to the Fc oligosaccharide region of the MAb, SDS-PAGE in the presence of mercaptoethanol was performed. As shown in Figure 4, all of the heavy chain from the purified conjugates migrated to a region of higher molecular weight than that seen for unmodified heavy chain. In contrast, unmodified light chain bands were found for both the conjugated and unconjugated MAbs. Prior to staining of the SDS-PAGE gels with silver stain only the modified heavy chain bands were

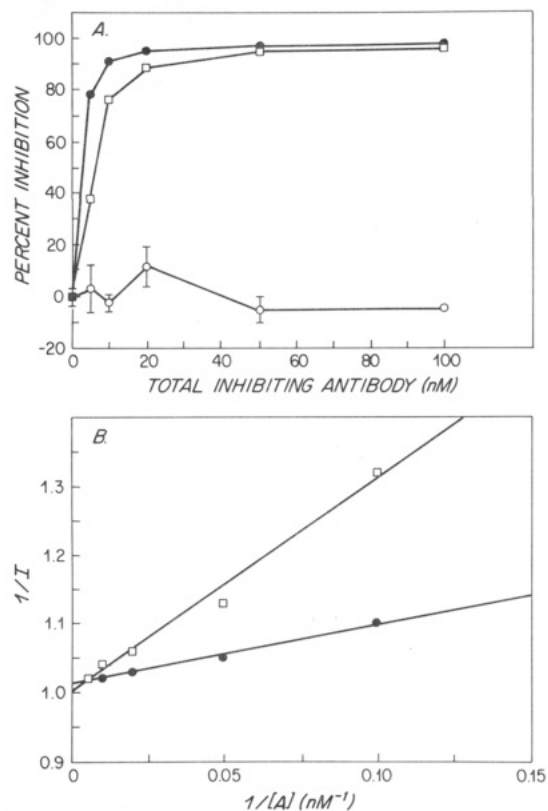


Figure 5. Inhibition of the binding of a 125 I-labeled antimalanoma 2.1 antibody to SK-MEL-2 human malignant melanoma cells by various unlabeled inhibitors. A nonsaturating amount of the radiolabeled MAb (total concentration 10 nM) and varying amounts of inhibitor were incubated with SK-MEL-2 cells in suspension. The data (mean \pm SD) are the results of triplicate samples for each concentration of inhibitor. (A) A plot of the inhibition of the binding reaction between 125 I-labeled 2.1 antibody and SK-MEL-2 cells by (\square) unlabeled antimalanoma 2.1-dextran-SnCe6 conjugate (SnCe6/MAb molar ratio 6.8:1), (\bullet) unlabeled antimalanoma 2.1 alone, (\circ) unlabeled antilymphoma 2.130-dextran-SnCe6 (SnCe6/MAb molar ratio 7.2:1) and (B) a linear transform of inhibition data plotted in panel A [(\square) unlabeled antimalanoma 2.1-dextran-SnCe6 conjugate (SnCe6/MAb molar ratio 6.8:1), slope = 3.07 nM; (\bullet) unlabeled antimalanoma 2.1 alone, slope = 0.85 nM] are shown. Solid lines represent the best fit to the data using linear least squares analysis ($r^2 = 0.994$).

observed to be green in color. This confirms the presence of the SnCe6-dextran carrier on the heavy chain of the MAb. The isoelectric point of the purified immun conjugates ranged between 3.8 and 4.0, close to the pI of 3.5 observed for SnCe6-dextran modules alone.

Conjugate antigen binding properties relative to non-conjugated controls were determined by competitive inhibition RIA using suspensions of SK-MEL-2 human malignant melanoma cells. Figure 5a shows that nonradiolabeled MAb 2.1 conjugate and unlabeled MAb 2.1 alone (unconjugated MAb) inhibited the binding of unconjugated 125 I-labeled MAb 2.1 in a similar manner. The non-binding conjugated prepared from antilymphoma 2.130 exhibited no inhibition of 125 I-labeled MAb 2.1 binding to SK-MEL-2 cell surface antigen (Figure 5a).

In order to quantitatively determine the effect of conjugation on MAb binding affinity, a linear transform of the Langmuir binding isotherm was applied. A plot of $1/I$ as a function of $1/A$ for the RIA data is shown in Figure 5b; where I is the percent of inhibition and A is the total inhibitor concentration. Analysis of the slopes of the inhibition curves shows that the ratio of the binding constants for the immun conjugate versus the unmod-

ified MAb ($K_{\text{conjugate}}/K_{\text{unmodified}}$) was found to be 0.28. Given an affinity constant for unconjugated MAb 2.1 of $3.9 \times 10^9 \text{ M}^{-1}$ (21), the average affinity constant for the MAb 2.1 conjugate was, therefore, $1.1 \times 10^9 \text{ M}^{-1}$.

DISCUSSION

In the present paper, we have described a reproducible method for the site-specific covalent attachment of multiple small molecules to immunoglobulins. The main features of this approach are (1) site-specific attachment of the carrier polymer to the MAb at a point distal to the antigen-binding site minimizes the modification of MAb binding properties (6); (2) multiple active agents can be attached to an antibody via the carrier polymer; (3) the use of a single, chain-terminal group for attachment to the MAb prevents Ab-Ab cross-linking; (4) the use of the hydrazide moiety as the functional group for coupling the carrier to the MAb obviates the use of reductive stabilization of the MAb-carrier bond as required in other techniques; and (5) the method is reproducible and can be generalized to a variety of active agents.

Attachment of the carrier to the Fc carbohydrate moiety of the MAb, in the majority of cases, confined the modification of the MAb to a point that is distal to the antigen-binding sites. In fact, Rodwell et al. (6) have demonstrated that MAb modification via the Fc oligosaccharide has less of an impact on both the antigen-binding affinity and immunoconjugate homogeneity than does a non-site-specific method. This phenomenon is supported by the present work. Competitive inhibition experiments with the antimelanoma MAb 2.1 immunoconjugates show only a slight decrease in the antigen-binding affinity with respect to the unmodified MAb. Thus, the reported technique appears to allow for coupling of multiple active agents to MAb via a dextran carrier while a major fraction of the binding activity of the MAb is retained.

A dextran carrier polymer was employed to increase the number of active agents coupled to the antibody. Dextran was chosen because it is water-soluble, nontoxic, contains multiple functional groups for active agent attachment, and possesses a single reducing terminus to which the antibody can be linked. The dextran carrier was end-functionalized with a hydrazide group, which served as the only point of attachment between the carrier and the Fc oligosaccharide moiety of the MAb. Because the carrier polymer possessed a single group for covalent coupling to the MAb, the likelihood of MAb cross-linking induced by multiple coupling groups on the carrier is minimized. It might have also been possible to use a carrier with several hydrazide groups and still obtain a single MAb-carrier bond. This approach would probably provide higher yields of conjugate but at the potential expenses of greater aggregate formation.

Using a method to measure the number of reactive Fc aldehyde groups generated by periodate oxidation (24), we have found that the number of reactive aldehyde groups per MAb varies with the identity of the MAb employed. Because the number of hydrazone bonds between the MAb aldehydes and the carrier hydrazide groups will be governed by equilibrium considerations, antibodies having fewer reactive Fc aldehyde groups may actually be able to tolerate an increased number of carrier coupling groups without significant aggregate formation. Evidence of the equilibrium nature of the MAb-carrier coupling reaction is found in the yield of immunoconjugates produced by the present method (Table I). Conjugate yield did not depend on SnCe6/dextran substitution ratio and was relatively constant for a particular MAb in the presence

of a molar large excess of carrier in the coupling reaction. For both MAbs, the number of dextran carriers bound per MAb was approximately two. Given that no unmodified heavy chain could be detected on SDS-PAGE (reducing conditions) of the purified immunoconjugates (Figure 4), the data suggest that each heavy chain is able to couple to one carrier chain. Because several reactive aldehyde groups have been found to exist per antibody (and, hence, probably more than one reactive aldehyde group per MAb heavy chain) (24), we conclude that the yield of the coupling reaction is governed by the equilibrium of intermolecular hydrazone formation in conjunction with steric considerations once the first hydrazone bond has been formed.

Attachment of the carrier to the MAb was accomplished via formation a hydrazone bond. The reaction was conducted at pH 4.75 in acetate buffer in the presence of a large excess of hydrazide-functionalized carrier polymer. Because the hydrazide group has a pK_a in the vicinity of 3.0 (25), at a pH of 4.75 the nucleophilic properties of the hydrazide are retained and the hydrazone formation rate is maximized (26). In addition, because the coupling is conducted at pH 4.75, possible Schiff base formation between Fc aldehyde and side-chain lysine amino groups on the MAb (4) is inhibited. Raising the pH to neutral before removal of the excess carrier polymer prevents hydrolysis of the hydrazone bond. The stability of the hydrazone bond at neutral pH is such that reduction of the hydrazone with NaCNBH_3 or NaBH_4 is not necessary to insure conjugate integrity (26). In fact, attempts in our laboratory to stabilize the conjugate hydrazone bond with NaCNBH_3 or NaBH_4 usually resulted in precipitation of the conjugate (data not shown). In contrast, attachment of MAb to amino-substituted carrier polymers (11, 12) requires stabilization of the resulting Schiff base due to susceptibility of the bond to hydrolysis at neutral pH.

Extension of the general method reported in this work to other active agents should be easily accomplished. The photosensitizer SnCe6 was used as the active agent for studies of antibody-target photolysis of malignant melanoma cells. However, any active agent (e.g. drug, toxin, radioisotope chelator) which can be derivatized with a suitable group for attachment to the carrier could be employed. Because the active agent-carrier conjugate is assembled separate from the MAb, synthetic conditions can be used to prepare the carrier which may be too severe to be used in the presence of the MAb. The number of active agents per carrier chain can be stoichiometrically controlled with an upper limit defined by agent structure and solubility. In the present work with SnCe6, an upper limit of 12.3 chromophores per dextran chain was found with a dextran of molecular weight $\sim 40 \text{ kDa}$. Attempts were made to prepare chlorin-dextran chains using metal-free chlorin e6 in place of the SnCe6 derivative (data not shown). While such compounds could be prepared, the limited aqueous solubility behavior of the Sn-free material made these carriers difficult to handle. At chlorin to dextran ratios as low as 2.0, the metal-free chains slowly precipitated from solution upon standing. The precipitation was accelerated by increasing the ionic strength of the solution or lowering the pH to mildly acidic conditions. The increased solubility of the metal-chlorin derivatives is most probably attributed to the metal in the chlorin macrocycle, and the subsequent formation of hydrated complexes in the resulting octahedral field. Active agents which are less bulky or more water soluble than SnCe6 may allow for increased substitution ratios to be realized.

While dextrans of differing size could be used, a practical upper limit to the size of the carrier polymer used might exist, depending on the application. In the case of immunoconjugate use in vivo, carrier polymers larger than ~40–70 kDa might impair immunoconjugate uptake because of transport limitations. In vitro conjugate use, on the other hand, would not be so hampered, and the use of larger carrier polymers may be allowed if greater amplification of the active agent effect is desired (e.g. fluorescent or radioisotope labels for diagnostic assay). However, because the yield of the conjugates appears to be determined by the equilibrium of intermolecular hydrazone formation, increasing the size of the carrier polymer may adversely effect the resultant immunoconjugate yield.

ACKNOWLEDGMENT

We thank Dr. Jerry C. Bommer of Porphyrin Products in Logan, UT, for his discussions concerning metalochlorin chemistry. Excellent technical assistance was provided by Emilio Cacciavillani and Stephen Warren. This work was supported by the Lucille P. Markey Charitable Trust, the Whitaker Foundation, and the Shriners Hospital for Crippled Children.

LITERATURE CITED

- (1) Blair, A. H., and Ghose, T. I. (1983) *J. Immunol. Methods* 59, 129–143.
- (2) Ghose, T. I., Blair, A. H., and Kulkarni, P. N. (1983) *Methods Enzymol.* 93, 280–333.
- (3) O'Shannessy, D. J., Quarles, R. H. (1987) *J. Immunol. Methods* 99, 153–161.
- (4) Muryama, A., Shimada, K., and Yamamoto, T. (1978) *Immunochemistry* 15, 523–528.
- (5) O'Shannessy, D. J., and Quarles, R. H. (1985) *J. Appl. Biochem.* 7, 347–355.
- (6) Rodwell, J. D., Alvarez, V. L., Lee, C., Lopes, A. D., Goers, J. W. F., King, H. D., Powsner, H. J., and McKearn, T. J. (1986) *Proc. Natl. Acad. Sci. U.S.A.* 83, 2632–2636.
- (7) Hurwitz, E., Wilchek, M., and Pitha, J. (1980) *J. Appl. Biochem.* 2, 25–35.
- (8) Garnett, M. C., Embelton, M. J., Jacobs, E., and Baldwin, R. W. (1983) *Int. J. Cancer* 31, 661–670.
- (9) Arnon, R., and Hurwitz, E. (1985) In *Monoclonal Antibodies for Cancer Detection and Therapy*. (R. W. Baldwin, and V. S. Byers, Eds.) pp 365–383, Academic, London.
- (10) Manabe, Y., Tsubota, T., Haruta, Y., Kataoka, K., Okazaki, M., Haisa, S., Nakamura, K., and Kimura, I. (1984) *J. Lab. Clin. Med.* 104, 445–454.
- (11) Oseroff, A. R., Ohuoha, D.; Hasan, T., Bommer, J. C., and Yarmush, M. L. (1986) *Proc. Natl. Acad. Sci. U.S.A.* 83, 8744–8748.
- (12) Shih, L. B., Sharkey, R. M., Primus, F. J., and Goldenberg, D. M. (1988) *Int. J. Cancer* 41, 832–839.
- (13) Djorck, L., and Kronvall, G. (1984) *J. Immunol.* 133, 969–974.
- (14) Bernfeld, P. (1955) *Methods Enzymol.* 1, 149–158.
- (15) Hurd, C. D., Buess, C. M., and Bauer, L. (1952) *J. Org. Chem.* 47, 865–876.
- (16) Barlos, K., Papaioannou, D., and Theodoropoulos, D. (1982) *J. Org. Chem.* 47, 1324–1326.
- (17) Janson, J. C., and Porath, J. (1966) *Methods Enzymol.* 8, 615.
- (18) Scott, T. A., and Melvin, H. (1953) *Anal. Chem.* 25, 1656.
- (19) Doane, W. M., Shasha, B. S., Stout, E. I., Russell, C. R., and Rist, C. E. (1968) *Carbohydr. Res.* 8, 266–274.
- (20) Saxton, R. E., Mann, D. L., and Burk, M. W. (1982) *Hybridoma* 1, 433–445.
- (21) Shockley, T. R., and Yarmush, M. L. *Mol. Immunol.*, submitted.
- (22) Fogh, J., and Trempe, G. (1975) In *Human Tumors Cells In Vitro*. (J. Fogh, Ed.) Plenum, New York.
- (23) Borch, R. F., Bernstein, M. D., and Durst, H. D. (1971) *J. Am. Chem. Soc.* 93, 2897–2904.
- (24) Rakestraw, S. L., Tompkins, R. G., and Yarmush, M. L. *Anal. Biochem.*, submitted.
- (25) Inman, J. K., and Dintzis, H. M. (1969) *Biochemistry* 8, 4704–4082.
- (26) King, T. P., Zhao, S. W., and Lam, T. (1986) *Biochemistry* 25, 5774–5779.

TECHNICAL NOTE

Simplified Method for Conjugating Macrocyclic Bifunctional Chelating Agents to Antibodies via 2-Iminothiolane

Michael J. McCall, Habibe Diril, and Claude F. Meares*

Chemistry Department, University of California, Davis, California 95616. Received February 8, 1990;
Revised Manuscript Received March 13, 1990

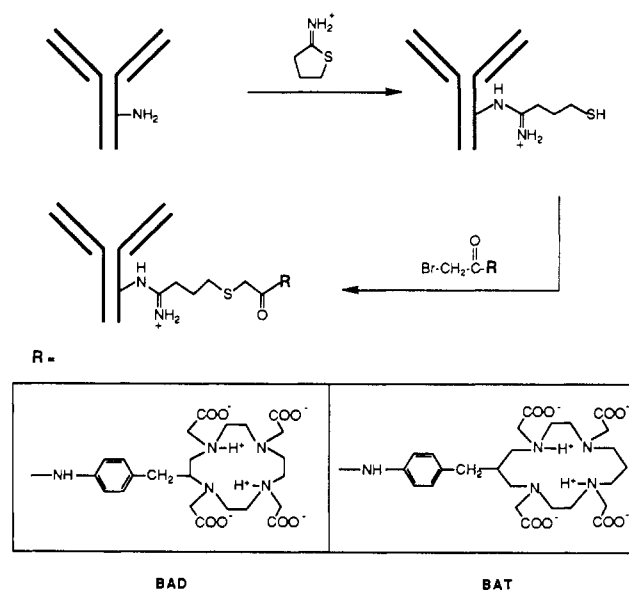
A one-step method for conjugating macrocyclic chelators to antibodies using the protein modification reagent 2-iminothiolane controls aggregation, maintains immunoreactivity, and produces consistent chelate/antibody ratios. Conjugation conditions have been investigated with the macrocyclic chelates 6-[*p*-(bromoacetamido)benzyl]-1,4,8,11-tetraazacyclotetradecane-*N,N',N'',N'''*-tetraacetic acid and 2-[*p*-(bromoacetamido)benzyl]-1,4,7,10-tetraazacyclododecane-*N,N',N'',N'''*-tetraacetic acid, with three different monoclonal antibodies. The bifunctional chelating agents are prepared by bromoacetylation of their amine precursors using a two-phase H₂O/CHCl₃ system, which improves product purity.

The attachment of metal ions to monoclonal antibodies (mAbs)¹ for medical applications demands extreme stability under physiological conditions, with no significant release of metal (1-4). Development of antibody-macrocyclic chelate conjugates for tumor localization and therapy has led to the following improvements.

In our earliest study of the conjugate of 6-[*p*-(bromoacetamido)benzyl]-1,4,8,11-tetraazacyclotetradecane-*N,N',N'',N'''*-tetraacetic acid (BAT) with the mouse mAb Lym-1 it was observed that, rather than linking the macrocyclic bifunctional chelating agent directly to the antibody, it was necessary to employ a spacer group between the two moieties (5). Without this spacer, no practical uptake of radiometal (copper or cobalt) was observed when radiolabeling was attempted after conjugation. For use with short-lived radionuclides, postconjugation radiolabeling is an important feature. As shown in Scheme I, linkage was accomplished in a two-step, overnight procedure using Traut's reagent (6) 2-iminothiolane (2IT), which reacts with amino groups to produce mercaptobutyrimidyl groups, followed by alkylation of the mercapto sulfur with BAT. For Lym-1, this method led to variable amounts of protein aggregation via cross-linking. The degree of aggregation was difficult to control, ranging from 10% to >50%. Also, the use of ≈0.4 M 2-mercaptoethanol in the Traut procedure (to prevent oxidation of the mercaptobutyrimidyl groups, which could form disulfide cross-links) could possibly reduce antibody disulfide bonds, and it was necessary to remove the 2-mercaptoethanol prior to the addition of BAT.

2-Iminothiolane has also been used as the cross-linking reagent in the synthesis of antibody-toxin conjugates. Since the disulfide bond between the antibody

Scheme I



and toxin proved to be unstable in vivo ($t_{1/2}$ = 6-8 h) (7), Carroll et al. (8) studied substituted 2IT's with a view to increasing the disulfide bond stability. In the latter study, the nascent mercaptobutyrimidyl groups reacted with the activated disulfide 5,5'-dithiobis(2-nitrobenzoic acid) to form a mixed disulfide. This work called our attention to the possibility that, since under mildly alkaline conditions bromoacetamide reagents react rapidly with sulfhydryl groups but only slowly with amino groups, the antibody, BAT, and 2IT solutions could be combined in a single reaction mixture. The method has been explored with three mAbs, Lym-1, 155H.7, and chimeric L6, and with either BAT or 2-[*p*-(bromoacetamido)benzyl]-1,4,7,10-tetraazacyclododecane-*N,N',N'',N'''*-tetraacetic acid (BAD) as the chelator.

EXPERIMENTAL PROCEDURES

Reagents. Lym-1, an anti B cell lymphoma IgG_{2a} mAb (9), was obtained from Damon Biotech (Needham Heights,

*Abbreviations used are as follows: mAb, monoclonal antibody; BAT, 6-[*p*-(bromoacetamido)benzyl]-1,4,8,11-tetraazacyclotetradecane-*N,N',N'',N'''*-tetraacetic acid; BAD, 2-[*p*-(bromoacetamido)benzyl]-1,4,7,10-tetraazacyclododecane-*N,N',N'',N'''*-tetraacetic acid; 2IT, 2-iminothiolane; NO₂Bn, *p*-nitrobenzyl; NH₂Bn, *p*-aminobenzyl; DOTA, 1,4,7,10-tetraazacyclododecane-*N,N',N'',N'''*-tetraacetic acid; TETA, 1,4,8,11-tetraazacyclotetradecane-*N,N',N'',N'''*-tetraacetic acid.

MA 02194; Encapcel murine mAb, lot # 3-171-860818). It was further purified by protein A affinity column chromatography prior to use. Chimeric (where the immunoglobulin constant domains, $C_{\gamma 2a}$ and C_{κ} , of the mouse mAb have been replaced by human $C_{\gamma 1}$ and C_{κ} domains) L6, a mAb against a carbohydrate antigen found at the surface of cells from human carcinomas of the lung, breast, colon, and ovary (10) (lot 88/42E), was obtained from Dr. I. Hellstrom, Oncogen, Seattle, WA. 155H.7, a murine antibody (IgG_{2a}) raised against a synthetic β -anomer of the Thomson-Friedenreich antigen (11) (lot 250588), was obtained from Dr. A. Noujaim, University of Alberta, Canada. Protein A on Sepharose-CL-4B and 2IT were purchased from Sigma Chemical Co. Cobalt-57 chloride was purchased from ICN (specific activity 7000 Ci/g). [1-¹⁴C]Bromoacetic acid was purchased from Amersham (specific activity 0.383 Ci/g). Pure water (resistance 18 M Ω , NANOpure II, Barnstead, MA) was employed throughout. All glass labware was washed with a mixed acid solution and thoroughly rinsed with deionized, distilled water (12). All plastic labware was washed with 3 M HCl and thoroughly rinsed with deionized, distilled water. All other reagents were the purest commercially available.

Thin-Layer Chromatography. TLC was run on plastic-backed silica gel plates (EM Science) using a 10% (w/v) ammonium acetate/methanol (1:1 v/v) solution as the eluent. In this system, unchelated cobalt and conjugate remain at the origin while free chelates migrate to R_f 0.5–0.6.

High-Performance Liquid Chromatography. Gel-filtration HPLC of the immunoconjugates was performed at room temperature with Spherogel G3000SW (Altex). Protein molecular weight markers (Bio-Rad) were used to calibrate the column. The eluent was 0.1 M sodium phosphate buffer, pH 7.0, containing 0.025% Na₂S₂O₅ by weight. The flow rate was 0.5 mL/min. The UV-absorbing fractions were detected at 280 nm.

Reversed-phase HPLC of BAT and BAD was performed at room temperature with a 10 \times 250 mm C₁₈ column (Alltech). A 20-min linear gradient, from 0.1 M sodium acetate, pH 7 (containing 1 mM EDTA), to 100% methanol, was used at a flow rate of 3.0 mL/min. The UV-absorbing fractions were detected at 254 nm.

Glycineamido-Bn-DOTA was purified by reversed-phase HPLC using a 21.4 \times 250 mm C₁₈ column (Dynamax). A 20-min linear gradient from 0.1 M ammonium acetate, pH 6, to 100% methanol was used at a flow rate of 12.5 mL/min, detected at 254 nm.

Ultraviolet Spectrophotometry. Optical density measurements at 280 nm were made on a Gilford Model 250 spectrophotometer using a 1 cm path length microcell. Antibody concentrations were determined with $E^{1\%}_{280} = 13.5$ (13) and a molecular weight of 155K. Optical densities were measured on dilutions suitable to give absorbance readings of 0.1–1.0.

Radiation Counting. Gamma counting was done in a Beckman Model 310 counter with the appropriate energy windows set for ⁵⁷Co. TLC plates containing radiolabeled materials were visualized with an AMBIS Radioanalytic Imaging System. Beta counting was done in Aquasol, using a Beckman LS 6800 liquid-scintillation counter with the energy windows set for ¹⁴C.

Macrocycles. 6-(*p*-Nitrobenzyl)-1,4,8,11-tetraazacyclotetradecane-*N,N',N'',N'''*-tetraacetic acid (NO₂Bn-TETA) and 2-(*p*-nitrobenzyl)-1,4,7,10-tetraazacyclododecane-*N,N',N'',N'''*-tetraacetic acid (NO₂Bn-DOTA) were prepared according to the method of Moi et al. (2, 5). Reduction of each to the respective *p*-amino compound

was accomplished in the following manner. NO₂Bn-DOTA (120 mg, 0.22 mmol) was dissolved in 30 mL of water and the pH was adjusted to 11.5 with 2 M sodium hydroxide. Ten percent palladium on carbon catalyst (25 mg) was added, and the reaction vessel was attached to an atmospheric-pressure hydrogenation apparatus, cooled in an ice bath, purged with N₂, and filled with H₂. The course of the reaction was monitored by observing the uptake of H₂ and noting the presence of a transient green color in the reaction mixture. When H₂ uptake had ceased (3–5 h), the reaction mixture was removed from the hydrogenation apparatus, the pH was adjusted to 6.8 with 1 M HCl, and the catalyst was removed by filtration through a double layer of Millipore GS membrane (0.22 μ m). The filtrate, which was positive for amino groups by a fluorescamine test (14), was lyophilized. Proton NMR showed a shift of the aromatic aa'bb' pattern from 7.5 and 8.2 ppm for NO₂Bn-DOTA to 6.8 and 7.1 ppm for NH₂Bn-DOTA. FAB mass spectrum: $M + 1$ peak at m/e 510 and $M + Na$ peak at m/e 532 for the product, as expected. NO₂Bn-TETA was reduced in the same manner and characterized by a fluorescamine test; the same shift of the aromatic proton NMR as seen in the DOTA analogue and the FAB mass spectrum $M + 1$ peak of m/e 538 were as expected. NO₂Bn-TETA was reduced in the same manner and characterized by a fluorescamine test; the same shift of the aromatic proton NMR as seen in the DOTA analogue and the FAB mass spectrum $M + 1$ peak of m/e 538 were as expected. Each lyophilized residue was further tested for metal binding capacity by a ⁵⁷Co assay (15).

Conversion of the *p*-amino compounds to the *p*-bromoacetamido macrocycles BAT and BAD used a modification of Mukkala's method (16) rather than the one-solvent system used previously (15). The lyophilization residue containing NH₂Bn-TETA (ca. 0.22 mmol) was dissolved in 8.6 mL of water, and 231 μ L (1.33 mmol) of *N,N*-diisopropylethylamine was added to adjust the pH to 8. Bromoacetyl bromide (159 μ L, 1.82 mmol) was dissolved in 8.6 mL of CHCl₃. The chloroform and aqueous solutions were mixed and stirred vigorously for 10 min. A fluorescamine test on the aqueous layer indicated that amine groups were still present. The pH of the aqueous layer was adjusted to 8 with *N,N*-diisopropylethylamine (1.1 mL in 100- μ L increments) and bromoacetyl bromide (two 100- μ L portions) was added until the aqueous layer no longer tested positive for primary amine groups. A 2-mL portion of water was added, the chloroform layer was removed, and the aqueous layer was extracted with CHCl₃ (8 \times 5 mL). The aqueous layer was acidified to pH 1 with 1 M HCl and again extracted with CHCl₃ until a test for alkylating groups using 4-(*p*-nitrobenzyl)pyridine (17) showed the absence of bromoacetic acid in the chloroform extracts. Following extraction, the aqueous solution's pH was adjusted to 6.4, and it was frozen in liquid N₂ and stored at –80 °C. FAB mass spectroscopy of the BAT solution gave the two expected $M + 1$ peaks of the product at 658 and 660 mass units, typical of a bromine (⁷⁹Br and ⁸¹Br) containing compound.

The macrocyclic chelate BAD was synthesized from NH₂Bn-DOTA by the same procedure. FAB mass spectroscopy results for BAD were unsatisfactory due to interference by matrix peaks.

In order to characterize BAD, an aqueous solution of BAD was treated with NH₃(g) to form the stable amino derivative glycineamido-Bn-DOTA. The derivative was purified by C₁₈ HPLC (see above) and lyophilized. It was positive for amino groups by fluorescamine test and

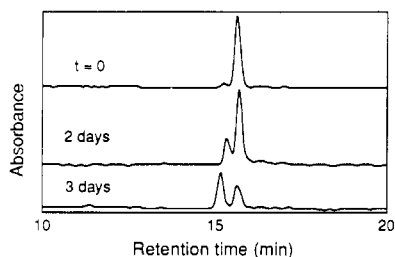


Figure 1. Reversed-phase HPLC of the macrocyclic chelate 2-[*p*-(bromoacetamido)benzyl]-1,4,7,10-tetraazacyclododecane-*N,N',N'',N'''*-tetraacetic acid (BAD), showing decomposition in aqueous solution at pH 7.6, room temperature (20–22 °C).

negative for alkyl bromide with 4-(*p*-nitrobenzyl)pyridine. FAB mass spectroscopy showed the expected $M + 1$ peak at m/e 567. ^1H NMR (D_2O , pH 4.1, 300 MHz): 7.2–7.4 ppm (4 H, aromatic aa'bb'), 3.9 ppm (2 H, s, $\text{NH}_2\text{CH}_2\text{C}=\text{O}$), 2.6–3.8 ppm (27 H, broad multiplet, expected 25 H).

HPLC analysis of BAD indicated a major peak at retention time 15.8 min and several minor peaks (total less than 10%). Upon lyophilization one of the minor peaks (retention time 15.2 min) increased, whereas the major peak decreased. Similarly the 15.2 min peak grew gradually when the sample was allowed to stand over a period of time (Figure 1). Both peaks tested positive for alkyl bromide with 4-(*p*-nitrobenzyl)pyridine, and both chelated ^{57}Co . To prevent this conversion, the sample should be frozen in liquid N_2 and stored at -80°C . BAT behaved similarly.

[^{14}C]BAD was synthesized from $\text{NH}_2\text{Bn-DOTA}$ by the procedures above except that [^{14}C]bromoacetyl chloride was substituted for bromoacetyl bromide used in the earlier preparation. The [^{14}C]bromoacetyl chloride was prepared by adding 1 mmol of bromoacetyl chloride to 2.00 mL of CHCl_3 containing approximately 246 μCi of [^{14}C]bromoacetic acid and allowing an exchange reaction to occur (12 days at room temperature in the dark) to form [^{14}C]bromoacetyl chloride. Aliquots of this compound were allowed to react with $\text{NH}_2\text{Bn-DOTA}$ as above to give the product [^{14}C]BAD. HPLC analysis of the product also gave a major and minor peak as with the unlabeled compound; the separation was too small for efficient isolation. The [^{14}C]BAD stock solution was standardized by ^{57}Co assay.

Lym-1-2IT-BAT Conjugation. The Lym-1 antibody solution (15–20 mg/mL) was prepared for conjugation with a centrifuged gel-filtration column (15, 18) with 0.1 M tetramethylammonium phosphate, pH 8, as the column buffer. To the collected effluent was added (in order) excess BAT in aqueous solution and freshly prepared 2IT in 50 mM triethanolamine hydrochloride, pH 8.7 (final approximate concentrations: Lym-1, 0.1 mM; BAT, 2 mM; 2IT, 1 mM). The pH of the solution was adjusted to 7.8 and the solution was incubated at 37°C for 30 min. Excess BAT and 2IT were removed and the conjugate was placed in a 0.1 M tetramethylammonium acetate solution, pH 7, with a centrifuged gel-filtration column.

Antibody-2IT-BAD Conjugation. Conjugations using the macrocycle BAD were done as above, with the following exception. Following the 30-min incubation at 37°C , 2-mercaptoethanol (1% v/v aqueous solution) was added in sufficient quantity to bring its final concentration to approximately 2 mM, and the solution was incubated at 37°C for 10 min more to reduce the level of any alkylated methionine adduct side products. The excess 2-mercaptoethanol was removed in the final centrifuged

Scheme II

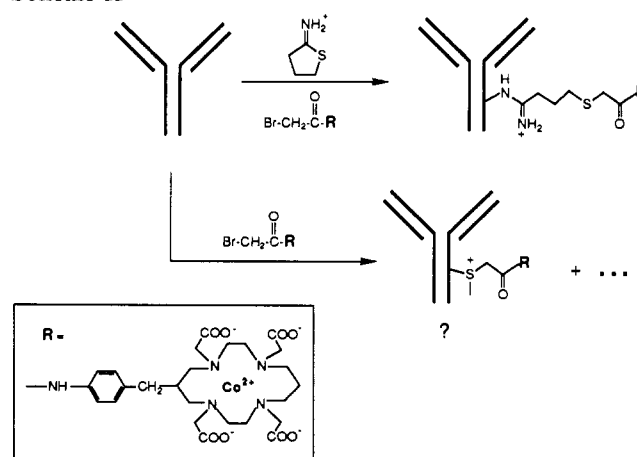


Table I. Lym-1-2IT-BAT Conjugation Reactions*

prep	chelates/mAb	% aggregates	% immunoreactivity
1	1.33	8.7	97
2	1.48	8.5	104
3	1.88	10	98
4	1.13	10	ND
avg \pm SD	1.45 \pm 0.32		

* Conditions: pH 7.8, 30 min, 37°C , 2 mM BAT, 1 mM 2IT, 0.1 mM Lym-1.

Table II. Antibody-2IT-BAD Conjugation Reactions*

antibody	chelates/mAb	% aggregates	% immunoreactivity	pH
155H.7	2.4	6.4	86.7	7.0
	4.5	7.8	56.7	8.0
	2.3	3.6	46.7	9.0
chimer L6	2.4	2.5	96	7.0
	4.2	3.8	96.5	8.0
	2.7	1.8	90.6	9.0
Lym-1	2.1	10	86.4	7.0
	3.6	4.2	88.5	8.0
	2.2	2.9	101.4	9.0

* Conditions as in Table I, except for pH.

gel-filtration column. Further experiments have shown that this 2-mercaptoethanol incubation was not necessary; the amount of readily dealkylated side products is quite small (see the Discussion Section).

Parallel Lym-1-2IT-BAT- ^{57}Co and Lym-1-BAT- ^{57}Co Conjugations (Scheme II). These were performed at pH 8 by the above procedures on two samples of Lym-1, with BAT which had been radiolabeled with ^{57}Co prior to conjugation (21.8 μCi ^{57}Co /mol BAT). One solution contained 2IT while the other did not. Relative concentrations of Lym-1 and BAT were maintained by adding the appropriate amount of buffer (50 mM triethanolamine hydrochloride) to the second conjugation solution. Relative chelate to antibody ratios were determined from UV absorbances and radioactivities of the conjugate products.

Immunoreactivity Assay. Solid-phase radioimmunoassays for immunoreactivity on either ^{111}In - or ^{57}Co -labeled conjugates were done as reported previously (19) using ^{125}I -labeled antibody as the standard. Immunoreactivity values given in Tables I and II are relative to ^{125}I -labeled antibody.

RESULTS

Table I shows the results of four Lym-1-2IT-BAT conjugations using the new procedure, while Figure 2, parts

A and B, show typical "old and new" HPLC traces of the conjugate solutions with the decrease in aggregation clearly evident. The new method gives usable, consistent ($\pm 20\%$) chelate/antibody ratios and consistently low aggregation compared to the earlier method, while high immunoreactivity is maintained.

Exploring the scope of the method using a different macrocyclic chelate (BAD vs BAT), three different antibodies, and three different pH's gave the results shown in Table II. To test for reproducibility, five or six conjugations (7–10 mg each) of each of the three antibodies with BAD were done at the pH affording the best immunoreactivity. Chelate/antibody ratios and degree of aggregation were consistent and comparable to the values in Table II.

The results of three Lym-1-2IT- ^{14}C]BAD conjugations at pH 8.0 gave 5.6 ± 0.4 available chelates per antibody by ^{14}C analysis. However, ^{57}Co metal binding assay revealed that only 3.6 ± 0.2 chelates per antibody were still capable of radiolabel uptake, in excellent agreement with the corresponding data point in Table II.

For the ^{57}Co]BAT experiments, TLC analyses of the product conjugates showed direct attachment of ^{57}Co]BAT to Lym-1 (yielding Lym-1-BAT- ^{57}Co) had occurred to a small but measurable extent (0.2 chelates/antibody) compared to indirect attachment (Lym-1-2IT-BAT- ^{57}Co , 4.1 chelates/antibody). Challenging each conjugate with 2-mercaptoethanol (final concentration 10 mM) and incubating at 37°C for 0.5 h showed by TLC that the directly alkylated Lym-1-BAT- ^{57}Co conjugate was unstable, losing 30–40% of its radiolabel. There was only a minor loss of radiolabel ($<2.5\%$) for Lym-1-2IT-BAT- ^{57}Co under the same conditions, with no change on further incubation up to 1.5 h.

DISCUSSION

As shown in Scheme I, the 2IT reacted with the antibody to form mercaptobutyrimidyl groups, which were then alkylated by BAT. By keeping the BAT concentration high with respect to the nascent thiol groups, alkylation by BAT became the preferred reaction pathway rather than thiol oxidation to disulfides. Thus, the need for 2-mercaptoethanol to prevent oxidation was eliminated, and antibody aggregation was kept to a minimum. As shown in Table I, this single-step method takes less than 1 h to complete and gives consistent yields with relatively little aggregation of Lym-1. For unknown reasons, aggregate formation with Lym-1 is greater than with the other antibodies under similar conditions (Table II). The chelate/antibody ratios are similar for each antibody, but depend on the reaction pH, with the maximum yield occurring around pH 8 in each case. The degree of Lym-1 aggregation in each case is lower than that encountered with the previous two-step method (consistently $\leq 10\%$ versus variable 10–50+%) and is lowest at pH 9. Changes in immunoreactivity with reaction pH are antibody dependent, with the best 155H.7 immunoreactivity seen with the pH 7 conjugate and the best Lym-1 immunoreactivity seen with the pH 9 conjugate. For chimeric L6, changing the reaction pH has only a minor effect on immunoreactivity.

To estimate the degree of direct attachment of BAT to Lym-1 and the efficiency of uptake of radiolabel by an attached versus a free chelate, a set of parallel Lym-1 + ^{57}Co]BAT experiments was conducted (Scheme II). One reaction contained 2IT and the other did not. No drastic differences in the rates of reaction were expected for ^{57}Co]BAT versus BAT since the location of change

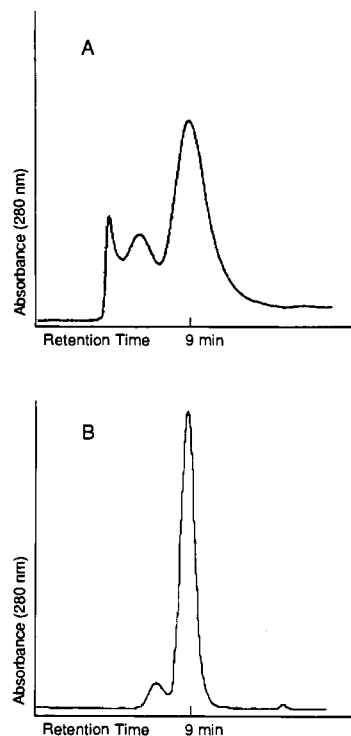


Figure 2. Gel filtration HPLC of Lym-1-2IT-BAT conjugates prepared (A) by the former method (1) and (B) by the one-step method. Here the immunoconjugate peak appears at a retention time of approximately 9 min, the peak preceding it contains the antibody dimer, and the peak preceding that in A consists of higher aggregates. The sample in A illustrates the variability of the former method, which could also yield results comparable to those of B.

in the chelate's structure is distant from the point of attachment to the antibody and since the binding of Co^{2+} is accompanied by the loss of 2H^+ (20).

As haloacetamides, BAT and BAD can attach to amine, sulfhydryl, imidazole, or thioether groups on amino acid side chains, with the sulfhydryl group being the most reactive (21). The relatively low pH of conjugation and the observed instability of the product Lym-1-BAT- ^{57}Co led to the suggestion that, in the absence of 2IT, side chains of methionines were alkylated by ^{57}Co]BAT to form sulfonium adducts, which would be susceptible to hydrolysis (thus releasing the chelate). In the case of Lym-1-2IT-BAT- ^{57}Co , the thioether linkage proved to be stable under the conditions employed. It is possible that a small number of methionine residues were alkylated during the preparation of Lym-1-2IT-BAT- ^{57}Co , and the minor loss of radiolabel may reflect the loss of these chelates by hydrolysis.

The differences in the chelate/antibody ratios of the Lym-1-2IT- ^{14}C]BAD (total 5.6 chelates/mAb versus 3.6 chelates/mAb available to bind metal) suggest that even the 2IT linker does not make all antibody-bound chelating groups accessible for postconjugation radiolabeling. This was not unexpected, since previous work with backbone-substituted ^{14}C]EDTA's has shown that not all attached EDTA groups may be available for metal binding (22). The differences in the chelate/antibody ratios of the Lym-1-2IT-BAT seen in the parallel reactions (pre-radiolabeling, 4.1 chelates/mAb) versus the standard procedure (postradiolabeling, 1.45 chelates/mAb) are generally consistent with the ^{14}C]BAD results. While the observed differences might be caused by metal contamination during processing, such was not the case in ref 22, and we feel that steric hindrance of the protein-bound chelate is a more likely cause.

Finally, comparison of Table II values for Lym-1 + BAD at pH 8.0 with those of Table I for Lym-1 + BAT at pH 7.8 shows differences in chelate/antibody ratios. One possible reason for this may be that the attached BAD is more efficient in taking up the ^{57}Co used in the metal binding assay to determine chelate/antibody ratios. Our experience with the two macrocyclic chelates indicates that BAD is a good ligand for a variety of metals, while BAT appears to be limited to Cu and Co. The use of other linkers may improve accessibility of the bound macrocycles.

ACKNOWLEDGMENT

We wish to thank Linda A. Kroger for performing the immunoreactivity analyses. This work was supported by National Cancer Institute Grant CA47829 and DOE Grant DE F903-84ER60233.

LITERATURE CITED

- (1) Deshpande, S. V., DeNardo, S. J., Meares, C. F., McCall, M. J., Adams, G. P., Moi, M. K., and DeNardo, G. L. (1988) Copper-67-Labeled Monoclonal Antibody Lym-1, A Potential Radiopharmaceutical for Cancer Therapy: Labeling and Biodistribution in RAJI Tumored Mice. *J. Nucl. Med.* 29, 217-225.
- (2) Moi, M. K., Meares, C. F., and DeNardo, S. J. (1988) The Peptide Way to Macrocyclic Bifunctional Chelating Agents: Synthesis of 2-(p-Nitrobenzyl)-1,4,7,10-tetraazacyclododecane- N,N',N'',N''' -tetraacetic Acid and Study of Its Yttrium (III) Complex. *J. Am. Chem. Soc.* 110, 6266-6267.
- (3) Morphy, J. R., Parker, D., Kataky, R., Harrison, A., Eaton, M. A. W., Millican, A., Phipps, A. and Walker, C. (1989) Towards Tumour Targeting with Copper-radiolabelled Macrocyclic-Antibody Conjugates. *J. Chem. Soc., Chem. Commun.* 792-794.
- (4) Kumar, K., Mirzadeh, S., and Gansow, O. A. (1989) Copper(II) Complexes of Polyazacycloalkane- N -Acetic Acids: Possible Use in Radiotherapy and Tumor Imaging. Nuclear Chemistry Division Abstract #96, Abstracts of Papers, 197th ACS National Meeting, American Chemical Society, Washington, D.C.
- (5) Moi, M. K., Meares, C. F., McCall, M. J., Cole, W. C., and DeNardo, S. J. (1985) Copper Chelates as Probes of Biological Systems: Stable Copper Complexes with a Macrocyclic Bifunctional Chelating Agent. *Anal. Biochem.* 148, 249-253.
- (6) Traut, R. R., Bollen, A., Sun, T.-T., Hershey, J. W. B., Sundberg, J., and Pierce, L. R. (1973) Methyl 4-Mercaptobutyrimidate as a Cleavable Cross-Linking Reagent and Its Application to the *Escherichia coli* 30S Ribosome. *Biochemistry* 12, 3266-3273.
- (7) Blakey, D. C., Watson, G. J., Knowles, P. P., and Thorpe, P. E. (1987) Effect of chemical deglycosylation of ricin A-chain on the in vivo fate and cytotoxic activity of an immunotoxin composed of ricin A-chain and anti-Thy 1.1 antibody. *Cancer Res.* 47, 947-952.
- (8) Carroll, S. F., Goff, D., Reardan, D., and Trown, P. W. (1989) Substituted 2-Iminothiolanes: Reagents for the Preparation of Disulfide-Crosslinked Conjugates with Increased Stability. Poster Abstract #73, Fourth International Conference on Monoclonal Antibody Immunoconjugates for Cancer, Mar. 30-Apr. 1, 1989, San Diego, CA.
- (9) Epstein, A. L., Zimmer, A. M., and Spies, S. M. (1985) Radioimmunodetection of human B-cell lymphomas with a radio-labeled tumor-specific monoclonal antibody (Lym-1). In *Malignant Lymphomas and Hodgkin's Disease: Experimental and Therapeutic Advances* (F. Cavalli, G. Bonadonna, and M. Rozencweig, Eds.) pp 569-577, Martinus Nijhoff Publishing Co., Boston.
- (10) Liu, A. Y., Robinson, R. R., Hellstrom, K. E., Murray, E. D., Jr., Chang, C. P., and Hellstrom, I. (1987) Chimeric mouse-human IgG₁ antibody that can mediate lysis of cancer cells. *Proc. Natl. Acad. Sci. U.S.A.* 84, 3439-3443.
- (11) Turner, C. J., Sykes, T. R., Longenecker, B. M., and Noujaim, A. A. (1988) Comparative Radiolabeling and Distribution of a Tumour-Directed Monoclonal Antibody. *Nucl. Med. Biol.* 15, 701-706.
- (12) Thiers, R. C. (1957) Contamination in Trace Element Analysis and Its Control. *Methods Biochem. Anal.* 5, 273-335.
- (13) Harlow, E., and Lane, D. (1988) *Antibodies: A Laboratory Manual* p 673, Cold Spring Harbor Laboratory, Cold Spring Harbor, NY.
- (14) Udenfriend, S., Stern, S., Bohlen, P., Dairman, W., Leimgruber, W., and Weigle, M. (1972) Fluorescamine: a reagent for assay of amino acids, peptides, proteins and primary amino acids in the picomolar range. *Science (Washington, D.C.)* 178, 871-872.
- (15) Meares, C. F., McCall, M. J., Reardan, D. T., Goodwin, D. A., Diamanti, C. I., and McTigue, M. (1984) Conjugation of Antibodies with Bifunctional Chelating Agents: Isothiocyanate and Bromoacetamide Reagents, Methods of Analysis, and Subsequent Addition of Metal Ions. *Anal. Biochem.* 142, 68-78.
- (16) Mukkala, V. M., Mikola, H., and Hemmila, I. (1989) The Synthesis and Use of Activated N -Benzyl Derivatives of Diethylenetriaminetetraacetic Acids: Alternative Reagents for Labeling of Antibodies with Metal Ions. *Anal. Biochem.* 176, 319-325.
- (17) Kramer, S. P., Goodman, L. E., Dorfman, H., Solomon, R., Gutenberg, A. M., Pineda, E., Nason, L. L., Ulfohn, A., Gaby, S. D., Bakal, D., Williamson, C. E., Miller, J. I., Sass, S., Witten, B., and Seligman, A. M. (1963) Enzyme alterable alkylating agents VI. Synthesis, chemical properties, toxicities and clinical trial of haloacetates and haloacetamides containing enzyme susceptible bonds. *J. Natl. Cancer Inst.* 31, 297-326.
- (18) Penefsky, H. S. (1979) A Centrifuged-Column Procedure for the Measurement of Ligand Binding by Beef Heart F₁. *Methods Enzymol.* 56, Part G, 527-530.
- (19) DeNardo, S. J., Peng, J.-S. B., DeNardo, G. L., Mills, S. L., and Epstein, A. L. (1986) Immunochemical Aspects of Monoclonal Antibodies Important for Radiopharmaceutical Development. *Nucl. Med. Biol.* 13, 303-310.
- (20) Stetter, H., and Frank, W. (1976) Complex Formation with Tetraazacycloalkane- N,N',N'',N''' -tetraacetic Acids as a Function of Ring Size. *Angew. Chem., Int. Ed. Engl.* 15, 686.
- (21) Means, G. E., and Feeney, R. F. (1971) *Chemical Modification of Proteins* pp 12-13, 105-110, Holden-Day, Inc., San Francisco, CA.
- (22) Leung, C. S.-H., Meares, C. F., and Goodwin, D. A. (1978) The Attachment of Metal-chelating Groups to Proteins: Tagging of Albumin by Diazonium Coupling and Use of the Products as Radiopharmaceuticals. *Int. J. Appl. Radiat. Isot.* 29, 687-692.

Registry No. 2IT, 6539-14-6; BAT, 121697-38-9; BAD, 126753-62-6; NO₂Bn-TETA, 126753-63-7; NO₂Bn-DOTA, 123317-51-1; NH₂Bn-DOTA, 123317-52-2; NH₂Bn-TETA, 126753-64-8; bromoacetyl bromide, 598-21-0.

Bioconjugate Chemistry

JULY/AUGUST 1990
Volume 1, Number 4

© Copyright 1990 by the American Chemical Society

Enzymatic Solid-Phase Assay for Biotin and a Biotin-Benzodiazepine Conjugate

Toshifumi Takeuchi and Garry A. Rechnitz*

Hawaii Biosensor Laboratory, Department of Chemistry, University of Hawaii at Manoa, Honolulu, Hawaii 96822.
Received November 8, 1989

A novel enzymatic ligand binding assay for biotin and its benzodiazepine conjugate is based on their binding to horseradish peroxidase-avidin conjugate (A-P) followed by the uptake of biotin-unsaturated A-P onto polystyrene beads coated with biotin-BSA. The detection limit is 1.3×10^{-16} mol per tube (300 μ L) with a 3.3×10^{-12} M A-P solution and varies with the conjugate concentration employed. The coefficient of variation for 10 repetitive assays of 10^{-15} mol of biotin is 6.22%.

INTRODUCTION

Biotin conjugates, used in conjunction with the binding protein avidin, have found widespread application for cytologic identification, amplified detection, affinity purification, and related disciplines (1) because of the extremely strong binding of biotin to avidin with a dissociation constant of 10^{-15} M (2). If biotin is used as a label for a target compound, a highly sensitive and selective method of determination is necessary. Currently, there are two approaches available for the determination of biotin, either a bioassay (3, 4) or a binding assay (5-24). Recently, the binding assay has gained preference, because the procedure is easier than that of bioassays with no sacrifice in sensitivity. These binding assays are based upon the competition of free and labeled ligands for a limited number of biotin binding sites on avidin. Diverse binding assays have been proposed, including isotopic (5-12), colorimetric (13-17), fluorometric (18-21), chemiluminescent (22), and potentiometric (23, 24) techniques.

The binding assays can be classified into two categories, homogeneous and heterogeneous. Homogeneous assays are faster and easier to perform than heterogeneous assays because no bound/free separation step is necessary. However, due to matrix effects, it is difficult to measure a very low concentration in a complicated sample by homogeneous assay. In practice, a heterogeneous enzymatic assay (16) has a detection limit 100-fold lower than the most sensitive homogeneous assay (21).

Consequently, we employed a heterogeneous system incorporating enzymatic amplification in an effort to develop a highly sensitive method for the determination of biotin and its conjugates, especially benzodiazepine drugs.

EXPERIMENTAL PROCEDURES

Materials. Nonporous polystyrene beads ($1/4$ in.) were purchased from Pierce (Rockford, IL). Horseradish peroxidase-avidin D (A-P, 1.5 mole of peroxidase per mol of avidin)¹ was obtained from Vector Laboratories (Burlingame, CA). Biotinamidocaproyl-bovine serum albumin (biotin-BSA, ca. 9.6 mol of biotin per mol of BSA), bovine serum albumin, fraction V (BSA), 3,3',5,5'-tetramethylbenzidine (TMB), and biotinamidocaproic acid *N*-hydroxysuccinimide ester (BAC-NHS) were obtained from Sigma Chemicals (St. Louis, MO). Hydrogen peroxide was bought from Aldrich Chemicals (Milwaukee, WI). A ben-

¹ Abbreviations used are as follows: A-P, horseradish peroxidase-avidin D; biotin-BSA, biotinamidocaproyl-bovine serum albumin; BSA, bovine serum albumin, fraction V; TMB, 3,3',5,5'-tetramethylbenzidine; BAC-NHS, biotinamidocaproic acid *N*-hydroxysuccinimide ester; HPLC, high-performance liquid chromatography; PBS, 10 mM phosphate buffer containing 0.1 M sodium chloride (pH 7.4); PBS-B, PBS containing 0.1% BSA; DMF, *N,N*-dimethylformamide; A_i , an initial enzyme activity of free A-P; A_s , an enzyme activity of free A-P after an incubation period.

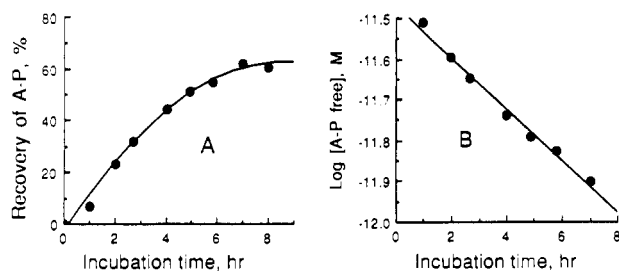


Figure 1. Uptake of A-P by the biotin beads. The beads are incubated with 3.3×10^{-12} M A-P at 4°C for 1–8 h, then the enzyme activity in solution is measured. The recovery is expressed as $100(A_i - A_s)/A_i$, where A_i is an initial enzyme activity and A_s is an enzyme activity of free A-P after a given incubation period.

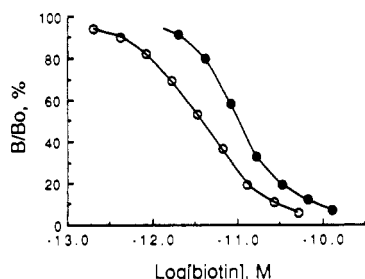


Figure 2. Standard curves of biotin: (●) using 3.3×10^{-11} M A-P; (○) using 3.3×10^{-12} M A-P; B , enzyme activity on the bead; B_0 , enzyme activity on the bead without biotin.

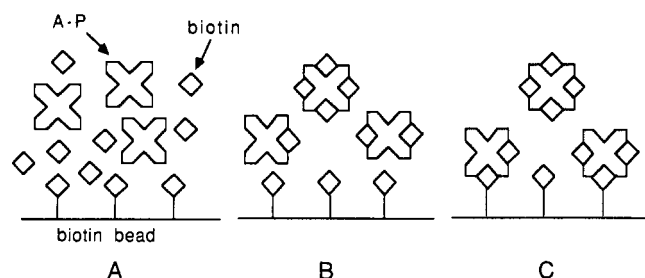


Figure 3. Schematic diagram of the binding assay: (A) the biotin bead is added to sample, and A-P is then added; (B) biotin is bound to A-P (the first stage); (C) immobilized biotin complexes biotin-unsaturated A-P (the second stage).

zodiazepine drug, 1012-S, was provided by Shionogi & Co., Ltd. (Osaka, Japan). The biotin-1012-S conjugate was prepared by mixing BAC-NHS and 1012-S (1.2:1 molar ratio) in 50 mM phosphate buffer at pH 7.0 and incubating it overnight at 4°C . The product was then purified by a reversed-phase HPLC with 30% (v/v) acetonitrile/50 mM ammonium acetate buffer at pH 4.5. Other chemicals were purchased from Fisher Scientific (Kent, WA) and used without further purification.

Immobilization of Biotin onto Polystyrene Beads. Before the immobilization, the beads were washed sequentially with detergent (Alconox), methyl alcohol, and water by using an ultrasonic bath and stored in 10 mM phosphate buffer (pH 7.4) containing 0.1 M sodium chloride (PBS) at 4°C . Fifty beads were soaked in 10 mL of 0.002% biotin-BSA PBS solution overnight at 4°C . To eliminate protein-binding sites, the beads were then incubated with 1% BSA in PBS. The biotin-immobilized polystyrene beads prepared (biotin beads) were stored in PBS containing 0.1% BSA (PBS-B) and 0.1% sodium azide at 4°C .

To determine an average amount of biotin-BSA per bead, three sets of five beads in 1 mL of 0.002% biotin-BSA were incubated overnight at 4°C . The concentration of biotin-BSA in the supernatant was determined by the Bio-Rad protein assay based on the Bradford method (25)

using biotin-BSA as the standard. The solution incubated without beads was also assayed. The amount of biotin-BSA was calculated from the difference in the concentrations.

Binding Assay Procedure. A sample (100 μL) and PBS-B (100 μL) were pipetted into a test tube (10 \times 75 mm) followed by addition of one biotin bead per tube. A-P (10^{-10} or 10^{-11} M, 100 μL) was then added and mixed immediately. The mixture was incubated overnight (ca. 16 h) at 4°C with continuous shaking at 80 oscillations/min by a Precision Model 25 shaker bath (Chicago, IL). After the bead was washed five times with PBS, the enzyme activity was measured.

In order to prevent the adsorption of A-P onto the test tube wall during complexation with biotin, the incubation mixture contained 0.033% BSA. It is empirically demonstrated that BSA does not affect the binding of biotin to A-P.

Measurement of Peroxidase Activity. A bead was placed in TMB solution (600 μL), prepared by dissolving 10 mg of TMB in 1 mL of DMF followed by mixing with 100 mL of 0.1 M sodium acetate buffer (pH 5.5), and the enzyme reaction was started by addition of 0.01% H_2O_2 (200 μL). The mixture was incubated for 5 min (for 6.3×10^{-11} – 4.0×10^{-10} M biotin) or 30 min (for 6.3×10^{-13} – 1.6×10^{-10} M biotin and 1.2×10^{-13} – 1.2×10^{-9} M biotin-1012-S) with shaking. After an incubation period, the reaction was then stopped by addition of 0.2 N sulfuric acid (200 μL) and the absorbance was measured at 450 nm with a Sequoia-Turner Model 340 spectrophotometer. The activity in solution was determined by taking a 100- μL aliquot of it and assaying it with the same procedure used for a bead.

Time Course of A-P Uptake by the Biotin Bead. Mixtures of 10^{-11} M A-P in PBS-B (100 μL) and PBS (200 μL) were incubated with one bead per mixture at 4°C for 1–8 h with continuous shaking at 80 oscillations/min. The enzyme activity in solution (A_s) was measured and the recovery of A-P with the biotin bead was calculated by $100(A_i - A_s)/A_i$, where A_i is the initial enzyme activity in the incubation mixture.

RESULTS AND DISCUSSION

Uptake of A-P with the Biotin Bead. For the characterization of the biotin bead prepared, biotin-BSA adsorbed on the polystyrene bead was determined, and experiments of A-P uptake by the bead were performed. The average amount of biotin-BSA immobilized was 0.81 ± 0.06 μg per bead, corresponding to about 10^{-10} mol of biotin per bead. Although all of the immobilized biotin would not be available for the binding of A-P, it is expected that biotin on the bead is in large excess compared to the amount of A-P in the assay system, which is between 10^{-14} and 10^{-15} mol. In order to estimate the availability of immobilized biotin, the biotin bead was incubated overnight at 4°C with 33 nM A-P dissolved in PBS-B (300 μL). After the incubation, 44% of the initial peroxidase activity remained in the solution. Nonspecific binding was estimated to be 8% by incubating the bead with biotin-saturated A-P. Therefore, it is estimated that 48% of A-P initially added is specifically bound to the bead, corresponding to approximately 5×10^{-12} mol. This figure represents a lower limit because additional experiments demonstrate that the bead has not yet been saturated with A-P under these experimental conditions. In the concentration range of A-P used in the assay procedure (0 – 3.3×10^{-11} M), the amount of A-P bound increased linearly with the concentration. Consequently,

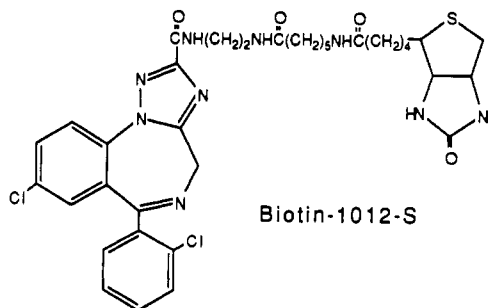
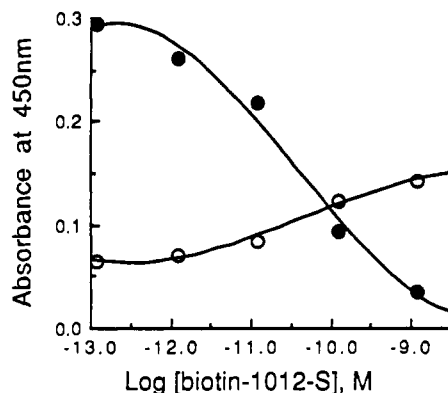


Figure 4. Standard curves of the biotin-benzodiazepine conjugate. Each biotin-1012-S conjugate was incubated overnight at 4 °C with 3.3×10^{-12} M A-P and the biotin bead, then the enzyme activity was measured on the bead (●) and in the liquid phase (○).

it is concluded that a sufficient amount of biotin-BSA is immobilized onto the beads for the purpose of this assay.

Various factors contribute to a decrease in the observed rate of A-P uptake by the biotin bead (Figure 1A), in contrast to the intrinsic association rate of avidin with biotin (2). Because the bead is nonporous, internal diffusion is not a factor. In a comparison of unstirred and vigorously agitated (80 oscillations/min) samples, the initial uptake rate observed was only twice as fast as that for the agitated sample. No further increase in the rate of uptake was observed for shaking at greater than 80 oscillation/min. This implies that external diffusion is not a significant factor in the observed slow rate of uptake by the biotin bead. Therefore, the slow overall rate observed most likely is due to factors associated with the intrinsic properties of the unstirred boundary layer, e.g. steric effects of BSA covalently bound to biotin and protein-protein interactions between BSA and A-P.

Biotin Binding Assay. The standard curves for biotin obtained by using 3.3×10^{-11} and 3.3×10^{-12} M A-P are depicted in Figure 2. The detection limit was 1.3×10^{-16} mol and the coefficient of variation of 10 replicate assays for 10^{-15} mol of biotin was 6.22%. The range of biotin to be determined could be varied by altering the concentration of A-P used in the assay. Nonspecific binding of A-P decreased linearly when the initial concentration of A-P added was reduced. It was negligible when the concentration was below 10^{-10} M, i.e. the absorbance is less than 0.002 for the enzyme activity of non-specifically bound A-P on the bead with an incubation period of 30 min.

In the experiments of uptake described above, when the log concentration of free A-P vs incubation time was plotted, a linear relationship was obtained (Figure 1B). These experimental data show that the overall uptake rate observed is first-order with respect to free A-P concentration under the experimental conditions employed and was independent of immobilized biotin. Comparison of biotin samples that were preincubated with A-P and those with no preincubation showed no significant difference in the results. Because of these results, it is likely that the present binding assay involves two noncompetitive binding steps (Figure 3): a fast step involving the binding of aqueous biotin by A-P (Figure 3B) and a slow step involving the complexation of unsaturated A-P with the biotin bead (Figure 3C). Thus, even without a preincubation step of samples with A-P, the experimental procedure gave quite reasonable results.

Bayer et al. reported a sensitive enzymatic method for biotin using immobilized streptavidin on biotinyl-BSA adsorbed microtiter plates and detection by a biotin-alkaline phosphatase conjugate (16). For the detection of

approximately 10^{-15} mol of biotin, they used 0.1 μ g of streptavidin per sample, which was an amount approximately 1700 times greater than that utilized in our system. Their incubation time for color formation by the enzyme reaction was recommended to be 20–24 h for the lower end of the biotin concentration range. In contrast, we employed the labeled avidin, allowing the amount of binding protein to decrease. In addition, we set up the procedure to include a long incubation for the uptake of the conjugate and a short incubation for the enzyme reaction. This gave high sensitivity and minimized errors associated with enzyme incubation.

Determination of Biotin-Benzodiazepine Conjugate. Our aim is to establish a sensitive method for the determination of biotin conjugate. In order to preliminarily demonstrate the applicability of the proposed method, a biotin-benzodiazepine conjugate (biotin-1012-S) concentration was determined. The structure of the conjugate and the absorbance change with the concentration of the conjugate are shown in Figure 4. Although the measurement of the activity in solution was easier than that on the bead because of no bead-washing step, the change was measurably smaller than that for the solid phase. For a sample with a low concentration, the measurement of the activity on the bead is preferable. In this assay, a colorimetric detection method was employed, so the detection limit was 1.3×10^{-16} mol. If more sensitivity is desired, a substrate with a fluorescent product like 3-(4-hydroxyphenyl)propionic acid is preferable.

In conclusion, a highly sensitive assay method has been developed for biotin and a biotinylated benzodiazepine without special equipment. This binding assay will be applicable to the determination of biotin-drug conjugates used as probes in complicated systems, such as benzodiazepine binding studies in conjunction with benzodiazepine receptor proteins. These experiments are currently in progress.

ACKNOWLEDGMENT

The financial support of NIH grant GM-25308 is gratefully acknowledged. We wish to thank Kentaro Hirai and Urara Katsuyama, Shionogi & Co., Ltd. for providing 1012-S. We also thank Glenn B. Martin, Hawaii Biosensor Laboratory, and Akira Saito, University of Delaware, for valuable discussions.

LITERATURE CITED

- 1) Bayer, E. A., and Wilchek, M. (1980) The Use of the Avidin-Biotin Complex as a Tool in Molecular Biology. *Methods of Biochemical Analysis* (D. Glick, Ed.) Vol. 26, pp 1–45, John Wiley & Sons, New York.

- (2) Green, N. M. (1975) Avidin. *Advances in Protein Chemistry* (C. B. Anfinsen, J. T. Edsall, and F. M. Richards, Eds.) Vol. 29, pp 85-133, Academic Press, New York.
- (3) Baker, H., Frank, O., Matovitch, V. B., Pasher, I., Aaronson, S., Hutner, S. H., and Sobotka, H. (1962) A New Assay Method for Biotin in Blood, Serum, Urine, and Tissues. *Anal. Biochem.* 3, 31-39.
- (4) Demoll, E., and Shive, W. (1986) Assay for Biotin in the Presence of Dethiobiotin with *Lactobacillus plantarum*. *Anal. Biochem.* 158, 55-58.
- (5) Horsburgh, T. and Gompertz, D. (1978) A Protein-Binding Assay for Measurement of Biotin in Physiological Fluids. *Clin. Chim. Acta* 82, 215-223.
- (6) Swack, J. A., Zander, G. L., and Utter, M. F. (1978) Use of Avidin-Sepharose to Isolate and Identify Biotin Polypeptides from Crude Extracts. *Anal. Biochem.* 87, 114-126.
- (7) Retteneauer, R. (1980) Biotin-Bestimmung in Lebergewebe nach dem Prinzip der Isotopen-Verdünnungsanalyse. *Anal. Chim. Acta* 113, 107-112.
- (8) Yankofsky, S. A., Gurevitch, R., Niv, A., Cohen, G., and Goldstein, L. (1981) Solid-Phase Assay for *d*-Biotin on Avidin-Cellulose Disks. *Anal. Biochem.* 118, 307-314.
- (9) Sanghvi, R., Lemins, R. M., Baker, H., and Thoene, J. G. (1982) A Simple Method for Determination of Plasma and Urinary Biotin. *Clin. Chim. Acta* 124, 85-90.
- (10) Mock, D. M., and Dubois, D. B. (1982) A Sequential, Solid-Phase Assay for Biotin in Physiologic Fluids That Correlates with Expected Biotin Status. *Anal. Biochem.* 153, 272-278.
- (11) Chan, P. W., and Barlett, K. (1986) A New Solid-Phase Assay for Biotin and Biocytin and Its Application to the Study of Patients with Biotinidase Deficiency. *Clin. Chim. Acta* 159, 185-196.
- (12) Livaniou, E., Evangelatos, G. P., and Ithakissios, D. S. (1987) Biotin Radioligand Assay with an ^{125}I -Labeled Biotin Derivative, Avidin, and Avidin Double-Antibody Reagents. *Clin. Chem.* 33, 1983-1988.
- (13) Green, N. M. (1965) A Spectrophotometric Assay for Avidin and Biotin Based on Bonding of Dyes by Avidin. *Biochem. J.* 94, 23c-24c.
- (14) Ngo, T. T., Lenhoff, H. M., and Ivy, J. (1982) Biotinyl-Glucose-6-Phosphate Dehydrogenase. Preparation, Kinetics, and Modulation by Avidin. *Appl. Biochem. Biotechnol.* 7, 443-454.
- (15) Niedbala, R. S., Gergits, F., III, and Schray, K. J. (1986) A Spectrophotometric Assay for Nanogram Quantities of Biotin and Avidin. *J. Biochem. Biophys. Methods* 13, 205-210.
- (16) Bayer, E. A., Ben-Hur, H., and Wilchek, M. (1986) A Sensitive Enzyme Assay for Biotin, Avidin, and Streptavidin. *Anal. Biochem.* 154, 367-370.
- (17) Daunert, S., and Bachas, L. G. (1988) Homogeneous Enzyme-Linked Competitive Binding Assay for Biotin Based on the Avidin-Biotin Interaction. *Anal. Chim. Acta* 208, 43-52.
- (18) Lin, H. J., and Kirsch, J. F. (1977) A Sensitive Fluorometric Assay for Avidin and Biotin. *Anal. Biochem.* 81, 442-446.
- (19) Al-Hakim, M. H. H., Landon, J., Smith, D. S., and Nargessi, R. D. (1981) Fluorimetric Assays for Avidin and Biotin Based on Biotin-Induced Fluorescence Enhancement of Fluorescein-Labeled Avidin. *Anal. Biochem.* 116, 264-267.
- (20) Mock, D. M., Langford, G., Dubois, D., Criscimagna, N., and Horowitz, P. (1985) A Fluorometric Assay for the Biotin-Avidin Interaction Based on Displacement of the Fluorescent Probe 2-Anilinonaphthalene-6-Sulfonic Acid. *Anal. Biochem.* 151, 178-181.
- (21) Schray, K. J., Artz, P. G., and Hevey, R. C. (1988) Determination of Avidin and Biotin by Fluorescence Polarization. *Anal. Chem.* 60, 853-855.
- (22) Williams, E. J., and Campbell, A. K. (1986) A homogeneous Assay for Biotin Based on Chemiluminescence Energy Transfer. *Anal. Biochem.* 155, 249-255.
- (23) Gebauer, C. R., and Rechnitz, G. A. (1980) Ion Selective Electrode Estimation of Avidin and Biotin Using a Lysozyme Label. *Anal. Biochem.* 103, 280-284.
- (24) Kjellström, T. L. and Bachas, L. G. (1989) Potentiometric Homogeneous Enzyme-Linked Competitive Binding Assay Using Adenosine Deaminase as the Label. *Anal. Chem.* 61, 1728-1732.
- (25) Bradford, M. M. (1976) A Rapid and Sensitive Method for the Quantitation of Microgram Quantities of Protein Utilizing the Principle of Protein-Dye Binding. *Anal. Biochem.* 72, 248-254.

Registry No. Biotin, 58-85-5; biotin-1012-S, 127709-42-6.

Synthesis and Tissue Distribution of Fluorine-18 Labeled Trifluorohexadecanoic Acids. Considerations in the Development of Metabolically Blocked Myocardial Imaging Agents

Susan Sondej Pochapsky,[†] Henry F. VanBrocklin,[‡] Michael J. Welch,[‡] and John A. Katzenellenbogen^{*†}

Department of Chemistry, University of Illinois, 1209 West California Street, Urbana, Illinois 61801, and Radiation Sciences Research, Mallinckrodt Institute of Radiology, Washington University School of Medicine, 510 South Kingshighway, St. Louis, Missouri 63110. Received February 6, 1990

A versatile method for the synthesis of trifluoro fatty acids, potential metabolically blocked myocardial imaging agents, has been developed. Two trifluorohexadecanoic (palmitic) acids have been prepared [6,6,16-trifluorohexadecanoic acid (I) and 7,7,16-trifluorohexadecanoic acid (II)], each of which bears two of the fluorine atoms as a *gem*-difluoromethylene unit on the fatty acid chain (at C-6 or C-7) and the third at the ω (C-16) position. The metabolic stability of carbon-fluorine bonds suggests the *gem*-difluoro group may block the β -oxidation pathway, while the terminal fluorine could be the site for labeling with fluorine-18. The convergent synthetic approach utilizes a 2-lithio-1,3-dithiane derived from 10-undecenal or 9-decenal, which is alkylated with the OBO (oxabicyclooctyl) ester of 5-bromopentanoic acid or 6-bromohexanoic acid, respectively. Hydroboration-oxidation and alcohol protection are followed by halofluorination to convert the 1,3-dithiane system to a *gem*-difluoro group. The third fluorine is introduced by fluoride ion displacement of a trifluoromethanesulfonate. This synthesis is adapted to the labeling of these trifluoro fatty acids with the short-lived radionuclide fluorine-18 ($t_{1/2} = 110$ min), with the third fluorine introduced as fluoride ion in the penultimate step. The radiochemical syntheses proceed in 3-34% radiochemical yield (decay corrected), with an overall synthesis and purification time of 90 min. Tissue distribution studies in rats were performed with I and II, as well as with 16- ^{18}F fluoropalmitic acid (III), ^{14}C palmitic acid, and ^{14}C octanoic acid. The heart uptake of the fluoropalmitic acids decreases with substitution, the 2-min activity level for 16-fluoropalmitic acid being 65% and that for both 6,6,16- and 7,7,17-trifluoropalmitic acids being 30% that of palmitic acid. Fluorine substitution results in some alteration in the retention of activity by the heart: 16-fluoropalmitate actually clears more rapidly than palmitate, but the two trifluoropalmitates (particularly 6,6,16-trifluoropalmitate, I) show somewhat slower clearance of activity, although the improvement of I over palmitate is only modest. There is considerable accumulation of activity in the bone after administration of the fluorine-18 labeled fatty acids, suggestive of metabolic defluorination. These results indicate that fluorine substitution alters the physicochemical properties of the fatty acid so that uptake by the myocardium is diminished. Furthermore, while the *gem*-difluoro substituents at C-6 and C-7 may block β -oxidation, the chain-terminal radiofluorine substituent is subject to ω -oxidation that releases it as fluoride ion.

INTRODUCTION

Well-oxygenated cardiac muscle uses free fatty acids as a nearly exclusive energy source. As a consequence, it is possible to assess the metabolic viability of the myocardium by its ability to take up and metabolize fatty acids (1). While the myocardium can be imaged with fatty acids labeled at C-1 with the positron-emitting radionuclide carbon-11, these images are somewhat transient: Rapid oxidative degradation of the fatty acid chain by β -oxidation releases the labeled carbon as acetyl CoA, which is then converted to carbon dioxide in the tricarboxylic acid cycle and released from the cell; thus, the initial image based on differential fatty acid uptake by the myocardium decays with the release of the radiolabel (2).

Various strategies have been used to block the metabolic release of the radiolabel in order to give more persistent

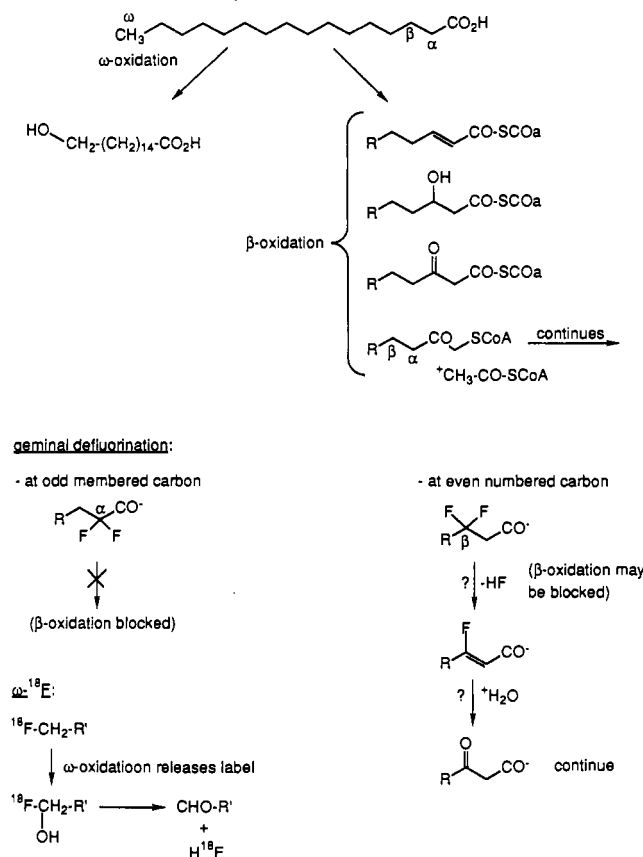
images. With fatty acids labeled at the carboxy carbon (C-1) with carbon-11, used for positron-emission tomography (PET), β -oxidation can be suppressed by methyl substitution at the β -carbon (C-3) (2, 3). Alternatively, agents labeled with radionuclides for single photon emission tomography (SPECT), such as iodine-123, may also suffer from metabolic release of the radiolabel; placement of the radiohalogen on a vinylic or aryl group at the terminus of the fatty acid chain (4) or incorporation of methyl substituents (5) or unusual atoms (e.g., tellurium) (6) in the polymethylene chain are strategies that have, either alone or in combination, been used to protect against metabolic release of the radiolabel. A number of these analogues give more persistent myocardial images, but the steric and functional perturbation of the fatty acid structure has raised concerns that they may not be proper analogues of the natural fatty acid and, therefore, that the images observed may not truly reflect the competency of the myocardium for natural fatty acid uptake and metabolism (7).

Fatty acids labeled with the positron-emitter fluorine-18 have been prepared with the radionuclide placed either

* Address correspondence to John A. Katzenellenbogen, Department of Chemistry, 1209 W. California St., Box 37, University of Illinois, Urbana, IL 61801.

[†] University of Illinois.

[‡] Washington University School of Medicine.

Scheme I. β - and ω -Oxidation of Fatty Acids. Effect of Geminal Difluorination

at a primary position (the ω -position) (8) or at a secondary position in the chain (on either C-6 or C-7) (9). The ω -fluoro fatty acid is metabolized rapidly, releasing fluoride ion, despite its position remote from the carboxylate, suggesting that β -oxidation may proceed rapidly down the whole chain or that other metabolic processes are occurring. The 6- or 7-fluoro fatty acid was prepared in the hopes of interrupting metabolism and retaining the label. In the preparation of these 6- or 7-fluoro fatty acids, however, considerable elimination occurs in competition with fluoride ion displacement at the secondary position, and the in vivo distribution of these compounds was not very favorable (10).

In the hopes of overcoming both of these difficulties, we have proposed the synthesis of a trifluoro fatty acid: Two of the fluorines form a difluoromethylene group in the fatty acid backbone; the third, which may be radio-labeled with fluorine-18, is situated at the ω -position, where it may be protected from metabolism by β -oxidation (see Scheme I). Because carbon-fluorine bonds are considered to be relative inert to metabolism (11) and because the covalent radius of fluorine (0.135 nm) is only slightly greater than that of hydrogen (0.120 nm) (12), we felt that the gem-difluoromethylene unit would be a nearly isosteric replacement for the methylene group that might be inert to metabolism and thus might be preferable to those systems in which β -oxidation is blocked by larger substituents. When situated at an even position, this difluoromethylene group would end up at a site α to the carboxyl group where it would block β -oxidation; situated at an odd site, it may also block metabolism, although oxidation could continue if hydrogen fluoride were eliminated and the β -fluoroenoate hydrolyzed to the β -keto acid.

In this report, we describe a versatile synthetic sequence for the preparation of two trifluoro fatty acids, 6,6,16-

trifluoro- and 7,7,16-trifluorohexadecanoic acids (I and II), prototypes of these potentially metabolically blocked myocardial imaging agents, and the adaptation of these routes so that the terminal fluorine substituent can be introduced by a simple, rapid fluoride ion displacement reaction, suitable for labeling with [^{18}F]fluorine ion. The tissue distribution of these compounds, labeled with fluorine-18, is studied in rats and is compared with that for 16-[^{18}F]fluoropalmitate, [^{14}C]palmitate, and [^{14}C]octanoate.

EXPERIMENTAL PROCEDURES

Chemical Syntheses. General Methods. ^1H NMR spectra were obtained on Varian XL200, General Electric QE300, and Nicolet NT360 spectrometers and are reported downfield from $(\text{CH}_3)_4\text{Si}$ (δ scale). ^{13}C NMR spectra were obtained on Varian XL200 and General Electric QE300 spectrometers at 50.3 and 75.44 MHz, respectively, and are also reported relative to TMS. ^{19}F NMR spectra were obtained on a Nicolet NT360 spectrometer at 338.76 MHz and are reported in parts per million with internal CFCl_3 at 0 ppm (ϕ scale). Melting points were taken on a Fischer-Johns melting point apparatus and are uncorrected. Low-resolution electron-impact mass spectra (LREI) were obtained on a Finnigan MAT CH5 instrument. High-resolution electron-impact (HREI) and field-ionization (FI) mass spectra were obtained on a Finnigan MAT 731 instrument. Low- and high-resolution chemical-ionization mass spectra (LRCI, HRCI) were obtained on a VG-70-SE-4F instrument. GC/MS data was obtained on a Finnigan MAT 311A instrument. IR spectra were obtained on a Nicolet 7199 FT-IR. Elemental analyses were performed by the Microanalytical Service Laboratory of the University of Illinois.

Analytical gas-liquid chromatography (GLC) was performed on a Hewlett-Packard 5793A instrument equipped with a flame-ionization detector. Analyses were performed on an Alltech RSL-150 capillary column (0.25 mm \times 30 m) or a Hewlett-Packard Ultra 1 capillary column (0.20 mm \times 12.5 m). Preparative thin-layer chromatography was performed on 2 mm \times 20 cm \times 20 cm E. Merck silica gel plates (60F-254). E. Merck silica gel (particle size 0.032–0.063 mm) was used for flash chromatography (13). High-pressure liquid chromatography for the radiochemical experiments was performed on a Spectra-Physics Model 8700 instrument equipped with a UV detector (operating at 215 nm) and a NaI(Tl) radioactivity detector. The preparative chromatography employed a C-18 column (Whatman Partisil M-9, 10 mm \times 50 cm). Radioactivity was determined in a dose calibrator.

Most starting materials were purchased from Aldrich Chemical Co. 16-Hexadecanolide was purchased from Lancaster Chemicals. Tetrahydrofuran was distilled from sodium, and methylene chloride was distilled from P_2O_5 . Other reagents and solvents were used without additional purification.

Caution. Pyridinium poly(hydrogen fluoride), while more convenient to use than anhydrous hydrogen fluoride, requires similar safety precautions. It is extremely corrosive to human tissue, and contact with the skin, even in dilute concentrations, can result in painful, slow-healing burns which may not be visible for several hours. This reagent should only be used in a well-ventilated hood with the user wearing protective clothing (lab coat, rubber gloves, etc.) and a full-face shield. Several treatments for hydrogen fluoride burns have been reported (14).

2-(9-Decenyl)-1,3-dithiane (2). 10-Decenal (1; 5.0 g, 29.7 mmol) and 5.96 mL (59.4 mmol) of 1,3-pro-

panedithiol were combined under nitrogen and stirred, followed by the addition of 4.12 mL (29.7 mmol) of $\text{BF}_3 \cdot 2\text{HOAc}$. The biphasic solution was allowed to stir vigorously for 1 h. The reaction mixture was diluted with hexane (30 mL) and washed with three 20-mL portions each of saturated NaHCO_3 solution, 15% NaOH solution, and brine. The organic extract was dried (Na_2SO_4) and concentrated. Purification by flash chromatography (10% diethyl ether/hexane) yielded 6.91 g (90%) of dithiane 2: ^1H NMR (CDCl_3) δ 1.22–1.54 (m, 12 H), 1.73–2.10 (m, 6 H), 2.85 (m, 4 H), 4.05 (t, 1 H, $J = 6.6$ Hz), 4.94 (dm, 1 H, $J = 10.3$ Hz), 4.99 (dm, 1 H, $J = 17.1$ Hz), 5.80 (tdd, 1 H, $J = 17.1, 10.3, 6.7$ Hz); MS (LREI, 70 eV) m/z (relative intensity) 258 (M^+ , 4), 119 (33), 69 (35), 55 (35), 41 (100). Anal. Calcd for $\text{C}_{14}\text{H}_{26}\text{S}_2$: C, 65.05; H, 10.14; S, 24.81. Found: C, 64.90; H, 10.09; S, 25.01.

5-Bromopentanoyl Chloride (5). 5-Bromopentanoic acid (4; 10 g, 55.2 mmol) and thionyl chloride (30 mL, 0.41 mol) were combined and allowed to heat at reflux for 1 h. Distillation at atmospheric pressure removed the excess SOCl_2 . Vacuum distillation produced 9.7 g (87%) of the pure acid chloride 5: bp 48–51 °C (0.5 mmHg); ^1H NMR (CDCl_3) δ 1.90 (m, 4 H), 2.92 (t, 2 H, $J = 7.2$ Hz), 3.40 (t, 2 H, $J = 6.4$ Hz); MS (LREI, 70 eV) m/z (relative intensity) 200 (M^+ , 2), 198 (2), 165 (100), 163 (100), 137 (85), 135 (85), 121 (29), 119 (83), 101 (56), 91 (52), 83 (100), 73 (45), 63 (38), 55 (100).

(3-Oxa-1-methylcyclobutyl)methyl 5-Bromovalerate (6). Dry pyridine (4.2 mL, 51.9 mmol) was added to 3-methyloxetane (5.2 mL, 52.1 mmol) in dry CH_2Cl_2 (20 mL) under nitrogen. The solution was cooled to 0 °C and 5-bromopentanoyl chloride (5; 9.44 g, 47.3 mmol) was added slowly via syringe. The solution was allowed to stir at 0 °C for 1 h. The mixture was diluted with CH_2Cl_2 (40 mL) and washed with three 50-mL portions of water. The organic extract was dried (Na_2SO_4) and concentrated to produce 12.06 g (96%) of oxetane ester 6 as a pale yellow oil. Preparatively, purification was not performed at this stage because silica gel chromatography resulted in significant loss of product due to decomposition: ^1H NMR (CDCl_3) δ 1.32 (s, 3 H), 1.82 (m, 2 H), 1.90 (m, 2 H), 2.39 (t, 2 H, $J = 7.12$ Hz), 3.41 (t, 2 H, $J = 6.46$ Hz), 4.16 (s, 2 H), 4.38 (d, 2 H, $J = 6.0$ Hz), 4.50 (d, 2 H, $J = 6.0$ Hz); MS (LREI, 70 eV) m/z (relative intensity) 285 (10), 283 (7), 165 (46), 137 (17), 135 (18), 83 (15), 55 (100). Anal. Calcd for $\text{C}_{10}\text{H}_{17}\text{O}_3\text{Br}$: C, 45.29; H, 6.48; Br, 30.13. Found: C, 45.59; H, 6.43; Br, 30.30.

1-(4-Bromobutyl)-4-methyl-2,6,7-trioxabicyclo[2.2.2]octane (7). The crude oxetane ester 6 (12.06 g, 45.5 mmol) was dissolved in dry CH_2Cl_2 (30 mL) under nitrogen. The reaction mixture was cooled to 0 °C and 1.6 mL (13.0 mmol) of boron trifluoride etherate was slowly added. The mixture was warmed to room temperature and allowed to stir for 1.5 h. The reaction mixture was quenched with triethylamine (1.82 mL, 13.0 mmol) and diluted with 50 mL of diethyl ether. The mixture was filtered to remove the amine- BF_3 complex, dried (Na_2SO_4), and concentrated. Traditional flash chromatography resulted in large yield losses (>50%), presumably due to cleavage of the OBO group on the silica. Rapid chromatography on silica pretreated with Et_3N /hexane (12.0 g of crude OBO compound loaded on 6 in. of silica in a 40-mm column, eluting with 500 mL hexane, followed by 1000 mL of 20% diethyl ether/hexane) produced 9.6 g of pure OBO compound 7 as a white waxy solid: mp 26–28 °C; ^1H NMR (CDCl_3) δ 0.80 (s, 3 H), 1.60 (m, 2 H), 1.70 (m, 2 H), 1.90 (m, 2 H), 3.39 (t, 2 H, $J = 6.7$ Hz), 3.89 (s, 6 H); MS (LREI, 70 eV) m/z (relative intensity) 266 (M^+ , 0.4), 264 (0.4), 165 (97), 163

(100), 137 (30), 135 (31), 91 (47), 72 (27), 55 (39). Anal. Calcd for $\text{C}_{10}\text{H}_{17}\text{BrO}_3$: C, 45.30; H, 6.46; Br, 30.14. Found: C, 44.94; H, 6.52; Br, 30.70.

1-[5,5-(Trimethylenedithio)-14-pentadecenyl]-4-methyl-2,6,7-trioxabicyclo[2.2.2]octane (8). All glassware used in this reaction was dried in an oven overnight and then assembled and flame-dried immediately before use. Dithiane 2 and OBO ester 7 had both been stored in a vacuum desiccator over P_2O_5 for 2 days. A 250-mL three-neck round-bottomed flask was equipped with a three-way stopcock and serum caps. The flask was alternately flushed with nitrogen and evacuated. Dithiane 2 (8.64 g, 33.4 mmol) was added via syringe and the flushing/evacuating sequence was repeated. Dry THF (130 mL, freshly distilled from Na) was added to the stirring dithiane and the flushing/evacuating sequence was repeated. Hexamethylphosphoramide (6.1 mL, distilled from CaH_2) was added and the flushing/evacuating sequence was repeated a final time. The solution was cooled to –78 °C and 24 mL of *n*-butyllithium (1.48 M in hexane) was added. After 10–15 min, the –78 °C bath was replaced by a –40 °C bath and the solution was allowed to stir an additional 90 min. At this time the solution, which had initially been dark green-brown, had turned clear orange-red, indicating the formation of the anion (confirmed by D_2O quench and ^1H NMR analysis). The reaction mixture was then cooled to –78 °C, and a 5% excess of the OBO compound in THF (9.31 mL, 35.1 mmol) was added by rapidly drizzling down the side of the flask. The reaction was complete after 30 min at –78 °C, as indicated by GLC analysis. The mixture was diluted with 100 mL of hexane and washed exhaustively with water (to remove HMPA). The organic extract was dried (Na_2SO_4), concentrated, and purified (by using the same rapid chromatography method reported for the purification of 7) to produce 13.6 g (92%) of pure fatty OBO compound 8 as a waxy white solid: mp 34–36 °C; ^1H NMR (CDCl_3) δ 0.80 (s, 3 H), 1.22–1.54 (m, 14 H), 1.62 (m, 2 H), 1.90 (m, 6 H), 2.05 (m, 2 H), 2.80 (m, 4 H), 3.95 (s, 6 H), 4.94 (dm, 1 H, $J = 10.3$ Hz), 4.99 (dm, 1 H, $J = 17.1$ Hz), 5.80 (tdd, 1 H, $J = 17.1, 10.3, 6.7$ Hz); MS (LREI, 70 eV) m/z (relative intensity) 442 (M^+ , 24), 336 (24), 335 (23), 303 (52), 257 (99), 225 (25), 223 (51), 165 (27), 163 (28), 157 (100), 144 (61), 85 (29). Anal. Calcd for $\text{C}_{24}\text{H}_{42}\text{S}_2\text{O}_3$: C, 65.11; H, 9.56; S, 14.48. Found: C, 65.14; H, 9.38; S, 14.36.

3-Hydroxy-2-(hydroxymethyl)-2-methylpropyl 6,6-(Trimethylenedithio)-15-hexadecenoate (9). A solution of fatty OBO ester 8, (2.46 mmol) in 48 mL of a mixture of glacial acetic acid, THF, and water (4:2:1) was allowed to stir at room temperature for 1.5 h. The solution was concentrated on a rotary evaporator, employing benzene to azeotropically remove the acetic acid. A quantitative yield of neopentyl ester 9 was obtained as a clear, colorless oil: ^1H NMR (CDCl_3) δ 0.90 (s, 3 H), 1.3–1.57 (m, 14 H), 1.69 (m, 2 H), 1.9 (m, 6 H), 2.05 (m, 2 H), 2.42 (t, 2 H, $J = 7.2$ Hz), 2.85 (m, 4 H), 3.52 (d, 2 H, $J = 11.3$ Hz), 3.60 (d, 2 H, $J = 11.3$ Hz), 4.22 (s, 2 H), 4.94 (dm, 1 H, $J = 10.3$ Hz), 4.99 (dm, 1 H, $J = 17.1$ Hz), 5.80 (tdd, 1 H, $J = 17.1, 10.3, 6.7$ Hz); MS (LREI, 70 eV) m/z (relative intensity) 460 (M^+ , 15), 321 (39), 258 (17), 257 (100), 201 (16), 107 (22), 106 (18), 95 (21), 85 (16), 81 (39), 74 (18), 73 (17), 69 (18), 67 (39), 55 (69); IR (solution, CHCl_3) 3630, 3500 (br), 2940, 2860, 1725, 1470, 1240, 1050, 910; HREI calcd for $\text{C}_{24}\text{H}_{44}\text{S}_2\text{O}_4$ 460.2684, found 460.2682.

Methyl 6,6-(Trimethylenedithio)-15-hexadecenoate (10). The neopentyl ester (2.46 mmol) was dissolved in dry methanol (30 mL) under nitrogen. Anhydrous K_2CO_3 (5.18 mmol) was added quickly, and the mixture was

allowed to stir at room temperature for 2 h. The cloudy solution was diluted with 60 mL of CH_2Cl_2 and washed with three 30-mL portions of water. The organic extract was dried (Na_2SO_4) and concentrated to provide 870 mg (95%) of the methyl ester 10, which was used in the next step without further purification: colorless oil; ^1H NMR (CDCl_3) δ 1.3–1.5 (m, 14 H), 1.65 (m, 2 H), 1.90 (m, 6 H), 2.06 (m, 2 H), 2.35 (t, 2 H, $J = 7.6$ Hz), 2.85 (m, 4 H), 3.68 (s, 3 H), 4.94 (dm, 1 H, $J = 10.3$ Hz), 4.99 (dm, 1 H, $J = 17.1$ Hz), 5.80 (tdd, 1 H, $J = 17.1, 10.3, 6.7$ Hz); MS (LREI, 70 eV) m/z (relative intensity) 372 (M^+ , 25), 257 (100), 233 (99), 101 (23), 95 (22), 81 (43), 74 (27), 67 (39), 55 (63); HREI calcd for $\text{C}_{20}\text{H}_{36}\text{O}_5\text{S}_2$ 372.2156, found 372.2156.

Methyl 6,6-(Trimethylenedithio)-16-hydroxyhexadecanoate (11). The unsaturated ester 10 (870 mg, 2.3 mmol) was dissolved in freshly distilled THF (2.5 mL) and allowed to stir under nitrogen. 9-Borabicyclo[3.3.1]nonane (9-BBN, 4.6 mmol) was added dropwise via syringe and the solution was allowed to stir at room temperature for 1 h. The reaction was complete after 1 h, as indicated by the absence of starting material in direct TLC analysis of the mixture. The solution was cooled to 0 °C and 1.54 mL of 3 M NaOH was slowly added via syringe, followed by the dropwise addition of 1.54 mL of 30% H_2O_2 . The mixture was allowed to stir for 30 min at 0 °C, followed by 1 h at room temperature (by monitoring the quench by TLC, the 1 h at room temperature was found to increase the yield of desired product). Dilution with CH_2Cl_2 (50 mL), extraction with three 20-mL portions of water, drying, and concentration produced 0.81 g (90%) of hydroxy fatty ester 11, which was used in the next step without further purification: colorless oil; ^1H NMR (CDCl_3) δ 1.3–1.7 (m, 16 H), 1.9 (m, 8 H), 2.35 (t, 2 H, $J = 7.6$ Hz), 2.85 (m, 4 H), 3.65 (t, 2 H, $J = 6.8$ Hz), 3.68 (s, 3 H); MS (LREI, 70 eV) m/z (relative intensity) 390 (M^+ , 13), 275 (63), 233 (92), 127 (51), 109 (62), 95 (30), 81 (58), 69 (34), 67 (90), 55 (100); HREI calcd for $\text{C}_{20}\text{H}_{38}\text{O}_3\text{S}_2$ 390.2252, found 390.2257.

Methyl 6,6-(Trimethylenedithio)-16-acetoxyhexadecanoate (12). Dry pyridine (1.7 mmol) was added in one portion to hydroxy ester 11, 1.0 mmol) in dry CH_2Cl_2 under nitrogen. Acetic anhydride (1.7 mmol) was added dropwise via syringe and the solution was allowed to stir overnight at room temperature. The mixture was diluted with CH_2Cl_2 (40 mL) and washed with two 20-mL portions each of saturated NaHCO_3 solution, saturated CuSO_4 solution, and brine. The organic extract was dried (Na_2SO_4) and concentrated. Purification by flash chromatography (20% ethyl acetate/hexane) yielded 850 mg (94%) of protected alcohol 12 as a colorless oil: ^1H NMR (CDCl_3) δ 1.3–1.50 (m, 16 H), 1.65 (m, 4 H), 1.90 (m, 6 H), 2.05 (s, 3 H), 2.35 (t, 2 H, $J = 7.6$ Hz), 2.85 (m, 4 H), 3.68 (s, 3 H), 4.05 (t, 2 H, $J = 6.8$ Hz); MS (LREI, 70 eV) m/z (relative intensity) 432 (M^+ , 16), 317 (77), 233 (95), 107 (15), 95 (24), 81 (40), 67 (38), 54 (47), 41 (100); IR (solution, CCl_4) 2940, 2860, 1743, 1438, 1365, 1240, 1170, 1040. Anal. Calcd for $\text{C}_{22}\text{H}_{40}\text{O}_4\text{S}_2$: C, 61.07; H, 9.32; S, 14.82. Found: C, 61.31; H, 9.20; S, 14.80.

Methyl 6,6-Difluoro-16-acetoxyhexadecanoate (13). 1,3-Dibromo-5,5-dimethylhydantoin (0.66 g, 2.3 mmol) was suspended in 5 mL of dry CH_2Cl_2 in a dry, polyethylene vial equipped with a rubber septum. The mixture (under nitrogen) was cooled to –78 °C and 0.60 mL (2.56 mmol, i.e., 50 equiv of F^-) of pyridinium poly(hydrogen fluoride) was added via polypropylene/polyethylene syringe. After stirring for 10 min, dithiane 12 (200 mg, 0.46 mmol) was slowly added via syringe. The orange mixture was allowed to stir for 15 min at –78 °C, followed by 15 min at room

temperature (at this point the deep red solution was homogeneous). The solution was diluted with CH_2Cl_2 (30 mL) and washed with three 20-mL portions each of saturated NaHCO_3 solution, saturated NaHSO_3 solution, saturated CuSO_4 solution, and brine. The organic extract was dried (Na_2SO_4) and concentrated to provide 142 mg (85%) of difluoro ester 13, which was used in the next step without further purification: colorless oil; ^1H NMR (CDCl_3) δ 1.30 (m, 12 H), 1.5–1.90 (m, 12 H), 2.05 (s, 3 H), 2.35 (t, 2 H, $J = 7.6$ Hz), 3.68 (s, 3 H), 4.05 (t, 2 H, $J = 6.8$ Hz); MS (LRCI) m/z (relative intensity) 365 ($\text{M} + \text{H}$, 13), 345 ($(\text{M} + \text{H}) - \text{HF}$, 100), 325 ($(\text{M} + \text{H}) - 2\text{HF}$, 10), 313 (100), 265 (33); ^{19}F NMR (CDCl_3) ϕ –98.499 (quintet, $J = 16.56$ Hz); HRCI calcd for $\text{C}_{19}\text{H}_{35}\text{F}_2\text{O}_4$ ($\text{M} + \text{H}$) 365.2479, found 365.2491.

Methyl 16-Hydroxy-6,6-difluorohexadecanoate (14). A small piece (~50–100 mg) of sodium (rinsed in hexane) was added to 30 mL of anhydrous methanol under nitrogen at 0 °C. After the sodium had dissolved, 142 mg (0.39 mmol) of difluoro ester 13 in methanol was added via syringe. The solution was allowed to stir for 2 h at room temperature. After diluting with CH_2Cl_2 (40 mL), the solution was washed with three 30-mL portions of water. The organic extract was dried (Na_2SO_4), concentrated, and purified by flash chromatography (40% ethyl acetate/hexane) to produce 107 mg (85%) of the hydroxy fluoro ester 14 as a colorless oil: ^1H NMR (CDCl_3) δ 1.3–1.9 (m, 24 H), 2.35 (t, 2 H, $J = 7.6$ Hz), 3.65 (t, 2 H, $J = 6.8$ Hz), 3.68 (s, 3 H); ^{13}C NMR (CDCl_3) δ 173.7 (CO_2CH_3), 124.9 (t, $J = 240$ Hz, C-6), 62.6 (CH_2OH), 51.4 (OCH_3), 36.2 (t, $J = 26$ Hz, C-7), 35.8 (t, $J = 26$ Hz, C-5), 33.6, 32.6, 29.4, 29.2, 29.1, 25.6, 24.7, 24.4, 24.2, 22.1 (t, $J = 5$ Hz, C-8), 21.7 (t, $J = 5$ Hz, C-4); MS (LRCI, 70 eV) m/z (relative intensity) 323 ($\text{M} + \text{H}$, 5), 303 ($(\text{M} + \text{H}) - \text{HF}$, 24), 283 ($(\text{M} + \text{H}) - 2\text{HF}$, 100), 271 (46), 265 (28), 251 (71), 233 (29); ^{19}F NMR (CDCl_3) ϕ –98.483 (quintet, $J = 16.64$ Hz); HRCI calcd for $\text{C}_{17}\text{H}_{33}\text{F}_2\text{O}_3$ ($\text{M} + \text{H}$) 323.2401, found 323.2399; calcd for $\text{C}_{17}\text{H}_{32}\text{FO}_3$ ($(\text{M} + \text{H}) - \text{HF}$) 303.2331, found 303.2333; calcd for $\text{C}_{17}\text{H}_{31}\text{O}_3$ ($(\text{M} + \text{H}) - 2\text{HF}$) 283.2293, found 283.2283.

Methyl 16-[[Trifluoromethyl)sulfonyl]oxy]-6,6-difluorohexadecanoate (15). 2,6-Lutidine (80 μL , 0.69 mmol, distilled from CaH_2 and stored over KOH) was added via syringe to the hydroxy difluoro ester 14 (100 mg, 0.31 mmol) under nitrogen. Dry CH_2Cl_2 (1 mL) was added and the stirred solution was cooled to –40 °C. Triflic anhydride (111 μL , 0.66 mmol, distilled from P_2O_5) was slowly added via syringe. The solution was allowed to stir at –40 °C for 15 min and then was diluted with 20 mL of cold CH_2Cl_2 . The dilute solution was quickly washed with two 10-mL portions each of cold 10% HCl solution, cold, saturated NaHCO_3 solution, and brine. The organic extract was dried (Na_2SO_4) and concentrated to provide 120 mg (86%) of triflate 15: pale yellow oil; ^1H NMR (CDCl_3) δ 1.30–1.90 (m, 24 H), 2.35 (t, 2 H, $J = 7.6$ Hz), 3.68 (s, 3 H), 4.54 (t, 2 H, $J = 6.8$ Hz).

Methyl 6,6,16-Trifluorohexadecanoate (16). Dry THF (1.5 mL) was added to triflate 15 (50 mg, 0.11 mmol) under nitrogen. The clear yellow solution turned amber upon the dropwise addition of tetrabutylammonium fluoride (0.55 mL, 1.0 M solution in THF). The solution was allowed to stir at room temperature for 15 min. The solution was diluted with CH_2Cl_2 (5 mL) and passed through a short plug of silica. Flash chromatography (10% diethyl ether/hexane) produced 32 mg (90%) of trifluoro ester 16: colorless oil; ^1H NMR (CDCl_3) δ 1.3–1.50 (m, 14 H), 1.60–1.90 (m, 10 H), 2.35 (t, 2 H, $J = 7.6$ Hz), 3.68 (s, 3 H), 4.45 (td, 2 H, $J_{\text{HF}} = 47.4$ Hz, $J_{\text{HH}} = 6.2$ Hz); MS

(LRCI, 70 eV) m/z (relative intensity) 325 ($M + H$, 0.7), 305 ($(M + H) - HF$, 90), 285 ($(M + H) - 2HF$, 18), 265 ($(M + H) - 3HF$, 42); ^{19}F NMR ($CDCl_3$) δ -98.44 (quintet, $J = 16.6$ Hz), -218.51 (tt, $J_{gem} = 47.4$ Hz, $J_{vic} = 24.9$ Hz); HRCI calcd for $C_{17}H_{31}F_2O_2$ ($(M + H) - HF$) 305.2308, found 305.2300; calcd for $C_{17}H_{30}FO_2$ ($(M + H) - 2HF$) 285.2259, found 285.2244; calcd for $C_{17}H_{29}O_2$ ($(M + H) - 3HF$) 265.2197, found 265.2182. Anal. Calcd for $C_{17}H_{31}F_2O_2$: C, 62.94; H, 9.63; F, 17.57. Found: C, 61.96; H, 9.43; F, 18.24.

6,6,16-Trifluorohexadecanoic Acid (I). Potassium hydroxide (1.0 mL, 5 M solution) was added to 20 mg of trifluoro ester 16 (0.06 mmol) in a Reactival. The vial was tightly capped and placed into a heating block at 138 °C for 5 min. After cooling, the mixture was acidified with 6 N HCl (1.5 mL) and extracted into CH_2Cl_2 (3 \times 3 mL). After drying (Na_2SO_4) and solvent evaporation, 17 mg (91%) of trifluoro acid I was obtained: colorless oil; 1H NMR ($CDCl_3$) δ 1.28–1.48 (m, 14 H), 1.54 (m, 2 H), 1.69 (m, 4 H), 1.82 (m, 4 H), 2.38 (t, 2 H, $J = 7.8$ Hz), 4.45 (td, 2 H, $J_{HF} = 47.4$ Hz, $J_{HH} = 6.2$ Hz); MS (LRCI) m/z (relative intensity) 311 ($M + H$, 3), 291 ($(M + H) - HF$, 32), 271 ($(M + H) - 2HF$, 27), 251 ($(M + H) - 3HF$, 17), 177 (89), 89 (100); ^{19}F NMR ($CDCl_3$) δ -98.49 (quintet, $J = 16.6$ Hz), -218.46 (tt, $J_{gem} = 47.4$ Hz, $J_{vic} = 24.9$ Hz); HRCI calcd for $C_{16}H_{29}F_2O_2$ ($(M + H) - HF$) 291.2141, found 291.2138; calcd for $C_{16}H_{28}FO_2$ ($(M + H) - 2HF$) 271.2081, found 271.2077.

9-Decenal (18). 9-Decen-1-ol (17; 10.3 mL, 57.7 mmol) in 40 mL of CH_2Cl_2 was added in one portion to pyridinium chlorochromate (18.6 g, 86.4 mmol) suspended in 100 mL of CH_2Cl_2 . The reaction mixture was allowed to stir at room temperature under nitrogen for 90 min. TLC analysis showed that the reaction was complete at this time. The mixture was diluted with diethyl ether (300 mL) and filtered. The solvent was evaporated and the mixture was purified by flash chromatography (10% diethyl ether/hexane) to provide 7.11 g (80%) of aldehyde 18: colorless oil; 1H NMR ($CDCl_3$) δ 1.33 (m, 8 H), 1.65 (m, 2 H), 2.05 (m, 2 H), 2.44 (td, 2 H, $J = 7.3$, 5 Hz), 4.94 (dm, 1 H, $J = 10.2$ Hz), 5.00 (dm, 1 H, $J = 17$ Hz), 5.81 (tdd, 1 H, $J = 17$, 10.2, 6.7 Hz), 9.77 (t, 1 H, $J = 5$ Hz); MS (LREI, 70 eV) m/z (relative intensity) 154 (M^+ , 0.3), 125 (6), 110 (33), 97 (48), 83 (66), 69 (100), 55 (100), 41 (100). Anal. Calcd for $C_{10}H_{18}O$: C, 77.84; H, 11.78. Found: C, 77.66; H, 11.65.

2-(8-Nonenyl)-1,3-dithiane (19). The dithiane was prepared by following the procedure for 2 on a 5-g scale (32 mmol) to produce (after chromatography) 5.6 g (72%) of dithiane 19: 1H NMR ($CDCl_3$) δ 1.35 (m, 10 H), 1.75 (m, 2 H), 2.05 (m, 4 H), 2.85 (m, 4 H), 4.05 (t, 1 H, $J = 6.5$ Hz), 4.94 (dm, 1 H, $J = 10.2$ Hz), 5.00 (dm, 1 H, $J = 17$ Hz), 5.81 (tdd, 1 H, $J = 17$, 10.2, 6.7 Hz); MS (LREI, 70 eV) m/z (relative intensity) 244 (M^+ , 12), 169 (17), 119 (100), 87 (10), 74 (11), 73 (13), 67 (13), 54 (18), 43 (16). Anal. Calcd for $C_{13}H_{24}S_2$: C, 63.87; H, 9.90; S, 26.23. Found: C, 63.44; H, 9.75; S, 26.38.

6-Bromohexanoyl Chloride (22). The acid chloride was prepared by following the procedure for 5 on a 15-g scale to produce 16.1 g (98%) of the pure acid chloride 22 (after distillation): 1H NMR ($CDCl_3$) δ 1.54 (m, 2 H), 1.75 (m, 2 H), 1.90 (m, 2 H), 2.94 (t, 2 H, $J = 7$ Hz), 3.41 (t, 2 H, $J = 6.2$ Hz); MS (LREI, 70 eV) m/z (relative intensity) 216 (M^+ , 1), 214 (2), 212 (2), 179 (100), 177 (100), 151 (20), 149 (21), 137 (57), 135 (65), 133 (37), 97 (100), 78 (100), 69 (100).

(3-Oxa-1-methylcyclobutyl)methyl 5-Bromohexanoate (23). The oxetane ester was prepared by following the procedure for 6 on a 4.4-g scale (21 mmol) to produce

4.8 g (83%) of the crude oxetane ester 23: 1H NMR ($CDCl_3$) δ 1.34 (s, 3 H), 1.50 (m, 2 H), 1.67 (m, 2 H), 1.89 (quintet, 2 H, $J = 7.2$ Hz), 2.38 (t, 2 H, $J = 7$ Hz), 3.40 (t, 2 H, $J = 6.2$ Hz), 4.16 (s, 2 H), 4.38 (d, 2 H, $J = 6$ Hz), 4.50 (d, 2 H, $J = 6$ Hz); MS (LREI, 70 eV) m/z (relative intensity) 281 ($M + H$, 0.4), 279 (0.4), 197 (20), 195 (20), 179 (100), 177 (100), 144 (24), 97 (34), 69 (100), 55 (59). Anal. Calcd for $C_{11}H_{19}O_3Br$: C, 47.35; H, 6.86; Br, 28.64. Found: C, 47.22; H, 6.97; Br, 28.42.

1-(5-Bromopentyl)-4-methyl-2,6,7-trioxabicyclo[2.2.2]octane (24). The OBO ester was prepared following the procedure for 7 on a 4.8-g scale (17 mmol) to produce (after chromatography) 3.4 g (70%) of OBO compound 24: colorless oil; 1H NMR ($CDCl_3$) δ 0.80 (s, 3 H), 1.46 (m, 4 H), 1.69 (m, 2 H), 1.88 (quintet, 2 H, $J = 7.2$ Hz), 3.40 (t, 2 H, $J = 7$ Hz), 3.90 (s, 6 H); MS (LREI, 70 eV) m/z (relative intensity) 280 (M^+ , 0.5), 278 (0.5), 250 (18), 248 (18), 179 (79), 177 (79), 72 (23), 69 (100), 54 (35). Anal. Calcd for $C_{11}H_{19}BrO_3$: C, 47.32; H, 6.87; Br, 28.62. Found: C, 47.24; H, 6.91; Br, 28.68.

1-[6,6-(Trimethylenedithio)-14-pentadecenyl]-4-methyl-2,6,7-trioxabicyclo[2.2.2]octane (25). The alkylated fatty acid precursor was prepared by following the procedure for 8 on a 5.4-g scale (22 mmol) to produce 8.5 g (87%) of the alkylated OBO compound 25 after chromatography: colorless oil; 1H NMR ($CDCl_3$) δ 0.80 (s, 3 H), 1.35 (m, 16 H), 1.67 (m, 2 H), 1.85 (m, 6 H), 2.05 (m, 2 H), 2.85 (m, 4 H), 3.90 (s, 6 H), 4.94 (dm, 1 H, $J = 10.2$ Hz), 5.00 (dm, 1 H, $J = 17$ Hz), 5.81 (tdd, 1 H, $J = 17$, 10.2, 6.7 Hz); MS (LREI, 70 eV) m/z (relative intensity) 442 (M^+ , 32), 336 (31), 303 (53), 257 (100), 223 (47), 157 (83), 144 (49), 81 (32), 69 (31), 67 (33), 57 (36), 55 (70). Anal. Calcd for $C_{24}H_{42}O_3S_2$: C, 65.11; H, 9.56; S, 14.48. Found: C, 65.18; H, 9.55; S, 14.38.

3-Hydroxy-2-(hydroxymethyl)-2-methylpropyl 7,7-(Trimethylenedithio)-15-hexadecenoate (26). The neopentyl ester was prepared in quantitative yield by the procedure for 9 and was used directly without purification or characterization.

Methyl 7,7-(Trimethylenedithio)-15-hexadecenoate (27). The methyl ester was prepared by the procedure for 10 to produce, after flash chromatography (10% diethyl ether/hexane), 3.5 g (85%) of pure methyl ester 27: 1H NMR ($CDCl_3$) δ 1.35 (m, 14 H), 1.65 (m, 2 H), 1.85 (m, 4 H), 1.95 (m, 2 H), 2.05 (m, 2 H), 2.32 (t, 2 H, $J = 7.5$ Hz), 2.82 (m, 4 H), 3.67 (s, 3 H), 4.94 (dm, 1 H, $J = 10.2$ Hz), 5.00 (dm, 1 H, $J = 17$ Hz), 5.81 (tdd, 1 H, $J = 17$, 10.2, 6.7 Hz); MS (LREI, 70 eV) m/z (relative intensity) 372 (M^+ , 9), 247 (21), 243 (22), 119 (17), 87 (20), 81 (25), 74 (100), 69 (19), 59 (23), 55 (35); HREI calcd for $C_{20}H_{36}O_2S_2$ 372.2141, found 372.2149.

Methyl 7,7-(Trimethylenedithio)-16-hydroxyhexadecanoate (28). The hydroxy compound was prepared by following the procedure for 11 on a 3.5-g scale to produce 3.3 g (89%) of the hydroxy compound 28, which was used in the next step without purification: 1H NMR ($CDCl_3$) δ 1.35 (m, 14 H), 1.60 (m, 6 H), 1.85 (m, 4 H), 1.95 (m, 2 H), 2.32 (t, 2 H, $J = 7.5$ Hz), 2.82 (m, 4 H), 3.65 (t, 2 H, $J = 6.8$ Hz), 3.67 (s, 3 H); MS (LREI, 70 eV) m/z (relative intensity) 390 (M^+ , 7), 261 (29), 247 (44), 127 (84), 109 (78), 95 (30), 81 (50), 67 (100), 55 (98); IR (solution, $CHCl_3$) 3615, 3010, 2930, 2860, 1733, 1438, 1235; HREI calcd for $C_{20}H_{38}O_3S_2$ 390.2268, found 390.2265.

Methyl 7,7-(Trimethylenedithio)-16-acetoxyhexadecanoate (29). The acetate was prepared by the procedure for 12 on a 3.0-g scale to produce, after flash chromatography (20% ethyl acetate/hexane), 3.1 g (93%) of acetate 29: pale yellow oil; 1H NMR ($CDCl_3$) δ 1.35 (m,

14 H), 1.65 (m, 6 H), 1.85 (m, 4 H), 1.95 (m, 2 H), 2.04 (s, 3 H), 2.32 (t, 2 H, $J = 7.5$ Hz), 2.82 (m, 4 H), 3.67 (s, 3 H), 4.05 (t, 2 H, $J = 6.7$ Hz); MS (LREI) m/z (relative intensity) 432 (M^+ , 5), 303 (24), 247 (33), 127 (67), 109 (42), 74 (21); HREI calcd for $C_{22}H_{40}O_4S_2$ 432.2360, found 432.2364.

Methyl 7,7-Difluoro-16-acetoxyhexadecanoate (30). The difluoro compound was prepared by the procedure for 13 on a 0.5-g scale to produce 0.35 g (83%) of difluoro compound 30, which was used in the next step without purification: 1H NMR ($CDCl_3$) δ 1.30–1.45 (m, 12 H), 1.55–1.9 (m, 12 H), 2.04 (s, 3 H), 2.32 (t, 2 H, $J = 7.5$ Hz), 3.67 (s, 3 H), 4.05 (t, 2 H, $J = 6.7$ Hz); MS (LRCI) m/z (relative intensity) 365 ($M + H$, 29), 345 ($(M + H) - HF$, 100), 325 ($(M + H) - 2HF$, 3), 313 (72), 265 (39); ^{19}F NMR ($CDCl_3$) ϕ -98.46 (quintet, $J = 16.57$ Hz); HRCI calcd for $C_{19}H_{34}FO_4$ 345.2458, found 345.2449; calcd for $C_{19}H_{33}O_4$ ($(M + H) - HF$) 325.2386, found 325.2382.

Methyl 16-Hydroxy-7,7-difluorohexadecanoate (31). The hydroxy difluoro compound was prepared by the procedure for 14 on a 0.35-g scale (0.96 mmol) to produce, after flash chromatography (40% ethyl acetate/hexane), 0.25 g (80%) of the hydroxy difluoro compound 31: 1H NMR ($CDCl_3$) δ 1.30–1.90 (m, 24 H), 2.32 (t, 2 H, $J = 7.5$ Hz), 3.65 (t, 2 H, $J = 6.8$ Hz), 3.67 (s, 3 H); MS (LRCI) m/z (relative intensity) 323 ($M + H$, 68), 303 ($(M + H) - HF$, 50), 283 ($(M + H) - 2HF$, 100), 265 (52), 251 (71); ^{19}F NMR ($CDCl_3$) ϕ -98.405 (quintet, $J = 16.6$ Hz); HRCI calcd for $C_{17}H_{33}O_3F_2$ ($M + H$) 323.2411, found 323.2404; calcd for $C_{17}H_{32}FO_3$ ($(M + H) - HF$) 303.2343, found 303.2339; calcd for $C_{17}H_{31}O_3$ ($(M + H) - 2HF$) 283.2287, found 283.2280.

Methyl 16-[(Trifluoromethyl)sulfonyl]oxy]-7,7-difluorohexadecanoate (32). The triflate was prepared by the procedure for 15 on a 0.25-g scale to produce 0.31 g (90%) of triflate 32: 1H NMR ($CDCl_3$) δ 1.35 (m, 16 H), 1.65 (m, 2 H), 1.82 (m, 6 H), 2.35 (t, 2 H, $J = 7.6$ Hz), 3.68 (s, 3 H), 4.55 (t, 2 H, $J = 6.8$ Hz).

Methyl 7,7,16-Trifluorohexadecanoate (33). The trifluoro ester was prepared by the procedure for 16 on a 50-mg scale to produce 30 mg (88%) of trifluoro ester 33: 1H NMR ($CDCl_3$) δ 1.30–1.50 (m, 14 H), 1.70 (m, 10 H), 2.32 (t, 2 H, $J = 7.5$ Hz), 3.67 (s, 3 H), 4.44 (td, 2 H, $J_{HF} = 47.2$ Hz, $J_{HH} = 6.1$ Hz); MS (LRCI) m/z (relative intensity) 325 ($M + H$, 5), 305 ($(M + H) - HF$, 83), 285 ($(M + H) - 2HF$, 39), 265 ($(M + H) - 3HF$, 72); ^{19}F NMR ($CDCl_3$) ϕ -98.43 (quintet, $J = 16.6$ Hz), -218.55 (tt, $J_{gem} = 47.4$ Hz, $J_{vic} = 24.9$ Hz); HRCI calcd for $C_{17}H_{32}O_2F_3$ ($M + H$) 325.2358, found 323.2356.

7,7,16-Trifluorohexadecanoic Acid (II). The trifluoro acid was prepared by the procedure for I on a 30-mg scale to provide 25 mg (90%) of trifluoro acid II: 1H NMR ($CDCl_3$) δ 1.30 (br m, 18 H), 1.44 (m, 2 H), 1.70 (m, 4 H), 2.35 (t, 2 H, $J = 7.6$ Hz), 4.44 (td, 2 H, $J_{HF} = 47.2$ Hz, $J_{HH} = 6.1$ Hz); MS (LRCI) m/z (relative intensity) 291 ($(M + H) - HF$, 13), 271 ($(M + H) - 2HF$, 36), 251 ($(M + H) - 3HF$, 40), 186 (88), 142 (56); ^{19}F NMR ($CDCl_3$) ϕ -98.42 (quintet, $J = 16.6$ Hz), -218.50 (tt, $J_{gem} = 47.3$ Hz, $J_{vic} = 24.9$ Hz); HRCI calcd for $C_{16}H_{29}O_2F_2$ ($(M + H) - HF$) 291.2130, found 291.2133; calcd for $C_{16}H_{28}O_2F$ ($(M + H) - 2HF$) 271.2075, found 271.2074; calcd for $C_{16}H_{27}O_2$ ($(M + H) - 3HF$) 251.2011, found 251.2012.

Methyl 16-Hydroxyhexadecanoate (35). 16-Hexadecanolide (34; 5.0 g, 19.7 mmol) was dissolved in dry methanol (200 mL) under nitrogen. Anhydrous K_2CO_3 (5.4 g, 39.4 mmol) was added quickly, and the mixture was allowed to stir at room temperature. GLC analysis indicated that the reaction was complete after 3 h. The

solution was diluted with CH_2Cl_2 (100 mL) and washed with three 50-mL portions of water. The organic extract was dried (Na_2SO_4) and concentrated to provide 5.1 g (90%) of the pure hydroxy ester 35 as a white, crystalline solid: mp 56 °C; 1H NMR ($CDCl_3$) δ 1.30 (br, 20 H), 1.46 (m, 2 H), 1.60 (m, 4 H), 2.31 (t, 2 H, $J = 7.5$ Hz), 3.65 (t, 2 H, $J = 6.8$ Hz), 3.67 (s, 3 H); MS (LREI, 70 eV) m/z (relative intensity) 286 (M^+ , 1), 268 ($M - H_2O$, 5), 256 (26), 98 (63), 87 (46), 75 (45), 74 (100). Anal. Calcd for $C_{17}H_{34}O_3$: C, 71.28; H, 11.96. Found: C, 71.28; H, 11.93.

Methyl 16-[(Trifluoromethyl)sulfonyl]oxy]hexadecanoate (36). 2,6-Lutidine (0.91 mL, 7.8 mmol, distilled from CaH_2 and stored over KOH) was added via syringe to hydroxy ester 35 (1.0 g, 3.5 mmol) under nitrogen. Dry CH_2Cl_2 (12 mL) was added and the stirred solution was cooled to -40 °C. Triflic anhydride (1.25 mL, 7.5 mmol, distilled from P_2O_5) was slowly added via syringe. The solution was allowed to stir at -40 °C for 15 min and then was diluted with 100 mL of cold CH_2Cl_2 . The dilute solution was quickly washed with two 50-mL portions each of cold 10% HCl solution, cold, saturated $NaHCO_3$ solution, and brine. The organic extract was dried (Na_2SO_4) and concentrated to provide 1.4 g (93%) of triflate 36: 1H NMR ($CDCl_3$) δ 1.2–1.4 (m, 20 H), 1.6 (m, 4 H), 1.83 (quintet, 2 H, $J = 7.3$ Hz), 2.31 (t, 2 H, $J = 7.5$ Hz), 3.67 (s, 3 H), 4.54 (t, 2 H, $J = 6.5$ Hz); MS (LREI, 70 eV) m/z (relative intensity) 418 (M^+ , 100), 387 (37), 345 (42), 281 (21), 268 (39), 240 (69), 239 (100), 212 (79); HREI calcd for $C_{18}H_{33}F_3O_5S$ 4110.3993, found 4110.3997.

Methyl 16-Fluorohexadecanoate (37). Dry THF (5 mL) was added to triflate 36 (229 mg, 0.55 mmol) under nitrogen. The clear yellow solution turned amber upon the dropwise addition of tetrabutylammonium fluoride (2.75 mL, 1.0 M solution in THF). The solution was allowed to stir at room temperature for 15 min. The solution was diluted with CH_2Cl_2 (20 mL) and passed through a short plug of silica. Flash chromatography (10% diethyl ether/hexane) produced 143 mg (90%) of fluoro ester 37: mp 36 °C; 1H NMR ($CDCl_3$) δ 1.3–1.4 (br, 20 H), 1.65 (m, 4 H), 1.75 (m, 2 H), 2.31 (t, 2 H, $J = 7.5$ Hz), 3.67 (s, 3 H), 4.45 (td, 2 H, $J_{HF} = 47.5$ Hz, $J_{HH} = 6$ Hz); MS (LREI, 70 eV) m/z (relative intensity) 288 (M^+ , 6), 143 (7), 87 (54), 75 (23), 74 (100), 69 (17), 57 (10), 55 (30); ^{19}F NMR ($CDCl_3$) ϕ -218.471 (tt, $J_{gem} = 47.51$ Hz, $J_{vic} = 24.9$ Hz). HREI calcd for $C_{17}H_{33}FO_2$ 288.2480, found 288.2472. Anal. Calcd for $C_{17}H_{33}FO_2$: C, 70.79; H, 11.53; F, 6.59. Found: C, 70.03; H, 11.30; F, 6.40.

16-Fluorohexadecanoic Acid (III). The ester hydrolysis was performed in a manner identical with that for I on the same scale, producing a similar yield (18 mg, 93%): 1H NMR ($CDCl_3$) δ 1.30 (br, 20 H), 1.65 (m, 6 H), 2.36 (t, 2 H, $J = 7.5$ Hz), 4.54 (dt, 2 H, $J_{HF} = 47.5$, $J_{HH} = 6$ Hz); MS (LREI, 70 eV) m/z (relative intensity) 274 (M^+ , 27), 255 (10), 236 (17), 129 (33), 104 (100); ^{19}F NMR ($CDCl_3$) ϕ -218.51 (tt, $J_{gem} = 47.4$ Hz, $J_{vic} = 24.9$ Hz); HRCI calcd for $C_{16}H_{32}O_2F$ ($M + H$) 275.2376, found 275.2381.

Radiochemical Synthesis. General Procedure for the Preparation of [^{18}F]Fatty Acids. Fluorine-18 was prepared from [^{18}O]H $_2$ O by the $^{18}O(p,n)^{18}F$ reaction (15). Tetrabutylammonium hydroxide (2 μ mol, 1 M aqueous solution) was added via microcapillary tube to the bottom of a Vacutainer (16). Water containing the [^{18}F]fluoride ion was added to the base, followed by the addition of 200 μ L of acetonitrile. The Vacutainer was allowed to heat in an oil bath at 110 °C while a gentle stream of nitrogen was used to assist in the azeotropic distillation of the water. As the volume decreased, additional acetonitrile was added, until there was only a very small volume remaining. The

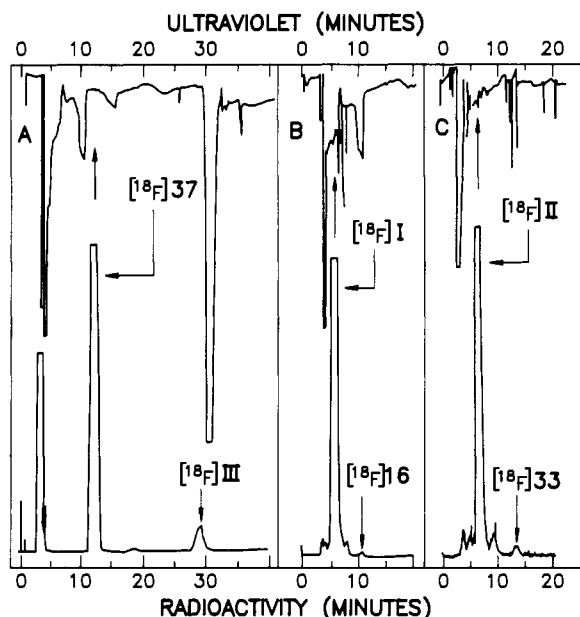


Figure 1. HPLC trace of the purification of the three fluorohexadecanoic Acids (I-III). Chromatography was performed with reverse-phase HPLC (Whatman Partisil M-9 column) eluting with 86% acetonitrile and 14% (1% trifluoroacetic acid in water). A shows the trace for 16-[^{18}F]fluorohexadecanoic acid (III): The large peak at the void volume of the column ($t_R = 3.2$ min) is $^{18}\text{F}^-$, the second large peak ($t_R = 12.5$ min) is the 16-[^{18}F]fluorohexadecanoic acid ([^{18}F]III), and the small peak at $t_R = 29$ min is the methyl 16-[^{18}F]fluorohexadecanoate ([^{18}F]37). B shows the trace for 6,6,16-[16- ^{18}F]trifluorohexadecanoic acid (I): The large peak ($t_R = 6.0$ min) is 6,6,16-[16- ^{18}F]trifluorohexadecanoic acid ([^{18}F]I) and the small peak at $t_R = 11.0$ min is methyl 6,6,16-[16- ^{18}F]trifluorohexadecanoate ([^{18}F]16). C shows the trace for 7,7,16-[16- ^{18}F]trifluorohexadecanoic acid (II): The large peak ($t_R = 6.8$ min) is 7,7,16-[16- ^{18}F]trifluorohexadecanoic acid ([^{18}F]II) and the small peak at $t_R = 13.5$ min is methyl 7,7,16-[16- ^{18}F]trifluorohexadecanoate ([^{18}F]33).

last minutes of the evaporation were performed without heat, since it has been found that overdrying the activity provides a much less active form of $^{18}\text{F}^-$.

After the water had been azeotropically removed, 200 μL of dry THF was used to transfer the concentrated activity from the Vacutainer to a vial (12 \times 75 mm, borosilicate glass, with Teflon-lined cap) containing the preweighed triflate. The vial was tightly capped and the mixture was allowed to heat at 105–110 $^\circ\text{C}$ for 20 min. After cooling (~ 1 min), the reaction mixture was transferred to a small plug of silica (1 cm), using an additional 400 μL of THF to rinse the vial and elute the silica. The mixture was eluted into a 1-mL Reactivial and concentrated by rotary evaporation or under a gentle stream of nitrogen (at room temperature). To the concentrated mixture was added 200 μL of 5 M KOH. The vial was tightly capped and allowed to heat at 135 $^\circ\text{C}$ for 5 min. After cooling (~ 2 min), 300 μL of 6 N HCl was added and the acidified mixture was transferred to a test tube. The aqueous layer was washed with CH_2Cl_2 until the cloudiness disappeared. The organic extract was passed through a 6.5-cm drying column (0.5 cm of MgSO_4 topped with 6.0 cm of Na_2SO_4) into a 25-mL pear-shaped flask. The solution was concentrated in vacuo, redissolved in 1.5 mL methanol, and purified by reverse-phase HPLC.

16-[^{18}F]Fluorohexadecanoic Acid ([^{18}F]III). [^{18}F]Fluoride (91 mCi) and triflate 36 (7.2 μmol) were allowed to react. The yields for each manipulation were as follows: resolubilization, 96%; displacement, 68%; hydrolysis, 45%; overall, 10% decay corrected at 90 min after the end of

bombardment. The product was purified by HPLC (cf. Figure 1A); the desired acid (III) eluted at 12.5 min.

6,6,16-[16- ^{18}F]Trifluorohexadecanoic Acid ([^{18}F]I). [^{18}F]Fluoride (176 mCi) and triflate 15 (6.2 μmol) were allowed to react. The yields for each manipulation were comparable to those listed for [^{18}F]III above; overall yield was ca. 10%. The product was purified by HPLC (cf. Figure 1B); the desired acid (I) eluted at 6.0 min.

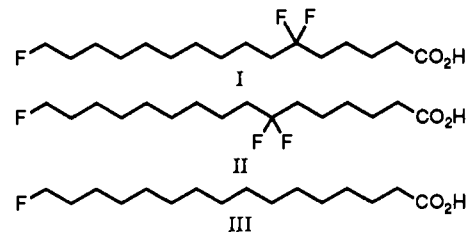
7,7,16-[16- ^{18}F]Trifluorohexadecanoic Acid ([^{18}F]II). [^{18}F]Fluoride (158 mCi) and triflate 32 (5.6 μmol) were allowed to react. The yields for each manipulation were somewhat less than those listed for [^{18}F]III above; overall yield was ca. 3%. The product was purified by HPLC (cf. Figure 1C); the desired acid (II) eluted at 6.8 min.

[^{11}C]Palmitate and [^{11}C]Octanoate. These compounds were prepared by methods described previously (17).

Biodistribution Studies. After HPLC, the fractions containing the three fluorinated fatty acids [^{18}F]I, [^{18}F]II, and [^{18}F]III were concentrated to dryness and then redissolved in 200 μL of ethanol. A 2.5% human serum albumin in saline solution (4 mL) was added and the resulting solution was filtered through a Millex-GV 0.22- μm filter unit. Sprague-Dawley rats (150–200 g) were allowed food and water and were anesthetized with ether just prior to injection. The radioactive compound was administered via femoral injection. At the indicated times, tissues were removed and the activity levels were determined by γ -counting.

RESULTS

The two prototype trifluoro fatty acids that we have synthesized are 6,6,16-trifluoro- and 7,7,16-trifluorohexadecanoic (palmitic) acid I and II. In addition, in order to provide a system that is not metabolically blocked in the same manner, we prepared 16-fluoropalmitic acid (III).

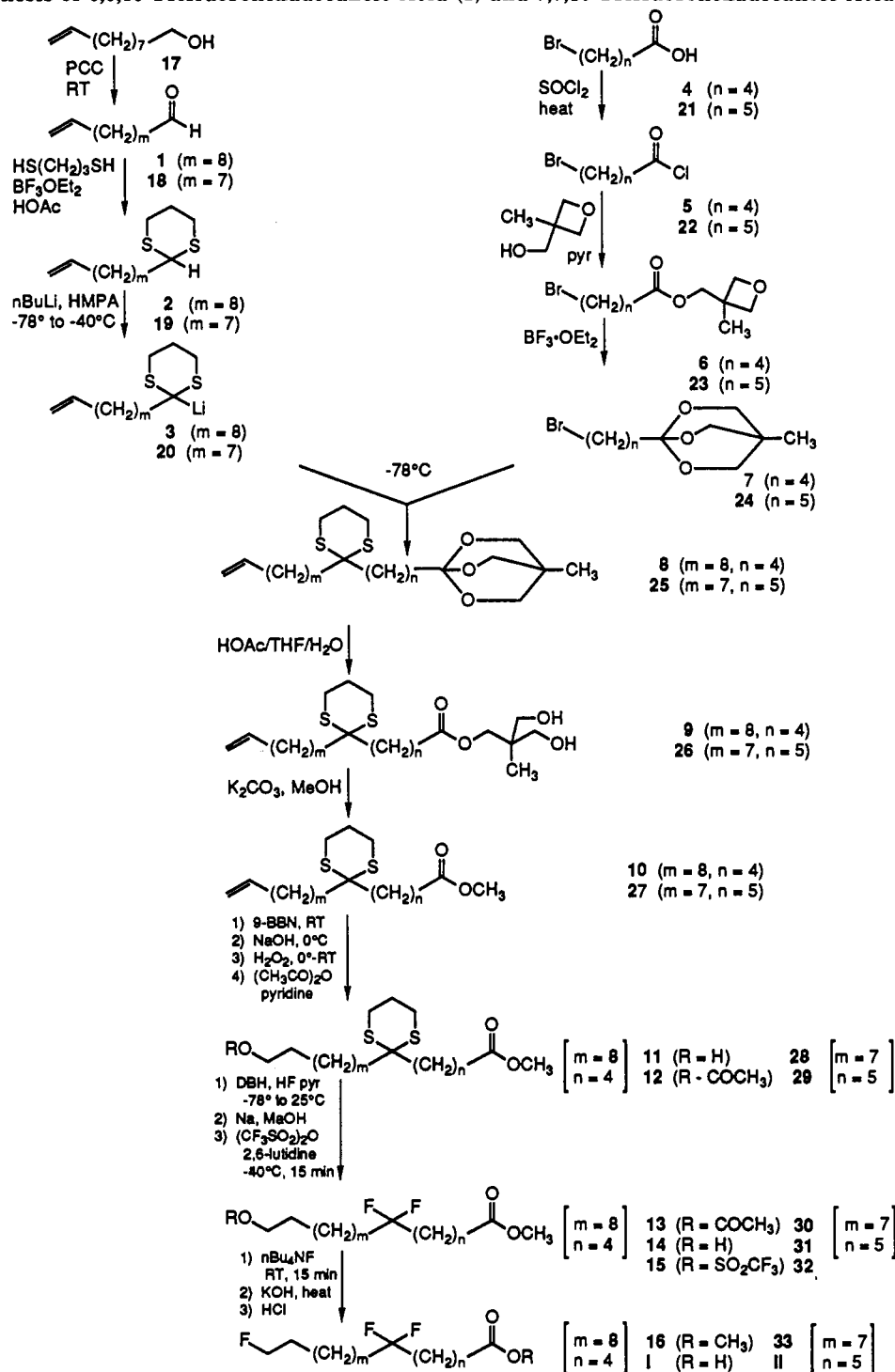


Chemical Synthesis. Because the trifluoro fatty acids I and II are to be labeled with fluorine-18 on the terminal carbon, the synthetic scheme was developed so that this fluorine could be introduced at a late stage in the sequence, by a simple fluoride ion displacement reaction. Since we have found that a *gem*-difluoromethylene group can be derived from a 1,3-dithiane (18), we selected a synthetic sequence whereby two carbon chains, each terminally functionalized, are joined by alkylation of a 2-lithio-1,3-dithiane.

Synthesis of 6,6,16-Trifluorohexadecanoic Acid (I). The synthetic route to 6,6,16-trifluorohexadecanoic acid (I) is shown in Scheme II. The 11-carbon fragment was derived from 10-undecenal (1), an inexpensive, commercially available starting material, by conversion to dithiane 2, under standard conditions. Thiylation of the olefin was observed after prolonged reaction time, but could be minimized by carefully monitoring the course of the reaction by TLC. Metalation of the dithiane with *n*-butyllithium was assisted by the presence of hexamethylphosphoramide (HMPA).

The five-carbon fragment was derived from 5-bromopentanoic acid (4). Corey's OBO (oxabicyclooctyl) ester (19) was chosen to allow selective displacement of the

Scheme II. Synthesis of 6,6,16-Trifluorohexadecanoic Acid (I) and 7,7,16-Trifluorohexadecanoic Acid (II)

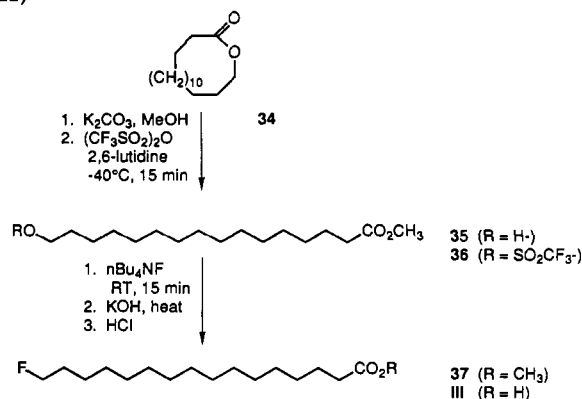


halide by the 2-lithio-1,3-dithiane without competing addition to an ester carbonyl. Initial attempts using other esters, acid salts, etc. to protect the ester functionality proved ineffective. Prior distillation of acid chloride 5 and use of an excess of pyridine were required to insure a reasonable yield of oxetane ester 6. As this ester is highly sensitive to acid, purification was postponed until the somewhat less acid-sensitive OBO stage (7); decomposition could be minimized by performing chromatography rapidly on silica pretreated with triethylamine. The chromatographic fractions were monitored by GLPC as the compound has no UV chromophore and does not stain with any of the usual TLC visualization methods.

Alkylation of lithio-1,3-dithiane 3 proceeded rapidly at -78°C , providing fatty acid precursor 8 in 90% yield. The

OBO compound was transformed into a methyl ester (10) in excellent yield in two steps, hydrolysis and transesterification, according to Fried's method (20). Olefin hydroboration with 9-borabicyclo[3.3.1]nonane (9-BBN), followed by the usual oxidative workup, provided a good yield of hydroxy fatty ester 11. Careful monitoring of the course of the hydroboration and quench steps by TLC was necessary to avoid side reactions such as oxidation at sulfur and methyl ester cleavage.

As fluorination of dithiane 18 converts alcohols to bromo compounds, the terminal alcohol was protected as acetate 12. Under optimized conditions (polyethylene reaction flask, -78°C to room temperature, buffered aqueous quench), fluorination of the protected dithiane 12 gave di-

Scheme III. Synthesis of 16-Fluorohexadecanoic Acid (III)

fluoro product 13 in 85% yield. Selective methanolysis of the acetate gave the hydroxy difluoro methyl ester 14.

Since the trifluoromethanesulfonate (triflate) 15 is quite thermally labile and decomposes rapidly on silica gel, it was necessary to control carefully the reaction conditions for its formation to minimize the generation of byproducts and obviate the need for purification. By combining a short reaction time at $-40^\circ C$ with a cold, aqueous quench, a good yield (86%) of triflate 15 ($\sim 98\%$ pure by 1H NMR) could be obtained. The triflate is stable for several months at $-20^\circ C$.

The displacement of the triflate by fluoride ion (tetrabutylammonium fluoride), gives excellent yields of trifluoro ester 16 within 5 min at room temperature. Finally, the methyl ester can be hydrolyzed under vigorous conditions to give trifluoro acid I in good yield. A major consideration in the selection of vigorous ester hydrolysis conditions was that the reaction be very fast, since, in the radiosynthesis, this step would follow the introduction of the short-lived radionuclide.

Synthesis of 7,7,16-Trifluorohexadecanoic Acid (II). The synthesis of 7,7,16-trifluorohexadecanoic acid (II) paralleled that of the 6,6,16-isomer I (Scheme II). Although 9-decenal (18) was not commercially available, it could be easily synthesized by oxidizing the available 9-decen-1-ol (17) with pyridinium chlorochromate. Subsequent dithiane formation and lithiation proceeded as before. 6-Bromohexanoic acid (21) was used as the six-carbon fragment.

Alkylation and the subsequent steps to produce 7,7,16-trifluorohexadecanoic acid (II) provided similar yields to those obtained in the synthesis of the 6,6,16-trifluoro isomer. In fact, in characterization of the products along this route, the mass spectra provided the only unique information, as the fragment ions clearly showed the position of the dithiane. The 1H NMR, ^{13}C NMR, IR, elemental analysis, and chromatographic behavior of the isomers were indistinguishable.

Synthesis of 16-Fluorohexadecanoic Acid (III). 16-Fluorohexadecanoic acid (III) was prepared as a model compound to be used for optimization of the radiochemical synthesis and as a standard for the subsequent biodistribution studies. Although 16-hydroxyhexadecanoic acid (juniperic acid) is commercially available, the lactone 16-hexadecanolide (34) is available at less than one-tenth the cost and can be efficiently converted to hydroxy ester 35 in one step (see Scheme III).

Identification of Fluoro Compounds. The fluorine-containing fatty acid analogues proved to be difficult to characterize by standard methods, with the level of difficulty generally increasing with the addition of each fluorine. In general, while aromatic fluoro compounds

provide large molecular ion peaks in mass spectral analysis, the molecular ion is usually very small or missing in aliphatic fluoro compounds, as elimination of F or HF occurs readily under electron-ionization conditions (21). The monofluoro compounds (III, 37) provided visible molecular ions, and the difluoro compounds (13, 14, 30, 31), very small molecular ions, but only when using chemical ionization. Molecular ions could not be obtained for the trifluoro compounds (16, I, 33, II), regardless of the ionization technique (field ionization, field desorption, chemical ionization, electron ionization, and fast-atom bombardment were attempted). However, the loss of each F as HF was clearly visible (i.e., $M - 20$, $M - 40$, $M - 60$).

1H NMR analysis provides definite evidence for the presence of the primary fluoride (downfield shift and characteristic geminal coupling of ~ 50 Hz); however, the position of the difluoro group cannot be determined clearly. Since the methylene protons α to the difluoromethylene group resonate in the same region as other methylenes in the molecule, the vicinal H-F coupling (~ 15 Hz) is usually obscured. The ^{13}C NMR provides very definite evidence for the number and types of fluorine atoms present in the molecule. The carbon atom of the difluoromethylene is split into a triplet ($J_{CF} \cong 240$ Hz), as are the carbon atoms α and β to the difluoromethylene group ($J_{CF} \cong 26$ and 5 Hz, respectively). ^{19}F NMR is the most useful tool for structural determination of the fluoro compounds. The chemical shift in ^{19}F NMR is highly dependent on structure, with the difluoro group resonating at ~ -98 ppm, while the primary monofluoride resonates at ~ -218 ppm. In addition, the clean spectrum allows the diagnostic coupling ($J_{HF-gem} = 35-50$ Hz, $J_{HF-vic} = 12-25$ Hz, $J_{FF-gem} = 100-150$ Hz) to be seen.

Radiochemical Synthesis. Model Reactions. The synthetic routes to the trifluoropalmitic acids I and II were designed so that the ω -terminal fluorine was introduced in the penultimate step by fluoride ion displacement of the corresponding trifluoromethanesulfonate (triflate) derivative (cf. Scheme II). To investigate conditions that would be effective for performing this displacement using tracer levels of [^{18}F] fluoride ion, we surveyed reaction conditions for [^{19}F] fluoride ion displacement on the readily available precursor 36 for the monofluoro analogue 16-fluorohexadecanoic acid (III).

Working on a 120- μ mol scale with 1 equiv of tetrabutylammonium fluoride (TBAF) in THF at room temperature, we obtained an 80% yield of the fluoro fatty acid ester 37; the reaction could be reduced to one-fourth the scale (29 μ mol), with only modest reduction in yield (55%). As solvent, THF, rather than CH_3CN or CH_2Cl_2 , provided the best yield. Even when fluoride ion was the limiting reagent (down to 0.1 equiv of fluoride ion), reasonable yields (ca. 30%, based on fluoride ion as limiting reagent) were obtained.

Radiochemical Synthesis. The three ^{18}F -labeled fatty acid analogues (I-III) were synthesized by the routes shown in Scheme II. A series of 20 radiochemical reactions were performed to investigate the required reaction conditions. The [^{18}F]fluoride, obtained from an [^{18}O]water target after proton bombardment (15), was combined with tetrabutylammonium hydroxide, and the water was removed by azeotropic distillation with acetonitrile at $90^\circ C$ in a Vaportainer (16). The dried activity was resolubilized in THF and transferred to a small, glass vial containing the triflate. The yields in the resolubilization step were consistently high (85-95%). Resolubilization yields were lower with potassium carbonate [2.2.2]kryptofix (22) as base in a platinum crucible. Although the triflate

Table I. Tissue Distribution of [¹⁴C]Palmitate in Adult Rats^a

tissue	2 min	5 min	15 min	30 min ^b	1 h ^c
			%ID/g		
blood	0.44 ± 0.17	0.13 ± 0.03	0.33 ± 0.09	0.60 ± 0.26	0.19 ± 0.05
lung	2.94 ± 1.47	2.06 ± 0.80	2.24 ± 0.70	1.91 ± 0.51	1.81 ± 0.42
liver	6.35 ± 1.07	7.28 ± 0.81	6.73 ± 1.05	4.81 ± 0.44	4.19 ± 0.56
muscle	0.31 ± 0.06	0.30 ± 0.07	0.31 ± 0.06	0.27 ± 0.04	0.33 ± 0.09
heart	3.75 ± 0.68	1.97 ± 0.38	2.09 ± 0.79	1.73 ± 0.40	1.70 ± 0.68
bone ^b	0.30 ± 0.06	0.30 ± 0.10	0.25 ± 0.12	0.34 ± 0.03 ^d	0.41 ± 0.11
			%ID/organ		
blood	4.67 ± 1.87	1.45 ± 0.37	3.55 ± 0.93	6.52 ± 2.74	2.03 ± 0.53
lung	3.03 ± 1.51	2.43 ± 0.80	2.40 ± 0.64	2.00 ± 0.29	2.04 ± 0.30
liver	41.03 ± 5.43	49.93 ± 3.67	45.18 ± 6.43	33.62 ± 3.29	27.27 ± 3.98
muscle	6.54 ± 1.17	6.51 ± 1.57	6.51 ± 1.21	6.46 ± 1.02	6.98 ± 1.59
heart	2.13 ± 0.43	1.12 ± 0.21	1.06 ± 0.29	1.00 ± 0.20	0.98 ± 0.39
bone ^b	4.91 ± 0.92	5.02 ± 1.47	4.09 ± 1.85	5.70 ± 0.23	6.87 ± 1.87

^a Mean ± standard deviation, *n* = 12, unless noted otherwise. ^b *n* = 8. ^c *n* = 13. ^d *n* = 4.

displacement reaction occurred rapidly at room temperature when using [¹⁹F]fluoride, it was necessary to heat the reaction mixture to obtain reasonable yields when using [¹⁸F]fluoride, and yields increased significantly when the reaction time was extended from 10 to 20 min.

The product from the displacement reaction was passed through a plug of silica gel and then evaporated under a stream of nitrogen. In some cases, a considerable quantity of activity was lost during this step. While the loss was first thought to be due to evaporation of an apolar, volatile byproduct, control experiments showed that the ester itself had significant volatility under a nitrogen stream; higher yields were obtained when solvent was removed by rotary evaporation.

Ester hydrolysis could be achieved with either 50% H₂SO₄ or 6 N hydrochloric acid; the latter gave fewer emulsion problems. The acid was isolated by extraction with dichloromethane. Overall yields (decay corrected) were 3–34%, with synthesis times of 60 min.

The ¹⁸F fatty acids used for animal studies were purified by reverse-phase HPLC (Figure 1). Since the fatty acid has no UV chromophore, mass detection was achieved with a UV detector set at 215 nm. This detection wavelength limited the choice of solvents. Reasonable separations, however, could be obtained with mixtures of acetonitrile and 1.0% trifluoroacetic acid in water. In order to obtain a fairly constant baseline at 215 nm, it was essential to degas the solvents and to premix the acetonitrile and water.

Tissue Distribution Studies. For animal uptake studies, the collected HPLC fractions were combined and concentrated in vacuo, adsorbed onto albumin, and injected intravenously into rats. At 2-, 5-, 15-, and 60-min intervals, the rats were sacrificed, and the tissue distribution of the fatty acids was determined. For comparative purposes, tissue-uptake studies were also performed with [¹⁴C]-palmitic acid, used clinically for myocardial imaging, and [¹⁴C]octanoic acid, a fatty acid not utilized by the heart: The tissue distribution data for each of the five fatty acids are presented in Tables I–V; uptake is also depicted graphically in Figures 2–4.

All of the palmitates show high uptake by the liver, fairly low uptake by muscle, and fairly low activity levels in blood (Figure 2; Tables I–IV). The clearance of activity from the liver with 7,7,16-trifluoropalmitate (II) is significantly faster than that with the other three. Activity in the liver, muscle, and lung tissue can reduce the quality of myocardial images. 7,7,16-Trifluoropalmitate (II) is the only compound which shows a higher uptake in lung tissue compared to heart tissue.

As expected, the uptake of [¹⁴C]octanoate is very different from that of the palmitates: Heart uptake is

Table II. Tissue Distribution of 16-[¹⁸F]Fluoropalmitate (II) in Adult Rats^a

tissue	2 min	5 min	15 min	60 min
			%ID/g	
blood	0.26 ± 0.05	0.14 ± 0.01	0.39 ± 0.10	0.27 ± 0.02
lung	1.71 ± 0.59	1.32 ± 0.18	1.12 ± 0.17	1.11 ± 0.28
liver	4.70 ± 1.75	4.89 ± 1.10	4.12 ± 1.08	3.06 ± 0.44
muscle	0.20 ± 0.05	0.21 ± 0.04	0.25 ± 0.05	0.28 ± 0.05
heart	2.44 ± 0.99	1.57 ± 0.27	1.21 ± 0.33	0.66 ± 0.07
bone	0.18 ± 0.04	0.18 ± 0.04	0.33 ± 0.07	1.08 ± 0.15
			%ID/Organ	
blood	3.40 ± 0.65	1.94 ± 0.19	5.05 ± 1.15	3.36 ± 0.26
lung	1.91 ± 0.61	1.56 ± 0.19	1.56 ± 0.38	1.32 ± 0.15
liver	33.60 ± 10.42	39.92 ± 8.44	33.44 ± 6.68	21.45 ± 3.58
muscle	5.31 ± 1.54	5.73 ± 1.02	6.54 ± 1.56	6.84 ± 1.05
heart	1.47 ± 0.53	0.97 ± 0.22	0.71 ± 0.15	0.38 ± 0.05
bone	3.63 ± 0.72	3.56 ± 0.86	6.68 ± 1.61	20.61 ± 3.51

^a Mean ± standard deviation, *n* = 5.

Table III. Tissue Distribution of 6,6,16-[¹⁸F]Trifluoropalmitate (I) in Adult Rats^a

tissue	2 min	5 min	15 min	60 min
			%ID/g	
blood	0.38 ± 0.10	0.24 ± 0.07	0.30 ± 0.06	0.37 ± 0.15
lung	1.40 ± 0.20	1.37 ± 0.34	1.17 ± 0.33	1.23 ± 0.44
liver	6.78 ± 1.76	8.21 ± 2.15	6.59 ± 0.50	5.12 ± 0.91
muscle	0.27 ± 0.06	0.24 ± 0.05	0.24 ± 0.03	0.30 ± 0.04
heart	1.14 ± 0.25	0.99 ± 0.22	0.70 ± 0.15	0.76 ± 0.18
bone	0.16 ± 0.02	0.14 ± 0.02	0.29 ± 0.02	1.28 ± 0.12
			%ID/Organ	
blood	4.72 ± 0.94	2.64 ± 0.65	3.79 ± 0.78	4.51 ± 1.73
lung	1.49 ± 0.26	1.60 ± 0.45	1.30 ± 0.48	1.31 ± 0.40
liver	43.88 ± 5.66	48.00 ± 6.23	46.85 ± 3.67	31.86 ± 2.57
muscle	6.83 ± 1.62	5.44 ± 1.32	6.07 ± 0.73	7.40 ± 0.80
heart	0.69 ± 0.11	0.56 ± 0.13	0.43 ± 0.10	0.44 ± 0.14
bone	3.12 ± 0.37	2.41 ± 0.23	5.82 ± 0.40	24.31 ± 3.43

^a Mean ± standard deviation, *n* = 5.

initially high, but clearance is rapid from all tissues (Table V). Among the palmitic acids, there are marked differences in uptake efficiency by the heart and more subtle differences in retention of activity by the heart. Compared to [¹⁴C]palmitate, the heart activity at 2 min with fluoropalmitate is somewhat lower and that with the two trifluoropalmitates is considerably lower (Tables I–IV). This decreasing uptake upon progressive fluorine substitution parallels the increasing polarity of these compounds (see the Discussion section).

The retention of activity by the heart can best be appreciated in Figure 3, where the activity in the heart at 5, 15, and 60 min is shown as a percentage of the activity at 2 min. Heart activity with octanoate is lost most rapidly; activity loss with fluoropalmitate is next most rapid. Gem-

Table IV. Tissue Distribution of 7,7,16-[16-¹⁸F]Trifluoropalmitate (II) in Adult Rats^a

tissue	2 min	5 min	15 min	60 min
	%ID/g			
blood	0.89 ± 0.13	0.54 ± 0.10	0.60 ± 0.06	0.44 ± 0.06
lung	1.56 ± 0.25	1.18 ± 0.30	1.16 ± 0.21	0.94 ± 0.16
liver	6.21 ± 1.38	4.97 ± 0.78	5.13 ± 1.04	2.16 ± 0.43
muscle	0.27 ± 0.05	0.28 ± 0.03	0.33 ± 0.04	0.30 ± 0.03
heart	1.18 ± 0.24	0.89 ± 0.14	0.61 ± 0.06	0.45 ± 0.03
bone	0.22 ± 0.05	0.27 ± 0.06	0.62 ± 0.06	1.87 ± 0.52
	%ID/Organ			
blood	10.53 ± 1.42	6.91 ± 0.85	7.11 ± 0.54	5.26 ± 0.45
lung	1.69 ± 0.34	1.40 ± 0.13	1.42 ± 0.36	0.96 ± 0.22
liver	43.28 ± 5.54	37.05 ± 3.51	33.32 ± 5.97	15.04 ± 3.43
muscle	6.41 ± 0.83	7.33 ± 0.51	7.68 ± 0.89	7.32 ± 0.54
heart	0.67 ± 0.14	0.54 ± 0.08	0.33 ± 0.02	0.27 ± 0.01
bone	4.06 ± 0.96	5.47 ± 0.83	11.41 ± 0.81	34.96 ± 7.93

^a Mean ± standard deviation, *n* = 5.

inal difluorination of the ¹⁸F-labeled palmitate does result in significantly increased retention of activity by the heart. This is particularly true for 6,6,16-trifluoropalmitate (I), which is the isomer in which the blockage of β -oxidation is most likely (see the Introduction, Scheme I). Nevertheless, the improvement in heart activity retention with this compound over palmitate itself is not great.

The accumulation of activity in the bone, following injection of the ¹⁸F-labeled palmitates, indicates active metabolism that produces free fluoride ion. The time course of bone accumulation with these three compounds is shown in Figure 4. Activity accumulates most rapidly with 7,7,16-trifluoropalmitate (II), but even with fluoropalmitate (III) and 6,6,16-trifluoropalmitate (I), total bone activity at 60 min represents 20–25% of the injected dose. A reexamination of Figure 2 reveals that there is a roughly reciprocal relationship between liver and bone activities for the three ¹⁸F-labeled palmitic acids. 7,7,16-Trifluoropalmitate (II), which shows the most rapid decline in liver activity, also shows the most rapid increase in bone activity. Thus, metabolic release of fluoride ion from the liver is the most likely source of bone activity.

DISCUSSION

We have described the synthesis and tissue distribution of two new fatty acids labeled with fluorine-18, 6,6,16-[16-¹⁸F]trifluoropalmitic acid (I) and 7,7,16-[16-¹⁸F]-trifluoropalmitic acid (II), and have compared them with 16-[¹⁸F]fluoropalmitate (III), 1-[¹¹C]palmitate, and 1-[¹¹C]-octanoate. The synthesis of the trifluoropalmitic acids utilized a method we have developed for the geminal difluorination of 1,3-dithianes by halofluorination (18); the dithiane also served as a convenient assembly point for the synthesis of the internally functionalized fatty acids. The terminal fluorine, site of radiolabeling, was introduced by fluoride ion displacement of a triflate, a reaction that is readily adapted to labeling with fluorine-18. In this manner, the radiolabel was introduced in the penultimate step; only ester hydrolysis and HPLC purification were required to prepare the material for use in animals.

The two new trifluoropalmitic acid derivatives were designed in the hope that they would be good analogues for palmitic acid in terms of uptake by the heart but would be resistant to metabolism in the heart that releases radiolabel and thereby compromises the initial pattern of uptake. As was explained in the Introduction (Scheme I), β -oxidation, which can result in rapid degradation of fatty acids, releasing radiolabel both at the C-1 and at internal and terminal positions, should be blocked by the 6,6-difluoro (and possibly also by the 7,7-difluoro) substitution

in these palmitate analogues. The tissue distribution studies indicate, however, that these fluorine-substituted palmitic acids have significantly reduced uptake by the heart and that their retention by the heart is, at best, marginally improved over that of palmitate itself.

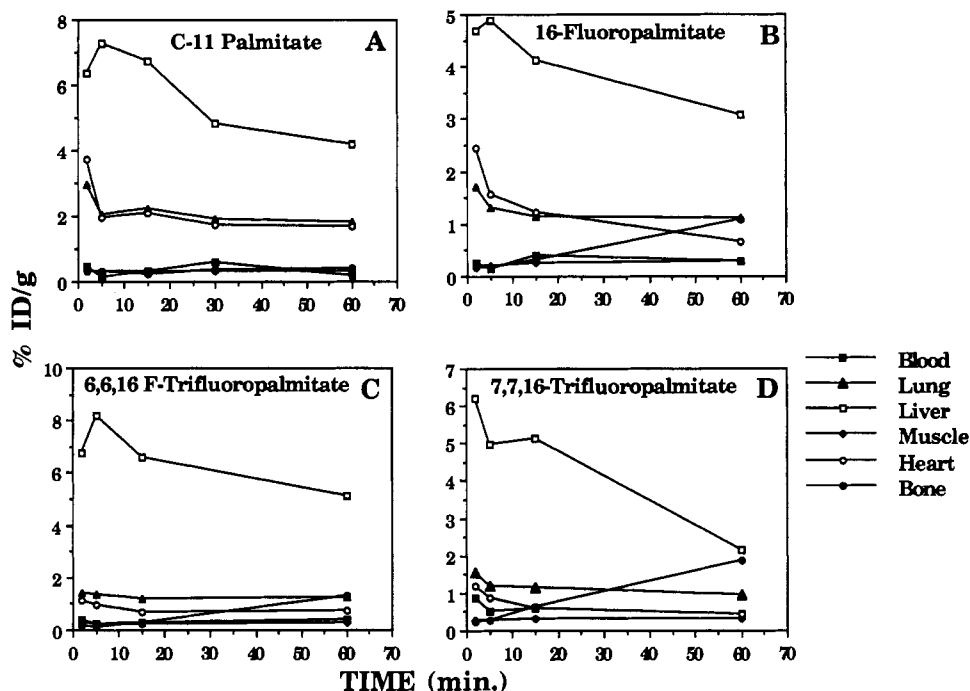
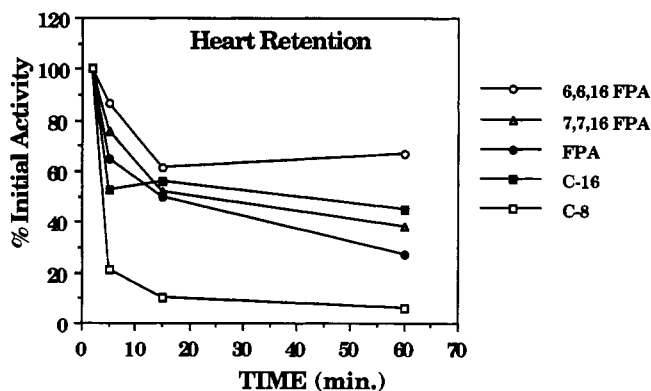
The reduced heart uptake of the fluoropalmitates vs palmitic acid itself could result from substantial physicochemical changes that occur upon fluorine substitution. Current literature contains many references to the increased lipophilicity imparted to molecules through incorporation of C–F bonds (23). While this is certainly true for aromatic C–F bonds, and while CF₃ is one of the most lipophilic groups available, the substitution of one or two fluorine atoms in place of hydrogen actually decreases the lipophilicity (24). This effect can be observed by comparing the HPLC traces of 16-[¹⁸F]fluoropalmitic acid and the corresponding C-6 and C-7 *gem*-difluoro analogues (Figure 1). The principles of reversed-phase HPLC dictate that more lipophilic compounds should be retained on the column as a result of favorable hydrophobic interactions between the compounds and the stationary phase. In fact, under conditions in which 16-fluoropalmitic acid elutes in 12.5 min, the trifluoropalmitic analogues elute in only 6 min, indicating that the *gem*-difluoro substitution creates a less lipophilic molecule. This reduced lipophilicity may be partially responsible for the lower heart uptake observed with these analogues.

Since transport of the fatty acids into the mitochondria (where β -oxidation occurs) occurs through a series of functionalization steps at the carboxyl group (25), we expected that substitution at any of the methylene groups in the middle of the chain would not affect the uptake and transport of the fatty acid. Recent reports, however, suggest that very specific interactions at particular points on the fatty acid chain may affect heart uptake. While Knapp and co-workers observed little discrimination between fatty acids substituted with tellurium at positions 6, 9, and 11 (6b), a dramatic decrease in myocardial uptake was observed when the tellurium atom was at position 13 (6a). Furthermore, in studies of *gem*-dimethyl-substituted fatty acids, substitution at C-4 produced at least a 2-fold increase in uptake compared to that with substitution at C-3, C-6, or C-9 (26). Obviously, the interactions involved in the uptake and transport of fatty acids are not straightforward, and the sites we have chosen for geminal difluorination (C-6 and C-7) could interfere with myocardial uptake and transport processes. Perhaps the *gem*-difluoromethylene substitution at a different position along the chain would lead to analogues possessing high heart uptake.

The retention of activity by the heart, following injection of the fluoropalmitates, is not dramatically different from that of palmitate itself: 16-[¹⁸F]fluoropalmitate is cleared somewhat more rapidly than palmitate itself; the two trifluoropalmitates have slower clearance patterns, particularly 6,6,16-trifluoropalmitate (I) (cf. Figure 3). The reduced clearance rates of the trifluoropalmitates vs 16-fluoropalmitate suggests that geminal difluorination may, indeed, be blocked in these compounds, particularly since clearance is slowest with the isomer (I) in which the blockage of β -oxidation is most likely (see the Introduction, Scheme I). Nevertheless, the clearance rate for 6,6,16-trifluoropalmitate (I) is not markedly slower than for palmitate itself and other modes of oxidation may be operating to release ¹⁸F label from these compounds. Other modes of oxidative degradation of fatty acids are known (ω and ω -1) (27). These involve cytochrome P-450 mixed function

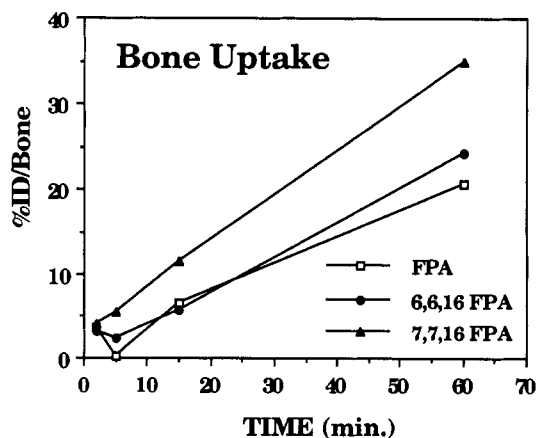
Table V. Tissue Distribution of [1-¹¹C]Octanoate in Adult Rats^a

tissue	2 min	5 min	15 min	30 min	60 min
	%ID/g				
blood	0.93 ± 0.14	0.48 ± 0.13	0.31 ± 0.03	0.23 ± 0.04	0.20 ± 0.03
lung	2.05 ± 0.43	1.76 ± 0.19	1.12 ± 0.16	0.71 ± 0.19	0.51 ± 0.01
liver	3.56 ± 0.62	2.66 ± 0.07	1.54 ± 0.45	1.02 ± 0.38	0.79 ± 0.29
muscle	0.17 ± 0.04	0.26 ± 0.09	0.24 ± 0.05	0.16 ± 0.02	0.14 ± 0.04
heart	4.02 ± 1.10	0.84 ± 0.28	0.41 ± 0.06	0.26 ± 0.03	0.24 ± 0.01
	%ID/Organ				
blood	11.97 ± 1.61	5.80 ± 1.22	3.94 ± 0.43	3.06 ± 0.59	2.58 ± 0.47
lung	2.99 ± 0.71	2.28 ± 0.63	1.27 ± 0.12	0.85 ± 0.15	0.55 ± 0.05
liver	22.07 ± 4.36	16.80 ± 1.33	9.10 ± 2.19	6.91 ± 2.52	5.34 ± 1.69
muscle	4.29 ± 0.82	6.33 ± 1.67	6.24 ± 1.18	4.26 ± 0.46	3.68 ± 1.06
heart	2.23 ± 0.54	0.44 ± 0.11	0.25 ± 0.06	0.18 ± 0.01	0.15 ± 0.01

^a Mean ± standard deviation, *n* = 4.**Figure 2.** Summary of tissue distribution of activity following the injection of 1-[¹¹C]palmitate and the fluorine-substituted palmitate analogues in the rat. In each case 150–200-g rats were injected iv with the indicated compound, and the tissue distribution was determined at the indicated times. Data are taken from Tables I–IV; further details are given in the text and the Experimental Procedures.**Figure 3.** Summary of heart retention of activity after injection of 1-[¹¹C]octanoate (C-8), [1-¹¹C]palmitate (C-16), and the [¹⁸F]-fluoropalmitate analogues (16-FPA, 6,6,16-FPA, and 7,7,16-FPA). Data taken from Tables I–V.

oxidases and have been most well-characterized in liver (25) but may also occur in heart as well as in other tissues (27).

The fact that 20–35% of the injected dose of all three of the fluorine-18 labeled fatty acids ends up in bone at 60 min indicates that a substantial fraction of metabolism,

**Figure 4.** Summary of accumulation of activity in bone after injection of 16-[¹⁸F]fluoropalmitate (FPA), 6,6,16-[16-¹⁸F]-trifluoropalmitate (6,6,16-FPA), and 7,7,16-[16-¹⁸F]trifluoropalmitate (7,7,16-FPA). Data are taken from Tables II–IV.

probably occurring principally in the liver, results in the release of free fluoride ion (28). While the strength of the carbon-fluorine bond (106 kcal/mol) (12) is frequently cited as a reason for the metabolic inertness of certain

fluorine-substituted compounds, metabolic inertness is more a characteristic of perfluorinated rather than monofluorinated substances. In fact, the electronic characteristics of fluorine are unusual, being electron withdrawing by an inductive effect but electron supplying through resonance. As a result, a cationic center α to a fluorine substituent is stabilized (29), the stabilizing effect of fluorine on carbocations lying between that of a hydrogen and a methyl group. So, whereas sites β to fluorine substitution are deactivated toward an electrophilic oxidative metabolic event (because the β -position experiences only the inductive, electron-withdrawing effect of fluorine), the site α to fluorine might actually be activated (due to the resonance contribution).

CONCLUSION

The development of improved myocardial metabolic imaging agents remains an intriguing goal. Structural and functional alterations in the fatty acid molecule, introduced to provide greater resistance to release of the label through metabolism, need to preserve both the physicochemical properties of the molecule, as well as the detailed sites of its interaction with proteins involved in uptake and transport in the myocardium. The trifluoropalmitic acids we have prepared here are not better myocardial imaging agents than palmitate, largely because their uptake by the heart is low (probably because of their increased polarity). On the basis of our design and results, it is reasonable to assume that geminal difluorination of an internal methylene group of a fatty acid has interrupted β -oxidation (at least with I), the principal oxidative metabolic route of fatty acids in the heart, and the retention of ^{18}F label by the heart is somewhat improved by geminal difluorination (I > II > III; although the retention of I is still not markedly better than that of palmitate itself). High bone activity signals the fact that the chain-terminal ^{18}F is still vulnerable to other oxidative, metabolic processes (possibly ω -oxidation), and while most bone activity probably results from metabolism of these fatty acids in the liver, these other oxidative processes may also contribute to the loss of label from the heart.

ACKNOWLEDGMENT

We are grateful for support of this work through grants from the National Institute of Health (Grant PHS 5RO1 CA 25836 to J.A.K.) and the Department of Energy (Grant DE FG02 84ER 60218 to M.J.W.). We are most appreciative for the assistance of Carla J. Mathias and Carmen S. Dence.

LITERATURE CITED

- (1) Council on Scientific Affairs (1988) Application to Positron Emission Tomography in the Heart. *J. Am. Med. Assoc.* 259, 2438-2445.
- (2) Jones, G. S., Livni, E., Strauss, H. W., Hanson, R. N., and Elmaleh, D. R. (1988) Synthesis and Biologic Evaluation of 1-[^{11}C]-3,3-Dimethylheptadecanoic Acid. *J. Nucl. Med.* 29, 68-72 and references cited therein.
- (3) Livni, E., Elmaleh, D. R., Levy, S., Brownell, G. L., and Strauss, W. H. (1982) Beta-methyl 1-[^{11}C]heptadecanoic Acid: A New Myocardial Metabolic Tracer for Positron Emission Tomography. *J. Nucl. Med.* 27, 521-531.
- (4) (a) Freundlieb, C., Höck, A., Vyska, K., Feinendegen, L. E., Machulla, H.-J., and Stöcklin, G. (1980) Myocardial Imaging and Metabolic Studies with [17- ^{129}I]Iodoheptadecanoic Acid. *J. Nucl. Med.* 21, 1043-1050. (b) Reske, S. N., Knapp, F. F., Jr., and Winkler, C. (1986) Experimental Basis of Metabolic Imaging of the Myocardium with Radioiodinated Aromatic Free Fatty Acids. *A. J. Physiol. Imaging* 1, 214-229. (c) Eisenhut, M., and Liefhold, J. (1988) Radioiodinated *p*-Phenylene Bridged Fatty Acids as New Myocardial Imaging Agents: Syntheses and Biodistribution in Rats. *Appl. Radiat. Isot.* 39, 639-649.
- (5) (a) Knapp, F. F., Goodman, M. M., Callahan, A. P., and Kirsch, G. (1986) Radioiodinated 15-(*p*-Iodophenyl)-3,3-Dimethylpentadecanoic Acid: A Useful New Agent to Evaluate Myocardial Fatty Acid Uptake. *J. Nucl. Med.* 23, 169-175. (b) Ambrose, K. R., Owen, B. A., Goodman, M. M., and Knapp, F. F., Jr. (1987) Evaluation of the Metabolism in Rat Hearts of Two New Radioiodinated 3-Methyl-Branched Fatty Acid Myocardial Imaging Agents. *Eur. J. Nucl. Med.* 12, 486-491. (c) Som, P., Oster, Z. H., Kubota, K., Goodman, M. M., Knapp, F. F., Jr., Sacker, D. F., and Weber, D. A. (1989) Studies of a New Fatty Acid Analog (DMIVN) in Hypertensive Rats and the Effect of Verapamil Using ARG Microimaging. *Nucl. Med. Biol.* 16, 483-490.
- (6) (a) Knapp, F. F., Goodman, M. M., Callahan, A. P., Ferren, L. A., Kabalka, G. W., and Sastry, K. A. R. (1983) New Myocardial Imaging Agents: Stabilization of Radioiodine as a Terminal Vinyl Iodide Moiety on Tellurium Fatty Acids. *J. Med. Chem.* 26, 1293-1300. (b) Knapp, F. F., Ambrose, K. R., Callahan, A. P., Ferrin, L. A., Grigsby, R. A., and Irgolic, K. J. (1981) Effects of Chain Length and Tellurium Position on the Myocardial Uptake of Tellurium-123m Labeled Fatty Acids. *J. Nucl. Med.* 22, 988-993.
- (7) Abendschein, D. R., Fox, K. A. A., Ambos, K. R., Sobel, B. E., and Bergmann, S. R. (1987) Metabolism of Beta-Methyl-[1- ^{14}C]Heptadecanoic Acid in Canine Myocardium. *Nucl. Med. Biol.* 14, 579-585.
- (8) Knust, E. J., Kupfernagel, Ch., and Stöcklin, G. (1979) Long-Chain F-18 Fatty Acids for the Study of Regional Metabolism in Heart and Liver; Odd-Even Effects of Metabolism in Mice. *J. Nucl. Med.* 20, 1170-1175.
- (9) Berridge, M. S., Tewson, T. J., and Welch, M. J. (1983) Synthesis of ^{18}F -Labeled 6- and 7-Fluoropalmitic Acids. *Int. J. Appl. Radiat. Isot.* 34, 727-730.
- (10) Berridge, M. S. (1980) The Synthesis of Radiopharmaceuticals Labeled with Short-Lived Isotopes. Ph.D. Dissertation, Washington University, St. Louis, Missouri.
- (11) Palmer, A. J., Clark, J. C., and Goulding, R. W. (1977) The Preparation of Fluorine-18 Labeled Radiopharmaceuticals. *Int. J. Appl. Radiat. Isot.* 28, 53-65.
- (12) Smith, F. A. (1973) Biological Properties of Compounds Containing the C-F Bond. *Chemtech* 422-429.
- (13) Still, W. C., Kahn, M., and Mitra, A. (1978) Rapid Chromatographic Technique for Preparative Separations with Moderate Resolution. *J. Org. Chem.* 43, 2923-2925.
- (14) (a) Steere, N. V., Ed. (1971) *CRC Handbook of Laboratory Safety* 2nd ed. pp 45-57, CRC Press, Boca Raton, FL. (b) Committee on Hazardous Substances in the Laboratory (1981) *Prudent Practices for Handling Hazardous Chemicals in Laboratories* pp 43-45, National Academy Press, Washington, DC.
- (15) Kilbourn, M. R., Jerabek, P. A., and Welch, M. J. (1985) An Improved [^{18}O]Water Target for [^{18}F]Fluoride Production. *Int. J. Appl. Radiat. Isot.* 36, 327-28.
- (16) Brodack, J. W., Kilbourn, M. R., Welch, M. J., and Katzenellenbogen, J. A. (1986) NCA 16 α -[^{18}F]Fluoroestradiol-17 β : The Effect of Reaction Vessel on Fluorine-18 Resolubilization, Product Yield, and Effective Specific Activity. *Int. J. Appl. Radiat. Isot.* 37, 217.
- (17) Welch, M. J., Dence, C. S., Marshall, D. R., and Kilbourn, M. R. (1983) Remote System for Production of Carbon-11 Labeled Palmitic Acid. *J. Labeled Compd. Radiopharm.* 20, 1087-1095.
- (18) Sondej, S. C., and Katzenellenbogen, J. A. (1986) gem-Difluoro Compounds: A Convenient Preparation from Ketones and Aldehydes by Halogen Fluoride Treatment of 1,3-Dithiolanes. *J. Org. Chem.* 51, 3508-3513.
- (19) Corey, E. J., and Raju, N. (1983) A New General Synthetic Route to Bridged Carboxylic Ortho Esters. *Tetrahedron Lett.* 24, 5571-5574.
- (20) Fried, J., Kwok, P.-Y., Muellner, F. W., and Chen, C.-K. (1987) Total Synthesis of 7,7-, 10,10-, and 13,13-Difluoroarachidonic acids. *J. Am. Chem. Soc.* 109, 3684-3692.

- (21) (a) Beynon, J. H., Saunders, R. A., and Williams, A. E. (1988) *The Mass Spectra of Organic Molecules* pp 382-383, Elsevier, Amsterdam. (b) Beynon, J. H. (1960) *Mass Spectrometry and its Applications to Organic Chemistry* pp 413-415, Elsevier, Amsterdam.
- (22) Hamacher, K., Coenen, H. H., and Stöcklin, G. (1986) Efficient Stereospecific Synthesis of No-Carrier-Added 2- ^{18}F -fluoro-2-deoxy-D-glucose Using Aminopolyether Supported Nucleophilic Substitution. *J. Nucl. Med.* 27, 235-238.
- (23) Mann, J. (1987) Modern Methods for the Introduction of Fluorine into Organic Molecules: An Approach to Compounds with Altered Chemical and Biological Activities. *J. Chem. Soc. Rev.* 16, 381-436.
- (24) Hansch, C., and Leo, A. (1979) *Substituent Constants for Correlation Analysis in Chemistry and Biology* Wiley & Sons: New York.
- (25) White, A., Handler, P., and Smith, E. L. (1978) *Principles of Biochemistry* 6th ed. McGraw-Hill: New York.
- (26) Goodman, M. M., Goudonnet, A., and Knapp, F. F. (1987) The Position of Geminal Dimethyl-Substitution Affects Myocardial Uptake and Clearance Kinetics of DMIPP Analogs in Fasted Rats. *J. Nucl. Med.* 28, 570.
- (27) (a) Masters, B. S. S., Okita, R. T., Williams, D. E., Hale, S. E., Muerhoff, A. S., and Hevner, R. F. Prostaglandin and Fatty Acids ω and (ω -1) Hydroxylation Cytochromes P-450 in Extrahepatic Tissues. *Microsomes and Drug Oxidations, Proceedings of the 6th International Symposium*, 1984 (1985) (A. R. Boobis, Ed.) pp 74-83, Taylor and Francis: London, U.K. (b) Wahle, K. W., Hare, W. R., and Paterson, S. M. (1978) Aspects of ω and (ω -1) Oxidation of Fatty Acids by Microsomal Preparations from Sheep. *Biochem. Soc. Trans.* 6, 1158-1159.
- (28) Wallace-Durbin, P. (1954) The Metabolism of Fluorine in the Rat Using ^{18}F as a Tracer. *J. Dental Res.* 33, 789-800.
- (29) (a) Lowry, T. H., and Richardson, K. S. (1980) *Mechanism and Theory in Organic Chemistry* 2nd ed., pp 130-145, Harper and Row, New York. (b) Olah, G. A., and Mo, Y. K. (1973) Fluorinated Carbocations. *Adv. Fluorine Chem.* 7, 69-112. (c) Johnson, W. F., Daub, G. W., Lyle, T. A., and Niwa, M. (1980) Vinyl Fluoride Function as a Terminator of Biomimetic Polyene Cyclizations Leading to Steroids. *J. Am. Chem. Soc.* 102, 7800-7802.
- Registry No.** 1, 112-45-8; 2, 73813-71-5; 3, 127946-90-1; 4, 2067-33-6; 5, 4509-90-4; 6, 113331-76-3; 7, 113331-77-4; 8, 127946-91-2; 9, 127971-23-7; 10, 127946-92-3; 11, 127946-93-4; 12, 127946-94-5; 13, 127946-95-6; 14, 127946-96-7; 15, 127946-97-8; 16, 127946-98-9; 17, 13019-22-2; 18, 39770-05-3; 19, 127946-99-0; 20, 127947-00-6; 21, 4224-70-8; 22, 22809-37-6; 23, 127947-01-7; 24, 127947-02-8; 25, 127947-03-9; 26, 127947-04-0; 27, 127947-05-1; 28, 127947-06-2; 29, 127947-07-3; 30, 127947-08-4; 31, 127947-09-5; 32, 127947-10-8; 33, 127947-11-9; 34, 109-29-5; 35, 36575-67-4; 36, 127947-12-0; 37, 127947-13-1; I, 127947-14-2; ^{18}F -I, 127947-15-3; II, 127947-16-4; ^{18}F -II, 127947-17-5; III, 3109-58-8; ^{18}F -III, 71029-19-1; $\text{HS}(\text{CH}_2)_3\text{SH}$, 109-80-8; $(\text{CF}_3\text{SO}_2)_2\text{O}$, 358-23-6; 3-methyloxelane, 3143-02-0; ^{11}C palmitate, 59694-42-7; ^{11}C octanoate, 65251-17-4.

Preparation of Antigastric Cancer Monoclonal Antibody MGb₂-Mitomycin C Conjugate with Improved Antitumor Activity

Song Li,*† Xue-Yong Zhang,† Su-Yin Zhang,† Xi-Tao Chen,† Ling-Ji Chen,† Yu-Hua Shu,† Jia-Liu Zhang,† and Dai-Ming Fan†

Laboratory of Gastroenterology, Xijing Hospital, Xi'an, Shaanxi Province 710032, China, and Shanghai Institute of Materia Medica, Chinese Academy of Sciences, Shanghai 200031, China. Received February 28, 1990

In the present study, an antigastric cancer monoclonal antibody, MGb₂, was chosen to prepare antibody-mitomycin C conjugate with dextran T-40 as intermediary. Up to 20 molecules of mitomycin C were specifically bound per molecule of antibody, without significantly impairing the antigen-binding capacity of the antibody and the pharmacological activity of mitomycin C. The conjugate showed selective cytotoxicity upon human gastric cancer cell line SGC-7901 in vitro. Radioimmunoimaging and biodistribution studies indicated that, after conjugation with mitomycin C via dextran T-40 as intermediary, the tumor localization capacity of the antibody was well-retained. When tested in nude mice inoculated with human gastric carcinoma GAI in bilateral subrenal capsules, intraperitoneal injection of the conjugate twice a week for 3 weeks at the dose of 1 mg/kg of drug gave a tumor inhibitory rate of 152.29%, the result being far better than that of free mitomycin C or an irrelevant conjugate. A similar result was found in another nude mouse model of human gastric carcinoma SGC-7901. Meanwhile, after conjugation with antibody, the toxicity of mitomycin C on tested animals was significantly reduced.

INTRODUCTION

Although it has been years since anticancer therapy developed, there are still many problems in the treatment of gastric cancer. Most cases are inoperable in the late stage. Conventional chemotherapy also has a drawback, that is, agents effective in killing neoplastic cells also have detrimental effects on normal cells, thus limiting the amount of drugs given (1). One possible approach to overcome these limitations is to attach anticancer agents to monoclonal antibodies against gastric cancer so that the toxicity could be selectively restricted to tumor cells. It could improve therapeutic effect, minimize toxic effect, and overcome the resistance of tumors against free drugs (2). Recently, a hybridoma cell line which produces an antigastric cancer IgG₁ monoclonal antibody (MGb₂) was established in our laboratory (3). Previous studies showed that it was highly specific against tumor cells and could be well-localized in the tumor tissues in nude mice bearing human gastric carcinoma xenografts and even in the patients with gastric cancer (4). In the present study, MGb₂ was chosen to prepare antibody-MMC¹ conjugate via dextran T-40 as intermediary; the in vitro and in vivo cytotoxic effect of the conjugate upon human gastric cancer cells was investigated.

EXPERIMENTAL PROCEDURES

Cells and Medium. Human gastric cancer cell line SGC-7901 was obtained from Dr. X. W. Feng, Academy of Military Medical Sciences, Beijing, China. Human normal embryonic lung cell line SL₇ was kindly provided by Dr. L. S. Tan, Shanghai First Pulmonary Disease Hospital, Shanghai, China. They were grown as mono-

layers in RPMI 1640 (GIBCO) supplemented with 10% fetal calf serum (Lan Zhou Institute of Biological Products, Lan Zhou, China). The cells were routinely passaged after detachment with trypsin/0.2% EDTA.

Animals and Tumor Models. Nude mice of Swiss-DF-nu/nu and BALB/c-nu/nu genetic background (Shanghai Institute of Materia Medica, Shanghai, China) were used for the passage, tumor inoculation, and the in vivo studies. They were maintained under SPF conditions.

SGC-7901 cloned human gastric carcinoma previously established in ascitic form from cultured cell line and maintained in Swiss-DF nude mice was used as a source of solid tumor. The solid tumor was induced by inoculating the tumor cell suspension (in ascitic fluid) subcutaneously. It was revealed to possess fast growth and a short latent period of 3-4 days. Ten days after the inoculation, the tumor could reach 1 cm in diameter.

The human gastric carcinoma GAI was established in the Department of Pathology of Beijing Medical University and maintained in BALB/c nude mice by serial transplantation with a duration of 4-5 weeks.

Monoclonal Antibody MGb₂. The monoclonal antibody (IgG₁) was prepared in BALB/c mice by hybridoma clone established in our laboratory and purified from ascitic fluid by (NH₄)₂SO₄ precipitation and ion-exchange chromatography on DEAE-cellulose (DE-52).

Preparation of Immunoconjugates. Dextran T-40 was oxidized by the following Malaprade reaction (5). Dextran T-40 (Pharmacia) (1.0 g) was mixed with sodium periodate (0.33 g) in 200 mL of distilled water and incubated overnight at room temperature in the dark. The oxidized dextran was then dialyzed extensively against distilled water and lyophilized. Sixty milligrams of PAD was incubated with 20 mg of MGb₂ in 2 mL of 0.1 M PBS, pH 7.2, for 24 h at 4 °C, following which 12 mg of MMC (Kyowa Hakko Co., Tokyo, Japan) in 4 mL of PBS was added. The solution was stirred for another 24 h. The Schiff bases thus formed were then reduced by the addition of 0.1 mL of sodium borohydride PBS solution (1 mg/mL). The

* Xijing Hospital.

† Chinese Academy of Sciences.

¹ Abbreviations: MMC, mitomycin C; PAD, polyaldehyde dextran; PBS, phosphate-buffered saline; SPECT, single photon emission computed tomography; SPF, specific pathogen free.

reaction mixture was incubated with the reducing agent for 2 h at 4 °C and then applied to a Sephadex G-200 column (1.8 × 65 cm) equilibrated with PBS. The antibody peak was collected and analyzed for the MMC/IgG molar ratio. The concentration of MMC was determined by measuring the absorbance at 363 nm. Dextran concentration was determined by the modified anthrone-sulfuric acid method (6). The IgG concentration was measured by the Bio-Rad protein assay (7).

Similarly, normal mouse IgG-PAD-MMC (irrelevant conjugate) was prepared.

Determination of Antibody Activity in the Conjugate. Indirect enzyme linked immunosorbent assay was employed to evaluate the antigen-binding capacity of the conjugate. Human gastric cancer cells SGC-7901 were plated in a tissue-culture plate with 40 flat-bottomed wells and fixed with 0.25% glutaraldehyde. Different dilutions of conjugate and free antibody in 0.1 mL was added. Following incubation at 37 °C for 1 h, rabbit antimouse immunoglobulin G antibody labeled with horseradish peroxidase (Tianjing Institute of Hematology, Tianjing, China) was added. The peroxidase reaction was initiated by the addition of *o*-phenylenediamine and the optical density at 495 nm of each well was recorded.

Cytotoxicity Assay. The tetrazolium dye colorimetric assay was used in the cytotoxicity test with human gastric cancer cell line SGC-7901 as target and human normal embryonic lung cell line SL₇ as nontarget as described previously (8). The cytotoxic effect of MGB₂-PAD-MMC was compared with that of free MMC and irrelevant conjugate.

Stability Study. To assess the release of MMC from the antibody-PAD-MMC conjugate, MGB₂-PAD-MMC conjugate was incubated under the physiological conditions of pH 7.4 and 37 °C. The MMC remaining in the conjugate was determined after gel filtration on Sephadex G-25. MGB₂ IgG content in the conjugate after gel filtration was also determined.

Iodination of MGB₂-PAD-MMC Conjugate. MGB₂-PAD-MMC was labeled with ¹²⁵I (Institute of Atomic Energy, Beijing, China) by the chloramine-T method (9) to a specific activity of 3.4 μCi/μg of protein.

Imaging and Biodistribution Study. For the imaging and biodistribution study, six Swiss-DF nude mice bearing human gastric carcinoma SGC-7901 about 1.5 cm × 1.5 cm in size at 2 weeks posttransplantation of 1–2 mm³ tissues into their right flank were used. The mice were divided into two groups and were then given intraperitoneal injections of radiolabeled MGB₂-PAD-MMC and irrelevant conjugate respectively at a dose of 10 μCi per mouse. Ninety-six hours following the administration, the mice had SPECT taken and were then sacrificed. Blood, tumor, and tissue samples were taken, weighed, and assayed for radioactivity. The result of analysis was expressed as the ratio of radioactivity per milligram of tumor to that per milligram of blood or tissue (T/NT).

Inhibitory Effect of MGB₂-PAD-MMC on the Growth of Human Gastric Carcinoma SGC-7901. The subrenal capsule assay was used to investigate the in vivo therapeutic effect of the conjugate (10, 11). Treatment was initiated soon after fragments (about 1 mm³ in size) of tumor tissue were inoculated under bilateral renal capsules. MGB₂-PAD-MMC, free MMC, free MGB₂, a mixture of MMC and MGB₂, irrelevant conjugate, and saline were given intraperitoneally daily for 6 days at the dose of 1 mg/kg of drug. Eight days after the tumor inoculation, the mice were sacrificed by cervical dislocation. Kidneys were removed and the final in situ tumor size

Table I. Enzyme Linked Immunosorbent Assay of Binding of MGB₂-PAD-MMC and Free MGB₂ to Human Gastric Cancer Cells SGC-7901

concn, nmol/L	absorbance at 495 nm ^a	
	MGB ₂ -PAD-MMC	MGB ₂
300	1.24	1.53
30	0.87	1.04
3	0.43	0.73
0.3	0.14	0.27

^a (*A*_{495nm})_{control} = 0.043.

measurements were taken. The in vivo antitumor activity of the tested agents were evaluated by analyzing the change in tumor size pre- and posttreatment.

Similarly, the inhibitory effect of MGB₂-PAD-MMC and MMC in different dose level (1, 2, 3 mg/kg) on the tumor growth was also studied.

Inhibitory Effect of MGB₂-PAD-MMC on the Growth of Human Gastric Carcinoma GAIL. The subrenal capsule assay was also employed to assess the in vivo cytotoxic effect of MGB₂-PAD-MMC conjugate on a slow-growing human gastric carcinoma GAIL. Treatment was initiated the day after tumor inoculation. MGB₂-PAD-MMC, MGB₂, MMC, irrelevant conjugate, and saline were given twice a week for 3 weeks at the dose of 1 mg/kg of drug. Eighteen days after tumor inoculation, the mice were sacrificed. The next steps were performed as described above.

RESULTS

Preparation of Conjugate and Its Immunoreactivity. According to the methods described above, MGB₂-PAD-MMC was successfully prepared. It was calculated that the MGB₂/PAD/MMC molar ratio in the conjugate was about 1:1.4:20 with the protein-recovery rate being 72%. On this basis, it was estimated that the average molecular weight of the MGB₂-PAD-MMC conjugate was around 220 kDa. This was confirmed by the gel-filtration profile of MGB₂-PAD-MMC on Sephadex G-200 (data not shown).

Table I shows the antibody activity of the conjugate, as measured by indirect enzyme linked immunosorbent assay. The MGB₂-PAD-MMC conjugate retained up to 50% of the antibody activity, compared with that of equimolar amount of unmodified antibody. At the concentration of 3 nmol/L, the conjugate could still be bound to tumor cells.

Cytotoxic Effect of MGB₂-PAD-MMC Conjugate. The 48-h cytotoxic effect of MGB₂-PAD-MMC, free MMC, and irrelevant conjugate on target cells and nontarget cells is shown in Figure 1. The cytotoxicity of MGB₂-PAD-MMC on human gastric cancer cell line SGC-7901 was quite similar to that of free MMC, but greater than that of irrelevant conjugate (*p* < 0.01). Compared with free MMC, the MGB₂-PAD-MMC conjugate had only a little effect on nontarget cells, similar to that of irrelevant conjugate (*p* > 0.05).

Figure 2 shows the cytotoxic activity of MGB₂-PAD-MMC on target cells and nontarget cells after a 30-min exposure to the conjugate. The cytotoxic effect of MGB₂-PAD-MMC on target cells was greater than that of free MMC (*p* < 0.01). In contrast, MGB₂-PAD-MMC showed statistically less cytotoxic effect than MMC against nontarget cells (*p* < 0.01). MMC exhibited comparable cytotoxicity to target cells and nontarget cells.

Stability of the Conjugate. Figure 3 shows the time course for MMC remaining in the conjugate. The release of MMC from the conjugate was less than 10% of the original content in the conjugate during incubation in PBS

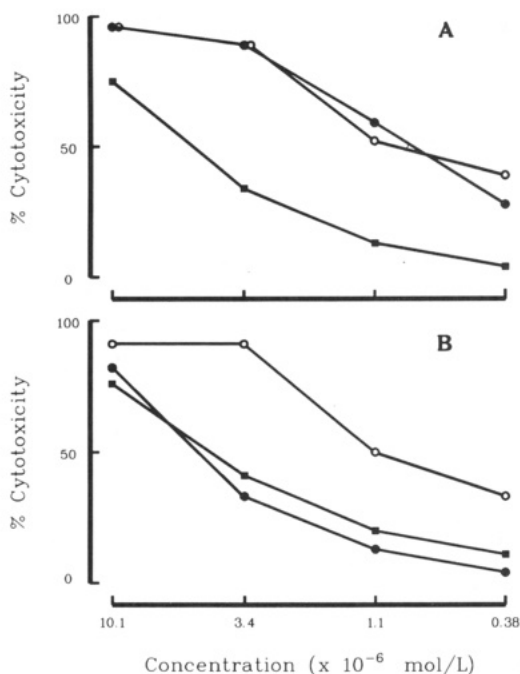


Figure 1. Cytotoxic effects of antigastric cancer monoclonal antibody MGB₂-PAD-MMC (●), free MMC (○), and normal mouse IgG-PAD-MMC (■) on (A) human gastric cancer cell line SGC-7901 and (B) human normal embryonic lung cell line SL7. Cells (2×10^5 /mL) were cultured with the test drugs for 48 h.

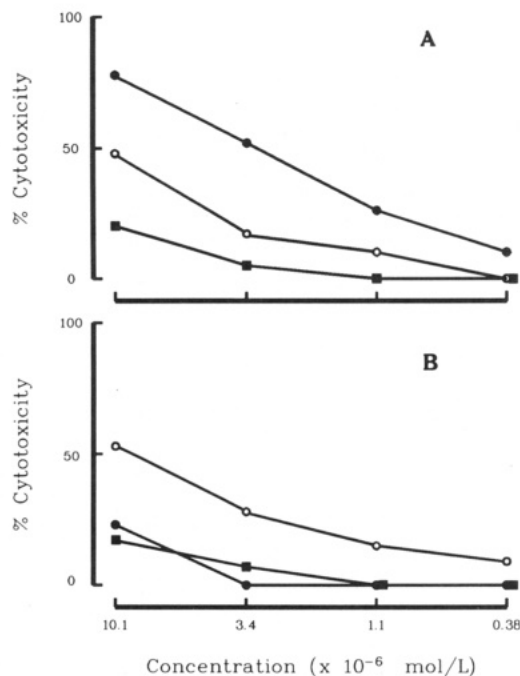


Figure 2. Cytotoxic effects of antigastric cancer monoclonal antibody MGB₂-PAD-MMC (●), free MMC (○), and normal mouse IgG-PAD-MMC (■) on (A) human gastric cancer cell line SGC-7901 and (B) human normal embryonic lung cell line SL7. Cells (2×10^5 /mL) were cultured for 48 h after a 30-min drug exposure.

at 37 °C for 3 days. MGB₂ IgG content in the conjugate was not changed, suggesting that MGB₂-MMC coupled by a dextran bridge was stable.

Tumor Localization of MGB₂-PAD-MMC Conjugate in Nude Mice with Tumor Xenografts. Table II shows the result of biodistribution study of ¹²⁵I-MGB₂-PAD-MMC and ¹²⁵I-normal mouse IgG-PAD-MMC conjugate. It could be seen that MGB₂-PAD-MMC conjugate was taken up by the tumor preferentially. SPECT imaging confirmed the result of biodistribution

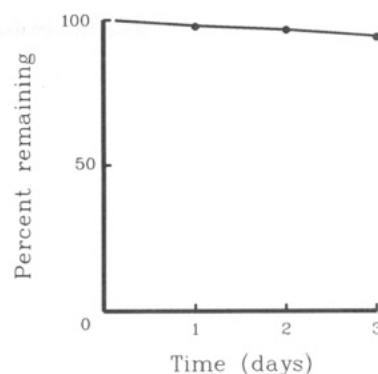


Figure 3. Time course of MMC in MGB₂-PAD-MMC conjugate. MGB₂-PAD-MMC in 0.1 M PBS, pH 7.4, was incubated at 37 °C. The MMC remaining in the conjugate was determined after gel filtration on Sephadex G-25.

Table II. Biodistribution of ¹²⁵I-MGB₂-PAD-MMC and ¹²⁵I-Normal Mouse IgG-PAD-MMC Conjugate in Swiss-DF Nude Mice Bearing Human Gastric Carcinoma SGC-7901

tissues	T/NT ^a	
	MGB ₂ -PAD-MMC	normal mouse IgG-PAD-MMC
blood	0.79 ± 0.03	0.19 ± 0.013
heart	2.62 ± 0.72	0.83 ± 0.240
lung	1.65 ± 0.14	0.34 ± 0.100
liver	3.46 ± 0.56	1.03 ± 0.270
spleen	3.46 ± 0.71	0.93 ± 0.210
kidney	4.11 ± 0.88	0.86 ± 0.190
stomach	5.50 ± 1.38	1.31 ± 0.320

^a Ratio of radioactivity per milligram of tumor to that per milligram of nontumor tissues.

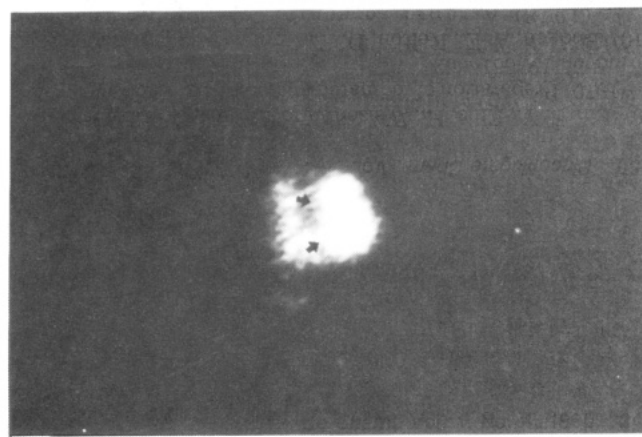


Figure 4. Immunoscintigraphy performed by emission computed tomography (SPECT) at 96 h after injection of 10 μCi of ¹²⁵I-MGB₂-PAD-MMC conjugate.

study. ¹²⁵I-MGB₂-PAD-MMC could visualize tumors clearly while ¹²⁵I-normal mouse IgG-PAD-MMC showed negative results (Figure 4).

In Vivo Inhibitory Effect of MGB₂-PAD-MMC on the Growth of Human Gastric Carcinoma SGC-7901. Table III shows the response of SGC-7901 gastric carcinoma growing under the renal capsules of nude mice to MGB₂-PAD-MMC conjugate, irrelevant conjugate, free MGB₂, free MMC, MMC mixed with but not conjugated to MGB₂, and saline. Significant responses were found in those groups treated with MGB₂-PAD-MMC conjugate, free MMC, and a mixture of MMC with MGB₂, while MGB₂-PAD-MMC conjugate showed greater inhibitory effect on tumor growth than MMC or the mixture of MMC with MGB₂ did. No synergetic effect was found with regard to the mixture of MMC with MGB₂.

Table III. Inhibitory Effects of MGb₂-PAD-MMC, MGb₂, MMC, a Mixture of MGb₂ with MMC, and Normal Mouse IgG-PAD-MMC on the Growth of Human Gastric Carcinoma SGC-7901 Implanted under Renal Capsules in Swiss-DF Nude Mice^a

agents tested	dose, mg/kg	tumor size (omu ^b)		change in tumor size (day 8-day 0)	% inhibition rate
		initial	final		
MGb ₂ -PAD-MMC	1	11.13 ± 0.75	20.88 ± 1.10	9.75 ± 1.26	68.55 ^{c,d}
MGb ₂	10	12.63 ± 0.63	39.88 ± 2.93	27.25 ± 2.40	12.00
MMC	1	12.63 ± 0.63	30.38 ± 3.45	17.75 ± 2.40	42.74 ^c
MGb ₂ + MMC	1	13.00 ± 1.08	29.88 ± 1.80	16.88 ± 1.84	45.50 ^c
normal mouse IgG-PAD-MMC	1	11.00 ± 0.91	37.88 ± 3.82	26.88 ± 4.26	13.29
saline control		11.50 ± 0.95	42.50 ± 3.85	31.00 ± 3.92	

^a Two mice (four capsules) per test group; four mice (eight capsules) in control group. ^b Omu, ocular micrometer units; 1 mm = 10 omu. ^c $p < 0.001$ (vs control). ^d $p < 0.001$ (conjugate vs mixture of MMC and MGb₂).

Table IV. Inhibitory Effects of MGb₂-PAD-MMC and Free MMC of Different Dose Levels on Human Gastric Carcinoma SGC-7901 Implanted under Renal Capsules in Swiss-DF Nude Mice^a

agents tested	dose, mg/kg	tumor size (omu)		change in tumor size (day 8-day 0)	% inhibition rate
		initial	final		
MGb ₂ -PAD-MMC	1	13.25 ± 1.85	25.25 ± 8.00	12.00 ± 6.86	68.00 ^c
MMC	1	11.88 ± 3.00	31.88 ± 4.00	20.00 ± 3.24	46.67
MGb ₂ -PAD-MMC	2	12.38 ± 1.25	11.88 ± 1.49	-0.50 ± 2.16	101.33
MMC	2	12.50 ± 0.82	19.88 ± 7.16	7.38 ± 6.80	80.32
MGb ₂ -PAD-MMC	3	12.50 ± 1.00	12.00 ± 1.78	-0.50 ± 1.47	101.33 ^b
MMC	3	12.75 ± 1.85	13.00 ± 0.00	0.25	99.33 ^d
saline control		12.06 ± 1.01	49.56 ± 9.66	37.50 ± 9.44	

^a Two mice (four capsules) per test group; four mice (eight capsules) in control group. ^b $p < 0.01$. ^c $p < 0.001$ (MGb₂-PAD-MMC vs MMC). ^d One of the two mice tested died of toxicity.

Table V. Inhibitory Effects of MGb₂-PAD-MMC, MGb₂, MMC, Normal Mouse IgG, and Normal Mouse IgG-PAD-MMC on the Growth of Human Gastric Carcinoma GAI1 Implanted under Renal Capsules in BALB/c Nude Mice^a

agents tested	dose, mg/kg	tumor size (omu)		change in tumor size (day 18-day 0)	% inhibition rate
		initial	final		
MGb ₂ -PAD-MMC	1	12.13 ± 2.46	8.25 ± 4.19	-3.88 ± 2.49	152.29 ^{b,c}
MGb ₂	10	11.38 ± 1.65	21.38 ± 4.23	10.00 ± 5.79	
MMC	1	12.00 ± 1.41	16.00 ± 2.48	4.00 ± 2.97	46.19
normal mouse IgG	10	12.63 ± 2.17	24.63 ± 2.32	12.00 ± 3.94	
normal mouse IgG-PAD-MMC	1	11.63 ± 1.18	17.00 ± 2.08	5.38 ± 3.20	27.49
saline control		12.58 ± 1.35	20.00 ± 2.99	7.42 ± 3.10	

^a Two mice (four capsules) per test group; six mice (12 capsules) in control group. ^b $p < 0.001$ (vs control). ^c $p < 0.001$ (vs MMC).

Table IV shows the effect of various doses of MGb₂-PAD-MMC conjugate in comparison with the chemotherapeutic ability of free MMC. With increasing dose, the in vivo cytotoxic effect of both conjugate and free MMC was augmented, but compared to free drug, the conjugate exhibited higher activity. Besides, at the dose above 3 mg/kg, one of the two mice in the free MMC-treated group died of toxicity. No lethal toxicity was found in the conjugate-treated group.

In Vivo Inhibitory Effect of MGb₂-PAD-MMC on the Growth of Human Gastric Carcinoma GAI1. Table V shows the suppressive effect of MGb₂-PAD-MMC on the growth of human gastric carcinoma GAI1. It could be seen that MMC alone had some effect on GAI1. However, when coupled to antgastric cancer monoclonal antibody MGb₂, its activity was significantly increased. At the dose of 1 mg/kg of drug, the conjugate could completely inhibit the tumor growth. MGb₂ alone and irrelevant conjugate demonstrated no inhibition on GAI1.

DISCUSSION

MMC, an antibiotic, has potent antitumor activity and has been used in the treatment of various solid tumors including gastric cancer and colorectal carcinoma. However, its clinical use is limited by its detrimental effect on normal cells especially rapidly proliferating cells such

as those in bone marrow (12). One possible approach to overcome this defect is to link MMC with antibodies against tumors so that the toxicity could be selectively restricted to tumor cells. Suzuki et al. (13) first prepared an antibody-MMC conjugate with cyanogen bromide as the coupling agent. But, only one molecule of MMC could be introduced into each molecule of antibody. Kato et al. (14) presented an active ester method by which the molar ratio of antibody/MMC in the conjugate reached 1:8 with the protein-recovery rate being as high as 85–90%. However, with direct linkage, the number of drug molecules that could be attached to antibody molecule without significantly damaging its activity is limited. Attempts to increase the drug/antibody molar ratio not only decreased the yield of immunoconjugate but also dramatically damaged antibody activity (15, 16).

In order to get active conjugate with increased drug content, an indirect linkage method was adopted. We chose dextran T-40 in the present study as intermediary to prepare antibody-MMC conjugate because it is highly soluble and it may be able to decrease the recipient's immune response to foreign proteins (17).

Dextran of different molecular size have been used as a carrier system in the past. However, the conjugates obtained varied greatly in their in vitro and in vivo antitumor potency (18–20). This may be due to, among other factors, the degree of oxidation of dextran and the extent

of reduction of Schiff bases by sodium borohydride. We adopted 25% oxidation of dextran and partial reduction by sodium borohydride to prepare the MGB₂-PAD-MMC conjugate. In this manner, no severe loss of antigen-binding capacity of the antibody and the pharmacological activity of MMC occurred. The MGB₂-PAD-MMC conjugate was also proved to be quite stable.

The MGB₂-PAD-MMC conjugate exhibited selective cytotoxicity upon human gastric cancer cells SGC-7901 in vitro. This cytotoxicity was apparent in the 30-min pretreatment cytotoxicity assay in which conjugate was only briefly exposed to cells, a situation closely mimicking the in vivo action of a conjugate where there may be only a brief encounter with tumor or normal tissue followed by prolonged association with antigen-positive cells. We once chose another antigestric cancer monoclonal antibody, MG₁₁, to prepare the antibody-MMC conjugate. The cytotoxicity of MG₁₁-PAD-MMC conjugate on human gastric cancer cell line SGC-7901 was weaker than that of MGB₂-PAD-MMC (Li et al., unpublished observation). This may be due to the quantitative difference of the corresponding antigens on tumor cells, suggesting that the selective cytotoxicity of the immunoconjugates on target cells be mediated by the antibodies chosen.

Retention of tumor localization capacity is an important component of the therapeutic approaches with monoclonal antibodies and their anticancer agent conjugates. Different methods of conjugation may affect greatly the in vivo distribution behavior of the conjugates obtained (21). Our imaging and biodistribution studies demonstrated clearly that the MGB₂-PAD-MMC conjugate could be satisfactorily localized in the tumor tissue in nude mice bearing human gastric carcinoma xenografts. Compared with unmodified antibody, no obvious increase in the uptake of conjugate by liver was observed, as noted in the conjugate of antibody with ricin toxin A chain (22) or the conjugate of antibody with methotrexate utilizing serum albumin as intermediary (23).

Having firmly established the specific in vitro cytotoxic effect of MGB₂-PAD-MMC conjugate and its in vivo tumor localization capacity, studies were carried out to appraise its in vivo antitumor activity. The subrenal capsule (SRC) assay method was used. Because of the rich blood flow in the renal capsules and thus the relative rapid growth of tumor xenografts and the easy access of tested agents to the tumor tissues, SRC required much less time as compared to the tumor models of subcutaneous or ascitic form which were widely used to test the therapeutic effect of immunoconjugates (24, 25). By inoculating the tumor tissues in bilateral capsules instead of in the left one, as introduced in the literature (10), fewer nude mice were used. Furthermore, because of the graft size and site of implantation, it mimics the residual metastases more closely, it is the metastases against which immunochemotherapy is directed after removal of primary tumor loci (26). The result of SRC assay showed that MMC alone had some inhibitory effect on human gastric carcinoma xenografts in nude mice. However, when coupled to monoclonal antibody MGB₂, its antitumor activity was significantly augmented, which was more obviously manifested in GAIL, a slow-growing human gastric carcinoma model. Meanwhile, by conjugation with antibody, the toxicity of MMC on nude mice was also reduced. This should allow a greater amount of immunoconjugates to be given to achieve better therapeutic effect. Of course, one should bear in mind the high sensitivity of SRC assay when appraising the in vivo therapeutic efficacy of the immunoconjugate.

We are aware of the fact that the oxidized dextrans are multifunctional with many reactive aldehyde groups per molecule, just as immunoglobulin is with many reactive amine groups. Therefore, the coupling between those two types of molecules may yield a complex mixture of products differing in their molecular size. However, the chromatographic analyses of the products showed that they were not grossly heterogenous and that products as those with one molecule of dextran and two molecules of immunoglobulins or more were not formed. The thing which should be more taken into account is perhaps the heterogeneity in their coupling sites. If the sites necessary for antigen-binding were involved, great reduction to the immunological activity of antibody may occur. The site specific linkage method presented by Shih et al. (27) may provide a solution to this problem.

In summary, an antigestric cancer monoclonal antibody-MMC conjugate was prepared with dextran T-40 as intermediary. In vitro studies demonstrated that the immunoconjugate exhibited selective cytotoxicity upon human gastric cancer cells SGC-7901. The conjugate was proved to be quite stable and could be well-localized in the tumor tissue in nude mice xenografted with human gastric carcinoma. SRC assay indicated that MGB₂-PAD-MMC conjugate could inhibit the growth of transplanted tumor much more effectively than unconjugated MMC or irrelevant conjugate. Recent studies showed that the MGB₂-PAD-MMC conjugate could be satisfactorily localized in the tumor tissue in the patients with gastric cancer. Even the metastatic lymph nodes could be recognized by the immunoconjugate, the tumor to nontumor uptake ratio ranging from 2.6 to 5.7 (Li et al., manuscript in preparation). The above results are encouraging us to make continuous effort to further improve this conjugate and perform a clinical trial.

ACKNOWLEDGMENT

We thank Mrs. Xiao-Yan Cao for her assistance in preparing this manuscript.

LITERATURE CITED

- (1) Zhang, X. Y. (1984) Further study on the etiology, mechanism and early diagnosis of gastric cancer. *Chin. J. Dig.* 4, 29.
- (2) Baldwin, R. W. (1985) Monoclonal antibody targeting of anticancer agents. *Eur. J. Cancer Clin. Oncol.* 21, 1231-1235.
- (3) Fan, D. M., Zhang, X. Y., Chen, X. T., Mu, Z. X., Hu, J. L., Qiao, T. D., and Chen, B. J. (1988) Mouse and human monoclonal antibodies against gastric cancer: Preparation and clinical application. *Chin. Med. J.* 101, 488-489.
- (4) Deng, J. L., Jiang, M. D., Tan, X. Y., Gao, R. Z., Chen, M., Fan, D. M., Hu, J. L., Zhang, X. Y., Chen, X. T., and Mu, Z. X. (1990) Tumor localization and radioimmunoimaging by monoclonal antibodies in nude mice and patients with gastric cancer. *Chin. J. Dig.*, in press.
- (5) Bernstein, A., Hurwitz, E., Maron, R., Arnon, R., Sela, M., and Wilchek, M. (1978) Higher antitumor efficacy of daunomycin when linked to dextran: In vivo and in vitro studies. *JNCI, J. Natl. Cancer Inst.* 60, 379-384.
- (6) Bradford, N. M. (1976) A rapid and sensitive method of quantitation of microgram quantities of protein utilizing the principle of protein-dye binding. *Anal. Biochem.* 72, 248-253.
- (7) Termyn, M. A. (1975) Increasing the sensitivity of the anthrone method for carbohydrate. *Anal. Biochem.* 68, 332-335.
- (8) Li, S., Zhang, X. Y., Chen, X. T., Fan, D. M., Tan, L. S., Pan, H. Z., and Huang, L. Q. (1989) Preparation and characterization of immunotoxin with blocked galactose-binding sites of ricin. *Chin. J. Pharmacol. Toxicol.* 3, 81-84.

- (9) Lin, S. Y., Ellis, H., Weisenblum, B., and Goodfriend, T. L. (1970) Preparation of iodinated angiotensins. *Biochem. Pharmacol.* 19, 651-662.
- (10) Bodgen, A. E., Kelton, D. E., Cobbb, W. R., and Esber, H. J. (1978) A rapid screening method for testing chemotherapeutic agents against human tumor xenografts. In *Proceedings of the Symposium on the Use of Athymic (Nude) Mice in Cancer Research* (D. P. Houchens, and A. A. Over-Jera, Eds.) pp 231-256, Gustav Fisher, New York.
- (11) Zhang, S. Y., Shu, Y. H., Zhang, J. L., Lin, Z. Q., and Xu, C. W. (1989) Effects of 8 antitumor drugs against the growth of human lung adenocarcinoma (LAX-83) transplanted under the kidney capsule of nude mice. *Acta Pharmacol. Sin.* 10, 450-453.
- (12) Comis, R. L., and Carter, S. K. (1974) A review of chemotherapy in gastric cancer. *Chem. Pharm. Bull.* 34, 1576-1586.
- (13) Suzuki, T., Sato, E., Goto, K., Katsurada, Y., Unno, K., and Takahashi, T. (1981) The preparation of mitomycin C, adriamycin and daunomycin covalently bound to antibodies as improved chemotherapeutic agents. *Chem. Pharm. Bull.* 29, 844-848.
- (14) Kato, Y., Tsukada, Y., Hara, T., and Hirai, H. (1983) Enhanced antitumor activity of mitomycin C conjugated with anti- α -fetoprotein antibody by a novel method of conjugation. *J. Appl. Biochem.* 6, 297-307.
- (15) Kulkarni, P. N., Blair, A. H., and Ghose, T. I. (1981) Covalent binding of methotrexate to immunoglobulins and the effect of antibody-linked drug on tumor growth in vivo. *Cancer Res.* 41, 2700-2706.
- (16) Li, S., Zhang, X. Y., Chen, X. T., Zhang, S. Y., Chen, L. J., and Zhang, J. L. (1990) Selective killing of tumor cells by anti-gastric cancer monoclonal antibody-mitomycin C conjugate. *Acta Pharmacol. Sin.*, in press.
- (17) King, T. P., Kochoumian, L., Ishizaka, K., Lichtenstein, L. M., and Norman, P. S. (1975) Immunochemical studies of dextran coupled ragweed pollen allergen, antigen E. *Arch. Biochem. Biophys.* 169, 464-473.
- (18) Ghose, T. I., Blair, A. H., and Kulkarni, P. (1983) Preparation and application of antibody-linked cytotoxic agents. *Methods Enzymol.* 93, 280-333.
- (19) Manabe, Y., Tsubota, T., Haruta, Y., Kataoka, K., Okazaki, M., Haisa, S., Nakamura, K., and Kimura, I. (1985) Production of a monoclonal antibody-mitomycin C conjugate, utilizing dextran T-40, and its biological activity. *Biochem. Pharmacol.* 34, 289-291.
- (20) Iwasa, S., Konishi, E., Kondo, K., Suzuki, T., Akaza, H., and Nijijima, T. (1987) Selective cytotoxicity of drug-monomonal antibody conjugates against murine bladder tumor cells. *Chem. Pharm. Bull.* 35, 1128-1137.
- (21) Koizumi, M., Endo, K., Kunimatsu, M., Sakahara, H., Nakashima, T., Kawamura, Y., Watanabe, Y., Sega, T., Konishi, J., Yamamuro, T., Hosoi, S., Toyama, S., Arano, Y., and Yokoyama, A. (1988) ^{67}Ga -Labeled antibodies for immunoscintigraphy and evaluation of tumor targeting of drug-antibody conjugates in mice. *Cancer Res.* 48, 1189-1194.
- (22) Bourrie, B. J. P., Casellas, P., Blythman, H. E., and Jansen, F. K. (1986) Study on the plasma clearance of antibody-ricin A chain immunotoxins. Evidence for specific recognition sites on the A chain that mediate rapid clearance of the immunotoxin. *Eur. J. Biochem.* 155, 1-10.
- (23) Pimm, M. V., Clegg, J. A., Caten, J. E., Ballantyne, K. D., Perkins, A. C., Garnett, M. C., and Baldwin, R. W. (1987) Biodistribution of methotrexate-monomonal antibody conjugates and complexes: experimental and clinical studies. *Cancer Treat. Rev.* 14, 411-20.
- (24) Smyth, M. J., Pietersz, G. A., Classon, B. J., and McKenzie, F. C. (1986) Specific targeting of chlorambucil to tumors with the use of monoclonal antibodies. *JNCI, J. Natl. Cancer Inst.* 76, 503-510.
- (25) FitzGerald, D. J., Bjorn, M. J., Ferris, R. J., Winkelhake, J. L., Frankel, A. E., Hamilton, T. C., Ozols, R. F., Willingham, M. C., and Pastan, I. (1987) Antitumor activity of an immunotoxin in a nude mouse model of human ovarian cancer. *Cancer Res.* 47, 1407-1410.
- (26) Foon, K. A., and Morgan, C. (1986) Monoclonal antibody therapy of cancer: Animals models and human trials. In *Monoclonal Antibodies in Cancer: Advances in Diagnosis and Treatment* (J. A. Roth, Ed.) pp 141-171, Futura Publishing Co., Inc., Mount Kisco, NY.
- (27) Shih, L. B., Sharkey, R. M., Primus, F. J., and Goldenberg, D. M. (1988) Site-specific linkage of methotrexate to monoclonal antibodies using an intermediate carrier. *Int. J. Cancer* 41, 832-839.

Electrophilic Analogues of Daunorubicin and Doxorubicin¹

Leonard O. Rosik and Frederick Sweet*

Department of Obstetrics and Gynecology, Washington University School of Medicine, St. Louis, Missouri 63110.
Received March 19, 1990

Daunorubicin (DNR) or doxorubicin (DOX) was modified with one of four "linker reagents" to produce electrophilic drug analogues for synthesis of bioconjugates. Synthesis and characterization of two new reagents [*p*-isothiocyanatobenzoyl chloride and 3-(*p*-isothiocyanatophenyl)propionyl chloride] are described here for the first time. Adding one of the new reagents, bromoacetyl bromide, or *p*-(fluorosulfonyl)-benzoyl chloride in chloroform to an alkaline aqueous solution of DNR (or DOX) provided excellent yields of the corresponding, electrophilic 3'-*N*-amide analogue. The DNR and DOX analogues were characterized by thin-layer chromatography, nuclear magnetic resonance spectroscopy, and infrared spectroscopy. Bioconjugates were produced with the electrophilic DNR or DOX analogues by mixing them with bovine serum albumin (BSA), mouse IgG, or a monoclonal antibody (OC125, which specifically binds to the CA125 antigen from human ovarian carcinoma). The relative reactivity of the 3'-*N*-substituents toward protein is *p*-(fluorosulfonyl)benzoyl > phenylisothiocyanato > bromoacetyl. Overall, the new phenyl isothiocyanate acid chlorides are superior to *p*-(fluorosulfonyl)benzoyl chloride or bromoacetyl bromide as reagents with which to produce electrophilic DNR or DOX analogues for conjugation with monoclonal antibodies. The bioconjugates DNR-OC125 and DOX-OC125 are selectively toxic to two human ovarian cancer cell lines in vitro (1) and bind with high specificity to human ovarian tumor sections (2) that express the CA125 antigen.

Rapidly growing numbers of bioconjugates derived from drugs and monoclonal antibodies have been synthesized and tested on human cancers in vitro and in vivo with varying degrees of success (3-8). Recent developments in bioconjugate chemistry focus on new methods for attaching drugs to monoclonal antibodies while preserving characteristic drug toxicity and antibody binding. Preservation of these characteristics requires that the structural integrity of both drug and antibody be maintained (9, 10). Efforts have also been made to produce drug-antibody conjugates in which the linkage can be cleaved by the target cells (11). The history and developments in bioconjugate chemistry have recently been described in excellent review articles (12, 13).

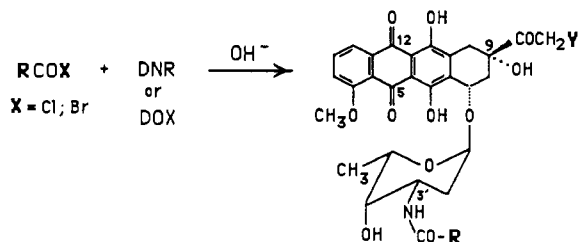
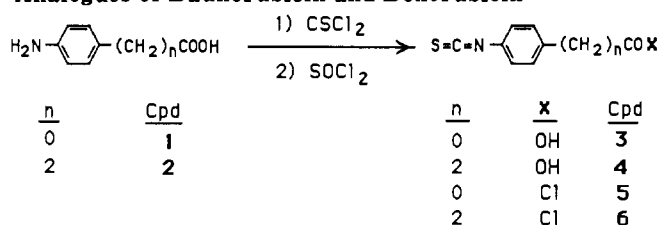
Doxorubicin (DOX) is used for treating ovarian cancer, making it a logical choice for conjugation with monoclonal antibodies that bind to the cancer. DOX and daunorubicin (DNR) have tetracycline anthraquinone rings containing an amino sugar and ketonic carbonyl at the C-7- and C-9-positions, respectively (Chart I). The structural difference between DNR and DOX is a hydroxy group in the side chain at the C-9-position. Hurwitz et al. earlier attempted to link DNR and DOX to an antibody by first oxidizing the carbohydrate moiety in the drugs with NaIO₄ to produce corresponding dialdehydes. The oxidized, tetracyclic anthraquinones were assumed to conjugate with amino groups in the antibody protein through formation of Schiff base, subsequently "stabilized" with NaBH₄. However, opening of the amino sugar ring by NaIO₄ (probably accompanied by removal of the α -hydroxyketonic side chain at C-9) caused major structural changes in the drug with consequent loss of its desired toxicity (14).

Recently, progress has been made by modifying the 3'-amino group on the intact sugar moiety or the methyl ketone side chain at the C-9-position in DNR and DOX, intended for conjugation with antibodies (15-17).

It seemed worthwhile to explore methods for modifying the 3'-amino group in DNR and DOX with new "linker reagents" so designed that at some later time a desired bioconjugate can be synthesized simply by mixing the electrophilic drug analogues with a suitable protein. These objectives have been accomplished in principle with electrophilic, affinity-labeling analogues of biologically active steroids, nucleosides, and other compounds. Electrophilic groups [e.g. bromoacetyl or *p*-(fluorosulfonyl)-benzoyl] have been used in the synthesis of affinity-labeling analogues that become covalently bound to specific enzyme, transport, or receptor proteins (18). Our reason for selecting the presently reported reagents for bioconjugate synthesis is that each of them contains two different electrophilic groups. The two groups in each reagent greatly vary from one another in their rates of reaction with nucleophiles. Accordingly, during the first reaction the more reactive of the two electrophilic groups forms a stable, covalent bond (i.e., amide linkage) between the reagent and the anticancer drug. The second electrophilic group in the drug analogue remains reactive. After isolating the drug analogue, at some later time the electrophilic group can be used to form stable, covalent bonds with nucleophilic amino acid residues in proteins.

In the present study, we chose the acid halide for the more rapidly reacting of the two electrophilic groups in the reagents. The relatively slower reacting, second electrophilic groups were bromoacetyl, (fluorosulfonyl)-phenyl, and phenylisothiocyanato (Chart I). It seemed worthwhile to include the phenyl isothiocyanate group in the new reagents because other aromatic isothiocyanates have been successfully used in bioconjugate chemistry. For example, fluorescein isothiocyanate (FITC)

¹ Presented in part at the Fourth International Conference on Monoclonal Antibody Immunoconjugates for Cancer, San Diego, CA, March 30-April 1, 1989 and at the Society for Gynecologic Investigation 37th Annual Meeting, St. Louis, MO, March 21-24, 1990.

Chart I. Synthesis and Structures of Electrophilic Analogues of Daunorubicin and Doxorubicin

R	Compound [% yield]	
	(Y = H)	(Y = OH)
	7 [99]	
	8 [94]	9 [87]
	10 [98]	11 [88]
	12 [95]	

(19–21) or chelator reagents for making tumor imaging substances (22–24) each produce stable conjugates when the aromatic isothiocyanate reacts with a suitable protein. In the present case, Schotten–Baumann reaction conditions were expected to cause the assorted acid halides to selectively react with the lone 3'-N-amino group in the polyfunctional DNR (or DOX) to produce the desired electrophilic analogues of the anticancer drugs.

This report describes syntheses of DNR and DOX analogues that contain an electrophilic group, made by reacting two new phenyl isothiocyanate acid chlorides and also known dual electrophilic acid halides with the anthracycline antibiotics. The electrophilic analogues of DNR and DOX are sufficiently stable to be stored and then later used for producing desired monoclonal antibody–anticancer drug conjugates simply by mixing the analogues with a monoclonal antibody. Preliminary results with this approach have provided bioconjugates that exhibit specific binding to human ovarian tumor sections (2) and selective toxicity for human ovarian cancer cells (1).

EXPERIMENTAL PROCEDURES

General Procedures. *p*-(Fluorosulfonyl)benzoyl chloride and *p*-aminobenzoic acid were from Aldrich (Milwaukee, WI). 3-(*p*-Aminophenyl)propionic acid was from Pfaltz and Bauer (Waterbury, CT). Thiophosgene was from Fluka (Ronkonkoma, NY). Bromoacetyl bromide was from Eastman Kodak (Rochester, NY). Daunorubicin was from Wyeth (Princeton, NJ) and doxorubicin was from Adria (Columbus, OH). Mouse IgG was from Sigma (St. Louis, MO) and anti-CA-125 monoclonal antibody (OC-125) was from Centocor (Malvern, PA). Nuclear magnetic

resonance spectra were obtained with a Varian XL-300 spectrometer. Infrared spectra were performed with thin-film NaCl plates (unless otherwise noted) and a Beckman Acculab 4 spectrophotometer. Elemental analyses were performed by Galbraith Laboratories (Knoxville, TN). Thin-layer chromatograms (TLC) were obtained with 2.5 × 7.5 cm plates of silica gel G (Eastman Kodak), developed with chloroform/methanol (95:5 v/v). R_f values are reported for characteristic mobilities of the DNR and DOX analogues.

***p*-Isothiocyanatobenzoic Acid (3).** A solution of *p*-aminobenzoic acid (13.7 g, 0.10 mol) in 110 mL of 1 M aqueous potassium hydroxide was added dropwise during 30 min to a vigorously stirred mixture of thiophosgene (12.6 g, 0.11 mol) in 200 mL of water at room temperature. During addition, formation of a thick mixture required that sufficient water be added to maintain smooth stirring. The total volume of the reaction mixture was ca. 1 L at the end of the addition. Then the reaction mixture was stirred for one additional hour and filtered under vacuum, and the collected white solid was washed 10 times with 100-mL portions of water. The product (16.6 g, 93%) was dried in a vacuum desiccator for 48 h. A sample of the dry product was recrystallized twice from ethyl acetate to provide crystalline material that melted with decomposition above 235 °C: ^1H NMR (CDCl_3) δ 8.10 (d, J = 8.4 Hz, 2 H), 7.31 (d, J = 8.7 Hz, 2 H); IR (KBr) 2080 (SCN), 1665 (CO), 1590, 1412, 1280, 850 cm^{-1} . Anal. Calcd for $\text{C}_8\text{H}_5\text{NO}_2\text{S}$: C, 53.62; H, 2.81; N, 7.82; S, 17.89. Found: C, 53.58; H, 2.73; N, 7.72; S, 17.93.

3-(*p*-Isothiocyanatophenyl)propionic Acid (4). Compound 4 was prepared in 77% yield from 2 by the procedure described above for the synthesis of 3. An analytical sample of 4 was recrystallized twice from benzene: mp 140–141 °C; ^1H NMR (CDCl_3) δ 7.20 (d, J = 8.7 Hz, 2 H), 7.16 (d, J = 8.7 Hz, 2 H), 2.95 (t, J = 7.5 Hz, 2 H), 2.67 (t, J = 7.5 Hz, 2 H); IR (KBr) 2095 (SCN), 1690 (CO), 1502, 1440, 1221, 829, cm^{-1} . Anal. Calcd for $\text{C}_{10}\text{H}_9\text{NO}_2\text{S}$: C, 57.96; H, 4.38; N, 6.76; S, 15.47. Found: C, 58.12; H, 4.29; N, 6.75; S, 15.33.

General Synthesis of Electrophilic Analogues of Anthracycline Antibiotics. A solution of an acid halide (1.1–2.1 equiv) in chloroform or benzene was added at room temperature to DNR or DOX (1 equiv) in a vigorously stirred mixture of water, chloroform and/or benzene, and potassium bicarbonate (10–20 equiv). After stirring the resulting mixture for 10–30 min, the liquid layers were allowed to separate, the organic layer was removed, and then the aqueous layer was extracted with several portions of chloroform. The combined chloroform extracts were washed with water, dried over anhydrous sodium sulfate, and filtered, and then the solvent was removed under reduced pressure. The residue (10–15 mg) was flash chromatographed in chromatographic columns made from cotton-plugged Pasteur pipets and ca. 1 g of flash silica gel. After applying the crude material in chloroform to a column, three or four 1-mL portions of chloroform were percolated through the column, then the product was eluted with methanol/chloroform (2–3% of methanol). The fractions containing product (according to TLC) were pooled and the solvent was removed under reduced pressure.

3'-N-(*p*-Isothiocyanatobenzoyl)daunorubicin (7). Acid chloride 5 was prepared by heating a mixture of 3 (180 mg, 1 mmol), thionyl chloride (100 μL , 1.4 mmol), 4 drops of DMF, and 5 mL of chloroform, under reflux (drying tube) for 2 h. Solvents and excess thionyl chloride were removed under vacuum (water aspirator). The

residue was twice dissolved in a few milliliters of chloroform and the solvent was removed under vacuum. The resulting residue was dissolved in 5 mL of chloroform. An aliquot (150 μ L, 30 μ mol) of the solution containing **5** was added to DNR·HCl (11 mg, 19.5 μ mol) in a mixture of 500 μ L of water, 400 μ L of chloroform, and potassium bicarbonate (15 mg, 150 μ mol), and then the mixture was stirred for 10 min at room temperature. Flash chromatography provided 13.39 mg (99%) of pure **7**: R_f = 0.64; ^1H NMR (CDCl_3) δ 7.71 (d, J = 8.4 Hz, 2 H), 7.22 (d, J = 8.4 Hz, 2 H), 6.48 (d, J = 7.8 Hz, 1 H, 3'-NH), 4.34 (br, 1 H 3'-CH); IR 3500, 3410, 2940, 2090 (SCN), 1719 (9 C=O), 1642 (amide), 1622 (5, 12 C=O) 1583, 1499, 1417, 1290, 1211, 1012, 988, 716 cm^{-1} .

3'-N-[3-(*p*-Isothiocyanatophenyl)propionyl]daunorubicin (8**).** Acid chloride **6** was prepared by stirring **4** (10 mg, 48 μ mol) in a solution of thionyl chloride (200 μ L, 1.37 M) in benzene for 5 h at room temperature. After removal of the solvent and excess thionyl chloride under vacuum, the residue was dissolved in benzene and the solvent was removed in vacuo. Crude **6** was dissolved in chloroform (200 μ L) and the resulting solution was added to a stirred mixture of DNR·HCl (22 mg, 39 μ mol) in 1.0 mL of water, chloroform (200 μ L), and potassium bicarbonate (100 mg, 1 mmol). After rinsing of the residual acid chloride into the reaction mixture with 200 μ L of chloroform, the resulting mixture was stirred for 30 min. Flash chromatography provided pure **8** (26.2 mg, 94%); R_f = 0.61; ^1H NMR (CDCl_3) δ 7.15 (d, J = 9 Hz, 2 H), 7.11 (d, J = 9 Hz, 2 H), 5.69 (d, J = 8.1 Hz, 1 H, 3'-NH), 4.15 (br, 1 H, 3'-CH), 2.89 (t, J = 7.6 Hz, 2 H), 2.41 (dt, J = 2.8, 7.8 Hz, 2 H); IR 3490, 3400, 2945, 2120 (SCN), 1720 (9 C=O), 1660 (amide), 1629 (5, 12 C=O), 1590, 1421, 1295, 1218, 1020, 993, 826 cm^{-1} .

3'-N-[3-(*p*-Isothiocyanatophenyl)propionyl]-doxorubicin (9**).** By the method described above, **6** was prepared from **4** (12.1 mg, 58 μ mol). The a solution of **6** in 500 μ L of chloroform was added to a stirred mixture of DOX·HCl (15.7 mg, 27 μ mol) in 1.0 mL of water, chloroform (200 μ L), and potassium bicarbonate (24 mg, 240 μ mol). Residual acid chloride was rinsed into the reaction mixture with 500 μ L of chloroform and the mixture was stirred for 30 min. Flash chromatography provided pure **9** (17.2 mg, 87%); R_f = 0.37; ^1H NMR (CDCl_3) δ 7.15 (d, J = 8.9 Hz, 2 H), 7.12 (d, J = 8.9 Hz, 2 H), 5.70 (d, J = 8.5 Hz, 1 H, 3'-NH), 4.12 (br, 1 H, 3'-CH), 2.90 (t, J = 7.4 Hz, 2 H), 2.41 (dt, J = 3.0, 7.4 Hz, 2 H); IR 3400, 2950, 2120 (SCN), 1730 (9 C=O), 1660 (amide), 1630 (5, 12 C=O), 1590, 1419, 1296, 1219, 1028, 997 cm^{-1} .

3'-N-(Bromoacetyl)daunorubicin (10**).** A solution of bromoacetyl bromide (110 μ L, 0.11 M in benzene) was added to a stirred mixture of DNR·HCl (6.0 mg, 10.6 μ mol) in 500 μ L of water, 500 μ L of chloroform, and potassium bicarbonate (10 mg, 100 μ mol). The reaction mixture was stirred for 30 min at room temperature. Chromatography gave 6.8 mg (98%) of pure **10**: R_f = 0.44; ^1H NMR (CDCl_3) δ 6.76 (d, J = 8.2 Hz, 1 H, 3'-NH), 4.14 (br, 1 H, 3'-CH), 3.82 (s, 2 H, BrAc); IR 3490, 3400, 2940, 1711 (9 C=O), 1656 (amide), 1619 (5, 12 C=O), 1580, 1412, 1285, 1207, 1020, 985, 762 cm^{-1} .

3'-N-(Bromoacetyl)doxorubicin (11**).** Bromoacetyl bromide solution (200 μ L, 22 μ mol) was added to a mixture of DOX·HCl (6.2 mg, 10.7 μ mol) in 1.0 mL of water, chloroform (800 μ L), and potassium bicarbonate (24 mg, 240 μ mol) that was stirred for 30 min. Flash chromatography provided pure **11** (6.25 mg, 88%); R_f = 0.25; ^1H NMR (CDCl_3) δ 6.76 (d, J = 8.1 Hz, 1 H, 3'-NH), 4.14 (br, 1 H, 3'-CH), 3.82 (s, 2 H, BrAc); IR 3500,

3400, 2945, 1725 (9 C=O), 1661 (amide), 1625 (5, 12 C=O), 1585, 1416, 1290, 1214, 1023, 994 cm^{-1} .

3'-N-[*p*-(Fluorosulfonyl)benzoyl]daunorubicin (12**).** *p*-(Fluorosulfonyl)benzoyl chloride (5.5 mg, 25 μ mol) in 0.5 mL of benzene was added to DNR·HCl (12.6 mg, 22.5 μ mol) in 1 mL of water, 0.5 mL of chloroform, and potassium bicarbonate (24 mg, 240 μ mol), and the mixture was stirred at room temperature for 30 min. Flash chromatography gave 15.4 mg (95%) of pure **12**: R_f = 0.58; ^1H NMR (CDCl_3) δ 8.05 (d, J = 8 Hz, 2 H), 7.95 (d, J = 8.3 Hz, 2 H), 6.61 (d, J = 8 Hz, 1 H, 3'-NH), 4.42 (br, 1 H, 3'-CH); IR 3500, 3420, 2945, 1720 (9 C=O), 1650 (amide), 1625 (5, 12 C=O), 1587, 1420, 1295, 1220, 1020, 991, 793, 768, 614 cm^{-1} .

Conjugating DNR or DOX Analogues with Antibody or Other Proteins. A solution of a DNR (or DOX) analogue in acetonitrile (330–660 μ M, 100 μ L) was added to a mixture of 500 μ L of stock antibody solution in PBS (1–2 mg/mL) and 500 μ L of 0.1 M phosphate buffer (pH 8), stirred with a vortex apparatus. After standing at room temperature for 24 h, the resulting mixture was placed in a dialysis bag and dialyzed for 3 days at 0 $^\circ\text{C}$ against daily changes of 250 mL of a buffer, according to the following scheme: first day, 0.05 M phosphate buffer, pH 8 (containing 10% acetonitrile); second day, 0.05 M phosphate buffer, pH 7 (containing 10% acetonitrile); and third day, 0.05 M phosphate buffer, pH 7. This scheme is essential for preventing precipitation of the crude product during its purification by dialysis.² The ratios of DNR (or DOX) to antibody in the retentate were calculated from the measured light absorption at 490 nm (ϵ = 11 000) due to DNR (or DOX) and the antibody protein concentration, by the method of Lowry et al. (17) from light absorption at 750 nm (referred to a standard curve from known concentrations of mouse IgG).

RESULTS AND DISCUSSION

Synthesis of Electrophilic Analogues of DNR and DOX. Phenyl isothiocyanates **3** and **4** (Chart I) were obtained in good yields (93% and 77%, respectively) by treating *p*-aminobenzoic acid (**1**) or 3-(*p*-aminophenyl)-propionic acid (**2**) with thiophosgene in an aqueous alkaline solutions. Although **4** was readily converted to **6** with thionyl chloride in chloroform at room temperature, **3** remained unchanged under these conditions. Most likely, the carboxylic acid group in **3** is deactivated due to its conjugation with the electron-withdrawing phenyl isothiocyanate group. Accordingly, the more vigorously reactive DMF/thionyl chloride (Vilsmeier reagent (**26**)) was required for converting **3** to **5**. The acid chlorides that remained after removing excess reagent and the volatile byproducts served as the "linker reagents" for synthesizing the electrophilic anthracycline antibiotic analogues.

p-(Fluorosulfonyl)benzoyl chloride in DMF failed to react with the 3'-amino group in DNR. Under similar conditions bromoacetyl bromide reacts with 5'-amino-5'-deoxyadenosine in DMF to give the corresponding 5'-*N*-(bromoacetyl)amide (**27**), and *p*-(fluorosulfonyl)benzoyl chloride gives the corresponding 3'-ester with adenosine (**28**). However, adding **5**, **6**, bromoacetyl bromide, or *p*-(fluorosulfonyl)benzoyl chloride in chloroform (or benzene) to a vigorously stirred, aqueous alkaline (potassium

² It was suggested during review of this paper that instead of adding a cosolvent to the dialysis mixture, addition of glutathione (or cysteine) for the bromoacetamide, and glycine (or glutamic acid) for the isothiocyanate (or sulfonyl fluoride) may facilitate efficient removal of the excess, lipophilic reagents during purification of the conjugates.

bicarbonate) solution of DNR or DOX gave excellent yields of a 3'-N-substituted electrophilic analogue of the anthracycline antibiotic (Chart I). The electrophilic analogues of DNR or DOX are stable for months under dry, cool, and dark conditions.

At first, crystalline hydrochlorides of DNR or DOX were used to synthesize the electrophilic anthracycline antibiotic analogues. After discovering that the lactose (added to stabilize the drugs) in pharmaceutical preparations does not interfere with the N-acylation reactions, equivalent amounts of cerubicin (DNR-HCl, buffer, and lactose) provided the same yields as aqueous solutions of crystalline DNR-HCl. While working up the acylation reaction mixtures, lactose remains in the aqueous phase and the electrophilic DNR analogues are isolated in the organic extracts.

Anthracycline antibiotics are intensely red (ν_{\max} 490 nm; ϵ = 11 000), causing less than 1 μ g of the compounds to be visible on a TLC plate. Chloroform/methanol (95:5) is ideal for separating DOX (R_f = 0.03) and DNR (R_f = 0.06) from the corresponding 3'-N-amide analogues. The analogues have mobilities with R_f values of 0.25–0.37 and 0.44–0.64 for the various N-substituted derivatives of DOX and DNR, respectively. Accordingly, flash chromatography is the method of choice for final purification of the anthracycline antibiotic analogues.

Characteristic ^1H signals (29, 30) and IR bands (31–33) from the DNR and DOX moieties of the N-substituted analogues were in complete agreement with the established spectra. Thus we reported here only those ^1H NMR signals for DNR and DOX that reflect changes at the 3'-NH (amide) and the 3'-CH (sugar) positions, in addition to the signals produced by the various 3'-N-substituents. The IR spectrum of DNR-HCl contains a characteristic pattern of bands at 1715, 1623, 1588, 1416, 1293, 1217, 1125, and 995 cm^{-1} . This pattern was observed in the IR spectra of the DNR and DOX analogues. The phenyl isothiocyanate group in 3 and 4 produces characteristically strong absorption bands at 2080–2120 cm^{-1} , also observed in the IR spectra of the corresponding N-substituted analogues (7–9) of DNR and DOX. A synthesis of 3'-N-(iodoacetyl)-doxorubicin in 75% yield has been reported (17), but this material was only characterized by TLC and therefore the spectra could not be compared with those of the present DOX analogues.

Reactions of Electrophilic DNR and DOX Analogues with Proteins. The DNR analogues were tested with bovine serum albumin (BSA) to assess the reactivity of the N-substituents toward proteins and the stability of the resulting DNR-BSA conjugates. Concentrations of BSA were 1–4 mg/mL (ca. 12–50 μM), and that of a DNR analogue were approximately 300 μM . Various conjugation reactions were carried out between pH 7 and 8 (in 0.1 M phosphate buffer, containing 10% acetonitrile as cosolvent). The best results were obtained at pH 8. 1,2-Dimethoxyethane and dioxane were tested as cosolvents, but they were not as effective as acetonitrile for dissolving the N-substituted DNR analogues at the high concentrations required for efficient conjugation reactions with proteins in aqueous solutions.

Dialysis, gel-filtration chromatography, and polyacrylamide gel electrophoresis (PAGE) were used to determine the conjugation efficiency of the various DNR analogues. The conjugates prepared with DNR analogues containing a phenyl isothiocyanate group were expected to be reactive like FITC toward proteins. Thus these conjugates were only subjected to dialysis. Dialysis of the crude conjugation reaction mixture against water alone caused a major portion

of the protein and DNR analogue to precipitate. When phosphate buffer alone was used for dialysis, the DNR analogue precipitated while the DNR-protein conjugate remained in solution. However, dialysis of the reaction mixture for 2 days against phosphate buffer containing 10% acetonitrile and for an additional day against phosphate buffer alone removes all of the unreacted DNR analogue (mostly on the first day of dialysis). During the third day of dialysis, the organic cosolvent is removed. The pH of the buffer is lowered to 7 on the second and third days of dialysis because the conjugate is most stable at the lower pH during storage. Storing a conjugate at 0 $^{\circ}\text{C}$ for 2–3 months at pH 8 produces a bathochromic shift in the visible spectrum (from 490 to 500–505 nm) of the anthracycline moiety. This may result from the higher rate of oxidation of the hydroquinone function in the anthracycline group promoted by the alkaline conditions.

The above dialysis scheme provides a bright red solution of a DNR-protein conjugate in the retentate. The dialysates of the conjugates made from 10 and 12 appeared as light red solutions. The red material was extracted with chloroform from the dialysate of the dialyzed 10-BSA. TLC analysis of the extracted, red material showed it to be unreacted 10. The red dialysate from 12-BSA (dialyzed at pH 8) was repeatedly extracted with chloroform, but no colored material appeared in the organic layer. After acidification of the dialysate, the red material was extracted from the aqueous solution by chloroform. Presumably, the red extract contained the sulfonic acid form of 12, that had undergone hydrolysis. When 7 or 8 were conjugated with BSA, the bright red products remained in the retentate throughout the 3 days of dialysis. Only a trace of red material could be extracted from the faintly red dialysates.

Two red bands emerged from a Sephadex G25-50 column during chromatography of crude 10- or 12-BSA conjugates (eluted with 0.1 M phosphate buffered at pH 8, containing 10% acetonitrile). The more rapidly eluted red conjugate was followed by a second red band of unconjugated starting material. Polyacrylamide gel electrophoresis was performed on the following samples: (1) BSA (reference), (2) 12-BSA (dialyzed), (3) 12-BSA (gel filtered), and (4) 12-BSA (crude reaction mixture). Lanes 2–4 exhibited the major, bright red bands that migrated with the BSA in the reference lane. Lane 4 contained a red spot at the origin. After staining the gels for protein (Coomassie Blue), the major, migrating red bands in lanes 1–4 were vividly stained, but the red spot at the origin did not stain. The results suggest that either dialysis or gel filtration are effective in separating the DNR-protein conjugates from the unreacted (or hydrolyzed) DNR analogue.

The relative reactivity with BSA of the electrophilic substituents in the analogues of DNR and DOX is the order *p*-(fluorosulfonyl)benzoyl > phenylisothiocyanate > bromoacetyl. However, the *p*-(fluorosulfonyl)benzoylamide 12 undergoes hydrolysis in competition with protein conjugation. Unreacted 3'-N-bromoacetyl-DNR is always observed in the dialysates from the conjugation reaction mixtures. Accordingly, the phenyl isothiocyanates are ideally reactive substituents for producing bioconjugates. The resulting conjugates are entirely stable at pH 7 for at least days at room temperature and for months at 0 $^{\circ}\text{C}$.

DNR- and DOX-Antibody Conjugates. The electrophilic analogues of DNR were conjugated with OC125 (a monoclonal antibody that binds to the CA125 antigen in human ovarian cancer cells). During the conjugation reactions the protein concentration of OC125 was 0.5–

1.0 mg/mL (3.3–6.6 μ M), the concentration of the electrophilic DNR analogues was 33–66 μ M, and the reactions were conducted in 0.05 M phosphate buffer at pH 8 (containing 10% acetonitrile). The conjugates were purified by dialysis in the manner described above for the DNR–BSA conjugates, and they exhibited similar stability. The measured ratios of DNR/OC125 in the conjugates were between 0.5:1 and 19:1. Conjugates with ratios higher than 19:1 precipitated during dialysis. DNR–OC125 conjugates used in earlier in vitro experiments had drug/antibody ratios of 3:1 to 6:1 (1, 2). Human ovarian cancer cells were used to test the cytotoxicity of DNR–OC125 conjugates (1) in which 8–OC125 had low (2–3:1) and high (10–14:1) ratios. The cytotoxicities of these bioconjugates appear to be independent of the drug/antibody ratio in that the low and high ratio of the DNR–OC125 conjugates exhibit equal toxicities for equivalent, nominal concentrations of DNR (34).

The relative stability of the 3'-N linkage formed between 1 or 2 and DNR is interesting. In experiments that preceded the present work, *N*-hydroxysuccinimide esters of the *N*-trityl derivatives of 1 or 2 were condensed with DNR to provide moderate yields of the corresponding 3'-N-substituted phenylpropionyl- or benzoylamides (34). Both amides were completely stable in neutral solutions. However, when detritylation was conducted in acetic acid (pH 4) the benzoyl amide derivative formed free DNR and 1, but the detritylated 3'-N-[3-(*p*-aminophenyl)propionyl]-amide–DNR remained intact. Clearly, the aromatic ring that is conjugated with the carboxamide group promotes hydrolysis of the 3'-N-amide linkage. By contrast, in 3'-N-[3-(*p*-aminophenyl)propionyl]amide–DNR the two additional carbon atoms prevent this effect of the aromatic ring by electronically insulating the carboxamide group. Furthermore, the aliphatic amide linkages in the 3'-N-(bromoacetyl) and 3'-N-[3-(*p*-isothiocyanatophenyl)propionyl] derivatives (8–11) are analogous to natural peptide linkage systems containing alanine and phenylalanine, respectively. By this analogy, the 3'-N-amide linkage in these conjugates are expected to possess greater (i.e., "natural") stability in acidic environments (i.e., pH 4) than the corresponding 3'-N linkage in protein conjugates from 7 or 12.

The relative toxicities in vitro of the DNR–antibody conjugates made from 7 or 8 and OC125 may be related to certain bond-stability factors (discussed above). Under equivalent conditions of concentration and incubation periods, 8–OC125 is consistently about twice as toxic as 7–OC125 to two different cell lines derived from human ovarian tumors (1). Additional experimental work must be undertaken on this theme to precisely relate the chemical nature of the 3'-N-amide linkage in the DNR–antibody conjugates of 7 and 8 with the observed differences in their toxicities. Nevertheless, the reactivity of the reagent, stability of the linkage, and toxicity of the resulting OC125 conjugate make 6 the preferred reagent for producing electrophilic analogues of drugs intended for synthesis of bioconjugates.

The present report describes a variety of reagents that efficiently provide stable electrophilic analogues of DNR and DOX that can be isolated, characterized, and stored. A stable anticancer drug–antibody conjugate can be produced by mixing the analogues with a monoclonal antibody. The potential use of the present DNR–OC125 bioconjugates for treating a variety of antibody-targeted cancers is suggested by results from in vitro tests. The bioconjugates are both selectively toxic to human ovarian cancer cell lines (1) and also specifically bind to tissue

sections from human ovarian cancers (2) that express the CA125 antigen.

ACKNOWLEDGMENT

We gratefully acknowledge the technical assistance of Qingxuan Chen (PAGE), in vitro toxicity testing by John L. Collins and Deanne Perry, the generosity of Adria Laboratories of Columbus, OH, for providing Doxorubicin, Wyeth Laboratories of Princeton, NJ, for daunorubicin, and Centocor Laboratories of Malvern, PA, for the OC125 monoclonal antibody used in this study. NMR spectra were recorded at the Washington University High-Resolution NMR Facility that is partly funded by NIH Shared Instrument Grant No. 1-S10-RR02004. This research was supported by a grant from the Fraternal Order of Eagles (MO).

LITERATURE CITED

- (1) Sweet, F., Rosik, L. O., Sommers, G. M., and Collins, J. L. (1989) Daunorubicin conjugated to a monoclonal anti-CA-125 antibody selectively kills human ovarian cancer cells. *Gynecol. Oncol.* 34, 305–311.
- (2) Dezső, B., Török, I., Rosik, L. O., and Sweet, F. (1990) Human ovarian tumors specifically bind daunorubicin–OC125 antibody conjugates: an immunofluorescence study. *Gynecol. oncol.*, in press.
- (3) Ghose, T. I., Blair, A. H., Vaughan, K., and Kulkarni, P. (1983) *Targeted Drugs* (E. P. Goldberg, Ed.) pp 1–22, J. Wiley and Sons, New York.
- (4) Reisfeld, R. A., and Cherish, D. A. (1985) Human tumor-associated antigens: targets for monoclonal antibody-mediated cancer therapy. *Cancer Surv.* 4, 271–290.
- (5) Frankel, A. E., Houston, L. L., Issell, B. F., and Fathman, G. (1986) Prospects for immunotoxin therapy in cancer. *Ann. Rev. Med.* 37, 125–142.
- (6) Ghose, T., and Blair, A. H. (1987) The design of cytotoxic-antigen–antibody conjugates. *Crit. Rev. Ther. Drug Carrier Syst.* 3, 263–359.
- (7) Pietrersz, G. A., Kanellos, J., Smyth, M. J., Zalberg, J., and McKenzie, I. F. C. (1987) The use of monoclonal antibody conjugates for the diagnosis and treatment of cancer. *Immunol. Cell Biol.* 65, 111–125.
- (8) Rodwell, J. D. (1988) *Antibody-Mediated Delivery Systems* Marcel Dekker, New York.
- (9) Rodwell, J. D., Alvarez, V. L., Lee, C., Lopes, A. D., Goers, J. W. F., King, H. D., Powsner, H. J., and McKearn, T. J. (1986) Site-specific covalent modification of monoclonal antibodies: in vitro and in vivo evaluations. *Proc. Natl. Acad. Sci. U.S.A.* 83, 2632–2636.
- (10) Laguzza, B. C., Nichols, C. L., Briggs, S. L., Cullinan, G. J., Johnson, D. A., Starling, J. J., Baker, A. L., Bumol, T. F., and Corvalan, J. R. F. (1989) New antitumor monoclonal antibody–vinca conjugates LY203725 and related compounds: Design, preparation, and representative in vivo activity. *J. Med. Chem.* 32, 548–555.
- (11) Diener, E., Diner, U. E., Sinha, A., Xie, S., and Vergidis, R. (1986) Specific immunosuppression by immunotoxins containing daunomycin. *Science* 231, 148–150.
- (12) Means, G. E., and Feeney, R. E. (1990) Chemical Modifications of Proteins: History of Applications. *Bioconjugate Chem.* 1, 2–12.
- (13) Koppel, G. A. (1990) Recent Advances with Monoclonal Antibody Drug Targeting for the Treatment of Human Cancer. *Bioconjugate Chem.* 1, 13–23.
- (14) Hurwitz, E., Levy, R., Maron, R., Wilchek, M., Arnov, R., and Selig, M. (1975) The covalent binding of daunomycin and adriamycin to antibodies with retention of both drug and antibody activities. *Cancer Res.* 35, 1175–1181.
- (15) Gallego, J., Price, M. R., and Baldwin, R. W. (1984) Preparation of four daunomycin–monoclonal antibody 79IT/36 conjugates with anti-tumor activity. *Int. J. Cancer* 33, 737–744.

- (16) Yang, H. M., and Reisfeld, R. A. (1988) Doxorubicin conjugated with monoclonal antibody directed to a human melanoma-associated proteoglycan suppresses the growth of established tumor xenographs in nude mice. *Proc. Natl. Acad. Sci. U.S.A.* 85, 1189-1193.
- (17) Pietersz, C. A., Smyth, M. J., and McKenzie, I. F. C. (1988) The use of anthracycline-antibody complexes for the specific antitumor activity. In *Antibody-Mediated Delivery Systems* (J. D. Rodwell, Ed.) Marcel Dekker, New York.
- (18) Sweet, F., and Murdock, G. L. (1987) Affinity labeling of hormone-specific proteins. *Endocr. Rev.* 8, 154-184.
- (19) Riggs, J. L., Seiwald, R. J., Burckhalter, J. H., Downs, C. M., and Metcalf, T. G. (1958) Isothiocyanate compounds as fluorescent labeling agents for immune serum. *Am. J. Pathol.* 34, 1081-1097.
- (20) McKinney, R. M., Spillane, J. T., and Pearce, G. W. (1964) Factors affecting the rate of reaction of fluorescein isothiocyanate with serum proteins. *J. Immunol.* 93, 232-242.
- (21) Nairn, R. C. (1976) *Fluorescent Protein Tracing* Churchill Livingstone, New York.
- (22) Meares, C. F., McCall, M. J., Reardan, D. T., Goodwin, D. A., Diamanti, C. I., and McTigue, M. (1984) Conjugation of Antibodies with Bifunctional Chelating Agents: Isothiocyanate and Bromoacetamide Reagents, Methods of Analysis, and Subsequent Addition of Metal Ions. *Anal. Biochem.* 142, 68-78.
- (23) Westerberg, D. A., Carney, P. L., Rogers, P. E., Kline, S. J., and Johnson, D. K. (1989) Synthesis of novel bifunctional chelators and their use in preparing monoclonal antibody conjugates for tumor targeting. *J. Med. Chem.* 32, 236-243.
- (24) Mirzadeh, S., Brechbiel, M. W., Atcher, R. W., and Gansow, O. A. (1990) Radiometal Labeling of Immunoproteins: Covalent Linkage of 2-(4-Isothiocyanatobenzyl)diethylene-triaminepentacetic Acid Ligands to Immunoglobulin. *Bioconjugate Chem.* 1, 59-65.
- (25) Lowry, O. H., Rosebrough, N. J., Farr, A. L., and Randall, R. J. (1951) Protein measurement with folin phenol reagent. *J. Biol. Chem.* 193, 265-275.
- (26) Fieser, L. F., and Fieser, M. (1967) *Reagents for Organic Synthesis* pp 286-287, J. Wiley and Sons, New York.
- (27) Samant, B. R., and Sweet, F. (1983) 5'-Bromoacetamido-5'-deoxyadenosine. A novel reagent for labeling adenine nucleotide sites in proteins. *J. Biol. Chem.* 258, 12779-12782.
- (28) Pal, P. K., Wechter, W. J., and Colman, R. F. (1975) Affinity labeling of a regulatory site of bovine liver glutamate dehydrogenase. *Biochemistry* 14, 707-715.
- (29) Iwamoto, R. H., Lim, P., and Bhacca, N. S. (1968) The structure of daunomycin. *Tetrahedron Lett.* 3891-3894.
- (30) Arcamone, F., Cassinelli, G., Franceschi, G., Orezzi, P., and Mondelli, R. (1968) Total absolute configuration of daunomycin. *Tetrahedron Lett.* 3353-3356.
- (31) Arcamone, F., Franceschi, G., Orezzi, P., Cassinelli, G., Barbieri, W., and Mondelli, R. (1964) Daunomycin I. The structure of daunomycinone. *J. Am. Chem. Soc.* 86, 5334-5335.
- (32) Wong, C. M., Schwenk, R., Popien, D., and Ho, T.-L. (1973) The total synthesis of daunomycinone. *Can. J. Chem.* 51, 466-467.
- (33) Arcamone, F., Franceschi, G., and Penco, S. (1969) Adriamycin, a novel antitumor antibiotic. *Tetrahedron Lett.* 1007-1010.
- (34) Unpublished results.
- Registry No.** 1, 150-13-0; 2, 2393-17-1; 3, 2131-62-6; 4, 127793-04-8; 5, 53611-24-8; 6, 127793-05-9; 7, 110409-19-3; 8, 127793-06-0; 9, 127793-07-1; 10, 47831-81-2; 11, 127793-08-2; 12, 127793-09-3; thiophosgene, 463-71-8; bromoacetyl bromide, 598-21-0; *p*-(fluorosulfonyl)benzoyl chloride, 402-55-1; daunorubicin hydrochloride, 23541-50-6; doxorubicin hydrochloride, 25316-40-9.

Electrochemical Investigations of the Interaction of Metal Chelates with DNA. 3. Electrogenenerated Chemiluminescent Investigation of the Interaction of Tris(1,10-phenanthroline)ruthenium(II) with DNA

Michael T. Carter[†] and Allen J. Bard*

Department of Chemistry, The University of Texas at Austin, Austin, Texas 78712. Received March 28, 1990

The electrogenerated chemiluminescence (ECL) that results from the oxidation of tris(1,10-phenanthroline)ruthenium(II), at a gold electrode in the presence of oxalate, was used to investigate the interaction of the Ru(II) chelate with calf thymus DNA. The decrease in ECL emission from the excited state, $\text{Ru}(\text{phen})_3^{2+*}$, in the presence of DNA, is ascribed to binding of the chelate to the DNA strand. An ECL titration of the metal complex with DNA allowed determination of the equilibrium constant (K) and binding-site size (s) for association of $\text{Ru}(\text{phen})_3^{2+}$, under the assumption that only the free metal complex contributes to the observed emission. In 25 mM $\text{Na}_2\text{C}_2\text{O}_4$, 2 mM phosphate buffer, pH 5, 0.05% Tween-20, 0.05% Triton X-100, regression based on the McGhee/von Hippel model, which accounts for free base pair gaps between binding sites, yielded $K = 8.1 (\pm 0.2) \times 10^3 \text{ M}^{-1}$ and $s = 4 \text{ bp}$.

INTRODUCTION

We describe the application of electrogenerated chemiluminescence (ECL) measurements to an investigation of the binding of tris(1,10-phenanthroline)ruthenium(II), $\text{Ru}(\text{phen})_3^{2+}$, to calf thymus DNA. ECL has been used to investigate electrode reactions that lead to excited states, with applications to analytical problems (1). Many studies have been carried out on ECL systems based on chelates of Ru(II), e.g. $\text{Ru}(\text{bpy})_3^{2+}$ (bpy = 2,2'-bipyridine), $\text{Ru}(\text{phen})_3^{2+}$, and their derivatives, which yield emissions characteristic of the RuL_3^{2+*} excited state via direct annihilation of the 1+ and 3+ oxidation states in cyclic potential step experiments (2-6), or via generation of the excited state in a single potential step, in the presence of a reactant such as oxalate or peroxydisulfate that generates a strong oxidant or reductant intermediate (e.g., $\text{CO}_2^{\cdot-}$ or $\text{SO}_4^{\cdot-}$) (7-10). Analytical methods, e.g., for oxalate or with Ru chelate tags (10), based on ECL have been reported. An ECL analysis is carried out in an electrochemical cell containing appropriate reagents (e.g., the Ru species, oxalate, buffer). The imposition of the appropriate electrical signal to the working electrode causes light emission. The fact that no excitation light is employed in ECL, as it is in photoluminescence, leads to high sensitivities in ECL detection. Moreover, the specific nature of the ECL reaction, with control over both electrochemical and spectroscopic variables, promotes high selectivity.

Barton has reported (11-13) the use of enantiomers of $\text{Ru}(\text{phen})_2^{2+}$ (14), $\text{Ru}(\text{phen})_3^{2+}$, $\text{Ru}(\text{DIP})_3^{2+}$ (DIP = 4,7-diphenyl-1,10-phenanthroline) (15-19), and $\text{Ru}(\text{TMP})_3^{2+}$ (TMP = 3,4,7,8-tetramethyl-1,10-phenanthroline) (20) as chiral probes for the B, Z, and A conformations of DNA. Metal-activated cleavage of DNA strands can also be accomplished by Ru(II) chelates (21, 22). Because of the wide interest in $\text{Ru}(\text{phen})_3^{2+}$ and related complexes in the study of DNA conformation and cleavage and of chemiluminescent systems to biological problems (23-25), we have chosen to investigate the ECL of $\text{Ru}(\text{phen})_3^{2+}$ in the

presence of DNA, as a means of characterizing the binding of the luminescor to the DNA strand.

To our knowledge, ECL studies of equilibria for binding of metal chelates to DNA have not been reported previously. ECL provides a useful extension of our previously reported voltammetric studies of the binding of metal chelates to DNA (26, 27). Detection of luminescence can be achieved with high precision and has the advantage compared to voltammetric and spectrophotometric measurements that very low concentrations of complex (e.g., micromolar to nanomolar) can be used. As shown below, analysis of the binding data from titration experiments is simplified, in the case of the $\text{Ru}(\text{phen})_3^{2+}$ -oxalate ECL system, where the oxalate species does not interact with DNA.

EXPERIMENTAL PROCEDURES

Materials. Calf thymus DNA was purchased from Sigma Chemical Co. (St. Louis, MO) and used as received. Previous studies with this material (26, 27) have shown no differences in binding studies with as-received and purified material. The details of the handling of the DNA have been described previously (26, 27). Tris(1,10-phenanthroline)ruthenium(II) dichloride, $\text{Ru}(\text{phen})_3\text{Cl}_2$, was purchased from Aldrich Chemical Co. (Milwaukee, WI). The as-received material was dissolved in hot water to filter out an unidentified, insoluble, black substance. The filtrate was concentrated to a small volume and allowed to evaporate to dryness at room temperature to obtain the metal complex. Tween-20 was obtained from Sargent-Welch (Irving, TX) and Triton X-100 was from Fluka Chemical Corp. (Ronkonkoma, NY). Tripropylamine (TPRA) (98%) was obtained from Aldrich and used as received. All other chemicals for preparation of electrolytes were reagent grade and used without further purification. Solutions were prepared with high-purity water from a Millipore Milli-Q reagent water system.

Procedures. Experiments were carried out with solutions of $\text{Ru}(\text{phen})_3^{2+}$ with either oxalate or TPRA buffered to the pH for optimum ECL response. Concentrations of DNA were measured in electrolyte 1 [25

[†] Present address: The State University of New York at Buffalo, Department of Chemistry, Buffalo, NY 14214.

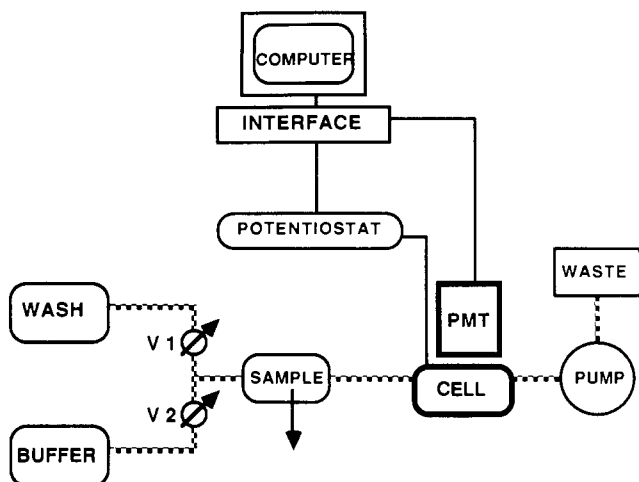


Figure 1. Block diagram of an Origen Analyzer.

mM $\text{Na}_2\text{C}_2\text{O}_4$, 2 mM H_3PO_4 , 0.05% (w/v) Tween-20, 0.05% w/v Triton X-100, adjusted to pH 5 with NaOH] and electrolyte 2 (25 mM TPrA, 7.2 mM H_2SO_4 , 16.1 mM Na_2SO_4 , 0.05% Tween-20, 0.05% Triton X-100, adjusted to pH 5 with NaOH) assuming $\epsilon_{260} = 6600 \text{ M}^{-1} \text{ cm}^{-1}$ (28). Concentrations of $\text{Ru}(\text{phen})_3^{2+}$ in electrolytes 1 and 2 were measured by assuming $\epsilon_{447} = 19\,000 \text{ M}^{-1} \text{ cm}^{-1}$ (29). Solutions of DNA and $\text{Ru}(\text{phen})_3^{2+}$ in electrolytes 1 and 2 showed the same absorbances at λ_{max} as in equimolar solutions in 50 mM NaCl. The surfactants Tween-20 and Triton X-100 were added to prevent bubble formation in the flow ECL cell in the analyzer and to promote more effective cleaning of the cell in the flushes with pure electrolyte between samples (32). In a recent ECL study of the interaction of another metal chelate with DNA, to be reported elsewhere, we have found procedures where addition of surfactant can be avoided.

For ECL measurements, 0.6 mL of the solution of interest (8–9 μM $\text{Ru}(\text{phen})_3^{2+}$ containing different excesses of nucleotides) was pumped through the flow cell of the ECL analyzer described below, in a flow stream of the appropriate electrolyte. Measurements were taken during a potential sweep, under quiescent solution conditions. The potential applied to the potentiostat was scanned linearly from 0.565 to 2.4 V vs Ag/AgCl, at 438 mV/s. The ECL cell configuration used in the analyzer resulted in a significant uncompensated resistance between working and reference electrodes, so the actual working electrode potential was less positive, but clearly encompassed the $\text{Ru}(\text{II})$ oxidation wave. Luminescence from the $\text{Ru}(\text{phen})_3^{2+}$ excited state was measured in 34-ms intervals, during a scan. All measurements were obtained on air-equilibrated samples, at the ambient temperature of the laboratory (23–25 °C). Five replicate measurements were performed on each sample.

Stock solutions of DNA (2–3 mM nucleotide phosphate, NP) and $\text{Ru}(\text{phen})_3^{2+}$ (1 mM) were prepared fresh for each series of experiments and discarded immediately after use. All glassware was silanized with a 5% solution of trimethylchlorosilane in toluene.

Instrumentation. Electrogenerated chemiluminescence (ECL) was measured on an Origen 1 Analyzer (IGEN, Inc., Rockville, MD), an automated, computer-controlled (IBM PS/2 Model 25) flow system for ECL analysis of different types of samples (Figure 1). In this system the sample is introduced into a flow stream of the appropriate solution and is pumped into an electrochemical flow cell, equipped with a Plexiglas window where the working electrode surface is viewed by a photomultiplier tube

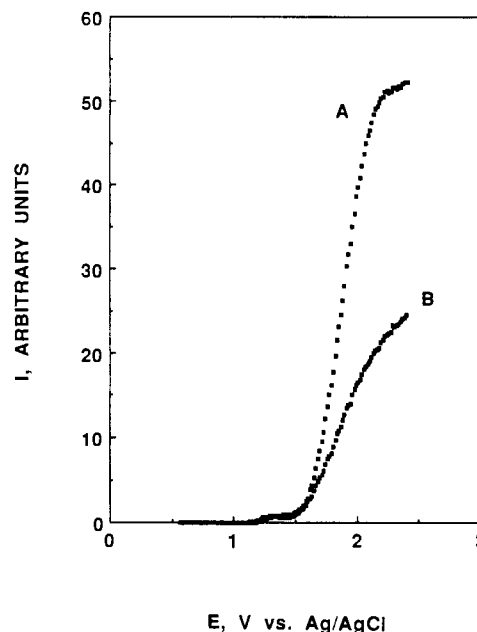


Figure 2. Typical intensity-potential curves for 9.2 μM $\text{Ru}(\text{phen})_3^{2+}$ (A) in the absence and (B) in the presence of 0.28 mM nucleotide phosphate.

(PMT). The working and counter electrodes were gold disks (geometric area = 0.071 cm^2) and the reference electrode was Ag/AgCl (3 M NaCl) located downstream of the flow cell. Cell resistances were 2600Ω (working-to-counter electrode) and $7.2 \times 10^4 \Omega$ (working-to-reference electrode leads), in electrolyte 1, as measured with a Yellow Springs Instruments Model 35 conductance meter. The thickness of the solution layer in the cell was ca. 0.5 mm. During analysis, the flow was stopped and a programmed potential sweep was applied to the working electrode. ECL during the sweep was detected with a Hamamatsu R 1104 PMT, operated at 850 V.

Spectroscopic measurements were done on a Hewlett-Packard Model 8450A dual-beam spectrophotometer. Cyclic voltammetry (CV) and square wave voltammetry (SWV) were performed on a Bioanalytical Systems (BAS) Model 100 electrochemical analyzer. SWV was performed with square wave amplitude = 25 mV and step height = 5 mV. The square wave frequency was 15 Hz. Working electrodes for voltammetry were either a BAS glassy carbon disk (geometric area = 0.071 cm^2) or a gold disk sealed in glass (geometric area = 0.03 cm^2). A Pt flag served as the counter electrode and the reference was a saturated calomel electrode (SCE). Analysis of titration data from ECL experiments was performed using nonlinear-regression routines available from the SAS statistical software package (The SAS Institute, Cary, NC) on an IBM 3081D computer.

RESULTS

Effect of DNA on ECL Emission. A typical intensity (I)-potential curve for the $\text{Ru}(\text{phen})_3^{2+}$ -oxalate system (electrolyte 1) is shown in Figure 2, for a total concentration (C_t) of $\text{Ru}(\text{phen})_3^{2+}$ of 9.2 μM . The potentials shown in Figure 2 should be considered as values applied to the potentiostat because of the large, uncompensated resistance of the electrochemical cell. Onset of ECL from $\text{Ru}(\text{phen})_3^{2+}$ occurred at ca. 1.25 V vs Ag/AgCl and reached a maximum at ca. 2.0 V, in the absence of DNA. In the presence of 0.28 mM nucleotide phosphate [NP] (Figure 2B, i.e., at a ratio of nucleotide phosphate, NP, to metal complex, R, of 30), the intensity decreased to 48% of that in the absence of DNA. Since the solution layer through

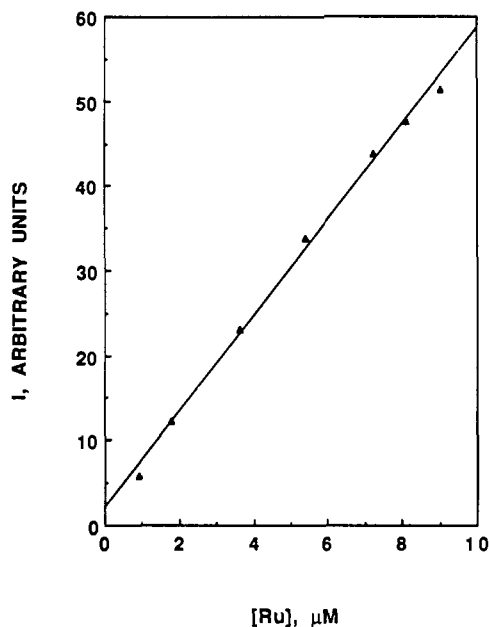


Figure 3. Detector response for concentrations of $\text{Ru}(\text{phen})_3^{2+}$ varied between 9.02 and 0.9 μM , in DNA-free solution.

which the emitted light passes is thin (ca. 0.5 mm), the decrease in ECL in the presence of DNA cannot be attributed to scattering by DNA. Additionally, at higher photomultiplier voltages, where background emission from electrolyte could be measured, the presence of a large concentration of DNA caused no decrease in the background. For example, at $[\text{NP}] = 0$, the emission intensity, I , was 33 (arbitrary units), and at $[\text{NP}] = 1.4 \text{ mM}$, $I = 55$. Thus, in the presence of DNA, background emission actually increased slightly. Significant adsorption of DNA onto the gold electrode during a measurement would be expected to have the opposite effect, especially if light scattering occurred. Irreversible adsorption of DNA would also be expected to yield decreases in intensity upon repetitive runs on the same $\text{Ru}(\text{II})/\text{DNA}$ mixture. However, all measurements during a series of experiments were reproducible, regardless of the order in which the solutions were sampled.

A plot of the peak ECL emission intensity, I , against concentration of $\text{Ru}(\text{II})$, in the absence of DNA, was linear, as shown in Figure 3. Here, the concentrations of $\text{Ru}(\text{II})$ were chosen to span the range of observed decreases in ECL intensity, as a function of DNA concentration, in titration experiments (see below). Linearity of the response to $\text{Ru}(\text{II})$ concentration is important in this system, since it bears directly upon the model used to fit titration data. The small intercept represents background emission in the oxalate, as previously observed at other electrode materials in studies of $\text{Ru}(\text{bpy})_3^{2+}$ system ECL (10). It has been ascribed to effects of traces of undefined impurity or to inverse photoemission from the metal electrode.

Cyclic Voltammetry in Oxalate Electrolyte. Cyclic voltammograms of electrolyte 1 showed an oxidation wave at 0.7 V vs SCE on the first positive-going scan at a gold disk. Upon subsequent scans, the wave disappeared. The oxidation wave observed on the initial scan corresponds to oxidation of the gold electrode surface. On the second and subsequent scans this wave is absent because the oxide is not reduced by the oxalate in the solution. The oxidation wave only reappeared upon scanning the potential of the electrode from 0.0 to -1.0 V, but subsequent positive-going scans again showed a diminished oxidation wave upon repeated scanning. Direct oxidation of oxalate on

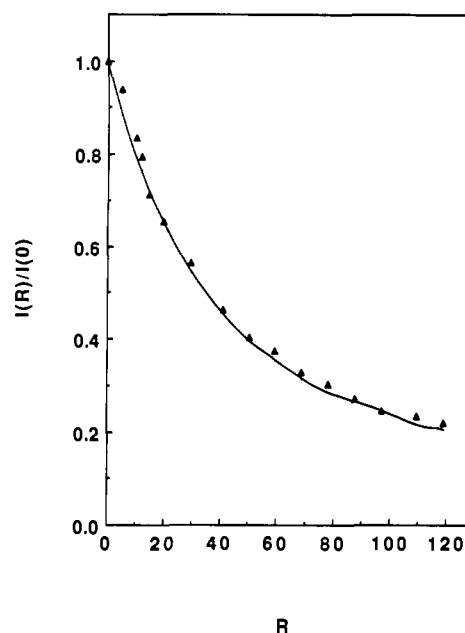


Figure 4. ECL titration of 8.7 μM $\text{Ru}(\text{phen})_3^{2+}$ with DNA, in electrolyte 1. Normalized emission intensity vs R , where $R = [\text{nucleotide phosphate}]/[\text{total Ru}] = [\text{NP}]/C_t$. Points are experimental data and the solid curve represents that calculated based on the equilibrium model of McGhee and von Hippel.

the oxidized gold electrode does not occur until oxidation of $\text{Ru}(\text{phen})_3^{2+}$ takes place at +1.1 V vs SCE.

Experimental Titration Results. Results of a titration of 8.7 μM $\text{Ru}(\text{phen})_3^{2+}$ with DNA, in electrolyte 1, are shown in Figure 4. Experimental data are plotted as peak emission intensity, I , normalized to I at $R = 0$, $[I(0)]$ vs R where

$$R = [\text{nucleotide phosphate}]/[\text{total Ru}] = [\text{NP}]/C_t$$

The data were regressed onto eq 3, below, with K determined from a one-parameter fit, for integer values of s (15, 27). The best fit for the experimental curve was $K = 8.1 (\pm 0.2) \times 10^3 \text{ M}^{-1}$ and $s = 4 \text{ bp}$ (solid curve of Figure 4). Extensive sonication of a solution containing 9.0 μM $\text{Ru}(\text{phen})_3^{2+}$ and 0.86 mM NP (electrolyte 1) resulted in only ca. 14% increase in ECL intensity after 65 min of treatment. ECL of a solution containing only $\text{Ru}(\text{phen})_3^{2+}$ was not affected when sonicated for the same amount of time.

Experiments were performed in which 25 mM tri-*n*-propylamine (TPPrA) was cooxidized with $\text{Ru}(\text{phen})_3^{2+}$ to produce ECL (electrolyte 2) (32, 33). The ionic strength and pH of this system was the same as those for electrolyte 1. Since binding of $\text{Ru}(\text{phen})_3^{2+}$ to DNA is dependent on ionic strength (18), no difference in normalized ECL intensity would be expected, at the same C_t and R , between the $\text{Ru}(\text{phen})_3^{2+}$ -oxalate and $\text{Ru}(\text{phen})_3^{2+}$ -TPPrA systems, assuming equal interactions of TPPrA and oxalate with DNA. However, $I(R)/I(0)$ was larger, at all R investigated, in the TPPrA system than for the corresponding experiment in the oxalate system. For example, at $R = 40$ (8.8 μM $\text{Ru}(\text{II})$), $I(R)/I(0) = 0.47$ for oxalate vs 0.63 for TPPrA, and at $R = 80$, $I(R)/I(0) = 0.30$ for oxalate vs 0.49 for TPPrA. As shown in Figure 2, the detector response to ECL in the $\text{Ru}(\text{phen})_3^{2+}$ -TPPrA system was linear with concentration of $\text{Ru}(\text{II})$, over a concentration range bracketing the observed decrease in intensity with addition of DNA.

An Equilibrium Binding Model. The peak intensity, I , is a linear function of $\text{Ru}(\text{phen})_3^{2+}$ concentration, in the absence of DNA

$$I/I_0 = C/C_0 \quad (1)$$

where I and I_0 are the peak intensities at concentrations of Ru(II) C and C_0 , respectively. A treatment of binding data, based on a modification of the classical Scatchard binding isotherm (34), has been reported by McGhee and von Hippel. This model (35) accounts for the presence of free gaps on DNA which are less than s bp long and thus cannot participate in binding of the metal complex (i.e., the DNA strand cannot be saturated with metal complex). The relevant equation for noncooperative binding, based on an analogous one of Barton et al. (15), with $\nu = C_b/[NP]$, is

$$\frac{\nu}{C_f} = \frac{K}{2}(1 - 2s\nu) \left[\frac{1 - 2s\nu}{1 - 2(s-1)\nu} \right]^{s-1} \quad (2)$$

where C_b and C_f are the equilibrium concentrations of DNA-bound and free metal complex, respectively, K is the microscopic binding constant, and s is the binding-site size, in base pairs, bp. This may be rewritten to give the normalized ECL intensity as a function of C_t and R :

$$\frac{I(R)}{I(0)} = \left\{ \frac{RC_t K}{2} [1 - 2s(X_b/R)] \times \left[\frac{1 - 2s(X_b/R)}{1 - 2(s-1)(X_b/R)} \right]^{s-1} + 1 \right\}^{-1} \quad (3)$$

where $I(R)$ and $I(0)$ are the intensities measured at R and $R = 0$, respectively, $C_t = C_b + C_f$, and $X_b = C_b/C_t$, under the assumption that only the free metal complex contributes to ECL. The value of s for the titration data of Figure 4 is in excellent agreement with that determined by Barton (15). K is ca. 30% larger than in the previous determination ($K = 6.3 \times 10^3 \text{ M}^{-1}$, in 50 mM NaCl, 5 mM Tris, pH 7.1) (15).

Comparison to the Voltammetric Binding Model.

We have previously shown that the concentration of bound metal, C_b , as a function of total metal concentration, C_t , binding constant, K , and binding-site size, s , is (26, 27)

$$C_b = \{b - [b^2 - (2K^2 C_t [NP]/s)]^{1/2}\} / 2K \quad (4a)$$

$$b = 1 + KC_t + K[NP]/2s \quad (4b)$$

Equation 4 assumes (1) nonspecific, (2) noncooperative binding, and (3) existence of a single, discrete binding site. Assumption 3 may be interpreted as the ability to saturate the DNA strand with metal complex (i.e., all base pairs can participate in binding). With this model the ECL intensity is given by

$$I(R) = A_f C_f + A_b C_b \quad (5)$$

where A_f and A_b are constants of proportionality for ECL arising from free and bound metal complex, respectively. This may be rewritten as

$$I(R) = A_f C_f + X A_f C_b \quad (6a)$$

$$I(0) = A_f C_t \quad (6b)$$

where X ($0 \leq X \leq 1$) represents the fraction of total ECL due to bound metal. Combining eqs 6a and 6b gives

$$I(R)/I(0) = r(1 - X) + X \quad (7a)$$

$$r = C_f/C_t \quad (7b)$$

Equation 7 reduces to the equivalent of eq 1 when $X = 0$ (i.e., bound metal does not contribute to ECL emission). Note that this assumption allows calculation of binding constant and binding-site size without knowledge of the diffusion coefficients of the free and DNA-bound metal

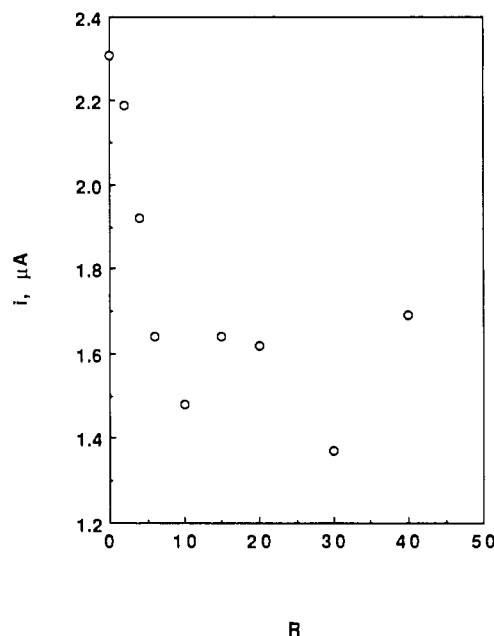


Figure 5. Square wave voltammetric titration of $9.2 \times 10^{-5} \text{ M}$ $\text{Ru}(\text{phen})_3^{2+}$ with DNA. The electrolyte was 25 mM $\text{Na}_2\text{C}_2\text{O}_4$, 2 mM H_3PO_4 , pH 5.0.

complex (D_f and D_b) or of the ECL efficiency for the $\text{Ru}(\text{phen})_3^{2+}$ -oxalate system. The magnitudes of the binding parameters were calculated via eq 7, again fitting K for integer values of s (26, 27). A plot of the experimental data, superimposed on the best-fit curve, was essentially identical to that shown in Figure 4, except as noted below. The best fit of the experimental data to the simple binding model given above was $K = 9.0 (\pm 0.4) \times 10^4 \text{ M}^{-1}$ and $s = 10$ bp (when $X = 0$), suggesting that some segments of the DNA strand are unavailable for binding. The binding-site size here is much larger than that determined previously for binding of racemic $\text{Ru}(\text{phen})_3^{2+}$ (in 50 mM NaCl, 5 mM Tris, pH 7.1) to calf thymus DNA (15). While the agreement between experiment and calculations from the two models is about the same for $R \leq 60$, there is slightly better agreement at $R > 60$ when eq 3 is used, vs eq 7. The implications of the titration results are discussed below.

To test further the validity of the assumption that bound metal does not contribute significantly to ECL, additional two-parameter fits were performed in which K and X were determined for $s = 10$ bp. These calculations gave $K = 9.6 (\pm 0.8) \times 10^4 \text{ M}^{-1}$ and $X = 0.02$. The sum of squares deviation obtained here agreed with that from the one-parameter fit of K , above, to within 3%. Thus, we can estimate that at least 98% of the ECL is due to free metal complex and that the assumptions used in fitting titration data are valid, within the error of the measurement.

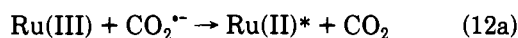
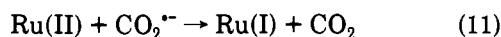
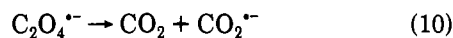
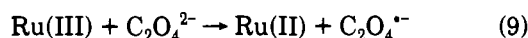
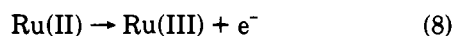
Square Wave Voltammetry. To test the possibility that the surfactants present in the electrolyte used for ECL measurements may interfere with binding of $\text{Ru}(\text{phen})_3^{2+}$ to DNA, independent measurements of binding were performed by using square wave voltammetry (SWV). SWV was employed, rather than the cyclic voltammetry or differential pulse voltammetry used in earlier electrochemical experiments (26, 27), because very small concentrations of $\text{Ru}(\text{II})$ were used to keep the concentration range equivalent to that in the ECL experiments. Measurements cannot be carried out conveniently with electrolytes without added surfactants in the ECL apparatus described above. Typical results are shown in Figure 5, where the peak current in SWV for oxidation of $\text{Ru}(\text{phen})_3^{2+}$ to the 3+ ion is plotted

as a function of R . The electrolyte here was electrolyte 1, but without added Triton X-100 or Tween-20. Although SWV measurements at these concentrations are not very precise and the data show appreciable scatter, particularly at larger values of R where the concentration of unbound Ru(phen)_3^{2+} is small, the titration curve in Figure 5 indicates that the binding-site size (s), in the absence of surfactants, is smaller than that found in ECL measurements. A value of $s = 10$ bp would correspond to $R = 20$ in Figure 5. The data indicate a value of s closer to 5 bp.

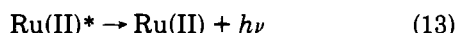
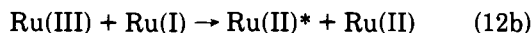
The peak potential of the $\text{Ru(phen)}_3^{2+/3+}$ redox couple is severely overlapped by the background oxidation of the electrolyte. Although the data shown in Figure 5 represent background-subtracted peak currents, the background current in the region of Ru(II) oxidation is not particularly reproducible. The result is the scatter in the data shown. Thus, while this experiment suggests that the absence of surfactant causes the apparent value of s to decrease, we could not obtain quantitative results from nonlinear-regression analysis, based on a SWV analogue of our previously reported voltammetric titration method (26, 27). Voltammetric measurements under the electrolyte conditions of the ECL measurements, i.e., with added Triton X-100 or Tween-20, could not be carried out because electroactive components in the surfactant stock solutions interfered with the Ru(II) oxidation wave.

DISCUSSION

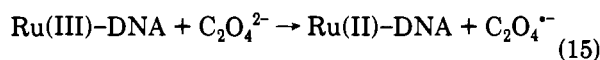
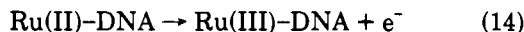
ECL in electrolyte 1 originates from oxidation of Ru(phen)_3^{2+} , in the presence of oxalate, according to the following sequence of reactions (8, 10):



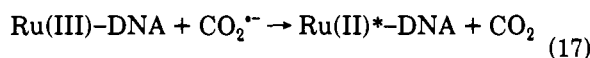
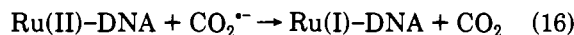
or



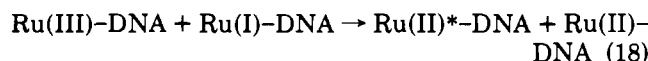
where Ru(II) and Ru(III) represent Ru(phen)_3^{2+} and Ru(phen)_3^{3+} . In the presence of DNA, the corresponding reaction sequence is



followed by eq 10 and



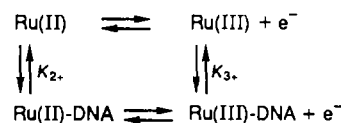
or



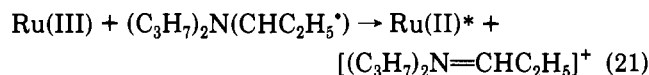
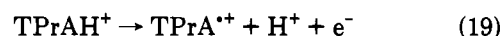
followed by eq 13, where -DNA denotes a metal complex bound to DNA. However the results indicate that emission does not result from Ru(II) bound to DNA. This might be caused by inaccessibility of DNA-bound Ru species to $\text{CO}_2^{\bullet -}$ or $\text{C}_2\text{O}_4^{2-}$ (e.g. because of steric constraints or electrostatic effects due to the negative charge on the DNA

double helix, as discussed below). This reduces this series of reactions to eqs 8–14. The ECL intensity is controlled by the equilibrium binding of the metal chelate to DNA. Combining eqs 8 and 14, by analogy with our previous work (26, 27) and electrochemical studies of the interaction of electroactive species with micelles (36, 37), gives Scheme I.

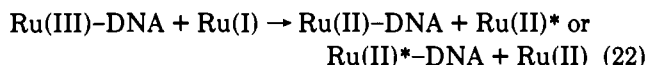
Scheme I



The mechanism of light emission in the Ru(phen)_3^{2+} -TPPrA system has not been elucidated but probably proceeds through a reaction sequence similar to that of Ru(phen)_3^{2+} -oxalate, with cooxidation of Ru(phen)_3^{2+} and TPPrAH^+ producing the excited state-chelate by eq 8, followed by (32, 33, 38)



Binding of cations to DNA is driven by release of counterions from the helix (e.g., Na^+) (39, 40). In view of the experimental results described above for the differences in behavior of the oxalate and TPPrA systems, it is reasonable that the ECL is essentially due to free Ru(phen)_3^{2+} . Since TPPrA is fully protonated at pH 5.0 ($\text{pK}_a = 10.6$), these results suggest that bound Ru(phen)_3^{2+} can participate to a small extent in ECL in electrolyte 2, because TPPrAH^+ can approach the anionic sugar-phosphate backbone of DNA. In electrolyte 1, however, oxalate exists as 84% dianionic and 16% monoanionic forms. Oxalate would not be expected to interact with DNA as strongly as TPPrAH^+ , because of coulombic repulsion. While the reactant $\text{TPPrA}^{\bullet +}$ in eqs 20 and 21 is uncharged, TPPrA is initially delivered to the bound Ru species as the protonated form. The results support the assumption that the ECL component from bound metal in the oxalate system can be neglected and are consistent with our previous observations on the lack of influence of DNA on the diffusion of anions, such as Mo(CN)_6^{4-} and Fe(CN)_6^{3-} (26, 27) as well as observations on luminescence quenching of Ru(phen)_3^{2+} , bound to DNA, by ferrocyanide (17). The photoluminescence of Ru(phen)_3^{2+} is enhanced upon binding to DNA (15, 17, 18, 41), in the absence of added quencher. The excited state of another intercalator, ethidium, bound to DNA is effectively quenched by cationic species, e.g. methylviologen (42, 43), whereas Ru(phen)_3^{2+} bound to DNA is protected from quenching by anionic species such as Fe(CN)_6^{4-} (17). The enhanced luminescence of Ru(phen)_3^{2+} intercalated into DNA was attributed to "greater rigidity and lower collisional frequency of the molecule when stacked within the helix". This same decreased collisional frequency, with $\text{C}_2\text{O}_4^{2-}$, HC_2O_4^- and $\text{CO}_2^{\bullet -}$, would decrease excited-state formation. The lower diffusion coefficient of Ru(phen)_3^{2+} when bound to DNA would also decrease the contribution from bound Ru(phen)_3^{2+} . The small increase in ECL, in experiments where the metal complex-DNA mixture was sonicated, may be due to a small contribution from cross-reactions, e.g.



in which degradation of the DNA strand by ultrasound would enhance ECL production by increasing the diffusion coefficient of the bound metal.

The simple equilibrium binding model, used previously for analysis of titration curves from voltammetric experiments involving diffusion of an equilibrium mixture of free and DNA-bound metal complex (26, 27), yields values of K and s in this study that appear to be unreasonably large, compared to those of previous studies. This model assumes that the DNA strand can be saturated with metal complex (i.e., gaps of $< s$ bp are rare or nonexistent). While this model was successful in analyzing binding data in uncomplicated solutions, e.g. 50 mM NaCl (26, 27), in the present case, the presence of surfactants may affect the binding of Ru(phen)_3^{2+} . For example, the nonionic surfactant Triton X-100 could associate hydrophobically with the DNA helix, preventing some base pairs from interaction with Ru(phen)_3^{2+} . The structurally similar 5-alkylresorcinols (44) and a number of other lipophilic species (45) bind to DNA via association with the hydrophobic interior of the strand. While the simple model cannot take this into account, direct detection of free and DNA-bound Ru(II) in ECL allows the use of the model of McGhee and von Hippel. The agreement between our results and previous determination of s for the Ru(phen)_3^{2+} -DNA system provides additional evidence for the validity of the assumptions used. Finally we might mention that similar ECL studies with Ru(bpy)_3^{2+} show no binding effect of DNA, consistent with the known lack of intercalative interaction of this species with DNA (46). Further related studies with other metal chelates are in progress.

CONCLUSIONS

Electrogenerated chemiluminescence (ECL) can be applied to the study of the binding of certain luminescent metal complexes to DNA. Selection of the proper ECL-generating system, e.g. with an anionic precursor ($\text{C}_2\text{O}_4^{2-}$) of a strong reductant ($\text{CO}_2^{\bullet-}$), allows the independent determination of free and DNA-bound complex. ECL data from titration experiments can be applied directly to the same binding models used in equilibrium dialysis and spectrophotometric determinations, without the need to consider diffusion coefficients (required for voltammetric measurements) or ECL efficiencies. While the range of useful metal chelates that show ECL is small, these should provide useful tags of DNA and are capable of measurements at very low metal chelate concentrations.

ACKNOWLEDGMENT

The support of the National Science Foundation (Grant No. CHE8901450) is gratefully acknowledged.

LITERATURE CITED

- (1) Faulkner, L. R., and Bard, A. J. (1977) Techniques of electrogenerated chemiluminescence. In *Electroanalytical Chemistry*, Vol. 10 (A. J. Bard, Ed.) pp 1-95 and references therein, Marcel Dekker, New York.
- (2) Tokel, N. E., and Bard, A. J. (1972) Electrogenerated chemiluminescence IX. Electrochemistry and emission from systems containing tris(2,2'-bipyridine)ruthenium(II) and dichloride. *J. Am. Chem. Soc.* 94, 2862.
- (3) Tokel-Takvoryan, N. E., Hemingway, R. E., and Bard, A. J. (1973) Electrogenerated chemiluminescence XIII. Electrochemical and electrogenerated chemiluminescence studies of ruthenium chelates. *J. Am. Chem. Soc.* 95, 6582.
- (4) Luttmer, J. D., and Bard, A. J. (1981) Electrogenerated chemiluminescence 38. Emission intensity-time transients in the tris(2,2'-bipyridine)ruthenium(II) system. *J. Phys. Chem.* 85, 1155.
- (5) Abruña, H. D., and Bard, A. J. (1982) Electrogenerated chemiluminescence. 40. A chemiluminescent polymer based on the tris(4-vinyl-4'-methyl-2,2'-bipyridyl)ruthenium(II) system. *J. Am. Chem. Soc.* 104, 2641.
- (6) Gonzales-Velasco, J., Rubinstein, I., Crutchley, R. J., Lever, A. B. P., and Bard, A. J. (1983) Electrogenerated chemiluminescence. 42. Electrochemistry and electrogenerated chemiluminescence of the tris(2,2'-bipyrazine)ruthenium(II) system. *Inorg. Chem.* 22, 822.
- (7) Chang, M.-M., Saji, T., and Bard, A. J. (1977) Electrogenerated chemiluminescence. 30. Electrochemical oxidation of oxalate ion in the presence of luminescers in acetonitrile solutions. *J. Am. Chem. Soc.* 99, 5399.
- (8) Rubinstein, I., and Bard, A. J. (1981) Electrogenerated chemiluminescence. 37. Aqueous electrogenerated chemiluminescence systems based on $\text{Ru(2,2'-bipyridine)}_3^{2+}$ and oxalate or organic acids. *J. Am. Chem. Soc.* 103, 512.
- (9) White, H. S., and Bard, A. J. (1982) Electrogenerated chemiluminescence. 41. Electrogenerated chemiluminescence and chemiluminescence of $\text{Ru(2,2'-bipyridine)}_3^{2+}$ -peroxydisulfate system in acetonitrile-water solutions. *J. Am. Chem. Soc.* 104, 6891.
- (10) Ege, D., Becker, W. G., and Bard, A. J. (1984) Electrogenerated chemiluminescent determination of Ru(bpy)_3^{2+} at low levels. *Anal. Chem.* 56, 2413.
- (11) Barton, J. K. (1983) Tris(phenanthroline) metal complexes: probes for DNA helicity. *J. Biomol. Struct. Dyn.* 1, 621.
- (12) Barton, J. K. (1985) Simple coordination complexes: drugs and probes for DNA structure. *Comments Inorg. Chem.* 3, 321.
- (13) Barton, J. K. (1986) Metals and DNA: molecular left-handed complements. *Science* 233, 727.
- (14) Barton, J. K., and Lolis, E. (1985) Chiral discrimination in the covalent binding of Bis(phenanthroline)dichlororuthenium(II) to B-DNA. *J. Am. Chem. Soc.* 107, 708.
- (15) Barton, J. K., Danishefsky, A. T., and Goldberg, J. M. (1984) Tris(phenanthroline)ruthenium(II): stereoselectivity in binding to DNA. *J. Am. Chem. Soc.* 106, 2172.
- (16) Barton, J. K., Basile, L. A., Danishefsky, A., and Alexandrescu, A. (1984) Chiral probes for the handedness of DNA helices: enantiomers of tris(4,7-diphenylphenanthroline)-ruthenium(II). *Proc. Natl. Acad. Sci. U.S.A.* 81, 1961.
- (17) Kumar, C. V., Barton, J. K., and Turro, N. J. (1985) Photophysics of ruthenium complexes bound to double helical DNA. *J. Am. Chem. Soc.* 107, 5518.
- (18) Barton, J. K., Goldberg, J. M., Kumar, C. V., and Turro, N. J. (1986) Binding modes and base specificity of tris(phenanthroline)ruthenium(II) enantiomers with nucleic acids: tuning the stereoselectivity. *J. Am. Chem. Soc.* 108, 2081.
- (19) Goldstein, B. M., Barton, J. K., and Berman, H. M. (1986) Crystal and molecular structure of a chiral-specific DNA-binding agent: tris(4,7-diphenylphenanthroline)ruthenium(II). *Inorg. Chem.* 25, 842.
- (20) Mei, H.-Y., and Barton, J. K. (1986) A chiral probe for A-form helices of DNA and RNA: tris(tetramethylphenanthroline)-ruthenium(II). *J. Am. Chem. Soc.* 108, 7414.
- (21) Basile, L. A., and Barton, J. K. (1987) Design of a double-strand DNA cleaving agent with two polyamine metal-binding arms: Ru(DIP)_2 macro $^{n+}$. *J. Am. Chem. Soc.* 109, 7548.
- (22) Basile, L. A., Raphael, A. L., and Barton, J. K. (1987) Metal activated hydrolytic cleavage of DNA. *J. Am. Chem. Soc.* 109, 7550.
- (23) Adam, W., and Cilento, G. (Eds.) (1982) *Chemical and Biological Generation of Excited States* Academic Press, New York.
- (24) Cormier, M. J., Hercules, D. M., and Lee, J. (Eds.) (1973) *Chemiluminescence and Bioluminescence* Wiley, New York.
- (25) Schölerich, J., Andreesen, R., Kapp, A., Ernst, M., and Woods, W. G. (1987) *Bioluminescence and Chemiluminescence* Wiley, Chichester.

- (26) Carter, M. T., and Bard, A. J. (1987) Voltammetric studies of the interaction of tris(1,10-phenanthroline)cobalt(II) with DNA. *J. Am. Chem. Soc.* 109, 7528.
- (27) Carter, M. T., Rodriguez, M., and Bard, A. J. (1989) Voltammetric studies of the interaction of metal chelates with DNA. 2. Tris-chelated complexes of cobalt(III) and iron(II) with 1,10-phenanthroline and 2,2'-bipyridine. *J. Am. Chem. Soc.* 111, 8901.
- (28) Reichmann, M. E., Rice, S. A., Thomas, C. A., and Doty, P. (1954) A further examination of the molecular weight and size of desoxypentose nucleic acid. *J. Am. Chem. Soc.* 76, 3047.
- (29) Lin, C.-T., Böttcher, W., Chou, M., Creutz, C., and Sutin, N. (1976) Mechanism of the quenching of the emission of substituted polypyridineruthenium(II) complexes by iron(III), chromium(III), and europium(III) ions. *J. Am. Chem. Soc.* 98, 6536.
- (30) Jacobsen, E., and Sawyer, D. T. (1968) Electrochemical oxidation of oxalate ion in dimethylsulfoxide at a gold electrode. *J. Electroanal. Chem.* 16, 361.
- (31) Anson, F. C., and Schultz, F. A. (1963) Effect of adsorption and electrode oxidation on the oxidation of oxalic acid at platinum electrodes. *Anal. Chem.* 35, 1114.
- (32) Leland, J. K. IGEN, Inc., private communication.
- (33) Noffsinger, J. B., and Danielson, N. D. (1987) Generation of chemiluminescence upon reaction of aliphatic amines with tris(2,2'-bipyridine)ruthenium(III). *Anal. Chem.* 59, 865.
- (34) Scatchard, G. (1949) The attractions of proteins for small molecules and ions. *Ann. N. Y. Acad. Sci.* 51, 660.
- (35) McGhee, J. D., and von Hippel, P. H. (1974) Theoretical aspects of DNA-protein interactions: co-operative and non-co-operative binding of large ligands to a one-dimensional homogeneous lattice. *J. Mol. Biol.* 86, 469.
- (36) Kaifer, A. E., and Bard, A. J. (1985) Micellar effects on the reductive electrochemistry of methyl viologen. *J. Phys. Chem.* 89, 4876.
- (37) Ouyang, J., and Bard, A. J. (1988) Electrogenated chemiluminescence 50. Electrochemistry and electrogenerated chemiluminescence of micelle solubilized $\text{Os}(\text{bpy})_3^{2+}$. *Bull. Chem. Soc. Jpn.* 61, 17.
- (38) Smith, P. J., and Mann, C. K. (1969) Electrochemical dealkylation of aliphatic amines. *J. Org. Chem.* 34, 1821.
- (39) Manning, G. (1978) The molecular theory of polyelectrolyte solutions with applications to the electrostatic properties of polynucleotides. *Q. Rev. Biophys.* 11, 179.
- (40) Berg, O. G., and von Hippel, P. H. (1985) Diffusion controlled macromolecular interactions. *Ann. Rev. Biophys. Chem.* 14, 131.
- (41) Kelly, J. M., Tossi, A. B., McConnell, D. J., and OhUigin, C. (1985) A study of the interactions of some polypyridylruthenium(II) complexes with DNA using fluorescence spectroscopy, topoisomerisation and thermal denaturation. *Nucleic Acids Res.* 13, 6017.
- (42) Fromhertz, P., and Rieger, B. (1986) Photoinduced electron transfer in DNA matrix from intercalated ethidium to condensed methyl viologen. *J. Am. Chem. Soc.* 108, 5361.
- (43) Atherton, S. J., and Beaumont, P. C. (1987) Laser flash photolysis of DNA-intercalated ethidium bromide in the presence of methyl viologen. *J. Phys. Chem.* 91, 3993.
- (44) Scannell, R. T., Barr, J. R., Murty, V. S., Reddy, K. S., and Hecht, S. M. (1988) DNA strand scission by naturally occurring 5-alkylresorcinols. *J. Am. Chem. Soc.* 110, 3650.
- (45) Baguley, B. C. (1982) Nonintercalative DNA-binding antitumor compounds. *Mol. Cell. Biochem.* 43, 167.
- (46) Schmidt, N., and Bard, A. J., unpublished results.

Registry No. $\text{Ru}(\text{phen})_3^{2+}$, 22873-66-1.

Antitumor Activity of a Thioether-Linked Immunotoxin: OVB3-PE

David FitzGerald,* Thierry Idziorek, Janendra K. Batra, Mark Willingham, and Ira Pastan

Laboratory of Molecular Biology, National Cancer Institute, National Institutes of Health, 9000 Rockville Pike, Bethesda, Maryland 20892. Received April 6, 1990

A thioether-linked immunotoxin was made between *Pseudomonas* exotoxin and the monoclonal antibody OVB3. This conjugate, OVB3-PE, was cytotoxic for the human ovary cancer cell line OVCAR-3 (ID of 2.5×10^{-12} M) and it was therefore tested for antitumor activity in a nude mouse model of ovarian cancer. This model employs the injection of a lethal number of OVCAR-3 cells into the peritoneal cavity of nude mice. When 0.2–1 μ g of OVB3-PE was injected intraperitoneally on three successive days beginning 3–5 days after OVCAR-3 cell implantation, the survival of the tumor-bearing mice was increased 2–4-fold compared to that of untreated control mice. Median survival times for control mice ranged from 44 to 50 days while survival times of 150 days or greater were seen in mice treated with OVB3-PE. When OVB3-PE administration was delayed until 2–4 weeks after tumor cell implantation, OVB3-PE treatment also showed antitumor activity, but the duration of survival was less than with the early treatments. OVB3-PE was also cytotoxic for MCF-7 breast carcinoma cells, HT-29 colon carcinoma cells, and A431 epidermoid carcinoma cells.

INTRODUCTION

Ovarian cancer is an important cause of death in women. New approaches, such as immunotoxin therapy (1, 2), are needed because ovarian cancer is frequently resistant to chemotherapy and because it often spreads to the peritoneal cavity before it is discovered so that surgery cannot remove all the tumor. In order to treat this disorder, we have developed a monoclonal antibody, OVB3, that has reacted with all adenocarcinomas of the ovary examined so far (25/25) as well as some adenocarcinomas of the breast and colon (3). This antibody was coupled previously to *Pseudomonas* exotoxin (PE)¹ by a disulfide bond (3, 4) and the resulting conjugate, OVB3-PE, was shown to kill ovarian cancer cells in tissue culture and to prolong the life of immunodeficient mice with human ovarian cancer implants (3). Here we extend our original findings and describe a method to conjugate PE to OVB3 by a thioether bond. Thioether conjugates may have advantages in animals over disulfide conjugates since the carbon-sulfur bond is likely to be more stable in vivo.

In this study we have prepared a thioether conjugate of OVB3 and PE and evaluated its cell-killing activity in tissue culture and in a tumor model. In vitro it inhibited protein synthesis with an ID₅₀ of $2-3 \times 10^{-12}$ M. The antitumor activity of the thioether conjugate was tested in the OVCAR-3 nude mouse model of human ovarian cancer. Mice implanted with 25×10^6 OVCAR3 cells die about 40 days after tumor implantation with massive ascites (5), but mice treated 3–5 days after implantation with OVB3-PE survive to 100 days or longer, with a few animals living for over 175 days. Furthermore, administration of OVB3-PE at day 26 after tumor implantation, when significant ascites and a large tumor load is present, causes the disappearance of ascites and prolongation of the life of the tumor-bearing animals.

Because OVB3-PE has been shown to be active against human ovarian cancer growing in mice, a phase I study using OVB3-PE has begun in women. The information contained in this paper was used to plan the initial protocol.

EXPERIMENTAL PROCEDURES

Reagents. Purified PE was purchased from Swiss Serum and Vaccine Institute, Berne, Switzerland. The OVB3 antibody was produced by in vitro culture at Damon Biotech. Purified antiTac antibody was a gift from T. Waldmann (NCI). Cross-linking and protein-modification reagents were obtained from Pierce Chemical Co.

Construction of OVB3-PE by Thioether Linkage. To couple PE to OVB3 by a thioether bond, PE was first reacted with sulfo-SMPB (sulfosuccinimidyl 4-(*p*-maleimidophenyl)butyrate). Typically PE at 2–3 mg/mL in borate buffer, pH 8.0, was reacted with a 3-fold molar excess of sulfo-SMPB. Immediately prior to use sulfo-SMPB was dissolved in dimethyl formamide (DMF) to a final concentration of 5–10 mg/mL (as appropriate). Usually 5 μ L or less of the sulfo-SMPB solution was added per milliliter of PE solution. The reaction, which proceeded at 37 °C for 30 min, was quenched by the addition of excess glycine. PE modified in this manner was then resolved from low molecular weight reactants by HPLC gel-filtration chromatography (TSK-250, Bio-Rad, 21.5 \times 600 mm). The running buffer for this column was 0.2 M NaPO₄, 1 mM EGTA, pH 7.0. With this chromatography system, both PE and chemically modified PE elute at approximately 140 mL. OVB3 was reacted for 1 h at 37 °C with a 3-fold molar excess of 2-iminothiolane in 0.2 M NaPO₄, 1 mM EGTA at pH 8.0. Reaction with 2-iminothiolane introduced approximately 0.9 mol of SH per mol of OVB3. This was determined with 5,5'-dithiobis(2-nitrobenzoic acid) (4). As with PE, excess glycine was used to quench the reaction. Chemically modified antibody was recovered by gel filtration on a TSK-250 (21.5 \times 600 mm) column. The running buffer was the same as described above and the antibody eluted at 117 mL. Finally, PE, having a reactive maleimide group, was mixed

¹ Abbreviations: PE = *Pseudomonas* exotoxin, MST = median survival time, ip = intraperitoneally, H and E = hematoxylin and eosin, SMCC = succinimidyl 4-(*N*-maleimidomethyl)cyclohexane-1-carboxylate, SDS-PAGE = sodium dodecyl sulfate-polyacrylamide gel electrophoresis.

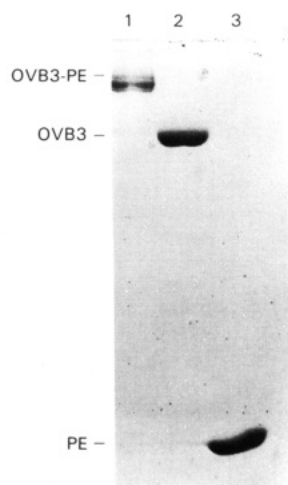


Figure 1. SDS-PAGE run under nonreducing conditions, using 10% acrylamide: lane 1, OVB3-PE (made by thioether linkage); lane 2, OVB3; and lane 3, PE.

with OVB3-SH. The two proteins were allowed to react at room temperature overnight and then further purified by gel filtration. The 1:1 conjugate which eluted at 105 mL was recovered and used in all subsequent experiments (see Figure 1 for SDS-page analysis of the final product). Protein concentration for the 1:1 conjugate was determined with the following conversion factor: absorbance of 1.3 at 280 nm was equivalent to 1.0 mg/mL of total protein.

AntiTac-PE was also made by thioether linkage and served as a control immunotoxin. AntiTac-PE (thioether) was made by using a similar protocol to the one used for the thioether-linked OVB3 immunotoxin. However, the one-to-one conjugate was purified by using a different separation strategy. The final reaction mixture was applied to a MonoQ (Pharmacia/LKB) column and eluted with a linear NaCl gradient. This separated unreacted antibody (which eluted at approximately 0.2 M NaCl) from a complex mixture that contained the immunotoxin and unreacted PE (this complex mixture eluted between 0.25 and 0.28 M NaCl). The one-to-one conjugate was then separated from high molecular weight material and unreacted PE on a HPLC sizing column. To ensure the conjugate was made correctly, it was tested on target HUT102 cells and had an ID₅₀ value of 0.5 ng/mL.

Tissue Culture. OVCAR-3, MCF-7, A431, and HT-29 cells were maintained in DMEM, 10% FCS. HUT-102 cells were maintained in RPMI 1640, 10% FCS. For cytotoxicity studies, cells were plated at $1-2 \times 10^5$ cells/well in 24-well Costar tissue-culture plates (6). Adherent cells were seeded approximately 24 h before the addition of immunotoxin. HUT-102 cells were washed 3 or 4 times with tissue-culture medium and used the same day.

Cytotoxic Activity. Cytotoxic activity was determined by measuring inhibition of protein synthesis. Immunotoxins were added to cells in culture for 20 h. At the end of this period, [³H]leucine at 10 μ Ci/mL was added for a further hour. Cells were washed with PBS, solubilized with 0.1 M NaOH, precipitated with excess TCA, and counted. Experiments were done with triplicate samples and usually repeated on 3 or 4 separate occasions.

Animal Experiments. B75 female mice 6–9 weeks old were used to grow OVCAR-3 ascites tumors. Usually, 25×10^6 washed cells were injected into recipient mice on day 1. Untreated, these mice died from their tumor burden 40–50 days later (5, 7). To prevent undue suffering, mice beginning to show distress from their tumor burden were killed prematurely. Tumor-bearing mice were treated by

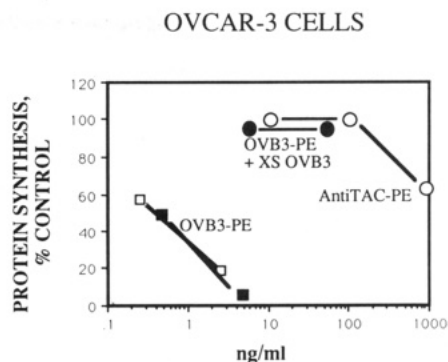


Figure 2. Inhibition of protein synthesis by OVB3-PE. Various concentrations of OVB3-PE (two individual experiments are shown) or antiTac-PE shown as total protein in ng/mL were added to OVCAR-3 cells for approximately 20 h. Following this, [³H]leucine was added to individual wells to a final concentration of 10 μ Ci/mL for 1 h. Inhibition of protein synthesis was determined by measuring the radioactivity in TCA-precipitable material in immunotoxin-treated wells compared to that of untreated wells. Parallel experiments were conducted where excess OVB3 (75 μ g/mL) was added to cells immediately prior to the addition of the OVB3-PE.

Table I. Cytotoxic Activity of OVB3-PE for Various Adenocarcinomas

cell line	OVB3-PE ID ₅₀ , ^a ng/mL	cell line	OVB3-PE ID ₅₀ , ^a ng/mL
OVCAR-3	0.5	A431	0.4
MCF-7	0.3	HT-29	0.5

^a ID₅₀s were assessed after an overnight incubation with immunotoxin.

ip administration of immunotoxins. The early-treatment protocols (experiments 1–5) involved giving injections of OVB3-PE beginning on days 3–5 and various numbers of individual injections were administered. For the late-treatment protocol (experiment 6), immunotoxin treatments were initiated 19–33 days after the injection of the tumor cells. In the case of late treatments, five injections were given approximately every other day. All immunotoxin preparations were formulated in normal saline/human serum albumin (10 mg/mL), filter sterilized (0.22 μ M, GV-Millipore), and injected ip in a volume of 0.5 mL.

RESULTS

OVB3-PE (Thioether): Evaluation of Cytotoxic Activity. To assess the cytotoxic potential of a thioether-linked immunotoxin, a one-to-one conjugate was made between the monoclonal antibody OVB3 and *Pseudomonas* exotoxin (PE). OVB3-PE was purified by gel-filtration chromatography and evaluated for its cytotoxic activity by adding various concentrations of the immunotoxin to OVCAR-3 cells. After a 20-h incubation, inhibition of protein synthesis was determined. As shown in Figure 2 and Table I, the ID₅₀ was 0.5 ng/mL (2.5×10^{-12} M). When the control immunotoxin, antiTac-PE, which does not bind OVCAR-3 cells was added, an ID₅₀ of greater than 1000 ng/mL was noted. Also excess OVB3 competed at least 100-fold for the cytotoxic activity of OVB3-PE. OVB3-PE was also assessed for cytotoxic activity against other cancer cell lines and for its antitumor activity against OVCAR-3 tumors growing in nude mice (see below).

Antitumor Activity Mediated by Early Treatment with OVB3-PE. The thioether conjugate of OVB3-PE was tested for antitumor activity in the same nude mouse model of human ovarian cancer previously used to test the

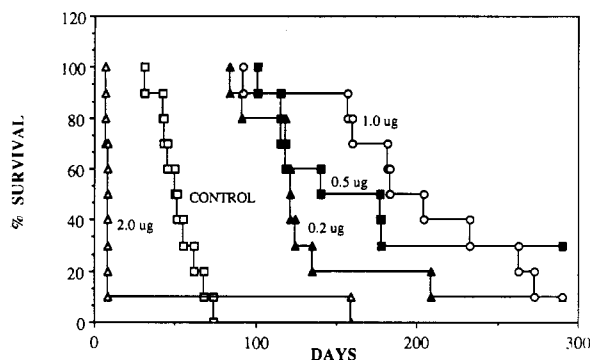


Figure 3. Inhibition of tumor growth by OVB3-PE. OVCAR-3 (25×10^6) cells were injected into the peritoneal cavity of B75 athymic nude mice on day 1. On days 3, 4, and 5, various amounts of OVB3-PE (ranging from 0.2 to 2.0 μg) were injected ip in 0.5 mL of sterile normal saline, 10 mg/mL of human serum albumin. The survival of each group of mice was then followed. There were 10 mice in each group.

antitumor activity of the OVB3-PE disulfide conjugate (3) and various other immunotoxins (7, 8). In this model, 25×10^6 OVCAR-3 cells were injected intraperitoneally into athymic nude mice on day 1, and immunotoxin treatment was begun on day 3 or later. The immunotoxin was also given by the ip route. The mice were then monitored for immunotoxin-mediated antitumor effects. The OVCAR-3 tumor was lethal and untreated mice usually died between days 40 and 50. At death these mice had one or two large tumor masses, studding of the abdominal cavity with small tumor implants, and 5–7 mL of ascites fluid containing approximately 500×10^6 unattached tumor cells.

When OVB3-PE was injected on days 3, 4, and 5 after the injection of the tumor cells, there was a large increase in the duration of survival compared to that of the untreated animals. The duration of increased survival was generally related to the amount of immunotoxin given (Figure 3 and Table II, experiment 1). In this experiment, the median survival time (MST) was increased from 50 days in control mice to 121 days for mice receiving three injections of 0.2 μg , to 158 days for mice receiving 0.5 μg , and to 193 days for mice receiving 1.0 μg of immunotoxin. The injection of three doses of 1.0 μg of OVB3-PE was the maximum tolerated daily dose. Injection of 2.0 μg per day for 3 days was lethal for at least 50% of the mice.

Two experiments (nos. 2 and 3 of Table II) were carried out where OVB3-PE was first administered on day five and injections were given on days 5, 6, and 7. In both cases a significant antitumor effect was seen (Table II). Additional experiments were then carried out to determine (1) whether a greater number of immunotoxin injections would increase median survival and (2) whether beginning OVB3-PE treatment 2 days after tumor inoculation would be more effective than beginning 5 days after inoculation. The results of experiment 4 indicated that seven injections were no more effective than three when 0.2 μg of immunotoxin were given but were marginally better when 0.5 μg were administered. Experiment 5 indicated that at early times after tumor inoculation there was little or no differences in survival when treatment was initiated 2 days after inoculation or 5 days after inoculation.

Antitumor Activity Mediated by Late Treatment with OVB3-PE. To determine if it were possible to achieve antitumor effects even when the OVCAR-3 tumors had reached a large size and significant ascites was present, the first injection of OVB3-PE was delayed by 2–4 weeks after the injection of tumor cells. In one experiment (Table

Table II. Median Survival Times (MST) of Tumor-Bearing Mice Treated with OVB3-PE

group	OVB3-PE, $\mu\text{g}/\text{injection}$	MST, days	no. of injections	day of injection
Experiment 1 ($n = 10$)				
1	0	50	3	3, 4, 5
2	0.2	121	3	3, 4, 5
3	0.5	158	3	3, 4, 5
4	1.0	193	3	3, 4, 5
5	2.0	8 ^a	3	3, 4, 5
Experiment 2 ($n = 10$)				
1	0	44	3	5, 6, 7
2	0.2	87	3	5, 6, 7
3	0.5	87	3	5, 6, 7
4	2.0	42 ^a	3	5, 6, 7
Experiment 3 ($n = 10$)				
1	0	48	3	5, 6, 7
2	0.05	56.5	3	5, 6, 7
3	0.1	70.0	3	5, 6, 7
4	0.2	64.5	3	5, 6, 7
5	0.5	69.5	3	5, 6, 7
6	1.0	91.5 ^b	3	5, 6, 7
Experiment 4 ($n = 7$)				
1	0	53	3	5, 6, 7
2	0.2	81	3	5, 6, 7
3	0.5	83	3	5, 6, 7
4	2.0	10 ^a	3	5, 6, 7
5	0.2	83	7	5, 6, 7, 9, 10, 11, 12
6	0.5	118	7	5, 6, 7, 9, 10, 11, 12
7	2.0	10 ^a	7	5, 6, 7, 9, 10, 11, 12
Experiment 5 ($n = 10$)				
1	0	46	5	2, 3, 5, 7, 10
2	1.0	90 ^c	5	2, 3, 5, 7, 10
3	1.0	90	5	5, 7, 10, 12, 14

^a At least 50% of mice in this group died from dose-related toxicity.

^b Three mice alive past day 160. ^c Four mice alive past day 140.

Table III. Survival of Tumor-Bearing Mice Receiving Early and Late Treatments with OVB3-PE

experiment 6 ($n = 10$); group	OVB3-PE, $\mu\text{g}/\text{injection}$	MST, days	no. of injections	day of injection
1	0	37	5	5, 6, 7, 10, 11
2	1.0	156	5	5, 6, 7, 10, 11
3	1.0	63	5	19, 20, 21, 24, 25
4	1.0	63	5	26, 27, 28, 31, 32

III, experiment 6), five daily injections of 1 μg of OVB3-PE were administered to tumor-bearing mice beginning on day 19 or 26. As a control for early treatment, OVB3-PE (1 μg) was also administered starting on day 5. The results indicated that the administration of OVB3-PE beginning on day 19 or 26 resulted in both antitumor activity and increased survival compared to control mice receiving only diluent (Figure 4 and Table III). The increase in survival time for mice beginning treatment on day 19 or 26 was approximately 26 days. In contrast, the increase in survival for mice beginning treatment on day 5 was greater than 100 days.

To follow tumor growth, each mouse was weighed and scored for abdominal girth on a weekly basis. An increase in body weight began two weeks after injection of the tumor cells. By day 26, most of the mice had gained 10 g and had an abdominal girth score of 3–4+ (scale of 0–4+). The increase in body weight was due to the build-up of ascites fluid within the abdominal cavity. The body weight of the untreated mice continued to increase until death (Figure 4A). In the group of mice that received OVB3-PE (1 $\mu\text{g}/\text{injection} \times 5$ between days 26 and 32) there was a rapid decrease in body weight (Figure 4B), a reduction in abdominal girth, and a 26-day prolongation of survival (Figure 4C). Similar survival data to that shown in Figure

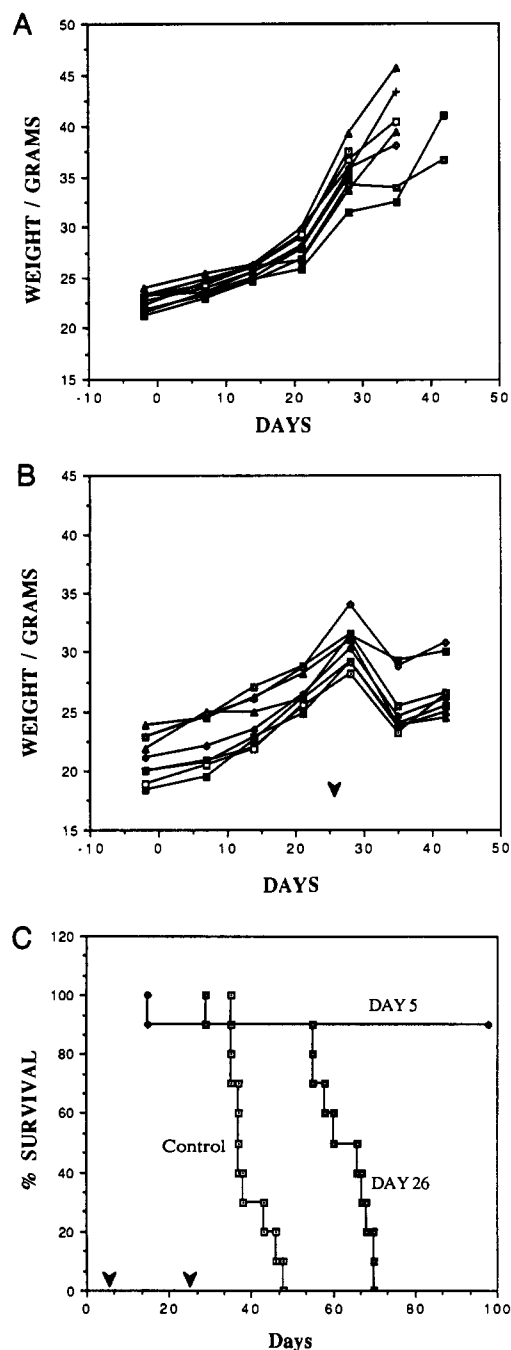


Figure 4. Antitumor effect of OVB3-PE on mice bearing large tumor burden with ascites. OVCAR-3 (25×10^6) cells were injected into the peritoneal cavity on day 1. Beginning on day 26, five individual injections (see Table III for exact days) of OVB3-PE were given to mice with prominent distention from ascites accumulation. As a control for early treatment, one group of mice was treated beginning on day 5. A shows the progressive increase in weight of control mice that were not treated with immunotoxin (data for individual mice are shown). B shows the weight of mice treated with OVB3-PE beginning on day 26. The arrow indicates the day when immunotoxin treatment was initiated. C shows the survival curves for mice treated with OVB3-PE ($1 \mu\text{g}/\text{injection}$) beginning on day 26 (■) or day 5 (◆) or untreated (□). The arrows indicate the days when immunotoxin treatment was initiated. Additional details are provided in Table III (experiment 6).

4C were obtained for the mice that were treated with OVB3-PE between days 19 and 25 (Table III).

An additional experiment was performed to determine the fate of large tumors treated with cytoreductive doses of OVB3-PE. In this experiment, the tumors grew slower than in the previous experiment so treatment was delayed

until day 33. To estimate the tumor burden at the time when OVB3-PE was injected, three mice were sacrificed on day 33. By aspirating the peritoneal cavity an average of 4×10^8 OVCAR-3 tumor cells per mouse was recovered from ascites fluid. In addition, there was a single solid tumor mass in each mouse (approximately 1.0×1.0 cm in size). A comparison that was made with the tumor burden present on days 0–5 showed there were roughly 50–100 times more tumor cells present on day 33 than on days 0–5. Five immunotoxin injections were given beginning on day 33. To assess the effect of this treatment, two mice from this treatment group were killed and examined for evidence of viable tumor 4 days after the final injection of immunotoxin. Gross anatomical examination revealed that the immunotoxin treatment eliminated the ascites fluid and unattached tumor cells. However, the solid tumor mass remained evident in both mice and the tumor had similar dimensions to the pretreatment solid tumor. This posttreatment tumor mass was examined microscopically following fixation and H and E staining. The tumor cells appeared viable.

Cell Killing of OVB3-PE on Breast and Colon Cancer Cells. The reactivity of OVB3 for various human tumor samples was reported previously and has been extended here (3). With use of immunocytochemistry on frozen sections of cancer specimens, OVB3 has been found to react with 25/25 ovarian carcinomas and approximately 25% of breast cancers and colon tumors. Because of this reactivity with tumors other than ovarian, we investigated the cytotoxicity of OVB3-PE on cell lines derived from breast and colon tumors. OVB3-PE was found to have an ID_{50} of less than $1 \text{ ng}/\text{mL}$ for both a breast cancer cell line, MCF-7, and a colon cancer cell line, HT-29 (Table I). Thus OVB3 has potential for use in the treatment of other adenocarcinomas besides ovarian cancers. OVB3-PE was also tested on epidermoid carcinomas and found to have potent cell-killing activity for A431 cells (Table I) and to a lesser extent, KB cells (data not shown). Recently, OVB3-PE was shown to have antitumor activity against HT-29 tumors (9).

DISCUSSION

We show here that it is possible to make a very potent immunotoxin by conjugating native PE to OVB3 by a thioether linkage.

OVB3 was originally selected as an ovarian-specific monoclonal antibody. We have examined many tumors for reactivity with OVB3 and found that OVB3 has preferential reactivity for ovarian cancer (25/25), but it also reacts with a significant percentage of adenocarcinomas of the breast and colon. As shown in Table I, OVB3 is also active against a breast (MCF-7), a colon (HT-29), and an epidermoid carcinoma (A431) cell line. While OVB3-PE inhibited these cell lines with an ID_{50} of $0.5 \text{ ng}/\text{mL}$, a 200-fold higher concentration was needed to kill HUT-102 cells (data not shown). Thus, the cytotoxicity of OVB3-PE was relatively specific for cells bearing the OVB3 antigen.

Immunotoxin therapy has been shown to be effective in treating intraperitoneal tumor models of human cancer (7–10). Here we show in some instances that OVB3-PE can increase survival of nude mice bearing OVCAR-3 tumors by greater than 100 days. The injection of irrelevant immunotoxins such as antiTac-PE has no antitumor activity in this model (7). For OVB3-PE, $1 \mu\text{g}$ per injection gave the most pronounced antitumor effects. The median survival times of 193 days in experiment 1 and 156 days in experiment 6 represent some of the longest

survival times reported to date for an immunotoxin-mediated antitumor effect. We have also shown that OVB3-PE prolongs the life of tumor-bearing mice when given 19–33 days after OVCAR-3 implantation at a time when ascites had developed and large tumor implants were present.

In every experiment where OVB3-PE was administered at a dose of 0.5 or 1.0 μg /injection, there was a significant increase in the survival of mice bearing OVCAR-3 tumors. However, from experiment to experiment, we have noted some variability in the median survival times of the various treatment groups. For example, the MST for the 0.5 μg per injection dose ranged from 158 days in experiment 1 to 69 days in experiment 3 and for 1.0 μg from 193 days in experiment 1 to 91 days in experiment 3. We have noted intermediate MSTs in other experiments. Various lots of immunotoxins were checked for changes in cell-killing activity upon storage. No systemic loss of activity was noted. We do not have an explanation for the variability in the mouse experiments except to suggest that animal-to-animal variation may be greater than the small variations seen in tissue-culture systems.

The administration of OVB3-PE 2–4 weeks after initiating tumor growth was carried out to test for antitumor activity against a large established tumor. OVB3-PE was effective when injections were begun either 19, 26, or 33 days after the injection of tumor cells. Antitumor activity was characterized by increased survival time, decreased body weight, diminished abdominal girth, and a reduced number of tumor cells recovered immediately posttreatment. The antitumor effect was most pronounced against ascites tumor cells. In two mice that were autopsied 5 days posttreatment, ascites tumor cells were not evident. However, in those same mice, the solid tumor was of similar size to tumors examined immediately prior to treatment. It would appear that the large solid tumor was poorly permeable to the immunotoxin.

Bjorn et al. had reported that it was possible to produce active immunotoxins when PE was thioether-linked to various monoclonal antibodies (11). In this report, we have described a novel method to make thioether-linked PE immunotoxins which is different from that of Bjorn et al. By first reacting PE with sulfo-SMPB, and OVB3 with 2-iminothiolane we have made a very potent immunotoxin with an ID_{50} of 2.5×10^{-12} M. In more recent experiments we have used SMCC in place of sulfo-SMPB and shown no difference in conjugate potency (data not shown). In this report, only data using native PE coupled to OVB3 is presented. We have made OVB3 conjugates with PE40, a recombinant form of PE lacking the toxin's binding domain, but these showed little or no cytotoxicity for cells and were not pursued further (data not shown).

The dosing schedule used in these experiments has been designed with certain clinical parameters in mind. Patients receiving PE conjugated to antibodies have been found to develop neutralizing antibodies to PE 10–12 days after the initial immunotoxin injection. Because of this, our injection protocol did not span more than 2 weeks. Thus, we achieved antitumor responses with an injection schedule that could be directly applied to patient treatment. Likewise, after the initial evidence that thioether conjugates

mediated an antitumor response when the immunotoxin was given 3–5 days after tumor implantation, we decided to treat more advanced tumors. While it is difficult to relate the staging of human disease to mouse tumor load, it was clear that we could achieve a significant antitumor effect when the tumor burden had increased by a minimum of 50-fold. OVB3-PE gave an antitumor effect in the dose range of 5–50 μg /kg in mice when administered at early times after tumor implantation. When administered after 3 weeks of tumor growth, 50 μg /kg also gave a significant antitumor response. At 100 μg /kg OVB3-PE was often lethal. Mice died 24–72 h after injection of severe liver toxicity.

ACKNOWLEDGMENT

Thanks to E. Lovelace, A. Rutherford, and M. Hazen for excellent technical assistance, to S. Neal for photography, and to A. Schombert, J. Evans, and A. Gad-dis for typing the manuscript.

LITERATURE CITED

- (1) Vitetta, E. S., Fulton, R. J., May, R. D., Till, M., and Uhr, J. W. (1987) Redesigning nature's poisons to create antitumor reagents. *Science* 238, 1098–1104.
- (2) Pastan, I., Willingham, M. C., and FitzGerald, D. J. (1986) Immunotoxins. *Cell* 47, 641–648.
- (3) Willingham, M. C., FitzGerald, D. J., and Pastan, I. (1987) *Pseudomonas* exotoxin coupled to a monoclonal antibody against ovarian cancer inhibits the growth of human ovarian cancer cells in a mouse model. *Proc. Natl. Acad. Sci. U.S.A.* 84, 2474–2478.
- (4) FitzGerald, D. J. P. (1987) Construction of immunotoxins using *Pseudomonas* exotoxin A. *Methods Enzymol.* 151, 139–145.
- (5) Hamilton, T. C., Young, R. C., Louie, K. G., Behrens, B. C., McCoy, W. M., Grotzinger, K. R., and Ozols, R. F. (1984) Characterization of a xenograft model of human ovarian carcinoma which produces ascites and intraabdominal carcinomatosis in mice. *Cancer Res.* 44, 5286–5290.
- (6) Pirker, R., FitzGerald, D. J. P., Hamilton, T. C., Ozols, R. F., Willingham, M. C., and Pastan, I. (1985) Anti-transferrin receptor antibody linked to *Pseudomonas* exotoxin as a model immunotoxin in human ovarian carcinoma cell lines. *Cancer Res.* 45, 751–757.
- (7) FitzGerald, D. J., Willingham, M. C., and Pastan, I. (1986) Antitumor effects of an immunotoxin made with *Pseudomonas* exotoxin in a nude mouse model of human ovarian cancer. *Proc. Natl. Acad. Sci. U.S.A.* 83, 6627–6630.
- (8) FitzGerald, D. J., Bjorn, M. J., Ferris, R. J., Winkelhake, J. L., Frankel, A. E., Hamilton, T. C., Ozols, R. J., Willingham, M. C., and Pastan, I. (1987) Antitumor activity of an immunotoxin in a nude mouse model of human ovarian cancer. *Cancer Res.* 47, 1407–1410.
- (9) Pearson, J. W., FitzGerald, D. J. P., Willingham, M. C., Wiltrout, R. H., Pastan, I., and Longo, D. L. (1989) Chemoimmunotoxin therapy against a human colon tumor (HT-29) xenografted into nude mice. *Cancer Res.* 49, 3562–3567.
- (10) Griffin, T. W., Richardson, C., Houston, L. L., LePage, D., Bogden, A., and Raso, V. (1987) Antitumor activity of intraperitoneal immunotoxins in a nude mouse model of human malignant mesothelialoma. *Cancer Res.* 47, 4266–4270.
- (11) Bjorn, M. J., Groetsma, G., and Scalapino, L. (1986) Antibody-*Pseudomonas* exotoxin A conjugates to human breast cancer cells in vitro. *Cancer Res.* 46, 3262–3267.

Protein Radiohalogenation: Observations on the Design of *N*-Succinimidyl Ester Acylation Agents

Ganesan Vaidyanathan and Michael R. Zalutsky*

Duke University Medical Center, Department of Radiology, Box 3808, Durham, North Carolina 27710.

Received April 11, 1990

In previous studies we have demonstrated that antibodies radioiodinated with *N*-succinimidyl 3-iodobenzoate (SIB) are less susceptible to loss of radioiodine *in vivo* than antibodies iodinated directly by electrophilic substitution on their tyrosine residues with Iodogen. Since the Bolton-Hunter reagent, *N*-succinimidyl 3-(4-hydroxy-3-iodophenyl)propionate, is identical with SIB except that it contains a hydroxyl group on the aromatic ring and a two-methylene spacer, a comparison of their coupling chemistry and *in vivo* behavior was performed to better understand the structural requirements for a useful iodinated acylation agent. Protein concentration and pH had a significant effect on the coupling efficiency of both SIB and the Bolton-Hunter reagent; however, protein-labeling yields with SIB were generally higher by a factor of 2. Paired-label biodistribution studies in mice demonstrated that thyroid uptake (a monitor of dehalogenation) of antibody labeled by the Bolton-Hunter method was twice that of antibody labeled with SIB but only 7% of that observed for antibody labeled with Iodogen. These results suggest that even minor differences in iodination site can profoundly alter the retention of label on a protein *in vivo*.

INTRODUCTION

Radioiodination of monoclonal antibodies (MAbs)¹ is a labeling approach which offers certain advantages over the use of metallic nuclides such as ¹¹¹In (1). Because of the availability of multiple γ -emitting iodine nuclides, direct comparison of different MAbs, labeling methods, or routes of injection is possible by paired-label analyses, greatly facilitating the investigation of the basic processes influencing MAb distribution. In addition, the nuclear properties of ¹²³I are nearly ideal for either planar imaging or single-photon emission tomography (2).

Conventional methods for the radioiodination of proteins such as the Iodogen method (3) involve direct electrophilic substitution of the iodine ortho to the hydroxyl group on tyrosine residues (4). MAbs labeled by this approach undergo rapid deiodination after administration *in vivo* (4), a factor which is a major impediment to the utilization of radiohalogenated MAbs. In an attempt to develop improved methods for protein radioiodination, our laboratory has been investigating the influence of the chemical nature of the MAb iodination site on subsequent behavior *in vivo*.

Because of the better biologic properties generally associated with proteins labeled by the Bolton-Hunter method (5) (presumably because of the nonoxidative conditions which are employed), this reagent, *N*-succinimidyl 3-(4-hydroxy-3-[¹²⁵I]iodophenyl)propionate (BH, Chart I) was utilized as the point of departure for the design of other protein iodination reagents. For example, we have developed a conceptually similar compound, *N*-succinimidyl 3-iodobenzoate (SIB) (Chart I), which is obtained by the iododestannylation of *N*-succinimidyl 3-(tri-*n*-butylstannyl)benzoate (ATE) (Chart I) (6). Subsequent reports by other investigators have described

Chart I. Structures of ATE, SIB, and Bolton-Hunter Reagent

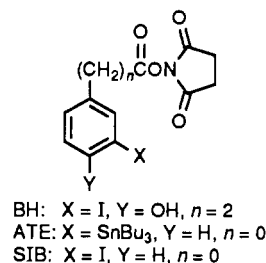
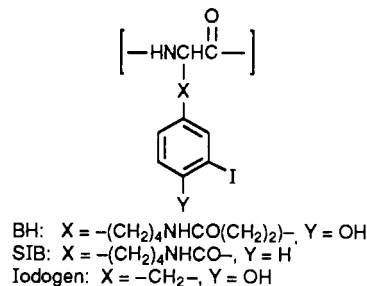


Chart II. Iodination Site on Protein



the use of *N*-succinimidyl 4-iodobenzoate for labeling proteins (7, 8). As illustrated in Chart II, labeling proteins using both BH and SIB results in modification of lysine residues on the protein. However, two structural differences were incorporated into the design of SIB in an attempt to make this reagent more useful for *in vivo* applications (Chart I). First, the two-carbon spacer between the aromatic ring and the activated ester was removed in order to increase protein coupling yields by minimizing competitive hydrolysis. And second, unlike BH, SIB lacks the phenolic hydroxyl group ortho to the iodine atom. It was speculated that the extensive deiodination of proteins which is observed *in vivo* could be minimized by decreasing the structural similarity of the protein iodination site to thyroid hormones, for which multiple dehalogenases are known to exist (9-11).

* Abbreviations used: MAbs, monoclonal antibodies; BH, *N*-succinimidyl 3-(4-hydroxy-3-[¹²⁵I]iodophenyl)propionate; SIB, *N*-succinimidyl 3-iodobenzoate; ATE, *N*-succinimidyl 3-(tri-*n*-butylstannyl)benzoate.

Several paired-label studies have documented the fact that intact MABs and their $F(ab')_2$ fragments labeled by using the ATE method are more inert to dehalogenation than those labeled by direct electrophilic substitution on tyrosine residues (Iodogen method) (12, 13). These experiments facilitated the comparison of our results to those reported in the literature for directly labeled MABs; however, testing the original design hypothesis for SIB requires a direct comparison to MABs labeled with BH. In this study, we have compared the protein-coupling chemistries of SIB and BH. In addition, data will be presented which suggests that presence or absence of a hydroxyl group ortho to the site of iodination is not necessarily the primary factor influencing the loss of radioiodine from MABs in vivo.

EXPERIMENTAL PROCEDURES

Reagents. ATE was synthesized and purified by using previously published procedures (6). The mono[^{125}I]-iodinated form of the Bolton-Hunter reagent was obtained from Amersham Corp. (Arlington Heights, IL) and sodium [^{131}I]iodide was purchased from Du Pont-New England Nuclear (Boston, MA). Goat immunoglobulin (IgG) was purchased from Sigma Chemical Co. (St. Louis, MO). MAb 81C6 is of the IgG_{2b} isotype and reacts with an epitope of the extracellular matrix antigen tenascin (14). It was obtained as a gift from Dr. Darell Bigner, Department of Pathology, Duke University Medical Center.

Synthesis of *N*-Succinimidyl 3-[^{131}I]Iodobenzoate (SIB). Radioiodination of ATE was accomplished as described in an earlier publication (15). Briefly, to 1–2 μL of [^{131}I] in 0.1 N NaOH in a glass, conical vial was added twice the volume of 3% acetic acid in CHCl_3 followed by 15 μL of *tert*-butyl hydroperoxide (10% in CHCl_3) and 5 μL of ATE (0.5 μmol in CHCl_3). After stirring for 30 min at room temperature, [^{131}I]SIB was isolated by HPLC. The separation system consisted of an Alltech silica gel column eluted with hexane/ethyl acetate/acetic acid (70:29.88:0.12).

General Method for Labeling IgG Using SIB and BH. The standard labeling conditions used were as follows: For the ATE method, the HPLC fractions containing [^{131}I]SIB were concentrated to about 50–100 μL and transferred, with the aid of a small volume of ethyl acetate, to a 0.5-dram glass vial. The solvent was evaporated with a gentle stream of argon. In the case of BH, an appropriate volume of the benzene/DMF solution containing the [^{125}I]-labeled active ester was transferred to a 0.5-dram vial and evaporated with a gentle stream of argon.

Goat IgG or 81C6 MAB (75 μL , 150 μg) in 0.1 M borate buffer, pH 8.5, was added to the vial containing either [^{131}I]SIB or [^{125}I]BH, and the mixture was incubated on ice at 4 °C for a period of 20 min with gentle shaking. The reaction was terminated by the addition of 300 μL of 0.2 M glycine in 0.1 M borate. The radioiodinated protein was isolated from lower molecular weight impurities with a Sephadex G-25 column. Protein-associated activity, determined by precipitation with 20% trichloroacetic acid, was greater than 95% for all preparations.

Labeling 81C6 IgG with [^{131}I] Using Iodogen. For use in some of the biodistribution studies, 81C6 MAB was labeled with [^{131}I] by using a variation of the original Iodogen method (3). MAB 81C6 (200 μg in 220 μL 100 mM phosphate buffer, pH 7.4) was added to sodium [^{131}I]iodide in a glass vial coated with 10 μg of Iodogen (Pierce Chemical Co., Rockford, IL). After a 10-min reaction at room temperature, radioiodinated 81C6 was purified by

chromatography over a Sephadex G-25 column. The trichloroacetic acid precipitability of this preparation was 99%.

Effect of pH. Goat IgG at a concentration of 2 mg/mL was prepared in 0.1 M borate buffers with pH in the range 8.5–10.0. To both [^{131}I]SIB and [^{125}I]BH was added 75 μL of the various protein solutions. Protein coupling efficiency was calculated by dividing the activity eluting in the void volume of the Sephadex G-25 column by the total activity added to the column. Activity levels were measured with a Capintec CRC-7 dose calibrator. Two to five determinations were performed at each pH.

Effect of Protein Concentration. Goat IgG in pH 8.5, 0.1 M borate buffer was prepared at concentrations of 1, 2, 3, 4, and 10 mg/mL. To both [^{131}I]SIB and [^{125}I]BH was added 75 μL of each goat IgG solution. Methods employed for separating the labeled protein and determining coupling efficiency were as described above. Two to five determinations were performed at each protein concentration.

Biodistribution Studies. MAB 81C6 was labeled with [^{125}I] by using BH and with [^{131}I] by using SIB as described above. Specific activities for the preparations, determined by measuring the protein concentration spectrophotometrically and the radioactivity level with the dose calibrator, were approximately 1 $\mu\text{Ci}/\mu\text{g}$. BALB/c mice weighing 20–25 g were injected in the tail vein with 3 μg each of [^{125}I] and [^{131}I]-labeled 81C6. Groups of 5 or 6 mice were sacrificed by ether overdose at 3, 4, 5, 6, and 7 days after injection for paired-label biodistribution analysis. This protocol was repeated twice. An additional set of mice was injected with 2 μg each of 81C6 labeled with [^{125}I] by using BH and with [^{131}I] by using Iodogen. Animals were dissected; tissues of interest were removed, weighed, washed with saline, and counted for both [^{125}I] and [^{131}I] activity with an LKB Model 1282 dual-channel γ -counter. Counting data were corrected for crossover of [^{131}I] activity into the [^{125}I] counting window. The percent injected dose in each tissue for both nuclides was calculated by comparison to injection standards of appropriate count rate. Blood was assumed to represent 6% of total body weight.

Statistical Analysis. Comparisons between the coupling efficiencies of SIB and BH were made by using the Student's *t* test (16). Since the tissue distribution experiments were performed in paired-label format, a direct comparison of the different iodination methods, with each animal serving as its own control, was possible. Data were analyzed by using a paired *t* test (16). In both analyses, only $p < 0.05$ has been considered to be statistically significant.

RESULTS AND DISCUSSION

Proteins can be radioiodinated either directly by electrophilic substitution on tyrosine residues or by conjugation of a labeled compound to the ϵ -amino group of lysines, thus permitting the labeling of proteins lacking a reactive tyrosine residue. An additional advantage is that conjugation radioiodination methods avoid exposing the protein to oxidants. In studies comparing the biologic activity of several proteins and peptides labeled directly and by using the Bolton-Hunter method, use of the latter yielded greater retention of immunological activity (5, 17). Since preservation of immunocompetence after radiolabeling is a critical factor in the labeling of MABs, acylation agents of this type might be useful for radioimmunosciintigraphic and therapeutic applications.

In an attempt to create a Bolton-Hunter analogue that would be more suitable for routine use in vivo, a method

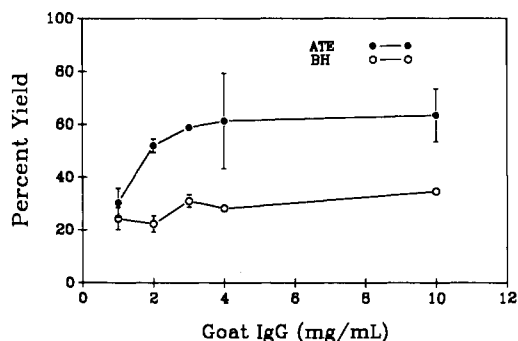


Figure 1. Effect of protein concentration on protein-labeling efficiency for the ATE and Bolton-Hunter methods. Reaction conditions, pH = 8.5 for 20 min at 4 °C.

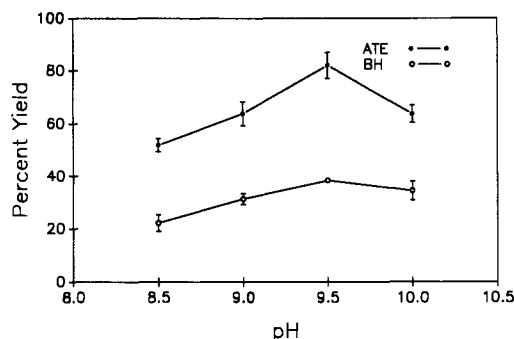


Figure 2. Effect of pH on protein-labeling efficiency for the ATE and Bolton-Hunter methods. Reaction conditions, 150 μ g of goat IgG per 75 μ L, 20 min at 4 °C.

was developed for synthesizing *N*-succinimidyl 3-iodobenzoate (SIB) from *N*-succinimidyl 3-(tri-*n*-butylstannyl)benzoate via electrophilic destannylation (6). The purpose of the present study was to evaluate by direct comparison to the Bolton-Hunter reagent two hypotheses used in the design of SIB.

Coupling Chemistry. A major difficulty with the Bolton-Hunter reagent and other conjugation labeling methods (18) is that conjugation efficiencies are low, generally on the order of 15–30% (18, 19). We speculated that omitting the two-carbon spacer between the aromatic ring and the *N*-succinimidyl ester moiety should increase conjugation efficiency to the protein by minimizing loss of labeled ester as a consequence of hydrolysis.

In Figure 1, the coupling efficiency for BH and SIB at pH 8.5 and a reaction time of 20 min is compared. At 1 mg/mL goat IgG in a 75 μ L reaction volume, the yield with SIB was $30.3 \pm 5.4\%$, a value 1.25 times that obtained with the BH reagent ($24.3 \pm 4.2\%$, difference not significant, $p = 0.06$). With both BH and SIB, coupling yield increased with increasing protein concentration until 3 mg/mL, after which a plateau was reached. In both cases, the results do not appear to represent first-order dependence of the reaction rate on protein concentration. It is important to note that, at all concentrations above 1 mg/mL, the coupling yields obtained with SIB were 1.8–2.3 times greater than those observed with BH ($p < 0.005$).

Over the pH range 8.5–10.0, at a fixed protein concentration of 2 mg/mL, maximum yields were obtained for both BH and SIB at a pH of 9.5 (Figure 2). It seems likely that the increased coupling efficiency at higher pH is a consequence of greater deprotonation of lysine ϵ -amino groups at higher pH, resulting in more amine sites available for reaction with the *N*-succinimidyl esters. Lower yields at pH 10 could be the result of competitive hydrolysis and/or partial precipitation of goat IgG at this pH. Again,

conjugation efficiency for SIB was about twice that of BH at all pH's ($38.3 \pm 0.4\%$ BH; $82.0 \pm 4.9\%$ SIB at pH 9.5; $p < 0.005$).

Yields obtained for coupling of SIB to goat IgG are in excellent agreement with our previous studies using goat IgG (6) and 81C6 MAb (13, 15) and are similar to those extrapolated from those of Wilbur et al. (7) and Khawli and Kassis (8) using slightly different reaction conditions. Likewise, coupling yields for BH are in qualitative agreement with those reported previously (5, 19). However, since coupling efficiencies have been shown to be dependent on pH, protein concentration, and even the nature of the protein (19), the current study was performed to compare the utility of BH and SIB for the radioiodination of a protein under identical reaction conditions.

The results of these experiments indicate that modifying the structure of the Bolton-Hunter reagent increased protein labeling yields by a factor of 2. It is presumed that the deletion of the two-carbon spacer between the *N*-succinimidyl ester and the aromatic ring resulted in a greater availability of active ester for amide-bond formation due to a decreased rate of ester hydrolysis. Indeed, when the Bolton-Hunter and SIB esters were exposed to PBS in the absence of protein, TLC analysis indicated that conversion to the corresponding acid was twice as fast for the Bolton-Hunter reagent. These results are in agreement with previous studies which have shown that the rate of hydrolysis of ethyl benzoates is considerably lower than that for ethyl esters of aryl compounds containing methylene spacers between the benzene ring and the ester functionality (20–22).

Loss of Label in Vivo. Since we have hypothesized that the dehalogenation of conventionally radioiodinated proteins in vivo is facilitated by the presence of a hydroxyl group ortho to the iodine on an aromatic ring, iodination using the ATE reagent is accomplished via destannylation in order to avoid this potential problem. The reasons for this speculation are that lack of a hydroxyl group ortho to the iodine (a) decreases the structural similarity to iodotyrosine and thyroxine, known substrates for multiple dehalogenases (9–11), and (b) increases the strength of the C–I bond (23).

Paired-label biodistribution studies were performed in normal mice to compare the pharmacokinetics of 81C6 MAb labeled by using both the ATE and Bolton-Hunter methods. As summarized in Table I, the tissue distribution of radioiodine generally is quite similar for MAb labeled using the two methods. However, as shown in Figure 3, thyroid uptake of radioiodine from MAb labeled by using the Bolton-Hunter method was significantly higher ($p < 0.01$ – 0.001) than that observed in the same mice for 81C6 labeled by using the ATE method, suggesting more rapid dehalogenation of MAb labeled by using the Bolton-Hunter method.

Although differential dehalogenation of MAb labeled using the two different acylation agents was not unexpected, the fact that the ATE method offered only a 2-fold advantage was somewhat surprising in light of our previous studies (13) comparing this same MAb radioiodinated with ATE and with Iodogen. These results demonstrated that the thyroid uptake for 81C6 labeled with Iodogen was 40–100-fold higher than MAb labeled with ATE. Wilbur et al. (7) have reported that neck uptake of radioiodine was 2–8-fold lower for NR-ML-95 MAb labeled with *p*-iodophenyl benzoate compared to chloramine-T; however, for a F(ab')₂ fragment at similar time points, 25–100-fold differences were seen.

In order to confirm the unexpectedly low thyroid uptake observed for 81C6 labeled with BH, the tissue distribution

Table I. Paired-Label Tissue Distribution of Radioiodine in Normal Mice Following Injection of 81C6 Labeled with [¹²⁵I]BH and with [¹³¹I]SIB

tissue	% injected dose per organ				
	3 days	4 days	5 days	6 days	7 days
Labeled with SIB					
liver	3.44 ± 0.32	1.98 ± 0.46	1.81 ± 0.22 ^a	1.64 ± 0.80	1.52 ± 0.37 ^b
spleen	0.21 ± 0.02	0.13 ± 0.02	0.12 ± 0.01	0.09 ± 0.04	0.09 ± 0.01
lung	1.94 ± 0.77	0.76 ± 0.24	1.24 ± 0.42	0.81 ± 0.27	0.73 ± 0.47
heart	0.28 ± 0.07	0.17 ± 0.05	0.21 ± 0.05	0.15 ± 0.07	0.13 ± 0.03
kidney	1.22 ± 0.10	0.72 ± 0.13	0.67 ± 0.11	0.53 ± 0.21	0.50 ± 0.09
stomach	0.30 ± 0.08	0.16 ± 0.05	0.14 ± 0.01	0.13 ± 0.07	0.10 ± 0.03
small intestine	1.59 ± 0.15	1.00 ± 0.24	0.97 ± 0.11	0.67 ± 0.29	0.73 ± 0.09
large intestine	0.89 ± 0.17 ^a	0.46 ± 0.14 ^c	0.45 ± 0.04	0.37 ± 0.16	0.30 ± 0.04
muscle	7.88 ± 0.49	5.63 ± 1.01	4.63 ± 0.63	3.15 ± 1.29	3.07 ± 0.18
bone	3.26 ± 0.22	3.04 ± 0.69	2.61 ± 0.69	1.39 ± 0.59	1.40 ± 0.18
blood	13.28 ± 1.51 ^a	7.78 ± 0.65 ^a	8.41 ± 1.61 ^a	5.87 ± 2.56 ^c	5.45 ± 0.75 ^a
brain	0.11 ± 0.02	0.06 ± 0.02	0.06 ± 0.01	0.05 ± 0.02	0.05 ± 0.02
Labeled with BH					
liver	3.28 ± 0.29	1.87 ± 0.42	1.64 ± 0.19	1.46 ± 0.71	1.34 ± 0.33
spleen	0.21 ± 0.02	0.13 ± 0.02	0.11 ± 0.01	0.08 ± 0.03	0.08 ± 0.01
lung	1.80 ± 0.69	0.73 ± 0.22	1.11 ± 0.32	0.71 ± 0.23	0.64 ± 0.42
heart	0.27 ± 0.07	0.16 ± 0.04	0.19 ± 0.05	0.13 ± 0.06	0.11 ± 0.03
kidney	1.23 ± 0.12	0.73 ± 0.12	0.66 ± 0.10	0.52 ± 0.20	0.49 ± 0.09
stomach	0.30 ± 0.09	0.16 ± 0.05	0.13 ± 0.01	0.12 ± 0.06	0.09 ± 0.02
small intestine	1.74 ± 0.13	1.07 ± 0.24	0.96 ± 0.12	0.66 ± 0.28	0.72 ± 0.11
large intestine	1.18 ± 0.25	0.59 ± 0.20	0.51 ± 0.08	0.44 ± 0.17	0.35 ± 0.07
muscle	7.61 ± 0.41	5.38 ± 0.85	4.47 ± 1.16	2.85 ± 1.13	2.96 ± 0.51
bone	3.09 ± 0.18	2.88 ± 0.58	2.34 ± 0.65	1.19 ± 0.52	1.31 ± 0.25
blood	11.93 ± 1.44	6.92 ± 0.59	7.30 ± 1.44	4.96 ± 2.18	4.51 ± 0.68
brain	0.10 ± 0.02	0.06 ± 0.01	0.06 ± 0.01	0.04 ± 0.02	0.04 ± 0.02

Significance of difference determined by two-sided paired *t* test: ^a *p* < 0.01; ^b *p* < 0.05; ^c *p* < 0.02; other tissues, no significant difference (*p* > 0.05)

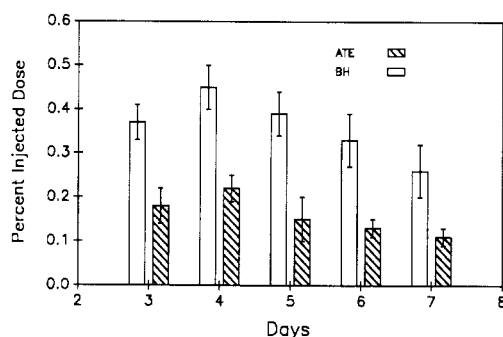


Figure 3. Comparison of the percent injected dose of radioiodine localized in the thyroids of normal mice following the injection of 81C6 monoclonal antibody labeled with ¹²⁵I and ¹³¹I by using the Bolton–Hunter and ATE methods, respectively.

of 81C6 labeled by using the Bolton–Hunter and Iodogen methods were compared directly in normal mice 3 days after injection. As shown in Table II, significant differences in radioiodine uptake were observed between the two nuclides in only thyroid and stomach, the two tissues normally reflecting free-iodide uptake (12). Thyroid uptake associated with MAb labeled with the Bolton–Hunter reagent was about 13 times lower than for MAb labeled with Iodogen.

In comparing the results obtained in this study with those reported previously, it is important to bear in mind that many factors can influence the magnitude of thyroid accumulation. Although the thyroid uptake observed for 81C6 labeled with SIB are in good agreement with a previous study, also performed in normal mice (24), they are 2–3-fold higher than those observed in athymic mice for both 81C6 and a nonspecific MAb in tumor-bearing athymic mice (13). Similarly, the thyroid uptake observed in the current study 3 days after injection of 81C6 labeled with Iodogen (5.97 ± 0.73%) was also higher than that seen (13) in athymic mice (4.14 ± 0.67%), suggesting that differences may exist in the catabolism of labeled MABs

Table II. Paired-Label Tissue Distribution of Radioiodine in Normal Mice 3 Days following Injection of 81C6 Labeled with [¹²⁵I]BH and with [¹³¹I]Iodogen

tissue	% injected dose per organ	
	BH	Iodogen
liver	2.81 ± 0.50	2.88 ± 0.60
spleen	0.19 ± 0.03	0.19 ± 0.03
lung	0.72 ± 0.20	0.75 ± 0.22
heart	0.22 ± 0.04	0.23 ± 0.04
kidney	1.05 ± 0.06	1.15 ± 0.06
stomach	0.22 ± 0.05 ^a	0.46 ± 0.05
small intestine	1.46 ± 0.25	1.29 ± 0.18
large intestine	0.95 ± 0.15	0.87 ± 0.21
thyroid	0.44 ± 0.06 ^a	5.97 ± 0.73
muscle	7.42 ± 2.38	6.84 ± 1.04
bone	3.04 ± 0.31	3.56 ± 0.48
blood	12.50 ± 1.78	13.50 ± 2.02
brain	0.09 ± 0.03	0.09 ± 0.01

Significance of difference determined by two-sided paired *t* test: ^a *p* < 0.001; other tissues, no significant difference (*p* > 0.05).

in normal versus athymic mice. In addition, Dumas et al. (25) has reported that the deiodinase activity of sheep liver microsomes in vitro for aryl iodides varied from lot to lot and was dependent on the nutritional and physiological state of the animal. Thus, paired-label protocols are essential to compare directly the catabolism of label from MABs radioiodinated by using different methods.

Although many antibodies and other proteins have been labeled by using the Bolton–Hunter method for in vitro applications, little data are available concerning their behavior in vivo. To our knowledge, no systematic study of MABs labeled by using the Bolton–Hunter method has been reported which includes a determination of thyroid uptake. Although the pharmacokinetics of auroiomycin would not be expected to be similar to those of an antibody, it is worth noting that Anatha Samy and co-workers (26) have reported that, 8 h after injection of this antibiotic labeled with ¹²⁵I by using the Bolton–Hunter method, uptake of ¹²⁵I activity in the thyroid was only

0.13% of the injected dose. In addition, Schiff et al. (27) have reported that the radioactive catabolites formed following the cellular internalization of asialoglycoprotein labeled by the Bolton-Hunter and the iodine monochloride methods are different.

While use of the ATE method for MAb radiohalogenation results in the lowest degree of thyroid accumulation, only a 2-fold advantage was observed relative to the Bolton-Hunter method in contrast to as much as a 100-fold advantage when compared to the Iodogen method. It thus appears that presence or absence of a hydroxyl group ortho to the iodination site is not the sole factor determining the thyroid uptake and presumably the dehalogenation of radioiodinated proteins.

The specificity of deiodinases from sheep thyroidal and hepatic microsomes for 19 aryl iodides has been investigated by Dumas et al. (25). While 3-iodo-L-tyrosine was almost completely dehalogenated, 3-iodo-D-tyrosine, 3-iodo- α -methyl-DL-tyrosine, and 3-iodo-tyramine were not, indicating a high degree of structural specificity for these deiodinases. In a subsequent study performed in rats injected with 11 of these compounds, a similar pattern of deiodination specificity was reported (28). The relevance of these results to the catabolism of label from radioiodinated MAbs is unclear, particularly since in the in vitro study it was reported that *N*-acetyl-3,5-diiodo-L-tyrosine, the compound with the closest structural similarity to an iodinated tyrosine residue on a protein (Chart II), was inert to dehalogenation (25). Experiments are currently underway investigating the catabolism of label from a series of aromatic iodides and their MAb conjugates in order to be able to design better acylation agents for the radioiodination of MAbs.

ACKNOWLEDGMENT

The excellent technical assistance of Donna Affleck and Susan Slade is greatly appreciated. Ann Tamariz provided editorial assistance. This research was supported by National Institutes of Health Grants CA 42324, NS 20023, CA 14236, and by Grant DEFG05-89ER60789 from the Department of Energy.

LITERATURE CITED

- (1) Larson, S. M., and Carrasquillo, J. A. (1988) Advantages of radioiodine over radioindium labeled monoclonal antibodies for imaging solid tumors. *Nucl. Med. Biol.* 15, 231-233.
- (2) Delaloye, B., Bischof-Delaloye, A., Buchegger, F., von Flidner, V., Grob, J.-P., Volant, J.-C., Pettavel, J., and Mach, J.-P. (1986) Detection of colorectal carcinoma by emission-computerized tomography after injection of ^{125}I -labeled Fab or F(ab')_2 fragments from monoclonal anti-carcinoembryonic antigen antibodies. *J. Clin. Invest.* 77, 301-311.
- (3) Fracker, P. J., and Speck, J. C. (1987) Protein and cell membrane iodination with a sparingly soluble chloramide 1,3,4,6-tetrachloro-3 α -6 α -diphenylglycouril. *Biochem. Biophys. Res. Commun.* 80, 849-857.
- (4) Eary, J. F., Krohn, K. A., Kishore, R., and Nelp, W. B. (1989) Radiochemistry of Halogenated Antibodies. In *Antibodies in Radiodiagnosis and Therapy* (M. R. Zalutsky, Ed.) pp 83-102, CRC Press, Inc., Boca Raton, Florida.
- (5) Bolton, A. M., and Hunter, R. M. (1973) The labeling of proteins to high specific radioactivities by conjugation to a I-125 containing acylating agent. *Biochem. J.* 133, 529-539.
- (6) Zalutsky, M. R., and Narula, A. S. (1987) A method for the radiohalogenation of proteins resulting in decreased thyroid uptake of radioiodine. *Appl. Radiat. Isot.* 38, 1051-1055.
- (7) Wilbur, D. S., Hadley, S. W., Hylarides, M. D., Abrams, P. G., Beaumier, P. A., Morgan, A. C., Reno, J. M., and Fritzberg, A. R. (1989) Development of a stable radioiodinating reagent to label monoclonal antibodies for radiotherapy of cancer. *J. Nucl. Med.* 30, 216-226.
- (8) Khawli, L. A., and Kassis, A. I. (1989) Synthesis of ^{125}I labeled *N*-succinimidyl *p*-iodobenzoate for use in radiolabeling antibodies. *Nucl. Med. Biol.* 16, 727-733.
- (9) Gershengorn, M. C., Glinioer, D., and Robbins, J. (1980) Transport and Metabolism of Thyroid Hormones. In *The Thyroid Gland* (M. DeVisscher, Ed.) pp 81-121, Raven Press, New York.
- (10) Koehrle, J., Aufmkolk, M., Rokos, H., Hesch, R.-D., and Cody, V. (1986) Rat liver iodothyronine ligand-binding site. *J. Biol. Chem.* 261, 11813.
- (11) Smallridge, R. C., Burman, K. D., Ward, K. E., Wartofsky, L., Dimond, R. C., Wright, F. D., and Latham, K. R. (1981) 3',5-Diiodothyronine to 3'-monoiodothyronine conversion in the fed and fasted rat: enzyme characteristics and evidence for two distinct 5'-diiodinases. *Endocrinology* 108, 2336-2345.
- (12) Zalutsky, M. R., and Narula, A. S. Radiohalogenation of a monoclonal antibody using an *N*-succinimidyl-3-(tri-*n*-butylstannyl)benzoate intermediate. *Cancer Res.* 48, 1446-1450.
- (13) Zalutsky, M. R., Noska, M. A., Colapinto, E. V., Garg, P. K., and Bigner, D. D. (1989) Enhanced tumor localization and in vivo stability of a monoclonal antibody radioiodinated using *N*-succinimidyl-3-(tri-*n*-butylstannyl)benzoate. *Cancer Res.* 49, 5543-5549.
- (14) Bourdon, M. A., Wikstrand, C. J., Furthmayr, H., Matthews, T. J., and Bigner, D. D. (1983) Human glioma-mesenchymal extracellular matrix antigen defined by monoclonal antibody. *Cancer Res.* 43, 2796-2805.
- (15) Garg, P. K., Archer, G. E., Jr., Bigner, D. D., and Zalutsky, M. R. (1989) Synthesis of radioiodinated *N*-succinimidyl iodobenzoate: optimization for use in antibody labelling. *Appl. Radiat. Isot.* 40, 485-490.
- (16) Remington, R. D., and Schork, M. A. (1985) *Statistics with Applications to the Biological Sciences* pp 135-190, Prentice-Hall, Englewood Cliffs, NJ.
- (17) Bolton, A. E., Lee-Own, V., Kramer McLean, R., and Chaland, G. S. (1979) Three different radioiodination methods for human spleen ferritin compared. *Clin. Chem.* 25, 1826-1830.
- (18) Wood, F. T., Wu, M. M., and Gerhart, J. C. (1975) The radioactive labeling of proteins with an iodinated amidation reagent. *Anal. Biochem.* 69, 339-349.
- (19) Bolton, A. E., Bennie, J. G., and Hunter, W. M. (1976) Innovations in labeling techniques for radioimmunoassays. *Protides Biol. Fluids* 24, 687-693.
- (20) Euranta, E. K. (1969) Esterification and Ester Hydrolysis. *The Chemistry of Carboxylic Acids and Esters* (S. Patai, Ed.) pp 506-581, Interscience, New York.
- (21) Jaffe, H. H., (1953) A reexamination of the Hammett equation. *Chem. Rev.* 53, 191-261.
- (22) Kindler, K. (1926) Haftfestigkeit organischer radikale und reaktionsfahigkeit. II. *Justus Liebigs Ann. Chem.* 452, 90-120.
- (23) Cottrell, T. C. (1958) *The Strengths of Chemical Bonds*, Butterworths, London.
- (24) Garg, P. K., Slade, S. K., Harrison, C. L., and Zalutsky, M. R. (1989) Labeling proteins using aryl iodide acylation agents: influence of meta vs para substitution on in vivo stability. *Nucl. Med. Biol.* 16, 669-673.
- (25) Dumas, P., Maziere, B., Autissier, N., and Michel, R. (1973) Specificite de l'iodotyrosine desiodase des microsomes thyroïdiens et hépatiques. *Biochim. Biophys. Acta* 293, 36-47.
- (26) Anantha Samy, T. S., Siegel, P. J., Hopper, W. E., and Krishnan, A. (1984) Experimental pharmacology of auroiomycin in L1210 tumor cells in vitro and in vivo. *Cancer Res.* 44, 3202-3207.
- (27) Schiff, J. M., Fisher, M. M., and Underdown, B. J. (1984) Receptor-mediated biliary transport of immunoglobulin A and asialoglycoprotein: sorting and missorting of ligands revealed by two radiolabeling methods. *J. Cell. Biol.* 98, 79-89.
- (28) Dumas, P. (1979) Deshalogenation de divers deries iodes phenoliques chez le rat normal et thyroïdectomise. *Biochem. Pharmacol.* 22, 1599-1605.

Registry No. ATE, 112725-22-1; [^{131}I]SIB, 127733-21-5; BH, 65114-37-6.

Antibody-Directed Fibrinolysis: A Bispecific (Fab')₂ That Binds to Fibrin and Tissue Plasminogen Activator

Marschall S. Runge,[†] Christoph Bode,[‡] Christopher E. Savard, Gary R. Matsueda, and Edgar Haber*

Cardiac Unit, Massachusetts General Hospital and Harvard Medical School, Boston, Massachusetts 02114.

Received December 22, 1989

A bispecific (Fab')₂ molecule was constructed by linking the monovalent Fab' from an anti-fibrin monoclonal antibody to the Fab' from an anti tissue plasminogen activator (tPA, single chain) monoclonal antibody by means of inter-heavy-chain disulfide bonds. An immunochemical complex composed of the bispecific (Fab')₂ molecule bound to tPA [tPA-bispecific (Fab')₂ complex] was then generated and purified. Its molecular weight was 170 kDa [less than half the molecular weight of a previously described tPA-bispecific antibody complex containing the entire anti-fibrin and anti-tPA immunoglobulin molecules; Runge, M. S., et al. (1987) *Trans. Assoc. Am. Phys.* 100, 250-255]. The tPA-bispecific (Fab')₂ complex was 8.6-fold more efficient in fibrinolysis than tPA alone and 94-fold more potent than urokinase. This enhancement in the fibrinolytic potency of tPA compares favorably with that observed for the bispecific whole-antibody complex. These results suggest that this smaller, less immunogenic molecule is capable of binding both fibrin and tPA with high affinity and of enhancing the thrombolytic efficiency of exogenous and, perhaps, endogenous tPA.

INTRODUCTION

Treating myocardial infarction with plasminogen activators has been shown to result in a reduction in infarct size (1, 2) and mortality (3, 4). For optimal results, treatment must be initiated as soon as possible after the onset of symptoms (3). This mandates a rapid therapeutic decision and heightens the need for a thrombolytic agent that is free of serious side effects.

A bispecific antibody capable of binding both fibrin and single-chain tissue plasminogen activator (tPA)¹ has been described (5-7). We assembled it by forming a disulfide bond between *N*-succinimidyl 3-(2-pyridyldithio)-propionate modified anti-fibrin monoclonal antibody 59D8 and 2-iminothiolane-modified anti-tPA monoclonal antibody TCL8. The bispecific antibody enhances the fibrinolytic potency of tPA in vitro and in vivo. Here we describe the production and characterization of a molecule assembled by linking an Fab' fragment from each of the two antibodies. The bispecific (Fab')₂ similarly enhances the fibrinolytic potency of tPA, but unlike the bispecific whole antibody, the bispecific (Fab')₂ has a well-defined structure, is much smaller, and lacks the highly immunogenic Fc portions of its component antibodies.

EXPERIMENTAL PROCEDURES

The tPA used in these studies was derived from melanoma cells purchased from BioResponse (Hayward, CA). Two-chain, low molecular weight urokinase (Abokinase) was purchased from Abbott Laboratories and Sepharose 4B-CL was obtained from Pharmacia P-L Biochemicals. The ¹²⁵I-labeled fibrinogen came from Am-

ersham; the plasma came from the local blood bank. Chromogenic substrate H-D-isoleucyl-L-prolyl-L-arginine-*p*-nitroanilide dihydrochloride (S-2288) was obtained from Helena Laboratories. Human placenta factor XIII was purchased from Green Cross (Osaka, Japan); the Superose 12 resin for fast protein-liquid chromatography was from Pharmacia. All other chemicals came from Sigma.

Antibodies. tPA-specific monoclonal antibody TCL8 and fibrin-specific monoclonal antibody 59D8 were raised and purified as described (5, 8).

Protein Concentration. Protein concentration was determined by the method of Bradford (9).

Preparation of tPA-Sepharose. Twenty milligrams of recombinant tPA was solubilized in 10 mL of water and passed through a Sephadex G-25 column (30 × 2 cm) equilibrated with 0.2 M NaHCO₃, 1.5 M sodium chloride, and 0.1% Tween-80 (coupling buffer). The protein was immediately incubated with 15 mL of cyanogen bromide activated Sepharose (Pharmacia P-L Biochemicals) and coupled according to the manufacturer's instructions. After incubation for 24 h at 4 °C, residual binding sites on the Sepharose were blocked with 10 mL of 1.0 M ethanolamine (titrated with HCl to pH 8.0) for an additional 8 h.

Production and Purification of Bispecific (Fab')₂. The bispecific (Fab')₂ molecule was prepared by linking the monovalent Fab's of antibodies 59D8 and TCL8 through the intrinsic heavy-chain cysteines, which usually form disulfide bonds in native (Fab')₂ molecules (10). Each antibody was first digested with pepsin (11): 10 mL of antibody solution (2.0 mg/mL in 0.01 M sodium phosphate, 0.15 M sodium chloride, pH 7.4) was mixed with 1 mL of 1.0 M sodium citrate (pH 2.75) and 1 mL of pepsin solution (0.3 mg/mL in water), the final pH was adjusted to 3.5, and the mixture was incubated for 2 h at 37 °C. The reactions were stopped by the addition of 1.0 mL of 3.0 M Tris HCl, pH 8.5. In pilot experiments, these conditions had produced optimal yields of 59D8 Fab' and TCL8 Fab'. Pepsin concentrations had varied between 0.05 and 0.5 mg/mL, the final pH was between 2.5 and 5.0, and the duration of incubation was between 30 min and 8 h.

[†] Present address: Cardiology Division, Emory University, Post Office Drawer LL, Atlanta, GA 30322.

[‡] Present address: Medizinische Klinik III (Kardiologie) der Universität Heidelberg, 6900 Heidelberg, Federal Republic of Germany.

¹ Abbreviations: tPA, tissue plasminogen activator (single chain); S-2288, chromogenic substrate H-D-isoleucyl-L-prolyl-L-arginine-*p*-nitroanilide dihydrochloride.

(Fab')₂ were purified from the 59D8 and TCL8 digests by chromatography against their respective affinity ligands. For the former, β peptide (Gly-His-Arg-Pro-Leu-Asp-Lys-Cys, corresponding to the seven amino-terminal residues of the β chain of fibrin) coupled to Sepharose (β peptide-Sepharose) was used; for the latter, tPA coupled to Sepharose (see Preparation of tPA-Sepharose) was used. After elution from the affinity matrices with 0.2 M glycine (pH 2.8), each (Fab')₂ solution was collected into tubes containing a neutralizing amount of 3.0 M Tris HCl (pH 8.5), dialyzed into 0.1 M sodium phosphate (pH 6.8), and reconcentrated in an ultrafiltration chamber to 2 mg/mL. Reduction of the 59D8 and TCL8 fragments was then carried out at room temperature in 1 mM 2-mercaptoethylamine, 1 mM ethylenediaminetetraacetic acid, and 10 mM sodium arsenite, followed by the addition of solid Ellman's reagent to a concentration of 5 mM. After 3 h at room temperature, excess reagent was removed from the two Fab' solutions by gel filtration on a Sephadex G-25 column (30 \times 2 cm) equilibrated with 0.1 M sodium phosphate (pH 6.8). The thiol form of anti-fibrin 59D8 Fab' was then regenerated by treatment with 10 mM 2-mercaptoethylamine for 30 min, followed by gel filtration as above. After that the anti-fibrin 59D8 Fab' was incubated with the thionitrobenzoate derivative of the anti-tPA TCL8 Fab' for 16 h at room temperature in 0.1 M sodium phosphate and 1 mM ethylenediaminetetraacetic acid (pH 6.8). The desired (Fab')₂ heterodimer was purified from the reaction mixture by sequential affinity chromatography on β peptide-Sepharose and tPA-Sepharose. The final yield of bispecific (Fab')₂ was 7 mg, or about 25% of the theoretical yield of the coupling of two different Fab' molecules.

Preparation of Immunochemical Complex. An immunochemical complex made up of tPA and the bispecific (Fab')₂ [tPA-bispecific (Fab')₂ complex] was formed by mixing 3.5 mg of tPA (0.5 mg/mL) with 5 mg of bispecific (Fab')₂ (0.5 mg/mL) for 2 h at room temperature. After concentration to a volume of 9 mL, chromatography on Sephacryl S-300 [preequilibrated with 0.1 M sodium phosphate, 0.1 M NaCl, 0.01% sodium azide, pH 7.4 (PBSA)] revealed a peak of approximately 170 kDa [tPA bound to the bispecific (Fab')₂] and a second peak of approximately 70 kDa (unbound tPA). On the basis of enzymatic activity (assayed by S-2288, see below), approximately 1 mol of tPA appeared to bind per mole of bispecific (Fab')₂.

Measurement of Plasminogen Activator Activity. To compare the activity of native tPA with that of tPA as part of an immunochemical complex, the amidolytic activities and molar amounts of tPA in the various preparations were measured in the following manner. Standardized samples of melanoma tPA or recombinant tPA (as aliquots from a freshly resuspended vial of tPA, in international units) were analyzed in the S-2288 assay with a substrate concentration of 1×10^{-3} mol/L and an enzyme concentration of 8×10^{-9} mol/L in 0.15 M Tris, 0.15 M NaCl, pH 8.4. For tPA, 1 international unit was assumed to equal 6.3×10^{-6} nmol. The correlation between the reported change in absorbance/minute for the assay preparations² and our samples was excellent, such that 100 units of tPA (6.3×10^{-6} mmol) gave an absorbance change at 405 nm of approximately 0.060/min. On the basis of these results, the activity (in appropriate units as above) or the molar amount of active enzyme of an unknown sample of urokinase or tPA was determined by diluting the sample until assay with S-2288 as described above

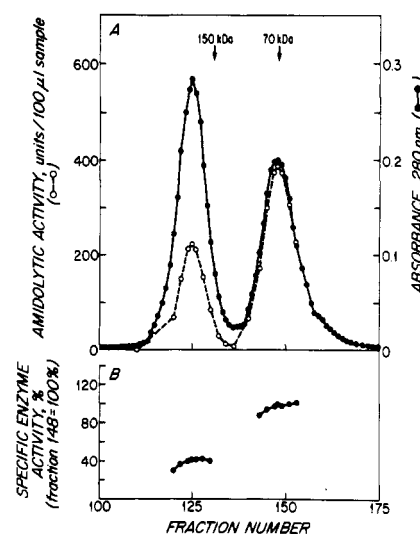


Figure 1. Gel filtration on a calibrated Sephacryl S-300 column of the tPA-bispecific (Fab')₂ complex. (A) The gel filtration resulted in two protein peaks, both of which contained enzymatic activity. Profiles of absorbance at 280 nm (closed circles) and amidolytic activity (open circles) are shown. On the basis of molecular weights and the relative specific enzymatic activities of the two peaks (B), peak 1 (170 kDa) was judged to contain a 1:1 molar conjugate of bispecific (Fab')₂ and tPA and peak 2 was judged to contain unbound tPA.

produced an absorbance change of 0.060/min at 405 nm. The linear range of enzyme concentration to absorbance change was from 4×10^{-9} to 3.2×10^{-8} mol/L in our hands. If concentrations outside this range were used in any of the assays described here, appropriate dilutions were made from stock solutions that contained either 8×10^{-9} or 8×10^{-8} mol/L (an aliquot of which had been tested at a 1:10 dilution in the S-2288 assay).

Measurement of Fibrinolytic Potency. Relative fibrinolytic potency was calculated (on a molar tPA basis) by measuring the lysis of ¹²⁵I-labeled fibrin monomer covalently linked to cyanogen bromide activated Sepharose 4B-CL (quantitative fibrinolysis assay) (12). To facilitate direct statistical comparison between fibrinolysis with a plasminogen activator alone and fibrinolysis with a plasminogen activator in the presence of the bispecific antibody, a fit-function program (13) was applied to the data from each assay and the curves were compared by the *t* test, as previously described (14).

RESULTS

Figure 1A shows the characterization of the tPA-bispecific (Fab')₂ complex on a calibrated Sephacryl S-300 column. The first peak eluted at an apparent molecular size slightly higher than 150 kDa (IgG was used as marker protein), which corresponds to the presumed size (170 kDa) of an immunochemical complex made up of the heterodimer (Fab')₂ and tPA. The second peak eluted at 70 kDa, corresponding to recombinant tPA. Both peaks contained enzymatic activity, as assessed by the S-2288 chromogenic substrate assay. The calculated theoretical specific activity of a 1:1 complex of bispecific (Fab')₂ and tPA is 41.2% of the specific activity of tPA alone. Figure 1B shows that the specific enzymatic activity of fractions from peak 1 was about 40% that of the fractions from peak 2.

The results of SDS-PAGE on a sample from the first peak shown in Figure 1A (pooled fractions 123–128) are shown in Figure 2. Under nonreducing conditions (panel A), the tPA-bispecific (Fab')₂ complex displayed two bands: one corresponding to the size of an (Fab')₂ molecule,

² KabiVitrum, 1986.

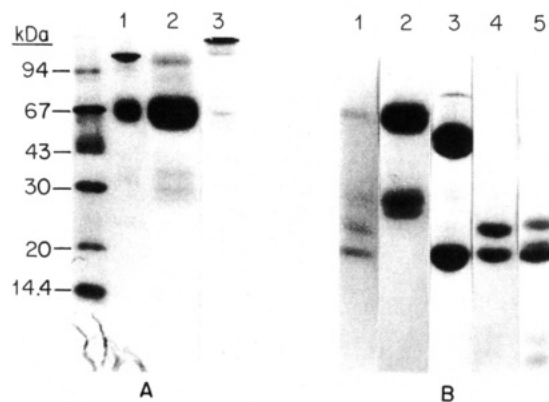


Figure 2. SDS-PAGE of tPA-bispecific (Fab')₂ complex. Ten percent polyacrylamide gels were run under nonreducing (panel A) and reducing (panel B) conditions. (A) numbers on the left correspond to molecular weight standards (Pharmacia): lane 1, tPA-bispecific (Fab')₂ complex; lane 2, single-chain recombinant tPA; and lane 3, anti-tPA antibody. (B) Lanes 1–3 as in A; lane 4, antifibrin 59D8 (Fab')₂; Lane 5, anti-tPA TCL8 (Fab')₂.

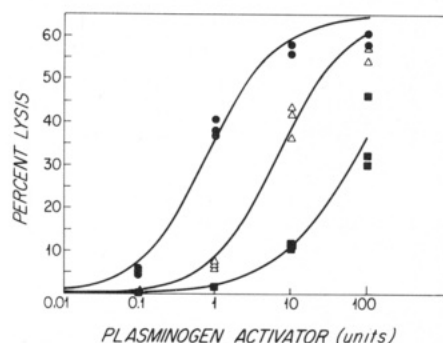


Figure 3. Release of radioactive peptides from ¹²⁵I-labeled fibrin-Sepharose by the tPA-bispecific (Fab')₂ complex (filled circle), by tPA alone (open triangle), and by urokinase alone (filled square). Lysis is expressed as the quotient of released radioactivity over total radioactivity. Each point represents the mean of three determinations. A three-parameter inverse logit function was used to fit the curves to the original triplicate points.

the other to the size of a tPA molecule. Under reducing conditions (panel B), bands corresponding in size to the two chains of the Fab' molecules and to single-chain tPA could be seen, and there was evidence of traces of two-chain tPA.

The tPA-bispecific (Fab')₂ complex was compared with tPA alone and with urokinase in the quantitative fibrinolysis assay (Figure 3). In these experiments, the tPA-bispecific (Fab')₂ complex was 8.6-fold more efficient in fibrinolysis than tPA alone ($p < 0.0001$), and 94-fold more potent than urokinase ($p < 0.0001$). Here tPA was 11-fold more efficient than urokinase, a finding similar to that of previous experiments (5). It is of particular interest that the tPA-bispecific (Fab')₂ complex showed an enhancement in the fibrinolytic activity of tPA similar to that of the tPA-bispecific antibody complex (5).

DISCUSSION

Here we describe a bispecific (Fab')₂ that has affinity for both fibrin and tPA. The rationale for producing this bispecific (Fab')₂ was based on promising results obtained when intact anti-fibrin and anti-tPA antibodies were coupled. We previously demonstrated (5–7) that a bispecific antibody containing intact anti-fibrin and anti-tPA antibodies is capable of concentrating tPA and enhancing the fibrinolytic potency of tPA in vitro, in human plasma, and in vivo in the rabbit jugular vein model. In model experiments, the bispecific antibody was able to

concentrate the low amounts of tPA normally present in human plasma and effect fibrinolysis. This increased potency is probably related to the fact that the antifibrin antibody has an affinity for fibrin 1800 times greater than that of tPA: the K_D of tPA for fibrin is 0.14×10^{-6} M (15), whereas that of antibody 59D8 is 0.77×10^{-10} M.³ However, one limitation to the clinical utility of the bispecific whole antibody is that the coupling chemistry used to create it does not yield a homogeneous product.

The bispecific (Fab')₂ is a better-defined molecule than the bispecific whole antibody because the linkage between the component Fab's in the fragment antibody occurs only at the disulfide bonds of the hinge region, with the practical result that only (Fab')₂ molecules are present after the coupling reaction. To ensure that only molecules possessing both fibrin and tPA binding properties (in a 1:1 molar ratio) were present in the final reaction mixture, we subjected the products of the coupling reaction to sequential affinity chromatography against the two antigens. The gel-filtration data presented in Figure 2 suggest that tPA binds to the bispecific (Fab')₂ in a 1:1 complex. Our calculations indicate that almost all the bispecific (Fab')₂ reacted with the tPA. This suggests that the purification process selects for functionally active molecules. The ability of the bispecific (Fab')₂ to enhance the fibrinolytic potency of tPA is apparently identical with that of the bispecific whole antibody. Thus monovalent binding to both antigens appears to be sufficient to effect increased potency. Because of its increased diffusibility, the smaller bispecific (Fab')₂, as opposed to the bispecific whole antibody, may provide advantages for later in vivo studies. More importantly, the (Fab')₂ can be synthesized in a reproducible manner that does not require the introduction of cross-linking reagents, which have the potential to act as immunogenic epitopes.

ACKNOWLEDGMENT

M.S.R. is a recipient of a Merck Fellowship from the American College of Cardiology. C.B. is a recipient of a fellowship from Boehringer Ingelheim Fonds and a grant from the Sandoz Foundation. This work was supported by National Institutes of Health Grants HL-19259 and HL-28015 and by a grant from the Schering Corp.

LITERATURE CITED

- (1) Collen, D., Topol, E. J., Tiefenbrunn, A. J., Gold, H. K., Weisfeldt, M. L., Sobel, B. E., Leinbach, R. C., Brinker, J. A., Ludbrook, P. A., Yasuda, I., Bulkley, B. H., Robison, A. K., Hutter, A. M., Jr., Bell, W. R., Spadaro, J. J., Jr., Khaw, B. A., and Grossbard, E. B. (1984) Coronary thrombolysis with recombinant human tissue-type plasminogen activator: a prospective, randomized, placebo-controlled trial. *Circulation* 70, 1012–1017.
- (2) Simoons, M. L., Serruys, P. W., van de Brand, M., Bär, F., de Zwaan, C., Res, J., Verheugt, F. W. A., Krauss, X. H., Remme, W. J., Vermeer, F., and Lubsen, J. (1985) Improved survival after early thrombolysis in acute myocardial infarction. A randomized trial by the Interuniversity Cardiology Institute in The Netherlands. *Lancet* 2, 578–581.
- (3) Gruppo Italiano per lo Studio della Streptochinasi nell'Infarto miocardico (GISSI) (1986) Effectiveness of intravenous thrombolytic treatment in acute myocardial infarction. *Lancet* 1, 397–402.
- (4) The ISAM Study Group (1986) A prospective trial of intravenous streptokinase in acute myocardial infarction (ISAM). *N. Engl. J. Med.* 314, 1465–1471.

³ Bohdan J. Kudryk, personal communication.

- (5) Bode, C., Runge, M. S., Branscomb, E. E., Newell, J. B., Matsueda, G. R., and Haber, E. (1989) Antibody-directed fibrinolysis: An antibody specific for both fibrin and tissue plasminogen activator. *J. Biol. Chem.* 264, 944-948.
- (6) Runge, M. S., Bode, C., Matsueda, G. R., and Haber, E. (1987) Antibody-enhanced thrombolysis: capture of tissue plasminogen activator by a bispecific antibody and direct targeting by an antifibrin-tPA conjugate in vivo. *Trans. Assoc. Am. Phys.* 100, 250-255.
- (7) Runge, M. S., Quertermous, T., Matsueda, G. R., and Haber, E. (1988) Increasing selectivity of plasminogen activators with antibodies. *Clin. Res.* 56, 501-506.
- (8) Hui, K. Y., Haber, E., and Matsueda, G. R. (1983) Monoclonal antibodies to a synthetic fibrin-like peptide bind to human fibrin but not fibrinogen. *Science* 222, 1129-1132.
- (9) Bradford, M. M. (1976) A rapid and sensitive method for the quantitation of microgram quantities of protein utilizing the principle of protein-dye binding. *Anal. Biochem.* 72, 248-254.
- (10) Brennan, M., Davison, P. F., and Paulus, H. (1985) Preparation of bispecific antibodies by chemical recombination of monoclonal immunoglobulin G₁ fragments. *Science* 229, 81-83.
- (11) Parham, P. (1983) On the fragmentation of monoclonal IgG₁, IgG_{2a}, and IgG_{2b}, from BALB/c mice. *J. Immunol.* 131, 2895-2902.
- (12) Bode, C., Matsueda, G. R., Hui, K. Y., and Haber, E. (1985) Antibody-directed urokinase: a specific fibrinolytic agent. *Science* 229, 765-767.
- (13) BBN Research Systems (1983) *RS/1 User's Guide*, book 2, release 2, serial V-14342, pp 180-187, Bolt Beranek and Newmann, Cambridge, MA.
- (14) Bode, C., Runge, M. S., Newell, J. B., Matsueda, G. R., and Haber, E. (1987) Thrombolysis by a fibrin-specific antibody Fab'-urokinase conjugate. *J. Mol. Cell. Cardiol.* 19, 335-341.
- (15) Hoylaerts, M., Rijken, D. C., Lijnen, H. R., and Collen, D. (1982) Kinetics of the activation of plasminogen by human tissue plasminogen activator. Role of fibrin. *J. Biol. Chem.* 257, 2912-2919.

Registry No. Plasminogen activator, 105913-11-9.

Kinetics of the Dissociation of Indium-(*p*-Substituted-benzyl)ethylenediaminetetraacetic Acid Hapten Analogues from the Monoclonal Anti-Hapten Antibody CHA255

Damon L. Meyer,* Mark Fineman, Barbara W. Unger, and James M. Frincke

Hybritech Incorporated, P.O. Box 269006, San Diego, California 92126. Received March 16, 1990

Half-lives were measured for the dissociation of a series of 20 indium-benzyl-EDTA derivatives from a monoclonal antibody that binds to them. Most haptens gave expected monoexponential dissociation curves with half-lives ranging from ~ 8 to ~ 100 min at 22 ± 1 °C. Precise ($\pm \sim 2.5\%$) determinations were made using centrifugal ultrafiltration to separate free from bound hapten. A strong pH dependence of the dissociation half-life was found for the two haptens studied. Activation enthalpies were identical (23 ± 1 kcal/mol) for the dissociation of four haptens, suggesting that, in contrast to individual rate constants, this parameter is insensitive to hapten modification. The dissociation half-lives provided evidence for the location of a positive charge in the binding site, but gave no clear indication of the role of hydrophobic interactions or of steric requirements in hapten binding. While variations in ionic strength had no effect on the dissociation rate, lowering surface tension with dioxane increased the rate somewhat. Three hapten-antibody complexes showed biexponential dissociation rates. It is postulated that this results from distinct conformations of the complex dissociating at different rates. The dissociation rate constant was found to be an extremely sensitive indicator of the hapten-antibody interaction that can be measured very precisely.

INTRODUCTION

In vivo, anti-hapten monoclonal antibodies can be used to control the pharmacokinetic parameters of haptens and molecules to which a hapten moiety has been chemically attached (1, 2). For small hydrophilic haptens, the presence of anti-hapten antibodies dramatically extends the serum and whole-body lifetime of the hapten. "Hybrid" or "bifunctional" antibodies which have one binding site with high affinity for a hapten and the other binding site with high affinity for a cell marker, such as a tumor-associated antigen, not only prolong the lifetime of the hapten but also cause the hapten to preferentially accumulate at the target in nude mouse tumor models and in humans (3). We have begun animal experiments aimed at exploiting these properties for delivery of radioimaging agents, radiotherapy agents, and chemotherapy agents (2).

The biodistribution of a radiolabeled hapten is observed to change if the hapten structure is modified, even though the hapten is complexed to an anti-hapten antibody over 100 times its molecular weight. Some of this variability may be attributed to differences in the binding characteristics of the antibody to the related haptens. Therefore, an understanding of how hapten derivatization will affect antibody binding is useful in designing a hapten-antibody system. Particularly important is the dissociation rate constant, since this parameter should limit the rate at which a hapten leaves the carrier antibody either to diffuse away from the target site or to be ingested into a target cell. Retention time at the target, which may affect therapeutic dose and target/background ratio, is a function of the complex half-life.

Information about charge location in, and the size of, the binding site should emerge from knowledge of the dissociation rate constants for a properly selected group of hapten analogues. Dissociation rates can be used to screen clones for particular applications and to detect changes in binding due to site-specific mutation. The

information can also be used to direct the synthesis of new haptens for use in a particular application. Thus, we elected to develop a simple procedure to measure monoclonal antibody dissociation rate constants for a series of chemically related haptens with the intent of applying the information to an in vivo delivery system.

For pharmacological prediction and evaluation, rate constant values at 37 °C are of primary importance, but it was found in the course of this study that the dissociation rates in our system can be measured much more precisely at room temperature than at 37 °C. Consequently, the temperature dependence of the dissociation rate was measured for selected haptens to see whether a relative ordering of dissociation rates at room temperature would extrapolate to body temperature. In addition, a knowledge of the activation parameters for the dissociation provides further insight into the physical nature of the anti-hapten antibody system for future applications. In fact, it has been concluded (4) that the activation energy for the dissociation reaction is the primary determinant of the affinity constant.

Dissociation and association rate constants have been reported for monoclonal (5-7) and polyclonal (7-10, review: 4) antibodies. It is concluded that antibody affinities correlate inversely with dissociation rate constants and that variations in association rate constants are relatively small (11, 12, 4). Also, Hansch and co-workers (13-16) have developed structure-activity relationships for hapten derivatives binding to polyclonal antibodies. However, no studies have been reported that show quantitatively the sensitivity of the dissociation rate constant to variation in the hapten structure or to variation in solvent conditions for a well-defined anti-hapten monoclonal antibody system. Methods used previously to separate free hapten from complex include adsorption on activated carbon (7) and filtration through cellulose acetate (8, 9, 4). In this study, we used the Centrifree micropartition apparatus (Ami-

con Corp.) to separate the unbound hapten from the complex and found this to be a convenient and reproducible method.

In this paper, we describe the measurement of the dissociation rate constants for a series of chemically related haptens, all derivatives of the In^{3+} complex of benzyl-EDTA, that bind to an anti-hapten monoclonal antibody, designated CHA255. The immunogen from which CHA255 was obtained is a conjugate of (*p*-thioureidobenzyl)-EDTA-In (3) (17), linked to the ϵ -amino group of a lysine side chain of keyhole limpet hemocyanin. (*p*-Isothiocyanatobenzyl)-EDTA and similar (aminobenzyl)-EDTA derivatives (e.g., 4) provide a convenient synthetic route (18) to a wide range of compounds whose indium chelates are all complexed by the antibody. (Benzyl-EDTA chelates of metal ions other than indium are also bound by CHA255 but with significantly lower affinity (19).) Our results indicate that the dissociation rate constant is an extremely sensitive indicator of the antibody-hapten interaction and that it can be measured conveniently with high precision.

EXPERIMENTAL PROCEDURES

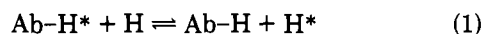
Hapten Derivatives. Several of the bifunctional chelates used as hapten derivatives or intermediates were prepared as described previously: 1, 2, 4 (18); 3 (20); 6 and 22 (2). Compound 18 was prepared by treating 17 with glutaric anhydride. Hapten derivatives 7–17, 19, and 20 were prepared by treating 3 with the appropriate amine at pH ~ 9 . Synthesis of the remaining hapten derivatives (5, 21) will be described elsewhere. Purification was conveniently accomplished by ion-exchange chromatography on DEAE Sephadex A25 eluted with a volatile buffer such as triethylammonium formate, followed by lyophilization, or by binding to AG1 ion-exchange resin in 0.5 M formic acid and elution with 8.0 M formic acid.

Hapten derivatives were characterized by HPLC retention time with a Hewlett-Packard 10-cm microbore ODS column using a 10-min linear gradient from 50 mM triethylammonium acetate containing 10 mM EDTA to 100% methanol at a flow rate of 0.4 mL/min. Indium-loaded and metal-free chelates were analyzed with this system, giving two characteristic retention times for each hapten. Chelates not containing In^{3+} were further characterized by their ^1H and ^{13}C NMR spectra, obtained on a Varian XL-300 Spectrophotometer.

These chelates were loaded with In^{3+} in either ammonium or triethylammonium citrate (18).

Antibodies. The antibody used throughout this work was CHA255, a murine antibody of the IgG1 type. The immunizations which led to the isolation of CHA255 were performed with a keyhole limpet hemocyanin conjugate of the In^{3+} complex of 3 (17). The "bifunctional" antibody ECH037 was derived from a fusion of the CHA255 cell line and an anti-CEA monoclonal antibody producing cell line designated CEM231.

Kinetic Scheme. It can be shown (21) that isotope-exchange reactions (eq 1) obey first-order kinetics. As



applied to antibody-hapten exchange, the general equation is

$$\ln(1-x) = \frac{R}{[\text{H}]_{\text{tot}}[\text{Ab}]_{\text{tot}}} ([\text{H}]_{\text{tot}} + [\text{Ab}]_{\text{tot}})t \quad (2)$$

where x is the fraction of exchange that has occurred and R is the "gross rate of exchange" of labeled and unlabeled hapten (constant for a given reaction mixture). Since,

in the case of antibodies and haptens, the affinity constant is very high, the dissociation rate constant is many orders of magnitude smaller than the association rate constant. Consequently, the gross rate of exchange is controlled by the dissociation rate, and if dissociation is a first-order process (eq 3)



and hapten is present in excess, then

$$\begin{aligned} R &= -k_{-1}([\text{Ab-H}] + [\text{Ab-H}^*]) \\ &= -k_{-1}[\text{Ab}]_{\text{tot}} \end{aligned}$$

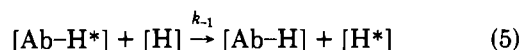
Hence

$$\ln(1-x) = \frac{-k_{-1}}{[\text{H}]_{\text{tot}}} ([\text{H}]_{\text{tot}} + [\text{Ab}]_{\text{tot}})t$$

Experimental conditions have been arranged so that $[\text{Ab}]_{\text{tot}}$ is much less than $[\text{H}]_{\text{tot}}$, so

$$\ln(1-x) = -k_{-1}t \quad (4)$$

If dissociation were a different process, e.g. bimolecular (eq 5)



but with other experimental conditions the same, then

$$R = -k_{-1}[\text{Ab}]_{\text{tot}}[\text{H}]_{\text{tot}}$$

and

$$\ln(1-x) = -k_{-1}[\text{H}]_{\text{tot}}t \quad (6)$$

Hence, dependence of the observed rate constant on $[\text{H}]_{\text{tot}}$ distinguishes the dissociation mechanisms.

Two simultaneous first-order processes leading to indistinguishable products can be described (22) by equation 7:

$$1-x = A[f \exp(-k_{-1}t) + (1-f) \exp(-k_{-2}t)] \quad (7)$$

where A is the fraction of isotope originally bound to antibody (approximately 1), f is the fraction of complex dissociating with rate constant k_{-1} , and $(1-f)$ is the fraction of complex dissociating with rate constant k_{-2} .

Assay Method. Hapten-antibody dissociation rates were determined by measuring the quantity of $^{111}\text{In}^{3+}$ chelate released from the antibody-hapten complex as a function of time after addition of a 100-fold excess (over antibody binding sites) of unlabeled hapten. Thus, for each hapten, a set of 700- μL reaction solutions were prepared containing (1) antibody at a concentration of 160 nM, (2) indium-loaded hapten, trace labeled with ^{111}In (total concentration = 160 nM), (3) normal serum albumin at a total concentration of 1.5 mg/mL, and (4) isotonic phosphate-buffered saline, pH 7.4. At time T_0 indium-loaded, unlabeled hapten was added to a final concentration of 32 μM . Reactions were stirred by placing the sample containers in a rack mounted on a vortexer head.

At various times after addition of the excess hapten, 400- μL portions of the reaction solutions were transferred to Centrifree tubes and centrifuged at 100g for 8–10 min. The reaction time was taken to be the time between addition of the excess hapten and the time the centrifuge reached

the desired velocity.¹ Six time points, each in duplicate, were obtained over a range of about two reaction half-lives for each rate constant determination. A 200- μ L portion from each centrifuged and uncentrifuged solution was then counted for ¹¹¹In. The relative concentration of free hapten was taken to be the ratio of counts in the centrifuged solution (filtered) to the uncentrifuged solution at each time point. Times were recorded to the nearest 1/10 min.

Room temperature rate constants were measured at ambient temperature, which remained at 22 \pm 1 $^{\circ}$ C. Rate constants at 4 $^{\circ}$ C (or 5 $^{\circ}$ C) were measured in a refrigerated room. The rate constant at 0 $^{\circ}$ C was measured in an ice-water bath in a refrigerated room. Rate constants above room temperature were measured in a water bath controlled to \pm 1 $^{\circ}$ C. Stirring was maintained throughout the reactions.

Rate constants and standard deviations for the mono-exponential dissociations were obtained from a plot of the logarithm of the relative complex concentration (e.g. $1 - x$ in eq 4) vs time. These data were analyzed by using the linear-regression module of the RS/3 program (BBN Software Products Corp.). Biexponential data were fit to eq 7, with uniform weighting of each time point, using the RS/3 program. (For the purposes of curve-fitting, duplicates were averaged before being plotted.)

Control samples were included in each experiment to determine (A) that the initial condition of 100% of labeled hapten bound to antibody was met and (B) that in the absence of antibody, 100% of the counts were able to penetrate the Centrifree membrane.

If control A showed that a significant portion of the counts did not bind to antibody initially, the average number of counts in the control duplicates was subtracted from all centrifuged and uncentrifuged sample solutions. If control B showed that not all of the counts penetrated the membrane, each count ratio (i.e., the relative concentration of free hapten) was divided by the average of the fraction penetrating the membrane in the control duplicates.

RESULTS

Dissociation rates were calculated from linear first-order plots (Figure 1) for a series of benzyl-EDTA derivatives para-substituted with nitro, amino, thiourea, or acetamide functional groups (Table I). (Compounds 3 and 4 are intermediates in the synthesis of other haptens, and their dissociation rates were not measured.) The room temperature rate constants show that modification of the hapten at the para position does have a sizable effect on the dissociation rate, and that the method used is capable of distinguishing between very similar haptens. For example, the difference in dissociation rate between benzyl- and phenyl-substituted thiourea derivatives (11 and 12) is considerable. Also, the dissociation rates for the series of alkyl carboxylates 13–15 are strikingly different.

Statistical treatment of the errors for the room temperature half-life determinations shows that the average relative error for the method is $2.4 \pm 1.2\%$. Precise

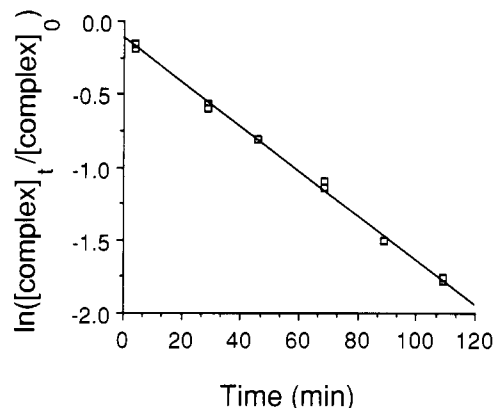


Figure 1. First-order plot of the dissociation of compound 17 from CHA255 at 22 $^{\circ}$ C.

determinations were obtained for reactions with half-lives as short as 5.5 min and as long as 1400 min.

The reaction rate shows no direct dependence on the concentration of excess hapten (Table II), indicating that the dissociation is a first-order process.

The temperature dependence of the dissociation rate for compounds 14, 17, 18, and 20 follows the expected Arrhenius relationship (Table III) and is experimentally identical for the four compounds. Hapten derivatives for which rate constants are available at only two temperatures (7, Table I) show a similar variation with temperature. This trend suggests that hapten derivative 22, which gave a biexponential dissociation plot at 22 $^{\circ}$ C, binds much more tightly than the other hapten derivatives.

Only a minor dependence of the dissociation rate of 20 on ionic strength could be detected (Table IV). A strong dependence was expected, given the charge and multiplicity of sites available for hydrogen bonding in this set of hapten derivatives. Decreasing the surface tension by including an organic cosolvent increased the dissociation rate by a factor of 2.

In contrast to the ionic-strength dependence, the dissociation rates of 20 and 13 show dramatic and different pH profiles (Figure 2), which suggest the involvement of several ionizable residues.

Compounds 10 and 22 reproducibly exhibited dissociation rate plots fit by biexponential curves at 22 $^{\circ}$ C (e.g., Figure 3). Compound 10 bound to albumin under the conditions of the standard method but gave a biexponential plot when albumin was omitted from the procedure.² Compound 7 also exhibited a biexponential plot at 5 $^{\circ}$ C. For compounds 7 and 22, the biexponential curvature occurred at temperatures at which the dissociation was very slow, and the plots became monoexponential at higher temperature. However, not all haptens gave biexponential plots under conditions of slow dissociation. Also, for compound 10, the biexponential curvature was observed when the dissociation rate was in the range of the other haptens measured. Its behavior was not explored at higher temperature.

DISCUSSION

The dissociation rate constants for para-substituted derivatives in In^{3+} -benzyl-EDTA vary over an unexpect-

¹ Since the separation is not instantaneous, the choice of what point in the process to use for the time values is somewhat arbitrary. Fortunately, the slope of the first-order dissociation rate plot (and the $t_{1/2}$) is dependent only on the interval between measurements so that, as long as the separations all require the same amount of time, any point in the process can serve to identify a measurement time.

² A control experiment was performed in which a mixture of labeled and cold hapten, at the concentration used in the standard assay but in the absence of antibody and albumin, were filtered in the Centrifree apparatus. Approximately 94% of the label penetrated the membrane in multiple experiments, showing that compound 10 does not bind to container surfaces to an extent that interferes with the assay.

Table I. Hapten Derivative Dissociation Rate Data

no.	structure	$t_{1/2},^a$ min (σ)		
		38 °C	22 °C	5 °C
p -R ₁ R ₂ NC ₆ H ₄ CH ₂ -EDTA-In				
1 ^b	R ₁ = R ₂ = H		13.0	
2	R ₁ = R ₂ = O		8.1 (1.5)	
3 ^c	R ₁ ,R ₂ = CS			
XCH ₂ CONHC ₆ H ₄ CH ₂ -EDTA-In				
4	X = Br ^e			
5	X = S(CH ₂) ₄ SCH ₂ CONH- p -C ₆ H ₄ CH ₂ -DTPA		50.3 (0.7)	
6	X = S(CH ₂) ₄ S-Co-bleomycin		51.3 (1.7)	
YNHCSNHC ₆ H ₄ CH ₂ -EDTA-In				
7	Y = H	9.7 (1.3)	84.2 (2.5)	
8	Y = Et		72.6 (1.3)	
9	Y = n -Bu		90.6 (2.0)	
10 ^d	Y = n -Oct			
11	Y = Ph		78.0 (0.8)	
12	Y = CH ₂ C ₆ H ₄		94.2 (3.0)	
13 ^e	Y = CH ₂ CO ₂ H		49.7 (2.5)	
14	Y = (CH ₂) ₂ CO ₂ H	11.6 (0.2)	87.8 (2.6)	1181 (32)
15	Y = (CH ₂) ₃ CO ₂ H		74.3 (1.8)	
16	Y = p -C ₆ H ₄ CH ₂ CO ₂ H		71.5 (0.8)	
17	Y = (CH ₂) ₂ NH ₂	5.5 (0.2) ^f	45.6 (0.8)	611 (16) ^g
18	Y = (CH ₂) ₂ NHCO(CH ₂) ₃ CO ₂ H	14.3 (0.3)	98.8 (1.2)	1446 (21)
19	Y = (CH ₂) ₄ C(NHCOCH ₃)HCONH ₂		90.9 (1.2)	
20	Y = (CH ₂) ₂ OH	8.8 (0.2)	59.7 (1.5)	749 (11)
21	Y = p -C ₆ H ₄ CH ₂ -DTPA	22.9 (0.8)		
22	Y = N1A-mitomycin C	40.9 (0.8) ^f		

^a Correlation coefficients were between -0.993 and -0.999, except for 2, $r = -0.978$, and 17, 0 °C, $r = -0.983$. ^b Half-life estimated from only two time points. ^c Compounds 3 and 4 are intermediates in the synthesis of the other hapten derivatives; their half-lives were not measured. ^d Compound 10 bound to albumin under standard conditions and gave a nonlinear first-order plot when albumin was omitted. ^e Values are an average of four determinations. ^f Actually 37 °C. ^g Actually 4 °C.

Table II. 22 °C Dissociation Half-Life of 20 as a Function of Excess Hapten Level

excess unlabeled hapten/Ab binding site, mol/mol	$t_{1/2}$, min	σ
20	57.8	1.3
100	56.2	2.1
100	58.9	1.1
1000	50.9	1.1

Table III. Activation Parameters for Selected Haptens

hapten	H^* , kcal/mol	σ	S^* , eu	σ	$-r$
14	22.9	0.9	1.2	1.6	0.999
17	22.7	0.8	2.4	1.4	0.999
18	23.5	1.0	2.9	3.6	0.999
20	22.6	0.7	0.4	1.2	0.999

Table IV. 22 °C Dissociation Half-Life of Compound 20 as a Function of Solvent

relative ionic strength	% dioxane	pH	$t_{1/2}$, min	σ	$-r$
1 ^a	0	7.4	59.7	1.5	0.997
5	0	7.5	46.2	1.5	0.995
10	0	7.5	52.4	1.2	0.997
1	20	7.5	24.7	1.9	0.978

^a 1 = 150 mM NaCl, 15 mM NaPO₄.

edly wide range. Determination of these rate constants proved to be convenient and precise. Consequently, measurement of the dissociation rate constant is a very sensitive method of detecting a change in antibody binding. As such, it may be useful for detecting chemical modification or site-specific mutation of antibodies, for predicting behavior of various in vitro or in vivo systems, or for screening new antibodies or haptens.

First-order dissociation rate plots for the exchange reaction could be obtained either from the unimolecular dissociation mechanism of eq 3 or from the bimolecular reaction of eq 5. That eq 5 is not the observed reaction (i.e., that dissociation of the antibody-hapten complex is

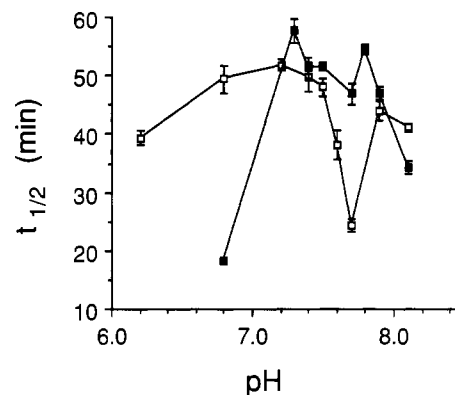


Figure 2. Dissociation half-life of compounds 13, open squares, and 20, filled squares, at 22 °C as a function of pH. Error bars indicate standard deviation of a single determination, except for 13 at pH 7.4 (which represents four determinations) and pH 7.5 and 7.7 (which each represent duplicate determinations) and 20 at pH 6.8 (duplicate determinations) and 7.5 (seven determinations). (The value of the dissociation rate constant at pH 7.7 for 13 was unexpectedly low. It was repeated, and a value at pH 7.6 obtained under identical conditions confirmed the trend.)

a unimolecular process) was shown by performing the assay at three levels of unlabeled hapten. Since k_{obsd} is the same in the three cases (Table III), the reaction is not pseudo-first-order and the data fit the mechanism of eq 3.

The data reveal several interesting facets of the relationship between the hapten and the antibody binding site. Since the original immunogen was a conjugate of 3 with keyhole limpet hemocyanin, the resultant antibody is expected to have the tightest binding to, and the slowest dissociation from, haptens that contain a thioacyl substituent in the para position. Further, according to Hansch and co-workers (13, 14), additional steric bulk in the para position should lead to tighter antibody binding. Clearly, interaction occurs at the para substituent in the

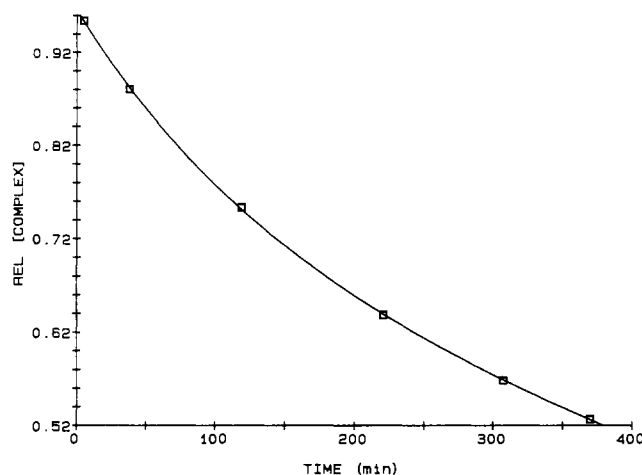


Figure 3. Dissociation plot for Compound 22 at 22 °C overlaid with biexponential curve of formula in eq 7. Compound 7 also exhibited a biexponential plot at 5 °C. For compounds 7 and 22, the biexponential curvature occurred at temperatures at which the dissociation was very slow, and the plots became monoexponential at higher temperature. However, not all haptens gave biexponential plots under conditions of slow dissociation. Also, for compound 10, the biexponential curvature was observed when the dissociation rate was in the range of the other haptens measured. Its behavior was not explored at higher temperature.

current instance. The para substituents of 1 and 2 (NO_2 and NH_2 , respectively), for example, have different electronic effects and opposite contributions to the binding interactions of the aromatic ring, but both haptens dissociate rapidly relative to other haptens that have either an acyl or a thioacyl substituent on the nitrogen. Hence, the thioacyl substituent present in the immunogen does contribute to the CHA255 binding. Also, the two acetamides tested dissociate faster than almost all the thioureas, suggesting that there is some specificity in the antibody recognition of the thiourea functionality.

On the other hand, the antibody binding site apparently does not specifically recognize substituents five carbons removed from the thiourea functionality of haptens 7–22. Compound 19 was prepared to resemble as closely as possible the original CHA255 immunogen. The α -N-acetyl substituent and the amide derivative of the carboxyl group of 19 mimic the backbone of the immunogen carrier protein, yet the dissociation rate for 19 is as fast or faster than several haptens that have much different functionality. For example, compound 9, with only a hydrocarbon substituent, has no functionality available for binding other than hydrophobic interactions but has the same dissociation rate as 19. An explanation for this observation may be that the binding site for the original immunogen surrounds and includes that which is involved with hapten binding but that it does not extend into the backbone of the immunizing carrier protein.

Another discernible relationship between hapten and binding site involves charged residues. Comparison of half-lives for 14 and 17, which put opposite charges at approximately the same location, suggest that this region of the binding site contains a positive charge. Neutralization of the positive charge on 17 by acylation (18) gives a much slower dissociation rate. Placing the negative charge further from the thiourea, as in compounds 15 and 16, essentially neutralizes the interaction (compound 15 vs compound 8). Placing the negative charge closer to the thiourea (13) may interfere with recognition of the thiourea itself. It is possible that the relatively rapid dissociation of 20 is due to unfavorable interaction of the hydroxyl proton with the positively charged amino acid residue.

Table V. Curve-Fit Parameters for the Biexponential Dissociation Reaction of Eq 7

no.	A	f	$t_{1/2}, 1^a$	$t_{1/2}, 2^a$	$\sum \chi^2/\text{parameters}$
7 ^b	0.929 (0.005) ^c	0.10 (0.02)	76 (24)	952 (30)	0.84
10	0.899 (0.014)	0.30 (0.02)	9.5 (1.3)	113 (7)	0.44
22	0.966 (0.003)	0.19 (0.05)	81 (19)	624 (79)	0.81

^a Rate constants k_{-1} and k_{-2} , respectively, expressed as half-lives, in minutes. ^b Compound 7 data were collected at 4 °C; data for compounds 10 and 22 were collected at 22 °C. ^c Numbers in parentheses are standard errors for each parameter.

The nature of the charge environment in the CHA255 binding site is not clarified by the pH dependence of the dissociation half-life (Figure 2). The effect of pH over the relatively narrow range from 6.2 to 8.1 is strong and unexpectedly complex. It suggests that at least three amino acid residues, which change ionization state in the pH range 6–8, are significantly involved in binding 13. (Compounds 13 and 20 do not change ionization state in this pH range.)

The importance of hydrophobic interactions and steric crowding in hapten–CHA255 binding are difficult to identify. Comparison of the half-lives for 11 and 12 suggests that steric repulsion in the region close to the thiourea has a noticeable effect on the rate, but both 21 and 22 are bulky in this region yet exhibit very slow dissociation at room temperature (see below). It is likely that steric effects that are present are manifest weakly, if at all, in dissociation rates, since once a ligand is bound, steric interactions could either hasten or hinder its dissociation if conformational changes in the binding site must be reversed for dissociation to occur. Nonetheless, 22 appears to exhibit both the slowest dissociation and the highest affinity (data not shown) even though it is highly sterically crowded in the area close to the thiourea, which is clearly involved in binding.

In an effort to determine which forces (4) are primarily responsible for the slow dissociation (high affinity) of CHA255 and indium–benzyl–EDTA's, half-life measurements were performed for compound 20 at three levels of ionic strength and in the presence of a solvent which lowers surface tension (Table IV). That ionic strength variation causes no variation in dissociation rate is surprising since the pH profile implicates charged residues in binding. The involvement of van der Waal's forces in binding is reflected in the decrease in dissociation half-life in the presence of dioxane. However, this does not provide a complete explanation for the affinity (19) of the antibody for this set of haptens.

Measurement of the dissociation rate constants for selected haptens at different temperatures (Tables IV and V) shows that even though the rates themselves vary significantly (as a function of hapten structure), the temperature dependence of the rate constants is remarkably similar. The activation enthalpies and entropies of the four compounds are experimentally identical, despite opposite para-substituent charges (14, 17) and vastly different room temperature rate constants (14, 18, 20).³ The temperature dependence of the rate constants for 7 appears to parallel 18, 14, 20, and 17.

The temperature dependence of antibody dissociation rate constants is infrequently explicitly measured. The

³ The fact that the rate constants are clearly distinguishable while the activation parameters are experimentally identical points out the precision with which rate constants can be measured. The interpretation must be that the activation enthalpies and entropies are not identical, but the differences are too small to be easily measurable. This is clearly shown in a comparison of the standard error for the rate constants and the activation parameters.

activation enthalpies measured in this system (~ 23 kcal/mol) are higher than those reported by Pontarotti et al. (~ 16.1 and 18.7 kcal/mol; ref 7) for a series of anti-vinca antibodies by about 5 kcal/mol. The negligible activation entropy (Table III) may result from a combination of large opposite terms or may simply suggest that the constraint in the transition state resembles that in the fully bound complex. It does, however, argue against the requirement for major antibody conformational changes in the dissociation reaction.

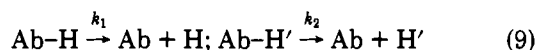
Nonlinear first-order dissociation rate plots for certain haptens were disconcerting when first encountered, despite a report of a similar finding in kinetic investigation of antibody binding to cellular antigens (6). Prolonged preincubation of the complex did not produce linear first-order plots, eliminating the possibility that the "secondary binding" phenomenon (4) reported for polyclonal interactions was responsible. We also increased the buffer ionic strength to test the possibility that nonspecific hydrophobic interactions were responsible, but we saw no change. Eliminating albumin from the assay made no change, and using a larger concentration of excess unlabeled hapten also did not produce linear first-order dissociation rate plots.

Curve fits were attempted with several different functions. The best fits were of biexponential form (eq 7). The best fit parameters with their standard errors, for the three observed cases, are listed in Table V. Fits that were of statistically equivalent quality were obtained with a monoexponential function of the form of eq 8. However,

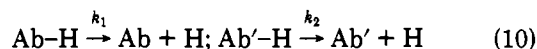
$$1 - x = Ae^{-kt} + B \quad (8)$$

the values of A and B required by this fit imply that close to 50% of the hapten becomes irreversibly bound to the antibody. While a covalent reaction may be conceivable for 22, it is certainly unlikely for 10 and 7. Furthermore, if such a reaction did occur, it would be very difficult to explain the return to simple first-order dissociation at higher temperature (for 7 and 22). While the relative standard error for the curve-fit parameters is large, each case suggests a minor fast-dissociating component and a major slow-dissociating component. The ratio of the rate constants of fast-/slow-dissociating components is constant within experimental error, for the three cases.

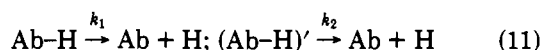
The fact that these dissociations were fit by biexponential curves offers the explanation that two simultaneous first-order dissociations contribute to the observed dissociation (see the Experimental Procedures). This circumstance would occur if (1) the hapten were impure, so that two different labeled haptens dissociated with different rate constants (eq 9), (2) two slightly different



forms of antibody binding site released the hapten with different rate constants (eq 10), or (3) two conformations

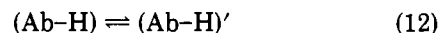


of the antibody-hapten complex dissociated at different rates (eq 11). The first of these possibilities is excluded



by analytical data. The second possibility cannot be eliminated but seems unlikely since such a small percentage of the conditions tested (hapten derivatives \times temperature)

exhibited the phenomenon. The most likely explanation, that two forms of complex exist for these particular hapten derivatives, also offers a potential explanation for the fact that the dissociations become first-order at higher temperature: if the two conformations are in equilibrium (eq 12), with the proper kinetic barrier to interconver-



sion, then at low temperature independent dissociation of the two forms should be observed, whereas at higher temperature, rapid equilibration between the two forms should lead to dissociation of an "average" form. However, there is no direct evidence for the two-conformation model, and there is no clear rationalization for the fact that only these particular hapten derivatives bind in more than one conformation.

A hybrid bifunctional antibody has been prepared that recognizes the benzyl-EDTA hapten with one binding site and the tumor-associated antigen CEA with the other binding site. We have found that this antibody causes hapten derivatives to accumulate at CEA-bearing tumor sites (3). To show whether the hapten binding site of the bifunctional antibody is different from that of its parent, CHA255, the dissociation rate constant for compound 17 was measured with the bifunctional antibody. The room temperature complex dissociation half-life with the bifunctional antibody is 49.6 ± 1.3 min, which is close to the value with the parent antibody (45.6 ± 0.8 min). This result confirms that the binding sites are identical. Thus, measurement of a dissociation rate constant with the parent antibody appears to yield a value that is representative of the bifunctional antibody.

We have found that the dissociation rate constant is useful for comparing small changes in the interaction between a monoclonal antibody and a hapten. Although the rate constants cannot be directly related to affinity constants, the convenience and precision with which rate constants can be measured, as described in this paper, makes them attractive indicators of the interaction between haptens and antibodies. Also, when considering the behavior of a formed hapten-antibody complex under conditions of infinite dilution (e.g., in vivo), the dissociation rate constant assumes importance independent of affinity.

Interpreting these relative half-lives based on the generalization (4) that dissociation rates are inversely correlated with affinities, we conclude that there is a positive charge in a certain location of the binding site, and that van der Waal's forces are more important than ionic forces in binding hapten and antibody. In addition, questions have emerged about the observed pH dependence and the small amount of binding energy that could be accounted for by tests for ionic and van der Waals's contribution and by the biexponential rate plots for particular hapten derivatives. To test these conclusions and answer these questions, the structure of the antibody binding site is being investigated through X-ray crystal-structure analysis of the complex of CHA255 F(ab)' with selected hapten derivatives.

ACKNOWLEDGMENT

We would like to acknowledge contributions to this work made by S. Christensen, who performed several of the rate determinations and helped with the development of the procedure, and T. Battersby and L. Anderson, who prepared many of the haptens and performed some of the radiolabeling. Also, M. Pellegrino, C. Ahlem, P. Sundstrom, and W. Butler provided helpful discussion and criticism of the manuscript.

LITERATURE CITED

- (1) Frincke, J. M., Unger, B. W., Burnett, K., Hersh, E., Rosenblum, M., and Gutterman, G. (1984) Antibody Compositions of Therapeutic Agents and Extended Serum Half-life, U.S. Pat. Ser. No. 732, 154.
- (2) Frincke, J. M., David, G. S., Bartholomew, R. M., and Meyer, D. L. (1986) Antibody Complexes of Hapten-Modified Diagnostic or Therapeutic Agents, U.S. Pat. Ser. No. 906, 728.
- (3) Anderson, L. D., Meyer, D. L., Battersby, T. R., Frincke, J. M., Mackensen, D., Lowe, S., and Connolly, P. (1988) Optimization of Ligand Structure for Imaging with a Bifunctional Antibody. *J. Nucl. Med.* 29, 835.
- (4) Absolom, D. R., and van Oss, C. J. (1987) The Nature of the Antigen-Antibody Bond and the Factors Affecting its Association and Dissociation. *CRC Crit. Rev. Immunol.* 6, 1-46.
- (5) Birnbaum, D., and Kourilsky, F. M. (1981) Differences in the Cell Binding Affinity of a Cross-Reactive Monoclonal Anti-Ia Alloantibody in Mice of Different H-2 Haplotypes. *Eur. J. Immunol.* 11, 734-738.
- (6) Mason, D. W., and Williams, A. F. (1980) The Kinetics of Antibody Binding to Membrane Antigens in Solution and at the Cell Surface. *Biochem. J.* 187, 1-20.
- (7) Pontarotti, P. A., Rahmani, R., Martin, M., and Barbet, J. (1985) Monoclonal Antibodies to Antitumor *Vinca* Alkaloids: Thermodynamics and Kinetics. *Mol. Immunol.* 22, 277-284.
- (8) Barbet, J., Rougon-Rapuzzi, G., Cupo, A., and Delaage, M. A. (1981) Structural Requirements for Recognition of Vasopressin by Antibody; Thermodynamics and Kinetic Characteristics of the Interaction. *Mol. Immunol.* 18, 439-446.
- (9) Denizot, F. C., Hirn, M. H., and Delaage, M. A. (1979) Relationship Between Affinity and Kinetics in a Hapten-Antibody Reaction. Studies on Anti-Cyclic ATP Antibodies. *Mol. Immunol.* 16, 509-513.
- (10) Hornick, C. L., and Karush, F. (1972) Antibody Affinity-III. The Role of Multivalence. *Immunochemistry* 9, 325-340.
- (11) Eisen, H. A. (1974) *Immunology. An Introduction to the Molecular and Cellular Principles of the Immune Response*, pp 365, 366, Harper and Row Publishers, Incorporated, Hagerstown, MD.
- (12) Froese, A. (1968) *Immunochemistry* 5, 253-264.
- (13) Kutter, E., and Hansch, C. (1969) The Use of Substituent Constants in the Quantitative Treatment of Hapten-Antibody Interaction. *Arch. Biochem. Biophys.* 135, 126-135.
- (14) Hansch, C., and Moser, P. (1978) Structure-Activity Relationships in Immunochemistry—The Interaction of Phenylsuccinates and Pyridine Haptens with Anti-3-Azopyridine Antibody. *Immunochemistry* 15, 535-540.
- (15) Hansch, C., Yoshimoto, M., and Doll, M. H. (1976) Structure-Activity Relationships in Immunochemistry. 4. Inhibition of Complement by Benzylpyridinium Ions. On the Predictive Value of Correlation Equations. *J. Med. Chem.* 19, 1089-1093.
- (16) Yoshimoto, M., Hansch, C., and Jow, P. Y. C. (1975) Structure Activity Relationships in Immunochemistry. III. Inhibition of Complement by Benzyl Pyridinium Ions. *Chem. Pharm. Bull.* 23, 437-444.
- (17) Goodwin, D. A., Meares, C. F., David, G. F., McTigue, M., McCall, M. J., Frincke, J. M., Stone, M. R., Bartholomew, R. M., and Leung, J. P. (1986) Monoclonal Antibodies as Reversible Equilibrium Carriers of Radiopharmaceuticals. *Nucl. Med. Biol.* 13, 383-391.
- (18) Meares, C. F., McCall, M. J., Reardan, D. J., Goodwin, D. A., Diamanti, C. I., and McTigue, M. (1984) Conjugation of Antibodies with Bifunctional Chelating Agents: Isothiocyanate and Bromoacetamide Reagents, Methods of Analysis and Subsequent Addition of Metal Ions. *Anal. Biochem.* 142, 68-78.
- (19) Reardan, D. J., Meares, C. F., Goodwin, D. A., McTigue, M., David, G. S., Stone, M. R., Leung, J. P., Bartholomew, R. M., and Frincke, J. M. (1985) Antibodies Against Metal Chelates. *Nature* 316, 265-267.
- (20) DeRiemer, L. H., Meares, C. F., Goodwin, D. A., and Diamanti, C. I. (1981) Bledta II: Synthesis of a New Tumor Visualizing Derivative of Co(III)-Bleomycin. *J. Labelled Compd. Radiopharm.* 18, 1517-1534.
- (21) Moore, J. W., and Pearson, R. G. (1981) *Kinetics and Mechanism*, 3rd ed., pp 311-313, John Wiley and Sons, New York.
- (22) See ref 21, pp 286-288.

A Conjugate of 5-Fluorouridine-Poly(L-lysine) and an Antibody Reactive with Human Colon Carcinoma

E. Hurwitz,*† I. Stancovski,† M. Wilchek,† D. Shouval,§ H. Takahashi,|| J. R. Wands,|| and M. Sela†

Departments of Chemical Immunology and Biophysics, The Weizmann Institute of Science, Rehovot 76100, Israel, Liver Unit, Department of Medicine, A. Hadassa University Hospital, Jerusalem 91120, Israel, and Molecular Hepatology Center, Massachusetts General Hospital, Boston, Massachusetts 02114. Received March 13, 1990

The ribose moiety of 5-fluorouridine (FUR) was oxidized with periodate and the product was bound through a poly(L-lysine) bridge to monoclonal antibodies, denoted SF25MAb, reactive with a human colon carcinoma LS180. The antibody was linked via its polysaccharide (previously oxidized with periodate) to the poly(L-lysine)-drug conjugate. The linking of FUR-poly(L-lysine) to the antibody markedly increased the latter's binding to the tumor cells. A relatively lower increase was also observed with conjugates of nonrelated antibodies, such as anti-hepatitis B surface antigen and anti-epidermal growth factor receptor antibodies. The pharmacological activity of the specific conjugate FUR-poly(L-lysine)-SF25MAb was higher than that of the drug-substituted polymer alone. The poly(L-lysine) bridge caused toxic effects *in vivo*, even though substituted both by FUR and by antibody. Therefore, the additional unreacted lysyl residues were blocked by succinylation. Partial blocking of free amino groups on the conjugate rendered it nontoxic but decreased its cell-binding capacity, though to a level still higher than that of the original unmodified antibody. The pharmacological activity of the specific conjugate after blocking was also reduced and necessitated prolonged incubation periods or higher concentrations. Following periodate oxidation and reduction, FUR was as effective as the clinically preferred compound 5-fluoro-2'-deoxyuridine *in vitro* and *in vivo*, against the LS180 colon carcinoma. Experiments in nude mice, with LS180 tumor subcutaneous xenotransplants, showed that FUR-poly(L-lysine)-SF25MAb (blocked by succinylation) was not toxic and was effective in the retardation of tumor growth. In a metastatic form of the colon carcinoma, the conjugate caused a marginal delay in the median survival time as well as the prevention of the development of metastases in a small but consistent number of mice. Intraperitoneal injection of the specific conjugate (unblocked by succinylation) was not toxic but was also not effective. The drug-substituted polymer (without the antibody) was not therapeutically effective in the succinylated form. However, in the unblocked form, it diminished the size of an already existing tumor when injected directly into the tumor site.

INTRODUCTION

Fluorinated derivatives of uracil, such as 5-fluorouracil (FU) and 5-fluoro-2'-deoxyuridine (FUDR), are clinically employed against various tumors, particularly against those of the gastrointestinal tract. The ribosylated derivative of FU, 5-fluorouridine (FUR), is not in use primarily because of its greater toxicity (1, 2).

We have previously demonstrated the binding of periodate-oxidized FUR through a dextran-hydrazone bridge to a murine antibody directed against an experimental B cell lymphoma (3). In the following study we have employed the same drug derivative, periodate-oxidized FUR, conjugating it to a monoclonal antibody directed against a human colon carcinoma. The conjugation was performed via a poly(L-lysine) (pLys) bridge. pLys was extensively employed as a carrier for a variety of anticancer drugs, such as methotrexate (4), adriamycin, daunomycin, 6-aminonicotinamide (5, 6), and a derivative of FUDR (7). It was shown to increase the uptake of the drugs into tumor cells even in cases in which such entry was barred, thereby turning drug-resistant cells to

susceptible ones (4). In addition, pLys was found to be effective by itself against certain tumors and was demonstrated to be an anticancer agent when used below its general cytotoxic range (5). The monoclonal antibody SF25MAb, which was originally prepared against a human hepatoma (FOCUS), binds to a unique antigen expressed on LS180 colon adenocarcinoma cells. The antibody was capable of concentrating at the tumor site transplanted into nude mice (9). The pharmacological activity of the conjugate, as shown by its cytotoxicity to the human colon carcinoma cells, is maintained. The antibody-specific binding of the conjugate to the relevant tumor cells is markedly increased. Polymers of L-lysine were shown to cause mortality upon *in vivo* administration (5, 10), which could be prevented by complexing them with heparin (10, 11). In the following studies FUR-pLys derivatives were not toxic when injected intraperitoneally or subcutaneously. Intravenous administration of the conjugates caused mortality which was prevented by blocking the conjugates by succinylation. The *in vivo* effectivity of FUR-pLys-SF25MAb was tested against LS180 colon carcinoma transplants in nude mice.

EXPERIMENTAL PROCEDURES

The monoclonal antibody (MAb) reactive with colon and hepatocarcinomas, SF25MAb (IgG 1), was previously described (8, 9). The immunoglobulin was obtained from the ascitic fluid of hybridoma-bearing mice by affinity chro-

* Department of Chemical Immunology, The Weizmann Institute of Science.

† Department of Biophysics, The Weizmann Institute of Science.

§ Department of Medicine, A. Hadassa University Hospital.

|| Massachusetts General Hospital.

matography on protein A-Sepharose CL-4B (Pharmacia, Uppsala, Sweden) or by precipitation with $(\text{NH}_4)_2\text{SO}_4$ at 45% saturation.

Tumor Line. LS180, a human adenocarcinoma, was obtained from the American Type Culture Collection (Rockville, MD). The cells were maintained in culture in Earl's Modified Eagle's Medium (Gibco, Grand Island, NY) supplemented with 10% fetal calf serum (inactivated at 56 °C). The cells were harvested from the monolayer by incubation in a mixture of 0.17% trypsin and 0.07% versane for 45–60 min (in order to obtain single cell suspensions).

Oxidation of 5-Fluorouridine. 5-Fluorouridine (FUR) (Sigma, St. Louis, MO) was oxidized as previously described (3) with some modifications. Half the equimolar amounts of sodium metaperiodate (Merck, Darmstadt, West Germany) were added to FUR at a final concentration of 0.05 M in 0.1 M sodium acetate buffer at pH 5.5. The mixture was kept in the dark for 4 h at 4 °C. The oxidized compound was lyophilized and then extracted with methanol. Residual NaIO_3 and other salts were insoluble in the solvent and the nucleotide was separated in the methanolic fraction which was then evaporated to dryness. $[5\text{-}^3\text{H}]\text{Uridine}$ (25 Ci/mmol, Amersham Buckinghamshire, England) was oxidized along with FUR in order to serve as a marker. The oxidized product was identified by thin-layer chromatography in silica gel 60 F254 (Merck, Darmstadt, West Germany) in ethyl acetate/methanol at a ratio of 2:1. The R_f of FUR was 0.68, while that of oxidized FUR (FUR(oxi)) was 0.8. FUR(oxi) was reduced, for some of the experiments, by the addition of equimolar amounts of NaBH_4 at a final concentration of 0.03 M. The reduced product was designated FUR(oxi-red).

Binding of FUR(oxi) to Poly(L-lysine). Poly(L-lysine) (pLys) [MW 12 000 (90-mer polymerization degree, synthesized at the Weizmann Institute, Rehovot, Israel), 100 mg] was dissolved in 6 mL of 0.07 M sodium carbonate buffer at pH 9.5 and mixed with 80 mg of FUR(oxi) in a volume of 2 mL of water. The mixture was left at 4 °C for 72 h. The product was reduced by NaCNBH_3 (0.9 mL of 10 mg/mL in water) in 1 h at 37 °C. Unbound FUR(oxi) was removed by dialysis against water. The degree of substitution of FUR(oxi) on pLys was 6–11 mol/mol drug to polymer.

Binding of FUR-pLys to SF25MAb Antibody. The polymer binding to the antibody was performed as previously described (12, 13). Briefly, antibody at a concentration of 5 mg/mL was reacted for 1 h with 10 mM NaIO_4 in 0.1 M acetate buffer at pH 5.5. The oxidation was terminated by dialysis against phosphate buffer saline (0.15 M NaCl, 0.01 M phosphate buffer, at pH 7.2, PBS). The oxidized SF25MAb antibody was diluted to a concentration of 0.9 mg/mL with 0.2 M acetate buffer at pH 5.5 in 0.15 M NaCl and mixed into a volume of FUR-pLys which contained an excess of 10–20 mol of pLys over 1 mol of antibody. After 72 h at 4 °C, the product was subjected to fractionation on Sephadex G-100 in order to separate any unbound FUR-pLys and FUR from the antibody-conjugated polymer (^{125}I -labeled antibody, $[^3\text{H}]\text{-FUR-pLys}$, and $[^3\text{H}]\text{FUR}$ were each applied separately for the calibration of the column). Between 67 and 78% of the FUR-pLys was conjugated to the antibody in different preparations. The antibody content in each preparation was determined by the Bradford colorimetric assay (Bio-Rad, Richmond, CA) and the FUR bound was determined by its radioactive label.

Succinylation of the FUR-pLys and FUR-pLys-

SF25MAb. In order to prevent the in vivo toxicity of the pLys derivatives (lethal when injected intravenously), a partial succinylation of the compounds was performed. Succinic anhydride (25 mg, 0.25 mmol) was dissolved in 1 mL of dimethyl sulfoxide and added in small aliquots to FUR-pLys or FUR-pLys-SF25MAb (0.11 mmol of pLys) solutions, in a total volume of 12 mL. The solution was maintained at pH 8–9 (by sodium carbonate buffer at pH 9.5 at a final buffer concentration of 0.05–0.1 M). The extent of the succinylation was aimed at blocking 40–50% of the free amino groups in the pLys (calculated according to the total amount of pLys in the conjugate).

Binding of Antibody and Its Conjugates to LS180 Cells. The binding of the SF25 MAb was assayed indirectly with ^{125}I -labeled goat antimouse immunoglobulin (Ig). The iodination was performed with Iodo Beads (Pierce, Rockford, IL) according to the manufacturer's instructions. Antibody binding was tested either on live LS180 cells in 24-well plates (Nunc, Kamstrup, Denmark) ($0.5\text{--}1 \times 10^5$ cells/well, 48 h after plating) or on 0.15% formalin-fixed cells (1×10^5 cells/well in a 96-well microtiter soft plate) (Dynatech Labs, Alexandria, VA). The antibody-containing solution was added to the cells for 1 h at 24 °C. Then, after three washes, ^{125}I -labeled goat antimouse Ig ($1\text{--}2 \times 10^5$ cpm/well) was added and the mixture was left at 24 °C for another 1–2 h. In the live-cell assay, the cells were washed three times in PBS containing 1% BSA and then dissolved in 1 N NaOH and transferred into counting vials. In the fixed-cell assay, the wells containing the cells were dried, cut, and counted. The bound ^{125}I was determined in a Kontron γ -counter (Munchenstein, Switzerland).

Cytotoxic Activity of the FUR-MAb Conjugates. The cytotoxicity of the conjugates was determined by two methods.

(1) *Inhibition of $[^3\text{H}]\text{Leucine}$ Incorporation as a Measure of Protein Synthesis.* LS180 cells (5×10^4 /well) were plated in 0.1-mL aliquots on 96-well multititer plates (Nunc, Kamstrup, Denmark). The drugs 2'-deoxy-5-fluorouridine (FUDR), FUR, FUR(oxi), FUR(oxi-red), and the various FUR(oxi)-polymer derivatives were added 4 h later and incubated with the cells for 1–48 h. The inhibitors were then replaced by fresh medium and incubation was continued for another 48 h. Following incubation, the medium was replaced by 0.1 mL of PBS containing 0.5 μCi of $[^3\text{H}]\text{leucine}$ (Amersham, Buckinghamshire, England) and the plate was reincubated for 4 h at 37 °C, after which the labeled cells were detached from the wells by the trypsin versane mixture and harvested for counting. In experiments where longer periods of incubation were required, the drug or its conjugates were not replaced with fresh medium for further incubation. Incorporated $[^3\text{H}]\text{leucine}$ was determined in Lumax scintillation fluid (Landgraaf, Netherlands) in a β -counter (Kontron, Munchenstein, Switzerland).

(2) *Effect of FUR-pLys Conjugates in a Tumor Colony Assay.* The colonization assay was performed according to Flentje et al. (14) with some modifications. LS180 cells (10^5) were plated in 0.1 mL of medium per well (round-bottom 96-well plate). The derivatives were added in 0.1-mL aliquots and the plate was left at room temperature for 1 h. This was followed by washing and plating of 500–2000 cells in 6-cm tissue-culture dishes (Nunc, Kamstrup, Denmark). The number of colonies was counted after 14 days following fixation with 4% formalin and staining with hematoxylin.

In Vivo Experiments. Athymic BALB/c nu/nu mice (4–6 weeks old) were obtained from Bomholtgaard and CD₁

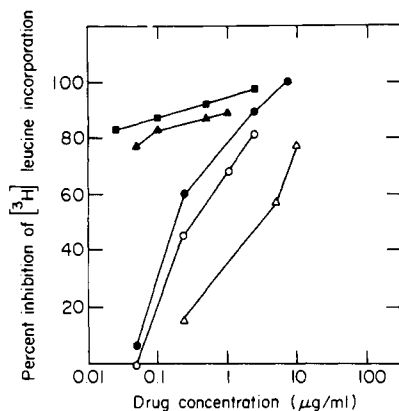


Figure 1. The activity of the FUR drug family on LS180 cells. The drugs, FUR (■), FUR(oxi) (▲), FUR(oxi-red) (○), FUDR (●), and FU (△), were incubated with LS180 cells for 15 h. This was followed by an incubation for 48 h with fresh medium, addition of [³H]leucine for 4 h, harvesting, and counting.

nu/nu mice were from the Weizmann Institute Animal Center. LS180 colon carcinoma cells ($1-3 \times 10^6$) were injected subcutaneously (sc). Treatments by the specific conjugate FUR-pLys-SF25MAb and various controls were started 2-3 days after tumor implantation and repeated four or five times, every 3-4 days. Lymph node metastasis of the colon carcinoma was obtained by the intravenous (iv) injection of 2×10^6 LS180 cells, 10 days after the mice received 400 rad (cobalt-60) of irradiation. The metastatic tumor caused death within about 50 days. Treatments were given iv as described above. The results are shown as the increase in life span (ILS), namely, the increase in the median survival time (MST) of the treated group divided by the MST of the placebo-receiving group ($\times 100$).

RESULTS

FUR, which was used as the reference drug in the following studies, was shown to be very inhibitory to LS180 colon carcinoma cells (Figure 1). The oxidation of FUR, which opened its ribosyl sugar to a dialdehyde derivative, did not affect its activity. Reduction of the aldehydes to alcoholic groups decreased the effectivity of the drug, making it comparable to the clinically used compound FUDR. Both of them, FUR(oxi-red) and FUDR, were about 10 times more effective than 5-fluorouracil (FU), which has to undergo metabolic conversions to the active substance.

Preparation of FUR-pLys-MAb Conjugates. FUR(oxi) was bound via its aldehyde groups to the amino groups of a pLys backbone. Binding could be performed under either acidic (pH 5.5) or basic (pH 9.5) conditions. The latter resulted in higher substitution rates. The maximal binding of drug to pLys was 11 mol/mol. The antibody was bound to the pLys bridge through its periodate-oxidized polysaccharide chain. The oxidized SF25MAb (obtained under mild oxidation conditions) was unaffected in its antigen-binding capacity (Table I). FUR-pLys was then linked through residual unsubstituted amino groups on the pLys to aldehydic groups on the oxidized SF25MAb. The conjugates obtained had a molar ratio of 45-100 mol of drug per mol of antibody, linking about 5-9 mol of pLys per mol antibody.

Binding of FUR-pLys-MAb Conjugates to LS180 Cells. The linking of the drug-pLys bridge to the antibody markedly increased its antigen-binding capacity (Table I). Since pLys has the capability of sticking nonspecifically to molecules and surfaces, the FUR-pLys derivative was used as a control in the binding assay to the tumor cells.

Table I. SF25MAb Binding to LS180 Cells*

antibody concn, μg/mL	bound cpm				
	SF25- MAb	SF25MAb oxidized	SF25MAb + DMSO	FUR-pLys-SF25MAb succinylated	un- succinylated
0.1	1160	ND ^b	ND ^b	4540	35590
0.5	4620	ND ^b	ND ^b	9250	59700
2.0	8230	6409	8120	14450	81270
10.0	8620	10654	9092	24010	106970
25.0	8910	8858	9500	27280	105250

* SF25MAb alone or after various treatments and conjugation with FUR-pLys was added at increasing concentrations to LS180 cells. The extent of binding to the cells was assayed indirectly with [¹²⁵I]-labeled goat antimouse Ig. ^b ND = not determined.

At high concentrations of FUR-pLys, equivalent to about 50 μg/mL pLys, nonspecific binding occurred both to the tumor cells and to the second antibody (¹²⁵I-labeled goat antimouse Ig). However, these concentrations were above those used with the specific antibody conjugates in the binding assay.

In order to determine whether the linking of FUR-pLys to unrelated antibody could also increase nonspecific binding to the LS180 tumor cells, two unrelated antibody-drug conjugates were prepared: FUR-pLys-monoclonal anti-epidermal growth factor (EGF) receptor and anti-hepatitis B surface (HBS) MAb. The binding properties of the conjugates were compared with those of both respective unconjugated antibody and with the conjugated specific antibody SF25MAb. LS180 cells were fixed with 0.15% formaldehyde (conditions which did not affect the antibody binding epitope of the cells). Indeed, the pLys bridge between drug and antibody increased the non-specific attachment of unrelated antibodies to the tumor cells. Yet, the increased binding capacity was much higher with conjugates of the specific antibody (Figure 2). In order to abolish any cytotoxicity by the pLys bridge, additional lysyl residues were blocked. This was achieved by treating the pLys conjugates at pH 8-9 with succinic anhydride, in dimethyl sulfoxide. The succinylation procedure decreased the conjugates binding capacity, but it was still higher than that of the original antibody (Table I). Dimethyl sulfoxide mixed with the antibody at final concentrations of 5% had no effect on its antigen binding (Table I).

Cytotoxic Activity of the FUR-pLys Conjugates. The drug activity of the conjugates was tested by inhibition of protein synthesis of LS180 colon carcinoma cells. The inhibitors were incubated with tumor cells for 15 h. The specific conjugate FUR-pLys-SF25MAb was a more efficient inhibitor than FUR-pLys (Figure 3). Yet, the free drug, FUR(oxi), was a better inhibitor than both conjugates. Another control for testing the cytotoxic activity of the conjugates was pLys substituted with uridylic acid. This conjugate, uridylic acid-pLys, was inhibitory only at very high concentration (40 times higher than that needed for 50% inhibition of protein synthesis by FUR-pLys-SF25MAb). Succinylation reduced the activity of both FUR-pLys and its antibody conjugate and completely abolished any activity of uridylic acid-pLys. Shorter incubation periods with the drug derivatives showed similar, only lower, inhibitory effects with all the compounds. The assays were performed with tumor cells prior to their adherence to the plates since firm surface binding reduced the susceptibility to the inhibitory action of the drugs. The SF25MAb antibody alone had no inhibitory or stimulatory effect on the cells in this assay.

Inhibition of LS180 Colony Formation by FUR-

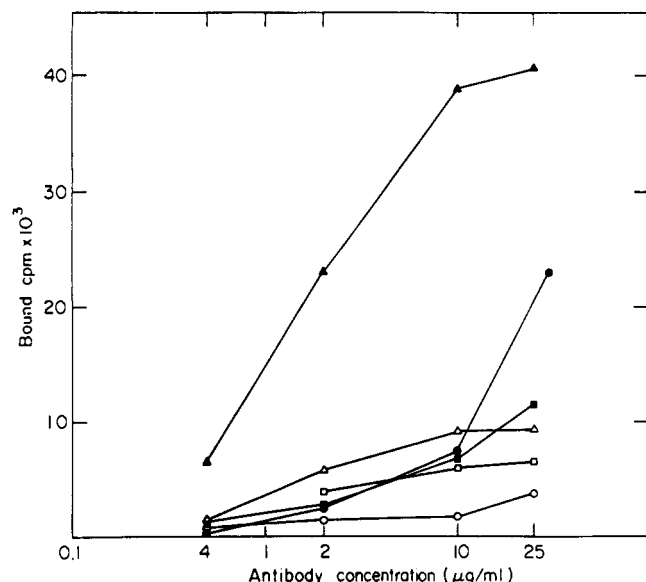


Figure 2. The binding of FUR-pLys-SF25MAb and FUR-pLys bound to control antibodies to LS180 cells. LS180 (5×10^4) cells were fixed with 0.15% formalin in the wells of a multititer soft plate. Increasing concentrations of antibodies or their derivatives were added for 1 h at 25 °C. The antibody solutions were then removed. The wells were washed and incubation with ^{125}I -labeled goat antimouse followed for 1 h at 25 °C. At the termination of the experiment the wells were dried, cut, and counted: SF25MAb (Δ), FUR-pLys-SF25MAb (\blacktriangle), anti-EGF receptor MAb (\square), FUR-pLys-anti-EGF receptor (\blacksquare), anti-HBS MAb (\circ), FUR-pLys-anti-HBS (\bullet).

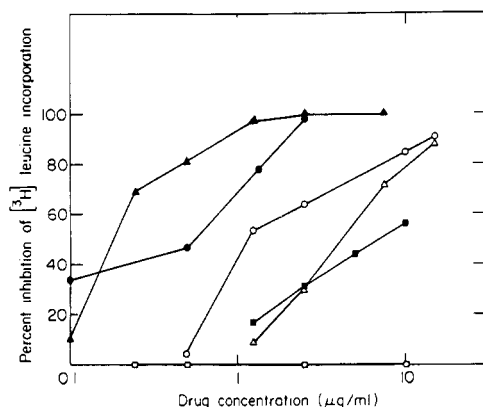


Figure 3. The cytotoxic activity of the FUR-pLys-antibody derivatives. The experiment was performed as that described in Figure 1: FUR-pLys-SF25MAb (\blacktriangle), succinylated FUR-pLys-SF25MAb (Δ), FUR-pLys (\bullet), succinylated FUR-pLys (\circ), uridylic acid-pLys (\blacksquare), succinylated uridylic acid-pLys (\square).

pLys-SF25MAb. Results describing the effects of the specific conjugates and various controls on the colony-formation capacity of LS180 cells are given in Table II and Figure 4. The specific conjugate was a better inhibitor than FUDR but was less effective than FUR(oxi-red) and FUR-pLys. The succinylated specific conjugate needed slightly higher doses for 50% inhibition of colony formation than the parent compound FUR-pLys-SF25MAb. A succinylated nonspecific conjugate with anti-HBS antibody was effective only at 10 times higher concentrations.

In Vivo Therapeutic Effectivity of FUR-pLys-SF25MAb. The intravenous injection of FUR-pLys-SF25MAb containing 0.5–1 mg of pLys caused immediate death. The same dose was not toxic if delivered intraperitoneally. Succinylation of the FUR-pLys derivatives enabled us to repeat intravenous injections without causing any obvious side effects. The therapeutic effectivity of FUR-pLys-SF25MAb (succinylated) on a subcutaneous

Table II. Inhibition of LS180 Colony Formation by FUDR, FUR(oxi-red), and FUR-pLys-Antibody*

compound	concn for 50% inhibn, $\mu\text{g/mL}$		
	drug	pLys	MAb
FUR(oxi-red)	0.26	—	—
FUDR	1.7	—	—
FUR-pLys	1.0	7.7	—
FUR-pLys-SF25MAb	2.6	11.9	2.9
succinylated	3.0	13.7	3.4
FUR-pLys-SF25MAb succinylated	25.0	114.5	28.6
FUR-pLys-anti-HBS MAb			

* LS180 cells were incubated for 1 h with FUR derivatives. Cells were washed and plated, and the number of colonies formed was counted; after 7 days SF25MAb at a concentration of 12 $\mu\text{g/mL}$ had no effect on the clone number.

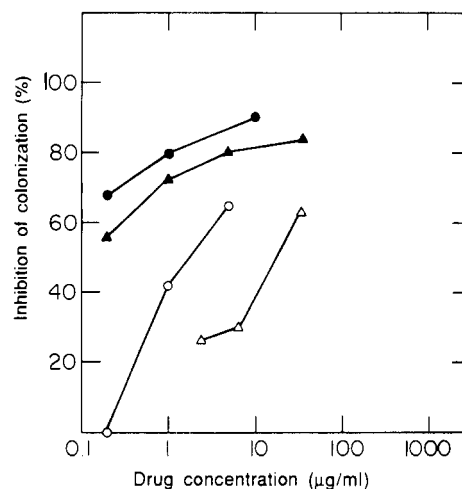


Figure 4. The inhibition of LS180 tumor cell colony formation by FUR-pLys conjugates. LS180 cells (10^5 /tube) were treated with FUR(oxi) and its antibody derivatives for 1 h at 24 °C. The cells were plated after washings at dilutions made to 500 cell/culture dish (triplicates for each treatment). After 14 days the number of colonies was counted: FUR(oxi-red) (\bullet), FUDR (\circ), FUR-pLys-SF25MAb (Δ), succinylated FUR-pLys-SF25MAb (\blacktriangle).

LS180 tumor growth is shown in Figure 5, parts A and B. The specific conjugate was compared to FUR-pLys, uridylic acid-pLys, and SF25MAb alone and is significantly more effective in retarding the tumor growth than any of the controls (Figure 5A). In the experiment described in Figure 5B, the controls were FUR-pLys, FUR(oxi-red), and a mixture of the specific antibody and the drug. In this experiment, the combined effect of the drug and the antibody was similar to that of the specific conjugate. The in vivo antitumor effectivity of FUR(oxi-red) was compared to that of FUDR. Both showed a similar reduction in tumor size as compared to that of the control, phosphate-buffered saline (PBS). A total dose of 750 μg injected three times intravenously every 3 days from the 3rd day after the tumor implantation resulted in a tumor size reduction to 30% of that of the control. A lower dose (375 μg) was almost ineffective (the experiment was performed with CD₁ nude mice). Succinylated FUR-pLys-SF25MAb tested against a metastatic tumor by repeated intravenous injections marginally, yet significantly ($p = 0.005$), increased the median survival time (Table III). The effect was only slightly better than that obtained by the antibody alone while none of the controls was effective (the mice in the metastatic model were CD₁ nudes).

DISCUSSION

A specific drug-antibody conjugate, FUR-pLys-SF25MAb, was prepared. In contrast to a previously used

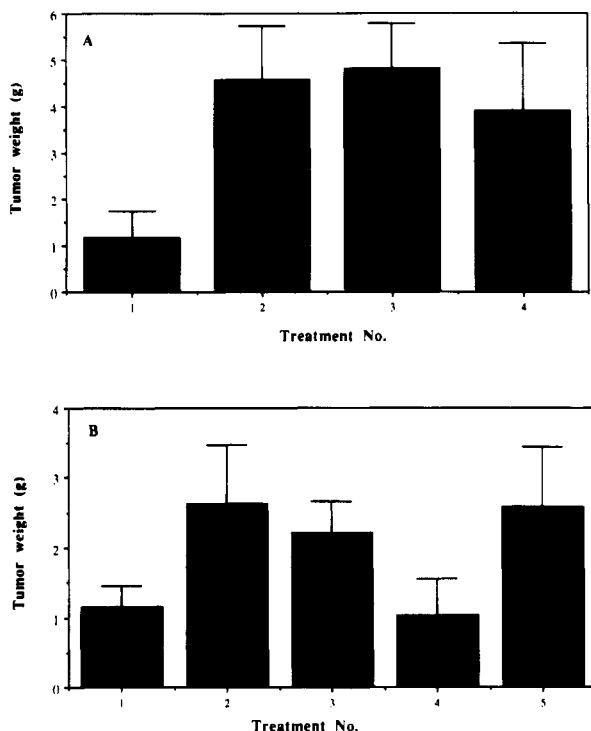


Figure 5. The effect of treatment by succinylated FUR-pLys-SF25MAb and control derivatives on LS180 colon carcinoma growth in athymic mice (Balb/c nu/nu). (A) LS180 (2×10^6) cells were injected sc. The treatment groups were (1) FUR-pLys-SF25MAb at a total dose of 0.34 mg of FUR/1.2 mg of pLys/3 mg of SF25MAb, and the controls (2) FUR-pLys, (3) uridylic acid-pLys, and (4) SF25MAb, at the respective doses, were injected intravenously on days 3, 7, 10, and 17. Tumor weights were determined after 30 days. (B) conditions were the same as for A except 3×10^6 LS180 cells were injected and treatment groups were (1) FUR-pLys-SF25MAb at a total dose of 0.54 mg of FUR/4.4 mg of pLys/2.5 mg of Ab, (2) FUR-pLys, (3) FUR(oxi-red), (4) a mixture of FUR(oxi-red) and SF25MAb, and (5) phosphate-buffered saline, injected on days 2, 7, 9, 13, and 16. The statistical analysis was by Anova and Duncan's multiple comparison test (15).

Table III. The Effect of FUR pLys-SF25MAb on a Metastatic Growth of LS180 Colon Carcinoma^a

compound	MST ^b	% ILS ^c	% survival
FUR-pLys-SF25MAb	64	28	23
FUR-pLys-anti-DNP	51	2	0
FUR(oxi-red)	59	18	0
FUR-p(Lys)	54	8	10
SF25MAb	67	34	8
PBS	50		

^a Results are an average of four experiments with six mice per group at a dose range of FUR 0.5–0.87 mg of FUR/3.5–8 mg of pLys/1.6–1.8 mg of Ab. ^b MST = median survival time. ^c ILS = increase in life span.

bridge for the conjugation of FUR to antibody (3), the use of pLys enabled high substitution rates (45–100 mol/mol). In addition, it was anticipated that such a bridge, capable by itself to be active against tumors (5), could add to the overall effectivity of the product. In vitro, this conjugate was indeed very active both in its binding capacity to the target cells and its cytotoxic effect. Poly-(L-lysine)-containing antibody conjugates, regardless of the antibody specificity, always showed increased level of nonspecific binding to the cells tested. Yet, the relative increase was much higher with an antibody which recognized and bound to the pertinent cells, colon carcinoma LS180 (Table I, Figure 2). The in vitro chemotherapeutic activity of the specific conjugate was comparable to that of FUDR and FUR(oxi-red) (Figures

1 and 2) and was appreciably higher than the previously prepared conjugate, with a dextran-hydrazide bridge (3). The activity of the latter was comparable to that of FU, which was the least active (Figure 1). The starting compound, FUR, although the most active compound from this group of fluorinated nucleotides (Figure 1), is not used clinically because of its toxicity to many normal tissues. Its periodate-oxidized and borohydrate-reduced derivative (which was used as the control compound both in vitro and in vivo) was similar in its overall activity to the clinically most widely used drug, FUDR. FUR(oxi-red) was superior to its in vitro cytotoxicity compared to the pLys-bound drug derivatives, probably because of its rapid penetration into the cells. FUR-pLys-SF25MAb was consistently more effective than FUR-pLys, although the differences between the two were slight (Figure 3). In vivo, FUR-pLys-SF25MAb was toxic when delivered intravenously. Injection as a heparin complex (11) was tried yet found to be unsuitable; the complex caused precipitations of the material unless minute amounts were used. Thus, additional free amino groups on the pLys bridge had to be blocked, which was achieved by succinylation. The blocking process also required reduction of the Schiff bases formed between the amino groups of pLys and aldehyde groups of the oxidized FUR groups. The resulting product was a much slower reacting derivative (Figure 4). Total killing of the cells was obtained, but longer incubation periods were required. The binding of the blocked conjugate to the LS180 cells was similar to that of the original antibody (Table I). In vivo, FUR-pLys-SF25MAb was effective in the retardation of a subcutaneous tumor development (Figure 5). The conjugate also caused a small increase in the median survival time of a metastatic tumor (Table III). The conjugate was more effective than the antibody or the drug alone (Figure 5A). Yet, the effect of the conjugate was not superior to that of the mixture of the drug and antibody (Figure 5B). FUR-pLys-SF25MAb was not toxic by injection intraperitoneally. Yet, delivered by this route, the capacity of the conjugate to inhibit the subcutaneous tumor growth was not superior to that obtained by the antibody alone (data not shown). In conclusion, pLys as a bridge produced high substitution rates of drug on antibody, and such conjugates showed high cell bindings and cytotoxic activities in vitro. In the model animals, however, these advantages could not be manifested. In the unblocked form, FUR-pLys-SF25MAb delivered intraperitoneally, perhaps because of nonspecific attachment of the pLys moiety to other cells of tissues, interfered with its tumor-targeting capacity. Succinylated FUR-pLys-SF25MAb could be injected intravenously. However, the blocked conjugate no longer possessed the original pLys qualities, which made it inhibitory to the cells by its own merits and therefore could not show additional activity to the combined effects of FUR and the specific antibody.

LITERATURE CITED

- (1) Heidelberger, C., and Ansfield, F. J. (1963) Experimental and clinical use of fluorinated pyrimidines in cancer chemotherapy. *Cancer Res.* 23, 1226–1243.
- (2) Montgomery, J. A., and Struck, R. F. (1973) The relationship of metabolism of anti-cancer agents to their activity. *Arzneim-Forsch. (Drug Res.)* 17, 320–410.
- (3) Hurwitz, E., Kashi, R., Arnon, R., Wilchek, M., and Sela, M. (1985). The covalent linking of two nucleotide analogues to antibody. *J. Med. Chem.* 28, 137–140.
- (4) Ryser, H. J.-P., and Shen, W.-C. (1986) Drug-poly(lysine) conjugates: their potential for chemotherapy and for the study of endocytosis. In *Targeting of drugs with synthetic systems*

- (G. Gregoriadis, J. Senior, and G. Poste, Eds.) pp 103-113, Plenum Press-NATO (ASI series) Life Sciences, New York.
- (5) Arnold, L. J., Jr., Dagan, A., and Kaplan, N. O. (1983) Poly-L-lysine as an antineoplastic agent and tumor specific drug carrier. In *Targeted Drugs* (E. P. Goldberg, Ed.) pp 89-112, J. Wiley & Sons, New York.
- (6) Zunino, F., Savi, G., Giuliani, F., Gambetta, R., Supino, R., Tinelli, S., and Pezzoni, G. (1984) Comparison of anti-tumor effects of daunorubicin covalently linked to poly-L-amino acid carrier. *Eur. J. Cancer Clin. Oncol.* 20, 421-425.
- (7) Onishi, H., Kawaguchi, T. and Nagai, T. (1987) In vitro drug release from macromolecule-drug conjugates of 3'-(7-carboxyheptanoyl)-5-fluoro-2'-deoxyuridine with decylenediamine-dextran T70 of poly-L-lysine. *Chem. Pharm. Bull.* 35, 3370-3374.
- (8) Takahashi, H., Carlson, R., Ozturk, M., Sun, S., Motte, P., Strauss, W., Isselbacher, K. J., Wands, J. R., and Shouval, D. (1989) Radioimmunolocalization of hepatic and pulmonary metastases of human colon adenocarcinoma. *Gastroenterology* 96, 1317-1329.
- (9) Takahashi, H., Wilson, B., Ozturk, M., Motte, P., Strauss, W., Isselbacher, K. J., and Wands, J. R. (1988) In vivo localization of human colon adenocarcinoma by monoclonal antibody binding to highly expressed cell surface antigen. *Cancer Res.* 48, 6573-6579.
- (10) Katchalski, E., and de Vries, A. (1953) Action of polysine on blood in vitro and in vivo. *Acta Med. Orient.* 12, 288-293.
- (11) Morad, N., Ryser, H. J.-P., and Shen, W.-C. (1984) Binding sites and endocytosis of heparin and poly-lysine are changed when the two molecules are given as a complex to Chinese hamster ovary cells. *Biochim. Biophys. Acta* 801, 117-126.
- (12) Hurwitz, E., Wilchek, M., and Pitha, J. (1980) Soluble macromolecules as carriers for daunorubicin. *J. Appl. Biochem.* 2, 25-35.
- (13) Galun, E., Shouval, D., Adler, R., Shahaar, M., Wilchek, M., Hurwitz, E., and Sela, M. (1990) The effect of anti-alpha-fetoprotein adriamycin conjugate on a human hepatoma. *Hepatology* 11, 578-584.
- (14) Flentje, M., Flentje, D., and Schlag, P. (1986) Comparison of FUR versus FUDR activity in human colorectal cancer using an in vitro clonogenic assay (HTCA). *Cancer Chemother. Pharmacol.* 18, 223-225.
- (15) Duncan, D. B. (1955) Multiple range and multiple *F* tests. *Biometrics*, 11, 1-42.

Succinylated Polylysine as a Possible Link between an Antibody Molecule and Deferoxamine

M. A. Slinkin,[†] A. L. Klibanov,[†] B. A. Khaw,[‡] and V. P. Torchilin^{*†}

U.S.S.R. Cardiology Research Center, Academy of Medical Sciences, Moscow, U.S.S.R., and Nuclear Medicine Department, Massachusetts General Hospital, Boston. Received March 7, 1990

Modification of antibodies with chelating polymers may be helpful for radioimmunoimaging, radioimmunotherapy, and NMR tomography. Succinylated polylysine was activated with carbodiimide/*N*-hydroxysulfosuccinimide in dimethyl sulfoxide and isolated as a dry solid. Sulfosuccinimide-esterified polymer was used for the two-stage coupling of an amino-containing chelating agent (deferoxamine) to monoclonal R11D10 (IgG) or its Fab fragment. Conjugates were separated from free components by using gel-chromatography and anion-exchange chromatography. Antibody-coupling efficiency and the loss of its immunoreactivity upon modification have been studied for polymers with different deferoxamine content. Specific binding of ⁶⁷Ga to the corresponding antigen via the conjugate has been demonstrated.

INTRODUCTION

Different monoclonal antibodies are already used in radioimmunoscintigraphy for the noninvasive diagnosis of tumors (1), necrotic tissues (2), and thrombi (3). Usually it takes 24–48 h to achieve sufficiently high target-to-background ratio because of slow antibody clearance and relatively high nonspecific binding with nontarget tissues (4). Different approaches have been developed to shorten the time of diagnostic procedures (5–7). Thus, for example, Fab fragments of antibodies with relatively low molecular weight have been used for this purpose (4).

We have recently shown that the time interval for diagnosis of experimental myocardial infarction in a canine model can be significantly shortened (up to 3–4 h), when ¹¹¹In-labeled anticardiac myosin R11D10 Fab coupled to a highly negatively charged chelating polymer is used (8). The approach decreased the background radioactivity in normal myocardium and in nontarget organs such as liver and kidneys, thus enhancing myocardial infarct visualization.

The same approach may be very useful for obtaining diagnostic images in a few hours after administration of any preparation labeled with short-lived isotopes, which can be used both for radioimmunoimaging (^{113m}In) and for positron tomography (⁶⁸Ga).

The most popular chelating agent for different isotopes of Ga is deferoxamine (DFA) (9, 10). The major object of the present paper is the development of the convenient and reliable method of DFA conjugation with antibodies via polymer with the express purpose to prepare Ga-labeled negatively charged polymeric conjugates of antibodies. In our experiments we have used ⁶⁷Ga instead of ⁶⁸Ga: the latter isotope has very short half-period and is not too convenient to work with.

When developing the method for the preparation of polymeric conjugates of antibodies with DFA, we also kept in mind that the direct labeling of protein with DFA can cause antibody inactivation (10). Modification of an antibody with a chelating polymer can allow the coupling (without loss of its immunoreactivity) of many more chelating units (and, consequently, metal atoms) than is possible by direct modification with low molecular weight chelators. This aspect is especially important for immu-

nocontrast in NMR tomography (11) and for radioimmunotherapy (12).

EXPERIMENTAL PROCEDURES

Monoclonal anticardiac myosin antibody R11D10 was prepared by the method described by Khaw et al. (2). The purified antibody was then treated with papain (13) to produce the Fab.

Preparation of Succinylated Polylysine (PLS).¹ To prepare PLS, dry succinic anhydride (70 mg) was added with stirring to a PL bromide (Sigma, MW 17000, 20 mg) solution in 2 mL of 0.1 M carbonate buffer, pH 8.0. The pH was continuously adjusted to 8.0 with concentrated NaOH solution. The degree of PL amino group modification was controlled by spectrophotometric amino group titration with TNBS (14).

The PLS solution was extensively dialyzed against water. The solution after dialysis was acidified with 1 N HCl to pH 3.0 to precipitate the free PLS acid. The suspension obtained was lyophilized. Yield: 19 mg.

Preparation of the SSI Ester of PLS (PLS Ester). PLS was dissolved in dry DMSO up to the concentration of 40 mg/mL. A DMSO solution (46 μ L) of HSSI (1.84 mg, 8.5 μ mol) and 40 μ L of a DMSO solution of EDC (1.6 mg, 8.4 μ mol) were subsequently added to 100 μ L of a PLS solution (4 mg, 18 μ mol of monomer units) at 25 °C. The mixture was incubated for 1.5 h. Then the activated polymer was precipitated with dry ethanol (2 mL). After centrifugation and ethanol evaporation under an argon stream, the PLS ester was isolated as a white solid. Yield: 3.5 mg.

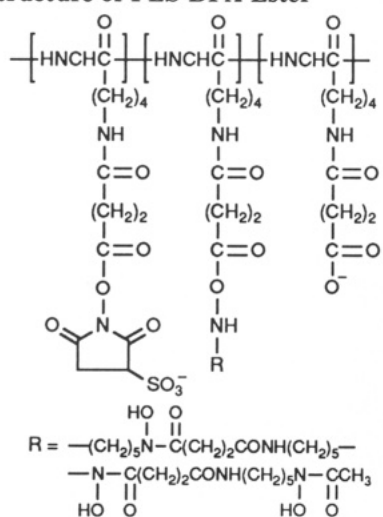
Assay for the Active Ester Content of the PLS Ester. The PLS ester was dissolved in DMSO up to a concentration of 20 mg/mL. A 1- μ L portion of this solution was added to 350 μ L of 0.1 M borate buffer, pH 8.0; the rate of *N*-hydroxysulfosuccinimide appearance was followed spectrophotometrically at 259 nm at 25 °C. After the reaction was completed (~60 min) and the increase in the absorbance leveled off, the active ester concentration

[†] Academy of Medicinal Sciences.

[‡] Massachusetts General Hospital.

¹ Abbreviations: DFA, deferoxamine (mesylate); PL, polylysine; PLS, succinylated polylysine; EDC, 1-ethyl-3-[3'-(dimethylamino)propyl]carbodiimide; HSSI, *N*-hydroxysulfosuccinimide; AEC, anion-exchange chromatography; TNBS, trinitrobenzenesulfonic acid; TEA, triethylamine; BAC, biologically active compound.

Chart I. Structure of PLS-DFA Ester



was calculated with $\epsilon_{259} = 7500 \text{ M}^{-1} \text{ cm}^{-1}$ (our data).

To calculate the percent of esterified COOH group in the PLS ester, the following equations were used:

$$220an + 413(1-a)n = 20$$

$$an = [\text{ester}] \quad (1)$$

where 220 and 413 are the molecular weights of nonesterified and esterified monomer units, respectively; n is the total amount of moles of monomer units per liter; a is the ratio of DFA-modified monomer units to the total number of monomer units; and 20 is the amount of PLS ester per liter in grams.

Preparation of DFA-Modified PLS Ester (PLS-DFA Ester) and its Conjugate with Antibodies. Different volumes of DFA solution in DMSO (1–4 μL , 0.036–0.14 μmol , concentration 24 mg/mL) were added to 5 μL of a PLS ester solution in DMSO (100 μg , 0.15 μmol of SSI-esterified units). The mixture was incubated for 1 h at 25 $^{\circ}\text{C}$ in the presence of triethylamine (TEA; molar ratio TEA/DFA = 1:1).

The coupling efficiency of DFA was estimated following spectrophotometric titration of primary amino groups with TNBS. Briefly, a 1- μL aliquot of the reaction mixture was mixed with 300 μL of 0.05 M borate buffer, pH 9.2, and 150 μL of a TNBS solution in water (2 mg/mL) was then added. After 1-h incubation, 150 μL of 2 M NaH_2PO_4 solution, containing 2.3 mg/mL of Na_2SO_3 , was added into the system, and the optical density (OD) at 420 nm was measured.

The reaction mixture obtained was quickly added to an antibody solution in 0.065–0.1 M borate buffer, pH 8.0 (1–2 mg protein/mL), and incubated for 3–4 h at 25 $^{\circ}\text{C}$. Then the solution was centrifuged and dialyzed against water (before gel electrophoresis), 0.05 M phosphate buffer, pH 6.0 (before AEC on DEAE-Sephadex A-25), or 0.05 M PBS, pH 7.5 (before ^{67}Ga -labeling and GC).

Assay of PLS-DEA-Antibody Conjugates. 1. SDS-polyacrylamide gel electrophoresis (SDS-PAGE) under nonreducing and reducing conditions (15) has been used to evaluate the ability of polymers with different DFA content to be coupled with antibody molecules. Reaction mixtures after PLS-DFA-antibody conjugation and dialysis of the mixture obtained against water have been used for SDS-PAGE.

2. AEC on DEAE-Sephadex A-25 has been used for separating free antibodies from conjugates and free polymers. A 2-mL column of DEAE-Sephadex A-25 was equilibrated with 0.05 M phosphate buffer, pH 6.0. Then

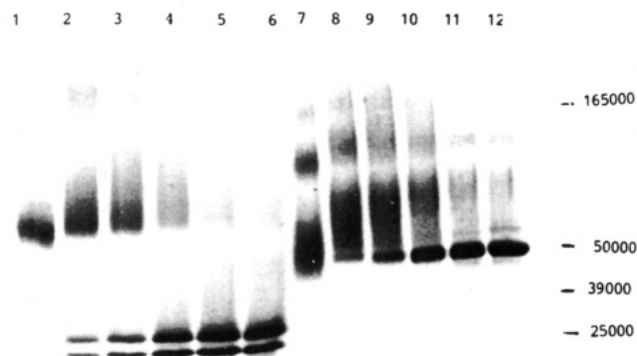


Figure 1. 10% SDS-polyacrylamide gel electrophoresis in reducing and nonreducing conditions of R11D10 Fab, modified with PLS ester (1, 7), PLS-DFA₁₁ ester (2, 8), PLS-DFA₂₃ ester (3, 9), PLS-DFA₃₄ ester (4, 10), PLS-DFA₄₆ ester (5, 11), and PLS-DFA₅₅ ester (conditional designation; 6, 12). Samples were (1–6) or were not (7–12) reduced with dithiothreitol. The positions of molecular weight markers are indicated along the right side of the gel.

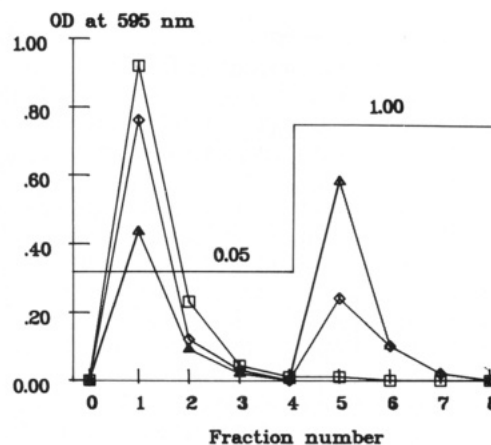


Figure 2. AEC on DEAE-Sephadex A-25 (1 \times 2 cm): (\square) R11D10 IgG; (Δ , \diamond) reaction mixtures after conjugation of R11D10 IgG with PLS-DFA₁₁ ester and PLS-DFA₃₅ ester, respectively. Conditions: start buffer, 0.05 M sodium phosphate, pH 6.0; step gradient, 0.05 M sodium phosphate + 0.95 M sodium chloride, pH 6.0; $V_{fr} = 2 \text{ mL}$.

the reaction mixture after dialysis containing all three species was loaded onto the column and eluted with 4 column volumes of the equilibrating buffer. Free Fab or IgG was eluted in the wash. The mixture of PLS-DFA-antibody and PLS-DFA was then eluted with a 1 M step gradient, containing 0.05 M sodium phosphate + 0.95 M NaCl, pH 6.0 (see Figure 2). Antibody concentration in fractions was estimated with the Bio-Rad protein assay reagent (polymer does not influence the results obtained). The immunoreactivity of antibody in conjugates was then determined by using a solid-phase radioimmunoassay (2).

3. GC on Sephadex G-75 or G-100 was used to estimate the coupling efficiency of polymer to R11D10 Fab or R11D10 IgG, respectively. This was done after labeling of the dialyzed reaction mixture with ^{67}Ga in 0.05 M PBS, pH 7.5, for 2–3 h.

Isolation, Labeling, and Assay of Pure PLS-DFA-Antibody Conjugates. The isolation of conjugates was performed by using a two-step purification procedure including (1) GC on Sephadex G-75 (for Fab-based conjugate) or G-100 (for IgG-based conjugate), allowing the separation of free polymer from the mixture of free antibodies and conjugate; and (2) AEC on DEAE-Sephadex A-25, allowing the separation of free antibodies from the conjugate (see Figure 2 for the illustration).

The labeling of purified conjugates with ^{67}Ga was performed for 2–3 h in eluent buffer, its pH being adjusted to 7.5, with fresh [^{67}Ga]gallium citrate. After the separation of nonbound ^{67}Ga with a PD-10 column of Sephadex G-50, the conjugate was subjected to direct solid-phase radioimmunoassay (2). Specific radioactivities of the labeled IgG- and Fab-based conjugates were close to each other and equal to 1 mCi/mg of protein.

RESULTS

Spectrophotometrically it was shown that the PLS ester solution in DMSO (20 mg/mL) contained 29 mM ester groups. From this value and eq 1 given in the Experimental Procedures, it was calculated that 45% of PLS ester monomer units were esterified and were present as the SSI ester.

The titration of DFA amino groups with TNBS has shown that the coupling efficiency of DFA with the PLS ester exceeds 95%, when ester groups are present in molar excess with respect to DFA. This condition corresponds to the following ratio between DFA and the PLS ester: 94 μg of DFA/100 μg of PLS ester (145 nm of active ester groups).

Polymers with different DFA-content were designated according to the molar percent of DFA-containing units in the polymer chain. For example, polymer obtained at DFA/PLS ester weight ratio 48/100 contains ~23% of DFA-containing units and was designated as PLS-DFA₂₃ ester.

Despite the high yield of the coupling reaction between DFA and the PLS-ester, the labeling efficiency of PLS-DFA with ^{67}Ga is very low, if nonbound DFA is not separated from the polymer prior to labeling. For example, when adding 48 μg of DFA to a DMSO solution containing 100 μg of PLS, ca. 95% of DFA is bound to PLS. At the same time, the efficiency of the labeling with ^{67}Ga of non-dialyzed PLS-DFA thus obtained is just ca. 5%. The strong effect of free DFA can probably be explained by the preferential binding of ^{67}Ga to free DFA molecules, which are not sterically hindered. After separating free DFA by dialysis, the efficiency of labeling the polymer with ^{67}Ga was about 90%.

The increase in DFA content in the PLS-DFA ester reagent drastically reduced the ability of polymer to couple with an antibody molecule. SDS-PAGE pattern of the reaction mixtures after dialysis (see Figure 1) demonstrates this trend for the coupling reaction between different PLS-DFA esters and R11D10 Fab. From this pattern one can see that the most intensively stained bands from the conjugates (see columns 2–4) correspond to the molecular weight (MW) just above 50000, i.e. to the conjugate of Fab R11D10-PLS-DFA type with the average molar polymer-to-antibody ratio of 1:1. Two closely situated bands with the approximate MW 25000 (columns 1–6) correspond to the single chains of reduced Fab, whereas the intensively stained band with MW 50000 corresponds to the whole nonreduced Fab.

The same trend of decreasing the coupling efficiency of a polymer resulting from the increase in its DFA content can be demonstrated by AEC of reaction mixtures containing both the conjugate PLS-DFA-antibody and free components on DEAE-Sephadex A-25. Figure 2 shows the difference between AEC profiles for free R11D10 IgG and reaction mixtures obtained upon its conjugation with PLS-DFA ester containing different amounts of DFA. A similar picture was observed when R11D10 Fab was used instead of R11D10 IgG.

Direct evidence for conjugate formation between the antibody molecule and a PLS-DFA ester has been obtained

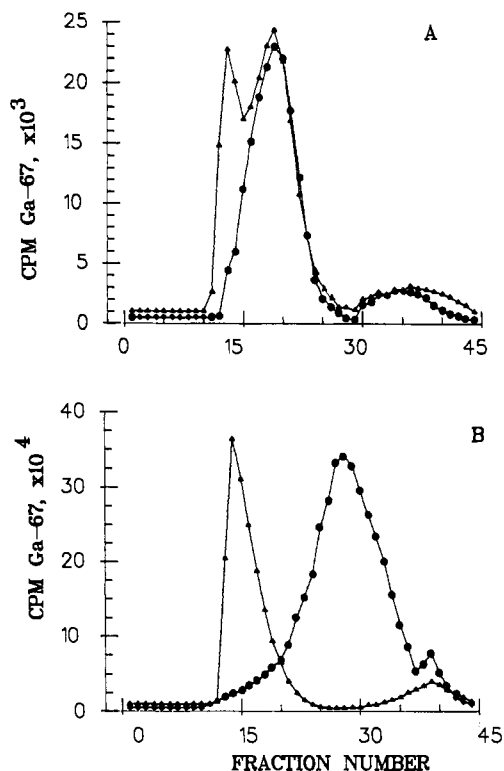


Figure 3. GC on Sephadex G-75 (A) or G-100 (B) (1 × 25 cm): A, (▲) reaction mixture after conjugation of PLS-DFA₁₁ ester with R11D10 Fab and its ^{67}Ga -labeling; B, (▲) purified ^{67}Ga -labeled R11D10 Fab-PLS-DFA₁₁; A and B, (●) ^{67}Ga -labeled PLS-DFA₁₁; V_{fr} = 0.6 mL; eluent, 0.05 M acetate + 0.15 M NaCl, pH 6.5.

with GC on Sephadex G-75 or G-100 (see Figure 3). When performing GC of R11D10 IgG conjugate on a Sephadex G-100 column, the peaks' separation was practically complete, whereas chromatographic peaks (Sephadex G-75) corresponding to R11D10 Fab conjugate and free PLS-DFA partially overlapped. Nevertheless, even in the latter case the pooling of fractions 11–14 (Figure 3a) allowed the separation of almost all of the free polymer from the conjugate. The absence of the free polymer in the R11D10 Fab-PLS-DFA₁₁ has been demonstrated after labeling of the purified conjugate with ^{67}Ga and GC of the labeled sample on Sephadex G-100 (see Figure 3b).

The immunoreactivity was estimated for conjugates derived from PLS-DFA esters with different DFA content. Fractions eluted from DEAE-Sephadex with a 1 M step gradient (see Figure 2) were used for immunoreactivity tests.

As one can see from Figure 4, there is some loss of immunoreactivity upon conjugation for both R11D10 Fab and R11D10 IgG. Intact antibodies denature to a lesser extent than do their fragments. DFA content in the polymer has some effect on the immunoreactivity of the conjugated antibody in the case of R11D10 Fab, but not R11D10 IgG. The higher the content of DFA residues in the PLS-DFA ester is, the better the preservation of immunoreactivity of R11D10 Fab upon conjugation. But even for PLS-DFA₂₃ ester, 15–25-fold loss of Fab immunoreactivity is observed. The loss of whole IgG immunoreactivity upon the conjugation with PLS-DFA₁₁ ester is less than 4–5-fold.

Despite some loss of antigen-binding activity, conjugated antibodies retain the capacity for specific delivery of ^{67}Ga to myosin-coated microtiter wells. Figure 5 shows an increase in the binding of ^{67}Ga -labeled R11D10 Fab-PLS-DFA₁₁, whereas ^{67}Ga -labeled R11D10 IgG-PLS-DFA₁₁ at

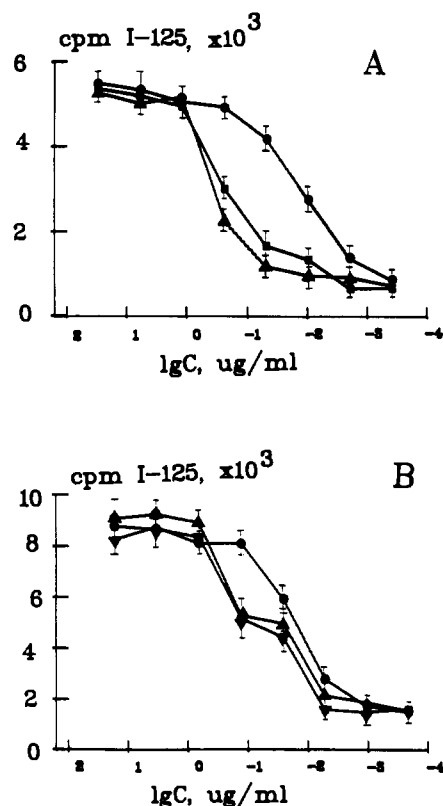


Figure 4. Solid-phase radioimmunoassay of R11D10 Fab (A) and R11D10 IgG (B): (●) nonmodified antibodies; antibodies conjugated with PLS-DFA₁₁ (▲), PLS-DFA₂₃ (■), PLS-DFA₃₅ (▼). C is the protein concentration in the well.

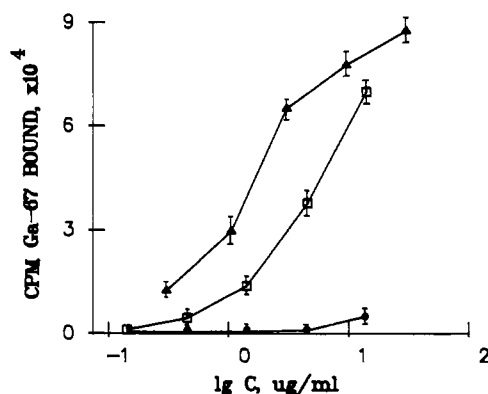


Figure 5. Comparative binding to myosin-coated microtiter wells of serial dilutions of ⁶⁷Ga-R11D10 Fab-PLS-DFA₁₁ (□) and ⁶⁷Ga-R11D10 IgG-PLS-DFA₁₁ (Δ), and (●) binding of ⁶⁷Ga-R11D10 IgG-PLS-DFA₁₁ to BSA-coated wells. C is the protein concentration in the well.

the same protein concentrations demonstrates binding saturation. This is not surprising taking into account that Fab immunoreactivity in the conjugate is less than that of IgG.

DISCUSSION

The use of polymers capable of carrying a large number of chelating groups for the modification of antibodies (and other proteins) via a limited number of reactive amino acid residues has already been described by us and other authors (17–20). Two principal approaches were developed: the direct binding of the chelating polymer with an antibody (17, 18) or the binding of the chelating polymer with an antibody via a nonchelating polymer which is used as a link between the protein molecule and chelating agents (19). Thus, following the latter approach, Yamamoto et

al. prepared a conjugate between DFA, dialdehyde starch, and fibrinogen (21). However, Schiff base formation in the aqueous media used (21) has some disadvantages from the chemical point of view. This reaction is relatively slow and it is hardly possible to control the number of DFA residues introduced into the polymeric chain. Besides, dialdehyde starch at physiological pH is practically a neutral polymer and cannot be used for charge modification of an antibody, which is often desirable (8).

One of the most reliable and convenient methods of amino group modification is the use of *N*-hydroxysuccinimide ester groups. On the other hand, polymer carriers based on polylysine are known to be nontoxic and biodegradable and were used earlier for the preparation of polymeric forms of biologically active substances (BAS) (22). PL derivatives such as PLS have a net negative charge. Therefore we decided to use PLS with an active ester groups as a polymer link.

The method of PLS activation in organic solvent (DMSO) suggested in this paper allows isolation of the activated polymer, containing approximately 50% of SSI esterified units, as a dry, white solid (HSSI was used instead of *N*-hydroxysuccinimide because PLS activated with EDC/*N*-hydroxysuccinimide is not soluble in water). As far as we know, this approach to the activation of COOH-containing carriers for BAC has not been previously described. In our earlier work the activation of a COOH-containing polymer based on polylysine and DTPA with HSSI/EDC mixture was performed in an aqueous medium (20). In this case, however, to decrease the degree of protein (R11D10 Fab) inactivation upon modification, one had to separate the activated polymer from free EDC by, for example, centrifugation in minicolumns (8).

Another approach to the introduction of succinimide esters into a polymeric chain is copolymerization of the corresponding monomers, such as acrylamide and *N*-acryloyloxysuccinimide (23). However, this approach results in the formation of acrylic polymers which are not biodegradable and therefore less preferable as compared with PLS.

The active groups of a PLS ester can react with amine-containing compounds in DMSO, providing an equimolar (with regard to amino groups) amount of TEA is present in the solution. We have shown that under these conditions the reaction between DFA mesylate and PLS ester proceeds practically quantitatively within 1 h. Residual active ester groups of the polymer can subsequently react with the amino groups of a protein after the formation of a PLS-DFA ester is completed. This allows the use of a PLS ester as a polymeric link in the two-stage coupling of DFA to protein molecules.

Upon modification of 11% of PLS ester (MW ~20 kDa) units a polymer with 10 DFA residues per single polymeric chain can be obtained. Subsequently, the corresponding PLS-DFA₁₁ ester in the second stage modifies ~50% of R11D10 Fab (Figure 1) and ~60% of R11D10 IgG (Figure 2); the initial polymer-to-protein ratios (w/w) in the reaction mixtures being 1:1 and 1:2, respectively. From the electrophoresis patterns, the average composition of the Fab-polymer conjugate can be estimated as 1:1. Hence, the average number of DFA residues per protein molecule in such conjugates is about 10. The 2–3-fold increase of DFA content in the polymeric chain results in a drastic reduction of the polymer coupling yield during its conjugation with an antibody but has only slight effect on the immunoreactivity of conjugated antibodies. Figure 4 demonstrates this effect for the case of R11D10-Fab: the higher the number of DFA residues in the polymeric chain

is, the higher the immunoreactivity of the conjugated Fab. Such effects can be regarded as a feature of the polymeric link, which permits an increase in antibody substitution with chelating groups, without inactivation. When using low molecular weight chelators, such as DTPA derivatives (24) and DFA (25), an increase in the number of chelating groups per protein molecule results in a reduction of the immunoreactivity of the modified antibodies.

The approach developed in this paper can also be used for the conjugation of proteins with other amine-containing chelating agents and is applicable to the binding a wide spectrum of different heavy metal ions. Among such chelators are (S)-p-aminobenzyl-EDTA (26), C-1-(p-aminobenzyl)-DTPA (27), 6-(p-aminobenzyl)-1,4,8,11-tetraazacyclotetradecane-N,N',N'',N'''-tetraacetic acid (28), etc. Thus, α -, β -, and γ -isotopes of heavy metals can be tightly bound to antibody molecules by using this approach. We hope that these conjugates of antibodies with negatively charged polymers will demonstrate reduced nontarget organ activity and find application both for radioimmunomaging, positron tomography, and radioimmunotherapy.

LITERATURE CITED

- (1) Mitchell, E. P., and Schlom, J. (1988) Monoclonal antibodies in gastrointestinal cancers. *Semin. Oncol.* 15, 170-180.
- (2) Khaw, B. A.; Mattis, J. A.; Melincoff, G.; Strauss, H. W.; Gold, H. K., and Haber, E. (1984) Monoclonal antibody to cardiac myosin: imaging of experimental myocardial infarction. *Hybridoma* 3, 11-23.
- (3) Knight, L. C.; Maurer, A. H.; Ammar, I. A.; Shealy, D. J., and Mattis, J. A. (1988) Evaluation of Indium-111-labeled anti-fibrin antibody for imaging vascular thrombi. *J. Nucl. Med.* 29, 494-502.
- (4) Khaw, B. A.; Yasuda, T.; Gold, H. K.; Leinbach, R. C.; Johns, J. A.; Kanke, M.; Barlaikovach, M.; Strauss, H. W., and Haber, E. (1987) Acute myocardial infarct imaging with indium-111-labeled monoclonal antimyosin Fab. *J. Nucl. Med.* 28, 1671-1678.
- (5) Sharkey, R. M.; Primus, F. P., and Goldenberg, D. M. (1984) Second antibody clearance of radiolabeled antibody in cancer radioimmunodetection. *Proc. Natl. Acad. Sci. U.S.A.* 81, 2483-2486.
- (6) Wahl, R. L.; Parker, C. W., and Philpott, G. W. (1983) Improved radioimmunomaging and tumor localization with monoclonal F(ab')₂. *J. Nucl. Med.* 24, 316-325.
- (7) Klivanov, A. L.; Martynov, A. V.; Slinkin, M. A.; Sakharov, I. Yu.; Smirnov, M. D.; Muzykantov, V. R.; Danilov, S. M., and Torchilin, V. P. (1988) Blood clearance of radiolabeled antibody: enhancement by lactoseamination and treatment with biotin-avidin or anti-mouse IgG antibodies. *J. Nucl. Med.* 29, 1951-1956.
- (8) Khaw, B. A.; Klivanov, A. L.; O'Donnell, S. M.; Saito, T.; Nossiff, N. D.; Strauss, H. W., and Torchilin, V. P. (1989) Charge modification of monoclonal antibodies for enhanced target visualization. *J. Nucl. Med.* 30, 762 (abstract).
- (9) Yokoyama, A.; Ohmomo, Y.; Horiuchi, K.; Saji, H.; Tanaka, H.; Yamamoto, K.; Yasushi, I., and Torizuka, K. (1982) Deferoxamine, a promising bifunctional chelating agent for labeling proteins with gallium: Ga-67 DF-HSA: Concise communication. *J. Nucl. Med.* 23, 909-914.
- (10) Motta-Hennessy, C.; Eccles, S. A.; Dean, C., and Coghlan, G. (1985) Preparation of ⁶⁷Ga-labeled human IgG and its Fab fragments using deferoxamine as chelating agent. *Eur. J. Nucl. Med.* 11, 240-245.
- (11) Anderson-Berg, W. T.; Strand, M.; Lempert, T. E.; Rosenbaum, A. E., and Joseph, P. M. (1986) Nuclear magnetic resonance and gamma camera imaging using Gd-labeled monoclonal antibodies. *J. Nucl. Med.* 27, 829-833.
- (12) Mach, J. P.; Buchegger, F.; Bischof-Delaloye, A.; Curchod, S.; Studer, A.; Douglas, P.; Leyvraz, S.; Grob, J.; Mosimann, F.; Givel, J.-C.; Pettavel, J., and Delaloye, B. (1988) Progress in diagnostic immunoscintigraphy and first approach to radioimmunotherapy of colon carcinoma. *Radiolabeled Monoclonal Antibodies for Imaging and Therapy* (S.C. Srivastava, Ed.) pp 95-110, Plenum Publishing Corp., New York.
- (13) Porter, R. R. (1959) The hydrolysis of rabbit gamma-globulin and antibodies with crystalline papain. *Biochem. J.* 73, 119-126.
- (14) Spadaro, A. C. C.; Draghetta, W.; Del Lama, S. N.; Camargo, A. C. M., and Green, L. J. (1979) A convenient manual trinitrobenzenesulfonic acid method for monitoring amino acids and peptides in chromatographic column effluents. *Anal. Biochem.* 96, 317-321.
- (15) Laemmli, U. K. (1970) Cleavage of structural proteins during the assembly of the head of bacteriophage T4. *Nature (London)* 227, 680-685.
- (16) Shreve, P., and Aisen, A. E. (1986) Monoclonal antibodies labeled with polymeric paramagnetic ion chelates. *Magn. Reson. Med.* 3, 336-340.
- (17) Manabe, Y.; Longley, C., and Furmanski, P. (1986) High-level conjugation of chelating agents onto immunoglobulins: use of an intermediary poly(L-lysine)-diethylenetriaminepentacetic acid carrier. *Biophys. Biochem. Acta* 883, 460-467.
- (18) Torchilin, V. P.; Klivanov, A. L.; Nossiff, N. D.; Slinkin, M. A.; Strauss, H. W.; Haber, E.; Smirnov, V. N., and Khaw, B. A. (1987) Monoclonal antibody modification with chelate-linked high-molecular-weight polymers: major increases in polyvalent cation binding without loss of antigen binding. *Hybridoma* 6, 229-240.
- (19) Torchilin, V. P.; Klivanov, A. L.; Slinkin, M. A.; Danilov, S. M.; Levitsky, D. O., and Khaw, B. A. (1989) Antibody-linked chelating polymers for radioimmunomaging in vivo. *J. Controlled Release* 11, 297-303.
- (20) Klivanov, A. L.; Slinkin, M. A., and Torchilin, V. P. (1989) Conjugation of proteins with chelating polymers via water-soluble carbodiimide and N-hydroxysulfosuccinimide. *Appl. Biochem. Biotech.* 22, 45-58.
- (21) Yamamoto, K.; Senda, M.; Fujita, T.; Kumada, K.; Fukui, K.; Yonekura, Y.; Yokoyama, A., and Torizuka, K. (1988) Positive imaging of venous thrombi and thromboemboli with ⁶⁷Ga DFO-DAS-fibrinogen. *Eur. J. Nucl. Med.* 14, 60-64.
- (22) Arnold, L. J.; Dagan, A., and Kaplan, N. O. (1983) Poly(L-lysine) an antineoplastic agent and tumor-specific drug carrier. *Targeted Drugs* (E. P. Goldberg, Ed.) pp 89-112, Wiley-Interscience, New York.
- (23) Pollak, A.; Blumenfeld, H.; Wax, M., and Baughn, R. L.; Whitesides, G. M. (1980) Enzyme immobilization by condensation copolymerization into cross-linked polyacrylamide gels. *J. Am. Chem. Soc.* 102, 6324-6336.
- (24) Sakahara, H.; Endo, K.; Nakashima, T.; Koizumi, M.; Ohta, H.; Torizuka, K.; Furukawa, T.; Ohmomo, Y.; Yokoyama, A.; Okada, K.; Yoshida, O., and Nishi, S. (1985) Effect of DTPA conjugation on the antigen binding activity and biodistribution of monoclonal antibodies against α -fetoprotein. *J. Nucl. Med.* 26, 750-755.
- (25) Koizumi, M.; Endo, K.; Kunimatsu, M.; Sakahara, H.; Nakashima, T.; Kawamura, Y.; Watanabe, Y.; Ohmomo, Y.; Arano, Y.; Yokoyama, A., and Torizuka, K. (1987) Preparation of ⁶⁷Ga-labeled antibodies using deferoxamine as a bifunctional chelate. An improved method. *J. Immunol. Methods* 104, 93-102.
- (26) Meares, C. F.; McCall, M. J.; Reardan, D. T.; Goodwin, D. A.; Diamanti, C. I., and McTigue, M. (1984) Conjugation of antibodies with bifunctional chelating agents: isothiocyanate and bromoacetamide reagents, methods of analysis, and subsequent addition of metal ions. *Anal. Biochem.* 142, 68-78.
- (27) Brechbiel, M. W.; Gansow, O. A.; Atcher, R. W.; Schlom, J.; Esteban, J.; Simpson, D. E., and Colcher, D. (1986) Synthesis of 1-(p-isothiocyanatobenzyl) derivatives of DTPA and EDTA. Antibody labeling and tumor-imaging studies. *Inorg. Chem.* 25, 2772-2781.
- (28) Moi, M. K.; Meares, C. F.; McCall, M. J.; Cole, W. C., and DeNardo, S. J. (1985) Copper chelates as probes of biological systems: stable copper complexes with a macrocyclic bifunctional chelating agent. *Anal. Biochem.* 148, 249-253.

The Oxidative Cleavability of Protein Cross-Linking Reagents Containing Organoselenium Bridges

Troels Koch,[†] Elisabeth Suenson,[‡] Ulla Henriksen,[†] and Ole Buchardt^{*†}

Research Center for Medical Biotechnology, Chemical Laboratory II, The H. C. Ørsted Institute, University of Copenhagen, Universitetsparken 5, DK-2100 Copenhagen, Denmark, and Department of Clinical Chemistry, Rigshospitalet, Blegdamsvej 9, DK-2100 Copenhagen, Denmark. Received April 23, 1990

The intensive use of cleavable cross-linking reagents to study macromolecular biological interactions has shown a demand for optimizing these reagents in such a way that the involved macromolecules remain intact. The present work focuses on the development of selenium linkers that are cleavable by mild oxidation. The efficiency of cross-linking and subsequent cross-linker cleavage with a new series of such homo- or heterobifunctional cross-linking reagents have been tested in a simple model system, consisting of albumin and cytochrome *c*. Resultant, or residual, covalent complex formation is examined by SDS-polyacrylamide gel electrophoresis. From this work it can be concluded that diallyl selenides are readily cleaved by mild oxidation, whereas dialkyl selenides and benzyl alkyl selenides can only be cleaved when the alkyl part of the selenide has an electron-withdrawing group next to the β -carbon from selenium.

INTRODUCTION

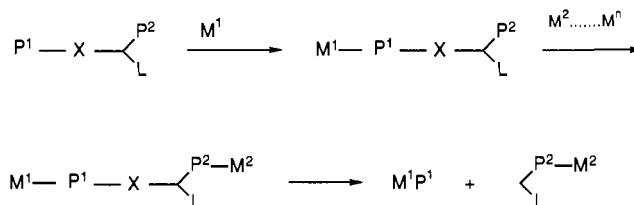
Bifunctional cross-linking reagents are important tools for studying molecular interactions between biological macromolecules (Lundblad & Noyes, 1984; Ji, 1983; Peters & Richards, 1977; Bayley & Knowles, 1977; Buchardt et al., 1989). They allow two-step reactions whereby the interaction between various biological entities can be examined.

Such reagents must contain some or all of the following components (Scheme I): (a) two different reactive probes (P^1 and P^2) (when one of the probes can be activated photochemically, such reagents allow examination of temporal sequences in dynamic macromolecular interactions (Wisniewski & Bramhall, 1981; Ishida et al. 1983)); (b) a linker which preferentially contains a cleavable site ($-X-$); and (c) a label ($-L-$) for detecting cross-linker-modified (entities in) macromolecules and their complexes, as well as allowing their quantification. In Scheme I this is illustrated: A biomolecule M^1 is modified via P^1 . Upon interaction of the modified M^1 with biomolecule M^2 and irradiation, M^1 and M^2 are crosslinked via the photo-probe P^2 . Subsequent cleavage results in label transfer to M^2 (Maassen, 1979; Schwartz et al., 1982).

Cleavability has so far mainly been obtained with $-S-S-$, 1,2-diol, azo-, or ester linkages (Ji & Ji, 1989). Most recently, reagents containing acetals, which are cleaved by treatment with mild acid, have been prepared (Srinivasachar & Neville, 1989). However, the cleavage of conventional linkers is often deleterious to the modified macromolecules. For instance, the molecular structure of many proteins is lost when $-S-S-$ bridges are cleaved (reduction). Thus novel types of cleavable linkers are warranted, and in this paper we present some results with selenium containing linkers.

The basic idea behind the synthesis of selenide containing linkers (selenium bridges) is that selenides can easily be oxidized to yield selenoxides. These oxides are

Scheme I



labile at room temperature and react intramolecularly by β -elimination or rearrangement to cause cleavage of the linker. The mild oxidation necessary to initiate this reaction is in many cases less deleterious to protein structure and activity than alternative procedures (e.g. reduction or hydrolysis).

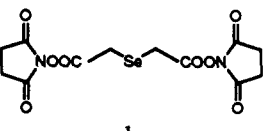
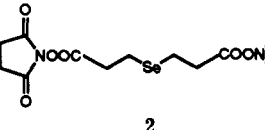
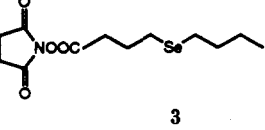
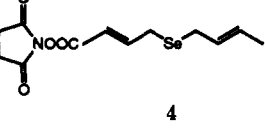
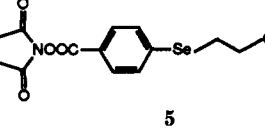
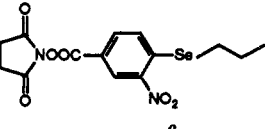
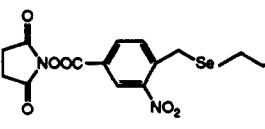
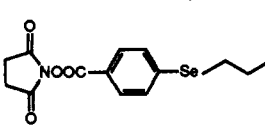
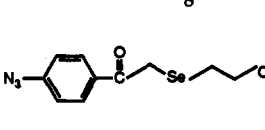
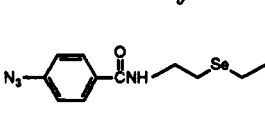
Selenoxide chemistry has been used in a number of different systems (Sharpless & Lauer, 1973; Sharpless et al., 1973; Reich, 1987; 1979; Liotta, 1984), e.g., in double bond precursors in the synthesis of natural products (Grieco et al., 1975; 1976). The necessary elimination/rearrangement reactions have usually been carried out in aprotic organic solvents, and the selenides are typically oxidized with potent oxidants such as hydrogen peroxide, ozone, organic peracids, or periodate.

In order to study the behavior of selenium bridges in protein systems, we have prepared a series of different selenide containing reagents (Table I). Most of the reagents are homobifunctional with amino specific *N*-hydroxysuccinimide thermoprobes (1-8). However, we have also prepared two heterobifunctional reagents (9, 10) on the basis of the well-known 4-azidobenzoyl photoprobes (Lundblad & Noyes, 1984; Ji, 1983; Peters & Richards, 1977; Buchardt et al., 1984; 1989). Upon photolysis of the azide, the generated excited singlet loses nitrogen and ring expands to a dehydroazepine (Nielsen & Buchardt, 1982; Shields et al., 1987; 1988). The dehydroazepine reacts further by addition of nucleophilic groups such as mercapto, amino, or hydroxy. Besides this, which causes cross-linking, other reactions can occur (Nielsen & Buchardt, 1982; Shields et al., 1987).

[†] University of Copenhagen.

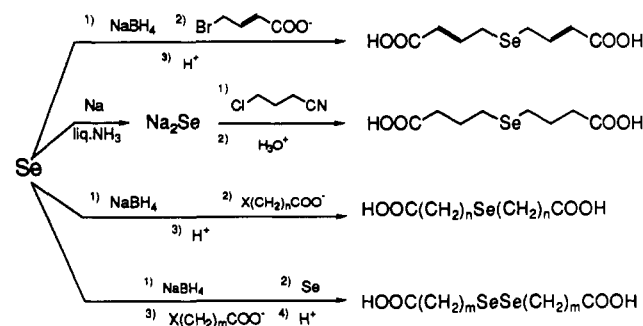
[‡] Rigshospitalet.

Table I

compound	cross-link. eff.	cleavage ^a	
		- amines	+ amines
	+	-	-
1			
	++	++	++
2			
	++	-	-
3			
	++	+	++
4			
	++	-	-
5			
	++	-	-
6			
	++	++	++
7			
	++	-	-
8			
	+	-	-
9			
	+	-	-
10			

^a Designations are as follows: efficient (++), observable (+), absent (-).

The compounds were tested in a model system, consisting of cytochrome *c* (from equine mitochondria) which is a basic protein (*pI* 10.7) with a positive net charge at neutral pH, and albumin (from human serum), which is negatively charged at neutral pH (*pI* 4.7-5.5). Their electrostatic interaction at low ionic strength has previously been demonstrated (Buchardt et al., 1986). *N*-Chloroben-

Scheme II^a

^a X = Cl, Br; *n* = 1, 2; *m* = 2, 3.

zenesulfonamide (chloramine-T) immobilized on polystyrene beads (Iodo-Beads) was used as the oxidizing reagent.

EXPERIMENTAL PROCEDURES

Chemistry. Chemicals for synthesis were commercially available from FLUKA and/or EGA. ¹H and ⁷⁷Se NMR spectra were recorded on a JEOL FX 90Q spectrometer (90 MHz) and mass spectra on a Masslab VG 12-250 instrument. Elemental analyses were performed on a Perkin-Elmer 240 elemental analyzer. Melting points were recorded on a Büchi apparatus and are uncorrected.

The introduction of selenium into organic molecules was done by substitution of halogen by reduced selenium species. The preferred way to produce selenium nucleophiles was analogous to the Klayman and Griffin procedure (Klayman & Griffin, 1973), reduction of elementary selenium in water by sodium borohydride (Scheme II). This worked out well when the selenium anions were subjected to sufficiently reactive molecules: (A) allylic bromo compounds (e.g. 4-bromocrotonic acid), (B) short-chained bromo compounds (e.g. 3-bromopropanoic acid), or (C) activated short-chained chloro compounds (e.g. 2-chloroacetic acid). Diselenides, in contrast to the corresponding monoselenides, substitute chlorine in less reactive molecules (e.g. 4-chlorobutanoic acid) due to their enhanced nucleophilicity.

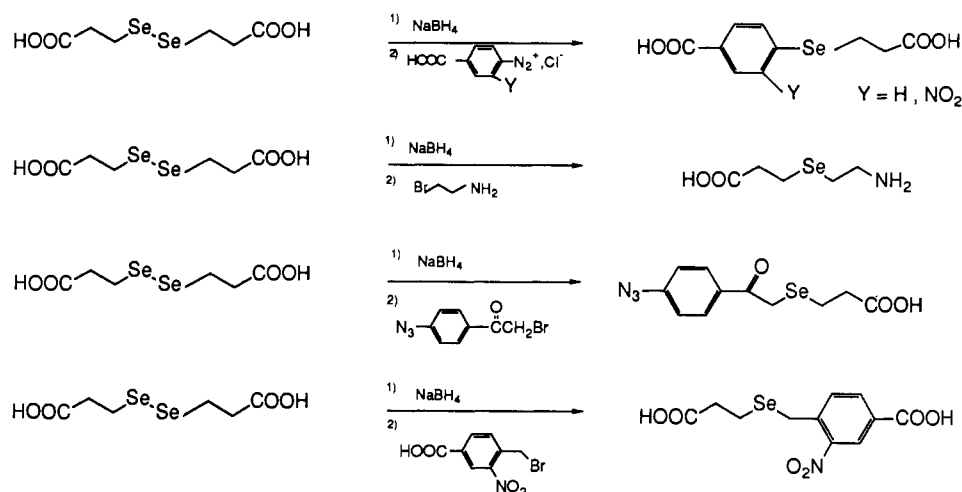
The Klayman and Griffin condition (sodium borohydride reductions in protic solvents) lowers the nucleophilicity of selenium anions, due to the formation of boron complexes of the selenium anions and strong solvation of these (Liotta et al., 1977; 1981; Liotta & Santiesteban, 1977). However, the reduction is very easy and quick to perform, and should be considered when the reaction conditions are suitable.

Substitution of nonactivated chlorine by monoselenides (e.g., in 4-chlorobutyronitrile) requires activation of the selenium species. This can be done by reducing elementary selenium with sodium in liquid ammonia (Agénäs & Lindgren, 1969; Fredga & Bendz 1949). These non-complexed selenide ions are very powerful nucleophiles and readily substitute any aliphatic halogen (Scheme II).

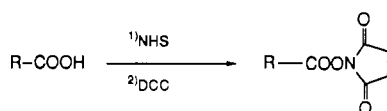
The asymmetric selenides were prepared by reducing diselenides and subjecting these to subsequent reaction with electrophiles (Scheme III). 4-(Bromomethyl)-3-nitrobenzoic acid and 4-azidophenacyl bromide were prepared according to the literature (Hixton & Hixton, 1975; Hephner & Wagner, 1962; Rich & Gurwara, 1975). The amino group specific *N*-hydroxysuccinimide esters were prepared from the corresponding acids by standard procedures (Scheme IV).

Synthesis. Compounds 1 and 2 were prepared analogously to Buchardt et al., 1986. It was found that 1 and

Scheme III



Scheme IV



2 were more conveniently purified by using ethanol in the recrystallization step.

3,3'-Diselenodipropionic Acid. Selenium (3.0 g, 38 mmol) was suspended in degassed water (25 mL). Sodium borohydride (3.0 g, 79 mmol) was dissolved in degassed water (25 mL) and gradually added to the selenium suspension. When the solution was clear, selenium (3.0 g, 38 mmol) was added. The dark red solution was heated to about 40 °C. The whole sequence was carried out under nitrogen. The sodium salt of 3-bromopropionic acid (12.1 g, 79 mmol in water (25 mL)) was added to the selenide solution, and the reaction was stirred over night. After this the solution was filtered and acidified with 4 N HCl and the yellow suspension extracted twice with ethyl acetate. The ethyl acetate solution was filtered, extracted twice with water, dried, and evaporated. The resulting diselenide was recrystallized from ethyl acetate, yield 7.0 g (61%) after recrystallization to analytical purity. ^1H NMR (d_6 -DMSO): δ 2.7 (t, 2 H), 3.1 (t, 2 H). ^{77}Se NMR (d_6 -DMSO): δ 327.7. Mp 128–129 °C (lit. mp 134–135 °C (Agenäs & Lindgren, 1969)). MS m/z : 302/306 ($^{78}\text{Se}/^{80}\text{Se}$). Anal. Calcd for $\text{C}_6\text{H}_{10}\text{O}_4\text{Se}_2$: C, 23.68; H, 3.29. Found: C, 23.85; H, 3.40.

4,4'-Diselenodibutanoic acid was prepared from the sodium salt of 4-chlorobutanoic acid (76 mmol) as described above for 3,3'-diselenodipropionic acid. After addition of 4-chlorobutanoic acid the reaction mixture was refluxed overnight. The workup was similar to that for 3,3'-diselenodipropionic acid. The crude diselenide was recrystallized from aqueous ethanol, yield 4.5 g (36%) after recrystallization to analytical purity. ^1H NMR (d_6 -DMSO): δ 1.91 (m, 2 H), 2.36 (t, 2 H), 2.95 (t, 2 H). ^{77}Se NMR (d_6 -DMSO): δ 301.7. Mp 78–79 °C (lit. mp 85–86 °C (Agenäs & Lindgren, 1969)). MS m/z : 330/334 ($^{78}\text{Se}/^{80}\text{Se}$). Anal. Calcd for $\text{C}_8\text{H}_{14}\text{O}_4\text{Se}_2$: C, 28.94; H, 4.32. Found: C, 28.92; H, 4.42.

4,4'-Selenodibutanoic Acid. Selenium (7.9 g, 0.1 mol) was suspended in liquid ammonia (300 mL), and sodium (4.6 g, 0.2 mol) was slowly added. The reaction was carried out under nitrogen. The color of the suspension was initially black, then light blue, and finally colorless. The ammonia was evaporated, and methanol (300 mL) carefully degassed and kept under nitrogen was added to the light

yellow sodium selenide salt (the solution turned black). 4-Chlorobutyronitrile (19.2 mL, 0.20 mol) was dissolved in methanol (25 mL) and added to the selenide solution. The sodium was refluxed overnight and was almost decolorized after 2 h. Water (100 mL) was added, and the methanol distilled off with use of a column. When 100 mL of methanol had been collected, concentrated aqueous HCl (100 mL) was added, and the solution was refluxed for 6 h. After this the solution was cooled, and the generated precipitate was collected by filtration and recrystallized from water, yield 4 g (16%) after recrystallization to analytical purity. ^1H NMR (CD_3OD): δ 1.92 (m, 2 H), 2.41 (t, 2 H), 2.53 (t, 2 H). Mp 92–93 °C (lit. mp 97–98 °C (Agenäs & Lindgren, 1969)). Anal. Calcd for $\text{C}_8\text{H}_{14}\text{O}_4\text{Se}$: C, 37.95; H, 5.53. Found: C, 37.63; H, 5.48.

4,4'-Selenodibutanoic acid bis(*N*-succinimidyl ester) (3) was prepared from 4,4'-selenodibutanoic acid (1.0 g, 4 mmol), NHS¹ (1.0 g, 8.8 mmol), and DCC (2.0 g, 9.6 mmol), as described for compound 1. The product was recrystallized from methanol, yield 822 mg (46%) after recrystallization to analytical purity. ^1H NMR (CDCl_3): δ 2.01 (m, 2 H), 2.68 (t, 2 H), 2.75 (t, 2 H), 2.83 (s, 4 H). Mp 96.5–98 °C. Anal. Calcd for $\text{C}_{16}\text{H}_{20}\text{N}_2\text{O}_8\text{Se}$: C, 42.95; H, 4.47; N, 6.26. Found: C, 42.72; H, 4.44; N, 6.01.

4-Bromo-2(*E*)-butenoic Acid Methyl Ester. Methyl crotonate (Jeffrey & Vogel, 1948) (50 g, 0.5 mol) was mixed with carbon tetrachloride (75 mL) and *N*-bromosuccinimide (84 g, 0.47 mol) was added. The suspension was refluxed for 21 h during which time it turned red and the succinimide gathered at the surface of the solvent. The succinimide was removed by filtration, and the title compound was purified by vacuum distillation (90–93 °C at 15 mmHg), yield 58 g (65%). ^1H NMR (CCl_4): δ 3.78 (s, 3 H), 4.01 (d, 2 H), 5.95 (d, 1 H), 6.95 (d, 1 H). Anal. Calcd for $\text{C}_5\text{H}_7\text{O}_2\text{Br}$: C, 33.81; H, 3.91; Br, 44.69. Found: C, 32.2; H, 3.79; Br, 45.40.

4,4'-Selenodi-2(*E*)-butenoic Acid Methyl Ester. 4-Bromo-2(*E*)-butenoic acid methyl ester (5.0 g, 28 mmol) was added to a selenium solution (1.1 g of selenium and 1.1 g of sodium borohydride) as described for 2,2'-

¹ Abbreviations: d, deuterium; DCC, dicyclohexylcarbodiimide; DCU, dicyclohexylurea; DMF, dimethylformamide; DMSO, dimethyl sulfoxide; lit., literature reference; mp, melting point; m/z , molecular weight determined by mass spectroscopy (EI); NHS, *N*-hydroxysuccinimide; NMR, nuclear magnetic resonance; SDS, sodium dodecyl sulfate; THF, tetrahydrofuran; s, singlet; d, doublet; dd, doublet of doublets; t, triplet; q, quartet; m, multiplet; δ , chemical shift.

selenodiacetic acid. The water phase was extracted twice with ether. After drying, the ether was evaporated to give an oil (the title compound). This was directly hydrolyzed to the corresponding acid without further purification. However, ^1H NMR and mass spectroscopy confirmed that the oil predominantly contained the title compound. ^1H NMR (CDCl_3): δ 3.32 (d, 4 H), 3.82 (s, 6 H), 6.78 (d, 2 H), 6.97 (m, 2 H). MS m/z : 276/278 ($^{78}\text{Se}/^{80}\text{Se}$).

4,4'-Selenodi-2(E)-butenoic Acid. 4,4'-Selenodi-2-(E)-butenoic acid methyl ester (15 g, 54 mmol) was suspended in 25% aqueous ethanol (150 mL). The suspension was cooled to 2 °C. Barium hydroxide octahydrate (14 g, 44 mmol) was slowly added. The suspension was stirred at 2 °C for 15 h, and for 2 h at room temperature. Water (150 mL) was added to the red suspension, after which it was extracted twice with ether. The water phase was filtered and acidified with 4 N HCl. The brown precipitate was collected by filtration and recrystallized from ethyl acetate, yield 2.5 g (18%) after recrystallization to analytical purity. ^1H NMR ($(\text{CD}_3)_2\text{CO}$): δ 3.39 (d, 4 H), 5.78/5.95 (d, 2 H), 7.96 (m, 2 H). Mp 171–173 °C. MS m/z : 248/250 ($^{78}\text{Se}/^{80}\text{Se}$). Anal. Calcd for $\text{C}_8\text{H}_{10}\text{O}_4\text{Se}$: C, 38.55; H, 4.02. Found: C, 38.48; H, 4.04.

4,4'-Selenodi-2(E)-butenoic acid bis(N-succinimidyl ester) (4) was prepared from 4,4'-selenodi-2-(E)-butenoic acid (500 mg, 2.01 mmol), NHS (506 mg, 4.40 mmol), and DCC (988 mg, 4.79 mmol) as described for 1. The compound was suspended in boiling chloroform, and ethanol was added until a clear solution was obtained, from which the product crystallized upon cooling, yield 445 mg (50.0%) after recrystallization to analytical purity. ^1H NMR (CDCl_3): δ 2.85 (s, 8 H), 3.34 (d, 4 H), 6.0 (d, 2 H), 7.16 (m, 2 H). Mp 162–164 °C. MS m/z : 442/444 ($^{78}\text{Se}/^{80}\text{Se}$). Anal. Calcd for $\text{C}_{16}\text{H}_{16}\text{O}_8\text{N}_2\text{Se}$: C, 43.34; H, 3.61; N, 6.32. Found: C, 42.98; H, 3.54; N, 6.18.

3-[(4-Carboxyphenyl)seleno]propanoic Acid. 4-Aminobenzoic acid (2.7 g, 18 mmol) was dissolved in water (40 mL) and concentrated HCl (4.5 mL) to which sodium nitrite (1.2 g) in water (10 mL) was added dropwise. 3,3'-Diselenodipropanoic acid (2.74 g, 9.01 mmol) was suspended in water (10 mL) and sodium borohydride (about 3 g) was added until the diselenide was dissolved and the solution decolorized. The reduced diselenide was added dropwise at 4 °C to the solution containing the diazonium salt, and a light yellow precipitate was formed. This was collected by filtration and recrystallized from chloroform/ethanol (1/1 v/v). ^1H NMR (d_6 -DMSO): δ 2.74 (t, 2 H), 3.14 (t, 2 H), 7.55 (d, 2 H), 7.84 (d, 2 H). Mp 187–189 °C. MS m/z : 272/274 ($^{78}\text{Se}/^{80}\text{Se}$). Anal. Calcd for $\text{C}_{10}\text{H}_{10}\text{O}_4\text{Se}$: C, 43.95; H, 3.66. Found: C, 43.34; H, 3.51.

3-[[4-[(Succinimidyl)oxy]carbonyl]phenyl]seleno]propanoic acid N-succinimidyl ester (5) was prepared from 3-(4-carboxyphenyl)selenopropanoic acid (80 mg, 0.30 mmol), NHS (80 mg, 0.60 mmol), and DCC (124 mg, 0.60 mmol) analogously to the method described for compound 1, yield 79 mg (57%) after recrystallization to analytical purity. ^1H NMR (CDCl_3): δ 2.84 (s, 4 H), 2.90 (s, 4 H), 3.20 (t, 2 H), 3.40 (t, 2 H). MS m/z : 466/468 ($^{78}\text{Se}/^{80}\text{Se}$). Anal. Calcd for $\text{C}_{18}\text{H}_{16}\text{O}_8\text{N}_2\text{Se}$: C, 46.30; H, 3.50; N, 6.00. Found: C, 47.11; H, 3.65; N, 6.10.

3-[(4-Carboxy-2-nitrophenyl)seleno]propanoic Acid. 4-Amino-3-nitrobenzoic acid (Lucius and Bruning, 1902; Kaiser, 1885; Ullman and Mauthner, 1903) (4.0 g, 22 mmol) was suspended in 4 N H_2SO_4 (30 mL) and diazotized with sodium nitrite (1.5 g, 26 mmol) in water (8 mL) (below 4 °C). The solution was filtered before further use, and 3,3'-diselenodipropanoic acid was reduced and added to the

diazonium salt as described above for 3-[(4-carboxyphenyl)seleno]propanoic acid. The precipitate was collected by filtration and dissolved in ethyl acetate. The ethyl acetate phase was extracted twice with 0.02 M sodium hydrogen carbonate. The alkaline water phase was acidified with 4 N HCl and a precipitate was formed, which was collected, dried, and recrystallized from aqueous ethanol, yield 2.1 g (31%) after recrystallization to analytical purity. ^1H NMR (d_6 -DMSO): δ 2.76 (t, 2 H), 3.23 (t, 2 H), 7.87 (d, 1 H), 8.14 (d, 1 H), 8.66 (s, 1 H). ^{77}Se (d_6 -DMSO): δ 394.0. Mp 257–260 °C. MS m/z : 317/319 ($^{78}\text{Se}/^{80}\text{Se}$). Anal. Calcd for $\text{C}_{10}\text{H}_9\text{O}_6\text{NSe}$: C, 37.74; H, 2.83; N, 4.40. Found: C, 37.63; H, 2.92; N, 4.65.

3-[[[(4-Succinimidyl)oxy]carbonyl]-2-nitrophenyl]seleno]propanoic acid N-succinimidyl ester (6) was prepared from 3-[(4-carboxy-2-nitrophenyl)seleno]propanoic acid (655 mg, 2.04 mmol), NHS (515 mg, 4.50 mmol), and DCC (843 mg, 4.04 mmol) as described for compound 1. The title compound was crystallized from chloroform/ethanol (9/1, v/v) by adding a little petroleum ether (bp > 80 °C), yield 690 mg (66%) after recrystallization to analytical purity. ^1H NMR (d_6 -acetone): δ 2.89 (s, 4 H), 2.99 (s, 4 H), 3.25 (t, 2 H), 3.56 (t, 2 H), 8.23 (d, 1 H), 8.37 (d, 1 H), 8.93 (s, 1 H). ^{77}Se NMR (d_6 -acetone): δ 414.4. Mp 189–191 °C. MS m/z : 511/513 ($^{78}\text{Se}/^{80}\text{Se}$). Anal. Calcd for $\text{C}_{18}\text{H}_{15}\text{O}_{10}\text{N}_3\text{Se}$: C, 42.15; H, 2.93; N, 8.20. Found: C, 41.64; H, 2.97; N, 8.06.

5-(2-Nitro-4-carboxyphenyl)-4-selenapentanoic Acid. 4-(Bromomethyl)-3-nitrobenzoic acid (Rich & Gurvara, 1975) (3.0 g, 11.4 mmol) was dissolved in degassed DMF (75 mL). 3,3'-Diselenodipropanoic acid (1.8 g, 5.76 mmol) was suspended in degassed water, and sodium borohydride (432 mg, 11.4 mmol) was added. The reduced diselenide was then added to the DMF solution which turned yellow at once. Subsequently water (300 mL) was poured into the solution, which was acidified with 4 N HCl and extracted three times with ether. The combined ether phases were washed once with water and dried (MgSO_4). The solvent was removed by evaporation, in vacuo, and the light yellow residue was recrystallized from water, yield 3.51 g (93%) after recrystallization to analytical purity. ^1H NMR (d_6 -DMSO): δ 2.51 (t, 2 H), 2.59 (t, 2 H), 4.16 (s, 2 H), 8.21 (d, 1 H), 8.45 (d, 1 H), 8.4 (s, 1 H). Mp 173–174 °C. Anal. Calcd for $\text{C}_{11}\text{H}_{11}\text{O}_6\text{NSe}$: C, 39.79; H, 3.30; N, 4.22. Found: C, 40.27; H, 3.24; N, 4.33.

5-[2-Nitro-4-[(succinimidyl)oxy]carbonyl]phenyl]-4-selenapentanoic acid N-succinimidyl ester (7) was prepared from 5-(2-nitro-4-carboxyphenyl)-4-selenapentanoic acid (1.0 g, 3.0 mmol), NHS (762 mg, 6.60 mmol), and DCC (1.48 g, 7.20 mmol) analogously to the method described for 1, and recrystallized from ethanol/ethyl acetate (1:1), yield 1.14 g (72%) after recrystallization to analytical purity. ^1H NMR (CDCl_3): δ 2.85 (s, 4 H), 2.88 (t, 2 H), 2.92 (s, 4 H), 3.03 (t, 2 H), 7.60 (d, 1 H), 8.27 (d, 1 H), 8.76 (s, 1 H). Anal. Calcd for $\text{C}_{19}\text{H}_{17}\text{N}_3\text{O}_{10}\text{Se}$: C, 43.34; H, 3.23; N, 7.98. Found: C, 43.55; H, 3.31; N, 7.94.

4-[(4-Carboxyphenyl)seleno]butanoic acid was prepared from 4-aminobenzoic acid (0.82 g, 6 mmol) dissolved in water (13.5 mL) and concentrated HCl (1.5 mL), and diazotized with sodium nitrite (0.40 g, 5.8 mmol in 4 mL water). 4,4'-Diselenodibutanoic acid (1 g, 3 mmol) was reduced and added to the diazonium salt as described for 3-[(4-carboxyphenyl)seleno]propanoic acid. The collected material was recrystallized from chloroform/ethanol, yield 600 mg (35%) after recrystallization to analytical purity. ^1H NMR (CDCl_3): δ 2.15 (m, 2 H), 2.33 (t, 2 H), 2.95 (t, 2 H), 7.53 (d, 2 H), 7.77 (d, 2 H). Mp

197–200 °C. MS m/z : 286/288 ($^{78}\text{Se}/^{80}\text{Se}$). Anal. Calcd for $\text{C}_{11}\text{H}_{12}\text{O}_4\text{Se}$: C, 45.98; H, 4.18. Found: C, 45.43; H, 4.09.

4-[[[(4-Succinimidyl)oxy]carbonyl]phenyl]seleno]butanoic acid *N*-succinimidyl ester (8) was prepared from 4-[(4-carboxyphenyl)seleno]butanoic acid (100 mg, 0.29 mmol), NHS (80 mg, 0.6 mmol), and DCC (124 mg, 0.6 mmol) as described for 1 and purified on a silica gel column (eluent $\text{CH}_2\text{Cl}_2/\text{ethanol}$ 19/1, v/v), yield, 61 mg (51%). ^1H NMR (CDCl_3): δ 2.16 (m, 2 H), 2.78 (t, 2 H), 2.84 (s, 4 H), 2.93 (s, 4 H), 3.12 (t, 2 H), 7.55 (d, 2 H), 7.98 (d, 2 H). Mp 125–129 °C. MS m/z : 480/482 ($^{78}\text{Se}/^{80}\text{Se}$). Anal. Calcd for $\text{C}_{19}\text{H}_{18}\text{O}_8\text{N}_2\text{Se}$: C, 47.40; H, 3.74; N, 5.82. Found: C, 46.96; H, 3.70; N, 5.73.

3-[(4-Azidophenacyl)seleno]propanoic Acid. 4-Azidophenacyl bromide (Hixton & Hixton, 1975; Hephher & Wagner, 1962) (1.5 g, 6.3 mmol) was dissolved in DMF (100 mL). 3,3'-Diselenodipropionic acid (0.95 g, 3.1 mmol) was suspended in degassed water and reduced with sodium borohydride (to decolorization). This solution was acidified with 4 N HCl and added to the DMF solution from above. After 5 min water (200 mL) was added to the reaction mixture to give a suspension which was extracted twice with ether. The ether phase was extracted twice with 0.5 M sodium hydrogen carbonate. The aqueous phase was acidified and extracted twice with ether. The ether phase was washed once with distilled water and dried, and the ether was evaporated. The white product was recrystallized from water/ethanol 1/1 (v/v), yield 1.02 g (52%) after recrystallization to analytical purity. ^1H NMR (d_6 -DMSO): δ 2.6 (t, 4 H), 3.96 (s, 2 H), 7.22 (d, 2 H), 8.04 (d, 2 H). ^{77}Se NMR (CDCl_3): δ 239.3. Mp 94–95 °C. MS m/z : 311/313 ($^{78}\text{Se}/^{80}\text{Se}$). Anal. Calcd for $\text{C}_{11}\text{H}_{11}\text{O}_3\text{N}_3\text{Se}$: C, 42.31; H, 3.53; N, 13.46. Found: C, 42.25; H, 3.56; N, 13.30.

3-[(4-Azidophenacyl)seleno]propanoic acid *N*-succinimidyl ester (9) was prepared from 3-[(4-azidophenacyl)seleno]propanoic acid (700 mg, 2.24 mmol), NHS (281 mg, 2.44 mmol), and DCC (461 mg, 2.24 mmol) as described for 1. When the THF was removed an oil remained. Petroleum ether (50 mL, bp 30–50 °C) was added and evaporated whereafter crystals remained. These were recrystallized from ethanol/chloroform, yield 540 mg (59%) after recrystallization to analytical purity. ^1H NMR (CDCl_3): δ 2.83 (s, 4 H), 2.97 (t, 2 H), 3.05 (t, 2 H), 3.83 (s, 2 H), 7.08 (d, 2 H), 7.97 (d, 2 H). ^{77}Se NMR (CDCl_3): δ 293.4. Mp 98–100 °C. MS m/z : 408/410 ($^{78}\text{Se}/^{80}\text{Se}$). Anal. Calcd for $\text{C}_{15}\text{H}_{14}\text{O}_5\text{N}_4\text{Se}$: C, 44.01; H, 3.43; N, 13.59. Found: C, 43.84; H, 3.43; N, 13.61.

3-[(2-Aminoethyl)seleno]propanoic Acid. 3,3'-Diselenodipropionic acid (1 g, 3.3 mmol) was dissolved in 30 mL of degassed ethanol and reduced with sodium borohydride under nitrogen to decolorization. 2-Bromoethanamine (6.6 mmol) was added and the reaction mixture was stirred overnight, concentrated and applied to a column of Dowex 50X8 ion-exchange resin (acidic form). The column was washed with water and eluted with 0.5 N aqueous ammonia. The solution was evaporated and the residue was recrystallized from methanol and used without further purification, yield 850 mg (66%). ^1H NMR (D_2O): δ 2.68 (m, 6 H), 3.20 (t, 2 H).

3-[[2-(4-Azidobenzamido)ethyl]seleno]propanoic Acid. *N*-Succinimidyl 4-azidobenzoate (520 mg, 2 mmol) and 3-[(2-aminoethyl)seleno]propanoic acid (392 mg, 2 mmol) were dissolved in dry dioxane/methanol (1:1, v/v, 15 mL) containing triethylamine (0.5 mL) and allowed to stand overnight at ambient temperature. The reaction mixture was evaporated, 4 N HCl was added, and the

solution was extracted with chloroform. After evaporation, the residue was recrystallized from chloroform/ether and used without further purification, yield 380 mg (56%). ^1H NMR (d_6 -DMSO): δ 2.70 (t, 4 H), 2.73 (t, 2 H), 3.46 (q, 2 H), 7.20 (d, 2 H), 7.90 (d, 2 H), 8.67 (t, 1 H).

3-[[2-(4-Azidobenzamido)ethyl]seleno]propanoic Acid *N*-Succinimidyl Ester (10). NHS (115 mg, 1 mmol), DCC (227 mg, 1.1 mmol), and 3-[[2-(4-azidobenzamido)ethyl]seleno]propanoic acid (341 mg, 1 mmol) were dissolved in dry dioxane and allowed to stand overnight at ambient temperature. After filtration, the solution was evaporated, and the residue was washed with ether and recrystallized from 2-propanol, yield 225 mg (51%). ^1H NMR (CDCl_3): δ 2.88 (s, 4 H), 2.9 (m, 6 H), 3.71 (q, 2 H), 6.85 (t, 1 H), 7.06 (d, 2 H), 7.81 (d, 2 H). Mp 110–111 °C. Anal. Calcd for $\text{C}_{16}\text{H}_{17}\text{N}_5\text{O}_5\text{Se}$: C, 43.84; H, 3.92; N, 15.98. Found: C, 43.90; H, 3.86; N, 15.90.

Biochemistry. Albumin (human, "essentially globulin free"), and cytochrome *c* (type IV, horse heart), were from the Sigma Chemical Company. Iodo-Beads were from Pierce. Calibration proteins for SDS-polyacrylamide gel electrophoresis, Low Molecular Markers (LMW: phosphorolase (M_r 94 000), albumin (M_r 67 000), ovalbumin (M_r 43 000), carbonic anhydrase (M_r 30 000), trypsin inhibitor (M_r 20 100), and α -lactalbumin (M_r 14 400)) were from Pharmacia, Uppsala, Sweden.

Lyophilized albumin and cytochrome *c* were weighed and their respective molecular weights, 67 000 and 13 000 Da, used to calculate their concentration in solution. SDS-polyacrylamide gel electrophoresis was performed as described by Weber, Pringle, and Osborn (Weber et al., 1975) in homogeneous 7.5% polyacrylamide gel slabs. Prior to electrophoresis SDS and urea were added to the protein (reaction) mixtures to final concentrations of 35 mM and 6 M, respectively. The standard marker proteins of variable molecular weight were reduced by the further addition of dithioerythritol to a final concentration of 100 mM. All reaction mixtures were hereafter incubated for 45 min at 56 °C. Following electrophoresis, gels were fixed and stained for 0.5 h at 55 °C in 7% acetic acid containing 0.02% Commassie Brilliant Blue R 250 and destained in 7% acetic acid.

Cross-linking efficiency and cleavability were qualitatively determined by the degree of staining of the albumin-cytochrome *c* complex band(s). Optimal degrees of cross-linking (denoted ++, in Table I) were, in addition to the intensity of the complex bands, chosen by the criterion that a band reflecting a trimolecular complex of albumin and two molecules of cytochrome *c* was clearly distinguishable.

Cross-linking of proteins was carried out in sodium phosphate buffer (6.93 mM, $I = 0.02$, pH = 8.0), containing 15 μM albumin and 30 μM cytochrome *c*, and 0.25 mM cross-linking reagent. Stock solutions (25 mM or 15 mM) of the cross-linking reagents were prepared in DMSO and/or acetonitrile. The volume of organic solvents was less than 1.5% of the volume of the final reaction mixture. The protein complexes were incubated for 1 h at room temperature with the crosslinking reagents. Photoactivated reagents were irradiated for 5 min in a Rayonet reactor equipped with 300-nm light tubes.

Cleavage of the cross-linked proteins was done by incubating the reaction mixtures with two Iodo-Beads per 150 μL reaction mixture alone or with 10 mM diisopropylamine for 1 h.

RESULTS

The synthesized compounds are shown in Table I, which also summarizes their cross-linking efficiency and cleav-

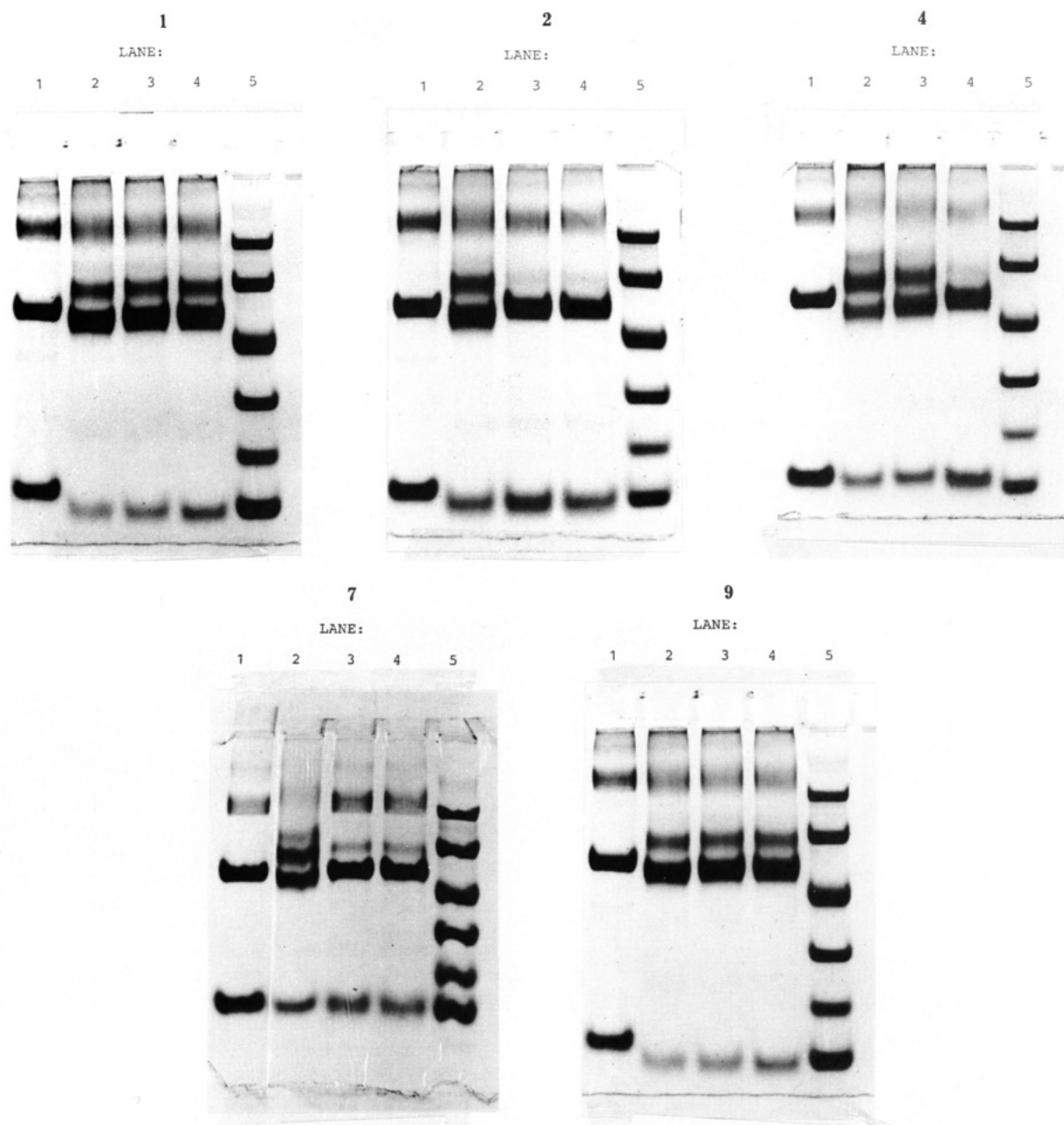


Figure 1. Polyacrylamide electrophoreses of experiments with selected compounds: 1, 2, 4, 7, 9. For each compound five lanes have been run: lane 1, noncross-linked proteins; lane 2, cross-linked proteins; lane 3, cross-linked material oxidized with Iodo-Beads; lane 4, cross-linked material oxidized with Iodo-Beads in the presence of diisopropylamine (10 mM); lane 5, reduced low molecular markers (LMW), with the following molecular masses: 94 000, 67 000 (albumin), 43 000, 30 000, 20 100, and 14 000, run following reduction with 75 mM dithioerythritol as described in the Experimental Procedures.

ability. Examples of the primary data obtained (with reagents 1, 2, 4, 7, and 9) upon examination of the model protein electrophoretic system are shown in Figure 1. Control electrophoresis of the two proteins involved in complex formation reveals high molecular weight bands which by separate experiments were shown to stem from the albumin preparation and likely represent albumin polymers, especially albumin dimer. (Their mobilities do not interfere with those of albumin-cytochrome *c* complexes and it was therefore deemed superfluous to remove them from the commercial albumin preparation.)

The mobility of albumin in SDS-polyacrylamide gel electrophoresis is influenced by reduction and by cross-linking. Reduction results in impeded mobility (compare the mobility of albumin in lanes 5 and 1 of all gel slabs, Figure 1), whereas efficient cross-linking increases albumin mobility. Cross-linker cleavage reverses this latter effect, (see for example experiments with reagent 4).

Cross-Linking. The homobifunctional reagents (1–8) are generally more efficient cross-linkers than the two heterobifunctional reagents with aryl azide photoprobes (9 and 10). The different homobifunctional reagents cross-link to about the same extent, although 4 and 7 seem to be particularly efficient (Figure 1, reagents 2, 4, and 7) and 1 is less efficient.

Cross-Linker Cleavage. Proteins cross-linked with reagents 2, 4, and 7 were found to be readily cleaved by oxidation with Iodo-Beads. Those cross-linked with reagent 4 can only be totally cleaved in the presence of amines, whereas no amine effect is found on the cleavage of proteins cross-linked with reagents 2 and 7. Proteins cross-linked with the other reagents were not cleavable.

Stronger oxidizing reagents (e.g. hydrogen peroxide, sodium periodate) were found to be deleterious to the proteins (results not published). The protein bands in the

gels disappeared even at oxidant concentrations smaller than that of the cross-linker reagents originally used (0.25 mM).

We tested three secondary amines as cleavage enhancers and found that diisopropylamine was the best.

DISCUSSION

The Model Electrophoretic System and Its Usefulness in Determining Cross-Linker Efficiency and Cross-Linker Cleavage. Both reduction of albumin with dithioerythritol and cross-linking are shown to influence its mobility (Figure 1). The fact that reduction results in impeded mobility compared to nonreduced samples is not surprising (Weber et al., 1972).

The reversible influence of cross-linking particularly on albumin mobility in the electrophoretic system is most probably caused by intramolecular cross-linking. This may exert conformational constraints (just as do disulfide bridges) fixing the protein in a tighter conformation than exposure to SDS (and urea) otherwise would allow.

The relatively marginal change in mobility caused by cross-linking however does not prevent distinct identification of the albumin band as well as the bands of dimolecular complex formation between albumin and cytochrome *c* or trimolecular complex formation between albumin and two molecules of cytochrome *c*, (Figure 1, reagents 2, 4, and 7; Buchardt et al., 1986).

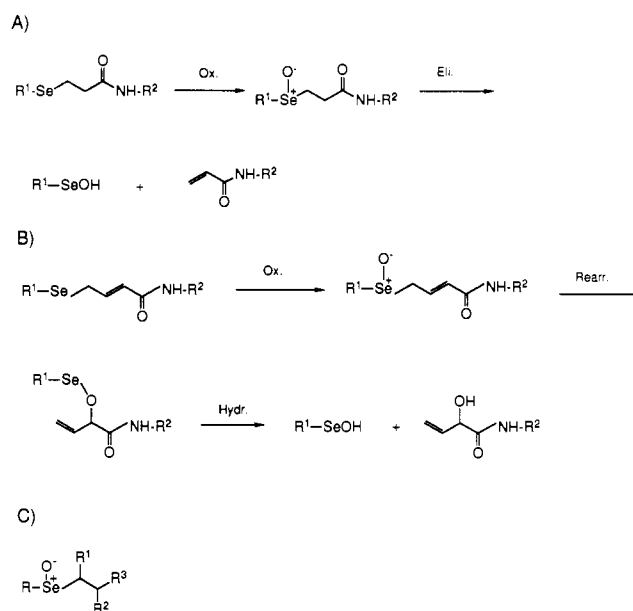
Cross-Linking. The relatively inefficient cross-linking found with the heterobifunctional reagents is probably a result of the nonproductive reactions of aryl azide upon photolysis (Shields et al., 1987), which will always reduce the yield for such reagents. However, the yield is good enough for practical use. The lower cross-linking efficiency of reagent 1 may be related to its relatively short linker length.

Cross-Linker Cleavage. It is necessary to look at the fundamental selenium chemistry in order to explain the cleavability pattern. Successful cleavage of selenium bridges and permanent separation of the previously cross-linked proteins involve three successive steps: (1) oxidation to selenoxide; (2) elimination or rearrangement of the selenoxide; (3) prevention of reunion of the separated proteins induced by the cleavage products.

Oxidation of the selenide (step 1) is known to be feasible even by mild oxidation (as has previously been demonstrated for reagent 2 (Buchardt et al., 1986)). Mild oxidation conditions are requisite to the preservation of protein structure and function which in turn are necessary for their (optimal) detection and identification. This is the case with immunological procedures and with analyses based on e.g. intrinsic enzymatic activity or receptor function. In aqueous solution the *N*-chlorosulfonamide component of Iodo-Beads hydrolyses to give rise to low concentrations of the actual oxidizing species, HOCl (Seever & Counsell, 1982; Jennings, 1974). However, this may also have deleterious effects on the involved proteins (Stagg et al., 1970; Alexander, 1973), probably as a result of histidine, tyrosine, and/or tryptophan residue modification.

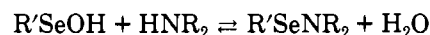
In the second step of cleavage, two mechanisms may be operating (Scheme V): (A) The selenoxides formed after use of reagents 2, 3, and 5–10 are able to undergo β -elimination equivalent to the Cope and sulfoxide eliminations. The two latter require elevated temperatures, in contrast to the selenoxide elimination, which often runs smoothly at room temperature (Sharpless & Lauer, 1973; Sharpless et al., 1973; Reich, 1979; 1987; Liotta, 1984). (B) The allylic selenoxide from reagent 4 can undergo 2,3-

Scheme V



sigmatropic rearrangement which proceeds even more easily than elimination (Scheme V part B). Thus, for selenoxides where both β -elimination and 2,3-sigmatropic rearrangement are possible, the latter is the most abundant (Reich, 1987).

Reunion of the proteins after cleavage (step 3) may be caused by an addition of the selenenic acid and the olefin products. This produces α -hydroxy selenides, which will not eliminate under mild conditions (see below). However, this side reaction can be avoided by trapping the selenenic acid with amines:



Although selenenamides are hydrolyzable, an excess of amine will eliminate the selenium electrophiles by forcing the equilibrium to the right. These general rules are obeyed for cleaving of reagents 2, 4, and 7.

However, for the other reagents, which are noncleavable under the general conditions, unwanted interference in the cleaving sequence is taking place. Use of reagent 1, which contains no β -hydrogens (hydrogens attached to the carbon β to selenium, Scheme V part C), cannot lead to cleavage, and it was prepared as a negative control. However reagent 3, which contains hydrogens β to selenium and therefore is theoretically able to cleave, does not. This shows that available hydrogens β to selenium are not the only necessary requisite for cleavability. It has been shown that electron-withdrawing substituents in the β -position (R^2 or R^3 , Scheme V part C) strongly accelerate the rate of elimination (cf. Reich et al., 1978; Back, 1987). The opposite is found for electron-donating substituents which decrease the rate of elimination, whereas α -alkyl groups (R^1) increase the rate of elimination. The β -effect is clearly demonstrated by the difference in cleavability with 2 and 3: 2 has a carbonyl group in the β -position and cleaves, whereas 3 has an alkyl group and does not. The lack of cleavage with 8 is also related to this.

In aqueous systems this need to "activate" the alkyl parts of the reagents (electron-withdrawing groups in the β -position) is necessary, because water will markedly decrease the rate of selenoxide elimination by forming powerful hydrogen bonds to the selenoxide (Reich et al., 1978).

The position of electron-attracting groups in the β -position is not the only prerequisite for cross-linker

cleavage. Note that proteins cross-linked with 5 and 6 are noncleavable. Such aryl alkyl selenides are generally known to give higher elimination yields when oxidized than dialkylselenides (Labar et al., 1978; 1978). This is particularly true for alkyl selenoxides bearing an electron-withdrawing group on the benzene ring (Sharpless & Young, 1975). It is therefore surprising that proteins cross-linked by 5 or 6 were not cleaved in our system. Aryl alkyl selenoxides are known to be very labile and any stabilization of the selenoxide by the solvent, via hydrogen bonding, can also be excluded as the cause of inefficient cleavage with 5 and 6 because this effect is comparable to the solvent effects exerted on cleavable reagents such as 2 and 7. Most likely, the cleavage sequence is simply not initiated, i.e. these aryl alkyl selenides are not oxidized under the circumstances.

The two heterobifunctional reagents 9 and 10 were found to give noncleavable adducts (Figure 1, reagent 9). It is also believed that the noncleavability with 9 is due to lack of selenium oxidation under the reaction conditions.

The lack of cleavage with 10 is not believed to be an oxidation problem (results not published). Reagent 10 was constructed such that the electronic surroundings of the selenium atom were analogous to those of reagent 2 which was readily cleaved. It is expected that an oxidant is unable to discriminate between selenium in the structure $-\text{CH}_2-\text{CH}_2-\text{Se}-\text{CH}_2-\text{CH}_2-$ in 10 and in 2, which could indicate that 10 is readily oxidized. Furthermore, 10 contains a carbonyl group in the right position which should promote cleavage. The effect of amines was insignificant, and therefore reunion of separated species is not acting here. Selenoxides are very polarized species, which count for the hydration (Reich et al., 1978), but this effect should not be more significant here than with reagents 2 and 7. However, another and more powerful stabilization of selenoxides is due to intramolecular hydrogen bonding, which presumably is exerted here between the selenoxide and the amide group. Such intramolecular hydrogen bonding between selenoxides and amides has been shown to block elimination completely (Detty, 1980; Toshimitsu et al., 1981).

The rates of 2,3-sigmatropic rearrangements of selenoxides at room temperature are very high. We therefore prepared a cross-linking reagent containing allylic selenides. This reagent led to easy cleavage, and, consequently, the three demands set up at the beginning of the discussion are fulfilled. However, efficient cleavage can only be obtained in the presence of excess amine. This is presumably due to the presence of unconjugated double bonds, which add selenic acids. This addition is blocked by amines.

CONCLUSION

This work describes which structural features of selenium linkers in cross-linking reagents are requisite to their cleavage by mild oxidation. We find that: (1) Dialkyl selenides can be cleaved effectively upon moderate oxidation as a result of rearrangement if amines are added. (2) Dialkyl and benzyl alkyl selenides will eliminate if the alkyl part has an acidifying group next to the β -hydrogen. (3) Aryl alkyl selenides are found not to eliminate. (4) It is confirmed that groups (such as the amido groups in reagent 10) that exert a stabilizing effect on the selenoxide must be avoided.

ACKNOWLEDGMENT

Support by the Danish Research Center for Medical Biotechnology and the Danish Medical Science Research Council (Grant No. 12-8557 to E.S.) is gratefully ac-

knowledgeed. We thank Mogens Andersen for helpful discussions and Birgitte Korsholm for technical assistance.

LITERATURE CITED

- Agenäs, L.-B., and Lindgren, B. (1969) Mass spectrometry of organo-selenium compounds. IV. Mass spectra of a series of straight chain seleno- and diseleno-dicarboxylic acids. *Ark. Kemi* 30, 529-547.
- Alexander, N. M. (1973) Oxidation and oxidative cleavage of tryptophanyl peptide bonds during ionization. *Biochem. Biophys. Res. Comm.* 52, 614-621.
- Back, T. G. (1987) Preparative uses of organoselenium and organotellurium compounds. In *The Chemistry of Organoselenium and Tellurium Compounds* (S. Patai, Ed.) Vol. 2, pp 94-194, J. Wiley and Sons Ltd, New York.
- Bayley, H., and Knowles, J. R. (1977) Photoaffinity labeling, in *Meth. Enzymol.* (W. B. Jacoby and M. Wilchek, Eds.) 46, 69-114.
- Buchardt, O., Erbar, U., Larsen, C., et al. (1984) Designing photoaffinity labeling reagents for chromatin studies. *J. Org. Chem.* 49, 4123-4127.
- Buchardt, O., Elsner, H. I., Nielsen, P. E., et al. (1986) Protein crosslinking reagents containing a selenoethylene linker are cleaved by mild oxidation. *Anal. Biochem.* 158, 87-92.
- Buchardt, O., Henriksen, U., Koch, T. and Nielsen, P. E. (1989) Photolabeling Reagent Design, in *Photochemical Probes in Biochemistry* (P. E. Nielsen, Ed.) Vol. 272, pp 1-9, NATO. ASI Series, Kluwer Academic Publishers, Lancaster, UK.
- Denny, J. B., and Blobel, G. (1984) ^{125}I -labeled crosslinking reagent that is hydrophilic, photoactivable, and cleavable through an azo linkage. *Proc. Natl. Acad. Sci. U.S.A.* 81, 5286-5290.
- Detty, M. R. (1980) Oxidation of selenides and tellurides with positive halogenating species. γ -Seleno derivatives of butyric acid. *J. Org. Chem.* 45, 274-279.
- Fredga, A., and Bendz, G. (1949) *Sven. Kem. Tidskr.* 7, 119-225.
- Grieco, P. A., Hiroi, K., Reap, J. J., et al. (1975) Model studies directed toward the total synthesis of vernolepin, III. Synthesis of the α -methylene- δ -valerolactone AB ring model. *J. Org. Chem.* 40, 1450-1453.
- Grieco, P. A., Gilman, S. and Nishizawa, M. (1976) Organoselenium chemistry. A facile one-step synthesis of alkyl aryl selenides from alcohols. *J. Org. Chem.* 41, 1485-1486.
- Hepher, M., and Wagner, H. M. (1962) Light-sensitive layer for photomechanical reproduction. *Chem. Abstr.* 57, 3016i.
- Hixton, S. H., and Hixton, S. S. (1975) *p*-Azidophenacyl bromide, a versatile photolabile bifunctional reagent. Reaction with glyceraldehyde-3-phosphate dehydrogenase. *Biochemistry* 14, 4251-4254.
- Ishida, B., Cawley, D. B., Reue, K., et al. (1983) Lipid-protein interactions during ricin toxin insertion into membranes. *J. Biol. Chem.* 258, 5933-5937.
- Jeffery, G. H., and Vogel, A. I. (1948) Physical properties and chemical constitution. Part XVI. Ethylenic compounds. *J. Chem. Soc.* 658-673.
- Jennings, V. J. (1974) Analytical applications of chloramine-T. *Crit. Revs Anal. Chem.* 407-419.
- Ji, T. H. (1983) Bifunctional Reagents. *Methods Enzymol.* (C. H. W. Hirs and S. B. Timasheff, Eds.) 91, 580-601.
- Ji, T. H. and Ji I. (1989) Heterobifunctional photoaffinity labeling reagents. *Pharm. Ther.* 43, 321-332.
- Kaiser, A. (1885) Mono-nitro derivatives of *p*- and *m*-acetamidobenzoic acid and their reduction products (anhydro acids). *Chem. Ber.* 19, 2942-2945.
- Klayman, D. L., and Griffin, T. S. (1973) Reaction of selenium with sodium borohydride in protic solvents. A facile method for the introduction of selenium ions into organic molecules. *J. Am. Chem. Soc.* 95, 197-199.
- Labar, D., Dumont, W., Hevesi, L., et al. (1978) Synthetic connective route to allyl alcohols from carbonyl compounds. *Tetrahedron Lett.* 13, 1145-1148.
- Labar, D., Hevisi, L., Dumont, W., et al. (1978) Olefin synthesis from selenides and selenoxides. *t*-Butylhydroperoxide-alumina, a powerful reagent for selenide oxidation-elimination. *Tetrahedron Lett.* 13, 1141-1144.

- Liotta, D. (1984) New organoselenium methodology. *Acc. Chem. Res.* 17, 28-34.
- Liotta, D., Sunay, U., Santiesteban, H., et al. (1981) Phenyl selenide anion, a superior reagent for the S_N2 cleavage of esters and lactones. *J. Org. Chem.* 46, 2605-2610.
- Liotta, D., Markiewicz, W., and Santiesteban, H. (1977) The generation of uncomplexed phenyl selenide anion and its applicability to S_N2 -type ester cleavages. *Tetrahedron Lett.* 50, 4365-4368.
- Liotta, D., and Santiesteban, H. (1977) Nucleophilic ring opening of lactones via S_N2 -type reaction with uncomplexed phenyl selenide anion. *Tetrahedron Lett.* 50, 4369-4372.
- Lucius, M., and Bruning, (1902) D.R.P. No. 129000. *Chem. Centr. Blatt*, 1, 686-687.
- Lundblad, R. L., and Noyes, C. M. (1984) The chemical crosslinking of peptide chains. In *Chemical Reagents for Protein Modification*, Vol. II, pp 123-170, CRC Press, Boca Raton FL.
- Maassen, J. A. (1979) Cross-linking of ribosomal proteins by 4-(6-formyl-3-azidophenoxy)butyrimidate, a Heterobifunctional, cleavable cross-linker. *Biochemistry* 18, 1282-1288.
- Nielsen, P. E., and Buchardt, O. (1982) Aryl azides as photoaffinity labels. A photochemical study of some 4-substituted aryl azides. *Photochem. Photobiol.* 35, 317-323.
- Peters, K., and Richards, F. M. (1977) Chemical crosslinking reagents and problems in studies of membrane structure. *Ann. Rev. Biochem.* 46, 523-551.
- Reich, H. J. (1979) Functional group manipulation using organoselenium reagents. *Acc. Chem. Res.* 12, 22-30.
- Reich, H. J. (1987) [2,3]Sigmatropic rearrangement of organoselenium compounds. In *Organoselenium Chemistry* (D. Liotta, Ed.), pp 371-395, John Wiley and Sons, New York.
- Reich, H. J., Wollowitz, S., Trend, J. E., et al. (1978) Syn elimination of alkyl selenoxides. Side reactions involving selenenic acids. Structural and solvent effects on rates. *J. Org. Chem.* 43, 1697-1705.
- Rich, D. H., and Gurwara, S. K. (1975) Preparation of a new *o*-nitrobenzyl resin for solid-phase synthesis of *tert*-butyloxycarbonyl-protected peptide acids. *J. Am. Chem. Soc.* 97, 1575-1579.
- Schwartz, M. A., Das, O. P., and Hynes, R. O. (1982) A new radioactive cross-linking reagent for studying the interactions of proteins. *J. Biol. Chem.* 257, 2343-2349.
- Seever, R. H., and Counsell, R. E. (1982) Radioiodination techniques for small organic molecules. *Chem. Rev.* 82, 575-590.
- Sharpless, K. B., Lauer, R. F., and Teramishi, A. Y. (1973) Electrophilic and nucleophilic organoselenium reagents. New routes to α,β -unsaturated carbonyl compounds. *J. Am. Chem. Soc.* 95, 6137-6139.
- Sharpless, K. B., and Lauer, R. F. (1973) A mild procedure for the conversion of epoxides to allylic alcohols. The first organoselenium reagent. *J. Am. Chem. Soc.* 95, 2697-2699.
- Sharpless, K. B., and Young, M. W. (1975) Olefin synthesis. Rate enhancement of the elimination of alkyl aryl selenoxides by electron-withdrawing substituents. *J. Org. Chem.* 40, 947-949.
- Shields, C. J., Falvey, D. E., Schuster, G. B. et al. (1988) Competitive singlet-singlet energy transfer and electron transfer activation of aryl azides: Application to photocrosslinking experiments. *J. Org. Chem.* 53, 3501-3507.
- Shields, C. J., Chrisope, D. R., Schuster, G. B., et al. (1987) Photochemistry of aryl azides: Detection and characterization of a dehydroazepine by time-resolved infrared spectroscopy and flash photolysis at room temperature. *J. Am. Chem. Soc.* 109, 4723-4725.
- Srinivasachar, K., and Neville, D. M. (1989) New protein crosslinking reagents that are cleaved by mild acid. *Biochemistry* 28, 2501-2509.
- Stagg, B. H., Temperley, J. M., Rochman, H., et al. (1970) Iodination and the biological activity of gastrin. *Nature* 228, 58-59.
- Toshimitsu, A., Owada, H., Aoi, T., et al. (1981) Selenoxide fragmentation leading to allylic amides. *J. Chem. Soc., Chem. Comm.* 1, 546-547.
- Ullman, F., and Mauthner, F. (1903) Oxidation of substituted *o*-phenylenediamines. *Chem. Ber.* 36, 4026-4034.
- Weber, K., Pringle, J. R., and Osborn, U. (1972) Measurements of molecular weights by electrophoresis on SDS-acrylamide gel. In *Methods in Enzymology*, (Hirs, C. H. W. and Timasheff, S. N., Eds.) Vol. 26, pp 3-27, Academic Press, New York and London.
- Wisniewski, B. J., and Bramhall, J. S. (1981) Photolabeling of cholera toxin subunits during membrane penetration. *Nature*, 289, 319-321.

Bioconjugate Chemistry

SEPTEMBER/OCTOBER 1990
Volume 1, Number 5

© Copyright 1990 by the American Chemical Society

LETTERS

Using Starburst Dendrimers as Linker Molecules To Radiolabel Antibodies

Jeanette C. Roberts,^{*,†} Yvonne E. Adams,[†] Donald Tomalia,[‡] Janet A. Mercer-Smith,[§] and David K. Lavallee^{||}

Department of Medicinal Chemistry, University of Utah, Salt Lake City, Utah 84112, Michigan Molecular Institute, 1910 W. St. Andrews Road, Midland, Michigan 48640, INC-11 MS J514, Los Alamos National Laboratory, Los Alamos, New Mexico 87545, and Department of Chemistry, Hunter College—CUNY, 695 Park Avenue, New York, New York 10021. Received August 6, 1990

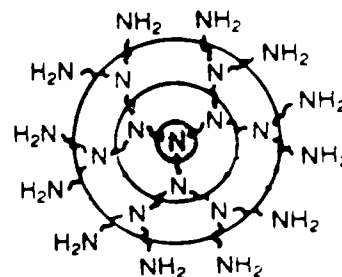
Starburst dendrimers, spherical polymers constructed from methyl acrylate and ethylenediamine, were successfully used to covalently couple synthetic porphyrins to antibody molecules. The dendrimers, as linker molecules, have great potential for increasing the specific activity of radiolabeled antibodies for tumor therapy and diagnosis.

Modifying antibodies with radioisotopes, toxins, or cytotoxic drugs is becoming of increasing value in the ongoing search for site-selective or -specific chemotherapeutic agents. Antibodies are of potentially great value in targeted drug therapy because of the inherent specificity of the antibody-antigen interaction. Unfortunately, modification of the antibody molecule with the cytotoxic agent often diminishes or eliminates the biological activity of the macromolecule, thus negating any targeting potential.

For these reasons, methods must be developed to maximize drug loading while minimizing the deleterious effects of such loading on the biological integrity of the antibody. An attractive approach is to use intermediate linker molecules which can be highly modified with drug, but which will only modify a single site on the surface of the antibody.

Several systems are being investigated for their ability to function as linkers in this scenario. Dextran, pep-

tides, proteins, and synthetic polymers may all be useful. Current work in our laboratory is concentrating on starburst dendrimers (1) as the linker molecule capable of being highly modified, then attached to antibody.



Starburst dendrimer, 1
(schematic)

Starburst dendrimers are spherical polymers that possess known molecular weights, dimensions, and number of terminal functional groups depending on the "generation"

* To whom correspondence should be addressed.

† University of Utah.

‡ Michigan Molecular Institute.

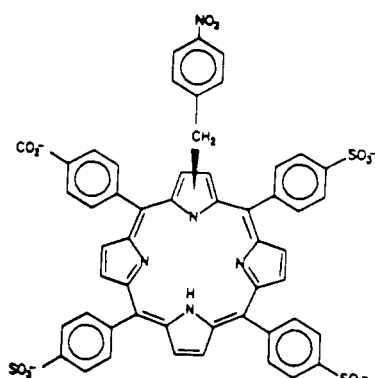
§ Los Alamos National Laboratory.

|| Hunter College—CUNY.

of the dendrimer (1). The dendrimers offer optimal properties for a linker molecule and are likely to be useful in a number of related applications. We used either third- or fourth-generation dendrimers in the current studies. Third-generation dendrimers have a molecular weight of 5147 Da and possess 24 terminal amines, while fourth-generation have 10 632 as their molecular weight with 48 amine groups.

Along with using linker molecules, selectively modifying the carbohydrate region of antibodies, a site remote from the antigen binding domain, is another promising method to assure minimal effects of covalent modification on antibody integrity.

The system under study uses *N*-(4-nitrobenzyl)-5-(4-carboxyphenyl)-10,15,20-tris(4-sulfophenyl)porphine (*N*-bzHCS₃P, 2) as a chelating agent with excellent ability to



N-bzHCS₃P, 2

chelate radiocopper ions (2-4); in particular, copper-67 is being used in these studies because of its attractive nuclear decay properties (5). *N*-bzHCS₃P has the added advantage of the benzyl substitution on one of the pyrrole nitrogens. This modification distorts the normally planar arrangement of the porphyrin macrocycle, which allows metal ion incorporation under very mild conditions (neutral pH, aqueous systems, 40 °C) that are compatible with antibody integrity.

In our pilot studies, *N*-bzHCS₃P was coupled to the dendrimer molecule by using 1-ethyl-3-[3'-(dimethylamino)propyl]carbodiimide (EDAC) in the presence of *N*-hydroxysuccinimide (NHS) (2-4). This method involves the initial activation of the carboxylate group on the porphyrin, followed by coupling to terminal amino groups on the dendrimer. The dendrimer-porphyrin conjugates were then coupled to the antibody after oxidizing the sugar residues in the carbohydrate region of the glycoprotein with NaIO₄. The resulting aldehydes were reacted with remaining free amines on the dendrimer, and the intermediate Schiff base was reduced with NaCNBH₃ (6). Figure 1 outlines the overall synthetic scheme for producing the antibody-dendrimer-porphyrin conjugate. These complexes were analyzed by sodium dodecylsulfate-polyacrylamide gel electrophoresis (SDS-PAGE) to determine the extent of antibody labeling. Bound and unbound porphyrin are easily separated by SDS-PAGE and can be quantitated by the absorbance at 435 nm. Purification of the conjugates was effected by gel filtration chromatography to yield the tertiary complex ready for radiolabeling. Conjugates without the linker molecule, viz., with porphyrin randomly coupled over the surface of the antibody, were synthesized for comparative biological studies.

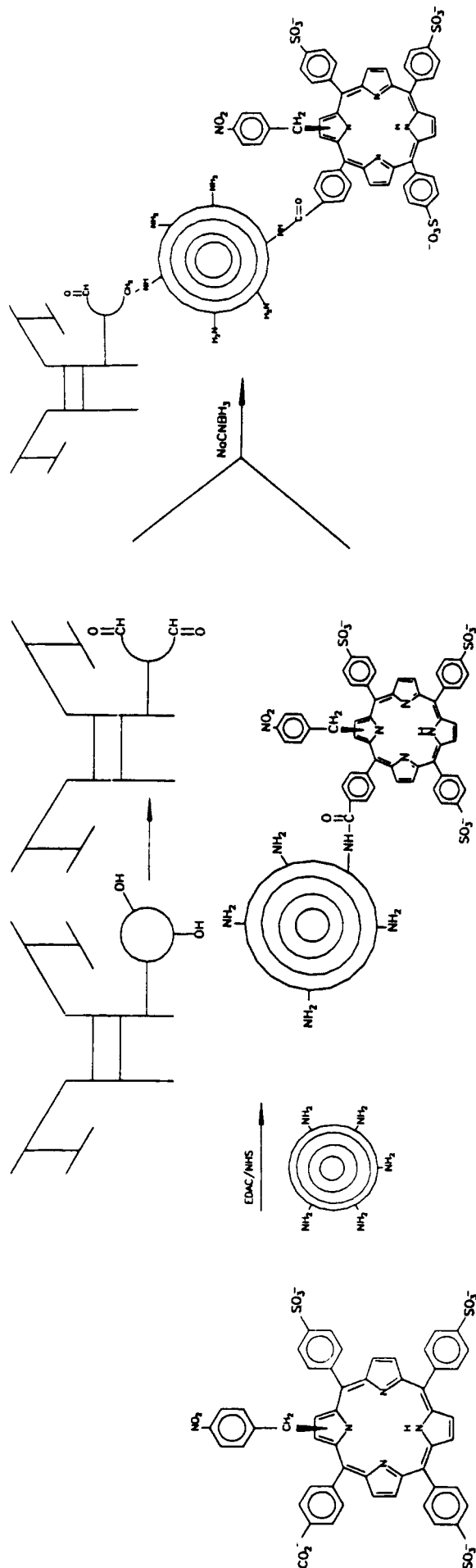


Figure 1. Schematic representation of synthetic process used to produce antibody-dendrimer-porphyrin conjugates.

Table I. Need for Reduction of the Schiff Base for Stability of Antibody-Dendrimer-Porphyrin Conjugate

day	% <i>N</i> -bzHCS ₃ P bound to antibody ^a day	
	with NaCNBH ₃	without NaCNBH ₃
0	23	30
3	21	9
8	22	5
10	20	5

^a Determined by SDS-PAGE.

To investigate the need to reduce the intermediate Schiff base formed in the reaction sequence, conjugates were synthesized both in the presence and absence of NaCNBH₃ and subjected to SDS-PAGE analysis on days 0, 3, 8, and 10. Table I illustrates the rapid loss of the porphyrin-dendrimer from the antibody when the reducing agent is not included.

Preliminary biological evaluation of the conjugates involved an investigation of the site of attachment (2) on the antibody surface to confirm coupling to the carbohydrate region. We observed 100% of the porphyrin bound to the heavy chain of the antibody, as expected. In contrast, only 69% of porphyrin was attached to the heavy chain by using the random-labeling technique; 31% of the porphyrin was attached to the light chain which is concentrated in the vicinity of antigen recognition. Also, an enzyme-linked immunosorbent assay (ELISA) was carried out to investigate the immunoreactivity remaining in the modified conjugates (2). The dendrimer conjugates were found to contain 90% of the immunoreactivity of unmodified antibody; conjugates labeled by the random-coupling method yielded 82% of the immunoreactivity of unmodified antibody. Both preparations contained two porphyrins per antibody, a labeling level chosen to compare the two methods. Negative control antibody showed 1% immunoreactivity.

In radiolabeling experiments, copper-67 was incorporated into the conjugates by incubating the radioisotope (as ⁶⁷CuCl₂) with modified antibody. Final purification was effected by vacuum dialysis against phosphate-buffered saline (PBS), pH 7.4, containing sodium citrate to complex any remaining free copper-67. The dendrimer-containing conjugates showed a high radiolabeling level, with 80% of the copper-67 being bound. This is in contrast to studies with conjugates synthesized with the random-coupling method that show an average of 55–60% radiochemical yield (4).

In summary, the starburst dendrimer represents a novel linker molecule that possesses favorable chemical and physical properties useful for antibody modification. Dendrimers can be synthesized with a specific molecular weight and a specific number of terminal functional groups, making them a homogeneous reagent. This property is a distinct advantage over commonly used polymers, in which a range of molecular weights and modifiable groups are produced.

The pilot studies described herein offer evidence for the use of starburst dendrimers coupled to synthetic porphyrins for antibody radiolabeling. Experiments with higher generation dendrimers that are highly modified with drug or radioisotope will continue to explore the ultimate utility of this system in cancer imaging and therapy.

EXPERIMENTAL PROCEDURES

All reagents were obtained from Sigma Chemical Co. (St. Louis, MO) and were used without further purification.

Gel electrophoresis reagents were purchased from Bio-Rad (Richmond, CA). Starburst dendrimers (1) and *N*-bzHCS₃P (3) were prepared as previously described. Porphyrin-containing reactions were carried out in the dark to avoid photooxidation. Protein was measured by the Bradford method (7).

Preparation of Dendrimer-Porphyrin Conjugates. The carboxylate on the porphyrin was activated by combining 20 μ L of *N*-bzHCS₃P (1.8 mg in 200 μ L of DMF), 10 μ L of EDAC (2.6 mg in 100 μ L of 12 mM NaH₂PO₄, pH 6.0), and 10 μ L of NHS (1.5 mg in 100 μ L of 12 mM NaH₂PO₄, pH 6.0). After stirring for 1.5 h at room temperature, 160 μ L of a fourth generation dendrimer stock solution (3.8 mg in 1 mL of 100 mM borate buffer, 80 mM NaCl, pH 8.5) was added, and the mixture was stirred for an additional 3.5 h at room temperature.

Preparation of Antibody-Dendrimer-Porphyrin Conjugates. In 1 mL of sodium acetate buffer (30 mM, 150 mM NaCl, pH 5.5), 7.5 mg of rabbit immunoglobulin G (RIgG) was combined with 1.0 mg of NaIO₄. The mixture was kept in the dark for 8 h at room temperature with occasional agitation. The antibody mixture was dialyzed into phosphate buffer (20 mM, pH 6.0). This solution was combined with the porphyrin-dendrimer reaction mixture in the presence of 1.3 mg NaCNBH₃. The mixture was stirred in the dark for an additional 8 h (6). The molar ratio of reactants used was 2:1:1 (porphyrin:dendrimer:antibody).

Aliquots (10 μ L) of the reaction mixture were analyzed by SDS-PAGE in tube gels composed of an initial 5% acrylamide region followed by a 12% acrylamide region. The gels were run at 2 mA per gel, then were scanned at 435 nm for porphyrin absorbance. The amount of porphyrin covalently attached to antibody was calculated from the areas under the peaks.

Purification of the product conjugate was carried out by gel filtration chromatography on Sephadex G-25.

Preparation of Antibody-Porphyrin Conjugates. Antibody conjugates with no linker molecules and, therefore, porphyrin randomly attached to the surface were prepared as previously described (4).

Preparation of Radiolabeled Antibody-Dendrimer-Porphyrin Conjugates. ⁶⁷CuCl₂ was prepared and purified as previously described (3). The radioisotope was taken up into DMF, and a 1:1 ratio of no-carrier-added ⁶⁷CuCl₂:porphyrin was incubated with the antibody conjugates for 60 min at 40 °C. The radiolabeled material was purified by vacuum dialysis against PBS (0.01 M sodium phosphate, 0.15 M NaCl, pH 7.4) containing 0.05 M sodium citrate to chelate any uncomplexed radiocopper.

Site of Attachment. Antibody conjugates were incubated for 3 min in a boiling-water bath with a solution containing 2-mercaptoethanol to reduce the intrachain disulfide linkages (2). The chains were separated, and the amount of porphyrin attached to each chain was quantitated by gel electrophoresis as described above.

ELISA. ELISA was carried out as described (2) with rabbit anti-conalbumin as the antibody and conalbumin as the antigen. Modified and unmodified antibodies were compared on each plate, with unmodified antibody representing 100% immunoreactivity. Negative control (RIgG) antibody was included to determine nonspecific interaction.

ACKNOWLEDGMENT

We wish to acknowledge the financial support supplied by the American Association of Colleges of Pharmacy and

the University of Utah College of Pharmacy. Support from DOE/OHER and NIH Grant CA25427 is also appreciated.

LITERATURE CITED

- (1) Tomalia, D. A., Naylor, A. M., and Goddard, W. A. (1990) Starburst dendrimers—Molecular-level control of size, shape, surface chemistry, topology, and flexibility from atoms to macroscopic matter. *Angew. Chem. Int. Ed. Engl.* 29, 138–175.
- (2) Roberts, J. C., Figard, S. D., Mercer-Smith, J. A., Svitra, Z. V., Anderson, W. L., and Lavalley, D. K. (1987) Preparation and characterization of copper-67 porphyrin-antibody conjugates. *J. Immunol. Methods* 105, 153–164.
- (3) Mercer-Smith, J. A., Roberts, J. C., Figard, S. D., and Lavalley, D. K. (1988) The Development of Copper-67-Labeled Porphyrin-Antibody Conjugates. *Antibody-Mediated Delivery Systems* (J. D. Rodwell, Ed.) pp 317–352, Marcel Dekker, Inc., New York.
- (4) Roberts, J. C., Newmyer, S. L., Mercer-Smith, J. A., Schreyer, S. A., and Lavalley, D. K. (1989) Labeling antibodies with copper radionuclides using *N*-4-nitrobenzyl-5-(4-carboxyphenyl)-10,15,20-tris(4-sulfophenyl)porphine. *Appl. Radiat. Isot.* 40, 775–781.
- (5) Raman, S., and Pinajian, J. J. Decay of ^{67}Cu . *Nucl. Phys. A131*, 393–397.
- (6) Chua, M.-M., Fan, S.-T., and Karush, F. (1984) Attachment of immunoglobulin to liposomal membrane via protein carbohydrate. *Biochim. Biophys. Acta* 800, 291–300.
- (7) Bradford, M. M. (1976) A rapid and sensitive method for the quantitation of microgram quantities of protein utilizing the principle of protein-dye binding. *Anal. Biochem.* 72, 248–254.

ARTICLES

Synthesis and Characterization of Digoxin-Phospholipid Conjugates^{1,†}

D. R. Hwang,* M. E. Scott,† and E. Hedaya

Immunology Department, Research and Development Division, Technicon Instruments Corporation, Tarrytown, New York 10591. Received June 27, 1990

The preparation of immunoreactive derivatives of digoxin for analytical applications is most often carried out by periodate cleavage of the terminal sugar ring (digitoxose) followed by reaction with an enzyme, protein, carrier, or related biological molecules. Here we report an improved and more efficient synthesis which was developed to provide digoxin-phospholipid conjugates useful for liposome immunoassay. The approach used involved the linking of the cleaved digitoxose through a carboxymethyl oxime functionality, which provides much improved yields of readily purified products. The synthetic modification should be applicable to the preparation of analogous phospholipid conjugates involving linkage through a sugar ring (digitoxin, ouabain, and related cardiac glycosides) or to those involving steroids (i.e., 3-digoxigenone) which can be modified to form oxime derivatives remote from key functionalities important for immunorecognition by specific antibody. The characterization of the digoxin-phospholipid conjugates with high-resolution NMR and fast atom bombardment mass spectrophotometry will also be discussed.

Digoxin is a potent cardiac glycoside. Toxic amounts of digoxin exert undesirable and potentially lethal electrophysiological effects (2). Accordingly, various immunoassay methods for cardiac glycosides are now widely used for determination of appropriate dosage schedules for patients receiving these drugs. Because digoxin is too small a molecule to be antigenic by itself, it is necessary to conjugate digoxin covalently as a hapten to an antigenic carrier, for example, human serum albumin (HSA), bovine serum albumin (BSA), or keyhole limpet hemocyanin (KLH), in order to elicit digoxin-specific antibodies in experimental animals for use in immunoassay. The preparation of immunoreactive digoxin derivatives is typically carried out by the procedures of Butler and Chen (3) which is based on the work of Erlanger and Beiser (4). The reaction sequence involved periodate cleavage of the terminal sugar ring (digitoxose or rhamnose) followed by reaction with an amino functionality from a protein carrier, enzyme, or related biological molecule, and finally reductive amination of the intermediate Schiff base with sodium borohydride. Thus, digoxin-HSA (3), digoxin-BSA (5), mellitin-ouabain (6), and digoxin-dibenzo-18-crown-6 (7) conjugates have been prepared by using the aforementioned reaction sequence.

We have attempted to adopt the procedure of Butler and Chen (3) to prepare digoxin-dipalmitoyl phosphatidylethanolamine (digoxin-DPPE) conjugates for use in homogeneous liposome immunoassays for determination of haptens such as digoxin (9). In our hands, following the procedure of Butler (3) and Cole (8) gave a very complex mixture from the reaction, and thus the reaction

sequence via the Schiff base was not useful for our purpose. Here, we report an improved and more efficient synthesis for digoxin-DPPE conjugates which were immunoreactive and useful for liposome immunoassay.

RESULTS AND DISCUSSION

The synthetic sequence is outlined in Scheme I. The terminal digitoxose in digoxin is cleaved to give dialdehyde in quantitative yield by using sodium periodate under nitrogen atmosphere. The condensation reaction of digoxin dialdehyde and carboxymethoxylamine hemihydrochloride proceeds rapidly in sodium acetate/ethanol under a nitrogen atmosphere. A quantitative yield of the bis[*O*-(carboxymethyl)oxime] was obtained (11). The digoxin dioxime derivative was used immediately in the next reaction step, where the carboxy functionalities of the dioxime is reacted with *N*-hydroxysuccinimide in the presence of dicyclohexylcarbodiimide to give an active ester. The dioxime active ester is then condensed with a stoichiometric amount of dipalmitoyl phosphatidylethanolamine (DPPE) with gentle heating for 12 h. The reaction was monitored closely by TLC. Thin-layer chromatography with the solvent system chloroform/methanol/water 75/25/3 by volume showed two major components at *R_f* 0.20 and 0.13 along with *N*-hydroxysuccinimide at *R_f* 0.30. The phospholipid moiety of the conjugates was detected by molybdenum spray (11).

The excess *N*-hydroxysuccinimide was removed from the reaction mixture by preparative LPLC. Pure digoxin-di-DPPE conjugate (0.1348 g, 20%; *R_f* 0.30) and digoxin-mono-DPPE conjugate (0.1424 g, 26.5%; *R_f* 0.15) were isolated from crude reaction mixture by preparative TLC in chloroform/methanol/water (75/25/3 by volume). Two other minor products were also isolated which were not identified. It should be noted that when twice the stoichiometric amount of dipalmitoyl phosphatidylethanolamine was used for condensation reaction with the digoxin dioxime active ester, only digoxin-di-DPPE was

* To whom correspondence should be addressed.

† Chemistry Department, University of Akron.

Abbreviations: DPPE, dipalmitoyl phosphatidylethanolamine; HSA, human serum albumin; BSA, bovine serum albumin; KLH, keyhole limpet hemocyanin; TLC, thin-layer chromatography; IR, infrared spectroscopy; UV, ultraviolet spectroscopy; NMR, nuclear magnetic resonance; FAB, fast atom bombardment; LPLC, low-pressure liquid chromatography.

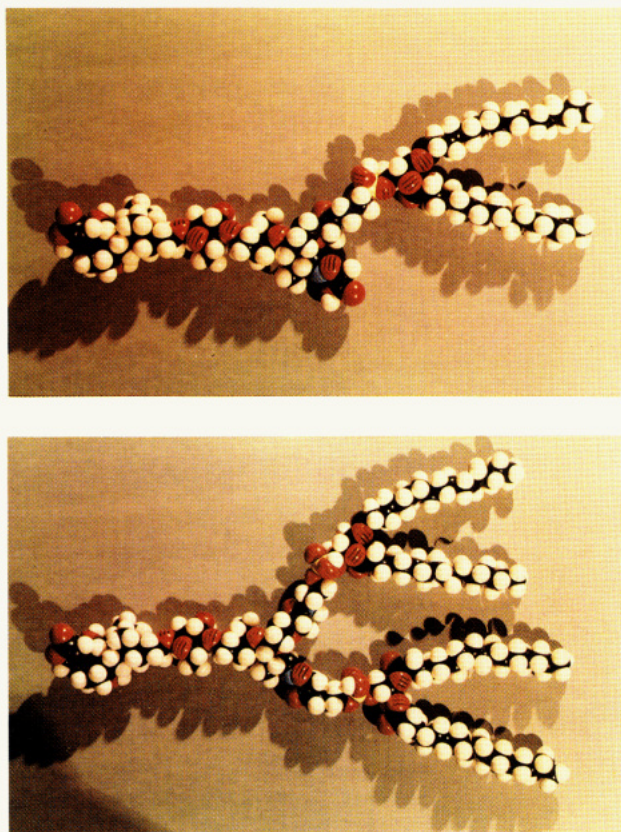


Figure 1. Digoxin-mono-DPPE (top) and digoxin-di-DPPE (bottom) are shown.

denum spray was prepared according to the procedure of Dittmer and Lester (11). FT NMR spectra were obtained with the 7 T spectrometer at the Rockefeller University. FAB mass spectra were obtained with the MS-50 high-resolution mass spectrometer at the Middle Atlantic Regional Mass Spectrometer Center at Johns Hopkins University. Preparative low-pressure liquid chromatography (LC) was carried out on a home-built LC system using a Kieselgel 60 (200 g, 0.040–0.063 mm) glass column (2.5 × 50 cm).

Digoxin Dialdehyde. Digoxin (0.4985 g, 0.64 mmol) is dissolved in 10 mL of chloroform/methanol (3/1.5) and placed into a 100-mL two-necked flask. Sodium periodate (0.3102 g, 1.4 mmol) is dissolved in a 4 mL of distilled water and placed into a pressure-equalized addition funnel. The periodate solution is slowly added to the flask while the reaction mixture is stirred under nitrogen. A white precipitate is immediately formed and the reaction is complete within 15 min after addition of the periodate. Reaction progress is monitored by TLC (E. M. Merck, pre-coated TLC sheets, silica gel 60 F254, 0.2 mm thickness) in chloroform/methanol (10/1 by volume, R_f 0.16 = dialdehyde, one homogeneous spot; R_f 0.07 = digoxin). Both spots became dark brownish when the TLC plate is sprayed with methanol/concentrated sulfuric acid (9/1 by volume) and placed in a 100 °C oven for 5 min. The reaction mixture is evaporated on a rotary evaporator and dissolved in 30 mL of chloroform and 3 mL of water. The cloudy solution is extracted and the aqueous layer is washed three times with 10 mL of chloroform. The organic phases are combined (60 mL) and dried over magnesium sulfate. The organic solvents are evaporated to dryness. A light yellow brownish, oily material is left. Satisfactory NMR spectra have been obtained. The aldehydic protons appear as two complex multiplets near 9.68 and 9.77 ppm (Figure 2a). The J values are relatively small. This material is used

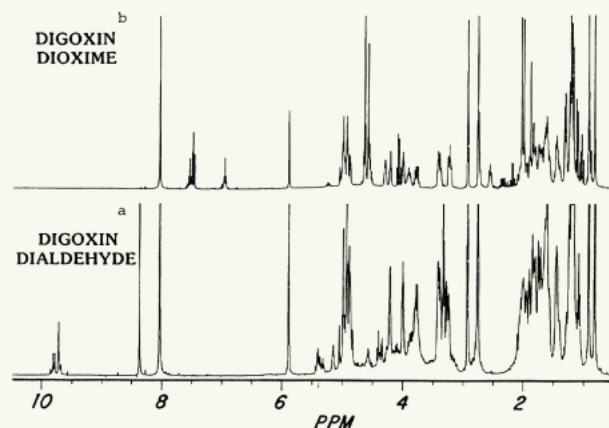


Figure 2. NMR of (a) digoxin dialdehyde and (b) digoxin dioxime.

immediately in the next reaction. No attempt was made to isolate the dialdehyde because of its lability.

Digoxin Bis[O-(carboxymethyl)oxime] Carboxymethoxylamine hemihydrochloride (0.3119 g, 1.4 mmol) and sodium acetate (0.2260 g, 1.6 mmol) are dissolved in 3 mL of water and placed into a 50-mL two-necked flask. The digoxin dialdehyde, dissolved in 1.3 mL of methanol, is placed into a pressure-equalized funnel and slowly added to the flask while the reaction mixture is stirred under nitrogen. The reaction is completed within 10 min (TLC chloroform/methanol, 6/1 by volume, R_f 0.09–0.13). The reaction mixture is evaporated to dryness and dissolved in 20 mL of ethyl acetate and 3 mL of water. The organic layer is separated and the aqueous layer is washed three times with 5.0 mL of ethyl acetate. The organic layers are combined and dried over anhydrous magnesium sulfate. The solution is filtered and evaporated to dryness. The residue is dried for 30 min under high vacuum (0.1 mmHg) and used immediately for the next step. Satisfactory elemental analysis and NMR spectra were obtained for the residual product. Elemental anal. for $C_{45}H_{68}O_{18}N_2 \cdot 2H_2O$ (calcd): C, 56.65 (56.22); N, 7.39 (7.56); O 33.22 (33.70); H, 2.91 (2.91). The aldehydic protons of the dioxime appeared as two multiplets near 6.94 and 7.5 ppm (Figure 2b).

N-Hydroxysuccinimide Ester of Digoxin Bis[O-(carboxymethyl)oxime]. Dicyclohexylcarbodiimide (DCC, 0.2805 g, 1.3 mmol) is dissolved in 6 mL of dry DMF and placed into a 50-mL two-necked flask. The solution is cooled in an ice-water bath (4 °C). Digoxin (bis[O-(carboxymethyl)oxime], dissolved in 80 mL of DMF, is slowly added while the reaction mixture is stirred under nitrogen. Immediately afterward, *N*-hydroxysuccinimide (NHS) solution (0.1500 g, 1.3 mmol, in 6 mL of DMF) is likewise added. Reaction progress is monitored by TLC [chloroform/methanol/water, 75/25/3 by volume, R_f 1.0 (DCC), 0.75 (dioxime NHS active ester), 0.34 (NHS), 0.1 (dioxime)]. The reaction continues at 4 °C under nitrogen for 18 h. The white solid precipitate in the mixture is removed by filtration. The filtrate is then evaporated with a rotary evaporator under vacuum (0.1 mmHg). An oil material is left.

The desired product possesses the following TLC characteristics: (1) homogeneous UV detectable spot (short wavelength), (2) the homogeneous spot turns brownish when the TLC plate is sprayed with methanol/concentrated sulfuric acid (9/1 by volume) and warmed briefly in a 100 °C oven.

Digoxin-DPPE Conjugates. The crude dioxime active ester (17 mL of reaction mixture) is placed into a 100-

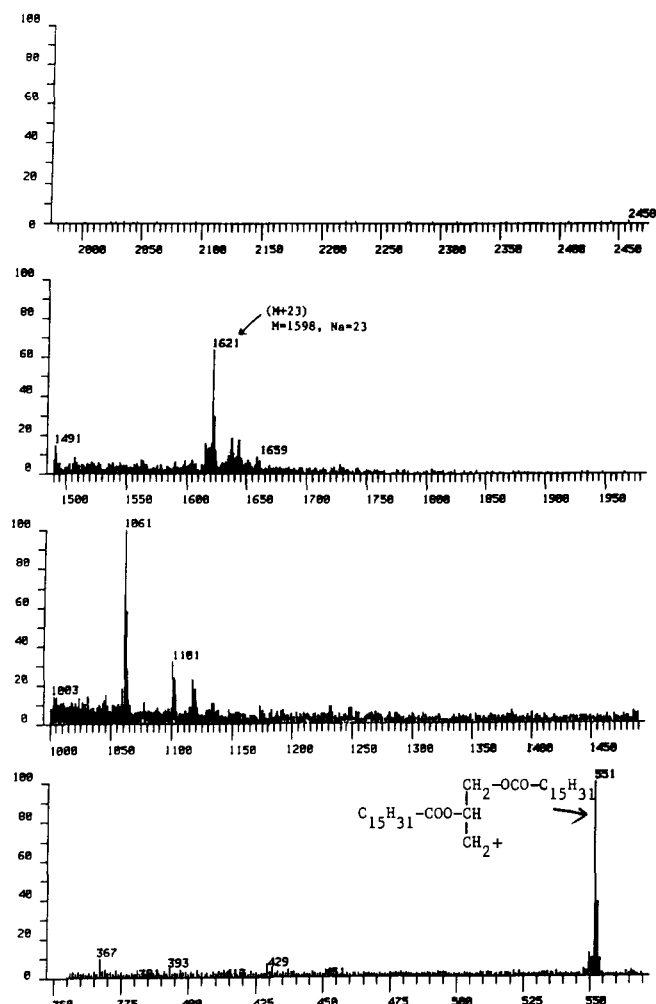


Figure 3. FAB MS of digoxin-mono-DPPE.

mL two-necked flask. A suspension of DPPE (0.4431 g, 0.64 mmol, dispersed in 30 mL of dry chloroform and 0.87 mL of triethylamine) is placed into an addition funnel and slowly added to the flask while the reaction mixture is stirred under nitrogen and protected from light. The mixture was heated gently (40–50 °C) and this continues for 72 h. The reaction was monitored by TLC [solvent system chloroform/methanol/water, 75/25/3 by volume, R_f 0.75 (active ester), 0.52 (unknown 1), 0.45 (unknown 2), 0.30 (NHS), 0.21 (DPPE), 0.20 (disubstituted conjugate), 0.13 (monosubstituted conjugate)]. The phospholipid moiety of the conjugates was detected by molybdate blue spray. The reaction mixture was evaporated and brought up in 10 mL of chloroform/methanol/water (2/8/1). The *N*-hydroxysuccinimide was removed from the mixture by LPLC [Kieselgel, 200 g, glass column (2.5 cm × 50 cm), solvent system chloroform/methanol/water (2/8/1 by volume)]. Pure mono- and disubstituted conjugates can be obtained by preparative TLC in chloroform/methanol/water [75/25/3 by volume; R_f 0.30 (disubstituted), 0.15 (monosubstituted)]. Pure digoxin-di-DPPE conjugate (0.1349 g, 20%) and digoxin-mono-DPPE conjugate (0.1424 g, 26.5%) were obtained. Two other minor products were also isolated. The structures of the minor products were not identified. The molecular ion for digoxin-mono-DPPE is 1621 ($M + Na$)⁺ (Figure 3) and the molecular ion for digoxin-di-DPPE is 2311 ($M + K$)⁺ (Figure 4).

CONCLUSION

An important advantage of the above synthetic procedure is the use of the relatively stable, storable, yet ac-

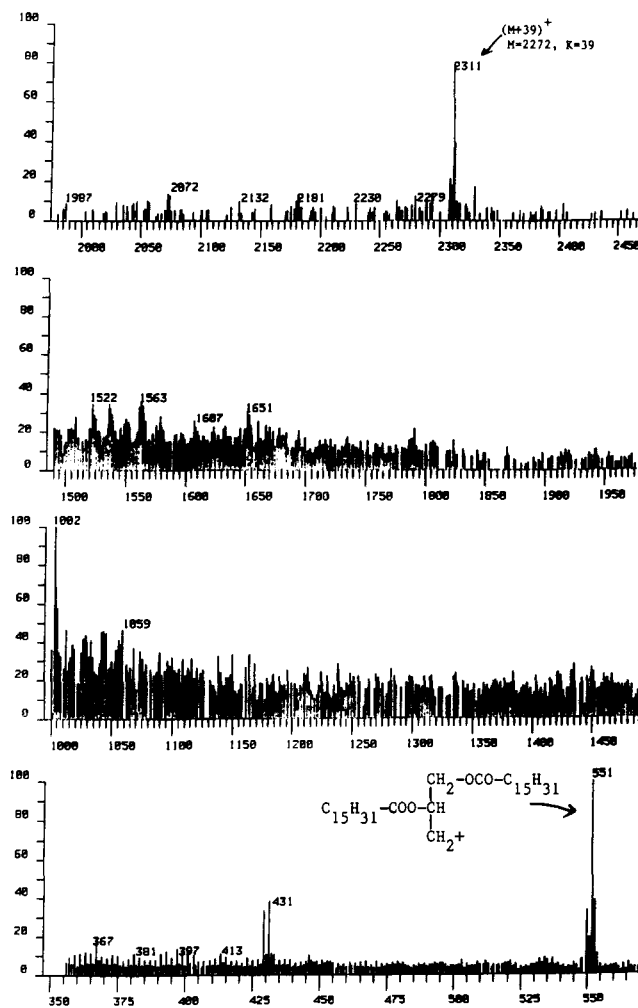


Figure 4. FAB MS of digoxin-di-DPPE.

tivatable, oxime intermediate. This intermediate overcomes the disadvantages inherent in the Butler et al. procedure discussed earlier. These include the propensity for the dialdehyde intermediate to undergo deleterious side reactions, particularly in the presence of amine derivatives of lesser reactivities such as phospholipids. An additional advantage is that the improved procedure provides products which can be readily isolated, characterized, and purified, in contrast to that of Butler, which, to our knowledge, yields a sufficiently complex mixture, thwarting the desired product characterization.

The objective of this work has been to provide digoxin-phospholipid conjugates which are ultimately incorporated in liposome diagnostic reagents. It is interesting to compare the digoxin-mono- and -di-DPPE conjugates prepared here with respect to their incorporation within a liposome bilayer membrane as well as their comparative impact on diagnostic utility, even though these considerations go beyond the scope of this preparative report. CPK models of the digoxin-mono- and -di-DPPE derivatives (see Figure 1) suggest that the di-DPPE derivatives should be more effectively incorporated in a bilayer membrane, owing its four fatty acid legs. Data bearing on this and related diagnostic applications will be reported separately.

The synthetic method described here is also applicable to the preparation of analogous phospholipid conjugates involving linkage through a sugar ring such as digitoxin, gitoxin, ouabain, digitonin, and related cardiac glycosides, or those involving steroids (i.e., 3-ketodigoxigenin) which can be modified to form oxime derivatives

remote from key functionalities important for immunorecognition by specific antibodies. For example, digoxigenin-DPPE was prepared efficiently from digoxigenin 3-[(carboxymethyl)oxime] and dipalmitoyl phosphatidylethanolamine via a NHS active ester. The digoxigenin 3-[(carboxymethyl)oxime] was prepared quantitatively from the reaction of 3-digoxigenone and carboxymethoxylamine hemihydrochloride. The preparation of 3-digoxigenone from digoxigenin was performed by previous methods (12).

ACKNOWLEDGMENT

The technical assistance from Francis Picart of Rockefeller University is highly appreciated. D.H. extends his appreciation to Drs. Robert Cotler and David Heller of the Middle Atlantic Regional Mass Spectrometry Center at Johns Hopkins University for the FAB mass spectra.

LITERATURE CITED

- (1) Preliminary account of this study was present at the 189th ACS National Meeting at Miami Beach, Florida, 1985; Bioorganic section paper 229.
- (2) Hoffman, B. F., and Bigger, J. T., Jr. (1980) in *The Pharmacological Basis of Therapeutics*, 6th ed. p 729, (A. G. Gilman, L. S. Goodman, and A. Gilman, Eds.) McMillan, New York.
- (3) (a) Butler, V. P., Jr., and Chen, J. P. (1967) Digoxin-specific antibodies. *Proc. Natl. Acad. Sci. U.S.A.* 57, 71-78. (b) Butler, V. P., Jr., and Tse-Eng, D. (1982) In immunoassay of digoxin and other cardiac glycosides. *Methods Enzymol.* 84, 558-577.
- (4) Erlanger, B. F., and Beiser, S. M. (1964) Antibodies specific for ribonucleosides and ribonucleotides and their reaction with deoxyribonucleic acid (DNA). *Proc. Natl. Acad. Sci. U.S.A.* 52, 68-74.
- (5) Smith, T. W., Butler, V. P., Jr., and Huber, E. (1970) Characterization of antibodies of high affinity and specificity for the ditigalys glycoside digoxin. *Biochemistry* 9, 331-337.
- (6) Freytag, J. W. and Litchfield, J. (1984) Liposome-mediated immunoassays for small haptens (digoxin) independent of complement. *J. Immunol. Method* 70, 133-140.
- (7) Keating, M. Y., and Rechnitz, G. A. (1984) Potentiometric digoxin antibody measurements with antigen-ionophore based membrane electrodes. *Anal. Chem.* 56, 801-806.
- (8) Cole Francis, X. U.S. Patent 4,342,826, Aug. 3, 1982. [immunoassay products and methods (see examples IX and X) and references cited therein].
- (9) Adolfsen, R., Hedaya, E., Mark, C., and Schwarzberg, M. U.S. patent 4,839,276, June 13, 1989 (interference-resistant liposome specific binding assay).
- (10) There was only one product according to extensive TLC studies. Whereas, the NMR spectra of digoxin dioxime showed two multiplets (6.94 and 7.5 ppm) separated by 0.56 ppm which were assignable to the aldehydic proton. (Phillips, W. D. (1958) Studies of hindered internal rotation in organic molecules by nuclear magnetic resonance. *Ann. N. Y. Acad. Sci.* 70, 817-832.) The existence of two separated proton resonances could be explained by the simultaneous existence of syn and anti isomers. Area ratio of proton resonances provided the efficient determination of the equilibrium concentration of the isomers. The isomer ratio (syn/anti) was calculated to be 2.
- (11) Ditter, J. D., and Lester, R. L. (1964) A simple, specific spray for the detection of phospholipids on thin-layer chromatograms. *J. Lipid Res.* 24, 126.
- (12) (a) Shimiju, Y., and Mitushashi, M. (1968) Studies on C-NOR-D homosteroids-1 X solvolysis of 14B-hydroxy-12B tosyloxy steroids. *Tetrahedron* 24, 4207. (b) Tamm, Ch., and Gubler, A. (1959) Microbiological conversion of cardiac active glycosides and aglycones. *Chimia* 13, 116-117.

Misonidazole Conjugates of the Colorectal Tumor Associated Monoclonal Antibody 17-1A

Deborah L. Pierce,[†] Ned D. Heindel,^{*†‡} Keith J. Schray,[†] Michele M. Jetter,[†] Jacqueline G. Emrich,[‡] and David V. Woo[‡]

Institute for Health Sciences, Lehigh University, Bethlehem, Pennsylvania 18015, and Department of Radiation Oncology & Nuclear Medicine, Hahnemann University, Philadelphia, Pennsylvania 19102.

Received October 16, 1989

The radiation sensitizer misonidazole has been linked to the monoclonal antibody 17-1A which recognizes a nonshed antigen of a human gastrointestinal tumor. Linkage was accomplished through a hemisuccinate of misonidazole attached by a mixed anhydride coupling and gave a conjugate whose plasma half-life (for drug cleavage) was ca. 70 h. The degree of substitution on the antibody could be precisely regulated by varying the reactant ratios. The binding avidities of the resulting conjugates to the SW1116 colorectal tumor cells decrease logarithmically with increasing drug load. Four to six misonidazoles per antibody represented the optimum drug loading on this system. Enzymatic cleavage of the conjugate-drug union took place at both the ester and the amide linkages with the former scission predominating.

Radiation sensitizers such as misonidazole, desmethylnisonidazole, and metronidazole enhance radiation lethality on hypoxic tumor cells in culture but have been much less successful in clinical trials because of their marked dose-limiting neuropathies and minimal tumor affinities (1-6). The tumor-delivery successes reported for the use of monoclonal antibody conjugates in diagnosis (radioimmunoimaging) and in drug targeting (immunochemotherapy) offer a solution to enhancement of the clinical utility of sensitizers (7-9).

In an earlier study we reported the conjugation of misonidazole to the anti-colorectal carcinoma monoclonal antibody 19-9 (10). This antibody was derived from a hybridoma 1116-NS-19-9, produced by fusion of the 653 variant of P3X63 Ag8 murine myeloma cells with splenocytes from a mouse immunized with the human colorectal carcinoma cell line SW1116 (11). These studies showed that an optimum number of 10-12 misonidazoles could be attached to the IgG with retention of approximately 40% immunorecognition. However, since the antigenic determinant recognized by 19-9 is found not only on the cell but is also shed into the blood of patients with colorectal cancer, only a fraction of the sensitizer-antibody conjugate would bind at the tumor target (12).

The antibody 17-1A recognizes a nonshed antigen and was originally derived from the injection of the SW1083 human colon carcinoma line into BALB/c mice with subsequent fusion of the splenocytes with P3x63/Ag8 myeloma cells (11, 12). 17-1A recognizes a membrane receptor on colon carcinoma, primary pancreatic cancer, and metastatic adenocarcinomas and has already been used to deliver toxins and boron compounds for neutron therapy to tumors (7, 13, 14).

In the following discussion, the synthesis, characterization, and in vitro evaluation of misonidazole-antibody conjugates with 17-1A are described. Antibody-drug conjugates have been prepared with retained binding avidity and sufficient resistance to plasma-enzyme hy-

drolysis to permit targeting. This preliminary investigation indicates that monoclonal transport of sensitizers may constitute an effective way to enhance radiation therapy of hypoxic tumors.

EXPERIMENTAL PROCEDURES

Materials. Misonidazole was obtained from Dr. Peter Sorter of Hoffmann-La Roche, Nutley, NJ. The monoclonal antibody 17-1A was obtained from Centocor, Malvern, PA. Human plasma employed in the hydrolysis studies was donated by one of the authors (D.L.P.).

Conjugation of Misonidazole Hemisuccinate to 17-1A. Ratios of sensitizer molecules/IgG from 44 to 1 could be obtained by altering the reaction ratios of the sensitizer and the antibody as well as the contact times of the reactants. Table I shows the relationship between reactant ratios and loading factors at a fixed reaction time (15 h). A typical preparation which resulted in a drug load of six sensitizers per antibody is described.

Individual stock solutions were prepared of misonidazole hemisuccinate (10), triethylamine, and isobutyl chloroformate each at a 0.05 M concentration in anhydrous acetonitrile. Aliquots of 0.031 mL (1.55×10^{-3} mmol) of the triethylamine and the misonidazole hemisuccinate stock solutions were mixed at 4 °C for 15 min to form a light yellow reaction mixture. To this was added 0.031 mL (1.55×10^{-3} mmol) of isobutyl chloroformate stock solution with the resulting colorless mixture incubated at 4 °C for 1 h. This reaction solution was added dropwise to a solution of 4.65 mg of 17-1A (3.1×10^{-5} mmol) in 4.5 mL of 0.1 M phosphate buffered saline, pH 7.7 (PBS). The reaction was allowed to proceed for 15 h at 4 °C during which time the pH decreased to 7.5, whereafter the product was isolated and purified as described below. This particular conjugate had a loading factor of 6 and a binding avidity of 62%.

Purification of the Antibody Conjugates. The requisite antibody conjugate was isolated from the crude reaction mixture by chromatography on Sephadex G-25 (Pharmacia PD-10 columns, Pharmacia Laboratory Separation Division, Uppsala, Sweden), equilibrated, and

* To whom requests for reprints should be addressed.

[†] Lehigh University.

[‡] Hahnemann University.

Table I. Reactant Ratios, Loading Factors, and Binding Avidities of Misonidazole Hemisuccinate Conjugation to 17-1A

conjugate	reactant ratio ^a	loading factor ^b	% avidity
1	20:1	1.4	88
2	35:1	5	67
3	50:1	6	62
4	100:1	12	9.3
5 ^c	90:1	14	6.0
6	150:1	21	4.7
7	500:1	44	<1

^a Moles of misonidazole hemisuccinate to moles of 17-1A. ^b Moles of misonidazole hemisuccinate bound per mole of 17-1A. ^c Reactant contact time = 26 h; all other runs = 15 h.

eluted with 0.9% aqueous sodium chloride at room temperature. Fractions of 3.0 mL were collected and analyzed at the λ_{\max} for the drug and the antibody (vide infra). The desired antibody conjugate was collected in fractions 1 and 2 and unconjugated drug followed in fractions 4 and 5. The conjugate was further purified and concentrated with Centricon 30 Microconcentrators (Amicon, Danvers, MA), which allow molecules of less than 30 kD to pass through the membrane. Purity was then assessed by high-performance liquid chromatography (HPLC) on a Du Pont GF-250 Bioseries column (Zorbax PSM-150, 9.4 mm \times 24 cm id; Du Pont Instruments, Wilmington, DE) employing 0.2 M PBS, pH 7.2, at a 1.0 mL/min flow rate with monitoring at 325 nm. Elution times for 17-1A and free-drug standards were 8.3 and 11.8 min.

Determination of Loading Factor. Antibody loading factor, i.e. number of moles of drug per mole of antibody, was determined by UV difference spectrometry. Standard solutions of drug and antibody in 0.9% sodium chloride solution were prepared and standard curves were determined to provide extinction coefficients (ϵ) for insertion to eq 1 and 2. Herein, A_{325} and A_{280} correspond to the

$$A_{325} = \epsilon_{\text{at } 325 \text{ for drug}}[\text{drug}] + \epsilon_{\text{at } 325 \text{ for MoAb}}[\text{MoAb}] \quad (1)$$

$$A_{280} = \epsilon_{\text{at } 280 \text{ for drug}}[\text{drug}] + \epsilon_{\text{at } 280 \text{ for MoAb}}[\text{MoAb}] \quad (2)$$

absorbances of a purified conjugate at these wavelength maxima, [drug] is the moles/liter concentration of misonidazole present in the conjugate, and [MoAb] is the moles/liter of the antibody present in the conjugate. The molar concentrations of drug and antibody in a conjugate were calculated by measuring that conjugate's absorption (A) at both wavelengths, and solving these equations simultaneously to obtain the loading factor as [drug]/[MoAb].

Evaluation of Antibody Conjugate Activity. *Maintenance of Cells in Culture.* SW1116 cells are human colon adenocarcinoma cells established by the Scott-White Clinic of Temple, TX. This cell line was originally derived from a Broders Grade II, Dukes' A adenocarcinoma of the colon of a 73-year-old, white male (15). The cells were maintained in a growth medium of three parts RPMI 1640 and one part Liebovitz's L-15 medium which was supplemented with 20% fetal bovine serum. Cells were maintained in Corning polystyrene tissue-culture flasks in a humidified 5% CO₂ chamber at 37 °C. The cultures were tested periodically for mycoplasma and found to be free by Mycotrim T.C. test kits (Hana Media, Berkeley, CA).

Cells in log phase were harvested by removing the medium and washing with 0.05% trypsin, 0.02% EDTA, 5 μ g/mL DNAase solution, and they were subsequently incubated with a second aliquot of the solution for 0.5 h at 37 °C. The cells were washed by suspending in pH 7.4 PBS with 5 μ g/mL of DNAase, centrifuging for 10 min at 1200 rpm, separating, and discarding the supernatant.

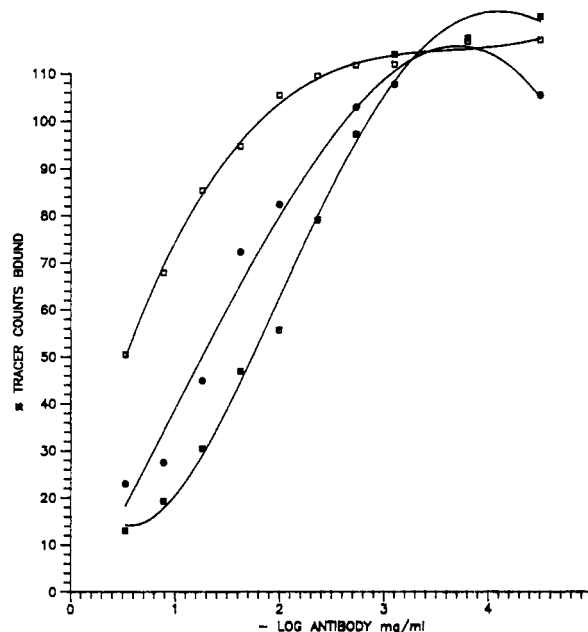


Figure 1. Radioimmunoassay evaluation of misonidazole-labeled 17-1A antibody conjugates. Varying dilutions of unmodified 17-1A (■) and misonidazole-antibody conjugate with a loading factor of 5 (●) and 12 (□) were incubated competitively with ¹²⁵I-labeled antibody for binding to SW1116 cells.

These cells were then resuspended to a concentration of 1×10^7 per mL in the PBS-DNAase medium and used in the free cell binding study.

Cell Binding of Modified Conjugates. Antibody conjugate and unmodified 17-1A were diluted serially from a stock solution of 0.3 mg/mL in PBS. Twelve dilutions were prepared with PBS containing 1.0% bovine serum albumin (BSA) as the diluent: 1–8 being 2.33-fold serially and 9–12 being 5.00-fold serially diluted. To 0.2 mL of the above solutions was added 0.1 mL (3.0×10^6 cpm/mL) of ¹²⁵I-17-1A prepared and purified by our published method (17). The specific activity of the ¹²⁵I-17-1A was 10 μ Ci/ μ g. From each of the above antibody conjugate/¹²⁵I-17-1A solutions, 0.05 mL was added to a solution of SW1116 cells (0.05 mL at 1×10^7 cells/mL) and the mixture was incubated for 18 h at 4 °C in 96-well microtiter plates. All assays were done in triplicate. An additional control binding assay was used to determine the maximal cpm bound using the same cell concentration and only ¹²⁵I-17-1A at the same radioactive concentration. The plates were centrifuged and the pelleted cells were washed three times with PBS containing 1% BSA. Cell pellets were then removed with cotton swabs and counted in a Searle Autogamma counter set for ¹²⁵I.

The relative binding avidity of each conjugate was compared to unmodified 17-1A by using a competitive binding assay. Various concentrations of antibody conjugates were allowed to bind to antigen containing SW1116 cells in the presence of a fixed quantity of radiolabeled ¹²⁵I-17-1A. A binding curve was then determined in which the percent counts bound of ¹²⁵I-17-1A was plotted against the negative log of the antibody conjugate concentration (see Figure 1). The percent counts bound was determined by dividing the actual spm of antibody binding (at various antibody conjugate concentrations) by the maximal possible cpm bound of ¹²⁵I-17-1A alone. The percent avidity was determined as the concentration of the conjugate at 50% bound divided by the concentration of the control (unmodified 17-1A) at 50% bound. The percent avidities of the conjugate are shown in Table I.

Evaluation of Conjugate Stability to Plasma

Enzymes. Conjugates were evaluated both for stability to cleavage by plasma enzymes and to storage in saline. Freshly drawn human blood (40 mL in evacuated containers coated with sodium heparin) was centrifuged to separate the plasma phase. Three milliliters of plasma was transferred to a sterile vial and a misonidazole-17-1A conjugate (loading factor = 39) was added to achieve a final concentration of 2 mg/mL. The mixing of the two solutions from preequilibrated stocks was taken as time zero. The solutions and the reaction mixture were maintained at 37 °C in a VWR-1910 incubator. Samples were withdrawn at the indicated times (see Figure 4) and were injected onto a Du Pont Bioseries GF-250 column packed with Zorbax PSM 150 (9.4 mm × 25 cm id; Du Pont Instruments, Wilmington, DE) mounted on a Perkin-Elmer Series 2 HPLC with UV monitoring at 325 nm and a mobile phase of 0.2 M PBS at pH 7.4 flowing at 1.0 mL/min. The main analytical column was protected by a guard column (2.1 mm × 2.0 cm id) of identical packing material. The peaks were identified by separate injection and coinjection of standards. Storage stability of the conjugate was determined by this HPLC method with conjugate at a concentration of 2 mg/mL in saline at 4 °C and at 25 °C.

Biodistributions. Conjugate 3 (Table I) was labeled with ^{111}In -DTPA by the Hnatowich method (18) and evaluated for tumor/muscle/blood distribution at 2 days postdosing by serial necropsy in three Harlan Sprague-Dawley nude mice bearing the SW1116 tumor as a flank implant. Animals were 8–10-week-old females implanted 9 days previously with 1.5×10^7 cells and maintained in colony until the tumors developed to an average weight of 125–200 mg. Biodistributions were performed in the previously reported fashion (12, 19). Labeled conjugate 3 (0.5 uCi) was administered i.v. into the lateral tail vein. At 48 h 0.2 mL of blood was withdrawn by cardiac puncture just before necropsy.

RESULTS AND DISCUSSION

Loading factor is remarkably sensitive to the relative concentrations of the misonidazole hemisuccinate and 17-1A in the coupling medium, allowing the controlled syntheses of a whole spectrum of conjugates (see Table I). Roughly 7–10 drug moieties become affixed to the IgG for each successive 10 mol equiv increase in the relative hemisuccinate-to-antibody ratio. Binding avidity, however, decreases rapidly with increasing radiosensitizer burden, falling by ca. 50% between 6 and 12 misonidazoles attached (Figure 2).

For *in vivo* radiosensitization application the amount of misonidazole delivered to the tumor site would depend on the number of drugs that are covalently attached to the antibody as well as on the avidity retained by a given misonidazole-antibody conjugate to the target antigen. The plot of loading factor times binding avidity versus loading factor (Figure 3) may be used to determine the optimal drug/antibody ratio for therapeutic usage. Binding avidities employed in this calculation are derived from the least-squares line (Figure 2). It can be seen from Figure 3 that the curve reaches a maximum at a loading factor of ca. 6, indicating that the optimal load for conjugates when used for immunoradiotherapy lies between 4 and 8.

The stability of a misonidazole-antibody conjugate (loading factor = 39) was evaluated by HPLC methods in human plasma and in saline at room temperature (25 °C) and at 4 °C. It can be seen from Figure 4 that a marked difference exists in the stability of the antibody conjugate in plasma vs saline. The amount of misonidazole that remains attached to the antibody decreases more rapidly

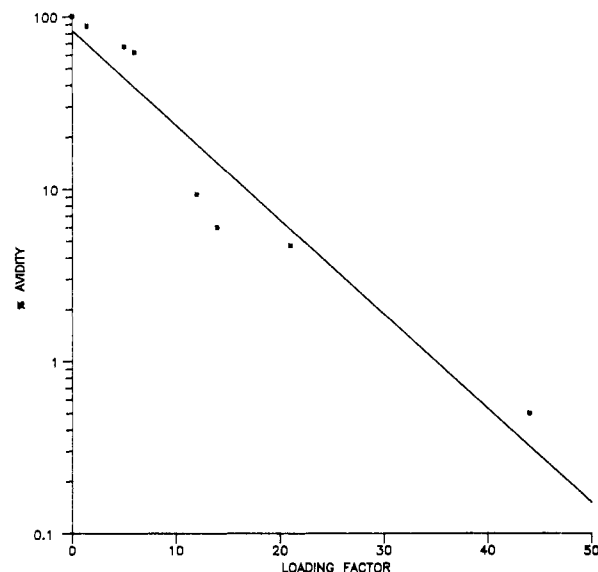


Figure 2. Relationship between percentage of antibody-binding avidity as measured by radioimmunoassay (Table I), and loading factor.

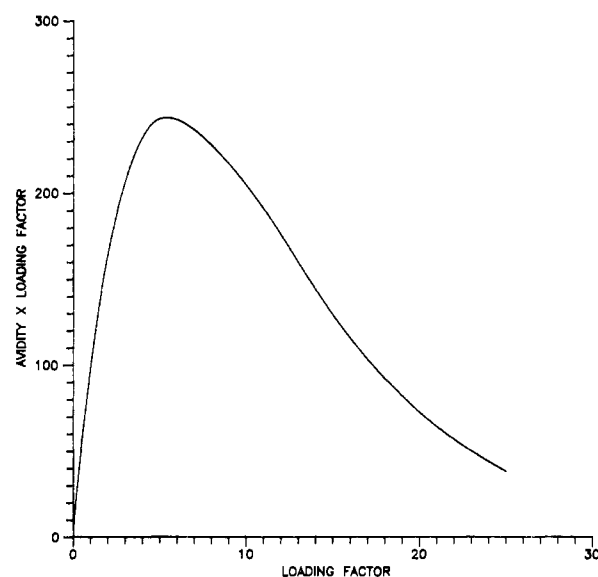


Figure 3. Product of fractional antibody avidity times loading factor, obtained from Table I, versus loading factor.

in plasma than in a standard buffer solution. The drug may be cleaved as misonidazole hemisuccinate (amide bond cleavage) or as misonidazole itself (ester bond cleavage). Obviously, in plasma the mechanism by which the drug is cleaved from the antibody involves not only simple hydrolysis but also includes the action of peptidases and esterases on the conjugate. At all times the amount of free drug in the form of misonidazole was greater than that in the form of misonidazole hemisuccinate, indicating the relative instability of the ester bond vs amide bond toward cleavage. The peak in the HPLC chromatogram corresponding to the intact misonidazole-antibody conjugate (Figure 5, peak A) appears to resolve into multiple peaks at longer incubation times as the drug is freed either as misonidazole or its hemisuccinate.

Evaluation of Conjugate Stability to Plasma Enzymes. Figure 5 displays an HPLC chromatogram of the cleavage products of the misonidazole-17-1A conjugate (loading factor = 39) in plasma at 37 °C at an incubation time of 24 h. The analysis was conducted as indicated in the Experimental Procedures. An antibody fraction (peak

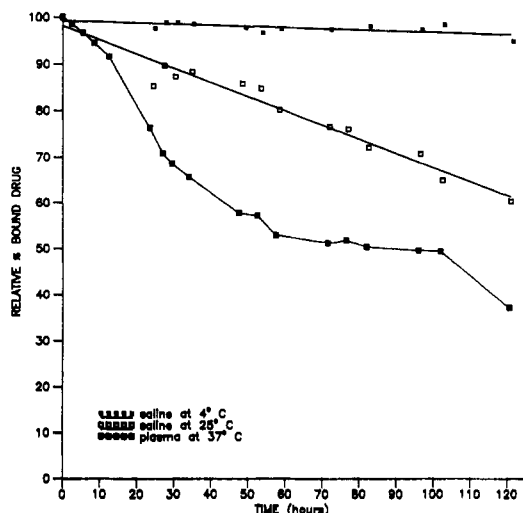


Figure 4. HPLC analysis of release rates of drug from misonidazole-17-1A-antibody conjugate (loading factor = 39) in plasma at 37 °C (■), saline at 25 °C (□), and saline at 4 °C (●). Bound drug refers to the remaining percent of misonidazole which is considered bound to the antibody.

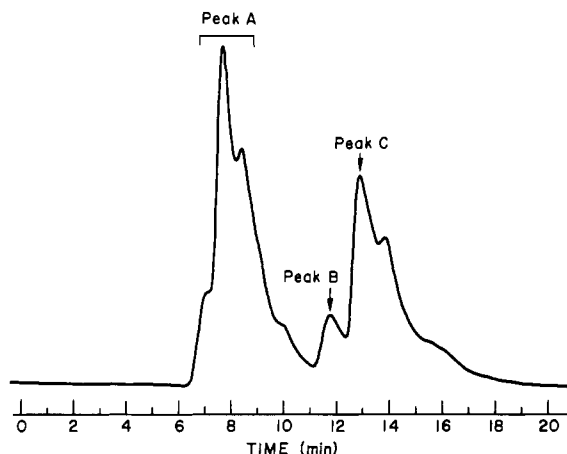


Figure 5. HPLC chromatogram of misonidazole-antibody conjugate (loading factor = 39) in serum at 37 °C at $t = 24.5$ h.

A)—containing the initial antibody conjugate, its cross-linked homologues, and its partially hydrolyzed derivatives—eluted as a multiple-component peak from ca. 6.5–10 min. By peak-enhancement techniques the original, unhydrolyzed conjugate in plasma was established to elute at 7.7 min. A shoulder at 7.1 min is apparently cross-linked antibody since it is generated in the synthesis of the original antibody conjugate. Other shoulders eluting after the original unhydrolyzed conjugate in the antibody portion (peak A) at longer incubation times are attributed to antibody remaining after fractional hydrolytic/enzymatic scission of misonidazole and/or misonidazole hemisuccinate. Peak-enhancement techniques identify peak B, eluting at 11.8 min, as misonidazole hemisuccinate and peak C, eluting at 13.0 min, as misonidazole. The shoulder at 13.9 min is attributed to a metabolite of misonidazole since it is found only at longer incubation times in plasma and is not present in saline.

Because the fragment peaks and their metabolites arise from multiple possible sources, i.e. original antibody-conjugate or misonidazole hemisuccinate cleaved therefrom, it is not possible to determine distinct kinetic parameters for each product. However, the relative percent drug bound to the antibody could be measured by subtraction of the summation of the individual chromatographic peak integrations for all fragment species (misonidazole, mis-

onidazole hemisuccinate, and their respective metabolites) from total peak integration for all antibody bound and unbound species with the subsequent expression of this quantity as a percentage of total integration. With the HPLC UV detector measuring at 325 nm, the peaks are completely attributable to the imidazole chromophore, and therefore to drug concentration. Antibody is transparent at this wavelength.

Figure 4 shows the percent drug bound to antibody vs time in plasma at 37 °C. As indicated, 76% of the drug remains antibody-bound at 24 h, but by 120 h the bound drug has decreased to <40%. Although the drug release rate is not a simple function, a half-life of 70 h can be extracted from the data. HPLC evaluation of the stability of the antibody-drug conjugate demonstrates proteolytic cleavage of the amide linkage between the antibody and the misonidazole hemisuccinate as well as preferential enzymatic/hydrolytic cleavage of the misonidazole ester.

Corresponding analyses were performed in saline at 4 °C and at 25 °C to determine stability of the conjugate to various storage conditions. At 25 °C the hydrolysis showed linear kinetics with a half-life of 162 h. At the lower temperature, however, the conjugate was virtually unchanged over >120 h, indicating that 4 °C saline solution represents an effective medium for storage.

Although the optimum loading of 4–6 misonidazoles (Figure 3) is less for 17-1A than for 19-9 (10–12 misonidazoles) (16) and the hydrolysis rate for drug release is slightly greater, the immunotargeting potential could undoubtedly be enhanced by removing a fraction of inactive antibody by affinity chromatography. As it stands, preliminary biodistribution to evaluate tumor uptake, performed in tumor-bearing nude mice with six-drug-load conjugate, was encouraging. At 48 h postdosing this did show a tumor/blood ratio of 5.4 and a tumor/muscle ratio of 11.0 with absolute levels of $3.31 \pm 0.92\%$ dose/gram in tumors of the conjugate-dosed mice. An earlier study of the uptake of radioiodinated (^{131}I) 17-1A in a similar nude mouse tumor reported 8% dose/gram at 1 day postdosing and 12% dose/gram at 5 days postdosing (12). In this study, the drug-substitution rates which could be obtained without substantial loss of antibody activity were too low to justify in vivo radiosensitizing testing. Additional studies with more potent sensitizers conjugated to polymeric spacers on antibody fragments are underway in these laboratories.

ACKNOWLEDGMENT

This project was supported by a grant to N.D.H. from the W. W. Smith Charitable Trust and by fellowship support to D.L.P. from the Quaker Chemical Foundation.

LITERATURE CITED

- (1) Brown, J. M., Hall, E. J., Hirst, D. G., Kinsella, T. J., Kligerman, M. M., Mitchell, J. B., Travis, E. J., and Valeriote, F. (1988) Chemical modification of radiation and chemotherapy. *Am. J. Clin. Oncol.* 11, 288–303.
- (2) Brady, L. W. (Ed.) (1980) *Radiation Sensitizers*, Masson Publishing USA, Inc., New York.
- (3) Brown, J. M., Yu, N. Y., Cory, M. J., Bricknell, R. B., and Taylor, D. L. (1978) *In vivo* evaluation of the radiosensitizing and cytotoxic properties of newly synthesized electron affinic drugs. *Br. J. Cancer* 37 (Suppl. 3), 206–211.
- (4) Bleehen, N. M. (1980) The Cambridge glioma trial of misonidazole and radiation therapy with associated pharmacokinetic studies. *Cancer Clin. Trials* 3, 267–273.
- (5) Dische, S. (1980) Misonidazole in the clinic at Mt. Vernon. *Cancer Clin. Trials* 3, 175–178.

- (6) Dische, S., Saunders, M. L., Anderson, P., Urtasun, R. C., Karcher, K. H., Kogelnik, H. D., Bleehe, N. M., Phillips, T. L., and Wasserman, T. H. (1978) Neurotoxicity of misonidazole: pooling of data from five centers. *Br. J. Radiol.* 51, 1023-1024.
- (7) Ram, B. P., and Praveen, T. (1987) Immunoconjugates: applications in targeted drug delivery for cancer therapy. *Pharmacol. Res.* 4, 181-188.
- (8) Chatal, J.-F., Saccavini, J.-C., Fumoleau, P., Douillard, J.-Y., Curtet, C., Kremer, M., Le Mevel, B., and Koprowski, H. (1984) Immunoscintigraphy of colon cancer. *J. Nucl. Med.* 25, 307-314.
- (9) Woo, D. V., Markoe, A. M., Brady, L. W., Koprowski, C., Koprowski, H., Heindel, N. D., and Mattis, J. (1988) Monoclonal antibodies for use in radiotherapy and diagnosis. *Am. J. Clin. Oncol.* 11, 355-361.
- (10) Borlinghaus, K. P., Fitzpatrick, D. A., Heindel, N. D., Mattis, J. A., Mease, B. A., Schray, K. J., Shealy, D. J., Walton, H. L., and Woo, D. V. (1987) Radiosensitizer conjugation to the carcinoma 19-9 monoclonal antibody. *Cancer Res.* 47, 4071-4075.
- (11) Koprowski, H., Steplewski, Z., Mitchell, K., Herlyn, M., Herlyn, D., and Fuhrer, P. (1979) Colorectal carcinoma antigens detected by hybridoma antibodies. *Somatic Cell Genet.* 5, 957-971.
- (12) Douillard, J. Y., Chatal, J.-F., and Saccavini, J. C. (1983) Radio-Pharmacokinetic Studies in Nude Mice with Monoclonal Antibodies Specific to Human Gastro-intestinal Cancers. *Bull. Cancer (Paris)* 70, 169-171.
- (13) Mach, J.-P., Chatel, J.-F., Lumbroso, J.-D., Buchegger, F., Forni, M., Ritschard, J., Berche, C., Douillard, J.-Y., Carrel, S., Herlyn, M., Steplewski, Z., and Koprowski, H. (1983) Tumor localization in patients by radiolabeled monoclonal antibodies against colon carcinoma. *Cancer Res.* 43, 5593-5600.
- (14) Mafune, N., Barth, R. F., Alam, F., Soloway, A. H., Blue, T. E., Adams, D., Sautins, I., Curran, J. F., and Steplewski, Z. (1987) Purification and characterization of B-10 linked monoclonal antibody conjugates for neutron capture therapy. *Proc. Am. Assoc. Cancer Res.* 28, 391.
- (15) Herlyn, M., Steplewski, Z., Herlyn, D., and Koprowski, H. (1979) Colorectal carcinoma-specific antigen: detection by means of monoclonal antibodies. *Proc. Natl. Acad. Sci. U.S.A.* 76, 1438-1442.
- (16) Brady, L. W., Woo, D. V., Heindel, N. D., Markoe, A. M., and Koprowski, H. (1981) Therapeutic and diagnostic uses of modified monoclonal antibodies. *Int. J. Radiat. Oncol. Biol. Phys.* 13, 1535-1544.
- (17) Woo, D. V., Li, D., Mattis, J. A., and Steplewski, Z. (1989) Selective chromosomal damage and cytotoxicity of ^{125}I -labeled monoclonal antibody 17-1A in human cancer cells. *Cancer Res.* 49, 2952-2958.
- (18) Hnatowich, D. J., Layne, W. W., and Childs, R. L. (1982) Preparation and Labeling of DTPA-Coupled Albumin. *Int. J. Appl. Radiat. Isot.* 33, 327-332.
- (19) Herlyn, D., Powe, J., Alavi, A., Mattis, J. A., Herlyn, M., Ernst, C., Vaun, R., and Koprowski, H. (1983) Radioimmuno-detection of human tumor xenografts by monoclonal antibodies. *Cancer Res.* 43, 2731-2735.

Synthesis and Interactive Properties of an Oligonucleotide with Anthraquinone at the Sugar Fragment

Kazushige Yamana,* Yoshitaka Nishijima, Tadashi Ikeda, Tadao Gokota, Hiroaki Ozaki,† Hidehiko Nakano, Osamu Sangen, and Takeo Shimidzu†

Department of Applied Chemistry, Himeji Institute of Technology, 2167 Shosha, Himeji, Hyogo 671-22, Japan, and Division of Molecular Engineering, Graduate School of Engineering, Kyoto University, Yoshida, Sakyo-ku, Kyoto 606, Japan. Received May 30, 1990

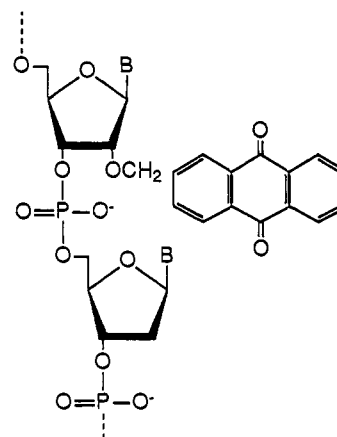
The synthesis of a self-complementary oligonucleotide possessing an anthraquinonylmethyl substituent at the designated sugar fragment, 5'-CCU(2'AQ)AGCTAGG (1), is described. The anthraquinonylmethyl group was introduced to 2'-hydroxyl moiety of uridine, which was then converted to the protected phosphorobisdiethylamidite derivative. This reagent was used for the solid-phase synthesis of the modified oligonucleotide 1. The UV and CD melting behaviors indicate that the modified oligonucleotide 1 can form a duplex in aqueous buffer solution similar to the unmodified strand 5'-CCTAGCTAGG (7). The observed melting temperatures for the duplexes 1 and 7 were 57.4 and 40.0 °C, respectively. The temperature-dependent change in the intensity of the induced CD at around 335 nm reflected directly to the melting behaviors of duplex 1, indicating that the anthraquinone groups intercalate into the base pairs in the duplex. The intercalation-induced stability of the duplex translates into a free energy cost of 5.2 kcal/mol. The present work provides a novel method for enhancing the affinity of oligonucleotides for their complementary sequences.

There is current interest in conjugation of oligonucleotides with intercalating agents that stabilize the complexes with the complementary sequences without losing the specificity of recognition (1-11). It has been previously shown that oligonucleotide-acridine or -anthraquinone conjugates can be used for inhibiting mRNA translation or viral expression (5-8). The synthesis of oligonucleotide-intercalator conjugates has been accomplished by linking oligonucleotides via linker arms to intercalating agents at a terminal position (1-8), an internal phosphorus (9, 10), or a pyrimidine C-5 (11).

We describe here the synthesis of an oligonucleotide with an anthraquinone selectively incorporated to the sugar at a specific residue. Our strategy involves the preparation of a 2'-anthraquinone-modified uridine derivative that is suitable for a solid-phase synthesis of oligonucleotides. Molecular models allowed us to consider that an anthraquinone group could be incorporated via a relatively short linker to the 2'-sugar position in an oligonucleotide, the resulting oligonucleotide binds to complementary sequence, and the anthraquinone intercalates between the base pairs adjacent to the sugar in the duplex. To test the validity of our consideration, we synthesized self-complementary oligonucleotide 5'-CCU(2'AQ)AGCTAGG (1),¹ containing the anthraquinone-modified uridine (Figure 1). Spectroscopic and thermodynamic studies indicate that a single oligonucleotide-anthraquinone conjugate 1 binds to another in aqueous buffer solution forming a duplex with an enhanced thermal stability by intercalation.

* Kyoto University.

¹ Abbreviations: U(2'AQ), 2'-O-(2-anthraquinonylmethyl)-uridine; BzU(2'AQ), 2'-O-(2-anthraquinonylmethyl)-N³-benzoyluridine; DMT, 4,4'-dimethoxytrityl; BzC, N⁴-benzoyldeoxycytidine; iBz, N²-isobutyryldeoxyguanosine; CPG, controlled-pore glass; oligonucleotide-anthraquinone conjugate, 5'-CCU(2'AQ)AGCTAGG [an oligodeoxyribonucleotide containing an anthraquinone-modified uridine [U(2'AQ)] at position 7]; tm, melting temperature, poly(rA), poly(riboadenylic acid).



5'-CCU(AQ)AGCTAGG 1

Figure 1. The oligonucleotide containing an anthraquinone at the sugar fragment.

EXPERIMENTAL PROCEDURES

Melting and boiling points were uncorrected. Elemental analyses were performed at the Analytical Center of Kyoto University. ¹H NMR and ³¹P NMR spectra were obtained on a JEOL-JNM-GX400 spectrometer, using tetramethylsilane as internal standard and 85% H₃PO₄ as external standard, respectively. Assignment of ¹H NMR signals was done by analysis of 2D NMR spectra. High-performance liquid chromatography (HPLC) was performed on a Waters ALC/GPC 600E model equipped with a 254 nm fixed-wavelength detector, using a reversed-phase Cosmosil 5C₁₈-300 column (0.46 × 15 cm). Column chromatography and thin-layer chromatography (TLC) were carried out on Wako silica gel C-200 and Merck 60 PF₂₅₄, respectively. Ultraviolet (UV) spectra were recorded with a Shimadzu UV-300 spectrophotometer equipped with

a thermoelectrically controlled cell holder. Circular dichroism (CD) spectra were obtained on a JASCO CD J-600 spectrometer equipped with a thermoelectrically controlled cell holder.

Materials and Solvents. *N*³-Benzoyluridine (12), 2-(bromomethyl)anthraquinone (13), and *N*-(trimethylsilyl)diethylamine (14) were prepared by the literature procedures. Protected deoxyribonucleoside β -cyanoethyl phosphoramidites and CPG support were purchased from Applied Biosystems. The oligodeoxyribonucleotide 5'-CCTAGCTAGG was synthesized by using a DNA synthesizer (Applied Model 380A). Snake venom phosphodiesterase and alkaline phosphatase were obtained from Boehringer-Mannheim. Dimethylformamide (DMF) was stirred in the presence of CaH₂, distilled, and stored over CaH₂. Dichloromethane, acetonitrile, and diethylamine were dried by refluxing with CaH₂ at least for 5 h and then distilled and stored over CaH₂ or molecular sieves.

Synthesis of 5'-DMT-U(2' AQ) (5). *N*³-Benzoyluridine (2; 2.1 g, 6 mmol) was allowed to react with di-*n*-butyltin oxide (1.5 g, 6 mmol) in methanol (300 mL) under reflux for 2 h (15). The solvent was removed to dryness, giving 2',3'-*O*-dibutylstannylene-*N*³-benzoyluridine (3). Dibutylstannylene derivative 3 was dried over P₂O₅ under vacuum for 12 h. To a solution of 3 in dry DMF (36 mL) were added 2-(bromomethyl)anthraquinone (4.5 g, 15 mmol) and CsF (1.8 g, 12 mmol), and the mixture was stirred at room temperature for 45 h. Ethyl acetate (200 mL) was added to the reaction mixture and the resulting solution was washed with water (50 mL \times 3) and then dried over Na₂SO₄. The solution was concentrated to a minimum volume and then applied to a silica gel column (4.5 \times 30 cm); elution with CH₂Cl₂-MeOH (20:1, v/v) gave fractions which contain a mixture of BzU(2' AQ) (4) and its 3'-isomer (1.9 g, 55% combined yield). The mixture (1.9 g, 3.3 mol) was allowed to react with DMT chloride (1.2 g, 3.6 mmol) in dry pyridine (20 mL) at room temperature for 6 h. Concentrated ammonium hydroxide (5 mL) was added to the solution and the solution was stirred at room temperature for 16 h. The solution was concentrated to dryness, dissolved in CH₂Cl₂ (50 mL), and then washed with water (20 mL). The organic solution was dried over Na₂SO₄, the solvent was removed, and then the residue was applied to a silica gel column (3 \times 45 cm); elution with CH₂Cl₂-MeOH (20:1, v/v) gave two major fractions which were separated to 5'-DMT-U(2' AQ) (5; 0.8 g, 31%) and its 3'-isomer (1.1 g, 54%). 5: mp 138–139 °C; TLC (CH₂Cl₂-MeOH 9:1, v/v) *R*_f 0.69; ¹H NMR (DMSO-*d*₆) δ 3.30 (m, 2 H, H_{5'}), 3.72 (s, 6 H, CH₃O of DMT), 4.09 (m, 1 H, H_{4'}), 4.10 (dd, 1 H, H_{2'}), 4.28 (ddd, 1 H, becoming dd with D₂O, H_{3'}), 4.92 (d, 2 H, *J*_{gem} = 13.68 Hz, ArCH₂), 5.24 (d, 1 H, uracil H₅), 5.47 (d, 1 H, diminished with D₂O, 3-OH), 5.95 (d, 1 H, *J*_{1',2'} = 3.66 Hz, H_{1'}), δ 7.26 (d, 1 H, uracil H₆), 7.80, 7.94, and 8.20 (m, total 7 H, Ar of anthraquinone). Anal. Calcd for C₄₅H₃₈N₂O₁₀: C, 70.49; H, 4.99; N, 3.65. Found: C, 69.97; H, 4.90; N, 3.58. 3'-isomer of 5: mp 140–141 °C; TLC (CH₂Cl₂-MeOH 9:1, v/v) *R*_f 0.55; ¹H NMR (DMSO-*d*₆) δ 3.27 (m, 2 H, H_{5'}), 3.68 (s, 6 H, CH₃O of DMT), 4.13 (m, 1 H, H_{4'}), 4.14 (dd, 1 H, H_{3'}), 4.42 (ddd, 1 H, becoming dd with D₂O, H_{2'}), 4.82 (d, 2 H, *J*_{gem} = 13.19 Hz, ArCH₂), 5.24 (d, 1 H, uracil H₅), 5.72 (d, 1 H, diminished with D₂O, 2'-OH), 5.80 (d, 1 H, *J*_{1',2'} = 4.15 Hz, H_{1'}), 7.78 (d, 1 H, uracil H₆), 7.78, 7.95, and 8.20 (m, total 7 H, Ar of anthraquinone). Anal. Calcd for C₄₅H₃₈N₂O₁₀: C, 70.49; H, 4.99; N, 3.65. Found: C, 69.40; H, 4.77; N, 3.52.

Conversion of 5 to U(2' AQ). 5'-DMT-U(2' AQ) (76.6 mg, 0.1 mmol) was treated with 10 mL of 80% CH₃COOH

in water at room temperature for 2 h. The solvent was removed to dryness. The residue was dissolved in CH₂Cl₂ (10 mL) and the solution was washed with aqueous 5% NaHCO₃. A pale yellow crystalline solid appeared from the organic solution. The product was filtered and then dried in vacuo over P₂O₅ to yield 38 mg (82%): TLC (CH₂Cl₂-MeOH 9:1, v/v) *R*_f 0.42; ¹H NMR (DMSO-*d*₆) δ 3.63 (m, 2 H, H_{5'}), 3.96 (m, 1 H, H_{4'}), 4.10 (dd, 1 H, H_{2'}), 4.20 (ddd, 1 H, H_{3'}), 4.85 (d, 2 H, *J*_{gem} = 13.19 Hz, ArCH₂), 5.56 (d, 1 H, uracil H₅), 5.97 (d, 1 H, *J*_{1',2'} = 4.87 Hz, H_{1'}), 7.90, 7.94, and 8.20 (total 8 H, Ar of anthraquinone and uracil H₆); ϵ ₂₆₀ (25 °C, H₂O-EtOH 1:1, v/v) 3.50 \times 10⁵, ϵ ₃₃₅ (25 °C, H₂O-EtOH 1:1, v/v) 0.46 \times 10⁵.

Synthesis of Bis(diethylamino)phosphorochloridite. To PCl₃ (11.6 mL, 0.13 mol) cooled at 0 °C with stirring was added *N*-(trimethylsilyl)diethylamine (53.6 mL, 0.28 mol). The reaction was carried out for 60 min. The produced trimethylsilyl chloride was removed by distillation at atmospheric pressure. The remaining liquid was distilled under reduced pressure to give bis(diethylamino)phosphorochloridite as a colorless liquid (20 g, 72%): bp 68–71 °C at 3 mmHg; *d*₂₅ 1.018; ³¹P NMR δ 161.5. Anal. Calcd for C₄H₁₀N₂PCl: C, 45.16; H, 9.57; N, 13.30; P, 14.70. Found: C, 45.19; H, 9.92; N, 13.09; P, 14.78.

Synthesis of 5'-DMT-U(2' AQ) Phosphorobisdiethylamidite (6). To a solution of 5 (35.2 mg, 0.046 mmol) in dry CH₂Cl₂ (0.25 mL) containing triethylamine (1 equiv) was added a solution (92 μ L) of bis(diethylamino)phosphorochloridite (1 equiv vs 5) in CH₂Cl₂. The solution was stirred at room temperature for 15 min. Diethylamine (0.23 mmol) in CH₂Cl₂ (0.7 mL) was added to the solution and the solution was washed with aqueous, saturated NaCl (1 mL). The organic solution was dried over Na₂SO₄ and then the solvent was removed in vacuo to dryness. The residual powder was dissolved in dry CH₃CN and then analyzed by ³¹P NMR. The one major peak appeared at 134 ppm, indicating that bisamidite 6 thus obtained could be used for the solid-phase oligonucleotide synthesis. 5'-DMT-BzC phosphorobisdiethylamidite was synthesized by essentially the same procedure described above.

Synthesis of Oligonucleotide-Anthraquinone Conjugate 5'-CCU(2' AQ)AGCTAGG (1). The synthesis of oligonucleotide-anthraquinone conjugate 1 was accomplished by the manual solid-phase phosphoramidite (16, 17) and phosphorobisamidite (18, 19) methods, beginning with 5'-DMT-ibG (0.2 μ mol) bound to a CPG support. The fully protected 5'-DMT-AGCTAGG-CPG was synthesized by using deoxyribonucleoside β -cyanoethyl phosphoramidites (16, 17). Bisamidite 6 was coupled in the seventh addition cycle as follows: 6 (0.046 mmol) was activated with 0.5 equiv of (*p*-nitrophenyl)tetrazole in CH₃CN (0.2 mL) and coupled (15 min) to the protected, CPG-bound, 5'-detritylated AGCTAGG. After the hydrolysis with aqueous tetrazole (18), DMT cation released from the CPG was monitored spectroscopically, indicating a coupling yield of 87% for U(2' AQ). The remainder of the oligonucleotide synthesis cycles using 5'-DMT-BzC phosphorobisdiethylamidite were as previously described (18), resulting in each coupling yield of 96%. Thus an overall yield for the 10-mer 1 based on DMT cation was approximately 70%. The remaining H-phosphonate linkage was oxidized with iodine-water (18) and then CPG-bound 10-mer 1 was treated with concentrated ammonium hydroxide at 55 °C for 12 h. The purification of oligomer 1 was performed with reversed-phase HPLC eluting with a CH₃CN linear gradient (1% /min) from 3% CH₃CN in 0.1 M triethylammonium acetate (pH 7.0) at a flow rate

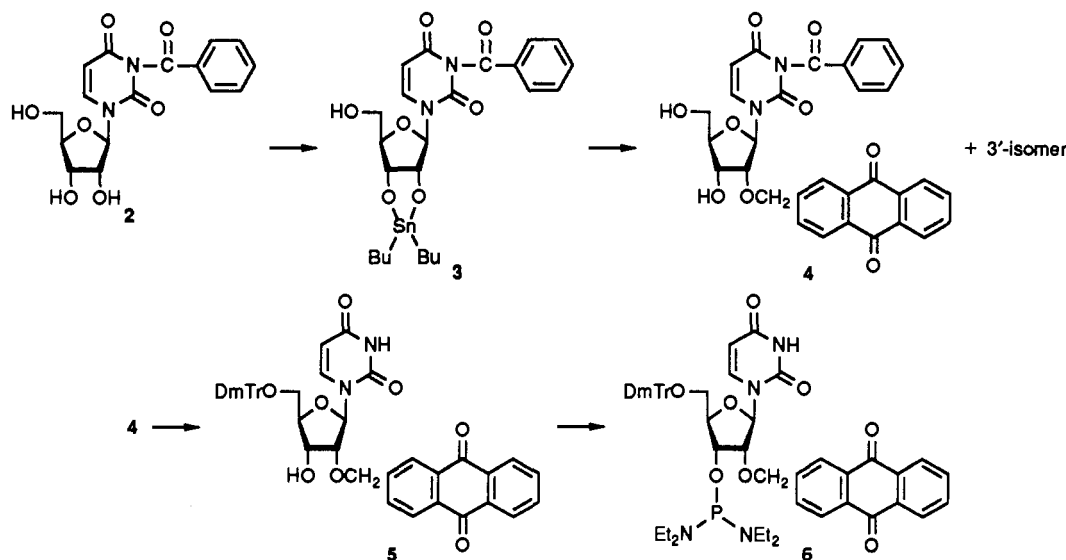


Figure 2. Synthesis of the anthraquinone-modified uridine derivative.

of 1.0 mL/min. The major peak ($t_R = 23.2$ min) was collected and lyophilized, affording 8.0 A_{260} units of purified oligomer 1.

The purified oligonucleotide 1 (ca. 0.1 A_{260} unit) was subjected to digestion with snake venom phosphodiesterase (0.3 unit/mL) and alkaline phosphatase (100 unit/mL) in 50 μ L of Tris-HCl buffer (pH 7.2) at 37 °C for 2 h (20). The reaction mixture was analyzed by reversed-phase HPLC; elution with 0.05 M ammonium formate containing a 15% CH_3CN gradient (20 min) at a flow rate of 1.5 mL/min gave deoxyribonucleosides in an expected molar ratio of dG:dC:dA:T = 3.29:3.15:1.95:1.00. The nucleoside U(2'AQ) was detected from the mixture with 30% CH_3CN in the buffer as the eluent. The purified oligomer 1 exhibits the absorption band at around 335 nm similar to U(2'AQ), indicating that U(2'AQ) is present in this sequence.

Preparation of Oligonucleotide Solutions for Physical Measurements. All solutions were prepared by using a buffer containing 0.01 M sodium phosphate and 0.1 M NaCl, adjusted to pH 7.0. Oligonucleotide concentrations were determined based on the measured absorbance at 260 nm and the following single-strand extinction coefficients ($\epsilon \times 10^{-5} \text{ M}^{-1} \text{ cm}^{-1}$ at 25 °C): oligonucleotide-anthraquinone conjugate 1, 1.23; oligonucleotide 5'-CCTAGCTAGG (7), 0.95. Each ϵ value was determined by calculations based on a nearest neighbor model (21). Since oligomers studied here have a self-complementary sequence, the calculations for oligomer concentrations were carried out by taking account of the hypochromic effect on the absorbance at 25 °C: for oligomer 1, 11%; for oligomer 7, 14%.

Except for thermodynamic studies, all duplex melting curves by UV and CD spectra were measured at a common strand concentration ($1.5 \times 10^{-5} \text{ M}$). Temperature-dependent induced CD curves were obtained at the same concentration. The thermodynamic data for duplex formation were obtained from UV melting curves by plotting inverse melting temperature versus $\log C$, where C is the total strand concentration (22).

RESULTS

Synthesis of 5'-DMT-U(2'AQ) Phosphorobisdiethylamidite (6). The synthesis of 5'-DMT-U(2'AQ) phosphorobisdiethylamidite (6) is shown in Figure 2. N^3 -Benzoyluridine (2) was converted according to Moffatt's

procedure (15) to 2',3'-O-dibutylstannylene derivative 3, which was allowed to react directly with 2-(bromomethyl)anthraquinone in the presence of CsF as a catalyst, affording a mixture of BzU(2'AQ) (4) and its 3'-isomer. These nucleosides were treated with DMT chloride followed by ammonium hydroxide, giving two products which were separated by a silica gel chromatography, 5'-DMT-U(2'AQ) (5) and its 3'-isomer. Nucleoside 5 was phosphitylated with bis(diethylamino)phosphorochloridite, yielding 5'-DMT-U(2'AQ) phosphorobisdiethylamidite (6).

Synthesis of Oligonucleotide-Anthraquinone Conjugate (1). The oligonucleotide 5'-CCU(2'AQ)-AGCTAGG (1) was synthesized by the manual solid-phase phosphoramidite and phosphorobisamidite methods (16–19). Phosphorobisdiethylamidite 6 was used directly for introduction of U(2'AQ) into the sequence of 1. DMT cation measurements indicated coupling efficiencies of 96–98% for the phosphoramidites and the phosphorobisamidite, although a slightly lower efficiency (87%) was observed in the coupling of DMT-U(2'AQ) phosphorobisdiethylamidite (6). The protected oligonucleotide 1 bound to the support was treated with concentrated ammonium hydroxide in a usual manner to give deprotected oligomer 1. Final purification of 1 was effected by reversed-phase HPLC. The nucleoside composition of oligonucleotide 1 was verified by enzymatic digestion analysis. The purified oligonucleotide 1 exhibits a UV absorption band at around 335 nm due to the 2-substituted anthraquinone.

Oligonucleotide Duplex. Figure 3 shows the UV melting curves for the anthraquinone-modified duplex 1 and the corresponding unmodified oligonucleotide duplex 5'-CCTAGCTAGG (7). Analyses of the UV melting curves provide the melting temperature (t_m) values which are listed in Table I. Table I also summarizes the thermodynamic data derived from the analysis of dependency of inverted t_m values on logarithm of the total oligonucleotide concentrations. Figure 4 indicates the two families of temperature-dependent CD spectra for duplex 1 and 7. The CD melting curves for duplexes 1 and 7 are shown in each box in Figure 4. The t_m values yielded from the CD melting curves were identical with those derived from the UV melting profiles. The families of the induced CD spectra for duplex 1 between 300 and 400 nm at different temperatures are presented in Figure 5. The intensity of

Table I. Spectroscopically Measured T_m Values and Thermodynamic Parameters for Duplexes 5'-CCU(2'-AQ)AGCTAGG (1) and 5'-CCTAGCTAGG (7)^a

duplex	t_m	Δt_m	ΔG°	$\Delta\Delta G^\circ$	ΔH°	$\Delta\Delta H^\circ$	ΔS°	$\Delta\Delta S^\circ$
1	57.4	17.4	-15.1	-5.3	-80.9	-31.0	-219.2	-85.5
7	40.0		-9.8		-49.9		-133.7	

^a T_m was measured at a strand concentration of 1.5×10^{-5} M. The free energy and enthalpy data are in kcal/mol; the entropy data are in cal/mol·K. ΔG° and $\Delta\Delta G^\circ$ are at 27 °C.

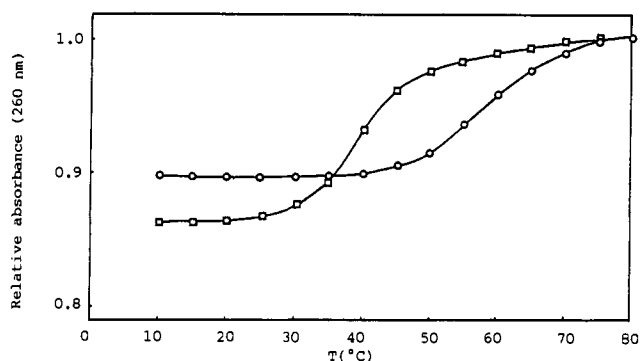


Figure 3. UV melting curves measured at 260 nm for duplexes [O, 5'-CCU(2'-AQ)AGCTAGG (1); □, 5'-CCTAGCTAGG (7)] at a common strand concentration (1.5×10^{-5} M). The buffer used contained 0.1 M NaCl and 0.01 M sodium phosphate, adjusted to pH 7.0.

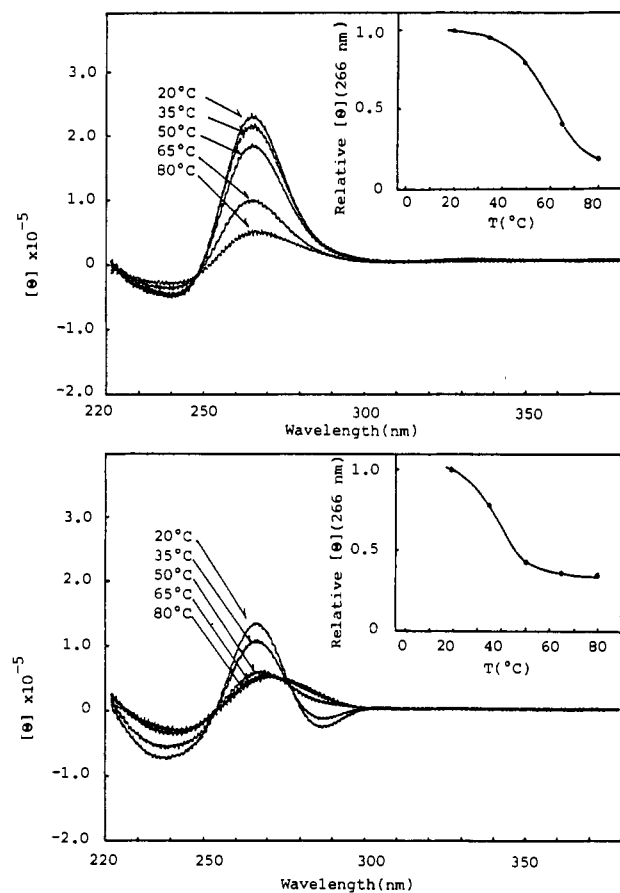


Figure 4. Temperature-dependent CD spectra and CD melting curves at 266 nm for duplexes (upper, 1; lower, 7) at a common strand concentration (1.5×10^{-5} M). The buffer used contained 0.1 M NaCl and 0.01 M sodium phosphate, adjusted pH 7.0. the ellipticity at around 335 nm decreased with increase in temperature. For unmodified duplex 7, no induced CD can be detected.

DISCUSSION

Synthesis of Oligonucleotide–Anthraquinone Conjugate (1). Our strategy for introduction of an an-

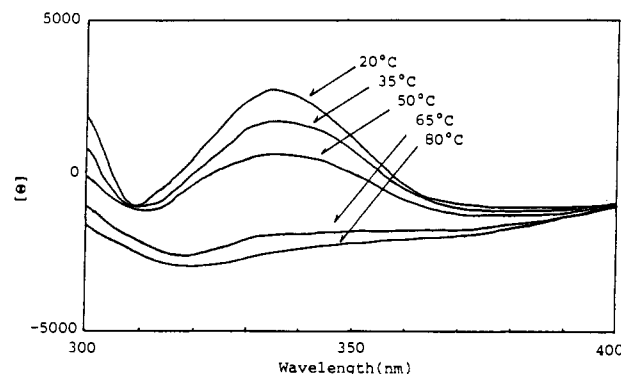


Figure 5. Expanded CD spectra for duplex 1 between 300 and 400 nm as a function of the indicated temperature. The measurements were carried out at a strand concentration of 1.5×10^{-5} M in a pH 7.0 buffer containing 0.1 M NaCl and 0.01 M sodium phosphate.

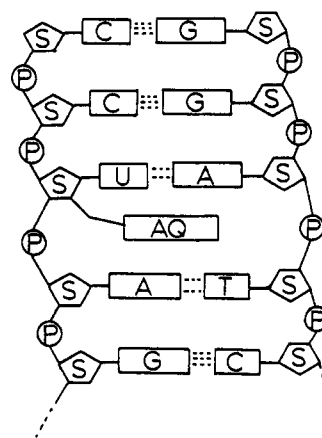


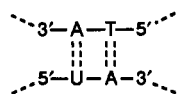
Figure 6. Model of the duplex of oligonucleotide–anthraquinone conjugate. Dotted lines indicate hydrogen bondings between Watson–Crick base pairs.

thraquinone group into the specific sugar residue of an oligonucleotide was based on the preparation of a modified ribonucleoside with anthraquinonylmethyl group at 2'-hydroxyl moiety. Benzyl substitution at the 2'- or 3'-hydroxyl moiety of the ribonucleoside can be achieved by reaction of 2',3'-O-dibutylstannylene ribonucleoside with benzyl bromide (15). This reaction has proved to be useful for introduction of the anthraquinonylmethyl group into the uridine 2'- or 3'-hydroxyl moieties, yielding 4 and its 3'-isomer. It should be noted that use of an *N*-acyl group as a protecting group of uridine and CsF as a catalyst is important for obtaining the desired product by the above reaction. After 5'-dimethoxytritylation and debenzoylation, 5'-DMT-U(2'AQ) (5) can be isolated in a pure form by a silica gel chromatography.

5'-DMT-U(2'AQ) phosphorobisdieethylamidite (6), prepared by phosphorylation of 5 with bis(diethylamino)-phosphorochloridite, is a suitable monomer for phosphorobisamidite oligonucleotide synthesis procedures that we have recently developed (18, 19). Coupling reactions of deoxyribonucleoside phosphorobisdieethylamidites are almost equally effective as standard deoxyribonucleoside phosphoramidite reagents, although 6 was found to

be slightly less efficient in the coupling probably because of the bulky 2'-substituent.

Duplex Stability. Model-building studies show that the duplex formation of oligonucleotide-anthraquinone conjugate (1) by Watson-Crick base pairing should allow two anthraquinone moieties to intercalate into both the base pairs of



in the resulting duplex (Figure 6). The UV and CD melting behaviors, where the shapes of the melting profiles for duplex 1 exhibit sigmoidal curves similar to those for 7, indicate the formation of oligonucleotide duplex for 1. The temperature-dependent change in the intensity of the induced CD at around 335 nm reflects directly the melting behaviors of duplex 1. These observations suggest that the intercalation of the anthraquinone moieties occurs in a cooperative manner with Watson-Crick base pairing.

Inspection of the melting profiles in Figure 3 and the t_m values in Table I reveals that the modification with anthraquinonylmethyl at the 2'-sugar hydroxyl moiety of the oligonucleotide double helix increases the duplex melting temperature by 17 °C relative to the corresponding unmodified duplex. The thermodynamic data in Table I show that this modification-induced increase in thermal stability translates into a free energy cost ($\Delta\Delta G^\circ$) of 5.3 kcal/mol for duplex at 27 °C. The magnitude of $\Delta\Delta G^\circ$ per one anthraquinone molecule can be estimated to be ca. 2.7 kcal/mol, which is larger than that reported for the oligonucleotide duplex with anthraquinone at the thymidine C-5 (7).

Close examination of the thermodynamic data reveals that the stabilizing influence ($\Delta\Delta G^\circ$) results from negative reductions in both the transition enthalpy ($\Delta\Delta H^\circ$) and the transition entropy ($\Delta\Delta S^\circ$). Anthraquinone-modified duplex 1 exhibits different CD spectral properties from the unmodified duplex 7 in the region between 200 and 300 nm, indicating that the modification with the anthraquinone at the sugar alters the global conformation of the double helix. This alteration must be considered for interpreting the enthalpy and the entropy effects that we have obtained for the duplex formation of oligonucleotide-anthraquinone conjugate 1. Nevertheless, the overall gain in the transition enthalpy may be derived mainly from intercalation between anthraquinone and the adjacent base pairs. Similar enthalpy effects have been reported on stabilizing complexes of oligonucleotides containing 5'-linked anthraquinone with poly(rA) (11). Further studies may be necessary to elucidate more detailed effects of the anthraquinone intercalation on the duplex stability.

A general procedure has been developed for incorporation of an anthraquinone to a specific sugar residue in oligonucleotide sequences. The oligonucleotide-anthraquinone conjugate has an increased affinity for the complementary sequence. The anthraquinone moiety should locate in between the base pairs adjacent to the designated sugar in the duplex. The present procedure would provide a useful method for preparation of oligonucleotide derivatives to deliver an anthraquinone group specifically to a given nucleotide sequence in DNA or RNA as well as for enhancement of the affinity of oligonucleotides for their complementary sequences.

ACKNOWLEDGMENT

We are grateful to Dr. H. Sugiyama for instruction in enzyme digestion analysis and to Dr. Y. Kuroda for the use of the CD spectrometer. A part of this work was

supported by a Grant from the Ministry of Education, Science, and Culture of Japan.

LITERATURE CITED

- (1) Asseline, U., Delarue, M., Lancelot, G., Toulme, F., Thuong, N. T., Montenay-Garestier, T., and Helene, C. (1984) Nucleic Acids-Binding Molecules with High Affinity and Base Sequence Specificity: Intercalating Agents Covalently Linked to Oligodeoxyribonucleotides. *Proc. Natl. Acad. Sci. U.S.A.* 81, 3297-3301.
- (2) Lancelot, G., Asseline, U., Thuong, N. T., and Helene, C. (1985) Proton and Phosphorus Nuclear Magnetic resonance Studies of an Oligothymidylate Covalently Linked to an Acridine Derivative and of Its Binding to Complementary Sequences. *Biochemistry* 24, 2521-2529.
- (3) Thuong, N. T., Asseline, U., Roig, V., Takasugi, M., and Helene, C. (1987) Oligo (α -deoxyribonucleotide)s Covalently Linked to Intercalating Agents: Differential Binding to Ribonucleotides and Deoxypolynucleotides and Stability Towards Nuclease Digestion. *Proc. Natl. Acad. Sci. U.S.A.* 84, 5129-5133.
- (4) Sun, J.-S., Francois, J.-C., Montenay-Garestier, T., Saison-Behmoaras, T., Roig, V., Thuong, N. T., and Helene, C. (1989) Sequence-Specific Intercalating Agents: Intercalation at Specific Sequences on Duplex DNA via Major Groove Recognition by Oligonucleotide-Intercalator Conjugates. *Proc. Natl. Acad. Sci. U.S.A.* 86, 9198-9202.
- (5) Toulme, J. J., Krisch, M. M., Loreau, N., Thuong, N. T., and Helene, C. (1986) Specific Inhibition of mRNA Translation by Complementary Oligonucleotides Covalently Linked to Intercalating Agents. *Proc. Natl. Acad. Sci. U.S.A.* 83, 1227-1231.
- (6) Verspieren, P., Cornelissen, A. W. C. A., Thuong, N. T., Helene, C., and Toulme, J. J. (1987) An Acridine-Linked Oligodeoxyribonucleotide Targeted to the Common 5'-End of Trypanosome mRNAs Kills Cultures Parasites. *Gene* 61, 307-315.
- (7) Zerial, A., Thuong, N. T., and Helene, C. (1987) Selective Inhibition of the Cytopathic Effect of Type A Influenza Virus by Oligodeoxyribonucleotides Covalently Linked to An Intercalating Agent. *Nucleic Acids Res.* 15, 9909-9919.
- (8) Mori, K., Subasinge, C., and Cohen, J. S. (1989) Oligodeoxyribonucleotide Analogs with 5'-Linked Anthraquinone. *FEBS Lett.* 249, 213-218.
- (9) Letsinger, R. L., and Schott, M. E. (1981) Selectivity in Binding a Phenthridinium-Dinucleotide Derivative to Homopolynucleotides. *J. Am. Chem. Soc.* 103, 7394-7396.
- (10) Yamana, K., and Letsinger, R. L. (1985) Synthesis and Properties of Oligonucleotides Bearing a Pendant Pyrene Group. *Nucleic Acids Res. Symposium Series No. 16*, 169-172.
- (11) Telser, J., Cruickshank, K. A., Morrison, L. E., Netzel, T. L., and Chan, C. (1989) DNA Duplexes Covalently Labeled at Two Sites: Synthesis and Characterization by Steady-State and Time-Resolved Optical Spectroscopies. *J. Am. Chem. Soc.* 111, 7226-7232.
- (12) Welch, C. J., and Chattopadhyaya, J. (1983) N^3 -Acyluridines: Preparation and Properties of a New Class of Uracil Protecting Group. *Acta Chem. Scand.* B37, 147-150.
- (13) Kemp, D. S., and Reczek, J. (1977) New Protective Groups for Peptide Synthesis-III The MAQ Ester Group Mild Reductive Cleavage of 2-Acyloxymethylantraquinone. *Tetrahedron Lett.* 12, 1031-1034.
- (14) Pike, R. A., and Schank, R. L. (1962) Preparation of β -Cyanoethyltrichlorosilane Using Silylamine Catalysts. *J. Org. Chem.* 27, 2190-2192.
- (15) Wagner, D., Verheyden, J. P. H., and Moffatt, J. G. (1974) Preparation and Synthetic Utility of Some Organotin Derivatives of Nucleosides. *J. Org. Chem.* 39, 24-30.
- (16) Caruthers, M. H. (1985) Gene Synthetic Machines: DNA Chemistry and Its Uses. *Science*, 230, 281-284.
- (17) Atkinson, T., and Smith, M. (1984) Solid-phase Synthesis of Oligodeoxyribonucleotides by the Phosphite Triester Method. In *Oligonucleotide Synthesis: A Practical Approach*

- (M. J. Gait, Ed.) pp 35–81, IRL Press, Oxford, UK.
- (18) Yamana, K., Nishijima, Y., Oka, A., Nakano, H., Sangen, O., Ozaki, H., and Shimidzu, T. (1989) A Simple Preparation of 5'-O-Dimethoxytrityl Deoxyribonucleoside 3'-O-Phosphorobisdiethylamidites as Useful Intermediates in the Synthesis of Oligodeoxyribonucleotides and Their Phosphorobisdiethylamidate Analogs on a Solid Support. *Tetrahedron* 45, 4135–4140.
- (19) Yamana, K., Nishijima, Y., Nakano, H., Sangen, O., Ozaki, H., and Shimidzu, T. (1989) A Phosphorobisamidite Approach to the Synthesis of Oligodeoxyribonucleotides and Their Analogues. *Nucleic Acids Res. Symposium Series* No. 21, 31–32.
- (20) Sugiyama, H., Kawabata, H., Fujiwara, T., Dannou, Y., and Saito, I. (1990) Specific Detection of C₄'-Hydroxylated Abasic Sites Generated by Bleomycin and Neocarzinostatin in DNA. *J. Am. Chem. Soc.* 112, 5252–5257.
- (21) Fasman, G. D., Ed. (1985) *Handbook of Biochemistry and Molecular Biology: Nucleic Acids*, 2nd ed., Vol. I, p 589 CRC Press, Cleveland, OH.
- (22) Turner, D. H., and Sugimoto, N. (1988) RNA Structure Prediction. *Annu. Rev. Biophys. Chem.* 17, 167–192.

Antibody Conjugates with Morpholinodoxorubicin and Acid-Cleavable Linkers

Barbara M. Mueller,*† Wolf A. Wrasidlo,† and Ralph A. Reisfeld†

Scripps Clinic and Research Foundation, La Jolla, California 92037, and Biotechnetics, San Diego, California 92121.

Received June 7, 1990

Antibody-morpholinodoxorubicin conjugates were prepared for targeted immunotherapy of human melanoma. Spacer molecules that differ in hydrolytic stability were employed between the C-13 of the drug and amino residue of lysine on the monoclonal antibody. Antibody-drug conjugates were made with five structurally different morpholinodoxorubicin derivatives including oxime, phenylhydrazone, (sulfonylphenyl)hydrazone, and acylhydrazone moieties. Hydrolytic stability of the antibody conjugates directly correlated with their in vitro cytotoxicity against melanoma cells. Derivatives or conjugates with the greatest hydrolytic stability showed the least cytotoxicity.

INTRODUCTION

Anthracyclines are effective antitumor antibiotics that have been used extensively in the treatment of different cancers (1-5). Although anthracyclines are among the most potent anticancer drugs known, their clinical application is limited by their cardiotoxicity. One possibility to overcome the toxicity of drugs to normal tissues is to attach the drug to a carrier system, such as monoclonal antibodies (Mab¹), which are capable of targeting tumor cells. In this way, the drug concentration will be selectively enhanced in tumor tissues, while the systemic concentration is reduced, thereby eliminating some of the toxic side effects of chemotherapy. To this end, anthracyclines were conjugated to a variety of Mab and these chemoimmunoconjugates were analyzed in several preclinical in vitro and in vivo studies (6-13).

Among the extensive list of anthracycline derivatives synthesized, morpholino doxorubicin and its 3-cyano analogue were shown to exhibit cytotoxic potencies against human tumor cell lines that can be from 2- to 10 000-fold higher than those of any other anthracyclines (14-16). This increase in potency, however, is not accompanied by an increase in cardiotoxicity. An additional advantage of these anthracycline analogues is that, due to different intracellular mechanisms of action than that of their parental drug doxorubicin (DXR), they are able to overcome multiple drug resistance (17-20). Recently, while preparing chemoimmunoconjugates of these compounds and Mab, we found that their potency could be varied over several orders of magnitude, depending on the nature of the spacer molecules employed in the conjugation reactions (21). These findings prompted us to investigate the linker chemistry of these immunoconjugates in greater detail. We describe here conjugates between MRA-HCl and Mab LM609 directed against the vitronectin receptor $\alpha_v\beta_3$ on human melanoma cells (22, 23). The human melanoma cell line used in this study (M21) has 2.5×10^5 binding

sites per cell for LM609 and internalizes LM609 with an endocytotic rate constant (k_e) of 1×10^{-2} (21). This implies that at saturation and 37 °C, 2500 antibody molecules are internalized into each cell per minute. We describe here the synthesis of MRA-HCl-LM609 conjugates with different acid-cleavable linkers and report the results of a study on the hydrolytic stability and cytotoxicity of these conjugates.

EXPERIMENTAL PROCEDURES

3'-Deamino-3'-(4-morpholinyl)doxorubicin (MRA-HCl). MRA-HCl was prepared by a method similar to that described in the literature (14). DXR was first reacted via 2,2'-oxybisacetaldehyde, followed by a reaction with sodium cyanoborohydride to form the morpholino- and (cyanomorpholino)doxorubicin mixtures. These mixtures were separated by silica gel column fractionation and after purification provided morpholino and cyanomorpholino derivatives in 45% and 20% yield, respectively. Homogeneity of these compounds was determined by silica gel thin-layer chromatography (TLC) (19:1 chloroform/methanol) and the purity was found to be 98% by reverse-phase HPLC analysis (20 mM ammonium acetate, pH 4.5/methanol).

3'-Deamino-3'-(4-morpholinyl)doxorubicin 13-[O-(Carboxymethyl)oxime] (Compound V). A solution of 6.1 mg (9.7×10^{-5} mol) of MRA-HCl in 500 μ L of anhydrous dimethylacetamide (DMA) and 3 μ L of triethylamine (1.1 molar excess) was stirred in the dark at 50 °C. A stock solution of 45 μ L of carboxymethoxylamine (4.66 mg; 2.13×10^{-5} mol in 200 μ L of dimethylacetamide) was then added with stirring. The course of the reaction was followed by reverse-phase HPLC and the elution time of the MRA-HCl was 20.29 min and that of its acid derivative equaled 15.89 min. The reaction was complete after 90 min and the product was 95% pure by HPLC analysis. Visible spectrophotometric analysis of the product showed peaks at 530, 488, 474, and 382 nm, characteristic of the doxorubicin chromophores.

13-[(4-Carboxyphenyl)hydrazono]-3'-deamino-3'-(4-morpholinyl)doxorubicin (Compound IV). MRA-HCl (4.3 mg, 6.6×10^{-6} mol) in 200 μ L of DMA was stirred in the dark and 10 μ L of a 10 mg/100 μ L stock solution of 4-hydrazinobenzoic acid was added. The clear reddish

* To whom correspondence should be addressed.

† Scripps Clinic and Research Foundation.

‡ Biotechnetics.

¹ Abbreviations: Mab, monoclonal antibody; DXR, doxorubicin; MRA-HCl, 3'-deamino-3'-(4-morpholinyl)doxorubicin; NHS, N-hydroxysuccinimide; EcDi, carbodiimide; FBS, fetal bovine serum; DMA, dimethylacetamide.

solution was heated for 60 min at 43 °C. Then another 2 μ L of reagent was added and the reaction continued for 60 min. HPLC analysis revealed quantitative conversion to the hydrazone derivative. The visible spectrum of this compound showed peaks at 530, 495, 478, and 389 nm, which are characteristic of doxorubicin, plus an additional absorption peak at 324 nm which is due to the phenylhydrazone moiety.

13-[(4-Carboxyphenyl)sulfonyl]hydrazono]-3'-deamino-3'-(4-morpholinyl)doxorubicin (Compound III). A solution of 7.16 mg (1.12×10^{-5} mol) of MRA-HCl in 180 μ L of dimethylacetamide was stirred in the dark and 20 μ L or 1.14×10^{-5} mol of a stock solution of 3-(hydrazinosulfonyl)benzoic acid (25 mg in 200 μ L of DMA) was added with stirring for 22 h at ambient temperature. After this period, HPLC analysis revealed the complete disappearance of free drug and showed a single new absorption band of the hydrazone derivative. Analysis of the visible spectrum indicated absorption bands at 528, 489, 474, and 385 nm attributable to doxorubicin and a new band at 338 nm due to the (hydrazinosulfonyl)-phenyl chromophore.

13-[(Hydrazinoadipyl)hydrazono]-3'-deamino-3'-(4-morpholinyl)doxorubicin (Compound II). A mixture of 6.5 mg (1×10^{-5} mol) of MRA-HCl in 300 μ L of DMA, 15 mg (1.1×10^{-5} mol) of adipic dihydrazide in 200 μ L of dimethylacetamide, and 3 mg of lithium chloride was stirred in the dark. Then, 3 μ L of acetic acid was added and the clear red solution was stirred for 18 h. After this period, TLC (19:1 chloroform/methanol) revealed the absence of free starting material.

The slightly turbid solution was passed through a silica gel plug using methanol as an eluant. The product was purified via preparative silica gel TLC (3:1 chloroform/methanol). Reverse-phase HPLC analysis (20 mM ammonium acetate, pH 4.5/methanol) of this compound showed a purity of 93% and visible spectral analysis revealed bands at 531, 486, 474, and 385 nm.

13-[(3-Carboxy-1-oxopropyl)hydrazono]-3'-deamino-3'-(4-morpholinyl)doxorubicin (Compound I). A mixture of 4.9 mg (7.5×10^{-6} mol) of MRA-HCl in 250 μ L of DMA and 3.2 mg (2.4×10^{-5} mol) of succinic acid monohydrazide was stirred in the dark at 45 °C for 18 h. The resultant turbid solution was filtered and the product was purified by preparative silica gel TLC (3:1 chloroform/methanol). The purity of this material by HPLC was 97%. The compound showed the characteristic visible spectrum with maxima at 534, 488, 474, and 380 nm.

Coupling Reactions with Mabs. Mab LM609 used in this study is directed against the vitronectin receptor expressed on human melanoma cells. LM609 is of IgG1 isotype and was purified from tissue culture supernatants by protein A Sepharose affinity chromatography. The doxorubicin derivatives were coupled to the NH_2 of the lysine side chains of this antibody via the carboxyl terminals by *N*-hydroxysuccinimide (NHS) activation. In a typical coupling procedure, the compound was dissolved in DMA and reacted with equal molar quantities of carbodiimide (Ecdi) and NHS in the dark at 4 °C with stirring for 18 h. Conversion rates to the NHS esters were nearly quantitative under these reactions conditions, as determined by HPLC analysis.

Solutions of the active esters were then added to Mab LM609 dissolved at approximately 10 mg/mL of solution in 100 mM phosphate-buffered saline (PBS) in a 30-fold molar excess at pH 7.8–8.0. After stirring for 3 h, the drug-antibody conjugates were purified by Sephadex G-50 column chromatography, filtered, and stored at 4 °C until

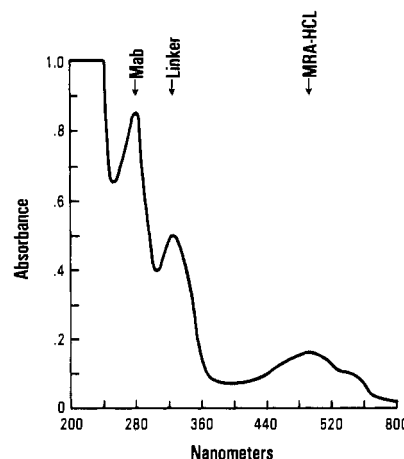


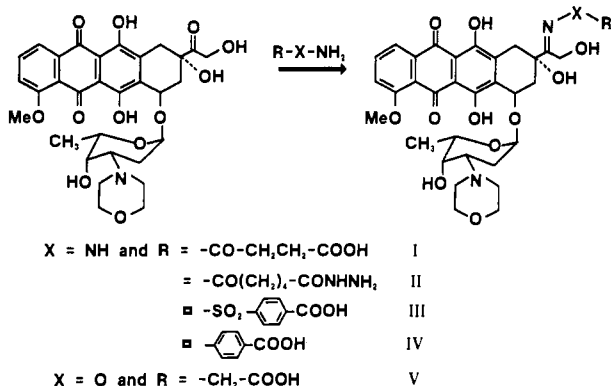
Figure 1. UV absorption spectrum of MRA-NNHC₆H₄CONH-Mab conjugate showing three distinct maxima corresponding to Mab (at 280 nm), linker (at 324 nm), and drug (at 488 nm) chromophores.

further use. The drug to antibody ratios were determined by spectroscopy (see Figure 1) at 280 and 480 nm using extinction coefficients of 9.9 and 13 $\text{mM}^{-1} \text{cm}^{-1}$, respectively.

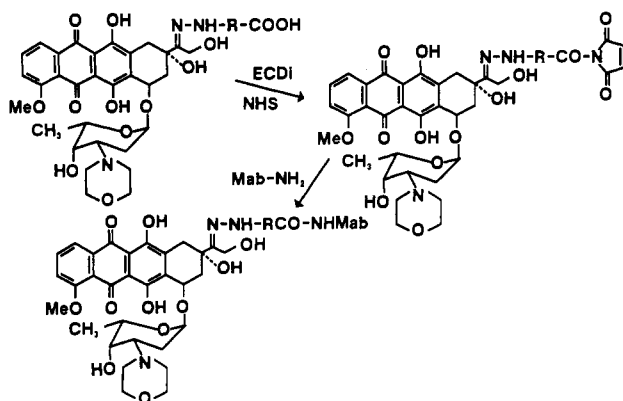
Stability Experiments. The stability of various preparations was tested by incubating samples in PBS under controlled conditions of temperature and pH by determining the extent of degradation by HPLC analysis of aliquots that were periodically removed from the preparation. Typically, 10 μ L of such aliquots were diluted with 30 μ L of methanol prior to injection on a Bondapak C18 column (Waters Assoc.). The elution was carried out with a gradient of 10 mM potassium phosphate, pH 5.6, and 60% methanol. The extent of degradation was determined by the ratios of areas under the peaks for the derivatized versus the free drug. Degradation studies of the antibody-drug conjugates were done by incubating samples at 37 °C, removing 100- μ L aliquots, and separating free drug from the conjugate by Sephadex G-50 gel chromatography. The residually bound drug was then determined by fluorescence spectroscopy (Perkin-Elmer LS-SR spectrophotometer) at an excitation frequency of 480 nm and drug concentration was measured at an emission frequency of 585 nm.

In Vitro Cytotoxicity. The human melanoma cell line UCLA-SO-M21 was kindly provided by Dr. D. L. Morton (UCLA, Los Angeles, CA) and a subclone (M21) established from these cells in our laboratory was used for our studies. M21 has 2.5×10^5 binding sites for Mab LM609 and internalizes LM609 with an endocytotic rate constant (k_e) of 1×10^{-2} (21). The M21 cells were grown in RPM1 tissue-culture media supplemented with 10% fetal bovine serum (FBS). The adherent growing cell line was detached with 0.5 mM EDTA, 0.15 M NaCl, 0.02 M HEPES and plated at 10^4 cells in 100 μ L of RPMI containing 10% FBS in each well of a 96-well tissue-culture plate. These cells were allowed to adhere overnight and then dilutions of drug, antibody, or conjugate were added in 10- μ L volumes and incubated with the cells for 2 h. Thereafter, the plates were washed three times in tissue-culture media and incubated overnight. Each well received 1 μ Ci of [³H]-thymidine and after a 16-h incubation, the cells were harvested onto glass-fiber filters with a Skatron cell harvester. The filters were placed in Ecolume scintillation solution (ICN, Irvine, CA) and were counted in a β -scintillation counter. [³H]Thymidine incorporation, as percentage of untreated control cells, is used to express cytotoxicity.

Scheme I



Scheme II



RESULTS

The C-13 substituted morpholinoanthracylines were prepared according to Scheme I. Conversions of the parent MRA-HCl to the hydrazones took place in near quantitative yields (>90%) under mild reaction conditions and the derivatives were readily purified by preparative TLC. With the exception of compound II, all other derivatives were conjugated to Mabs via their *N*-hydroxysuccinimide esters as shown in Scheme II. The intermediate NHS esters were determined by HPLC by first converting small aliquots to stable derivatives with ethanolamine. Then the intermediate NHS esters were linked directly to Mabs without any further purification.

Immunoconjugates were prepared by the addition of about 30 molar excess of NHS ester to antibody and the Sephadex G-50 purified preparations yielded drug to Mab ratios of 3 to 6. In these conjugates, the specific binding characteristics of the antibody were not significantly affected as measured by testing serial dilutions of Mab and conjugate in an ELISA assay with goat antimouse horseradish peroxidase as secondary reagent (data not shown).

Compounds I-V were tested for hydrolytic stability at pH 4.5 and 7 at 37 °C. HPLC analysis of samples taken periodically showed retention times corresponding to free MRA-HCl without any secondary hydrolysis products being present. The results of these experiments are shown in Figures 2 and 3. Except for the oxime derivative (Compound V), which was completely stable under these conditions, all other derivatives exhibited hydrolysis at rates that depended on the structure of the R group incorporated into these compounds. At pH 7, only the aliphatic acylhydrazone showed significant hydrolytic instability, while the other hydrazone derivatives exhibited relatively good resistance to hydrolytic degradation. At pH 4.5 both acyl (I and II) and sulfonylhydrazones (III)

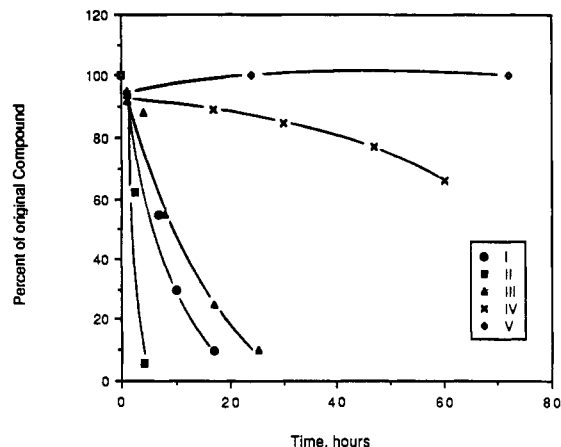


Figure 2. Hydrolytic stability of MRA-HCl derivatives expressed as percent of nonhydrolyzed derivative after incubation for various times at pH 4.5 and 37 °C.

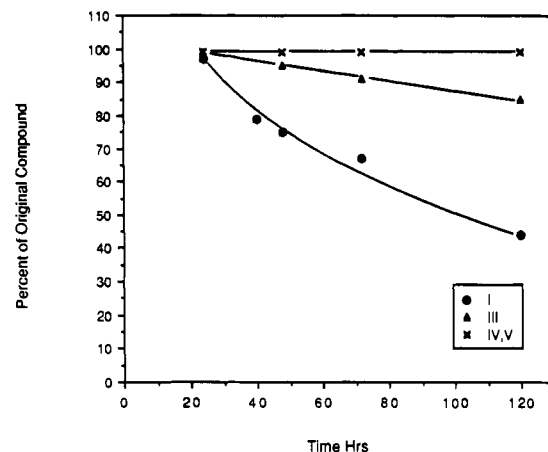


Figure 3. Hydrolytic stability of MRA-HCl derivatives expressed as percent of nonhydrolyzed derivative after incubation for various times at pH 7.0 and 37 °C.

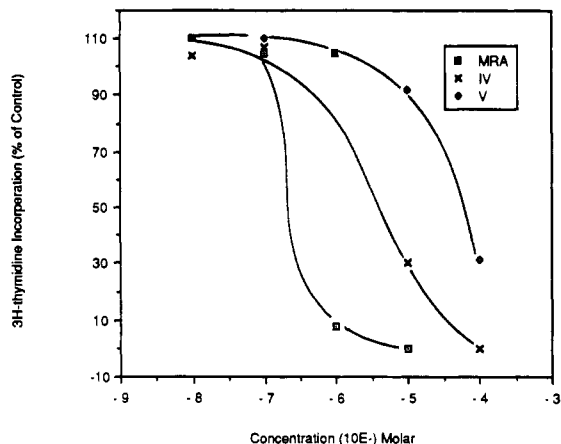


Figure 4. Cytotoxicity of MRA-HCl and its hydrazone derivatives on the human melanoma cell line M21. Cells were incubated with drugs for 2 h and their ability to incorporate [³H]thymidine was measured 24 h later.

exhibited relative rapid hydrolytic reversal rates to free MRA-HCl and only the oxime derivative remained stable.

Figure 4 depicts the cytotoxicity of MRA-HCl and its hydrazone and oxime derivatives on the human melanoma cell line M21. These substitutions of the C-13 position of the original drug result in a loss of cytotoxicity of 1 and 2 log units, respectively.

Hydrolysis data for antibody-drug conjugates of I, III,

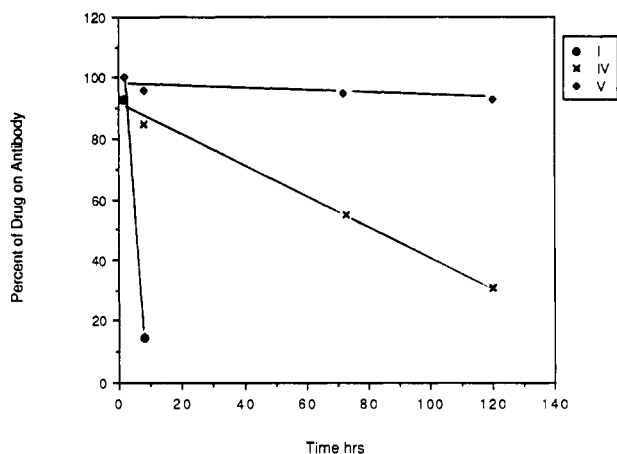


Figure 5. Hydrolytic stability of LM609-MRA conjugates expressed as percent of MRA-HCl bound to Mab after incubation for various times at pH 4.5 and 37 °C.

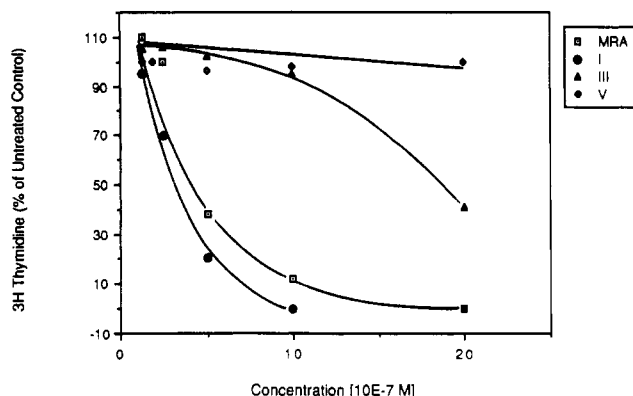


Figure 6. Effect of linker stability on the cytotoxicity of LM609-MRA conjugates. M21 cells were incubated with LM609-MRA conjugates for 2 h and their ability to incorporate [³H]-thymidine was measured 24 h later.

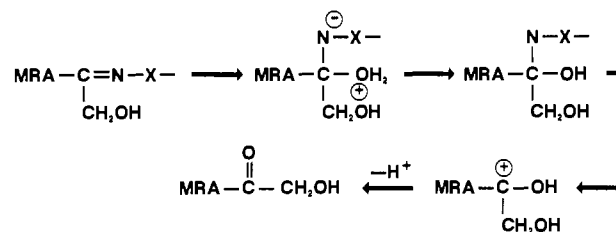
and V with Mab LM609 are summarized in Figure 5. The results obtained are similar to those shown in Figures 2 and 3. The acylhydrazone I conjugate dissociated about 90% within the first 8 h of incubation at pH 4.5 and 37 °C. However, under these same conditions, the acylsulfonyl-MRA-HCl-antibody (III) conjugate hydrolyzed at a rate of 1 order of magnitude slower, while the oxime-MRA-HCl-antibody conjugate (V) remained essentially unchanged.

The effect of linker structure on the cytotoxicity of these conjugates was also investigated. Plots of [³H]thymidine incorporation into M21 melanoma cell as a function of molar concentration of the free drug MRA-HCl or molar equivalents of drug linked to Mab LM609 are shown in Figure 6. The hydrolytically stable oxime V conjugate did not exhibit any significant cytotoxicity over the time period investigated, while both the hydrazones III and I were cytotoxic, with the acylhydrazone being significantly more so, approaching the cytotoxicity of free MRA-HCl.

DISCUSSION

The most significant result from this study has been the direct correlation between hydrolytic stability of the intermediate drug derivatives and their antibody conjugate with the cytotoxicity against human tumor cells. In every case, derivatives or conjugates with the greatest hydrolytic stability showed the least cytotoxicity. Since the amino group of daunosamine, which is commonly used when modifying anthracyclines with a linkable group, is unavailable in the morpholino derivatives of anthracy-

Scheme III



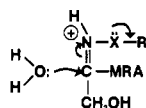
clines, we choose to react these through their C-13 carbonyl group. It has been shown previously (24) that the carbonyl group of daunomycin can be reacted with hydrazines and semicarbazide, yielding the corresponding hydrazones and semicarbazone, respectively. We found that morpholinoanthracyclines could be readily modified for antibody conjugation through their C-13 carbonyl group. Furthermore, condensation reactions with hydrazines or oximes yielded the corresponding hydrazono and hydroxyimino derivatives under mild reaction conditions in near quantitative yields. The use of heterobifunctional linkers of the general formula $\text{H}_2\text{NNHRCOOH}$ or $\text{H}_2\text{NORCOOH}$ resulted in derivatives with terminal carboxy functionalities as shown in Scheme I. These reactive derivatives could readily be activated via carbodiimide/*N*-hydroxysuccinimide intermediates and conjugated to lysine residues of monoclonal antibodies via the reactions of Scheme II.

Our initial effort involved the reaction of both morpholino- and (cyanomorpholino)doxorubicin with carboxymethoxylamine and subsequent conjugation to several Mabs directed against different tumor-associated antigens expressed on human melanoma cells, including the vitronectin receptor, chondroitin sulfate proteoglycan, gangliosides, and epidermal growth factor receptor.

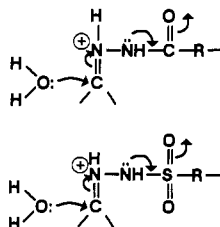
In vitro assays with these chemoimmunoconjugates indicated good immunoreactivity and specificity. However, a substantial loss of 2 orders of magnitude in cytotoxicity was observed with both intermediate oxime derivatives, as well as their final antibody conjugates. These findings are similar to those of earlier studies (25) which indicated that the cytotoxic properties of daunorubicin are lost whenever the drug is attached to carrier proteins in an irreversible manner. Thus, we were prompted to investigate other hydrazino derivatives and, in particular, to study the stability of these new derivatives and their respective immunoconjugates. Of particular interest to us was the stability observed at 37 °C under acidic conditions, since previous studies of acid-labile linkers (26–28) suggested that cleavage in the acidic milieu of the endosomes of cancer cells could release the toxic agent from the conjugate which then could transverse the endosome membrane and cause cell death.

The results of hydrolysis studies of five structurally different MRA-HCl derivatives, summarized in Figure 2, indicated that oxime or phenylhydrazone derivatives were quite stable while those with either sulfonyl or acyl groups in the linker were readily hydrolyzed to regenerate the carbonyl moiety. The general mechanism of hydrolysis of carbon-nitrogen double bonds involves initial addition of water, followed by elimination of the nitrogen moiety (29, 30). Thus, the hydrolytic regeneration of MRA-HCl from the derivatized conjugates can be viewed as shown in Scheme III. For the acid-catalyzed reaction, the specific mechanism shown in Scheme IV would apply. Thus, the nature of X should have a significant influence on the above mechanism. The relatively good hydrolytic stability of the oxime and phenylhydrazone can be attributed to the

Scheme IV



Scheme V



presence of the neighboring oxygen and NH groups in the linker. On the other hand, the relative ease of hydrolysis of the acyl and sulfonyl derivatives can be attributed to the delocalization of the lone electron pair of the neighboring carbonyl or sulfonyl groups (Scheme V). Of the five compounds investigated, the acylhydrazone derivative (structure I) was the least stable. In fact, slow hydrolysis was evident with this compound even at neutral pH, which could pose a storage problem with immunconjugates, as well as result in premature drug release of these antibody conjugates in in vivo experiments.

Ideally, the optimal drug-linker-antibody system is one which exhibits the greatest stability under physiological conditions, followed by rapid cleavage after endocytosis. From the data presented here, it appears that the best candidate is intermediate III, which is quite stable at pH 7 and 37 °C (Figure 3) and when conjugated with Mab LM609 is reasonably cytotoxic against the M21 human melanoma cell line.

ACKNOWLEDGMENT

We wish to thank George L. Tong for his help in synthesizing morpholinodoxorubicin and Lynne Kottel for preparing this manuscript. This work was supported in part by a grant from the National Cancer Institute, Outstanding Investigator Award 1R35CA42508. This is the Research Institute of Scripps Clinic Manuscript Number 6425-IMM.

LITERATURE CITED

- (1) DiMarco, A., Gaetani, M., and Scarpinato, B. (1969) Adriamycin (NCS-123,127): A new antibiotic with antitumor activity. *Cancer Chemother. Rep.* 53, 133-137.
- (2) Bonadonna, G., De Lena, M., and Beretta, G. (1971) Preliminary clinical screening with adriamycin in lung cancer. *Eur. J. Cancer* 7, 365-367.
- (3) Davis, H. L., and Davis, T. E. (1979) Daunorubicin and adriamycin in cancer treatment: An analysis of their roles and limitations. *Cancer Treat. Rep.* 63, 809-815.
- (4) Oki, T. (1984) Structure-activity relationship of antitumor anthracycline antibiotics and drug development. *Stud. Biophys.* 104, 169-200.
- (5) Weiss, R. B., Sarosy, G., Clagett-Carr, K., Russo, M., and Leyland-Jones, B. (1986) Anthracycline analogues: The past, present, and future. *Cancer Chemother. Pharmacol.* 18, 185-197.
- (6) Hurwitz, E., Maron, R., Arnon, R., Wilchek, M., and Sela, M. (1978) Daunomycin-immunoglobulin conjugates, uptake and activity in vitro. *Eur. J. Cancer* 14, 1213-1220.
- (7) Hurwitz, E., Maron, R., Bernstein, A., Wilchek, M., Sela, M., and Arnon, R. (1978) The effect in vivo of chemotherapeutic drug-antibody conjugates in two murine experimental tumor systems. *Int. J. Cancer* 21, 747-755.
- (8) Belles-Isles, M., and Page, M. (1980) In vitro activity of daunomycin-anti-alpha fetoprotein conjugate on mouse hepatoma cells. *Br. J. Cancer* 41, 841-842.
- (9) Belles-Isles, M., and Page, M. (1981) Anti-oncofetal proteins for targeting cytotoxic drugs. *Int. J. Immunopharmacol.* 3, 97-102.
- (10) Gallego, J., Price, M. R., and Baldwin, R. W. (1984) Preparation of four daunomycin-monooclonal antibody 791T/36 conjugates with antitumor activity. *Int. J. Cancer* 33, 737-744.
- (11) Tsukada, T., Ohkawa, K., and Hibi, N. (1985) Suppression of human alpha-fetoprotein-producing hepatocellular carcinoma growth in nude mice by an anti alpha-fetoprotein antibody-daunorubicin conjugate with a poly-L-glutamic acid derivative as intermediate drug carrier. *Br. J. Cancer* 52, 111-116.
- (12) Yang, H. M., and Reisfeld, R. A. (1988) Doxorubicin conjugated with a monoclonal antibody directed to a human melanoma-associated proteoglycan suppresses the growth of established tumor xenografts in nude mice. *Proc. Natl. Acad. Sci. U.S.A.* 85, 1189-1193.
- (13) Aboud-Pirak, E., Hurwitz, E., Bellot, F., Schlessinger, J., and Sela, M. (1989) Inhibition of human tumor growth in nude mice by a conjugate of doxorubicin with monoclonal antibodies to epidermal growth factor receptor. *Proc. Natl. Acad. Sci. U.S.A.* 86, 3778-3781.
- (14) Acton, E. M., Tong, G. L., Mosher, C. W., and Wolgemuth, R. L. (1984) Intensely potent morpholinyl anthracyclines. *J. Med. Chem.* 27, 638-645.
- (15) Giuliani, F. C., Barbieri, B., Geroni, C., Facchinetti, T., Casazza, A. M., and Acton, E. M. (1984) Properties of cyanomorpholinyl-doxorubicin, a new anthracycline active against P388 resistant leukemia. *Proc. Am. Assoc. Cancer Res.* 25, 305.
- (16) Sikic, B. I., Ehsan, M. N., Harker, W. G., Friend, N. F., Brown, B. W., Newman, R. A., Hacker, P. M., and Acton, E. M. (1985) Dissociation of antitumor potency from anthracycline cytotoxicity in a doxorubicin analogue. *Science* 228, 1544-1546.
- (17) Westerndorf, J., Marquardt, H., and Marquardt, H. (1984) Structure activity relationship of anthracycline-induced genotoxicity in vitro. *Cancer Res.* 44, 5599-5604.
- (18) Streeter, D. G., Johl, J. S., Gordon, G. R., and Peters, J. H. (1986) Uptake and retention of morpholinyl anthracyclines by adriamycin-sensitive and -resistant P388 cells. *Cancer Chemother. Pharmacol.* 16, 247-252.
- (19) Scudder, S. A., Brown, J. M., and Sikic, B. I. (1988) DNA cross-linking and cytotoxicity of the alkylating cyanomorpholino derivative of doxorubicin in multidrug-resistant cells. *JNCI, J. Natl. Cancer Inst.* 80, 1294-1298.
- (20) Wassermann, K., Newman, R. A., Davis, F. M., Mullins, T. D., and Rose, K. M. (1988) Selective inhibition of human ribosomal gene transcription by the morpholinyl anthracyclines cyanomorpholinyl- and morpholinyl-doxorubicin. *Cancer Res.* 48, 4101-4106.
- (21) Mueller, B. M., Reisfeld, R. A., Silveira, M. H., Duncan, J. D., and Wrasidlo, W. A. Pre-clinical therapy of human melanoma with morpholino-doxorubicin conjugated to a monoclonal antibody directed against an integrin on melanoma cells. *Antibody Immunoconjugates Radiopharm.* in press.
- (22) Cheresch, D. A., and Spiro, R. C. (1987) Biosynthesis and functional properties of an Arg-Gly-Asp-directed receptor involved in human melanoma cell attachment to vitronectin, fibronectin, and von Willebrand factor. *J. Biol. Chem.* 262, 17703-17711.
- (23) Smith, J. W., and Cheresch, D. A. (1990) Integrin (alpha3 beta3)-ligand interaction. Identification of a heterodimeric RGD binding site on the vitronectin receptor. *J. Biol. Chem.* 265, 2168-2172.
- (24) Yamamoto, K., Acton, E. M., and Henry, D. W. (1972) Antitumor activity of some derivatives of daunorubicin at the amino and methyl ketone functions. *J. Med. Chem.* 15, 872-875.
- (25) Hurwitz, E., Levy, R., Maron, R., Wilchek, M., Arnon, R., and Sela, M. (1975) The covalent binding of daunomycin and adriamycin to antibodies with retention of both drug and antibody activities. *Cancer Res.* 35, 1175-1181.
- (26) Shen, W.-C., and Ryser, H. J.-P. (1981) Cis-acetyl spacer

- between daunomycin and macromolecular carriers: A model of pH-sensitive linkage releasing drug from a lysosomotropic conjugate. *Biochem. Biophys. Res. Commun.* 102, 1048–1054.
- (27) Diener, E., Diner, U. E., Sinha, A., Xie, S., and Vergidis, R. (1986) Specific immunosuppression by immunotoxins containing daunomycin. *Science* 231, 148–150.
- (28) Blattler, W. A., Kuenzi, B. S., Lambert, T. M., and Senter, P. D. (1985) New heterobifunctional protein cross-linking reagent that forms an acid labile link. *Biochemistry* 24, 1517–1524.
- (29) Reeves, R. L. (1962) Schiff bases: Kinetics of hydrolysis of *p*-trimethylammoniumbenzylidene-*p'*-hydroxyaniline chloride in aqueous solution from pH 1 to 11.5. *J. Am. Chem. Soc.* 84, 3332–3337.
- (30) Cordes, E. H., and Jencks, W. P. (1963) The mechanism of hydrolysis of Schiff bases derived from aliphatic amines. *J. Am. Chem. Soc.* 85, 2843–2848.

Immunotoxin Construction with a Ribosome-Inactivating Protein from Barley

Ray F. Ebert* and Lucinda A. Spryn†

Akzo Pharma/Organon Teknika Corporation, Biotechnology Research Institute, 1330-A Piccard Drive, Rockville, Maryland 20850-4373. Received June 22, 1990

The aim of this study was to determine the suitability of a ribosome-inactivating protein (RIP) from barley endosperm for use as an immunotoxin. This barley RIP is identical with the 30-kDa protein first reported by Coleman and Roberts [(1982) *Biochim. Biophys. Acta* 696, 239] and sequenced by Asano and co-workers [(1986) *Carlsberg Res. Commun.* 51, 75]. Use of the terms barley toxin I, II, and III is proposed to describe the three isoforms resolved by cation-exchange chromatography. An improved procedure for isolating the protein involving the steps of aqueous extraction, ammonium sulfate precipitation, and cation-exchange HPLC is described. Barley toxin II retained activity after exposure to ca. 40% acetonitrile and 0.1% trifluoroacetic acid or lyophilization. In a comparative study using the rabbit reticulocyte lysate assay, the protein was about 68% and 30% as potent as gelonin and ricin A-chain (RTA), respectively. Introduction of SH groups with 2-iminothiolane resulted in a substantial loss of activity as the number of thiol groups approached four. Therefore, it was necessary to limit thiolation to an average of one to two SH groups per toxin molecule. Anti-transferrin receptor-based immunotoxins constructed with RTA, gelonin, and barley toxin II exhibited comparable cytotoxicity against a human colon tumor cell line. We conclude that the availability of raw material, ease of purification, and stability of barley toxin II to lyophilization and denaturing conditions render it a suitable protein for the construction of immunotoxins.

Type 1 ribosome-inactivating proteins (RIP¹) are a class of plant-derived polypeptides, possibly involved in disease resistance, that lack cell-binding (B-chain) domains and function by inactivating eukaryotic ribosomes (1). A translation inhibitor with these characteristics was first isolated from pearled (dehusked) barley (*hordeum vulgare*) by Coleman and Roberts in 1982 (2). Like other RIP's from the family *Gramineae*, the barley protein synthesis inhibitor was found to be a basic ($pI > 10$), 30-kDa protein that was relatively nontoxic to intact cells. A subsequent report (3) disclosed that fungal ribosomes are approximately 10 times more sensitive than eukaryotic ribosomes to the barley RIP.

Independently, Asano and co-workers isolated and characterized three isoforms of a 30-kDa protein synthesis inhibitor from barley seeds (4, 5). They also determined the sequence for the most prevalent of these isoforms, "barley protein synthesis inhibitor II" (6). A direct comparison of this protein with RTA disclosed a 21% homology overall, with an extraordinary conservation of residues in the putative active-site region (7). Comparative evaluation of RTA and this "barley toxin" demonstrated that both proteins inactivate ribosomes via the same mechanism: enzymatic hydrolysis of the *N*-glycosidic bond at A⁴³²⁴ of 28S rRNA (8).

The available evidence indicates that the protein synthesis inhibitor/30-kDa antifungal protein described by Roberts and co-workers (2, 3), the protein synthesis inhibitor sequenced by Asano and colleagues (4-6), and the toxin evaluated by Endo et al. (8) represent the same enzyme. In this report we shall refer to this protein as "barley toxin" and, where appropriate, use the descriptors I, II, and III to denote the three isoenzyme peaks eluting from cation-exchange columns.

The aim of the present study was to determine the suitability of barley toxin II for use as an immunotoxin. We describe an improved, three-step purification procedure for isolating the protein and an optimized method for conjugating it to an anti-transferrin receptor monoclonal antibody. A comparison between this immunotoxin and similarly constructed conjugates with RTA and gelonin disclosed comparable in vitro cytotoxicity against a colon tumor cell line.

EXPERIMENTAL PROCEDURES

Materials. RTA was from Vector Laboratories, Burlingame, CA. Gelonin was kindly provided by Dr. Walter Blättler, ImmunoGen, Inc., Cambridge, MA. Ammonium sulfate (enzyme grade) was from Bethesda Research Laboratories, Gaithersburg, MD. SPDP and 2-iminothiolane were from Pierce Chemical Co., Rockford, IL. DTNB (Ellman's reagent) was from Aldrich Chemical Co., Milwaukee, WI. Medium, pearled barley was a product of The Quaker Oats Co., Chicago, IL, and was purchased at a local grocery store. Tritiated leucine was purchased from Amersham Corp., Arlington Heights, IL. SDS-PAGE molecular weight standards were purchased from Bio-Rad, Inc., Rockville Centre, NY.

Isolation of Barley Toxin. Barley RIP's were isolated essentially as described by Roberts and Selitrennikoff (3),

* To whom requests for reprints should be addressed.

† Portions of this work were submitted to The American University in partial fulfillment of the requirements for the Master of Science degree.

¹ Abbreviations: DTNB, 5,5'-dithiobis(2-nitrobenzoic acid); ID₅₀, concentration at which protein synthesis is inhibited by 50%; PBS, Dulbecco's phosphate-buffered saline (pH 7.3); Na₂HPO₄ (10 mM), KH₂PO₄ (1.8 mM), KCl (3.4 mM), and NaCl (171 mM); RIP, ribosome-inactivating protein; RTA, ricin A-chain; SDS-PAGE, sodium dodecyl sulfate-polyacrylamide gel electrophoresis; SPDP, *N*-succinimidyl 3-(2-pyridyldithio)propionate.

except that the conventional carboxymethyl-Sepharose cation-exchange step was replaced with a high-performance cation-exchange procedure. This modification yielded homogeneous barley toxin and eliminated the need for size-exclusion chromatography. To summarize, 3–5 kg of pearled barley was ground into a coarse dry powder in a blender and stirred for 1–2 h at 4 °C in 7.5 L of a 10 mM sodium phosphate buffer (pH 7.4) containing 130 mM NaCl. All remaining procedures were performed at 4 °C, and all centrifugation steps were at 10000g for 10 min. The extraction mixture was filtered through cheesecloth and clarified by centrifugation. The supernatant was brought to 55% (w/v) saturation by slow addition of solid $(\text{NH}_4)_2\text{SO}_4$. After stirring for 2 h, the precipitate was removed by centrifugation and the supernatant was filtered through Whatman #1 paper. The filtrate was brought to 80% (w/v) saturation with solid $(\text{NH}_4)_2\text{SO}_4$, stirred overnight, and centrifuged. This 55–80% $(\text{NH}_4)_2\text{SO}_4$ precipitate, which contains barley toxins I, II, and III, was resuspended in 200–400 mL of 25 mM sodium phosphate (pH 7.0) containing 50 mM NaCl (eluent A) and dialyzed against 4 L of eluent A with four changes at 7–14-h intervals. The dialysate was clarified by centrifugation and stored at –70 °C. Fractions containing approximately 0.8–1.0 g of protein were thawed and applied to a 0.94×20 cm cation-exchange HPLC column (PolyCAT-A, PolyLC Inc., Columbia, MD) that had been equilibrated with eluent A. After sufficient washing with eluent A to remove nonadsorbed protein, the column was developed with a gradient from 50 to 300 mM NaCl (in 25 mM sodium phosphate, pH 7.0) over a period of 60 min at 2 mL/min. Between runs, the column was regenerated with 2–4 volumes of 0.5 M NaCl in 25 mM sodium phosphate, pH 7.0. Approximately four runs were needed to process the 55–80% $(\text{NH}_4)_2\text{SO}_4$ precipitate resulting from an extract of 3–5 kg of pearled barley.

Anti-Human Transferrin Receptor Monoclonal Antibody. An hybridoma secreting monoclonal antibody 5E9C11 (anti-human transferrin receptor; ref 9) was obtained from the American Type Culture Collection (ATCC HB-21), Rockville, MD. The antibody was generated in pristane-primed BALB/c mice and purified from ascites fluid by protein A affinity chromatography or by ion-exchange HPLC on a Bakerbond ABx column (0.775×10 cm; Baker Chemical Co., Phillipsburg, NJ) according to the manufacturer's instructions. The antibody preparation used to construct immunotoxins was judged to be >95% pure on the basis of SDS-PAGE.

Thiolation of Barley Toxin and Gelonin. Traut's reagent (2-iminothiolane) was used to introduce sulfhydryl groups into barley toxin and gelonin, both of which lack cysteine. The toxins were dialyzed against a 100 mM potassium phosphate buffer (pH 8.0) containing 1 mM EDTA and adjusted to a final concentration of 2–4 mg/mL. After prewarming to 30 °C, a sufficient amount of 0.4 M 2-iminothiolane was added to yield a 50-fold molar excess over the toxin. After incubation for 10–30 min at 30 °C, the solutions were dialyzed against a 10 mM potassium phosphate buffer (pH 7.0) containing 1 mM EDTA (three changes, 8–12 h each) to remove low molecular weight components. This procedure resulted in the addition of one or two sulfhydryl groups per toxin molecule, as estimated with the Ellman method (10). Higher substitution ratios were obtained by incubating the reaction mixture as above for 30–60 min.

Activation and Conjugation of the Anti-Transferrin Receptor Monoclonal Antibody. Antibody HB-21 (M_R 180 000) was dialyzed into a buffer containing 50

mM potassium phosphate (pH 7.5) and 200 mM NaCl (coupling buffer) and incubated for 30 min at room temperature with a 3-fold molar excess of SPDP. Excess reactants and non-protein products were removed by dialysis at 4 °C against coupling buffer. Under these conditions, approximately two pyridinedithiol groups were incorporated per monoclonal antibody. The activated monoclonal antibody was incubated overnight at room temperature with thiolated toxin at a concentration 5 times higher than that of the antibody-linked 2-pyridinedithiol. The immunoconjugate was separated from unreacted toxin by gel-permeation HPLC using a Zorbax GF-250 column (2.12×25 cm, E. I. du Pont de Nemours & Co., Wilmington, DE) equilibrated with PBS.

Reticulocyte Lysate Assay. Inhibition of protein synthesis in a cell-free system was used to measure toxin activity. Reagents provided in a translation kit (Promega Biotec, Madison, WI) were employed with a modified assay procedure (Note: conjugates were not reduced prior to assay, nor were reducing agents present in the reaction mixture). A solution of kit reagents consisting of one part 1 mM amino acid mixture minus leucine, one part 0.5 $\mu\text{g}/\mu\text{L}$ Brome mosaic virus mRNA, one part glass-distilled water, and five parts [^3H]leucine (5 $\mu\text{Ci}/\text{mL}$) was made. Each assay tube contained 8 μL of this solution, 35 μL of lysate, and 10 μL of sample. All dilutions were made with a 40 mM sodium phosphate buffer (pH 7.4) containing 150 mM NaCl (sample buffer), and molar concentrations of the immunotoxins were based on an assumed molecular weight of 240 000 (antibody plus two toxin molecules). The solutions were mixed and centrifuged in a microfuge apparatus for 5 s to ensure that all liquid was at the bottom of the tubes. After 1 h at 37 °C, 50 μL of assay mixture was transferred to a microtiter plate (Immulon II, Dynatech Laboratories, Chantilly, VA) that had been blocked with 1% bovine serum albumin in sample buffer. The translated protein was transferred to glass-fiber filters by means of a cell harvester (PhD, Cambridge Technology, Inc., Cambridge, MA). The filters were then dried and radioactivity was determined in a liquid-scintillation counter. The percent inhibition of protein synthesis was calculated relative to a control to which no toxin had been added. One unit of toxin activity is defined as the sample dilution that inhibits protein synthesis by 50%.

Cytotoxicity Assay. A human colon adenocarcinoma cell line, HT-29, was obtained from the American Type Culture Collection (Rockville, MD) and used to evaluate the cytotoxicity of immunoconjugates. Microtiter plates (96 well, Immulon II, Dynatech Laboratories, Chantilly, VA) were inoculated (day 1) with 200 $\mu\text{L}/\text{well}$ of cells ($2.5 \times 10^5/\text{mL}$) suspended in Eagle's MEM (GIBCO, Grand Island, NY) plus 10% fetal calf serum plus 0.1% gentamicin. All incubations were in a constant humidity chamber set at 37 °C and 94% $\text{O}_2/6\%$ CO_2 . On day 2, the medium was replaced (100 $\mu\text{L}/\text{well}$), and test samples (50 μL in sterile PBS) were added. All samples were assayed in quadruplicate. On day 4 the cells were washed with PBS and 100 μL of Eagle's MEM leucine-free medium was added to each well. After a 1–3-h incubation at 37 °C, 50 μL of [^3H]leucine (0.04 $\mu\text{Ci}/\mu\text{L}$) in PBS was added. After 3–4 h at 37 °C, the medium was aspirated from the wells; cells were released by addition of 0.1% trypsin (100 $\mu\text{L}/\text{well}$), harvested on glass-fiber filters as above, and evaluated for radioactivity by liquid scintillation counting. The molar concentrations of the immunotoxins were based on an assumed molecular weight of 240 000 (antibody plus two toxin molecules).

Reversed-Phase (RP) HPLC of Barley Toxin. RP-

Table I. Purification of Barley Toxin

step	mg of protein	total units (10 ⁶) ^a	sp act., units/ μ g	% yield
aqueous extract	10100	140	14	100
55–80% (NH ₄) ₂ SO ₄ ppt	3570	318	89	227
cation-exchange HPLC	174	107	618	76

^a One unit of toxin activity is defined as the sample dilution that inhibits protein synthesis by 50% in a reticulocyte lysate assay system. Total units are obtained by multiplying this dilution factor by the quotient of the total sample volume (in mL) divided by 0.01 mL (the volume of sample in the reticulocyte lysate assay).

HPLC of purified barley toxin was performed with a Vydac TP-C4 (butylsilane) HPLC column (1.0 \times 25 cm, The Separations Group, Hesperia, CA). Eluents A and B were water and acetonitrile, respectively, each containing 0.1% trifluoroacetic acid. The column was equilibrated with eluent A and the protein was eluted by a gradient (1.5% / min) from 30% to 50% B. Protein was detected by absorbance at 280 nm. Protein-containing peaks were collected manually, evaporated to dryness in a SpeedVac concentrator (Savant Instrument Co., Farmingdale, NY), and redissolved in a 40 mM potassium phosphate buffer (pH 7.4) containing 150 mM NaCl.

Electrophoresis. SDS-PAGE was carried out in the buffer system of Laemmli (11) using a 5% stacking gel and a gradient of 5–15% polyacrylamide (0.8% bisacrylamide) in the separating gel. The gels were stained with Coomassie Brilliant Blue R-250.

Other Assays. All protein concentrations were determined with the method of Lowry et al. (12) using bovine serum albumin as the protein standard.

RESULTS

Isolation and Characterization of Barley Toxin.

The three-step purification procedure comprised aqueous extraction of triturated barley endosperm, differential ammonium sulfate precipitation, and cation-exchange HPLC. The results of a representative lot are summarized in Table I: an aqueous extract of 3.17 kg of pearled barley yielded 10.1 g of crude protein, from which 174 mg of barley toxin was isolated. The recovery of toxin activity in the 55–80% ammonium sulfate fraction consistently exceeded 100%. The possibility that this was due to removal of an inhibitor was not explored further.

The introduction of a highly selective cation-exchange HPLC step (Figure 1) obviated the need to remove contaminants by gel filtration, as has been required following conventional cation-exchange chromatography (3, 4, 13). The major peak of RNA *N*-glycosidase activity (peak II) corresponded to a major *A*₂₈₀ peak at about 43 min (Figure 1). Ribosome-inactivating activity also was detected in protein eluting at approximately 25–30 min and at approximately 55 min. These were presumed to represent barley toxins I and III, respectively (4).

The isolated protein migrated as a single 30-kDa protein band on SDS-PAGE (Figure 2), from which purity was estimated to be >99%. However, when evaluated by RP-HPLC, barley toxin II eluted as two protein peaks (Figure 3). Each protein peak was collected, lyophilized, redissolved in PBS, and compared in the reticulocyte lysate assay with cation-exchange-purified material that had not been lyophilized. The results (Figure 4) disclosed virtually no difference between the two RP-HPLC peaks, nor was there any substantial loss of activity upon exposure to the reversed-phase solvents (0.1% TFA and acetonitrile). Thus, barley toxin II appears to be stable to acid, organic solvent, and lyophilization.

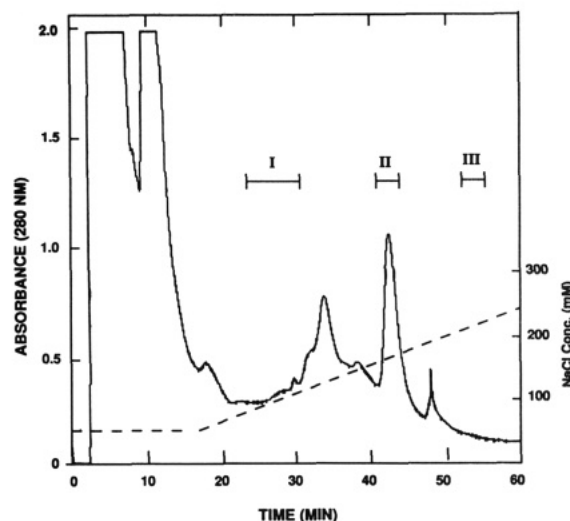


Figure 1. Cation-exchange HPLC of a 55–80% (NH₄)₂SO₄ precipitate prepared from an aqueous extract of pearled barley. See Experimental Procedures for chromatographic conditions. The NaCl gradient is indicated by the dashed line. The bars denote regions in which toxin activity was detected in a reticulocyte lysate (cell-free) protein synthesis assay.

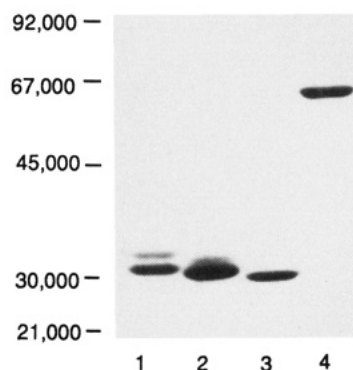


Figure 2. Comparative SDS-PAGE of RIP's. A 5–15% polyacrylamide gradient gel under nonreducing conditions was used: lane 1, ricin A-chain; lane 2, gelonin; lane 3, barley toxin II; lane 4, *Pseudomonas* exotoxin.

For the preparation described in Table I, barley toxin II comprised about 1.3% of the protein in the aqueous extract. In general, the toxin represented 1–2% of the protein in these extracts. On average ($N = 3$), 55 mg of toxin were obtained per kg of pearled barley. Specific activities of the isolated protein ranged from 400 to 1600 units/ μ g (mean = 980 units/ μ g), and the concentration at which cell-free protein synthesis was inhibited by 50% ranged from 0.52 to 2.1 nM (mean = 1.1 nM; $N = 4$).

In agreement with the observations of Asano and co-workers (4), carbohydrate was not detected on the barley toxin. Also in agreement with a previous report (6), the N-terminus of the toxin was blocked. Sequencing of CNBr-derived peptides (not shown) confirmed the identity of barley toxin with the protein synthesis inhibitor described by Asano et al. (4–6). In a comparative study using the rabbit reticulocyte lysate assay, barley toxin ($ID_{50} = 0.47$ nM) was found to be about 75% and 30% as potent as gelonin ($ID_{50} = 0.32$ nM) and RTA ($ID_{50} = 0.14$ nM), respectively (Figure 5).

Effect of Thiolation on Barley Toxin II Activation.

Prior to conjugation with SPDP-activated antibody, sulfhydryl groups were introduced via 2-iminothiolane. We found that as the average number of thiol groups approached four, RIP activity was severely inhibited (Figure

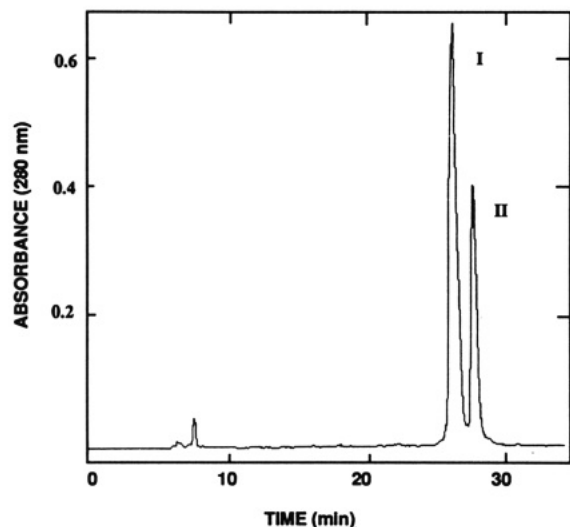


Figure 3. Reversed-phase (butylsilane) HPLC. Isolated barley toxin II (200 μ g) was applied to a butylsilane column and eluted with a gradient of acetonitrile (30–50%; 1.5% /min) as described in Experimental Procedures. Peaks I and II were collected manually, lyophilized, and evaluated for activity as described in Results.

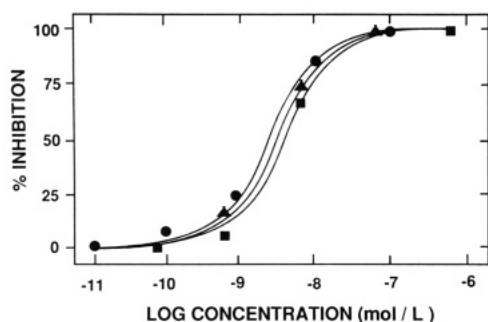


Figure 4. Activity of barley toxin II preparations in the reticulocyte lysate assay: barley toxin II purified via cation-exchange HPLC (●); isolated barley toxin II after reversed-phase HPLC (see Figure 3), peak I (■), peak II (▲).

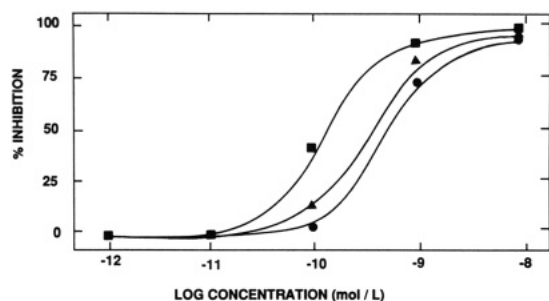


Figure 5. Comparison of ribosome-inactivating activity in the reticulocyte lysate assay of barley toxin II (●), gelonin (▲), and ricin A-chain (■). Details of the assay are described in Experimental Procedures. ID_{50} values were 0.47, 0.32, and 0.14 nM, respectively, for barley toxin II, gelonin, and RTA.

6). Accordingly, it was necessary to limit thiolation to an average of one to two SH groups per toxin molecule.

Evaluation of Immunotoxins. SDS-PAGE was used to determine the approximate number of toxin molecules linked to the anti-transferrin receptor monoclonal antibody. In this system the unconjugated antibody migrated at M_R 180 000 (Figure 7, lanes 3 and 6). The results for barley toxin II and gelonin conjugates (Figure 7, lanes 2 and 5) disclosed a minor protein band with the same electrophoretic mobility as unconjugated antibody, major bands at M_R 210 000, 240 000, and 270 000, and higher molecular weight multimers. From this we estimate that these im-

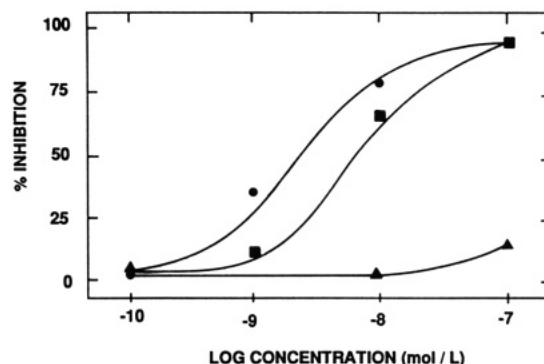


Figure 6. Effect of thiolation on barley toxin II activity in the reticulocyte lysate assay: control (unmodified) barley toxin II (●), thiolated barley toxin II at 1.4 (■) and 4.4 (▲) SH groups per molecule. See Experimental Procedures for additional details.

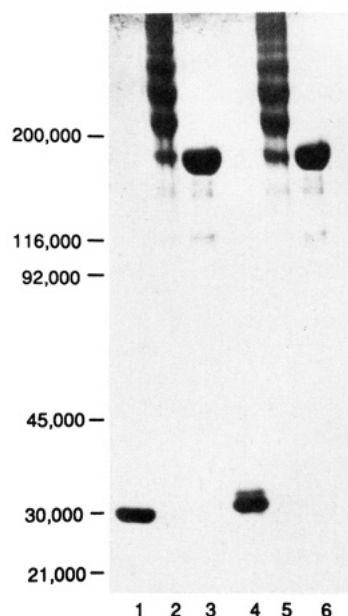


Figure 7. SDS-PAGE of immunotoxins constructed with an anti-transferrin receptor (α TFR) monoclonal antibody and gelonin or barley toxin II. All samples were run under nonreducing conditions: lane 1, barley toxin II; lane 2, barley toxin II- α TFR monoclonal antibody conjugate; lanes 3 and 6, unconjugated (control) α TFR monoclonal antibody; lane 4, gelonin; lane 5, gelonin- α TFR monoclonal antibody conjugate.

munotoxin preparations consisted of less than 10% unconjugated antibody, with a major fraction comprised of one to three toxin molecules per antibody. Similar results were obtained for the RTA conjugate (not shown).

Anti-transferrin receptor-based immunotoxins constructed with RTA, gelonin, and barley toxin were evaluated for ribosome-inactivating activity in the rabbit reticulocyte lysate assay. In this cell-free system the barley toxin conjugate exhibited comparable activity to the gelonin conjugate (ID_{50} values of 4.5 and 3.3 nM, respectively); however, it was only about one-tenth as active as the RTA conjugate ($ID_{50} = 0.32$ nM).

When tested *in vitro* against a colon tumor cell line (Figure 8), all three immunotoxins exhibited comparable, cytotoxicity, with the RTA conjugate remaining the most potent, followed by the gelonin and barley toxin II conjugates. From these data ID_{50} values of 4.2, 7.6, and 10 nM, respectively, were calculated for the RTA, gelonin, and barley toxin II containing immunotoxins.

DISCUSSION

Our interest in evaluating barley toxin for suitability as an immunotoxin stems from several considerations: (i) it

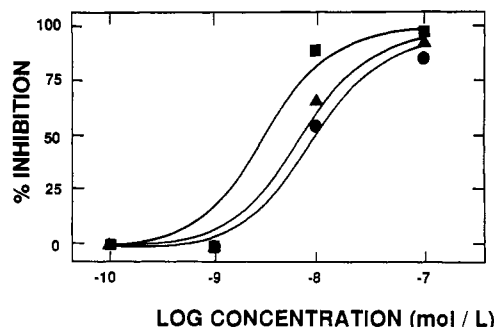


Figure 8. In vitro cytotoxicity of conjugates constructed with the anti-transferrin receptor monoclonal antibody and barley toxin II (●), gelonin (▲), and ricin A-chain (■). Details of the assay are described in Experimental Procedures. ID_{50} values of 10, 7.6, and 4.2 nM were calculated for barley toxin II, gelonin, and ricin A-chain, respectively.

is an abundant, easily-isolated, and well-characterized RIP; (ii) since it is a type 1 RIP, purified barley toxin is free of B-chain contamination and therefore will be relatively nontoxic to intact cells; (iii) barley toxin is not glycosylated (4); therefore, the plasma half-life of immunotoxins constructed therewith will not be reduced via the asialoglycoprotein receptor pathway; and (iv) since it is now recognized that patients undergoing RTA-immunotoxin therapy may develop (in addition to a human anti-mouse antibody response) an anti-RTA immune response (14–16), immunoconjugates with barley toxin II may represent an alternative approach for a follow-up course of treatment.

An improved purification procedure for isolating barley toxin II yielded an electrophoretically homogeneous preparation that nevertheless was resolvable into two isoforms by reversed-phase HPLC. The possibility that this heterogeneity represents a failure to resolve barley toxin II from barley toxins I and III has not been ruled out, but appears to be unlikely because activity corresponding to the latter two proteins was detected in two other regions of the cation-exchange elution profile (Figure 1).

Our average recovery of 55 mg of barley toxin II per kg of seeds is substantially different from the estimate by Coleman and Roberts (2) of 1365 mg/kg but is similar to the yields of barley toxin II reported by Asano et al. (37.5 mg/kg; 4), and Barbieri et al. (95 mg/kg; 13). The observation that our recoveries of toxin activity in the 55–80% ammonium sulfate precipitate exceeded 100% raises the intriguing possibility that a specific toxin inhibitor is present in the barley endosperm.

Barley toxin II is a remarkably stable protein, unaffected by exposure to 0.1% TFA, 40% acetonitrile, or lyophilization (Figure 4). In our hands, RTA did not tolerate these conditions. However, we observed a significant loss of barley toxin II activity in the thiolation step as the number of alkylated amino groups approached four (Figure 6). This characteristic is in apparent contrast to the effect of thiolation on the activity of gelonin: Lambert et al. (17) observed only a slight loss of activity in 2-iminothiolane-treated gelonin preparations containing 2.93 sulfhydryl groups per molecule.

Evaluation of RTA, gelonin, and barley toxin II in a cell free (reticulocyte) protein synthesizing system disclosed that the native type I RIP's exhibited about one-third the potency of RTA (Figure 5). However, when conjugated to a monoclonal antibody, the type I RIP's were only about one-tenth as potent as the corresponding RTA conjugate. This indicates that the active sites of gelonin and barley toxin II are less exposed than that of RTA after the

conjugation step. Other factors that may account for these discrepancies between the type I and type II toxins include (i) fundamental differences in substrate specificity and (ii) reduction in the activity of the type I RIP's as a result of the covalent modification required to introduce SH groups.

Interestingly, the major differences between immunotoxins containing type I vs type II RIP's were considerably attenuated when they were assessed in vitro against a colon tumor cell line that expresses the transferrin receptor. In this case the immunotoxins constructed with barley toxin II and gelonin were about equivalent in potency and 42–76% as effective as the RTA immunotoxin. We may speculate that efficient translocation of the conjugates via receptor-mediated endocytosis partially compensated for the differences in (cell-free) toxin activity of the immunotoxins. Notwithstanding this effect, the general trend in potency [RTA >> gelonin \approx barley toxin II] persisted.

In conclusion, among the type I and type II plant RIP's evaluated in this report, RTA remains the toxin of choice, due to its potency in both cell-free and intact-cell inhibition assays. Gelonin and barley toxin II were found to be about equivalent in their activity, but the latter apparently is more sensitive to covalent modifications through amino groups. Nevertheless, we conclude that the availability of raw material, ease of purification, and stability of barley toxin II to denaturing conditions render it a suitable protein for the construction of immunotoxins.

LITERATURE CITED

- (1) Stirpe, F., and Barbieri, L. (1986) Ribosome-inactivating proteins up to date. *FEBS Lett.* 195, 1–8.
- (2) Coleman, W. H., and Roberts, W. K. (1982) Inhibitors of animal cell-free protein synthesis from grains. *Biochim. Biophys. Acta* 696, 239–244.
- (3) Roberts, W. K., and Selitrennikoff, C. P. (1986) Isolation and partial characterization of two antifungal proteins from barley. *Biochim. Biophys. Acta* 880, 161–170.
- (4) Asano, K., Svensson, B., and Poulsen, F. M. (1984) Isolation and characterization of inhibitors of animal cell-free protein synthesis from barley seeds. *Carlsberg Res. Commun.* 49, 619–626.
- (5) Asano, K., Svensson, B., Poulsen, F. M., Nygard, O., and Nilsson, L. (1986) Influence of a protein synthesis inhibitor from barley seeds upon different steps of animal cell-free protein synthesis. *Carlsberg Res. Commun.* 51, 75–81.
- (6) Asano, K., Svensson, B., Svendsen, I., and Poulsen, F. M. (1986) The complete primary structure of protein synthesis inhibitor II from barley seed. *Carlsberg Res. Commun.* 51, 129–141.
- (7) Ready, M. P., Katzin, B. J., and Robertus, J. D. (1988) Ribosome-inhibiting proteins, retroviral reverse transcriptase, and RNase H share common structural elements. *Proteins* 3, 53–59.
- (8) Endo, Y., Tsurugi, K., and Ebert, R. F. (1988) The mechanism of action of barley toxin: a type 1 ribosome-inactivating protein with RNA N-glycosidase activity. *Biochim. Biophys. Acta* 954, 224–226.
- (9) Haynes, B. F., Hemler, M., Cotner, T., Mann, D. L., Eisenbarth, G. S., Strominger, J. L., and Fauci, A. S. (1981) Characterization of a monoclonal antibody (5E9) that defines a human cell surface antigen of cell activation. *J. Immunol.* 127, 347–351.
- (10) Ellman, G. L. (1959) Tissue sulfhydryl groups. *Arch. Biochem. Biophys.* 82, 70–77.
- (11) Laemmli, U. K. (1970) Cleavage of structural proteins during the assembly of the head of bacteriophage T4. *Nature* 227, 680–685.
- (12) Lowry, O. H., Rosebrough, N. J., Farr, A. L., and Randall, R. J. (1951) Protein measurement with the Folin phenol reagent. *J. Biol. Chem.* 193, 265–275.
- (13) Barbieri, L., Stoppa, C., and Bolognesi, A. (1987) Large scale chromatographic purification of ribosome-inactivating proteins. *J. Chromatogr.* 408, 235–243.

- (14) Hertler, A. A., Schlossman, D. M., Borowitz, M. J., Poplack, D. G., and Frankel, A. E. (1988) An immunotoxin for the treatment of T-acute lymphoblastic leukemic meningitis: Studies in rhesus monkeys. *Cancer Immunol. Immunother.* 28, 59-66.
- (15) Kernan, N. A., Byers, V., Scannon, P. J., Mischak, R. P., Brochstein, J., Flomenberg, N., Dupont, B., and O'Reilly, R. J. (1988) Treatment of steroid-resistant acute graft-vs-host disease by in vivo administration of an anti-T ricin A chain immunotoxin. *J. Am. Med. Assoc.* 259, 3154-3157.
- (16) Mischak, R. P., Foxall, C., Rosendorf, L. L., Knebel, K., Scannon, P. J., and Spitler, L. E. (1990) Human antibody responses to components of the monoclonal antimelanoma antibody ricin A chain immunotoxin XomaZyme-MEL. *Mol. Biother.* 2, 104-109.
- (17) Lambert, J. L., Blätter, W. A.; mCIntyre, G. D., Goldmacher, V. S., and Scott, C. F. (1988) Immunotoxins containing single chain ribosome-inactivating proteins. In *Immunotoxins* (A. E. Frankel, Ed.) pp 175-209, Kluwer Academic Publishers, Boston.

A Photoactive Phosphonamide Derivative of GTP for the Identification of the GTP-Binding Domain in β -Tubulin¹

Ashok J. Chavan,[†] Hyuntae Kim,[‡] Boyd E. Haley,^{*,‡} and David S. Watt^{*,†}

Department of Chemistry and Department of Biochemistry, University of Kentucky, Lexington, Kentucky 40506.
Received June 22, 1990

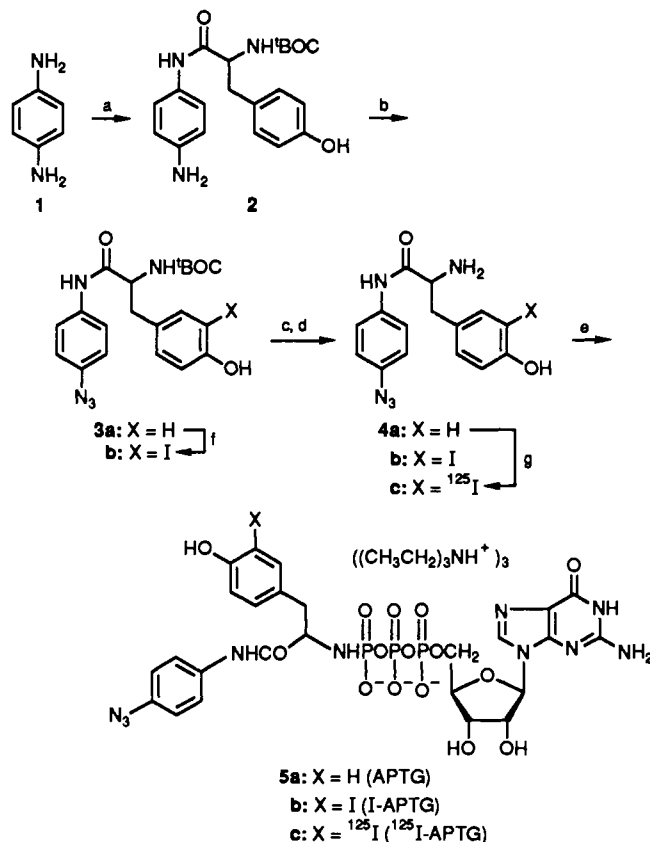
A GTP photoaffinity probe (¹²⁵I-APTG) was developed that incorporated an [¹²⁵I]-*N*-(4-azidophenyl)-2-amino-3-(4-hydroxy-3-iodophenyl)propionamide group at the γ -position of GTP through a phosphonamide linkage. A combination of saturation and GTP protection studies (90% protection at 25 μ M GTP with an apparent K_d of 5 μ M) validated the use of this new probe as a satisfactory GTP mimic. This probe offered the advantage of possessing an ¹²⁵I radiolabel external to the GTP moiety, in contrast to the previously reported [γ -³²P]-8-N₃GTP that possessed an internal ³²P radiolabel. This novel feature accommodated the purification of photolabeled peptides using a combination of ion-exclusion, gel filtration, and HPLC techniques. [¹²⁵I]APTG was used to identify a peptide (β :65-79) in the exchangeable GTP-binding domain of the β -subunit of tubulin.

INTRODUCTION

Tubulin, a ubiquitous structural protein, possesses a guanine base binding region at the exchangeable GTP binding site that has been localized on the β -subunit with [γ -³²P]-8-N₃GTP² (1) or by direct photoaffinity labeling using [α -³²P]GTP (2, 3). A problem, however, encountered with these probes is the loss of the ³²P radiolabel through adventitious enzymatic or chemical hydrolysis that occurs during purification of the photolabeled peptides. In order to avoid this problem, a new photoaffinity probe, [¹²⁵I]-APTG² (5c), shown in Scheme I, was developed that, unlike the previous probes, carried the photoactive and radiolabeled moieties *external* to the GTP portion of the probe.

It was anticipated that this arrangement of photoactive and radioiodine substituents would offer unique advantages in the purification of cross-linked peptides following photoinsertion of ¹²⁵I-APTG into a GTP-binding domain and trypsin digestion. Specifically, the presence of the triphosphate group on the photolabeled peptides would permit the separation of these negatively

Scheme I.^a Synthesis of APTG, I-APTG, and ¹²⁵I-APTG



^a Reagents: (a) *t*-BOCTyr, DCC; (b) NaN₃, HCl followed by NaHCO₃; (c) HCl gas, HOAc; (d) NaHCO₃; (e) GTP and CDI with HCl addition commencing after pH exceeded 5.6, followed by the addition of amine; (f) NaI, *t*-BuOCl; (g) [¹²⁵I]NaI, *t*-BuOCl.

charged photolabeled peptides, as well as other negatively charged acidic peptides, from the bulk of the other positively charged, nonphotolabeled peptides by anion-exclusion chromatography. This initial purification would be followed by a deliberate hydrolysis that would remove the triphosphate group from the photolabeled peptides without disturbing the radiolabel. A second anion-

* Authors to whom correspondence should be addressed: David S. Watt, Department of Chemistry, University of Kentucky, Lexington, KY 40506; telephone, (606) 257-5294; FAX, (606) 258-1069; or Boyd E. Haley, Department of Biochemistry; telephone, (606) 257-4481; FAX, (606) 257-4000.

[†] Department of Chemistry.

[‡] Department of Biochemistry.

¹ Part of this work was disclosed at the following meetings: American Chemical Society Meeting, Los Angeles, CA, September 1988 and Meeting of the American Society for Biochemistry and Molecular Biology, New Orleans, LA, June 1990, Abstract #849.

² The abbreviations used are as follows: ¹²⁵I-APTG, monoanhydride of guanosine 5'-(trihydrogen diphosphate) tris-(triethylammonium) salt and [¹²⁵I]-*N*-(4-azidophenyl)-2-phosphoramido-3-(4-hydroxy-3-iodophenyl)propionamide; buffer A, 100 mM 2-(*N*-morpholino)ethanesulfonic acid (MES), 1 mM magnesium chloride, 1 mM EGTA (pH = 6.7); buffer B, 10 mM sodium phosphate, 1 mM magnesium chloride, 1 mM EGTA (pH 6.7); CDI, 1-cyclohexyl-3-(2-morpholinoethyl)carbodiimide metho-*p*-toluenesulfonate; DEAE cellulose, [(*N,N*-diethylamino)ethyl]-cellulose; EGTA, ethylene glycol bis(β -aminoethyl ether)-*N,N,N',N'*-tetraacetic acid; GTP, guanosine 5'-triphosphate; MAP, microtubule-associated protein; 8-N₃GTP, 8-azidoguanosine 5'-triphosphate; THF, tetrahydrofuran.

exclusion chromatography would then separate the negatively charged, acidic peptides from the desired photolabeled peptides. In order to evaluate this approach, we performed validation studies that confirmed [^{125}I]-APTG (5c) as a suitable mimic for GTP itself, we examined the photoinsertion of 5c into the exchangeable GTP-binding domain of β -tubulin that proceeded with limited but acceptable efficiency, and we utilized the unique properties of this probe that permitted the isolation of a peptide (β : 65–79) that was previously identified with [$\gamma^{32}\text{P}$]-8- N_3GTP .

EXPERIMENTAL PROCEDURES

General Chemical Procedures. Chemicals were purchased from Aldrich or Sigma with the exception of [^{125}I]NaI, which was purchased from Amersham. Silica gel 60 F-254 TLC plates were purchased from Brinkman Instruments. Trypsin-TPCK was purchased from Cooper Biomedical. Infrared spectra were recorded on a Perkin-Elmer Model 357 spectrometer. Nuclear magnetic resonance spectra were determined on a Varian 400-MHz or Gemini 200-MHz NMR spectrometer. Chemical shifts are reported in parts per million relative to tetramethylsilane as an internal standard in the case of ^1H and ^{13}C NMR and relative to 85% phosphoric acid in the case of ^{31}P NMR. Mass spectra were determined on a VG ZAB spectrometer. Elemental analyses were performed by Atlantic Microlabs, Norcross, GA. Column chromatography using Macherey Nagel silica gel 60 is referred to as "chromatography on silica gel", preparative-layer chromatography on Macherey Nagel silica gel F254 is referred to as "chromatography on a silica gel plate", and the drying of an organic phase over anhydrous magnesium sulfate is simply indicated by the phrase "dried".

***N*-(4-Aminophenyl)-2-(*tert*-butoxycarboxamido)-3-(4-hydroxyphenyl)propionamide (2).** To 0.52 g (4.8 mmol, 1.0 equiv) of *p*-phenylenediamine (1) in 20 mL of THF² under a nitrogen atmosphere was added 1.5 g (5.3 mmol, 1.1 equiv) of *N*-(*tert*-butoxycarbonyl)tyrosine and 1.1 g (5.3 mmol, 1.1 equiv) of *N,N'*-dicyclohexylcarbodiimide (DCC). The solution was stirred at 25 °C for 4 h, diluted with ethyl acetate, and filtered. The urea byproduct was washed with additional ethyl acetate. The combined filtrates were concentrated to obtain 2 that was sufficiently pure to use in the next step: mp 95–97 °C; IR (KBr) 1690, 1660 cm^{-1} ; ^1H NMR (acetone- d_6) δ 1.37 (s, 9, $\text{C}(\text{CH}_3)_3$), 2.92 (dd, $J = 14$, 8.2 Hz, 1, CH_2), 3.07 (dd, $J = 14$, 6 Hz, 1, CH_2), 4.39–4.50 (m, 1, CH), 6.60 (d, $J = 8.5$ Hz, 2, ArH), 6.74 (d, $J = 8.8$ Hz, 2, ArH), 7.09 (d, $J = 8.5$ Hz, 2, ArH), 7.29 (d, $J = 8.8$ Hz, 2, ArH), 8.85 (s, 1, OH); exact mass calcd for $\text{C}_{20}\text{H}_{25}\text{N}_3\text{O}_4$ 371.1846, found 371.1846.

***N*-(4-Azidophenyl)-2-(*tert*-butoxycarboxamido)-3-(4-hydroxyphenyl)propionamide (3a).** To a solution of 1.9 g (5.1 mmol, 1.0 equiv) of 2 in 44 mL of 1:1 water-THF and 4 mL of concentrated hydrochloric acid was added 0.39 g (5.6 mmol, 1.1 equiv) of sodium nitrite in 1.5 mL of water at 0–5 °C. The solution was stirred at 0–5 °C for 45 min. To this solution was added 0.36 g (5.6 mmol, 1.1 equiv) of sodium azide in 1.5 mL of water. The solution was stirred for an additional 1 h and the temperature of the reaction mixture was allowed to rise to 25 °C. The mixture was extracted with ethyl acetate. The combined extracts were washed with two 15-mL portions of saturated sodium bicarbonate solution and brine. The ethyl acetate extracts were dried and evaporated to get the crude product which was chromatographed on silica gel using 1:1 hexane-ethyl acetate to afford 1.24 g (61%)

of 3a: mp 85–86 °C; IR (KBr) 2120, 1680, 1620 cm^{-1} ; ^1H NMR (acetone- d_6) δ 1.37 (s, 9, $\text{OC}(\text{CH}_3)_3$), 2.92 (dd, $J = 14$, 8.2 Hz, 1, CH_2), 3.07 (dd, $J = 14$, 6 Hz, 1, CH_2), 4.40–4.54 (m, 1, CH), 6.19 (br d, 1, CHNH), 6.75 (d, $J = 8.5$ Hz, 2, ArH), 7.01 (d, $J = 8.8$ Hz, 2, ArH), 7.11 (d, $J = 8.5$ Hz, 2, ArH), 7.66 (d, $J = 8.8$ Hz, 2, ArH), 8.18 (s, 1, CONH), 9.32 (s, 1, OH); exact mass calcd for $\text{C}_{20}\text{H}_{23}\text{N}_5\text{O}_4$ 397.1750, found 397.1752.

***N*-(4-Azidophenyl)-2-(*tert*-butoxycarboxamido)-3-(4-hydroxy-3-iodophenyl)propionamide (3b).** To a solution of 500 mg (1.26 mmol, 1.0 equiv) of 3a and 226 mg (1.51 mmol, 1.2 eq) of sodium iodide (nonradiolabeled) in 4.5 mL of acetonitrile and 0.9 mL of water at 0 °C was added 180 μL (1.51 mmol, 1.2 equiv) of *tert*-butyl hypochlorite dropwise. The solution was stirred for 30 min at 0 °C and diluted with 50 mL of ethyl acetate. The organic solution was washed successively with 5% sodium thiosulfate solution and brine, dried, and concentrated to afford 703 mg of crude product, which was chromatographed on a silica gel column using 10:2 dichloromethane-ethyl acetate to afford 105 mg (16%) of 3b: mp 188–189 °C dec; IR (KBr) 2120, 2100, 1680, 1670 cm^{-1} ; ^1H NMR (DMSO- d_6) δ 1.32 (s, 9, $\text{OC}(\text{CH}_3)_3$), 2.74 (dd, $J = 14$, 8 Hz, 1, CH_2), 2.88 (dd, $J = 14$, 5.2 Hz, 1, CH_2), 4.16–4.30 (m, 1, CH), 6.76 (d, $J = 8.8$ Hz, 1, ArH), 6.96–7.14 (m, 3, ArH), 7.60–7.70 (m, 3, ArH); ^{13}C NMR (DMSO- d_6) δ 28.14, 56.69, 78.10, 84.18 (C-I), 114.44, 119.39, 120.73, 130.36, 130.45, 133.86, 136.13, 139.10, 155.03, 155.37, 170.64; exact mass calcd for $\text{C}_{20}\text{H}_{22}\text{IN}_5\text{O}_4 - \text{N}_2 + \text{H}_2$ 497.0812, found 497.0785. In addition, 317 mg (39%) of *N*-(4-azidophenyl)-2-(*tert*-butoxycarboxamido)-3-(4-hydroxy-3,5-diiodophenyl)propionamide was isolated: mp 105–106 °C; IR (KBr) 2100, 1690, 1670, 1600 cm^{-1} ; ^1H NMR (acetone- d_6) δ 1.37 (s, 9, $\text{OC}(\text{CH}_3)_3$), 2.90 (dd, $J = 14$, 8 Hz, 1, CH_2), 3.13 (dd, $J = 14$, 5.2 Hz, 1, CH_2), 4.42–4.54 (m, 1, CH), 6.29 (br s, 1, CHNH), 7.05 (d, $J = 8.9$ Hz, 2, ArH), 7.69 (d, $J = 8.7$ Hz, 2, ArH), 7.72 (s, 2, ArH), 7.94 (br s, 1, CONH), 9.41 (br s, 1, OH); ^{13}C NMR (acetone- d_6) δ 28.51, 36.10, 57.32, 79.55, 84.17 (C-I), 120.10, 121.94, 122.04, 134.72, 135.83, 136.87, 141.24, 156.27, 170.69; exact mass calcd for $\text{C}_{20}\text{H}_{21}\text{I}_2\text{N}_5\text{O}_4 - \text{N}_2 + \text{H}_2$ 622.9779, found 622.9753.

***N*-(4-Azidophenyl)-2-amino-3-(4-hydroxyphenyl)propionamide (4a).** To 2.0 g (5 mmol) of 3a was added 20 mL of glacial acetic acid saturated with hydrogen chloride. The solution was allowed to stand for 30 min at 25 °C and was diluted with 150 mL of ether to precipitate 726 mg (45%) of the hydrochloride salt of 4a: IR (KBr) 2120, 1680, 1615 cm^{-1} ; ^1H NMR (DMSO- d_6) δ 2.90–3.16 (m, 2, CH_2), 4.05–4.20 (m, 1, CH), 6.69 (d, $J = 8.4$ Hz, 2, ArH), 7.07 (d, $J = 3.6$ Hz, 2, ArH), 7.11 (d, $J = 4$ Hz, 2, ArH), 7.62 (d, $J = 8.8$ Hz, 2, ArH), 8.31 (br s, 3, NH_3^+), 9.36 (br s, 1, CONH), 10.80 (s, 1, OH); exact mass calcd for $\text{C}_{15}\text{H}_{16}\text{ClN}_5\text{O}_2 - \text{N}_2$ 305.0931, found 305.0931.

***N*-(4-Azidophenyl)-2-amino-3-(4-hydroxy-3-iodophenyl)propionamide (4b).** The procedure described for the preparation of 4a was repeated with 30 mg (0.06 mmol, 1.0 equiv) of 3b and 5 mL of glacial acetic acid saturated with hydrogen chloride gas to afford, after stirring for 30 min, adjusting the pH of the solution to 7 by the addition of saturated sodium bicarbonate solution, extraction with ethyl acetate, and concentration, 21 mg (87%) of 4b: IR (KBr) 3280, 3070, 2100, 1675, 1605 cm^{-1} .

GTP Photoaffinity Probe APTG (5a): Monoanhydride of Guanosine 5'-(Trihydrogen diphosphate) Tris(triethylammonium) Salt with *N*-(4-Azidophenyl)-2-phosphoramido-3-(4-hydroxyphenyl)propionamide. The hydrochloride salt of 4a was converted to the free base immediately before use by

dissolution in a saturated sodium bicarbonate solution, extraction with ethyl acetate, and concentration. To 1.0 mL of water was added 10 mg (0.018 mmol, 1.0 equiv) of guanosine triphosphate disodium salt at 10–15 °C and 74.5 mg (0.18 mmol, 10 equiv) of CDI.² The pH of the mixture was maintained at 5.5–6 during the addition of CDI by titration with 0.05 M hydrochloric acid. No appreciable rise in pH was noted after adding 12 equiv of CDI. To this was added 5.2 mg (0.018 mmol, 1.0 equiv) of amine **4a** in 100 μ L of pyridine. The mixture was stirred for 4 h at 10–15 °C and purified, first on DEAE cellulose² using a linear gradient of 250 mL of 50 mM and 250 mL of 700 mM triethylammonium bicarbonate buffer at the rate of 3 mL/10 min to afford **5a** (fractions 104–106, R_f = 0.55 on Macherey Nagel F-254 silica gel plate; 7:3 ethanol–1 M ammonium bicarbonate) and unreacted GTP and secondly on a SEP-PAK C₁₈ cartridge (Waters Associates) to afford 6.9 mg (35%) of **5a** as the tris(triethylammonium) salt: IR (KBr) 3330 (br), 2975, 2491, 2120, 1694, 1605, 1476 cm^{-1} ; ³¹P NMR (D₂O) δ -3.65 (d, J = 19.8 Hz, 1, γ -P), -10.85 (d, J = 19.5 Hz, 1, α -P), -22.14 (t, J = 19.8 Hz, 1, β -P). Ion-exchange chromatography of the tris(triethylammonium) salt of **5a** using Bio-Rex 70 (Bio-Rad) afforded the trisodium salt of **5a**: ¹H NMR (D₂O with TSP-*d*₄) δ 2.80 (dd, J = 8 and 13 Hz, 1, CH₂), 3.17 (dd, J = 4 and 13 Hz, 1, CH₂), 4.05–4.14 (m, 1, CH), 5.76 (d, J = 5.3 Hz, 1, C-1' H), 6.68 (d, J = 7.8 Hz, 2, ArH), 6.88 (d, J = 8 Hz, 2, ArH), 7.02 (d, J = 7.8 Hz, 2, ArH), 7.12 (d, J = 8 Hz, 2, ArH), 7.91 (s, 1, C-8 H).

GTP Photoaffinity Probe I-APTG (5b): Monoanhydride of Guanosine 5'-(Trihydrogen diphosphate) Tris(triethylammonium) Salt with N-(4-Azidophenyl)-2-phosphoramido-3-(4-hydroxy-3-iodophenyl)propionamide. The procedure described for the preparation of **5a** was repeated with 10 mg (0.018 mmol, 1.0 equiv) of guanosine triphosphate disodium salt, 74.5 mg (0.18 mmol, 10 equiv) of CDI, and 14.0 mg (0.033 mmol, 1.8 equiv) of **4b** to afford 6.8 mg (32%) of **5b**: IR (KBr) 2130, 1700, 1610 cm^{-1} ; ³¹P NMR (D₂O) δ -3.82 (d, J = 18.5 Hz, 1, γ -P), -10.95 (d, J = 18.9 Hz, 1, α -P), -22.31 (t, 1, β -P). Ion-exchange chromatography of the tris(triethylammonium) salt of **5b** using Bio-Rex 70 (Bio-Rad) afforded the trisodium salt of **5b**: ¹H NMR (D₂O with TSP-*d*₄) δ 5.94 (d, J = 6.4 Hz, 1, C-1' H), 6.60 (d, J = 8.2 Hz, 1, ArH), 7.02 (dd, J = 8.2, 2 Hz, 1, ArH), 7.11 (d, J = 8.9 Hz, 2, ArH), 7.29 (d, J = 8.9 Hz, 2, ArH), 7.51 (d, J = 2 Hz, 1, ArH), 8.15 (s, 1, C-8 H).

¹²⁵I-APTG (5c). To 11.3 μ L of [¹²⁵I]NaI (6.1 mCi, 2.8 nmol, Amersham) in a Reacti-vial was added 10 μ L of potassium phosphate buffer (pH = 7.5), 5 μ L (84 nmol, 30 equiv) of a solution of the hydrochloride salt of **4a** in water, and 6.7 μ L (11.2 nmol, 4 equiv) of a solution of *tert*-butyl hypochlorite (J. T. Baker) in acetonitrile. The mixture was allowed to stand at 25 °C for 1 h with occasional vortex stirring. The reaction was quenched by adding 20 μ L of 5% aqueous sodium thiosulfate solution. Approximately 0.5 μ L of the mixture was placed on an analytical silica gel TLC plate (Macherey Nagel F254) and eluted with 10:1 ethyl acetate–methanol. Autoradiography of the plate confirmed the presence of the desired product (R_f = 0.36). The mixture was extracted with three 100- μ L portions of ethyl acetate. The ethyl acetate was evaporated under a stream of nitrogen (in a hood) to afford a mixture of mono- and diradioiodinated amines.

The procedure described for the preparation of **5a** was repeated with 10 mg (0.016 mmol, 1 equiv) of guanosine triphosphate trisodium salt and 68 mg (0.16 mmol, 10 equiv) of CDI to obtain the trimetaphosphate intermediate

in 650 μ L of water. To the mixture of radioiodinated amines in 10 μ L of pyridine was added 325 μ L of the solution of the trimetaphosphate. The mixture was stirred at 5–10 °C for 4 h. Approximately 0.5 μ L of the mixture containing **5c** and a small sample of nonradiolabeled **5b** were placed on an analytical silica gel TLC plate (Macherey Nagel F254) and eluted with 7:3 ethanol–1 M ammonium bicarbonate. Autoradiography of the plate confirmed the presence of the desired product **5c** (R_f = 0.56). The crude product was purified on a DEAE cellulose column (12 \times 1 cm) using a linear gradient of 125 mL of water and 125 mL of 400 mM triethylammonium bicarbonate buffer at a rate of 1 mL/min during which time 6-mL fractions were collected. Fractions 22–28 were combined and concentrated to 5 mL that was chromatographed on a C₁₈ SEP-PAK cartridge. The excess GTP was eluted with 10 mL of 20 mM triethylammonium bicarbonate buffer solution, and the desired probe **5c**, which is a mixture of mono- and diiodinated materials, was eluted with absolute methanol. The specific activity of the probe **5c** was 10–50 mCi/ μ mol.

Tubulin Preparations. Microtubule protein was isolated from fresh bovine or ovine brain by two cycles of reversible assembly (4). Microtubules obtained from the second cycle of polymerization were stored at -70 °C until needed. Prior to use, pellets were thawed and purified by gel filtration on Sephadex G-25 (medium) using either buffer A² for the polymerization assay or buffer B² for the photolabeling experiments. MAPs² are present in these preparations but represent less than 5% of the total protein weight.

Polymerization Assay. Microtubule formation was followed by a light-scattering assay using a Beckman Model 25 spectrophotometer equipped with a cuvette chamber heated to 37 °C (5). Solutions were monitored at 350 nm.

Photoaffinity Labeling. Appropriate specific activities of ¹²⁵I-APTG were obtained by diluting it with I-APTG (3000–5000 cpm/pmol). Tubulin solutions (5 μ g) in buffer B containing ¹²⁵I-APTG in 30- μ L final volume were incubated for 5–10 min at 0 °C and subsequently irradiated with a hand-held UV light with the glass face removed (4600 μ W/ cm^2 , Model UVS-11, Ultra-violet Products, Inc.) at a distance of 4 cm for 1 min at 0 °C. Protein mixtures were solubilized in a protein solubilizing mixture (6). The α - and β -tubulin monomers were separated on 10% SDS-PAGE. Protein bands were stained with Coomassie Brilliant Blue and cut from the gel, and the radioactivity was determined in a Minaxi Gamma Counter 5000 series (Packard Instruments Co.).

RESULTS

Synthesis of GTP Probes. A new GTP phosphonamide photoaffinity probe, ¹²⁵I-APTG (**5c**), as well as its noniodinated and nonradioiodinated analogues (**5a** and **5b**) were synthesized as shown in Scheme I. *N*-(4-azidophenyl)tyrosine (**4a**) and the corresponding iodinated and radioiodinated analogues (**4b** and **4c**) were coupled to GTP to obtain APTG (**5a**), I-APTG (**5b**), and ¹²⁵I-APTG (**5c**), respectively. The coupling sequence involved the activation of GTP as a trimetaphosphate (11–13), as confirmed by ³¹P NMR (13) at 10–15 °C which displayed a multiplet at δ -23.35 relative to 85% H₃PO₄ in D₂O, using CDI while the pH was maintained in the 5.5–6.0 range (14) and the trapping of the trimetaphosphate by the immediate addition of an appropriate amine (4) at temperatures of 10–15 °C. The direct radioiodination of the tyrosyl residue in APTG (**5a**) was not successful, and consequently, the radioiodination was performed on **4a** that was subsequently

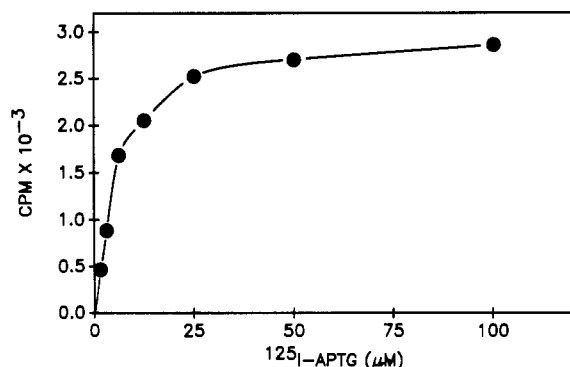


Figure 1. Saturation of labeling of $^{125}\text{I-APTG}$ with β -tubulin. Tubulin ($5 \mu\text{g}$) was incubated with increasing concentrations of $^{125}\text{I-APTG}$ (2400 cpm/pmol, 5 min, 0°C), photolyzed (1 min, 0°C), and analyzed on 10% SDS-PAGE. The gel was sliced and the appropriate protein bands were counted with a Minaxi γ -counter.

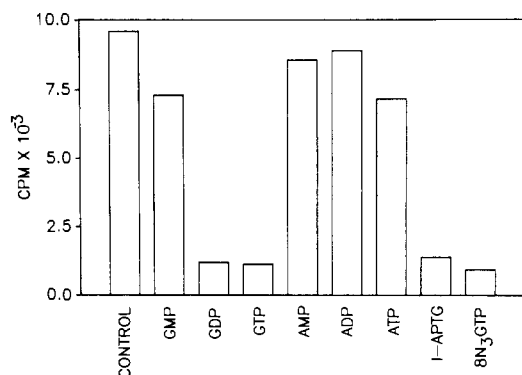


Figure 2. Bar graph showing competition of $^{125}\text{I-APTG}$ binding to β -tubulin with other nucleotides and nucleotide analogues. Tubulin ($5 \mu\text{g}$) was incubated with various nucleotides or GTP analogues ($100 \mu\text{M}$, 10 min, 0°C) and then with $^{125}\text{I-APTG}$ (5000 cpm/pmol, $5 \mu\text{M}$, 10 min, 0°C), photolyzed (1 min, 0°C), and analyzed on 10% SDS-PAGE. The gel was sliced, and the appropriate protein bands were counted with a Minaxi γ -counter.

coupled to GTP. The APTG and I-APTG probes were characterized by ^1H and ^{31}P NMR, UV photodecomposition studies, and infrared spectroscopy. $^{125}\text{I-APTG}$ and I-APTG possessed identical R_f values on thin-layer silica gel chromatography as judged by detection by UV activity and autoradiography.

Validation Studies: Saturation. The development of a new GTP photoaffinity probe requires studies that confirm that the probe mimics the natural substrate, GTP, in terms of saturation, specificity, and competition. The tubulin solutions were incubated with increasing concentrations of $^{125}\text{I-APTG}$ and photolyzed (see the Experimental Procedures) to produce the results shown in Figure 1. The β -tubulin showed saturation of labeling at a $25 \mu\text{M}$ concentration of $^{125}\text{I-APTG}$ with an apparent K_d of $5 \mu\text{M}$. Considerably less photoincorporation was seen in the α -subunit and appeared to be nonsaturable (data not shown). At an $^{125}\text{I-APTG}$ concentration of $25 \mu\text{M}$, 0.023 pmol of $^{125}\text{I-APTG}$ were cross-linked per pmol of β -tubulin.

Validation Studies: Specificity. The specificity of protection of photolabeling by $^{125}\text{I-APTG}$ ($5 \mu\text{M}$) was tested with several nucleotides and nucleotide analogues ($100 \mu\text{M}$). The bar graph in Figure 2 showed that GDP, GTP, 8-N₃GTP, and I-APTG protected (as expected) against photolabeling by $^{125}\text{I-APTG}$ whereas GMP, AMP, ADP, and ATP did not protect against photolabeling.

Validation Studies: Competition. Tubulin solutions were photolyzed with $^{125}\text{I-APTG}$ ($10 \mu\text{M}$) in the presence

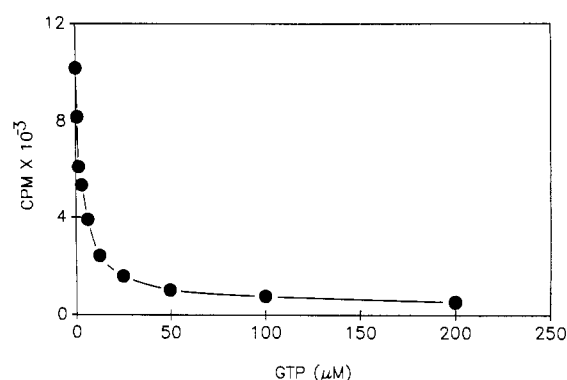


Figure 3. Competition of $^{125}\text{I-APTG}$ binding to β -tubulin with GTP. Tubulin ($5 \mu\text{g}$) was incubated with increasing concentrations of GTP (5 min, 0°C) and then with $^{125}\text{I-APTG}$ (5000 cpm/pmol, $10 \mu\text{M}$, 5 min, 0°C), photolyzed (1 min, 0°C), and analyzed on 10% SDS-PAGE. The gel was sliced and the appropriate protein bands were counted with a Minaxi γ -counter.

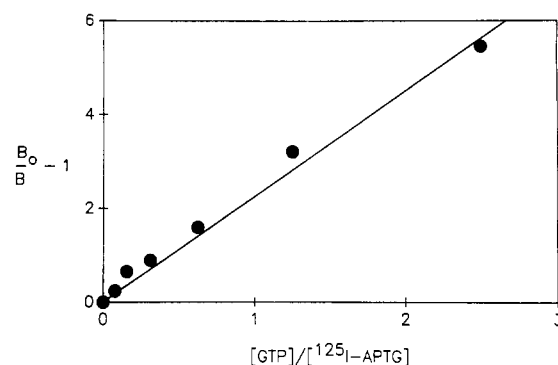


Figure 4. Relative dissociation constants of $^{125}\text{I-APTG}$ and GTP.

of increasing concentrations of GTP as shown in Figure 3. In β -tubulin, approximately 90% of the photoincorporation was competitively removed by GTP concentrations in the 25 – $50 \mu\text{M}$ range with half-maximal protection observed at ca. $5 \mu\text{M}$ GTP concentration. Photoincorporation in the β -subunit was 8-fold higher than that observed in the α -subunit with no competitor present (data not shown). The relative affinities of $^{125}\text{I-APTG}$ and GTP were examined with the relationship $(B_0/B) - 1 = K_r[\text{GTP}]/[^{125}\text{I-APTG}]$ (7) as shown in Figure 4, where B_0 and B represent the degrees of photolabeling in the absence and the presence of GTP, respectively. Using this Ofengand analysis, the relative dissociation constant for $^{125}\text{I-APTG}$ was determined to be 1.7 times that of GTP.

Polymerization Studies. APTG alone was incapable of sustaining tubulin polymerization, but it was a potent inhibitor of GTP-supported tubulin polymerization as shown in Figure 5.

Cross-Linked Peptide Purification. Isolation of the cross-linked peptides from the photolabeling experiments used a combination of anion-exclusion chromatography and gel filtration. A purified tubulin solution in a plastic weighing boat (1.5 – 2 mg/mL , 10 – 15 mg total) in buffer B was incubated with $20 \mu\text{M}$ $^{125}\text{I-APTG}$ (1500 – 4500 cpm/pmol) for 30 min at 0°C and photolyzed (as described in the Experimental Procedures) for 5 min at 0°C . The reaction was quenched by adding 1 mM β -mercaptoethanol, and the protein was precipitated with ice-cold acetone and collected by centrifugation. The pellet was resuspended in 100 mM ammonium bicarbonate and digested with trypsin (1% w/w and an additional 1% w/w after 1 h) for 4 h at 25°C . The tryptic digest was subjected to anion-exclusion chromatography on a $27 \times 1.5 \text{ cm}$ SP-25 Sephadex column using 50 mM sodium formate ($\text{pH} = 3.5$)

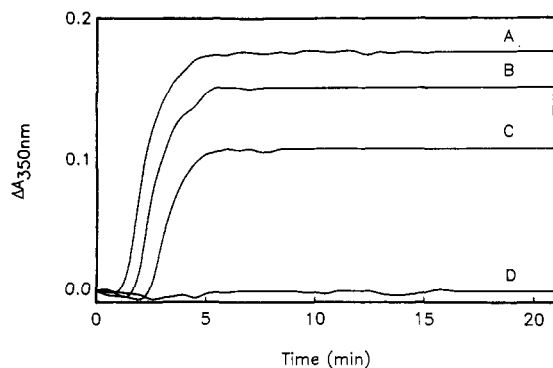


Figure 5. Polymerization of tubulin. Change in absorbance at 350 nm by incubating tubulin (0.9 mg/mL) in buffer A at 37 °C in the presence of (A) 200 μ M GTP, (B) 200 μ M GTP and 200 μ M APTG, (C) 200 μ M GTP and 400 μ M APTG, and (D) 200 μ M APTG.

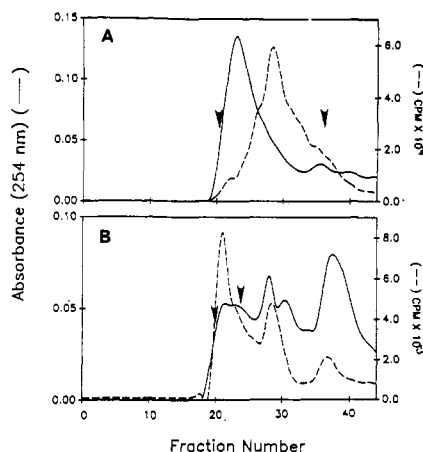


Figure 6. Anion-exclusion chromatography for the tryptic digest of the photolabeled tubulin: (A) fractions collected of tryptic digest purified on 27 \times 1.5 cm SP-25 Sephadex, (B) fractions collected from 27 \times 1.5 cm G-10 Sephadex column of the radioactive peaks between the arrows in A after formic acid hydrolysis.

at a rate of 1 mL/min to separate the photolabeled peptides from positively charged peptides. The fractions containing radioactivity (between the arrows in Figure 6A) were pooled and analyzed by HPLC. Sequencing of selected peptides established, as expected, that several carboxylic acid rich peptides contaminated the fractions with the photolabeled peptides still bearing the negatively charged triphosphate group of 125 I-APTG.

Separation of these carboxylic acid rich peptides from the desired photolabeled peptides was accomplished as follows. The fractions (between the arrows in Figure 6A) were reduced to 600 μ L with a Speed-vac, and 200 μ L of 88% formic acid was added (pH = 1–2). The solution was incubated for 1 h at 25 °C to hydrolyze deliberately the phosphonamide (P–N) bond, thereby releasing the negatively charged phosphates but retaining the 125 I radiolabel. Purification on a 27 \times 1.5 cm G-10 Sephadex column using 50 mM sodium formate (pH = 3.5) at a rate of 1 mL/min now separated the positively charged, radiolabeled peptides from the small, negatively charged, carboxylic acid rich peptides as shown in Figure 6B. The fractions from the G-10 column that correspond to major radioactive peak (between the arrows in Figure 6B) were pooled, and the volume was reduced to 800 μ L. This material was again subjected to anion-exclusion chromatography on a 27 \times 1.5 cm SP-25 Sephadex column using 50 mM sodium formate (pH = 3.5) at a rate of 1 mL/min. This last step separated the radiolabeled peptides

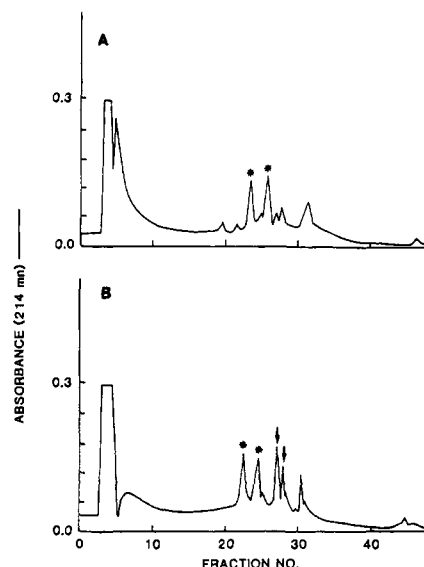


Figure 7. Reversed-phase HPLC purification of the photolabeled peptides: (A) HPLC elution profile of control experiment, (B) HPLC elution profile of major radioactive peak from the second SP-25 Sephadex column (see the Results section).

from the remaining carboxylic acid rich peptides, and two radioactive peaks were obtained. One minor peak migrated with a retention time similar to that observed in Figure 6A, and perhaps representing incomplete hydrolysis of the GTP group from the photolabeled peptide. The major peak eluted 6 mL later as expected for a photolabeled peptide now lacking the GTP group.

The major radioactive peak from the last SP-25 Sephadex column was pooled and analyzed by HPLC (LKB, equipped with diode-array spectral detector) with an Aquapore RP 300 C₈ reverse-phase (250 \times 4.6 mm) column and a gradient of 0.1% trifluoroacetic acid in water at 0 min, 0.1% trifluoroacetic acid in water at 5 min, and 0.1% trifluoroacetic acid in 70% acetonitrile at 65 min. Figure 7A shows a control experiment which lacked the photolabeling step but otherwise was subjected to the purification scheme described above. Figure 7B is the HPLC elution profile for the pooled fractions of the major radioactive peak that shows the photolabeled peptides (peaks marked by arrows) that were absent in the control experiment (Figure 7A). The fractions corresponding to the unique peaks (marked by arrows) in Figure 7B, but missing in the control experiment in Figure 7A, contained 50% of the radioactivity.

The purified peptides were analyzed first on a Beckman 6300 high-performance amino acid analyzer and subsequently sequenced with an Applied Biosystems 477A pulse liquid protein sequencer with on-line 120A PTH identification. The two major peaks (marked by arrows) isolated from the photolabeling experiments (Figure 7B) were collected in a single fraction and contained a total of three peptides having 15, 15, and 18 residues and containing 3, 3, and 2 acidic residues, respectively. The major peptide isolated by this procedure was determined to consist of residues 65–79 of the β -subunit. The percent photoincorporation, as deduced from final peptide yields, was determined to be 0.4%. In contrast, two major peaks (marked by asterisks) isolated in the control experiments (Figure 7A) were, as expected, carboxylic acid rich peptides (α :431–448 and α :431–444).

DISCUSSION

A new GTP photoaffinity probe, 125 I-APTG, was developed to explore the merits of having a radiolabel

external to the GTP portion of the probe. Photoaffinity labeling experiments using the previously reported photoaffinity probes such as $[\gamma\text{-}^{32}\text{P}]\text{-8-N}_3\text{GTP}$ (1, 8, 9) and direct photoaffinity labeling using $[\alpha\text{-}^{32}\text{P}]\text{-GTP}$ (2, 3) suffered from the loss of the ^{32}P radiolabel from photo-labeled peptides during peptide purification. In order to circumvent this problem, a different radiolabel (^{125}I) was selected for incorporation in a position that would be resistant to loss through adventitious enzymatic or chemical hydrolysis. The retention of biological activity in fluorescent analogues of GTP modified at the γ -phosphate suggested that radiolabeled, photoactive phosphonamide derivatives of GTP would be suitable photoaffinity probes for GTP (10). Consequently, the desired probe, ^{125}I -APTG (5c), shown in Scheme I, incorporated both an ^{125}I radiolabel of high specific activity and an azide group in a photoactive fragment that was attached to the γ -phosphate of GTP. The probe was synthesized in a straightforward fashion, shown in Scheme I, and this route provided ^{125}I -APTG (5c) that had high specific activity (10–50 mCi/ μmol) and could be stored in absolute methanol at -20°C for an extended period.

The studies that validated the use of ^{125}I -APTG as a photoaffinity probe for GTP included the following: a demonstration of saturation effects and the prevention of ^{125}I -APTG photoinsertion by GTP at concentrations that agreed with the known K_d of GTP for tubulin. Specifically, with tubulin prepared from bovine or ovine brain (3), it was demonstrated that the photoaffinity reagent ^{125}I -APTG exhibited saturation of the exchangeable GTP-binding site on the β -subunit of tubulin with an apparent K_d of 5 μM , as shown in Figure 1. This value compares favorably with that obtained with $[\gamma\text{-}^{32}\text{P}]\text{-8-N}_3\text{GTP}$, another valid GTP photoaffinity probe (9).

Selectivity was demonstrated for the photoinsertion of ^{125}I -APTG since it was competitive with GTP, GDP, and GTP analogues such as 8- N_3GTP and I-APTG, but the photoinsertion was not affected by other nucleotides (e.g., ATP, ADP, AMP, GMP) as shown in Figure 2. With these concentrations of ^{125}I -APTG, little photoinsertion into the α -subunit of tubulin was observed. The half-maximal prevention of ^{125}I -APTG photoinsertion into β -tubulin was obtained with ca. 5 μM GTP as shown in Figure 3. The Ofengand treatment of the data for the β -subunit indicated that the K_d for ^{125}I -APTG is 1.7 times that for GTP (Figure 4), indicating that the substantial modification of the γ -phosphate in ^{125}I -APTG had not altered substantially its ability to bind to the GTP-binding domain in β -tubulin. This value is in close agreement with 1.4 determined for 8- N_3GTP (9). APTG alone would not support tubulin polymerization in agreement with observations (10) that other GTP derivatives modified at the γ -phosphate were incompetent polymerization analogues of GTP even though they bound at the GTP site. The results shown in Figure 5 indicated that APTG could successfully compete with the GTP-binding site on tubulin since APTG increased the lag time before polymerization started and decreased the total amount of polymers formed.

^{125}I -APTG was designed to provide unique advantages in purifying photolabeled peptides. The incubation of ^{125}I -APTG at 20 μM concentration with purified tubulin for 30 min at 0°C and photolysis at 0°C effected a specific photoinsertion into the β -subunit of tubulin that was completely consistent with the ability of the probe to mimic GTP. Following the photochemical step, the radiolabel exhibited the desired hydrolytic stability. Acetone precipitation, resuspension in 100 mM ammonium bicarbonate solution, and trypsin digestion of the photo-

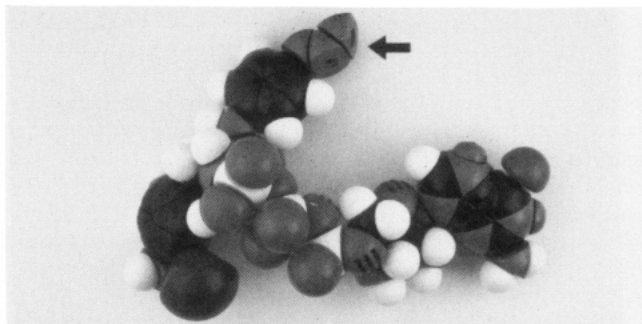


Figure 8. CPK model of ^{125}I -APTG. The arrow denotes the photoactive azide group.

labeled tubulin led to a mixture of peptides. A dramatic purification of the photolabeled peptides from this mixture was achieved by anion-exclusion chromatography on SP-25 Sephadex using 50 mM sodium formate (pH = 3.5) as the eluting buffer that removed the bulk of the nonphotolabeled peptides. This produced a void volume containing a mixture of the desired photolabeled peptides bearing the anionic triphosphate group and the acidic peptides from the C-terminal regions of the α - and β -chains (Figure 6A).

In the next step in this purification process, the addition of formic acid reduced the pH to ca. 1 and hydrolyzed the labile, negatively charged GTP portion of the photoinserted probe but left the radiolabel attached. Gel filtration on a Sephadex G-10 column separated the radiolabeled peptides from small, acidic peptides (Figure 6B). In the third step in the purification process, a second anion-exclusion chromatography on SP-25 Sephadex using 50 mM sodium formate separated the additional acidic peptides from the photolabeled peptides that now lacked the anionic triphosphate moiety and consequently eluted in later fractions. Final HPLC analysis of the photolabeled peptides on an Aquapore RP-300 C₈ reversed-phase column provided two radiolabeled peaks. On HPLC, radioactivity was observed in two locations. One (50%) was with the void volume where no peptides were found and probably represents breakdown of photoinserted label. The second (50%) comigrated with the two peaks marked by arrows in Figure 7B. Additional evidence that these radiolabeled peptides represented true photolabeled peptide derivatives was obtained by comparing the elution profiles by diode-array spectroscopy for the peptides recovered from photolabeled tubulin (Figure 7B) and peptides generated in a control experiment in which the probe was not present (Figure 7A).

The radiolabeled peaks (denoted by arrows in Figure 7B) were isolated in a single fraction and sequenced to reveal a peptide near the N-terminus of the β -subunit: AILVDLEPGTMDSV(R) (β :65–79). The isolation of this sequence was also noted with $[\gamma\text{-}^{32}\text{P}]\text{-8-N}_3\text{GTP}$ (1), and as shown in Figure 8, a CPK model of ^{125}I -APTG indicated that conformations were available to ^{125}I -APTG that would place the reactive azide (see arrow in Figure 8) in the same spacial domain as the azide group in $[\gamma\text{-}^{32}\text{P}]\text{-8-N}_3\text{GTP}$. Although the syn conformation is preferred for bulky C-8 substituted nucleotides (16), the 8-azidoguanosine in $[\gamma\text{-}^{32}\text{P}]\text{-8-N}_3\text{GTP}$ can adopt the anti conformation shown in Figure 8. We do not, however, represent ^{125}I -APTG as a general probe for defining the guanine base binding region but again emphasize that ^{125}I -APTG is a probe for defining the GTP-binding domain of various proteins. Although we lack precise evidence as to the specific amino acids that $[\gamma\text{-}^{32}\text{P}]\text{-8-N}_3\text{GTP}$ and ^{125}I -APTG cross-linked in AILVDLEPGTMDSV(R) (β :65–79), it was assumed, in the case

of ^{125}I -APTG, that a reactive dehydroazepine intermediate (17, 18), generated on photolysis of the aryl azide, intercepted a basic arginine (R) residue to establish the putative covalent linkage. Consistent with this observation, the terminal R residue in AILVDLEPGTMDSV(R) was not detected, as indicated by the parentheses in the above sequence. In addition, minor quantities of peptides in the same fraction containing AILVDLEPGTMDSV(R) (β : 65–79) were identified as AVFVDLEPTVIDEV(R) (α : 65–79) and VGINYEPPTVVPGGDLA(K) (α : 353–370) from the α -chain. The appearance of these minor quantities of peptides from the α -subunit raises the interesting possibility that another conformation of the photoactive subunit in ^{125}I -APTG can reach a domain on the α -subunit that lies in proximity to the β -subunit, but current data are clearly insufficient to warrant this conclusion.

We have noted that the overall photoincorporation based on the purified peptide AILVDLEPGTMDSV(R) (β : 65–79) was low (0.4%), and yet we are confident that this peptide represents a true photolabeled peptide and not an artifact. The usual practice in calculating photoincorporation "yields" is to report the percentage of label incorporated prior to the purification of the actual peptide(s). If we had followed this convention, the photoincorporation yield using ^{125}I -APTG would have been 2.3% since, as expected, considerable material is lost physically or through chemical deterioration in the course of the purification steps. Reporting a yield based on the final purified peptide underestimates the true photoincorporation yield.

In addition to the loss of material during the purification process, there is one additional feature that complicated the use of ^{125}I -APTG. Although we have indicated that the radiolabel was stable after the photolysis step, we discovered during the course of related studies that photodeiodination (15) was a concurrent process in the photolysis of aryl azides. We assume, on the basis of the observed loss of label, that this process also intervened in the course of the photolysis of ^{125}I -APTG and tubulin. It was rather surprising to discover that the photochemical cleavage of the carbon-iodine bond was faster than the photochemical conversion of the aryl azide to a reactive dehydroazepine (15), and of course, this undesired reaction further served to underestimate the true value of the photoincorporation "yield" since the deiodinated product APTG would also photoinsert. In the absence of the radiolabel, there was no way to estimate the extent of this process. Although the photochemical loss of radiolabel clearly limits the overall utility of ^{125}I -APTG as a general reagent, another experiment suggested that there would be merit in exploring this class of GTP probes further. ^{125}I -APTG was used to photolabel the proteins in whole homogenates of normal and Alzheimer's diseased brains (Figure 9). In normal brain, the photolabeling of β -tubulin, as well as four other unidentified proteins, was noted whereas, in Alzheimer's diseased brains, only two proteins were significantly photolabeled. It was of interest that the β -subunit of tubulin in homogenates of Alzheimer's diseased brains was one of the proteins that was not photolabeled, in agreement with another report on the aberrant properties of tubulin from Alzheimer's diseased brain (19). It was of interest that ^{125}I -APTG exhibited selectivity for β -tubulin even in the face of numerous other proteins and thereby further testified to its validity as a GTP probe. However, in the absence of detailed studies of the other labeled proteins, we can say only that this observation underscores the merit of developing other phosphonamide GTP photoaffinity probes with photostable radio-

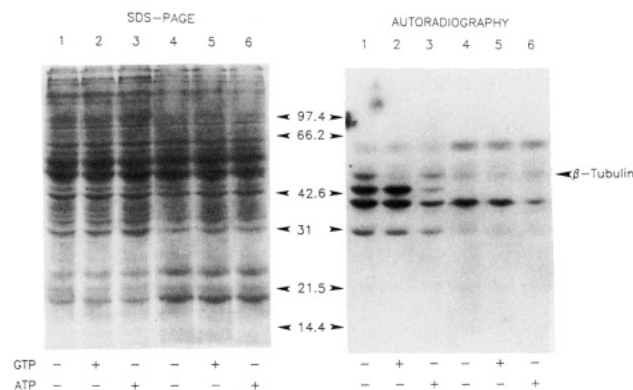


Figure 9. Photolabeling of normal and Alzheimer's diseased brain homogenate with ^{125}I -APTG. Normal brain homogenate (lanes 1, 2, and 3) (20%) and Alzheimer's diseased brain homogenate (lanes 4, 5, and 6) (20%) were incubated successively with GTP (100 μM) or ATP (100 μM) at 0 $^{\circ}\text{C}$ (2 min) and with ^{125}I -APTG (10 μM) at 0 $^{\circ}\text{C}$ (2 min), photolyzed at 0 $^{\circ}\text{C}$ (2 min), and analyzed on 10% SDS-PAGE. Autoradiography was performed for 12 h.

labels. Current efforts are focused on the incorporation of a photostable ^{35}S radiolabel.

ACKNOWLEDGMENT

We thank the National Institutes of Health (Grant P50 AG05144, GM-33150 and GM-35806) for their generous financial support.

LITERATURE CITED

- (1) Kim, H., Ponstingl, H., and Haley, B. E. (1987) Identification of the guanosine interacting peptide of the GTP binding site of β -tubulin using $8\text{N}_3\text{GTP}$. *Fed. Proc.* 46, 2229.
- (2) Linse, K., and Mandelkow, E.-M. (1988) The GTP binding peptide of β -tubulin. *J. Biol. Chem.* 263, 15205–15210.
- (3) Nath, J. P., and Himes, R. (1986) Localization of the exchangeable nucleotide binding domain in β -tubulin. *Biochem. Biophys. Res. Commun.* 135, 1135–1143.
- (4) Shelanski, M. L., Gaskin, F., and Cantor, C. R. (1973) Microtubule assembly in the absence of added nucleotides. *Proc. Nat. Acad. Sci. U.S.A.* 70, 765–768.
- (5) Gaskin, F., Cantor, C. R., and Shelanski, M. L. (1974) Turbidimetric studies of the in vitro assembly and disassembly of porcine neurotubules. *J. Mol. Biol.* 89, 737–758.
- (6) Laemmli, U. K., and Favre, M. (1973) Maturation of the head of bacteriophage T4. *J. Mol. Biol.* 80, 575–599.
- (7) Ofengand, J., and Henes, C. (1969) The function of pseudouridylic acid in transfer ribonucleic acid. *J. Biol. Chem.* 244, 6241–6253.
- (8) Geahlen, R. L., and Haley, B. E. (1977) Interactions of a photoaffinity analog of GTP with the proteins of microtubules. *Proc. Natl. Acad. Sci. U.S.A.* 74, 4375–4377.
- (9) Geahlen, R. L., and Haley, B. E. (1979) Use of a GTP photoaffinity probe to resolve aspects of the mechanism of tubulin polymerization. *J. Biol. Chem.* 254, 11982–11987.
- (10) Yarbrough, L. R., and Kirsch, M. (1981) Binding of fluorescent analogs of GTP to the exchangeable nucleotide binding site of tubulin. *J. Biol. Chem.* 256, 112–117.
- (11) Glonek, T., Kleps, R. A., and Myers, T. C. (1974) Cyclization of the phosphate side chain of adenosine triphosphate: formation of monoadenosine 5'-trimetaphosphate. *Science* 185, 352–354.
- (12) Babkina, G. T., Zarytova, V. F., and Knorre, D. G. (1975) Preparation of γ -amides of nucleoside-5'-triphosphate in aqueous solution with the aid of a water-soluble carbodiimide. *Bioorg. Khim.* 1, 611–615.
- (13) Knorre, D. G., Kurbatov, V. A., and Samukov, V. V. (1976) General method for the synthesis of ATP-GAMMA derivatives. *FEBS Lett.* 70, 105–108.
- (14) Babkina, G. T., Jonak, J., and Rychlik, I. (1982) Interaction of elongation factor EF-Tu with γ -amides of GTP and β -amides of GDP bearing the azidoaryl group or the chloroethylaminoaryl group placed at the terminal phosphate. *Biochim. Biophys. Acta* 698, 116–127.

- (15) Watt, D. S., Kawada, K., Leyva, E., and Platz, M. S. (1989) Exploratory photochemistry of iodinated aromatic azides. *Tetrahedron Lett.* 30, 899-902.
- (16) Saenger, W. (1984) *Principles of Nucleic Acid Structure*, pp 21-23, Springer-Verlag, New York.
- (17) Torres, M. J., Zayas, J., and Platz, M. S. (1986) A formal CH insertion reaction of an aryl nitrene into an alkyl CH bond. Implications for photoaffinity labelling. *Tetrahedron Lett.* 27, 791-794.
- (18) Shields, C. J., Chrisope, D. R., Schuster, G. B., Dixon, A. J., Poliakoff, M., and Turner, J. J. (1987) Photochemistry of aryl azides: detection and characterization of a dehydroazepine by time-resolved infrared spectroscopy and flash photolysis at room temperature. *J. Am. Chem. Soc.* 109, 4723-4726.
- (19) Khatoon, S., Campbell, S. R., Haley, B. E., Slevein, J. T. (1989) Aberrant guanosine triphosphate- β -tubulin interaction in Alzheimer's disease. *Ann. Neurol.* 26, 210-215.
- Registry No.** 1, 106-50-3; 2, 129571-94-4; 3a, 126083-05-4; 3b, 129571-95-5; 4a, 126083-06-5; 4b, 129571-96-6; 5a, 129592-78-5; 5b, 129592-80-9; 5c, 129592-82-1; GTP, 86-01-1; AILVDLEPGT-MDSVR, 111261-75-7; *N*-(*tert*-butoxycarbonyl)tyrosine, 3978-80-1; guanosine triphosphate disodium salt, 56001-37-7.

Synthesis and Evaluation of Two New Bifunctional Carboxymethylated Tetraazamacrocyclic Chelating Agents for Protein Labeling with Indium-111

Gerd Ruser, Walter Ritter, and Helmut R. Maecke*

Department of Nuclear Medicine, University Hospital Basel, 4031 Basel, Switzerland. Received July 16, 1990

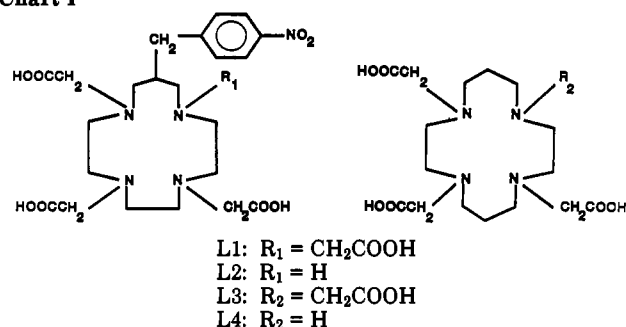
The synthesis of two new N- and C-functionalized tetraazamacrocyclic ligands intended to be covalently linked to biomolecules like monoclonal antibodies and to bind the γ -emitting isotope indium-111 in a thermodynamically and/or kinetically inert way is described. 12-(*p*-Nitrobenzyl)-1,4,7,10-tetraazacyclotridecane-1,4,7,10-tetraacetic acid (L1) was synthesized by means of bimolecular cyclization with the appropriate malonic acid diethyl ester and triethylenetetraamine, followed by reduction with diborane and alkylation of the cyclic tetraamine with bromoacetic acid. The corresponding triscarboxymethylated ligand L2 was made by statistical alkylation of the tetraamine. Both ligands fulfill the criteria for antibody labeling using the bifunctional chelate approach, namely fast chelate formation, high radiochemical yield, and high stability under physiological conditions. Surprisingly the heptadentate ligand L2 confers higher stability to In^{3+} and exhibits faster complex formation than octadentate L1. ^{13}C NMR spectra in solution indicate that the difference in stability is not due to incomplete coordination of all four carboxylate groups in In -L1.

The application of radiolabeled monoclonal antibodies (MoAb) is a potentially powerful tool in nuclear medicine for tumor diagnosis and therapy (1-6). The use of metallic radionuclides has the special advantage that the lyophilized antibody-ligand conjugates can be prepared and stored in advance. A specific radiopharmaceutical can then be prepared by simply adding a buffered solution of the radiometal prior to application. This circumvents technical and logistical problems associated with the iodine isotopes. Many MoAb show optimal tumor localization only after few days. For this reason the γ -emitting isotope ^{111}In was proposed (7-11). Its appropriate nuclear characteristics, a 68 h half-life, and γ -energies of 173 keV and 247 keV make it ideally suited to tumor diagnosis. For a successful use of the isotope in antibody labeling it has to be coupled to the MoAb by using the bifunctional chelate approach. Thereby the following prerequisites have to be fulfilled: (i) fast complex formation and high radiochemical yield, (ii) high kinetic inertness, to avoid label transfer in vivo to the competing serum protein transferrin and concomitant transferrin-mediated liver uptake, and (iii) preserved immunoreactivity of the antibody complex conjugate.

We report here on the achievement of the first two aspects with two new bifunctional carboxymethylated tetraazamacrocycles (L1, L2, Chart I).

Our earlier work on In^{3+} chemistry has shown the Na_2In -(DTPA)- $3\text{H}_2\text{O}$ complex to have coordination number eight with antiprismatic geometry (12). This geometry also holds for $\text{NaIn}(\text{DOTA})\cdot 3\text{H}_2\text{O}$ (13). The complex with the tetracarboxymethylated macrocycle now is more compact and very symmetric and the In^{3+} -nitrogen and In^{3+} -oxygen bonds are somewhat shorter. This is reflected in increased kinetic stability of $\text{In}(\text{DOTA})^-$ compared to the open chain polyaminopolycarboxylato- In^{3+} complex (14). We have therefore continued our studies toward the synthesis of C-functionalized tetraazamacrocycles and describe the approach with C-functionalized carboxymethylated derivatives of 1,4,7,10-tetraazatridecane.

Chart I



So far bifunctional derivatives of open chain polyaminopolycarboxylates as EDTA (15) and DTPA (7, 11) were tested in animal models and patients. These ligands certainly confer high thermodynamic stability to the corresponding ^{111}In complexes. Because of the possible importance of kinetic inertness, bifunctional macrocycles may be of additional benefit in antibody labeling with ^{111}In .

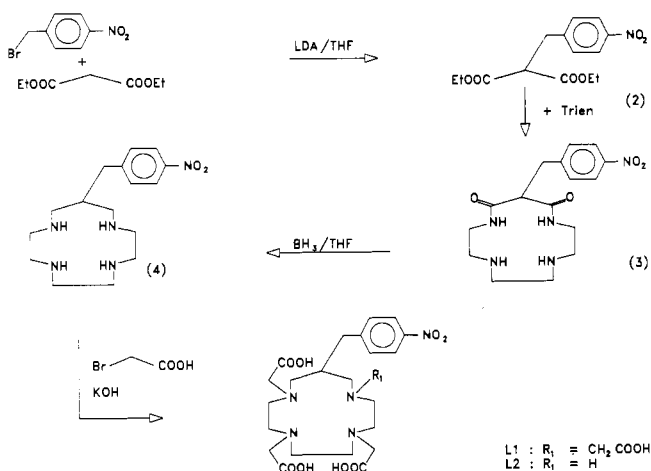
Bifunctional DOTA has recently been shown to stabilize $^{88}\text{Y}^{3+}$ in human serum extremely well (16) and a bifunctional triazamacrocyclic was proposed for antibody labeling with $^{111}\text{In}^{3+}$ (17).

EXPERIMENTAL PROCEDURES

Material and Methods. All reagents and solvents were obtained from commercial sources and were used without further purification.

Infrared spectra were recorded on a Perkin-Elmer 983 instrument with KBr pellets. Proton and carbon-13 nuclear magnetic resonance spectra were recorded at 25 °C on a Bruker spectrometer at 360 and 91 MHz, respectively, and a Varian VXR-400 spectrometer at 400 and 101 MHz. Chemical shifts reported are relative either to TMS (CDCl_3) or sodium 3-(trimethylsilyl)tetradecatriopropionate (TSP, D_2O). Mass measurements were obtained on a VG 70-SE mass spectrometer, using 8 kV

Scheme I



in a thioglycerol matrix. Elemental analysis were performed at CIBA-GEIGY Analytical Services Laboratories. $^{111}\text{InCl}_3$ was obtained from Mallinckrodt Diagnostica (10 mCi/mL in pH 1 HCl). γ -Counting was performed on a Packard A 5000 D well counter and a homemade continuous flow-through γ -detector based on a Picker Model 628018 NaJ detector and a Canberra AMP ITSCA amplifier.

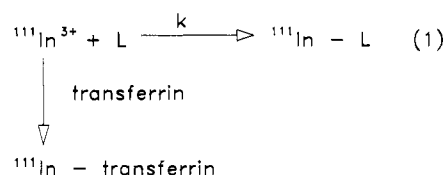
Synthesis. The ligands L1 and L2 were synthesized according to Scheme I.

(*p*-Nitrobenzyl)malonic Acid Diethyl Ester 2. A mixture of 58 g (0.36 mol) of diethyl malonate and 21.4 g (0.18 mol) of lithium diisopropylamide in 210 mL of THF was cooled to -62°C and 39.1 g (0.18 mol) of *p*-nitrobenzyl bromide in 30 mL of THF was added slowly. Stirring was continued for 1 h. A solid was removed by filtration and the remaining solution was evaporated to dryness. Warm ethanol was added to the solid and filtered from the side products (mp 160°C , disubstituted malonic acid diethyl ester). The pure product was obtained by crystallization from the filtrate (yield 70%, mp $58\text{--}59^\circ\text{C}$). IR (KBr): 3110–3080 (ar-C-H), 1735 (C=O), 1600 (ar-C-C), 1510 and 1345 cm^{-1} (NO_2). ^1H NMR: δ 1.20 (t, 8 H), 3.50 (m, 3 H), 4.20 (q, 4 H), 7.4 (d, 2 H), 8.10 (d, 2 H). Elemental Anal. Calcd for $\text{C}_{14}\text{H}_{17}\text{N}_1\text{O}_6$ (295.29): C, 56.9; H, 5.8; N, 4.7; O, 32.5. Found: C, 57.0; H, 5.9; N, 4.7; O, 32.5.

12-(*p*-Nitrobenzyl)-1,4,7,10-tetraazacyclotridecane-11,13-dione (3) was synthesized by aminolysis of 38.69 g (0.131 mol) of 2 with 19.7 (0.135 mol) of 1,4,7,10-tetraazadecane. The mixture was heated in 500 mL of ethanol for 5 days. The product could be crystallized by slow evaporation of the solvent (yield 28%, mp 265°C dec). Mass spectrum (FAB): m/e 350 (M + H). IR (KBr): 3310 (N-H), 3310–3060 (ar-C-H), 1670 (C=O), 1510 and 1345 cm^{-1} (NO_2). ^1H NMR: δ 2.6–3.6 (m, 15 H), 7.41 (d, 2 H), 8.13 (d, 2 H). ^{13}C NMR: δ 34.92, 39.59, 46.87, 47.79, 57.30, 128.80, 129.80, 146.60, 146.90, 169.30. Elemental Anal. Calcd for $\text{C}_{16}\text{H}_{23}\text{N}_5\text{O}_4$ (349.39): C, 55.0; H, 6.6; N, 20.0; O, 18.3. Found: C, 54.8; H, 6.7; N, 20.0; O, 18.1.

12-(*p*-Nitrobenzyl)-1,4,7,10-tetraazacyclotridecane (4) was obtained by reducing 7.06 g (20.2 mmol) of 3 in 100 mL of THF with a large excess of diborane (220 mmol) and heating under reflux for 24 h. Repeated treatment with methanol and evaporation followed by 3 h of heating under reflux with concentrated hydrochloric acid gave, after evaporation to $1/3$ the volume, 71% of the cyclic tetraamine as a tetrahydrochloride salt. The free tetraamine was obtained by addition of KOH (pH 12) and extraction with CH_2Cl_2 (yield 95%). Mass spectrum

Scheme II



(FAB): m/e 322 (M + H). IR (KBr): 3400 (NH_2^+), 1600 (ar-C-C), 1510 and 1350 cm^{-1} (NO_2). ^1H NMR: δ 2.81 (t, 1 H), 3.04 (d, 2 H), 3.50 (m, 16 H), 7.57 (d, 2 H), 8.16 (d, 2 H). ^{13}C NMR: δ 37.92, 38.52, 46.43, 47.44, 47.74, 50.71, 126.84, 133.06, 148.26, 149.36. Elemental Anal. Calcd for $\text{C}_{16}\text{H}_{27}\text{N}_5\text{O}_2 \cdot 1.23\text{H}_2\text{O} \cdot 4\text{HCl}$ (489.43): C, 39.26; H, 6.89; N, 14.30; O, 10.55; Cl, 28.97; H_2O , 4.53. Found: C, 39.55; H, 6.71; N, 14.48; O, 10.24; Cl, 29.11; H_2O , 4.54.

Tris- and tetracarboxymethylation of the tetraamine was afforded in aqueous solution at a pH of between 9.5 and 10.5.

12-(*p*-Nitrobenzyl)-1,4,7,10-tetraazacyclotridecane-1,4,7,10-tetraacetic acid (L1) was obtained at 70°C and pH 10.5 by the slow addition of 5 equiv of bromoacetic acid. The pH was controlled by use of a pH-stat. After stirring for 3 h at 70°C , the yellow solution was loaded onto an anion-exchange column (Dowex 1 \times 4, formate form, $2.6 \times 30\text{ cm}$). The column was washed with water and the ligand was eluted with a 0.02–5 M gradient of formic acid. A side product (triscarboxymethylated tetraamine) eluted at 0.05 M HCOOH, the product at 0.5 M HCOOH. The solution was evaporated and crystallized from HCl/acetone (yield 65%). Mass spectrum (FAB): m/e 554 (M + H). IR (KBr): 1725 (C=O), 1510 and 1345 cm^{-1} (NO_2). ^1H NMR: δ 2.70 (q, 1 H), 2.83 (d, 2 H), 3.05–4.15 (m, 24 H), 7.54 (d, 2 H), 8.19 (d, 2 H). ^{13}C NMR: δ 33.018, 37.446, 51.005, 52.004, 53.937, 54.370, 54.659, 60.777, 124.939, 131.156, 147.125, 147.472, 171.946. Elemental Anal. Calcd for $\text{C}_{24}\text{H}_{35}\text{N}_5\text{O}_{10} \cdot 1.85\text{H}_2\text{O} \cdot 3.5\text{HCl}$ (714.2): C, 40.67; H, 5.97; N, 9.86; Cl, 17.05. Found: C, 40.93; H, 6.04; N, 9.94; Cl, 17.95.

12-(*p*-Nitrobenzyl)-1,4,7,10-tetraazacyclotridecane-1,4,7-triacetic acid (L2) was obtained by statistical alkylation of 4 with 3.5 equiv bromoacetic acid at pH 9.5, 70°C (3 h), and purification as above (yield 45%). Mass spectrum (FAB): m/e 496.6 (M + H). IR (KBr): 1725 (C=O), 1510 and 1345 cm^{-1} (NO_2). ^1H NMR: δ 2.52 (s, 1 H), 2.79 (d, 2 H), 2.83–3.93 (m, 22 H), 7.49 (d, 2 H), 8.22 (d, 2 H). ^{13}C NMR: δ 35.251, 37.579, 46.375, 50.062–56.468 (m), 82.194, 125.088, 131.304, 147.808, 147.712, 169.441, 176.574, 176.449. Elemental Anal. Calcd for $\text{C}_{22}\text{H}_{33}\text{N}_5\text{O}_8 \cdot 1.25\text{H}_2\text{O} \cdot 2.8\text{HCl}$ (624.64): C, 42.30; H, 6.26; N, 11.26; O, 24.33; Cl, 15.90; H_2O , 4.33. Found: C, 42.26; H, 6.38; N, 11.15; O, 24.57; Cl, 16.21; H_2O , 4.26. 1,4,8,11-Tetraazacyclotetradecane-1,4,8,11-tetraacetic acid (TETA, L3) and 1,4,8,11-tetraazacyclotetradecane-1,4,8-triacetic acid (TE3A, L4) were synthesized according to published procedures (18, 14).

Rate of Formation of ^{111}In Chelates. The rate of $^{111}\text{In}^{3+}$ complex formation was measured by scavenging of free $^{111}\text{In}^{3+}$ with transferrin according to Scheme II. The measurements were performed under relevant antibody labeling conditions. A carrier-free solution of 150 μL of $^{111}\text{InCl}_3$ in 0.1 N HCl (0.5–2 mCi indium-111, depending on specific activity) was mixed with 2 mL of 0.05 M sodium citrate (pH 6.5). This solution (400 μL) was mixed with 10 μL of ligand solution in H_2O (final ligand concentration 9–50 μM). The reaction (1) was quenched after appropriate time intervals by mixing 10- μL aliquots of this reaction mixture with 200 μL of human serum or 200 μL of 2×10^{-5}

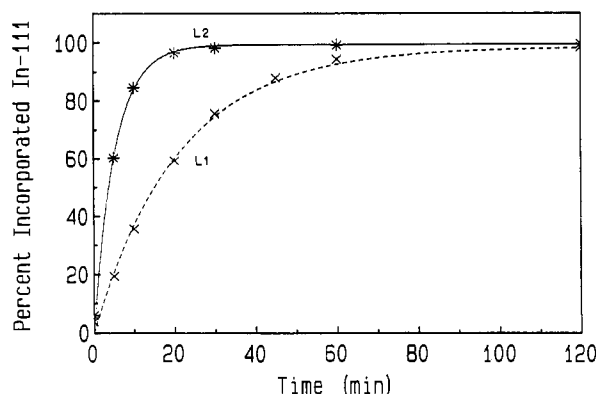


Figure 1. Rate of formation of ^{111}In chelates with L1 and L2. Ligand concentrations were $10\ \mu\text{M}$ $1\ \text{mCi } ^{111}\text{InCl}_3$, with $k_{\text{obs}} = 8 \times 10^{-4}\ \text{s}^{-1}$ for L1 and $3.1 \times 10^{-3}\ \text{s}^{-1}$ for L2.

M transferrin in 0.1 M carbonate buffer, pH 7.4. This causes scavenging of free In^{3+} . The mixture was subject to gel filtration (Sephadex G-50, $1 \times 15\ \text{cm}$ column). The column was eluted with 0.01 M PBS buffer (pH 7.4) at a flow rate of 37 mL per h. Samples were taken for 30 s after a dead volume of 4 min. After a total of 36 samples, >98% of the radioactivity was eluted from the column. In later experiments radioactive fractions were detected with a homemade continuous flow-through γ -detector based on a Picker Model 628018 sodium iodide detector and a Canberra AMP/TSCA amplifier. Transferrin and other serum proteins were detected with a flow-through cell (1 mm) and a Beckman UV/VIS spectrophotometer set at 280 nm. $^{111}\text{InCl}_3$ given to human serum or transferrin both eluted off the column between 5 and 9 min whereas ^{111}In chelates eluted between 10 and 25 min. The reaction between $^{111}\text{In}^{3+}$ and transferrin is complete within 2–3 min. The percentage of $^{111}\text{In}^{3+}$ scavenged by transferrin was used as a measure of free In^{3+} . It was calculated from the radioactivity of the respective fractions (Figure 1).

Rate of $^{111}\text{In}^{3+}$ Exchange with Transferrin in Human Serum. This rate was measured by using similar strategies as described above (19, 20). After an incubation time of 30 min–2 h for L1 and L2 with indium-111 (at least 30 h for L3 and L4 and 10 times higher ligand concentrations are necessary) the complex formation was complete. A 200- μL aliquot of this mixture was given to 2–8 mL of sterile human serum and incubated up to 7 days at $37\ ^\circ\text{C}$ in a chamber maintained at 5% CO_2 and 95% air. At appropriate time intervals, 25 μL of this mixture was taken and subjected to gel filtration as described above. The percentage of $^{111}\text{In}^{3+}$ transferred to transferrin as a function of time is shown in Figure 2.

^{13}C NMR of In-L1 and In-L2. Solutions of the complexes for NMR measurements were made up in D_2O and the pD was adjusted with NaOD. The final pD was determined by using the equation $\text{pD} = \text{pH} + 0.4$ (21). L1 (20 mg, $2.84 \times 10^{-5}\ \text{mol}$) and 7.35 mg ($1.42 \times 10^{-5}\ \text{mol}$) of $\text{In}_2(\text{SO}_4)_3$ were dissolved in 750 μL of D_2O . The pD was kept at 4.2 with NaOD. The incorporation was complete within 1 h. TSP was added and the desired pD was adjusted with NaOD or DCl, respectively. In-L2 was synthesized likewise.

RESULTS

Two new bifunctional macrocyclic ligands (L1, L2) based on 12-(*p*-nitrobenzyl)-1,4,7,10-tetraazatridecane have been synthesized by extensive or statistical alkylation with bromoacetic acid. The overall yield of the four-step synthesis was 9.8% for L1 and 6.9% for L2. The ligands were

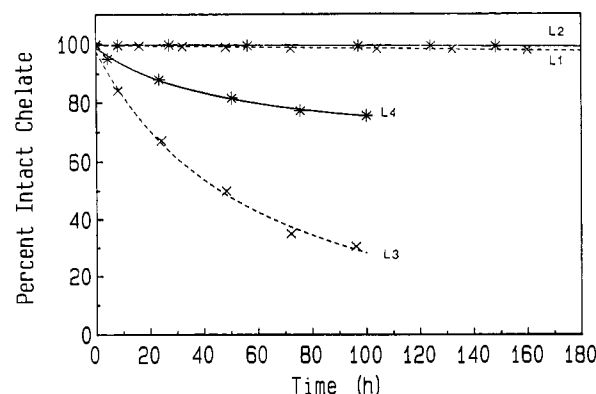


Figure 2. Dissociation of ^{111}In chelates in human serum at $37\ ^\circ\text{C}$, in air/ CO_2 (95/5%). The data points are from at least two ligand concentrations between 8×10^{-7} and $3 \times 10^{-6}\ \text{M}$ and/or two complex concentrations. The deviations were between 10 and 20%.

characterized by the usual analytical procedures: NMR, IR, mass spectra, and elemental analysis. The analytical data are in accordance with the structures depicted in Chart I. L2 appears to be a single compound as can be judged from TLC, ion-exchange chromatography, and reversed-phase HPLC. This is somewhat surprising as two isomers are possible [12-(*p*-nitrobenzyl)-1,4,7,10-tetraazacyclotridecane-1,4,7-triacetic acid or 12-(*p*-nitrobenzyl)-1,4,7,10-tetraazacyclotridecane-1,4,10-triacetic acid]. Extensive NMR studies (2D, COLOC, HCCORR) did not give any conclusion as to the isomeric form.

The rate of In^{3+} chelate formation was determined as shown in Scheme II. The data are plotted in Figure 1. The experimental data points follow pseudo-first-order kinetics with $k_{\text{obs}} = 8 \times 10^{-4}\ \text{s}^{-1}$ for L1 and $3.1 \times 10^{-3}\ \text{s}^{-1}$ for L2, respectively, at $10\ \mu\text{M}$ ligand concentration. Both complexes form at ligand concentrations $>30\ \mu\text{M}$ within 30 min, giving >98% radiochemical yield. The stability of these chelates in human serum is shown in Figure 2. Four complexes (In-L1 through In-L4) are compared in this plot. L2, the heptadentate bifunctional tetraazamacrocyclic, loses In^{3+} with a pseudo-first-order rate constant of $k \approx 1 \times 10^{-8}\ \text{s}^{-1}$ (i.e. <0.1% loss of In^{3+} within 24 h) whereas octadentate L1 decays with $k \approx 4 \times 10^{-8}\ \text{s}^{-1}$. Both rate constants do not change significantly with ligand and complex concentration. The monofunctional 14-membered tetraazamacrocyclics TETA (L3) and TE3A (L4) are too unstable for the purpose of in vivo use. They form only after prolonged incubation times and much higher ligand excess. They decay with rate constants $k(\text{L3}) = 3 \times 10^{-6}\ \text{s}^{-1}$ and $k(\text{L4}) = 9.3 \times 10^{-7}\ \text{s}^{-1}$.

Structural factors which may be responsible for the difference of stability were elucidated by using ^{13}C NMR in solution. Earlier work has shown that the relative chemical shifts of the $^{13}\text{COO}^-$ resonances are useful to distinguish between bound and free carboxylate groups (12). Especially the question if all carboxylate groups are bound to In^{3+} in In-L1 was of interest in this context. The four COO^- groups exhibit four signals within 0.8 ppm around 180 ppm with an approximate intensity of 4:4:1:1 (Table I). The spectrum does not change with pD between 2.5 and 7.0. For the heptadentate ligand L2 six signals around 180 ppm with an intensity of 2:2:2:1:1:1 were found. As a comparison the $^{13}\text{COO}^-$ chemical shifts of octahedral hexacoordinate $\text{Ga}(\text{DTPA})^{2-}$ at different pD values is given in Table I (12). Free, noncoordinated carboxylate groups can clearly be distinguished by their downfield shifts and line broadening. Moreover at low pD values

Table I. Carbon-13 NMR Data for the CO₂⁻ Group in In³⁺ Complexes

compd	CN ^a	pD	chemical shifts ^b of ¹³ CO ₂ ⁻ groups, ppm	assign.
In-L1	8	2.5	180.07, 179.87, 179.63, 179.29	4 COO ⁻ -In ³⁺
		5.5	181.05, 180.74, 180.55, 180.29	intensity: 4:4:1:1
		7.2	181.02, 180.72, 180.52, 180.26	
In-L2	7(8)	4.0	181.2, 180.87, 180.65, 180.61	3 COO ⁻ -In ³⁺
			180.4, 180.37	intensity: 1:2:2:2:1:1
Ga(DTPA) ²⁻	6	3.0	172.92	2 free COOH
			178.02, 177.77, 177.18	3 COO ⁻ -Ga ³⁺
		8.4	181.25	2 free COO ⁻
			178.73, 178.68, 178.62	3 COO ⁻ -Ga ³⁺

^a CN = coordination number. ^b Sodium 3-(trimethylsilyl)tetra-deuteriopropionate as internal standard.

where protonation of these carboxylates is expected, a further dramatic upfield shift can be found.

DISCUSSION

In-L1 and In-L2 fulfill the criteria of fast chelate formation, high radiochemical yield, and high stability under physiological conditions and are currently being tested for antibody labeling with indium-111. The rate of indium transfer to transferrin is clearly complex- and ligand-concentration independent and represents the high kinetic stability of the two complexes. Surprisingly the heptadentate ligand L2 confers higher stability to In³⁺ and exhibits faster complex formation than octadentate L1. The reasons for these unexpected results are unclear. This trend is certainly ring-size dependent as In(DOTA)⁻ is slightly more stable than In(DO3A) (14, 22), but In(TE3A) (heptadentate ligand) again is more stable than In(TETA)⁻ (octadentate ligand). The stability difference between the octadentate and heptadentate ligand is reversed in the open chain polyaminocarboxylates. In(DTPA)²⁻ exhibits higher stability than In(DTPA-mono-*n*-butylamide)⁻ (13, 23). The results indicate that preformed ligand conformation rather than ligand denticity determine complex stability in the complexes studied.

The results of ¹³C NMR studies of In-L1 are in good accordance with the assumption of four bound carboxylate groups in an all-trans configuration and two isomeric complexes depending on the axial or equatorial position of the *p*-nitrobenzyl group. An alternative explanation of the ¹³COO⁻ pattern is the assumption of two carboxylate groups having faster relaxation times due to a looser binding to In³⁺. The pD independence of the ¹³COO⁻ pattern down to pD 2.5 clearly shows the stability of the complex in the pD region studied. More pronounced is the splitting of the ¹³COO⁻ resonances in In-L2. Six signals are found and this is most simply explained with the assumption of two isomeric species. The splitting of the remaining 13 ¹³C resonances into doublets is again in accordance with this explanation.

It will be of great interest to see the differences of the two compounds in living systems. L2 forms a neutral complex which is more stable toward acid-catalyzed hydrolysis. Furthermore, a neutral complex may alter the proteins's surface less than a charged species and may therefore show more favorable pharmacokinetics. Moreover having two almost equally well-suited ligands which differ by charge, may be of importance in a future clinical application. The coupling of small chelates to large biomolecules may render them immunogenic and the problem of human antichelate antibody response (HACA) may emerge. This problem may be solved by the use of different bifunctional chelates if repeated injections of labeled antibody are necessary.

ACKNOWLEDGMENT

The helpful discussions on NMR data with Prof. U. Sèquin are gratefully acknowledged as well as the expert technical help of N. Ulmer and C. Leuenberger. This work was supported by the Swiss National Science Foundation (Grant No. 3.060-0.87), the Swiss Cancer League (FOR.329.88.2), and the Sandoz-Stiftung.

LITERATURE CITED

- (1) Rainsbury, R. M., Westwood, J. H., Coombes, R. C., Neville, A. M., Ott, R. J., Kalirai, T. S., McCready, V. R., and Gazet, J. C. (1983) Location of Metastatic Breast Carcinoma by a Monoclonal Antibody Chelate Labeled with Indium-111. *Lancet*, 934.
- (2) Beatty, J. D., Duda, R. B., Williams, L. E., Sheibasi, K., Paxton, R. J., Beatty, B. G., Philben, V. J., Werner, J. L., Shively, J. E., Vlahos, W. G., Kokal, W. A., Riihimatti, D. U., Terz, J. J., and Wagman, L. D. (1986) Preoperative Imaging of Colorectal Carcinoma with 111-In-Labeled Anticarcinoembryonic Antigen Monoclonal Antibody. *Cancer Res.* 46, 6494.
- (3) Carrasquillo, J. A., Bunn, P. A., Keenan, A. M., Reynolds, J. C., Schroff, R. W., Foon, K. A., Ming-Hsu, S., Gazdar, A. F., Mulshine, J. L., Oldham, R. K., Perentesis, P., Horowitz, M., Eddy, J., James, P., and Larson, S. (1986) Radioimmuno-detection of Cutaneous T-Cell Lymphoma with 111-In-Labeled T 101 Monoclonal Antibody. *N. Engl. J. Med.* 315, 673.
- (4) Mach, J. P., Correl, S., Forni, M., Ritschard, J., Donath, A., and Alberto, P. (1980) Tumor Localization of Radiolabelled Antibodies against Carcinoembryonic Antigen in Patients with Carcinoma. *N. Engl. J. Med.* 303, 5.
- (5) Macklis, R. M., Kinsey, B. M., Kassis, A. I., Ferrara, J. L. M., Atcher, R. W., Hines, J. J., Coleman, C. N., Adelstein, S. J., Burakoff, S. J. (1988) Radioimmunotherapy with α -Particle-Emitting Immunoconjugates. *Science* 240, 1024.
- (6) Baldwin, R. W., and Byers, V. S. (1986) Monoclonal Antibodies in Cancer Treatment. *Lancet* 603.
- (7) Hnatowich, D. J., Layne, U. U., Childs, R. I., Lateigne, D., Davis, M. A., Griffin, T. W., and Doherty, P. W. (1983) Radioactive labeling of antibody: a simple and efficient method. *Science* 220, 613.
- (8) Paik, C., Herman, D. E., Eckelman, W. C., and Reba, R. C. (1980) Synthesis, plasma clearance and in vitro stability of protein containing a conjugated indium-111 chelate. *J. Radioanal. Chem.* 57, 553.
- (9) Khaw, B. A., Fallon, J. T., Strauss, H. W., and Haber, E. (1980) Myocardial infarct imaging of antibodies to canine cardiac myosin with indium-111-diethylenetriamine pentaacetic acid. *Science* 209, 295.
- (10) Sundberg, M. W., Meares, C. F., Goodwin, D. A., and Diamanti, C. I. (1974) Chelating agents for the binding of metal ions to macromolecules. *Nature (London)* 250, 587.
- (11) Brechbiel, M. W., Gansow, O. A., Atcher, R. W., Schlom, J., Esteban, J., Simpson, D. E., and Colcher, D. (1986) Synthesis of 1-(*p*-isothiocyanatobenzyl) derivatives of DTPA and EDTA. Antibody labeling and tumor imaging studies. *Inorg. Chem.* 25, 2772.
- (12) Maacke, H. R., Riesen, A., and Ritter, W. (1989) The Molecular Structure of Indium-DTPA. *J. Nucl. Med.* 30, 1235.
- (13) Ritter, W. (1989) Ph.D. thesis, University of Basel, Basel

- (paper in preparation). DOTA = 1,4,7,10-tetraazacyclododecane-1,4,7,10-tetraacetic acid.
- (14) Riesen, A., Kaden, Th. A., Ritter, W., and Maecke, H. R. (1989) Synthesis and characterization of seven coordinate macrocyclic In^{3+} complexes with relevance to radiopharmaceutical applications. *Chem. Commun.*, 460.
- (15) Meares, C. F., McCall, M. J., Reardan, D. T., Goodwin, D. A., Diamanti, C. I., and McTigue, M. (1984) Conjugation of Antibodies with Bifunctional Chelating Agents: Isothiocyanate and Bromoacetamide Reagents, Methods of Analysis, and Subsequent Addition of Metal Ions. *Anal. Biochem.* 142, 68.
- (16) Moi, M. K., Meares, C. F., and DeNardo, S. J. (1988) The Peptide Way to Macrocyclic Bifunctional Chelating Agents: Synthesis of 2-(*p*-Nitrobenzyl)-1,4,7,10-tetraazacyclododecane-*N,N',N'',N'''*-tetraacetic Acid and Study of Its Yttrium(III) Complex. *J. Am. Chem. Soc.* 110, 6266.
- (17) Craig, S. A., Helps, I. M., Jankowski, K. J., Parker, D., Beeley, N. R. A., Boyce, B. A., Eaton, M. A. W., Millican, A. T., Millar, K., Phipps, A., Rhind, S. K., Harrison, A., and Walker, T. (1989) Towards Tumour Imaging with Indium-111 Labeled Macrocyclic Antibody Conjugates. *Chem. Commun.* 794.
- (18) Stetter, H., and Frank, W. (1976) Complex formation with tetraazacycloalkane-*N,N',N'',N'''*-tetraacetic acids as a function of ring size. *Angew. Chem., Int. Ed. Engl.* 15, 686.
- (19) Yeh, S. M., Meares, C. F., and Goodwin, D. A. (1979) Decomposition Rates of Radiopharmaceutical Indium Chelates in Serum. *J. Radioanal. Chem.* 53, 327.
- (20) Meares, C. F., Goodwin, D. A., Leung, C. S. H., Girgis, A. Y., Silvester, D. J., Nunn, A. D., and Lavender, P. J. (1976) Covalent attachment of metal chelates to proteins: The stability in vivo and in vitro of the conjugate of albumin with a chelate of 111-indium. *Proc. Natl. Acad. Sci. U.S.A.* 73, 3803.
- (21) Mikkelsen, K., and Nielsen, S. O. (1960) *J. Phys. Chem.* 64, 632.
- (22) DO3A = 1,4,7,10-tetraazacyclododecane-1,4,7-triacetic acid.
- (23) Meares, C. F., and Wensel, T. G. (1984) Metal Chelates as Probes of Biological Systems. *Acc. Chem. Res.* 17, 202.

Registry No. 2, 7598-70-1; 3, 128924-89-0; 4, 128924-90-3; L1, 128924-91-4; L2, 128924-92-5; ^{111}In , 15750-15-9; diethyl malonate, 510-20-3; *p*-nitrobenzyl bromide, 100-11-8; 1,4,7,10-tetraazadecane, 112-24-3.

Rapid Routes of Synthesis of Chemically Reactive and Highly Radioactively Labeled α - and β -Oligonucleotide Derivatives for in Vivo Studies

A. S. Boutorine,^{†,‡} T. Le Doan,^{*†} J. P. Battioni,[§] D. Mansuy,[§] D. Dupré,[§] and Claude Hélène[†]

Laboratoire de Biophysique, Muséum National d'Histoire Naturelle, 43 rue Cuvier, 75231 Paris Cedex 05, France, Institute of Bioorganic Chemistry, Siberian Division of the USSR Academy of Sciences, Lavrentyev Prosp. 8, 630090 Novosibirsk, U.S.S.R., and Laboratoire de Chimie et Biochimie Pharmacologique et Toxicologique, CNRS URA400 Université René Descartes, 45 rue des Saints-Pères, 75270 Paris Cedex 06, France.

Received July 17, 1990

Development of the antisense oligonucleotide strategy for the regulation of gene expression in vivo poses several problems: the stability of oligonucleotides toward intracellular nucleases, labeling of oligonucleotides with high specific radioactivity, improvements of penetration of oligonucleotides into living cells, and enhancement of antisense action by coupling of chemically active groups. In the present paper synthesis of highly radioactively labeled [³²P]- and [³⁵S]oligonucleotide derivatives is described starting from both natural (β) and nuclease-resistant (α) anomers of oligonucleotides. Conditions for preparative phosphorylation and thiophosphorylation suitable for oligonucleotides of various lengths, base composition, and anomeric forms were established. The stability of the phosphoramidate bond under in vivo experimental conditions was checked. The methods of terminal phosphate chemical activation and terminal thiophosphate alkylation were applied to synthesize oligonucleotides equipped with hydrophobic, intercalating, alkylating, and photoactivatable groups. In the case of porphyrin-oligonucleotide conjugates, a series of new monofunctional porphyrin derivatives bearing a free aliphatic amino group was developed.

INTRODUCTION

Synthetic oligonucleotides and their chemically reactive derivatives are widely used for sequence-specific artificial regulation of gene expression (for review see refs 1 and 2). The efficiency of antisense oligonucleotides to specifically inhibit gene expression has been demonstrated in various systems (3-10). However a large part of these studies was confined to in vitro experiments. Further extension of the antisense strategy to cell cultures or to animals encountered several problems which need to be solved before considering in vivo applications. These include the poor penetration of oligonucleotides into living cells (11, 12), their degradation in biological media (13), and difficulties in following their fate inside cells.

In order to make the oligonucleotides resistant to nucleases, several modifications of the phosphodiester backbone have been described (see ref 2 for a review). All these modifications (methylphosphonates, phosphotriesters, phosphorothioates, phosphoramidates, etc.) introduce a chirality at the phosphorus atom. To avoid this problem, oligonucleotides consisting of α -anomers of nucleotides instead of the natural β -anomers were synthesized (14, 15). However, all modified oligonucleotides developed until now, except oligophosphorothioates, do not exhibit efficient antisense activity because the complexes formed by the modified oligonucleotides with messenger RNAs are no longer substrates for ribonuclease H, which selectively cleaves RNA in the complexes and thereby blocks translation.

To solve these problems different chemical groups were attached to the oligonucleotide termini. Blocking of the

oligonucleotide ends improves their resistance to exonuclease attack. Double labeling of the oligonucleotides by attaching a highly radioactive phosphate or thiophosphate group at the 3'- or 5'-end followed by linkage of different chemical moieties yields highly radioactive materials that possess a better ability to cross cell membranes and are no longer sensitive to dephosphorylation by intracellular phosphatases (12, 13, 16, 17). Introduction of chemically reactive moieties into the oligonucleotides can help to increase the antisense effect of these molecules especially in the absence of RNase H activity. Oligonucleotide derivatives that exhibit such characteristics are particularly useful for cell uptake and intracellular compartmentation studies but also for biodistribution experiments in animals.

Several synthetic methods have been devised in the past to perform chemical modification of protected (12, 18) and nonprotected (16, 19-22) oligonucleotides. A very efficient method of derivatization in organic media was described for the synthesis of nonprotected oligonucleotides with attached liposoluble group (20). Another approach is based on reaction of thiophosphorylated oligonucleotides with bromoalkyl or iodoalkyl derivatives of chemically active molecules (23), thiophosphate group being introduced into oligonucleotides by chemical (18, 23) or enzymatic (24) means. Exchange reactions between thiols and disulfides can also be used for coupling of thiol- or disulfide-containing molecules.

In the present paper we have optimized conditions for the enzymatic preparation of radioactively labeled oligonucleotides including nuclease-resistant α -oligomers. We also investigated the conditions for the chemical synthesis of different derivatives starting from nonprotected oligonucleotides and checked the stability of the phosphoramidate bond under physiological conditions. On the basis of these studies we propose an easy-to-handle and versatile

* To whom correspondence should be addressed.

[†] Muséum National d'Histoire Naturelle.

[‡] Siberian Division of the USSR Academy of Sciences.

[§] CNRS URA400 Université René Descartes.

method of derivatization of oligonucleotides which could be applied to conventional but also to modified oligonucleotides, especially the nuclease-resistant α -oligomers. Covalent linkage of various chemical groups to the oligonucleotides was performed including hydrophobic (cholesterol), intercalating (acridine derivatives), alkylating, and photoactivable compounds such as porphyrins and azido derivatives.

EXPERIMENTAL PROCEDURES

Chemicals. Chemicals used in the present work were from Aldrich, Sigma, or Fluka; T4-polynucleotide kinase was from Ozyme, [γ - 32 P]ATP (110 TBq/mmol) and [35 S]-ATP- γ -S (22 TBq/mmol) were from Amersham, and cystamine chloride was from Merck. Dimethylformamide (DMF) and dimethyl sulfoxide (DMSO) were distilled under reduced pressure. Propionic acid, pyrrole, benzaldehyde, 4-carboxybenzaldehyde, 4-pyridine- or 3-pyridinecarboxyaldehyde, 1,6-diaminohexane, 1,8-diaminooctane, di-*tert*-butyl dicarbonate ([Boc] $_2$ O), and 1,1'-carbonyldiimidazole were commercially available and used without further purification. Mono-Boc-1,6-diaminohexane and -1,8-diaminooctane were prepared as previously described (25–28). (pT) $_{16}$ and T(pT) $_{15}$ were purchased from Pharmacia and the oligodeoxynucleotide HO-CACACCGACGGC was from Institut Pasteur. α - and β -anomers of octathymidylate T(pT) $_7$, the α -anomer of T(pT) $_{19}$, β -CACCACTTCTTCCACA (β -17-mer), and α -ACACCTTCTTCAACCAC (α -17-mer) were gifts of Dr. N. T. Thuong (Orléans, France). 4-[N-(2-chloroethyl)-N-methylamino]benzylmethylamine was obtained from Novosibirsk Institute of Bioorganic Chemistry (Novosibirsk, USSR). Azidoproflavine synthesis was described in ref 23.

Physical Measurements. UV-visible absorption spectra of porphyrins in CH $_2$ Cl $_2$ -CH $_3$ OH (96/4, v/v) solution and oligonucleotide-porphyrin conjugates in water were recorded in the 360–800-nm range on a Uvikon 820 (Kontron) spectrophotometer; λ_{\max} are given in nanometers and ϵ (in parentheses) are in mM $^{-1}$ cm $^{-1}$. 1 H NMR spectra for porphyrins were run at 20 °C, on a Bruker WM 250 spectrometer operating at 250 MHz; chemical shifts are reported in ppm downfield from Me $_4$ Si with J values in hertz. Mass spectrometry were recorded on a VG 70-250 double-focusing instrument equipped with a fast-bombardment gun operating at 7.5 kV and 1.2 mA.

Synthesis of Monofunctional Porphyrin. The starting porphyrins, (PhCOOH)(4-Py) $_3$ PH $_2$ (P1) and (PhCOOH)Ph $_3$ PH $_2$ (P4), were prepared according to the mixed-aldehyde method (28–30). A scheme of the porphyrin derivatives synthesis is presented in Figure 1.

5-[4-[[[8-(Boc-amino)octyl]amino]carbonyl]phenyl]-10,15,20-tris(4-pyridyl)porphyrin, (PhCONH-(CH $_2$) $_8$ NHCO $_2$ -*t*-C $_4$ H $_9$)(4-Py) $_3$ PH $_2$ (P2). (a) *Activation of the Carboxylic Acid.* A 50/50 (v/v) DMF-DMSO solution was used as the solvent. At 0 °C and under argon, a solution of 130 mg (0.2 mmol) of porphyrin P1 in 60 mL of solvent was added dropwise to 100 mg (0.6 mmol) of 1,1'-carbonyldiimidazole in 25 mL of solvent. The reaction mixture was stirred for 6 h, at this temperature.

(b) *Coupling with N-Boc-1,8-diaminooctane.* To this solution was added 250 mg (1 mmol) of *N*-Boc-1,8-diaminooctane dissolved in 60 mL of solvent, at 0 °C in 30 min. The solution was stirred overnight at room temperature. The solvent was removed and porphyrin P2 was purified on a SiO $_2$ chromatography column (CH $_2$ Cl $_2$ -CH $_3$ OH, 96/4, v/v). The solvent was removed and the crude product was dissolved in CH $_2$ Cl $_2$ and precipitated

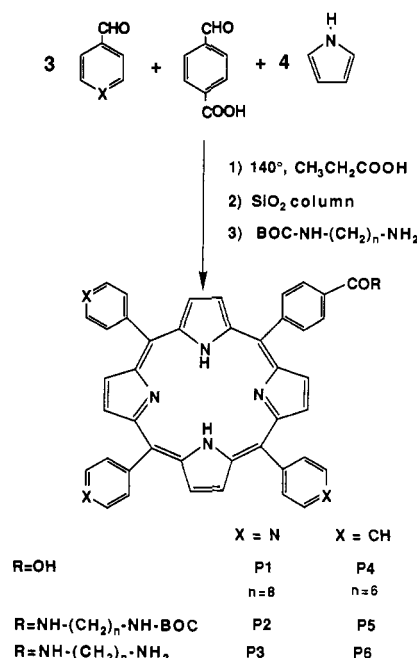


Figure 1. Scheme for the synthesis of porphyrin derivatives bearing free aliphatic amino groups.

by addition of an excess of diethyl ether. After filtration, the violet powder was dried in the oven at 70 °C (88 mg, 50% yield). MS: m/e = 888 (M^+ + 1), 813 (M^+ - O-*t*-C $_4$ H $_9$ - 1). UV-vis: 418 (370), 514 (18), 540 (6), 589 (6), 624 (3). 1 H NMR (DCCl $_3$): 9.03 (3,5-Py, 6 H, m), 8.83 (Pyr, 8 H, m), 8.26 (*o*-Ph, 2 H, d, J = 7.5), 8.16 (*m*-Ph, 2 H, d, J = 7.5), 8.13 (2,6-Py, 6 H, m), 6.48 (CONH, 1 H, t, J = 5.5), 4.52 (NHCO, 1 H, m), 3.62 ((CH $_2$) $_8$, 2 H, m), 3.12 ((CH $_2$) $_6$, 2 H, m), 1.8–1.5 ((CH $_2$) $_6$, 12 H, br m), 1.44 (*t*-C $_4$ H $_9$, 9 H, s), -2.90 (NH $_{\text{pyrr}}$, 2 H, s). Anal. Calcd for C $_{55}$ H $_{53}$ N $_9$ O $_3$ ·3H $_2$ O: C, 70.12; H, 6.31; N, 13.38. Found: C, 70.69; H, 6.49; N, 13.32.

5-[4-[[[8-(Boc-amino)octyl]amino]carbonyl]phenyl]-10,15,20-tris(4-pyridyl)porphyrin, (PhCONH-(CH $_2$) $_8$ NHCO $_2$ -*t*-C $_4$ H $_9$)(4-Py) $_3$ PH $_2$ (P3). To 85 mg (0.096 mmol) of porphyrin P2 in 5 mL of CH $_2$ Cl $_2$ and 10 mL of CH $_3$ OH was added 5 mL of concentrated HCl. After 2 h of stirring, the solution was neutralized by a CH $_2$ Cl $_2$ -CH $_3$ OH-concentrated NH $_4$ OH (60/30/10, v/v/v) solution and the ammonium salt was filtered. The solvents were removed, and the resulting powder was dissolved in a solution of CH $_2$ Cl $_2$ -CH $_3$ OH (90/10, v/v), from which the crude porphyrin was obtained by addition of diethyl ether. Purification on a SiO $_2$ chromatography column (CH $_2$ Cl $_2$ -CH $_3$ OH-concentrated NH $_4$ OH, 75/25/5, v/v/v), evaporation of solvents, and precipitation from CH $_2$ Cl $_2$ -CH $_3$ OH solution by addition of diethyl ether gave a violet powder which was dried under high vacuum (66 mg, 86% yield). MS: m/e = 788 (M^+ + 1, 95), 661 (M^+ for P $_1$, 100). UV-vis: 418 (350), 514 (16), 545 (5), 588 (5), 642 (3). 1 H NMR (DCCl $_3$): 8.94 (3,5-Py, 6 H, m), 8.78 (Pyr, 8 H, m), 8.20 (*o*-Ph, 2 H, d, J = 7.5), 8.13 (*m*-Ph + 2,6-Py, 8 H, br m), 7.36 (CONH, 1 H, t, J = 5), 3.53 ((CH $_2$) $_8$, 2 H, m), 2.89 ((CH $_2$) $_6$, 2 H, m), 1.71 ((CH $_2$) $_2$, 4 H, m), 1.38 ((CH $_2$) $_4$, 8 H, br m), -2.99 (NH $_{\text{pyrr}}$, 2 H, s).

5-[4-[[[6-(Boc-amino)hexyl]amino]carbonyl]phenyl]-10,15,20-triphenylporphyrin, (PhCONH-(CH $_2$) $_6$ NHCO $_2$ -*t*-C $_4$ H $_9$)Ph $_3$ PH $_2$ (P5). A procedure similar to the one used for porphyrin P2, starting with 216 mg (0.33 mmol) of porphyrin P4 and 165 mg (0.98 mmol) of 1,1'-carbonyldiimidazole and then 560 mg (2.6 mmol) of *N*-Boc-1,6-diaminohexane, gave 203 mg (72% yield) of porphy-

rin P5. MS: $m/e = 857$ ($M^+ + 1$). UV-vis: 417 (420), 516 (18), 550 (6), 590 (6), 645 (4). ^1H NMR (CD_2Cl_2 - CD_3OD): 8.83 and 8.79 (Pyr, 8 H, m), 8.27 (*o*-Ph-C, 2 H, d, $J = 7.5$), 8.15 (*m*-Ph-C, 2 H, d, $J = 7.5$), 8.10 (*o*-Ph, 6 H, m), 7.75 (*m*- and *p*-Ph, 9 H, m), 6.70 (CONH, 1 H, s), 4.58 (NH-Boc, 1 H, s), 3.61 ($(\text{CH}_2)_\alpha$, 2 H, m), 3.19 ($(\text{CH}_2)_\omega$, 2 H, m), 1.76 ($(\text{CH}_2)_2$, 4 H, m), 1.56 ($(\text{CH}_2)_2$, 4 H, m), 1.45 (*t*-C₄H₉, 9 H, s), -2.79 (NH_{pyrr}, 2 H, s). Anal. Calcd for C₅₆H₅₂N₆O₃: C, 78.48; H, 6.12; N, 9.81. Found: C, 77.89; H, 6.26; N, 9.34.

5-[4-[[6-Aminohexyl]amino]carbonyl]phenyl]-10,15,20-triphenylporphyrin, (PhCONH(CH₂)₆NH₂)-Ph₃PH₂ (P6). A procedure similar to the one used for porphyrin P3, starting from 85 mg (0.1 mmol) of porphyrin P5, gave 40 mg (51% yield) of porphyrin P6. UV-vis: 417 (400), 514 (16), 549 (7), 589 (5), 644 (3.5). ^1H NMR (CD_2Cl_2 - CD_3OD): 8.74 (Pyr, 8 H, m), 8.18 (*o*-Ph-C, 2 H, m), 8.14 (*o*-Ph and *m*-Ph-C, 8 H, br m), 7.70 (*m*-Ph and *p*-Ph, 9 H, br m), 6.74 (CONH, 1 H, s), 3.51 ($(\text{CH}_2)_\alpha$, 2 H, m), 3.2 ($(\text{CH}_2)_\omega$, 2 H, m), 1.73 ($(\text{CH}_2)_2$, 4 H, m), 1.48 ($(\text{CH}_2)_2$, 4 H, br m), -2.8 (NH_{pyrr}, s).

5-[N-(8-Bromooctyl)-3-pyridinio]-15-(N-methyl-3-pyridinio)-10,20-diphenylporphyrin Dichloride, [(N-(CH₂)₈Br-3-Py)(N-Me-3-Py)Ph₂PH₂]²⁺ Cl₂ (P7). This porphyrin derivative was prepared from 5,15-bis(3-pyridyl)-10,20-diphenylporphyrin (31) by successive alkylations with dibromooctane and methyl tosylate. The resulting dialkylated porphyrin was passed through an ion-exchange column (amberlite IRA 400, Cl⁻) to obtain chloride as a counterion (32).

Phosphorylation and Thiophosphorylation of Oligonucleotides. In analytical experiments the conditions of Maniatis et al. (33) were used except for an excess of [γ -³²P]ATP (50 pmol per 6 pmol of oligonucleotide). The yield of labeling was determined by analysis of a known quantity of labeled oligonucleotide by electrophoresis on denaturing 20% polyacrylamide gels followed by excision of the radioactive bands and liquid-scintillation counting in a LKB scintillation counter by Cherenkov effect (for ³²P) or liquid scintillation (for ³⁵S).

For preparative phosphorylation of 5'-nonphosphorylated oligonucleotides with simultaneous radioactive labeling, 30–500 μCi of [γ -³²P]ATP was dried and dissolved in 100 μL of a mixture containing 100–600 μg of 5'-OH-oligonucleotide and 30–40 units of T4-polynucleotide kinase in kinase buffer (0.01 M MgCl₂, 5 mM DTT, 0.1 mM spermidine, 0.1 mM EDTA, 0.05 M Tris HCl, pH 7.6). After 30 min of incubation at 37 °C, 4 μL of 0.1 M ATP and 40 units of T-4 polynucleotide kinase in 50 μL of kinase buffer were added, and the mixture was incubated at 37 °C for 1 h. The inactivation of kinase was achieved by adding EDTA (10 mM) and heating 3 min at 90 °C. Purification of the labeled oligomer was carried out by gel filtration on Sephadex G-25 in 0.01 M Tris HCl, pH 7.5–0.1 mM EDTA buffer, lyophilization, and precipitation by ethanol. For radioactive labeling of phosphorylated oligonucleotides, 30–500 μCi of [γ -³²P]ATP were dried and dissolved in 60 μL of a mixture containing 15–20 μg of 5'-P-oligonucleotide and 40 units of T4-polynucleotide kinase in exchange kinase buffer (0.01 M MgCl₂, 5 mM DTT, 0.1 mM spermidine, 0.1 mM EDTA, 0.05 M imidazole hydrochloride, pH 6.6) in the presence of 0.08 mM ADP. The mixture was incubated for 40 min at 37 °C, and then the same isolation procedure as described above was used.

Thiophosphorylation of 5'-OH-oligonucleotides was performed under the same conditions as phosphorylation except for the time of incubation. A mixture of 50–150 pmol of [³⁵S]ATP- γ -S, 10–40 nmol of oligonucle-

otide, and 40 units of T4-polynucleotide kinase was incubated in the kinase buffer at 37 °C during 3 h. Nonradioactive ATP- γ -S (4 μmol) and 40 units of polynucleotide kinase in kinase buffer were added, and the mixture was incubated for 8 h at 37 °C. The isolation procedure was as described above.

Chemical Derivatization of Oligonucleotides. Coupling of amino-containing compounds to the activated 5'-phosphate of oligonucleotides was performed by the method of Godovikova et al. (20). A 50–200- μg portion of oligonucleotide was dissolved in 25 μL of water and precipitated by 2–5 μL of 8% cetyltrimethylammonium bromide. The precipitate was dried in vacuo and redissolved in dry dimethyl sulfoxide with 0.3 M dipyrilidyl disulfide, 0.3 M triphenylphosphine, and 0.5 M *N*-methylimidazole (total volume 100 μL). After 15 min of incubation, 3–5 mg of amine compound in the form of free amine was added and the mixture was incubated at room temperature for 20 min. The product was precipitated by 3% LiClO₄. For coupling of porphyrins the method was modified. After conversion of phosphate into a *N*-methylimidazole derivative, 2 μL of triethylamine and 0.5–1 mg of porphyrin derivative were added, and the mixture was heated at 60 °C during 2 h. Then a mixture of chloroform–0.1% SDS in water was added and the oligonucleotide derivative was isolated by successive extractions with water, 0.3 M LiClO₄–0.1% Triton X-100 (1:1 v/v), and 0.05% tetraphenylboron. The water phase was recovered; the oligonucleotide–porphyrin conjugate was precipitated with acetone and purified by electrophoresis in 20% denaturing acrylamide gel, followed by excision of the colored band and extraction or electroelution of the derivative.

Cystamine derivatives of oligonucleotides were reduced by 0.7 M DTT, which was then removed by several ethanol precipitations. Synthesis of radioactive 3-amino-6-[(ω -bromoalkyl)amino]proflavine derivatives and coupling of bromoalkyl derivatives to SH-containing or thiophosphorylated oligonucleotides was carried out as described earlier (23).

For synthesis of the cholesterol derivative, 3-thiocholesterol was used. It was reacted during 1 h at 37 °C in pyridine solution with excess of dipyrilidyl disulfide; the product was precipitated by DMSO, dissolved in pyridine, and left overnight to react with the cetyltrimethylammonium salt of the oligonucleotide–cysteamine derivative. All the products were purified by HPLC on a L5C-18-25R column (Interchim, France) in an acetonitrile gradient. Proflavine, azidophenacyl, and 4-[[N-(2-chloroethyl)-*N*-methylamino]benzyl]phosphamido derivatives were eluted by 12–15% CH₃CN; cholesterol and porphyrin derivatives were eluted by 80% and 60% CH₃CN, respectively.

Coupling by direct alkylation of the terminal SH group of a modified oligonucleotide by 3-iodocholesterol was also used following previously published procedures (24).

RESULTS AND DISCUSSION

Methods for coupling reagents to the oligonucleotide ends are mainly based on the activation of the 5'-terminal phosphate. So, the first problem to solve was preparative phosphorylation of oligonucleotides with simultaneous radioactive labeling. Solid-phase automatic synthesis of oligonucleotides yields 5'-nonphosphorylated molecules. Methods for introducing radioactive [³²P]-phosphate or [³⁵S]thiophosphate with T4 polynucleotide kinase catalyzed reaction has been described (24, 33). In the present work we studied the kinetics and the yield of the phosphorylation and thiophosphorylation reactions

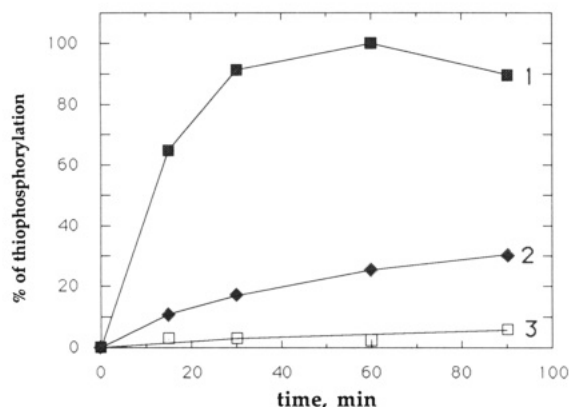


Figure 2. Kinetics of thiophosphorylation of oligonucleotides [(1) β -T(pT)₁₅, (2) β -17-mer, (3) α -17-mer] in standard conditions in 20 μ L of solution. Concentrations are as follows: 0.25×10^{-6} M [35 S]-ATP- γ -S, 0.20×10^{-6} M oligonucleotide, 0.75 units/ μ L kinase.

Table I. Yield of Phosphorylation and Thiophosphorylation of Oligonucleotides under Standard Conditions at the Reaction Plateau^a

oligonucleotide	label	% phosphorylation at plateau
β -T(pT) ₇	³² P	69
α -T(pT) ₇	³² P	50
β -17-mer	³² P	100
α -17-mer	³² P	57
β -T(pT) ₁₅	³² P	100
α -T(pT) ₁₉	³² P	60
β -17-mer	³⁵ S	30
α -17-mer	³⁵ S	5.8
β -T(pT) ₁₅	³⁵ S	100
α -T(pT) ₁₉	³⁵ S	0.9

^a Concentrations were as follows: 0.75 units/mL kinase, 0.2×10^{-6} M oligonucleotides, 0.5×10^{-6} M ATP.

as a function of the length, base composition, and α - or β -anomeric configuration under the standard conditions described by Maniatis et al. (33). Results are presented in Figure 2 and Table I. It is seen that (i) longer oligonucleotides are phosphorylated better, (ii) the yield of phosphorylation and thiophosphorylation is not identical for oligonucleotides with different base composition, (iii) thiophosphorylation of oligonucleotides proceeds much more slowly than phosphorylation, and (iv) reactions are not always quantitative under standard conditions. The most dramatic difference was between α - and β -anomers. The nonnatural α -oligonucleotides were phosphorylated not more than 60% and their thiophosphorylation was too low to be considered as a preparative method.

We have studied the effect of changing the concentrations of the reaction components on the kinetics and yield of the reaction and found that it is possible to increase the plateau level of reactions by raising the concentration of oligonucleotides, ATP, and kinase. The most pronounced effect of kinase concentration on thiophosphorylation of β -17-mer is shown in Figure 3. At high excess of ATP (50 times) and high concentration of substrates (10^{-4} – 10^{-3} M) complete phosphorylation of α -oligonucleotides can be achieved.

We elaborated a two-step method for preparative phosphorylation of both α - and β -oligonucleotides (see the Experimental Procedures). During the first step the effect of high oligonucleotide and polynucleotide kinase concentration was used to introduce radioactive phosphate, specific radioactivity depending only on the quantity and activity of [γ -³²P]ATP. Gel filtration of the sample on Sephadex G50 (Figure 4) showed that almost 90% of

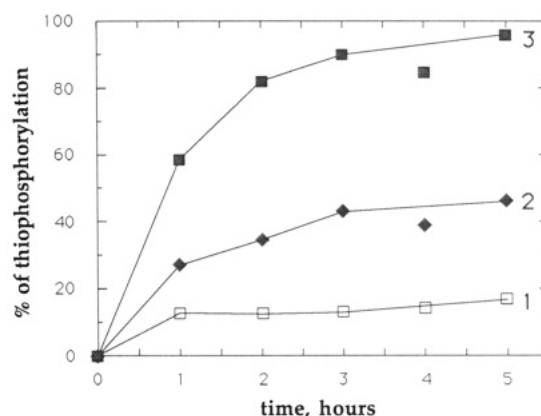


Figure 3. Effect of kinase concentration on thiophosphorylation of β -17-mer in 20 μ L of buffer. Concentrations are as follows: 0.25×10^{-6} M [35 S]ATP- γ -S; 0.20×10^{-6} M oligonucleotide; (1) 0.75 units/ μ L, (2) 1.25 units/ μ L, (3) 1.75 units/ μ L kinase.

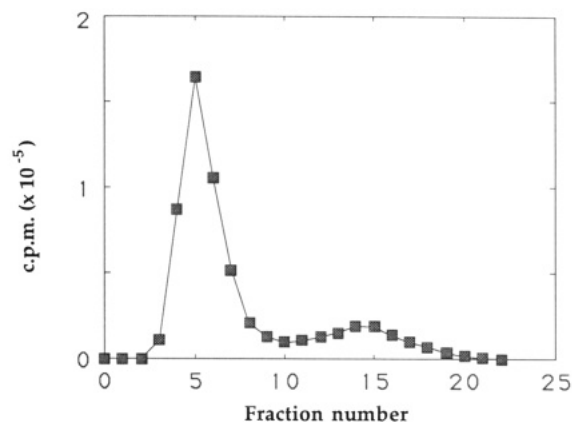


Figure 4. Gel filtration of phosphorylated β -T(pT)₁₅ on Sephadex G-50 in 0.01 M Tris HCl, pH 7.6–0.1 mM EDTA on a 0.6×10 cm column.

radioactive phosphate was incorporated into the oligonucleotide. During the second step a high excess of "cold" ATP and additional kinase were added to phosphorylate all the remaining 5'-OH groups. Complete phosphorylation of oligonucleotide was checked by HPLC and gel electrophoresis (data not shown).

We performed similar kinetic studies of phosphate exchange reaction catalyzed by T4-polynucleotide kinase (33) and found that by using concentrations of oligonucleotides 80–100 times higher and concentrations of ADP 3–4 times lower than under standard conditions more than 80% radioactive phosphate could be incorporated into the oligonucleotide (see the Experimental Procedures).

Similar results were obtained in the preparative thiophosphorylation of β -oligonucleotides by ATP- γ -S. The only difference was the time of incubation (3 h for the first step and 8 h for the second). Enzymatic incorporation of thiophosphate into α -oligonucleotides gave a very poor yield, even with high concentrations of the reactants and addition of successive amounts of kinase. For these reasons we used an alternative method to introduce SH groups into α -oligomers (see below).

In the following experiments we used preparations of ³²P- and ³⁵S-labeled oligonucleotides with a specific activity of up to several TBq/mmol, but this specific radioactivity was not an upper limit because its value depends on the ratio of oligonucleotide and radioactive ATP put into the reaction mixture.

The next step was to elaborate a simple and easy method for coupling of chemical reagents to the nonprotected oli-

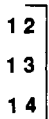
gonucleotides. Thiophosphorylation of oligonucleotides opened a way to couple bromoalkyl or iodoalkyl derivatives of chemically active substances according to ref 23. For coupling of nucleophilic (e.g. amino group containing) compounds, we have chosen a method based on the activation of terminal phosphate in organic solutions (20). This method allowed us to work both with water-soluble and organic-soluble substances. In addition, coupling of a chemical moiety to a terminal phosphate protected the oligonucleotide against the action of intracellular phosphatases.

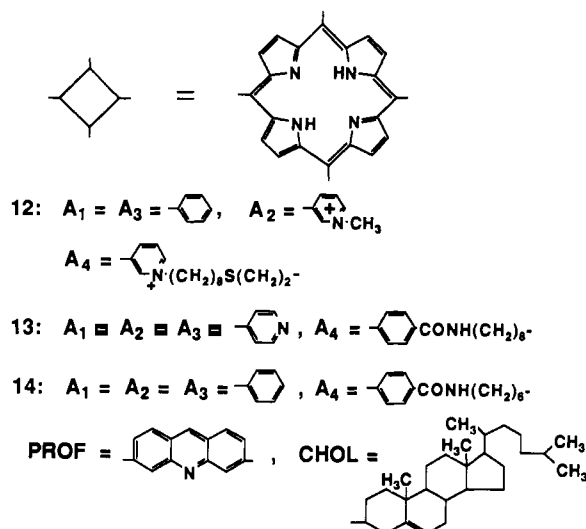
Table II represents a set of radioactive oligonucleotide conjugates synthesized from nonprotected α - and β -anomers of oligonucleotides, listed in the Experimental Procedures. Among them we would like to draw attention to the porphyrin derivatives of oligonucleotides. These derivatives have been shown to be efficient reagents for nucleic acid modification by either chemical or photochemical activation (34–36). Moreover their lipophilic character makes them good candidates for cell-penetration studies. To apply the method of 5'-phosphate activation for coupling of a porphyrin moiety, a series of new monofunctional porphyrin derivatives bearing a free aliphatic amino group was developed. Porphyrins P3 and P6 were prepared via coupling reaction between *N*-mono-Boc- α,ω -diaminoalkane and the corresponding porphyrins P1 and P3, followed by the cleavage of the protecting group. Porphyrins P1 and P3 were obtained according to the mixed-aldehyde method (28–30) (see Figure 1). All the spectral data (especially ^1H NMR) of porphyrins P1–P6 (which all gave only one spot in TLC) were in good agreement with the structures assigned.

Extrapolation of the technique to amino-containing porphyrin derivatives faced the problems of yield and product isolation (the conjugate was coprecipitated by water with free porphyrin in attempts to isolate it). Longer time and higher temperatures of incubation helped to increase the yield, and an isolation procedure based on successive extractions by a mixture of chloroform and a water-SDS solution allowed 80–90% extraction of the derivative in the water phase. We used preparative gel electrophoresis for final purification followed by extraction of the product from the gel or electroelution. The conjugate was characterized by retardation of the band compared to the original oligonucleotide in gel electrophoresis, the yellow color of the product, the characteristic red fluorescence of the band under UV-light irradiation, the solubility of the product in water, and the UV-visible spectra of the derivatives (Figure 5). The stoichiometry of the oligonucleotide-porphyrin conjugate was estimated to be 1/1 (molar ratio) from absorption bands of the porphyrin at 420 nm and of the oligonucleotide part at 260 nm.

The coupling of cystamine to 5'-phosphate of oligonucleotides followed by reduction of the S–S bond by DTT represented an alternative method for the introduction of SH groups into oligonucleotides radioactively labeled with ^{32}P . This method also allowed us to synthesize SH derivatives of nonprotected α -oligonucleotides which could not be directly thiophosphorylated by polynucleotide kinase, as mentioned above. In such a way we could also perform alkylation by bromo- or iodoalkyl derivatives or use the SS–SH exchange to attach proflavin, photoactive aromatic azido compounds, cholesterol, and alkylating reagents. Reaction of cysteamide oligonucleotide derivative with 5-[*N*-(8-bromooctyl)-3-pyridinio]-15-(*N*-methyl-3-pyridinio)-10,20-diphenylporphyrin yielded another radioactive porphyrin derivative of an oligonucleotide that could be easily synthesized from nonpro-

Table II. List of Oligonucleotide Derivatives Synthesized for in Vitro and in Vivo Applications

1	$\text{CH}_3\text{CH}_2\text{CH}_2\text{CH}_2\text{NH}-\boxed{^{32}\text{P}}\text{O}_2\text{O}-\text{Nu}(\text{pNu})_n$	q
2	$\text{H}_2\text{N}(\text{CH}_2)_m\text{NH}-\boxed{^{32}\text{P}}\text{O}_2\text{O}-\text{Nu}(\text{pNu})_n$	q
3	$\text{HO}(\text{CH}_2)_m\text{NH}-\boxed{^{32}\text{P}}\text{O}_2\text{O}-\text{Nu}(\text{pNu})_n$	q
4	$\text{HS}(\text{CH}_2)_2\text{NH}-\boxed{^{32}\text{P}}\text{O}_2\text{O}-\text{Nu}(\text{pNu})_n$	q
5	$\text{N}_3-\text{C}_6\text{H}_4-\text{COCH}_2\text{S}(\text{CH}_2)_2\text{NH}-\boxed{^{32}\text{P}}\text{O}_2\text{O}-\text{Nu}(\text{pNu})_n$	q
6	$\text{N}_3-\text{C}_6\text{H}_4-\text{COCH}_2-\boxed{^{35}\text{S}}\text{PO}_2\text{O}-\text{Nu}(\text{pNu})_n$	80%
7	$\text{N}_3\text{-PROF-NH}(\text{CH}_2)_3\text{S}(\text{CH}_2)_2\text{NH}-\boxed{^{32}\text{P}}\text{O}_2\text{O}-\text{Nu}(\text{pNu})_n$	37%
8	$\text{N}_3\text{-PROF-NH}(\text{CH}_2)_3-\boxed{^{35}\text{S}}\text{PO}_2\text{O}-\text{Nu}(\text{pNu})_n$	30%
9	$\text{CHOL-SS}(\text{CH}_2)_2\text{NH}-\boxed{^{32}\text{P}}\text{O}_2\text{O}-\text{Nu}(\text{pNu})_n$	58%
10	$\text{CHOL-S}(\text{CH}_2)_2\text{NH}-\boxed{^{32}\text{P}}\text{O}_2\text{O}-\text{Nu}(\text{pNu})_n$	20%
11	$\text{Cl}(\text{CH}_2)_2\text{N}(\text{CH}_3)-\text{C}_6\text{H}_4-\text{CH}_2\text{NH}-\boxed{^{32}\text{P}}\text{O}_2\text{O}-\text{Nu}(\text{pNu})_n$	80%
12		15–22%
13		
14		
15		



^a Derivatives 1–5, 7, and 9–14 were synthesized starting from α - and β -oligonucleotides, products 6 and 8 only were from β -oligonucleotides. The yield of product is indicated; q = quantitative yield (no initial material was found by electrophoresis). Derivatives 1–3 could be used as phosphatase-protected oligonucleotide analogues and for further synthesis. Derivative 4 was used for coupling alkylating and thiol-containing molecules. Derivatives 5–8 and 12–14 could be used for photochemical modification, 11 could be used for chemical modification and 12–14 could be used for metal-catalyzed modification of biopolymers in vivo and in vitro. All of them could be suitable for cell-penetration studies. The radioactive label is boxed.

tected oligonucleotides. All the derivatives were characterized by HPLC, gel electrophoresis, and UV spectroscopy.

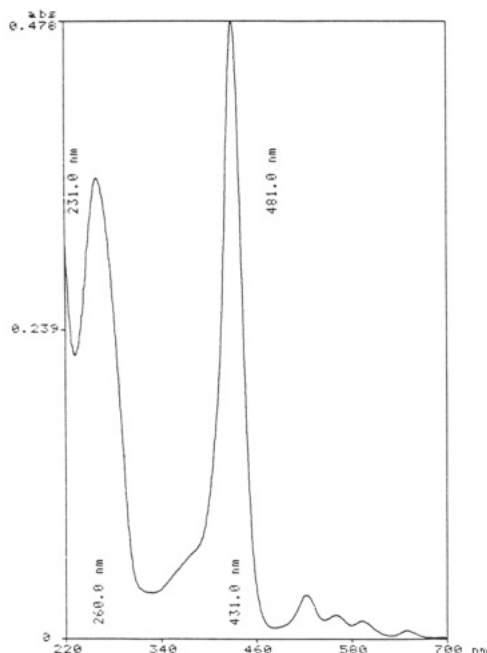


Figure 5. UV-visible spectrum of oligonucleotide-porphyrin conjugate $\text{PH}_2\text{Ph}_3\text{PhCONH}(\text{CH}_2)_6\text{NH-pT}(\text{pT})_{15}$ (Table II, 14) in aqueous solution.

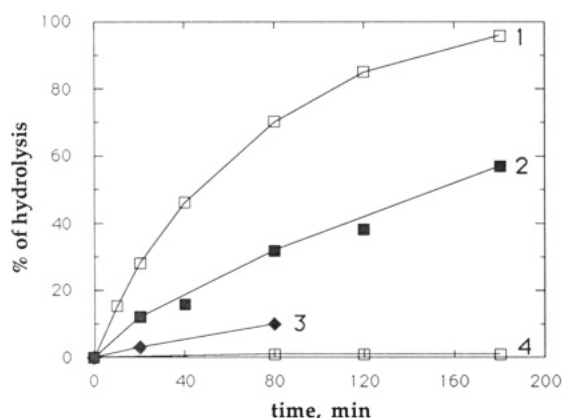


Figure 6. Kinetics of phosphamide bond hydrolysis in acidic solutions at 37 °C. Curves 1-4 correspond to pH values 1-4.

Working with a large majority of the reagents described above requires some cautions. For example, cysteamide derivative 4 (Table II) exhibited a tendency to dimerize due to oxidation by air. All the experiments should be done in degassed or helium-saturated solutions. The high reactivity of photoactive reagents 5-8 and 12-14 necessitates working in the dark. The absorption band at $\lambda = 427$ nm of reagent 12 was considerably diminished when the reagent was manipulated under daylight or luminescent light. Alkylating reagent 11 had to be used quickly or kept at very low temperature because even in the precipitated state at -20 °C it showed a pronounced tendency toward self-alkylation (13).

Finally we have studied the stability of phosphamide bond in the conditions used for in vivo and in vitro experiments including incubation in the culture medium, phenol extraction, heating up to 100 °C, and pH shift. No cleavage of phosphamide bonds was observed under these conditions except at low pH, but as it is seen from Figure 6, only very acidic pH led to significant hydrolysis of this bond. This pH never exists in living cells, but the acid hydrolysis of the bond could be useful to regenerate oligonucleotides, to remove the oligonucleotide in vitro from

the modified site, and to provide evidence for chemical modification and not metabolism of the reagent.

ACKNOWLEDGMENT

We gratefully thank Drs. V. P. Starostin and T. M. Ivanova for synthesis of alkylating reagent, Drs. N. T. Thuong and U. Asseline for synthesis of α -oligonucleotides, and Drs. J. L. Decout, N. Habboub, and J. Lhomme for the synthesis of azidoproflavine. A. S. Boutorine was supported by Institut National de la Santé et de la Recherche Médicale (France).

LITERATURE CITED

- (1) Knorre, D. G., and Vlassov, V. V. (1985) *Prog. Nucleic Acids Res. Mol. Biol.* 32, 291-322.
- (2) Toulmé, J. J., and Hélène, C. (1988) *Gene* 72, 51-58.
- (3) Kulka, M., Smith, C. C., Aurelian, L., Fischelevich, R., Meade, K., Miller, P., and Tso, P. O. P. (1989) *Proc. Natl. Acad. Sci. U.S.A.* 86, 6868-6872.
- (4) Letsinger, R. L., Zhang, G., Sun, D. K., Ikeuchi, T., and Sarin, P. S. (1989) *Proc. Natl. Acad. Sci. U.S.A.* 86, 6553-6556.
- (5) Goodchild, J., Agrawal, S., Civiera, M. P., Sarin, P. S., Sun, D., and Zamecnik, P. C. (1988) *Proc. Natl. Acad. Sci. U.S.A.* 85, 5507-5511.
- (6) Wickström, E. L., Bacon, T. A., Gonzalez, A., Freeman, D. L., Lyman, G. H., and Wickström, E. (1988) *Proc. Natl. Acad. Sci. U.S.A.* 85, 1028-1032.
- (7) Zerial, A., Thuong, N. T., and Hélène, C. (1987) *Nucleic Acids Res.* 15, 9909-9919.
- (8) Verspieren, P., Cornelissen, A. W. C. A., Thuong, N. T., Hélène, C., and Toulmé, J. J. (1987) *Gene* 61, 307-315.
- (9) Cazenave, C., Stein, C. A., Loreau, N., Thuong, N. T., Neckers, L. M., Subasinghe, C., Hélène, C., Cohen, J. S., and Toulmé, J. J. (1989) *Nucleic Acids Res.* 17, 4255-4273.
- (10) Leonetti, J. P., Machy, P., Degols, G., Lebleu, B., and Leserman, L. (1990) *Proc. Natl. Acad. Sci. U.S.A.* 87, 2448-2451.
- (11) Abramova, T. V., Lebedev, A. V., and Rytte, A. S. (1988) *Mol. Biol. (USSR)* 22, 1285-1292.
- (12) Boutorin, A. S., Guskova, L. V., Ivanova, E. M., Kobetz, N. D., Zarytova, V. F., Rytte, A. S., Yurchenko, L. V., and Vlassov, V. V. (1989) *FEBS Lett.* 254, 129-132.
- (13) Babkin, I. V., Boutorin, A. S., Ivanova, E. M., and Rytte, A. S. (1988) *Biokhimiya* 53, 384-393.
- (14) Morvan, F., Rayner, B., Imbach, J. L., Chang, D. K., and Lown, J. W. (1986) *Nucleic Acids Res.* 14, 5019-5035.
- (15) Thuong, N. T., Asseline, U., Roig, V., Takasugi, M., and Hélène, C. (1987) *Proc. Natl. Acad. Sci. U.S.A.* 84, 5129-5133.
- (16) Lemaitre, M., Bayard, B., and Lebleu, B. (1987) *Proc. Natl. Acad. Sci. U.S.A.* 84, 648-652.
- (17) Stevenson, M., and Iversen, P. L. (1989) *J. Gen. Virol.* 70, 2673-2682.
- (18) Asseline, U., and Thuong, N. T. (1989) *Tetrahedron Lett.* 30, 2521-2524.
- (19) Chu, B. C. F., Wahl, G. W., and Orgell, L. E. (1983) *Nucleic Acids Res.* 11, 6513-6529.
- (20) Godovikova, T. S., Zarytova, V. F., and Khalimskaya, L. M. (1986) *Bioorg. Khim.* 12, 475-481.
- (21) Fedorova, O. S., Savitskii, A. P., Shoikhet, K. G., and Ponomarev, G. V. (1990) *FEBS Lett.* 259, 335-337.
- (22) Teare, J., and Wollenzein, P. (1989) *Nucleic Acids Res.* 17, 3359-3372.
- (23) Praseuth, D., Le Doan, T., Chassignol, M., Decout, J. L., Habboub, N., Lhomme, J., Thuong, N. T., and Hélène, C. (1988) *Biochemistry* 27, 3031-3038.
- (24) Oshevsky, S. I. (1982) *FEBS Lett.* 143, 119-123.
- (25) Callahan, J. F., Ashton-Shue, D., Bruyan, H. G., Bryan, W. M., Heckman, G. D., Kinter, L. B., McDonald, J. E., Moore, M. L., Schmidt, D. B., Silvestri, J. S., Stassen, F. L., Sulat, L., Yim, N. C. F., and Huffman, W. F. (1989) *J. Med. Chem.* 32, 391-396.
- (26) Hansen, J. B., Nielsen, M. C., Ehrbar, U., and Buchardt, O. (1982) *Synthesis* 404-405.
- (27) Stahl, G. L., Walter, R., and Smith, C. W. (1978) *J. Org. Chem.* 43, 2285-2286.

- (28) Little, R. G., Anton, J. A., Loach, P. A., and Ibers, J. A. (1975) *J. Heterocycl. Chem.* **12**, 343-349.
- (29) Anton, J. A., Kwong, J., and Loach, P. A. (1976) *J. Heterocycl. Chem.* **13**, 717-725.
- (30) Schmidt, D., and Steffen, H. (1984) Eur. Pat. 127, 797; *Chem. Abstr.* (1985) **102**, 109374a.
- (31) Sari, M. A., Battioni, J. P., Dupré, D., Mansuy, D., and Le Pecq, J. B. (1990) *Biochemistry* **29**, 4205-4215.
- (32) Sari, M. A. (1988) Thèse de Doctorat de l'Université Pierre et Marie Curie Paris 6, Paris, France.
- (33) Maniatis, T., Fritsch, E. F., and Sambrook, J. (1982) *Molecular Cloning. A Laboratory Manual*, Cold Spring University Press, Cold Spring Harbor.
- (34) Le Doan, T., Perrouault, L., Hélène, C., Chassignol, M., and Thuong, N. T. (1986) *Biochemistry* **25**, 6736-6739.
- (35) Le Doan, T., Perrouault, L., Chassignol, M., Thuong, N. T., and Hélène, C. (1987) *Nucleic Acids Res.* **15**, 8643-8659.
- (36) Le Doan, T., Praseuth, D., Perrouault, L., Chassignol, M., Thuong, N. T., and Hélène, C. (1990) *Bioconjugate Chem.* **1**, 108-113.

N-Terminal Modification of Immunoglobulin Polypeptide Chains Tagged with Isothiocyanato Chelates

Tariq M. Rana and Claude F. Meares*

Chemistry Department, University of California, Davis, California 95616. Received July 25, 1990

Conjugates of monoclonal antibodies with drugs, toxins, radionuclides, and other agents are in widespread use in therapeutic trials and as clinical research tools. The characterization of these immunoconjugates generally does not include determining the individual sites at which such agents are attached. We have begun to explore the attachment of the bifunctional chelating agent isothiocyanatobenzyl-EDTA (CITC¹) to the N-termini of the light chains of the Lym-1 monoclonal antibody. The similarity between this bifunctional chelating agent and Edman's reagent, phenyl isothiocyanate, led us to develop methods to distinguish between chelate-conjugated α -amino groups and ϵ -amino groups by Edman degradation. Practically all the N-terminal Asp α -NH₂ groups of Lym-1 can be modified at neutral pH, while attachment at lysine side chains predominates at pH 9. Comparison of the immunoreactivities of Lym-1-CITC conjugates with and without N-terminal conjugation shows that both are almost fully active. This implies that modification of light-chain N-termini has little or no effect on immunoreactivity, despite the fact that these residues lie near the antigen-binding sites.

Monoclonal antibody technology allows the specificity of an antibody for its antigen to be used in targeting cancer cells. Radiolabeled monoclonal antibodies (mAbs) have shown considerable promise for the early detection and therapy of cancer (1-3). As the clinical use of radiolabeled monoclonal antibodies proceeds, relatively few antibodies have been found to be useful in vivo for both diagnosis and therapy of human patients. In order to make these work better, we need improved understanding of the conjugation chemistry of immunoglobulin molecules.

With the notable exception of Rodwell and co-workers (4), most researchers in this area have used reagents that react principally with lysine residues on antibodies. In fact, very little data is available exploring the relationship between sites of conjugation and biological activity of antibodies (other than iodination of tyrosine (5)). Since antibodies and their conjugates with drugs, toxins, radionuclides, and other useful agents are in widespread use as clinical research tools and in therapeutic trials, many of these approaches might benefit from experimenters knowing which sites on the peptide chains of the antibody can be modified successfully.

The antibodies of primary interest to us are mouse immunoglobulin G (IgG) molecules, which have two pairs of polypeptide chains (light and heavy), with a total molecular weight of approximately 150K. The overall shape of an IgG molecule resembles a T or a Y (6), with the N-termini of the four polypeptide chains located near the antigen-binding sites. While the particular amino acids in the six hypervariable loops comprising the antigen-binding sites vary with antigen specificity, most of the residues in the light and heavy chains do not change from one antibody to another. Thus, the chemical properties of one IgG should provide a useful guide to others.

The reactive groups we consider here are NH₂ groups

located at lysine side chains and at the polypeptide chain termini (the α -amino groups of polypeptide chains react with the same reagents as lysine ϵ -amino groups). Mouse IgG2a mAb Lym-1 contains 30 lysines in each of its γ 2a heavy chains and 13 lysines in each of its κ V light chains, for a total of 86 lysines in the molecule (7). The lysines are distributed throughout the light and heavy chains of the antibody. In mouse immunoglobulins 95% of the expressed light chains are of the κ type, and 80% of these contain Asp as the N-terminal residue (8, 9). The vast majority of subgroup κ V light chains (95%) have Asp as their N-terminal residue (9). Light chains of Lym-1 also showed Asp as their N-terminal residue during sequence analysis (Table II).

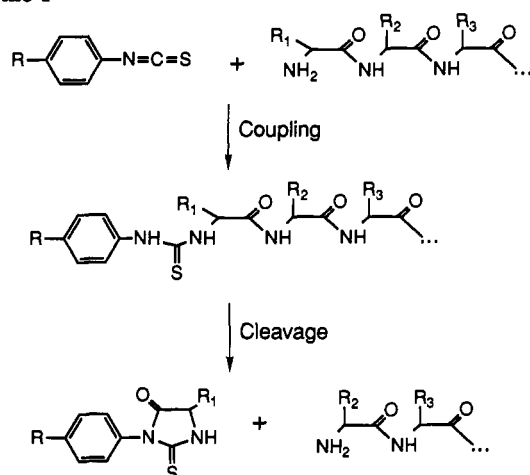
Heavy chains of Lym-1 have Gln as the N-terminal residue and showed no sequence during automated Edman sequence analyses. The primary structural analyses of many naturally occurring proteins and peptides including gastrin, fibrinopeptides, collagen, and immunoglobulins have been hindered by the presence of pyrrolidonecarboxylic acid (pyroglutamic acid) as an amino terminal residue (10, and references therein). It is believed that cyclization of terminal glutaminyl or glutamyl residues leads to the formation of pyroglutamic acid. Sanger and Thompson (11) observed the spontaneous formation of pyroglutamyl peptides during the isolation and proteolysis of peptides containing glutamine as N-terminal residues. Since the automated Edman sequence analysis depends on the availability of an α -amino group, the proteins beginning with pyroglutamic acid pose problems in their direct sequencing.

Because the NH₂ termini of the Lym-1 heavy chains are blocked, the only α -amino groups available for conjugation are on the light chains.

The usual strategy with monoclonal antibodies is to seek labeling conditions that will not block the antigen-binding sites. Because an IgG antibody molecule contains so many lysine residues, and because the great majority of these are not found in the antigen-binding sites (82/86 for Lym-1), lysine ϵ -amino groups are usually considered good targets.

¹ Abbreviations: *t*-Boc, *tert*-butoxycarbonyl; CAPS, 3-(cyclohexylamino)-1-propanesulfonic acid; CITC, isothiocyanatobenzyl-EDTA; DNFB, 2,4-dinitrofluorobenzene; DNP, dinitrophenyl; mAb, monoclonal antibody; MCA, 7-amino-4-methylcoumarin; PTH, phenylthiohydantoin.

Scheme I



1. PTH-amino acids (R = H)
2. CITC-Gly (R = CH₂EDTA, R₁ = H)
3. CITC-Asp (R = CH₂EDTA, R₁ = CH₂COOH)

To a first approximation, it might be expected that chemistry directed toward a particular residue such as lysine would produce a statistical mixture of products (12). For example, if all lysines were equally reactive, then modifying one of the 86 lysines in Lym-1 would involve a lysine in an antigen-binding site with a probability of only 4/86, or 4.6%. Assuming that any hit in an antigen-binding site inactivates the antibody, but any other hit has no effect, this would produce a conjugate with about 95% of its original immunoreactivity.

We have frequently observed results contrary to that simple expectation. Conjugation yields and immunoreactivity of conjugates vary with reaction conditions in complex ways that depend strongly on the pH of the reaction, among other factors (13, 14). Since the pK_a of α-amino groups is 7.6–8, while the pK_a of ε-amino groups is 9.3–9.5, and since it is the unprotonated RNH₂ groups that react with electrophilic reagents (15), one possibility to be investigated is whether conjugation of the α-amino groups with bifunctional chelating agents affects antigen binding. This is particularly interesting, since these α-amino groups lie within ~10 Å of the antigen-binding sites (16).

Typical conjugation reactions in our laboratory involve addition of isothiocyanatobenzyl-EDTA (CITC) to an antibody (17). The similarity between this bifunctional chelating agent and Edman's reagent, phenyl isothiocyanate (Scheme I), suggested to us that we could distinguish between chelate-conjugated α-amino groups and ε-amino groups by Edman degradation. The literature contains numerous examples of the use of analogues of phenyl isothiocyanate bearing fluorescent tags for protein microsequencing (e.g. 18–22). Here, we report experiments demonstrating how a chelate isothiocyanate can reveal N-terminal conjugation and some of the properties of such conjugates.

EXPERIMENTAL PROCEDURES

Chemicals. Diglycine, triglycine, and Asp-Ala peptides were purchased from Sigma Chemical Co. The peptide *t*-Boc-Gly-Lys-Arg-MCA was purchased from Peptides International. Bromophenol blue and 2,4-dinitrofluorobenzene (DNFB) were purchased from Aldrich. Lym-1, an anti B cell lymphoma IgG_{2a} mAb (23), was obtained from Damon Biotech (Needham Heights, MA; Encapcel murine mAb, lot # 3-171-860813). It was further purified

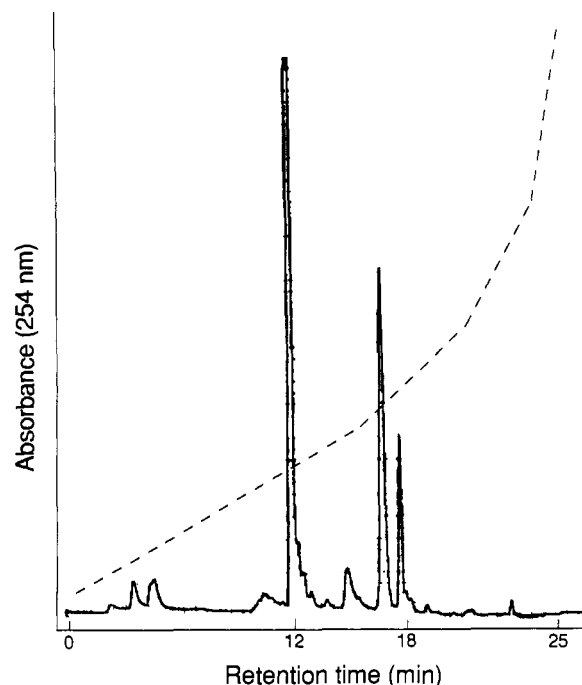


Figure 1. HPLC profile of the products of Edman degradation of CITC-triglycine, after treatment with DNFB. Retention times of authentic compounds are indicated: DNP-diglycine, 12 min; DNFB, 18 min. The peak at 17 min is presumably the CITC-Gly Edman product. The shape of the solvent gradient is indicated by the dashed line; see Experimental Procedures for details.

by protein A affinity column chromatography prior to use. Protein A on Sepharose-CL-4B, NaDodSO₄, Tris, CAPS, and Coomassie Blue R-250 were obtained from Sigma Chemical Co. PVDF membranes (Immobilon transfer), 0.45 μm pore size, were obtained from Millipore. Cobalt-57 chloride was purchased from ICN (specific activity 7000 Ci/g). Pure water (resistance 18 MΩ, NANOpure II, Barnstead, MA) was used throughout the experiments. All glass labware was washed with a mixed acid solution and thoroughly rinsed with pure water (24). All plastic labware was washed with 3 M HCl and thoroughly rinsed. All other chemicals were the purest grade available.

Thin-Layer Chromatography. TLC was run on plastic-backed silica gel plates (EM Science) using a solution composed of equal volumes of 10% (w/v) aqueous ammonium acetate and methanol as the eluent. In this system, protein conjugates remain at the origin while free chelates and smaller peptide-chelate conjugates migrate to *R*_f 0.4–0.8.

High-Performance Liquid Chromatography. Reversed-phase HPLC for analyses of CITC-peptide conjugates, DNP-diglycine, DNP-triglycine, and reaction mixtures after Edman degradation was performed at room temperature with a 10 × 250 mm C₁₈ column (Alltech). A 20-min linear gradient, from 0.1 M ammonium acetate, pH 7.0 (containing 1 mM EDTA), to 100% methanol, was used for analyses of CITC conjugates. A gradient system shown in Figure 1, from 0.1 M ammonium acetate, pH 7.0 (0.1 mM EDTA), to 90% acetonitrile, was used to isolate DNP derivatives, at a flow rate of 3.0 mL/min. The UV-absorbing fractions were detected at 254 nm.

Purification of peptide-CITC conjugates, DNP-diglycine, and DNP-triglycine was done by reversed-phase HPLC using a 21.4 × 250 mm C₁₈ column (Dynamax). Gradients and solvent systems were the same as described above, with a flow rate of 12.5 mL/min.

Radiation Counting. γ-Counting was done in a Beck-

man Model 310 counter with the energy window set for ^{57}Co . TLC plates containing radiolabeled materials were visualized with an AMBIS radioanalytical imaging system.

Spectroscopy. Proton NMR spectra were recorded on a QE 300 spectrometer at 300 MHz. IR spectra were recorded on an IBM IR/32 spectrometer. Exact mass measurements were obtained by running low- and high-resolution mass spectra on a ZAB-HS-2F mass spectrometer (VG Analytical, Wythenshawe, UK). During mass spectroscopic measurements, either 3-nitrobenzyl alcohol or dithiothreitol:dithioerythritol (3:1 w/w) was used as a matrix along with small amounts of *p*-toluenesulfonic acid. High-resolution FAB spectra contained polyethylene glycol or polyethylene glycol methyl ether as reference compound.

Preparation of the Peptide-Conjugates. DNP-diglycine and DNP-triglycine were prepared according to Sanger's method (25). Each peptide (0.4 g) and 0.8 g of NaHCO_3 were dissolved in 10 mL of water, and a solution of 0.8 g of DNFB in 10 mL of ethanol was added to this mixture. The mixture was shaken for 3 h at room temperature, concentrated under reduced pressure to remove the ethanol, dissolved in water, and extracted with ether to remove the excess DNFB. The aqueous solution was acidified, causing the separation of an oil that immediately solidified in amorphous form. DNP-peptides were purified by HPLC, and characterization was done by proton NMR and TLC.

Isothiocyanatobenzyl-EDTA (CITC) was prepared as described by Meares et al. (17). Triglycine (0.5 mmol) was dissolved in 0.1 M sodium phosphate, pH 8.0, to give a 0.1 M triglycine solution; 0.5 mmol of CITC was dissolved in the same buffer to the same final concentration. Conjugation was started by mixing both solutions and adjusting the final pH to 9.0. The reaction was carried out with constant stirring at 40 °C for 18 h. The course of the reaction was monitored by fluorescamine test (26) for the free amine terminus of triglycine. The reaction product gave one spot on TLC with R_f 0.6. The product was purified by HPLC, and characterized by proton NMR, FTIR (absence of SCN stretch at 2100 cm^{-1}), and FAB-MS (m/e 629, $M + 1$).

t-BOC-Gly-Lys-Arg-MCA peptide (8.5 μmol) was dissolved in 0.1 M sodium phosphate, pH 8.0, to give a 20 mM peptide solution; CITC was dissolved in the same buffer to the same final concentration. CITC was attached to the ϵ -amino group of the single lysine residue in the peptide by mixing the two solutions and adjusting the final pH to 9.0. The reaction was carried out with constant stirring at pH 9.0 and 40 °C for 5 h. The course of the reaction was monitored by fluorescamine test. The product was purified by HPLC and confirmed by FAB-MS (m/e 1056, $M + 1$).

Asp-Ala peptide (24.5 μmol) was dissolved in 0.1 M sodium phosphate, pH 8.0, to give a 20 mM peptide solution; CITC was dissolved in the same buffer to the same final concentration. The conjugate of CITC and Asp-Ala was prepared by mixing the two solutions and adjusting the final pH to 9.0 with saturated Na_3PO_4 (aqueous). The reaction was carried out with constant stirring at pH 9.0 and 40 °C for 10 h. The course of the reaction was monitored by fluorescamine test for the free amino terminus of aspartate. The product was purified by HPLC and confirmed by FAB-MS (m/e 644, $M + 1$).

Edman Degradation of Peptide-CITC Conjugates. This was carried out by the method of Chang (27) with the following modifications. CITC-triglycine conjugate was dried under reduced pressure and 1–5 μmol was dissolved in 500 μL of anhydrous trifluoroacetic acid in

Table I. Lym-1-CITC Conjugation Reactions^a

reaction pH	chelates/Lym-1	% immunoreactivity ^b
7.0	2.6	91.6 \pm 3.6
9.0	2.9	96.3 \pm 4.8

^a Reaction conditions described in Experimental Procedures. ^b Average values \pm SD from triplicate immunoreactivity assays.

an Eppendorf tube; the tube was flushed with N_2 , capped, and heated at 54 °C for 15 min. The trifluoroacetic acid was evaporated, 200 μL of water was added, and the pH was adjusted to 9.0. After the cleavage reaction, diglycine was converted to DNP-diglycine by adding an excess of DNFB to the reaction mixture. This conversion was carried out by stirring the reaction mixture at room temperature and pH 9.0 for 3 h. Excess DNFB was extracted with ether, and the aqueous layer was analyzed by HPLC.

Edman degradation of the *t*-Boc-Gly-Lys(CITC)-Arg-MCA conjugate was done as described above. The products were analyzed by FAB-MS.

Edman degradation of the CITC-Asp-Ala conjugate was performed as described above. After the cleavage reaction, cleaved CITC-Asp was converted to PTH-like derivative 3 (shown in Scheme I) by adding 25% aqueous TFA and heating at 54 °C for 5 min, evaporated to dryness, and analyzed by FAB-MS and Applied Biosystems 470A gas-phase sequencer.

Preparation of Lym-1-CITC Conjugates. Lym-1-CITC conjugates were prepared at different pH conditions. The number of chelates per antibody was determined by ^{57}Co assay (17). The Lym-1 antibody solution (15–20 mg/mL) was prepared for conjugation with a centrifuged gel-filtration column (28) with 0.1 M sodium phosphate, pH 8.0 or 6.0, as the column buffer. The conjugation reactions were carried out as described below. Excess CITC was removed, and conjugates were transferred to 0.1 M ammonium citrate, pH 6.0, by centrifuged gel-filtration column chromatography. The course of the conjugation reactions was followed by subjecting aliquots of the reaction mixtures to ^{57}Co assay.

pH 9.0 Conjugate. CITC was dissolved in 0.1 M sodium phosphate buffer, pH 8.0, and added to Lym-1 antibody solution in the same buffer (final concentrations: Lym-1, 0.1 mM; CITC, 0.6 mM). The pH of the solution was adjusted to 9.0 and the reaction mixture was incubated at 37 °C for 3 h.

pH 7.0 Conjugate. CITC solution in 0.1 M sodium phosphate buffer, pH 8.0, and Lym-1 antibody solution in the same buffer were mixed together (final concentrations: Lym-1, 0.1 mM; CITC, 25 mM), and the final pH was adjusted to 7.0. The reaction mixture was incubated at 37 °C for 2 h.

Immunoreactivity Assay. Solid-phase radioimmunoassays for immunoreactivity of either ^{111}In - or ^{57}Co -labeled conjugates were done in triplicate as reported previously (29) with ^{125}I -labeled antibody as the standard. Immunoreactivity values given in Table I are relative to ^{125}I -labeled antibody.

NaDodSO₄-Polyacrylamide Gel Electrophoresis. The protein gels used in these experiments employed the NaDodSO₄ system of Laemmli (30). The running gel was 20% acrylamide with a thickness of 0.5 mm and a length of 7 cm. Gels were run in a Bio-Rad Mini-PROTEAN II system for 1 h at 80 V and then at 200 V until the bromophenol blue tracking dye had run off the bottom of the gel (ca. 1 h). After electrophoresis was complete, the gels were rinsed in electroblotting transfer buffer (see below).

Table II. Comparison of N-Terminal Sequences of Two Lym-1-CITC Conjugates

cycle	pH 9.0 ^a		pH 7.0			
	AA	pmol	AA	pmol	AA	pmol
1	Asp	150	"Trp"	"30"	Ile	16
2	Ile	120	Ile	42	Gln	10
3	Gln	100	Gln	31	Met	13
4	Met	70	Met	30	Thr	22
5	Thr	120	Thr	37	Gln	18
6	Gln	90	Gln	33	Ser	40
7	Ser	50				
8	Pro	70				

^a The pH 9.0 conjugate shows the normal sequence.

Electroblotting. Transfer of proteins from polyacrylamide gels to PVDF membranes was carried out according to the procedure of Matsudaira (31). The membrane was cut to the same size as the gel, wetted with a brief rinse in 100% methanol, and then equilibrated by soaking in transfer buffer for 10–15 min. The transfer buffer employed was 10 mM CAPS, 10% methanol, pH 11.0, to reduce the level of Tris and glycine in the medium. The gel, sandwiched between a sheet of PVDF membrane and several sheets of blotting paper, was assembled into a Bio-Rad Trans Blot apparatus and electroeluted for 30 min at 10 °C and 0.5 A in transfer buffer. A backing sheet of nitrocellulose was included to catch any protein that passed through the first membrane. The PVDF membrane was washed in deionized water for 5 min, stained with 0.1% Coomassie Blue R-250 in 50% methanol for 5 min, and then destained in 50% methanol, 10% acetic acid for 10 min at room temperature. The membrane was finally rinsed in deionized water for 10 min, air-dried, and stored at –20 °C.

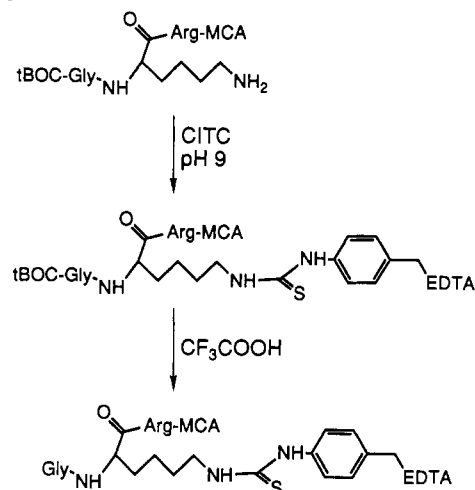
Edman Degradation of Lym-1-CITC Conjugates. Sequencing of Lym-1 and Lym-1-CITC conjugates was performed by automated Edman degradation with subsequent identification of the PTH-amino acids by chromatographic methods. This was done on an Applied Biosystems 470A gas-phase sequencer. Data reduction was achieved with Nelson Analytical software on an IBM AT computer.

RESULTS AND DISCUSSION

Isothiocyanatobenzyl-EDTA (CITC) can cleave N-terminal amino acids in the same way as phenyl isothiocyanate, the Edman degradation reagent. This was confirmed by labeling the N-terminus of triglycine with CITC. The N-terminal labeled triglycine-CITC conjugate was subjected to Edman degradation conditions in anhydrous trifluoroacetic acid at 54 °C for different time periods, and the cleavage products were analyzed by TLC.

The N-terminal labeled triglycine-CITC conjugate gave one UV-quenching spot on TLC with R_f 0.6 which was radioactive (when CITC was labeled with ⁵⁷Co), but fluorescamine negative, which shows the absence of free amino groups. After 5 min of trifluoroacetic acid treatment two spots appeared on the TLC, one UV-quenching, and fluorescamine-negative spot with the same R_f (0.8) as CITC (which was radioactive when ⁵⁷Co-CITC was used) and the other a nonquenching, nonradioactive, fluorescamine-positive spot at the R_f (0.5) of diglycine. In this TLC system, triglycine gave one fluorescamine-positive spot at R_f 0.4. After trifluoroacetic acid treatment for 10 min, the cleavage was complete. Extended treatment with trifluoroacetic acid for 15 min did not affect the intensity of the two product spots.

The experimental outline for Edman chemistry on the peptide-CITC conjugates and the structures of the

Scheme II

products are shown in Scheme I. After cleavage of N-terminal glycine, diglycine was converted into DNP-diglycine as described in Experimental Procedures. DNP derivatives of triglycine and diglycine were synthesized, and their retention times on C₁₈ reversed-phase HPLC were identified. HPLC analysis showed that one of the cleavage products had the same retention time as DNP-diglycine (Figure 1). These results indicate that the N-terminal glycine residue was removed from CITC-triglycine during trifluoroacetic acid treatment.

The chelate CITC does not cleave amino acids from peptides when attached to the ε-amino group of lysine. This was confirmed by a control experiment performed by conjugation of the CITC to a lysine-containing peptide with a blocked N-terminus. The experimental steps are outlined in Scheme II. A conjugate of CITC and *t*-Boc-Gly-Lys-Arg-MCA was synthesized and treated with trifluoroacetic acid under anhydrous conditions at 54 °C for 15 min. The reaction products were dried and analyzed by FAB-MS (m/e 957, $M + 1$). The results showed that the *t*-Boc group was lost from the peptide (as expected), but CITC was still attached.

Lym-1-CITC conjugates were prepared at pH 7 and 9 as described in Experimental Procedures. Heavy and light chains of Lym-1 were isolated by NaDodSO₄ gel electrophoresis and electroblotted onto Immobilon membranes for sequencing. The heavy chain of unmodified Lym-1 has a blocked N-terminus, therefore sequencing of Lym-1-CITC conjugates was carried out for the light chain only. The light chain of the Lym-1-CITC conjugate prepared at pH 9, which had 2.9 chelates/mAb, showed the normal sequence of the light chain through eight Edman cycles: Asp-Ile-Gln-Met-Thr-Gln-Ser-Pro (Table II).

On the other hand, the light chain of the Lym-1-CITC conjugate prepared at pH 7, with a chelate/mAb ratio of 2.6, showed no Asp at all in the first Edman cycle.

As shown in Table II, a mixture of two amino acids was observed: one eluted near Trp and the other was Ile (a "preview" of the actual second residue in the chain). The second Edman cycle showed a mixture of the expected Ile and a preview of the next residue Gln, and so on. These data indicate that practically all the N-terminal Asp α -NH₂ groups were modified during the pH 7 conjugation. Further, they indicate that the resulting adduct is somewhat unstable, since a significant number of the light chains analyzed had lost their original N-terminal residue. Finally, they show that the CITC-Asp Edman product elutes near Trp during sequence analysis.

Further identification and characterization of the CITC-Asp Edman degradation product was done by synthesizing a CITC-Asp-Ala conjugate. After HPLC purification, the CITC-Asp-Ala conjugate was subjected to Edman degradation and the UV-absorbing product was isolated and analyzed by FAB-MS (m/e 555, $M + 1$). These results confirm that CITC-Asp was cleaved from the CITC-Asp-Ala conjugate during trifluoroacetic acid treatment and cyclized to a PTH-like derivative **3** (shown in Scheme I). The CITC-Asp Edman product eluted near Trp on the protein sequencer, as did the first Edman degradation cycle product of the Lym-1-CITC conjugate prepared at pH 7.0.

The instability of the N-terminal CITC-Asp adduct is worthy of comment. The pH 7 conjugate was not exposed to strongly acidic conditions prior to Edman analysis. However, Asp residues in peptides are well-known to promote hydrolysis of adjacent peptide bonds under mildly acidic conditions (32–35), presumably through the interaction of the un-ionized side chain COOH of Asp with the amide carbonyl oxygen. This internal acid might promote Edman degradation of the N-terminal CITC-Asp adduct under very mild conditions, providing a possible explanation. As shown in Table II, N-terminal analysis of the immunoconjugate readily reveals the presence or absence of the CITC-Asp adduct.

To the extent that it would lead to loss of radiolabel from a target-bound antibody, such instability is not desirable for most in vivo applications. However, separation of chelate from antibody might be advantageously accelerated in the (pH 5) intracellular compartments of the liver. Further investigation is required to determine which effect is more important.

Comparison of the immunoreactivities of the pH 7 and 9 Lym-1-CITC conjugates is also instructive. Respectively, they were 91% and 96% of control ¹²⁵I-Lym-1 (Table I). Since practically all of the light-chain N-termini were modified in the pH 7 conjugate, but practically none in the pH 9 conjugate, this implies that modification of light-chain N-termini has little or no effect on immunoreactivity, despite the fact that these residues lie near the antigen-binding sites. Further experiments with the preferential labeling of these N-termini with other reagents could lead to stable immunoconjugates retaining all the antibody effector functions found in the constant regions that lie far away from the N-termini.

ACKNOWLEDGMENT

We thank Daniel Jones for running the FAB-MS, Gary Mirick for performing the immunoassays, John Gardner for sequencing the proteins, Michael McCall for the preparation of CITC and technical advice on numerous aspects of these experiments, and Sally and Gerald DeNardo for helpful discussions. Supported by NIH Grant P01-CA47829 (G. L. DeNardo, P. I.).

LITERATURE CITED

- (1) Cope, D. A., Dewhirst, M. W., Friedman, H. S., Bigner, D. D., and Zalutsky, M. R. (1990) Enhanced delivery of a monoclonal antibody F(ab')₂ fragment to subcutaneous human glioma xenografts using local hyperthermia. *Cancer Res.* 50, 1803–1809.
- (2) Williams, J. A., Wessels, B. W., Edwards, J. A., Kopher, K. A., Wanek, P. M., Wharam, M. D., Order, S. E., and Klein, J. L. (1990) Targeting and therapy of human glioma xenografts in vivo utilizing radiolabeled antibodies. *Cancer Res.* 50 (3 Suppl.), 974s–979s.
- (3) Fritzberg, A. R., Berninger, R. W., Hadley, S. W., and Wester, D. W. (1988) Approaches to radiolabeling of antibodies for diagnosis and therapy of cancer. *Pharm. Res.* 5, 325–334.
- (4) Rodwell, J. D., Alvarez, V. L., Lee, C., Lopes, A. D., Goers, J. W. F., King, H. D., Powsner, H. J., and McKearn, T. J. (1986) Site-specific covalent modification of monoclonal antibodies: in vitro and in vitro evaluations. *Proc. Natl. Acad. Sci. U.S.A.* 83, 2632–2636.
- (5) Roholt, O. A., and Pressman, D. (1967) Differential method for determining the relative reactivity to iodination of different tyrosyl residues in a protein molecule. *Biochim. Biophys. Acta* 147, 1–14.
- (6) Silverton, E. W., Navia, M. A., and Davies, D. R. (1977) Three-dimensional structure of an intact human immunoglobulin. *Proc. Natl. Acad. Sci. U.S.A.* 74, 5140–5144.
- (7) Wellman, A. A., and Meares, C. F. (1990) Sequences of the Lym-1 Antibody Heavy and Light Chain Variable Regions. *Nucl. Acids Res.* 18, Issue 17. EMBL Accession Numbers X53483 and X53484.
- (8) Zachau, H. G. (1989) Immunoglobulin Light-Chain Genes of the κ Type in Man and Mouse. *Immunoglobulin Genes* (T. Honjo, F. W. Alt, and T. H. Rabbitts, Eds.) pp 91–109, Academic Press, London.
- (9) Kabat, E. A., Wu, T. T., Reid-Miller, M., Perry, H. M., and Gottesman, K. S., (Eds.) (1987) *Sequences of Proteins of Immunological Interest*, 4th ed, Public Health Service, National Institutes of Health, Bethesda, MD.
- (10) Podell, D. N., and Abraham, G. N. (1978) A Technique for the Removal of Pyroglutamic Acid from the Amino Terminus of Proteins Using Calf Liver Pyroglutamate Amino Peptidase. *Biochem. Biophys. Res. Commun.* 81, 176–185.
- (11) Sanger, F., and Thompson, E. O. P. (1953) The Amino-acid Sequence in the Glycyl Chain of Insulin. *Biochem. J.* 53, 366–374.
- (12) Chang, C.-H., Meares, C. F., and Goodwin, D. A. (1982) Bifunctional Chelating Agents: Linking Radiometals to Biological Molecules. In *Applications of Nuclear and Radiochemistry* (Lambrecht, R. M., and Morcos, C. N., Eds.) pp 103–114, Pergamon, New York.
- (13) Mirzadeh, S., Brechbiel, M. W., Atcher, R. W., and Gansow, O. A. (1990) Radiometal Labeling of Immunoproteins: Covalent Linkage of 2-(4-Isothiocyanatobenzyl)diethylenetriaminepentaacetic Acid Ligands to Immunoglobulin. *Bioconjugate Chem.* 1, 59–65.
- (14) McCall, M. J., Diril, H., Meares, C. F. (1990) Simplified Method for Conjugating Macrocyclic Bifunctional Chelating Agents to Antibodies via 2-iminothiolane. *Bioconjugate Chem.* 1, 222–226.
- (15) Means, Gary E., and Feeney, Robert E. (1971) *Chemical Modification of Proteins*, pp 11–17, Holden-Day, Inc., San Francisco, CA.
- (16) Segal, D. M., Padlan, E. A., Cohen, G. H., Rudikoff, S., Potter, M., and Davies, D. R. (1974) The Three-Dimensional Structure of Phosphorylcholine-Binding Mouse Immunoglobulin Fab and the Nature of the Antigen Binding Site. *Proc. Natl. Acad. Sci. U.S.A.* 71, 4298–4302.
- (17) Meares, C. F., McCall, M. J., Reardon, D. T., Goodwin, D. A., Diamanti, C. I., and McTigue, M. (1984) Conjugation of Antibodies with Bifunctional Chelating Agents: Isothiocyanate and Bromoacetamide Reagents, Methods of Analysis, and Subsequent Addition of Metal Ions. *Anal. Biochem.* 142, 68–78.
- (18) Chang, J. Y. (1988) A complete quantitative N-terminal analysis method. *Anal. Biochem.* 170, 542–556.

- (19) Vergeres, G., Winterhalter, K. H., and Richter, C. (1989) Identification of the membrane anchor of microsomal rat liver cytochrome P-450. *Biochemistry* 28, 3650-3655.
- (20) Tsugita, A. (1987) Developments in protein microsequencing. *Adv. Biophys.* 23, 81-113.
- (21) Amoscato, A. A., Babcock, G. F., Sramkoski, R. M., Hynd, B. A., and Alexander, J. W. (1987) Synthesis of two biologically active fluorescent probes of thymopentin. *Int. J. Pep. Protein Res.* 29, 177-186.
- (22) Miyano, H., Nakajima, T., and Imai, K. (1987) Microscale sequence analysis from the N-terminus of peptides using the fluorogenic Edman reagent 4-*N,N*-dimethylamino-1-naphthyl isothiocyanate. *Biomed. Chromatog.* 2, 139-144.
- (23) Epstein, A. L., Zimmer, A. M., and Spies, S. M. (1985) Radioimmunoassay of human B-cell lymphomas with a radiolabeled tumor-specific monoclonal antibody (Lym-1). In *Malignant Lymphomas and Hodgkin's Disease: Experimental and Therapeutic Advances* (F. Cavalli, G. Bonadonna, and M. Rozencweig, Eds.) pp 569-577, Martinus Nijhoff Publishing Co., Boston.
- (24) Thiers, R. C. (1957) Contamination in Trace Element Analysis and Its Control. *Methods Biochem. Anal.* 5, 273-335.
- (25) Sanger, F. (1945) The Free Amino Groups of Insulin. *Biochem. J.* 39, 507-515.
- (26) Udenfriend, S., Stern, S., Bohlen, P., Dairman, W., Leimgruber, W., and Weigle, M. (1972) Fluorescamine: a reagent for assay of amino acids, peptides, proteins, and primary amino acids in the picomole range. *Science (Washington, D.C.)* 178, 871-872.
- (27) Chang, J.-Y. (1983) Manual Micro-Sequence Analysis of Polypeptides Using Dimethylaminoazobenzene Isothiocyanate. *Method Enzymol.* 91, 455-466.
- (28) Penefsky, H. S. (1979) A Centrifuged-Column Procedure for the Measurement of Ligand Binding by Beef Heart F1. *Methods Enzymol.* 56, Part G, 527-530.
- (29) DeNardo, S. J., Peng, J.-S. B., DeNardo, G. L., Mills, S. L., and Epstein, A. L. (1986) Immunochemical Aspects of Monoclonal Antibodies Important for Radiopharmaceutical Development. *Nucl. Med. Biol.* 13, 303-310.
- (30) Laemmli, U. K. (1970) Cleavage of Structural Proteins During the Assembly of the Head of Bacteriophage T4. *Nature* 227, 680-685.
- (31) Matsudaira, P. (1987) Sequence from Picomole Quantities of Proteins Electrophoretically Blotted onto Polyvinylidene Difluoride Membranes. *J. Biol. Chem.* 262, 10035-10038.
- (32) Fraser, K. J., Poulsen, K., and Haber, E. (1972) Specific cleavage between variable and constant domains of rabbit antibody light chains by dilute acid hydrolysis. *Biochemistry* 11, 4974-4977.
- (33) Hanford, R., Doonan, H. J., Doonan, S., Vernon, C. A., Walker, J., Bossa, F., Barra, D., Carloni, M., Fasella, P., and Riva, F. (1974) Primary structure of aspartate aminotransferase from pig heart muscle. Peptides produced by cleavage with cyanogen bromide and with dilute acid. *Atti Accad. Naz. Lincei, Cl. Sci. Fis., Mat. Nat., Rend.* 56, 73-83.
- (34) Jauregui-Adell, J., and Marti, J. (1975) Acidic cleavage of the aspartyl-proline bond and the limitations of the reaction. *Anal. Biochem.* 69, 468-473.
- (35) Inglis, A., McKern, N., Roxburgh, C., and Strike, P. (1980) Cleavage of proteins at aspartic acid residues using dilute acid. *Methods of Peptide and Protein Sequence Analysis. Proceedings of the 3rd International Conference; Meeting Date 1979* (Bir, Christian, Ed.) pp 329-343. Elsevier Amsterdam, Netherlands.

TECHNICAL NOTES

4-Azido[3,5-³H]phenacyl Bromide, a Versatile Bifunctional Reagent for Photoaffinity Radiolabeling. Synthesis of Prostaglandin 4-Azido[3,5-³H]phenacyl Esters

Bradley D. Smith,[†] Koji Nakanishi,^{*,†} Kikuko Watanabe,[‡] and Seiji Ito[‡]

Department of Chemistry, Columbia University, New York, New York, 10027, and Osaka Bioscience Institute, 6-2-4 Furuedai, Suita, Osaka 565, Japan. Received August 9, 1990

4-Azido[3,5-³H]phenacyl bromide was synthesized in three steps from 4-amino-3,5-diiodoacetophenone and coupled to the prostaglandins PGE₂ and PGD₂ to provide potential photoaffinity compounds.

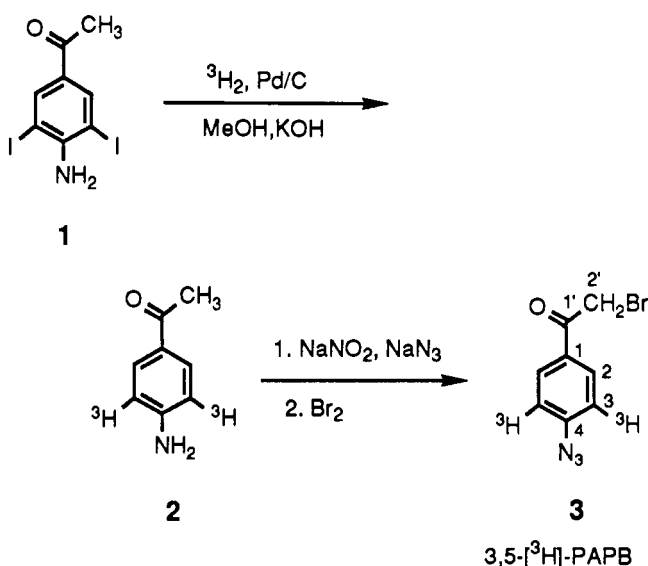
Since its introduction in 1973 (1,2), 4-azidophenacyl bromide (PAPB) has become a useful bifunctional reagent for the modification of both large and small molecules for photolabeling experiments (3). A current literature survey includes more than 25 photoaffinity studies using this compound. Generally, PAPB has been used to selectively alkylate reactive thiol residues in proteins, which have subsequently been used in photo-cross-linking experiments (4, 5). In analogous studies, it has been incorporated into polynucleotides via thiophosphate (6) and thiopyrimidine (7) linkages. Smaller molecules have been modified via attachment to thiol (8), carboxyl (9) and amino (9, 10) moieties to provide photolabile derivatives useful for labeling enzyme and receptor binding sites. In many cases, detection of the photolabeled compounds was achieved by using immunoassay techniques that were specific for each respective system.

We were interested in PAPB as a reagent to modify prostaglandin (PG) compounds for use in photoaffinity experiments (11). We reasoned that a suitable radioactive form of PAPB would provide an efficient way of introducing both the radio- and photolabile groups into the PG molecule. Radiolabeled PAPB has previously been reported

as its 1'-¹⁴C (2) and 2'-³H (12) labeled forms. However, both derivatives were considered unsuitable for our purposes; the specific activity of the ¹⁴C compound was too low, while synthesis of the ³H compound required specialized handling. Also considered as unsuitable were any potential derivatives labeled with ¹²⁵I, since it has been noted that arylazido compounds substituted with iodine sometime result in low incorporation of the photoprobe (13).

We therefore decided to synthesize [3,5-³H]PAPB (3), which was achieved by the sequence described in Scheme I. The tritium was introduced by catalytic dehalogenation of 4-amino-3,5-diiodoacetophenone (1; obtained by reaction of 4-aminoacetophenone with 2 equiv of iodine monochloride) using tritium gas and Pd/C catalyst in methanol/KOH.¹ Under these conditions the incorporation of tritium was high (specific activity of 50 Ci/mmol) and no concomitant reduction of the aryl ketone function was observed. Without purification, the tritiated 4-aminoacetophenone (2) was converted to [3,5-³H]-PAPB (3) in a simple, high-yielding, two-step process.² As

Scheme I



¹The following was carried out by Amersham Corp., tritium labeling service (TR3 method): 4-amino-3,5-diiodoacetophenone (40 mg), 10% Pd/C (4 mg), methanol (8 mL), and 1 N KOH aqueous methanol solution (0.50 mL) were hydrogenated at room temperature under 1 atm of tritium gas for 3 h. The catalyst and solvent were removed, and the tritiated product 2 (14 mg, 5 Ci, 50 Ci/mmol) was taken up in ethanol (30 mL).

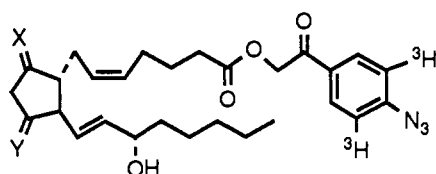
²To a 2.5-mL aliquot of the stock ethanol solution of tritiated 2 (500 mCi, 1.2 mg) was added unlabeled 4-aminoacetophenone (10.0 mg) and 5% aqueous H₂SO₄ (5 mL). The solution was cooled in ice, treated with aqueous NaNO₂ solution (18 mg in 200 μ L), and stirred for 20 min before a chilled solution of NaN₃ (24 mg in 200 μ L) was added. After stirring for a further 10 min, ether (10 mL) was added, and the phases separated. The organic layer was washed (2 \times 3 mL water), dried (MgSO₄), and evaporated to give crude 4-azido[3,5-³H]acetophenone. This residue was taken up in ether (1 mL) and treated with acetic acid (1 drop) and bromine solution (60 μ L, 1 N CCl₄ solution). After 40 min, TLC indicated the bromination was complete [*R_f* for 4-azidoacetophenone and monobromo and dibromo products (eluent, CH₂Cl₂) were 0.56, 0.74, 0.82; product ratios were 0.05, 0.90, 0.05, respectively]. Ether (15 mL) and water (3 mL) were added, and the organic layer separated and was dried. Removing of the solvent and purification by flash chromatography (1.5 \times 30 cm column packed with 12 cm of silica; eluent, 1:1 CH₂Cl₂/hexane) gave [3,5-³H]PAPB (3) [8.0 mg (38%), 160 mCi, 4.8 Ci/mmol; UV MeOH, λ_{\max} 292 nm, ϵ = 2.08 \times 10⁴ (2)], which was taken up in toluene (5 mL) and stored at -78 $^{\circ}$ C.

[†] Columbia University.

[‡] Osaka Bioscience Institute.

a bifunctional reagent, [3,5-³H]PAPB has the following advantages: (i) Its synthesis is straightforward and inexpensive, producing large amounts of labeled material of high specific activity. (ii) [3,5-³H]PAPB is stable to long-term storage at low temperature and therefore, in principle, one sample can be utilized for a variety of labeling targets. Even unreactive amino and alcohol groups can be attached via linker groups (5). (iii) The presence of the radio- and photolabels on the same ring eliminates the possibility of them becoming separated in any postlabeling digestive workup.

We have used [3,5-³H]PAPB to esterify the carboxyl functions of PGE₂ and PGD₂ to produce potential PG photoaffinity compounds 4 and 5, respectively.³ These PG compounds are currently being used in photolabeling experiments designed to characterize the structural aspects of PG synthase enzymes (14) and PG receptors (15).



4 X = O; Y = α -OH, β -H

5 X = α -OH, β -H; Y = O

ACKNOWLEDGMENT

This study was supported by NIH 10187. B.D.S. gratefully acknowledges a fellowship from Merck, Sharp and Dohme. We are grateful to Professor O. Hayaishi for discussions and encouragement.

Note Added in Proof: The procedures described in footnotes 2 and 3 have been successfully repeated on a 10-fold smaller scale to allow the carrier-free synthesis of [3,5-³H]PAPB and prostaglandin ester 4 at a specific activity of 50 Ci/mmol.

LITERATURE CITED

- Hixson, S. S., and Hixson, S. H. (1973) Photochemical labeling of yeast alcohol dehydrogenase with an azide analogy of NAD⁺. *Photochem. Photobiol.* 18, 135-8.
- Hixson, S. H., and Hixson, S. S. (1975) *p*-Azidophenacyl bromide, a versatile photolabile bifunctional reagent. Reaction with glyceraldehyde-3-phosphate dehydrogenase. *Biochemistry* 14, 4251-4.
- Bayley, H. (1983) *Photogenerated Reagents in Biochemistry and Molecular Biology*, Elsevier, New York.
- Some examples: First, E. A., and Taylor, S. S. (1988) Subunit interaction sites between the regulatory and catalytic subunits of cAMP-dependent protein kinase. Heterobifunctional cross-linking reagents lead to photodependent and photoindependent cross-linking. *J. Biol. Chem.* 263, 5170-5. Lunn, C. A., and Pigiet, V. P. (1986) Chemical cross-linking of thioredoxin to hybrid membrane fraction in *Escherichia coli*. *J. Biol. Chem.* 261, 832-8. Dupuis, A., and Vignais, P. V. (1985) Photolabeling of mitochondrial F1-ATPase by an azido derivative of the oligomycin-sensitivity conferring protein. *Biochem. Biophys. Res. Commun.* 129, 819-25.
- Erecinska, M. (1980) The use of photoaffinity labels in the study of mitochondrial function. *Ann. N. Y. Acad. Sci.* 346, 444-57.
- Praseuth, D., Perroualt, L., Trung, D., Chassagnol, M., Nguyen, T., and Helene, C. (1988) Sequence Specific binding and photocrosslinking of α and β oligonucleotides to the major groove of DNA via triple helix formation. *Proc. Natl. Acad. Sci. U.S.A.* 85, 1349-53. Hanna, M. M., and Meares, C. F. (1983) Topography of transcription: Path of the leading end of nascent RNA through the *Escherichia coli* transcription complex. *Proc. Natl. Acad. Sci. U.S.A.* 80, 4238-42. Hanna, M. M., and Meares, C. F. (1983) Synthesis of a cleavable dinucleotide photoaffinity probe of ribonucleic acid polymerase: Application to trinucleotide labeling of an *Escherichia coli* transcription complex. *Biochemistry*, 22, 3546-51.
- Some examples: Hanna, M. M., Dissinger, S., Williams, B. D., and Colston, J. E. (1989) Synthesis and characterization of 5-(4-azidophenacyl)thiouridine 5'-triphosphate, a cleavable photo-cross-linking nucleotide analog. *Biochemistry*, 28, 5814-20. Hsu, L. M., Lin, F. L., Nurse, K., and Ofengand, J. (1984) Covalent cross-linking of *Escherichia coli* phenylalanyl-tRNA and valyl-tRNA to the ribosomal A site via photoaffinity probes attached to the 4-thiouridine residue. *J. Mol. Biol.* 172, 57-76.
- Some examples: Kunst, M., Sies, H., and Akerboom, T. P. (1989) S-(4-azidophenacyl)[³⁵S]-glutathione photoaffinity labeling of rat liver plasma membrane-associated proteins. *Biochem. Biophys. Acta* 982, 15-23. Matthew, M. S., Lewis, R. V., and Barden, R. E. (1986) Photoaffinity labeling of carnitine acetyltransferase with S-(*p*-azidophenacyl)thiocarnitine. *Biochem. J.* 237, 533-40.
- Yurchenko, R. I., and Malitskaya, V. P. (1977) Syntheses based on *p*-azido- ω -haloacetophenones. *Zh. Org. Khim.* 13, 1980-7.
- Deushkin, Y. V., and Kotelevtsev, Y. V. (1982) Photoaffinity modification by azidocytisine of the nicotine acetylcholine receptor from optic ganglia of the squid. *Bioorg. Khim.* 13, 1980-7.
- Michalak, M., Wandler, E. L., Strynadka, K., Lopaschuk, G. L., Njue, W. M., Liu, H.-J., and Olley, P. M. (1990) Photolabeling of the prostaglandin E₂ receptor in cardiac sarcolemmal vesicles. *FEBS Lett.* 265, 117-20.
- Muccino, R. R., and Serico, L. (1978) Alumina catalysed exchange of enolizable hydrogens. *J. Labelled Compd. Radiopharm.* 15, 523-7.
- Watt, D. S., Kawada, K., Leyva, E., and Platz, M. S. (1989) Exploratory photochemistry of iodinated aromatic azides. *Tetrahedron Lett.* 30, 899-902.
- Watanabe, K., Fujii, Y., Nakayama, K., Ohkubo, H., Kuramitsu, S., Kagamiyama, H., Nakanishi, S., and Hayaishi, O. (1988) Structural similarity of bovine lung prostaglandin F synthase to lens ϵ -crystallin of the european common frog. *Proc. Natl. Acad. Sci. U.S.A.* 85, 11-5.
- Negishi, M., Ito, S., Tanaka, T., Yokohama, H., Hayashi, H., Katada, T., Ui, M., and Hayaishi, O. (1988) Covalent cross-linking of prostaglandin E receptor from bovine adrenal medulla with a pertussis toxin-insensitive guanine nucleotide-binding protein. *J. Biol. Chem.* 262, 12077-84.

[3,5-³H]PAPB (3; 4 mg, 16 mmol, 80 mCi) was treated with a solution of PGD₂ (10 mg, 28 mmol) in THF (0.50 mL) and diisopropylethylamine (5 μ L, 29 mmol). The solution was stirred overnight at room temperature, the solvent was evaporated and the residue was purified by flash chromatography (1 \times 20 cm column packed with 6 cm of silica; eluent, 1:1 ethyl acetate/hexane) to give PGD₂ 4-azido[3,5-³H]phenacyl ester 5 [4.8 mg, 45 mCi, 4.8 Ci/mmol]. PGE₂ 4-azido[3,5-³H]phenacyl ester 4 was synthesized by using the same procedure except the chromatography eluent was 4:1 ethyl acetate/hexane.

Bioconjugate Chemistry

NOVEMBER/DECEMBER 1990
Volume 1, Number 6

© Copyright 1990 by the American Chemical Society

Polymeric Contrast Agents for Magnetic Resonance Imaging: Synthesis and Characterization of Gadolinium Diethylenetriaminepentaacetic Acid Conjugated to Polysaccharides

Frances E. Armitage,[†] David E. Richardson,^{*,†,‡} and King C. P. Li[§]

Department of Chemistry, and Radiology Department, College of Medicine, University of Florida, Gainesville, Florida 32611. Received March 20, 1990

The synthesis and characterization of polysaccharides esterified with gadolinium diethylenetriaminepentaacetic acid (GdDTPA) are described. The results of several synthetic methods are presented for esterification of dextrans and inulin with DTPA. One method results in highly conjugated products labeled with an average of 0.4 mol of GdDTPA/mol of glucopyranose unit in dextrans of up to 70 800 average molecular weight and 0.5 mol of GdDTPA/mol of fructofuranose unit in inulin. Chromatographic and potentiometric evidence supporting the absence of significant chelate cross-linking of the conjugated polysaccharides is presented. The thermodynamic stability constant, $\log K$ ($Gd^{3+} + L^{4-} \rightarrow GdL^{-}$), of the complexes was 18.0 ± 0.2 based on an independent chelate model. In vitro ester hydrolysis of the GdDTPA-dextran 70 800 (at 37 °C, pH = 7.4 phosphate buffer) occurs with a half-life of 21 h. The agents exhibit T_1 relaxivities ranging from 1.5 to 2.3 times that of GdDTPA at 100 MHz, and decreasing in vitro relaxivity with increasing molecular weight of the dextran carrier was observed. Phantom MRI studies indicate that the T_1 and T_2 effects of the complexes differ from those of GdDTPA, with the polysaccharide-bound complexes exhibiting a considerably faster drop in relative signal intensity with increased concentration in T_1 and T_2 weighted pulse sequences.

Magnetic resonance imaging (MRI) has rapidly become the method of choice for the initial screening of patients suspected of a variety of physiological disorders including certain types of cancer (1-3). The gadolinium(III) complex of diethylenetriaminepentaacetic acid (GdDTPA) (4-8) and other paramagnetic compounds (9-11) have been used successfully to enhance the imaging of several types of carcinomas, particularly those of the brain. GdDTPA undergoes rapid renal excretion following extracellular bio-distribution with a blood-concentration half-life of 20 min (12). The short persistence and rapid extravascular distribution of GdDTPA make the contrast agent

ineffective for situations where a lengthy blood-pool persistence of the agent may be required.

Several alternatives to GdDTPA have been proposed, including agents that contain different paramagnetic metals and chelating ligands (11, 13-15). GdDTPA exhibits a large spin-lattice relaxation effect (16, 17), and the DTPA chelate affords the complex great ($K = 10^{22.5}$) thermodynamic stability (18). One approach to overcome the limitations of monomeric GdDTPA described above involves the covalent attachment of the clinically evaluated GdDTPA to macromolecular carriers, for example, bovine serum albumin (19). The use of macromolecular carriers can result in compounds that have a greater effect on T_1 relaxation of surrounding water molecules (20) as well as enhanced blood-pool persistence and possible tissue specificity relative to GdDTPA.

Although using macromolecular carriers with contrast agents can provide advantages, the biological effect and

* Author to whom correspondence should be addressed.

[†] Department of Chemistry.

[‡] A.P. Sloan Research Fellow, 1988-1990.

[§] Radiology Department.

fate of the carrier and carrier-complex must also be considered. Proteins as carrier molecules (19, 21, 22) are often antigenic, and the level of loading of the paramagnetic agent on the protein may be too low to make the agent clinically useful. Polysaccharides are possible alternatives to protein carriers, and reports concerning the synthesis and imaging properties of polysaccharide-conjugated DTPA have appeared (23–26). As carrier macromolecules, dextrans have the desirable qualities of low expense, hydrophilicity, pH stability, precedence in drug delivery, and increased plasma persistence of the conjugated moiety. The reported preparations of GdDTPA-dextrans (23–25) yield products with variable chelate loading levels and, in at least one case (23), significant amounts of chelate cross-linking of the polysaccharide chains. In two reports (24, 25), synthetic details and chemical properties of the conjugates are not provided.

In contrast to protein carriers, dextrans are not homogeneous in molecular weight. However, different average molecular weight preparations are available that could in principle be used to control the biodistribution of conjugated MRI contrast agents (e.g., by altering blood-pool persistence and renal-clearance rates). Cross-linking of the dextran carrier broadens the molecular weight distribution and reduces the potential for selecting desired molecular weight ranges in the polymeric contrast agents (although cross-linked products can be prepared to produce different average molecular weight products (23)). In the synthetic method of Gibby et al. (23), increasing the degree of chelate loading on dextran results in increased cross-linking. The thermodynamic stability constants for the various published DTPA-dextran conjugates (23–25) have not been reported, and cross-linking may reduce the stability of Gd^{3+} binding by removal of two carboxylate binding sites.

The goal of the present study was the synthesis of non-cross-linked dextrans ranging in average molecular weight from 9400 to 487 000 that have been extensively labeled with GdDTPA by a single ester linkage. An improved method for esterification of polysaccharides that yields conjugates with a higher loading of chelating agent than reported previously (23–25) is described. The binding constant for Gd^{3+} has been determined by potentiometric titration for one of the products. Spectroscopic, chemical, and physical characterization of the esters provides evidence for macromolecular products that are not significantly cross-linked by the chelate, and solvent T_1 and T_2 relaxation effects by the conjugated gadolinium complexes are investigated.

EXPERIMENTAL PROCEDURES

General Considerations. Water was purified by using a Barnstead Nanopure apparatus. All glassware was washed with 1 M EDTA and repeatedly rinsed with purified water before use. All chemicals used were reagent grade unless otherwise noted. The gadolinium complexes of EDTA (HGdEDTA) and DTPA ($H_2GdDTPA$) were prepared by the method outlined for $H_2GdDTPA$ by Wenzel et al. (27). The hexahydrate of $GdCl_3$ (Aldrich, 99.9%) was used instead of Gd_2O_3 in the preparations and acetone was used to precipitate the solids.

Preparation of Anhydrides. The isobutyl formate and ethyl formate mixed anhydrides of DTPA were prepared by the method of Krejcarek and Tucker (28). A 1:5 mole ratio of H_5DTPA (Aldrich) to triethylamine (Kodak) in anhydrous acetonitrile (Aldrich) was used. Isobutyl chloroformate (Aldrich) or ethyl chloroformate (Kodak) was allowed to react with the triethylamine salt. Following

precipitation of solid triethylamine hydrochloride, the cold mixture was filtered and solid washed by cold filtering with acetonitrile. The washings were added to the filtrate, and the solution was rotary-evaporated to form a white paste. Repeated washing and decantation with anhydrous ethyl ether resulted in a white powder following vacuum drying in a desiccator.

The dicyclic anhydride of DTPA was prepared and isolated by the method of Eckelman (29). Acetic anhydride (Fisher) was allowed to react in a 4:1 mole ratio with H_5DTPA in ACS-grade pyridine (Aldrich). It was found that heating at 65 °C for 24 h resulted in significant product discoloration. Heating at 45 °C did not result in the formation of the dark brown solid/solution and this temperature was used in all subsequent cyclic anhydride preparations.

Modifications of Eckelman's method (29) were used to produce the mixtures of mono- and dicyclic anhydrides of DTPA. H_5DTPA (Aldrich) was allowed to react with acetic anhydride (Fisher Scientific) in anhydrous pyridine (Aldrich) at 45 °C for 24 h. Reaction mixtures containing mole ratios of DTPA to acetic anhydride of 1.0:1.0, 1.0:2.0, or 1.0:3.2 were used. In a typical preparation of 1.0:3.2 DTPA to acetic anhydride ratio, 10.0 g (25.4 mmol) of H_5DTPA and 8.3 g (81.4 mmol) of acetic anhydride were dissolved in 800 mL of pyridine and heated at 45 °C for 24 h. After cooling to room temperature, the heterogeneous mixture was filtered, and the collected light beige solid washed with acetic anhydride, followed by anhydrous ethyl ether, and vacuum dried in a desiccator.

Halpern's method (30) of synthesis and isolation was also used to produce the reported monocyclic anhydride. Thionyl chloride (Fisher) was allowed to react with H_5DTPA in the presence of excess trifluoroacetic anhydride (Fisher).

Preparation of Polysaccharide-DTPA Esters. General Procedures. All glassware was oven-dried prior to the preparation of acid esters of the polysaccharides. All reactions were conducted in flasks equipped with a condensing or vigreux column topped with a calcium chloride drying tube. All preparations which required the use of trifluoroacetic anhydride or acetic anhydride were, following the reaction heating time, heated sufficiently to distill off their respective acids. All polysaccharides, inulin, dextran 9400, 40 200, 70 800, or 487 000 (average molecular weights, Sigma Chemical Co.), were lyophilized for 3 h prior to use. Acetone was used to precipitate products and hydrated cyclic anhydrides in all preparations involving the reaction of mono- or dicyclic anhydrides of DTPA. Methanol or ethanol was used to precipitate products and DTPA in all preparations in which the mixed anhydrides were used. In all reaction conditions tried, a ratio of 1 mol of mixed or cyclic anhydride/mol of repeating glucopyranose or fructofuranose unit of the polysaccharide was used.

Several methods for esterifying polysaccharides with DTPA were investigated. The reaction conditions are summarized in Tables I and II.

Preparation of Polysaccharide-DTPA Esters. Optimized Procedure. Highly loaded polysaccharide DTPA esters were prepared by placing the polysaccharide in 1:1 volume mixture of formamide (Kodak, previously dried over molecular sieves) and anhydrous pyridine. Glucopyranose repeating unit concentrations in all preparations were 0.1 M, and the glucopyranose:DTPA anhydride molar ratio was 1:1. In a typical procedure, 4.7 g (0.50 mmol) of polysaccharide, 26 mmol of glucopyranose of dextran 9400 was placed in a flask with 250 mL of a 1:1 volume mixture of formamide and pyridine (28).

Table I. Mixed Anhydride Reactions with Polysaccharides

reactant anhydride	polysac ^a	solvent ^b	temp/time	catalyst added	% reacted ^c
isobutyl	D	pyr/DMSO	reflux/2 h	none	0
isobutyl	I	pyr/DMSO	reflux/2 h	none	7
ethyl	I	pyr	reflux/1 h	none	7
isobutyl	D†	DMSO	5 °C/15 min	none	5–25
ethyl	D†*	benzene	RT/12 h	none	0
ethyl	I†*	benzene	RT/12 h	none	1–5
ethyl	D	1:1 pyr/form.	RT/60 h	none	<1
ethyl	D	1:1 pyr/form.	60 °C/3 h	ZnCl ₂	24
isobutyl	D	1:1 pyr/form.	60 °C/17 h	ZnCl ₂	22

^a D = dextran 9400, I = inulin, †polysaccharide activated by *n*-butyllithium; *heterogeneous reaction conditions, all other reactions were homogeneous. ^b Pyr = pyridine; DMSO = dimethyl sulfoxide; form. = formamide; unless a ratio is given, all solvent mixtures were prepared such that the more polar solvent was added to the mixture of polysaccharide in the less polar solvent until the polysaccharide dissolved. ^c Obtained from HPLC elution profiles, all values ± 2 .

Table II. Cyclic Anhydride Reactions with Polysaccharides

reactant ^a anhydride	polysac ^b	solvent	temp/time	catalyst ^c added	% reacted ^d
d-dicy	D*	toluene	reflux/3 h	TFAA	0
d-dicy	D	1:1 pyr/form	60 °C/24 h	none	0
d-dicy	D	1:1 pyr/form	60 °C/3.5 h, RT/2 h	ZnCl ₂	[88]
d-dicy	I	1:1 pyr/form	60 °C/3.5 h, RT/2 h	ZnCl ₂	[67]
d-1:3.2	D	1:1 pyr/form	65 °C/24 h	TFAA	16 [8]
d-mocy	D	1:1 pyr/form	65 °C/4 h, RT/24 h	ZnCl ₂	42 [7]
d-1:1.0	D	1:1 pyr/form	60 °C/3 h, RT/12 h	ZnCl ₂	23
d-1:2.0	D	1:1 pyr/form	60 °C/3.5 h, RT/12 h	none	0
d-1:2.0	D	1:1 pyr/form	60 °C/1 h, RT/12 h	ZnCl ₂	34
d-1:3.2	D	1:1 pyr/form	50 °C/4 h, RT/2 h	ZnCl ₂	59
d-1:3.2	D (402)	1:1 pyr/form	50 °C/4 h, RT/2 h	ZnCl ₂	60
d-1:3.2	I	1:1 pyr/form	50 °C/4 h, RT/2 h	ZnCl ₂	72

^a d-dicy = DTPA dicyclic anhydride (Aldrich); d-mocy = DTPA monocyclic anhydride prepared as outlined by Halpern et al. (30); ratios indicate moles of DTPA to moles of acetic anhydride used to prepare the cyclic anhydride. ^b D = dextran 9400; D(402) = dextran 40 200; I = inulin; * = heterogeneous reaction conditions, all other reactions homogeneous. ^c TFAA = trifluoroacetic anhydride; ZnCl₂ added as either solid ZnCl₂ or a mixture with anhydrous pyridine. ^d Obtained from HPLC elution profiles, bracketed numbers represent percent reacted anhydride which formed cross-linked product (if two percentages are reported) or the percent reacted anhydride which formed products with very broad elution profiles. All values are $\pm 2\%$.

The flask contents were stirred while being heated at 40 °C for 1/2 h to dissolve the polysaccharide. After addition of 0.5 mg of anhydrous zinc chloride (Aldrich), heating was continued for 1/2 h. The prepared cyclic anhydride (10.2 g, 26 mmol) was added to the solution. The flask contents were stirred while being heated at 50 °C for 4 h under anhydrous conditions. After cooling to room temperature over a period of 3 h, the homogeneous solution was rotary-evaporated to approximately half the original volume. The solution was cooled in an ice bath and acetone was added to precipitate the solid. The solid was filtered, washed with cold acetone followed by anhydrous ethyl ether, and dried under vacuum in a desiccator. The crude solids were dissolved in deionized water and exhaustively dialyzed against water to remove unreacted DTPA. The solid esterified polysaccharides were then obtained by lyophilization of the dialysis bag contents following rotary evaporation to reduce volume.

The above method was used to esterify dextrans (9400, 40 200, and 70 800 average molecular weight) and inulin with DTPA. Elemental analyses of the unmodified dextrans were conducted independently so the effect of polysaccharide branching on the average repeating glucopyranose analysis could be incorporated. The following calculated and observed elemental analysis results were obtained for conjugates from typical preparations, and the analyses are calculated for (attached DTPA unit)_y-(average esterified glucopyranose unit)₁. The amount of DTPA in a given sample of DTPA-esterified polysaccharide is uniquely determined by the nitrogen analysis, and this allows for the direct determination of the number of moles of DTPA per mole of repeating saccharide unit. DTPA-dextran conjugates are identified in the text by the average molecular weight of the unmodified dextran. **DTPA-dextran 9400:** Anal. Calcd for (C₁₄H₂₂N₃O₉)_{0.42}-

(C₆H_{10.95}O_{6.04}): C, 42.24; H, 6.02; N, 5.22. Found: C, 42.93; H, 6.22; N, 5.28. **DTPA-dextran 40 200:** Anal. Calcd for (C₁₄H₂₂N₃O₉)_{0.38}(C₆H_{11.04}O_{5.85}): C, 41.01; H, 6.27; N, 5.12. Found: C, 41.92; H, 6.04; N, 4.92. **DTPA-dextran 70 800:** Anal. Calcd for (C₁₄H₂₂N₃O₉)_{0.36}(C₆H_{10.83}O_{5.75}): C, 42.71; H, 6.09; N, 4.87. Found: C, 42.64; H, 6.20; N, 4.86. The following calculated and observed elemental analysis results were obtained for the conjugate from a typical preparation of DTPA-inulin and the analysis is calculated for (attached DTPA unit)_y-(average esterified fructofuranose unit)₁. **DTPA-inulin:** Anal. Calcd for (C₁₄H₂₂N₃O₉)_{0.53}-(C_{5.5}H_{9.06}O_{5.11}): C, 43.54; H, 5.86; N, 6.25. Found: C, 43.82; H, 6.05; N, 6.07.

An example of the conjugate of dextran 487 000 as synthesized by the general method above resulted in the following calculated and observed elemental analysis. **DTPA-dextran 487 000:** Anal. Calcd for (C₁₄H₂₂N₃O₉)_{0.06}-(C₆H_{11.23}O_{6.05}): C, 40.52; H, 6.24; N, 1.24. Found: C, 41.12; H, 6.57; N, 1.25. For the product prepared as above except that the reaction solution was allowed to stir at room temperature for 30 h prior to precipitation and isolation of product, the analysis was as follows. Anal. Calcd for (C₁₄H₂₂N₃O₉)_{0.82}(C₆H_{10.83}O_{6.05}): C, 43.02; H, 5.98; N, 7.06. Found: C, 42.94; H, 6.05; N, 7.08.

Preparation of Gadolinium Conjugates. Metalation of the esterified polysaccharides was achieved by dissolving the DTPA-dextran conjugates in water to produce solutions of approximately 0.1 M glucopyranose followed by the addition of a 20% stoichiometric excess of the hexahydrate of GdCl₃ (Aldrich, 99.9%). The solutions were stirred at room temperature for 1 h, placed in dialysis tubing, and exhaustively dialyzed against water until the wash solutions tested negative for free Gd³⁺ with xylenol orange indicator. After the products were isolated by rotary evaporation and lyophilization, the compounds

were analyzed by inductively coupled plasma emission spectroscopy (ICP) and elemental analysis. The solids were then dissolved in water and dialyzed for 48 h against 0.1 M EDTA at room temperature followed by dialysis against water. The final product was isolated by rotary evaporation of the dialysis bag contents followed by lyophilization.

For typical preparations of the metal complexes, elemental analysis and ICP analysis results were obtained, and the results were compared with those calculated for $Gd_x(\text{attached DTPA unit})_y(\text{average esterified glycopyranose unit})_1$ or $Gd_x(\text{attached DTPA unit})_y(\text{average esterified fructofuranose unit})_1$. These formulae were derived by fit of the elemental analysis data. **GdDTPA-dextran 9400**: Anal. Calcd for $Gd_{0.36}(C_{14}H_{17}N_3O_9)_{0.36}(C_6H_{11.21}O_{6.04}) \cdot 0.3H_2O$: Gd, 15.06; C, 35.28; H, 4.81; N, 4.02. Found: Gd, 15.4 ± 0.4 ; C, 35.16; H, 5.18; N, 3.92. **GdDTPA-dextran 40 200**: Anal. Calcd for $Gd_{0.31}(C_{14}H_{17}N_3O_9)_{0.36}(C_6H_{11.06}O_{5.85}) \cdot 0.4H_2O$: Gd, 13.30; C, 36.19; H, 4.95; N, 4.13. Found: Gd, 13.7 ± 0.6 ; C, 36.52; H, 5.44; N, 4.03. **GdDTPA-dextran 70 800**: Anal. Calcd for $Gd_{0.36}(C_{14}H_{17}N_3O_9)_{0.36}(C_6H_{10.83}O_{5.75}) \cdot 0.8H_2O$: Gd, 14.91; C, 34.92; H, 4.92; N, 3.98. Found: Gd, 14.6 ± 0.5 ; C, 35.11; H, 5.43; N, 4.00. **GdDTPA-inulin**: Anal. Calcd for $Gd_{0.52}(C_{14}H_{17}N_3O_9)_{0.57}(C_{5.5}H_{9.02}O_{5.11}) \cdot 2.0H_2O$: Gd, 17.24; C, 31.60; H, 4.82; N, 5.05. Found: Gd, 17.16 ± 1.43 ; C, 31.77; H, 4.77; N, 4.90.

For a typical preparation of the metalated dextran 487 000 conjugate the elemental and ICP analysis results for **GdDTPA-dextran 487 000** were as follows. Calcd for $Gd_{0.04}(C_{14}H_{17}N_3O_9)_{0.06}(C_6H_{11.23}O_{6.05}) \cdot 0.1H_2O$: Gd, 2.99; C, 39.02; H, 5.96; N, 1.20. Found: Gd, 2.6 ± 0.3 ; C, 39.02; H, 6.17; N, 1.02. For the conjugate product in which the highly loaded DTPA-dextran 487 000 was used (prepared by modification of the general method) the analyses was as follows. Anal. Calcd for $Gd_{0.78}(C_{14}H_{17}N_3O_9)_{0.79}(C_6H_{10.50}O_{6.05}) \cdot 1.5H_2O$: C, 32.92; H, 4.36; N, 5.33. Found: C, 32.40; H, 4.59; N, 5.34. The product could not be evaluated by ICP analysis as it was too insoluble in deionized water for solution preparation.

Characterization of Contrast Media. All high-performance liquid chromatography (HPLC) experiments were conducted with pH = 7.0 phosphate buffer of 0.1 M ionic strength as the eluting solvent. A Waters Model 6000A solvent delivery system was used with a Waters Protein-Pac 125 column. Detection was at 230 nm and a flow rate of 0.5 mL/min was used for all elutions. One-milliliter fractions of eluting solution were obtained for pooling and carbohydrate analysis.

A series of blanks were prepared for HPLC analysis for comparison with the esterified polysaccharides. The unmodified polysaccharides were heated under identical reaction conditions but without the presence of the cyclic anhydride or zinc chloride. The polysaccharides were isolated, dissolved in buffer with free DTPA present (to provide a reference elution peak), and analyzed by HPLC.

A carbohydrate assay of the fractions was used to produce polysaccharide elution profiles by the reaction of 1-mL aliquots of the eluent with 1 mL concentrated sulfuric acid in the presence of 20 μ L of 80% phenol (31). Solution absorbances at 490 nm (IBM Model 9430 spectrophotometer) were recorded within 1 h of preparation and results were superimposed on the HPLC elution-absorbance profiles for each sample.

The mass percent gadolinium in aqueous samples was determined with ICP (Perkin-Elmer PlasmaII emission spectrometer) with solutions that contained approximately 200 ppm Gd^{3+} from each of the polysaccharide complexes

in deionized water. Infrared spectroscopy (Nicolet 5DXB FTIR) of the esters and their respective Gd^{3+} complexes were obtained as Nujol mulls.

Potentiometric titrations were conducted at 25.0 °C with a pH meter (Orion Research Digital pH/Millivolt Meter 611) and a calibrated semimicro combined pH electrode (Orion Research gel filled). All solutions were purged with argon for $1/2$ h prior to use. Solutions (100 mL) containing from 0.12 to 0.17 mmol of DTPA or esterified DTPA were prepared in 0.1 M KNO_3 . Titration of the esters with a standard solution of 18.8 mM Gd^{3+} in 0.01 M HNO_3 was used to prepare the metalated complexes in solution for subsequent potentiometric titration. The mole ratio of Gd^{3+} added per DTPA moiety was 1:1. The titration was conducted with 0.100 M KOH and constant ionic strength was maintained with KNO_3 . Approximate $\log K_a$ values for the ligands were obtained by using the computer program PKAS (32), and refinement of these values and the approximated thermodynamic stability constants for the metal complexes was achieved with the computer program BEST (32).

Kinetic decomposition studies to determine ester hydrolysis stability for each of the GdDTPA esters were conducted at 37.0 ± 0.1 °C. Solutions containing 30 mM GdDTPA in the dextran complexes were prepared in pH = 7.4 phosphate buffer of 0.15 M ionic strength and placed in a water bath maintained at 37.0 °C for 4 days. Portions of each solution were removed at regular intervals and analyzed by HPLC using pH = 7.4 phosphate buffer at 0.15 M ionic strength to elute the samples. HPLC detection was at 235 nm. The relative areas under the curves in each elution profile for the intact (elution peak for GdDTPA-dextran) and hydrolyzed esters (elution peak for GdDTPA) were used to calculate the percent decomposition.

NMR Relaxation Studies. T_1 relaxivities were assessed by the inversion recovery technique at 25 °C using a 100-MHz JOEL Fourier transform NMR. Solutions of a range of gadolinium concentrations in pH = 7.4 phosphate buffer, ionic strength of 0.15 M, were prepared, and the gadolinium content was determined by ICP analysis. At internal coaxial reference tube containing D_2O and methanol was used. The pulse sequence used was 180° followed by variable time τ then 90° . A minimum of 10 τ values were used per sample and the longer τ value (1 s) was a minimum of 7 times the T_1 of the sample. The samples were scanned four times over a 500-MHz range with 4096 data points collected per scan (4.09 s/scan), and an average plot was obtained for each τ value. Solutions of GdDTPA, GdEDTA, buffer alone, and buffer with unmodified polysaccharides at concentrations comparable with that present in the GdDTPA-polysaccharide solutions were prepared and evaluated. Solutions containing the gadolinium complexes with concentrations of unmodified dextran comparable with the esterified-dextran complex solutions were similarly prepared and evaluated. The raw data (water proton signal intensity and τ values) were analyzed as described by Brown and Johnson (33) and relaxivity plots of $1/T_1$ vs gadolinium concentration were obtained. Relaxivities (R_1 in $mM^{-1} s^{-1}$) were obtained from linear least squares determination of the slopes of $1/T_1$ vs gadolinium concentration plots.

In Vitro Phantom Studies. Phantom solutions were prepared in deionized water. Solution concentrations of GdDTPA-polysaccharides and GdDTPA (Magnevist, Berlex Imaging) ranging from 0.33 to 33.3 mM were studied. A tube containing deionized water alone was used as a standard. A General Electric Sigma (Milwaukee, WI) 1.5

T (63.91-MHz proton Larmor frequency) clinical MR imager with a standard knee coil was used. To use the gray scale as fully as possible without data truncation, the receiver attenuation was adjusted manually before each scan acquisition (manual prescan) to maximize signal intensity at 70–75% of the dynamic range. Signal intensity values for various pulse sequences were therefore in arbitrary units and could not be compared directly with each other. The raw data (ROI (region of interest) intensities and their standard deviations) were normalized by the calculation of relative intensity for each sample. The relative intensity = $ROI_{\text{sample}}/ROI_{\text{standard}}$, where the standard was the water phantom. The pulse sequences evaluated were T_1 and T_2 weighted spin echo ($T_R/T_E = 300/20$ and $2500/80$, respectively).

RESULTS AND DISCUSSION

Syntheses. The synthesis of GdDTPA-polysaccharides involved three steps: preparation of a reactive anhydride of DTPA, reaction of the anhydride with the polysaccharide in a suitable anhydrous mixed-solvent system under conditions that did not result in polysaccharide degradation, and metalation of the DTPA-esterified polysaccharide with gadolinium(III).

HPLC was used following all esterification reactions to evaluate the extent of esterification of the polysaccharide, evaluate the product purity following dialysis, and evaluate the integrity of the polysaccharide following reaction. The extent of esterification was determined from the relative areas of the HPLC elution profiles for the esterified product relative to the unreacted DTPA acid. This procedure is convenient for polysaccharides since they do not absorb at the detection wavelength.

The percentages of ethyl and isobutyl mixed anhydrides of DTPA that react under various reactions conditions are shown in Table I. The results strongly suggest that homogeneous reaction conditions are required for high reactivity of the anhydrides with the polysaccharides. The following additional observations were made: (1) solvents that provided homogeneous reaction conditions for reactions involving inulin did not necessarily provide the same for dextran preparations; (2) the activation of the polysaccharides with *n*-butyllithium did not provide reproducible results; (3) inulin, with a much greater number of primary alcohol functions available for esterification relative to glucopyranose based polysaccharides, reacted to a significantly greater extent than dextran 9400 under the same reaction conditions. The moderate heating of either the isobutyl or ethyl mixed anhydride with dextran in a 1:1 volume ratio of pyridine and formamide in the presence of $ZnCl_2$ resulted in significant esterification as shown in Table I. The zinc(II)-catalyzed reaction provided a calculated degree of loading of approximately 0.2 mol of DTPA/mol of repeating unit of the polysaccharide.

The use of a mixture of anhydrous pyridine and formamide results in homogeneous reaction conditions for the esterification of dextrans (34) and inhibits the competitive hydration of the cyclic anhydrides encountered in aqueous media. The degree of DTPA conjugation was also significantly affected by the presence of $ZnCl_2$ in the reaction mixture. When added to the solvated polysaccharide before the addition of the reactant anhydride, $ZnCl_2$ resulted in a 30-fold increase in the level of DTPA loading relative to when no zinc was present. Based on the yield of ester product formed, the calculated turnover number for the $ZnCl_2$ catalyst is on the order of 10^3 . The mechanism by which the $ZnCl_2$ accelerates the esterifi-

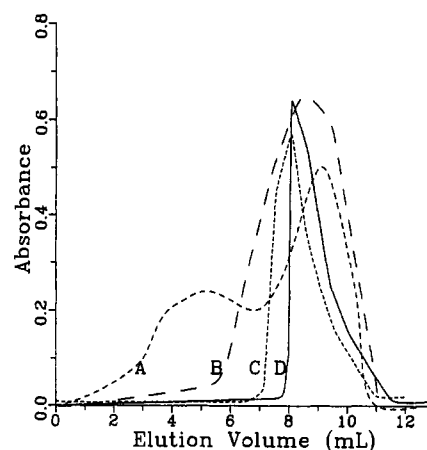


Figure 1. HPLC elution profiles for dextran 9400 from sugar assay (solid line, D), dextran 9400 after reaction with prepared cyclic anhydride in the presence of trace quantities of trifluoroacetic anhydride (dashed line, B), and dextran 9400 after reaction with dicyclic anhydride (dashed line, A) and as prepared by optimized method developed in this work (dashed line, C).

cation may involve Lewis acid catalysis or some other unknown mechanism.

As indicated in Table II, the highest level of DTPA conjugation to polysaccharides without chromatographic evidence for cross-linking was observed for products obtained from the reaction of an anhydride prepared by using a 1:3.2 mol ratio of DTPA to acetic anhydride in 1:1 volume ratio of pyridine and formamide with $ZnCl_2$ present. These reaction conditions were used subsequently for all large-scale preparations of DTPA-esterified polysaccharides. The DTPA cyclic anhydride prepared in this fashion was a mixture containing both dicyclic and monocyclic anhydride as supported by infrared carbonyl stretching frequencies of 1821, 1772, 1758, and 1640 cm^{-1} . The two higher frequencies are attributed to characteristic anhydride carbonyl stretching frequencies ($-C(O)-O-C(O)-$) and the lowest wavenumber represents the central carboxyl group carbonyl stretch ($-C(O)OH$) (35). The band at 1758 cm^{-1} is assigned as a terminal carboxyl group stretch (35) ($-C(O)OH$) that has been shifted in energy relative to that of DTPA at 1738 cm^{-1} .

As shown in Table II, a high percentage of the anhydride also reacted when the commercially available dicyclic anhydride was used to esterify dextran and inulin in 1:1 volume ratio of pyridine and formamide in the presence of $ZnCl_2$; however, HPLC elution band broadness indicated that significant cross-linking had occurred (chromatogram A in Figure 1). This result is consistent with the work of Gibby et al. (23), where the use of the dicyclic anhydride to prepare highly cross-linked products resulted in considerable elution-band broadness on a Sephacryl 400 column. A similar result, shown as B in Figure 1, was observed when the prepared mixture of cyclic anhydrides was allowed to react with the polysaccharides in the presence of trace quantities of trifluoroacetic anhydride (36). In contrast, no chelate cross-linking of the esterified polysaccharides prepared by the "optimized procedure" was detected by HPLC chromatograms (C in Figure 1), which showed neither band broadness nor distinctly separate peaks at lower elution volumes relative to the unmodified polysaccharides.

The DTPA-esterified dextrans of 9400, 40 200, and 70 800 average molecular weight are water soluble, and several preparations by the optimized procedure resulted in levels of loading averaging 0.38 ± 0.05 mol of DTPA/mol of repeating glucopyranose unit. The optimized es-

Table III. Infrared Carbonyl Frequencies for DTPA, DTPA-Polysaccharide Conjugates, and Gadolinium Complexes

compound	wavelength, ^a cm ⁻¹		
DTPA	1630	1696	1737
DTPA-inulin	1626		1734
DTPA-dextran 9400	1639		1737
DTPA-dextran 40 200	1631		1737
DTPA-dextran 70 800	1628		1736
DTPA-dextran 487 000	1628		1738
H ₂ GdDTPA	1581	1704	
GdDTPA-inulin	1596	1700	1738
GdDTPA-dextran 9400	1606	1696	sh
GdDTPA-dextran 40 200	1598	sh	1737
GdDTPA-dextran 70 800	1594	1702	1723
GdDTPA-dextran 487 000	1602	sh	sh

^a Sh = shoulder of lower wavenumber absorption band.

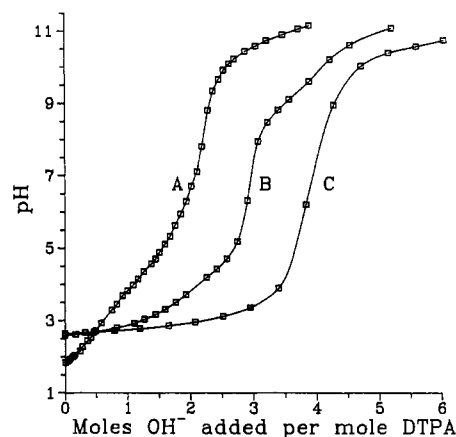
terification method produced DTPA-dextran 487 000 with an average of 0.10 ± 0.02 mol of DTPA/mol of repeating glucopyranose unit. A modification in the method was applied to subsequent preparations involving dextran 487 000, wherein the heated reactants were cooled to room temperature and allowed to stir for 30 h prior to product isolation. This procedure resulted in the reproducible production of substantially higher levels of loading (0.80 ± 0.06 mol of DTPA/mol of glucopyranose repeating unit). The resulting product was, however, considerably less water soluble than the product prepared by the optimized method.

On the basis of elemental analysis combined with ICP analysis, the metalated dextran esters contain an average of 0.38 ± 0.06 mol of GdDTPA attached/mol of glucopyranose unit in dextrans of 9400, 402 000, and 70 800 average molecular weight and 0.52 ± 0.08 mol of DTPA/mol of fructofuranose repeating unit in the inulin conjugate. The conjugates contain an average of 1.00 ± 0.04 mol of Gd³⁺/mol of DTPA. Following dialysis against 0.1 M EDTA, the mass percent gadolinium in the GdDTPA-dextran 9400 and 40 200 complexes was not altered more than 0.5%.

The level of loading of GdDTPA on dextrans of up to 70 800 average molecular weight is roughly 10 times that obtained by Ranney (24), who prepared the conjugate by the reaction of the bisanhydride of DTPA with dextran 70 000 in aqueous media. The level of loading is also more than twice that reported for Gibby's (23) preparations, which involved the synthesis of a mixture of cross-linked products from the bisanhydride reaction with dextran 17 000, 77 000, or 150 000 in anhydrous media. High loading is a desirable goal for macromolecule-bound contrast agents as plasma expansion is minimized (37). For the present conjugates, the average molecular weight per gadolinium is only 13% greater than that of monomeric GdDTPA.

Infrared Spectroscopy. The infrared carbonyl stretching frequencies of the complexes and the nonmetalated DTPA-polysaccharide esters in the present work were compared with that of GdDTPA and DTPA. As shown in Table III, the stretching frequencies of the DTPA-polysaccharide esters are nearly identical with those of DTPA. Similarities of carbonyl stretching frequencies for GdDTPA and the GdDTPA-polysaccharides is consistent with chelation of Gd³⁺ by the DTPA-esterified polysaccharides.

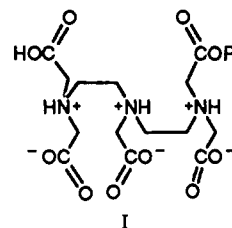
Potentiometric Titrations. Further evidence to support the lack of significant cross-linking in the DTPA-esterified dextrans as synthesized by the optimized method was obtained through potentiometric titration studies. As shown in Figure 2, DTPA exhibits a sharp inflection at 3

**Figure 2.** Potentiometric titration at 25.0 °C with 0.1 M KOH of DTPA-esterified dextran (A), DTPA (B), 1:1 Gd:DTPA-dextran (C).**Table IV. Acid Dissociation Constants for DTPA-Dextrans^a and Propyl Esters of DTPA^b**

	DTPA-dextran ^a	DTPA-PE ₁ ^b	DTPA-PE ₂ ^b
pK ₁	10.0	9.8	9.6
pK ₂	6.7	6.6	4.8
pK ₃	4.8	3.8	3.6
pK ₄	1.7	1.8	

^a Obtained by potentiometric titration (0.1 M KNO₃, 25.0 °C) in this work. All values are ± 0.1 . ^b Obtained by A. D. Sherry, et al. (1988) *Mag. Reson. Med.* 8, 180. All values are ± 0.1 , determined potentiometrically (0.1 M NaCl, 25 °C). Monopropyl and dipropyl esters of DTPA are DTPA-PE₁ and DTPA-PE₂, respectively.

mol of OH⁻ added/mol of acid function and a less definite inflection between 3 and 5 mol of OH⁻/mol of acid function (38). The potentiometric behavior of the free acid has been explained on the basis of the assumed trizwitterionic nature of the ligand in solution as shown in I (R = H in DTPA or saccharide ester in DTPA-dextran).



In the mole ratio (mol of OH⁻/mol of acid function) interval from 0 to 3, two carboxyl protons and one ammonium proton are removed, and the remaining ammonium protons are removed in the interval between 3 and 5 equiv (35). In the presence of a 1:1 mole ratio of Gd³⁺ to DTPA, the single sharp inflection at 5 mol of OH⁻/mol of acid function represents the neutralization of 5 mol of hydronium ion displaced by ligand chelation with 1 mol of Gd³⁺ (18).

All of the dextran-modified ligands in this work exhibited inflections at 2 mol of OH⁻/mol of acid function (Figure 2). Computer fitting of the potentiometric data yields values for pK_n (n = 1–4, Table IV). In the presence of 1:1 molar ratio of Gd³⁺ to dextran-conjugated DTPA, 4 mol of hydronium ions are neutralized in the titration and this represents the displacement of 4 mol of hydronium ions/mol of Gd³⁺ chelated. This result strongly suggests that the DTPA-esterified dextrans produced in this work are not significantly cross-linked since a sharp potentiometric inflection at 3 equiv of base would be expected for 1:1 Gd³⁺:DTPA-dextran, in cross-linked products (assuming

diester cross-link). However, a relatively small amount of cross-linking would not be detected in this type of experiment.

The observed absence of significant metal transfer to EDTA in dialysis with the prepared polymeric complexes suggests that the level of loading by DTPA on the polysaccharides is preventing significant nonspecific metal binding to the polysaccharides (39, 40). The thermodynamic stability constant for the GdDTPA-dextran, as obtained from the potentiometric titrations and assuming independent metal binding by the chelating groups, was 18.0 ± 0.2 ($\log K$ for $\text{Gd}^{3+} + \text{L}^{4-} \rightarrow \text{GdL}^-$). Neither Gibby et al. (23) nor Ranney et al. (24) reported stability constants for their products; however, recent work by Sherry et al. (41) involving the assessment of thermodynamic stabilities for mono- and dipropyl esters of DTPA resulted in $\log K$ values of 18.91 and 16.30, respectively. The higher stability constant for the DTPA-dextran complexes compared to that of the dipropyl ester of DTPA (41) and the comparisons for the free ligands in Table IV suggest that DTPA is monoesterified in the conjugates; however, the observed K value for DTPA-dextran is somewhat less than that observed for the monopropyl ester of DTPA, so no firm conclusions can be drawn. Further comparison studies are needed for cross-linked products prepared by the method of Gibby et al. (23) and non-cross-linked products obtained by the mixed-anhydride method to assess the trends in stability constants for polysaccharide conjugates.

Ester Hydrolysis. The nature of the bond between metal chelate and carrier is an important issue in the development of macromolecule-bound contrast agents since the rate of bond cleavage *in vivo* will to a large extent determine the biological fate of the agent. The covalent attachment of GdDTPA to proteins such as bovine serum albumin (BSA) has been via the formation of stable peptide bonds between the carrier and metal chelate (42). The dextrans of the complexes reported here are covalently attached to the metal chelate by a less hydrolytically stable ester linkage. Lewis acid assisted ester hydrolysis has been studied (43), and the effect of different lanthanide ions, including Gd³⁺, has been evaluated for amino acid esters of diacetic acids (44). The assumed mechanism for these metal-promoted hydrolysis reactions involves OH⁻ attack at the ester carbonyl group with carbonyl activation by metal binding to the ester carbonyl oxygen. Alternatively, metal-bound hydroxide may act as the nucleophile (43).

The half-lives for the ester bonds in the dextran conjugates were obtained from slopes of logarithmic decomposition plots (first order in conjugate concentration). The half-life of GdDTPA-dextran 70 800 (21 h) was significantly shorter than the non-metalated DTPA-dextran 70 800 ester (85 h). The presence of free GdDTPA in solutions containing the GdDTPA-dextran complexes did not decrease the half-life of the complexes, and these results suggest that gadolinium chelated by the conjugated DTPA is necessary for metal-assisted ester hydrolysis to occur. In studies of propyl ester models of DTPA, Gerald et al. (45) presented nuclear magnetic resonance dispersion (NMRD) evidence for the metal coordination of the ester carbonyl oxygen in gadolinium complexes, and such an interaction is consistent with acceleration of ester hydrolysis by metal-carbonyl interaction (44). No evidence for ester carbonyl-metal coordination in the present work was obtained, as an expected stretching mode shift to lower frequencies of the metal-bound ester carbonyl relative to the free ester carbonyl (32) could not be ascertained from the broad infrared peaks.

Table V. T_1 Relaxivities at 100 MHz^a

compound	relaxivity, (mM s) ⁻¹
GdDTPA	3.8 ± 0.1
GdDTPA-inulin	8.3 ± 1.0
GdDTPA-dextran 9400	8.7 ± 0.6
GdDTPA-dextran 40 200	8.1 ± 0.3
GdDTPA-dextran 70 800	7.1 ± 0.7
GdDTPA-dextran 487 000	5.8 ± 0.5

^a 1–5 mM Gd solutions.

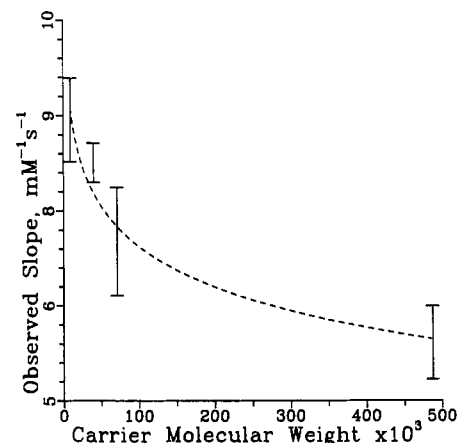


Figure 3. Plot of dextran carrier average molecular weight versus T_1 relaxivity at 100 MHz for the GdDTPA-dextran complexes.

Relaxivities of the New Complexes. As shown in Table V, the T_1 relaxivities of the GdDTPA-polysaccharides ranged from 1.5 to 2.3 times that of GdDTPA at 100 MHz (25 °C), a lower increase than found for relaxivities reported for other covalently attached GdDTPA-macromolecules (19). Possible explanations for the observed increased relaxivities, relative to GdDTPA, include (i) an increase in rotational correlation time (possibly due to microviscosity) (20) by virtue of the attachment of the metal chelate to the polymer, (ii) an increase in the number of inner sphere coordinated water molecules and/or their rate of exchange with bulk water molecules (46) as a result of reduction in the denticity of the chelate upon esterification, (iii) an increase in the number of outer sphere coordinated water molecules and/or their rate of exchange (47) via entrapment by the polysaccharide, or (iv) some combination of all these effects. Additionally, the mechanism of inner sphere water ligand exchange with bulk water molecules may be significantly altered relative to GdDTPA by the presence of hydrogen bonding between the coordinated water molecules and the macromolecular carrier (48).

The observed relaxivities decreased with increasing dextran carrier molecular weight (Figure 3). As shown in Figure 4, the polysaccharide alone made no significant contribution to the solvent relaxation over the concentration range (less than 200 mM glucopyranose) used in the T_1 studies and increased solvent relaxation to $>1 \text{ s}^{-1}$ only at high concentrations. It was therefore concluded that overall solution viscosity did not contribute to this apparent trend nor could the observed increased relaxivities, relative to GdDTPA, be attributed to solution viscosity effects.

The GdDTPA-dextran complexes exhibited significant reductions in relaxivity in the presence of equimolar concentrations of unmodified dextran (Table VI). This reduction was not observed for GdDTPA but was observed for GdEDTA solutions in the presence of free dextran at concentrations equal to bound-dextran concentrations in the GdDTPA-dextran solutions (Table VI). The results

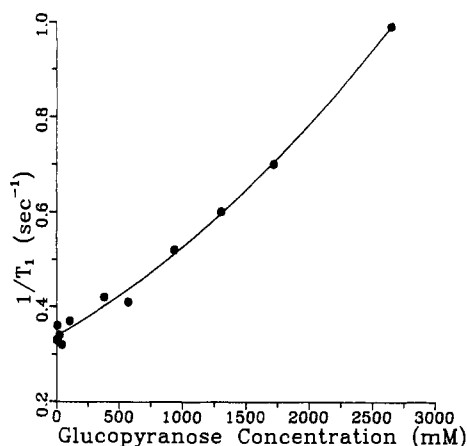


Figure 4. Plot of glucopyranose concentration (in dextran 9400) versus solution T_1 relaxivity in pH = 7.4 phosphate buffer, 0.15 M ionic strength, 100 MHz, 25 °C.

Table VI. Effect of Free Polysaccharide on T_1 Relaxivities of Gd^{3+} Chelates

compound	T_1 relaxivity, (mM s) $^{-1}$
GdDTPA-dextran 40 200	8.1 ± 0.3
GdDTPA-dextran 40 200 with free dextran	5.2 ± 0.1
GdDTPA	3.8 ± 0.1
GdDTPA with free dextran	4.4 ± 0.5
GdEDTA	4.6 ± 0.1
GdEDTA with free dextran	3.3 ± 0.1

suggest that the GdDTPA-dextran complexes may be better emulated with respect to metal-polysaccharide interactions by GdEDTA, which has two inner sphere coordinated water molecules (49). The GdEDTA complex readily exchanges coordinated water molecules for other available ligands (15), and it is possible that the observed effect free dextran has on GdEDTA and GdDTPA-dextran solutions may be due to coordinative displacement of water molecules by the hydroxyl groups of the polysaccharide. The observations can also be explained by hydrogen bonding between the coordinated water molecule(s) and the polysaccharide. The rate of exchange between ligand and bulk water molecules can be significantly reduced by hydrogen-bonding interaction of this nature (48).

In Vitro Imaging Results (Phantom Studies). The phantom studies were undertaken to provide a comparison to the NMR T_1 relaxivity measurements and ascertain the concentration dependence of signal intensity for the new complexes compared with GdDTPA (Magnevist, Berlex Imaging) using various pulse sequences. In selecting a concentration range for study, the following considerations were applied. The average blood volume of a 2-kg rabbit is 60 mL/kg and a dosage of 0.2 mmol of Gd^{3+} /kg (twice the recommended dosage of GdDTPA) results in an intravascular concentration of 3.3 mM, assuming that the contrast agent is distributed only in the intravascular space. Therefore, gadolinium concentrations in the range 0.33–33.0 mM were used to provide data with potential relevance to in vivo applications.

In T_1 weighted images, the GdDTPA-dextran complexes all exhibited suppression in relative signal intensity (sample signal intensity/solvent signal intensity) at concentrations greater than 3.33 mM relative to GdDTPA (Figure 5). This type of effect has been attributed (50) to the counteracting effects by macromolecular complexes on solvent T_2 . In spin echo experiments there is a direct proportionality between signal intensity and T_1 and an inverse propor-

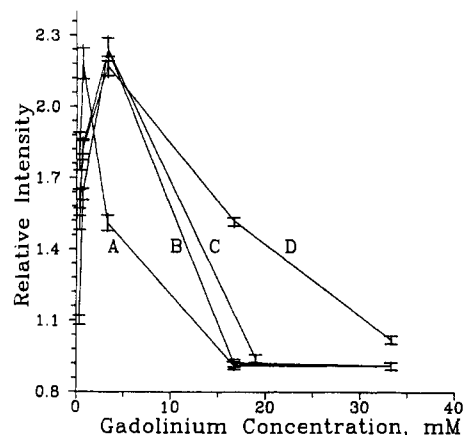


Figure 5. Plot of relative signal intensity versus gadolinium concentration for phantom solutions of GdDTPA-dextran 9400 (A), GdDTPA-dextran 70 800 (B), GdDTPA-dextran 487 000 (C), and GdDTPA (D) using T_1 weighted (SE, 300/20) pulse sequence.

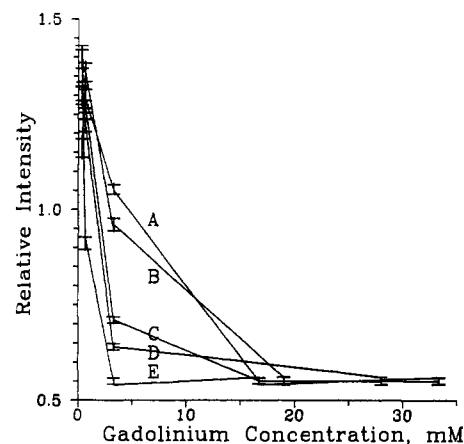


Figure 6. Plot of relative signal intensity versus concentration for phantom solutions containing GdDTPA (A), GdDTPA-dextran 487 000 (B), GdDTPA-dextran 70 000 (C), GdDTPA-dextran 40 200 (D), and GdDTPA-dextran 9400 (E) using T_2 weighted (SE, 2500/80) pulse sequence.

tionality between signal intensity and T_2 (51). The results indicate that at concentrations sufficiently greater than 3.33 mM, the contribution to signal intensity by paramagnetic effect on the solvent T_2 outweighs the T_1 contribution.

A trend in T_1 relaxivity for the samples was obtained from the relative signal intensities (sample signal intensity/solvent signal intensity) for each of the T_1 weighted phantoms at concentrations up to 3.33 mM, assuming that the T_2 of these solutions was equal to pure solvent T_2 . At low concentrations (less than or equal to 3.33 mM) the T_1 weighted phantoms (at 63 MHz) exhibited the same trend in T_1 relaxivity as observed in the 100-MHz T_1 relaxivity studies (i.e. reduction in T_1 relaxivity with increased carrier molecular weight).

The T_2 weighted phantom study resulted in the rapid increase of relative signal intensity up to concentrations of 3.33 mM for the GdDTPA-dextran compounds and Magnevist (Figure 6). This trend was followed by a more rapid decrease in signal intensity for the complexes relative to Magnevist with increasing concentration. With T_1 values approximated from the T_1 weighted images, the calculated solvent T_2 decreased less rapidly with increasing concentration of the higher molecular weight dextran-conjugated gadolinium complexes than the lower molecular weight complexes. The apparent inverse relationship between dextran carrier average molecular weight and T_1 relaxivity by the complexes was not observed for the cross-

linked products reported in the work of Gibby et al. (23). Since there is generally increased branching of the polysaccharide as the molecular weight increases (52), it is speculated that the observed trend of decreased T_1 with increased dextran molecular weight observed here is related to the structural differences between various molecular weights of the dextrans.

CONCLUSIONS

The synthetic method developed in this work for the production of polysaccharide conjugates of GdDTPA results in reproducibly higher levels of conjugation via ester linkage of the paramagnetic chelate on the carrier than previously reported methods (23–25). The method resulted in no apparent degradation of the polysaccharide, and no evidence for significant chelate-based polysaccharide cross-linking was observed. The conjugates are water soluble, exhibit carbonyl stretching frequencies indicative of gadolinium(III) chelation, and, along with their respective nonmetalated chelates, exhibit potentiometric behavior consistent with products in which only one of the carboxyl functions of DTPA has been modified for the majority of conjugated chelates.

The thermodynamic stability of the new complexes is somewhat lower than that of GdDTPA. Although high thermodynamic stability may suggest low in vivo toxicities of metal chelates, there is no necessary correlation between thermodynamic stability of metal complexes and toxicity (53). The GdDTPA–dextran complexes undergo ester hydrolysis (producing monomeric GdDTPA) considerably faster than the nonmetalated chelates. Although the toxicity of the new complexes has not been assessed, metal-promoted hydrolysis may be important to the excretory pathway these new compounds exhibit in vivo. The in vitro T_1 relaxivities of the polysaccharide complexes are significantly greater than that of GdDTPA at 100 MHz and appear to be inversely dependent on the average molecular weight of the carrier polysaccharide.

GdDTPA–dextrans produced in this work have been applied to in vivo imaging of normal rabbits, and results of these studies will be described in detail elsewhere (54). In general, the contrast agents did not exhibit any apparent toxic side effects. The contrast agents showed the expected blood-pool persistence and are potentially useful vascular imaging agents. Gibby and co-workers (26) and Wikstrom et al. (25) have reported similar observations in vivo studies of the cross-linked polysaccharide contrast agents in rats. Observations thus far suggest that the basic Gd–chelate–polysaccharide structure may lead to useful MRI contrast agents that can be produced in a variety of molecular weight formulations. Chelating agents with lower tendency to release Gd³⁺ in vivo (e.g., DOTA) could be used in dextran conjugates to counteract the effects of a longer in vivo residence time.

ACKNOWLEDGMENT

Partial support of this project was provided by the Florida Division of the American Cancer Society (Hazel C. M. Kerr Research Grant) and the Division of Sponsored Research of the University of Florida. The ICP instrument was purchased with a Biomedical Research Support Grant funded by the National Institutes of Health and administered by the Division of Sponsored Research, University of Florida. Imaging studies were funded by internal grants from the Department of Radiology, University of Florida College of Medicine.

LITERATURE CITED

- (1) Damadian R. (1971) Tumor detection by nuclear magnetic resonance. *Science* 171, 1151.
- (2) Brant-Zawadzki, M., Norman, D., Newton, T. H., Kelly, W. M., Kjos, B., Mills, C. M., Dillon, W., Sobel, D., and Crooks, L. E. (1984) Magnetic resonance of the brain: the optimal screening technique. *Radiology* 152, 71.
- (3) Partain, C. L., James, A. E., Rollo, F. D., and Price, R. R. (1983) *Nuclear Magnetic Resonance (NMR) Imaging*, Saunders, Philadelphia.
- (4) Gadian, D. G., Payne, J. A., Bryant, D. J., Young, I. R., Carr, D. H., and Bydder, G. M. (1985) Gadolinium–DTPA as a contrast agent in MR imaging—theoretical projections and practical observations. *J. Comput. Assist. Tomogr.* 9, 242.
- (5) Graif, M., and Steiner, R. E. (1986) Contrast enhanced magnetic resonance imaging of tumours of the central nervous system: a clinical review. *Brit. J. Radiol.* 59, 865.
- (6) Runge, V. M., Schoerner, W., Niendorf, H. P., Lanai, M., Koehler, D., Claussen, C., Felix, R., and James, A. E. (1985) Initial clinical evaluation of gadolinium–DTPA for contrast enhanced magnetic resonance imaging. *Magn. Reson. Imaging* 3, 27.
- (7) Brasch, R. C., Weinmann, H. J., and Wesbey, G. E. (1984) Contrast-enhanced NMR imaging: animal studies using gadolinium–DTPA complex. *Am. J. Roentgenol.* 142, 625.
- (8) Carr, D. H., Brown, J., Bydder, G. M., Steiner, R. E., Weinmann, H. J., Speck, U., Hal, A. S., and Young, I. R. (1984) Gadolinium–DTPA as a contrast agent in MRI: initial clinical experience in 20 patients. *Am. J. Roentgenol.* 143, 215.
- (9) Runge, V. M., Clanton, J. A., Herzer, W. A., Gibbs, S. J., Price, A. C., and Partain, C. L., James, A. E. (1984) Intravascular contrast agents suitable for magnetic resonance imaging. *Radiology* 153, 171.
- (10) Carr, D. H., Brown, J., Leung, A. W.-L., and Pennock, J. M. (1984) Iron and gadolinium chelates as contrast agents in NMR imaging: preliminary studies. *J. Comput. Assist. Tomogr.* 8, 385.
- (11) Widder, D. J., Greif, W. L., Widder, K. L., Edelman, R. E., and Brady, T. J. (1987) Magnetic albumin microspheres: a new MR contrast material. *Am. J. Roentgenol.* 148, 399.
- (12) Weinmann, H. J., Brasch, R. C., Press, W. R., and Wesbey, G. E. (1984) Characteristics of gadolinium–DTPA: a potential NMR contrast agent. *Am. J. Roentgenol.* 142, 619.
- (13) Bino, A., Johnston, D. C., Goshom, D. P., Halbert, T. R., and Steifel, E. I. (1988) $[\text{Cr}_4\text{S}(\text{O}_2\text{CCH}_3)_8(\text{H}_2\text{O})_4](\text{BF}_4)_2 \cdot \text{H}_2\text{O}$: Ferromagnetically Coupled Cr_4S Cluster with Spin 6 Ground State. *Science* 241, 1479.
- (14) Meyer, D., Schafer, M., and Bonnemain, B. (1988) Gd–DOTA, a potential MRI contrast agent: current status of physicochemical knowledge. *Invest. Radiol.* 23 (Suppl. 1), S232.
- (15) Tweedle, M. F., Gaughan, G. T., Hagan, J., Wedeking, P. W., Sibley, P., Wilson, L. J., and Lee, D. W. (1988) Considerations involving paramagnetic coordination compounds as useful NMR contrast agents. *Nucl. Med. Biol.* 15, 31.
- (16) Strich, G., Hagan, P. L., Gerber, K. H., and Slutsky, R. A. (1985) Tissue distribution and MRI spin lattice relaxation in NMR imaging of gadolinium–DTPA. *Radiology* 154, 723.
- (17) Carr, D. H., Brown, J., Bydder, G. M., Weinmann, H. J., Speck, U., Thomas, D. J., and Young, I. R. (1984) Intravenous chelated gadolinium as a contrast agent in NMR imaging of cerebral tumors. *Lancet*. 1, 484.
- (18) Perrin, D. D., Ed., (1979) *Stability Constants of Metal Ion Complexes. Part B: Organic Ligands*, Pergamon Press, Oxford.
- (19) Lauffer, R. B., and Brady, T. J. (1985) $1/T_1$ NMRD profiles of solutions of Mn^{2+} and Gd^{3+} protein–chelate conjugates. *Magn. Reson. Imaging* 3, 11.
- (20) Koenig, S. H., and Brown, R. D. (1987) Relaxometry of magnetic resonance imaging contrast agents. *Magn. Reson. Ann.* 1987, 263.
- (21) Ogan, M., Grodd, W., Paaanen, H., Huberty, J., Revel, D., Eriksson, U., Tozer, T., Sosnovsky, G., White, D., Engelstad, B., and Brasch, R. C. (1985) Approaches to chemical synthesis of macromolecular MR imaging contrast media for perfusion-dependent enhancement (abstract). *Radiology* 157 (P), 100.

- (22) Schmiedl, U., Ogan, M. D., Moseley, M. E., and Brasch, R. C. (1986) Comparison of contrast enhancing properties of albumin-(Gd-DTPA) and Gd-DTPA at 2.0 tesla: an experimental study in rats. *Am. J. Roentgenol.* 147, 1263.
- (23) Gibby, W. A., Bogdan, A., and Ovitt, T. W. (1989) Cross-linked DTPA polysaccharides for magnetic resonance imaging. *Invest. Radiol.* 24, 302.
- (24) Ranney, D. F., Weinreb, J. C., Cohen, J. M., Srikanthan, S., K-Breeding, L., Kulkarni, P., and Antich, P. (1986) Gd-DTPA polymers and microspheres for improved enhancement of liver, solid tumor, and the cardiovascular blood pool. In *Contrast Agents in Magnetic Resonance Imaging, Proceedings of an International Workshop January 1986* (V. M. Runge, C. Clausson, R. Felix, and A. E. James, Jr., Eds.) pp 81-87, Excerpta Medica: San Diego.
- (25) Wikstrom, M., Wang, S. C., White, D. L., Moseley, M. E., Rongved, P., Klaveness, J., and Brasch, R. C. (1989) Gadolinium-labeled dextran as an intravascular MR contrast agent: imaging characteristics in normal rat tissues. *Abstracts*. 1989 Society of Magnetic Resonance in Medicine Meeting, p 533.
- (26) Gibby, W. A., Billings, J., Hall, J., and Ovitt, T. W. (1990) Biodistribution and Magnetic Resonance Imaging of Cross-linked DTPA Polysaccharides. *Invest. Radiol.* 25, 164-172.
- (27) Wenzel, T. J., Ashley, M. E., and Sievers, R. E. (1982) Water-soluble paramagnetic relaxation reagents for carbon-13 nuclear magnetic resonance spectrometry. *Anal. Chem.* 54, 615.
- (28) Krejcarek, G. E., and Tucker, K. L. (1977) Covalent attachment of chelating groups to macromolecules. *Biochem. Biophys. Res. Commun.* 77, 581.
- (29) Eckelman, W. C., Karesh, S. M., and Reba, R. C. (1975) New compounds: fatty acid and long chain hydrocarbon derivatives containing a strong chelating agent. *J. Pharm. Sci.* 64, 704.
- (30) Halpern, S., Stern, P., Hagan, P., Chen, A., Frinke, J., Bartholomew, R., David, G., and Adams, T. (1983) Labeling of monoclonal antibodies with indium-111. In *Radioimmunoimaging and Radioimmunotherapy* (S. W. Burchiel, and B. A. Rhodes, Eds.) pp 197-205 Elsevier Science Publishers, New York.
- (31) Dubois, M., Giles, K. A., Hamilton, J. K., Rebers, P. A., and Smith, F. (1956) Colorimetric method for determination of sugars and related substances. *Anal. Chem.* 28, 351.
- (32) Martell, A. E., and Motekaitis, R. J. (1988) *Determination and Use of Stability Constants*, VCH, New York.
- (33) Brown, M. A., and Johnson, G. A. (1984) Transition metal-chelate complexes as relaxation modifiers in nuclear magnetic resonance. *Med. Phys.* 11, 67.
- (34) Bombardieri, G., Rotilio, G., Crifo, C., and DeMarco, C. (1968) Studies on dextran and dextran derivatives XIV: metal binding properties of succinyl and phthalyl derivatives. *Arch. Biochem. Biophys.* 127, 766.
- (35) Hnatowich, D. J., Friedman, B., Clancy, B., and Novak, M. (1981) Labeling of preformed liposomes with Ga-67 and Tc-99m by chelation. *J. Nucl. Med.* 22, 810.
- (36) Fordyce, C. R. (1945) Cellulose esters of organic acids. *Adv. Carbohydr. Chem.* 1, 309.
- (37) Melton, R. G., Wiblin, C. N., Baskerville, A., Foster, R. L., and Sherwood, R. F. (1987) Covalent linkage of carboxypeptidase G₂ to soluble dextrans—II. *Biochem. Pharmacol.* 36, 113.
- (38) Harder, R., and Chaberek, S. (1959) The interaction of rare earth ions with diethylenetriaminepentaacetic acid. *J. Inorg. Nucl. Chem.* 11, 197.
- (39) Rendleman, J. A., Jr. (1966) Complexes of alkali metals and alkaline-earth metals with carbohydrates. *Adv. Carbohydr. Res.* 21, 209.
- (40) Cox, J. S. G., King, R. E., and Reynolds, G. F. (1965) Valency investigations of iron dextran (imferon). *Nature* 207, 1202.
- (41) Sherry, A. D., Cacheris, W. P., and Kuan, K.-T. (1988) Stability constants for Gd³⁺ binding to model DTPA conjugates and DTPA-proteins: implications for their use as magnetic resonance contrast agents. *Magn. Reson. Med.* 8, 180.
- (42) Hnatowich, D. J., Layne, W. W., and Childs, R. L. (1982) The preparation and labeling of DTPA-coupled albumin. *J. Appl. Radiat. Isot.* 33, 327.
- (43) Hay, R. W., and Morris, P. J. (1976) Metal Ion-Promoted Hydrolysis of Amino Acid Esters and Peptides. In *Metal Ions in Biological Systems*, (H. Sigel, Ed.) Vol 5, Marcel Dekker, New York.
- (44) Leach, B. E., and Angelici, R. J. (1968) Metal-ion catalysis of the hydrolysis of some amino acid ester *N,N*-diacetic acids. *J. Am. Chem. Soc.* 90, 2504.
- (45) Gerald, C. F. G. C., Sherry, A. D., Cacheris, W. P., Kuan, K.-T., Brown, R. D., Koenig, S. H., and Spiller, M. (1988) Number of inner sphere water molecules in Gd³⁺ and Eu³⁺ complexes of DTPA-amide and DTPA-ester conjugates. *Magn. Reson. Med.* 8, 191.
- (46) Lauffer, R. B. (1987) Paramagnetic metal complexes as water proton relaxation agents for NMR imaging: theory and design. *Chem. Rev.* 87, 901.
- (47) Koenig, S. H., Baglin, C., and Brown, R. D. (1984) Magnetic field dependence of solvent proton relaxation induced by Gd³⁺ and Mn²⁺ complexes. *Magn. Reson. Med.* 1, 496.
- (48) Koenig, S. H., and Brown, R. D. (1984) Relaxation of solvent protons by paramagnetic ions and its dependence on magnetic field and chemical environment: implications for NMR imaging. *Magn. Reson. Med.* 1, 478.
- (49) Weinmann, H.-J. (1986) Chelated contrast agents. In *Contrast Agents in Magnetic Resonance Imaging, Proceedings of an International Workshop January 1986* (V. M. Runge, C. Clausson, R. Felix, and A. E. James, Jr., Eds.) pp 19-23, Excerpta Medica: San Diego.
- (50) Koenig, S. H., and Gillis, P. (1988) Transverse relaxation (1/T₂) of solvent proton induced by magnetized spheres and its relevance to contrast enhancement in MRI. *Invest. Radiol.* 23 (Suppl. 1), S224.
- (51) Pykett, I. L., Newhouse, J. H., Buonanno, F. S., Brady, T. J., Goldman, M. R., Kistler, J. P., and Pohost, G. M. (1982) Principles of nuclear magnetic resonance imaging. *Radiology* 143, 157.
- (52) Sandford, P. A. (1979) Exocellular microbial polysaccharides. *Adv. Carbohydr. Chem. Biochem.* 36, 265.
- (53) Cole, W. C., DeNardo, S. J., Meares, C. F., McCall, M. F., DeNardo, G. L., Epstein, A. L., O'Brien, H. A., and Moi, M. K. (1987) Comparative serum stability of radiochelates for antibody radiopharmaceuticals. *J. Nucl. Med.* 28, 83.
- (54) Quisling, R. G., King, C. P., Armitage, F. E., Richardson, D. E., and Mladinich, C., in preparation.
- Registry No.** DTPA dicyclic anhydride, 23911-26-4; DTPA monocyclic anhydride, 106145-40-8; Gd, 7440-54-2; inulin, 9005-80-5; dextran, 9004-54-0; DTPA isobutyl formate anhydride, 92927-81-6; DTPA ethyl formate anhydride, 130434-29-6.

Synthesis and Characterization of Gentiobiose Heptaacetate Conjugate Vaccines That Produce Endotoxin-Neutralizing Antibodies^{1,2}

Apurba K. Bhattacharjee,*† Jerald C. Sadoff,† Hugh Collins,† Alan S. Cross,† Ali H. Khalil,† Marcia M. Bieber,‡ Craig Wright,§ and Nelson N. H. Teng‡

Department of Bacterial Diseases, Walter Reed Army Institute of Research, Washington, DC 20307-5100, Cancer Biology Research Laboratory, Stanford University School of Medicine, Stanford, California 94305, and Univax Biologics, Inc., Rockville, Maryland 20852. Received July 23, 1990

We have prepared aminoethyl (AE), aminopropyl (AP), and aminopentyl (APT) derivatives of gentiobiose heptaacetate (GH). These spacer compounds (AEGH, APGH, APTGH) have been coupled to succinylated diphtheria toxoid (Suc-DT) to produce conjugate vaccines. These conjugates all bind to the anti-lipid A human monoclonal antibody A6(H4C5) in an ELISA binding assay. Rabbits immunized with the APGH conjugate vaccine in either Freund's complete adjuvant or aluminum hydroxide gel produced antibody levels of 5120 and 3600 ELISA units, respectively, compared to an antibody level of less than 20 ELISA units for the prebleed sera. Sera from mice immunized with either the amino-propyl or the aminopentyl conjugate had antibody levels of 5120 and 2560 ELISA antibody units, respectively. These antibodies neutralized endotoxin in a *Limulus* lysate neutralization assay. Protection against the local Schwartzman reaction was demonstrated ($p < 0.05$) in eight out of nine rabbits immunized with the Suc-DT-APGH conjugate vaccine compared to three out of 10 rabbits immunized with the carrier protein Suc-DT. Passive transfer experiments demonstrated that four out of five rabbits receiving immune serum were protected from Schwartzman reaction compared to one out of five rabbits receiving normal serum ($p < 0.1$). These results indicated that epitopes contained in gentiobiose heptaacetate when properly presented as conjugate vaccines were capable of inducing neutralizing antibodies against endotoxin.

Endotoxin is the causative agent for shock in Gram-negative bacteremia. It has been estimated that septic shock is responsible for about 30 000 deaths in the United States every year (1, 2). The problem of treatment is compounded by the increase in antibiotic resistance in these organisms (3, 4).

Attempts have been made to develop vaccines to protect against endotoxic shock. Immunization of animals with Gram-negative bacilli protects them against infection with homologous organisms (5-7). Rough mutants of Gram-negative bacilli contain LPS determinants in their core portion that are shared by most Gram-negative bacteria (8, 9). Immunization with LPS of some rough mutants such as the Re mutant of *Salmonella* and the J5 (Rc) mutant of *Escherichia coli* have been shown to provide cross-protection against challenge with heterologous organisms (10-14). Ziegler et al. (15) have shown that antisera obtained from healthy human volunteers immunized with the J5 mutant lowered mortality of patients from Gram-negative bacteremia and endotoxic shock. Teng et al. (16) have developed a human IgM monoclonal antibody, A6(H4C5), against a J5 LPS epitope. This antibody was shown to react to a wide variety of Gram-negative

organisms in ELISA and with a wide variety of isolated LPS, including a strong reaction with lipid A. In the mouse mucin model of lethal bacteremia this antibody showed significant protection against lethal challenge with *Pseudomonas aeruginosa*, *E. coli*, and *Klebsiella pneumoniae*, but not against the Gram-positive organism *Streptococcus pneumoniae* (16). Protection against the local Schwartzman reaction induced by *E. coli* and *Klebsiella* endotoxin was also demonstrated with this monoclonal antibody. In a recent report DeMaria et al. (17) showed that immunization of human volunteers with vaccines prepared from unheated and boiled *Salmonella minnesota* R595 (Re chemotype) produced antibodies that showed enhanced protective activity in mice against challenge with viable Gram-negative bacilli and endotoxin.

Bieber et al. (Bieber, M. M., Ozguc, M., and Teng, N. N. H., unpublished results) have shown that the binding between human anti-J5 monoclonal A6(H4C5) and lipid A could be inhibited (98%) with gentiobiose octaacetate (a structure similar to the core disaccharide present in lipid A), compared to 80% inhibition with β -glucose pentaacetate and no inhibition with galactose pentaacetate. These results indicated that a 1,6-linked β -glucose disaccharide was required for the antibody binding and that acetate groups fulfilled the requirements for acyl substitution at C2 and C3. We decided to prepare a synthetic vaccine using gentiobiose heptaacetate as the epitope and linking it to carrier proteins through spacer arms of different lengths. In this report we describe the preparation of such conjugate vaccines and the immunogenicity of these vaccines in rabbits and mice. Antisera raised in rabbits were tested for endotoxin-neutralizing activity

* To whom correspondence should be addressed.

† Walter Reed Institute of Research.

‡ Stanford University School of Medicine.

§ Univax Biologics, Inc.

¹ The views of the authors do not purport to reflect the position of the Department of the Army or the Department of Defense.

² In conducting the research described in this paper, the investigators adhered to the *Guide for Laboratory Animal Facilities and Care* as promulgated by the committee of the guide for laboratory animal facilities and care of the institute of laboratory animal resources, National Research Council.

with J5 LPS and for protective activity against local Shwartzman reaction with *E. coli* O6 LPS and *E. coli* 0111: B4 LPS.

EXPERIMENTAL PROCEDURES

2-Aminoethanol, 3-aminopropanol, 5-aminopentanol, gentiobiose octaacetate, silica gel, TLC plates, and 1,4-dioxane were purchased from Sigma Chemical Co. (St. Louis, MO). Diphtheria toxoid and tetanus toxoid were obtained from Massachusetts Biologic Laboratories (Boston, MA). Chloroform, dichloromethane, and ethyl acetate were purchased from Aldrich Chemical Co. (Milwaukee, WI). Phosphatase-labeled anti-human, anti-rabbit, and anti-mouse immunoglobulins were purchased from Kirkegaard and Perry Laboratories (Gaithersburg, MD). HBr (33%) in glacial acetic acid was purchased from Fluka Chemical Corp. (Hauppauge, NY). Succinic anhydride and 1-ethyl-3-[3-(dimethylamino)propyl]-carbodiimide (EDC) were purchased from Pierce Chemical Co. (Rockford, IL). Melting points were recorded with a Fisher Johns melting point apparatus and are corrected.

Preparation of Acetobromogentiobiose. Gentiobiose octaacetate (I; 1 g) was dissolved in dichloromethane (2.5 mL) and 33% HBr in glacial acetic acid (5 mL) was added to this solution. After 45 min at 5 °C, dichloromethane (30 mL) and ice water (30 mL) were added. The organic phase was separated, successively washed with aqueous sodium hydrogen carbonate solution and water, dried (sodium sulfate), and evaporated to dryness. Acetobromogentiobiose II was crystallized from diethyl ether. The crystalline compound gave a single spot on TLC in ethyl acetate/*n*-hexane (2:1) moving slightly faster than gentiobiose octaacetate.

Preparation of 2,3,4,2',3',4',6'-Hepta-O-acetylgentiobioside (AEGH). The acetobromogentiobiose (284 mg) was dissolved in dry chloroform (5 mL), and Drierite (0.5 g) was added followed by 2-aminoethanol (0.2 mL in 0.8 mL of chloroform). The reaction mixture was stirred in the dark at room temperature for 16 h and filtered and the filtrate was washed with ice water (2 × 10 mL), dried (sodium sulfate), and evaporated to dryness. The solid was dissolved into dichloromethane (0.9 mL) and AEGH was purified by chromatography on silica gel using ethyl acetate/ethanol (19:1) as the eluant. The purified AEGH was crystallized from hot ethanol (yield 41%), mp 176–177 °C. Anal. Calcd for C₂₈H₄₀O₁₈N: C, 49.56; H, 5.94; N, 2.06. Found: C, 49.44; H, 6.05; N, 2.10.

3-Aminopropyl 2,3,4,2',3',4',6'-hepta-O-acetylgentiobioside (APGH) was synthesized the same way as described above except that 3-aminopropanol was used in place of 2-aminoethanol (yield 62%). The crystalline APGH had mp 166–167 °C. Anal. Calcd for C₂₉H₄₂O₁₈N: C, 50.25; H, 6.06; N, 2.02. Found: C, 50.31; H, 6.21; N, 1.90.

5-Aminopentyl 2,3,4,2',3',4',6'-hepta-O-acetylgentiobioside (APTGH) was synthesized the same way with 5-aminopentanol as the aglycon (yield 40%). The crystalline APTGH had mp 145–146 °C. Anal. Calcd for C₃₁H₄₆O₁₈N: C, 51.67; H, 6.43; N, 1.94. Found: C, 51.57; H, 6.49; N, 1.93.

Succinylation of Diphtheria Toxoid. Diphtheria toxoid (DT) solution (10 mL, 8.0 mg of protein/mL) was dialyzed against 1 L of 0.05 M NaCl at 5 °C for 16 h. Succinic anhydride (60 mg) was added to the dialyzed DT slowly with stirring during 2 h while the pH was maintained between 8 and 8.5 by adding small amounts of 3 M NaOH solution. The reaction mixture was dialyzed against three changes of water (3 × 1 L) in 24 h and then lyophilized to yield 70 mg (88%). Estimation by the TNBS reagent (18) showed the presence of less than 1% primary amine.

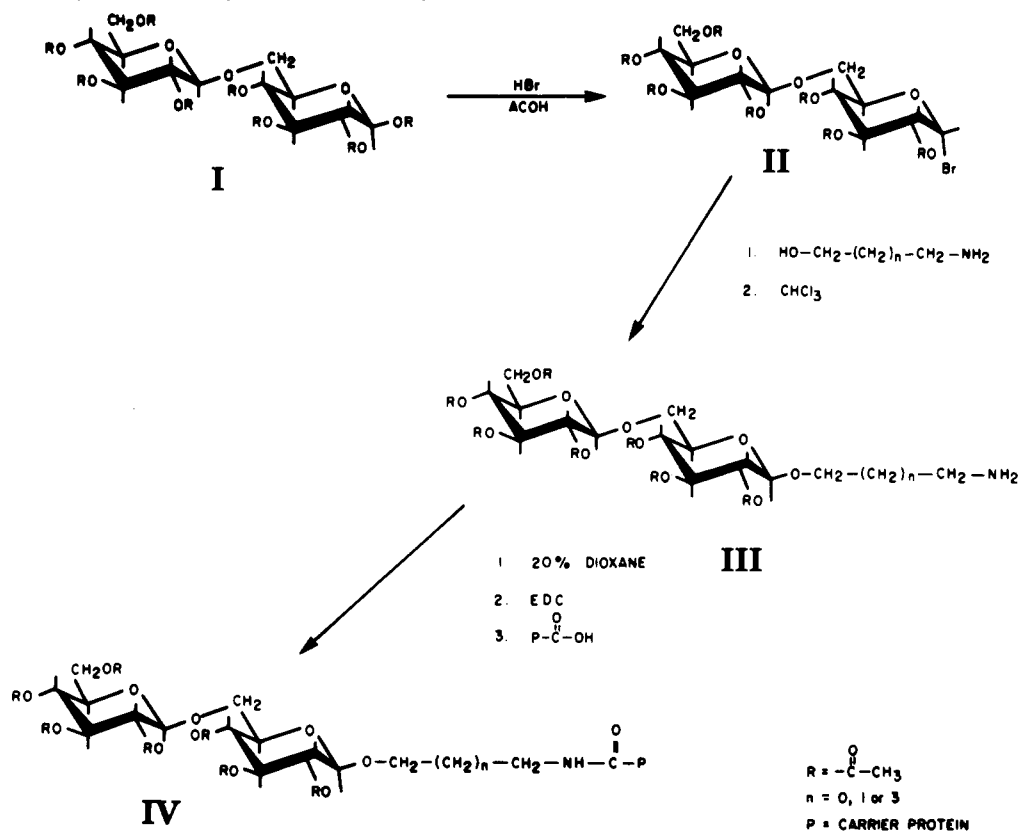
Preparation of Conjugate Vaccine. Succinylated diphtheria toxoid (Suc-DT, 50 mg) was dissolved in 20% dioxane (10 mL) and EDC (200 mg) was added to it followed by a solution (8 mL) of APGH (25 mg) in 20% dioxane. The pH of this reaction mixture was maintained between 5.5 and 5.9 by intermittent addition of 0.1 N HCl for 1 h at room temperature. A second 200 mg of EDC was added and the reaction continued for one more hour. The reaction mixture was dialyzed extensively against several changes of distilled water for 2 days at 5 °C and was then freeze-dried (yield 32 mg, 61%). The conjugate Suc-DT-APGH was found to contain 5.25% APGH by the phenol sulfuric acid method (19). Several batches of conjugate vaccines were prepared the same way as described above. Suc-DT-APTGH was prepared the same way as described above. The reaction sequence is shown in Scheme I. Tetanus toxoid (TT) was coupled to APTGH by the same procedure to give the conjugate TT-APTGH.

Enzyme Linked Immunosorbent Assay (ELISA). The ELISA was performed in 96-well flat-bottom polystyrene microtiter plates (Costar, Cambridge, MA) essentially by the method of Engvall and Perlmann (20). The wells were coated with the conjugate TT-APTGH at a concentration of 10 µg/mL in PBS (0.01 M NaH₂PO₄, 0.14 M NaCl, 0.02% NaN₃, pH 7.4) at 37 °C for 3 h. Excess reactive groups were blocked with 1% casein (Fisher Scientific, Columbia, MD) in PBS at 37 °C for 1 h. The wells were washed with PBS between steps to remove unbound material. The antigen-coated plates were incubated with serial 2-fold dilutions of antibodies for 16 h at room temperature (25 °C). Incubation with the second antibody was done for 16 h at room temperature. Disodium *p*-nitrophenyl phosphate (Sigma Chemical Co.) at a concentration of 1 mg/mL in 1.0 M diethanolamine buffer (with 1 mM MgCl₂), pH 9.8, was used as substrate. Absorbance was read on a Dynatech plate reader (Dynatech Laboratories, Alexandria, VA) at 410 nm. Antibody units were calculated as the mean of the product of the optical density (in the range of 0.3–1.0) and the reciprocal serum dilution at three different 2-fold dilutions.

SDS-PAGE and Western Transfer. Sodium dodecyl sulfate (SDS)-polyacrylamide gel electrophoresis (PAGE) was performed by the method of Laemmli (21) as described previously (22). Western transfer of electrophoretically separated glycoproteins to nitrocellulose membrane (Bio-Rad Laboratories, Richmond, CA) was performed in a transblot apparatus (Bio-Rad) as described before (22).

Immunization of Rabbits. New Zealand white rabbits, obtained from Hazelton Research Products (Denver, PA) (2–2.5 kg), were injected intramuscularly with Suc-DT-APGH (lot no. IIIA-103, 100 µg) in Freund's complete adjuvant. Booster injections were given with the conjugate (100 µg) in saline. Four New Zealand white rabbits (2–2.5 kg) were immunized with Suc-DT-APGH (lot no. IIIA-171, 100 µg) mixed with aluminum hydroxide gel with a gel to protein ratio of 20:1 (w/w). The first booster injection was given with the same adjuvant. The subsequent injections were given with Suc-DT-APGH (50 µg) in saline.

Immunization of Mice. One group of C57 black mice (5–6 weeks old), obtained from Charles River Laboratories (Wilmington, MA), were immunized intraperitoneally with Suc-DT-APTGH (lot no. V-13, 10 µg) mixed with aluminum hydroxide gel with a gel to protein ratio of 20:1 (w/w). A second group of C57 black mice (five mice in a group) were immunized the same way with Suc-DT-APGH (lot no. IIIA-171). The first booster injections were

Scheme I.^a Synthesis of hepta-*O*-acetyl-gentiobiose conjugate vaccines

^a I, Gentiobiose octaacetate; II, acetobromogentiobiose; III, aminoalkylhepta-*O*-acetylgentiobioside; IV, carrier protein conjugate of (aminoalkyl)hepta-*O*-acetylgentiobiose.

given the same way as the primary immunization. The subsequent injections were given with conjugate (10 μg) in saline.

Production of the Local Shwartzman Reaction.

The skin sites in 1.5-kg New Zealand white rabbits were prepared by intracutaneous injection of 0.1 mL of endotoxin (*E. coli* O6 LPS, or *E. coli* 0111:B4 LPS prepared by the hot phenol extraction method) in saline containing 0.1 mg of LPS. The reaction was provoked 23 h later by injection of 0.1 mL of endotoxin (0.025 mg) solution into the marginal ear vein. For the active immunization experiment, nine rabbits were immunized with Suc-DT-APGH vaccine as described in the methods, and 10 rabbits were immunized with the carrier protein Suc-DT the same way to be used as the control.

For the passive protection experiment, 15 mL of immune serum (2500 ELISA units/mL) was given intravenously to each of the test rabbits and 15 mL of normal rabbit serum was given intravenously to each of the control rabbits 2 h before the provocative dose. Any hemorrhage or necrosis of the skin occurring after the provocative dose was recorded as a positive reaction.

Preparation of APGH-Coupled Affinity Adsorbent.

Affigel-15 (Bio-Rad Laboratories, Richmond, CA) was washed three times with ethanol to remove additives. APGH (10 mg) was taken into ethanol (2 mL) when it gave a suspension. 1,4-Dioxane was added to a final concentration of 20% when the solution became clear. This solution was added to 2 mL of washed Affigel-15 and the mixture was shaken for 4 h at room temperature. The gel was filtered, washed once with ethanol, suspended into 0.1 M tris-Cl buffer, pH 7.4, and shaken for another 4 h to block excess active groups. The gel suspension was filtered, washed with PBS, pH 7.4, and packed into a column.

Affinity Chromatography. The Affigel-15-APGH

column (2 mL) was washed with 0.05 M NaCl (10 mL). Immune rabbit serum (1.0 mL) was cycled (3 \times) through the column. The column was then washed with PBS until the OD of the effluent was <0.01. Specific antibody was eluted with 0.2 M glycine hydrochloride, pH 2.5. The eluted fractions were immediately neutralized to pH 7.0 with 0.2 M tris. The column wash fractions and eluted fractions were tested by ELISA.

Neutralization of Bacterial Lipopolysaccharide by Nonimmune and Immune Serum. The ability of the postimmunization serum to neutralize endotoxic activity was tested in a previously described *Limulus* lysate neutralization assay (23). Briefly, dilutions of commercially provided endotoxin were added to microtiter wells over a dosage range of 2500–20 pg/mL. To the endotoxin was added an equal volume of nonpyrogenic normal saline or preimmune or postimmune rabbit sera. This mixture was then incubated for 3 h at 37 $^{\circ}\text{C}$, at the end of which time *Limulus* lysate was added (Associates of Cape Cod, Woods Hole, MA) and the plate incubated further at 37 $^{\circ}\text{C}$. The optical density of the mixture was read at 20 and 40 min at 405 nm (OD 405), and the results were plotted against the concentration of LPS added. A 50% *Limulus* gelation response (LR_{50}) was then calculated. Controls consisted of lapine sera alone and normal saline alone to which the *Limulus* lysate was added.

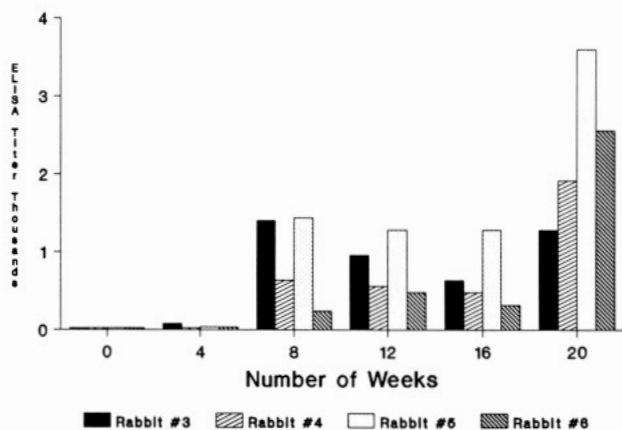
RESULTS

Preparation of Conjugate Vaccines. Derivatives of gentiobiose heptaacetate were prepared and coupled to carrier proteins as shown in Scheme I. Gentiobiose octaacetate (I) was treated with HBr/acetic acid to give acetobromogentiobiose II. The acetobromo sugar reacted with amino alcohols to give the hepta-*O*-acetyl ami-

Table I. Characteristics of the Gentioibiose Heptaacetate Conjugate Vaccines

vaccine	lot no.	molar ratio ligand:protein	ELISA titer, ^a OD units
Suc-DT-AEGH	AKB-III-92	4.5:1	48
Suc-DT-APGH	AKB-III-103	5.4:1	1120
Suc-DT-APGH	AKB-III-171	5.0:1	560
Suc-DT (control)	AKB-III-102		0
Suc-DT-APTGH	AKB-V-13	5.0:1	848

^a ELISA titers were measured against anti-J5 human monoclonal A6(H4C5).

**Figure 1.** Antibody response of four rabbits immunized with Suc-DT-APGH conjugate vaccine using aluminum hydroxide as adjuvant. Injections were given at 0, 4, 8, 12, and 16 weeks.

noalkyl glycosides (III). The aminoalkyl glycosides were coupled to the carrier proteins by a carbodiimide-mediated coupling reaction (24) to give the conjugate vaccines (IV). Three different spacers (two to five carbon in length) were used, namely, aminoethyl, aminopropyl, and aminopentyl, to link the acetobromogentioibiose to carrier proteins. The diphtheria toxoid was succinylated before conjugation to increase the number of reactive carboxyl groups. The ELISA binding of these conjugates to the anti-lipid A human monoclonal antibody A6-(H4C5) is shown in Table I. The conjugate Suc-DT-AEGH showed a weak binding to this antibody (48 ELISA units) and therefore was not pursued further. Two lots of the conjugate Suc-DT-APGH showed titers of 560 and 1120 ELISA units, respectively. The conjugate Suc-DT-APTGH showed a titer of 848 ELISA units. The human monoclonal antibody showed no binding to Suc-DT.

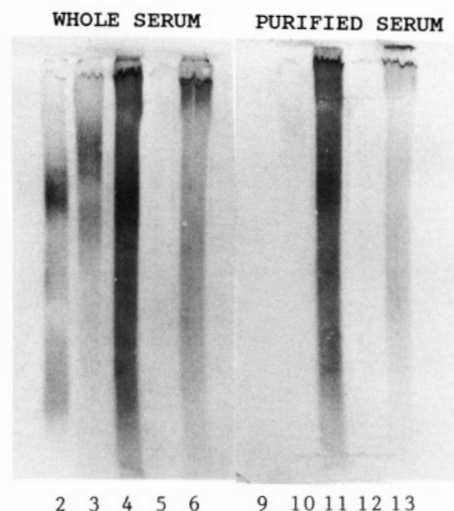
Immunization of Rabbits. The results of immunization of rabbits with Suc-DT-APGH using Freund's complete adjuvant for primary immunization (not shown) showed that there was a 12–30-fold rise in antibody level after the second immunization as determined by the ELISA using TT-APTGH as the antigen on the plate. The antibody levels could be maintained with repeated injections of conjugate in saline. The highest levels being 2400 ELISA units for rabbit 1 and 5120 ELISA units for rabbit 2. Results of immunization of rabbits with Suc-DT-APGH using aluminum hydroxide gel as adjuvant are shown in Figure 1. The primary antibody response was 2–4 times the preimmunization level. The secondary antibody response was variable and reached the highest level after the fifth injection.

Immunization of Mice. Antibody levels of sera from two groups of mice immunized with conjugate vaccines Suc-DT-APTGH and Suc-DT-APGH, respectively, are shown in Table II. The mice in group A which were immunized with the conjugate containing the five carbon spacer APTGH reached an antibody level of 2560 ELISA

Table II. Antibody Levels of Sera from Two Groups of Mice^a

no. of days ^b	ELISA antibody units	
	group A	group B
0	8	16
36	1200	1200
51	1600	2400
85	2560	1920
119	2560	5120

^a Mice from group A were immunized with the conjugate vaccine Suc-DT-APTGH with Al(OH)₃ gel with a gel to protein ratio of 20:1 (w/w). Mice from group B were immunized with conjugate vaccine Suc-DT-APGH with Al(OH)₃ gel and a gel to protein ratio of 20:1 (w/w). Al(OH)₃ was used for the first two injections only. All subsequent injections were in saline. ^b Injections were given on days 0, 24, 42, 74, and 107.

**Figure 2.** Western blot analysis of immune rabbit serum and affinity-purified anti-APGH antibodies. Antigens used are as follows: (lanes 2, 9) DT, (lanes 3, 10) Suc-DT, (lanes 4, 11) Suc-DT-APGH, (lanes 5, 12) TT, (lanes 6, 13) TT-APGH.

units which was comparable to the highest antibody level reached by mice in group B, which were immunized with the conjugate containing the three carbon spacer APGH (5120 ELISA units). Equal amounts of sera from all five mice in each group were pooled for these tests, and therefore, the antibody levels represent average values.

SDS-PAGE and Western Transfer. Electrophoretically separated glycoproteins (Suc-DT-APGH and TT-APGH) and carrier proteins (DT, Suc-DT, and TT) were transferred onto nitrocellulose membrane in duplicate. One part of the membrane was developed with immune whole rabbit serum and the other part was developed with affinity-purified anti-APGH antibodies (Figure 2). The affinity-purified antibodies bound only to the conjugates containing the synthetic epitope (lanes 11 and 13). The whole serum bound both the conjugates and the carrier proteins. None of the sera reacted with the tetanus toxoid (lanes 5 and 12).

Prevention of Local Shwartzman Reaction. As shown in Table III, the prevention of local Shwartzman reaction by active immunization with the vaccine Suc-DT-APGH showed that eight out of nine (90%) rabbits were protected in the immunized group compared to three out of 10 (30%) rabbits in the control group immunized with the carrier protein Suc-DT. The test for prevention of the local Shwartzman reaction by passive transfer of immune serum showed that four out of five (80%) rabbits that received immune serum were protected as compared to one out of five (20%) rabbits in the control group.

Limulus Lysate Neutralization. As previously

Table III. Protection of Rabbits against Local Schwartzman Reaction

	no. of rabbits protected				<i>p</i> ^a
	test group	%	control group	%	
active immunization ^b	8/9	90	3/10	30	<0.05
passive transfer ^c	4/5	80	1/5	20	<0.10

^a By χ^2 analysis. ^b Rabbits were challenged with *E. coli* O111:B4 LPS. ^c Rabbits were challenged with *E. coli* O6 LPS.

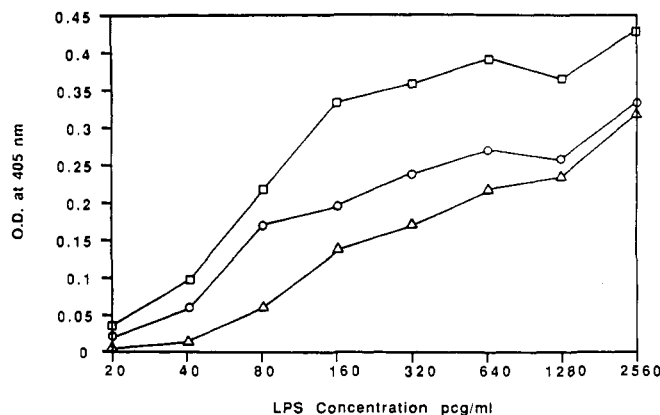


Figure 3. *Limulus* lysate neutralization assay of normal rabbit serum and immune rabbit serum: O, normal serum; Δ, immune serum; □, saline control.

described, the addition of normal serum was able to neutralize LPS when compared to the standard curve generated in the presence of normal saline (23). In one representative assay (Figure 3), normal sera increased the LR_{50} from 80 to 210 pg/mL. In the presence of the immune serum, the LR_{50} increased further to 540 pg/mL. This approximate 2-fold increase in LR_{50} was consistently reproducible and highly significant on multiple assays. The range of LR_{50} values recorded in multiple assays were for normal saline (86–76 pg/mL), for normal serum (222–212 pg/mL), and for immune serum (566–464 pg/mL).

DISCUSSION

The synthesis of derivatives of gentiobiose heptaacetate was designed with the knowledge that gentiobiose octaacetate is commercially available and that C1 glycosides could be prepared by the use of an acetobromo sugar (25). Since this reaction is performed in dry chloroform, it was necessary to select an aglycon that was soluble in chloroform and had the required functional groups. The amino alcohols satisfied these conditions as the hydroxy group would react in the base-catalyzed glycosidation, leaving the primary amino group free for subsequent coupling to the carrier protein. During preliminary experiments it was found that the amino alcohols acted as base and acid acceptors in this reaction and glycosidation was accomplished with 40–62% yield. The aminoalkyl glycosides were crystalline compounds and tested positive for primary amino groups on spraying with ninhydrin reagent (26). The carbodiimide-mediated coupling reactions (24) of these aminoalkyl glycosides to carrier proteins were performed in 20% dioxane since these glycosides were insoluble in water.

The conjugate vaccines we prepared showed binding to the anti-J5 human monoclonal antibody A6(H4C5) (Table I). This is significant since this human monoclonal has been shown to protect animals against Gram-negative bacteremia (16).

Results of immunizations with these conjugates (Table II, and Figure 1) show that (a) aluminum hydroxide gel can be used as adjuvant for immunization and give antibody levels similar to those achieved by immunizing with Freund's complete adjuvant (FCA) (This is important since aluminum hydroxide, unlike FCA, can be used in humans.) and (b) conjugate vaccines containing both three and five carbon spacer groups worked equally well.

Western blot analysis of conjugate vaccines and carrier proteins with immune rabbit serum and affinity-purified anti-APGH antibodies showed (Figure 2) that the immune serum had antibodies directed against the synthetic epitope APGH and the carrier protein Suc-DT. The affinity-purified antibodies reacted only with the conjugates containing the synthetic epitope showing the presence of APGH-specific antibodies in the polyclonal serum.

Protection against the local Schwartzman reaction in rabbits was demonstrated both by active immunization (eight out of nine rabbits had no lesions; $p < 0.05$) and by passive transfer of immune serum (four out of five rabbits had no lesions; $p < 0.10$). Since the number of animals used in the passive transfer experiment was small, the protection was not highly significant. Further work will be required to obtain these data. In addition to the neutralization of the local Schwartzman reaction, the immune sera generated by this vaccine also had the ability to neutralize the *Limulus* lysate reactivity of endotoxin, which is one measure of reduction of endotoxic activity.

Our results show that conjugate vaccines prepared with gentiobiose heptaacetate elicit antibodies in mice and rabbits that neutralize endotoxin. We have also shown that these sera have antibodies directed against the synthetic epitope (APGH). Further work is in progress to determine the immunoglobulin isotypes of the protective antibodies. These vaccines, if successful, will provide the first available synthetic vaccine for use in preventing endotoxic shock. Our active and passive immunization studies with these conjugates confirm that antibodies against this epitope have properties similar to those of A6-(H4C5). We, therefore, believe that these vaccines have potential for inducing protective antibodies in humans against endotoxin.

LITERATURE CITED

- (1) Kreger, B. E., Craven, D. E., Carling, P. C., and McCabe, W. R. (1980) Gram-negative bacteremia. III. Reassessment of etiology, epidemiology and ecology in 612 patients. *Am. J. Med.* 68, 332–343.
- (2) Kreger, B. E., Craven, D. E., and McCabe, W. R. (1980) Gram-negative bacteremia. IV. Reevaluation of clinical features and treatment in 612 patients. *Am. J. Med.* 68, 344–355.
- (3) Sanders, C. C., and Sanders, W. E., Jr. (1985) Microbial resistance to new generation of β -lactam antibiotics: clinical and laboratory implications. *J. Infect. Dis.* 151, 399–406.
- (4) Finland, M. (1970) Changing ecology of bacterial infections as related antibacterial therapy. *J. Infect. Dis.* 122, 419–431.
- (5) Freter, R. (1955) The fatal enteric cholera infection in the guinea pig, achieved by inhibition of normal enteric flora. *J. Infect. Dis.* 97, 57–65.
- (6) Sanford, J. P., Hunter, B. W., and Souda, L. L. (1962) The role of immunity in the pathogenesis of experimental hematogenous pyelonephritis. *J. Exp. Med.* 115, 383–410.
- (7) Markley, K., and Smallman, E. (1968) Protection by vaccination against *Pseudomonas* infection after thermal injury. *J. Bacteriol.* 96, 867–874.
- (8) Luderitz, O., Staub, A. M., and Westphal, O. (1966) Immunochemistry of O and R antigens of *Salmonella* and related enterobacteriaceae. *Bacteriol. Rev.* 30, 192–255.

- (9) Chedid, L., Parant, M., Parant, F., and Boyer, F. (1968) A proposed mechanism for natural immunity to enterobacterial pathogens. *J. Immunol.* 100, 292-301.
- (10) Braude, A. I., and Douglas, H. (1972) Passive immunization against the local Shwartzman reaction. *J. Immunol.* 108, 505-512.
- (11) McCabe, W. R., and Greely, A. (1972) Immunization with R mutants of *S. minnesota*. I. Protection against challenge with heterologous Gram-negative bacilli. *J. Immunol.* 108, 601-610.
- (12) Braude, A. I., Douglas, H., and Davis, C. E. (1973) Treatment and prevention of intravascular coagulation with antiserum to endotoxin. *J. Infect. Dis.* 128 (Suppl.), S157-S164.
- (13) Ziegler, E. J., Douglas, H., Sherman, J. E., Davis, C. E., and Braude, A. I. (1973) Treatment of *E. coli* and *Klebsiella* bacteremia in agranulocytic animals with antiserum to a UDP-Gal epimerase deficient mutant. *J. Immunol.* 111, 433-438.
- (14) Ziegler, E. J., and Douglas, H. (1979) *Pseudomonas aeruginosa* vasculitis and bacteremia following conjunctivitis: a simple model of fatal pseudomonas infection in neutropenia. *J. Infect. Dis.* 139, 288-296.
- (15) Ziegler, E. J., McCutchan, J. A., Fierer, J., Glauser, M. P., Sadoff, J. C., Douglas, H., and Braude, A. I. (1982) Treatment of Gram-negative bacteremia and shock with human antiserum to a mutant *Escherichia coli*. *N. Engl. J. Med.* 307, 1225-1230.
- (16) Teng, N. N. H., Kaplan, H. S., Hebert, J. M., Moor, C., Douglas, H., Wunderlich, A., and Braude, A. I. (1985) Protection against Gram-negative bacteremia and endotoxemia with human monoclonal IgM antibodies. *Proc. Natl. Acad. Sci. U.S.A.* 82, 1790-1794.
- (17) DeMaria, A., Johns, M. A., Berberich, H., and McCabe, W. R. (1988) Immunization with rough mutants of *Salmonella minnesota*: Initial studies in human subjects. *J. Infect. Dis.* 158, 291-300.
- (18) Kemp, H. A., and Morgan, M. R. A. (1986) Studies on the detrimental effects of bivalent binding in a microtitration plate ELISA and possible remedies. *J. Immunol. Methods* 94, 65-77.
- (19) Dubois, M., Gilles, K. A., Hamilton, J. K., Rebers, P. A., and Smith, F. (1956) Colorimetric method for determination of sugars and related substances. *Anal. Chem.* 28, 350-356.
- (20) Engvall, E., and Perlmann, P. (1972) Enzyme-linked immunosorbent assay, ELISA. III. Quantitation of specific antibodies by enzyme-labeled anti-immunoglobulin in antigen-coated tubes. *J. Immunol.* 109, 129-135.
- (21) Laemmli, U. K. (1970) cleavage of structural proteins during the assembly of the head of bacteriophage T4. *Nature (London)* 227, 680-685.
- (22) Zollinger, W. D., Moran, E. E., Connely, H., Mandrel, R. E., and Brandt, B. (1984) Monoclonal antibodies to serotype 2 and serotype 15 outer membrane proteins of *Neisseria meningitidis* and their use in serotyping. *Infect. Immun.* 46, 260-266.
- (23) Warren, H. S., Novitsky, T. J., Ketchum, P. A., Roslansky, P. F., Kania, S., and Siber, G. R. (1985) Neutralization of bacterial lipopolysaccharides by human plasma. *J. Clin. Microbiol.* 22, 590-595.
- (24) Yamada, H., Imoto, T., Fujita, K., Okazaki, K., and Motomura, M. (1981) Selective modification of aspartic acid-101 in lysozyme by carbodiimide reaction. *Biochemistry* 20, 4836-4842.
- (25) Hanes, L. J., and Newth, F. H. (1955) The glycosyl halides and their derivatives. *Advances in Carbohydrate Chemistry* (M. L. Wolfrom, Ed.) pp 207-255, Academic Press Inc., New York.
- (26) Aminoff, D., and Morgan, W. T. J. (1948) Hexosamine components of the human blood group substances. *Nature (London)* 162, 579-580.

Registry No. I, 58769-76-9; AEGH, 130469-08-8; APGH, 130495-62-4; APTGH, 130469-09-9; acetobromogentiobiose, 14187-83-8; 2-aminoethanol, 141-43-5; 3-aminopropanol, 156-87-6; 5-aminopentanol, 2508-29-4.

Substituted 2-Iminothiolanes: Reagents for the Preparation of Disulfide Cross-Linked Conjugates with Increased Stability¹

Dane A. Goff and Stephen F. Carroll*

Department of Biological Chemistry, XOMA Corporation, 2910 Seventh Street, Berkeley, California 94710.
Received July 30, 1990

Much attention has been focused recently on the stability of immunotoxin (antibody-toxin) conjugates linked by a disulfide bridge. Conflicting reports have appeared regarding the *in vivo* stability of such conjugates prepared with the two most commonly used cross-linking reagents, SPDP and 2-iminothiolane. We have developed (i) a series of reagents based on 2-iminothiolane substituted at the 4- and/or 5-positions (X2ITs) which, based on model studies with simple amines, should show enhanced disulfide stability when conjugated with antibodies or other proteins and (ii) a real-time method for monitoring the rate and extent of conjugation of these reagents with amino groups. Depending upon the substituent, the stability of model-activated disulfides relative to unsubstituted 2-iminothiolane was increased from 5- to 4000-fold as measured by glutathione-induced release of thionitrobenzoic acid. This family of cross-linking reagents should allow the construction of disulfide cross-linked toxin, drug, or enzyme conjugates with enhanced stability *in vivo*.

INTRODUCTION

Immunotoxins are a class of therapeutic agents typically composed of an antibody, capable of binding to specific cell-surface antigens on target cells, covalently cross-linked to a cytotoxic protein. For most immunotoxins prepared to date, the cytotoxic protein is ricin A chain (RTA),² which requires a reducible disulfide linkage with the targeting antibody for maximal expression of cytotoxic activity (1, 2). However, while some studies have indicated that the disulfide linkages prepared with RTA or other toxins and two of the most commonly used cross-linking reagents, 2-iminothiolane (2IT) and *N*-succinimidyl 3-(2-pyridyldithio)propionate (SPDP), are stable *in vivo* (3, 4), others (5, 6) have suggested that such linkages may be unstable. In addition to decreasing the circulating levels of the antibody-toxin conjugate, such deconjugation would liberate free antibody which can then compete with the conjugate for binding to target cells.

Worrell et al. (7) and Thorpe et al. (8, 9) have shown that hindering access to the disulfide bond linking the antibody and toxin by introducing a methyl group adjacent to the sulfur atom of reagents based upon SPDP increases the stability of the resultant conjugate both *in vitro* and *in vivo*. Moreover, alterations in spacer length have been found to alter the stability of conjugates *in vitro* (10). When combined with the experimental discrepancies noted above, these results suggest that the *in vivo* stability of immunotoxins may be influenced by the specific antibody-toxin pairing and can be enhanced by alterations in residues immediately adjacent to the disulfide bridge.

* Author to whom correspondence should be addressed.

¹ A preliminary report of a portion of this work has appeared (Abstracts from the Fourth International Conference on Monoclonal Antibody Immunoconjugates for Cancer, San Diego, 1989).

² The abbreviations used are as follows: DTNB, 5,5'-dithiobis(2-nitrobenzoic acid); PBS-EDTA, phosphate-buffered saline, pH 7.2, containing 0.5 mM EDTA, ethylenediaminetetraacetic acid; RTA, ricin toxin A chain; SPDP, *N*-succinimidyl 3-(2-pyridyldithio)propionate; TNB, 5-mercapto-2-nitrobenzoic acid; 2IT, 2-iminothiolane; X2IT, 4- and/or 5-substituted 2-iminothiolanes.

In an effort to more critically evaluate the requirements for improving disulfide bond stability *in vivo*, we have synthesized a series of sterically hindered reagents based on 2IT (11). 2IT offers several advantages over other possible linking reagents (Figure 1): (i) it reacts with primary amines to form stable amidinium derivatives, retaining the positive charge; (ii) inclusion of an aromatic disulfide such as 5,5'-dithiobis(2-nitrobenzoic acid) (DTNB) in the reaction mixture both activates the newly exposed 2IT thiol and allows real-time spectrophotometric monitoring of the labeling reaction; and (iii) substitution on the 2-IT ring at the 4- and/or 5-positions can be used to introduce various groups into proximity with the disulfide bond, thus allowing alterations in the degree of steric hindrance. Here we have prepared a series of sterically hindered 2IT molecules (X2ITs, Table I) and have evaluated their reactivity with amino groups and the disulfide stability of model conjugates.

EXPERIMENTAL SECTION

Materials. 2IT and DTNB were obtained from Sigma. Anhydrous solvents, 10 M *n*-butyllithium in hexane, and all other reagents were from Aldrich Chemical Co., except as noted.

General Procedures. Melting points are uncorrected and were measured on a Fisher-Johns apparatus. ¹H NMR spectra were recorded at 60 MHz on a Varian EM-360 or at 400 MHz on a Bruker AM-400 spectrometer. Peaks are given as δ values relative to tetramethylsilane as internal standard. Coupling constants (*J*) are given in hertz. IR spectra were obtained either as KBr disks or as neat films on NaCl plates on a Perkin-Elmer Model 1330 spectrophotometer. The abbreviations used to describe the spectral peaks are v = very, s = strong, b = broad, sh = sharp, m = medium, w = weak. Wavelengths are given in inverse centimeters. Ultraviolet spectra were recorded on a Shimadzu Model 160 spectrophotometer. Flash chromatography was performed on silica gel 60 (Merck, 230-400 mesh) with apparatus supplied by J.T. Baker. Elemental analyses were performed by Desert Analytics, Tucson, AZ.

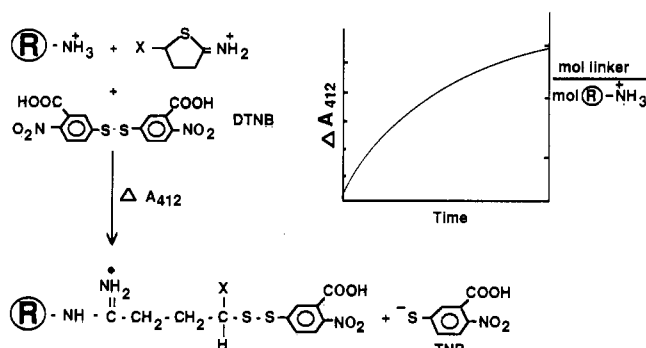


Figure 1. Chemistry of the X2ITs. Compounds containing a primary amine ($R-NH_2$) react with the X2ITs to create an amidinium linkage without neutralizing the positive charge. If the reaction is performed in the presence of DTNB, the newly exposed iminothiolane thiol cleaves DTNB in a disulfide-exchange reaction. This cleavage both activates the linker thiol (in preparation for conjugation) and releases free TNB, allowing real-time spectrophotometric monitoring of the rate and extent of reaction.

Table I. Structures of Substituted X2ITs

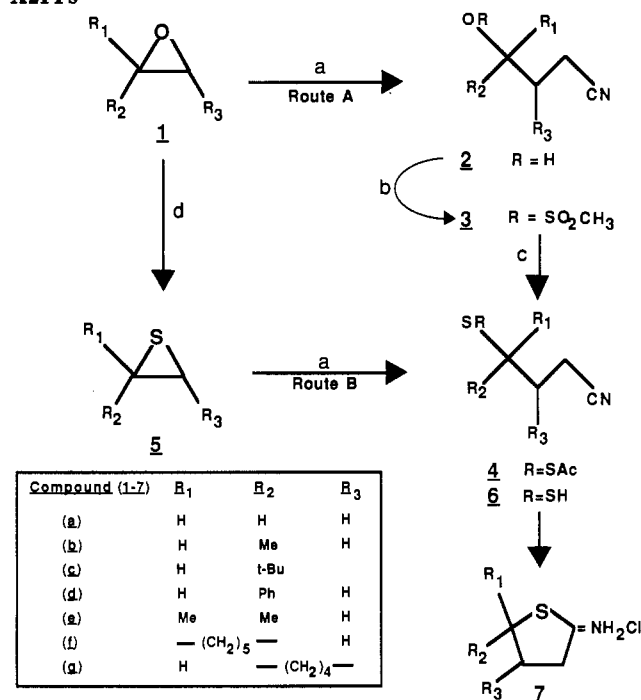
compd	substitution	no. ^a	structure
2IT	—	7a	
M2IT	5-methyl	7b	
TB2IT	5-tert-butyl	7c	
Ph2IT	5-phenyl	7d	
DM2IT	5,5-dimethyl	7e	
S2IT	5-spiro	7f	
R2IT	4,5-ring	7g	

^a Refers to the structures shown in Scheme I. ^b The fused ring structures are shown here with the numbering system common to the iminothiolane family.

All synthetic reactions were stirred magnetically under an inert atmosphere; argon for reactions with *n*-butyllithium, otherwise nitrogen. The expression "dried" refers to passage of the organic layer through a pad of anhydrous sodium sulfate. Concentration of solutions in vacuo was performed under water aspiration with a Büchi R110 Rotavapor. Reactions were performed at room temperature unless otherwise noted. For each compound, the boldfaced designation in parentheses (e.g. **6b**) denotes the corresponding structure shown in Scheme I.

4-Mercaptopentanenitrile (6b). To dry THF (100 mL) cooled to -75°C was added 10.0 M *n*-butyllithium (15.0 mL), followed carefully dropwise with a solution of CH_3CN (7.84 mL, 0.15 mol) in THF (20 mL). After 15 min 2-methylthiirane (11.75 mL, 0.15 mol) was added dropwise. The white suspension stirred a further 5 min at -75°C and then the cooling bath was removed. An exothermic reaction ensued to give a pale yellow homogeneous solution. After 2 h the reaction was quenched with 1/1 concentrated $\text{HCl}/\text{H}_2\text{O}$ (30 mL) and extracted (7 \times 50 mL) with Et_2O .

Scheme I.^a Synthetic Scheme for the Preparation of X2ITs



^a Details can be found in Experimental Procedures. Reagents: (a) $\text{LiCH}_2\text{CN}/\text{THF}$; (b) $\text{ClSO}_2\text{CH}_3/\text{benzene}/\text{Et}_3\text{N}$; (c) CsSAc/DMF ; (d) $\text{KSCN}/\text{EtOH}/\text{H}_2\text{O}$ or 3-methylbenzothiazole-2-thione/ $\text{TFA}/\text{CH}_2\text{Cl}_2$; (e) $\text{HCl(g)}/\text{MeOH}$. The products of the reactions are indicated by underlined number (stage of synthesis), letter (R groups) combinations. For example, 7a refers to the final X2IT hydrochloride where $R_1 = R_2 = R_3 = \text{H}$ (2IT).

The combined organic layers were dried and concentrated in vacuo to give a crude amber liquid (10.1 g, 59%). Distillation in vacuo gave **6b** as a colorless liquid (6.1 g, 35%): ^1H NMR (60 MHz, CDCl_3) 2.72–3.28 (m, 1 H, CH), 2.53 (t, $J = 7$, 2- CH_2), 1.62–2.18 (m, 2 H, 3- CH_2), 1.48 (d, 1 H, $J = 7$, exchanges with D_2O , SH), 1.40 (d, 3 H, $J = 6$, 5- CH_3); IR (film) 2550 (SH), 2245 (CN).

4-Mercapto-4-methylpentanenitrile (6e). To a 20 mL of dry THF cooled at -75°C was added 10.9 M *n*-BuLi (3.0 mL), followed dropwise by a solution of CH_3CN (1.60 mL, 30 mmol) in THF (5 mL). After addition was complete the mixture, containing a white precipitate of LiCH_2CN , was stirred for 10 min. Then 2,2-dimethylthiirane (19) (2.7 g, 30 mmol) was added dropwise. The cooling bath was removed and an exothermic reaction ensued to give a pale yellow homogeneous solution. After 1.5 h the reaction was quenched by the addition of 5 mL of 1/1 concentrated $\text{HCl}/\text{H}_2\text{O}$. The mixture was extracted (3 \times 10 mL) with EtOAc . The combined organic layers were dried and concentrated in vacuo to give a pale yellow liquid (3.66 g, 92%) with a strong thiol stench, which was used without further purification: ^1H NMR (60 MHz, CDCl_3) 2.88 (t, 2 H, $J = 7$, 2- CH_2), 2.05 (t, 2 H, $J = 7$, 3- CH_2), 1.53 (s, 6 H, 2 CH_3); IR (film) 2250 (w), 2190 (m).

4-Hydroxy-4-phenylbutanenitrile (2d) (13). Sodium amide (10.61 g, 0.271 mol) was transferred to a tared 500-mL three-neck round-bottom flask in a glove bag under Ar. An addition funnel and thermometer were added, then 150 mL of dry THF was cannulated in. The suspension was cooled to -30°C on a $\text{CCl}_4/\text{dry ice}$ bath and then CH_3CN (13.5 mL, 0.259 mol) was added dropwise, while the temperature was kept $<-20^\circ\text{C}$. This was followed by addition of styrene oxide (26.0 mL, 0.228 mol) over 30 min. The mixture was allowed to warm to 0°C over 80 min, and then to room temperature over 75 min. The mixture

was then recooled to -35°C and quenched with saturated aqueous NH_4Cl (35 mL). The mixture was diluted with EtOAc (200 mL), and the layers were separated. The aqueous layer was extracted (2×50 mL) with EtOAc . The combined organic layers were dried and concentrated in vacuo. TLC indicated two major products. Repeated flash chromatography on silica (hexanes/ EtOAc) gave **2d** as a pale yellow oil (3.48 g, 10%): TLC (70/30 hexanes/ EtOAc) $R_f = 0.52$; ^1H NMR (60 MHz, CDCl_3) 7.30 (s, 5 H, ar), 4.73 (m, 1 H, benzylic), 2.16–2.80 (m, 2 H), 1.70–2.16 (m, 2 H); IR (film) 3420 (vs, b, OH), 2240 (CN).

4-Phenyl-4-(thioacetyl)butanenitrile (4d). Hydroxy nitrile **2d** (3.48 g, 21.6 mmol) in benzene (20 mL) with Et_3N (3.13 mL, 22.5 mmol) was cooled to 0°C and treated dropwise with methanesulfonyl chloride (2.54 g, 22.2 mmol) in benzene (15 mL). The ice bath was removed and stirring continued for 30 min. The Et_3NHCl was filtered off and the filtrate concentrated in vacuo to give cyanomesylate **3d**: ^1H NMR (60 MHz, CDCl_3) 7.37 (s, 5 H, ar), 5.58 (m, 1 H, benzylic), 2.72 (s, 3 H, SO_2CH_3), 2.03–2.67 (m, 4 H). Crude **3d** was dissolved in dry DMF (5 mL) and treated with a solution of CsSAc (22 mmol, prepared according to the method of Kellog and Strijtveen, ref 15) in DMF (10 mL). After overnight stirring the mixture was diluted with Et_2O (150 mL) and rinsed (5×20 mL) with H_2O . The organic layer was dried and concentrated in vacuo to give a brown liquid which was purified by flash chromatography (hexanes/ EtOAc). Thioacetate **4d** was obtained as an orange oily liquid (3.37 g, 72%): TLC (90/10 hexanes/ EtOAc) $R_f = 0.21$; ^1H NMR (60 MHz, CDCl_3) 7.27 (s, 5 H, ar), 4.58 (m, 1 H, benzylic), 2.30 (s, 3 H, SAc), 2.10–2.30 (m, 4 H); IR (film) 2250 (CN), 1688 ($\text{C}=\text{O}$).

2-(Cyanomethyl)-1-mercaptopcyclohexane (6g). To dry THF (30 mL) at -75°C was added 10.0 M $n\text{-BuLi}$ (3.59 mL), followed dropwise by CH_3CN (1.88 mL, 35.9 mmol). Ten minutes after addition was complete, cyclohexene sulfide (**17**) (3.90 g, 34.2 mmol) in THF (10 mL) was added dropwise. When addition was complete the cooling bath was removed. After 2 h the mixture was recooled to 0°C and quenched by addition of a mixture of concentrated HCl (6 mL) and H_2O (15 mL). The layers were separated, and the aqueous layer was extracted (2×25 mL) with EtOAc . The combined organic layers were dried and concentrated in vacuo, followed by vacuum distillation to give **6g** as a colorless liquid (2.26 g, 43%): bp $85\text{--}89^{\circ}\text{C}$ (0.3 mm); ^1H NMR (60 MHz, CDCl_3) 2.68 (d, 2 H, $\text{CH}_2\text{-CN}$), 2.32 (s, 1 H), 1.00–2.30 (m, 10 H); IR (film) 2250 (CN).

1-(2-Cyanoethyl)-1-mercaptopcyclohexane (6f). To a solution of 10.0 M $n\text{-BuLi}$ (0.67 mL) in THF (10 mL) at -75°C was added CH_3CN (0.35 mL, 0.67 mmol) dropwise. After 10 min, 7-thiaspiro[5.2]octane [0.86 g, 0.67 mmol, prepared from 7-oxaspiro[5.2]octane (**20**) according to the method of ref 16] in 2 mL of dry THF was added. The cooling bath was removed and after 2 h the reaction was quenched with a mixture of concentrated HCl (1.5 mL) and H_2O (3.5 mL). The layers were separated, and the aqueous layer was extracted twice with EtOAc (25 mL). The combined organic layers were dried and concentrated in vacuo to give crude **6f** as a foul-smelling oil (0.48 g), which was used without further purification.

5,5-Dimethyl-4-mercaptophexanenitrile (6c). To a solution of 10.0 M $n\text{-BuLi}$ (5.6 mL) in dry THF (50 mL) at -75°C was added CH_3CN (2.9 mL, 56 mmol) dropwise. After 10 min, a solution of 2-*tert*-butylthiirane (**16**) (5.94 g, 51 mmol) in dry THF (5 mL) was added dropwise. After 10 min the cooling bath was removed and the mixture stirred for 2 h, whereupon it was recooled to 0°C and quenched with 1/1 concentrated $\text{HCl}/\text{H}_2\text{O}$ (12 mL).

The mixture was diluted with CH_2Cl_2 , and the layers were separated. The organic layer was rinsed four times with H_2O , dried, and concentrated in vacuo to give a pale yellow liquid (4.96 g). Kugelrohr distillation [$90\text{--}100^{\circ}\text{C}$ (0.6 mm)] gave 2.94 g (34%) of colorless **6c**: ^1H NMR (60 MHz, CDCl_3) 3.70 (dd, 1 H, $J = 6, 10$, CH), 2.36–3.36 (m, 3 H), 1.70–2.36 (m, 2 H), 1.03 (s, 9 H, *t*-Bu); IR (film) 3200–3300 (s, b), 2960 (vs, b), 2250 and 2210 (both sh, m, CN), 1620, 1475, 1375.

General Procedure for the Synthesis of Substituted 2-Iminothiolanes (7b–g). The appropriate 4-mercaptocyanitrile (**6**) or 4-(thioacetyl)nitrile (**4**) was dissolved in dry MeOH (ca. 10 mL/g) and bubbled vigorously with HCl (g) for 3–5 min. The mixture was stirred overnight or until IR spectroscopy showed complete loss of the nitrile absorbance at 2200 cm^{-1} . The solvent was removed in vacuo. The residue was slurried in EtOAc and then warm EtOH was added until a solution was obtained. The mixture was cooled to -20°C . If crystallization did not occur within several hours, Et_2O was added. Further cooling gave the following hydrochlorides.

5-Methyl-2-iminothiolane hydrochloride (M2IT·HCl, 7b): yield 6.67 g (83%); mp $114.5\text{--}115.5^{\circ}\text{C}$ (EtOAc/EtOH); ^1H NMR (400 MHz, $\text{DMSO}-d_6$) 7.46 (t, 1 H, $J = 50.7$, NH), 4.13–4.22 (m, 1 H, 5-H), 3.31–3.39 (m, 1 H), 3.19–3.28 (m, 1 H), 2.39–2.47 (m, 1 H), 1.88–1.97 (m, 1 H), 1.45 (d, 3 H, $J = 6.7$, 5- CH_3); IR (KBr) 3410, 2810 (vs, vb), 1615 (s, $\text{C}=\text{N}$), 1535, 1450, 1415, 1240 1025, 990, 885, 690. Anal. Calcd for $\text{C}_5\text{H}_{10}\text{ClNS}$: C, 39.60; H, 6.65; N, 9.24; S, 21.14. Found: C, 39.63; H, 6.62; N, 9.02; S, 21.34.

5-(1,1-Dimethylethyl)-2-iminothiolane hydrochloride (TB2IT·HCl, 7c): yield 1.22 g (41%); mp $224\text{--}226^{\circ}\text{C}$; ^1H NMR (400 MHz, $\text{DMSO}-d_6$) 7.43 and 7.40 (2 t, $J = 50.7$, major t centered at 7.40, combined integral 1.7 H, NH_2^+), 4.12 (dd, 1 H, $J = 5.2, 10.9$, H-5), 3.17–3.33 (m, 2 H, 3- CH_2), 2.28–2.32 (m, 1 H, H-4), 1.96–2.06 (m, 1 H, H-4), 1.01 (s, 9 H, *t*-Bu); IR (KBr) 2800–3000 (vs, vb), 1630 (s, $\text{C}=\text{N}$), 1535, 1475, 1410, 1375, 1260, 1185, 1000, 895, 695. Anal. Calcd for $\text{C}_8\text{H}_{16}\text{ClNS}$: C, 49.60; H, 8.32; N, 7.23; S, 16.55. Found: C, 49.52; H, 8.37; N, 7.37; S, 16.34.

5-Phenyl-2-iminothiolane hydrochloride (Ph-2IT·HCl, 7d): yield 1.22 g (44%); mp 172°C dec; ^1H NMR (400 MHz, $\text{DMSO}-d_6$) 7.52 (d, 2 H, $J = 6.9$), 7.36–7.45 (m, 3 H), 5.35 (dd, 1 H, $J = 5.5, 10.4$, 5-H), 3.30–3.44 (m, 2 H, 3- CH_2), 2.64–2.71 (m, 1 H), 2.39–2.48 (m, 1 H); IR (KBr) 3360, 2870 (vs, vb), 1615 (s, br, $\text{C}=\text{N}$), 1515, 1495, 1450, 1405, 1325, 1020, 985, 830, 770, 760, 700, 675. Anal. Calcd for $\text{C}_{10}\text{H}_{12}\text{ClNS}$: C, 56.20; H, 5.66; N, 6.55; S, 15.08. Found: C, 55.94; H, 5.54; N, 6.60; S, 15.05.

5,5-Dimethyl-2-iminothiolane hydrochloride (DM2IT·HCl, 7e): yield 3.0 g (65%); mp $156\text{--}159^{\circ}\text{C}$; ^1H NMR (400 MHz, $\text{DMSO}-d_6$) 7.43 (t, 1 H, $J = 51.3$, NH), 3.43 (t, 2 H, $J = 7.1$, 3- CH_2), 2.18 (t, 2 H, $J = 7.1$, 4- CH_2), 1.59 (s, 6 H, 2 CH_3); IR (KBr) 2900 (vs, vb), 1610 (s, b, $\text{C}=\text{N}$), 1510, 1325, 1240, 1215, 1120, 990, 875, 845, 690. Anal. Calcd for $\text{C}_6\text{H}_{12}\text{ClNS}$: C, 43.50; H, 7.30; N, 8.45; S, 19.35. Found: C, 43.08; H, 7.45; N, 8.63; S, 18.88.

8-Imino-7-thiaspiro[5.4]decane hydrochloride (S2IT·HCl, 7f): yield 0.17 g (35%); mp $130\text{--}135^{\circ}\text{C}$; ^1H NMR (400 MHz, $\text{DMSO}-d_6$) 7.37 (t, $J = 50.8$) and 7.34 (t, $J = 50.7$) (the major t is at 7.34, the combined integral of both 1.8 H, NH_2^+), 3.39 (t, 2 H, $J = 7.1$, 3- CH_2), 2.20 (t, 2 H, $J = 7.1$, 4- CH_2), 2.00 (m, 2 H), 1.69–1.79 (m, 4 H), 1.58 (m, 1 H), 1.33–1.38 (m, 3 H); IR (KBr) 2500–3500 (vs, vb), 1610 (s, $\text{C}=\text{N}$), 1525, 1445, 1405, 1130, 1100, 1020, 990, 875, 690.

***t*-8-Imino-7-thiabicyclo[4.3.0]nonane hydrochloride**

(**R2IT-HCl**, **7g**): yield 3.13 (59%); mp 254–255 °C dec; ^1H NMR (400 MHz, DMSO- d_6) 7.34 (t, 1 H, $J = 50.7$), 3.57 (td, 1 H, $J = 11.5, 3.4$, H-9), 3.24 (dd, 1 H, $J = 17.0, 5.7$, H-3_{eq}), 2.91 (dd, 1 H, $J = 17.0, 13.1$, H-3_{ax}), 2.22 (m, 1 H), 1.94–2.03 (m, 2 H), 1.75–1.84 (m, 2 H), 1.45–1.54 (m, 1 H), 1.28–1.39 (m, 3 H); IR (KBr) 2840 (vs, vb), 1624 (s, C=N), 1528, 998, 895, 880, 694. Anal. Calcd for $\text{C}_8\text{H}_{14}\text{ClNS}$: C, 50.12; H, 7.36; N, 7.31; S, 16.72. Found: C, 50.02; H, 7.29; N, 7.21; S, 16.79.

Preparation of Thiol-Activated Model Compounds. TNB-activated X2ITs were prepared by aminolysis in the presence of the aromatic disulfide DTNB. Each X2IT (final concentration 0.5 mM) was added to a solution of 1.0 mM DTNB in 30 mM NH_4HCO_3 , pH 8.0. After 1 h at 25 °C, the reactions were terminated, and solvent was removed, by lyophilization. The activated model compounds ($\text{NH}_2\text{-X2IT-TNB}$) were resuspended in 0.5 mL of 25 mM sodium citrate, pH 3.2, and applied to separate 1-mL columns of S-Sepharose Fast Flow (Pharmacia) equilibrated in the same buffer. Each column was washed with citrate buffer until the absorbance at 412 nm approached zero, and the model disulfides were then eluted with PBS-EDTA.

Preparation of IND1-M2IT-RTA. A mixture of the murine IgG2a IND1 antibody (20 μM , 3 mg/mL, 2 mL), DTNB (5.0 mM), and M2IT (3.4 mM) in PBS-EDTA was incubated at 25 °C until the absorbance of the reaction mixture at 412 nm reached 0.54. Excess reagents and reaction byproducts were then removed by desalting on a 1 cm \times 20 cm column Sephadex G25F equilibrated at 4 °C in PBS-EDTA. The thiolated IND1-M2IT-TNB antibody so prepared (6.4 μM , 5 mL) was mixed with a 5-fold molar excess of RTA, and the mixture was incubated at 4 °C for 16 h. The IND1-M2IT-RTA immunotoxin was subsequently purified by size-exclusion chromatography on a 1 cm \times 32 cm column of AcA44 equilibrated in PBS at 4 °C.

RESULTS

Synthesis and Characterization of Substituted 2-Iminothiolanes. The X2IT-HCl analogues (Table I) were prepared by cyclization of γ -mercapto or γ -thioacetyl nitriles in methanolic HCl (Scheme I). Both the parent unsubstituted 2IT (**7a**) and M2IT (**7b**) have been previously prepared in this way (11, 12). The nitriles were prepared either by ring opening of the appropriate epoxide with sodium or lithium acetonitrile (13, 14), followed by mesylation of the γ -hydroxy nitrile and displacement with cesium thioacetate (15) (route A), or by ring opening of a thiirane with lithium acetonitrile (route B). The thiiranes were prepared from the corresponding epoxides either with potassium thiocyanate in EtOH (or MeOH)/ H_2O (16) or with 3-methylbenzothiazole-2-thione (17). Route B was useful when nucleophilic substitution of a mesylate would be difficult [TB2IT (**7c**) and DM2IT (**7e**)]. Similarly, the cis-fused bicyclic R2IT (*cis*-**7g**) could not be prepared by substitution of mesylate **3g** or the corresponding triflate with cesium thioacetate, but the trans-fused (*trans*-**7g**) compound was readily prepared via cyclohexene sulfide (route B). The reaction of lithioacetonitrile with 2-phenylthiirane proceeded poorly, so in this case Ph2IT (**7d**) was prepared via route A. The preparation of nonracemic 5-substituted X2ITs was not investigated, but should be feasible from commercially available chiral epoxides such as (*R*)-(+)-styrene oxide and (*S*)-(-)-propylene oxide or the derived thiiranes (16, 18).

The X2IT-HCl compounds (**7a-g**) were characterized by ^1H NMR, IR, and UV spectroscopy and elemental

Table II. Properties of Substituted 2-Iminothiolanes

linker	λ_{max}	ϵ , 1 mM, 248 nm	reaction rates (25 °C); k , s^{-1}	
			hydrolysis ^a ($\times 10^{-5}$)	glycine ^b ($\times 10^{-3}$)
2IT	247	8.72	1.4	5.3
R2IT	250	9.07	1.7	3.4
M2IT	247	9.27	0.7	4.8
Ph2IT	246	9.00	0.2	5.2
TB2IT	248	11.7	0.8	4.4
DM2IT	247	10.8	0.9	3.5
S2IT	248	10.7	0.7	3.0

^a The X2ITs (100 μM) were incubated at 25 °C in PBS-EDTA and changes in the absorbance at 248 nm were monitored. Plots of $\log [\text{X2IT}]$ vs time were linear, and first-order rate constants were calculated from the slopes. ^b The rates of reaction of the X2ITs (100 μM) with glycine (160 mM) in PBS-EDTA were examined by coupling the reaction with 0.5 mM DTNB and monitoring changes at 412 nm. First-order rate constants were determined from the linear slopes of $\log [\text{X2IT}]$ vs time plots.

analysis. The recrystallized X2ITs are easily handled and stable for at least 6 months when stored dry at 4 °C. The compounds are readily soluble in H_2O or polar solvents such as DMSO. The ^1H NMR spectra of the X2ITs are straightforward, showing signals for the 4- CH_2 from 1.9 to 2.7 ppm, for the 3- CH_2 from 2.9 to 3.4 ppm, and for the 5-CH (when present) from 3.5 to 5.4 ppm. The trans ring fusion of R2IT (**7g**) was assigned on the basis of the assumed anti opening of cyclohexene sulfide with lithioacetonitrile and by the 11.5 Hz coupling observed between the bridgehead protons.

The UV spectra of the X2ITs have a maximum at 246–250 nm with mM extinction coefficients of ca. 10 (Table II). The UV absorbance of the X2ITs is lost upon ring opening and this provides a convenient method of monitoring hydrolysis or aminolysis rates. The rates of aqueous hydrolysis of the X2ITs (**7a-g**) in PBS could therefore be followed by (i) the loss of absorbance at 248 nm or (ii) coupling the reaction with DTNB. As shown in Table II, aqueous hydrolysis of the X2ITs was relatively slow, followed first-order kinetics, and showed little dependence upon ring substitution. The rates shown are for the direct optical assay; similar values were obtained when the released thiol was trapped with DTNB and the reaction monitored at 412 nm (data not shown). The rates of X2IT hydrolysis were thus unaffected by the presence of DTNB.

Reactivity with Glycine. Reaction of the X2ITs with amino groups was analyzed by incubating each cross-linker with glycine at pH 7.2. In order to better mimic the reaction with proteins, these reactions were performed in the presence of DTNB, thus allowing both real-time monitoring of the reaction, as well as activation of the newly exposed iminothiolane thiol. Each X2IT was therefore incubated with glycine and DTNB, and changes in the absorbance at 412 nm were monitored. Under these conditions, the reaction rates were first-order and were again unaffected by the ring substituent (Table II). Similar rates were also obtained when the reactions were monitored optically at 248 nm in the absence of DTNB (data not shown). Under the experimental conditions employed, the rates of reaction of the X2ITs with glycine were typically 5000-fold greater than the rates of aqueous hydrolysis.

Preparation and Stability of Model Disulfides. In order to assess the effect of the various ring substituents on subsequent disulfide bond stability, TNB-activated model conjugates were prepared by reacting each X2IT with ammonium bicarbonate in the presence of DTNB. Aminolysis with ammonium bicarbonate was chosen for these experiments because excess NH_3 and buffer could

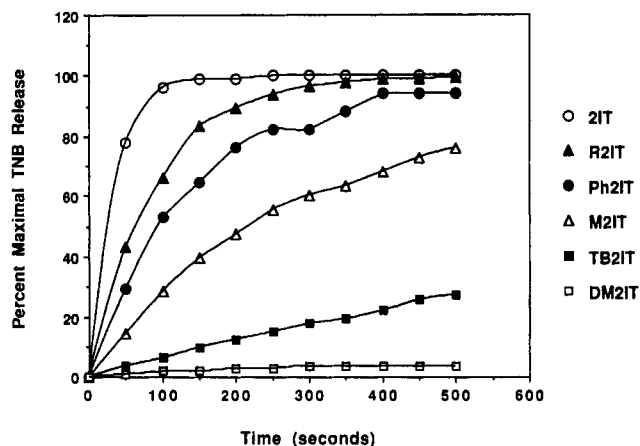


Figure 2. Glutathione-induced release of TNB from NH_2 -X2IT-TNB model conjugates. Samples of the activated model conjugates ($20 \mu\text{M}$) in PBS-EDTA were placed in a cuvette thermostated to 25°C and, at $T = 0$, reduced glutathione was added to a final concentration of $200 \mu\text{M}$. The release of TNB was monitored optically at 412 nm for 500 s , and 2-mercaptoethanol was then added to a final concentration of 200 mM to determine maximal release of TNB. The plots for the different linkers were normalized by determining percent maximal TNB release, as calculated by dividing the amount of TNB released at any timepoint by the amount released with 2-mercaptoethanol.

Table III. Relative Stability of TNB-Activated NH_2 -Iminothiolanes

	TNB release rate (25°C), ^a $k (\times 10^{-4}), \text{s}^{-1}$	stability increase relative to 2IT ^b
NH_2 -2IT-TNB	318	1.0
NH_2 -R2IT-TNB	113	2.8
NH_2 -Ph2IT-TNB	70.0	4.5
NH_2 -M2IT-TNB	32.5	9.8
NH_2 -TB2IT-TNB	3.22	99
NH_2 -DM2IT-TNB	0.076	4184

^a Reactions contained $20 \mu\text{M}$ NH_2 -X2IT-TNB in PBS-EDTA at 25°C and were initiated by the addition of reduced glutathione as described in the legend to Figure 2. The concentration of added glutathione was varied between $50 \mu\text{M}$ and 200 mM in order to achieve linear plots of $\log [\text{NH}_2\text{-X2IT-TNB}]$ vs time, and first order rate constants were then determined. ^b Calculated by dividing the rate constant for TNB release for each model conjugate by that obtained for NH_2 -2IT-TNB.

be removed by lyophilization, thereby minimizing ionic effects. Conditions were chosen such that each linker was quantitatively converted to the corresponding activated model conjugate (NH_2 -X2IT-TNB). Following lyophilization, the model conjugates were purified by cation-exchange chromatography to remove unreacted DTNB and TNB. The relative stabilities of these mixed disulfides were then examined by reacting the model conjugates with reduced glutathione. The release of TNB was monitored at 412 nm , providing a direct measure of glutathione-induced disulfide bond cleavage.

A comparative rate plot for the activated X2IT model conjugates ($20 \mu\text{M}$) incubated with $200 \mu\text{M}$ glutathione is shown in Figure 2. By varying the concentration of glutathione (0.05 to 250 mM) for the different compounds, first-order rate constants for TNB release were determined (Table III). The results indicate that the relative stability of the disulfide bonds formed by the X2ITs vary by a factor of roughly 4000, with DM2IT being the most stable, followed by TB2IT and M2IT.

Preparation of Protein-Protein Conjugates. To confirm the utility of the X2IT reagents for the preparation of antibody-toxin conjugates, one of the linkers (M2IT) was reacted with the murine IgG2a antibody IND1 (21)

in the presence of DTNB. The reaction was monitored optically at 412 nm and was terminated when the absorbance indicated 1.9 activated thiols/mol of protein. Following purification, an aliquot was removed and treated with 0.1 mM DTT; the activated IND1-M2IT-TNB antibody contained 2.0 TNB/mol . Subsequent conjugation with RTA gave IND1-M2IT-RTA in high yield.

DISCUSSION

The X2ITs described here represent a new family of cross-linking reagents that should prove useful in the preparation of stabilized protein conjugates linked by a disulfide bridge. Like 2IT (11), the X2ITs are highly water soluble, they react with amino groups to produce a stable amidinium linkage (thereby preserving the positive charge), and the reaction rate and extent can be monitored in real time by including an aromatic disulfide in the reaction mixture. In addition, the relative stability of the conjugate disulfides can be controlled by appropriate substitution on the 2IT ring, particularly at the 5-position. With the model conjugates prepared here, disulfide bond stability was increased from 6- to 4000-fold relative to unsubstituted 2IT and was well-correlated with the degree of steric hindrance (see below). Importantly, these increases were achieved without adversely affecting either the rate of reaction with glycine or the aqueous lability of the linker.

In designing cross-linking reagents for the preparation of disulfide-linked immunoconjugates, several features critical to actual therapeutic use must be evaluated (1). Some considerations (and consequences) include (i) the effect of linker derivatization on protein function (reduced binding or enzymatic activity, altered charge, etc.), (ii) variations in subsequent conjugation efficiency (lower efficiency necessitates higher linker/protein ratios and reagent needs), and (iii) relative stability in vivo (rapid deconjugation reduces the effective serum concentration and liberates competitive ligand). Whereas some of these concerns are empirical (i.e., the effect of linker derivatization), the remainder can be readily controlled by appropriate linker chemistry and selection.

Each of the above concerns can be minimized by the use of a linking reagent that allows both efficient conjugation with thiol-containing compounds, as well as the ability to control disulfide bond stability. Thus, the absolute number of linkers/molecule can be minimized, reducing the probability that protein function will be affected. Preliminary results suggest that the efficiency of conjugation (i.e., the efficiency with which the aromatic leaving groups are replaced by the protein thiol) for the X2ITs ranges between 60 and 100%, depending upon the diaryl disulfide present in the reaction mixture (unpublished data). These results, together with the preservation of positive charge and the controlled bond stability, support the use of the X2ITs in the preparation of human therapeutics.

Mechanistically, the observed increases in the stability of model X2IT disulfides conferred by α -alkylation can be rationalized by assuming that the incoming thiolate nucleophile (glutathione in this case) must attack the sulfur atom derived from the X2IT (see Figure 1). It has been postulated that this thiol-exchange process is a nucleophilic substitution with the attacking thiolate approaching along the extension of the S-S bond (22). According to this model, the $\sigma^*(\text{S-S})$ orbital interacts with the approaching nucleophile. Molecular modeling indicates that α -methyl groups do provide significant shielding of the adjacent S and that this shielding increases with increased steric bulk ($\text{H} < \text{methyl} < \text{tert-butyl} < \text{dime-}$

thyl). That this increased shielding closely parallels the measured increases in disulfide bond stability (1-, 10-, 100-, and 4000-fold, respectively) strongly argues in favor of steric protection.

The model reactions and conjugations described here have been successfully extended to the construction of other conjugates between monoclonal antibodies and RTA (manuscript in preparation). Preliminary data suggest that these conjugates are more stable to reduction than the corresponding SPDP conjugates. Within this context, it will be of interest to compare the relative stabilities of such conjugates with those of the model compounds described here. It should be emphasized, however, that the utility of the X2ITs is not limited to the construction of immunotoxins, but extends to the preparation of other protein-protein, protein-drug, and protein-enzyme conjugates where control of disulfide bond stability and maximum conjugation efficiency are essential.

LITERATURE CITED

- (1) Blakey, D. C., Wawrzynczak, E. J., Wallace, P. M., and Thorpe, P. E. (1988) Antibody toxin conjugates: A perspective. *Prog. Allergy* 45, 50-90.
- (2) Masuho, Y., Kishida, K., Saito, M., Umemoto, N., and Hara, T. (1982) Importance of the antigen-binding valency and the nature of the cross-linking bond in ricin A-chain conjugates with antibody. *J. Biochem.* 91, 1583-1591.
- (3) Ramakrishnan, S., and Houston, L. L. (1985) Immunochemical and biological stability of immunotoxins in vivo as studied by the clearance of disulfide-linked pokeweed antiviral protein-antibody conjugates from blood. *Cancer Res.* 45, 2031-2036.
- (4) Bourrie, B. J. P., Casellas, P., Blythman, H. E., and Jansen, F. K. (1986) Study of the plasma clearance of antibody-ricin A-chain immunotoxins. Evidence for specific recognition sites on the A-chain that mediate rapid clearance of the immunotoxin. *Eur. J. Biochem.* 155, 1-10.
- (5) Worrell, N. R., Cumber, A. J., Parnell, G. D., Ross, W. C. J., and Forrester, J. A. (1986) Fate of an antibody-ricin A chain conjugate administered to normal rats. *Biochem. Pharmacol.* 35, 417-423.
- (6) Thorpe, P. E., Blakey, D. C., Brown, A. N. F., Knowles, P. P., Knyba, R. B., Wallace, P. M., Watson, G. J., and Wawrzynczak, E. J. (1987) Comparison of two anti-Thy 1.1-abrin A-chain immunotoxins prepared with different crosslinking agents: antitumor effects, in vivo fate, and antitumor mutants. *JNCI, J. Natl. Cancer Inst.* 79, 1011-1111.
- (7) Worrell, N. R., Cumber, A. J., Parnell, G. D., Mirza, A., Forrester, J. A., and Ross, W. C. J. (1986) Effect of linkage variation on pharmacokinetics of ricin A chain-antibody conjugates in normal rats. *Anti-Cancer Drug D.* 1, 179-188.
- (8) Thorpe, P. E.; Wallace, P. M.; Knowles, P. P.; Relf, M. G.; Brown, A. N. F.; Watson, G. J.; Knyba, R. E.; Wawrzynczak, E. J., and Blakey, D. C. (1987) New Coupling Agents for the Synthesis of Immunotoxins Containing a Hindered Disulfide Bond with Improved Stability in vivo. *Cancer Res.* 47, 5924-5931.
- (9) Thorpe, P. E., Wallace, P. M., Knowles, P. P., Relf, M. G., Brown, A. N. F., Watson, G. J., Blakey, D. C., and Newell, D. R. (1988) Improved Antitumor Effects of Immunotoxins Prepared with Deglycosylated A-Chain and Hindered Disulfide Linkages. *Cancer Res.* 48, 6396-6403.
- (10) Dosio, F., Cogliati, T., Canevari, S., Mezzanzanica, D., Brusa, P., Delprino, L., Colnaghi, M. I., and Cattel, L. (1989) Antibody-toxin conjugation preparation: Effects of the linker on activity and stability. *Antibody Immunoconjugate Radiopharm.* 2, 101-115.
- (11) Traut, R. R., Bollen, A., Sun, T.-T., Hershey, J. W. B., Sundberg, J., and Pierce, L. R. (1973) Methyl 4-Mercapto-butyrimidate as a Cleavable Cross-Linking Reagent and Its Application to the *Escherichia coli* 30S Ribosome. *Biochemistry* 12, 3266-3273.
- (12) Addor, R. W. (1967) U.S. Patents 3,318,910, 3,348,940.
- (13) Enoki, K., Yaio, T. (1984) Japan Kokai 74 14 424; *Chem. Abstr.* 81, 3392.
- (14) Menard, M., and Martel, A. (1981) U.S. Patent 4,272,437.
- (15) Strijtveen, B., and Kellogg, R. M. (1986) Synthesis of (Racemization Prone) Optically Active Thiols by S_N2 Substitution Using Cesium Thiocarboxylates. *J. Org. Chem.* 3664-3671.
- (16) Dumas, P., Spassky, N., and Sigwalt, P. (1972) Preparation and Polymerization of Racemic and Optically Active *tert*-Butyl Thiirane. *Makromol. Chem.* 156, 55-64.
- (17) Calo, V., Lopez, L., Marchese, L., and Pesce, G. (1975) A Simple Method for Converting Oxirans into Thiirans Stereospecifically. *J. Chem. Soc. Chem. Commun.* 621-622.
- (18) Gottarelli, G., Samori, B., Moretti, I., and Torre, G. (1977) Optical Activity of the 260 nm Transition of Chiral Thiirans. *J. Chem. Soc. Perkin Trans. 2* 1105-1111.
- (19) Snyder, H. R., Stewart, J. M., and Ziegler, J. B. (1947) The synthesis of amino mercaptans from olefin sulfides. *J. Am. Chem. Soc.* 69, 2672-2674.
- (20) Fullerton, D. S., Chen, C. M., and Hall, I. H. (1976) Trichothecene Analogues. 1. 1,5-dioxaspiro[2.5]octanes. *J. Med. Chem.* 19, 1391-1395.
- (21) Scannon, P. J., Spitler, L. E., Lee, H. M., Kawahata, R. T., and Mischak, R. P. (1986) Melanoma specific immunotoxins. U.S. Patent 4,590,071.
- (22) Rosenfield, R. E., Jr., Parthasarathy, R., and Dunitz, J. D. (1977) Directional Preferences of Nonbonded Atomic Contacts with Divalent Sulfur. 1. Electrophiles and Nucleophiles. *J. Am. Chem. Soc.* 99, 4860-4862.

Radioiodination of Antibodies via *N*-Succinimidyl 2,4-Dimethoxy-3-(trialkylstannyl)benzoates

Ganesan Vaidyanathan and Michael R. Zalutsky*

Duke University Medical Center, Department of Radiology, Box 3808, Durham, North Carolina 27710.
Received August 20, 1990

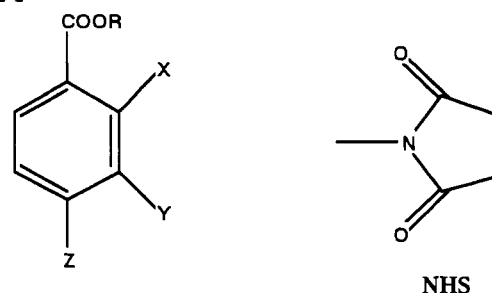
We have previously shown that use of *N*-succinimidyl 3-iodobenzoate (SIB) for radioiodination of monoclonal antibodies (MAbs) decreases the loss of radioiodine *in vivo* compared to MAbs labeled by using conventional methods. Herein, the synthesis of *N*-succinimidyl 2,4-dimethoxy-3-(trialkylstannyl)benzoates (alkyl = Me, Bu) are described as is their use as precursors for the radiosynthesis of *N*-succinimidyl 2,4-dimethoxy-3-iodobenzoate (SDMIB). A MAbs F(ab')₂ fragment labeled with SDMIB retained its ability to bind specifically to tumor homogenates. Paired-label tissue distribution studies indicate that the thyroid uptake (an indicator of deiodination) of hydrolyzed SDMIB was about 20 times that of hydrolyzed SIB. In contrast, thyroid uptake for SDMIB, when conjugated to a MAbs, was only 1.4–2.8 times that for SIB and was considerably lower than levels reported in the literature for MAbs labeled by using direct, electrophilic iodination methods. Although MAbs labeled with SDMIB are significantly more inert to dehalogenation than those labeled by conventional methods, compared to the original SIB reagent, addition of two methoxy groups decreased retention of label *in vivo*.

When radiolabeled monoclonal antibodies (MAbs)¹ are administered to patients intravenously, uptake of radioactivity is low, generally about 0.005% of the injected dose per gram (1). For this reason, single photon emission tomography is often required to obtain satisfactory sensitivity for tumor detection (2). Of the nuclides under active investigation for use in radioimmunoscintigraphy, 6-h ^{99m}Tc and 13-h ¹²³I have the most suitable nuclear properties for single photon emission tomography, particularly when quantitation of tracer uptake for dosimetric calculations is required. For many applications of labeled MAbs, the added expense and inconvenience of using ¹²³I may be more than offset by the greater compatibility of its physical half-life with MAbs pharmacokinetics.

Methods for the direct radioiodination of proteins have been available for many years (3). However, use of oxidants such as Iodogen or chloramine-T results primarily in the formation of iodinated tyrosine residues (4), and MAbs labeled by this approach have been observed to undergo extensive loss of label *in vivo* (5–7). Since numerous deiodinases exist with varying specificities for iodotyrosines and thyronines (8–10), MAbs dehalogenation probably is related to recognition of iodotyrosines on the MAbs by these enzymes.

In an attempt to minimize MAbs dehalogenation by providing an iodination site with a different chemical structure, we developed a method which involves reaction of the MAbs with *N*-succinimidyl 3-iodobenzoate (SIB, 1, Chart I), which is prepared by the iododestannylation of *N*-succinimidyl 3-(tri-*n*-butylstannyl)benzoate (ATE, 2)

Chart I



1. SIB R = NHS, X = Z = H, Y = I
2. ATE R = NHS, X = Z = H, Y = SnBu₃
- 3a. DMATE-Me R = NHS, X = Z = OCH₃, Y = SnMe₃
- 3b. DMATE-Bu R = NHS, X = Z = OCH₃, Y = SnBu₃
4. SDMIB R = NHS, X = Z = OCH₃, Y = I
5. IBA R = X = Z = H, Y = I
6. DMIBA R = H, X = Z = OCH₃, Y = I

(11). Paired-label studies demonstrated that proteins labeled via the ATE method had significantly lower uptake of activity in the thyroid and stomach (tissues known to avidly accumulate free iodide) compared to the same proteins labeled by using the Iodogen method (11–13). Similar results have been reported by other groups using MAbs and fragments labeled with 4-iodophenyl conjugates (14, 15), confirming the influence of the nature of the MAbs iodination site on *in vivo* stability.

Further improvements in protein radiohalogenation methodology will be facilitated by gaining a better understanding of the structural features required for minimizing dehalogenation. For example, although both the Bolton–Hunter and Iodogen methods involve radioiodination ortho to a hydroxyl group on an aromatic ring,

¹ Abbreviations: MAbs, monoclonal antibodies; SIB, *N*-succinimidyl 3-iodobenzoate; ATE, *N*-succinimidyl 3-(tri-*n*-butylstannyl)benzoate; DMATE-Bu, *N*-succinimidyl 2,4-dimethoxy-3-(tri-*n*-butylstannyl)benzoate; DMATE-Me, *N*-succinimidyl 2,4-dimethoxy-3-(trimethylstannyl)benzoate; DCC, dicyclohexylcarbodiimide; SDMIB, *N*-succinimidyl 2,4-dimethoxy-3-iodobenzoate; IBA, 3-iodobenzoic acid; DMIBA, 2,4-dimethoxy-3-iodobenzoic acid.

MAbs labeled by using the Bolton–Hunter method are considerably more inert to dehalogenation *in vivo* (16). In the present study, we investigated the utility of labeling MAbs via the iododestannylation of *N*-succinimidyl 2,4-dimethoxy-3-(tri-*n*-butylstannyl)benzoate (DMATE-Bu, **3b**) (17) and its trimethylstannyl analogue **3a** (DMATE-Me). The primary objective of this investigation was to determine whether substitution of electron-rich methoxy groups ortho to the iodine on the aromatic ring would decrease the probability of nucleophilic displacement of the iodine, thereby enhancing the *in vivo* stability of the carbon–iodine bond.

EXPERIMENTAL PROCEDURES

General Procedures. NMR spectra were obtained in CDCl₃ solution with a General Electric midfield GN-300 spectrometer. The proton chemical shifts are reported in ppm downfield from internal TMS (0.00 ppm). IR spectra were obtained on a BOMEM MB-100 variable-resolution FTIR spectrophotometer. Mass spectral data were obtained on a VG 70S (VG Analytical, Danvers, MA) instrument operating in the EI mode. Melting points were determined on a Haake Buchler variable-heat apparatus and are uncorrected.

All reagents were of reagent grade or better. THF was distilled over LiAlH₄. ATE was prepared as reported before (11). DMATE-Bu was synthesized with slight modifications of the previously described procedure (17), and DMATE-Me was prepared in a similar fashion, the details of which are given below.

Sodium [¹²⁵I]iodide and sodium [¹³¹I]iodide, both in 0.1 N NaOH, were obtained from Du Pont–New England Nuclear (North Billerica, MA). MAb C110 is a murine IgG1 reactive with carcinoembryonic antigen (18) and was obtained as a gift from Dr. David Johnson of Abbott Laboratories. Me1-14 is a murine IgG2a reactive with the tumor-associated chondroitin sulfate present in melanomas and gliomas (19). The procedure for generation of Me1-14 F(ab')₂ fragments has been described (20). This fragment was obtained as a gift from Dr. Darell D. Bigner of the Department of Pathology, Duke University Medical Center.

Thin-layer chromatography was done on EM Science analytical silica plates. Flash chromatography was done with 230–400 mesh silica gel from VWR Scientific, Marietta, GA. High-pressure liquid chromatography was conducted with an LKB Model 2150 pump, an LKB Model 2151 variable-wavelength UV detector, and a Beckman Model 170 radioisotope detector. Peak analysis was performed with a Nelson analytical software package on an AT&T 6300 computer. The column used was an Alltech silica gel column (Partisil 10 silica 10 μm, 250 × 4.6 mm). Radioactivity counting was performed with a LKB 1282 dual channel γ-counter.

Synthesis of DMATE-Me (3a). A solution of 3-bromo-2,4-dimethoxybenzoic acid, prepared as previously described (17) (786 mg, 3 mmol) in 96 mL of dry THF, was cooled in an ether/liquid nitrogen bath (–100 °C). To this solution was added dropwise 3.8 mL of butyllithium (1.6 M in hexane; 2 equiv), and the mixture was stirred at –100 °C for another 30 min. A solution of trimethylstannyl chloride (1.56 g, 7.85 mmol) in THF (5 mL) was added. The reaction mixture was allowed to warm to room temperature and stirred overnight. All of the above operations were done under an argon atmosphere. At the end of the reaction, the reaction mixture was partitioned between water and ether (100 mL of each). The aqueous layer was further extracted with ether (3 × 50 mL). The

combined ethereal layer was washed with brine (2 × 10 mL), dried over sodium sulfate, and evaporated to yield 1.2 g of a white solid. This was purified by silica gel flash chromatography with a gradient elution of 0–30% ethyl acetate in hexane to give 460 mg (45% yield) of a white, crystalline solid. Mp: 108–111 °C. NMR: (CDCl₃) δ 0.37 (s, 9 H, SnCH₃), 3.82 (s, 3 H, 4-OCH₃), 3.85 (s, 3 H, 2-OCH₃) 6.75 and 8.14 (dd, 2 H, aromatic, *J* = 8.65 Hz). (Note: NMR indicates this is the free acid in contrast to the tin ester obtained in the case of the butyl analogue. No attempt was made to further characterize it prior to proceeding to the next step.) To 250 mg (0.72 mmol) of the above solid in 10 mL of dry THF were added 120 mg (1.04 mmol) *N*-hydroxysuccinimide and 180 mg (0.87 mmol) of DCC under an argon atmosphere. The mixture was stirred overnight at room temperature. Precipitated dicyclohexylurea was filtered and washed with THF. The filtrate containing the product was evaporated in a rotary evaporator, and the residue was flash chromatographed on silica gel using a 0–30% ethyl acetate in hexane gradient to give 180 mg (58% yield) of a white, crystalline solid. Mp: 85–86 °C. NMR: (CDCl₃) δ 0.33 (s, 9 H, SnMe₃), 2.89 (br s, 4 H, NHS), 3.78 (s, 3 H), 3.80 (s, 3 H), 6.65 and 8.10 (dd, 1 H each, *J* = 8.71 Hz). IR: (KBr) cm^{–1} 3328, 2931, 2853, 1773, 1737, 1578. MS: *m/z* 428 (M – CH₃), 329 (M – ONHS), 299. Anal. Calcd for C₁₅H₁₈O₆NSn (M – CH₃) 428.0156, found 428.0163. TLC: 30% EtOAc/hexane, *R_f* = 0.16. HPLC: more than 99% pure; retention volume is 11.2 mL (EtOAc/hexane/HOAc 50:50:2; 0.8 mL/min, 10 bar).

Radioiodination Procedure. [¹²⁵I]SIB was synthesized from ATE and purified as described before (21). For the synthesis of [¹³¹I]SDMIB (4), sodium [¹³¹I]iodide (ca. 100 μCi) in about 5 μL of 0.1 N NaOH was transferred to a 1-mL conical glass vial and evaporated with a gentle stream of argon. (No loss of ¹³¹I activity was observed.) A 3% solution of acetic acid in CHCl₃, in a volume twice that of the ¹³¹I solution, was added, followed by 15 μL of *tert*-butyl hydroperoxide solution (10% dry basis in CHCl₃) and 5 μL (0.5 μmol) of either DMATE-Bu or DMATE-Me. The mixture was stirred for 1–30 min. The percent yield of [¹³¹I]SDMIB was determined by injecting an aliquot onto the HPLC and determining the fraction of the ¹³¹I which eluted with a retention time corresponding to that of a cold SDMIB standard (*t_R* = 14.0 min).

For biological experiments, higher amounts (0.5–1.5 mCi) of radioactivity were used. Free acids IBA (5) and DMIBA (6) were prepared by hydrolyzing the corresponding *N*-succinimidyl esters overnight in phosphate-buffered saline. The extent of hydrolysis was checked by acidifying an aliquot with acetic acid, extracting with EtOAc, and analyzing the EtOAc layer by HPLC.

Labeling of MAbs by Reaction with [¹²⁵I]SIB or [¹³¹I]SDMIB. The general methodology used for MAb labeling was similar to that reported previously (16, 21). In brief, the HPLC fractions containing [¹³¹I]SDMIB or [¹²⁵I]SIB (300–1000 μCi) were concentrated to <100 μL and transferred to a 1/2-dram vial. A gentle stream of argon was used to evaporate the remaining solvent. C110 MAb or Me1-14 F(ab')₂ (75–150 μL, 2–3.5 mg/mL) in 0.1 M borate buffer of pH 8.5 was added to the dried activity and incubated at room temperature for 20 min. Glycine solution, 0.2 M in the above buffer, was added at the end of 20 min to consume unreacted ester, and the mixture was incubated further for 5 min. The labeled protein was purified by gel filtration on Sephadex G-25 eluted with phosphate-buffered saline. The coupling yield was determined by calculating the percent of activity loaded

on the column that eluted in the void volume. Protein-associated activity was determined by trichloroacetic acid precipitation.

Evaluation of Immunoreactivity. F(ab')₂ fragments of Me1-14 were labeled with ¹³¹I by reaction with [¹³¹I]-SDMIB and their immunoreactivity was evaluated by determination of their specific binding in vitro to D-54 MG human glioma tumor homogenates. Between 50 and 100 ng of ¹³¹I-labeled Me1-14 F(ab')₂ in 1 mL of phosphate buffer (pH 7.4) was incubated in triplicate with 300 mg of both D-54 MG glioma and normal pork liver homogenates. After a 4-h incubation at room temperature, the homogenates were washed three times with phosphate buffer containing 2% human serum albumin. Specific binding was calculated by subtracting the percentage ¹³¹I bound to liver from the percentage bound to tumor.

Tissue Distribution Measurements. Three different sets of paired-label studies were performed in BALB/c mice weighing between 25 and 30 g. To investigate the inertness of DMIBA to dehalogenation, five or six animals per time point were injected through the tail vein with 6 μ Ci of [¹³¹I]DMIBA and 8 μ Ci of [¹²⁵I]iodide; groups of mice were killed by halothane overdose at 1, 2, 5, 6, and 24 h. In the second experiment, animals were injected with 4 μ Ci of [¹³¹I]DMIBA and 6 μ Ci of [¹²⁵I]IBA and groups of five or six mice were killed at 1, 2, 4, 6, and 24 h. In the third experiment, animals received 6 μ Ci (2 μ g) of MAb C110 IgG1 labeled with ¹³¹I prepared with ATE and 7.5 μ Ci (4 μ g) of MAb C110 labeled with ¹²⁵I by using DMATE-Bu as described above. Groups of five or six animals were killed by halothane overdose 1, 2, 3, and 4 days after labeled MAb administration. An additional experiment was performed in two groups of five mice who were injected with 5 μ Ci of [¹²⁵I]iodide and 4 μ Ci of [¹³¹I]DMIBA and sacrificed 4 h after injection. One group of animals had been given 0.1% potassium iodide as their drinking water starting 3 days prior to the experiment to block thyroid uptake of free iodide.

In all cases, the animals were dissected at the appropriate time points and tissues of interest were removed, washed with saline, and weighed. Activity in each organ was counted in a dual-channel γ -counter. Counting data were automatically corrected for ¹³¹I crossover into the ¹²⁵I window and decay of both nuclides. The percent injected dose of both ¹²⁵I and ¹³¹I in each tissue was calculated by comparison to injection standards of appropriate count rates.

Statistical Analysis. A direct comparison of the tissue distribution of the ¹²⁵I- and ¹³¹I-labeled compounds was possible since a paired-label format was used, with each animal serving as its own control. A paired *t* test with one-sided alternative was used to analyze the data (22). Only cases with *P* < 0.05 have been considered to be statistically significant.

RESULTS

Chemical Synthesis. DMATE-Me was prepared in two steps in ca. 25% overall yield. First, 3-bromo-2,4-dimethoxybenzoic acid was reacted with *n*-BuLi and trimethylstannyl chloride to yield an intermediate whose NMR spectrum, after purification over silica gel, was consistent with the formation of 2,4-dimethoxy-3-trimethylstannylbenzoic acid. (This is in contrast to **3b**, the corresponding tributyl tin ester of which is stable to chromatography.) The desired compound **3a** was produced by treatment of this intermediate with *N*-hydroxysuccinimide and dicyclohexylcarbodiimide. The assigned structure for **3a** was in full agreement with its spectral data.

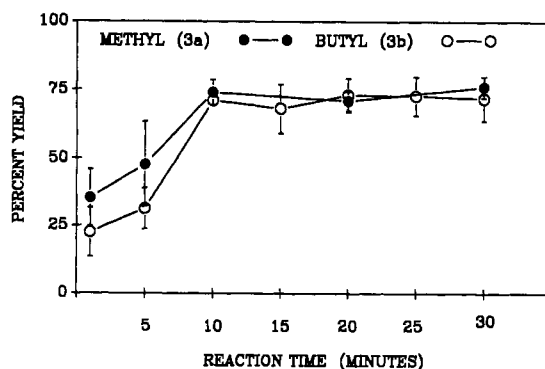


Figure 1. Yields for the radioiodination of DMATE-Bu and DMATE-Me as a function of reaction time.

Purity of **3a** (and **3b**) was determined to be greater than 98% by HPLC.

Radioiodination of 3a and 3b. The radioiodination of the *N*-succinimidyl active esters **3a** and **3b** was performed in chloroform/acetic acid with *tert*-butyl hydroperoxide as the oxidant. The kinetics of radioiodo-destannylation are illustrated in Figure 1. Yields were determined by calculating the percent of activity injected on the HPLC column that eluted with the retention time of an authentic sample of **4** and dividing by the activity added to the column. At early time points, yields for synthesis of **4** via the destannylation of **3a** were higher than those from **3b** (35 \pm 11% and 48 \pm 16% for DMATE-Me and 23 \pm 9% and 31 \pm 8% for DMATE-Bu at 1 and 5 min, respectively); however, these differences were not significant (*P* = 0.067 at 1 min and *P* = 0.059 at 5 min; Student's *t* test). With both DMATE-Me and DMATE-Bu, average radioiodination yields of 70–75% were obtained for reaction times of 10 min or more. When paired experiments were performed with both DMATE-Bu and ATE, radioiodination yields were similar.

Protein Coupling and in Vitro Binding. Conjugation efficiencies for C110 IgG1 at a pH of 8.5 and a concentration of 2 mg/mL ranged between 48 and 68%. The ¹²⁵I-labeled preparation used for the biodistribution studies had a specific activity of 2 μ Ci/ μ g. Coupling of SDMIB to Me1-14 F(ab')₂, also at 2 mg/mL, proceeded in 40–45% yield.

The immunoreactivity of ¹³¹I-labeled Me1-14 F(ab')₂ was assessed by measuring its binding to antigen-positive D-54 MG glioma and antigen-negative pork liver homogenates. In vitro binding to tumor was 65.7 \pm 1.5% and binding to liver was 2.4 \pm 0.3%, resulting in a specific binding percentage of 63.3 \pm 1.5%.

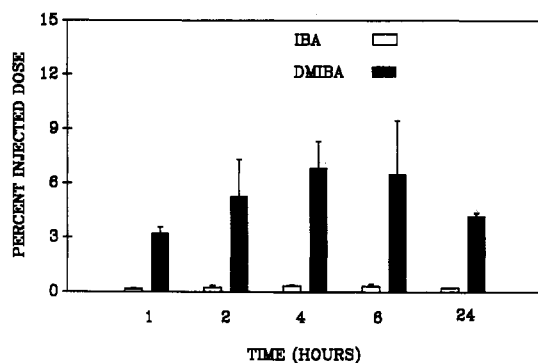
Biodistribution Studies. Paired-label studies were performed in normal mice injected with both DMIBA, a potential catabolite of MAbs labeled with DMATE, and either iodide or IBA, a potential catabolite of MAbs using the ATE reagent. In Table I, the tissue distribution of [¹²⁵I]iodide and [¹³¹I]DMIBA at 1 h and 6 h are compared (data for other time points available upon request). Most striking is the fact that the percent injected dose taken up by thyroid of DMIBA is only 2–3-fold lower than that of iodide (6.46 \pm 0.98% DMIBA, 15.65 \pm 2.09% iodide, *P* < 0.005, at 6 h). Stomach accumulation of iodide was higher than that of DMIBA, but in general when significant differences existed, tissue retention of ¹³¹I was higher than that of ¹²⁵I.

Mice were injected with both [¹³¹I]DMIBA and [¹²⁵I]-IBA to investigate the effect of the two methoxy groups on tissue distribution of radioiodine. As shown in Figure 2, thyroid uptake of ¹³¹I is about 20 times higher than that of ¹²⁵I, suggesting a significantly lower inertness to de-

Table I. Paired-Label Tissue Distribution of Radioiodine in Normal Mice following Injection of [^{131}I]DMIBA and [^{125}I]iodide^a

tissue	% injected dose per organ			
	1 h		6 h	
	DMIBA	iodide	DMIBA	iodide
liver	3.60 \pm 0.53	1.62 \pm 0.63	0.45 \pm 0.09	0.50 \pm 0.12 ^b
spleen	0.08 \pm 0.02	0.13 \pm 0.06	0.04 \pm 0.02	0.05 \pm 0.01 ^b
lung	0.52 \pm 0.16	0.49 \pm 0.21 ^b	0.19 \pm 0.06	0.10 \pm 0.06
heart	0.16 \pm 0.03	0.13 \pm 0.04 ^b	0.06 \pm 0.01	0.03 \pm 0.02
kidney	3.65 \pm 0.89	0.79 \pm 0.22	0.24 \pm 0.08	0.18 \pm 0.09
stomach	5.90 \pm 1.27	13.64 \pm 2.25	0.34 \pm 0.19	0.49 \pm 0.11
small intestine	3.04 \pm 1.07	5.14 \pm 2.10	0.50 \pm 0.17	0.77 \pm 0.33
large intestine	1.08 \pm 0.13	1.38 \pm 0.16	0.64 \pm 0.26	1.08 \pm 0.41
muscle	5.28 \pm 1.43	6.21 \pm 2.71 ^b	2.27 \pm 0.23	1.65 \pm 0.42
bone	2.20 \pm 0.61	3.49 \pm 1.30	0.60 \pm 0.22	0.65 \pm 0.35 ^b
blood	4.06 \pm 0.59	3.79 \pm 1.44 ^b	1.38 \pm 0.26	0.78 \pm 0.38
brain	0.18 \pm 0.04	0.08 \pm 0.03	0.10 \pm 0.02	0.04 \pm 0.03
thyroid	2.58 \pm 0.72	7.10 \pm 1.90	6.46 \pm 0.98	15.65 \pm 2.09

^a Results are mean \pm SD. ^b Differences not significant ($P > 0.05$) by paired t test.

**Figure 2.** Comparison of the percent injected dose of radioiodine localized in the thyroids of normal mice injected with [^{131}I]DMIBA and [^{125}I]IBA.

halogenation of DMIBA compared with IBA. As to other tissues, excepting the data for bone at 2 h, retention of ^{131}I was significantly higher ($P < 0.01$) than that of ^{125}I in all tissues at all time points (Table II). The uptake differential was greatest in stomach, where a 20-fold higher accumulation of ^{131}I activity was seen at 1 and 2 h.

Paired-label biodistribution measurements were also performed in normal mice to compare the in vivo distribution of MAb C110 IgG1 labeled with ^{125}I by using SDMIB and with ^{131}I by using SIB. As shown in Figure 3, thyroid uptake of ^{125}I ($0.64 \pm 0.12\%$) and ^{131}I ($0.45 \pm 0.12\%$) were comparable at 1 day postinjection (Figure 3); however, by days 3 and 4, accumulation of radioiodine from MAb labeled with SDMIB was 2.5-fold that of MAb labeled with SIB (significance of difference, $P < 0.005$). As shown in Table III, in general, uptake of both nuclides was similar in all tissues at all time points except for the stomach and large intestine, where SDMIB was higher, and blood, where use of SDMIB to label the MAb resulted in significantly lower activity levels ($P < 0.01$).

In order to evaluate the effect of substitution of two methoxy groups ortho to the iodination site, thyroid uptake ratios were calculated for the carboxylic acids and their MAb conjugates. The DMIBA/IBA uptake ratio ranged between 20 and 25:1 for data obtained at 1–24 h compared with only 1.4–2.8:1 for the MAb conjugates. To investigate whether this difference was related to the active uptake of DMIBA or its labeled catabolite or if it reflected dehalogenation and production of free iodide, DMIBA and

iodide were given to mice receiving blocking doses of potassium iodide in their drinking water. With [^{125}I]iodide, iodide blocking decreased thyroid uptake from $8.2 \pm 1.0\%$ to $0.05 \pm 0.01\%$; for [^{131}I]DMIBA, iodide blocking likewise decreased thyroid accumulation from $2.9 \pm 0.6\%$ to $0.07 \pm 0.01\%$.

DISCUSSION

As part of our continuing efforts to develop better radiohalogenation agents for use in labeling MABs, in this study we have investigated whether increasing electron density at the carbon bearing the radioiodine in the aromatic ring would decrease dehalogenation in vivo. In order to test this hypothesis, analogues of the original ATE reagent containing methoxy groups on both positions ortho to the trialkylstannyl group were synthesized.

Both DMATE-Bu and DMATE-Me were synthesized in order to determine whether decreasing the bulk of the alkyltin substituent increased the rate of iododestannylation. This was of particular interest because it was thought that the ortho methoxy groups might provide steric interference in the radioiodination reaction. Previous studies have shown that changing the alkyl substituent on the tin from Bu to Me can increase the rate of iododestannylation (21, 23). Our results indicate that for reaction times less than 10 min, labeling of [$^{125}\text{I}/^{131}\text{I}$]SDMIB proceeded more rapidly with the Me precursor; however, the differences were not statistically significant. With regard to the influence of the methoxy groups on the rate of destannylation, paired studies indicated that labeling yields using DMATE and ATE were similar, suggesting a balance between steric and electronic effects.

The specific binding of the F(ab')₂ fragment of Me1-14 F(ab')₂ after labeling with ^{131}I by using DMATE-Bu was determined to be 63%. This compares favorably with a range of 40–61% reported for this fragment labeled by using Iodogen (24) and identical with that observed (25) with the ATE method. Thus, at least for this particular MAb fragment, use of DMATE for MAB radioiodination provides a labeled protein with immunoreactivity greater than that obtained by using a conventional, direct electrophilic iodination approach.

In addition to retaining immunoreactivity, an additional factor of importance in evaluating new labeling methods is the pharmacokinetics of potential labeled catabolites. For example, we have reported previously that an advantage of using the ATE method for labeling MABs is the more rapid tissue clearance of IBA compared to that of iodide (12). Because of the altered lipophilicity induced by the substitution of the two methoxy groups (IBA, $\log k' = 0.81$; DMIBA, $\log k' = 0.53$; determined by reverse-phase HPLC as described in ref 26), it was anticipated that the tissue retention of activity of radioiodine from DMIBA would be different than that of IBA. In addition, DMIBA itself might be useful in approaches at reducing normal tissue background utilizing antibodies directed against small radioactive molecules with favorable blood-clearance rates (27).

The results of paired-label experiments suggest that substitution of the two methoxy groups ortho to the iodination site significantly retards the tissue clearance of DMIBA relative to IBA. The observation that thyroid uptake of DMIBA is about 20 times that of IBA and about 40% that of iodide suggests either extensive in vivo dehalogenation or active thyroid uptake of DMIBA or its labeled catabolite. In order to exclude the latter possibility, a paired-label experiment was performed in mice receiving both iodide and DMIBA, with and without a blocking dose

Table II. Paired-Label Tissue Distribution of Radioiodine in Normal Mice following Injection of [¹²⁵I]IBA and [¹³¹I]DMIBA^a

tissue	% injected dose/organ				
	1 h	2 h	4 h	6 h	24 h
[¹³¹I]DMIBA					
liver	3.18 ± 0.48	1.68 ± 0.42	0.89 ± 0.41	0.40 ± 0.12	0.17 ± 0.05
spleen	0.12 ± 0.02	0.10 ± 0.05	0.05 ± 0.02	0.02 ± 0.01	0.01 ± 0.00
lung	0.47 ± 0.11	0.32 ± 0.08	0.20 ± 0.09	0.11 ± 0.04	0.05 ± 0.01
heart	0.16 ± 0.02	0.10 ± 0.03	0.07 ± 0.03	0.04 ± 0.01	0.02 ± 0.00
kidney	2.53 ± 0.27	0.99 ± 0.13	0.46 ± 0.22	0.21 ± 0.04	0.09 ± 0.01
stomach	7.43 ± 2.42	6.19 ± 2.10	2.73 ± 1.68	0.48 ± 0.31	0.03 ± 0.01
small intestine	4.13 ± 0.18	2.50 ± 0.58	1.18 ± 0.57	0.43 ± 0.17	0.09 ± 0.04
large intestine	1.50 ± 0.45	1.45 ± 0.29	0.92 ± 0.07	0.52 ± 0.29	0.07 ± 0.01
muscle	5.71 ± 1.05	4.50 ± 1.15	2.69 ± 1.01	1.15 ± 0.41	1.27 ± 0.83
bone	2.82 ± 0.21	2.67 ± 1.16 ^b	1.22 ± 0.58	0.37 ± 0.18	0.10 ± 0.07
blood	4.20 ± 0.40	2.63 ± 0.55	2.01 ± 0.91	0.90 ± 0.21	0.36 ± 0.03
brain	0.16 ± 0.01	0.11 ± 0.01	0.10 ± 0.02	0.06 ± 0.01	0.04 ± 0.02
[¹²⁵I]IBA					
liver	0.21 ± 0.07	0.19 ± 0.06	0.09 ± 0.04	0.06 ± 0.01	0.02 ± 0.01
spleen	0.01 ± 0.00	0.02 ± 0.01	0.01 ± 0.00	0.00 ± 0.00	0.00 ± 0.00
lung	0.05 ± 0.02	0.05 ± 0.02	0.03 ± 0.01	0.03 ± 0.01	0.01 ± 0.00
heart	0.02 ± 0.00	0.01 ± 0.00	0.01 ± 0.00	0.01 ± 0.00	0.00 ± 0.00
kidney	0.10 ± 0.02	0.06 ± 0.01	0.04 ± 0.00	0.03 ± 0.00	0.01 ± 0.00
stomach	0.38 ± 0.09	0.32 ± 0.10	0.11 ± 0.04	0.03 ± 0.01	0.00 ± 0.00
small intestine	0.29 ± 0.05	0.20 ± 0.06	0.09 ± 0.04	0.04 ± 0.01	0.01 ± 0.00
large intestine	0.12 ± 0.05	0.15 ± 0.04	0.07 ± 0.01	0.04 ± 0.02	0.00 ± 0.00
muscle	0.71 ± 0.27	2.07 ± 1.53	0.36 ± 0.09	0.13 ± 0.02	0.06 ± 0.01
bone	1.07 ± 0.53	2.04 ± 1.46	0.19 ± 0.09	0.06 ± 0.02	0.02 ± 0.01
blood	0.45 ± 0.03	0.31 ± 0.12	0.30 ± 0.06	0.25 ± 0.02	0.09 ± 0.02
brain	0.01 ± 0.00	0.01 ± 0.00	0.01 ± 0.00	0.00 ± 0.00	0.00 ± 0.00

^a Results are mean ± SD. ^b Difference determined not to be statistically significant ($P > 0.05$) by paired t test; all other tissues, $P < 0.01$.

Table III. Paired-Label Tissue Distribution of Radioiodine in Normal Mice following Injection of MAb C110 IgG Labeled with ¹²⁵I by Using [¹²⁵I]SDMIB and with ¹³¹I by Using [¹³¹I]SIB^a

tissue	% injected dose per organ			
	1 day	2 days	3 days	4 days
Labeled with [¹³¹I]SIB				
liver	6.92 ± 0.61	7.17 ± 0.31	6.21 ± 0.57	5.97 ± 0.97
spleen	0.37 ± 0.04	0.40 ± 0.04	0.36 ± 0.05	0.27 ± 0.31
lung	4.00 ± 1.94	2.45 ± 0.57	2.90 ± 1.49	2.30 ± 0.93
heart	0.64 ± 0.07	0.50 ± 0.03	0.60 ± 0.06	0.47 ± 0.08
kidney	2.04 ± 0.17	2.12 ± 0.15	2.15 ± 0.12	1.88 ± 0.22
stomach	0.37 ± 0.05 ^b	0.49 ± 0.08	0.42 ± 0.07 ^b	0.44 ± 0.07 ^b
small intestine	2.88 ± 0.20	2.58 ± 0.05	2.53 ± 0.30	2.32 ± 0.16
large intestine	1.39 ± 0.27 ^b	1.62 ± 0.16	1.16 ± 0.12 ^b	1.64 ± 0.13 ^b
muscle	11.77 ± 0.83	15.27 ± 1.65	15.07 ± 2.83	14.83 ± 1.20
bone	4.19 ± 0.57	4.53 ± 1.14	4.05 ± 0.60	4.40 ± 0.52
blood	23.13 ± 2.53 ^b	25.88 ± 1.91 ^b	26.34 ± 1.82 ^b	22.46 ± 1.50 ^b
brain	0.20 ± 0.04	0.16 ± 0.03	0.17 ± 0.01	0.17 ± 0.01
Labeled with [¹²⁵I]SDMIB				
liver	6.84 ± 0.56	7.02 ± 0.30	6.14 ± 0.55	5.96 ± 0.96
spleen	0.38 ± 0.04	0.41 ± 0.04	0.37 ± 0.04	0.28 ± 0.04
lung	3.96 ± 1.85	2.44 ± 0.55	2.86 ± 1.41	2.29 ± 0.88
heart	0.65 ± 0.08	0.50 ± 0.03	0.60 ± 0.06	0.47 ± 0.07
kidney	2.10 ± 0.16	2.11 ± 0.16	2.15 ± 0.10	1.95 ± 0.21
stomach	0.39 ± 0.06	0.53 ± 0.08	0.48 ± 0.08	0.48 ± 0.06
small intestine	2.95 ± 0.21	2.59 ± 0.05	2.61 ± 0.28	2.40 ± 0.14
large intestine	1.80 ± 0.38	1.98 ± 0.09	1.75 ± 0.24	2.41 ± 0.38
muscle	12.27 ± 0.84	15.94 ± 1.93	15.69 ± 3.00	15.21 ± 1.03
bone	4.31 ± 0.54	4.54 ± 1.00	4.73 ± 1.23	5.19 ± 1.43
blood	21.84 ± 2.22	24.37 ± 1.83	24.77 ± 1.45	21.35 ± 1.26
brain	0.20 ± 0.04	0.16 ± 0.03	0.17 ± 0.02	0.18 ± 0.01

^a Results are mean ± SD. ^b Significance of difference determined by two-sided paired t test ($P < 0.01$); other tissues, no significant difference.

of potassium iodide. The decrease of thyroid activity to near-background levels for both DMIBA and iodide in mice receiving potassium iodide pretreatment is consistent with the possibility that thyroid uptake from DMIBA is related to its *in vivo* deiodination.

When tissue distribution of MAb conjugates of DMIBA and IBA were compared in mice, a greater similarity in radioiodine distribution was observed than with the benzoic acids. With the MAb conjugates, in most cases, normal tissue accumulation of the two nuclides was similar with

principal differences noted in tissues of the gastrointestinal tract and thyroid. However, thyroid uptake of DMIBA MAb conjugates was only 1.4–2.8 times that seen with MAb IBA conjugates, in contrast to the 20-fold difference noted above when DMIBA and IBA were compared. Thus inertness of an organic molecule in free form to dehalogenation does not necessarily reflect retention of label when the compound is coupled to a MAb.

The above results indicate that use of DMATE for radioiodination of MAbs offers no advantages over the

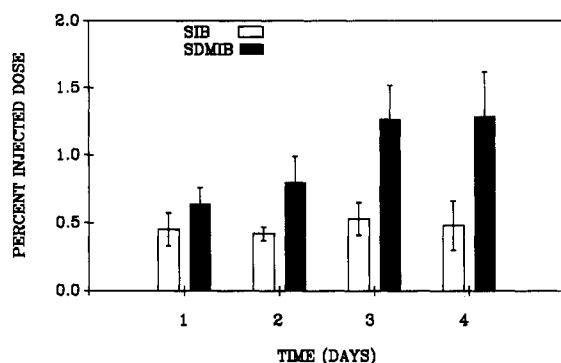


Figure 3. Comparison of the percent injected dose of radioiodine localized in the thyroids of normal mice injected with MAb C110 IgG1 labeled with ^{125}I and ^{131}I by using SDMIB and SIB, respectively.

original ATE reagent. It is important to point out, however, that the thyroid uptake for MAb C110 labeled with DMATE was 5–10-fold lower than that generally observed for other MABs and fragments labeled by using conventional methods (5, 11–14). The rationale for investigating the utility of SDMIB for use in MAB labeling was the hypothesis that substitution of methoxy groups could decrease deiodination either sterically by hindering an approaching nucleophile or electronically by increasing the electron density at the iodine-bearing carbon, making it less susceptible for nucleophilic attack.

Difference in bond strength is not a likely explanation for the more extensive deiodination of the dimethoxy derivatives, as substitution of methoxy groups for hydrogens may not significantly alter carbon–iodine bond strength (4- $\text{H}_3\text{COC}_6\text{H}_4\text{I}$, 59.2 ± 2.0 kcal/mol; $\text{C}_6\text{H}_5\text{I}$, 61.0 ± 1.8 kcal/mol) (28). A plausible explanation of the rapid deiodination of DMIBA is that the methoxy groups are demethylated to generate hydroxy groups. A number of investigations have shown that liver microsomes can dealkylate *O*-methyl compounds with the rate dependent on the structure (other substituents and position of substitution) and lipophilicity of the compound as well as the species of origin of the microsomes (29–32). In addition, rat liver microsomes have been shown to metabolize iodoanisoles by para and ortho hydroxylation (30). If enzymatic conversions of these types occurred with DMIBA or its MAB conjugate, the labeled catabolite could contain a hydroxyl group ortho to the iodine on the aromatic ring. The structural similarity of this product to thyroid hormones could then facilitate dehalogenation.

Experiments are in progress to investigate the nature of the labeled catabolites of DMIBA and its MAB conjugates. In addition, we are investigating whether potential iodination reagents containing methyl groups instead of methoxy groups ortho to the iodination site will have a more positive effect on deiodination in vivo.

ACKNOWLEDGMENT

The excellent technical assistance of Donna Affleck and Susan Slade is greatly appreciated. Ann Tamariz and Kelsea Parker provided editorial assistance. This research was supported by National Institutes of Health Grants CA 42324, NS 20023, CA 14236, and by Grant DEFG05-89ER60789 from the Department of Energy.

LITERATURE CITED

(1) Larson, S. M. (1990) Clinical radioimmunodetection, 1978–1988: Overview and suggestions for standardization of clinical trials. *Cancer Res. (Suppl.)* 50, 892s–898s.

(2) Delaloye, B., Bischof-Delaloye, A., Buchegger, F., von Fliedner, V., Grob, J.-P., Volant, J.-C., Pettavel, J., and Mach, J.-P. (1986) Detection of colorectal carcinoma by emission-computerized tomography after injection of ^{123}I -labeled Fab or F(ab')_2 fragments from monoclonal anti-carcinoembryonic antigen antibodies. *J. Clin. Invest.* 77, 301–311.

(3) McFarlane, A. S. (1958) Efficient trace-labelling of proteins with iodine. *Nature* 182, 53.

(4) Eary, J. F., Krohn, K. A., Kishore, R., and Nelp, W. B. (1989) Radiochemistry of Halogenated Antibodies. In *Antibodies in Radiodiagnosis and Therapy* (M. R. Zalutsky, Ed.) pp 83–102, CRC Press, Inc., Boca Raton, FL.

(5) Zalutsky, M. R., Colcher, D., Kaplan, W., and Kufe, D. (1985) Radioiodinated B6.2 monoclonal antibody: Further characterization of a potential radiopharmaceutical for the identification of breast tumors. *Int. J. Nucl. Med. Biol.* 12, 227–233.

(6) Hayes, D. F., Zalutsky, M. R., Kaplan, W., Noska, M., Thor, A., Colcher, D., Schlom, J., and Kufe, D. (1986) Pharmacokinetics of radiolabeled monoclonal antibody B6.2 in patients with metastatic breast cancer. *Cancer Res.* 46, 3157–3163.

(7) Carasquillo, J. A. (1989) Radioimmunoscintigraphy with polyclonal and monoclonal antibodies. In *Antibodies in Radiodiagnosis and Therapy* (M. R. Zalutsky, Ed.) pp 169–198, CRC Press, Boca Raton, FL.

(8) Smallridge, R. C., Burman, K. D., Ward, K. E., Wartofsky, L., Dimond, R. C., Wright, F. D., and Latham, K. R. (1981) 3',5'-Diodothyronine to 3'-monoiodothyronine conversion in the fed and fasted rat: Enzyme characteristics and evidence for two distinct 5'-diiodinases. *Endocrinology* 108, 2336–2345.

(9) Koehle, J., Aufmkolk, M., Rokos, H., Hesch, R.-D., and Cody, V. (1986) Rat liver iodothyronine ligand-binding site. *J. Biol. Chem.* 261, 11613.

(10) Gershengorn, M. C., Glinoe, D., and Robbins, J. (1980) Transport and Metabolism of Thyroid Hormones. In *The Thyroid Gland* (M. DeVisscher, Ed.) pp 81–121, Raven Press, New York.

(11) Zalutsky, M. R., and Narula, A. S. (1987) A method for the radiohalogenation of proteins resulting in decreased thyroid uptake of radioiodine. *Appl. Radiat. Isot.* 38, 1051–1055.

(12) Zalutsky, M. R., and Narula, A. S. Radiohalogenation of a monoclonal antibody using a *N*-succinimidyl-3-(tri-*n*-butylstannyl)benzoate intermediate. *Cancer Res.* 48, 1446–1450.

(13) Zalutsky, M. R., Noska, M. A., Colapinto, E. V., Garg, P. K., and Bigner, D. D. (1989) Enhanced tumor localization and in vivo stability of a monoclonal antibody radioiodinated using *N*-succinimidyl-3-(tri-*n*-butylstannyl)benzoate. *Cancer Res.* 49, 5543–5549.

(14) Wilbur, D. S., Hadley, S. W., Hylarides, M. D., Abrams, P. G., Beaumier, P. A., Morgan, A. C., Reno, J. M., and Fritzberg, A. R. (1989) Development of a stable radioiodinating reagent to label monoclonal antibodies for radiotherapy of cancer. *J. Nucl. Med.* 30, 216–226.

(15) Khawli, L. A., and Kassis, A. I. (1989) Synthesis of ^{124}I labeled *N*-succinimidyl *p*-iodobenzoate for use in radiolabeling antibodies. *Nucl. Med. Biol.* 16, 727–733.

(16) Vaidyanathan, G., and Zalutsky, M. R. (1990) Protein radiohalogenation: Observations on the design of *N*-succinimidyl ester acylation agents. *Bioconjugate Chem.* 1, 269–273.

(17) Narula, A. S., and Zalutsky, M. R. (1988) Synthesis of *N*-succinimidyl-2,4-dimethoxy-3-(tri-*n*-butylstannyl)benzoate via regioselectively generated lithium 2,4-dimethoxy-3-lithobenzoate. *Tetrahedron Lett.* 29, 4385–4388.

(18) Sumerdon, G. A., Rogers, P. E., Lombardo, C. L., Schnobrich, K. E., Melvin, S. L., Hobart, E. D., Tribby, I. I. E., Stroupe, S. D., and Johnson, D. K. (1990) An optimized antibody-chelator conjugate for imaging of carcinoembryonic antigen with indium-111. *Nucl. Med. Biol.* 17, 247–254.

(19) Carrel, S., Accolla, R. S., Carmagnola, A. L., and Mach, J.-P. (1980) Common human melanoma-associated antigen(s) detected by monoclonal antibodies. *Cancer Res.* 40, 2523–2528.

(20) Colapinto, E. V., Humphrey, P. A., Zalutsky, M. R., Groothuis, D. R., Friedman, H. S., de Tribolet, N., Carrel, S.,

- and Bigner, D. D. (1988) Comparative localization of murine monoclonal antibody Me1-14 F(ab')₂ fragment and whole IgG₂ in human glioma xenografts. *Cancer Res.* 48, 5701-5707.
- (21) Garg, P. K., Archer, G. E., Jr., Bigner, D. D., and Zalutsky, M. R. (1989) Synthesis of radioiodinated *N*-succinimidyl iodobenzoate: Optimization for use in antibody labeling. *Appl. Radiat. Isot.* 40, 485-490.
- (22) Remington, R. D., and Schork, M. A. (1985) *Statistics with Applications to the Biological Sciences* pp 135-190, Prentice-Hall, Englewood Cliffs, NJ.
- (23) Wursthorn, K. R., Kuivila, H. G., and Smith, G. F. (1978) Nucleophilic aromatic substitution by organostannylsodiums. A second-order reaction displaying a solvent cage effect. *J. Am. Chem. Soc.* 100, 2779-2789.
- (24) Zalutsky, M. R., Moseley, R. P., Benjamin, J. C., Colapinto, E. V., Fuller, G. N., Coakham, H. B., and Bigner, D. D. (1990) Monoclonal antibody and F(ab')₂ fragment delivery to tumor in patients with glioma: Comparison of intracarotid and intravenous routes of administration. *Cancer Res.* 50, 4105-4110.
- (25) Zalutsky, M. R., Garg, P. K., Friedman, H. S., and Bigner, D. D. (1989) Labeling monoclonal antibodies and F(ab')₂ fragments with the particle-emitting nuclide astatine-211: Preservation of immunoreactivity and in vivo localizing capacity. *Proc. Natl. Acad. Sci. U.S.A.* 86, 7149-7153.
- (26) Nunn, A. D., Loberg, M. D., and Conley, R. A. (1983) Structure-distribution-relationship approach leading to the development of Tc-99m mebrofenin: An improved cholescintigraphic agent. *J. Nucl. Med.* 24, 423-430.
- (27) Reardan, D. T., Meares, C. F., Goodwin, D. A., McTigue, M., David, G. S., Stone, M. R., Leung, J. P., Bartholomew, R. M., and Frinke, J. M. (1985) Antibodies against metal chelates. *Nature* 316, 265-268.
- (28) Vedeneyev, V. I., Gurvich, L. V., Kondrat'yev, V. A., Medvedev, V. A., and Frankevich, Y. L. (1966) *Bond Energies, Ionization Potentials, and Electron Affinities*, p 63, Edward Arnold, London.
- (29) Schmidt, H.-L., Möller, M. R., and Weber, N. (1973) Influence of substituents on the microsomal dealkylation of *N*-, *O*- and *S*-alkyl aromatic compounds. *Biochem. Pharmacol.* 22, 2989-2996.
- (30) Daly, J. (1970) Metabolism of acetanilides and anisoles with rat liver microsomes. *Biochem. Pharmacol.* 19, 2979-2993.
- (31) Nilsson, A., and Conner-Johnson, B. (1963) Cofactor requirements of the *o*-demethylating liver microsomal enzyme system. *Arch. Biochem. Biophys.* 101, 494-498.
- (32) Axelrod, J. (1956) Enzymic cleavage of aromatic ethers. *Biochem. J.* 63, 634-639.
- Registry No.** 1, 91487-18-2; 2, 112725-22-1; 3a, 130168-12-6; 3b, 122452-56-6; 4, 130168-13-7; 5, 618-51-9; 6, 3153-76-2; [¹²⁵I]-SIB, 125215-73-8; [¹³¹I]SDMIB, 130168-14-8; 3-bromo-2,4-dimethoxybenzoic acid, 39503-50-9.

Synthesis and Applications of an Aldehyde-Containing Analogue of SCH-23390

Theresa M. Filtz, Sumalee Chumpradit,[†] Hank F. Kung,[†] and Perry B. Molinoff*

Department of Pharmacology and Department of Radiology, University of Pennsylvania School of Medicine, Philadelphia, Pennsylvania 19104. Received September 5, 1990

SCH-23390 is a high-affinity antagonist selective for D1 dopamine receptors ($K_i = 2.5$ nM). It does not contain a functional group that can be conveniently coupled to commercially available resins for affinity chromatography or to prepare photolabels for photoaffinity labeling of receptors. To construct an affinity resin for purification of dopamine D1 receptors, an aldehyde analogue of SCH-23390, (\pm)-7-chloro-8-hydroxy-1-(4'-formylphenyl)-3-methyl-2,3,4,5-tetrahydro-1*H*-3-benzazepine (ASCH), was synthesized. 8-Methoxy-1-(4'-bromophenyl)-SCH-23390 was lithiated, formylated, and O-demethylated to form the aldehyde. NMR and IR analyses were performed to characterize the product. Assays were performed with the radioligand [¹²⁵I]SCH-23982 to define the biological activity of the aldehyde. ASCH displaced [¹²⁵I]SCH-23982 binding from caudate membranes with a K_i value of 7.1 nM. ASCH has been coupled through the aldehyde group on the phenyl ring to diaminodipropylamine-agarose for affinity chromatography. After solubilization of caudate membranes in 1% digitonin, the affinity resin retained binding sites for [¹²⁵I]SCH-23982 that were eluted with 10 mM SCH-23390. The aldehyde was also covalently coupled to biotin hydrazide for fluorescence labeling of dopamine D1 receptors. The biotin-conjugated aldehyde of SCH-23390 displaced [¹²⁵I]SCH-23982 binding from caudate membranes with a K_i value of 9.3 nM.

Dopamine receptors have been traditionally divided into two pharmacologically distinct classes, D1 and D2. Dopamine D1 receptors have been linked to stimulation of adenylyl cyclase activity (Kebabian & Calne, 1979; Kebabian et al., 1984) and stimulation of phosphoinositide hydrolysis (Felder et al., 1989) or not linked to adenylyl cyclase activity in some systems (DeKeyser et al., 1989). Additionally, D1 receptors were classified by displaying high affinity for the benzazepine derivatives SCH-23390, a receptor antagonist (Iorio et al., 1983), and SKF-38393, a receptor agonist (O'Boyle & Waddington, 1984). D2 receptors have been linked to inhibition of adenylyl cyclase activity (Kebabian et al., 1984) and display high affinity for a variety of compounds including neuroleptics of varying structures (Seeman et al., 1976). Recently the genetic and cDNA sequences of adenylyl cyclase linked human (Sunahara et al., 1990; Dearth et al., 1990; Zhou et al., 1990) and rat (Monsma et al., 1990) D1 receptors were reported. The elucidation of these sequences increases the methods available for studying D1 receptor structure and regulation. However, the D1 receptor has never been purified, and the appropriate start site of the D1 coding sequence is still a subject of debate.

Thus far, purification of dopamine D1 receptors has been incomplete. Solubilization of striatal membranes with 1% digitonin in a buffer with high ionic strength followed by lectin affinity chromatography led to the isolation of a binding site for SCH-23390 that copurified with a guanine nucleotide-binding protein (Niznik et al., 1986). Solubilization of D1 receptors with sodium cholate and partial purification using a sulfhydryl affinity column have been described, but reconstitution of binding sites into phospholipid vesicles was necessary for detection of binding activity (Sidhu, 1990). Gingrich et al. (1988) reported the

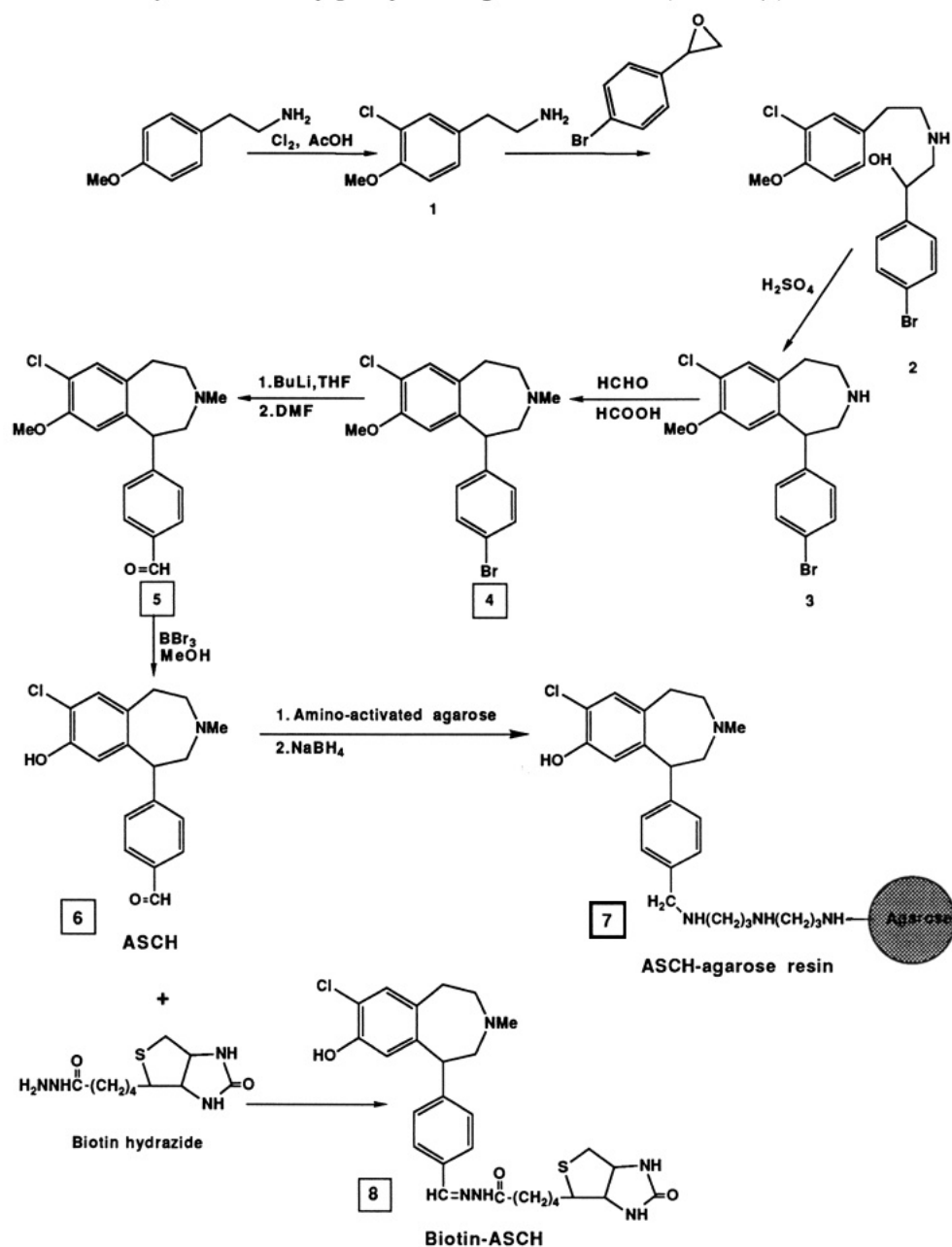
synthesis of an affinity resin for D1 receptors that involved coupling a 4'-aminophenyl derivative of SCH-23390 to an activated agarose resin. The affinity resin retained binding sites for SCH-23390 that were specifically eluted with (+)-butaclamol, but amino acid sequence data were not reported.

Autoradiographic studies of the binding of radiolabeled D1 antagonists [³H]SCH-23390 and [¹²⁵I]SCH-23982 to brain sections have revealed a high density of D1 receptors in the caudate nucleus, nucleus accumbens, and substantia nigra (Boyson et al., 1986; Dawson et al., 1988). Autoradiographic techniques do not, however, allow localization of dopamine receptor subtypes at the cellular or subcellular level (Schwarcz et al., 1978; Trugman et al., 1986; Palacios, 1986). Ariano et al. (1989) have recently reported the development of D1- and D2-selective receptor antagonists coupled directly to fluorescein, which may permit histofluorescent localization of these receptors. Final resolution of controversies surrounding dopamine receptor localization awaits the development of probes that can be used at the level of the electron microscope.

To develop a new, specific probe for the study of D1 receptors, we have synthesized a 4'-formylphenyl analogue of SCH-23390 (ASCH) that is easily coupled to primary amines through an aldehyde moiety. By linking the aldehyde to an amine-activated agarose resin, ASCH has been used to create an affinity resin for D1 receptors. We have also covalently coupled ASCH to biotin hydrazide, creating a D1 receptor ligand for use with avidin-linked compounds including fluorescein, rhodamine, horseradish peroxidase, and ferritin. The coupling of ASCH to biotin hydrazide increases the number of techniques that may potentially be used to study the distribution of D1 receptors. Derivatives of ASCH may ultimately permit resolution of the distribution of D1 receptors at the cellular level.

* Author to whom correspondence should be addressed.

[†] Department of Radiology.

Scheme I. Synthetic Pathway for a 4'-Formylphenyl Analogue of SCH-23390, ASCH (6)^a

^a ASCH was subsequently coupled to an amino-terminal agarose resin to produce a D1-receptor affinity resin (7) and to biotin hydrazide to produce a biotinylated analogue, biotin-ASCH (8).

EXPERIMENTAL PROCEDURES

Chemical Syntheses (Scheme I). The synthesis of (±)-7-chloro-8-methoxy-1-(4'-bromophenyl)-3-methyl-2,3,4,5-tetrahydro-1H-3-benzazepine (compound 4) was based on a protocol described by Wyrick and Mailman (1985) as utilized by Chumpradit et al. (1989).

Proton nuclear magnetic resonance spectroscopy (NMR) was recorded on a Varian EM 360A spectrometer. The chemical shifts were reported in ppm downfield from an internal tetramethylsilane standard. Infrared spectra were obtained with a Mattson Polaris FT-IR spectrometer. Melting points were determined with a Meltemp apparatus and are reported uncorrected for compounds 5 and 6. Fast-atom bombardment mass spectrometry was performed in the Department of Chemistry at the University of Pennsylvania, and all values are within 18 ppm of the theoretical values.

(±)-7-Chloro-8-methoxy-1-(4'-formylphenyl)-3-methyl-2,3,4,5-tetrahydro-1H-3-benzazepine

(Compound 5). Compound 4 (5 g, 13 mmol) was added to 100 mL of dried tetrahydrofuran (THF) and cooled to -78°C in a dry ice-acetone bath. *n*-Butyllithium (8.1 mL, 13 mmol) was added with stirring over 2 min, yielding a solution with a deep red color; 2.0 mL of dimethylformamide was added and the solution was stirred at -78°C for 1 h. The reaction was quenched by the addition of 5 mL of saturated ammonium chloride solution and allowed to warm to room temperature. THF was removed under reduced pressure and the residue was extracted with dichloromethane, dried over anhydrous sodium sulfate, and separated on a silica gel column eluted with a mixed solvent (dichloromethane-methanol-ammonium hydroxide 95:5:0.1) to yield 1.98 g of compound 5 (48% yield). The resulting product was further purified by recrystallization. Sodium bisulfite was added to 75% ethanol until the solution became cloudy and then water was added slowly until the mixture became clear. This solution was added directly to 1.98 g of reaction product and the

resulting crystals were filtered and dissolved in freshly prepared, saturated potassium carbonate. The mixture was extracted with dichloromethane and the solvent evaporated under reduced pressure to yield 0.75 g of compound **5** (18% overall yield): mp 134–140 °C; FT-IR (KBr) ν 1690 (s, C=O) 1600, 1570, 1500, 850, 830, 800 cm^{-1} ; ^1H NMR (DMSO- d_6) δ 9.95 (s, 1 H, HC=O), 7.90, 7.75, and 7.37, 7.22 (AA'BB', 4 H, ArH'), 7.10 (s, 1 H, ArH-6), 6.30 (s, 1 H, ArH-9), 4.50–4.25 (m, 1 H, CH), 3.65 (s, 3 H, OCH₃), 3.20–2.55 (m, 6 H, (CH₂)₃), 2.40 (s, 3 H, NCH₃) ppm; MS (FAB) (M + H)⁺ 330.1248, calcd for C₁₉H₂₀O₂NCl 330.1261.

(\pm)-7-Chloro-8-hydroxy-1-(4'-formylphenyl)-3-methyl-2,3,4,5-tetrahydro-1H-3-benzazepine (**6**, ASCH). (Formylphenyl)benzazepine **5** (100 mg, 0.303 mmol) in 10 mL of dried dichloromethane was cooled in a dry ice–2-propanol bath under argon. Boron tribromide (0.9 mL, 0.9 mmol) was added dropwise with stirring and the reaction was allowed to warm to room temperature with stirring for 2 h. Volatile substances were evaporated under nitrogen, after which 10 mL of methanol was added to the reaction mixture and stirred overnight at room temperature. Methanol was then removed under reduced pressure and the residue stirred with water. The pH of the mixture was increased with 10% NaOH and the precipitate filtered. The filtrate was adjusted to pH 7 with dilute HCl and extracted three times with ethyl acetate. The combined organic layers were dried over anhydrous sodium sulfate, and the solvent was removed under reduced pressure. The product ASCH (**6**; 30 mg, 32% yield) was recrystallized overnight in 100% ethanol. A C18 column for reverse-phase HPLC and isocratic elution with a mixture of 50% acetonitrile, 10 mM ammonium formate, pH 6.5, at a flow rate of 1 mL/min and a retention time of 4.45 min purified compound **6** (>99% purity): mp 170–172 °C; UV λ_{max} 256 nm (ϵ $5.9 \times 10^3 \text{ M}^{-1}\text{cm}^{-1}$); FT-IR (KBr) ν 2300–3300 (br OH) 1690 (C=O), 1600, 1570, 1500, 850, 830, 800 (para substituted phenyl) cm^{-1} ; ^1H NMR (DMSO- d_6) δ 9.95 (s, 1 H, HC=O), 7.95, 7.8, and 7.47, 7.33 (AA'BB', 4 H, ArH'), 7.10 (s, 1 H, ArH-6), 6.30 (s, 1 H, ArH-9), 4.55–4.30 (m, 1 H, CH), 3.27–2.60 (m, 6 H, (CH₂)₃), 2.40 (s, 3 H, NCH₃); MS (FAB) (M + H)⁺ 316.1036, calcd for C₁₈H₁₈O₂NCl 316.1104.

ASCH-Agarose Affinity Resin. Diaminodipropylamine-agarose (1 mL; Pierce, Rockford, IL) containing 10 μmol of primary amine was equilibrated into 100% ethanol by gradually increasing the concentration of ethanol over 10 washes of 10 mL each. ASCH (6.3 mg, 20 μmol) dissolved in 1 mL of 100% ethanol was incubated at room temperature overnight with the resin while the mixture was rotated end over end to insure constant mixing (setting 3, multipurpose rotator Model 151, Scientific Industries). Because the ligand was coupled to the resin through an imine bond, the ligand-coupled resin was washed with ethanol (200 mL) and reduced overnight with sodium borohydride (1.9 mL, 50 μmol) in ethanol (1 mL) at room temperature with rotation. The resin was washed extensively with 100% ethanol and gradually brought to 100% water by decreasing the concentration of ethanol in a series of washes. The resulting gel was washed thoroughly with water and stored.

Biotin-ASCH. Biotin hydrazide (50 mg, 0.092 mmol) and ASCH (29 mg, 0.092 mmol) were dissolved in 10 mL of methanol and refluxed overnight with stirring. The solvent was evaporated under reduced pressure and the resulting product purified by silica gel chromatography (dichloromethane–methanol–ammonium hydroxide 90:10:0.1).

Preparation of Tissue. Rabbit brains obtained on dry ice from Pel-Freez (Rogers, AK) were thawed on ice and the striata were removed and placed in 50 mM Tris, pH 7.4, containing 10 mM EDTA, 150 mM NaCl, and a mixture of protease inhibitors [1 $\mu\text{g}/\text{mL}$ of soybean trypsin inhibitor, leupeptin, aprotinin, and 10 $\mu\text{g}/\text{mL}$ of phenylmethanesulfonyl fluoride (PMSF)] at 10 mL/mg wet weight of striata. The tissue was homogenized with a Polytron homogenizer (setting 6) for 10 s, and membranes were pelleted by centrifugation for 10 min at 10000g. This was repeated twice and the tissue homogenate at 100 mg/mL was frozen in aliquots of 10 mL at –70 °C until needed.

Binding Assays for D1 Receptors. For assays with striatal membranes, tissue homogenates were thawed on ice and centrifuged at 10000g for 10 min. Pellets were suspended in 50 mM Tris, pH 7.4, containing 10 mM EDTA (ethylenediaminetetraacetic acid), 150 mM NaCl, 0.1% BSA (bovine serum albumin), and protease inhibitors as described above (buffer I) at 0.5 mg of tissue/mL of buffer. [¹²⁵I]SCH-23982 (New England Nuclear, Du Pont, Boston, MA) was used to assay for D1 receptors in a total assay volume of 0.25 mL with 0.1 mL of striatal membranes and 0.2 nM [¹²⁵I]SCH-23982 in buffer I. SCH-23390 (50 μM) was used to define nonspecific binding. Binding assays were carried out for 18 h at 4 °C and incubations were terminated by the addition of 5 mL of ice-cold 10 mM Tris containing 0.9% NaCl, pH 7.4 (wash buffer), followed by filtration over glass-fiber filters (#30, Schleicher and Schuell, Keene, NH) with two washes of 5 mL of wash buffer.

For binding assays on solubilized proteins, 0.2 mL of column eluate was used in a 1-mL assay with 0.2 nM [¹²⁵I]-SCH-23982. SCH-23390 (50 μM) was used to define nonspecific binding. Digitonin (0.1% w/v) was included in buffer I for assays of solubilized receptor. G-50 columns were used to separate bound radioligand from free. A 4-mL column of G-50 was equilibrated with buffer I plus 0.1% digitonin. A 1-mL sample was applied to each column and washed with 2.5 mL of buffer. The initial eluate (1.5 mL) was discarded and the next 2 mL collected.

Data Analysis. Competition curve-fitting was done by nonlinear least-squares regression analysis using the mathematical modeling program NEWFITSTATS on the NIH-sponsored PROPHET system (Lin et al., 1987).

Solubilization of Membrane Proteins. Tissue homogenates were thawed on ice and centrifuged at 10000g for 10 min. Pellets were suspended at 0.2 g/mL in 100 mM Tris (pH 7.4) and 20 mM EDTA containing protease inhibitors. An equal volume of 2% (w/v) digitonin was added to the tissue preparation and incubated on ice with gentle agitation for 1 h. Insoluble material was sedimented by centrifugation for 1 h at 100000g at 4 °C, and the supernatant was collected and used immediately.

Affinity-Resin Purification Protocol. Solubilized membranes (1 mL) were applied to columns containing either the affinity resin or uncoupled agarose. The columns were capped and rotated overnight at 4 °C to allow receptors to bind. Columns were washed with 9 mL of 0.1% digitonin in 50 mM Tris, pH 7.4, and 10 mM EDTA, and the eluate was collected in three fractions each containing 3 mL. Columns were then incubated with buffer including 500 mM NaCl at 4 °C for 12 h with rotation and washed with 9 mL of the high-salt solution, and again the eluate was collected. The resins were then incubated with 10 mM SCH-23390 in the presence of 500 mM NaCl overnight at 4 °C and washed with 9 mL of the SCH-23390 solution. Each fraction was applied to a G-50 column for desalting as described for binding to solubi-

lized proteins above. The eluate was assayed for the presence of D1 receptors.

HRP Assay for D1 Receptors. Homogenates were thawed on ice and centrifuged at 10000g for 10 min. The pellets were resuspended in phosphate buffer (138 mM NaCl, 4.1 mM KCl, 5.1 mM Na₂HPO₄, 1.5 mM KH₂PO₄, 11.1 mM glucose, pH 7.4) containing 3% BSA. Tissue (100 μ g) was incubated at 37 °C for 90 min with or without 50 μ M biotin-ASCH. SCH-23390 (50 μ M) was added to one set of tubes to define nonspecific binding. Assay tubes were centrifuged at 4 °C for 2 min at 14000g and the supernatant was discarded. Pelleted membranes were resuspended in 250 μ L of phosphate buffer containing 1 μ g/mL avidin-linked horseradish peroxidase (HRP) and 3% BSA and incubated on ice for 15 min. Tubes were centrifuged for 2 min, washed once with 250 μ L of phosphate buffer containing 3% BSA, and resuspended in 250 μ L of phosphate buffer. Soluble HRP stain (250 μ L; TMB peroxidase EIA substrate, Bio-Rad, Rockville Center, NY) was added to each assay tube and incubated for 2 min on ice before quenching with 100 μ L of 1 N H₂SO₄. The optical density of each sample was read at 450 nm.

Protein Determinations. Protein concentrations were determined by the method of Bradford (1976) using bovine γ globulin as a standard.

RESULTS

The four-step synthesis of 4'-bromo benzazepine 4 followed a protocol established by Wyrick and Mailman (1985) (Scheme I) as described by Chumpradit et al. (1989). The overall yield is low (9%) because of the low yield of the chlorination reaction and the production of a trialkylamine side product along with product 2. 4'-Bromo benzazepine was purified over a silica gel column prior to lithiation with *n*-butyllithium to replace the 4'-bromo group, producing an intensely red benzylic anion intermediate. Addition of 2 equiv of dimethylformamide (DMF) led to formation of 4'-formyl benzazepine 5, which was purified by silica gel chromatography to remove excess DMF and recrystallized as a sodium bisulfite adduct. The final product, 6 (ASCH), was prepared by O-demethylation of purified 5 with boron tribromide.

ASCH inhibited the binding of [¹²⁵I]SCH-23982 to rabbit caudate membranes with a K_i value of 7.1 nM. The affinity of the receptors for ASCH was almost as high as that for SCH-23390 (K_i = 2.5 nM), and the inhibition curve conformed to a one-site fit as analyzed by nonlinear-regression analysis using the PROPHEt system (Figure 1). ASCH was coupled to diaminodipropylamine-agarose as described in the Experimental Procedures to obtain an affinity resin for D1 receptors (Scheme I, compound 7). UV analysis of the ethanol column washes after coupling showed a recovery of 15 μ mol of ASCH, suggesting that approximately 50% of the resin-bound amine was coupled to ASCH. Final washes with ethanol revealed no free ASCH detectable by UV absorption spectroscopy. Prior to use, the affinity resin was washed extensively in 100% ethanol.

Binding sites for [¹²⁵I]SCH-23982 were eluted from the uncoupled agarose control column in the no-salt and high-salt washes (Figure 2). No additional binding sites were eluted by the addition of 10 mM SCH-23390, and recovery of binding sites for [¹²⁵I]SCH-23982 from the control column was nearly 100%. However, ca. 30% of the binding sites applied to the affinity resin could not be accounted for. They may have remained attached to the affinity resin after all washes or been destroyed during the absorption

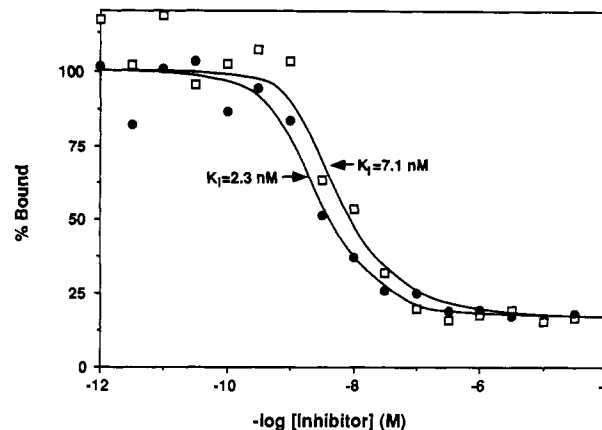


Figure 1. Inhibition of binding of [¹²⁵I]SCH-23982 to rabbit striatal membranes by ASCH (□) and SCH-23390 (●). The data shown are representative of results obtained in three similar experiments.

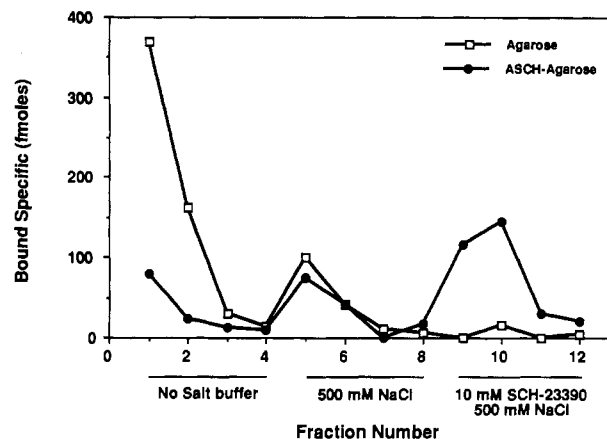


Figure 2. Elution profile of D1 receptors from ASCH-agarose resin (●) and uncoupled amine-agarose resin (□). Resins were incubated overnight with digitonin-solubilized rabbit striatal membranes and then washed and assayed for binding of [¹²⁵I]SCH-23982 to solubilized receptors. The resins were first washed with 50 mM Tris containing 10 mM EDTA, 0.1% digitonin, and protease inhibitors (no salt buffer) at 4 °C. The second wash was with the same buffer to which 500 mM NaCl had been added. The third wash included 500 mM NaCl and 10 mM SCH-23390 (in 0.01% ethanol). The profile is representative of results obtained in two similar experiments.

and elution procedures. In contrast to the control column, only 20% of the binding sites added to the affinity resin were eluted in no-salt and 500 mM NaCl washes. An additional 50% of the sites were eluted with 10 mM SCH-23390. The protein profile (data not shown) of ASCH-agarose affinity-resin washes showed that 25% of the total protein was eluted with 10 mM SCH-23390, which indicated a 2-fold purification of D1 receptors after affinity-resin chromatography.

ASCH was conjugated to biotin hydrazide in an attempt to create a probe for D1 receptors that could be coupled through avidin to many kinds of markers (fluorescent molecules, colloidal gold, horseradish peroxidase, etc.). Biotin-ASCH (Scheme 1, compound 8) was synthesized as described in the Experimental Procedures and was shown to inhibit the binding of [¹²⁵I]SCH-23982 with a K_i value of 9.3 nM. The inhibition curves conformed to a one-site fit as analyzed by nonlinear-regression analysis on the PROPHEt system. Biotin hydrazide at concentrations of up to 10 μ M did not inhibit binding of the radioligand to D1 receptors.

Experiments with biotin-ASCH were performed to determine whether avidin would bind to the biotin portion

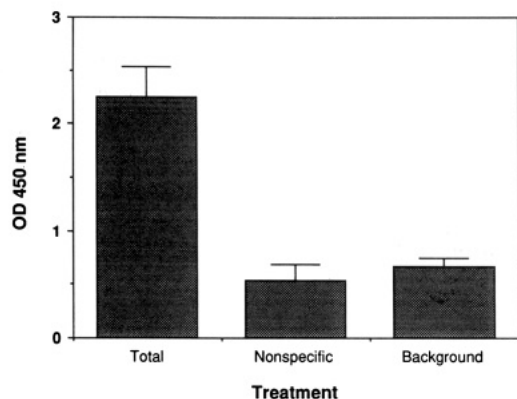


Figure 3. HRP assay for D1 receptors on rabbit striatal membranes using biotin-ASCH. Rabbit striatal membranes were incubated with 50 μ M biotin-ASCH (total), biotin-ASCH plus 50 μ M SCH-23390 (nonspecific), or assay buffer alone (background). Samples were then incubated with 1 μ g/mL of avidin-HRP. The membranes were sedimented to separate bound ligand from free ligand and resuspended in HRP substrate. The resultant color reaction was quantitated by measuring optical density (OD) at 450 nm. The data points represent the average of triplicate determinations with standard deviations and are representative of results obtained in three similar experiments.

of the molecule prebound to D1 receptors. An assay based on soluble horseradish peroxidase substrate and avidin-linked HRP was devised. Avidin-HRP, as assayed by the optical density of the soluble HRP substrate, bound to striatal membranes in the presence of biotin-ASCH (Figure 3). HRP staining was specifically blocked by the presence of SCH-23390. Thus, biotin-ASCH was capable of binding specifically to dopamine D1 receptors while simultaneously binding to avidin.

DISCUSSION

An analogue of the selective D1 receptor antagonist SCH-23390 that contains an aldehyde group at the 4'-phenyl position has been synthesized. The aldehyde was positioned on a phenyl ring distant from the portion of the molecule shown to be important for high-affinity binding to D1 receptors (McQuade et al., 1988). ASCH inhibited binding of [125 I]SCH-23982 with a K_i value of 7.1 nM, which is only 3-fold higher than the K_i value for SCH-23390 (2.5 nM). The synthesis involved an extension of the pathway established for the synthesis of SCH-23390. Addition of the aldehyde group was accomplished by an efficient reaction scheme through a lithium anion exchange, as suggested by Chumpradit et al. (1989). The cyclization step proceeded with good yield and did not involve the use of hydrogen fluoride or another strong acid. An analogue of SCH-23390 containing a primary amine has previously been synthesized through reduction of a nitro group at the 4'-phenyl position (Gingrich et al., 1988). The presence of the nitro group at the 4'-phenyl position makes cyclization much more difficult (S. Chumpradit, unpublished observation). ASCH was readily coupled to primary amines in dimethyl sulfoxide (unpublished observation), ethanol, or methanol to yield an affinity resin and biotinylated derivatives of ASCH.

Preliminary applications of ASCH to studies of D1 receptors included construction of an affinity resin that selectively retained binding sites for [125 I]SCH-23982. The affinity resin specifically retained approximately 80% of the binding sites for [125 I]SCH-23982, but removing specifically bound sites, once attached, was more difficult. Given that approximately 10 μ mol of ASCH was coupled to 1 mL of amine-agarose resin, the concentration of ASCH on the column was approximately 10 mM. Incubation with

SCH-23390 (10 mM, a nearly saturated solution) removed only 50% of the total binding sites from the ASCH-agarose resin. This may have been due to the high concentration of ASCH on the resin. Altering the duration and number of incubation times with NaCl and SCH-23390 might change the amount of protein or binding sites eluted from the column.

The use of ASCH may also provide information with regard to the location and structure of D1 receptors. The coupling of ASCH to biotin hydrazide resulted in a molecule able to simultaneously bind D1 receptors through the ASCH portion of the molecule and avidin through the biotin moiety. D1 receptors on rabbit striatal membranes prebound with biotin-ASCH were detected by HRP-linked avidin along with a soluble HRP substrate. A fluorescent avidin compound could be used in the same manner. Fluorescein-SCH-23390 has been synthesized and used to detect D1 receptors in whole brain tissue sections (Ariano et al., 1989). A biotin-coupled derivative of SKF-83566-NH₂ has been synthesized but has not been shown to simultaneously couple to avidin and D1 receptors (Madras et al., 1990). Visualizing D1 receptors through biotin-ASCH may have an advantage over the use of fluorescein-SCH-23390. Signal amplification can be obtained by having several fluorescent molecules coupled to one molecule of avidin bound through biotin to a D1 receptor. Such amplification is not possible with a ligand that is covalently coupled to fluorescein. Biotin-ASCH should make it possible to analyze the cellular distribution of D1 receptors in the striatum and other brain regions and possibly the subcellular localization of the receptors. For example, biotin-linked ω -conotoxin has been used with colloidal gold to localize voltage-dependent calcium channels to dendrites of hippocampal CA1 neurons by electron microscopy (Jones et al., 1989).

The coupling of ASCH through its aldehyde moiety to large antigenic proteins, such as keyhole limpet hemocyanin, may permit the production of anti-idiotypic anti-receptor antibodies to aid in structural analysis of the binding site and the purification of D1 receptors. The β -adrenergic receptor was studied in this manner with antibodies to alprenolol used to make anti-idiotypic antibodies cross-reacting with the β -receptor (Sawutz et al., 1987). With an aldehyde moiety capable of being easily coupled to a variety of molecules and a selectivity for D1 receptors, ASCH should be a valuable tool in further studies.

ACKNOWLEDGMENT

This work was supported by USPHS grants NS18591, NS18479, and NS24538 and a fellowship from the Pharmaceutical Manufacturers Association Foundation (TMF).

LITERATURE CITED

- Ariano, M. A., Monsma, F. J., Jr., Barton, A. C., et al. (1989). Direct Visualization and Cellular Localization of D₁ and D₂ Dopamine Receptors in Rat Forebrain by Use of Fluorescent Ligands. *Proc. Natl. Acad. Sci. U.S.A.* 86, 8570-8574.
- Boyson, S. J., McGonigle, P., and Molinoff, P. B. (1986). Quantitative Autoradiographic Localization of the D₁ and D₂ Subtypes of Dopamine Receptors in Rat Brain. *J. Neurosci.* 6, 3177-3188.
- Bradford, M. M. (1976). A Rapid and Sensitive Method for the Quantitation of Microgram Quantities of Protein Utilizing the Principle of Protein-Dye Binding. *Anal. Biochem.* 72, 248-254.
- Chumpradit, S., Kung, H. F., Billings, J., et al. (1989). (\pm)-7-Chloro-8-hydroxy-1-(4'-[125 I]iodophenyl)-3-methyl-2,3,4,5-

- tetrahydro-1H-3-benzazepine: A Potential CNS D-1 Dopamine Receptor Imaging Agent. *J. Med. Chem.* 32, 1431-1435.
- Dawson, T. M., Barone, P., Sidhu, A., et al. (1988). The D₁ Dopamine Receptor in the Rat Brain: Quantitative Autoradiographic Localization Using an Iodinated Ligand. *Neuroscience* 26, 83-100.
- Dearry, A., Gingrich, J. A., Falardeau, P., et al. (1990). Molecular Cloning and Expression of the Gene for a Human D₁ Dopamine Receptor. *Nature* 347, 72-77.
- DeKeyser, J., Walraevens, H., Ebinger, G., et al. (1989). In Human Brain Two Subtypes of D₁ Dopamine Receptors Can Be Distinguished on the Basis of Differences in Guanine Nucleotide Effect on Agonist Binding. *J. Neurochem.* 53, 1096-1102.
- Felder, C. C., Blecher, M., and Jose, P. A. (1989). Dopamine-1-Mediated Stimulation of Phospholipase C Activity in Rat Renal Cortical Membranes. *J. Biol. Chem.* 264, 8739-8745.
- Gingrich, J. A., Amlaiky, N., Senogles, S. E., et al. (1988). Affinity Chromatography of the D₁ Dopamine Receptor from Rat Corpus Striatum. *Biochemistry* 27, 3907-3912.
- Iorio, L. C., Barnett, A., Leitz, F. H., et al. (1983). SCH-23390, Potential Benzazepine Antipsychotic with Unique Interactions on Dopaminergic Systems. *J. Pharmacol. Exp. Ther.* 226, 462-468.
- Jones, O. T., Kunze, D. L., and Angelides, K. J. (1989). Localization and Mobility of ω -Conotoxin-Sensitive Ca²⁺ Channels in Hippocampal CA1 Neurons. *Science* 244, 1189-1193.
- Kebabian, J. W., Beaulieu, M., and Itoh, Y. (1984). Pharmacological and Biochemical Evidence for the Existence of Two Categories of Dopamine Receptor. *Can. J. Neurol. Sci.* 11, 114-117.
- Kebabian, J. W., and Calne, D. B. (1979). Multiple Receptors for Dopamine. *Nature* 277, 93-96.
- Lin, C., McGonigle, P., and Molinoff, P. B. (1987). Characterization of D-2 Dopamine Receptors in a Tumor of the Rat Anterior Pituitary Gland. *J. Pharmacol. Exp. Ther.* 242, 950-956.
- Madras, B. K., Canfield, D. R., Pfaelzer, C., et al. (1990). Fluorescent and Biotin Probes for Dopamine Receptors: D₁ and D₂ Receptor Affinity and Selectivity. *Mol. Pharmacol.* 37, 833-839.
- McQuade, R. D., Ford, D., Duffy, R. A., et al. (1988). Serotonergic Component of SCH-23390: In Vitro and In Vivo Binding Analyses. *Life Sci.* 43, 1861-1869.
- Monsma, F. J., Mahan, L. C., McVittie, L. D., et al. (1990). Molecular Cloning and Expression of a D₁ Dopamine Receptor Linked to Adenylyl Cyclase Activation. *Proc. Nat. Acad. Sci. U.S.A.* 87, 6723-6727.
- Niznik, H. B., Grigoriadis, D., Otsuka, N. Y., et al. (1986). The Dopamine D₁ Receptor: Partial Purification of a Digitonin-Solubilized Receptor-Guanine Nucleotide Binding Complex. *Biochem. Pharmacol.* 35, 2974-2977.
- O'Boyle, K. M., and Waddington, J. L. (1984). Selective and Stereospecific Interactions of R-SK&F 38393 with [³H]Piflutixol but Not [³H]Spiperone Binding to Striatal D₁ and D₂ Dopamine Receptors: Comparison with SCH 23390. *Eur. J. Pharmacol.* 98, 433-436.
- Palacios, J. M. (1986). Dopamine receptor disputes. *Nature* 323, 205.
- Sawatz, D. G., Koury, R., and Homcy, C. J. (1987). Enhanced Antigen-Antibody Binding Affinity Mediated by an Anti-Idiotypic Antibody. *Biochemistry* 26, 5275-5282.
- Schwarcz, R., Creese, I., Coyle, J. T., et al. (1978). Dopamine receptors Localised on Cerebral Cortical Afferents to Rat Corpus Striatum. *Nature* 271, 766-768.
- Seeman, P., Lee, T., Chau-Wong, M., et al. (1976). Antipsychotic Drug Doses and Neuroleptic/Dopamine Receptors. *Nature* 261, 717-719.
- Sidhu, A. (1990). A Novel Affinity Purification of D-1 Dopamine Receptors from Rat Striatum. *J. Biol. Chem.* 265, 10065-10072.
- Sunahara, R. K., Niznik, H. B., Weiner, D. M., et al. (1990). Human Dopamine D₁ Receptor Encoded by an Intronless Gene on Chromosome 5. *Nature* 347, 80-83.
- Trugman, J. M., Geary, W. A., and Wooten, G. F. (1986). Localisation of D-2 Dopamine Receptors to Intrinsic Striatal Neurons by Quantitative Autoradiography. *Nature* 323, 267-269.
- Wyrick, S. D., and Mailman, R. B. (1985). Tritium Labelled (\pm)-7-Chloro-8-hydroxy-3-methyl-1-phenyl-2,3,4,5-tetrahydro-1H-3-benzazepine (SCH-23390). *J. Labelled Comp. Radiopharm.* 22, 189-195.
- Zhou, Q.-Y., Grandy, D. K., Thambi, L., et al. (1990). Cloning and Expression of Human and Rat D₁ Dopamine Receptors. *Nature* 347, 76-79.

Thiol-Containing Cross-Linking Agent with Enhanced Steric Hindrance

Lawrence Greenfield,*† Will Bloch,† and Margaret Moreland‡§

PCR Department and Department of Chemistry, Cetus Corporation, 1400 53rd Street, Emeryville, California 94608.
Received September 17, 1990

Ricin A chain immunotoxins disulfide cross-linked with conventional, sterically unhindered reagents have unsatisfactorily short circulating life times in vivo. (Acetylthio)succinic anhydride, a thiolating reagent with partial steric hindrance of the sulfur atom, does not remedy this situation. Sulfosuccinimidyl *N*-[3-(acetylthio)-3-methylbutyryl]- β -alaninate, a new cross-linker in which the carbon α to the sulfur is doubly methylated, creates disulfide bonds 2 orders of magnitude more resistant to reduction than unhindered disulfides. Nevertheless, this deactivated thiolating agent rapidly and reliably cross-links ricin A chain and antibodies to create immunotoxins with in vitro cytotoxicities comparable to those of 2-iminothiolane-coupled conjugates.

INTRODUCTION

Immunotoxins are protein conjugates in which a toxin is covalently attached to a monoclonal antibody (reviewed in refs 1-3). These chimeric molecules contain up to four functional regions. The antibody targets the drug in vivo to the desired cell population. The toxin is the effector portion responsible for cell death once bound to the cell surface (for surface-acting toxins) or internalized into the cytosol (for toxins which act on the protein-synthesis machinery). Most toxins are thought to contain a translocation domain which facilitates entry of the catalytic portion into the cytosol. Finally, there is a cleavable linking region, which must confer stability to the conjugate in vivo while in the circulation, but later allow the release of the toxin to enable its entry into the cytosol.

Often the toxin moiety is one of a variety of proteins capable of catalytically inactivating the protein-synthesis machinery of eukaryotic cells. These include holotoxins consisting of a catalytically active A fragment and binding B fragment [e.g. diphtheria toxin (4, 5), *Pseudomonas* exotoxin A (6, 7), ricin (8, 9), and abrin (10, 11)], hemitoxins consisting of only the enzymatic A fragment [e.g. the A chain of diphtheria toxin (12, 13), ricin (1, 14), or abrin (15, 16)], and ribosome-inactivating proteins [e.g. gelonin (17, 18), pokeweed antiviral protein (19, 20), and saporin (21)]. In order to be effective in vivo, the toxin must remain attached to the antibody in the circulation. However, once the immunotoxin is inside the target cell, the release of the catalytic portion of the toxin is required in order to interact with its cytosolic target; A-chain-containing conjugates made with noncleavable thioether linkages are less than 1% as active as those containing easily reduced disulfide linkages (14, 22). The type of linkage required between the toxin and antibody depends on the form of the toxin used.

Conjugates made with the standard heterobifunctional cross-linking reagents, *N*-succinimidyl 3-(2-

pyridyldithio)propionate (SPDP)¹ and 2-iminothiolane (2-IT), are labile in circulation (23-26, 18). Premature cross-link cleavage reduces the amount of intact conjugate which can bind to target cells. In addition, the released antibody remains in the circulation longer than conjugate and can compete with the intact conjugate for target-cell binding (23, 24, 26-29). Finally, the slow, sustained release of ricin A chain may contribute to the increased toxicity of disulfide-linked conjugates compared to that of free ricin A chain, which is rapidly cleared by renal filtration (23, 30). All of these factors probably have reduced immunotoxin efficacy in various in vivo models for solid-tumor therapy.

Thorpe et al. (31) and Worrell et al. (32) synthesized cross-linking reagents capable of yielding more stable disulfide bonds, on the basis of the finding that substitution of the α -carbon decreases the reactivity of the adjacent sulfur atom (33). One linker, 4-[(succinimidyl-oxycarbonyl)- α -methyl- α -(2-pyridyldithio)toluene (SMPT), sterically hindered the disulfide with a methyl group and a benzene ring attached to the carbon adjacent to the sulfur atom (31). The other linker, *N*-succinimidyl 3-(2-pyridyldithio)butyrate, substituted a methyl group on the α -carbon (32). Conjugates made with these new cross-linkers were more difficult to reduce chemically and had longer circulating half-lives than immunotoxins bearing

¹ The abbreviations used are as follows: BSA, bovine serum albumin; DTDP, 4,4'-dithiodipyridine; DTNB, 5,5'-dithiobis(2-nitrobenzoic acid); DTT, dithiothreitol; EDTA, ethylenediaminetetraacetic acid; GSH, reduced glutathione; GSSTNB, 2-nitro-5-mercaptopbenzoic acid disulfide of glutathione; GSSTP, 4-mercaptoppyridine disulfide of glutathione; HEPES, 4-(2-hydroxyethyl)-1-piperazineethanesulfonic acid; HNSA, 4-hydroxy-3-nitrobenzenesulfonic acid; IAM, iodoacetamide; 2-IT, 2-iminothiolane; MEA, β -mercaptoethylamine; MTT, 3-(4,5-dimethylthiazol-2-yl)-2,5-diphenyltetrazolium bromide; NaP_i, sodium phosphate buffer; NHS, *N*-hydroxysuccinimide; PSH, penicillamine; PSSTNB, 2-nitro-5-mercaptopbenzoic acid disulfide of PSH; PSSTP, 4-mercaptoppyridine disulfide of PSH; rRA, recombinant ricin A chain; rRA-TNB, 2-nitro-5-mercaptopbenzoic acid disulfide of rRA; rRA-TP, 4-mercaptoppyridine disulfide of rRA; SAMSA, (acetylthio)succinic anhydride; SMPT, 4-[(succinimidyl-oxycarbonyl)- α -methyl- α -(2-pyridyldithio)toluene; sNHS, *N*-hydroxysulfosuccinimide; sNHS-ATMBA, sulfosuccinimidyl *N*-[3-(acetylthio)-3-methylbutyryl]- β -alaninate; SPDP, succinimidyl 3-(2-pyridyldithio)propionate; TCA, trichloroacetic acid; TFA, trifluoroacetic acid; TMBA, *N*-(3-mercaptop-3-methylbutyryl)- β -alanine; TNB, 2-nitro-5-mercaptopbenzoic acid; TP, 4-mercaptoppyridine.

* To whom correspondence should be addressed.

† PCR Department.

‡ Department of Chemistry.

§ Current address: Glycomed, 860 Atlantic Ave., Alameda CA, 94501.

the standard disulfide cross-links (31, 32). Conjugates made with SMPT were as cytotoxic in vitro as conjugates synthesized with SPDP or 2-IT and had improved efficacy in vivo (34). Attempts to make an active-ester cross-linking reagent from 3-(2-pyridyldithio)isovaleric acid, a compound containing two methyl substituents on the carbon α to the disulfide, failed (32).

During an effort to make immunotoxins which would resist undesired disulfide cleavage in circulation, we found that conjugates cross-linked with (acetylthio)succinic anhydride (SAMSA), in which the α -carbon is substituted with either a carboxylate or a methyl carboxylate, are unstable in vivo. Therefore, we developed a cross-linking reagent, sulfosuccinimidyl *N*-[3-(acetylthio)-3-methylbutyryl]- β -alaninate (sNHS-ATMBA), in which the α -carbon is substituted with two methyl groups. The disulfide bond involving the sulfur adjacent to the tertiary carbon is 2 orders of magnitude more difficult to reduce than the analogous glutathione disulfide bond. Nevertheless, most conjugates made with this cross-linker have in vitro cytotoxic activity similar to that of analogous conjugates made with 2-IT.

EXPERIMENTAL PROCEDURES

Reagents and Chemicals. (35 S)methionine (1086 Ci/mmol, cat. no. NEG-009A) and [1- 14 C]iodoacetamide (24.1 mCi/mmol) were purchased from New England Nuclear (Boston, MA); 2-IT, SAMSA, *N*-hydroxysulfosuccinimide (sNHS), 5,5'-dithiobis(2-nitrobenzoic acid) (DTNB), and 4,4'-dithiodipyridine (DTDP) were from Pierce (Rockford, IL); β -mercaptoethylamine (MEA), iodoacetamide (IAM), *tert*-butyl- β -alanine hydrochloride, *N*-hydroxysuccinimide (NHS), dicyclohexyl carbodiimide, and carboxymethylated BSA were from Sigma (St. Louis, MO); chloroform (CHCl_3), methanol (MeOH), and methylene chloride (CH_2Cl_2) were from Burdick and Jackson (Muskegon, MI); triethylamine, dimethylacryloyl chloride, thioacetic acid, trifluoroacetic acid (TFA), and D,L-penicillamine (α -amino- β -methyl- β -mercaptobutyric acid, PSH) were from Aldrich Chemical Co. (Milwaukee, WI); *N,N*-Dimethylformamide was from Fisher Scientific Co. (Fair Lawn, NJ); and activated Type 4A, 8–12 mesh molecular sieve was from J. T. Baker Chemical Co. (Phillipsburg, NJ). The 4-hydroxy-3-nitrobenzenesulfonic acid (HNSA) sodium salt was synthesized as previously described (35). Preparative chromatography was performed on a Chromatotron (Harrison Instruments, Palo Alto, CA).

Strains and Medium. Hybridoma cells were grown in HL-1 medium (Ventrex, Portland, ME) supplemented with Fungibact (Irvine Scientific, Santa Ana, CA) and 8 mM glutamine. When labeling the antibody metabolically by incorporation of (35 S)methionine, HL-1 medium deficient in methionine was used. For the in vitro kinetic studies, cells were grown in RPMI 1640 medium with and without methionine (Flow Laboratories, McLean, VA).

Mice. Female Balb/C nude (nu/nu) mice were obtained from Charles River Breeding Labs (Kingston, NY).

Hybridomas and Antibodies. The following mouse monoclonal antibodies and hybridomas were used in the study (14, 36–38).

antibody	isotype	antigen	Accession No.
113F1	IgG ₃ , κ	37/60/93/200 kDa	HB 8490
2G3	IgG ₁ , κ	HMW protein	HB 8491
260F9	IgG ₁ , κ	55 kDa	HB 8488
317G5	IgG ₁ , κ	44-kDa glycoprotein	HB 8484
454A12	IgG ₁ , κ	transferrin receptor	IVI 10075
520C9	IgG ₁ , κ	210 kDa	HB 8696
MOPC21	IgG ₁ , κ	none known	

Cell Lines. The human breast cancer cell line SK-Br-3 was a generous gift from Dr. J. Fogh (Sloan Kettering, New York, NY), and MCF-7 was obtained from E. G. & G. Mason Research Institute, Worcester, MA. The in vitro human breast cancer cell line MX-1 was a line adapted from the in vivo MX-1 tumor (39, 40) by C. Vitt and A. Creasey (Department of Cell Biology, Cetus Corp.). The newborn human foreskin cell line HS27F (ATCC CRL1634) was used as a negative control because it bound none of the antibodies.

Chemical Analysis. ^1H NMR spectra were taken on a Varian FT-80A spectrometer. Chemical shifts of compounds in CDCl_3 are reported in ppm downfield from internal tetramethylsilane.

Synthesis of ATMBA. The *tert*-butyl ester of β -alanine hydrochloride (structure II, Figure 1) (1.8 g, 10 mmol) in 10 mL of CH_2Cl_2 was neutralized with 1 equiv of triethylamine (1.4 mL, 10 mmol). The precipitated triethylamine hydrochloride was filtered. The solution of β -alanine *tert*-butyl ester and 1.4 mL of triethylamine was placed in a dropping funnel and added dropwise to a nitrogen-flushed 100-mL three-neck round-bottom flask containing dimethylacryloyl chloride (structure I, Figure 1) (1.1 mL, 10 mmol) dissolved in 10 mL of CH_2Cl_2 . The mixture was stirred at room temperature for 2 h. The reaction mixture was diluted to about 50 mL with CH_2Cl_2 , washed with water (15 mL \times 2) and brine (saturated aqueous sodium chloride), and dried over MgSO_4 . The crude product was purified by Chromatotron chromatography on a 4-mm silica gel plate. The plate was eluted first with 0.5% MeOH in CHCl_3 to remove an impurity, then with 2% MeOH in CHCl_3 to elute the product *tert*-butyl ester of dimethylacryloyl- β -alanine (structure III, Figure 1). ^1H NMR: δ 6.25 (br s, 1 H), 5.5 (s, 1 H), 3.45 (q, 2 H), 2.4 (t, 2 H), 2.2 (s, 3 H), 1.8 (s, 3 H), 1.45 (s, 9 H). Yield = 1.5 g (66%).

To 1.2 g (5.4 mmol) of the *tert*-butyl ester of dimethylacryloyl- β -alanine in a 25-mL round-bottom flask was added 5 mL of freshly distilled thioacetic acid. The reaction mixture was refluxed under nitrogen for 4 h. The solution was cooled and diluted with about 50 mL of ethyl ether. The ether solution was washed with 5% acetic acid, water, and brine and dried over MgSO_4 . Evaporation of the ether gave a colorless oil which was not further purified.

The crude product (structure IV, Figure 1) was dissolved in 10 mL of TFA and stirred at room temperature for 1 h. The TFA was evaporated and the crude product was purified by Chromatotron chromatography on a 4 mm silica gel plate. Chromatography was started in CHCl_3 and the product eluted with 5% MeOH in CHCl_3 . The product *N*-[3-(acetylthio)-3-methylbutyryl]- β -alanine (structure V, Figure 1) crystallized on evaporation of the solvent and was recrystallized from CHCl_3 -hexane. ^1H NMR: δ 8.3 (br s, 1 H), 6.4 (br t, 1 H), 3.5 (q, 2 H), 2.75 (s, 2 H), 2.55 (t, 2 H), 2.25 (s, 3 H), 1.5 (s, 6 H). Yield = 0.7 g (52%).

HNSA or sNHS Esters. *N*-[3-(Acetylthio)-3-methylbutyryl]- β -alanine (617 mg, 2.5 mmol) was weighed into a 10-mL round-bottom flask. Sodium HNSA (602 mg, 2.5 mmol) or sNHS (542 mg, 2.5 mmol) was dissolved in about 3 mL of dimethylformamide and added to the flask, followed by 515 mg of dicyclohexylcarbodiimide, and the mixture was stirred at room temperature for 18 h. The mixture was filtered to remove dicyclohexylurea and added dropwise to 50 mL of ethyl ether with rapid stirring. The ether was stirred for about 0.5 h, then the precipitate was allowed to settle. The ether was decanted and the precipitate was washed with fresh ether four times. The solid product (structure VI, Figure 1) was collected by filtration and dried. Yield (HNSA linker) = 535 mg (46%).

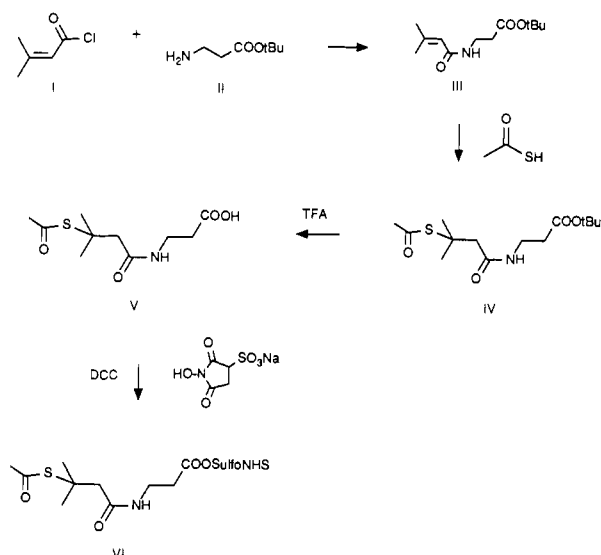


Figure 1. Synthesis of sNHS-ATMBA. The structures are (I) dimethylacryloyl chloride; (II) *tert*-butyl ester of β -alanine; (III) *tert*-butyl ester of (dimethylacryloyl)- β -alanine; (IV) *tert*-butyl ester of *N*-[3-(acetylthio)-3-methylbutyryl]- β -alanine; (V) *N*-[3-(acetylthio)-3-methylbutyryl]- β -alanine; and (VI) sulfosuccinimidyl ester of *N*-[3-(acetylthio)-3-methylbutyryl]- β -alanine.

NHS Ester. *N*-[3-(Acetylthio)-3-methylbutyryl]- β -alanine (494 mg, 2 mmol) was weighed into a 25-mL round-bottom flask. NHS (230 mg, 2 mmol), in 10 mL of CH_2Cl_2 , was added followed by 412 mg of dicyclohexylcarbodiimide. The reaction was stirred at room temperature for 18 h. The precipitated dicyclohexylurea was filtered off and the solvent evaporated to give a white powder. The product was recrystallized from ethanol. ^1H NMR: δ 6.3 (br s, 1 H), 3.6 (q, 2 H), 2.85 (s, 4 H), 2.8 (t, 2 H), 2.75 (s, 2 H), 2.25 (s, 3 H), 1.5 (s, 6 H). Yield = 350 mg (50%).

Characterization of Stock Concentrations of Linker. Stock 10 mM solutions of the HNSA ester of the linker were freshly prepared prior to use by dissolving ca. 2 mg in 500 μL of water. The concentration of active ester was determined in buffer (either 100 mM NaP_i , 1 mM EDTA, pH 7.6, or 100 mM HEPES, 0.2 M NaCl, 1 mM EDTA, pH 7.6) as described by Aldwin and Nitecki (35). Briefly, the free HNSA dianion concentration was measured at 406 nm with a molar extinction coefficient of $4.6 \times 10^3 \text{ M}^{-1} \text{ cm}^{-1}$. The initial concentration of the free HNSA dianion was determined. Following the addition of 5 N NaOH to a final concentration of 240 mM the total concentration of HNSA was determined. The concentration of ester was calculated from the difference in the initial and final values.

A stock (25 mM) solution of the NHS ester of the linker was prepared by dissolving 3 mg in acetonitrile and storing at -20°C . The amount of the anion of NHS was measured at 259 nm with an extinction coefficient of $8600 \text{ M}^{-1} \text{ cm}^{-1}$ (41, 42). To determine the concentration of ester, the stock solution was diluted into 0.25 M Tris-Cl, pH 8.0, and the absorbance at 259 nm was monitored with time. The ester concentration was determined from the difference between the final and initial (extrapolated) absorbances.

Stock (10 mM) solutions of the sNHS ester of the linker were made in dry dimethylformamide and stored at -70°C . Following dilution of the stock in 100 mM NaP_i , pH 6.0, the initial absorbance at 269 nm was measured. Hydroxylamine was added to a final concentration of 5 mM, and the measurement was repeated 1 min later. The aminolysis of the ester was complete in 10 s. Ester concentration was determined from the difference in the two

values, using a molar extinction coefficient at 269 nm of $6100 \text{ M}^{-1} \text{ cm}^{-1}$ at pH 6.0.

Kinetic Studies. Hydrolysis rates were studied spectrophotometrically in the indicated buffers as a function of time at 25°C . Reactions were carried out for 15 min and monitored at 15-s intervals. Hydrolysis was followed at 406 nm for the HNSA ester and at 269 nm for the sNHS ester. The total ester was determined as described above.

Second-order rate constants for thiol-disulfide exchange reactions with DTNB or DTDP, releasing 2-nitro-5-mercaptobenzoic acid (TNB) [molar extinction coefficient at 412 nm of $13\,600 \text{ M}^{-1} \text{ cm}^{-1}$ (43)] or 4-mercaptopyridine (TP) [molar extinction coefficient at 324 nm of $19\,800 \text{ M}^{-1} \text{ cm}^{-1}$ (44)], were determined by monitoring the reaction spectrophotometrically at 5-s intervals for 10 min at 23°C in 100 mM NaP_i , pH 7.0 or 8.0. When one reagent was in great excess, the reaction exhibited first-order kinetics with respect to the limiting reagent, and the pseudo-first-order rate constant was calculated from the initial linear part of the graph of \ln [unreacted reagent] vs time. The second-order rate constant was calculated by dividing the pseudo-first-order constant by the concentration of the excess species. For fast reactions, equal concentration of the two reagents were added, and the second-order rate constant was calculated from a plot of $(1/[A]) - (1/[A_0])$ vs time. Finally, when the concentrations of the two reagents were not equal but neither was in great excess, a plot of $(1/([A_0] - [B_0])) \times \ln([A] \times [B_0]/([A_0] \times [B]))$ vs time yielded the second-order rate constant.

The reactivity of the TMBA thiol was examined following derivatization of antibody, deacetylation with hydroxylamine, and desalting.

Synthesis of Immunoconjugates with 2-Iminothiolane. Recombinant ricin A (rRA) chain produced in *Escherichia coli* (45) and 2-IT conjugates were prepared by the Cetus Process and Product Development group using previously published methods (46, 47).

Synthesis of Radioactive Immunoconjugates with SAMSA. For the preparation of metabolically ^{35}S -labeled 260F9 antibody [(^{35}S) -260F9], hybridoma cells were grown in HL-1 medium at 37°C under 10% CO_2 for 2 days. Cells were harvested, washed, and resuspended in HL-1 medium deficient in methionine to a final cell density of 1×10^6 viable cells per mL. (^{35}S) methionine was added to a final specific activity of 50 $\mu\text{Ci/mL}$ (50 nM), and the culture was incubated an additional 24 h at 37°C under 10% CO_2 . The radiolabeled antibody was concentrated from the supernatant by chromatography over a Bio-Gel HPHT hydroxyapatite HPLC column (100 mm \times 7.8 mm, Bio-Rad Laboratories, Richmond, CA) using a sodium phosphate gradient. The antibody was further purified by chromatography over a BioGel TSK-phenyl-5-PW HPLC column (75 mm \times 7.5 mm, Bio-Rad, Richmond, CA) with a simultaneously descending gradient of ammonium sulfate (1.0–0 M) and ascending gradient of propylene glycol (0–30%) in phosphate buffer (100 mM NaP_i , pH 8.0). The antibody was at least 95% pure based on SDS-PAGE and autoradiography.

A stock solution (5 mM) of SAMSA was prepared in acetonitrile. (^{35}S) -260F9 (640 $\mu\text{g/mL}$, $1.1 \times 10^5 \text{ dpm}/\mu\text{g}$) was derivatized with a 15-fold excess of SAMSA in 10 mM HEPES, 0.2 M NaCl, 1 mM EDTA, pH 7.6, for 16 h to generate approximately 1.8 linkers per antibody, and the acetyl group was removed by treatment with 50 mM hydroxylamine at 23°C for 1 h. Following activation of the thiol by reaction with 1 mM DTNB at 23°C for 1 h, the preparation was dialyzed against 100 mM NaP_i , pH 8.0. rRA was freshly reduced in 100 mM NaP_i , pH 8.0, with

1 mM dithiothreitol (DTT) and desalted over a PD-10 column (Pharmacia, Piscataway, NJ) in 100 mM NaPi, pH 8.0. For conjugation, a 2.5 molar excess of rRA thiols over antibody thiols was reacted at 23 °C for 72 h under nitrogen. Conjugate containing one rRA per antibody (1-mer) was purified as described below.

Synthesis of Immunoconjugates with TMBA. Antibody (10 mg/mL) was derivatized in 100 mM HEPES, 200 mM NaCl, 0.1 mM EDTA, pH 7.6, with 3.3-fold excess of sNHS-ATMBA (or 8.5-fold excess of HNSA-ATMBA) for 16 h at 23 °C, resulting in 1.8–2 thiols per antibody. The linker thiol was deprotected by treatment of the modified antibody with 50 mM hydroxylamine at pH 8.0 for 1 h and the preparation desalted over a PD-10 column in 100 mM NaPi, pH 8.0. rRA was freshly reduced with 1 mM DTT and desalted over a PD-10 column, the thiol was activated by treatment with 1 mM DTNB, and the unreacted products were removed by dialysis. Conjugation proceeded by mixing 1.5 mol of activated rRA–TNB disulfides per titratable antibody thiol at 4 °C for 16 h. Unreacted thiols were blocked by addition of 40 mM IAM for 1 h at 23 °C, and the conjugate was purified as described by Ferris et al. (47).

Synthesis of Radioactive Immunoconjugate with TMBA. (³⁵S)-260F9 (850 µg, 1 mg/mL) in 10 mM HEPES, 200 mM NaCl, 1 mM EDTA, pH 7.6 was derivatized with 15-fold excess of HNSA-ATMBA at 23 °C for 18 h. The preparation was deacetylated and conjugated as described above. The conjugate mixture was chromatographed over a Bio-Gel TSK-phenyl-5-PW HPLC column (75 mm × 7.5 mm) and eluted at 1 mL/min with a simultaneously descending gradient of sodium chloride (1.5–0 M) and ascending gradient of propylene glycol (0–30%) in phosphate buffer (100 mM, pH 6.8). Fractions containing predominantly intact 1-mer, as determined by estimated molecular weight from SDS nonreducing PAGE and autoradiography, were pooled. Contaminating free rRA was removed by chromatography at 1 mL/min over a Zorbax Bio Series GF-250 HPLC column (25 cm × 9.4 cm, Du Pont, Wilmington, DE) equilibrated with 100 mM sodium phosphate, pH 6.8, 250 µg/mL human serum albumin (Travenol, Laboratores, Inc, Glendale, CA). The final conjugate had a specific activity of 7.5×10^5 dpm.

Detection of Cysteine Thiols following Deacetylation of 260F9–ATMBA. Monoclonal antibody 260F9 (33 mg/mL) was derivatized in 100 mM HEPES, 0.2 M NaCl, 1 mM EDTA, pH 7.6, with 6.7 molar excess of sNHS-ATMBA, deacetylated with 50 mM hydroxylamine, pH 8, and desalted over a PD10 column. DTNB analysis indicated 1.9 thiols per antibody. To 1 mg of underivatized antibody (260F9 in 397 µL), 1 mg of derivatized antibody prior to deacetylation (260F9–ATMBA, in 344 µL), or 1 mg of derivatized, deacetylated antibody (260F9–TMBA, in 166 µL) was added a 5 molar excess of [¹⁴C]-IAM (24.1 mCi/mmol, 16 µL) at 23 °C for 16 h. Unincorporated label was removed by desalting over a PD10 column equilibrated with 20 mM *N*-ethylmorpholine, pH 8.0. In addition, [¹⁴C]IAM was reacted with a 12-fold molar excess of cysteine and deacetylated TMBA. For acid hydrolysis, each sample was dried under vacuum, resuspended in 300 µL of 6 N HCl, sealed in glass capillary tubes under vacuum, and incubated at 100 °C for 16 h. Samples were chromatographed on a microcrystalline cellulose Baker-flex plate (J.T. Baker, Phillipsburg, NJ) in *n*-butanol–pyridine–glacial acetic acid–water (90:60:18:72), dried, and autoradiographed at –70 °C.

In Vitro MTT Assay. The in vitro activity of conjugates was measured by using a colorimetric assay based

on the ability of mitochondrial dehydrogenase enzymes to cleave the tetrazolium ring of the salt 3-(4,5-dimethylthiazol-2-yl)-2,5-diphenyltetrazolium bromide (MTT) to the violet crystal formazan (48). Assays were performed by the Cetus Assay Development group, using a procedure developed by C. Vitt of Cetus. Briefly, wells of a 96-well tissue culture plate were filled with 50 µL of MEM Eagles medium (Irvine Scientific, Santa Ana, CA) containing 10% fetal calf serum (Flow Laboratories, McLean, VA) and 1% penicillin–streptomycin (Irvine Scientific, Santa Ana, CA). Dilutions of the test conjugate were added in 25 µL followed by the addition of 100 µL of cell suspension (at 1×10^5 cells/mL). Following incubation at 37 °C (6% CO₂ for 72 h) 75 µg of MTT was added, and the plates were incubated for an additional 4–6 h at 37 °C under 5% CO₂. The liquid was removed by aspiration, 150 µL of 3% SDS, 0.04 N HCl–2-propanol was added, and the plates were incubated for 30–60 min to allow color development. The plates were read at 570 nm in a Titertek Multiscan plate reader.

Kinetics of in Vitro Cytotoxicity. OVCAR3 cells were trypsinized, counted, and seeded in 96-well plates at a cell density of 6.7×10^4 viable cells/mL followed by the addition of 10 nM conjugate. At the indicated times, the cells were washed, incubated for 45 min with methionine-deficient RPMI 1640 medium supplemented with 8 µCi/mL (³⁵S)methionine, washed, and harvested onto filter paper. Incorporated radioactivity was precipitated with TCA and counted.

Analysis of Radioactive Conjugates in Vitro. Six female Balb/C nude (nu/nu) mice were injected with 0.1 mL of (³⁵S)-260F9–SAMSA–rRA (6 µg, 5.4×10^5 dpm) in 100 mM NaPi, pH 7, 200 µg/mL carboxymethylated BSA. At 0.25, 1.25, 2.25, 4.25, 8.25, and 12.33 h, mice were bled retroorbitally with heparinized capillaries and sacrificed. Alternatively, eight mice were injected with 0.1 mL of (³⁵S)-260F9–TMBA–rRA (3.6 µg); four mice were bled and sacrificed at both 5 and 24 h. Samples of blood were counted, and plasma was electrophoresed on a 5–10% gradient polyacrylamide SDS gel, dried, and autoradiographed at –70 °C using an intensifying screen.

RESULTS

Analysis of (³⁵S)-260F9–SAMSA–rRA in Vitro. Thorpe et al. (31) and Worrell et al. (32) have reported that cross-linkers with a methyl substituent on the carbon α to the thiol stabilize conjugates in vivo. We investigated the commercially available reagent SAMSA, which is branched at the carbon α to the sulfur (Figure 2). Due to reagent asymmetry, the substituent following derivatization can either be a carboxymethyl or a carboxylate group (Figure 2). Despite the substitution, SAMSA conjugates were unstable in vivo (Figure 3), as has been observed with 2-IT (16, 23–25) and SPDP (11, 16, 26) conjugates. Because this substitution at the α -carbon failed to stabilize the conjugate in vivo, we investigated a new cross-linking reagent in which the α -carbon is substituted with two methyl groups.

Synthesis of ATMBA. Initially, penicillamine was chosen for the linker backbone (Figure 2). The 4-nitrophenyl ester of *N*-carbobenzoxy-*S*-benzylpenicillamine has been used in peptide synthesis (49). Preparation of several esters (NHS, HNSA, 2,4-dinitrophenol, and 4-nitrophenol) of *N,S*-diacetylpenicillamine was attempted. Only 4-nitrophenol yielded an ester product (data not shown). Unfortunately, this reagent, 4-nitrophenyl *N,S*-diacetylpenicillamine, was not sufficiently water soluble to be useful as a protein cross-linker.

The inability to esterify the penicillaminecarboxylate efficiently was ascribed to steric hindrance by the adjacent

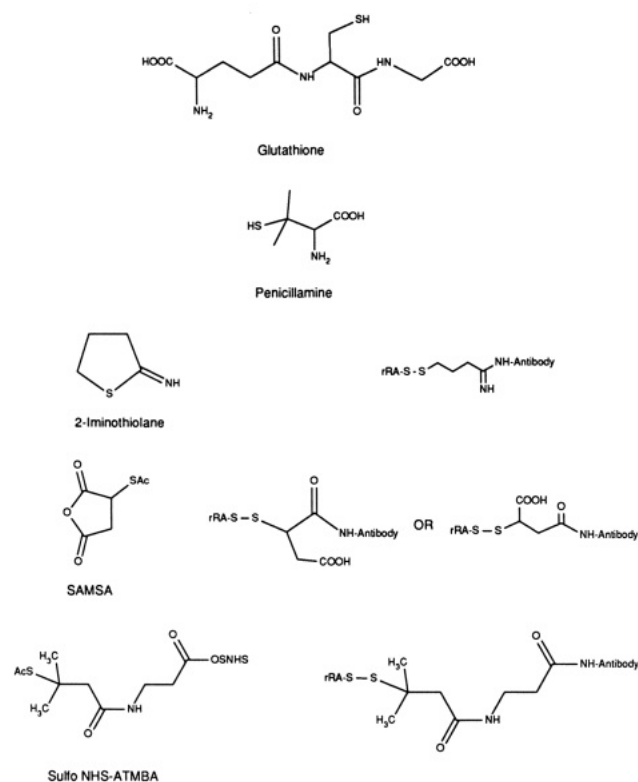


Figure 2. Chemical structures of thiol-containing compounds and cross-linkers. The thiol-containing compounds glutathione and penicillamine were used to compare the reactivity of sulfur atoms adjacent to a primary and tertiary carbon, respectively (Table I). The structures of the cross-linkers used in this study (2-IT, SAMSA, and TMBA) both before (left) and after (right) reacting with proteins are shown.

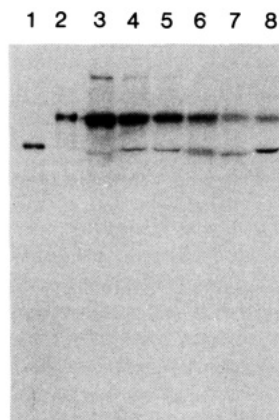


Figure 3. In vivo lability of 260F9-SAMSA-rRA conjugate. Six mice were injected intravenously with 6 μ g of (35 S)-260F9-SAMSA-rRA and sacrificed at 0.25 (lane 3), 1.25 (lane 4), 2.25 (lane 5), 4.25 (lane 6), 8.25 (lane 7) and 12.3 h (lane 8). Plasma was isolated and electrophoresed on a 5–10% gradient SDS polyacrylamide gel. The gel was dried and autoradiographed. Lane 1 is (35 S)-260F9 and lane 2 is (35 S)-260F9-SAMSA-rRA injectate.

doubly branched α -carbon. To avoid the problem, the linker backbone was elongated before the introduction of the sulfur, as outlined in Figure 1. On the basis of the approach of Worrell et al. (32), dimethylacryloyl chloride was used as the starting material but the linker backbone was extended by reacting with β -alanine *tert*-butyl ester. Thioacetic acid was added to the double bond, and the *tert*-butyl blocking group was removed. The carboxylate group, now five atoms removed from the sterically hindered site, was readily esterified with three different

Table I. Reactivity of Various Nucleophiles with Activated Thiols^a

activated thiol	k_2 , M ⁻¹ s ⁻¹			
	GSH	MEA	PSH	DTT
DTNB	2200 (5)	nd ^b	2100 (6)	nd
DTDP	1900 (3)	nd	1700 (4)	nd
GSSTNB	200 (2)	770 (1)	140 (3)	nd
GSSTP	360 (1)	890 (1)	210 (1)	nd
PSSTNB	1 (1)	3.2 (2)	0.73 (2)	1.7 (1)
PSSTP	1.6 (2)	1.8 (2)	nd	1.4 (1)
rRA-TNB	nd	nd	160 (1)	nd

activated thiol	k_2 , M ⁻¹ s ⁻¹		
	hydroxylamine	260F9-TMBA	520C9-TMBA
diacetyl-PSH	0.34 (1)	nd	nd
DTNB	nd	88 (8)	nd
sNHS-ATMBA	0.018 (6)	nd	nd
rRA-TNB	nd	nd	7 (1)
rRA-TP	nd	nd	3.6 (1)

^a The indicated two reagents were mixed and the release of the chromophore, TNB or TP, was followed spectrophotometrically at 23 °C as described in the Experimental Procedures. The concentration of the nucleophiles and the activated thiols ranged between 1×10^{-3} and 2×10^{-5} M. The rate of deacetylation of diacetyl-PSH (7×10^{-5} M) and sNHS-ATMBA (5×10^{-5} M) with hydroxylamine (50 mM) was monitored by measuring the exposed thiols by the inclusion of DTNB (1×10^{-4} M). The second-order rate constants (k_2) were determined during the initial part of the reaction. The number of determinations is indicated in parentheses. (rRA-TNB, rRA-2-nitro-5-mercaptobenzoate, rRA-TP, rRA-4-mercaptopyridine; 260F9-TMBA and 520C9-TMBA, derivatized antibody in which the thiol of the linker has been deblocked.) ^b Nd, not determined.

alcohols (HNSA, NHS, and sNHS). All three esters were evaluated for coupling efficiency.

Reactivity of Blocked Thiol. Penicillamine (Figure 2) was used to model the thiol reactivity of TMBA (Table I). The reactivity of the penicillamine (PSH) thiol with DTNB, DTDP, GSSTNB (2-nitro-5-mercaptobenzoic acid disulfide of glutathione), and GSSTP (4-mercaptopyridine disulfide of glutathione) was similar to those of reduced glutathione (GSH) and MEA (Table I). The reactivity of the penicillamine thiol with activated rRA, in which the thiol of rRA was activated with TNB ($k_2 = 160$ M⁻¹ s⁻¹). In contrast, the 2-nitro-5-mercaptobenzoic acid (PSSTNB) and 4-mercaptopyridine (PSSTP) disulfides of penicillamine were at least 2 orders of magnitude less reactive than the corresponding GSH derivatives toward reduction by GSH or MEA (Table I). Rabenstein and Thierault (50) have reported similar findings in which the penicillamine thiol acts as an efficient nucleophile while disulfide bonds involving the penicillamine sulfur resist cleavage.

Forms of Ester. Efficiency of protein modification with ATMBA is dependent upon competing aminolysis and hydrolysis reactions. As the hydrolysis rate is buffer dependent (Table II), more efficient derivatization could be achieved by selecting buffers which minimize this rate. It was found that HEPES buffer resulted in both a lower hydrolysis rate and a higher derivatization efficiency when compared to phosphate buffer (Tables II and III). This buffer effect on both hydrolysis rate and derivatization efficiency was greater for the HNSA ester than the sNHS ester (Tables II and III).

HNSA is a water-soluble and spectrophotometrically monitorable active-ester leaving group (35). Aldwin and Nitecki (35) found that the degree of derivatization assessed by HNSA release was higher than the actual number of groups introduced per protein despite correction for hy-

Table II. Hydrolysis and Aminolysis of ATMBA Esters^a

ester	buffer	$t_{1/2}$, min	app first-order rate constant, min ⁻¹
HNSA	100 mM NaPi, pH 7.6	76	0.0040
HNSA	100 mM NaPi, 1 mM EDTA, pH 7.6	71	0.0042
HNSA	10 mM HEPES, 0.2 M NaCl, pH 7.6	270	0.0011
HNSA	10 mM HEPES, 0.2 M NaCl, 1 mM EDTA, pH 7.2	330	0.00091
HNSA	10 mM HEPES, 0.2 M NaCl, 1 mM EDTA, pH 7.6	300	0.0010
	+ 10 mM 6-aminocaproic acid	50	0.0060
	+ 1 mM 6-aminocaproic acid	165	0.0018
	+ 0.1 mM imidazole	40	0.0075
	+ 0.01 mM imidazole	161	0.0019
HNSA	100 mM HEPES, 0.2 M NaCl, 1 mM EDTA, pH 7.6	270	0.0011
sNHS	100 mM NaPi, pH 6.0	39	0.0077
sNHS	100 mM HEPES, 0.2 M NaCl, 1 mM EDTA, pH 7.6	12	0.025

^a Reactions were monitored spectrophotometrically (HNSA ester at 406 nm, sNHS ester at 269 nm) at 15-s intervals for 15 min. The total concentration of ester was determined at the conclusion and the concentration of ester at each time point calculated. The rate constants represent the slope of the curve representing the \ln [ester] vs time. $t_{1/2} = \ln 2/k$. The $k_{\text{aminolysis}}$ is calculated from the equation $k_{\text{app}} = k_{\text{aminolysis}}[\text{amine}] + k_{\text{hydrolysis}}$ (53), where $k_{\text{aminolysis}}$ is the second-order aminolysis rate constant, [amine] is the concentration of the amino acid derivative, k_{app} is the experimentally measured pseudo-first-order rate constant for aminolysis and hydrolysis and $k_{\text{hydrolysis}}$ is the hydrolysis rate constant. The calculated $k_{\text{aminolysis}}$ for 6-aminocaproic acid was $0.65 \text{ M}^{-1} \text{ min}^{-1}$ and for imidazole was $78 \text{ M}^{-1} \text{ min}^{-1}$, using the total amine concentration. The respective pK_a values for the amines are 10.75 and 6.92.

drolysis. Histidine imidazoles are known to react with activated acyl groups to generate unstable acylimidazole intermediates which undergo subsequent hydrolysis (51–53). Not surprisingly, imidazole increased the rate of HNSA anion release from the ester (Table II). The displacement of the HNSA leaving group was higher with imidazole ($k_{\text{aminolysis}} = 78 \text{ M}^{-1} \text{ min}^{-1}$) than with 6-aminocaproic acid ($k_{\text{aminolysis}} = 0.65 \text{ M}^{-1} \text{ min}^{-1}$). This difference parallels the difference in pK_a values of the two compounds. Imidazole has a pK_a of 6.95 and is 82% un-ionized at pH 7.6, while the ϵ -aminocaproic acid amino group has a pK_a of 10.75 and is only 0.07% unprotonated at pH 7.6. Lysines are generally 2–3 times more abundant than histidines in most proteins (54) and are generally present on the protein surface (55). The counterbalancing ratios of abundance and side-chain reactivity combine to predict that histidine-catalyzed hydrolysis might compete effectively with lysine aminolysis in reactions intended to derivatize proteins. The quantitative outcome of this competition for a particular protein will depend on its amino acid composition and on side-chain microenvironment. In any event, this reaction may explain the discrepancy between the assessment of protein derivatization as determined by HNSA release as compared to titration of groups on the final product (data not shown) as well as the independence of derivatization efficiency from antibody concentration (Table III).

Despite the higher hydrolysis rates, sNHS esters derivatized antibody more efficiently than the corresponding HNSA esters. The derivatization reaction with the NHS ester was complete within 1 h (Figure 4). Because the sNHS ester is more soluble than the NHS ester, it is the preferred activated form of the linker.

Reactivity of the TMBA Thiol. Like SAMSA, ATMBA has a thiol blocked by an acetyl group. The acetyl

group was stable throughout the conjugation reaction (Table IV). Hydroxylamine completely deacetylated the blocked ATMBA thiol within 1 h (Figure 5; Table I). The TMBA thiol was 20-fold less reactive than the corresponding thiol of penicillamine as demonstrated by comparing their relative reactivities with DTNB ($k_2 = 88$ vs $2100 \text{ M}^{-1} \text{ s}^{-1}$), or rRA-TNB ($k_2 = 7$ vs $160 \text{ M}^{-1} \text{ s}^{-1}$) (Table I).

Efficient conjugation will occur only if the TMBA thiol reacts with the activated thiol of rRA faster than it autooxidizes. At the concentrations of rRA-TNB used during conjugation (5 mg/mL), the $t_{1/2}$ for the coupling reaction based on a k_2 of $7 \text{ M}^{-1} \text{ s}^{-1}$ (Table I) should be around 10 min. In contrast, the $t_{1/2}$ of TMBA thiol autooxidation was around 114 days (Figure 6), such that in a 24-h conjugation reaction, less than 0.6% of the antibody would be expected to dimerize.

Antibody derivatization did not alter the migration of the protein on SDS-PAGE (compare lanes 1 and 6 to lane 5 in Figure 7). However, when the thiol was deacetylated (Figure 7, lanes 2–4 and 7–9), there was a rapid appearance of a small amount of two new species. The apparent molecular weights of these bands suggested that they represent free light chain and an antibody molecule with two heavy chains and one light chain. These bands appeared only after deacetylation, suggesting that the TMBA thiol was somehow involved. The mechanism for this release probably involves the attachment of the linker to a lysine group in the vicinity of the disulfide bond connecting antibody heavy and light chains. Presumably, upon deacetylation of the linker thiol, a thiol–disulfide exchange resulted in release of the light chain. Thus the placement of the linker near this antibody disulfide is crucial to the proposed mechanism. The charge on the linker ester might influence which lysines are derivatized and hence the degree to which light chain release occurs. However, the appearance of these bands was independent of the ester form of the ATMBA used to derivatize the antibody (Figure 7).

No free thiols could be detected in the antibody either before or after derivatization prior to deacetylation (Table IV). If a rapid thiol–disulfide exchange reaction occurred after deacetylation, the ATMBA linker thiol must displace the light chain thiol from its disulfide bond, thereby freeing the light chain from the remainder of the antibody. As a result, the cysteine thiol of the light chain may become accessible.

The presence of free cysteine thiols was determined by labeling all free thiols with $[1\text{-}^{14}\text{C}]\text{IAM}$, cleaving the product by acid hydrolysis, and identifying the labeled species by thin-layer chromatography. Figure 8 demonstrates that following removal of the acetyl group from the ATMBA on the antibody, a population of cysteine thiols becomes available. The TMBA-IAM product resulted in one major and one minor species migrating close to the solvent front (lane 1). The cysteine-IAM product was a single spot close to the origin (lane 2) and the IAM product was a spot migrating at an intermediate position (lane 3). Thin-layer chromatography of the hydrolysate of underivatized antibody labeled with $[1\text{-}^{14}\text{C}]\text{IAM}$ (lane 4) and of ATMBA-antibody labeled with $[1\text{-}^{14}\text{C}]\text{IAM}$ (lane 5) resulted in barely detectable labeled species. In contrast, reaction of $[1\text{-}^{14}\text{C}]\text{IAM}$ with antibody that had been derivatized and deacetylated resulted in two groups of species (lanes 6 and 7): one migrating close to the solvent front similar in position to the TMBA control and one close to the origin as found with cysteine. In the absence of acid

Table III. Derivatization Efficiency with Different Esters of the ATMBA^a

ester	Ab	Ab conc mg/mL	buffer	efficiency	molar excess for 1.8 S/Ab
HNSA	260F9	1	0.1 M NaP _i , 1 mM EDTA, pH 6.8	0.010	177
HNSA	260F9	1	0.1 M NaP _i , 1 mM EDTA, pH 7.6	0.022	69
HNSA	260F9	1	0.01 M HEPES, 0.2 M NaCl, 1 mM EDTA, pH 7.6	0.11	15
HNSA	260F9	8	0.01 M HEPES, 0.2 M NaCl, 1 mM EDTA, pH 7.6	0.13	12
HNSA	260F9	9	0.1 M HEPES, 0.2 M NaCl, 1 mM EDTA, pH 7.6	0.13	14
NHS	260F9	8	0.01 M HEPES, 0.2 M NaCl, 1 mM EDTA, pH 7.6	0.54	3.8
sNHS	520C9	30	0.1 M HEPES, 0.2 M NaCl, 1 mM EDTA, pH 7.6	0.68	3.2
sNHS	520C9	30	0.1 M NaP _i , mM EDTA, pH 7.6	0.35	5.3

^a Antibody (Ab) at the indicated concentration (determined by absorbance) was incubated in buffer with increasing concentrations of ester for 16 h at 23 °C. The linker was deacetylated by the addition of hydroxylamine to 50 mM and NaP_i, pH 8.0, to 100 mM and incubation for 1 h; the mixture was desalted over a PD-10 column. The number of thiols per antibody was quantitated by assaying with DTDP and DTNB. The efficiency was determined by plotting the resulting thiols per antibody as a function of added esters per antibody and calculating the slope of the line via least-squares analysis. The number of linkers per antibody required to achieve 1.8 thiols per antibody molecule was determined by extrapolation.

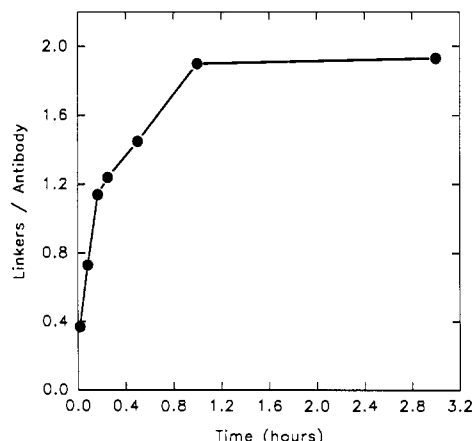


Figure 4. Derivatization of 520C9 with sNHS-ATMBA. 520C9 (30 mg/mL) was derivatized in 100 mM HEPES, 0.2 M NaCl, 1 mM EDTA, pH 7.6, with 3.3 molar excess of sNHS-ATMBA. At the indicated times, derivatization was stopped, the thiol deacetylated by the addition of 50 mM hydroxylamine for 1 h, the sample desalted on a PD-10 column, and the thiol content per antibody determined by DTNB analysis. At this concentration of hydroxylamine, any remaining sNHS ester was cleaved within 5 s.

Table IV. Free Thiol Content^a

sample	free thiols/antibody
260F9	0.04
260F9 treated with 50 mM hydroxylamine	0.02
260F9-ATMBA prior to hydroxylamine	0.10
260F9-ATMBA following hydroxylamine	2.2

^a Thiol content was assayed by DTNB analysis as indicated in the Experimental Procedures. Antibody, 260F9, was derivatized with HNSA-ATMBA at 23 °C for 16 h, followed by desalting on a PD10 column. The thiol content was measured on a fraction of the antibody. The remaining derivatized antibody was reacted with 50 mM hydroxylamine for 1 h, and the sample was desalted on a PD10 column. The thiol content was again measured. In addition, the thiol content was measured on the underivatized antibody as well as underivatized antibody treated with hydroxylamine for 1 h.

hydrolysis (lane 8), all radioactivity remained at the origin, indicating that all radioactivity was protein-associated.

Thin-layer chromatography of acid hydrolyzed, [1-¹⁴C]-IAM-labeled, deacetylated TMBA-antibody could not be used to quantitate the contribution of cysteine and TMBA to the final free thiols. The thiol content of TMBA-antibody determined by [1-¹⁴C]IAM ranged from 30 to 70% of that determined by both DTNB and DTDP analysis (data not shown). No free thiols could be detected with either DTNB or DTDP following reaction of TMBA-

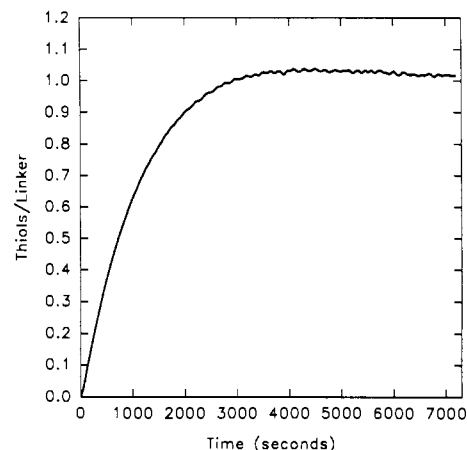


Figure 5. Deacetylation of ATMBA. 50 mM hydroxylamine was added to 50 μ M sNHS-ATMBA in 100 mM HEPES, 0.2 M NaCl, 1 mM EDTA, 50 mM NaP_i, pH 8, 50 μ M DTNB and the absorbance at 324 nm measured. The number of thiols per added linker was calculated with a molar extinction coefficient of 19 800 M⁻¹ cm⁻¹. In a control reaction, the hydrolysis of DTNB in the absence of linker was negligible.

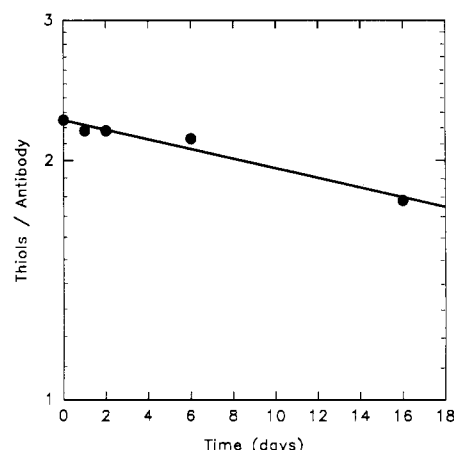


Figure 6. Oxidation of the TMBA thiol. Monoclonal antibody 260F9 (6.8 mg/mL) was reacted with HNSA-ATMBA, deacetylated with 50 mM hydroxylamine, desalted into 100 mM NaP_i, 1 mM EDTA, pH 7.0, and incubated at 23 °C for 16 days. Each point represents the average thiol content per antibody determined by both DTDP and DTNB analysis.

antibody with [1-¹⁴C]IAM. The reason for the discrepancy between radiolabeling stoichiometry and chromophoric thiol release is unclear.

In Vitro Cytotoxicities of Conjugates Made with ATMBA. Despite the increased stability of the disulfide adjacent to the tertiary carbon, the TMBA conjugates

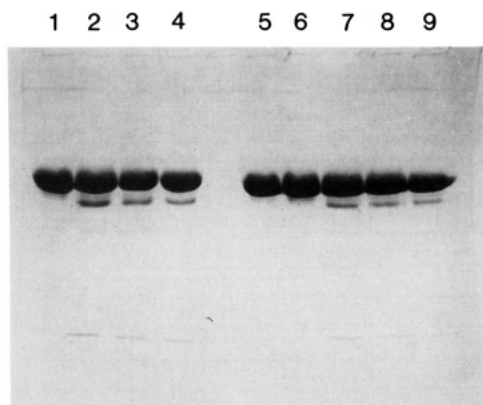


Figure 7. Thiol-disulfide exchange following deacetylation. 260F9 was derivatized with either sNHS-ATMBA (lanes 1-4) or HNSA-ATMBA (lanes 5-9) to add approximately 1.5 linkers per antibody. Following desalting over a PD-10 column, the preparations were deacetylated for 1 h in 50 mM hydroxylamine and again desalted over PD-10 columns. The thiol contents determined by DTNB analysis were 1.8 thiols per antibody (sNHS-ATMBA) and 1.3 thiols per antibody (HNSA-ATMBA). Samples were taken after each step and electrophoresed on a 6% SDS polyacrylamide gel: lanes 1, 6, following derivatization prior to deacetylation; lanes 2, 7, following deacetylation; lanes 3, 8, after final desalting; lanes 4, 9, blockage of free thiols by DTNB; lane 5, underivatized antibody.

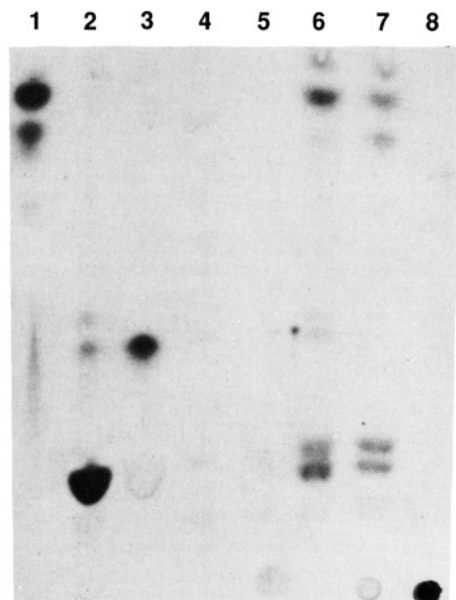


Figure 8. Availability of cysteine thiols following deacetylation of 260F9-ATMBA: TMBA (lane 1), cysteine (lane 2), 260F9 (lane 4) 260F9-ATMBA (lane 5), and 260F9-TMBA (lanes 6-8) were reacted with $[1-^{14}\text{C}]$ IAM, acid hydrolyzed (except lane 8) as described in the Experimental Procedures, and subjected to TLC, and the chromatogram was autoradiographed. Lane 3 is acid-hydrolyzed $[1-^{14}\text{C}]$ IAM, and lane 8 is 260F9-TMBA reacted with $[1-^{14}\text{C}]$ IAM without acid hydrolysis.

were specifically potent against breast cancer cell lines in vitro (Table V). The cytotoxicity of the TMBA conjugates relative to 2-IT conjugates depended on both the antibody and the cell line. In two cases (113F1 conjugates against MX-1 and SK-Br-3), TMBA increased the cytotoxicity by 1 order of magnitude, whereas in six cases (317G5 and 454A12 conjugates against MCF-7, 454A12 conjugates against MX-1, and 260F9, 317G5, and 454A12 conjugates against SK-Br-3) it decreased the cytotoxicity by at least 75%. Interestingly, replacing 2-IT had a "leveling" effect, reducing the cytotoxicity of the most active conjugate and increasing the cytotoxicity of most of the least active conjugates. This phenomenon might reflect differences

Table V. In Vitro Activity of Immunoconjugates^a

conjugate	TCID ₅₀ , nM			
	MCF-7	MX-1	SK-Br-3	HS27F
113F1-2-IT-rRA	1.2 (2)	31 (1)	510 (2)	390 (2)
113F1-TMBA-rRA	0.84 (7)	3.2 (7)	14 (4)	>69 (6)
2G3-TMBA-rRA	2.2 (6)	21 (6)	44 (2)	>200 (4)
260F9-2-IT-rRA	0.03 (26)	0.06 (16)	0.04 (14)	>380 (15)
260F9-TMBA-rRA	0.04 (30)	0.05 (12)	0.18 (6)	>350 (20)
317G5-2-IT-rRA	0.01 (2)	0.11 (1)	0.091 (2)	>320 (2)
317G5-TMBA-rRA	0.04 (8)	0.053 (8)	0.68 (5)	>1900 (8)
454A12-2-IT-rRA	0.002 (2)	0.002 (1)	0.029 (1)	220 (2)
454A12-TMBA-rRA	0.03 (6)	0.031 (4)	0.50 (8)	>160 (4)
520C9-2-IT-rRA	88 (6)	140 (7)	nd ^b	>1400 (6)
520C9-TMBA-rRA	130 (12)	110 (14)	0.58 (14)	>1000 (10)
MOPC21-TMBA-rRA	72 (6)	nd	nd	>890 (6)

^a The in vitro activity of conjugates made with seven different antibodies using the two linkers 2-IT and TMBA was measured against the three human breast cancer cell lines MCF-7, MX-1, and SK-Br-3 and a human fibroblast cell line (HS27F) as described in the Experimental Procedures. The concentration of conjugate which results in 50% of the MTT signal (TCID₅₀) is given, along with number of determinations in parentheses. ^b Nd, not determined.

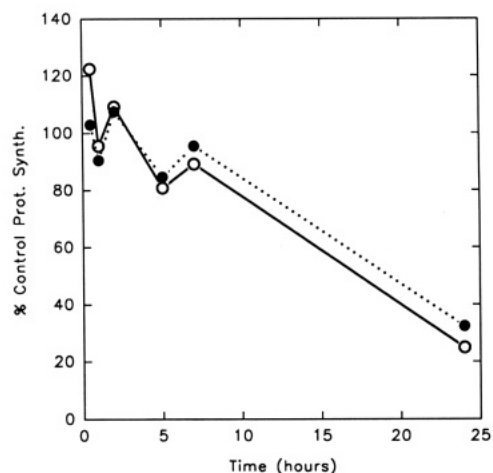


Figure 9. Kinetics of protein-synthesis inhibition by 260F9-TMBA-rRA (closed circles) and 260F9-2-IT-rRA (open circles). 260F9-2-IT-rRA or 260F9-TMBA-rRA at 10 nM was added to 1×10^4 OVCAR3 cells in 96-well microtiter plates and incubated at 37 °C under 10% CO₂. At the indicated times, the cells were pulsed for 45 min with (^{35}S) methionine and harvested. Each point represents an average of triplicate determinations. The TCID₅₀ values of 260F9-2-IT-rRA and 260F9-TMBA-rRA measured at 24 h by protein synthesis inhibition were 0.14 and 0.45 nM, respectively.

in the kinetics of killing. However, the kinetics of protein synthesis inhibition in OVCAR3 cells were similar for conjugates made with the two cross-linking reagents (Figure 9).

In Vivo Stability of Conjugates Made with TMBA.

The TMBA-linked conjugate was more resistant to breakdown in vivo than the SAMSA-linked conjugate (Figure 10). Whereas most of the SAMSA conjugate broke down to free antibody by 12.3 h (Figure 3), there was little breakdown of the TMBA conjugate even at 24 h. The radioactive material which migrated on SDS-PAGE at a position similar to that of antibody did not increase even at 168 h following in vivo administration (data not shown). A proportion of this material contained rRA as demonstrated by the presence of a similar band following SDS-PAGE analysis of plasma from animals injected with 260F9-TMBA- (^{35}S) rRA (data not shown). The terminal half-life of the TMBA conjugate in mice was 43 h compared to 24 h for the 2-IT conjugate (manuscript in preparation).

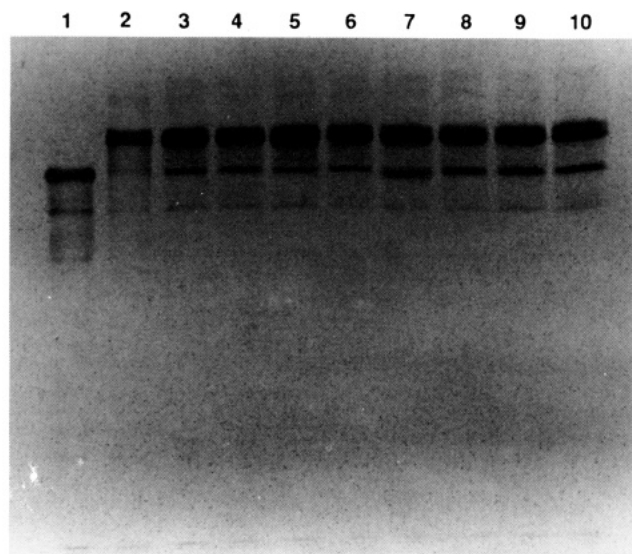


Figure 10. In vivo stability of 260F9-TMBA-rRA conjugate. Eight mice were injected intravenously with 3.6 μ g of (35 S)-260F9-TMBA-rRA and sacrificed at either 5 (lanes 3–6) or 24 (lanes 7–10) h. Plasma was isolated and electrophoresed on a 5–10% gradient SDS polyacrylamide gel. The gel was dried and autoradiographed. Lane 1 is (35 S)-260F9-TMBA and lane 2 is (35 S)-260F9-TMBA-rRA injectate.

DISCUSSION

The disulfide bond connecting ricin A chain to antibody using either SPDP (11, 16, 26) or 2-IT (16, 23–25) is labile in circulation on the time scale of hours. This fact has three important potential consequences. First, disulfide cleavage in the circulation reduces the amount of intact conjugate delivered to the tumor. Second, the released antibody, which has a longer circulating half-life than intact conjugate (16–18, 23, 24, 26, 27, 29, 30), can bind to the tumor, thereby potentially competing with the conjugate for binding to cell-surface epitopes if the latter are stoichiometrically limiting. Third, the slow continual release of the ricin A chain into the circulation may contribute to the increased toxicity of disulfide-linked conjugate compared to that of free ricin A chain, which is rapidly cleared by renal filtration (23, 30). These factors have undoubtedly contributed to the limited efficacy of immunoconjugates in vivo (56–59).

Thorpe et al. (31) and Worrell et al. (32) have shown that single substitution of the carbon adjacent to the sulfur makes the disulfide bond more difficult to reduce, leading to more stable conjugates in vivo. We investigated a commercially available cross-linking reagent, SAMSA, which, upon conjugation, has a carboxymethyl or a carboxylate group on the carbon adjacent to the sulfur, and found that the disulfide bond was still labile in vivo. We therefore developed a new cross-linking reagent with two methyl groups on the α -carbon.

Worrell et al. (32) demonstrated that reduction of the 3-(2-pyridyldithio)isovaleric acid disulfide was 50- and 600-fold less rapid than that of 3-(2-pyridyldithio)butyric acid and 3-(2-pyridyldithio)propionic acid, respectively, at pH 7.5. They were, however, unable to prepare the NHS ester of that acid, probably because of steric hindrance of the carboxylate group. We show here that elongation of the linker by addition of β -alanine to dimethylacryloyl chloride before introduction of the sulfur provides a carboxyl group which readily forms esters.

Three forms of ester were investigated. Aldwin and Nitecki (35) previously demonstrated the use of HNSA as a water-soluble ester leaving group that allows monitoring

of the derivatization reaction. We have found that the HNSA ester of TMBA is slow and inefficient in derivatizing antibody; spectrophotometric monitoring of HNSA release overestimates the degree of derivatization. Both NHS and sNHS esters lead to faster and more efficient derivatization, and the latter has the advantage of water solubility. The final form of the linker, sNHS-ATMBA, reacts rapidly and derivatizes antibody with approximately 70% efficiency.

The reactivity of sulfur atoms adjacent to a tertiary carbon was modeled with penicillamine. The penicillamine disulfide was over 2 orders of magnitude more inert than that of the corresponding nonhindered analogues (i.e. glutathione). In contrast, the nucleophilicity of the free penicillamine thiol was similar to that of the reduced glutathione thiol. These facts inspired an efficient conjugation strategy in which the linker sulfur served as the nucleophile and the ricin A chain thiol was activated with TNB. Table I also suggests that nucleophilic reactivity of a tertiary thiol toward a chromogenic disulfide is reduced about 95% by attachment to an immunoglobulin; this effect is too large to be explained solely by the effect of size on the diffusion coefficient, and therefore must reflect steric occlusion by the bulk of the immunoglobulin molecule.

ATMBA was synthesized with the thiol protected by an acetyl group, which can be efficiently removed by treatment with hydroxylamine at 23 $^{\circ}$ C for 1 h. Conjugation with activated rRA at 10 mg/mL at 23 $^{\circ}$ C occurs with an initial half-time of 5 min. However, a 16-h conjugation generally resulted in only 70–80% of the titratable TMBA thiols conjugated to rRA. This observation implies that there is a varying degree of accessibility among linker thiols attached to antibody. Following conjugation, unreacted thiols were blocked by IAM.

TMBA thiol autooxidation was very slow, with a half-life of approximately 114 days. Therefore, antibody dimerization during the conjugation reaction should not be a problem (and has not been in our experience to date). In contrast, 2-IT-modified monoclonal antibodies routinely exhibit some antibody dimerization. However, following exposure of the free TMBA thiol by deacetylation, a very rapid thiol–disulfide exchange between a small proportion of linker thiols and antibody disulfide bonds was demonstrated by the presence of free light chain on SDS-PAGE. This rapid reaction was complete during the deacetylation reaction, as longer incubation did not result in further release of antibody light chain.

Despite the resistance of the TMBA disulfide bond to reduction, conjugates made with this cross-linker were effective in vitro. The in vitro cytotoxicity of TMBA conjugates showed some differences when compared to the analogous 2-IT-conjugates. The relative potencies depended on the antibody and the cell line, and may reflect differences in the rate-controlling step for killing by conjugate made with different antibodies. For example, for those antibodies in which disulfide cleavage of the conjugate is rate-limiting, stabilization of the disulfide might decrease the in vitro toxicity. In contrast, for those antibodies in which internalization from the cell surface is slow, stabilization of the disulfide bond may decrease the vulnerability to cleavage prior to entry, either in the medium or on the cell surface, thereby increasing the in vitro cytotoxicity. In the one cell line so examined, OVCAR3, the kinetics of protein synthesis inhibition by the two conjugates were similar. It is interesting that, although model disulfides are deactivated by over 2 orders of magnitude by double α -substitution, the TCID₅₀ is

increased by no more than 1 order of magnitude. Thus such cross-linkers might make marginally effective immunotoxins better. Whether they worsen the performance of the best immunotoxins will depend on whether the pharmacokinetics or cellular events control efficacy in vivo.

The in vivo behavior of 2-iminothiolane and TMBA conjugates made with rRA has been studied (manuscript in preparation); the TMBA conjugates demonstrate a longer half-life, greater in vivo efficacy, and greater in vivo toxicity compared to the corresponding 2-iminothiolane conjugates.

In summary, we have developed a new, efficient cross-linking reagent which generates an unusually stable disulfide bond between antibody and ricin A chain, yet results in immunotoxins with in vitro potency similar to that of analogous conjugates made with 2-iminothiolane.

ACKNOWLEDGMENT

We wish to thank Danute Nitecki for suggesting penicillamine. We wish to thank Gregory Groetsema, Valerie Dumbrava, and Gregory Pattison for their excellent technical assistance; Anthony Chan for injecting mice; the Cetus Process and Product Development group for providing unlabeled antibody and rRA and 2-IT immunoconjugates; and the Cetus Assay Development group for performing the in vitro cytotoxicity assays on the conjugates. In addition, we thank Jonathan Raymond and Robert Ferris for careful review of the manuscript and Sharon Muir for the photography.

LITERATURE CITED

- (1) Blakey, D. C., and Thorpe, P. E. (1988) An Overview of Therapy with Immunotoxins Containing Ricin or Its A-Chain. *Antibody, Immunoconjugates Radiopharm.* 1, 1-16.
- (2) Blakey, D. C., Wawrzynczak, E. J., Wallace, P. M., and Thorpe, P. E. (1988) Antibody Toxin Conjugates: A Perspective. *Monoclonal Antibody Therapy. Progress in Allergy* 45 (H. Waldmann, Ed.) pp 50-90, S. Karger, Basel.
- (3) Vitetta, E. S., Fulton, R. J., May, R. D., Till, M., and Uhr, J. W. (1987) Redesigning Nature's Poisons to Create Anti-Tumor Reagents. *Science* 238, 1098-1104.
- (4) Thorpe, P. E., Ross, W. C. J., Cumber, A. J., Hinson, C. A., Edwards, D. C., and Davies, A. J. S. (1978) Toxicity of Diphtheria Toxin for Lymphoblastoid Cells Is Increased by Conjugation to Antilymphocytic Globulin. *Nature* 271, 752-755.
- (5) Moolten, F. L., Capparell, N. J., Cooperband, S. R. (1972) Antitumor Effects of Antibody-Diphtheria Toxin Conjugates: Use of Hapten-Coated Tumor Cells as an Antigenic Target. *J. Natl. Cancer Inst.* 49, 1057-1062.
- (6) Pirker, R., FitzGerald, D. J. P., Hamilton, T. C., Ozols, R. F., Willingham, M. C., and Pastan, I. (1985) Anti-Transferin Receptor Antibody Linked to *Pseudomonas* Exotoxin as a Model Immunotoxin in Human Ovarian Carcinoma Cell Lines. *Cancer Res.* 45, 751-757.
- (7) Bjorn, M. J., Groetsema, G., and Scalapino, L. (1986) Antibody-*Pseudomonas* Exotoxin A Conjugates Cytotoxic to Human Breast Cancer in Vitro. *Cancer Res.* 46, 3262-3267.
- (8) Youle, R. J., and Neville, D. M., Jr. (1980) Anti-Thy 1.2 Monoclonal Antibody Linked to Ricin Is a Potent Cell-Type-Specific Toxin. *Proc. Natl. Acad. Sci. U.S.A.* 77, 5483-5486.
- (9) Thorpe, P. E., Ross, W. C. J., Brown, A. N. F., Myers, C. D., Cumber, A. J., Foxwell, B. M. J., and Forrester, J. T. (1984) Blockade of the Galactose-Binding Sites of Ricin by Its Linkage to Antibody: Specific Cytotoxic Effects of the Conjugates. *Eur. J. Biochem.* 140, 63-71.
- (10) Godal, A., Fodstad, O., and Pihl, A. (1987) Studies on the Mechanism of Action of Abrin-9.2.27 Immunotoxin in Human Melanoma Cell Lines. *Cancer Res.* 47, 6243-6247.
- (11) Edwards, D. C., Ross, W. C. J., Cumber, A. J., McIntosh, D., Smith, A., Thorpe, P. E., Brown, A., Williams, R. H., and Davies, A. J. S. (1982) A Comparison of the in Vitro and in Vivo Activities of Conjugates of Anti-Mouse Lymphocyte Globulin and Abrin. *Biochim. Biophys. Acta* 717, 272-277.
- (12) Gilliland, D. G., Steplewski, Z., Collier, R. J., Mitchell, K. F., Chang, T. H., and Koprowski, H. (1980) Antibody-Directed Cytotoxic Agents: Use of Monoclonal Antibody To Direct the Action of Toxin A Chains to Colorectal Carcinoma Cells. *Proc. Natl. Acad. Sci. U.S.A.* 77, 4539-4543.
- (13) Trowbridge, I. S., and Domingo, D. L. (1981) Anti-Transferrin Receptor Monoclonal Antibody and Toxin-Antibody Conjugates Affect Growth of Human Tumour Cells. *Nature* 294, 171-173.
- (14) Bjorn, M. J., Ring, D., and Frankel, A. (1985) Evaluation of Monoclonal Antibodies for the Development of Breast Cancer Immunotoxins. *Cancer Res.* 45, 1214-1221.
- (15) Hwang, K. M., Foon, K. A., Cheung, P. H., Pearson, J. W., and Oldhan, R. K. (1984) Selective Antitumor Effect on L10 Hepatocarcinoma Cells of a Potent Immunoconjugate Composed of the A Chain of Abrin and a Monoclonal Antibody to a Hepatoma-Associated Antigen. *Cancer Res.* 44, 4578-4586.
- (16) Thorpe, P. E., Blakey, D. C., Brown, A. N. F., Knowles, P. P., Knyba, R. E., Wallace, P. M., Watson, G. J., and Wawrzynczak, E. J. (1987) Comparison of Two Anti-Thy 1.1-Abrin A-Chain Immunotoxins Prepared with Different Cross-Linking Agents: Antitumor Effects, in Vivo Fate, and Tumor Cell Mutants. *J. Natl. Cancer Inst.* 79, 1101-1112.
- (17) Scott, C. F., Jr., Lambert, J. M., Goldmacher, V. S., Blattler, W. A., Sobel, R., Schlossman, S. F., and Benacerraf, B. (1987) The Pharmacokinetics and Toxicity of Murine Monoclonal Antibodies and of Gelonin Conjugates of These Antibodies. *J. Immunopharm.* 9, 211-225.
- (18) Letvin, N. L., Goldmacher, V. S., Ritz, J., Yetz, J. M., Schlossman, S. F., and Lambert, J. M. (1986) In Vivo Administration of Lymphocyte-Specific Monoclonal Antibodies in Nonhuman Primates: In Vivo Stability of Disulfide-Linked Immunotoxin Conjugates. *J. Clin. Invest.* 77, 977-984.
- (19) Morgan, A. C., Jr., Bordonaro, J., Pearson, J. W., and Sivam, G. (1987) Immunotoxins to a Human Melanoma-Associated Antigen: Resistance to Pokeweed Antiviral Protein Conjugates in Vitro. *J. Natl. Cancer Inst.* 78, 1101-1106.
- (20) Ramakrishnan, S., and Houston, L. L. (1984) Comparison of the Selective Cytotoxic Effects of Immunotoxins Containing Ricin A Chain or Pokeweed Antiviral Protein and Anti-Thy 1.1 Monoclonal Antibodies. *Cancer Res.* 44, 201-208.
- (21) Thorpe, P. E., Brown, A. N. F., Bremner, J. A. G., Jr., Foxwell, B. M. J., and Stirpe, F. (1985) An Immunotoxin Composed of Monoclonal Anti-Thy 1.1 Antibody and a Ribosome-Inactivating Protein from *Saponaria officinalis*: Potent Antitumor Effects in Vitro and in Vivo. *J. Natl. Cancer Inst.* 75, 151-159.
- (22) Masuho, Y., Kishida, K., Saito, M., Umemoto, N., and Hara, T. (1982) Importance of the Antigen-Binding Valency and the Nature of the Cross-Linking Bond in Ricin A-Chain Conjugates with Antibody. *J. Biochem.* 91, 1583-1591.
- (23) Greenfield, L., and Dovey, H. Effects of Tagging Methods and Coupling Chemistry on the Pharmacology of Recombinant Ricin A Chain Immunotoxins, manuscript submitted.
- (24) Blakey, D. C., Watson, G. J., Knowles, P. P., and Thorpe, P. E. (1987) Effect of Chemical Deglycosylation of Ricin A Chain on the in Vivo Fate and Cytotoxic Activity of an Immunotoxin Composed of Ricin A Chain and Anti-Thy 1.1 Antibody. *Cancer Res.* 47, 947-952.
- (25) Wawrzynczak, E. J., and Thorpe, P. E. (1988) Effect of Chemical Linkage Upon the Stability and Cytotoxic Activity of A Chain Immunotoxins. *Immunotoxins* (A.E. Frankel, Ed.) pp 239-251, Kluwer Academic Publishers, Boston.
- (26) Worrell, N. R., Cumber, A. J., Parnell, G. D., Ross, W. C. J., and Forrester, J. A. (1986) Fate of an Antibody-Ricin A Chain Conjugate Administered to Normal Rats. *Biochem. Pharmacol.* 35, 417-423.
- (27) Fulton, R. J., Tucker, T. F., Vitetta, E. S., and Uhr, J. W. (1988) Pharmacokinetics of Tumor-Reactive Immunotoxins in Tumor-Bearing Mice: Effect of Antibody Valency and Deglycosylation of the Ricin A Chain on Clearance and Tumor Localization. *Cancer Res.* 48, 2618-2625.

- (28) Casellas, P., Bourrié, B., Canat, X., Blythman, H. E., and Jansen, F. (1987) Pharmacology of Antibody-Ricin-A-Chain Immunotoxins. *Membrane-Mediated Cytotoxicity: UCLA Symposia on Molecular and Cellular Biology, New Series*, 45 (B. Bonavida and R. J. Collier, Eds.) pp 185-193, Alan R. Liss, Inc., New York.
- (29) Bourrie, B. J. P., Casellas, P., Blythman, H. E., and Jansen, F. K. (1986) Study of the Plasma Clearance of Antibody-Ricin-A-Chain Immunotoxins: Evidence for Specific Recognition Sites on the A Chain that Mediate Rapid Clearance of the Immunotoxin. *Eur. J. Biochem.* 155, 1-10.
- (30) Blakey, D. C., Skilleter, D. N., Price, R. J., Watson, G. J., Hart, L. I., Newell, D. R., and Thorpe, P. E. (1988) Comparison of the Pharmacokinetics and Hepatotoxic Effects of Saporin and Ricin A-Chain Immunotoxins on Murine Liver Parenchymal Cells. *Cancer Res.* 48, 7072-7078.
- (31) Thorpe, P. E., Wallace, P. M., Knowles, P. P., Relf, M. G., Brown, A. N. F., Watson, G. J., Knyba, R. E., Wawrzynczak, E. J., and Blakey, D. C. (1987) New Coupling Agents for the Synthesis of Immunotoxins Containing a Hindered Disulfide Bond with Improved Stability in Vivo. *Cancer Res.* 47, 5924-5931.
- (32) Worrell, N. R., Cumber, A. J., Parnell, G. D., Mirza, A., Forrester, J. A., and Ross, W. C. J. (1986) Effect of Linkage Variation on Pharmacokinetics of Ricin A Chain-Antibody Conjugates in Normal Rats. *Anti-Cancer Drug Des.* 1, 179-188.
- (33) Jocelyn, P. C. (1972) *Biochemistry of the SH Group: The Occurrence, Chemical Properties, Metabolism and Biological Function of Thiols and Disulphides*, p 120, Academic Press, London.
- (34) Thorpe, P. E., Wallace, P. M., Knowles, P. P., Relf, M. G., Brown, A. N. F., Watson, G. J., Blakey, D. C., and Newell, D. R. (1988) Improved Antitumor Effects of Immunotoxins Prepared with Deglycosylated Ricin A-Chain and Hindered Disulfide Linkages. *Cancer Res.* 48, 6396-6403.
- (35) Aldwin, L., and Nitecki, D. E. (1987) A Water-Soluble, Monitorable Peptide and Protein Crosslinking Agent. *Anal. Biochem.* 164, 494-501.
- (36) Frankel, A. E., Ring, D. B., Tringale, F., and Hsieh-Ma, S. T. (1985) Tissue Distribution of Breast Cancer-Associated Antigens Defined by Monoclonal Antibodies. *J. Biol. Response Modif.* 4, 273-386.
- (37) Ring, D. B., Kassel, J. A., Hsieh-Ma, S. T., Bjorn, M. J., Tringale, F., Eaton, A. M., Reid, S. A., Frankel, A. E., and Nadji, M. (1989) Distribution and Physical Properties of BCA200, a M_r 200,000 Glycoprotein Selectively Associated with Human Breast Cancer. *Cancer Res.* 49, 3070-3080.
- (38) Ring, D. B., Kassel, J. A., Hsieh-Ma, S. T., Nadji, M., and Bjorn, M. J. Physical Properties and Distribution of the Carcinoma-Associated Antigen Recognized by Monoclonal Antibody 113F1, manuscript submitted.
- (39) Bogden, A. E., Houchens, D. P., Ovejera, A. A., and Cobb, W. R. (1982) Advances in Chemotherapy Studies with the Nude Mouse. *The Nude Mouse in Experimental and Clinical Research* (J. Fogh, and B. C. Giovanella, Eds.) Vol. 2, pp 367-400, Academic Press, New York.
- (40) Ovejera, A. A., Houchens, D. P., and Barker, A. D. (1978) Chemotherapy of Human Tumor Xenografts in Genetically Athymic Mice. *Ann. Clin. Lab. Sci.* 8, 50-56.
- (41) Adalsteinsson, O., Lamotte, A., Baddour, R. F., Colton, C. K., Pollak, A., and Whitesides, G. M. (1979) Preparation and Magnetic Filtration of Polyacrylamide Gels Containing Covalently Immobilized Proteins and a Ferrofluid. *J. Mol. Catal.* 6, 199-225.
- (42) Pollak, A., Blumenfeld, H., Wax, M., Baughn, R. L., and Whitesides, G. M. (1980) Enzyme Immobilization by Condensation Copolymerization into Cross-Linked Polyacrylamide Gels. *J. Am. Chem. Soc.* 102, 6324-6336.
- (43) Riddles, P. W., Blakeley, R. L., and Zerner, B. (1979) Ellman's Reagent: 5,5'-Dithiobis(2-nitrobenzoic acid)—A Reexamination. *Anal. Biochem.* 94, 75-81.
- (44) Grassetti, D. R., and Murray, J. F. Jr., (1967) Determination of Sulfhydryl Groups with 2,2'- or 4,4'-Dithiodipyridine. *Arch. Biochem. Biophys.* 119, 41-49.
- (45) Piatak, M., Lane, J. A., Laird, W., Bjorn, M. J., Wang, A., and Williams, M. (1988) Expression of Soluble and Fully Functional Ricin A Chain in *Escherichia coli* Is Temperature-Sensitive. *J. Biol. Chem.* 263, 4837-4843.
- (46) Ferris, R. (1987) Method of Recovering Microbially Produced Recombinant Ricin Toxin A Chain. United States Patent Number 4,689,401.
- (47) Ferris, R. and Laird, W. J. (1988) Method of Purifying Toxin Conjugates Using Hydrophobic Interaction Chromatography. United States Patent Number 4,771,128.
- (48) Mosmann, T. (1983) Rapid Colorimetric Assay for Cellular Growth and Survival: Application to Proliferation and Cytotoxicity Assays. *J. Immunol. Methods* 65, 55-63.
- (49) Schulz, H., and Vigneaud, V. du. (1966) Synthesis of 1-L-Penicillamine-Oxytocin, 1-D-Penicillamine-Oxytocin, and 1-Deaminopenicillamine-Oxytocin, Potent Inhibitors of the Oxytocic Response of Oxytocin. *J. Med. Chem.* 9, 647-650.
- (50) Rabenstein, D. R., and Theriault, Y. (1984) A Nuclear Magnetic Resonance Study of the Kinetics and Equilibria for the Oxidation of Penicillamine and N-acetylpenicillamine by Glutathione Disulfide. *Can. J. Chem.* 62, 1672-1680.
- (51) Lomant, A. J., and Fairbanks, G. (1976) Chemical Probes of Extended Biological Structures: Synthesis and Properties of the Cleavable Protein Cross-Linking Reagent [³⁵S]Dithiobis(succinimidyl propionate). *J. Mol. Biol.* 104, 243-261.
- (52) Jencks, W. P., and Carriuolo, J. (1959) Imidazole Catalysis: II. Acyl Transfer and the Reactions of Acetyl Imidazole with Water and Oxygen Anions. *J. Biol. Chem.* 234, 1272-1279.
- (53) Anjaneyulu, P. S. R., and Staros, J. V. (1987) Reactions of N-hydroxysulfosuccinimide Active Esters. *Int. J. Pept. Protein Res.* 30, 117-124.
- (54) Klapper, M. H. (1977) The Independent Distribution of Amino Acid Near Neighbor Pairs into Polypeptides. *Biochem. Biophys. Res. Commun.* 78, 1018-1024.
- (55) Chothia, C. (1976) The Nature of the Accessible and Buried Surfaces in Proteins. *J. Mol. Biol.* 105, 1-14.
- (56) Byers, V. S., Rodvien, R., Grant, K., Durrant, L. G., Hudson, K. H., Baldwin, R. W., and Scannon, P. J. (1989) Phase I Study of Monoclonal Antibody-Ricin A Chain Immunotoxin XomaZyme-791 in Patients with Metastatic Colon Cancer. *Cancer Res.* 49, 6153-6160.
- (57) Spitler, L. E., del Rio, M., Khentigan, A., Wedel, N. I., Brophy, N. A., Miller, L. L., Harkonen, W. S., Rosendorf, L. L., Lee, H. M., Mischak, R. P., Kawahata, R. T., Stoudemire, J. B., Fradkin, L. B., Bautista, E. E., and Scannon, P. J. (1987) Therapy of Patients with Malignant Melanoma Using a Monoclonal Antimelanoma Antibody-Ricin A Chain Immunotoxin. *Cancer Res.* 47, 1717-1723.
- (58) Hertler, A. A., Schlossman, D. M., Borowitz, M. J., Laurent, G., Jansen, F. K., Schmidt, C., and Frankel, A. E. (1988) A Phase I Study of T101-Ricin A Chain Immunotoxin in Refractory Chronic Lymphocytic Leukemia. *J. Biol. Response Modif.* 7, 97-113.
- (59) Gould, B. J., Borowitz, M. J., Groves, E. S., Carter, P. W., Anthony, D., Weiner, L. M., and Frankel, A. E. (1989) Phase I Study of an Anti-Breast Cancer Immunotoxin by Continuous Infusion: Report of a Targeted Toxic Effect Not Predicted by Animal Studies. *J. Natl. Cancer Inst.* 81, 775-781.

Hinge-Thiol Coupling of Monoclonal Antibody to Silanized Iron Oxide Particles and Evaluation of Magnetic Cell Depletion^{1,2}

P. Hermentin,* R. Doenges, U. Franssen, C. Bieva,† France J. Vander Brugghen,† P. Stryckmans,† H.-J. Friesen, Bettina Optaczy, Sabine Schneider, W. Ax, K. H. Enssle, R. Kurrle, and F. R. Seiler

Research Laboratories of Behringwerke AG, D-3550 Marburg/Lahn, Germany, and Institut Jules Bordet, Centre des Tumeurs de l'Université Libre de Bruxelles, Brussels, Belgium. Received October 22, 1990

Iron oxide particles of average size 0.5–1.5 μm , covered by a silane coat carrying amino groups (BioMag, Advanced Magnetics, Boston), were derivatized by reaction with *N*-[(γ -maleimidobutyl)oxy]succinimide (GMBS), *N*-hydroxysuccinimidyl iodoacetate (NHIA), 2-iminothiolane (2-It), or *N*-succinimidyl 3-(2-pyridyldithio)propionate (SPDP). The derivatized particles were suitable for the reaction with sulfhydryl groups and subsequently coated with monoclonal antibodies (MoAbs) of different classes and isotypes (IgM, IgG1, IgG2a, IgG2b, IgG3) as well as polyclonal rabbit anti-mouse IgG (RAM). The antibodies were reduced by dithiothreitol (DTT) and covalently conjugated to the BioMag derivatives via liberated sulfhydryls of the hinge region. The observed conjugation ratios, expressed as protein/iron ($\mu\text{g}/\text{mg}$), could be reproducibly varied for optimization. These ratios were dependent on the type and amount of antibody offered for coupling to the derivatized particles, decreasing as follows: polyclonal = IgM > IgG2b > IgG2a = IgG3 > IgG1. The conjugation ratios were also dependent on the type and amount of the spacer used to derivatize the BioMag particles, decreasing as follows: GMBS > NHIA > 2-It > SPDP. The magnetically responsive magnetite-antibody conjugates ("magnetobeads"), carrying MoAb BMA 081 (anti-CD8; IgG2a), MoAb BB10 (anti-CD10/CALLA; IgG2b), MoAb VIL-A1 (anti-CD10; IgM), and polyclonal RAM, coupled similarly via 3.6 μmol of GMBS spacer per mg of Fe, were further investigated with respect to a depletion effect on specific cell subsets. The rates of cell depletion were found to be strongly dependent on the individual characteristics of the antibody used. This might be due to conformational changes of the antibody after coupling to the particles and to the cell surface receptor that is recognized. Separate batches of GMBS- and NHIA-magnetobeads may prove to be useful in a purging technique for allogeneic and autologous bone marrow transplantation, where one of the objectives is the elimination of residual T- and leukemic cells, respectively, contaminating the graft.

INTRODUCTION

A number of methods are now available for removing T-cells or tumor cells from human bone marrow as a prerequisite prior to allogeneic or autologous marrow transplantation in various phases of malignant hemopathies (1). The most specific methods have largely benefited from the great specificities of MoAbs recognizing T- or tumor cells' surface receptors. Cytolysis may occur by a complement-mediated mechanism (2) or by the action of appropriate immunotoxins (3). More recently, a new procedure was issued, allowing specific coating of T- or

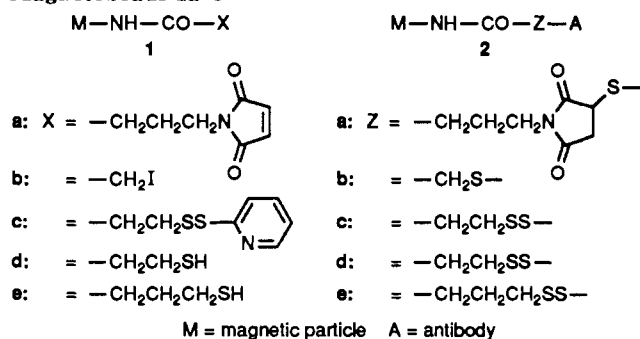
tumor cells by iron-containing polymer microspheres and removal of such cells by the use of a magnetic device (4–7).

For that purpose, styrene divinylbenzene copolymeric particles of 3 μm diameter have been developed (8) in which iron oxide was deposited by an in situ oxidation process (9). These particles have strong nonspecific binding capacity for protein and can be coated with antibodies by mere physical adsorption (10). However, the residual unspecific binding capacity must subsequently be blocked by incubation with e.g. fetal calf serum (10). The tendency to aggregate and bind specifically to cells seems to be correlated with the total surface area of the particles. These problems were largely overcome by filling the macroporous particles with polymer, while satisfactory binding capacity for antibody was retained (10). Such particles, coated with sheep or rabbit anti-mouse antibodies by mere physical adsorption, have been used in a two-step assay with respect to neuroblastoma (11), T-cell (12), and B-lymphoma cell depletion (7). However, desorption of physically adsorbed antibody or protein from the polystyrene microspheres was recognized as a major disadvantage, and covalent attachment of the antibody was requested in order to overcome leakage problems (11). This was achieved by covering the polystyrene particles by a polymer layer, carrying OH groups, concomitantly increasing the particle size from 3 to 4.5 μm (7). These hydroxyl groups can be activated by tosylation, thus enabling covalent attachment to proteins via accessible

* Centre des Tumeurs de l' Université Libre de Bruxelles.

¹ The abbreviations used are as follows: MoAb, monoclonal antibody; RAM, rabbit anti-mouse IgG; PBS, phosphate-buffered saline; PBL, peripheral blood lymphocytes; MNC, mononuclear cells; DTT, dithiothreitol; CD, cluster of differentiation; CALLA, common acute lymphoblastic leukemia antigen; GMBS, *N*-[(γ -maleimidobutyl)oxy]succinimide; NHIA, *N*-hydroxysuccinimidyl iodoacetate; SPDP, *N*-succinimidyl 3-(2-pyridyldithio)propionate; 2-It, 2-iminothiolane; DMF, dimethylformamide; CIMPA, cellular immunomagnetic purging assay.

² A preliminary report of the GMBS data has been presented at the 9th Presentation-Meeting of the German Society of Chemists (GdCh) (Immunoconjugates in Diagnosis and Therapy), Kaiserslautern, FRG, March 22–23, 1990 (abstracts of papers) and at the 6th Spring Meeting of the Society for Immunology, Marburg, FRG, March 22–24, 1990 (abstracts of papers, p 96).

Scheme I.^a Schematic Presentation of the Derivatized Magnetic Particles 1a-e and the Corresponding Magnetobeads 2a-e

^a a, GMBS-type; b, NHIA-type; c, SPDP-type; d, SPDP-type (after reduction of 1c and coupling); e, 2-It-type.

amino groups (7). However, it has turned out that covalent attachment of antibody to tosyl-activated beads is only feasible with polyclonal antibodies or monoclonal antibodies of the IgM class, whereas antibodies of the IgG class usually are inactivated and lose their immunoreactivity. Therefore, direct coating of MoAbs of the IgG class is not recommended for reasons of spatial orientation of the antigen binding site (13), and IgM class antibody or polyclonal sheep or rabbit anti-mouse IgG are coated preferably by physical adsorption rather than by chemical binding to tosyl-activated beads.

Ideally, the main strategy for clinical application consists in the use of a short direct assay to protect stem cells involving IgM but also IgG MoAbs currently available.

Recently, Bieva et al. (13) have shown that iron oxide particles of 0.5–1.5 μm , surrounded by a silane coat carrying amino groups (BioMag), allowed covalent attachment of monoclonal antibodies of various isotypes, using glutaraldehyde as cross-linking agent. These forms of conjugates were proved as suitable for distinct cell depletion, and this direct assay appeared superior to others already used in clinical trials and suitable for bone marrow depletions (Bieva et al., unpublished results). However, the ideal method of coupling would be one which allows the site-directed attachment of MoAb to the particles remote from the antibody combining site.

In this study we describe and compare four new methods for the site-directed (hinge-thiol) coupling of MoAbs to silanized magnetite of average size 0.5–1.5 μm , carrying amino groups as illustrated in Scheme I.

The first method involves the derivatization of the magnetite (M) by reaction with the heterobifunctional spacer GMBS, providing maleimido particles 1a. These can easily be reacted with free sulfhydryls of reduced MoAb, concomitant with the formation of "GMBS-magnetobeads" (2a), where the antibody is linked to the particles via stable thioether bonds.

In the second method the particles are reacted with the heterobifunctional spacer NHIA (or NHBra, unpublished results), leading to iodoacetyl particles 1b. These, upon reaction with MoAb hinge sulfhydryls, lead to "NHIA-magnetobeads" (2b), where the antibody is again coupled to the particles via stable thioether bonds, however via a shorter spacer.

In the third method, particles are derivatized by reaction with the heterobifunctional spacer SPDP. The pyridyldithio particles 1c obtained can again be reacted with MoAb hinge sulfhydryls, providing "SPDP-magnetobeads" (2c), where the antibody is coupled to the particles via disulfide bonds that are again susceptible to a reductive cleavage. Alternatively, analogous magnetobeads 2c can

also be gained by reductive conversion of the pyridyldithio particles 1c to sulfhydryl particles 1d. These can be reacted with nonreduced MoAb, resulting in the magnetobeads 2d, where the spacer is the same as in the "SPDP-magnetobeads" (2c)

In the fourth method, the particles are reacted with the heterobifunctional spacer 2-It, providing the sulfhydryl particles 1e. These can again be reacted with nonreduced MoAb, leading to the "2-It-magnetobeads" (2e), where the spacer is elongated by an additional CH_2 group, as compared to the "SPDP-magnetobeads" (2c), and can again be cleaved by reducing agents.

The four methods of coupling are compared with respect to their conjugation ratios, using MoAbs of various classes and isotypes, i.e., IgM, IgG1, IgG2a, IgG2b, and IgG3.

The GMBS- and NHIA-magnetobeads (2a and 2b), respectively, are compared with respect to their potential efficiency in bone marrow depletion before autologous or allogeneic transplantation.

EXPERIMENTAL PROCEDURES

Antibodies. The MoAbs BMA 0110 (anti-CD2; IgG2b), BMA 081 (anti-CD8; IgG2a), BMA 030 (anti-CD3; IgG2a), BMA 033 (anti-CD3; IgG3), BMA 0111 (anti-CD2; IgG1), and VIL-A1 (BMA 0150; anti-CD10; IgM) (Behringwerke AG) were provided lyophilized in a concentration of 1 mg/mL in a solution of 0.1 mol/L sodium citrate buffer, pH 6.6, and 50 g/L sucrose and redissolved in distilled water (0.5 mL). RAM (Behringwerke AG) was provided in PBS and adjusted to a concentration of 0.6 $\mu\text{g}/\text{mL}$.

MoAb BB10 (anti-CD10/CALLA; IgG2b) has broad specificity with ca. 100% of NALM-6, a human pre-B leukemia cell line as determined by indirect immunofluorescence. The MoAb was purified from ascites by affinity chromatography and used as IgG fraction.

BioMag Particles. BioMag particles (lot 2046-83) were purchased from Advanced Magnetics, Boston, MA. These particles were especially prepared for Behringwerke with respect to the need of clinical-grade material that may be used in bone marrow transplantations. This material is not identical with BioMag 4100, the regular trade product of Advanced Magnetics. The main difference consists in a higher silane content per iron and in a higher nitrogen (amino groups) content per iron.

Spacers and Chemicals. GMBS was a product of Calbiochem. SPDP and 2-It were products of Pierce, and DTT was purchased from Sigma. NHIA was synthesized according to Rector et al. (14). DMF was from Merck, Darmstadt, FRG.

General Method for the Introduction of the Spacers into BioMag Particles. A suspension of BioMag particles, corresponding to a total iron content of 5 mg, was washed three times in PBS, pH 7.2, and adjusted to a volume of 3 mL. To this suspension was added a freshly prepared solution of the heterobifunctional spacer reagent (0.9–14.5 μmol of spacer/mg of Fe) in dry DMF (2 mL), and the mixture was shaken at room temperature for 1 h. The particles were then removed by centrifugation at 3000g, washed three times with 10 mL of PBS, and resuspended in the appropriate volume of PBS, usually 5 mL.

General Procedure for Hinge-Thiol Coupling of Antibody to Derivatized Particles 1a-e. To 2 mg of antibody in 500 μL of salt solution were added 2 mg of DTT, and the mixture was incubated at room temperature for 30 min. The reduced antibody was isolated by gel filtration through a column ($d = 15 \text{ mm}$, $h = 90 \text{ mm}$) of Sephadex G25 in PBS pH 7.2 in a total elution volume

Table I. Conjugation Ratios Achieved in Various Coupling Experiments, Using Different Antibodies and Different Spacers at Different Concentrations

expt	antibody	isotype	specificity	mode of coupling	MoAb/Fe offered, mg/mg	spacer/Fe, $\mu\text{mol}/\text{mg}$	conj ratio protein/Fe, $\mu\text{g}/\text{mg}$
H1	RAM	IgG	aMIg	GMBS/SH	0.08	3.6	91
					0.16	3.6	162
					0.33	3.6	193
					0.66	3.6	204
					1.33	3.6	199
H2	BMA 0110	IgG2b	CD2	GMBS/SH	0.02	3.6	19
					0.04	3.6	38
					0.08	3.6	64
					0.16	3.6	132
H3	BMA 081	IgG2a	CD8	GMBS/SH	0.04	3.6	34
					0.08	3.6	56
					0.16	3.6	102
H4	VIL-A1	IgM	CD10	GMBS/SH	0.04	3.6	50
					0.08	3.6	76
					0.12	3.6	121
H6	RAM	IgG	aMIg	NHIA	0.07	7.1	74
					0.14	7.1	136
					0.21	7.1	171
H7	BMA 0110	IgG2b	CD2	NHIA	0.04	7.1	76
					0.12	7.1	156
					0.20	7.1	183
H8	BMA 081	IgG2a	CD8	NHIA	0.04	7.1	56
					0.12	7.1	107
					0.20	7.1	113
H9	RAM	IgG	aMIg	2-It/SS	0.10	14.5	110
					0.20	14.5	173
					0.30	14.5	229
H10a	BMA 0110	IgG2b	CD2	2-It/SS	0.10	14.5	107
					0.20	14.5	156
					0.30	14.5	178
H10b	BMA 0110	IgG2b	CD2	2-It/SS	0.10	3.6	65
					0.20	3.6	96
					0.30	3.6	112
H11	BMA 081	IgG2a	CD8	2-It/SS	0.10	14.5	73
					0.20	14.5	80
					0.30	14.5	91
H12	RAM	IgG	aMIg	SPDP/SH	0.06	3.2	25
					0.12	3.2	40
					0.18	3.2	55
H13	RAM	IgG	aMIg	SPDP/red.	0.10	3.2	27
					0.20	3.2	51
					0.30	3.2	74
H14	BMA 0110	IgG2b	CD2	SPDP/red.	0.10	3.2	27
					0.20	3.2	47
					0.30	3.2	57
H15	BMA 030	IgG2a	CD3	2-It/SS	0.20	14.5	71
					0.20	3.6	53
					0.20	0.9	26
H16	BMA 033	IgG3	CD3	2-It/SS	0.20	14.5	69
					0.20	3.6	56
					0.20	0.9	39
H17	BMA 0110	IgG2b	CD2	GMBS/SH	0.33	3.6	155
	BMA 081	IgG2a	CD8	GMBS/SH	0.33	3.6	139
	BMA 0111	IgG1	CD2	GMBS/SH	0.33	3.6	117

of ca. 4 mL and was immediately added to the derivatized particles at the desired ratio (see Table I). The mixture was incubated with gentle shaking at room temperature for 1 h. The particles were then removed by centrifugation at 3000g, washed three times with 10 mL of PBS, pH 7.2, each time, resuspended in the appropriate volume of PBS, pH 7.2, sterilized by X-ray at 12.000 rd, and finally stored at 4 °C.

Conjugation Ratios. The amount of protein coupled to the particles, expressed as nitrogen (μg)/iron (mg), was calculated from the nitrogen content determined by the Kjeldahl method (15) and was corrected by the nitrogen content per iron ($\mu\text{g}/\text{mg}$), determined for nonderivatized BioMag particles. The amount of iron was determined by atomic absorption (16, 17). The conjugation ratios were calculated by the formula

$$\frac{\mu\text{g of P-N}}{\text{mg of Fe}} = \frac{\mu\text{g of Tot-N}}{\text{mg of Fe}}(\text{sample}) - \frac{\mu\text{g of Tot-N}}{\text{mg of Fe}}(\text{control})$$

where the terms have the following meaning: P-N = protein nitrogen, Tot-N = total nitrogen.

The amount of protein bound to the particles, expressed as protein/iron ($\mu\text{g}/\text{mg}$), was calculated from the determined amount of protein nitrogen per iron ($\mu\text{g}/\text{mg}$) by multiplication by the factor 6.25 (18).

CD8+ Cell Depletion. Mononuclear cells (MNC) were isolated from fresh human blood on a Ficoll gradient as described by Bøyum (19). For the depletion assay, 3×10^7 MNC in 2 mL of PBS containing 1% BSA (w/v, Seromed) in plastic tubes (Falcon, No. 2051) were mixed with 1 mL of a suspension of 2 mg/mL BMA 081-magnetobeads 2a or 2b in PBS and incubated on a shaker at room temperature for 15 min. The magnetobeads and the cells

bound thereby were then separated from the mixture with a permanent magnet (Dynal, Norway). The cells remaining in the suspension were pelleted at 400g and resuspended in PBS. The depletion efficiency was evaluated by an indirect immunofluorescence assay.

For this purpose, 1×10^6 cells were, before and after treatment, labeled with 1 $\mu\text{g}/\text{mL}$ of BMA 081 as first antibody and then, after washings, with 20 $\mu\text{g}/\text{mL}$ of second antibody (RAM, F(ab)₂ fragment, FITC-labeled, Behringwerke). The amount of stained cells was estimated with a cytofluorograph (Ortho, Terrytown, NJ).

Depletion experiments with RAM-(GMBS)-magnetobeads were similarly performed after preincubation with BMA 081.

CD10+ Cell Depletion. Depletion of NALM-6 cells from PBL was performed, using the cellular immunomagnetic purging assay (CIMPA), recently described by Bieva et al. (13). Briefly, 5 mL of normal human cell suspensions containing 1×10^6 cells/mL were mixed with 10% of the vital dye Hoechst (H33342) stained NALM-6 (CD10+) cells. The cell line-blood mixture was incubated with BB10 (anti-CD10/CALLA; IgG2b)-(GMBS)-magnetobeads at concentrations ranging from 0.5 to 10 mg of Fe/mL. After a 30-min incubation at 4 °C with gentle stirring, separation was carried out by a magnetic device as described (13). The amount of CD10+ cells was analyzed before and after treatment by counting H33342-stained cells using a Leitz fluorescence microscope equipped with 200-W mercury lamp and UV excitation (350 nm)/blue fluorescence (460 nm) emission "D" cube.

RESULTS

Hinge-Thiol Coupling of Antibody to Derivatized Particles, Changing the Type and Amount of Antibody and Spacer. The various coupling experiments (Scheme I) are summarized in Table I. The amounts of heterobifunctional spacer reagents used for derivatization of BioMag particles are expressed as micromole of spacer per milligram of Fe. The amounts of antibody offered for the coupling to the derivatized particles are expressed as milligram/milligram (antibody/Fe). The conjugation ratios achieved in each coupling experiment are expressed as microgram/milligram (protein/Fe).

The results of antibody coupling to maleimido (GMBS) particles **1a** at 3.6 μmol of spacer/mg of Fe are summarized in experiments (expt) H1-H4 and H17 (Table I).

In all four experimental (exptl) series the conjugation ratios increased when increasing the amounts of reduced antibody offered for coupling, i.e. RAM (polyclonal IgG), VIL-A1 (IgM), BMA 0110 (IgG2b), and BMA 081 (IgG2a). A linear relation was observed when offering less than 0.17 mg of antibody/mg of Fe. At these antibody concentrations, virtually all offered RAM was coupled to the particles (Figure 1). When RAM was offered in amounts greater than 0.17 mg of RAM/mg of Fe, a borderline of 200 $\mu\text{g}/\text{mg}$ (protein/Fe) was reached as maximal load (Figure 1).

MoAb VIL-A1 (IgM) was coupled at almost identical ratios as RAM. Thus, when offering 0.12 mg of VIL-A1/mg of Fe, a conjugation ratio of 121 $\mu\text{g}/\text{mg}$ (protein/Fe) was achieved (expt H4).

The conjugation ratios observed for MoAb BMA 0110 (IgG2b) proved slightly smaller than those for RAM and VIL-A1 (IgM). Thus, when offering 0.16 and 0.33 mg of BMA 0110/mg of Fe, conjugation ratios of 132 (expt H2) and 155 $\mu\text{g}/\text{mg}$ (protein/Fe) (expt H17) were achieved, respectively, suggesting a borderline of 170 $\mu\text{g}/\text{mg}$ (protein/Fe) as maximal load for the IgG2b isotype (Figure 1).

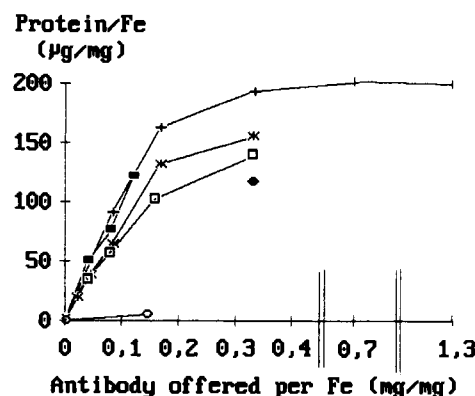


Figure 1. Coupling to maleimido (GMBS) particles **1a** at 3.6 μmol of spacer/mg of Fe (expt H1-H4 and H17, Table I): + = RAM, ■ = VIL-A1 (IgM), * = BMA 0110 (IgG2b), □ = BMA 081 (IgG2a), ● = BMA 0111 (IgG1), ○ = control (nonderivatized BioMag incubated with reduced MoAb BMA 0110).

The conjugation ratio achieved for BMA 081 (IgG2a) proved still smaller than that for the IgG2b isotype MoAb BMA 0110. When offering 0.16 and 0.33 mg of BMA 081/mg of Fe, conjugation ratios of 102 (expt H3) and 139 $\mu\text{g}/\text{mg}$ (protein/Fe) (expt H17) were achieved, respectively, suggesting a borderline of 150 $\mu\text{g}/\text{mg}$ (protein/Fe) as maximal load for the IgG2a isotype.

And even inferior was the conjugation of BMA 0111 (IgG1), where a conjugation ratio of 117 $\mu\text{g}/\text{mg}$ (protein/Fe) was achieved when offering 0.33 mg of BMA 0111/mg of Fe (expt H17).

The conjugation ratios were found to be clearly dependent on the antibody isotype, no matter which method of coupling was used, following the order RAM = IgM > IgG2b > IgG2a = IgG3 > IgG1 (Table I and Figure 1).

When reduced MoAb BMA 0110 was offered to nonderivatized BioMag particles as a control, the amount of antibody unspecifically adsorbed to the particles' surface was negligible (Figure 1).

In analogy to the GMBS coupling procedure, the conjugation ratios were increased when offering increasing amounts of reduced antibody for NHIA coupling (expt H6-H8, Table I) or of nonreduced antibody for 2-It coupling (expt H9, H10a, and H11, Table I). Also with the SPDP coupling an increase of the conjugation ratios was observed when increasing the amounts of antibody offered for coupling (expt H12-H14, Table I).

The conjugation ratios of RAM were comparable, no matter whether reacting reduced antibody with dithiopyridyl particles **1c** (SPDP/SH) or reacting nonreduced antibody with sulfhydryl particles **1d**, obtained from SPDP particles **1c** by reduction with DTT (SPDP/red.) (expt H12 and H13, Table I). Again, the conjugation ratios obtained for RAM were slightly higher than those observed for the IgG2b isotype (MoAb BMA 0110) (expt H13 and H14, Table I).

Although the amounts of spacer actually coupled to the beads per mg of Fe is not known and may vary from linker to linker, the conjugation ratios were shown to increase with increasing amounts of spacer coupled to the particles. Thus, when MoAb BMA 030 (IgG2a) was offered for coupling at constant ratios of 0.2 mg of MoAb/mg of Fe, the conjugation ratios were 71, 53, and 26 $\mu\text{g}/\text{mg}$ (protein/Fe), concomitant with the decrease of the amount of the 2-It spacer used for derivatization, i.e. 14.5, 3.6, and 0.9 μmol of 2-It/mg of Fe, respectively. And almost identical conjugation ratios were achieved for an IgG3 isotype MoAb BMA 033, i.e. 69, 56, and 39 $\mu\text{g}/\text{mg}$ (protein/Fe),

Table II. Comparison of Depletion of Peripheral Blood Lymphocytes with BMA 081 (anti-CD8; IgG2a)-Magnetobeads with GMBS and NHIA Spacer, Respectively, with Different Lots of Magnetobeads at Different Days

	antibody coupled to the beads	spacer	conjugation ratio, $\mu\text{g}/\text{mg}$	% CD8+ cells in the supernatant		remarks
				only second antibody	BMA 081 and second antibody	
experimental series A	BMA 081	-	-	0	14	22% CD8+ cells prior to depletion
		NHIA	56	<1	7	
		NHIA	107	<1	3	
		NHIA	113	<1	1	
		GMBS	139	<3	1	
experimental series B	BMA 081	NHIA	96	<1	<1	21% CD8+ cells prior to depletion
		GMBS	121	<1	<1	
experimental series C	RAM					17% CD8+ cells prior to depletion
		GMBS	140	<1	1	beads preincubated with BMA 081
		GMBS	122	0	<1	
		GMBS	140	<1	1	cells preincubated with BMA 081
		GMBS	122	<1	<1	

respectively, indicating that the conjugation ratios achieved for IgG2a and IgG3 isotypes appear comparable (expt H15 and H16, Table I).

A similar decrease of the conjugation ratio was observed for a series of experiments using variable amounts of MoAb BMA 0110 (IgG2b) and 14.5 and 3.6 μmol of 2-It spacer per mg of Fe, respectively (expt H10a and H10b, Table I).

When comparing the experimental series performed with BMA 0110 (IgG2b) as reference antibody and comparable concentrations of spacer, i.e. 3.2–3.6 μmol of spacer offered/mg of Fe (expt H2, H10b, and H14, Table I), the conjugation ratios decreased for different spacers in the order GMBS > 2-It > SPDP. On average, the conjugation ratios achieved with the 2-It coupling procedure were about 2-fold higher than those achieved with the SPDP method.

From the experimental data with polyclonal RAM as reference antibody, only experiments H1, H12, and H13 (Table I) were performed at comparable equivalents of spacer offered per milligram of Fe. The GMBS coupling procedure provided much higher conjugation ratios than the SPDP method in either variant.

The NHIA coupling procedure, using 7.1 μmol of NHIA/mg of Fe (expt H6, Table I), provided conjugation ratios almost identical with those of the GMBS method, using 3.6 μmol of GMBS/mg of Fe (exp. H1), as well as with those of the 2-It coupling procedure, using 14.5 μmol of 2-It/mg of Fe (expt H9).

However, when comparing the BMA 0110 experiments H2 and H10b (Table I), it is suggested that the GMBS coupling procedure may provide higher conjugation ratios than the 2-It method. Thus, a conjugation ratio of 132 $\mu\text{g}/\text{mg}$ (protein/Fe) was achieved with the GMBS method, offering 0.16 mg of reduced antibody/mg of Fe (expt H2), while 96 $\mu\text{g}/\text{mg}$ (protein/Fe) were measured for the 2-It method when offering 0.20 mg of nonreduced MoAb/mg of Fe (expt H10b). The same holds true for the IgG2a isotype MoAb BMA 081, comparing experiments H3 and H11 (Table I). A total of 102 $\mu\text{g}/\text{mg}$ (protein/Fe) were coupled via GMBS, offering 0.16 mg of reduced MoAb/mg of Fe at 3.6 μmol of spacer/mg of Fe (expt H3), while 80 $\mu\text{g}/\text{mg}$ (protein/Fe) were coupled via the 2-It method, offering 0.20 mg of nonreduced MoAb/per mg of Fe at 14.5 μmol of spacer/mg of Fe (expt H11).

Thus, it may be concluded that the conjugation ratios relate in the order GMBS > NHIA > 2-It > SPDP.

Depletion of CD8+ Cells. As can be seen from Table II (exptl series A), an increasing amount of MoAb BMA 081 coupled to the particles via the NHIA spacer resulted in an increased efficiency of the depletion of CD8+ cells from PBL. While BioMag alone provided an unspecific

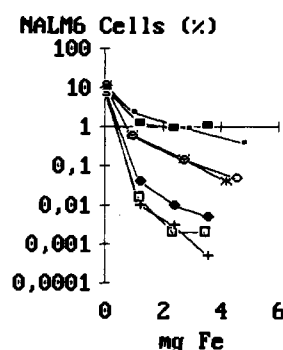


Figure 2. Comparison of NALM-6 Cell depletion using BB10 (anti-CD10; IgG2b)-(GMBS)-magnetobeads versus VIL-A1 (anti-CD10; IgM)-(GMBS)-magnetobeads. The conjugation ratios (protein/Fe) were as follows. BB10 (anti-CD10; IgG2b)-(GMBS)-magnetobeads: ● = 62 $\mu\text{g}/\text{mg}$, + = 90 $\mu\text{g}/\text{mg}$, □ = 133 $\mu\text{g}/\text{mg}$. VIL-A1 (anti-CD10; IgM)-(GMBS)-magnetobeads: ■ = 50 $\mu\text{g}/\text{mg}$, × = 76 $\mu\text{g}/\text{mg}$, ○ = 121 $\mu\text{g}/\text{mg}$. Control: ■ = non-derivatized BioMag.

decrease of CD8+ cells from 22 to 14%, less than 1% of residual CD8+ cells were detected in the supernatant after incubation with BMA 081 (anti-CD8; IgG2a)-(NHIA)-magnetobeads at a conjugation ratio of 113 $\mu\text{g}/\text{mg}$ (protein/Fe). Depleted cell populations or negative controls were <3%. The corresponding GMBS-type magnetobeads proved similarly effective, reducing the CD8+ cell subset down to <1% at a conjugation ratio of 139 $\mu\text{g}/\text{mg}$ (protein/Fe) (Table II, exptl series A). The absolute depletion efficiencies could not be determined by the flow cytometric assay as these values were below the background of immunofluorescence. The repetition of these experiments with different batches of magnetobeads at different days gave similar effects of depletion (Table II, exptl series B). These results were comparable to those obtained with RAM-(GMBS)-magnetobeads, preincubated with MoAb BMA 081 alone prior to CD8+ cell depletion (Table II, exptl series C). The same depletion efficiency was achieved if the PBL were preincubated with MoAb BMA 081 alone prior to depletion with RAM-(GMBS)-magnetobeads (Table II, exptl series C).

Depletion of CD10+ (NALM-6) Cells. Figure 2 illustrates the results of the cellular immunomagnetic purging assay (CIMPA) (13), using increasing amounts of BB10 (anti-CD10; IgG2b)-(GMBS)-magnetobeads for the depletion of NALM-6 cells, added to PBLs. The depletion efficiency increased with increasing amounts of magnetobeads added to the cells, reaching a borderline of about 4 log units of depletion, the maximal depletion that could be achieved in a single cycle. The depletion efficiency could be slightly improved when increasing the conjugation ratio

from 62 to 90 $\mu\text{g}/\text{mg}$ (protein/Fe) (Figure 2). However, a further increase of the conjugation ratio up to 133 $\mu\text{g}/\text{mg}$ (protein/Fe) did not further improve the results of depletion. Nonderivatized BioMag particles, used as a control, provided 1 log unit of depletion that was not increased with increasing amounts of particles added (Figure 2).

VIL-A1 (anti-CD10; IgM)-(GMBS)-magnetobeads were found less effective for NALM-6 cell depletion than the corresponding BB10 (anti-CD10; IgG2b)-(GMBS)-magnetobeads at conjugation ratios of 121 and 90 $\mu\text{g}/\text{mg}$ (protein/Fe), respectively (Figure 2).

DISCUSSION

Attempts to achieve T-cell depletion of human bone marrow have in the last few years been focused on the antibody-mediated coating of T-cells with iron-containing polymeric particles and the removal of such magnetic cells by the use of a magnetic device. As MoAb coupling to the particles via amino groups may potentially result in a certain loss of antibody reactivity, a site-directed attachment of MoAb to particles, remote from the antibody combining site, was requested.

In principle, two strategies appear feasible for the site-directed attachment of MoAbs to appropriate carrier systems. First, the carbohydrate chains of the CH_2 domain of the Fc portion, which are not involved in the antigen-binding properties of immunoglobulins, could be used for such purpose. Vicinal diols of these carbohydrate moieties are readily oxidized with periodate to form aldehyde groups which then are susceptible to further reactions (20). The created aldehyde groups could be reacted, for example, with hydrazide groups, followed by reduction of the Schiff base formed (21).

Another feasible approach involves partial reduction of the immunoglobulin with mercaptoethanol or dithiothreitol (22, 23), a reaction which cleaves the disulfide bonds between the heavy chains in the vicinity of the hinge between the Fab and Fc units. We have attempted to exploit this reaction for the site-directed (hinge-thiol) attachment of biotin (24), anthracyclines (25, 26), enzymes, and antibodies (Hermentin et al., unpublished data) without any detectable loss of antibody specificity and immunoreactivity.

This hinge-thiol coupling procedure, when used for the site-directed attachment of MoAb to silanized magnetite, proved very useful, simple, and straightforward. Antibodies of the IgM and IgG class and of isotypes IgG1, IgG2a, IgG2b, and IgG3 have been successfully coupled to BioMag particles that were derivatized by reaction with GMBS, NHIA, SPDP, and 2-It (Scheme I).

The new method of coupling was extensively evaluated with the maleimido (GMBS) particles 1a and RAM, MoAb BMA 0110 (anti-CD2; IgG2b), MoAb BMA 081 (anti-CD8; IgG2a), MoAb BMA 0111 (anti-CD2; IgG1), MoAb BB10 (anti-CD10/CALLA; IgG2b), and VIL-A1 (anti-CD10; IgM) as antibodies of choice.

As can be seen from Table I and Figure 1, increasing amounts of reduced antibody, offered for coupling, provided an almost linear increase of the conjugation ratios. For RAM, the maximal load ($\sim 200 \mu\text{g}$ of RAM/mg of iron) was achieved when offering about 0.3 mg of reduced RAM/mg of iron. This conjugation ratio could not be further enhanced, even when offering up to 1.4 mg of reduced RAM/mg iron, indicating that all maleimido groups were saturated.

While MoAb VIL-A1 (IgM) was coupled at almost identical ratios as RAM, the conjugation ratio of BMA 0110

(IgG2b) proved slightly smaller, approaching a borderline of 170 $\mu\text{g}/\text{mg}$ (protein/Fe). Even smaller was the conjugation ratio of BMA 081 (IgG2a), approaching a borderline of 150 $\mu\text{g}/\text{mg}$ (protein/Fe). And the least conjugation ratio was observed for BMA 0111 (IgG1). (When extrapolating the curves of Figure 1, a borderline in the range of 130 $\mu\text{g}/\text{mg}$ (protein/Fe) may be estimated for IgG1.)

Thus, the conjugation ratios were found to depend on the antibody class and isotype, following the order $\text{RAM} = \text{IgM} > \text{IgG2b} > \text{IgG2a} = \text{IgG3} > \text{IgG1}$ (Table I and Figure 1), which requires further confirmation.

This latter observation may reflect the flexibility of the hinge region of mouse monoclonal antibodies, which has been found to decrease in the order $\text{IgG2b} > \text{IgG2a} > \text{IgG1}$ (27). However, this most interesting hypothesis needs further evaluation.

A reduction by a factor of 5 in the amount of dithiothreitol used for antibody reduction did not significantly decrease the conjugation ratios (results not shown). The amount of DTT may, however, be of importance with respect to conformational changes which have been shown for human IgG subclasses (28). It may be expected that DTT concentrations and conditions that enable the reduction of only one instead of all hinge disulfide bonds (on an average) would certainly favor the preservation of the antibody combining site and thus improve the results of depletion. However, these conditions may have to be adjusted for a distinct antibody isotype or even for each individual antibody, depending on the number and the accessibility of the hinge disulfides and sulfhydryls, respectively.

The conjugation ratios were also found to depend on the type of spacer that was introduced to derivatize and activate the particles (Scheme I), decreasing in the order $\text{GMBS} > \text{NHIA} > 2\text{-It} > \text{SPDP}$ (Table I).

One could assume that an increasing length of the spacer arm attached to the particles would facilitate the access of the functional groups of the spacers to the hinge region and thus facilitate their reaction with the hinge sulfhydryls. This would explain the observed gradation in both the thioether ($\text{GMBS} > \text{NHIA}$) and the disulfide series ($2\text{-It} > \text{SPDP}$). However, further experiments are required in order to strengthen this kind of hypothesis.

The suitability of magnetoparticles for distinct cell depletions may depend on a variety of different parameters such as the concentration, the immunoreactivity and the isotype of the distinct antibody coupled to the particles, the concentration and the type of the spacer used, the particle support in terms of the size and the surface, and finally the cells, clusters, and epitopes to be recognized.

In a recent study Bieva et al. (13) have compared the depletion of NALM-6 cells from PBL, using two different types of magnetic support (Dynal beads versus BioMag particles) and the same anti-CD10 MoAb (BB10; IgG2b). In the first case, the anti-CD10 MoAb was coupled to tosyl-activated polystyrene beads of 3.5 μm diameter; in the second case, the anti-CD10 MoAb was coupled to BioMag particles via glutaraldehyde as cross-linking agent. Thus, the antibody was in both cases coupled via accessible amino groups. In this CIMPA study (13) the BioMag particles in combination with the glutaraldehyde cross-linkage proved clearly superior to the Dynal beads. Even when goat anti-mouse IgG was incorporated as a spacer arm between the MoAb and the Dynal beads, the depletion of NALM-6 cells was not satisfactory, presumably due to a low yield of coating or a particular conformation of the MoAb on the Dynal beads' surface (13).

In the present study, in which the same anti-CD10 MoAb (BB10; IgG2b) was coupled to derivatized BioMag particles **1a** via liberated sulfhydryls of the hinge region, a NALM-6 cell depletion of up to 4 log units was achieved at a conjugation ratio of 90 $\mu\text{g}/\text{mg}$ (protein/Fe) (Figure 2). The depletion efficiency was found to increase with increasing amounts of magnetoparticles added to identical aliquots of the cell suspension, which is in agreement with the results obtained by Bieva et al. (13). The NALM-6 cell removal was also dependent upon the conjugation ratio, again reflecting analogy to earlier results (13). However, in comparison to the glutaraldehyde cross-linkage (13), only about one-third of the amount of MoAb BB 10 was needed per mg of Fe in order to achieve comparable results of depletion in the CIMPA system. This is clearly in favor of the hinge-thiol coupling procedure, performed with the GMBS spacer. Interestingly, an increase of the conjugation ratio from 90 to 133 $\mu\text{g}/\text{mg}$ (protein/Fe) did not further increase the efficiency of depletion. Thus, a conjugation ratio of 60–90 $\mu\text{g}/\text{mg}$ (protein/Fe) appears optimal for NALM-6 cell removal with BB 10 (anti-CD10/CALLA; IgG2b)-(GMBS)-magnetobeads.

Our observation of a 1 log unit nonspecific depletion by nonderivatized BioMag in the CIMPA system (Figure 2) corresponds with a nonspecific depletion also slightly observed in the removal of CD8+ cells by a one-step depletion with a permanent magnet (Table 2, exptl series A). However, nonderivatized BioMag is not regarded as an appropriate control, and magnetoparticles carrying a MoAb of irrelevant specificity should be preferred (13).

When replacing MoAb BB10 (IgG2b) by MoAb VIL-A1 (IgM), the efficiency of NALM-6 cell depletion was significantly reduced (Figure 2). Thus, the antibody isotype, specificity, and immunoreactivity may contribute to the effects of depletion.

The results were similarly satisfying when using BMA 081 (anti-CD8; IgG2a)-magnetobeads for the depletion of CD8+ cells from PBL, no matter whether the GMBS- or the NHIA-type spacer was used (Table II). However, no depletion was achieved with BMA 081-magnetobeads in which 2-It or SPDP was incorporated as the spacer (results not shown). It is suggested that the spacer disulfide bonds present in the 2-It- and SPDP-type magnetoparticles **2e,c** may be cleaved by residual free hinge sulfhydryls and that these will have to be blocked by the addition of reagents such as *N*-ethylmaleimide or iodoacetamide.

A comparison between the BioMag particles of lot 2046-83, used in this study, and the commercially available BioMag 4100-amine has revealed that the methods of coupling described in this paper can similarly be applied to BioMag 4100-amine. Moreover, BioMag 4100-amine was found to be superior to the particles of lot 2046-83 with respect to unspecific adsorption of antibody to the beads' surface, unspecific cell depletion, and total cell recovery (Hermentin et al., unpublished results).

The results achieved in the present study may be summarized as follows: The hinge-thiol coupling procedure appears as a simple, reproducible, and useful method for the site-directed attachment of monoclonal antibody to derivatized BioMag particles **1a-e**. The GMBS and NHIA spacer reagents are suitable to provide high conjugation ratios and stable thioether bonds. The 2-It and SPDP spacer reagents lead to lower conjugation ratios and spacer disulfide bonds that can again be cleaved by neighboring sulfhydryls or reducing agent. The depletion efficiency achieved with GMBS- and NHIA-type magnetobeads appears to depend on the individual antibody that is coupled to the particles, i.e., its isotype, specificity, and

immunoreactivity. A distinct group of GMBS- and NHIA-magnetobeads (**2a** and **2b**) may prove useful in bone marrow depletion associated with allogeneic and autologous bone marrow transplantation as a therapeutic goal for malignant hemopathies.

LITERATURE CITED

- (1) Proceedings of the 1st International Workshop on Bone Marrow Purging. (1987) *Bone Marrow Transplant.* 2, Suppl. 2.
- (2) Bast, R. C., De Fabritiis, P., Lipton, J., Gelber, R., Maver, C., Nadler, L., Sallan, S., and Ritz, J. (1985) Elimination of malignant clonogenic cells from human bone marrow using multiple monoclonal antibodies and complement. *Cancer Res.* 45, 499–503.
- (3) Gorin, N. C., Douay, L., Laporte, J. P., et al. (1985) Autologous bone marrow transplantation with marrow decontaminated by immunotoxin T 101 in the treatment of leukemia and lymphoma: first clinical observations. *Cancer Treat. Rep.* 54, 953–959.
- (4) Kemshead, J. T., Heath, L., Gibson, F. M., Katz, F., Richmond, F., Treleaven, J., and Ugelstad, J. (1986) Magnetic microspheres and monoclonal antibodies for the depletion of neuroblastoma cells from bone marrow: Experiences, improvements and observations. *Br. J. Cancer* 54, 771–778.
- (5) Reynolds, C. P., Seeger, R. C., Dai Dang Vo, Black, A. T., Wells, J., and Ugelstad, J. (1986) Model system for removing neuroblastoma cells from bone marrow using monoclonal antibodies and magnetic immunobeads. *Cancer Res.* 46, 5882–5886.
- (6) Gee, A. P., Lee, C., Sleasman, J. W., Madden, M., Ugelstad, J., and Barrett, D. J. (1987) T lymphocyte depletion of human peripheral blood and bone marrow using monoclonal antibodies and magnetic microspheres. *Bone Marrow Transplant.* 2, 155–163.
- (7) Kvalheim, G., Fodstad, Ø., Pihl, A., Nustad, K., Pharo, A., Ugelstad, J., and Funderud, S. (1987) Elimination of B-lymphoma cells from human bone marrow: Model experiments using monodisperse magnetic particles coated with primary monoclonal antibodies. *Cancer Res.* 47, 846–851.
- (8) Ugelstad, J., Mørk, P. C., Kaggerud, K. H., Ellingsen, T., and Berge, A. (1980) Swelling of oligomer-polymer particles. New methods of preparation of emulsions and polymer dispersions. *Adv. Colloid Interface Sci.* 13, 101–140.
- (9) Ugelstad, J., Söderberg, L., Berge, A., and Bergström, J. (1983) Monodisperse polymer particles—A step forward for chromatography. *Nature* 303, 96–98.
- (10) Lea, T., Vartdal, F., Davies, C., and Ugelstad, J. (1985) Magnetic monosized polymer particles for fast and specific fractionation of human mononuclear cells. *Scand. J. Immunol.* 22, 207–216.
- (11) Treleaven, J. G., Gibson, F. M., Ugelstad, J., Rembaum, A., Philip, T., Caine, G. D., and Kemshead, J. T. (1984) Removal of neuroblastoma cells from bone marrow with monoclonal antibodies conjugated to magnetic microspheres. *Lancet* 1, 70–73.
- (12) Vartdal, F., Kvalheim, G., Lea, T. E., Bosnes, V., Gaudernack, G., Ugelstad, J., and Albrechtsen, D. (1987) Depletion of T-lymphocytes from human bone marrow. *Transplantation* 43, 366–371.
- (13) Bieva, C. J., Vander Bruggen, F. J., and Stryckmans, P. A. (1989) Malignant leukemic cell separation by iron colloid immunomagnetic adsorption. *Exp. Hematol.* 17, 914–920.
- (14) Rector, E. S., Schwenk, R. J., Tse, K. S., and Sehon, A. H. (1978) A method for the preparation of protein-protein conjugates of predetermined composition. *J. Immunol. Methods* 24, 321–336.
- (15) Ter Meulen, H. (1924) The determination of nitrogen in organic compounds by catalytic hydrogenation. *Recl. Trav. Chim.* 43, 643–644.
- (16) Sprague, S., and Slavin, W. (1965) Determination of iron, copper and zinc in blood serum by an atomic absorption method requiring only dilution. *At. Absorpt. Newsl.* 4, 228–233.

- (17) Rodgerson, D. O., and Helfer, R. E. (1966) Determination of iron in serum or plasma by atomic absorption spectrophotometry. *Clin. Chem.* 12, 338-349.
- (18) Molecular Biology of Human Proteins, Vol. 1, Chemical Methods (1966) p. 117; Schultze Heremans.
- (19) Boyum, A. (1976) Isolation of lymphocytes, granulocytes and macrophages. *Scand. J. Immunol.* 5 (Suppl. 5), 9-15.
- (20) O'Shannessy, D., and Quarles, R. H. (1987) Labeling of the oligosaccharide moieties of immunoglobulins. *J. Immunol. Methods* 99, 153-161.
- (21) Rodwell, J. D., Alvarez, V. L., Lee, C., Lopes, A. D., Goers, J. W. F., King, H. D., Powsner, H. J., and McKearn, T. J. (1986) Site-specific covalent modification of monoclonal antibodies: In vitro and in vivo evaluations. *Proc. Natl. Acad. Sci. U.S.A.* 83, 2632-2636.
- (22) Linford, J. H., Froese, G., Berczi, I., and Israels, L. G. (1974) An alkylating agent-globulin conjugate with both alkylating and antibody activity. *J. Natl. Cancer Inst.* 52, 1665-1667.
- (23) Youle, R. J., and Neville, D. M., Jr. (1980) Anti-Thy 1.2 monoclonal antibody linked to ricin is a potent cell-type-specific toxin. *Proc. Natl. Acad. Sci. U.S.A.* 77, 5483-5486.
- (24) Friesen, H.-J., Hermentin, P., and Gronski, P. (1986) Novel maleimido-biotins for the selective biotinylation of sulfhydryls. *Prot. Biol. Fluids* 34, 43-46.
- (25) Hermentin, P., Doenges, R., Gronski, P., Bosslet, K., Kraemer, H. P., Hoffmann, D., Zilg, H., Steinstraesser, A., Schwarz, A., Kuhlmann, L., Lueben, G., and Seiler, F. R. (1990) Attachment of rhodosaminylanthracyclinone-type anthracyclines to the hinge region of monoclonal antibodies. *Bioconjugate Chem.* 1, 100-107.
- (26) Hermentin, P., and Seiler, F. R. (1988) Investigations with monoclonal antibody drug (anthracycline) conjugates. *Behring Inst. Mitt.* 82, 197-215.
- (27) Oi, V. T., Vuong, T. M., Hardy, R., Reidler, J., Dangl, J., Herzenberg, L. A., and Stryer, L. (1984) Correlation between segmental flexibility and effector function of antibodies. *Nature (London)* 307, 136-140.
- (28) Michaelsen, T. E. (1988) Alteration of the conformation of human IgG subclasses by reduction of the hinge S-S bonds. *Mol. Immunol.* 25, 639-646.

Heterobifunctional Cross-Linking Agents Incorporating Perfluorinated Aryl Azides

Peter J. Crocker,[†] Nobuyuki Imai,[†] Krishnan Rajagopalan,[†] Michael A. Boggess,[†] Stefan Kwiatkowski,[†] Lori D. Dwyer,[‡] Thomas C. Vanaman,^{*,†} and David S. Watt^{*,†}

Department of Chemistry, and Department of Biochemistry, University of Kentucky, Lexington, Kentucky 40506.
Received October 31, 1990

New heterobifunctional cross-linking reagents were developed that possess a photoactive tetrafluorinated phenyl azide as the photoactive terminus and a chemically reactive succinimidyl ester as the electrophilic terminus. These reagents, succinimidyl *N*-(4-azido-2,3,5,6-tetrafluorobenzoyl)tyrosinate (**9**) and succinimidyl 2-(4-azido-2,3,5,6-tetrafluorophenyl)thiazole-4-carboxylate (**15**), were designed to possess either an ¹²⁵I or ³⁵S radiolabel, respectively. In a biochemical study, the latter reagent was coupled to Lys-75 of calmodulin (CaM), and the radioiodinated monoadduct was photochemically cross-linked, in a calcium-dependent manner, to the porcine erythrocyte plasma membrane Ca²⁺,Mg²⁺-ATPase. Densitometry scans of the gel indicated a reproducible 22% cross-linking of the CaM with one of the Ca²⁺,Mg²⁺-ATPase bands. Since the purification of the Ca²⁺,Mg²⁺-ATPase results in micelles having Ca²⁺,Mg²⁺-ATPase with its CaM binding site oriented both to the inside and outside of the micelle, the amount of Ca²⁺,Mg²⁺-ATPase available for cross-linking was reduced by approximately half, suggesting that the actual cross-linking efficiency was on the order of 40%.

INTRODUCTION

Interest in studying the interactions of the calcium-binding protein calmodulin (CaM) (*1*) with other proteins has led to the development of new heterobifunctional cross-linking reagents (*2, 3*). An effective reagent for studying intermolecular interactions of this type should possess three features: a photoactive terminus that cross-links with high efficiency to the target protein, an electrophilic terminus that establishes the initial covalent link to CaM,¹ and a radiolabel that will facilitate the identification of cross-linked peptides (*4*). In order to secure primary sequence data, the radiolabel must be readily introduced, possess a convenient half-life, and survive both the photochemical event and the subsequent purification process.

Several heterobifunctional reagents fulfill most of these requirements by incorporating both an aryl azide and an ¹²⁵I radiolabel. However, the putative cross-linking species produced in the photolysis of an aryl azide is not a singlet nitrene but rather an electrophilic dehydroazepine (*5-8*) that scavenges selectively for nucleophilic amino acid residues. The absence of such residues in the immediate vicinity of the photochemical event dramatically affects cross-linking efficiency. Moreover, the photolysis of aryl azides that possess an iodine substituent in the *same* ring as the azide leads to rapid photodeiodination (*9*), a competitive process that further reduces the observed cross-linking efficiency. For example, the cross-linking of radioiodinated CaM adducts of succinimidyl *N*-[2-(4-

azidosalicyl)ethyl]suberamate (*3*) with human erythrocyte plasma membrane Ca²⁺,Mg²⁺-ATPase proceeded with only 8% cross-linking efficiency.

In order to improve upon this limited efficiency, other photoactive reporter groups that might display an enhanced level of cross-linking were introduced in place of the simple aryl azides. Although the photoactive 3-aryl-3-(trifluoromethyl)diazirine (*10-12*) group generates a reactive carbene that might provide efficient cross-linking, an investigation of the photoproducts of 3-aryl-3-(trifluoromethyl)diazirines revealed that these products may not, in some cases, be stable toward conditions necessary for protein sequencing.² The photolysis of perfluorinated aryl azides (*13-18*) generates a singlet nitrene that inserts efficiently into a variety of bond types and promises to provide a solution to *both* the cross-linking efficiency and product stability problems. It was necessary, therefore, to investigate whether the perfluorinated azides could be incorporated in heterobifunctional reagents that would possess either a photostable ¹²⁵I or ³⁵S radiolabel (*19*) and to compare the cross-linking efficiency of these new reagents with their nonfluorinated counterparts.

² M. Platz and D. S. Watt, unpublished observations. For example, the photolysis of 3-(4-toluy1)-3-(trifluoromethyl)diazirine in diethylamine generated a carbene possessing a low-lying singlet state and a triplet ground state. The photoinsertion of the singlet carbene into various substrates was examined. Photoinsertion into the N-H bond of diethylamine produced the adduct *N,N*-diethyl-*N*-[(2,2,2-trifluoro-1-(4-toluy1)ethyl)-amine. Rapid elimination of hydrogen fluoride from this adduct under the conditions of the photolysis experiment afforded an enamine, 1'-(diethylamino)-2',2'-difluoro-4-methylstyrene. The subsequent hydrolysis of the enamine produced diethylamine and α,α -difluoro-4-methylacetophenone. This unexpected elimination and hydrolysis sequence had the net effect of reversing the photoinsertion process.

* Authors to whom correspondence should be addressed.

[†] Department of Chemistry.

[‡] Department of Biochemistry.

¹ The abbreviations used are as follows: CaM, calmodulin; DCC, *N,N'*-dicyclohexylcarbodiimide; DMSO, dimethyl sulfoxide; DSO, disuccinimidyl oxalate; EGTA, ethylene glycol bis(β -aminoethyl ether)-*N,N,N',N'*-tetraacetic acid; HEPES, 4-(2-hydroxyethyl)-1-piperazineethanesulfonic acid; NHS, *N*-hydroxysuccinimidyl; Pth, phenylthiohydantoin; TFA, trifluoroacetic acid; THF, tetrahydrofuran; TRIS, tris(hydroxymethyl)aminomethane.

EXPERIMENTAL PROCEDURES

General Chemical Procedures. Chemicals were purchased from Aldrich or Sigma. Infrared spectra were recorded on a Perkin-Elmer Model 357 spectrometer. Nuclear magnetic resonance spectra were determined on a Varian 400-MHz or Gemini 200-MHz NMR spectrometer. Chemical shifts are reported in parts per million relative to tetramethylsilane as an internal standard. Mass spectra were determined on a VG ZAB spectrometer. Elemental analyses were performed by Atlantic Micro-labs, Norcross, GA. Column chromatography using Macherey Nagel silica gel 60 is referred to as "chromatography on silica gel". Procedures for the preparation of the following compounds were developed concurrently in these laboratories but were recently published (14) elsewhere: methyl 4-amino-2,3,5,6-tetrafluorobenzoate (2), methyl 4-azido-2,3,5,6-tetrafluorobenzoate (3), 4-azido-2,3,5,6-tetrafluorobenzoic acid (4), and succinimidyl 4-azido-2,3,5,6-tetrafluorobenzoate (5).

Methyl *N*-(4-Azido-2,3,5,6-tetrafluorobenzoyl)-tyrosinate (6). To a solution of 2.05 g (6.21 mmol) of 5 and 1.58 g (6.83 mmol) of Tyr(OCH₃)·HCl in 50 mL of DMSO was added 1.25 g (12.4 mmol) of Et₃N. The solution was stirred for 23 h at 25 °C and diluted with EtOAc. The organic solution was washed with 2 N HCl solution and brine and dried over anhydrous MgSO₄. The crude product was chromatographed on silica gel using 1:1 EtOAc-hexane to afford 2.33 g (91%) of 6: mp 155–157 °C dec; IR (KBr) 2112, 1717, 1649 cm⁻¹; ¹H NMR (DMSO-*d*₆) δ 2.80–3.08 (m, 2, CH₂), 3.67 (s, 3, CH₃), 4.55–4.66 (m, 1, CH), 6.68 and 7.05 (2 d, *J* = 8.5 Hz, 4, ArH), 9.27 (s, 1, OH), 9.39 (d, *J* = 7.9 Hz, 1, NH). Anal. Calcd for C₁₇H₁₂F₄N₄O₄: C, 49.52; H, 2.93. Found: C, 49.63; H, 2.99.

Methyl *N*-(4-Azido-2,3,5,6-tetrafluorobenzoyl)-2,6-diiodotyrosinate (7). To a solution of 65 mg (0.16 mmol) of 6 in 2.4 mL of a 5:1 mixture of MeOH and TRIS buffer (pH 7.8) were added at 0 °C 60 mg (0.38 mmol) of NaI and 86 mg (0.38 mmol) of chloramine T hydrate. The mixture was stirred for 60 min at 0 °C and concentrated. The residue was dissolved in EtOAc, washed successively with 5% sodium thiosulfate solution, saturated NaHCO₃ solution, and brine, and dried over anhydrous MgSO₄. The product was chromatographed on silica gel using CHCl₃ to afford 85 mg (81%) of 7: mp 168–170 °C dec; IR (KBr) 2114, 1723, 1650 cm⁻¹; ¹H NMR (CD₃OD) δ 2.83–3.17 (m, 2, CH₂), 3.74 (s, 3, CH₃), 4.45–4.63 (m, 1, CH), 7.62 (s, 2, ArH). Anal. Calcd for C₁₇H₁₀F₄I₂N₄O₄: C, 30.75; H, 1.52. Found: C, 30.84; H, 1.56.

***N*-(4-Azido-2,3,5,6-tetrafluorobenzoyl)tyrosine (8).** To a solution of 1.15 g (2.79 mmol) of 6 in 33 mL of 10:1 MeOH-water was added 0.70 g (17 mmol) of LiOH·H₂O. The solution was stirred for 16 h at 25 °C and concentrated. The residual solid was acidified with 2 N HCl solution and extracted with EtOAc. The organic solution was washed with brine and dried over anhydrous MgSO₄. The product was crystallized from CHCl₃ to afford 576 mg (52%) of 8: mp 147–149 °C dec; IR (KBr) 2114, 1700, 1643 cm⁻¹; UV (95% EtOH) λ_{max} 256 nm (ε 19 000) (decay half-life was <10 s under 254 nm irradiation); ¹H NMR (acetone-*d*₆) δ 2.96–3.30 (m, 2, CH₂), 3.40 (br s, 1, CO₂H), 3.81 (s, 1, OH), 4.81–4.96 (m, 1, CH), 6.76 and 7.13 (2 d, *J* = 8.6 Hz, 4, ArH), 8.13 (d, *J* = 7 Hz, 1, NH). Anal. Calcd for C₁₆H₁₀F₄N₄O₄: C, 48.25; H, 2.53. Found: C, 48.41; H, 2.56.

Succinimidyl *N*-(4-Azido-2,3,5,6-tetrafluorobenzoyl)tyrosinate (9). To a solution of 274 mg (0.69 mmol) of 8 in 10 mL of anhydrous THF were added 114 mg (0.99 mmol) of *N*-hydroxysuccinimide and 170 mg (0.83 mmol) of DCC. After stirring for 22 h at 25 °C, the suspension

was filtered. To the filtrate was added 3 mL of DMSO, and the solution was concentrated. The resulting solution of the NHS ester 9 was used directly in coupling reactions with amines.

2-(4-Amino-2,3,5,6-tetrafluorophenyl)-4-carboxy-4,5-dihydrothiazole (11). A solution of 101 mg (0.53 mmol) of 4-amino-2,3,5,6-tetrafluorobenzonitrile (10), 64 mg (0.53 mmol) of L-cysteine, and 73 mg (0.53 mmol) of K₂CO₃ in 2.0 mL of 1:1 MeOH-water was heated at 65–70 °C for 14 h. The MeOH was removed under reduced pressure. The aqueous solution was extracted with ether to remove any unreacted 10 (19% recovery). The solution was acidified to pH 3–4 with 2 N HCl solution and extracted with EtOAc while the pH was checked and adjusted between extractions to maintain a value of 3–4. The EtOAc fractions were combined, washed with brine, and dried over anhydrous MgSO₄. The crude product was recrystallized from EtOAc-hexane to yield 63 mg (40%) of 11 as a pale yellow solid: mp 184–186 °C dec; [α]_D = 76.8° (*c* = 0.95, acetone); IR (KBr) 3000 (br), 1710, 1645 cm⁻¹; ¹H NMR (acetone-*d*₆) δ 3.77 (d, *J* = 9.1 Hz, 2, CH₂), 5.34 (t, *J* = 9.3 Hz, 1, CH), 5.98 (br s, 2, NH₂). Anal. Calcd for C₁₀H₆F₄N₂O₂S: C, 40.82; H, 2.06. Found: C, 40.70; H, 2.03.

2-(4-Azido-2,3,5,6-tetrafluorophenyl)-4-carboxy-4,5-dihydrothiazole (12). To a solution of 199 mg (0.68 mmol) of 11 in 3 mL of TFA at 0 °C was added 100 mg (1.5 mmol) of NaNO₂. The solution was stirred for 25 min at 0 °C and 150 mg (2.3 mmol) of NaN₃ was added. The solution was stirred an additional 1.5 h at 0 °C, warmed to 25 °C, and concentrated. The residue was diluted with 20 mL of water, and the pH was adjusted to ca. 4 with solid Na₂CO₃. The solution was extracted with EtOAc. The combined organic solutions were washed with brine and dried over anhydrous MgSO₄. The EtOAc solution was concentrated to afford 198 mg (91%) of 12: IR (thin film) 3000 (br), 2135 cm⁻¹; ¹H NMR (acetone-*d*₆) δ 3.87 (d, *J* = 9.2 Hz, 2, CH₂), 5.43 (t, *J* = 9.2 Hz, 1, CH), 6.97 (br s, 1, CO₂H). This material resisted efforts to prepare an analytically pure sample and was fully characterized as the methyl ester: IR (CHCl₃) 2135, 1738 cm⁻¹; ¹H NMR (CDCl₃) δ 3.68–3.99 (m, 2, CH₂), 3.86 (s, 3, OCH₃), 5.34 (t, *J* = 9.5 Hz, 1, CH); exact mass spectrum calcd for C₁₁H₆F₄N₄O₂S 334.0148, found 334.0146.

2-(4-Amino-2,3,5,6-tetrafluorophenyl)-4-carboxythiazole (13). A suspension of 415 mg (1.4 mmol) of 11 and 413 mg (2.0 mmol) of 9,10-phenanthrenequinone (20) in 8.4 mL of 5% HOAc in CHCl₃ was refluxed for 15 h. The solution was cooled, concentrated, and diluted with EtOAc. The solution was washed with several portions of 1 M NaOH solution. The combined aqueous solutions were extracted with CHCl₃ to remove much of the 9,10-phenanthrenequinone/-quinol. The aqueous solution was acidified to pH 3–4 and extracted with EtOAc while the pH was checked to maintain it at 3–4. These organic extracts were combined, washed with brine, dried over anhydrous MgSO₄, and concentrated to afford 430 mg of 13 that was used directly in the next reaction. In order to secure an analytical sample, traces of 9,10-phenanthrenequinone/-quinol were removed by trituration of the crude product with CHCl₃ and a subsequent recrystallization from EtOAc-hexane to yield 13 as an amorphous solid: mp >230 °C; IR (KBr) 3000 (br), 1704, 1655 cm⁻¹; ¹H NMR (acetone-*d*₆) δ 3.50 (br s, 1, CO₂H), 6.04 (br s, 2, NH₂), 8.60 (s, 1, CH). Anal. Calcd for C₁₀H₄F₄N₂O₂S: C, 41.10; H, 1.38. Found: C, 41.17; H, 1.39.

2-(4-Azido-2,3,5,6-tetrafluorophenyl)-4-carboxythiazole (14). To a solution of 415 mg (1.4 mmol) of 13 in

8.0 mL of TFA at 0 °C was added 149 mg (2.2 mmol) of NaNO_2 . The solution was stirred for 30 min at 0 °C, and 184 mg (2.8 mmol) of NaN_3 was added. The solution was stirred for 1.5 h at 0 °C, allowed to warm to 25 °C, and concentrated. The oil was diluted with EtOAc and washed with half-saturated NaHCO_3 solution to neutralize the residual TFA. The aqueous layer was separated, and the pH was adjusted to ca. 3. The aqueous solution was extracted with EtOAc. The combined organic solutions were washed with brine and dried over anhydrous MgSO_4 . The crude product was recrystallized from EtOAc to yield 172 mg (38%) of **14**: mp 172–174 °C dec; IR (KBr) 3105, 2800 (br), 2130, 1680, 1640 cm^{-1} ; UV (95% EtOH) λ_{max} 280 nm (ϵ 17 000) (decay half-life was <10 s under 254 nm irradiation); ^1H NMR (acetone- d_6) δ 3.50 (br s, 1, CO_2H), 8.74 (s, 1, CH). Anal. Calcd for $\text{C}_{10}\text{H}_2\text{F}_4\text{N}_4\text{O}_2\text{S}$: C, 37.75; H, 0.63. Found: C, 37.83; H, 0.64.

Succinimidyl 2-(4-Azido-2,3,5,6-tetrafluorophenyl)thiazole-4-carboxylate (15). To a suspension of 12 mg (0.037 mmol, 1.0 equiv) of **14**, 10 μL (0.13 mmol, 3.5 equiv) of anhydrous pyridine, and 1.0 mL of anhydrous CH_3CN was added 14 mg (0.05 mmol, 1.4 equiv) of DSO (**21**). The solution was stirred for 18 h at 25 °C, concentrated, diluted with 10 mL of water, and extracted with EtOAc. The EtOAc solution was separated and washed successively with half-saturated NaHCO_3 solution, water, and brine, dried over anhydrous MgSO_4 , and concentrated to afford 7.6 mg (49%) of **15**. The crude product was sufficiently pure to use directly or could be recrystallized from EtOAc-hexane to provide an analytically pure sample: mp 175–177 °C dec; IR (KBr) 2130, 1775, 1724 cm^{-1} ; ^1H NMR (CDCl_3) δ 2.94 (s, 4, CH_2CH_2), 8.68 (s, 1, CH). Anal. Calcd for $\text{C}_{14}\text{H}_5\text{F}_4\text{N}_5\text{O}_4\text{S}$: C, 40.48; H, 1.21. Found: C, 40.57; H, 1.22.

Preparation of Calmodulin. CaM was isolated from bovine testes according to the procedure of Jamieson and Vanaman (**22**).

Preparation of Porcine Erythrocyte Plasma Membrane Ca^{2+} , Mg^{2+} -ATPase. The ATPase was isolated from fresh porcine blood according to the procedure of Nigli (**23**).

Functionalization of CaM with Succinimidyl 2-(4-Azido-2,3,5,6-tetrafluorophenyl)thiazole-4-carboxylate (15). CaM was treated with succinimidyl 2-(4-azido-2,3,5,6-tetrafluorophenyl)thiazole-4-carboxylate (**15**) in the presence of 2 mM CaCl_2 or 2 mM EGTA. Reagent **15** was dissolved in HPLC-grade acetonitrile at a concentration of 1 mg/mL immediately prior to use. The reagent solution was added to a final concentration of 20 μM to a solution of 10 μM CaM, 30 mM HEPES (pH 7.4), and 2 mM CaCl_2 (or EGTA). The mixture was incubated at 25 °C for 2 h, and the reaction was quenched by adding lysine to a final concentration of 10 mM. The mixture was then applied to a C-4 column (Vydac bulk resin, 25 cm \times 0.4 cm) and progress of the reaction was monitored at 230 nm (protein) and 290 nm (tetrafluorinated phenyl azide) as shown in the HPLC traces in Figure 1.

The major calmodulin derivative observed in Figure 1 was prepared in quantities sufficient for further characterization and for use in photochemical cross-linking studies by increasing the volume of reaction mixtures and maintaining concentrations of all components to keep them identical with those used in Figure 1 (upper panel). For example, 3 mg of CaM was reacted with 133 μg of reagent **15** in 0.13 mL of acetonitrile in a total reaction volume of 18 mL. The mixture was then applied to a Pharmacia MONO Q anion-exchange FPLC column to separate the CaM-reagent **15** monoadduct from native and polymod-

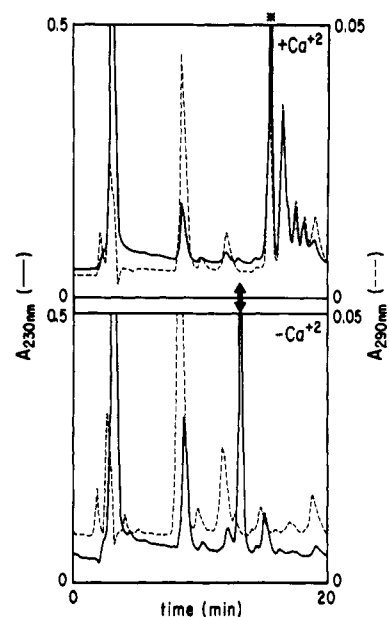


Figure 1. Reverse-phase HPLC profiles (C-4 column) of adducts of CaM and reagent **15** in the presence and absence of Ca^{2+} as monitored at 230 and 290 nm. The latter wavelength indicated the presence of the perfluoroaryl azide. Separation of the native CaM and its monoadducts was achieved with a 1% per min gradient of acetonitrile in 10 mM NaH_2PO_4 (pH 6) and 2 mM EGTA in which acetonitrile varied from 20% to 40%. The asterisk denotes the monoadduct at Lys-75. The arrow denotes the position at which native CaM would elute.

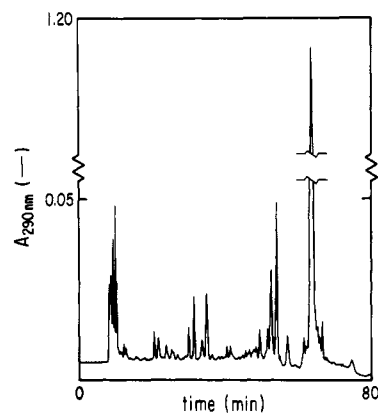


Figure 2. Phenyl μ Bondpak reverse-phase profiles of the tryptic digest of CaM-reagent **15** monoadduct as monitored at 290 nm. The separation was achieved with a gradient (starting at 5 min) of buffer A (10 mM NaH_2PO_4 , 2 mM EGTA). Buffer B (5 mM NaH_2PO_4 , 2 mM EGTA, 50% acetonitrile) was added from 0 to 50% (at 50% the gradient plateaus for 5 min before beginning a column wash cycle).

ified CaM. This was done with a gradient of buffer A [10 mM TRIS (pH 7.2) and 2 mM EGTA] and buffer B [10 mM TRIS (pH 7.2), 2 mM EGTA, and 0.8 M NaCl] from 45 to 60% B. The efficiency of the separation was monitored on a C-4 HPLC column.

The CaM-reagent **15** monoadduct was then digested with trypsin and applied to a Phenyl μ Bondpak HPLC (Waters) according to the method of Vanaman (**1**) in order to separate the CaM tryptic peptides. The separation was monitored at 290 nm in order to detect the peptide bearing the tetrafluorinated phenyl azide group. The resulting HPLC trace is shown in Figure 2. The major peak was collected, desalted, and applied to an Applied Biosystems Model 477a protein sequencer equipped for on-line HPLC analysis.

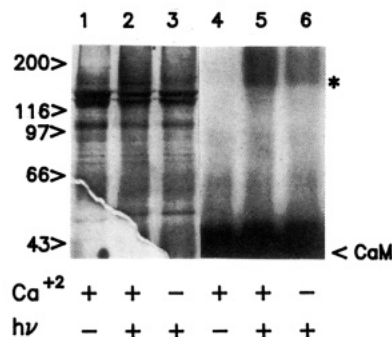


Figure 3. SDS-Polyacrylamide gel and autoradiogram of cross-linking experiments. Lanes 1–3 correspond to the silver-stained gel, and lanes 4–6 correspond to the autoradiogram of lanes 1–3, respectively. Molecular weight standards were run and their position is indicated by the numbers (kDa) at the left of lane 1. Lanes 2 and 5 correspond to the photolysis product of the ¹²⁵I-labeled monoadduct of CaM and Ca²⁺,Mg²⁺-ATPase in the presence of Ca²⁺. Lanes 1 and 4 correspond to the same mixture without photolysis. Lanes 3 and 6 correspond to the photolysis in the presence of 10 mM EGTA. The asterisk on the right indicates the position of the cross-linked species. The position of the non-cross-linked CaM is indicated at the lower right. The Ca²⁺,Mg²⁺-ATPase runs as a doublet at 138 and 128 kDa, and the cross-linked species runs at 151 kDa.

Preparation of ¹²⁵I-Labeled Monoadduct of CaM and Succinimidyl 2-(4-Azido-2,3,5,6-tetrafluorophenyl)-thiazole-4-carboxylate (15). Radioiodination of 1 mg of purified, monomodified CaM was achieved with 100 μ Ci of [¹²⁵I]NaI and Enzymobeads (Bio-Rad) according to the procedure supplied by Bio-Rad.

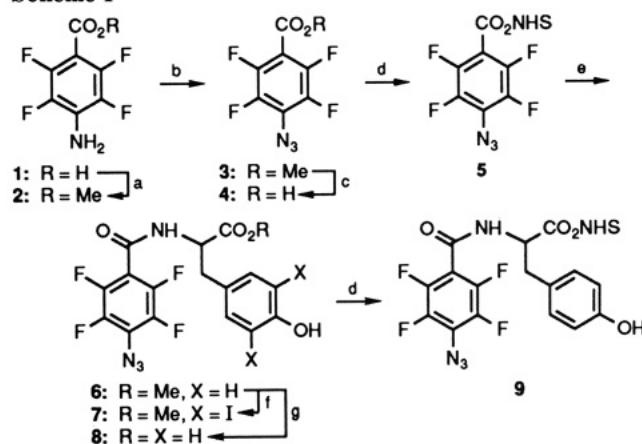
Photochemical Cross-Linking Experiments. A solution of 2 μ g of Ca²⁺,Mg²⁺-ATPase was incubated with 2 μ g of ¹²⁵I-labeled CaM–reagent 15 monoadduct (80 mCi/ μ mol) in 15 μ L of 30 mM HEPES (pH 7.4), 130 mM NaCl, 2 mM MgCl₂, 0.05% (v/v) Triton X-100, 5% (v/v) glycerol, 0.5 mg/mL phosphatidylcholine containing either 50 μ M CaCl₂ or 10 mM EGTA. The solution was photolyzed for 1 min with a hand-held ultraviolet light with the glass faceplate removed (4600 μ W/cm², Model UVS-11, Ultraviolet Products, Inc.) at a distance of 4 cm. The solution was suspended in a protein-solubilizing mixture of 65 mM Tris-HCl, 2% (v/v) SDS, 10% (v/v) glycerol, 5% (v/v) β -mercaptoethanol, and 0.001% bromophenol blue, and the solution was boiled for 5 min. The products were analyzed by 7.5% SDS-PAGE (24). The gel was dried, autoradiographed, resuspended, and silver stained. Autoradiography was performed for 4 h. Figure 3 shows the results of these experiments.

RESULTS

As shown in Scheme I, succinimidyl 4-azido-2,3,5,6-tetrafluorobenzoate (5) (14) was prepared from 4-amino-2,3,5,6-tetrafluorobenzoic acid (1) and coupled to methyl tyrosinate to obtain methyl ester 6. Methyl ester 6 underwent iodination under the usual conditions without any potential interference from nucleophilic aromatic substitution. Methyl ester 6 was converted to succinimidyl *N*-(4-azido-2,3,5,6-tetrafluorobenzoyl)tyrosinate (9) in the usual fashion.

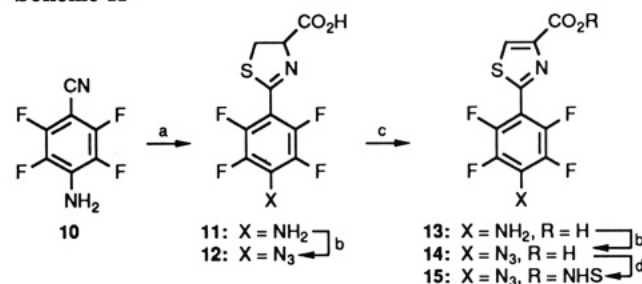
As shown in Scheme II, 2-(4-amino-2,3,5,6-tetrafluorophenyl)-4-carboxy-4,5-dihydrothiazole (11) was prepared in a condensation of 4-amino-2,3,5,6-tetrafluorobenzonitrile (10) with Cys. Although it was possible to convert thiazoline amine 11 to the corresponding thiazolinyl azide 12, the coupling of the NHS ester of 12 with various amines failed to produce the desired amides presumably as a consequence of competitive nucleophilic attack at the imino

Scheme I^a



^a Reagents: (a) HCl, MeOH; (b) (1) NaNO₂, TFA, 0 °C, (2) NaN₃; (c) LiOH·H₂O, 5:1 MeOH–H₂O; (d) NHS(OH), DCC, THF; (e) Tyr(OCH₃)-HCl, Et₃N, DMSO; (f) NaI, chloramine T, MeOH, TRIS buffer; (g) LiOH·H₂O, 10:1 MeOH–H₂O.

Scheme II^a



^a Reagents: (a) Cys, K₂CO₃, 1:1 MeOH–H₂O, 65 °C; (b) (1) NaNO₂, TFA, 0 °C, (2) NaN₃; (c) 9,10-phenanthrenequinone, 5% HOAc in CHCl₃, reflux; (d) DSO, Py, CH₃CN.

thioester carbon. Consequently, thiazoline amine 11 was oxidized to thiazole amine 13 with 9,10-phenanthrenequinone (20) and thiazole amine 13 was converted to the desired succinimidyl 2-(4-azido-2,3,5,6-tetrafluorophenyl)-thiazole-4-carboxylate (15).

Figure 1 shows reverse phase (C-4) HPLC separations, performed as described in the legend, of the products obtained when CaM (10 μ M) was treated with a 2-fold molar excess (20 μ M) of reagent 15 in the presence of 2 mM Ca²⁺ (upper panel) or 2 mM EGTA (lower panel). The double arrow denotes the elution position of unmodified, native CaM as displayed in a separate analysis. The effluent was monitored for UV absorption at 230 nm to detect protein and at 290 nm to detect the tetrafluorophenyl azide moiety. Calmodulin shows negligible UV absorption at the latter wavelength.

In the absence of Ca²⁺, a major peak displaying absorbance at 230 nm but lacking absorbance at 290 nm was obtained that possessed a retention time consistent with that of native CaM (Figure 1, lower panel). A number of early eluting peaks possessing both 230 and 290 nm absorption represented products of reagent hydrolysis and reaction with lysine that was added after incubation to quench further reaction with CaM. (This Lys adduct peak is substantially reduced in the upper trace where substantial CaM modification consumed reagent 15 prior to the addition of lysine.)

The reaction of CaM with reagent 15 in the presence of Ca²⁺ yielded a single major product denoted by the asterisk above the peak in Figure 1 (upper panel). This component, which was present in only small amounts in the lower trace, eluted slightly later than native CaM and possessed absorbance at both 230 and 290 nm. Native

CaM is nearly absent in the upper trace, indicating that chemical modification was nearly complete in the presence of Ca^{2+} under these conditions. A series of lesser peaks were also observed in the upper trace that eluted later than the major CaM monoadduct and that possessed a much higher ratio of the absorbance values at 290 and 230 nm, suggesting that these peaks were polymodified CaM adducts.

The modification reaction was successfully increased in scale. An anion-exchange FPLC separation yielded one major protein, again possessing both 230 and 290 nm UV absorption, that was isolated in a yield of 1.7 mg. An aliquot was further analyzed on C-4 reverse-phase HPLC (as in Figure 1) to yield a single peak identical in elution and UV absorbing properties with that labeled with the asterisk in Figure 1. Amino acid composition analysis confirmed that this material was a CaM adduct.

This adduct was digested with trypsin, and the resulting tryptic peptides were isolated by Phenyl μ Bondpak reverse-phase HPLC. Figure 2 shows the resulting elution profile obtained by monitoring the effluent at 290 nm. A single major peak (1.17 AU) was eluted at 65 min with 50% buffer B. Only minor peaks (<0.05 AU), probably representing Tyr-containing peptides, were observed earlier in the trace. It should be noted that the scale is magnified in the lower absorbance range. The 65-min peak was collected, desalted, and directly subjected to sequence analysis. The HPLC analysis of cycle 1 yielded no known Pth amino acid but had a major peak eluting at 10.95 min that presumably represented Pth-Lys modified by reagent 15 (vide infra). Cycle 2 gave 6.6 nmol of Pth-Met, and cycle 3 gave 4.8 nmol of Pth-Lys. The only sequence in CaM which could yield this tripeptide is residues 75–77, Lys-Met-Lys, with the ϵ -amino group of Lys-75 being the presumed site of modification by reagent 15.

Figure 3 shows the results of SDS-PAGE analysis of products obtained on photochemical cross-linking of the ^{125}I -labeled, Lys-75 CaM–reagent 15 monoadduct and a preparation of the porcine erythrocyte membrane Ca^{2+} , Mg^{2+} -ATPase. Lanes 1–3 represent the gel after silver staining, and lanes 4–6 display an autoradiogram of the same gel that was exposed prior to silver staining. Two major protein bands were observed at 128 and 138 kDa in lanes 1–3 representing the two different isoforms of the enzyme recently identified in erythrocytes (25). A major band of radioactivity is present in lane 5 with apparent M_r of 151 kDa (denoted by the asterisk), which is absent in a control sample run without photolysis (lane 4) and substantially diminished on photolysis of a sample that contained excess EGTA. Consequently, the cross-linking was both light- and calcium-dependent. The formation of this cross-linked species is also detectable in the silver-stained gel in lane 2. Densitometric scans of the silver-stained gel indicated that 22% of the Ca^{2+} , Mg^{2+} -ATPase was cross-linked in the presence of excess CaM monoadduct under these conditions.

DISCUSSION

These studies describe a new family of heterobifunctional, tetrafluorophenyl azide reagents that are designed for improved cross-linking efficiently (particularly with hydrophobic amino acid side chains) and that are capable of bearing a photostable radiolabel. Among the radioisotopes of high specific activity and reasonable half-life, ^{125}I and ^{35}S are logical candidates for inclusion in heterobifunctional cross-linking reagents. As shown in Schemes I and II, succinimidyl *N*-(4-azido-2,3,5,6-tetrafluorobenzoyl)tyrosinate (9), a photoactive perflu-

orinated aryl azide that could bear an ^{125}I -radiolabel, and succinimidyl 2-(4-azido-2,3,5,6-tetrafluorophenyl)thiazole-4-carboxylate (15), a perfluorinated aryl azide that could bear an ^{35}S -radiolabel, were prepared in a straightforward series of operations. The ^{35}S -radiolabeled NHS ester 15 is particularly attractive since the radiolabel is photostable whereas the ^{125}I -radiolabel suffers some photodeiodination (9) under certain circumstances. Before applying the radiolabeled version of reagent 15 in a detailed biochemical study, it seemed prudent to demonstrate that the tetrafluorophenyl azide moiety, incorporated into a donor protein, was capable of efficient photochemical cross-linking to an appropriate target enzyme and to assess the efficiency of this photoactive group relative to other reagents bearing just a simple phenyl azide.

In previous studies (2, 3), we have used the calmodulin (CaM) system to test two related heterobifunctional reagents bearing the simple phenyl azide group. These and a number of other studies (26, 27) demonstrated that most hydrophobic acylating reagents modify CaM at Lys-75 in a calcium-dependent manner and that reagent 15 demonstrated similar behavior. The photochemical cross-linking of the ^{125}I -labeled, Lys-75 CaM–reagent 15 monoadduct to the porcine erythrocyte membrane Ca^{2+} , Mg^{2+} -ATPase, shown in Figure 3, provided evidence for improved cross-linking efficiency for the tetrafluorinated phenyl azide. In our previous work with Lys-75 CaM monoadducts containing a simple phenyl azide, cross-linking to the human erythrocyte membrane Ca^{2+} , Mg^{2+} -ATPase gave an 8% yield (3) of cross-linked material under the same conditions where the tetrafluorophenyl azide gave at least 20% cross-linking. It should be noted that these studies were performed with a purified membrane enzyme solubilized in a detergent (Triton X-100) micelle. Assuming random insertion of the enzyme into the micelle, simple geometry dictates that approximately 50% of the molecules would have their cytoplasmic domains (where CaM binds) facing the interior and unavailable for interaction with the ^{125}I -labeled CaM–reagent 15 probe. This suggests that the cross-linking efficiency for accessible molecules is approximately twice that observed in densitometry readings.

The utilization of the tetrafluorophenyl azides in cross-linking agents addresses two other problems encountered with simple phenyl azide based cross-linking reagents: the selectivity of the reactive intermediate for hydrophobic versus hydrophilic amino acid residues in the target protein and chemical stability of the covalent attachment generated in the cross-linking process. The photolysis of a simple phenyl azide generates a substituted dehydroazepine as the reactive intermediate (5–8) that *selectively* traps nucleophilic substituents in certain hydrophilic amino acids. However, protein–protein interactions are largely dictated by hydrophobic forces and by van der Waal contacts that involve aliphatic and aromatic groups in hydrophobic amino acid side chains (28) and it would be preferable to have a reactive intermediate capable of intercepting such residues. Just such a hydrophobic site lies adjacent to Lys-75 in CaM and appears to be responsible for the calcium-dependent interaction with target enzymes as well as small hydrophobic compounds including the interaction of reagent 15 with CaM. Thus, the agents that rely on dehydroazepine-mediated cross-linking are unlikely to make efficient probes of protein–protein interaction sites as reflected in the minimal cross-linking experienced with a mixture of monoadducts of CaM and succinimidyl *N*-[2-(4-azidosalicyl)ethyl]suberamate (3).

On the other hand, the photolysis of the tetrafluorophe-

nyl azide group generates a reactive nitrene capable of inserting into carbon-hydrogen bonds in hydrophobic amino acid side chains. Photochemical studies with model perfluorinated azides in organic solvents have led to similar conclusions (13-18). In addition, such carbon-hydrogen insertion reactions generate stable adducts that are more likely to survive adventitious hydrolysis during the digestion and purification process. The enhanced cross-linking efficiency observed in the present study is consistent with perfluorinated phenyl azides generating a more reactive intermediate capable of covalently linking a wider variety of amino acid residues in the target protein than the corresponding simple phenyl azides. This study also demonstrates that enhanced reactivity is seen with interacting proteins even though they are surrounded by water as a bulk medium. Clearly, further studies will be required to determine the structure of the photoinsertion products obtained in studies of proteins using these tetrafluorophenyl azide-based probes.

In conclusion, we have prepared heterobifunctional cross-linking reagents that incorporate perfluorinated phenyl azides as the photoactive component and have the capacity to bear either an ^{125}I or ^{35}S radiolabel. One of these reagents displayed a cross-linking efficiency that suggest these perfluorinated azides will prove effective in biochemical studies, and detailed studies along these lines are in progress.

ACKNOWLEDGMENT

We thank the National Science Foundation (Grant CHE-8607441) and the National Institutes of Health (Grant NS-21868 to T.C.V.), for their financial support, and Degussa AG for a generous gift of amino acids.

LITERATURE CITED

- Vanaman, T. C. (1983) Chemical approaches to the calmodulin system. *Methods Enzymol.* 102, 296-310.
- Imai, N., Kometani, T., Crocker, P. J., Bowdan, J. B., Demir, A., Dwyer, L. D., Mann, D. M., Vanaman, T. C., Watt, D. S. (1990) Photoaffinity heterobifunctional cross-linking reagents based on *N*-(azidobenzoyl)tyrosines. *Bioconjugate Chem.* 1, 138-143.
- Imai, N., Dwyer, L. D., Kometani, T., Ji, T., Vanaman, T. C., Watt, D. S. (1990) Photoaffinity heterobifunctional cross-linking reagents based on azide-substituted salicylates. *Bioconjugate Chem.* 1, 144-148.
- Bayley, H. (1983) *Photogenerated Reagents in Biochemistry and Molecular Biology*, Elsevier, New York.
- Torres, M. J., Zayas, J., Platz, M. S. (1986) A formal CH insertion reaction of an aryl nitrene into an alkyl CH bond. Implications for photoaffinity labelling. *Tetrahedron Lett.* 27, 791-794.
- Leyva, E., Platz, M. S., Persy, G., Wirz, J. (1986) Photochemistry of phenyl azide: the role of singlet and triple phenylnitrene as transient intermediates. *J. Am. Chem. Soc.* 108, 3783-3790.
- Shields, C. J., Chrisope, D. R., Schuster, G. B., Dixon, A. J., Poliakoff, M., Turner, J. J. (1987) Photochemistry of aryl azides: Detection and characterization of a dehydroazepine by time-resolved infrared spectroscopy and flash photolysis at room temperature. *J. Am. Chem. Soc.* 109, 4723-4726.
- Schuster, G. B., Liang, T.-Y. (1987) Photochemistry of 3- and 4-nitrophenyl azides: Detection and characterization of reactive intermediates. *J. Am. Chem. Soc.* 109, 7803-7810.
- Watt, D. S., Kawada, K., Leyva, E., Platz, M. S. (1989) Exploratory photochemistry of iodinated aromatic azides. *Tetrahedron Lett.* 30, 899-902.
- Brunner, J., Senn, H., Richards, F. M. (1980) 3-(Trifluoromethyl)-3-phenyldiazirine: A new carbene generating group for photolabeling reagents. *J. Biol. Chem.* 255, 3313-3318.
- Baldini, G., Martoglio, B., Schachenmann, A., Zugliani, C., Brunner, J. (1988) Mischarging *Escherichia coli* tRNA^{Phe} with L-4'-[3-(trifluoromethyl)-3H-diazirin-3-yl]phenylalanine, a photoactivatable analogue of phenylalanine. *Biochemistry* 27, 7951-7959.
- Frey, A. B., Kreibich, G., Wadhwa, A., Clarke, L., Waxman, D. J. (1986) 3-(Trifluoromethyl)-3-(*m*-[^{125}I]iodophenyl)-diazirine photolabels a substrate-binding site of rat hepatic cytochrome P-450 form PB-4. *Biochemistry* 25, 4797-4803.
- Soundararajan, N., Platz, M. (1990) Descriptive photochemistry of polyfluorinated azide derivatives of methyl benzoate. *J. Org. Chem.* 55, 2034-2039.
- Keana, J. F. W., Cai, S. X. (1990) New reagents for photoaffinity labeling: Synthesis and photolysis of functionalized perfluorophenyl azides. *J. Org. Chem.* 55, 3640-3647.
- Keana, J. F. W., Cai, S. X. (1989) Functionalized perfluorophenyl azides: New reagents for photoaffinity labeling. *J. Fluorine Chem.* 43, 151-154.
- Cai, S. X., Keana, J. F. W. (1989) 4-Azido-2-iodo-3,5,6-trifluorophenylcarbonyl derivatives. A new class of functionalized and iodinated perfluorophenyl azide photolabels. *Tetrahedron Lett.* 30, 5409-5412.
- Young, M. J. T., and Platz, M. S. (1989) Polyfluorinated aryl azides as photoaffinity labelling reagents; The room temperature CH insertion reactions of singlet pentafluorophenyl nitrene with alkanes. *Tetrahedron Lett.* 30, 2199-2202.
- Leyva, E., Munoz, D., and Platz, M. S. (1989) Photochemistry of fluorinated aryl azides in toluene solution and in frozen polycrystals. *J. Org. Chem.* 54, 5938-5945.
- For an example of the use of [^{35}S]Cys in a radiolabeled thiazolidine, see: Mitchell, R. N., Harrison, E. H., Bowers, W. E. (1984) The use of radioactive cyteine methyl ester for labeling glycosylated molecules oxidized by periodate or neuraminidase plus galactose oxidase. *Arch. Biochem. Biophys.* 229, 544-554.
- Barton, M. A., Kenner, G. W., Sheppard, R. C. (1966) Peptides. Part XXI. Dehydrogenation of some thiazolines derived from cysteine. *J. Chem. Soc. C* 1061-1067.
- Takeda, K., Sawada, I., Suzuki, A., Ogura, H. (1983) A convenient synthesis of peptides using oxalates. *Tetrahedron Lett.* 24, 4451-4454.
- Jamieson, G. A., Vanaman, T. C. (1979) Calcium-dependent affinity chromatography of calmodulin on immobilized phenothiazine. *Biochem. Biophys. Res. Commun.* 90, 1048-1055.
- Niggli, V., Zurini, M., Carafoli, E. (1987) Purification, reconstitution, and molecular characteristics of the Ca^{2+} pump of plasma membranes. *Methods Enzymol.* 139, 791-808.
- Laemmli, U. (1970) Cleavage of structural proteins during the assembly of the head of Bacteriophage T4. *Nature* 227, 680-685.
- Strehler, E. E., James, P., Fischer, R., Heim, R., Vorherr, R., Filoteo, A. G., Penniston, J. R., Carifoli, E. (1990) Peptide sequence analysis and molecular cloning reveal two calcium pump isoforms in the human erythrocyte membrane. *J. Biol. Chem.* 265, 2835-2842.
- Mann, D. M., Vanaman, T. C. (1988) Modification of calmodulin on Lys-75 by carbamoylating nitrosoureas. *J. Biol. Chem.* 263, 11284-11290.
- Mann, D. M., Vanaman, T. C. (1989) Topographical mapping of calmodulin-target enzyme interaction domains. *J. Biol. Chem.* 264, 2373-2378.
- Janin, J., Chothia, C. (1990) The structure of protein-protein recognition sites. *J. Biol. Chem.* 265, 16027-16030.

Carrier Design: Biodistribution of Branched Polypeptides with a Poly(L-lysine) Backbone

J. A. Clegg,* F. Hudecz,† G. Mezö,† M. V. Pimm, M. Szekerke,† and R. W. Baldwin

Cancer Research Campaign Laboratories, University of Nottingham, University Park, Nottingham NG7 2RD, UK, and Research Group for Peptide Chemistry, Hungarian Academy of Science, L Eötvös University, Budapest 112, POB 32, Hungary 1518. Received September 5, 1990

The biodistribution has been examined in mice of a range of synthetic branched polypeptides which are based on a polylysine backbone but which differ in ionic charge, side-chain structure, and molecular size. Polycationic polypeptides, regardless of their size or primary structure at the branches, were cleared rapidly from the circulation, the liver being the major site of clearance. Polypeptides with glutamic acid in the side chain, which would be amphoteric under physiological conditions, showed a significantly prolonged blood survival, and this was seen with polypeptides in the range of molecular weights of 46 000 up to 213 000. Such polypeptides provide a useful system with which to investigate the effect of structural parameters on the pharmacokinetic properties of carrier molecules and would allow the selection of candidate carriers for a variety of uses.

INTRODUCTION

The use of macromolecular carriers for small molecules such as drugs has a wide range of applications, particularly in the field of drug delivery (1, 2). Promising results have been reported concerning the alteration of the pharmacokinetics of biologically active compounds by their conjugation to macromolecules (3, 4). In immunology, protein carriers are frequently applied to induce immune responses against covalently attached low molecular weight, nonimmunogenic epitopes, for monoclonal antibody production or for synthetic vaccine construction (5, 6). Conjugates of radionuclides and fluorophores to macromolecules could be useful in the development of biosensors and of various diagnostics.

Based on results with synthetic branched polypeptides, (7, 8) a model system was established to gain information for the rational design of macromolecular carriers with desired characteristics required for specific purposes. A new group of branched polypeptides was synthesized in order to investigate systematically chemical (charge, size, primary structure, conformation) (9, 10, 11) and biological (toxicity, immunogenicity, immunomodulatory potential, pyrogenicity, biodegradation) (12, 13, 14) parameters for an optimal carrier function (15).

As an extension of this line of research and in respect of the possibility of in vivo application of these synthetic compounds (and their conjugates), the present studies were designed to elucidate correlations between the structural features of branched polypeptides and their biodistribution profile. We examined the blood clearance, whole-body survival, and tissue distribution of branched polypeptides corresponding to the general formula poly[Lys-(X_i-DL-Ala_m)] or poly[Lys-(DL-Ala_m-X_i)]. These polypeptides are composed of a poly(L-Lys) backbone and of short side chains containing approximately three DL-Ala amino acid residues and one other (X) amino acid residue. The schematic presentation of these structures is shown in Figure 1. In order to dissect the effect of size from that

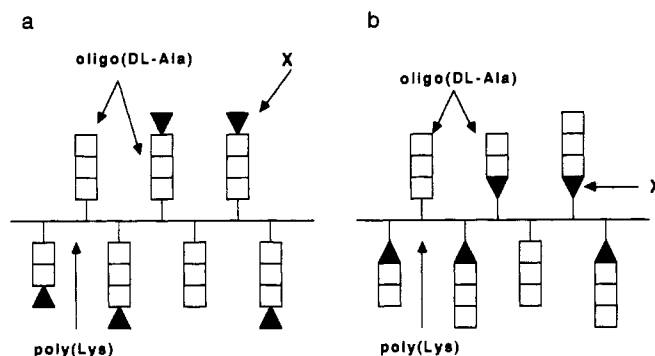


Figure 1. Schematic presentation of branched polypeptides with poly(L-Lys) backbone: (a) poly[Lys-(X_i-DL-Ala_m)] (XAK), (b) poly[Lys-(DL-Ala_m-X_i)] (AXK).

of other molecular characteristics, two groups of such polypeptides with basically identical side-chain composition, but with different size, were studied. In view of the importance of the side-chain structure in α -helix formation (9, 11) or in immunological properties (12, 13), we measured the biodistribution of polypeptides containing (i) amino acid residues of different identity (e.g., Leu, Pro, or Glu) at the side-chain terminal position, (ii) amino acid residues of different absolute configuration (L-Glu or D-Glu, L-Leu or D-Leu), (iii) amino acid residue X at the side-chain end or at the position next to the polylysine backbone. These comparative studies were used to identify factors which could influence the biodistribution of the branched polypeptides.

EXPERIMENTAL PROCEDURES

Abbreviations used in this paper follow the rules of the IUPAC-IUB Commission of Biochemical Nomenclature (16) in accord with the recommended nomenclature of graft polymers (17).

Branched polypeptides were synthesized as previously described (11, 18, 19). Briefly, poly(Lys) was prepared by the polymerization of *N*^ε-carboxy-*N*^ε-(benzyloxycarbonyl)-lysine anhydride under conditions that allowed an average degree of polymerization of either ca. 80–120 or ca. 400–

* To whom all correspondence should be addressed.

† L Eötvös University.

500. After cleavage of the protecting groups, either poly-[Lys-(DL-Ala_m)] (AK) was prepared by grafting of short oligomeric DL-Ala side chains onto the ϵ -amino groups of poly-(Lys) or benzyloxycarbonyl-protected leucine was coupled by the active-ester method. Poly[Lys-(X_i-DL-Ala_m)] (XAK) was synthesized by reacting a suitably protected amino acid pentachlorophenyl ester to the α -amino groups of AK. Blocking groups were removed completely with HBr in glacial acetic acid, as confirmed by UV spectroscopy at 254 nm. Poly[Lys-(DL-Ala_m-X_i)] (AXK) was prepared by the introduction of DL-Ala oligomers to the previously deprotected α -amino and ϵ -amino groups of poly[Lys-(Leu_i)] or poly[Lys-(Glu_i)] by the aid of *N*-carboxy-DL-alanine anhydride. The primary structure of polypeptides were studied by amino acid analysis, by the identification of the branch-terminating amino acid residue (19), and by the determination of the enantiomer composition of the side chains (20). The size of these compounds was analyzed by sedimentation and gel chromatography (18, 21).

Radioiodination of Branched Polypeptides. Branched polypeptides were labeled (35–40% efficiency) with [¹²⁵I]-*N*-succinimidyl 3-(4-hydroxyphenyl)propionate (Amersham International plc, Amersham, Bucks) using Bolton and Hunter's procedure (22). Reagent solution (10–20 μ L) was added to plastic Eppendorf tubes and evaporated to dryness under a stream of nitrogen. Then 500 μ L of polypeptide solution at 1 mg/mL in 0.1 M borate buffer (pH 8.6) was reacted with iodinated ester (2.5 mol of ester/mol of polypeptide). The reaction was allowed to proceed for 20 min at 0 °C and terminated by adding 500 μ L of 0.2 M glycine in the same buffer for 5 min at 0 °C. The ¹²⁵I-labeled polypeptide was purified on a G-25 Sephadex gel column using 0.066 M phosphate buffer (pH 7.6) containing 0.25% gelatin as eluent. Electrophoresis on native polyacrylamide gel with a continuous 8–25% gradient (PhastGel gradient 8-25 Pharmacia-LKB, Uppsala, Sweden) was applied to assess the low molecular weight labeled product content of the preparation.

Blood-Clearance and Tissue-Distribution Studies. Balb/c mice (female, 6–8 weeks old, Bantin and Kingman, Hull, UK) were used throughout these studies. Drinking water was supplemented with 0.1% w/v sodium iodide.

Groups of mice ($n = 3$) received a single injection (0.2 mL) of ¹²⁵I-labeled polypeptide (8 MBq/mg, 50–200 μ g/kg) via tail vein. Serial blood samples (10 μ L) were taken from the tail tip into microcapillary pipets (Drummond Microcaps, Drummond Scientific Co, Broomhall, PA), up to 6 h after injection. At this time the mice were killed and dissected. The blood samples, visceral organs, and residual carcasses were weighed and assayed for radioactivity in a conventional γ -counter. Results of the blood-clearance study were expressed as a percentage of the zero-time count rate assuming the blood volume of the mouse (mL) to be 11.2% of the body weight (g) (23). Area under the blood concentration–time curve up to 6 h following injection was calculated by the trapezoidal rule (24). Results of the tissue-distribution analysis were expressed as (i) percentage of the injected dose of radioactivity per gram of tissue or blood and (ii) ratios of radioactivity per gram of tissue to radioactivity per gram of blood (tissue to blood). Levels of statistical difference between groups of animals were assessed by Student's *t* test.

RESULTS AND DISCUSSION

Chemical Characteristics. A new type of branched polypeptide with poly(L-lysine) backbone was used in these studies (11, 18, 19). These polypeptides contain short side

chains composed of about three DL-alanine residues and one other amino acid residue (X) either at the end of the branches [poly[Lys-(X_i-DL-Ala_m)], XAK] or at the position next to the polylysine backbone [poly[Lys-(DL-Ala_m-X_i)], AXK], where $m \sim 3$ and $i \leq 1$.

These polypeptides represent a significantly modified version of multichain polypeptides used for immunological investigations by Sela et al. (25). In order to provide a simple, but versatile model system suitable for primary structure–conformation and chemical structure–carrier-function analysis, the length of the poly(DL-Ala) side chains has been markedly shortened, and instead of copolymers, single amino acids were introduced into the branches. Due to the limited solubility of branched polypeptides containing even only short side chains of L-Ala or D-Ala, racemic oligo(DL-Ala) grafts were applied.

Depending on the identity of the branch-terminating amino acid residue, these compounds have predominantly α -amino groups and express polycationic character (e.g., X = Leu, D-Leu, or Pro) or have α -amino groups as well as γ -carboxylic groups and proved to be amphoteric under physiological conditions (e.g., Glu or D-Glu). The size of these branched polypeptides was defined by the average relative molar masses (M_n , M_z , M_w), the relative molar mass distribution (M_z/M_w), and the average degree of polymerization (DP_n) determined by applying sedimentation analysis and gel chromatography. It was found that all polymers investigated possess a fairly narrow distribution of relative molar mass (21). We have attempted to dissect the effect of size from that of other molecular characteristics and therefore two groups of such polypeptides with almost identical side-chain composition were prepared.

The primary structure of these polypeptides was characterized by their amino acid composition and by the identification of the branch-terminating amino acid residue using HPLC analysis of the hydrolysates of dansylated polypeptides (20). The enantiomer composition of the side chains determined by reverse-phase HPLC and precolumn derivatization with Marfey's reagent indicated that no stereospecific or stereoselective polymerization took place during the synthesis and the coupling of D- or L-amino acid to the poly[Lys-(DL-Ala_m)] (AK) backbone did not result in racemization (26).

Conformational properties of polypeptides, studied by circular dichroism (CD) spectroscopy, showed significant differences correlating with the identity, hydrophilic or hydrophobic nature, and configuration of the side-chain-terminating amino acids and to the sequential order of amino acid residues in the side chains (9, 11, 27, 28). Chemical characteristics of the synthetic polypeptides are summarized in Table I.

At pH 7.3 in 0.2 M NaCl the CD spectra of polypeptides with oligo(DL-Ala) branches correspond to unordered spatial arrangement. Very similar CD properties have been observed in case of Pro-containing analogues (poly[Lys-(Pro_i-DL-Ala_m)] (28). Polymers with L-Leu and D-Leu in the side chain terminal position, which also have polycationic character, adopt helical or partially helical conformation, respectively (27). In the case of Leu polypeptides, reversal of the amino acid sequence in the side chains resulted in a pronounced change in the CD spectra at acidic pH. In spite of the fact that alk showed a stronger tendency to form ordered structure, under physiological conditions both polypeptides assume helical conformation (11). Polycationic polypeptides used in this study could assume helical conformation (Leu-containing polymers) and random coil structure (AK/ak and Pro-containing polypeptides), while amphoteric polypeptides (L-Glu or

Table I. Characteristics of Branched Polypeptides

polypeptide	abbreviation ^a	molar ratio of amino acids			\overline{DP}_n^c	M_w^d ($\pm 5\%$)
		Lys	DL-Ala _m	X _i ^b		
poly[Lys-(DL-Ala _m)]	AK	1	3.1		450	156 700
poly[Lys-(DL-Ala _m)]	ak	1	2.94		100	34 000
poly[Lys-(Leu _i -DL-Ala _m)]	LAK	1	3.1	0.98	450	206 600
poly[Lys-(Leu _i -DL-Ala _m)]	lak	1	2.94	0.81	100	42 800
poly[Lys-(DL-Ala _m -Leu _i)]	alk	1	2.9	0.79	92	38 900
poly[Lys-(D-Leu _i -DL-Ala _m)]	D-LAK	1	3.1	0.98	450	206 600
poly[Lys-(Pro _i -DL-Ala _m)]	PAK	1	3.1	0.96	450	198 700
poly[Lys-(Pro _i -DL-Ala _m)]	pak	1	2.94	0.94	100	42 800
poly[Lys-(Glu _i -DL-Ala _m)]	EAK	1	3.1	0.96	450	212 600
poly[Lys-(D-Glu _i -DL-Ala _m)]	D-EAK	1	3.1	0.95	450	212 000
poly[Lys-(Glu _i -DL-Ala _m)]	eak	1	2.94	0.93	100	45 800
poly[Lys-(DL-Ala _m -Glu _i)]	aek	1	2.67	1.0	100	44 610

^a Based on one-letter symbols of amino acids. Capital and small letters denote the size of the polypeptides. ^b X = Leu, D-Leu, Pro, Glu, or D-Glu. ^c Number average degree of polymerization. ^d Calculated from the average degree of polymerization of poly(L-Lys) and of the side-chain composition.

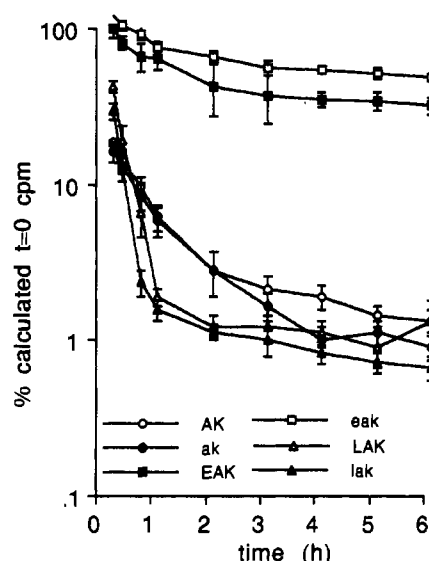


Figure 2. Blood-clearance profiles of ^{125}I -branched polypeptides following iv administration to BALB/c mice. $\text{AUC}_{0-6\text{h}}$ calculated from these data are given in Table II. Results are expressed as mean \pm standard deviation for groups of three animals.

D-Glu at the end of the side chains) could display dichroic curves relevant to unordered structure (28).

The branched polypeptides were readily radiolabeled by reaction of ^{125}I -labeled Bolton and Hunter reagent with their α -amino groups at the side-chain termini. The present studies with polylysine-based branched polypeptides have identified several factors which can influence the blood-survival and organ-clearance profiles of these carrier molecules.

Biological Studies. Blood Clearance. The blood-clearance profiles from both the large (157–213 kD) and small (34–46 kD) relative molecular mass series, up to 6 h after iv injection, are shown in Figure 2. The $\text{AUC}_{0-6\text{h}}$ values from these data are shown in Table II. There was no significant difference between the blood survival of the large and small relative molecular mass versions of polylysine with only DL-Ala side chains (AK/ak) or leucine-substituted alanylated polylysine poly[Lys-(Leu_i-DL-Ala_m)] (LAK/lak). However, for the amphoteric glutamic acid substituted polypeptide pair poly[Lys-(Glu_i-DL-Ala_m)] (EAK/eak) the blood survival of eak was longer than that for EAK. This was reflected in a significantly higher ($p < 0.01$) $\text{AUC}_{0-6\text{h}}$ for eak ($350 \pm 24.5\%$ calculated $t = 0$ cpm·h) compared to that for EAK ($248.1 \pm 45.1\%$ calculated $t = 0$ cpm·h).

Table II. Biodistribution Parameters of Branched Polypeptides

polypeptide	area under curve (0–6 h), % calcd $t = 0$ cpm·h, (mean \pm SD)	whole-body survival at $t = 24$ h, % injected dose (mean \pm SD)	% dose/g of blood at $t = 24$ h (mean \pm SD)
AK	28.9 ± 2.3	15.5 ± 1.6	0.24 ± 0.09
ak	26.8 ± 3.2	13.7 ± 1.6	0.17 ± 0.02
LAK	26.9 ± 1.8	8.9 ± 0.5	0.03 ± 0.01
lak	21.2 ± 1.2	9.1 ± 0.3	0.04 ± 0.01
alk	41.9 ± 2.7	36.64 ± 3.12	0.18 ± 0.03
D-LAK	<30	12.6 ± 0.19	0.02 ± 0.01
PAK	<30	6.8 ± 0.9	0.02 ± 0.01
pak	<30	11.3 ± 1.2	0.04 ± 0.01
EAK	248.1 ± 45.1	14.9 ± 0.74	5.64 ± 0.67
D-EAK	235.5 ± 45.8	22.3 ± 3.8	5.68 ± 1.45
eak	350.7 ± 24.5	28.1 ± 3.1	12.64 ± 3.0
aek	189.9 ± 1.7	9.8 ± 0.8	3.50 ± 0.13

In contrast, changes in side chain terminal amino acid in the branched polypeptides, resulting in a change in the overall charge of the compounds, had a dramatic effect on blood survival (Figure 2). The $\text{AUC}_{0-6\text{h}}$ for the relatively hydrophobic polycation lak was significantly ($p < 0.05$) lower than for alanylated polylysine (ak) (Table II). Moreover, a 10-fold increase in $\text{AUC}_{0-6\text{h}}$ was observed when glutamic acid was substituted in the terminal position in the alanine side chain (eak). This conferred an almost neutral charge to the polypeptide. Twenty-four hours after iv injection there was over 70 times more eak remaining in the circulation compared to ak (Table II).

The blood clearance of poly[Lys-(Glu_i-DL-Ala_m)] (EAK) and poly[Lys-(D-Glu_i-DL-Ala_m)] (D-EAK), containing L-Glu and D-Glu, respectively, are shown in Figure 3. The incorporation of the D-amino acid into the polypeptide had no significant effect on blood survival. The $\text{AUC}_{0-6\text{h}}$ for L-Glu-substituted polypeptide was 248.1 ± 45.1 calculated $t = 0$ cpm·h and for D-Glu substituted polypeptide $235.5 \pm 45.8\%$ calculated $t = 0$ cpm·h.

The effect of altering the position of the side chain substituted amino acid on the blood survival of the polypeptides was examined, with leucine and glutamic acid containing alanylated polylysines with small relative molecular mass. For the glutamic acid containing amphoteric pair of polypeptides poly[Lys-(Glu_i-DL-Ala_m)] (eak)/poly[Lys-(DL-Ala_m-Glu_i)] (aek) there was a 2-fold reduction in $\text{AUC}_{0-6\text{h}}$ (Table II) when glutamic acid is linked directly onto the polylysine backbone compared to substitution in the terminal side chain position (eak) (Figure 2). The $\text{AUC}_{0-6\text{h}}$ for eak and aek were $350.7 \pm 24.5\%$ calculated $t = 0$ cpm·h and $189.9 \pm 1.7\%$ calculated $t = 0$ cpm·h, respectively (Table II). In contrast, for the

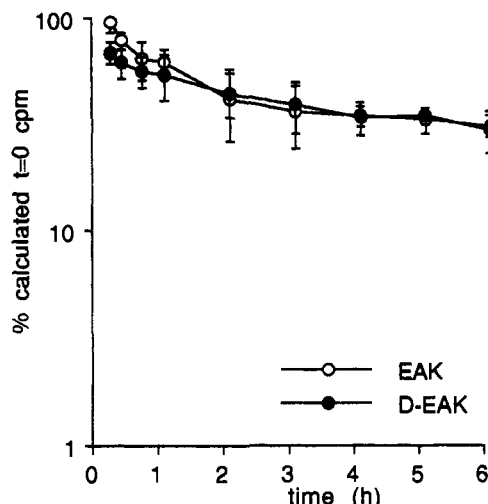


Figure 3. A comparison of the blood clearance of ^{125}I -labeled EAK and D-EAK in Balb/c mice following iv administration. $\text{AUC}_{0-6\text{h}}$ calculated from these data are given in Table II. Results are expressed as mean \pm standard deviation for groups of three mice.

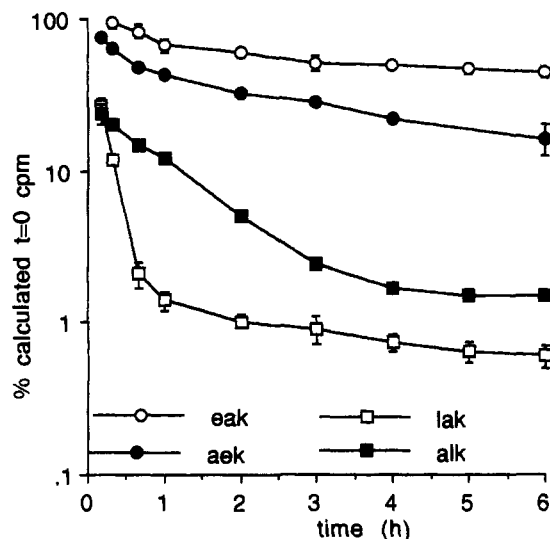


Figure 4. Blood clearance of ^{125}I -labeled eak, aek, lak, and alk following iv administration to Balb/c mice. $\text{AUC}_{0-6\text{h}}$ calculated from these data are given in Table II.

leucine-containing polycationic polypeptide pair poly-[Lys-(Leu-DL-Ala_m)] (lak)/poly[Lys-(DL-Ala_m-Leu_i)] (alk) a 2-fold increase in $\text{AUC}_{0-6\text{h}}$ was observed when leucine is directly linked to the polylysine backbone (alk) instead of substituted into the terminal side chain position (lak) (Figure 4, Table II). Twenty-four hours following injection there was a 4-fold difference in the amount of polypeptide surviving in the circulation (Table II).

Therefore, the blood survival for the series of branched polypeptides used in this study was primarily dependent on charge and side chain amino acid sequence. The glutamic acid containing amphoteric polypeptides showed the longest blood survival, the smaller peptide (eak, 46 kD) having a significantly higher blood survival than the larger peptide (EAK, 213 kD). This effect of size over the range 34–213 kD was not observed with the polycationic peptides ak/AK and lak/LAK, which all showed low blood survival. Similar observations have been reported with polycationic *N*-(2-hydroxypropyl)methacrylamide (29).

Tissue Distribution. The structural features of the branched polypeptides affecting tissue distribution were similar to those altering blood clearance. The effect of size

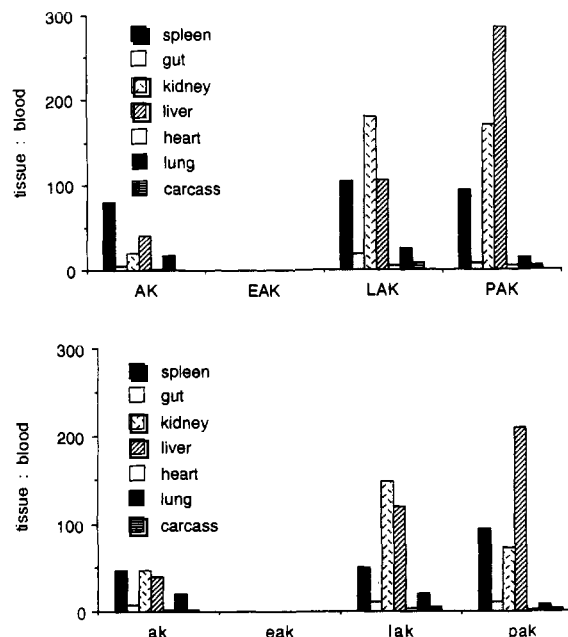


Figure 5. Tissue distribution of ^{125}I -branched polypeptides in Balb/c mice 24 h after iv administration. Results are expressed as mean for groups of three animals.

on tissue distribution 24 h after iv administration is shown in Figure 5. The data is expressed as a tissue to blood ratio, thus normalizing the results with respect to the absolute amount of the injected dose remaining in the blood. No significant difference was observed between the large and small relative molecular mass compounds of each individual polypeptide, but changes in the terminal side chain amino acid had a dramatic effect on tissue distribution. Figure 5 shows that the tissue distribution of eak, 24 h after iv administration, was very different from that of the other branched polypeptides studied. Alanylated polylysine (AK/ak) and the leucine (LAK/lak) and proline (PAK/pak) substituted polypeptides were taken out of the circulation, primarily into spleen, kidney, and liver. Much higher tissue to blood ratios were observed for LAK/lak and PAK/pak than for AK/ak. This is partly a reflection of the much lower blood survivals of these polypeptides compared to AK/ak (Table II). However, the glutamic acid substituted polypeptide (EAK/eak) was not preferentially taken up by any of the visceral organs. Tissue to blood ratios were less than 0.3 in all cases.

In contrast to observations in blood clearance studies, incorporation of the D-amino acid into the terminal side chain position resulted in an increase in the amount of polypeptide retained in the body (Table II), especially in the liver and spleen. This was seen for both amphoteric (EAK/D-EAK) and polycationic (LAK/D-LAK) peptides (Figure 6). This probably reflects the inability of the body to catabolize D-amino acids.

The effect of altering the position of the side chain substituted amino acid on the tissue distribution of the branched polypeptides is illustrated in Figure 7 and was in keeping with blood-survival data. For the amphoteric glutamic acid containing pair eak/aek the tissue-distribution profile was very similar although the whole-body survival for eak was significantly higher than for aek. Tissue to blood ratios were <1 in all tissues for both branched polypeptides. For the polycationic leucine-containing polypeptides the percentage injected dose per gram of alk in liver and spleen were much higher than for lak. It should be noted that although the blood clearance profile of ak and alk were very similar (Figures 2 and 4,

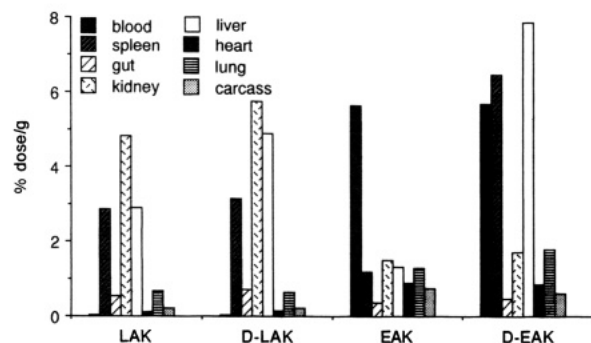


Figure 6. Effect of absolute configuration of terminal side chain amino acid on tissue distribution of ^{125}I -labeled branched polypeptides in Balb/c mice. Results shown are the mean of three animals.

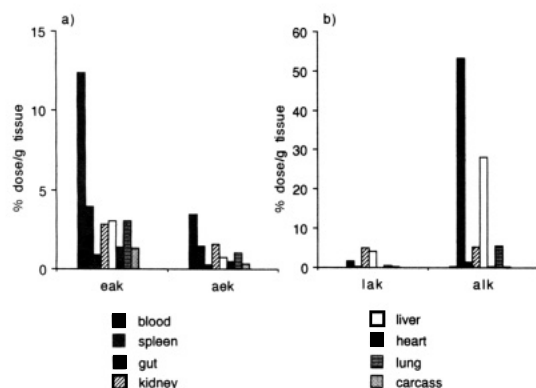


Figure 7. Effect of position of side-chain substitution on the biodistribution of ^{125}I -labeled branched polypeptides (a) eak/aek and (b) lak/alk. Data shown are the mean of three mice.

Table II), these two polypeptides showed dramatically different tissue-distribution profiles at 24 h. The amount of alk in spleen and liver was between 4- and 6-fold higher than for ak.

Whole-Body Survival. The whole-body survival (WBS) of the polypeptides 24 h after iv injection is summarized in Table II. There was no significant difference in the WBS of the large and small relative molecular mass versions of alanylated polylysine (AK/ak) and the leucine-substituted compound (LAK/lak). However, a significant ($p < 0.01$) 2-fold increase in WBS was observed with the small relative molecular mass polypeptides containing glutamic acid or proline.

The effect of alterations in charge, configuration of terminal amino acid, and side-chain sequence on the tissue distribution of the branched polypeptides were reflected in the WBS observed for these compounds. Indeed, as would be expected from the tissue distribution data the amphoteric polypeptides (EAK/eak) exhibited the highest WBS 24 h after administration. Incorporation of the D-amino acid at the side chain terminal position resulted in a 40–50% increase in WBS for both EAK and LAK. The dramatic alteration in blood-clearance and tissue-distribution profile observed when the side-chain amino acid sequence for the leucine-containing polycationic polypeptides was changed was also reflected in a much higher WBS for alk compared to lak.

In summary, these studies have indicated that it is primarily changes in the charge of the branched polypeptides, resulting from alterations in the identity of the terminal side chain amino acid, which contributed to the blood-clearance and tissue-distribution profiles in vivo. The amino acid sequence of the side chains of the branched polypeptides was also an important factor for both the

polycationic leucine-containing peptides and the amphoteric glutamic acid containing peptides studied. There was no correlation between conformation and biodistribution of the polypeptides, ordered (LAK/lak) and unordered polycations (PAK/pak) both being cleared rapidly.

In conclusion, the branched polypeptides with a poly-(L-lysine) backbone described in these studies provided a relatively simple system with which to investigate the effects of changes in molecular size, ionic charge, and primary structure on the biodistribution of carrier molecules and would allow suitable carriers to be selected according to their intended use. The polycationic peptides, exhibiting rapid blood clearance and high splenic uptake, have potential uses as carriers for haptens in antibody production and in the construction of synthetic vaccines. The amphoteric glutamic acid containing polypeptides would be good candidates for conjugation to cytotoxic drugs with potential use for site-specific drug delivery, either simply as drug-polypeptide conjugates or linked to monoclonal antibodies. This application is currently under investigation.

ACKNOWLEDGMENT

This work was partly supported by the Cancer Research Campaign, London, UK, and partly by an OTKA grant (2-86-1-484) from the Hungarian Academy of Science.

LITERATURE CITED

- (1) Ghose, T., and Blair, A. H. (1986) The design of cytotoxic agent-antibody conjugates. *CRC Crit. Rev. Ther. Drug Carrier Syst.* 3, 263.
- (2) Derrien, D., Midoux, P., Petit, C., Negre, E., Mayer, R., Mosigny, M., and Roche, A. C. (1989) Muramyl dipeptide bound to poly-L-lysine substituted with mannose and gluconoyl residues as macrophage activators. *Glycoconjugate J.* 6, 241.
- (3) Ferraiolo, B. L., and Benet, L. Z. (1985) Peptides and proteins as drugs. *Pharm. Res.* 151.
- (4) Pimm, M. V., Clegg, J. A., Garnett, M. C., and Baldwin, R. W. (1988) Biodistribution and tumour localisation of a methotrexate-monomonal antibody 791T/36 conjugate in nude mice with human tumour xenografts. *Int. J. Cancer* 41, 886.
- (5) Palfreyman, J. W., Aitchison, T. C., and Taylor, P. J. (1984) Guidelines for the production of polypeptide specific antisera using small synthetic oligopeptides as immunogens. *J. Immunol. Methods* 75, 383.
- (6) Balsari, A., Alzani, R., Parello, D., Morelli, D., Tagliabue, E., Gianni, L., Isetta, A. M., Bernard, S., Colnaghi, M. L., and Ghione, M. (1988) Monoclonal antibodies against doxorubicin. *Int. J. Cancer* 42, 798.
- (7) Szekerke, M., and Driscoll, J. S. (1977) The use of macromolecules as carriers of antitumour drugs. *Eur. J. Cancer* 13, 529.
- (8) Audibert, F., Jolivet, M., Chedid, L., Arnon, R., and Sela, M. (1982) Successful immunisation with a totally synthetic diphtheria vaccine. *Proc. Natl. Acad. Sci. U.S.A.* 79, 5042.
- (9) Hudecz, F., Votavova, H., Gaál, D., Šponar, J., Kajtár, J., Blaha, K., and Szekerke, M. (1985) Branched polypeptides with poly(L-lysine) backbone: synthesis, conformation and immunomodulation. *Polymeric Materials in Medication*, pp 265–289, Plenum Press, New York.
- (10) Hudecz, F., Kajtár, J., and Szekerke, M. (1988) Influence of side chain terminating moieties on the conformation of branched polypeptides and their conjugates with 4-(ethoxymethylene)-2-phenyl-5(4H)-oxazolone. *Biophys. Chem.* 31, 53.
- (11) Mezö, G., Hudecz, F., Kajtár, J., Szókan, G., and Szekerke, M. (1989) The influence of the side chain sequence on the structure-activity correlations of immunomodulatory branched polypeptides. *Biopolymers* 28, 1801.
- (12) Rajnavölgyi, É., Hudecz, F., Mezö, G., Szekerke, M., and Gergely, J. (1986) Isotype distribution and fine specificity of the antibody response on inbred mouse strains to four

- compounds belonging to a new group of synthetic branched polypeptides. *Mol. Immunol.* 23, 27.
- (13) Gaál, D., Hudecz, F., Kovács, A. L., and Szekerke, M. (1986) Immunomodulatory effect of synthetic branched polypeptides II. *Biol. Response Modif.* 5, 148.
- (14) Hudecz, F., Kutassi-Kovács, S., Mezö, G., and Szekerke, M. (1989) Biodegradability of synthetic branched polypeptide with poly-L-lysine backbone. *Biol. Chem. Hoppe-Seyler* 370, 1019.
- (15) Rajnavölgyi, É., Lányi, A., Hudecz, F., Kurucz, I., Kiss, K., László, G., Szekerke, M., and Gergely, J. (1989) Structural characteristics influencing the carrier function of synthetic branched polypeptides based on poly[Lys-(DL-Ala)₃] backbone. *Mol. Immunol.* 26, 949.
- (16) IUPAC-IUB Commission on Biochemical Nomenclature. (1972) *Biochem. J.* 127, 753.
- (17) IUPAC-IUB Commission on Biochemical Nomenclature. (1984) *Eur. J. Biochem.* 138, 9.
- (18) Hudecz, F., and Szekerke, M. (1980) Investigation of drug-protein interactions and the drug-carrier concept by the use of branched polypeptides as model systems. Synthesis and characterisation of the model peptides. *Collect. Czech. Chem. Commun.* 45, 933.
- (19) Hudecz, F., and Szekerke, M. (1985) Synthesis of new branched polypeptides with polylysine backbone. *Collect. Czech. Chem. Commun.* 50, 103.
- (20) Hudecz, F., and Szókán, Gy. (1985) Structure analysis of branched chain poly- and isopeptides based on HPLC of their dansyl derivatives. *Chromatography, the State of the Art*, pp 273-286, Akadémia Kiado, Budapest, Hungary.
- (21) Hudecz, F., Kovács, P., Kutassi-Kovács, S., and Kajtár, J. (1984) GPC, CD and sedimentation analysis of poly-Lys and branched chain poly-Lys-poly-DL-Ala peptides. *J. Colloid Polym. Sci.* 262, 208.
- (22) Bolton, A. E., and Hunter, W. M. (1973) The labelling of proteins to high specific radioactivities by conjugation to a ¹²⁵I-containing acylating agent. *Biochem. J.* 133, 529.
- (23) Pimm, M. V., Clegg, J. A., and Baldwin, R. W. (1987) Bio-distribution and tumour localisation of radiolabelled monoclonal antibody during continuous infusion in nude mice with human tumour xenografts. *Eur. J. Cancer Clin. Oncol.* 23, 521.
- (24) Rowland, M., and Tozer, T. N. (1989) Assessment of area. *Clinical Pharmacokinetics*, 32nd ed., pp 459-46, Lea and Fibiger, Philadelphia, PA.
- (25) Sela, M., Lupu, N., Yaron, A., and Berger, A. (1962) Water-soluble polypeptidyl gliadins. *Biochem. Biophys. Acta* 62, 594.
- (26) Szókán, Gy., Mezö, G., and Hudecz, F. (1988) Application of Marfey's reagent in racemization studies of amino acids and peptides. *J. Chromatogr.* 444, 115.
- (27) Votavova, H., Hudecz, F., Sponar, J., Szekerke, M., and Blaha, K. (1982) Conformation of branched polypeptides based on poly(L-lysine). Effect of the ionic strength and of the presence of alcohols. *Collect. Czech. Chem. Commun.* 47, 3437.
- (28) Votavova, H., Hudecz, F., Kajtár, J., Sponar, J., Blaha, K., and Szekerke, M. (1985) Conformation of branched polypeptides based on poly(L-lysine): the effect of terminal amino acids in the branches. *Collect. Czech. Chem. Commun.* 50, 228.
- (29) Seymour, L. W., Duncan, R., Strohm, J., and Kopecek, J. (1987) Effect of molecular weight (M_w) of *N*-(2-hydroxypropyl) methacrylamide copolymers on body distributions and rate of excretion after subcutaneous, intraperitoneal and intravenous administration to rats. *J. Biomed. Mater. Res.* 21, 1341.

Enhanced Kidney Clearance with an Ester-Linked ^{99m}Tc -Radiolabeled Antibody Fab'-Chelator Conjugate

Robert W. Weber,* Raymond H. Boutin, Mark A. Nedelman, John Lister-James,[†] and Richard T. Dean[†]

Chemistry Research, Centocor, Incorporated, 244 Great Valley Parkway, Malvern, Pennsylvania 19355.

Received April 9, 1990

Bifunctional chelators for labeling antibodies with ^{99m}Tc based on the N_3S core of (mercaptoacetyl)-triglycine having ester or amide linking moieties were synthesized and site-specifically attached to the sulfhydryl groups of the Fab' fragment of antimyosin. Protein labeling was quantitative after 15 min; postlabeling purification was not necessary. The radiolabeled conjugates exhibited no loss of immunoreactivity. Under basic conditions, the ester-linked conjugate lost 95% of the radiolabel in the form of the ^{99m}Tc complex of (mercaptoacetyl)triglycine as determined by RP-HPLC, while the radioactivity in the amide-linked conjugate remained completely bound to the protein. In a mouse biodistribution study, the ester-linked conjugate showed a 2-fold enhancement in clearance from the kidney when compared to the amide-linked product.

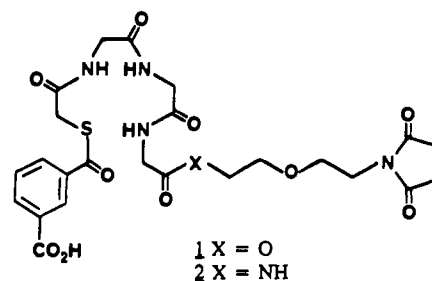
INTRODUCTION

The use of monoclonal antibodies as carriers of radioisotopes for diagnosis or therapy requires labeling methodologies which result in stable products with uncompromised immunoreactivity. Ideally, the radiolabeled product should be nonimmunogenic and exhibit rapid clearance from the blood, nontarget tissues, and excretory organs. For radiopharmaceuticals, the use of Fab or Fab' fragments of the monoclonal antibody offer several advantages over the IgG. These smaller fragments lack the Fc region of the IgG molecule and thus circumvent possible adverse effects due to this region. The fragments are better able to penetrate the target tissues, are less immunogenic, and are cleared from the circulation more rapidly than the intact IgG. The major route of clearance for these ~50,000 Da species is via the renal system, making the kidneys the critical organs in regard to absorbed radiation dosimetry. It would be advantageous if a mechanism to facilitate clearance from this organ could be constructed into the radiopharmaceutical product.

The goal of our research was to develop labeling methodology with ^{99m}Tc (the radionuclide of choice for diagnostic imaging) of antibody fragments which would allow quantitative, stable labeling with preservation of immunoreactivity in a short period of time (<30 min). In addition, the labeled product should show enhanced whole-body clearance, with an emphasis on clearance via the renal system.

Antibodies have been radiolabeled with ^{99m}Tc by attachment of ^{99m}Tc to native cysteine residues (direct labeling (1,2)), through the use of bifunctional chelators (3-9), and by conjugating a preformed ^{99m}Tc complex to the protein (10). The bifunctional chelator approach was chosen to achieve the above objectives as it appeared to offer the most structural versatility. The bifunctional chelators were to be site-specifically attached to the sulfhydryls of the C-terminus region of antibody Fab' fragments. As these sulfhydryls are located distal to the antigen binding region, the immunoreactivity of the product should

be preserved. To enhance the clearance of the radioactivity from nontarget tissues, an ester linkage was incorporated between the ^{99m}Tc complex and the antibody fragment. Mears (11, 12) and Paik (13, 14) have examined the effect of utilizing metabolizable esters when linking ^{111}In complexes to antibodies. In these studies, the ester-linked labeled conjugates typically exhibited a shorter biological half-life and an increase in the target to blood ratio. The N_3S core of (mercaptoacetyl)triglycine was chosen to bind the ^{99m}Tc , as this complex has been shown to form readily, is stable in vivo, and is rapidly excreted through the kidneys (15). Linkage of the chelator to the Fab' fragment through esterification of the C-terminal glycine of the N_3S system was proposed, as hydrolysis in vivo at this point would yield the ^{99m}Tc complex of (mercaptoacetyl)triglycine, which should be rapidly excreted through the kidneys. On the basis of the above considerations, the ester-linked bifunctional chelator 1 was targeted for synthesis, as well as the amide linked analogue 2 for comparative purposes.



Attachment of the chelators to antibody sulfhydryls occurs through Michael addition to the N-substituted maleimides of 1 and 2. The sulfhydryl group of the N_3S core required protection during the synthesis and subsequent protein conjugation step due to the presence of the maleimide. The *S*-isophthaloyl ester was chosen for this purpose to increase the hydrophilicity of the compound, as the protein conjugation was to be done under aqueous conditions. Solubility considerations led to the choice of the ether group in the chelator-antibody linking chain. Antimyosin antibody R11D10 Fab' was chosen as the model

[†] Present address: Diotech, Inc., 9 Delta Drive, Londonderry, NH 03053.

antibody for this study, as ^{111}In -labeled antimyosin Fab-DTPA has demonstrated utility in imaging myocardial necrosis (16).

This report describes the synthesis of chelators 1 and 2, their conjugation to antimyosin Fab', the deblocking of the sulfhydryl of the N_3S core, and subsequent $^{99\text{m}}\text{Tc}$ labeling. The labeled conjugates were compared in terms of immunoreactivity, stability in serum, and their susceptibility toward hydrolysis under basic conditions. Biodistribution studies in mice were also performed to determine the effect of the ester function on the clearance of the radiopharmaceutical.

EXPERIMENTAL PROCEDURES

Melting points were determined in open capillaries with a Thomas-Hoover melting point apparatus and are uncorrected. ^1H NMR spectra were recorded at 300 MHz on a General Electric QE-300 spectrometer and are reported in ppm (δ units) downfield of internal tetramethylsilane. Elemental analyses were performed by Galbraith Laboratories, Inc., Knoxville, TN. High-resolution FAB mass spectra were obtained at the University of California, Berkeley. Antimyosin (R11D10) F(ab')_2 was obtained from Centocor Europe, B.V. Phosphate buffer refers to 0.1 M sodium phosphate, pH 7.0, containing 1 mM EDTA. Protein concentration was determined from the absorption at 280 nm, $\epsilon_{0.1\%}^{1\text{cm}} = 1.4$. Equivalents of sulfhydryls were determined by Ellman's assay (17). Analytical gel-filtration HPLC was performed on a Waters unit with a Du Pont Zorbax GF-250 column, with both UV and radiometric detection. The running buffer was 0.2 M sodium phosphate, pH 6.8. Samples having free thiol groups were blocked with *N*-ethylmaleimide prior to injection. For reverse-phase HPLC, a Brownlee Labs ODS-MP Spheri-5 (100 \times 4.6 mm) column was used; the running buffer was 5% ethanol in 0.01 M sodium phosphate, pH 6.5. Silica gel impregnated paper (Gelman, cut to 1 \times 10 cm) was used for ITLC. After development, the strips were cut in half and the two halves counted in a well counter. Non protein bound $^{99\text{m}}\text{Tc}$ was determined by ITLC in 0.1 M citrate, pH 5.0, where the radiolabeled protein remained at the origin. Chromatographically immobile $^{99\text{m}}\text{Tc}$, assumed to be $^{99\text{m}}\text{Tc}$ colloids (e.g. TcO_2) were assayed for by ITLC in water/ethanol/aqueous ammonia 5:2:1. In this procedure, the ITLC strip was spotted with 5% bovine serum albumin (BSA) in phosphate-buffered saline (PBS, Dulbecco 'A') (20 μL) prior to application of the radiolabeled-protein solution (10 μL). In this system the $^{99\text{m}}\text{Tc}$ -labeled proteins migrated with the solvent.

2-(2-Maleimidoethoxy)ethanol (5). A solution of 2-(2-aminoethoxy)ethanol (4; 1.35 g, 13 mmol) in saturated NaHCO_3 (65 mL) was cooled in an ice bath and treated with *N*-(methoxycarbonyl)maleimide (3; 2.00 g, 13 mmol). After 20 min, the ice bath was removed and the solution was stirred at room temperature for 30 min. The solution was extracted with chloroform (3 \times 50 mL) and the combined extracts were dried (Na_2SO_4). Removal of the solvent under reduced pressure gave maleimido alcohol 5 as an oil (1.70 g, 71%) (18): NMR (CDCl_3) δ 2.32 (t, 1 H, OH), 3.54 (m, 2 H), 2.64 (m, 6 H), 6.72 (s, 2 H).

2-(2-Maleimidoethoxy)ethyl *N*-*t*-Boc-glycinate (6). A solution of maleimido alcohol 5 (21.2 g, 114 mmol) in methylene chloride (550 mL) was cooled in an ice bath and treated with 2,6-di-*t*-butyl-4-methylpyridine (23.4 g, 114 mmol) followed by trifluoromethanesulfonic anhydride (19.2 mL, 114 mmol). After stirring at 0 $^\circ\text{C}$ for 1 h, the resulting precipitate was removed by filtration. The filtrate containing the triflate was then added to a solution of *N*-*t*-

Boc-glycine (20.0 g, 114 mmol) and *N,N*-diisopropylethylamine (19.9 mL, 114 mmol) in methylene chloride (350 mL). After stirring at room temperature for 2 h, the mixture was washed with water (2 \times 400 mL) and the organic phase was dried (Na_2SO_4). Removal of the solvent under reduced pressure gave an oil which was chromatographed (SiO_2 , hexanes/ethyl acetate gradient) to provide ester 6 (9.6 g, 25%), as a watery white oil: NMR (CDCl_3) δ 1.45 (s, 9 H), 3.66 (m, 6 H), 3.94 (d, 2 H), 4.26 (t, 2 H), 5.14 (m, 1 H), 6.74 (s, 2 H).

2-(2-Maleimidoethoxy)ethyl Glycinate (7). *t*-Boc derivative 6 (8.3 g, 24 mmol) was stirred in trifluoroacetic acid (30 mL) for 1 h. Removal of excess TFA under vacuum gave amine 7 in quantitative yield as the TFA salt which was used directly in the coupling reaction with active ester 13: NMR ($\text{DMSO}-d_6$) δ 2.58 (m, 6 H), 3.84 (s, 2 H), 4.24 (m, 2 H), 7.04 (s, 2 H).

Succinimidyl 3-(*tert*-Butyloxycarbonyl)benzoate (9). A solution of mono-*tert*-butyl isophthalate (8 (19); 66.5 g, 300 mmol) in THF (1 L) was treated with *N*-hydroxysuccinimide (34.4 g, 300 mmol) followed by dicyclohexylcarbodiimide (60.9 g, 300 mmol). After stirring for 4 h, the mixture was allowed to stand at room temperature for 3 days. The precipitated urea was removed by filtration and the filtrate was concentrated under reduced pressure to give an oil which crystallized from 2-propanol to provide active ester 9 (67.7 g, 71%): mp 112–113 $^\circ\text{C}$; NMR (CDCl_3) δ 1.61 (s, 9 H), 2.94 (s, 4 H), 7.60 (m, 1 H), 8.30 (m, 2 H), 8.73 (m, 1 H). Anal. ($\text{C}_{16}\text{H}_{17}\text{NO}_6$) C, H, N.

2-[[3-(*tert*-Butyloxycarbonyl)benzoyl]thio]acetic Acid (10). To a solution of NHS ester 9 (67.2 g, 210 mmol) in methylene chloride (500 mL) was added 2-mercaptoacetic acid (14.6 mL, 210 mmol) followed by 4-(dimethylamino)pyridine (51.4 g, 420 mmol). After stirring at room temperature for 3.5 h, the mixture was washed with 1 N HCl (2 \times 250 mL). The organic phase was dried (Na_2SO_4) and the solvent was removed under reduced pressure. The resulting oil was chromatographed (SiO_2 , ethyl acetate/hexanes containing 1% acetic acid gradient) to provide acid 10 (29.5 g, 47%) as an oil which solidified upon drying under vacuum: mp 96–98 $^\circ\text{C}$; NMR (CDCl_3) δ 1.62 (s, 9 H), 3.96 (s, 2 H), 7.55 (m, 1 H), 8.05 (m, 1 H), 8.24 (m, 1 H), 8.57 (m, 1 H). Anal. ($\text{C}_{14}\text{H}_{16}\text{O}_5\text{S}$) C, H, S.

Succinimidyl 2-[[3-(*tert*-Butyloxycarbonyl)benzoyl]thio]acetate (11). A mixture of acid 10 (28.3 g, 95 mmol), *N*-hydroxysuccinimide (11.1 g, 95 mmol), and dicyclohexylcarbodiimide (19.8 g, 96 mmol) in THF (300 mL) was stirred at room temperature for 3 days. The urea was removed by filtration and the solvent was removed under reduced pressure. The resulting oil was crystallized from 2-propanol to yield 31.7 g (85%) of active ester 11: mp 118–120 $^\circ\text{C}$; NMR (CDCl_3) δ 1.62 (s, 9 H), 2.86 (s, 4 H), 4.21 (s, 2 H), 7.56 (m, 1 H), 8.12 (m, 1 H), 8.24 (m, 1 H), 8.56 (m, 1 H). Anal. ($\text{C}_{18}\text{H}_{19}\text{NO}_7\text{S}$) C, H, N, S.

[2-[[3-(*tert*-Butyloxycarbonyl)benzoyl]thio]acetyl]glycylglycine (12). To glycylglycine (12.3 g, 93 mmol) and NaHCO_3 (39 g, 464 mmol) in water (300 mL) was added NHS ester 11 (36.5 g, 93 mmol) in THF (300 mL). The resulting mixture was stirred at room temperature for 1 h followed by removal of the THF under reduced pressure. The solution was then diluted to 800 mL with water and acidified to pH 2 with 4 N HCl. The precipitate which formed was collected and recrystallized from aqueous acetone to afford dipeptide 12 (19.2 g, 50%): mp 188–189 $^\circ\text{C}$; NMR ($\text{DMSO}-d_6$) δ 1.58 (s, 9 H), 3.78 (m, 4 H),

3.94 (s, 2 H), 7.73 (m, 1 H), 8.20 (m, 2 H), 8.27 (m, 1 H), 8.39 (m, 1 H), 8.58 (m, 1 H). Anal. ($\text{C}_{18}\text{H}_{22}\text{N}_2\text{O}_7\text{S}$) C, H, N, S.

Succinimidyl [2-[[3-(*tert*-Butyloxycarbonyl)-benzoyl]thio]acetyl]glycylglycinate (13). A solution of dipeptide 12 (18.9 g, 46 mmol), *N*-hydroxysuccinimide (5.3 g, 46 mmol), and dicyclohexylcarbodiimide (9.5 g, 46 mmol) in DMF (200 mL) was stirred at room temperature for 20 h. The precipitated urea was filtered off and the DMF was removed under vacuum. The resulting oil was recrystallized from 2-propanol to afford active ester 13 (10.5 g, 45%) mp 122–124 °C; NMR ($\text{DMSO}-d_6$) δ 1.58 (s, 9 H), 2.82 (s, 4 H), 3.83 (m, 2 H), 3.94 (m, 2 H), 4.31 (m, 2 H), 7.73 (m, 1 H), 8.20 (m, 2 H), 8.39 (m, 1 H), 8.65 (m, 2 H). Anal. ($\text{C}_{22}\text{H}_{25}\text{N}_3\text{O}_4\text{S}$) H, N, S; C: calcd, 52.07; found, 51.21.

2-(2-Maleimidoethoxy)ethyl [2-[[3-(*tert*-Butyloxycarbonyl)benzoyl]thio]acetyl]glycylglycylglycinate (14). 2-(2-Maleimidoethoxy)ethyl glycinate 7 (5.8 g, 24 mmol free base based on 6) was mixed with a solution of NaHCO_3 (20.4 g, 243 mmol) in water (200 mL), followed by addition of active ester 13 (10.0 g, 20 mmol). After stirring at room temperature for 1 h, water (300 mL) and chloroform (300 mL) were added. An emulsion formed which was treated with water (100 mL), brine (50 mL), and 2-propanol (100 mL). The organic layer was separated, washed with brine, and dried (Na_2SO_4). Removal of the solvent gave crude material which was chromatographed (SiO_2 , chloroform/2-propanol gradient) to provide 4.2 g (33%) of maleimido tripeptide 14 as a waxy white solid: mp 98–100 °C; NMR ($\text{DMSO}-d_6$) δ 1.58 (s, 9 H), 3.57 (m, 4 H), 3.83 (m, 8 H), 3.95 (m, 2 H), 4.12 (m, 2 H), 7.05 (s, 2 H), 7.73 (m, 1 H), 8.20 (m, 2 H), 8.30 (m, 2 H), 8.39 (t, 1 H), 8.56 (t, 1 H); exact mass (FAB) calcd for $\text{C}_{28}\text{H}_{34}\text{N}_4\text{O}_{11}\text{S}$ (MH^+) 635.2022, found 635.2034. Anal. ($\text{C}_{28}\text{H}_{34}\text{N}_4\text{O}_{11}\text{S}$) C, H, N, S.

5-(*N*-Maleimido)-3-oxapentyl [2-[[3-Carboxybenzoyl]thio]acetyl]glycylglycylglycinate (1). *tert*-Butyl maleimido ester 14 (3.8 g, 6 mmol) was stirred with trifluoroacetic acid (30 mL) for 1 h at room temperature. The TFA was removed under reduced pressure and crystallization from aqueous acetone yielded bifunctional chelator 1 (2.70 g, 78%): mp 169–172 °C; NMR ($\text{DMSO}-d_6$) δ 3.56 (m, 6 H), 3.83 (m, 6 H), 3.94 (s, 2 H), 4.12 (m, 2 H), 7.04 (s, 2 H), 7.71 (m, 1 H), 8.20 (m, 4 H), 8.44 (t, 1 H), 8.55 (t, 1 H); exact mass (FAB) calcd for $\text{C}_{24}\text{H}_{26}\text{N}_4\text{O}_{11}\text{S}$ (MH^+) 579.1396, found 579.1404. Anal. ($\text{C}_{24}\text{H}_{26}\text{N}_4\text{O}_{11}\text{S} \cdot 1.7\text{H}_2\text{O}$) C, H, N, S, H_2O .

2-[*N*-(*tert*-Butyloxycarbonyl)amino]ethyl Cyano-methyl Ether (16). A solution of *N*-*t*-Boc-ethanolamine (15, 12.9 g, 80 mmol) in THF (400 mL) under Ar was cooled in an ice bath and treated dropwise with a solution of sodium bis(trimethylsilyl)amine (85 mL of 1 M in THF, 85 mmol) with mechanical stirring. Upon completion of the addition, the mixture was stirred an additional 15 min and treated dropwise with bromoacetonitrile (9.6 g, 80 mmol) in THF (50 mL). After warming to room temperature, the solvent was removed under reduced pressure and the residue was taken up in ethyl acetate and washed several times with water. The organic phase was dried (Na_2SO_4) and removal of the solvent gave an oil which was chromatographed (SiO_2 , hexanes/ethyl acetate gradient) to afford nitrile 16 (5.3 g, 33%) as an oil: NMR (CDCl_3) δ 1.54 (s, 9 H), 3.42 (t, 2 H), 3.70 (t, 2 H), 4.33 (s, 2 H), 4.94 (s, 1 H).

2-[*N*-(*tert*-Butyloxycarbonyl)amino]ethyl 2'-Aminoethyl Ether (17). A solution of nitrile 16 (3.9 g, 19.5 mmol) in acetic acid (60 mL) was treated with Pd/C

(0.8 g of 5%) and hydrogenated on a Parr apparatus at 45 psig for 1 h, during which time the shaker bottle was repressurized as necessary. The catalyst was removed by filtration through Celite and the majority of the acetic acid was removed under reduced pressure. The residue was taken up in water and the acidic solution was extracted twice with methylene chloride, and the extracts were discarded. The aqueous solution was brought to pH 12 with 50% NaOH and extracted with methylene chloride. The combined extracts were dried (Na_2SO_4) and removal of the solvent gave amine 17, (3.0 g, 76%) as an oil: NMR (CDCl_3) δ 1.56 (s, 9 H), 2.92 (t, 2 H), 3.39 (t, 2 H), 3.58 (m, 4 H), 5.12 (s, 1 H).

***N*-[5-[(*tert*-Butyloxycarbonyl)amino]-3-oxapentyl]-maleimide (18).** Amino ether 17 (2.0 g, 10 mmol), in saturated aqueous NaHCO_3 (50 mL) was cooled in an ice bath. *N*-(methoxycarbonyl)maleimide (3; 1.6 g, 10 mmol) was added in one portion. After stirring for 30 min, the ice bath was removed and stirring was continued for an additional 30 min. The aqueous mixture was extracted with methylene chloride, and the combined extracts were dried (Na_2SO_4), concentrated, and chromatographed (SiO_2 , hexanes/ethyl acetate) to yield maleimide 18 (1.7 g, 60%): NMR (CDCl_3) δ 1.53 (s, 9 H), 3.28 (m, 2 H), 3.53 (t, 2 H), 3.62 (t, 2 H), 3.75 (m, 2 H), 4.95 (s, 1 H), 6.72 (s, 2 H).

***N*-(5-Amino-3-oxapentyl)maleimide Trifluoroacetate (19).** *N*-Boc derivative 18 (1.6 g, 5.6 mmol) was stirred in TFA (10 mL) for 1 h. Excess TFA was removed under vacuum to give an oil which crystallized from ether to provide 1.5 g (90%) of amine salt 19: NMR ($\text{DMSO}-d_6$) δ 2.94 (m, 2 H), 3.60 (m, 6 H), 7.07 (s, 2 H).

[2-[[3-(*tert*-Butyloxycarbonyl)benzoyl]thio]acetyl]glycylglycylglycine (20). A solution of triglycine (4.1 g, 22 mmol) and NaHCO_3 (9.07 g, 108 mmol) in water (100 mL) was treated with THF (100 mL) followed by active ester 11 (8.5 g, 22 mmol). After stirring at room temperature for 1.5 h, the THF was evaporated under reduced pressure. The aqueous solution was diluted with water (350 mL) and the pH was brought to 2.5 with 4 N HCl. The resulting precipitate was collected and recrystallized from aqueous acetone to provide 5.5 g (54%) of triglycine derivative 20: mp 189–190 °C; NMR ($\text{DMSO}-d_6$) δ 1.58 (s, 9 H), 3.77 (m, 6 H), 3.94 (s, 2 H), 7.73 (t, 1 H), 8.20 (m, 4 H), 8.38 (t, 1 H), 8.55 (t, 1 H).

Succinimidyl [2-[[3-(*tert*-Butyloxycarbonyl)-benzoyl]thio]acetyl]glycylglycylglycinate (21). To triglycine 20 (1.8 g, 3.8 mmol) in DMF (20 mL) was added *N*-hydroxysuccinimide (0.44 g, 3.8 mmol) followed by dicyclohexylcarbodiimide (0.9 g, 4.3 mmol). After stirring at room temperature overnight, the mixture was filtered and the DMF was removed by vacuum pump. The oil which resulted yielded a precipitate from 2-propanol of the NHS ester 21 (1.4 g, 64%): NMR ($\text{DMSO}-d_6$) δ 1.58 (s, 9 H), 2.82 (s, 4 H), 3.80 (m, 4 H), 3.94 (s, 2 H), 4.29 (d, 2 H), 7.72 (t, 1 H), 8.19 (t, 2 H), 8.30 (t, 1 H), 8.38 (s, 1 H), 8.53 (m, 2 H).

***N*-[2-(2-Maleimidoethoxy)ethyl][2-[[3-(*tert*-butyloxycarbonyl)benzoyl]thio]acetyl]glycylglycylglycinamide (22).** Maleimide 19 (0.3 g, 1 mmol) in THF (20 mL) was treated with diisopropylethylamine (210 μL , 1.2 mmol) followed by active ester 21 (0.57 g, 1 mmol) in dichloromethane (20 mL). After stirring at room temperature for 1.5 h the mixture was filtered and concentrated. Chromatography (SiO_2 , dichloromethane/methanol gradient) provided amide 22 (0.25 g, 41%), which crystallized during removal of the solvent: mp 164–166 °C; NMR ($\text{DMSO}-d_6$) δ 1.60 (s, 9 H), 3.18 (s, 2 H), 3.48 (m, 6 H), 3.67 (m, 2 H), 3.79 (m, 4 H), 3.98 (m, 2 H), 7.03

(s, 2 H), 7.74 (m, 1 H), 7.82 (m, 1 H), 8.13 (m, 1 H), 8.22 (m, 3 H), 8.40 (m, 1 H), 8.59 (m, 1 H); exact mass (FAB) calcd for $C_{28}H_{35}N_5O_{10}S$ (MH⁺) 634.2182, found 634.2195.

N-(5-Maleimido-3-oxapentyl)[2-[(3-carboxybenzoyl)-thio]acetyl]glycylglycylglycinamide (2). *tert*-Butyl ester **22** (0.12 g, 0.19 mmol) was stirred in TFA (2 mL) at room temperature for 4 h. Removal of the TFA under vacuum afforded amide **2** (0.11 g, 100%) as a white solid: mp 177–180 °C; NMR (DMSO-*d*₆) δ 3.17 (m, 2 H), 3.41 (m, 2 H), 3.57 (m, 4 H), 3.75 (m, 6 H), 3.96 (s, 2 H), 7.02 (s, 2 H), 7.75 (m, 4 H), 8.09 (t, 1 H), 8.22 (m, 3 H), 8.44 (s, 1 H), 8.53 (t, 1 H); exact mass (FAB) calcd for $C_{24}H_{27}N_5O_{10}S$ (MH⁺) 578.1556, found 578.1569.

Preparation of Antimyosin Fab'. Antimyosin F(ab')₂ (5–10 mg/mL) was reduced with dithiothreitol (10 mM) for 1–1.5 h at room temperature. The antibody fragment solution was desalted by Sephadex G-25 chromatography with phosphate buffer. Protein-containing fractions were combined; GF-HPLC indicated complete reduction.

General Procedure for Preparation of the Antimyosin Fab' Conjugates of 1 and 2. The antimyosin Fab' (2–6 mg/mL) in phosphate buffer was treated with a solution of ester **1** or amide **2** (10 equiv per antibody SH) in DMF such that the final concentration of DMF in the antibody solution was 4% or less. After standing at room temperature for 1.5 h, the excess reagent was removed by gel filtration on Sephadex G-25 (medium). The antibody conjugate was eluted with phosphate buffer; no sulfhydryls were detected by Ellman's assay.

General Procedure for Cleavage of the Thiol Esters. The antimyosin Fab' conjugates were mixed with equal volumes of a solution of 1.0 M hydroxylamine in 0.5 M HEPES, at pH 7.5 (adjusted with 50% NaOH). After standing at room temperature for 5 min, the deblocked conjugate was purified by Sephadex G-25 (medium) chromatography with phosphate buffer. Protein-containing fractions were assayed for sulfhydryl content; typically 1.5–2.5 mol of SH/mol of Fab' were found.

^{99m}Tc Labeling of the Antimyosin Conjugates. A vial was charged with 1 mL of a solution containing potassium D-glucarate (12 mg/mL) and stannous chloride (100 μ g/mL) in 0.2 M NaHCO₃ at pH 6.8. Following lyophilization, the mixture was treated with sodium [^{99m}Tc]-pertechnetate solution (1 mL, 25 mCi, diluted with saline if necessary) from a ⁹⁹Mo/^{99m}Tc generator. After standing at room temperature for 15 min, an aliquot of the ^{99m}Tc glucarate solution was mixed with an equal volume of the deblocked antimyosin Fab' conjugate in phosphate buffer (1 mg/mL). The solution was mixed and allowed to stand at room temperature for 15 min. At this time, ITLC indicated that 99% of the radioactivity was protein bound (100% by HPLC, *t*_R = 9.7 min). No ^{99m}Tc colloids were observed by ITLC.

Immunoreactivity of the ^{99m}Tc-Labeled Antimyosin Fab' Conjugates. The ^{99m}Tc-labeled antibodies were diluted to 5 μ g/mL with 1% BSA in PBS. A 100- μ L aliquot was applied to an affinity column (1-mL bed volume, canine heart myosin coupled to CNBr-activated Sepharose 6B), which had been equilibrated with 1% BSA in PBS. After 15 min the column was eluted with 10 mL of 1% BSA in PBS followed by 10 mL of 0.1 M glycine, pH 2.5. Aliquots (1 mL) of both 10-mL fractions were counted in a NaI (T1) well counter. The percent immunoreactivity was calculated as

$$\% \text{ immunoreactivity} = \frac{\text{total net counts eluted by glycine}}{\text{total net counts eluted by glycine and BSA}} \times 100$$

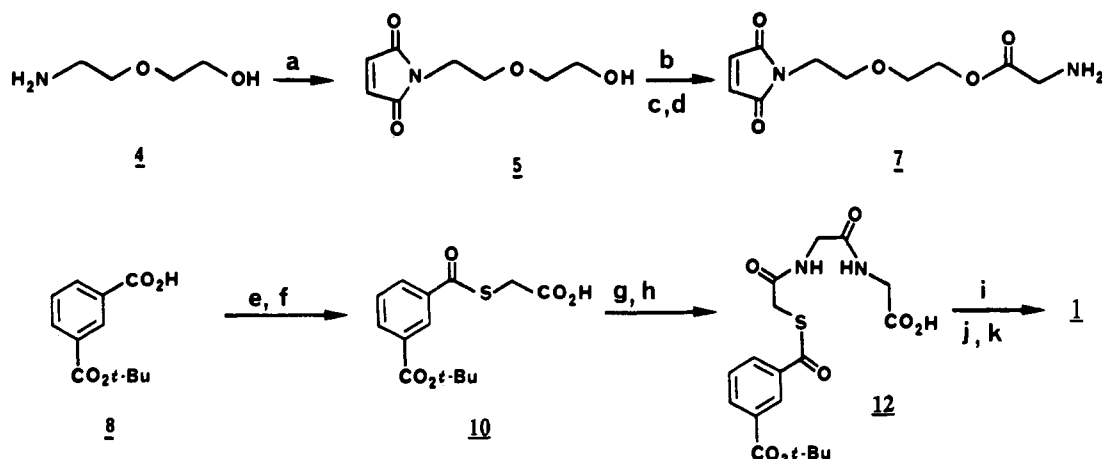
Evaluation of the Stability of the ^{99m}Tc-Labeled Conjugates and Base-Hydrolysis Studies. An aliquot of the ^{99m}Tc-labeled R11D10 conjugate was mixed with an equal volume of saline or fresh human serum (prepared from freshly drawn blood by centrifugation after clotting). The samples were then incubated at 37 °C. Aliquots were removed at various times and analyzed by HPLC. For the base-hydrolysis study, the radiolabeled Fab' fragments were buffer-exchanged into 0.1 M sodium phosphate pH 10 by passage through preequilibrated Sephadex G-25 columns. The samples were incubated at 37 °C and analyzed after 24 h by GF-HPLC, ITLC, and RP-HPLC.

Biodistribution Studies. Normal CF-1 female mice (8–10 weeks old) were injected intravenously via a lateral tail vein with 0.1 mL of each of the radiolabeled preparations (100 μ Ci/5 μ g). Mice were killed by cervical dislocation at 0.5, 1, 2, 5, and 24 h after injection in each of the studies (three mice per time point) and the following organs sampled: blood, heart, lung, liver, spleen, kidneys, stomach, small intestine, large intestine, muscle, and skin/fat. Tissue samples were rinsed of residual blood and blotted dry prior to weighing and counting for activity in a multichannel γ -scintillation counter (LKB). Data were calculated and represented as percent of the injected activity per gram (mean \pm 1 SD).

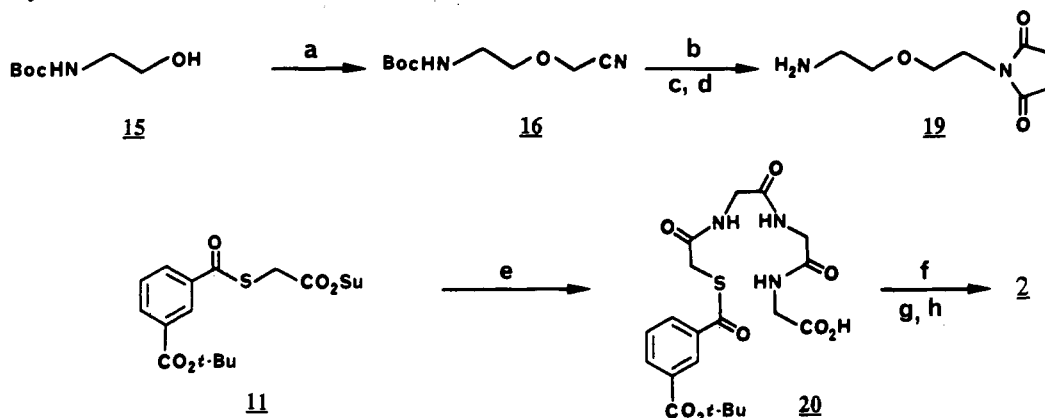
RESULTS AND DISCUSSION

The syntheses of the bifunctional chelators are outlined in Schemes I and II. The initial plan called for the construction of the tripeptide chelator followed by formation of the linker bond with the appropriate maleimide. The maleimides were readily prepared from *N*-(methoxycarbonyl)maleimide (**3**) and the corresponding amine according to the method of Keller and Rudinger (20). While this approach proved satisfactory for amide-linked ligand **2**, the direct esterification of triglycine derivative **20** gave poor yields of product and was difficult to scale up. The modified route illustrated in Scheme I was then developed. In this sequence, *N*-Boc-glycine was esterified via the triflate of alcohol **5**, followed by reaction with a diglycine derivative. The *m*-carboxyl of the *S*-isophthaloyl group was protected as the *tert*-butyl ester during the course of the syntheses, as the increased lipophilicity simplified manipulation of the intermediates.

The Fab' fragment of antimyosin was generated from the F(ab')₂ by reduction with dithiothreitol and typically contained 3–4 SH/Fab'. Although the inter-(truncated)-heavy-light chain disulfide bridge may be reduced, the strong interchain hydrophobic interaction causes the two chains to remain associated on GF-HPLC and in vivo (21). The Fab' sulfhydryls were alkylated by treating a buffered solution of the antibody fragment at pH 7 with a 10-fold excess of the ligand. By conducting the conjugation reaction at neutral pH, only the protein sulfhydryl groups will react with the maleimide; lysines will not be alkylated. This then limits the number of chelators which are attached to the antibody to the number of available sulfhydryls. Following the removal of excess chelator, no sulfhydryls were detected by Ellman's assay, indicating that all of the available sulfhydryls had been alkylated. The thiol esters of the antibody-chelator conjugate were cleaved through aminolysis with hydroxylamine (**22**), which typically yielded 1.5–2.5 SH/Fab' following gel filtration. In a control study, antimyosin Fab' was reacted with *N*-ethylmaleimide to block the sulfhydryls. Exposure of this material to hydroxylamine as above failed to produce any sulfhydryls, indicating that the sulfhydryls produced from the conjugated material must be from the ligands. This is of importance as any nonligand-associated thiols can

Scheme I^a. Synthesis of the Ester-Linked Chelator 1

Reagents: (a) NaHCO_3 , *N*-(methoxycarbonyl)maleimide; (b) $(\text{CF}_3\text{SO}_2)_2\text{O}$, base; (c) *N*-Boc-Gly, *i*-Pr₂NEt; (d) TFA; (e) HOSu, DCC; (f) $\text{HSCH}_2\text{CO}_2\text{H}$, DMAP; (g) HOSu, DCC; (h) Gly₂, NaHCO_3 ; (i) HOSu, DCC; (j) 7; (k) TFA.

Scheme II^a Synthesis of the Amide-Linked Chelator 2

Reagents: (a) NaHMDS , BrCH_2CN ; (b) H_2 , Pd/C; (c) NaHCO_3 , *N*-(methoxycarbonyl)maleimide; (d) TFA; (e) Gly₃, NaHCO_3 ; (f) HOSu, DCC; (g) 19; (h) TFA.

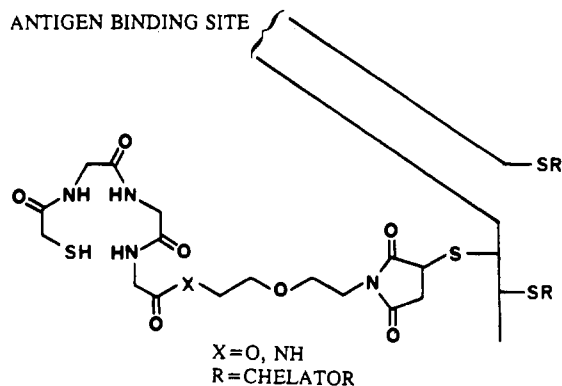


Figure 1. Structure of the Fab'-chelator conjugate.

successfully compete for the ^{99m}Tc during the radiolabeling procedure. The structure of the conjugates after deprotecting the ligand sulfhydryl is illustrated in Figure 1.

The ^{99m}Tc labeling of the conjugates was accomplished by ligand exchange. Pertechnetate from a commercial $^{99}\text{Mo}/^{99m}\text{Tc}$ generator was reduced with stannous chloride in the presence of the weakly chelating ligand D-glucuronate. The solution of ^{99m}Tc glucuronate thus formed was mixed with the antimyosin Fab' conjugates and incubated at room temperature. After 15 min, the progress of the radiolabeling was checked by ITLC and GF-HPLC (Figure 2). Both of these methods revealed that essentially all of the ^{99m}Tc was now protein bound. The small (4%) amount

Table I. Stability of ^{99m}Tc Antimyosin Fab' Ester and Amide-Linked Conjugates in Serum, Saline, and at pH 10, 37 °C

		% protein-bound radioactivity		
		1 h	4 h	20 h
^{99m}Tc Fab' ester conjugate	saline	100	99	80
	serum	95	95	92
	pH 10			5
^{99m}Tc Fab' amide conjugate	saline	100	100	100
	serum	97	96	100
	pH 10			100

of ^{99m}Tc -labeled F(ab')_2 observed for the ester-linked conjugate probably resulted from reoxidation of the Fab'. It is noteworthy that a purification step after the radiolabeling procedure is unnecessary. The immunoreactivity of the labeled antimyosin conjugates was determined by a canine myosin affinity column binding assay. Each of the two labeled conjugates retained 99% of their immunoreactivity in this assay.

To evaluate the stability of the ^{99m}Tc label, samples of the radioactive ester- and amide-linked Fab' were incubated for varying times in fresh human serum or saline. The results are presented in Table I. While the radiolabel of the amide-linked conjugate remained bound to the protein during the course of this study, the ester-linked conjugate showed a modest loss of the ^{99m}Tc from the protein. This is presumably due to hydrolysis of the ester.

To confirm that the ester-linked conjugate could undergo hydrolysis and to determine the nature of the hydrolysis

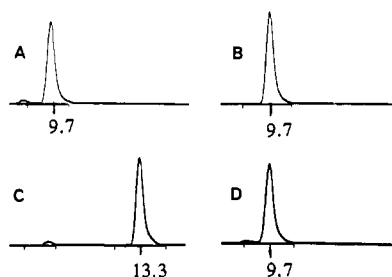


Figure 2. Radiometric GF-HPLC traces of ^{99m}Tc Fab' ester (A) and amide (B) linked conjugates and ester (C) and amide (D) linked material after 24 h at pH 10, 37 °C (t_R in minutes).

Table II. Mouse Biodistribution of ^{99m}Tc Antimyosin Fab' Ester 1^a

	15 min	1 h	2 h	5 h	24 h
blood	26.6(2.5)	13.7(0.8)	8.0(0.8)	3.6(0.6)	0.75(0.1)
heart	6.3(1.1)	4.2(0.3)	2.6(0.5)	1.2(0.2)	0.2(0.02)
lungs	6.9(1.5)	3.4(0.2)	2.4(0.2)	1.2(0.1)	0.3(0.02)
liver	5.5(0.5)	3.2(0.3)	2.3(0.1)	1.4(0.2)	0.7(0.03)
spleen	3.6(1.0)	1.9(0.3)	1.1(0.1)	0.7(0.1)	0.3(0.02)
kidney	29.4(4.0)	20.3(2.9)	12.8(1.4)	8.4(0.6)	4.4(0.2)
stomach	0.9(0.3)	0.8(0.1)	0.8(0.3)	2.0(0.7)	0.3(0.04)
small int	2.5(0.3)	4.7(1.8)	2.8(0.2)	1.9(0.3)	0.3(0.01)
large int	0.6(0.2)	0.8(0.2)	5.3(1.8)	7.2(2.4)	1.0(0.2)
muscle	0.5(0.07)	0.5(0.02)	0.6(0.06)	0.4(0.06)	0.06(0.01)
skin/fat	1.4(0.2)	1.1(0.1)	1.6(0.3)	1.0(0.2)	0.2(0.1)

^a Percent dose/gram; average \pm SD, $n = 3$.

product, the two radiolabeled proteins were subjected to basic conditions (pH 10, 37 °C, 24 h). Analysis by GF-HPLC (Figure 2) and ITLC revealed that 95% of the radioactivity was no longer bound to the protein of the ester-linked conjugate, being in the form of low molecular weight species, while the amide-linked material showed no loss of the radiolabel (see Table I). No Tc colloids were found by ITLC in either case. RP-HPLC was used to characterize the hydrolysis product. Direct injection of the ester-linked conjugate reaction mixture produced a single peak (radiometric detection) having $t_R = 1.75$ min. An authentic sample of the ^{99m}Tc complex of (mercaptoacetyl)triglycine was prepared from [(benzoylthio)acetyl]triglycine and [^{99m}Tc]pertechnetate by dithionite reduction according to the procedure of Fritzberg (15), and on RP-HPLC, this preparation yielded a major peak of $t_R = 1.75$ min. Coinjection of the authentic ^{99m}Tc complex of (mercaptoacetyl)triglycine and the hydrolysis product of the ester-linked conjugate again produced a single peak, thus confirming that in this experiment cleavage of the ester bond occurred and the expected ^{99m}Tc complex was obtained.

Biodistribution studies in mice were performed on the ^{99m}Tc -labeled ester- and amide-linked antimyosin Fab' conjugates; the results are presented in Tables II and III. Uptake by the major organs was very similar for the two products with the exception of the kidneys. In the kidneys, the ester and amide showed similar uptake at 15 min; however, at later time points the radioactivity from the ester-linked conjugate cleared the kidneys about twice as rapidly as that from the amide ($p < 0.01$). This result suggests that the ester linkage undergoes metabolic hydrolysis in the kidneys to produce a species which is readily excreted. The similar blood clearance observed (Tables II and III) for both of the labeled conjugates indicates that metabolism of the ester does not occur in the plasma. This is in agreement with the observed stability of the labeled ester-linked conjugate upon incubation in serum (Table I). Similarly, there is no significant difference in the levels of radioactivity found in the liver, or later, in the GI tract,

Table III. Mouse Biodistribution of ^{99m}Tc Antimyosin Fab' Amide 2^a

	15 min	1 h	2 h	5 h	24 h
blood	25.9(1.2)	13.2(1.4)	6.7(0.4)	2.8(0.4)	1.3(0.3)
heart	6.3(2.1)	3.5(0.3)	2.4(0.3)	1.0(0.2)	0.4(0.1)
lungs	5.3(0.8)	3.6(0.3)	2.3(0.4)	1.1(0.1)	0.5(0.1)
liver	5.8(0.5)	4.2(0.6)	2.6(0.2)	1.3(0.2)	1.5(0.1)
spleen	3.3(0.3)	2.0(0.3)	1.2(0.3)	0.6(0.03)	0.5(0.2)
kidneys	30.4(2.9)	33.8(5.9)	27.5(4.6)	18.7(2.4)	10.2(0.1)
stomach	1.2(0.1)	1.4(0.6)	0.8(0.2)	0.7(0.2)	0.4(0.1)
small int	2.5(0.4)	4.7(0.9)	2.9(0.6)	1.6(0.2)	0.5(0.1)
large int	0.8(0.1)	0.9(0.3)	3.0(1.5)	6.9(0.9)	2.3(0.7)
muscle	0.5(0.02)	0.6(0.1)	0.5(0.1)	0.4(0.03)	0.1(0.03)
skin/fat	1.8(0.2)	1.3(0.1)	1.4(0.1)	1.1(0.3)	0.3(0.1)

^a Percent dose/gram; average \pm SD, $n = 3$.

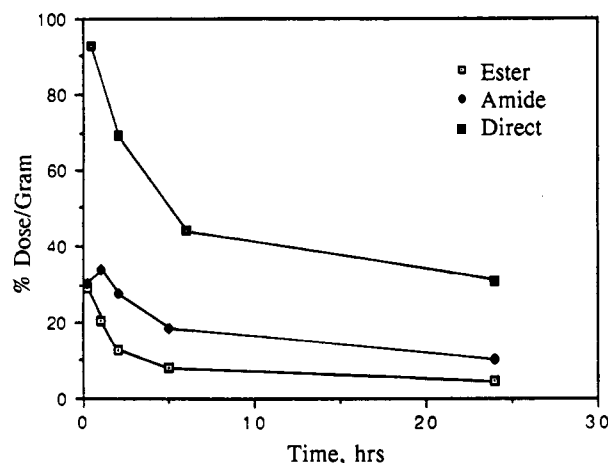


Figure 3. Mouse biodistribution kidney values.

which suggests that the hepatobiliary uptake and metabolism of the two labeled conjugates is equivalent. The kidney clearance is depicted graphically in Figure 3 along with data for antimyosin Fab' labeled directly with ^{99m}Tc via the native sulfhydryls (23). It can be seen from these data that the amide-linked conjugate also showed improved clearance kinetics from the kidney compared to the direct-labeled material. This effect may be due to the stability of the ^{99m}Tc -N₃S complex which forms on the chelator conjugate as opposed to the complex which forms upon direct labeling of the native protein sulfhydryls. It has been suggested (2) that the ^{99m}Tc which is released from the direct-labeled Fab' in the kidneys is taken up by metal-binding proteins in the tubules, resulting in the observed retention. As the kidney is the major organ for uptake of Fab' antibody fragments, the use of the ester-linked conjugate reduces the radiation dose to this organ and results in faster whole-body clearance. This effect has also been observed when ester 1 or related esters are used to radiolabel other antibody fragments such as antifibrin T2G1S (24).

In conclusion, we have developed a general method for labeling antibody Fab' fragments with ^{99m}Tc based on the ester-linked bifunctional chelator 1. The technology has been used successfully to prepare ^{99m}Tc -labeled antimyosin Fab' and may be applied to any antibody Fab' fragment as it is independent of the amino acid sequence. The use of the (mercaptoacetyl)triglycine type ligand resulted in quantitative radiolabeling; thus eliminating the need for a postlabeling purification step. Exchange labeling with D-glucarate allowed for rapid labeling at room temperature by a simple procedure which can be performed routinely in a clinical setting. The stability of the labeled conjugates in saline and in serum indicated the absence of "nonspecific" binding of the ^{99m}Tc to other sites on the

protein. The immunoreactivity of the product is preserved by the site-specific attachment of the chelator to the Fab' sulfhydryls. The presence of the ester linkage in 1 produced a 2-fold increase in the rate of clearance of the radioactivity from the kidneys over the corresponding amide-linked material, thus demonstrating that the biodistribution of ^{99m}Tc -labeled antibodies may be modified by the nature of the linking moiety.

LITERATURE CITED

- (1) Knight, L. C., Maurer, A. H., Ammar, I. A., Epps, L. A., Dean, R. T., Pak, K. Y., and Berger, H. J. (1989) Tc-99m Antifibrin Fab' Fragments for Imaging Venous Thrombi: Evaluation in a Canine Model. *Radiology* 173, 163-169.
- (2) Hansen, H. J., Jones, A. L., Sharkey, R. M., Grebenau, R., Blazejewski, N., Kunz, A., Buckley, M. J., Newman, E. S., Ostella, F., and Goldenberg, D. M. (1990) Preclinical Evaluation of an "Instant" Tc-99m-Labeling Kit for Antibody Imaging. *Cancer Research (Suppl.)* 50, 794s-798s.
- (3) Childs, R. L., and Hnatowich, D. J. (1985) Optimum Conditions for Labeling of DTPA-Coupled Antibodies with Technetium-99m. *J. Nucl. Med.* 28, 293-299.
- (4) Arano, Y., Yokoyama, A., and Magata, Y. (1985) Synthesis and Evaluation of a New Bifunctional Chelating Agent for Tc-99m labeling proteins: *p*-Carboxyethylphenylglyoxol-di(*N*-methylthiosemicarbazone) *Int. J. Nucl. Med. Biol.* 12, 425-430.
- (5) Franz, J., Volkert, W. A., Barefield, E. K., and Holmes, R. A. (1987) The Production of Tc-99m-Labeled Conjugated Antibodies Using a Cyclam-Based Bifunctional Chelating Agent *Nucl. Med. Biol.* 14, 569-572.
- (6) Morphy, J. R., Parker, D., Alexander, R., Bains, A., Carne, A. F., Eaton, M. A. W., Harrison, A., Millican, A., Phipps, A., Rhind, S. K., Titmas, R., and Weatherby, D. (1988) Antibody Labeling with Functionalised Cyclam Macrocycles. *Chem. Commun.* 156-158.
- (7) Tolman, G. L., Hadjian, R. J., Morelock, M. M., Jones, P. L., Neacy, W., Liberatore, F. A., Sands, H., and Gallagher, B. M. (1984) In Vivo Tumor Localization of Technetium-Labeled Metalothionein/Monoclonal Antibody Conjugates. *J. Nucl. Med.* 25, P24.
- (8) Lever, S. Z., Baidoo, K. E., Kramer, A. V., and Burns, D. H. (1988) Synthesis of a Novel Bifunctional Chelate Designed for Labeling Proteins with Technetium-99m. *Tetrahedron Lett.* 29, 3219-3222.
- (9) Nicolotti, R. A., and Dean, R. T. (1987) European Patent Application No. 87304716.1, December 12, 1987.
- (10) Fritzberg, A. R., Abrams, P. G., Beaumier, P. L., Kasing, S., Morgan, A. C., Rao, T. N., Reno, J. M., Sanderson, J. A., Srinivasan, A., Wilbur, D. S., and Vanderheyden, J. L. (1988) Specific and Stable Labeling of Antibodies with Technetium-99m with a Diamide Dithiolate Chelating Agent. *Proc. Natl. Acad. Sci. U.S.A.* 85, 4025-4029.
- (11) Haseman, M. K., Goodwin, D. A., Meares, C. F., Jaminski, M. S., Wensel, T. G., McCall, M. J., and Leuy, R. (1986) Metabolizable In-111 Chelate Conjugated Anti-idiotypic Monoclonal Antibody for Radioimmunodetection of Lymphoma in Mice. *Eur. J. Nucl. Med.* 12, 455-460.
- (12) Meares, C. F., McCall, M. J., Deshpande, S. V., DeNardo, S. J., and Goodwin, D. A. (1988) Chelate Radiochemistry: Cleavable Linkers Lead to Altered Levels of Radioactivity in the Liver. *Int. J. Cancer Suppl.* 2, 99-102.
- (13) Paik, C. H., Quadri, S. M., and Reba, R. C. (1989) Interposition of Different Chemical Linkages between Antibody and In-111 DTPA to Accelerate Clearance from Non-target Organs and Blood. *Nucl. Med. Biol.* 16, 475-481.
- (14) Paik, C. H., Yokoyama, K., Reynolds, J. C., Quadri, S. M., Min, C. Y., Shin, S. Y., Maloney, P. J., Larson, S. M., and Reba, R. C. (1989) Reduction of Background Activities by Introduction of a Diester Linkage Between Antibody and a Chelate in Radioimmunodetection of Tumor. *J. Nucl. Med.* 10, 1693-1701.
- (15) Fritzberg, A. R., Kasina, S., Eshima, D., and Johnson, D. L. (1986) Synthesis and Biological Evaluation of Technetium-99m MAG_3 as a Hippuran Replacement. *J. Nucl. Med.* 27, 111-116.
- (16) Johnson, L. L., and Seldin, D. W. (1989) The Role of Antimyosin Antibodies in Acute Myocardial Infarction. *Semin. Nucl. Med.* 29, 238-246.
- (17) Ellman, G. L. (1959) Tissue Sulfhydryl Groups. *Arch. Biochem. Biophys.* 82, 70-77.
- (18) Miyadera, T., Kosower, E. M., and Kosower, N. S. (1971) Receptor Site Labeling Through Functional Groups. Barbitol and Amphetamine Derivatives. *J. Med. Chem.* 14, 873-878.
- (19) Bookle, D. R., and Smith, H. (1971) An Improved Synthesis of Substituted Benzoyl Acetates. *J. Chem. Soc. (C)* 2821-2923.
- (20) Keller, O., and Rodinger, J. (1975) Preparation and Some Properties of Maleimido Acids and Maleoyl Derivatives of Peptides. *Helv. Chim. Acta* 58, 531-541.
- (21) Brown, J. Unpublished results, Centocor, Inc.
- (22) Suzuki, S., Hachimori, Y., and Matoba, R. (1970) The Chemical Modification of Biopolymers III. The Introduction of SH Groups into Taka-amylase A. *Bull. Chem. Soc. Jpn.* 43, 3849-3852.
- (23) Nedelman, M. A. Unpublished data, Centocor, Inc. The results for the ^{99m}Tc direct-labeled antimyosin Fab' were obtained from a biodistribution study at doses equivalent to those used with the labeled chelator conjugates.
- (24) Weber, R. W., Nedelman, M. A., Lister-James, J., and Dean, R. T. (1990) Comparison of Tc-99m Labeled Antibody Fab' Chelator Conjugates Having Mono, Di, and Triester Linkages. Eighth International Symposium on Radiopharmaceutical Chemistry, Princeton, NJ.